NAS 1.9/4:25/9

VOLUME 25 / NUMBER 9
MAY 8, 1987
ACC. NOS. N87-16784 TO N87-17656

U. S. DOCUMENT
DEPOSITORY SHIPMENT
MAY 04 1987
SHAFER LIBRARY
FINDLAY COLLEGE

STAR
AN ABSTRACT JOURNAL

Scientific and Technical Aerospace Reports

PRODUCED BY THE
SCIENTIFIC AND TECHNICAL
INFORMATION
BRANCH

NASA

NATIONAL AERONAUTICS AND SPACE ADMINISTRATION

WHAT YOU CAN DO FOR *STAR*

All users of this abstract service are urged to forward reports to be considered for announcement in *STAR*. This will aid NASA in its efforts to provide the fullest possible coverage of all scientific and technical publications that might support aeronautics and space research and development. If you have prepared relevant reports (other than those that you will transmit to NASA, DoD, or DOE through the usual contract- or grant-reporting channels), please send them for consideration to the NASA Scientific and Technical Information Facility, P.O. Box 8757, B.W.I. Airport, Maryland 21240.

Reprints of journal articles, book chapters, and conference papers are also welcome. These will be considered for announcement in *STAR*'s companion journal, *International Aerospace Abstracts*.

You may specify a particular source to be included in a report announcement if you wish; otherwise the report will be placed on public sale at the National Technical Information Service. Copyrighted publications will be announced but not distributed or sold.

PURCHASE OF *STAR*

The semimonthly issues are available for sale by the Superintendent of Documents, U.S. Government Printing Office, Washington, D.C. 20402.

PUBLISHED BY:

UNITED STATES GOVERNMENT
NATIONAL AERONAUTICS AND SPACE ADMINISTRATION
SCIENTIFIC AND TECHNICAL INFORMATION BRANCH
Scientific and Technical Aerospace Reports, Volume 25, is prepared by the NASA Scientific and Technical Information Facility operated for the National Aeronautics and Space Administration by RMS Associates.

The Administrator of the National Aeronautics and Space Administration has determined that the publication of this periodical is necessary in the transaction of the public business required by law of this Agency. Use of funds for printing this periodical has been approved by the Director of the Office of Management and Budget through March 22, 1988.

US ISSN 0036-8741

INTRODUCTION

Scientific and Technical Aerospace Reports (STAR) is a major component of a comprehensive National Aeronautics and Space Administration information system covering aeronautics, space, and supporting disciplines. *STAR* is issued on the 8th and 23rd of each month and announces current publications of the following types:

- NASA, NASA contractor, and NASA grantee reports
- Reports issued by other U.S. Government Agencies, domestic and foreign institutions, universities, and private firms
- Translations in report form
- NASA-owned patents and patent applications
- Dissertations and theses

Journal, book, and conference literature, cover-to-cover journal translations, and certain foreign dissertations are announced in a companion journal, *International Aerospace Abstracts (IAA)*, available on subscription from the American Institute of Aeronautics and Astronautics, Technical Information Service, 555 West 57th Street, 12th Floor, New York, New York 10019.

SUBJECT SCOPE

Subject scope of *STAR*, and *IAA* includes all aspects of aeronautics and space research and development, supporting basic and applied research, and applications. Aerospace aspects of earth resources, energy development, conservation, oceanography, environmental protection, urban transportation, and other topics of high national priority are also covered.

OTHER NASA PUBLICATIONS

Other NASA publications and information services are described in the publication, *The NASA Scientific and Technical Information System ... and How to Use It*, available without charge from the NASA Scientific and Technical Information Facility, P.O. Box 8757, B.W.I. Airport, Maryland 21240.

HOW TO USE *STAR* SUBJECT CATEGORIES

STAR is categorized by 10 major subject divisions divided into 76 specific subject categories and one general category/division. The major subject divisions are listed in the Table of Contents, together with a note for each that defines its scope and provides any cross-references. For example:

AERONAUTICS

Includes aeronautics (general); aerodynamics; air transportation and safety; aircraft communications and navigation; aircraft design, testing and performance; aircraft instrumentation; aircraft propulsion and power; aircraft stability and control; and research and support facilities (air).

For related information see also *Astronautics*.

Each major division is further divided into as many as nine specific categories, which are identified by category numbers.

Abstracts in *STAR* are grouped by specific category, the categories appearing in sequential order. Category breaks in the abstract section are identified by the category number and title, and a scope note. Cross-references to other categories are provided as appropriate. For example:

02 AERODYNAMICS

Includes aerodynamics of bodies, combinations, wings, rotors, and control surfaces; and internal flow in ducts and turbomachinery.

For related information see also *34 Fluid Mechanics and Heat Transfer.*

CROSS-REFERENCES

Individual *STAR* abstracts are not ordinarily cross-referenced, except for certain conference reports or book translations that have had separate abstracts written for their component papers or chapters. Citations and abstracts of the components follow immediately after those of the parent document. When the subject content of a component differs sufficiently from the general content of the parent, a cross-reference citation also is printed at the end of the category to which it normally would have been assigned if it were independent.

DOCUMENTS ON MICROFICHE

Documents on microfiche[1] are designated by a pound sign (#) following the accession number. The pound sign is used without regard to the source or quality of the microfiche.

AVAILABILITIES

One or more sources from which a document announced in *STAR* is available to the public is given in each citation. The most commonly indicated sources and their acronyms or abbreviations are listed below. If the publication is available from a source other than those listed, the publisher and his address will be displayed on the availability line or in combination with the corporate source line.

Avail: NTIS. Sold by the National Technical Information Service. Prices for hard copy (HC) and microfiche (MF) are indicated by a price code following the letters HC or MF in the *STAR* citation. Current values for the price codes are given in the tables on page vii.

Initially distributed microfiche under the NTIS SRIM (Selected Research in Microfiche) is available at greatly reduced unit prices. For this service and for information concerning subscription to NASA printed reports, consult the NTIS Subscription Section, Springfield, Va. 22161.

NOTE ON ORDERING DOCUMENTS: When ordering NASA publications (those followed by the * symbol), use the N accession number. NASA patent applications (only the specifications are offered) should be ordered by the US-Patent-Appl-SN number. Non-NASA publications (no asterisk) should be ordered by the AD, PB, or other *report* number shown on the last line of the citation, not by the N accession number. It is also advisable to cite the title and other bibliographic identification.

Avail: SOD (or GPO). Sold by the Superintendent of Documents, U.S. Government Printing Office, in hard copy. The current price and order number are given following the availability line. (NTIS will fill microfiche requests, as indicated above, for those documents identified by a # symbol.)

(1) A microfiche is a transparent sheet of film, 105 by 148 mm in size, containing as many as 60 to 98 pages of information reduced to micro images (not to exceed 26:1 reduction).

Avail: BLL (formerly NLL): British Library Lending Division, Boston Spa, Wetherby, Yorkshire, England. Photocopies available from this organization at the price shown. (If none is given, inquiry should be addressed to the BLL.)

Avail: DOE Depository Libraries. Organizations in U.S. cities and abroad that maintain collections of Department of Energy reports, usually in microfiche form, are listed in *Energy Research Abstracts*. Services available from the DOE and its depositories are described in a booklet, *DOE Technical Information Center - Its Functions and Services* (TID-4660), which may be obtained without charge from the DOE Technical Information Center.

Avail: ESDU. Pricing information on specific data, computer programs, and details on ESDU topic categories can be obtained from ESDU International Ltd. Requesters in North America should use the Virginia address while all other requesters should use the London address, both of which are on page vi.

Avail: Fachinformationszentrum, Karlsruhe. Sold by the Fachinformationszentrum Energie, Physik, Mathematik GMBH, Eggenstein Leopoldshafen, Federal Republic of Germany, at the price shown in deutschmarks (DM).

Avail: HMSO. Publications of Her Majesty's Stationery Office are sold in the U.S. by Pendragon House, Inc. (PHI), Redwood City, California. The U.S. price (including a service and mailing charge) is given, or a conversion table may be obtained from PHI.

Avail: NASA Public Document Rooms. Documents so indicated may be examined at or purchased from the National Aeronautics and Space Administration, Public Documents Room (Room 126), 600 Independence Ave., S.W., Washington, D.C. 20546, or public document rooms located at each of the NASA research centers, the NASA Space Technology Laboratories, and the NASA Pasadena Office at the Jet Propulsion Laboratory.

Avail: Univ. Microfilms. Documents so indicated are dissertations selected from *Dissertation Abstracts* and are sold by University Microfilms as xerographic copy (HC) and microfilm. All requests should cite the author and the Order Number as they appear in the citation.

Avail: US Patent and Trademark Office. Sold by Commissioner of Patents and Trademarks, U.S. Patent and Trademark Office, at the standard price of $1.50 each, postage free. (See discussion of NASA patents and patent applications below.)

Avail: (US Sales Only). These foreign documents are available to users within the United States from the National Technical Information Service (NTIS). They are available to users outside the United States through the International Nuclear Information Service (INIS) representative in their country, or by applying directly to the issuing organization.

Avail: USGS. Originals of many reports from the U.S. Geological Survey, which may contain color illustrations, or otherwise may not have the quality of illustrations preserved in the microfiche or facsimile reproduction, may be examined by the public at the libraries of the USGS field offices whose addresses are listed in this Introduction. The libraries may be queried concerning the availability of specific documents and the possible utilization of local copying services, such as color reproduction.

Avail: Issuing Activity, or Corporate Author, or no indication of availability. Inquiries as to the availability of these documents should be addressed to the organization shown in the citation as the corporate author of the document.

NASA PATENTS AND PATENT APPLICATIONS

Patents and patent applications owned by NASA are announced in *STAR* under appropriate subject categories and are referenced in the *STAR* indexes. In the Report/Accession Number Index, patents are indexed by the NASA Case Number (which appears in lieu of the report number in other indexes), the U.S. Patent Number, the U.S. Patent Application Serial Number, and the U.S. Patent Class. Patent applications for which patents have not yet been issued are indexed by the NASA Case Number and the U.S. Patent Application Serial Number.

NASA *patent application specifications* are sold in paper copy by the National Technical Information Service at price code A02. Microfiche are sold at price code A01. The US-Patent-Appl-SN- number should be used in ordering either paper copy or microfiche from NTIS. Printed copies of *patents* (which are not microfiched) are available for purchase at $1.50 per copy from:

Commissioner of Patents and Trademarks
U.S. Patent and Trademark Office
Washington, D.C. 20231

When ordering patents, the U.S. Patent Number should be used, and payment must be remitted in advance, preferably by money order or check payable to the Commissioner of Patents and Trademarks. Prepaid purchase coupons for ordering are also available from the Patent and Trademark Office. The patents and patent applications announced in *STAR* are owned by NASA and are available for royalty-free licensing. Requests for licensing terms and further information should be addressed to:

Assistant General Counsel for Patent Matters/Code GP
National Aeronautics and Space Administration
Washington, D.C. 20546

ELIGIBILITY AND REGISTRATION FOR NASA INFORMATION PRODUCTS AND SERVICES

A variety of services is available to organizations of the following types that have registered with NASA to receive specific services or products:

1. NASA offices, research centers, contractors, subcontractors, grantees, and consultants;
2. Other U.S. Government agencies and their contractors;
3. Libraries in the United States that have arrangements with NASA to maintain collections of NASA documents for public reference;
4. Other organizations in the United States having a need for NASA documents in work related to aeronautics and space research;
5. Organizations abroad that have established reciprocal document exchange arrangements with NASA.

Only the central service points or central points of document acquisition and control within qualified organizations are eligible to register for NASA products and services. Domestic organizations that may be eligible to receive various classes of NASA publications and services should address their requests for registration or for further information to:

NASA Scientific and Technical Information Facility
ATTN: Registration Activity
P.O. Box 8757
B.W.I. Airport, Maryland 21240

Organizations abroad should direct requests to the same address, but to the attention of: International Exchange Program.

AVAILABILITY OF *STAR* ABSTRACTS ON MICROFICHE

Microfiche of the abstract sections of this issue and other issues of *STAR* are available on annual subscription from NTIS, Attn: Subscriptions, 5285 Port Royal Road, Springfield, Virginia 22161. Annual subscription rates are $70.00 North America; $140.00 foreign. Abstract sections for previous years retroactive to 1964 are available at the current rates. Microfiche for individual *STAR* issue abstract sections are not available.

PUBLIC COLLECTIONS OF NASA DOCUMENTS

DOMESTIC: NASA and NASA-sponsored documents and a large number of aerospace publications are available to the public for reference purposes at the library maintained by the American Institute of Aeronautics and Astronautics, Technical Information Service, 555 West 57th Street, 12th Floor, New York, New York 10019

EUROPEAN: An extensive collection of NASA and NASA-sponsored publications is maintained by the British Library Lending Division, Boston Spa, Wetherby, Yorkshire, England for public access. The British Library Lending Division also has available many of the non-NASA publications cited in *STAR*. European requesters may purchase facsimile copy or microfiche of NASA and NASA-sponsored documents, those identified by both the symbols # and * from ESA - Information Retrieval Service European Space Agency, 8-10 rue Mario-Nikis, 75738 Paris CEDEX 15, France.

FEDERAL DEPOSITORY LIBRARY PROGRAM

In order to provide the general public with greater access to U.S. Government publications, Congress established the Federal Depository Library Program under the Government Printing Office (GPO), with 50 regional depositories responsible for permanent retention of material, inter-library loan, and reference services. At least one copy of nearly every NASA and NASA-sponsored publication, either in printed or microfiche format, is received and retained by the 50 regional depositories. A list of the regional GPO libraries, arranged alphabetically by state, appears on the inside back cover. These libraries are *not* sales outlets. A local library can contact a Regional Depository to help locate specific reports, or direct contact may be made by an individual.

ADDRESSES OF ORGANIZATIONS

American Institute of Aeronautics and Astronautics
Technical Information Service
555 West 57th Street, 12th Floor
New York, New York 10019

British Library Lending Division,
Boston Spa, Wetherby, Yorkshire,
England

Commissioner of Patents and Trademarks
U.S. Patent and Trademark Office
Washington, D.C. 20231

Department of Energy
Technical Information Center
P.O. Box 62
Oak Ridge, Tennessee 37830

ESA-Information Retrieval Service
ESRIN
Via Galileo Galilei
00044 Frascati (Rome) Italy

ESDU International, Ltd.
1495 Chain Bridge Road
McLean, Virginia 22101

ESDU International, Ltd.
251-259 Regent Street
London, W1R 7AD, England

Fachinformationszentrum Energie, Physik, Mathematik GMBH
7514 Eggenstein Leopoldshafen
Federal Republic of Germany

Her Majesty's Stationery Office
P.O. Box 569, S.E. 1
London, England

NASA Scientific and Technical Information Facility
P.O. Box 8757
B.W.I. Airport, Maryland 21240

National Aeronautics and Space Administration
Scientific and Technical Information Office (NTT-1)
Washington, D.C. 20546

National Technical Information Service
5285 Port Royal Road
Springfield, Virginia 22161

Pendragon House, Inc.
899 Broadway Avenue
Redwood City, California 94063

Superintendent of Documents
U.S. Government Printing Office
Washington, D.C. 20402

University Microfilms
A Xerox Company
300 North Zeeb Road
Ann Arbor, Michigan 48106

University Microfilms, Ltd.
Tylers Green
London, England

U.S. Geological Survey Library
National Center - MS 950
12201 Sunrise Valley Drive
Reston, Virginia 22092

U.S. Geological Survey Library
2255 North Gemini Drive
Flagstaff, Arizona 86001

U.S. Geological Survey
345 Middlefield Road
Menlo Park, California 94025

U.S. Geological Survey Library
Box 25046
Denver Federal Center, MS914
Denver, Colorado 80225

NTIS PRICE SCHEDULES

(Effective January 1, 1987)

Schedule A
STANDARD PRICE DOCUMENTS AND MICROFICHE

PRICE CODE	PAGE RANGE	NORTH AMERICAN PRICE	FOREIGN PRICE
A01	Microfiche	$ 6.50	$13.00
A02	001-025	9.95	19.90
A03	026-050	11.95	23.90
A04-A05	051-100	13.95	27.90
A06-A09	101-200	18.95	37.90
A10-A13	201-300	24.95	49.90
A14-A17	301-400	30.95	61.90
A18-A21	401-500	36.95	73.90
A22-A25	501-600	42.95	85.90
A99	601-up	*	*
NO1		45.00	80.00
NO2		48.00	80.00

Schedule E
EXCEPTION PRICE DOCUMENTS AND MICROFICHE

PRICE CODE	NORTH AMERICAN PRICE	FOREIGN PRICE
E01	$ 7.50	15.00
E02	10.00	20.00
E03	11.00	22.00
E04	13.50	27.00
E05	15.50	31.00
E06	18.00	36.00
E07	20.50	41.00
E08	23.00	46.00
E09	25.50	51.00
E10	28.00	56.00
E11	30.50	61.00
E12	33.00	66.00
E13	35.50	71.00
E14	38.50	77.00
E15	42.00	84.00
E16	46.00	92.00
E17	50.00	100.00
E18	54.00	108.00
E19	60.00	120.00
E20	70.00	140.00
E99	*	*

*Contact NTIS for price quote.

IMPORTANT NOTICE

NTIS Shipping and Handling Charges

U.S., Canada, Mexico — ADD $3.00 per TOTAL ORDER

All Other Countries — ADD $4.00 per TOTAL ORDER

Exceptions — Does NOT apply to:

ORDERS REQUESTING NTIS RUSH HANDLING

ORDERS FOR SUBSCRIPTION OR STANDING ORDER PRODUCTS *ONLY*

NOTE: Each additional delivery address on an order requires a separate shipping and handling charge.

VOLUME 25 NUMBER 9 / MAY 8, 1987

TABLE OF CONTENTS

AERONAUTICS

Includes aeronautics (general); aerodynamics; air transportation and safety; aircraft communications and navigation; aircraft design, testing and performance; aircraft instrumentation; aircraft propulsion and power; aircraft stability and control; and research and support facilities (air).

For related information see also *Astronautics.*

01 AERONAUTICS (GENERAL) 1135

02 AERODYNAMICS 1135

Includes aerodynamics of bodies, combinations, wings, rotors, and control surfaces; and internal flow in ducts and turbomachinery.

For related information see also *34 Fluid Mechanics and Heat Transfer*

03 AIR TRANSPORTATION AND SAFETY 1139

Includes passenger and cargo air transport operations; and aircraft accidents.

For related information see also *16 Space Transportation* and *85 Urban Technology and Transportation.*

04 AIRCRAFT COMMUNICATIONS AND NAVIGATION 1139

Includes digital and voice communication with aircraft; air navigation systems (satellite and ground based); and air traffic control.

For related information see also *17 Space Communications, Spacecraft Communications, Command and Tracking* and *32 Communications and Radar.*

05 AIRCRAFT DESIGN, TESTING AND PERFORMANCE 1140

Includes aircraft simulation technology.

For related information see also *18 Spacecraft Design, Testing and Performance* and *39 Structural Mechanics.* For land transportation vehicles see *85 Urban Technology and Transportation.*

06 AIRCRAFT INSTRUMENTATION 1141

Includes cockpit and cabin display devices; and flight instruments.

For related information see also *19 Spacecraft Instrumentation* and *35 Instrumentation and Photography.*

07 AIRCRAFT PROPULSION AND POWER 1141

Includes prime propulsion systems and systems components, e.g., gas turbine engines and compressors; and onboard auxiliary power plants for aircraft.

For related information see also *20 Spacecraft Propulsion and Power, 28 Propellants and Fuels,* and *44 Energy Production and Conversion.*

08 AIRCRAFT STABILITY AND CONTROL 1145

Includes aircraft handling qualities; piloting; flight controls; and autopilots.

For related information see also *05 Aircraft Design, Testing and Performance.*

09 RESEARCH AND SUPPORT FACILITIES (AIR) 1145

Includes airports, hangars and runways; aircraft repair and overhaul facilities; wind tunnels; shock tubes; and aircraft engine test stands.

For related information see also *14 Ground Support Systems and Facilities (Space).*

ASTRONAUTICS

Includes astronautics (general); astrodynamics; ground support systems and facilities (space); launch vehicles and space vehicles; space transportation; space communications, spacecraft communications, command and tracking; spacecraft design, testing and performance; spacecraft instrumentation; and spacecraft propulsion and power.

For related information see also *Aeronautics*

12 ASTRONAUTICS (GENERAL) 1146

For extraterrestrial exploration see *91 Lunar and Planetary Exploration.*

13 ASTRODYNAMICS 1147

Includes powered and free-flight trajectories; and orbital and launching dynamics.

14 GROUND SUPPORT SYSTEMS AND FACILITIES (SPACE) 1147

Includes launch complexes, research and production facilities; ground support equipment, e.g., mobile transporters; and simulators.

For related information see also *09 Research and Support Facilities (Air).*

15 LAUNCH VEHICLES AND SPACE VEHICLES 1147

Includes boosters; operating problems of launch/space vehicle systems; and reusable vehicles.

For related information see also *20 Spacecraft Propulsion and Power.*

16 SPACE TRANSPORTATION 1148

Includes passenger and cargo space transportation, e.g., shuttle operations; and space rescue techniques.

For related information see also *03 Air Transportation and Safety* and *18 Spacecraft Design, Testing and Performance.* For space suits see *54 Man/System Technology and Life Support.*

17 SPACE COMMUNICATIONS, SPACECRAFT COMMUNICATIONS, COMMAND AND TRACKING 1148

Includes telemetry; space communications networks; astronavigation and guidance; and radio blackout.

For related information see also *04 Aircraft Communications and Navigation* and *32 Communications and Radar.*

18 SPACECRAFT DESIGN, TESTING AND PERFORMANCE 1148

Includes satellites; space platforms; space stations; spacecraft systems and components such as thermal and environmental controls; and attitude controls.

For life support systems see *54 Man/System Technology and Life Support.* For related information see also *05 Aircraft Design, Testing and Performance, 39 Structural Mechanics,* and *16 Space Transportation.*

19 SPACECRAFT INSTRUMENTATION 1150

For related information see also *06 Aircraft Instrumentation* and *35 Instrumentation and Photography.*

20 SPACECRAFT PROPULSION AND POWER 1150

Includes main propulsion systems and components, e.g. rocket engines; and spacecraft auxiliary power sources.

For related information see also *07 Aircraft Propulsion and Power, 28 Propellants and Fuels, 44 Energy Production and Conversion,* and *15 Launch Vehicles and Space Vehicles.*

CHEMISTRY AND MATERIALS

Includes chemistry and materials (general); composite materials; inorganic and physical chemistry; metallic materials; nonmetallic materials; propellants and fuels; and materials processing.

23 CHEMISTRY AND MATERIALS (GENERAL) 1151

24 COMPOSITE MATERIALS 1151

Includes physical, chemical, and mechanical properties of laminates and other composite materials.

For ceramic materials see *27 Nonmetallic Materials.*

25 INORGANIC AND PHYSICAL CHEMISTRY 1153

Includes chemical analysis, e.g., chromatography; combustion theory; electrochemistry; and photochemistry.

For related information see also *77 Thermodynamics and Statistical Physics.*

26 METALLIC MATERIALS 1154

Includes physical, chemical, and mechanical properties of metals, e.g., corrosion; and metallurgy.

27 NONMETALLIC MATERIALS 1155

Includes physical, chemical, and mechanical properties of plastics, elastomers, lubricants, polymers, textiles, adhesives, and ceramic materials.

For composite materials see *24 Composite Materials.*

28 PROPELLANTS AND FUELS 1157

Includes rocket propellants, igniters and oxidizers; their storage and handling procedures; and aircraft fuels.

For related information see also *07 Aircraft Propulsion and Power, 20 Spacecraft Propulsion and Power,* and *44 Energy Production and Conversion.*

29 MATERIALS PROCESSING 1157

Includes space-based development of products and processes for commercial application.

For biological materials see *55 Space Biology.*

ENGINEERING

Includes engineering (general); communications and radar; electronics and electrical engineering; fluid mechanics and heat transfer; instrumentation and photography; lasers and masers; mechanical engineering; quality assurance and reliability; and structural mechanics.

For related information see also *Physics.*

31 ENGINEERING (GENERAL) 1157

Includes vacuum technology; control engineering; display engineering; cryogenics; and fire prevention.

32 COMMUNICATIONS AND RADAR 1158

Includes radar; land and global communications; communications theory; and optical communications.

For related information see also *04 Aircraft Communications and Navigation* and *17 Space Communications, Spacecraft Communications, Command and Tracking.* For search and rescue see *03 Air Transportation and Safety,* and *16 Space Transportation.*

33 ELECTRONICS AND ELECTRICAL ENGINEERING 1168

Includes test equipment and maintainability; components, e.g., tunnel diodes and transistors; microminiaturization; and integrated circuitry.

For related information see also *60 Computer Operations and Hardware* and *76 Solid-State Physics.*

34 FLUID MECHANICS AND HEAT TRANSFER 1170

Includes boundary layers; hydrodynamics; fluidics; mass transfer and ablation cooling.

For related information see also *02 Aerodynamics* and *77 Thermodynamics and Statistical Physics.*

35 INSTRUMENTATION AND PHOTOGRAPHY 1176

Includes remote sensors; measuring instruments and gages; detectors; cameras and photographic supplies; and holography.

For aerial photography see *43 Earth Resources and Remote Sensing.* For related information see also *06 Aircraft Instrumentation* and *19 Spacecraft Instrumentation.*

36 LASERS AND MASERS 1178

Includes parametric amplifiers.

For related information see also *76 Solid-State Physics.*

37 MECHANICAL ENGINEERING 1178

Includes auxiliary systems (nonpower); machine elements and processes; and mechanical equipment.

38 QUALITY ASSURANCE AND RELIABILITY 1186

Includes product sampling procedures and techniques; and quality control.

39 STRUCTURAL MECHANICS 1186

Includes structural element design and weight analysis; fatigue; and thermal stress.

For applications see *05 Aircraft Design, Testing and Performance* and *18 Spacecraft Design, Testing and Performance.*

GEOSCIENCES

Includes geosciences (general); earth resources and remote sensing; energy production and conversion; environment pollution; geophysics; meteorology and climatology; and oceanography.

For related information see also *Space Sciences.*

42 GEOSCIENCES (GENERAL) **1190**

43 EARTH RESOURCES AND REMOTE SENSING **1192**

Includes remote sensing of earth resources by aircraft and spacecraft; photogrammetry; and aerial photography.

For instrumentation see *35 Instrumentation and Photography.*

44 ENERGY PRODUCTION AND CONVERSION **1237**

Includes specific energy conversion systems, e.g., fuel cells; global sources of energy; geophysical conversion; and windpower.

For related information see also *07 Aircraft Propulsion and Power, 20 Spacecraft Propulsion and Power,* and *28 Propellants and Fuels.*

45 ENVIRONMENT POLLUTION **1239**

Includes atmospheric, noise, thermal, and water pollution.

46 GEOPHYSICS **1240**

Includes aeronomy; upper and lower atmosphere studies; ionospheric and magnetospheric physics; and geomagnetism.

For space radiation see *93 Space Radiation.*

47 METEOROLOGY AND CLIMATOLOGY **1243**

Includes weather forecasting and modification.

48 OCEANOGRAPHY **1245**

Includes biological, dynamic, and physical oceanography; and marine resources.

For related information see also *43 Earth Resources and Remote Sensing.*

LIFE SCIENCES

Includes life sciences (general); aerospace medicine; behavioral sciences; man/system technology and life support; and space biology.

51 LIFE SCIENCES (GENERAL) **N.A.**

52 AEROSPACE MEDICINE **1249**

Includes physiological factors; biological effects of radiation; and effects of weightlessness on man and animals.

53 BEHAVIORAL SCIENCES **N.A.**

Includes psychological factors; individual and group behavior; crew training and evaluation; and psychiatric research.

54 MAN/SYSTEM TECHNOLOGY AND LIFE SUPPORT **1249**

Includes human engineering; biotechnology; and space suits and protective clothing.

For related information see also *16 Space Transportation.*

55 SPACE BIOLOGY **N.A.**

Includes exobiology; planetary biology; and extraterrestrial life.

MATHEMATICAL AND COMPUTER SCIENCES

Includes mathematical and computer sciences (general); computer operations and hardware; computer programming and software; computer systems; cybernetics; numerical analysis; statistics and probability; systems analysis; and theoretical mathematics.

59 MATHEMATICAL AND COMPUTER SCIENCES (GENERAL) **1250**

60 COMPUTER OPERATIONS AND HARDWARE **1250**

Includes hardware for computer graphics, firmware, and data processing.

For components see *33 Electronics and Electrical Engineering.*

61 COMPUTER PROGRAMMING AND SOFTWARE **1251**

Includes computer programs, routines, algorithms, and specific applications, e.g., CAD/CAM.

62 COMPUTER SYSTEMS **1252**

Includes computer networks and special application computer systems.

63 CYBERNETICS **1253**

Includes feedback and control theory, artificial intelligence, robotics and expert systems.

For related information see also *54 Man/System Technology and Life Support.*

64 NUMERICAL ANALYSIS **1253**

Includes iteration, difference equations, and numerical approximation.

65 STATISTICS AND PROBABILITY **1256**

Includes data sampling and smoothing; Monte Carlo method; and stochastic processes.

66 SYSTEMS ANALYSIS **1256**

Includes mathematical modeling; network analysis; and operations research.

67 THEORETICAL MATHEMATICS **1257**

Includes topology and number theory.

PHYSICS

Includes physics (general); acoustics; atomic and molecular physics; nuclear and high-energy physics; optics; plasma physics; solid-state physics; and thermodynamics and statistical physics.

For related information see also *Engineering.*

70 PHYSICS (GENERAL) **1257**

For precision time and time interval (PTTI) see *35 Instrumentation and Photography;* for geophysics, astrophysics or solar physics see *46 Geophysics, 90 Astrophysics,* or *92 Solar Physics.*

71 ACOUSTICS 1257
Includes sound generation, transmission, and attenuation.
For noise pollution see *45 Environment Pollution.*

72 ATOMIC AND MOLECULAR PHYSICS 1258
Includes atomic structure, electron properties, and molecular spectra.

73 NUCLEAR AND HIGH-ENERGY PHYSICS 1259
Includes elementary and nuclear particles; and reactor theory.
For space radiation see *93 Space Radiation.*

74 OPTICS 1260
Includes light phenomena and optical devices.
For lasers see *36 Lasers and Masers.*

75 PLASMA PHYSICS 1262
Includes magnetohydrodynamics and plasma fusion.
For ionospheric plasmas see *46 Geophysics.* For space plasmas see *90 Astrophysics.*

76 SOLID-STATE PHYSICS 1263
Includes superconductivity.
For related information see also *33 Electronics and Electrical Engineering* and *36 Lasers and Masers.*

77 THERMODYNAMICS AND STATISTICAL PHYSICS N.A.
Includes quantum mechanics; theoretical physics; and Bose and Fermi statistics.
For related information see also *25 Inorganic and Physical Chemistry* and *34 Fluid Mechanics and Heat Transfer.*

SOCIAL SCIENCES

Includes social sciences (general); administration and management; documentation and information science; economics and cost analysis; law, political science, and space policy; and urban technology and transportation.

80 SOCIAL SCIENCES (GENERAL) 1265
Includes educational matters.

81 ADMINISTRATION AND MANAGEMENT 1265
Includes management planning and research.

82 DOCUMENTATION AND INFORMATION SCIENCE 1266
Includes information management; information storage and retrieval technology; technical writing; graphic arts; and micrography.
For computer documentation see *61 Computer Programming and Software.*

83 ECONOMICS AND COST ANALYSIS 1267
Includes cost effectiveness studies.

84 LAW, POLITICAL SCIENCE AND SPACE POLICY N.A.
Includes NASA appropriation hearings; aviation law; space law and policy; international law; international cooperation; and patent policy.

85 URBAN TECHNOLOGY AND TRANSPORTATION 1267
Includes applications of space technology to urban problems; technology transfer; technology assessment; and surface and mass transportation.
For related information see *03 Air Transportation and Safety, 16 Space Transportation,* and *44 Energy Production and Conversion.*

SPACE SCIENCES

Includes space sciences (general); astronomy; astrophysics; lunar and planetary exploration; solar physics; and space radiation.
For related information see also *Geosciences.*

88 SPACE SCIENCES (GENERAL) 1267

89 ASTRONOMY 1272
Includes radio, gamma-ray, and infrared astronomy; and astrometry.

90 ASTROPHYSICS 1275
Includes cosmology; celestial mechanics; space plasmas; and interstellar and interplanetary gases and dust.
For related information see also *75 Plasma Physics.*

91 LUNAR AND PLANETARY EXPLORATION 1278
Includes planetology; and manned and unmanned flights.
For spacecraft design or space stations see *18 Spacecraft Design, Testing and Performance.*

92 SOLAR PHYSICS 1287
Includes solar activity, solar flares, solar radiation and sunspots.
For related information see *93 Space Radiation.*

93 SPACE RADIATION 1287
Includes cosmic radiation; and inner and outer earth's radiation belts.
For biological effects of radiation see *52 Aerospace Medicine.* For theory see *73 Nuclear and High-Energy Physics.*

GENERAL

Includes aeronautical, astronautical, and space science related histories, biographies, and pertinent reports too broad for categorization; histories or broad overviews of NASA programs.

99 GENERAL 1288

Note: N.A. means that no abstracts were assigned to this category for this issue.

SUBJECT INDEX I-1
PERSONAL AUTHOR INDEX I-49
CORPORATE SOURCE INDEX I-57
CONTRACT NUMBER INDEX I-67
REPORT/ACCESSION NUMBER INDEX I-69

TYPICAL CITATION AND ABSTRACT

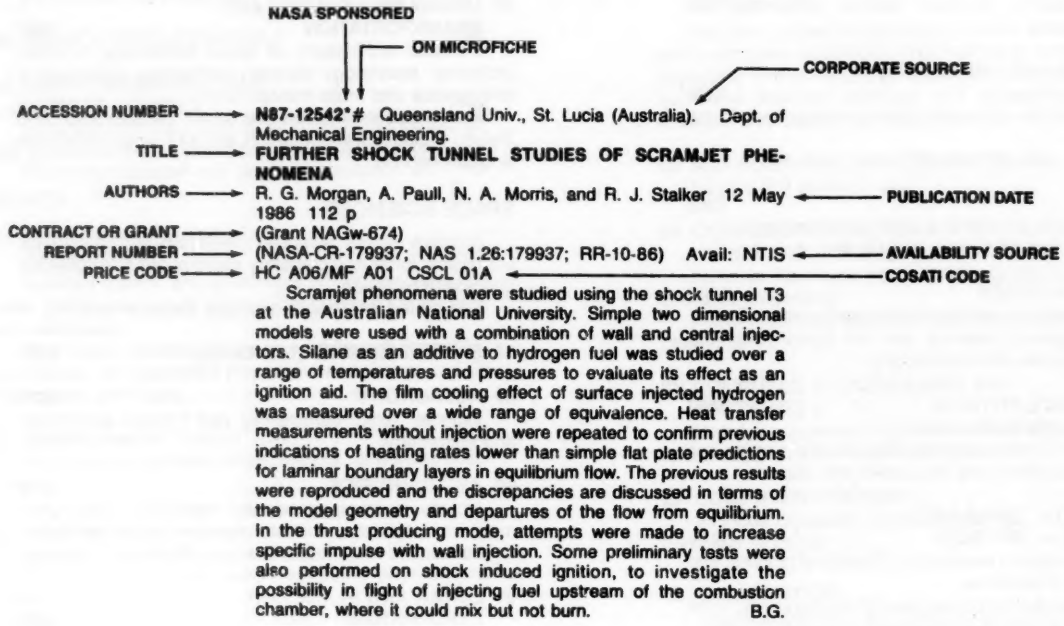
NASA SPONSORED
ON MICROFICHE
CORPORATE SOURCE
ACCESSION NUMBER
N87-12542*# Queensland Univ., St. Lucia (Australia). Dept. of Mechanical Engineering.
TITLE
FURTHER SHOCK TUNNEL STUDIES OF SCRAMJET PHENOMENA
AUTHORS
R. G. Morgan, A. Paull, N. A. Morris, and R. J. Stalker 12 May 1986 112 p
PUBLICATION DATE
CONTRACT OR GRANT
(Grant NAGw-674)
REPORT NUMBER
(NASA-CR-179937; NAS 1.26:179937; RR-10-86) Avail: NTIS
AVAILABILITY SOURCE
PRICE CODE
HC A06/MF A01 CSCL 01A
COSATI CODE
Scramjet phenomena were studied using the shock tunnel T3 at the Australian National University. Simple two dimensional models were used with a combination of wall and central injectors. Silane as an additive to hydrogen fuel was studied over a range of temperatures and pressures to evaluate its effect as an ignition aid. The film cooling effect of surface injected hydrogen was measured over a wide range of equivalence. Heat transfer measurements without injection were repeated to confirm previous indications of heating rates lower than simple flat plate predictions for laminar boundary layers in equilibrium flow. The previous results were reproduced and the discrepancies are discussed in terms of the model geometry and departures of the flow from equilibrium. In the thrust producing mode, attempts were made to increase specific impulse with wall injection. Some preliminary tests were also performed on shock induced ignition, to investigate the possibility in flight of injecting fuel upstream of the combustion chamber, where it could mix but not burn. B.G.

VOLUME 25 NUMBER 9 / MAY 8, 1987

Scientific and Technical Aerospace Reports

A Semimonthly Publication of the National Aeronautics and Space Administration

01 AERONAUTICS (GENERAL)

N87-16784*# National Aeronautics and Space Administration. Lewis Research Center, Cleveland, Ohio.
COMPARISON OF THREE EXPLICIT MULTIGRID METHODS FOR THE EULER AND NAVIER-STOKES EQUATIONS
Rodrick V. Chima, Eli Turkel, and Steve Schaffer 1987 15 p Presented at the 25th Aerospace Sciences Meeting, Reno, Nev., 12-15 Jan. 1987; sponsored by AIAA
(NASA-TM-88878; ICOMP-86-3; E-3126; NAS 1.15:88878) Avail: NTIS HC A02/MF A01 CSCL 01B

Three explicit multigrid methods, Ni's method, Jameson's finite-volume method, and a finite-difference method based on Brandt's work, are described and compared for two model problems. All three methods use an explicit multistage Runge-Kutta scheme on the fine grid, and this scheme is also described. Convergence histories for inviscid flow over a bump in a channel for the fine-grid scheme alone show that convergence rate is proportional to Courant number and that implicit residual smoothing can significantly accelerate the scheme. Ni's method was slightly slower than the implicitly-smoothed scheme alone. Brandt's and Jameson's methods are shown to be equivalent in form but differ in their node versus cell-centered implementations. They are about 8.5 times faster than Ni's method in terms of CPU time. Results for an oblique shock/boundary layer interaction problem verify the accuracy of the finite-difference code. All methods slowed considerably on the stretched viscous grid but Brandt's method was still 2.1 times faster than Ni's method. Author

02 AERODYNAMICS

Includes aerodynamics of bodies, combinations, wings, rotors, and control surfaces; and internal flow in ducts and turbomachinery.

For related information see also *34 Fluid Mechanics and Heat Transfer.*

N87-16785 Rutgers - The State Univ., New Brunswick, N. J.
CALCULATION OF SUPERSONIC FLOW OVER A COMPRESSION CORNER Ph.D. Thesis
Ching Cho Ong 1986 199 p
Avail: Univ. Microfilms Order No. DA8620068

A comparative study is made between the MacCormack explicit-implicit predictor-corrector and the Beam-Warming fully implicit algorithms for solving compressible viscous flow. The mass-averaged two-dimensional compressible Navier-Stokes equations in strong conservation law form and general curvilinear coordinates are solved numerically by marching forth in time on a body-fitted curvilinear grid for a shock wave-turbulent boundary layer interaction over a two-dimensional compression corner. Along the surface of the corner the boundary condition for the implicit part of the hybrid MacCormack algorithm is formulated using an approximation involving a lag in time of one-half step. Turbulence is simulated by means of the Baldwin-Lomax algebraic turbulent eddy viscosity model. Computations are done for a Mach number of 1.96 with a Reynolds number (based on the incoming boundary layer thickness) of 0.25 x 10 sub 6, and for a Mach number of 2.83 with a Reynolds number of 1.8 x 10 sub 6. The primary objectives of the study are: (1) to determine the extent to which the steady state solution obtained by the hybrid MacCormack algorithm is dependent upon the size of the time step employed in marching the calculation toward the steady state solution, (2) to compare the two algorithms regarding accuracy and efficiency, and (3) to further examine the efficacy of the Baldwin-Lomax algebraic eddy viscosity model through comparison with recent measurements of the Reynolds shear stress. Dissert. Abstr.

N87-16786 Stanford Univ., Calif.
THE AERODYNAMICS AND AEROACOUSTICS OF ROTATING TRANSONIC DISTURBANCES Ph.D. Thesis
John W. Rutherford 1986 122 p
Avail: Univ. Microfilms Order No. DA8619812

The aerodynamic flow field about a two-dimensional, transonically rotating disturbance is obtained using computational results from the transonic, small-disturbance, potential equation. A two-dimensional model, consisted of a circular-arc attached to the surface of a transonically, rotating cylinder, provides the same mechanism for the propagation of shocks into the far field as that found for a helicopter rotor blade in high tip speed hover. Current efforts to predict the high speed impulsive noise signature of a rotor blade have met with limited success above a limiting tip Mach number known as the delocalization Mach number. This is due to a radiating shock which forms even though the tip speed is subsonic. The two-dimensional model provides a simpler means of studying the flow field and predicting the pressure pulse without significantly altering the physics. A technique known as shock fitting is used to maintain the strong pressure discontinuity across the shock well into the flow field. Results are obtained out to nine cylinder radii, and a comparison of the pulse shape for shock fitting and shock capturing is also made. The method presented should be adaptable to the helicopter rotor problem due to experimental evidence showing the two-dimensionality of the radiating shock. Dissert. Abstr.

N87-16787 Virginia Polytechnic Inst. and State Univ., Blacksburg.
HYPERSONIC NONEQUILIBRIUM FLOW OVER AN ABLATING TEFLON SURFACE Ph.D. Thesis
Dong Joo Song 1986 173 p
Avail: Univ. Microfilms Order No. DA8620668

A complex chemical system of teflon/air mixture over an axisymmetric decoy at hypersonic reentry flight conditions has been analyzed by using the nonequilibrium viscous shock-layer method. The equilibrium catalytic wall boundary condition was used to obtain the species concentration at the wall. The species conservation equation for binary mixture (air/teflon) was solved to obtain the concentration of freestream air at the wall. Two test cases were chosen to demonstrate the capability of the current code. Due to

lack of experimental or theoretical data, the surface-measurable quantities from the current code (VSLTEF) were compared with the equivalent air injection and no-mass injection data obtained from VSL7S code. The current code predicts a higher total heat-transfer rate than that predicted by the seven species nonequilibrium air code (VSL7S) with the same injection rate due to the high diffusional heat-transfer rate. The wall pressure was not affected by blowing, while the skin-friction coefficient was decreased (i.e., 43% reduction for teflon ablation case; 53% for nonequilibrium air injection case at 125 kft) when compared with that of no-mass injection case. A shock-layer peak temperature drop (1512 R for 125 kft altitude and 848 R for 175 kft altitude) was observed at both cases. The temperature drops were chiefly due to endothermic reactions (dissociation) of the teflon ablation species. Dissert. Abstr.

N87-16788 Purdue Univ., West Lafayette, Ind.
MEASUREMENT OF THE THREE-DIMENSIONAL AERODYNAMICS OF AN ANNULAR CASCADE AIRFOIL ROW Ph.D. Thesis
Richie Charles Stauter 1986 247 p
Avail: Univ. Microfilms Order No. DA8622225

Aerodynamic design systems for turbomachine blade rows, which are evolving from simplified 2-D flow models to fundamentally 3-D models, necessarily use many assumptions. Such flow models must be validated by correlating their predictions with experimental data. The Purdue Annular Cascade Facility has been used to produce experimental data necessary to more fully understand the fundamentally 3-D nature of a turbomachine blade row flow field, and thus provide a database for flow model validation. The 3-D velocity field in the Purdue Annular Cascade Facility has been measured using a Laser Doppler Anemometer (LDA). A five degree-of-motion traversing system has been designed and fabricated to provide the various LDA probe volume orientations necessary to fully determine the velocity vector at any point in the flow field. Data produced by these experiments indicate significant three-dimensionality of the cascade passage flow field. Strong interaction is indicated between the vortices generated within the passage and the boundary layers on the passage surfaces. These interactions include transport of freestream fluid into the endwall regions and transport of fluid from the endwall regions onto the airfoil suction surface. These effects become more pronounced as the incidence angle increases. Dissert. Abstr.

N87-16789*# National Aeronautics and Space Administration. Lewis Research Center, Cleveland, Ohio.
MEASUREMENTS OF THE UNSTEADY FLOW FIELD WITHIN THE STATOR ROW OF A TRANSONIC AXIAL-FLOW FAN. 1: MEASUREMENT AND ANALYSIS TECHNIQUE
K. L. Suder, M. D. Hathaway (Army Research and Technology Labs., Cleveland, Ohio), T. H. Okiishi (Iowa State Univ. of Science and Technology, Ames.), A. J. Strazisar, and J. J. Adamczyk 1987 17 p Proposed for presentation at the 32nd International Gas Turbine Conference and Exhibition, Anaheim, Calif., 31 May - 4 Jun. 1987; sponsored by ASME
(NASA-TM-88945; E-3393; NAS 1.15:88945;
USAAVSCOM-TR-86-C-30) Avail: NTIS HC A02/MF A01 CSCL 01A

This two-part paper presents laser anemometer measurements of the unsteady velocity field within the stator row of a transonic axial-flow fan. The objective is to provide additional insight into unsteady blade-row interactions within high speed compressors which affect stage efficiency, energy transfer, and other design considerations. Part 1 describes the measurement and analysis techniques used for resolving the unsteady flow field features. The ensemble-average and variance of the measured velocities are used to identify the rotor wake generated and unresolved unsteadiness, respectively. (Rotor wake generated unsteadiness refers to the unsteadiness generated by the rotor wake velocity deficit and the term unresolved unsteadiness refers to all remaining contributions to unsteadiness such as vortex shedding, turbulence, mass flow fluctuations, etc.). A procedure for calculating auto and cross correlations of the rotor wake generated and unresolved unsteady velocity fluctuations is described. These unsteady-velocity correlations have significance since they also result from a decomposition of the Navier-Stokes equations. This decomposition of the Navier-Stokes equations resulting in the velocity correlations used to describe the unsteady velocity field will also be outlined in this paper. Author

N87-16790*# National Aeronautics and Space Administration. Lewis Research Center, Cleveland, Ohio.
MEASUREMENTS OF THE UNSTEADY FLOW FIELD WITHIN THE STATOR ROW OF A TRANSONIC AXIAL-FLOW FAN. PART 2: RESULTS AND DISCUSSION
M. D. Hathaway, K. L. Suder, T. H. Okiishi (Iowa State Univ. of Science and Technology, Ames), A. J. Strazisar, and J. J. Adamczyk 1987 16 p Prepared for presentation at the 32nd International Gas Turbine Conference and Exhibition, Anaheim, Calif., 31 May - 4 Jun. 1987; sponsored by ASME
(NASA-TM-88946; E-3394; NAS 1.15:88946;
USAAVSCOM-TR-86-C-31) Avail: NTIS HC A02/MF A01 CSCL 01A

Unsteady velocity field measurements made within the stator row of a transonic axial-flow fan are presented. Measurements were obtained at midspan for two different stator blade rows using a laser anemometer. The first stator row consists of double circular-arc airfoils with a solidity of 1.68. The second features controlled-diffusion airfoils with a solidity of 0.85. Both were tested at design-speed peak efficiency conditions. In addition, the controlled-diffusion stator was also tested at near stall conditions. The procedures developed here are used to identify the rotor wake generated and unresolved unsteadiness from the velocity measurements (rotor wake generated unsteadiness refers to the unsteadiness generated by the rotor wake velocity deficit and unresolved unsteadiness refers to all remaining unsteadiness which contributes to the spread in the distribution of velocities such as vortex shedding, turbulence, etc.). Auto and cross correlations of these unsteady velocity fluctuations are presented to show their relative magnitude and spatial distributions. Amplification and attenuation of both rotor wake generated and unresolved unsteadiness are shown to occur within the stator blade passage. Author

N87-16791*# National Aeronautics and Space Administration. Ames Research Center, Moffett Field, Calif.
COMPUTATION OF SEPARATION AHEAD OF BLUNT FIN IN SUPERSONIC TURBULENT FLOW
Ching-mao Hung Dec. 1986 9 p
(NASA-TM-89416; A-87047; NAS 1.15:89416) Avail: NTIS HC A02/MF A01 CSCL 01A

Separation ahead of a flat-face blunt fin in a supersonic turbulent boundary layer was studied numerically. The following observations and conclusions were made: (1) the length of separation increases to about 5.2 D, compared with about 2.0 to 2.5 D for the typical hemi-cylindrical results, and this numerical result confirms experimental observation; (2) even though there is a kink in pressure in the present case, there is no secondary separation under the main horseshoe vortices and there are three vortices, leading to the conclusion that the number of vortices is not always an even number; and (3) for the case investigated the separation point is connected to the inner (first) horseshoe vortex, rather than the outer (second) one. The four layers of fluid entrain in the three vortices, respectively. Author

N87-16792*# National Aeronautics and Space Administration. Lyndon B. Johnson Space Center, Houston, Tex.
EULER SOLUTIONS USING AN IMPLICIT MULTIGRID TECHNIQUE
Chien-peng Li Nov. 1986 19 p Presented at the 2nd Copper Mountain Multigrid Conference, 31 Mar. - 3 Apr. 1985
(NASA-TM-58276; NAS 1.15:58276) Avail: NTIS HC A02/MF A01 CSCL 01A

A coarse-grid correction algorithm has been implemented into an implicit upwind Euler solver and tested for transonic airfoil problems. The Euler solver uses split-flux formulation and penta-diagonal scalar equations, respectively, for the explicit and implicit

operators. The multigrid sequence starts at the fine grid level, then steps down to each coarse grid level to smooth error components using implicit operators. Estimate of residuals can be obtained by two approaches, which differ in the level where the residuals are collected. Both approaches will lead to a work reduction factor of 12 for a Mach 0.75 flow at 2 degrees incidence on a 65x26 grid. The work reduction factor is found to increase proportional to the number of grid levels. Author

N87-16793*# National Aeronautics and Space Administration. Langley Research Center, Hampton, Va.
GEOMETRIES FOR ROUGHNESS SHAPES IN LAMINAR FLOW Patent
Bruce J. Holmes, inventor (to NASA), Glenn L. Martin, inventor (to NASA) (Kentron International, Inc., Hampton, Va.), Christopher S. Domack, inventor (to NASA), Clifford J. Obara, inventor (to NASA), and Ahmed A. Hassan, inventor (to NASA) (Arizona State Univ., Tempe) Issued 28 Oct. 1986 9 p Filed 10 Nov. 1983 Supersedes N84-12092 (22 - 03, p 320)
(NASA-Case-LAR-13255-1; US-Patent-4,619,423; US-Patent-Appl-SN-550681; US-Patent-Class-244-130; US-Patent-Class-244-35R; US-Patent-Class-244-200; US-Patent-Class-244-204) Avail: U.S. Patent and Trademark Office CSCL 01A

A passive interface mechanism between upper and lower skin structures, and a leading edge structure of a laminar flow airfoil is described. The interface mechanism takes many shapes. All are designed to be different than the sharp orthogonal arrangement prevalent in the prior art. The shapes of the interface structures are generally of two types: steps away from the centerline of the airfoil with a sloping surface directed toward the trailing edge and, the other design has a gap before the sloping surface. By properly shaping the step, the critical step height is increased by more than 50% over the orthogonal edged step. NASA

N87-16794# Aeronautical Research Inst. of Sweden, Stockholm.
NAVIER-STOKES SOLUTION FOR LAMINAR TRANSONIC FLOW OVER A NACA0012 AIRFOIL
Bernhard Mueller 1986 101 p
(FAA-140) Avail: NTIS HC A06/MF A01

Laminar transonic flow at medium Reynolds numbers over a NACA0012 airfoil is numerically simulated by solving the two-dimensional compressible Navier-Stokes equations by means of the implicit central difference scheme of Beam and Warming. Recent improvements in efficiency, accuracy and convergence for the approximate factorization algorithm are employed, including local time stepping for steady-state calculations, combined 2nd and 4th order numerical damping, refined body and farfield boundary conditions, and linearization of the mixed derivatives. C-type meshes are generated by the transfinite interpolation method. The results cover the test cases for external flow of the GAMM Workshop on Numerical Simulation of Compressible Navier-Stokes Flows (1985) for Mach number M sub infinity=0.8, 0.85, 2, angles of attack alpha=0 deg and Reynolds numbers Re sub infinity=73 to 10 to the 4th power. Author

N87-16795# Weapons Systems Research Lab., Salisbury (Australia).
LINEARISED THEORY OF STABILITY AND RESONANCE FOR PROJECTILES WITH AERODYNAMICALLY INDUCED ROLL VARIATIONS
G. Jepps May 1986 50 p
(WSRL-0449-TR; AR-004-619) Avail: NTIS HC A03/MF A01

Equations of motion of an unguided projectile undergoing aerodynamically induced transient rolling motion are set up and linearized. A state variable formulation is used. Solutions for angle of attack are developed in the form of infinite series and in terms of confluent hypergeometric functions. Conditions for asymptotic stability are derived and two sets of criteria are found, depending on the relative magnitudes of the roll damping and axial force coefficients. Angle of attack response to a lateral moment that rolls with the projectile and which may lead to resonant coupling is also investigated. Author

N87-16796*# National Aeronautics and Space Administration. Langley Research Center, Hampton, Va.
LOADS AND AEROELASTICITY DIVISION RESEARCH AND TECHNOLOGY ACCOMPLISHMENTS FOR FY 1986 AND PLANS FOR FY 1987
James E. Gardner and S. C. Dixon Jan. 1987 123 p
(NASA-TM-89084; NAS 1.15:89084) Avail: NTIS HC A06/MF A01 CSCL 01A

The Loads and Aeroelasticity Division's research accomplishments for FY 86 and research plans for FY 87 are presented. The work under each Branch (technical area) is described in terms of highlights of accomplishments during the past year and highlights of plans for the current year as they relate to five year plans for each technical area. This information will be useful in program coordination with other government organizations and industry in areas of mutual interest. Author

N87-16797*# National Aeronautics and Space Administration, Washington, D.C.
STABILITY CHARACTERISTICS OF A SUPERSONIC BOUNDARY LAYER AND THEIR RELATION TO THE POSITION OF THE LAMINAR-TURBULENT TRANSITION POINT
V. I. Lysenko Jan. 1987 15 p Transl. into ENGLISH from Izvestiya Sibirskogo Otdeleniya Akademii Nauk SSSR, Seriya, Tekhnicheskikh Nauk (USSR), Issue 1, no. 4, 1985 p 79-86 Original language document was announced in IAA as A85-42123 Transl. by Kanner (Leo) Associates, Redwood City, Calif. Original document was prepared by USSR Academy of Sciences, Siberian Branch
(Contract NASw-4005)
(NASA-TM-88533; NAS 1.15:88533) Avail: NTIS HC A02/MF A01 CSCL 01A

By comparing the calculated results with experimental data, it is demonstrated that the position of the laminar-boundary transition point of a boundary layer can be estimated by using the e-exp-n method. The effect of the Mach number, pressure gradient, and heat transfer on the laminar-turbulent transition is discussed. It is found that under conditions of strong cooling, the effect of the pressure gradient on the position of the transition point is less pronounced than in the absence of heat transfer. Author

N87-16798*# National Aeronautics and Space Administration. Lewis Research Center, Cleveland, Ohio.
EULER ANALYSIS OF THE THREE DIMENSIONAL FLOW FIELD OF A HIGH-SPEED PROPELLER: BOUNDARY CONDITION EFFECTS
M. Nallasamy (Sverdrup Technology, Inc., Cleveland, Ohio), B. J. Clark, and J. F. Groeneweg 1987 18 p Proposed for presentation at the 32nd International Gas Turbine Conference and Exhibition, Anaheim, Calif., 31 May - 4 Jun. 1987; sponsored by ASME
(NASA-TM-88955; E-3399; NAS 1.15:88955) Avail: NTIS HC A02/MF A01 CSCL 01A

The results of an investigation of the effects of far field boundary conditions on the solution of the three dimensional Euler equations governing the flow field of a high speed single rotation propeller are presented. The results show that the solutions obtained with the nonreflecting boundary conditions are in good agreement with experimental data. The specification of nonreflecting boundary conditions is effective in reducing the dependence of the solution on the location of the far field boundary. Details of the flow field within the blade passage and the tip vortex are presented. The dependence of the computed power coefficient on the blade passage and the tip vortex are presented. The dependence of the computed power coefficient on the blade setting angle is examined. Author

N87-16799*# National Aeronautics and Space Administration. Lewis Research Center, Cleveland, Ohio.
SPATIALLY GROWING DISTURBANCES IN A TWO-STREAM, COPLANAR JET
Jeffrey H. Miles 1986 30 p Presented at the 24th Aerospace Sciences Meeting, Reno, Nev., 6-8 Jan. 1986; sponsored by AIAA
(NASA-TM-88949; E-3398; NAS 1.15:88949; AIAA-86-0041) Avail: NTIS HC A03/MF A01 CSCL 01A

The influence of the outer stream on the instability of a two-stream, coplanar jet with only the primary (central) stream heated for a nominal outer-to-primary velocity ratio of 0.3 was investigated by means of inviscid linearized stability theory. The instability properties of spatially growing axisymmetric and first order azimuthal disturbances were studied. It was found that the instability characteristics of the two stream jet are very different from those of a single stream jet. The presence of the outer stream enhanced the instability of the jet and increased the unstable frequency range for the first order azimuthal mode. Author

N87-16800*# National Aeronautics and Space Administration. Ames Research Center, Moffett Field, Calif.
TRANSONIC UNSTEADY AERODYNAMIC AND AEROELASTIC CALCULATIONS ABOUT AIRFOILS AND WINGS
Peter M. Goorjian and Guru P. Guruswamy Jan. 1987 9 p Prepared for presentation at the International Conference on Computational Eng. Mech., Beijing, China, 21-25 Jun. 1987
(NASA-TM-89417; A-87048; NAS 1.15:89417) Avail: NTIS HC A02/MF A01 CSCL 01A

Research in the area of computational unsteady transonic flows about airfoils and wings, including aeroelastic effects was surveyed. In the last decade, there were extensive developments in computational methods in response to the need for computer codes with which to study fundamental aerodynamic and aeroelastic problems in the critical transonic regime. For example, large commercial aircraft cruise most effectively in the transonic flight regime and computaticnal fluid dynamics (CFD) provides a new tool, which can be used in combination with test facilities to reduce the costs, time, and risks of aircraft development. Author

N87-16801*# National Aeronautics and Space Administration. Ames Research Center, Moffett Field, Calif.
COMPUTATIONAL, UNSTEADY TRANSONIC AERODYNAMICS AND AEROELASTICITY ABOUT AIRFOILS AND WINGS
Peter M. Goorjian and Guru P. Guruswamy Jan. 1987 9 p Prepared for presentation at the International Conference on Fluid Mechanics, Beijing, China, 16-19 Jun. 1987
(NASA-TM-89414; A-87042; NAS 1.15:89414) Avail: NTIS HC A02/MF A01 CSCL 01A

Research in the area of computational, unsteady transonic flows about airfoils and wings, including aeroelastic effects is reviewed. In the last decade, there have been extensive developments in computational methods in response to the need for computer codes with which to study fundamental aerodynamic and aeroelastic problems in the critical transonic regime. For example, large commercial aircraft cruise most effectively in the transonic flight regime and computational fluid dynamics (CDF) provides a new tool, which can be used in combination with test facilities to reduce the costs, time, and risks of aircraft development. Author

N87-16802*# National Aeronautics and Space Administration. Langley Research Center, Hampton, Va.
COMPENDIUM OF NASA LANGLEY REPORTS ON HYPERSONIC AERODYNAMICS
Frances E. Sabo, Aubrey M. Cary, and Shirley W. Lawson Jan. 1987 177 p
(NASA-TM-87760; NAS 1.15:87760) Avail: NTIS HC A09/MF A01 CSCL 01A

Reference is made to papers published by the Langley Research Center in various areas of hypersonic aerodynamics for the period 1950 to 1986. The research work was performed either in-house by the Center staff or by other personnel supported entirely or in part by grants or contracts. Abstracts have been included with the references when available. The references are listed chronologically and are grouped under the following general headings: (1) Aerodynamic Measurements - Single Shapes; (2) Aerodynamic Measurements - Configurations; (3) Aero-Heating; (4) Configuration Studies; (5) Propulsion Integration Experiment; (6) Propulsion Integration - Study; (7) Analysis Methods; (8) Test Techniques; and (9) Airframe Active Cooling Systems. Author

N87-16803*# Sverdrup Technology, Inc., Cleveland, Ohio.
A MULTIGRID LU-SSOR SCHEME FOR APPROXIMATE NEWTON ITERATION APPLIED TO THE EULER EQUATIONS Final Report
Seokkwan Yoon and Antony Jameson (Princeton Univ., N. J.) Sep. 1986 12 p
(Contract NAS3-24105)
(NASA-CR-179524; E-3104; NAS 1.26:179524) Avail: NTIS HC A02/MF A01 CSCL 01A

A new efficient relaxation scheme in conjunction with a multigrid method is developed for the Euler equations. The LU SSOR scheme is based on a central difference scheme and does not need flux splitting for Newton iteration. Application to transonic flow shows that the new method surpasses the performance of the LU implicit scheme. Author

N87-16804*# Sverdrup Technology, Inc., Cleveland, Ohio.
A HIGH RESOLUTION SHOCK CAPTURING SCHEME FOR HIGH MACH NUMBER INTERNAL FLOW Final Report
Seokkwan Yoon and Antony Jameson (Princeton Univ., N. J.) Sep. 1986 11 p
(Contract NAS3-24105)
(NASA-CR-179523; E-3103; NAS 1.26:179523) Avail: NTIS HC A02/MF A01 CSCL 01A

An accurate shock capturing scheme is developed for high speed flow. The flux limited dissipation scheme can be converted to a symmetric TVD scheme in the case of a scalar conservation law. Application to an oblique shock wave problem shows the improved resolution and accuracy when compared to the results obtained by the adaptive dissipation method, while exhibiting comparable computational efficiency. Author

N87-16805*# National Aeronautics and Space Administration. Lewis Research Center, Cleveland, Ohio.
UNSTEADY FLOWS IN A SINGLE-STAGE TRANSONIC AXIAL-FLOW FAN STATOR ROW Ph.D. Thesis - Iowa State Univ.
Michael D. Hathaway Dec. 1986 210 p
(NASA-TM-88929; E-3190; NAS 1.15:88929; USAAVSCOM-TR-86-C-29) Avail: NTIS HC A10/MF A01 CSCL 01A

Measurements of the unsteady velocity field within the stator row of a transonic axial-flow fan were acquired using a laser anemometer. Measurements were obtained on axisymmetric surfaces located at 10 and 50 percent span from the shroud, with the fan operating at maximum efficiency at design speed. The ensemble-average and variance of the measured velocities are used to identify rotor-wake-generated (deterministic) unsteadiness and turbulence, respectively. Correlations of both deterministic and turbulent velocity fluctuations provide information on the characteristics of unsteady interactions within the stator row. These correlations are derived from the Navier-Stokes equation in a manner similar to deriving the Reynolds stress terms, whereby various averaging operators are used to average the aperiodic, deterministic, and turbulent velocity fluctuations which are known to be present in multistage turbomachines. The correlations of deterministic and turbulent velocity fluctuations throughout the axial fan stator row are presented. In particular, amplification and attenuation of both types of unsteadiness are shown to occur within the stator blade passage. Author

N87-16806*# Sverdrup Technology, Inc., Cleveland, Ohio.
AN LU-SSOR SCHEME FOR THE EULER AND NAVIER-STOKES EQUATIONS Final Report
Seokkwan Yoon and Antony Jameson (Princeton Univ., N. J.) Dec. 1986 12 p Presented at the 25th Aerospace Sciences Meeting, Reno, Nev., 12-15 Jan. 1987; sponsored by AIAA
(Contract NAS3-24105)
(NASA-CR-179556; E-3105; NAS 1.26:179556; AIAA-87-0600) Avail: NTIS HC A02/MF A01 CSCL 01A

A new multigrid relaxation scheme, lower-upper symmetric successive overrelaxation (LU-SSOR) is developed for the steady-state solution of the Euler and Navier-Stokes equations. The scheme, which is based on central differences, does not require

flux splitting for approximate Newton iteration. Application to transonic flow shows that the new method is efficient and robust. The vectorizable LU-SSOR scheme needs only scalar diagonal inversions. Author

N87-16807*# Vigyan Research Associates, Inc., Hampton, Va.
CALCULATION OF SIDEWALL BOUNDARY-LAYER PARAMETERS FROM RAKE MEASUREMENTS FOR THE LANGLEY 0.3-METER TRANSONIC CRYOGENIC TUNNEL
A. V. Murthy Feb. 1987 36 p
(Contract NAS1-17919)
(NASA-CR-178241; NAS 1.26:178241) Avail: NTIS HC A03/MF A01 CSCL 01A

Correction of airfoil data for sidewall boundary-layer effects requires a knowledge of the boundary-layer displacement thickness and the shape factor with the tunnel empty. To facilitate calculation of these quantities under various test conditions for the Langley 0.3 m Transonic Cryogenic Tunnel, a computer program was written. This program reads the various tunnel parameters and the boundary-layer rake total head pressure measurements directly from the Engineering Unit tapes to calculate the required sidewall boundary-layer parameters. Details of the method along with the results for a sample case are presented. Author

N87-16808# Institut Franco-Allemand de Recherches, St. Louis (France).
COMBINED DENSITY AND VELOCITY MEASUREMENTS. APPLICATION TO THE INVESTIGATION OF A FREE JET [MESURES COMBINEES DE MASSE VOLUMIQUE ET DE VITESSE. APPLICATION A L'ETUDE DES JETS]
L. Bobin 27 Feb. 1986 25 p In FRENCH Presented at DRET/ONERA Colloque on Les Ecoulements Turbulents Compressibles, Poitiers, France, 10-12 Mar. 1986
(ISL-CO-206/86; ETN-87-98802) Avail: NTIS HC A02/MF A01

An experimental study was performed in order to establish for calculation programs an empirical estimate of the air flow rate in a turbulent flow with free boundaries. On a circular, vertical jet, fed by a compressed gas, combined and local measurements of the average axial velocity were performed by laser velocimetry and the average concentration of motor gas in the flow by spontaneous Raman diffusion. From these measurements the local and global air flow rates are deduced. The effect of diameter, jet velocity, volumetric mass, and viscosity of the gas motor were examined. The first results show a linear increase of the air flow rate with longitudinal distance. ESA

N87-16809# Instituto Nacional de Tecnica Aeroespacial, Madrid (Spain). Lab. de Ensayos Aerodinamicos.
THE EFFECTS OF HEAVY RAIN ON PROFILE AERODYNAMICS [EFECTOS DE LA LLUVIA INTENSA SOBRE LA AERODINAMICA DE UN PERFIL]
Alejandro Feo Palacios 1986 7 p In SPANISH; ENGLISH summary
(ETN-87-98848) Avail: NTIS HC A02/MF A01

The joint effects of rain and other meteorological phenomena on the aerodynamic characteristics of wing profiles is discussed. They may play a role in aircraft accidents taking place in take-off and landing conditions. Simulated trajectories were studied including heavy rain effects calculated under simplified conditions. It is shown that the simulations reproduce the paths of two accidents that happened approaching the runways. The relevant rain characteristics and the physical mechanisms under which degradations of the aerodynamic coefficients are produced are described. ESA

N87-16810# Instituto Nacional de Tecnica Aeroespacial, Madrid (Spain). Dept. de Aerodinamica y Navegabilidad.
PROFILE DESIGN IN TRANSONIC REGIME [DISENO DE PERFILES EN REGIMEN TRANSONICO]
Fernando Monge Gomez 1986 12 p In SPANISH; ENGLISH summary
(ETN-87-98849) Avail: NTIS HC A02/MF A01

Inverse design problem numerical methods are studied in order to solve difficulties encountered in their application to airfoils in transonic regime, due to the high pressure gradients across the shock wave. The MacFadden computer program is shown to behave poorly when supersonic points data are included. Modifications to alleviate computation problems are described. Suggestions to improve the usefulness of the MacFadden method are made. ESA

N87-16811# Aeronautical Research Inst. of Sweden, Stockholm. Aerodynamics Dept.
A COMPARISON OF SINGLE-BLOCK AND MULTI-BLOCK GRIDS AROUND WING-FUSELAGE CONFIGURATIONS
Torsten Berglind 20 Aug. 1986 34 p
(Contract FMV-F-K-82260-84-254-73-001)
(FFA-TN-1986-42; ETN-87-98906) Avail: NTIS HC A03/MF A01

Computational procedures for the generation of single and multiblock grids by transfinite interpolation around wing-fuselage configurations are presented. The single-block grid is generated from an initial grid around the wing alone, adapted to conform to the fuselage by transfinite interpolation. One of the grid lines also conforms to the cut between the fuselage and the symmetry plane. The single-block grid contains highly skewed grid cells outside the fuselage, especially if the fuselage is exposed far from the wing. It is better to divide the flow region into several subregions, each a geometrically simple figure. The flow region around the wing-fuselage configuration is divided into three subregions. The multiblock grid is better than a single-block grid to generate nearly orthogonal grids and to condense grid points in regions where the dependent variables change rapidly. ESA

03 AIR TRANSPORTATION AND SAFETY

Includes passenger and cargo air transport operations; and aircraft accidents.

For related information see also *16 Space Transportation* and *85 Urban Technology and Transportation.*

No abstracts in this category.

04 AIRCRAFT COMMUNICATIONS AND NAVIGATION

Includes digital and voice communication with aircraft; air navigation systems (satellite and ground based); and air traffic control.

For related information see also *17 Space Communications, Spacecraft Communications, Command and Tracking* and *32 Communications and Radar.*

N87-16812# Federal Aviation Administration, Washington, D.C. Air Traffic Control Radar Beacon System Analysis Team.
AIR TRAFFIC CONTROL RADAR BEACON SYSTEM TRANSPONDER PERFORMANCE STUDY AND ANALYSIS. VOLUME 2: APPENDIXES Final Report
Sep. 1986 397 p
(DOT/FAA/FS-86/1-Vol-2) Avail: NTIS HC A17/MF A01

Detailed test procedures, collected data, and other related background material on radar beacon system transponders are presented. Author

05 AIRCRAFT DESIGN, TESTING AND PERFORMANCE

Includes aircraft simulation technology.

For related information see also *18 Spacecraft Design, Testing and Performance* and *39 Structural Mechanics.* For land transportation vehicles see *85 Urban Technology and Transportation.*

N87-16813# Stanford Univ., Calif. Dept. of Aeronautics and Astronautics.

IDENTIFICATION OF A DYNAMIC MODEL OF A HELICOPTER FROM FLIGHT TESTS Ph.D. Thesis

Garth W. Milne Dec. 1986 297 p

Copyright. Avail: Issuing Activity

Techniques for identifying continuous models of dynamic systems were applied to the unstable longitudinal hover dynamics of a CH-47B Chinook helicopter. The equation error method with carefully filtered 7.18 Hz data produced good pitch transfer function models. Frequency response plots for increasing order models were used to determine the model order. The linear inter-sample equivalent produced better continuous models from identified ARMA models than the zero order hold assumption. The 300% overshoot in the vertical acceleration step response arising from dynamic inflow and rotor coning was also identified. The MIMO Maximum Likelihood identification method with process and measurement noise was then examined. High Kalman gain increases the high-frequency weighting, increasing sensitivity to unmodeled dynamics. Low-noise sensors and the absence of measurement noise above 3 Hz (following pre-filtering to remove rotor noise) resulted in high Kalman gains and singular measurement noise covariance estimates, requiring use of the Maine-Iliff MMLW3 algorithm formulation. A discrete gradient version of this algorithm was developed for the PC-MATLAB language on IBM-PC type computers, and was used for longitudinal derivative identification. The algorithm is attractive for instructional use. A User's Manual is included. Author

N87-16814 Michigan Univ., Ann Arbor.

OPTIMAL TURNING AT HIGH ANGLE OF ATTACK OF SUPERSONIC AND HYPERSONIC VEHICLES Ph.D. Thesis

Jaemyong Lee 1986 230 p

Avail: Univ. Microfilms Order No. DA8621320

The objective is to investigate the contribution of thrust angle of attack on the optimum turn of supersonic and hypersonic vehicles. The first part is concerned with the minimum time turning of a supersonic aircraft. Optimum trajectories including the effect of thrust angle of attack were studied using the Maximum Principle. Use of the domain of maneuverability, switching theory, and the Generalized Legendre Clebsch condition provides insight into the structure of the control and the optimality of the singular control. The problem of aerocruise of hypersonic vehicles with thrust angle was studied in the second part. A judicious choice of coordinate frame simplifies the relations between the aerodynamic turn and the corresponding changes in the inclination and the nodal angle. A new approach to solving the problem of achieving specified changes in both inclination and nodal angle without using numerical iterative methods is proposed. The influence of the key parameters, such as the initial argument of latitude, speed, cruise altitude, angle of attack, and thrust angle of attack is analyzed. The analytic solution giving the optimal thrust angle of attack is developed for the first time. It is shown to be accurate when compared with the numerical solution. Finally, an extremely accurate analytic solution for computing the trajectory with inclination changes of up to 40 deg. is developed. Dissert. Abstr.

N87-16815*# National Aeronautics and Space Administration. Langley Research Center, Hampton, Va.

FLIGHT INVESTIGATION OF THE EFFECT OF TAIL CONFIGURATION ON STALL, SPIN, AND RECOVERY CHARACTERISTICS OF A LOW-WING GENERAL AVIATION RESEARCH AIRPLANE

H. Paul Stough, III, James M. Patton, Jr., and Steven M. Sliwa Feb. 1987 125 p

(NASA-TP-2644; L-16194; NAS 1.60:2644) Avail: NTIS HC A06/MF A01 CSCL 01C

Flight tests were performed to investigate the stall, spin, and recovery characteristics of a low-wing, single-engine, light airplane with four interchangeable tail configurations. The four tail configurations were evaluated for effects of varying mass distribution, center-of-gravity position, and control inputs. The airplane tended to roll-off at the stall. Variations in tail configuration produced spins ranging from 40 deg to 60 deg angle of attack and turn rates of about 145 to 208 deg/sec. Some unrecoverable flat spins were encountered which required use of the airplane spin chute for recovery. For recoverable spins, antispin rudder followed by forward wheel with ailerons centered provided the quickest spin recovery. The moderate spin modes agreed very well with those predicted from spin-tunnel model tests, however, the flat spin was at a lower angle of attack and a slower rotation rate than indicated by the model tests. Author

N87-16816*# National Aeronautics and Space Administration. Lewis Research Center, Cleveland, Ohio.

IDENTIFICATION AND PROPOSED CONTROL OF HELICOPTER TRANSMISSION NOISE AT THE SOURCE

John J. Coy (Army Research and Technology Labs Cleveland, Ohio), Robert F. Handschuh, David G. Lewicki, Ronald G. Huff, Eugene A. Krejsa, and Allan M. Karchmer 1987 23 p Proposed for presentation at the NASA/Army Rotorcraft Technology Conference, Moffett Field, Calif., 17-19 Mar. 1987

(NASA-TM-89312; NAS 1.15:89312; USAAVCOM-TR-87-C-2) Avail: NTIS HC A02/MF A01 CSCL 01C

Helicopter cabin interiors require noise treatment which is expensive and adds weight. The gears inside the main power transmission are major sources of cabin noise. Work conducted by the NASA Lewis Research Center in measuring cabin interior noise and in relating the noise spectrum to the gear vibration of the Army OH-58 helicopter is described. Flight test data indicate that the planetary gear train is a major source of cabin noise and that other low frequency sources are present that could dominate the cabin noise. Companion vibration measurements were made in a transmission test stand, revealing that the single largest contributor to the transmission vibration was the spiral bevel gear mesh. The current understanding of the nature and causes of gear and transmission noise is discussed. It is believed that the kinematical errors of the gear mesh have a strong influence on that noise. The completed NASA/Army sponsored research that applies to transmission noise reduction is summarized. The continuing research program is also reviewed. Author

N87-16817# De Havilland Aircraft Co. of Canada Ltd., Downsview (Ontario).

PERFORMANCE DATA AEROC 8.2.AC.20, ISSUE 5, DASH 8, SERIES 100

Nov. 1986 90 p

Avail: NTIS HC A05/MF A01

The performance data for operations and route analysis are presented. The detailed description of the Dash 8 100 Series is given. All performance data are given with the deicing system off. All fuel consumption data are based on engine manufacture's specifications. Payload range, block fuel and time at constant cruise altitude is given, as is block time and fuel at optimum cruise altitude. Maximum permissible takeoff and landing weight is given along with takeoff and landing field lengths. Author

N87-16818# De Havilland Aircraft Co. of Canada Ltd., Downsview (Ontario).

PERFORMANCE DATA AEROC 8.2.AC.20(300), ISSUE 1

Sep. 1986 68 p

Avail: NTIS HC A04/MF A01

The performance data for operations and route analysis are presented. All performance data are given with the deicing system off. Block time and fuel data are given. Corrections for

weights, temperatures, and wind speeds are contained on the charts. B.G.

N87-16819*# National Aeronautics and Space Administration. Ames Research Center, Moffett Field, Calif.
AFTI/F-111 MAW FLIGHT CONTROL SYSTEM AND REDUNDANCY MANAGEMENT DESCRIPTION
Richard R. Larson Feb. 1987 72 p
(NASA-TM-88267; H-1368; NAS 1.15:88267) Avail: NTIS HC A04/MF A01 CSCL 01C

The wing on the NASA F-111 transonic aircraft technology (TACT) airplane was modified to provide flexible leading and trailing edge flaps; this modified wing is known as the mission adaptive wing (MAW). A dual digital primary fly-by-wire flight control system was developed with analog backup reversion for redundancy. This report discusses the functions, design, and redundancy management of the flight control system for these flaps. Author

N87-16820*# National Aeronautics and Space Administration. Dryden (Hugh L.) Flight Research Center, Edwards, Calif.
DESIGN AND INITIAL APPLICATION OF THE EXTENDED AIRCRAFT INTERROGATION AND DISPLAY SYSTEM: MULTIPROCESSING GROUND SUPPORT EQUIPMENT FOR DIGITAL FLIGHT SYSTEMS
Richard D. Glover Jan. 1987 93 p
(NASA-TM-86740; H-1296; NAS 1.15:86740) Avail: NTIS HC A05/MF A01 CSCL 01C

A pipelined, multiprocessor, general-purpose ground support equipment for digital flight systems has been developed and placed in service at the NASA Ames Research Center's Dryden Flight Research Facility. The design is an outgrowth of the earlier aircraft interrogation and display system (AIDS) used in support of several research projects to provide engineering-units display of internal control system parameters during development and qualification testing activities. The new system, incorporating multiple 16-bit processors, is called extended AIDS (XAIDS) and is now supporting the X-29A forward-swept-wing aircraft project. This report describes the design and mechanization of XAIDS and shows the steps whereby a typical user may take advantage of its high throughput and flexible features. Author

N87-16821*# National Aeronautics and Space Administration. Dryden (Hugh L.) Flight Research Center, Edwards, Calif.
DIGITAL PROGRAM FOR CALCULATING STATIC PRESSURE POSITION ERROR
J. Blair Johnson, Terry J. Larson, and Jules M. Ficke Feb. 1987 28 p
(NASA-TM-86726; H-1284; NAS 1.15:86726) Avail: NTIS HC A03/MF A01 CSCL 01C

A computer program written to calculate the static pressure position error of airspeed systems contains five separate methods for determining position error, of which the user may select from one to five at a time. The program uses data from both the test aircraft and the ground-based radar to calculate the error. In addition, some of the methods require rawinsonde data or an atmospheric analysis, or both. The program output lists the corrections to Mach number, altitude, and static pressure that are due to position error. Reference values such as angle of attack, angle of sideslip, indicated Mach number, indicated pressure altitude, stagnation pressure, and total temperature are also listed. Author

N87-16822# Fairchild Industries, Inc., Farmingdale, N.Y.
ASSESSMENT OF DAMAGE TOLERANCE REQUIREMENTS AND ANALYSIS. VOLUME 1: EXECUTIVE SUMMARY Final Technical Report, Sep. 1982 - Nov. 1985
Meir Levy Sep. 1986 429 p
(Contract F33615-82-C-3215)
(AD-A175110; AFWAL-TR-86-3003-Vol-1) Avail: NTIS HC A19/MF A01 CSCL 20/11

A structural test program of a typical aircraft structural configuration was conducted to assess the current Air Force damage tolerance design requirements defined in MIL-A-83444. The specimens, made of 2024-T3XX and 7075-T6XX, were subjected to randomized flight-by-flight spectra, representative of fighter/trainer and bomber/cargo-type loading spectra, respectively, and to constant amplitude loading spectrum. A total of 72 specimens were tested. The test results were correlated with analytical predictions using the crack growth method and combined method. As a result of this study, a recommendation is provided to the validity of MIL-A-83444, to develop guidelines for selection of critical crack locations, and to assess the state-of-the-art analytical capabilities in predicting crack growth and crack initiation time. This volume, Volume 1 of a five-volume report, presents an Executive Summary of the entire program. GRA

06 AIRCRAFT INSTRUMENTATION

Includes cockpit and cabin display devices; and flight instruments.

For related information see also *19 Spacecraft Instrumentation* and *35 Instrumentation and Photography.*

N87-16823# Rome Air Development Center, Griffiss AFB, N.Y.
ICNIA (INTEGRATED COMMUNICATIONS NAVIGATION IDENTIFICATION AVIONICS) HF TRANSMITTER SYSTEM PRELIMINARY STUDY Report, Apr. 1983 - Dec. 1984
George A. Pfeiffer Jul. 1986 31 p
(AD-A173013; RADC-TM-86-4) Avail: NTIS HC A03/MF A01 CSCL 17/2

The ICNIA HF Transmitter System Preliminary Study describes an investigation to determine if it is feasible to develop and fabricate an airborne HF/VHF power amplifier, antenna coupler, and antenna for high speed, high performance aircraft having future application in integrated CNI avionics systems. A key objective was to investigate and validate an airborne antenna with low reactive components that could be fabricated into an aircraft frame. The study shows that it is feasible to design and fabricate HF/VHF equipment for small high speed, high performance aircraft that can be integrated into CNI avionics systems. GRA

07 AIRCRAFT PROPULSION AND POWER

Includes prime propulsion systems and systems components, e.g., gas turbine engines and compressors; and onboard auxiliary power plants for aircraft.

For related information see also *20 Spacecraft Propulsion and Power, 28 Propellants and Fuels,* and *44 Energy Production and Conversion.*

N87-16824 Rolls-Royce Ltd., Derby (England).
LOW ASPECT RATIO TURBINE DESIGN AT ROLLS-ROYCE
S. E. Morgan 5 Aug. 1986 92 p Presented at a Von Karman Inst. for Fluid Dynamics Lecture, Rhode-Saint-Genese, Belgium, 10 May 1984
(PNR90338; ETN-87-98778) Copyright. Avail: NTIS HC A05

Low aspect ratio turbine design considerations are reviewed, and a computer aided design package is presented. A low aspect ratio HP stator design featuring a parabolic vortex distribution is described. ESA

N87-16825*# National Aeronautics and Space Administration. Lewis Research Center, Cleveland, Ohio.
OUTDOOR TEST STAND PERFORMANCE OF A CONVERTIBLE ENGINE WITH VARIABLE INLET GUIDE VANES FOR ADVANCED ROTORCRAFT PROPULSION
Jack G. McArdle Dec. 1986 25 p Prepared for presentation at the 1987 Rotorcraft Technology Conference, Moffett Field, Calif., 17-19 Mar. 1987; sponsored in part by NASA and Army
(NASA-TM-88939; E-3384; NAS 1.15:88939) Avail: NTIS

HC A02/MF A01 CSCL 21E

A variable inlet guide van (VIGV) type convertible engine that could be used to power future high-speed rotorcraft was tested on an outdoor stand. The engine ran stably and smoothly in the turbofan, turboshaft, and dual (combined fan and shaft) power modes. In the turbofan mode with the VIGV open fuel consumption was comparable to that of a conventional turbofan engine. In the turboshaft mode with the VIGV closed fuel consumption was higher than that of present turboshaft engines because power was wasted in churning fan-tip airflow. In dynamic performance tests with a specially built digital engine control and using a waterbrake dynamometer for shaft load, the engine responded effectively to large steps in thrust command and shaft torque. Previous mission analyses of a conceptual X-wing rotorcraft capable of 400-knot cruise speed were revised to account for more fan-tip churning power loss than was originally estimated. The new calculations confirm that using convertible engines rather than separate lift and cruise engines would result in a smaller, lighter craft with lower fuel use and direct operating cost. Author

N87-16826*# National Aeronautics and Space Administration. Lewis Research Center, Cleveland, Ohio.

PARTICLE-LADEN SWIRLING FREE JETS: MEASUREMENTS AND PREDICTIONS

D. L. Bulzan, J.-S. Shuen (Sverdrup Technology, Inc., Cleveland, Ohio), and G. M. Faeth (Michigan Univ., Dearborn) 1987 29 p Presented at the 25th Aerospace Sciences Meeting, Reno, Nev., 12-15 Jan. 1987; sponsored by AIAA

(NASA-TM-88904; E-3307; NAS 1.15:88904; AIAA-87-0303) Avail: NTIS HC A03/MF A01 CSCL 21E

A theoretical and experimental investigation of single-phase and particle-laden weakly swirling jets was conducted. The jets were injected vertically downward from a 19 mm diameter tube with swirl numbers ranging from 0 to 0.33. The particle-laden jets had a single loading ratio (0.2) with particles having a SMD of 39 microns. Mean and fluctuating properties of both phases were measured using nonintrusive laser based methods while particle mass flux was measured using an isokinetic sampling probe. The continuous phase was analyzed using both a baseline kappa-epsilon turbulence model and an extended version with modifications based on the flux Richardson number to account for effects of streamline curvature. To highlight effects of interphase transport rates and particle/turbulence interactions, effects of the particles were analyzed as follows: (1) locally homogeneous flow (LHF) analysis, where interphase transport rates are assumed to be infinitely fast; (2) deterministic separated flow (DSF) analysis, where finite interphase transport rates are considered but particle/turbulence interactions are ignored; and (3) stochastic separated flow (SSF) analysis, where both effects are considered using random-walk computations. Author

N87-16827*# National Aeronautics and Space Administration. Lewis Research Center, Cleveland, Ohio.

REPRESENTATION OF THE VAPORIZATION BEHAVIOR OF TURBULENT POLYDISPERSE SPRAYS BY EQUIVALENT MONODISPERSE SPRAYS

S. K. Aggarwal and J. S. Shuen (Sverdrup Technology, Inc., Cleveland, Ohio) Dec. 1986 16 p

(NASA-TM-88906; E-3300; NAS 1.15:88906) Avail: NTIS HC A02/MF A01 CSCL 21E

The concept of using an equivalent monodisperse spray to represent the vaporization behavior of polydisperse sprays has been examined by numerically solving two turbulent vaporizing sprays. One involves the injection of Freon-11 in a still environment, whereas the other is a methanol spray in a still but hot environment. The use of three different mean sizes, namely, Sauter mean diameter, volume median diameter, and surface-area mean diameter, has been investigated. Results indicate a good degree of correlation between the polydisperse spray and its equivalent monodisperse sprays represented by the volume median diameter and the Sauter mean diameter, the former giving slightly better results. The surface-area mean diameter does not provide as good a correlation as the other two mean diameters. Author

N87-16828*# National Aeronautics and Space Administration. Langley Research Center, Hampton, Va.

OVER-THE-WING PROPELLER Patent

Joseph L. Johnson, Jr., inventor (to NASA) and E. Richard White, inventor (to NASA) (Kentron International, Inc., Hampton, Va.) Issued 16 Dec. 1986 9 p Continuation of US-Patent-Appl-SN-661478, dated 16 Oct. 1984, abandoned

(NASA-Case-LAR-13134-2; US-Patent-4,629,147; US-Patent-Appl-SN-846462; US-Patent-Class-244-55; US-Patent-Class-244-130) Avail: US Patent and Trademark Office CSCL 21E

This invention is an aircraft with a system for increasing the lift drag ratio over a broad range of operating conditions. The system positions the engines and nacelles over the wing in such a position that gains in propeller efficiency is achieved simultaneously with increases in wing lift and a reduction in wing drag. Adverse structural and torsional effects on the wings are avoided by fuselage mounted pylons which attach to the upper portion of the fuselage aft of the wings. Similarly, pylon-wing interference is eliminated by moving the pylons to the fuselage. Further gains are achieved by locating the pylon surface area aft of the aircraft center of gravity, thereby augmenting both directional and longitudinal stability. This augmentation has the further effect of reducing the size, weight and drag of empennage components. The combination of design changes results in improved cruise performance and increased climb performance while reducing fuel consumption and drag and weight penalties. NASA

N87-16829*# Mississippi State Univ., Mississippi State. Dept. of Aerospace Engineering.

ADVANCED 3-D VISCOUS SSME TURBINE ROTOR STATOR CFD ALGORITHMS Final Report, 6 Sep. 1985 - 5 Sep. 1986

J. Mark Janus and David L. Whitfield Sep. 1986 31 p

(Contract NAS8-36486)

(NASA-CR-178997; NAS 1.26:178997) Avail: NTIS HC A03/MF A01 CSCL 21E

Current Space Shuttle Main Engine (SSME) high pressure fuel turbopump problems have generated a desire to analyze the flow field of rotating machinery. The status of Computational Fluid Dynamics (CFD) has reached the point that soon the capability to solve unsteady three-dimensional viscous flow fields will be at hand. The work presented involves upgrading the computational efficiency of an operational three-dimensional algorithm. The modifications include algorithm development, algorithm approximation and acceleration, and special coding optimizations. The overall result of these modifications has reduced processing time by nearly 80%. Author

N87-16830*# Garrett Turbine Engine Co., Phoenix, Ariz.

TRANSITION MIXING STUDY Final Report, Jul. 1984 - Sep. 1986

R. Reynolds and C. White Oct. 1986 185 p

(Contract NAS3-24340)

(NASA-CR-175062; NAS 1.26:175062; Garrett-21-5723) Avail: NTIS HC A09/MF A01 CSCL 21E

A computer model capable of analyzing the flow field in the transition liner of small gas turbine engines is developed. A FORTRAN code has been assembled from existing codes and physical submodels and used to predict the flow in several test geometries which contain characteristics similar to transition liners, and for which experimental data was available. Comparisons between the predictions and measurements indicate that the code produces qualitative results but that the turbulence models, both K-E and algebraic Reynolds Stress, underestimate the cross-stream diffusion. The code has also been used to perform a numerical experiment to examine the effect of a variety of parameters on the mixing process in transition liners. Comparisons illustrate that geometries with significant curvature show a drift of the jet trajectory toward the convex wall and weaker wake region vortices and decreased penetration for jets located on the convex wall of the liner, when compared to jets located on concave walls. Also shown were the approximate equivalency of angled slots and round holes and a technique by which jet mixing correlations

developed for rectangular channels can be used for can geometries. Author

N87-16831# United Technologies Research Center, East Hartford, Conn.
UNSTEADY AERODYNAMICS OF A ROTATING COMPRESSOR BLADE ROW IN INCOMPRESSIBLE FLOW. VOLUME 1: EXPERIMENTAL FACILITIES, PROCEDURES AND SAMPLE DATA Final Report, Jun. 1981 - Aug. 1985
Larry W. Hardin and Franklin O. Carta 31 Aug. 1985 98 p
(Contract F49620-81-C-0088)
(AD-A173043; UTRC/R85-915767-3; AFOSR-86-0863TR) Avail: NTIS HC A05/MF A01 CSCL 21/5

An experiment was conducted on a heavily instrumented isolated model compressor rotor to study the unsteady aerodynamic response of the blade row to a circumferential inlet flow distortion with non-oscillating blades, and to blade oscillation in an undistorted flow. To accomplish this, miniature pressure transducers were imbedded in the blades and the unsteady pressure time histories were recorded as the blades were subjected to these conditions. Both phases of the experiment were performed over a wide range of flow coefficient, from (c sub x)/(u sub m) = 0.6 to 0.95 in 0.05 steps, and data were taken at each condition for disturbances characterized by one, two, and four per revolution waves. Steady-state data were also acquired and were found to agree with baseline data obtained from an earlier experiment using the same model geometry. Volume 1 describes the purpose of the experiment, the test rig and model hardware, the data system, and the techniques used to acquire and reduce the data. Some sample data taken at the design condition, (c sub x)/(u sub m) = 0.8 are also included. GRA

N87-16832# United Technologies Research Center, East Hartford, Conn.
UNSTEADY AERODYNAMICS OF A ROTATING COMPRESSOR BLADE ROW AT LOW MACH NUMBER. VOLUME 2: ANALYSIS OF EXPERIMENTAL RESULTS AND COMPARISON WITH THEORY Final Report, Jun. 1981 - May 1986
Larry W. Hardin and Franklin O. Carta 6 Jun. 1986 176 p
(Contract F49620-81-C-0088)
(AD-A173044; UTRC/R86-915767-4) Avail: NTIS HC A09/MF A01 CSCL 20/4

This volume contains an analysis of the data and compares the steady and unsteady results of this experiment with both analytical predictions and experimental data from previous work. The bulk of the data analysis was made for results taken at the blade midspan. There were two major findings. It was found that the unsteady oscillatory pressures were in excellent agreement with the unsteady potential flow theory of Verdon and Caspar for all conditions in which the flow was essentially two-dimensional. Also, the measured steady pressures were in good agreement with the steady potential flow predictions (and with previous steady experimental data) when the measured exit angle was the imposed down stream boundary condition for the analysis. This volume also offers some hypotheses to explain some of the details observed in the pressure and skin friction gage time histories and relates some previously published flow visualization results to these observations. GRA

N87-16833# United Technologies Research Center, East Hartford, Conn.
UNSTEADY AERODYNAMICS OF A ROTATING COMPRESSOR BLADE ROW AT LOW MACH NUMBER. VOLUME 3: EXPERIMENTAL DATA BASE AND USERS MANUAL Final Report, Jun. 1981 - May 1986
Larry W. Hardin and Franklin O. Carta 27 May 1986 447 p
(Contract F49620-81-C-0088)
(AD-A173045; UTRC/R85-915767-5) Avail: NTIS HC A19/MF A01 CSCL 20/4

This last volume is intended to serve as an index and a users guide to the data obtained. It contains extensive plots of the unsteady data taken during the experiment, and a description of the data reduction procedures used to store the data in description of the data reduction procedures used to store the data in Fourier coefficient form. These data are stored on a set of archival tapes at AFOSR. This volume contains an index to the specific data files stored on the tapes, by name, as well as format information and instructions for reading the data into disk files. FORTRAN programs for reading and manipulating the data are also provided. GRA

N87-16834# Rolls-Royce Ltd., Leavesden (England).
IMPACT OF IPS AND IRS CONFIGURATION ON ENGINE INSTALLATION DESIGN
J. R. Ballard 2 Jun. 1986 14 p Previously announced as N87-10070 Sponsored by the UK Ministry of Defence Procurement Executive
(PNR90324; ETN-87-98773) Avail: NTIS HC A02/MF A01

It is argued that helicopter engine design should be coordinated with engine and airframe mounted separator performance characteristics to ensure that optimized designs can be offered to customers with very different operational requirements. A design method which allows the erosion reduction characteristics of engine and airframe IPS designs to be taken into account during engine design is outlined. An IPS design optimized for European operations can be efficiently adapted for extreme climate conditions; IRS designs can be integrated with IPS scavenge requirements to produce a low signature engine installation. ESA

N87-16835# Rolls-Royce Ltd., Derby (England).
MANUFACTURING CELL FOR THE V2500 VARIABLE VANES
J. McSherry and A. J. Hill 2 Apr. 1986 8 p Presented at the International Conference on Computer-Aided Production Engineering, Edinburgh, Scotland, 2 Apr. 1986
(PNR90330; ETN-87-98777) Avail: NTIS HC A02/MF A01

The conceptual design of a manufacturing cell for the production of the first four stages of stators of the variable pitch type for a turbofan aircraft engine is presented. The philosophies which were developed during the initial investigation covering aspects such as work holding, tooling, inspection, manning, and control systems are outlined. The technical solutions offered from stand alone numerical control machines to a full flexible manufacturing system are discussed. ESA

N87-16836# Rolls-Royce Ltd., Derby (England).
REDUCING THE COST OF AERO ENGINE RESEARCH AND DEVELOPMENT
P. C. Ruffles 5 Aug. 1986 12 p
(PNR90341; ETN-87-98779) Avail: NTIS HC A02/MF A01

Cost reductions in aircraft engine R and D due to computer aided design and fuller demonstration programs prior to full engine development are discussed. ESA

N87-16837# Rolls-Royce Ltd., Derby (England).
BURNER RIG AND ENGINE TEST EXPERIENCE OF PLATINUM ALUMINIDE COATINGS
D. F. Bettridge and R. G. Wing 12 Jun. 1986 34 p Presented at the 31st ASME International Gas Turbine Conference and Exhibit, Dusseldorf, West Germany, 12 Jun. 1986
(PNR90342; ETN-87-98780) Avail: NTIS HC A03/MF A01

Evaluation of platinum alumide coating systems for turbine blades under operating environments conducive to type 1 and 2 sulfidation and high temperature accelerated oxidation is outlined. Burner rig and engine test results are described together with relevant service experience for the two main types of platinum modified coatings. The influence of temperature on the compositional and structural stability of the platinum alumide layers, and the importance of a consistent standard of product from the coating vendors are discussed. Test results and operating experience show that platinum coatings are superior to conventional aluminizing. ESA

N87-16838# Rolls-Royce Ltd., Derby (England).
COMPONENT LIFING
A. C. Pickard 10 Jun. 1986 29 p Presented at the Inst. of Metals Conference on Mechanical Behavior of Superalloys, 10-11

Jun. 1986
(PNR90346; ETN-87-98781) Avail: NTIS HC A03/MF A01

Failure mechanisms which can occur in an aircraft engine component in service are categorized into low life failures, macroscopically nonlocalized damage accumulation, and macroscopically localized damage accumulation. The methods used to avoid these failure mechanisms are discussed. Fatigue life prediction is highlighted and the traditional initiation life calculation method is compared with fracture mechanics methods. The importance of performing full scale component tests for highly stressed gas turbine parts is emphasized, from the traditional lifing viewpoint and to validate fracture mechanics based calculations. Fracture mechanics fatigue life predictions are compared with full scale component rig test results. ESA

N87-16839# Rolls-Royce Ltd., Derby (England).
OBSERVATION OF ICE/WATER FORMATIONS ON A MODEL INTAKE SECTION SUBJECTED TO SIMULATED CLOUD CONDITIONS
S. J. Downs 6 May 1986 19 p Presented at the 3rd International Workshop on the Atmospheric Icing of Structures, Vancouver, British Columbia, 6-8 May 1986
(PNR90347; ETN-87-98782) Avail: NTIS HC A02/MF A01

A full-scale two-dimensional section of a typical aero engine intake was mounted downstream of a 15 in. icing tunnel and enclosed in ducting, the walls of which were shaped to simulate the airflow distribution for a typical descent flight condition. The tunnel was fitted with water spray nozzles of variable atomizing air pressure, enabling selection of the required water droplet size for a given water input, to simulate an icing cloud. The model was fitted with a mock-up section of anti-icing system. A tunnel total air temperature of 2 C and water droplet volume median diameter of 20 microns were maintained throughout testing. The temperature recorded by the thermocouple at entry to the piccolo pipe increases as ice built up, and falls as the ice shed, indicating that the ice acted as an insulator. Flowing water on the cowl surface tends to limit ice formation. The addition of air into the anti-icing system at 11 to 13 C does not change the water flow patterns, but where ice formed with no air input, ice accretion is severely limited. ESA

N87-16840# Rolls-Royce Ltd., Derby (England).
FUTURE TRENDS IN PROPULSION
S. C. Miller and H. W. Bennett 5 Aug. 1986 17 p Previously announced in IAA as A86-48979
(PNR90349; ETN-87-98784) Avail: NTIS HC A02/MF A01

Trends in civil and military aircraft propulsion are discussed. In civil designs, increase in bypass ratio will improve fuel consumption, the exact configuration being speed-dependent, but the advance must be achieved in a cost effective way. In military designs, while the configuration may be less likely to change, major improvements in weight and cost will appear. The V/STOL aircraft will move from subsonic to supersonic. Hypersonic propulsion will require radical new concepts. Computer assistance will increasingly apply to all phases from design through to production. ESA

N87-16841# Rolls-Royce Ltd., Derby (England).
AN APPROACH TO AE MONITORING DURING THE RIG SHOP TESTING OF LARGE CFRP AERO-ENGINE COMPONENTS
T. J. Holroyd and P. E. Cox 21 Jul. 1986 8 p Presented at the 2nd International Symposium on Acoustic Emission from Reinforced Composites, Montreal, Canada, 21-25 Jul. 1986 Sponsored by UK Ministry of Defence Procurement Executive
(PNR90350; ETN-87-98785) Avail: NTIS HC A02/MF A01

The detection and location of damage as it occurs during the rig shop testing of large CFRP aero-engine components using multichannel acoustic emission (AE) is discussed. Attenuative isolation using multiple high frequency transducers shows promise as a means of locating the AE activity from large composite structures. Good immunity from background noise can be achieved. High rates of activity do not cause such a system to latch up. The reduction of channel costs is important for such a system to be practical. Effective means of characterizing material attenuation and in-situ sensitivity are central to the success of this approach. Scanned gas jet attenuation mapping and the concepts of preamplifier substations and disposable transducers are important steps towards the implementation of the attenuative isolation approach. ESA

N87-16842# Rolls-Royce Ltd., Derby (England).
GAS TURBINE MATERIALS: A REVIEW
J. D. Alexander and D. Driver 2 Apr. 1986 23 p Presented at the Materials in Aerospace Conference, England, 2-4 Apr. 1986; sponsored by RAE
(PNR90356; ETN-87-98788) Avail: NTIS HC A02/MF A01

Developments in manufacturing methods for aircraft engine materials are discussed. The coupling of microstructural and process control is noted. Turbine disk materials, compressor disk materials, and turbine blade materials are described. Turbine blade thermal protection is illustrated. ESA

N87-16843# Rolls-Royce Ltd., Derby (England). Lubrication and Transmission Technology Div.
THE TECHNOLOGY OF ADVANCED PROP-FAN TRANSMISSIONS
J. Dominy and B. F. Rayner 23 Sep. 1986 8 p
(PNR90357; ICAS-86-3.10.1; ETN-87-98789) Avail: NTIS HC A02/MF A01

The advances in transmission technology that are necessary if the maximum installed efficiency of the powerplant is to be achieved by aerospace turboprop and ultra high bypass designs are outlined. Gears will continue to be designed to achieve a virtually infinite life thus life itself will not benefit from improved fatigue performance. This can, however, be used to carry higher loads while still meeting the necessary life criteria, but since life is inversely proportional to load to the third power, very substantial increases in fatigue performance are required to make any useful difference to the load capacity of a gear. Similarly, there is unlikely to be any significant rise in efficiency, partly because the current efficiency levels are already very high and partly because the new transmissions will be inherently less efficient than those currently in service. The greatest changes will be in the lubrication system and the lubricant itself. ESA

N87-16844# Rolls-Royce Ltd., Derby (England).
AIRCRAFT DERIVATIVE GAS TURBINE DEVELOPMENT IN CHINA
23 Sep. 1986 9 p Repr. from International Aviation, no. 4, 1986 p 15-16 In ENGLISH and CHINESE
(PNR90359; Transl-18511; ETN-87-98790) Avail: NTIS HC A02/MF A01

Use of aircraft engine derived gas turbines as electricity generator, prime mover for the automotive vehicle and locomotive, marine mechanical prime mover, water (suction) pump, and air compressor is described. The gas turbine employs much of the advanced technology and experience from the aero engine industry, so the cost of development is minimal. This type of gas turbine uses light oil (paraffin, diesel) natural gas crude oil, heavy oil, and low calorific value fuels. ESA

N87-16845# Rolls-Royce Ltd., Derby (England).
OPERATIONAL AIDS TO ENGINE DEVELOPMENT
D. S. Pearson 24 Sep. 1986 15 p
(PNR90362; ETN-87-98792) Avail: NTIS HC A02/MF A01

Computer aided design of aircraft engines is assessed. Economic, technical, and social factors are reviewed. ESA

N87-16846# Office National d'Etudes et de Recherches Aerospatiales, Paris (France). Direction de l'Energetique.
APPLICATION OF FLOW CALCULATION METHODS TO TRANSONIC AND SUPERSONIC AXIAL TURBOMACHINES [APPLICATION DES METHODES DE CALCUL D'ECOULEMENT DANS LES TURBOMACHINES AXIALES TRANSSONIQUES ET SUPERSONIQUES]
Georges Meauze 4 Mar. 1986 18 p In FRENCH

(Contract DRET-84-34-001)
(ONERA-RTS-80/7103-EY; ETN-87-98808) Avail: NTIS HC A02/MF A01

A three-dimensional (3D) inviscid calculation method was applied to a mobile compressor wheel and to a complete turbine stage. An important deficiency of the conservation of the flow rate between the upstream region, the interblade channel, and downstream in the 3D calculation of a compressor or turbine wheel, was strongly reduced by a treatment of the boundary conditions. The 3D calculation of a complete stage was improved and applied to several compressor and turbine configurations. This calculation uses certain simplifying hypotheses, such as periodicity for each interblade channel, and the identity of the radial evolutions of the azimuthal averages at the common frontier which separates the calculation domains relative to each wheel. ESA

08 AIRCRAFT STABILITY AND CONTROL

Includes aircraft handling qualities; piloting; flight controls; and autopilots.

For related information see also *05 Aircraft Design, Testing and Performance.*

N87-16847 Kansas Univ., Lawrence.
DEVELOPMENT OF A SENSITIVITY ANALYSIS TECHNIQUE FOR MULTILOOP FLIGHT CONTROL SYSTEMS Ph.D. Thesis
Alfredo Herrera-Vaillard 1986 175 p
Avail: Issuing Activity

The development and application of a sensitivity analysis technique for multiloop flight control systems is presented. This analysis yields very useful information on the sensitivity of the relative-stability criteria of the control system, with variations or uncertainties in the system and the controller elements. The sensitivity analysis technique developed is based on the computation of the singular values and singular-value gradients of a feedback-control system. The use of singular values to obtain a relative stability criterion for sampled-data systems is also explored with promising results. The sensitivity analysis technique was applied to a continuous yaw/roll damper stability augmentation system of a typical business jet, and the results show that the analysis is very useful in determining the system elements which have the largest effect on the relative stability of the closed-loop system. The relative stability criteria based on the concept of singular values were applied to a single-loop yaw damper system and a mutiloop yaw/roll damper system of a business jet.
Dissert. Abstr.

N87-16848*# National Aeronautics and Space Administration. Langley Research Center, Hampton, Va.
DESCRIPTION OF THE SPACECRAFT CONTROL LABORATORY EXPERIMENT (SCOLE) FACILITY
Jeffrey P. Williams and Rosemary A. Rallo (Purdue Univ., West Lafayette, Ind.) Jan. 1987 45 p
(NASA-TM-89057; NAS 1.15:89057) Avail: NTIS HC A03/MF A01 CSCL 01C

A laboratory facility for the study of control laws for large flexible spacecraft is described. The facility fulfills the requirements of the Spacecraft Control Laboratory Experiment (SCOLE) design challenge for laboratory experiments, which will allow slew maneuvers and pointing operations. The structural apparatus is described in detail sufficient for modelling purposes. The sensor and actuator types and characteristics are described so that identification and control algorithms may be designed. The control implementation computer and real-time subroutines are also described. Author

N87-16849*# National Aeronautics and Space Administration. Langley Research Center, Hampton, Va.
PILOTED SIMULATOR STUDY OF ALLOWABLE TIME DELAYS IN LARGE-AIRPLANE RESPONSE
William D. Grantham, Paul M. Smith (PRC Kentron, Inc., Hampton, Va.), Lee H. Person, Jr., Robert T. Meyer (Lockheed-Georgia Co., Marietta), and Stephen A. Tingas Feb. 1987 69 p
(NASA-TP-2652; L-16149; NAS 1.60:2652) Avail: NTIS HC A04/MF A01 CSCL 01C

A piloted simulation was performed to determine the permissible time delay and phase shift in the flight control system of a specific large transport-type airplane. The study was conducted with a six degree of freedom ground-based simulator and a math model similar to an advanced wide-body jet transport. Time delays in discrete and lagged form were incorporated into the longitudinal, lateral, and directional control systems of the airplane. Three experienced pilots flew simulated approaches and landings with random localizer and glide slope offsets during instrument tracking as their principal evaluation task. Results of the present study suggest a level 1 (satisfactory) handling qualities limit for the effective time delay of 0.15 sec in both the pitch and roll axes, as opposed to a 0.10-sec limit of the present specification (MIL-F-8785C) for both axes. Also, the present results suggest a level 2 (acceptable but unsatisfactory) handling qualities limit for an effective time delay of 0.82 sec and 0.57 sec for the pitch and roll axes, respectively, as opposed to 0.20 sec of the present specifications for both axes. In the area of phase shift between cockpit input and control surface deflection,the results of this study, flown in turbulent air, suggest less severe phase shift limitations for the approach and landing task-approximately 50 deg. in pitch and 40 deg. in roll - as opposed to 15 deg. of the present specifications for both axes. Author

09 RESEARCH AND SUPPORT FACILITIES (AIR)

Includes airports, hangars and runways; aircraft repair and overhaul facilities; wind tunnels; shock tubes; and aircraft engine test stands.

For related information see also *14 Ground Support Systems and Facilities (Space).*

N87-16850 Stanford Univ., Calif.
THE INFLUENCE OF WIND-TUNNEL WALLS ON DISCRETE FREQUENCY NOISE Ph.D. Thesis
Marianne Mosher 1986 243 p
Avail: Univ. Microfilms Order No. DA8619794

Enclosures partial or complete, significantly affect the sound field of a source contained in the enclosure. In particular, wind-tunnel walls effect measurements of the sound field of an aircraft model thereby complicating noise measurements of aircraft in wind tunnels. This work examines the effect of the wind tunnel on sound fields. The acoustic field from a known source in a wind tunnel has been modeled as an acoustic source in uniform subsonic flow, in an infinitely long duct with constant cross-section. The acoustic impedance boundary condition at the wall allows sound absorption. The problem of an aeroacoustic source in a duct is formulated as an inhomogeneous integro-differential equation for the acoustic pressure on the duct surface. Several sample programs are studied in a rectangular duct with and without flow. A simple model problem, for which an analytic approximation exists, demonstrates that the numerical calculation correctly solves the numerical model. The acoustic fields for many simple sources are examined. The acoustic field from a simple model of helicopter noise is studied in the duct. Results show that the presence of the duct significantly changes the acoustic field. For a given source, the region in the duct near the source resembling the free field increases as the wall adsorption increases. Outside this near field the sound depends mostly on the product of source wave number with duct cross dimension. Dissert. Abstr.

N87-16851*# National Aeronautics and Space Administration. Lewis Research Center, Cleveland, Ohio.
A DISTRIBUTED DATA ACQUISITION SYSTEM FOR AERONAUTICS TEST FACILITIES

Dennis L. Fronek, Robert N. Setter, Philip Z. Blumenthal, and Robert R. Smalley 1987 8 p Proposed for presentation at the International Instrumentation Symposium, Las Vegas, Nev., 3-8 May 1987; sponsored by the Instrument Society of America
(NASA-TM-88961; E-3417; NAS 1.15:88961) Avail: NTIS HC A02/MF A01 CSCL 14B

The NASA Lewis Research Center is in the process of installing a new data acquisition and display system. This new system will provide small and medium sized aeronautics test facilities with a state-of-the-art real-time data acquisition and display system. The new data system will provide for the acquisition of signals from a variety of instrumentation sources. They include analog measurements of temperatures, pressures, and other steady state voltage inputs; frequency inputs to measure speed and flow; discrete I/O for significant events, and modular instrument systems such as multiplexed pressure modules or electronic instrumentation with a IEEE 488 interface. The data system is designed to acquire data, convert it to engineering units, compute test dependent performance calculations, limit check selected channels or calculations, and display the information in alphanumeric or graphical form with a cycle time of one second for the alphanumeric data. This paper describes the system configuration, its salient features, and the expected impact on testing. Author

N87-16852# Royal Aircraft Establishment, Farnborough (England).
DEVELOPMENTS IN DATA ACQUISITION AND PROCESSING USING AN ADVANCED COMBUSTION RESEARCH FACILITY
J. B. Bullard, F. S. E. Whitcher, and R. V. Steeden Jul. 1986 22 p Presented at the AGARD Propulsion and Energetics Panel 67th Symposium on Advanced Instrumentation for Propulsion Components, Philadelphia, Pa., 19-23 May 1986
(RAE-TM-P1089; BR100238; ETN-87-98913) Avail: NTIS

A combustion rig to acquire rapid and detailed information on the combustion processes occurring within a sector of large annular gas turbine combustors operating over a range of inlet pressures and temperatures representative of engine conditions was designed. Gas samples are extracted using a probe positioned within the volume under examination and transferred to a system designed to perform analyses with a point-to-point cycle time less than 30 sec. A computer controls and synchronizes the probe positioning and gas analysis function, and presents coordinated results to rig controllers. The system is capable of automatic traversing within a prescribed volume or of control by a dummy traverse gear which permits tracing of air and fuel flows. ESA

N87-16853# Army Cold Regions Research and Engineering Lab., Hanover, N. H.
FROST ACTION PREDICTIVE TECHNIQUES FOR ROADS AND AIRFIELDS: A COMPREHENSIVE SURVEY OF RESEARCH FINDINGS
T. C. Johnson, R. L. Berg, E. J. Chamberlain, and D. M. Cole Dec. 1986 52 p
(Contract FHWA-8-3-0187)
(DOT/FAA/PM-85/23; CRREL-86-18) Avail: NTIS HC A04/MF A01

Findings from a six-year field and laboratory program of frost-action research in four principal areas are summarized. Research on the first topic, frost-susceptibility index tests, led to selection of the Corps of Engineers frost design soil classification system as a useful method at the simplest level of testing. At a much more complex level, a new freezing test combined with a CBR test after thawing is recommended as an index of susceptibility to both frost heave and thaw weakening. Under the second topic, a soil column and dual gamma system were developed and applied to obtain soil data used in improving and validating a mathematical model of frost heave, the objective of the third research topic. The model was effectively improved, a probabilistic component was added, and it was successfully tested against field and laboratory measurement of frost heave. A thaw consolidation algorithm was added, which was shown to be useful in predicting the seasonal variation in resilient modulus of granular soils, the objective of the fourth topic. A laboratory testing procedure was developed for assessing the resilient modulus of thawed soil at various stages of the recovery process, as a function of the applied stress and the soil moisture tension, which increases as the soil gradually desaturates during recovery. The procedure was validated. Author

N87-16854# G B Lab., Inc., Santa Ana, Calif.
DEVELOPMENT OF A DRAG MEASUREMENT SYSTEM FOR THE CERF 6-FOOT SHOCK TUBE Technical Report, 28 Sep. 1984 - 1 Mar. 1986
George H. Burghart 31 Mar. 1986 39 p
(Contract DNA001-84-C-0438; DNA Proj. Q93-QMXA)
(AD-A173087; GBL-86-036R; DNA-TR-86-119) Avail: NTIS HC A03/MF A01 CSCL 14/2

An instrumentation system was developed permitting the direct measurement of drag forces on flat plates in a precursed and/or dusty shock tube flow environment. The system was designed for very high frequency response to track the rapid changes in the shock tube flow. A fully self-contained data acquisition unit with solid state memory was also designed and built for this application. The system was fielded in the CERF 6-foot Shock Tube at Kirtland AFB, New Mexico. GRA

12 ASTRONAUTICS (GENERAL)

For extraterrestrial exploration see *91 Lunar and Planetary Exploration.*

N87-16855*# Martin Marietta Corp., Denver, Colo.
TETHERED ORBITAL REFUELING STUDY Final Report
Dale A. Fester, L. Kevin Rudolph, Erlinda R. Kiefel, Peter W. Abbott, and Pat Grossrode Apr. 1986 150 p
(Contracts NAS9-17059; NAS9-17422)
(NASA-CR-171953; NAS 1.26:171953; MCR-86-587; MCR-86-591)
Avail: NTIS HC A07/MF A01 CSCL 22A

One of the major applications of the space station will be to act as a refueling depot for cryogenic-fueled space-based orbital transfer vehicles (OTV), Earth-storable fueled orbit maneuvering vehicles, and refurbishable satellite spacecraft using hydrazine. One alternative for fuel storage at the space station is a tethered orbital refueling facility (TORF), separated from the space station by a sufficient distance to induce a gravity gradient force that settles the stored fuels. The technical feasibility was examined with the primary focus on the refueling of LO2/LH2 orbital transfer vehicles. Also examined was the tethered facility on the space station. It was compared to a zero-gravity facility. A tethered refueling facility should be considered as a viable alternative to a zero-gravity facility if the zero-gravity fluid transfer technology, such as the propellant management device and no vent fill, proves to be difficult to develop with the required performance. Author

N87-16856*# National Aeronautics and Space Administration, Washington, D.C.
A NEW DAY: CHALLENGER AND SPACE FLIGHT THEREAFTER
Jesco vonPuttkamer Mar. 1986 18 p Transl. into ENGLISH of 'Ein Neuer Tag: Challenger und die Raumfahrt Danach" Washington, D.C., 11 Feb. 1986 p 1-11
(Contract NASw-4005)
(NASA-TM-77717; NAS 1.15:77717) Avail: NTIS HC A02/MF A01 CSCL 22A

On January 28, 1986, at an altitude of 14 kilometers, the Space Shuttle Challenger was torn apart by an explosion of the external tank. The effects of the accident are undoubtedly far-reaching; they have broad repercussions that affect NASA's international partner organizations. The effects of the postponed shuttle flights on European space programs are discussed. A review of the German participation in the American space program is presented. The need to continue the future projects such as the space station is examined in light of its importance as a springboard for further exploration. B.G.

13 ASTRODYNAMICS

Includes powered and free-flight trajectories; and orbital and launching dynamics.

N87-16857 Rice Univ., Houston, Tex.
AEROASSISTED COPLANAR ORBITAL TRANSFER OF FLIGHT VEHICLES USING THE SEQUENTIAL GRADIENT RESTORATION ALGORITHM Ph.D. Thesis
Venkatesh K. Basapur 1985 98 p
Avail: Univ. Microfilms Order No. DA8617425

Classical and minimax problems of optimal control which arise in the study of coplanar aeroassisted orbital transfer are considered. The basic idea is to employ the hybrid combination of propulsive maneuvers in space and aerodynamic maneuvers via lift modulation in the sensible atmosphere. Within the framework of classical optimal control, the following problems were studied: minimize the energy required for orbital transfer; minimize the time integral of the heating rate; minimize the time of flight during the atmospheric portion of the trajectory; minimize the time integral of the square of the path inclination; minimize the time integral of the square of the difference between the altitude and a reference altitude to be determined; and minimize the sum of the squares of the initial and final path inclinations. Within the framework of minimax optimal control, the following problems were studied: minimize the peak heating rate; minimize the peak dynamic pressure; and minimize the peak altitude drop. Several numerical examples are presented, and their engineering implications are discussed. In particular, the merits of nearly grazing trajectories are discussed. Dissert. Abstr.

N87-16858 Colorado Univ., Boulder.
ORBIT DETERMINATION FOR LOW EARTH ORBIT SPACECRAFT BASED ON SATELLITE TO SATELLITE TRACKING TECHNIQUES VIA A UNIQUE VERY HIGH ALTITUDE RELAY CONSTELLATION Ph.D. Thesis
Douglas Roger Tighe 1986 145 p
Avail: Univ. Microfilms Order No. DA8619004

This study applies the work of John E. Draim in looking at an unique high altitude satellite constellation of elliptical orbits, which provides continuous global coverage, and considers the mission application of satellite to satellite tracking for this four satellite constellation. Such an application could provide precise, timely and affordable orbit determination services to a variety of low Earth orbit user satellites. The range of application for such services would be quite mission dependent. The required geometric access, precision, processing time, update interval and propagation interval are all factors which need to be considered. Here, the high altitude non-geosynchronous four satellite constellation developed by John Draim is described, its own orbit determination problem is examined and then the application and utility of orbit determination services to be provided to low Earth orbit users are examined and quantified. Depending on user mission requirements, use of such a high altitude relay constellation for orbit determination applications is shown to perform at levels which compare reasonably with other currently planned systems. In this investigation, orbit determination performance for a low Earth orbit user using the Draim constellation comparable to that indicated in the literature of NASA's TDRSS has been demonstrated. High accuracy performance to several feet or less, such as seems achievable with the Global Positioning System does not seem possible for the Draim constellation. Dissert. Abstr.

N87-16859# Royal Aircraft Establishment, Farnborough (England).
THE CONTRACTION OF SATELLITE ORBITS UNDER THE INFLUENCE OF AIR DRAG. PART 7: ORBITS OF HIGH ECCENTRICITY, WITH SCALE HEIGHT DEPENDENT ON ALTITUDE
D. G. King-Hele and Doreen M. C. Walker Feb. 1986 26 p
(RAE-TR-86013; RAE-Space-656; BR99688; ETN-87-98915) Avail: NTIS

Part 3 of this series of papers developed the theory of high-eccentricity orbits (e greater than 0.2) in an atmosphere having an exponential variation of air density with height, that is, with the density scale height H taken as constant. Part 4 derived the appropriate theory for low-eccentricity orbits (e less than 0.2) in a more realistic atmosphere where H varies linearly with height y (and mu = dH/dy less than 0.2). The present report treats the orbits of Part 3 when they meet the air drag specified by the atmospheric model of Part 4. Equations are derived showing how the perigee height varies with eccentricity, and the eccentricity varies with time, over the major part of the satellite's life. It is shown that the theory of Part 3 remains valid, to order mu sq, if H is evaluated at a specific height above perigee. ESA

14 GROUND SUPPORT SYSTEMS AND FACILITIES (SPACE)

Includes launch complexes, research and production facilities; ground support equipment, e.g., mobile transporters; and simulators.

For related information see also *09 Research and Support Facilities (Air).*

N87-17206# Flinders Univ., Bedford Park (Australia). Dept. of Environment and Planning.
THE FRS-68010: A NEW CONCEPT FOR THE ACQUISITION AND ANALYSIS OF NOAA HRPT DATA
M. Wegener *In* ESA Proceedings of the 1986 International Geoscience and Remote Sensing Symposium (IGARSS '86) on Remote Sensing: Today's Solutions for Tomorrow's Information Needs, Volume 1 Aug. 1986 p 253-258 (For primary document see N87-17163 09-43)
Avail: NTIS HC A99/MF E03; ESA, Paris, France, 3 volume set $90 Member States, AU, CN, and NO (+20% others)

15 LAUNCH VEHICLES AND SPACE VEHICLES

Includes boosters; operating problems of launch/space vehicle systems; and reusable vehicles.

For related information see also *20 Spacecraft Propulsion and Power.*

N87-16860*# Research Triangle Inst., Research Triangle Park, N.C. Center for Systems Engineering.
CONCEPT DEFINITION FOR SPACE STATION TECHNOLOGY DEVELOPMENT EXPERIMENTS. EXPERIMENT DEFINITION, TASK 2 Final Report
Apr. 1986 285 p
(Contract NAS1-17639)
(NASA-CR-178153; NAS 1.26:178153; RTI/3042/07-01F) Avail: NTIS HC A13/MF A01 CSCL 22B

The second task of a study with the overall objective of providing a conceptual definition of the Technology Development Mission Experiments proposed by LaRC on space station is discussed. During this task, the information (goals, objectives, and experiment functional description) assembled on a previous task was translated into the actual experiment definition. Although still of a preliminary nature, aspects such as: environment, sensors, data acquisition, communications, handling, control telemetry requirements, crew activities, etc., were addressed. Sketches, diagrams, block diagrams, and timeline analyses of crew activities are included where appropriate. Author

N87-16861*# National Aeronautics and Space Administration. Langley Research Center, Hampton, Va.
STRUCTURAL DYNAMICS AND ATTITUDE CONTROL STUDY OF EARLY MANNED CAPABILITY SPACE STATION CONFIGURATIONS
J. Kirk Ayers (PRC Kentron, Inc., Hampton, Va.), William M. Cirillo, Daniel P. Giesy, Jay C. Hitchcock, Martin J. Kaszubowski, and J. Philip Raney Jan. 1987 69 p

(NASA-TM-89078; NAS 1.15:89078) Avail: NTIS HC A04/MF A01 CSCL 22B

A study was performed to determine the vibration and attitude control characteristics of critical space station configurations featuring early manned capability during buildup from initial user support through the operations capability reference station. Five configurations were selected and were examined thus determining the changes that are likely to occur in the characteristics of the system as the station progresses from a single boom structure to a mature, dual keel, operations capability reference station. Both 9 foot and 5 meter truss bay sizes were investigated. All configurations analyzed were stable; however, the 5 meter truss bay size structure exhibited superior stability characteristics. Author

16 SPACE TRANSPORTATION

Includes passenger and cargo space transportation, e.g., shuttle operations; and space rescue techniques.

For related information see also *03 Air Transportation and Safety* and *18 Spacecraft Design, Testing and Performance.* For space suits see *54 Man/System Technology and Life Support.*

N87-16862*# Draper (Charles Stark) Lab., Inc., Cambridge, Mass.
REDUCING SHUTTLE-PAYLOAD DYNAMIC INTERACTION WITH NOTCH FILTERS M.S. Thesis
Brent D. Appleby Feb. 1987 122 p
(Contract NAS9-17560)
(NASA-CR-171958; NAS 1.26:171958; CSDL-T-939) Avail: NTIS HC A06/MF A01 CSCL 22B

The use of notch filters centered on the estimated bending frequencies to reduce the effect of low-frequency Shuttle-payload dynamic interaction is investigated. The Shuttle-payload dynamics that are studied are with payloads attached to the Shuttle Remote Manipulator System (RMS). Other payload-orbiter connection such as payloads pivoted out of the cargo bay on a tilt table can lead to low-frequency bending modes. Payloads attached to the RMS will, however, present greater problems in that the bending modes will be hard to predict and will tend to vary with time as the RMS changes in orientation. Author

17 SPACE COMM., SPACECRAFT COMM., COMMAND & TRACKING

Includes telemetry; space communications networks; astronavigation and guidance; and radio blackout.

For related information see also *04 Aircraft Communications and Navigation* and *32 Communications and Radar.*

N87-16863*# National Aeronautics and Space Administration. Langley Research Center, Hampton, Va.
SINGLE FREQUENCY MULTITRANSMITTER TELEMETRY Patent
Victor A. Carreno, inventor (to NASA) Issued 23 Dec. 1986 11 p Filed 28 Feb. 1983 Supersedes N83-20995 (21 - 11, p 1652)
(NASA-Case-LAR-13006-1; US-Patent-4,631,538;
US-Patent-Appl-SN-470113; US-Patent-Class-340-870.18;
US-Patent-Class-340-825.5; US-Patent-Class-371-63;
US-Patent-Class-375-88) Avail: U.S. Patent and Trademark Office CSCL 09F

The invention relates to a single frequency multitransmitter telemetry system that will deliver a substantial amount of data at low cost. The invention consists essentially of a plurality of sensor transmitter units at different locations, with individual signal conditioning and logic, which send sampled data signals to a single receiver. The transmitters operate independently on the same frequency in a frequency shift keying modulation system and are not synchronized to the receiver. The problem of reception of data from more than one transmitter simultaneously is solved by discarding the data - when there is overlap of data from two or more transmitters, the data is discarded and when there is no overlap the data is retained. The invention utilizes a unique overlap detection technique to determine if data should be retained or discarded. When data is received from a transmitter, it goes into a shift register. NASA

18 SPACECRAFT DESIGN, TESTING AND PERFORMANCE

Includes satellites; space platforms; space stations; spacecraft systems and components such as thermal and environmental controls; and attitude controls.

For life support systems see *54 Man/System Technology and Life Support.* For related information see also *05 Aircraft Design, Testing and Performance, 39 Structural Mechanics,* and *16 Space Transportation.*

N87-16864*# PRC Kentron, Inc., Hampton, Va.
SPACECRAFT ATTITUDE CONTROL MOMENTUM REQUIREMENTS ANALYSIS
Brent P. Robertson and Michael L. Heck (Analytical Mechanics Associates, Inc., Hampton, Va.) Jan. 1987 92 p
(Contracts NAS1-18000; NAS1-17958)
(NASA-CR-178219; NAS 1.26:178219) Avail: NTIS HC A05/MF A01 CSCL 22B

The relationship between attitude and angular momentum control requirements is derived for a fixed attitude, Earth orbiting spacecraft with large area articulating appendages. Environmental effects such as gravity gradient, solar radiation pressure, and aerodynamic forces arising from a dynamic, rotating atmosphere are examined. It is shown that, in general, each environmental effect contributes to both cyclic and secular momentum requirements both within and perpendicular to the orbit plane. The gyroscopic contribution to the angular momentum control requirements resulting from a rotating, Earth oriented spacecraft is also discussed. Special conditions are described where one or more components of the angular momentum can be made to vanish, or become purely cyclical. Computer generated plots for a candidate space station configuration are presented to supplement the analytically derived results. Author

N87-16865*# Lockheed Missiles and Space Co., Sunnyvale, Calif.
SPACE STATION HUMAN PRODUCTIVITY STUDY. VOLUME 4: ISSUES Final Report
Nov. 1985 178 p
(Contract NAS9-17272)
(NASA-CR-171963; NAS 1.26:171963; LMSC-F060784/4-Vol-4; DR-SE-1093T-Vol-4) Avail: NTIS HC A09/MF A01 CSCL 22B

The 305 Issues contained represent topics recommended for study in order to develop requirements in support of space station crew performance/productivity. The overall subject matter, space station elements affecting crew productivity, was organized into a coded subelement listing, which is included for the reader's reference. Each issue is numbered according to the 5-digit topical coding scheme. The requirements column on each Issue page shows a cross-reference to the unresolved requirement statement(s). Because topical overlaps were frequently encountered, many initial Issues were consolidated. Apparent gaps, therefore, may be accounted for by an Issue described within a related subelement. A glossary of abbreviations used throughout the study documentation is also included. Author

N87-16866*# Lockheed Missiles and Space Co., Sunnyvale, Calif.
SPACE STATION HUMAN PRODUCTIVITY STUDY. VOLUME 5: MANAGEMENT PLANS Final Report
Nov. 1985 517 p
(Contract NAS9-17272)
(NASA-CR-171964; NAS 1.26:171964; LMSC-F060784/5-Vol-5; DR-SE-1093T-Vol-5) Avail: NTIS HC A22/MF A01 CSCL 22B

The 67 Management Plans represent recommended study

approaches for resolving 106 of the 305 issues which were identified. Each study Management Plan is prepared in three formats: Management Plan Overview (lists the subsumed issues, study background, and related overview information); Study Plan (details the study approach by tasks, lists special needs, and describes expected study products); Schedule-Task Flow (provides a time-lined schedule for the study tasks and resource requirements). The Management Relationships Matrix, included in this volume, shows the data input-output relationships among all recommended studies. A listing is also included which cross-references the unresolved requirements to issues to management plans. A glossary of all abbreviations utilized is provided. Author

N87-16867*# Draper (Charles Stark) Lab., Inc., Boston, Mass.
REAL TIME IDENTIFICATION OF LARGE SPACE STRUCTURES Ph.D. Thesis - MIT
Janice E. Voss Feb. 1987 196 p
(Contract NAS9-17560)
(NASA-CR-171957; NAS 1.26:171957; CSDL-T-941) Avail: NTIS HC A09/MF A01 CSCL 22B

Identification of frequencies, damping ratios, and mode shapes of large space structures (LSSs) are examined in real time. Real time processing allows for quick updates of model processing after a reconfiguration of structural failure. Recursive lattice least squares (RLLS) was selected as the baseline algorithm for the identification. Simulation results on a one dimensional LSS demonstrated that it provides good estimates, was not ill-conditioned in the presence of under-excited modes, allowed activity by a supervisory control system which prevented damage to the LSS or excessive drift, and was capable of real-time processing for typical LSS models. A suboptimal version of RLLS, which is equivalent to simulated parallel processing, was derived. A NASTRAN model of the dual keel U.S. space station was used to demonstrate the input/identification algorithm package in a more realistic simulation. Because the first eight flexible modes were very close together, the identification was much more difficult than in the simple examples. Even so, the model was accurately identified in real time. Author

N87-16868*# Lockheed Missiles and Space Co., Sunnyvale, Calif.
SPACE STATION HUMAN PRODUCTIVITY STUDY. VOLUME 2: EXECUTIVE SUMMARY AND ORAL REVIEW PRESENTATION Final Report
Nov. 1985 81 p
(Contract NAS9-17272)
(NASA-CR-171962; NAS 1.26:171962; LMSC-F060784/2-Vol-2; DR-SE-1093T-Vol-2) Avail: NTIS HC A05/MF A01 CSCL 22B

Definition of design/operations requirements for support of human productivity, identification of problem areas lacking data for requirements definition, generation of management plans for conduct of studies to acquire needed data for timely space station program impact, and correlation of all issue study management plans with space station progam milestone need dates were addressed. B.G.

N87-16869*# Lockheed Missiles and Space Co., Sunnyvale, Calif.
SPACE STATION HUMAN PRODUCTIVITY STUDY, VOLUME 1 Final Report
Nov. 1985 71 p
(Contract NAS9-17272)
(NASA-CR-171961; NAS 1.26:171961; LMSC-F060784/1-Vol-1) Avail: NTIS HC A04/MF A01 CSCL 22B

The primary goal was to develop design and operations requirements for direct support of intra-vehicular activity (IVA) crew performance and productivity. It was recognized that much work had already been accomplished which provided sufficient data for the definition of the desired requirements. It was necessary, therefore, to assess the status of such data to extract definable requirements, and then to define the remaining study needs. The explicit objectives of the study were to: review existing data to identify potential problems of space station crew productivity and to define requirements for support of productivity insofar as they could be justified by current information; identify those areas that lack adequate data; and prepare plans for managing studies to develop the lacking data, so that results can be input to the space station program in a timely manner. Author

N87-16870*# Astro Aerpspace Corp., Carpinteria, Calif.
EVALUATION OF PACTRUSS DESIGN CHARACTERISTICS CRITICAL TO SPACE STATION PRIMARY STRUCTURE Final Report
John M. Hedgepeth 20 Feb. 1987 74 p
(Contract NAS1-17536)
(NASA-CR-178171; NAS 1.26:178171; AAC-TN-1147-Rev-A) Avail: NTIS HC A04/MF A01 CSCL 22A

Several aspects of the possible application of the Pactruss concept to the primary truss structure of the space station are investigated. Estimates are made of the loads and hinge moments in deploying diagonal members as full deployment is approached. Included are the effects of beam columning and compliance of the surrounding structure. Requirements for joint design are suggested and a two-stage mid-diagonal latching hinge concept is described or analyzed. The problems with providing the experimental and theoretical tools needed for assuring reliable synchronous deployment are discussed and a first attempt at high-fidelity analytical simulation with NASTRAN is described. An alternative construction scenario in which the entire dual-keel truss structure is deployed as a single Shuttle payload is suggested. Author

N87-16871# Integrated Systems, Inc., Palo Alto, Calif.
ADAPTIVE CONTROL TECHNIQUES FOR LARGE SPACE STRUCTURES Annual Report, 1 Jun. 1985 - 31 May 1986
Robert L. Kosut and Michael G. Lyons 15 Sep. 1986 117 p
(Contract F49620-85-C-0094)
(AD-A173083; ISI-85; AFOSR-86-0885TR) Avail: NTIS HC A06/MF A01 CSCL 22/1

The Large Space Structure (LSS) research program was originally formulated in response to increasing concern that performance robustness of Air Force LSS systems would be inadequate to meet mission objectives. Uncertainties in both system dynamics and disturbance spectra characterizations (both time varying and stochastic uncertainty) significantly limit the performance attainable with fixed gain, fixed architecture controls. Therefore, use of an adaptive system, where disturbances and/or plant models are identified prior to or during control, gives systems designers more options for minimizing the risk in achieving performance objectives. The aim of adaptive control is to implement in real time and on line as many as possible of the design functions now performed off line by the control engineer to give the controller intelligence. To realize this aim, both a theory of stability and performance of such inherently nonlinear controls is essential as well as a technology capable of achieving the implementation. The present research concentrated on: (1) on line robust design from identified models - what is referred to here as adaptive calibration; and (2) an analysis of slow-adaptation for adaptive control for LSS. GRA

N87-16872# Oklahoma Univ., Norman. Dept. of Mathematics.
ESTIMATION AND CONTROL OF DISTRIBUTED MODELS FOR CERTAIN ELASTIC SYSTEMS ARISING IN LARGE SPACE STRUCTURES Annual Report, 2 Jul. 1984 - 1 Jan. 1986
Luther W. White 1986 7 p
(Grant AF-AFOSR-0271-84)
(AD-A175019; AFOSR-86-2193TR) Avail: NTIS HC A02/MF A01 CSCL 20/11

This project is to study the estimation and control of elastic systems composed of beams and plates in order to develop efficient and accurate estimation and control algorithms. Results have been obtained for the estimation in static beams and plates, control and location of actuators for static beams and plates, and identifiability for discrete approximations of second order elliptic boundary value problems. Currently testing codes are being developed for numerical experimentation for estimation of damping and elastic coefficients in dynamic linear plate models, estimation of boundary parameters for second order elliptic problems,

estimation of elastic coefficients in cantilevered beams using perturbed boundary conditions, optimal location of actuators for the control of beams, and control of plates through forces at points and forces distributed over sets of small measure and curves. The plan is to next investigate boundary control and estimation, estimation and control in structures, use of friction as an active control, and parallelization of estimation and control algorithms.
GRA

N87-17145*# Jet Propulsion Lab., California Inst. of Tech., Pasadena.
PRESENT STATUE OF JAPANESE ERS-1 PROJECT
Yasufumi Ishiwada and Yoshiaki Nemoto *In its* The Second Spaceborne Imaging Radar Symposium 1 Dec. 1986 p 79-83 (For primary document see N87-17135 09-43)
Avail: NTIS HC A10/MF A01 CSCL 22B

19 SPACECRAFT INSTRUMENTATION

For related information see also *06 Aircraft Instrumentation* and *35 Instrumentation and Photography.*

N87-16873*# National Aeronautics and Space Administration. Langley Research Center, Hampton, Va.
INITIAL UTILIZATION OF THE CVIRB VIDEO PRODUCTION FACILITY
Russell V. Parrish, Anthony M. Busquets, and Thomas W. Hogge Feb. 1987 46 p
(NASA-TM-89036; NAS 1.15:89036) Avail: NTIS HC A03/MF A01 CSCL 14B

Video disk technology is one of the central themes of a technology demonstrator workstation being assembled as a man/machine interface for the Space Station Data Management Test Bed at Johnson Space Center. Langley Research Center personnel involved in the conception and implementation of this workstation have assembled a video production facility to allow production of video disk material for this propose. This paper documents the initial familiarization efforts in the field of video production for those personnel and that facility. Although the entire video disk production cycle was not operational for this initial effort, the production of a simulated disk on video tape did acquaint the personnel with the processes involved and with the operation of the hardware. Invaluable experience in storyboarding, script writing, audio and video recording, and audio and video editing was gained in the production process. Author

N87-17191# Dornier-Werke G.m.b.H., Friedrichshafen (West Germany).
DEVELOPMENT STATUS OF THE ERS-1 PAYLOAD INSTRUMENTS
E. H. Velten and G. H. Dieterle (European Space Agency. European Space Research and Technology Center, ESTEC, Noordwijk, Netherlands) *In* ESA Proceedings of the 1986 International Geoscience and Remote Sensing Symposium (IGARSS '86) on Remote Sensing: Today's Solutions for Tomorrow's Information Needs, Volume 1 Aug. 1986 p 161-166 (For primary document see N87-17163 09-43)
Avail: NTIS HC A99/MF E03; ESA, Paris, France, 3 volume set $90 Member States, AU, CN, and NO (+20% others)

N87-17192# European Space Agency. European Space Research and Technology Center, ESTEC, Noordwijk (Netherlands).
THE ESA APPROACH FOR ERS-1 SENSOR CALIBRATION AND PERFORMANCE VERIFICATION
J. Louet *In its* Proceedings of the 1986 International Geoscience and Remote Sensing Symposium (IGARSS '86) on Remote Sensing: Today's Solutions for Tomorrow's Information Needs, Volume 1 Aug. 1986 p 167-174 (For primary document see N87-17163 09-43)
Avail: NTIS HC A99/MF E03; ESA, Paris, France, 3 volume set $90 Member States, AU, CN, and NO (+20% others)

N87-17193# Marconi Space and Defence Systems Ltd. Portsmouth (England).
ON-GROUND VERIFICATION AND IN-ORBIT PERFORMANCE PREDICTION OF THE ERS-1 WIND SCATTEROMETER
D. J. Q. Carter *In* ESA Proceedings of the 1986 International Geoscience and Remote Sensing Symposium (IGARSS '86) on Remote Sensing: Today's Solutions for Tomorrow's Information Needs, Volume 1 Aug. 1986 p 175-180 (For primary document see N87-17163 09-43)
Avail: NTIS HC A99/MF E03; ESA, Paris, France, 3 volume set $90 Member States, AU, CN, and NO (+20% others)

N87-17194# European Space Agency. European Space Research and Technology Center, ESTEC, Noordwijk (Netherlands).
ERS-1 RADAR ALTIMETER: PERFORMANCE, CALIBRATION AND DATA VALIDATION
C. R. Francis *In its* Proceedings of the 1986 International Geoscience and Remote Sensing Symposium (IGARSS '86) on Remote Sensing: Today's Solutions for Tomorrow's Information Needs, Volume 1 Aug. 1986 p 181-184 (For primary document see N87-17163 09-43)
Avail: NTIS HC A99/MF E03; ESA, Paris, France, 3 volume set $90 Member States, AU, CN, and NO (+20% others)

N87-17195# Mullard Space Science Lab., Dorking (England).
AN AUTOMATIC TRACKING MODE SWITCHING ALGORITHM FOR THE ERS-1 ALTIMETER
D. J. Wingham *In* ESA Proceedings of the 1986 International Geoscience and Remote Sensing Symposium (IGARSS '86) on Remote Sensing: Today's Solutions for Tomorrow's Information Needs, Volume 1 Aug. 1986 p 185-190 (For primary document see N87-17163 09-43)
(Contract ESTEC-6375/85-NL-BI)
Avail: NTIS HC A99/MF E03; ESA, Paris, France, 3 volume set $90 Member States, AU, CN, and NO (+20% others)

N87-17205*# Operations Research, Inc., Rockville, Md.
THE SEQUENTIAL FILTER IMAGING RADIOMETER (SFIR), A NEW INSTRUMENT CONFIGURATION FOR EARTH OBSERVATIONS
M. S. Maxwell *In* ESA Proceedings of the 1986 International Geoscience and Remote Sensing Symposium (IGARSS '86) on Remote Sensing: Today's Solutions for Tomorrow's Information Needs, Volume 1 Aug. 1986 p 245-250 (For primary document see N87-17163 09-43)
(Contract NAS5-28057)
Avail: NTIS HC A99/MF E03; ESA, Paris, France, 3 volume set $90 Member States, AU, CN, and NO (+20% others) CSCL 14B

20 SPACECRAFT PROPULSION AND POWER

Includes main propulsion systems and components, e.g., rocket engines; and spacecraft auxiliary power sources.

For related information see also *07 Aircraft Propulsion and Power, 28 Propellants and Fuels, 44 Energy Production and Conversion,* and *15 Launch Vehicles and Space Vehicles.*

N87-16874*# Textron Bell Aerospace Co., Buffalo, N. Y.
SPACE STATION AUXILIARY THRUST CHAMBER TECHNOLOGY Final Report
J. M. Senneff Aug. 1986 196 p
(Contract NAS3-24656)
(NASA-CR-179552; NAS 1.26:179552; Rept-8911-950001) Avail: NTIS HC A09/MF A01 CSCL 21H

A program to design, fabricate and test a 50 lb sub f (222 N) thruster was undertaken (Contract NAS 3-24656) to demonstrate the applicability of the reverse flow concept as an item of auxiliary propulsion for the space station. The thruster was to operate at a mixture ratio (O/F) of 4, be capable of operating for 2 million lb

sub f- seconds (8.896 million N-seconds) impulse with a chamber pressure of 75 psia (52 N/square cm) and a nozzle area ratio of 40. Superimposed was also the objective of operating with a strainless steel spherical combustion chamber, which limited the wall temperature to 1700 F (1200 K), an objective specific impulse of 400 lb sub f sec/lbm (3923 N-seconds/Kg), and a demonstration of 500,000 lb sub f-seconds (2,224,000 N-seconds) of impulse. The demonstration of these objectives required a number of design iterations which eventually culminated in a very successful 1000 second demonstration, almost immediately followed by a changed program objective imposed to redesign and demonstrate at a mixture ratio (O/F) of 8. This change was made and more then 250,000 lb sub f seconds (1,112,000 N-seconds) of impulse was successfully demonstrated at a mixture ratio of 8. This document contains a description of the effort conducted during the program to design and demonstrate the thrusters involved. Author

N87-16875*# National Aeronautics and Space Administration. Lewis Research Center, Cleveland, Ohio.
HEAT EXCHANGER FOR ELECTROTHERMAL DEVICES Patent
Ralph J. Zavesky, inventor (to NASA), James S. Sovey, inventor (to NASA), Michael J. Mirtich, inventor (to NASA), Charalampus Marinos, inventor (to NASA), and Paul F. Penko, inventor (to NASA) 2 Sep. 1986 7 p Filed 31 Jul. 1984 Supersedes N84-32425 (22 - 22, p 3542
(NASA-Case-LEW-14037-1; US-Patent-4,608,821; US-Patent-Appl-SN-636463; US-Patent-Class-60-203.1; US-Patent-Class-219-275) Avail: U.S. Patent and Trademark Office CSCL 21H

An improved electrothermal device is disclosed. An electrothermal thruster utilizes a generally cylindrical heat exchanger chamber to convert electricity to heat which raises the propellant temperature. A textured, high emissivity heat element radiatively transfers heat to the inner wall of this chamber that is ion beam morphologically controlled for high absorptivity. This, in turn, raises the temperature of a porous heat exchanger material in an annular chamber surrounding the cylindrical chamber. Propellant gas flows through the annular chamber and is heated by the heat exchanger material. NASA

N87-16876*# National Aeronautics and Space Administration. Marshall Space Flight Center, Huntsville, Ala.
SPACE SHUTTLE MAIN ENGINE VIBRATION DATA BASE
Pat Lewallen Dec. 1986 37 p
(NASA-TM-86576; NAS 1.15:86576) Avail: NTIS HC A03/MF A01 CSCL 21H

The Space Shuttle Main Engine Vibration Data Base is described. Included is a detailed description of the data base components, the data acquisition process, the more sophisticated software routines, and the future data acquisition methods. Several figures and plots are provided to illustrate the various output formats accessible to the user. The numerous vibration data recall and analysis capabilities available through automated data base techniques are revealed. Author

N87-16877*# National Aeronautics and Space Administration. Marshall Space Flight Center, Huntsville, Ala.
STATISTICAL ANALYSIS OF 59 INSPECTED SSME HPFTP TURBINE BLADES (UNCRACKED AND CRACKED)
John T. Wheeler Jan. 1987 35 p
(NASA-TM-86584; NAS 1.15:86584) Avail: NTIS HC A03/MF A01 CSCL 21H

The numerical results of statistical analysis of the test data of Space Shuttle Main Engine high pressure fuel turbopump second-stage turbine blades, including some with cracks are presented. Several statistical methods use the test data to determine the application of differences in frequency variations between the uncracked and cracked blades. B.G.

N87-16878*# GT-Devices, Alexandria, Va.
INVESTIGATION OF A REPETITIVE PULSED ELECTROTHERMAL THRUSTER Contract Report, 24 May 1985 - 23 May 1986
R. L. Burton, D. Fleischer, S. A. Goldstein, D. A. Tidman, and N. K. Winsor 21 Aug. 1986 57 p
(Contract NAS3-24636)
(NASA-CR-179464; NAS 1.26:179464; GTD86-5) Avail: NTIS HC A04/MF A01 CSCL 21H

A pulsed electrothermal (PET) thruster with 1000:1 ratio nozzle is tested in a repetitive mode on water propellant. The thruster is driven by a 60J pulse forming network at repetition rates up to 10 Hz (600W). The pulse forming network has a .31 ohm impedance, well matched to the capillary discharge resistance of .40 ohm, and is directly coupled to the thruster electrodes without a switch. The discharge is initiated by high voltage breakdown, typically at 2500V, through the water vapor in the interelectrode gap. Water is injected as a jet through a .37 mm orifice on the thruster axis. Thruster voltage, current and impulse bit are recorded for several seconds at various power supply currents. Thruster to power ratio is typically T/P = .07 N/kW. Tank background pressure precludes direct measurement of exhaust velocity which is inferred from calculated pressure and temperature in the discharge to be about 14 km/sec. Efficiency, based on this velocity and measured T/P is .54 + or - .07. Thruster ablation is zero at the throat and becomes measurable further upstream, indicating that radiative ablation is occurring late in the pulse. Author

23 CHEMISTRY AND MATERIALS (GENERAL)

N87-16879*# Case Western Reserve Univ., Cleveland, Ohio. Dept. of Mechanical and Aerospace Engineering.
OIL FILM THICKNESS MEASUREMENT AND ANALYSIS FOR AN ANGULAR CONTACT BALL BEARING OPERATING IN PARCHED ELASTOHYDRODYNAMIC LUBRICATION M.S. Thesis. Final Report
Scott D. Hunter Sep. 1986 265 p
(Contract NCC3-30)
(NASA-CR-179506; E-3152; NAS 1.26:179506) Avail: NTIS HC A12/MF A01 CSCL 11H

The capacitance method is used to estimate the oil film thickness in the Hertzian contact zone of an angular contact ball bearing operating in parched elastohydrodynamic lubrication. The parched elastohydrodynamic lubrication regime is characterized by a transient film thickness and basic speed ratio (ball spin rate over combined race speed) and the formation of a friction polymer. The experimental apparatus tests 40 mm 108 H ball bearings in the counter rotating race mode at loads of 200 and 300 lb, a film parameter of 1.6 and nominal inner and outer race speeds of 38 and 26 rps, respectively. Experimental results are presented for the capacitance, thickness, and conductance of the oil film as functions of elapsed time and for the basic speed ratios as a function of elapsed time, load, and amount of lubricant applied to the test bearing. Results indicate that a friction polymer formed from the initial lubricant has an effect on the capacitance and basic speed ratio measurements. Author

24 COMPOSITE MATERIALS

Includes physical, chemical, and mechanical properties of laminates and other composite materials.
For ceramic materials see *27 Nonmetallic Materials.*

N87-16880*# National Aeronautics and Space Administration. Lewis Research Center, Cleveland, Ohio.
COMPOSITE SPACE ANTENNA STRUCTURES: PROPERTIES AND ENVIRONMENTAL EFFECTS
Carol A. Ginty and Ned M. Endres (Sverdrup Technology, Inc.,

Cleveland, Ohio) 1986 22 p Presented at the 18th International SAMPE Technical Conference, Seattle, Wash., 7-9 Oct. 1986
(NASA-TM-88859; E-3225; NAS 1.15:88859) Avail: NTIS HC A02/MF A01 CSCL 11D

The thermal behavior of composite spacecraft antenna reflectors has been investigated with the integrated Composites Analyzer (ICAN) computer code. Parametric studies have been conducted on the face sheets and honeycomb core which constitute the sandwich-type structures. Selected thermal and mechanical properties of the composite faces and sandwich structures are presented graphically as functions of varying fiber volume ratio, temperature, and moisture content. The coefficients of thermal expansion are discussed in detail since these are the critical design parameters. In addition, existing experimental data are presented and compared to the ICAN predictions. Author

N87-16881# Aeronautical Research Labs., Melbourne (Australia).
CARBON FIBRE COMPOSITE COUPONS: STATIC AND FATIGUE BEHAVIOUR AFTER IMPACT DAMAGE
G. Clark and T. J. VanBlaricum Aug. 1986 30 p
(ARL-STRUC-R-422; AR-004-495) Avail: NTIS HC A03/MF A01

Results from an experimental program involving the determination of static and fatigue properties of relatively thick (3 to 7 mm) carbon fiber composite laminates which was subjected to various levels of impact damage was described. The development of suitable compression testing procedures is described, as in the use of shadow Moire interference techniques for monitoring the development of delamination damage during fatigue tests. Author

N87-16882*# National Aeronautics and Space Administration. Langley Research Center, Hampton, Va.
EFFECT OF ADHEREND THICKNESS AND MIXED MODE LOADING ON DEBOND GROWTH IN ADHESIVELY BONDED COMPOSITE JOINTS
P. D. Mangalgiri (National Academy of Sciences - National Research Council, Washington, D. C.), W. S. Johnson, and R. A. Everett, Jr. (Army Aviation Research and Development Command, Hampton, Va.) Sep. 1986 46 p
(DA Proj. 1L1-61102-AH-45)
(NASA-TM-88992; NAS 1.15:88992; AVSCOM-TR-86-B-2) Avail: NTIS HC A03/MF A01 CSCL 11D

Symmetric and unsymmetric double cantilever beam (DCB) specimens were tested and analyzed to assess the effect of: (1) adherend thickness, and (2) a predominantly mode I mixed mode loading on cyclic debond growth and static fracture toughness. The specimens were made of unidirectional composite (T300/5208) adherends bonded together with EC3445 structural adhesive. The thickness was 8, 16, or 24 plies. The experimental results indicated that the static fracture toughness increases and the cyclic debond growth rate decreases with increasing adherend thickness. This behavior was related to the length of the plastic zone ahead of the debond tip. For the symmetric DCB specimens, it was further found that displacement control tests resulted in higher debond growth rates than did load control tests. While the symmetric DCB tests always resulted in cohesive failures in the bondline, the unsymmetric DCB tests resulted in the debond growing into the thinner adherend and the damage progressing as delamination in that adherend. This behavior resulted in much lower fracture toughness and damage growth rates than found in the symmetric DCB tests. Author

N87-16883*# Lockheed-California Co., Burbank.
FLIGHT SERVICE EVALUATION OF ADVANCED COMPOSITE AILERONS ON THE L-1011 TRANSPORT AIRCRAFT Annual Flight Service Report
R. H. Stone Jul. 1986 14 p
(Contract NAS1-15069)
(NASA-CR-178170; NAS 1.26:178170; LR-31032; AFSR-4) Avail: NTIS HC A02/MF A01 CSCL 11D

This report covers flight evaluation of composite inboard ailerons on the L-1011 under Contract NAS 1-15069 for a period of five years. This is the fourth annual report of the maintenance evaluation program, and covers the period from May 1985 when the third yearly inspections were completed, through July 1986. Four shipsets of graphite/epoxy composite inboard ailerons were installed on L-1011 aircraft for this maintenance evaluation program. These include two Delta aircraft and two TWA aircraft. A fifth shipset of composite ailerons was installed in 1980 on Lockheed's flight test L-1011. One instance of minor damage was observed on one of the composite ailerons and was repaired. No other maintenance actions have occurred on any of the composite parts except for repainting of areas with paint loss. Flight hours on the airline components at the time of inspection ranged from 12,051 to 14,046 hours, after approximately 4 years of service.
Author

N87-16884*# National Aeronautics and Space Administration. Langley Research Center, Hampton, Va.
COMPARISON OF COMPOSITE ROTOR BLADE MODELS: A COUPLED-BEAM ANALYSIS AND AN MSC/NASTRAN FINITE-ELEMENT MODEL
Robert V. Hodges (Army Aviation Systems Command, St. Louis, Mo.), Mark W. Nixon, and Lawrence W. Rehfield (Georgia Inst. of Tech., Atlanta) Mar. 1987 16 p
(DA Proj. 1L1-61102-AH-45)
(NASA-TM-89024; L-16207; NAS 1.15:89024;
AVSCOM-TM-87-B-2) Avail: NTIS HC A02/MF A01 CSCL 11D

A methodology was developed for the structural analysis of composite rotor blades. This coupled-beam analysis is relatively simple to use compared with alternative analysis techniques. The beam analysis was developed for thin-wall single-cell rotor structures and includes the effects of elastic coupling. This paper demonstrates the effectiveness of the new composite-beam analysis method through comparison of its results with those of an established baseline analysis technique. The baseline analysis is an MSC/NASTRAN finite-element model built up from anisotropic shell elements. Deformations are compared for three linear static load cases of centrifugal force at design rotor speed, applied torque, and lift for an ideal rotor in hover. A D-spar designed to twist under axial loading is the subject of the analysis. Results indicate the coupled-beam analysis is well within engineering accuracy. Author

N87-16885# Department of the Air Force, Washington, D.C.
A COMPOSITE ALUMINUM CONDUCTOR FOR PULSED POWER APPLICATIONS AT CRYOGENIC TEMPERATURES AND METHOD OF ITS MANUFACTURE Patent Application
Charles E. Oberly, inventor (to Air Force) Filed 10 Apr. 1986 24 p
(AD-D012501; US-Patent-Appl-SN-849989) Avail: NTIS HC A02/MF A01 CSCL 09/1

The conductor contains high-purity aluminum embedded in an aluminum-iron-cerium alloy matrix. It is not superconducting but still has extremely low electrical resistance at service temperatures. Selection of the aluminum-base alloy matrix with diffusionless alloying elements (iron and cerium) allows production of a multifilamentary conductor with the aluminum filaments maintaining their original high purity and consequently their very low electrical resistivity, even after a high temperature annealing cycle is applied. The composite conductor has good properties for both electromagnetic and thermal diffusion, which are critical to high power, fast-pulse operation. Author (GRA)

N87-16886# Lawrence Livermore National Lab., Calif.
MECHANICAL PROPERTIES OF GRAPHITE EPOXY USED FOR ZERO CTE PROGRAM
D. S. Hiromoto May 1986 12 p
(Contract W-7405-eng-48)
(DE86-013227; UCID-20805) Avail: NTIS HC A02/MF A01

Predictability of thermal expansion of materials has always been of concern for weapons applications. Incompatible coefficients of thermal expansion can significantly downgrade reliability and accuracy of any weapons system. This study, funded by Mechanical Engineering Research, supplied valuable data to verify theoretical predictions for mechanical properties of this fiber composite, also used in the Zero CTE Program. DOE

N87-16887# Rolls-Royce Ltd., Derby (England).
PRELIMINARY INVESTIGATIONS INTO THE MICROCRACKING OF PMR-15/GRAPHITE COMPOSITES. PART 1: EFFECT OF CURE TEMPERATURE
D. Wilson (British Petroleum Co. Ltd., Sunbury-on-Thames, England), J. K. Wells, J. N. Hay, D. Lind, G. A. Owens, and F. Johnson 8 Oct. 1986 13 p Presented at the SAMPE Conference, Seattle, Wash., 8-9 Oct. 1986
(PNR90348; ETN-87-98783) Avail: NTIS HC A02/MF A01

Laminates of the thermosetting polyimide PMR-15, a matrix resin for high temperature polymer composites, were prepared by curing at a range of temperatures. Mechanical and microcracking properties and thermo-oxidative stability of the laminates were determined. Results indicate that low temperature cure (280 to 290 C) of PMR-15 is possible to produce composites of acceptable mechanical properties that show a significantly reduced tendency to microcrack. ESA

N87-16888# Research Inst. of National Defence, Stockholm (Sweden). Dept. 2.
DAMAGE AND REPAIRING OF FIBER COMPOSITES, A SUMMARY
Lars Svensson Aug. 1986 28 p In SWEDISH; ENGLISH summary
(FOA-C-20620-2.5; ISSN-0347-3694; ETN-87-98907) Avail: NTIS HC A03/MF A01

The causes of fiber composite damage are outlined and various kinds of damage are surveyed, e.g., surface damage, delaminating, impact, edge defects, and temperature effects. Detection means are dealt with. Different repairing methods are described, especially for laminates and for delaminating damage. The strength of the repairs carried out by various methods are indicated: the mechanical resistance, as a rate of that of the undamaged part, varies from 30% to 50%, and exceptionally 85% when rivets can be used. ESA

25 INORGANIC AND PHYSICAL CHEMISTRY

Includes chemical analysis, e.g., chromatography; combustion theory; electrochemistry; and photochemistry.

For related information see also *77 Thermodynamics and Statistical Physics.*

N87-16889 Michigan Univ., Ann Arbor.
SIMULTANEOUS DENSITY VELOCITY MEASUREMENTS IN PREMIXED TURBULENT FLAMES TO ASSESS A THEORETICAL MODEL Ph.D. Thesis
Anil Gulati 1986 203 p
Avail: Univ. Microfilms Order No. DA8621292

Density and velocity are measured simultaneously for the first time in premixed turbulent flames using the techniques of Rayleigh scattering and laser velocimetry. The flame configuration used represents a significant improvement in that extraneous sources of turbulence were eliminated. Mean quantities, density-velocity correlations, Favre averaged velocities, and conditioned velocity measurements were used to assess the Bray-Moss-Libby model for premixed flames. Three of the five terms involved in turbulent kinetic energy budget in the flame are directly measured for the first time and compared with predictions of the model. The influence of heat release is also studied for the first time. Overall the model is found to be very successful in predicting trends of variation of most quantities correctly. Certain model improvements were suggested. Dissert. Abstr.

N87-16890*# San Diego State Univ., Calif. Dept. of Electrical and Computer Engineering.
MEASUREMENT OF HO2 CHEMICAL KINETICS WITH A NEW DETECTION METHOD Annual Technical Report, 1 Dec. 1985 - 30 Nov. 1986
Long C. Lee and Masako Suto 18 Dec. 1986 24 p
(Grant NAGw-661)
(NASA-CR-180114; NAS 1.26:180114) Avail: NTIS HC A02/MF A01 CSCL 07D

Reaction rate constants of HO2+O3 were measured at various temperatures using a newly developed HO2 detection method. HO2 was detected by the OH(A-X) emission produced from photodissociative excitation of HO2 at 147 nm. In order to examine the possible interference of other emitting species with the HO2 detection, the photoexcitation processes of all the chemical species existing in the discharge flow tube were also investigated. The results are summarized. For individual title, see N87-16891.

N87-16891*# San Diego State Univ., Calif. Dept. of Electrical and Computer Engineering.
CF2 AND CFCL FLUORESCENCE FROM VUV EXCITATION OF C2F3CL
J. B. Nee (National Central Univ., Chung-Li, Taiwan), Xiuyan Wang, Masako Suto, and Long C. Lee *In its* Measurement of HO2 Chemical Kinetics with a New Detection Method 18 Dec. 1986 16 p (For primary document see N87-16890 09-25)
Avail: NTIS HC A02/MF A01 CSCL 07D

The photoexcitation process of C2F3Cl molecule was investigated in the 106 to 230 nm region using synchrotron radiation as a light source. Photoabsorption and fluorescence cross sections were measured and used to determine the fluorescence quantum yield. Fluorescence yield starts to appear at 170 nm and increases to about 2% at 155 nm. The fluorescence spectra were dispersed to identify the emitting species. At the excitation wavelength of 155 nm, the emission system is CFCl (Hermitian conjugate of A - Hermitian conjugate of X), and at 123.9 nm, both the CF2 (Hermitian conjugate of A - Hermitian conjugate of X) and CFCl (Hermitian conjugate of A - Hermitian conjugate of X) systems are observed. The dissociation processes that produced these excited species are discussed. Author

N87-16892*# Nebraska Univ., Lincoln. Lab. of Physics.
TOTAL AND DISSOCIATIVE PHOTOIONIZATION CROSS SECTIONS OF N2 FROM THRESHOLD TO 107 eV
James A. R. Samson, T. Masuoka, P. N. Pareek, and G. C. Angel [1986] 17 p
(Grant NGR-28-004-021)
(NASA-CR-180172; NAS 1.26:180172) Avail: NTIS HC A02/MF A01 CSCL 07D

The absolute cross sections for the production of N(+) and N2(+) were measured from the dissociative ionization threshold of 115 A. In addition, the absolute photoabsorption and photoionization cross sections were tabulated between 114 and 796 A. The ionization efficiencies were also given at several discrete wave lengths between 660 and 790 A. The production of N(+) fragment ions are discussed in terms of the doubly excited N2(+) states with binding energies in the range of 24 to 44 eV. Author

N87-16893 Department of the Air Force, Washington, D.C.
FLAMEHOLDER WITH REMOVABLE FLAMEHOLDER ATTACHMENTS Patent
Steven B. Kushnick, inventor (to Air Force) and Gunther Eichhorn, inventor (to Air Force) Issued 17 Jun. 1986 4 p Supersedes US-Patent-Appl-SN-724720
(AD-D012466; US-Patent-4,594,851; US-Patent-Appl-SN-724720; US-Patent-Class-60-261) Avail: US Patent and Trademark Office CSCL 21/5

This patent discloses an improved flameholder which has a plurality of flameholder attachments removably mounted in cutouts in the downstream edge of a shroud of the flameholder. Each attachment includes a support plate which fits into one of the cutouts and a plurality of fan gutter flameholding elements rigidly mounted on the plate. A slip joint links the plate to the shroud and stiffeners which are fastened together connect each flameholding element to the shroud. GRA

N87-16894# Pennsylvania State Univ., University Park. Dept. of Mechanical Engineering.

TRANSIENT CATALYTIC COMBUSTION Annual Report, 30 Sep. 1984 - 30 Sep. 1985
D. A. Santavicca 10 Jan. 1986 29 p
(Grant AF-AFOSR-0224-84)
(AD-A173098; AFOSR-86-1004TR) Avail: NTIS HC A03/MF A01 CSCL 21/2

A study of the catalytic ignition of lean propane-air mixtures on platinum in a stacked-plate catalytic combustor is described. The effects of inlet temperature, equivalence ratio and gas velocity on the ignition transient were investigated. The ignition process was characterized in terms of the substrate axial temperature profile and the exhaust gas CO and CO2 concentrations measured as a function of time. Ignition was found to occur first near the leading edge of the catalyst as indicated by the more rapid heat-up of its front end. The downstream end heated up more slowly and was strongly dependent on convective heat transfer from the front. Increased inlet temperature, equivalence ratio and velocity were all found to shorten the ignition transient and to lead to increased steady state peak substrate temperatures. Increased velocity also caused the peak substrate temperature to move further toward the back of the catalyst. For the conditions studied, the initial ignition rate was found to be surface reaction rate controlled at high velocities (above 2 m/s) but at lower velocities (below 2 m/s) the initial ignition rate was found to depend both on surface reaction and mass transport rates. GRA

N87-16895# Spectron Development Labs., Inc., Costa Mesa, Calif.
DROPLET SIZING RESEARCH PROGRAM Final Report, 15 Jan. 1983 - 15 Jan. 1986
Cecil F. Hess 10 Mar. 1986 137 p
(Contract F49620-83-C-0060)
(AD-A173100; SDL-86-2286-15F; AFOSR-86-0875TR) Avail: NTIS HC A07/MF A01 CSCL 04/1

A three-year program in droplet sizing research has been completed. The major accomplishments include: (1) Establishing the errors and limitations associated with the Visibility technique; (2) Development of two new techniques utilizing absolute scattered light; (3) Extension of techniques to submicron particles; (4) Extension of techniques to nonspherical drops; (5) A solid spray diagnostic capability which has been synergistic with many programs from other agencies of the Air Force (AEDC, BMO, Wright-Patterson), the Government and Industry. The new techniques have been applied to the measurement of sprays and solid particles with accuracies better than 10% and dynamic ranges between 10 and 30. Complex bimodal, trimodal and quadramodal distributions have been measured with an accuracy and resolution exceeding all available techniques. GRA

N87-16896# Princeton Univ., N. J. Dept. of Mechanical and Aerospace Engineering.
LUMPED MODEL GENERATION AND EVALUATION: SENSITIVITY AND LIE ALGEBRAIC TECHNIQUES WITH APPLICATIONS TO COMBUSTION Annual Report, 10 Sep. 1985 - 31 Aug. 1986
F. L. Dryer, H. Rabitz, and R. Yetter 1 Oct. 1986 90 p
(Grant AF-AFOSR-0346-85)
(AD-A174984; AFOSR-86-2106TR) Avail: NTIS HC A05/MF A01 CSCL 07/1

This program dealt with the development and application of new approaches for producing and evaluating semi-empirical (lumped parameter) mathematical models of physical processes. Procedures using local sensitivity gradient methods were used to study the existing lumped kinetic models for the moist carbon monoxide oxidation to show that transport processes can cause oversimplified lumped models derived from homogeneous kinetics to fail when applied to flame propagation systems. New models are under development which will include the appropriate level of detail. A Lie group formalism was developed to address global parameter space mapping issues for first order differential equations. GRA

N87-16897# Princeton Univ., N. J. Dept. of Mechanical and Aerospace Engineering.
FUELS COMBUSTION RESEARCH Annual Technical Report, 1 Oct. 1985 - 30 Sep. 1986
F. L. Dryer, I. Glassman, and F. A. Williams 31 Oct. 1986 62 p
(Contract F49620-86-C-0006)
(AD-A175040; AFOSR-86-2107TR) Avail: NTIS HC A04/MF A01 CSCL 21/2

After great progress related to soot formation in normal diffusion flames, studies of near sooting inverse diffusion flames were begun to determine controlling precursors. Stable, temperature controlled inverse diffusion flames have been successfully developed and numerous chemical samples extracted and analyzed. Observed trends are being studied. The side chain oxidation of n-butyl benzene was found to follow the same processes as the smaller n-alkyl benzenes; abstraction, alkyl group displacement and thermal cleavage. The results have led to development of a simple general, mechanistic model for the oxidation of n-alkyl benzenes. Combustion property observations of isolated boron droplets were extended to boron/JP-10 slurries with various solid loadings. Some physical understanding of observed droplet-burning and disruption behavior was developed. Quasi-spherical hollow shells of the boron agglomerate with blowholes support the hypothesis of the formation of the impermeable shell and subsequent disruption of the primary slurry droplet. Boron suspension (cloud) combustion in the hot reaction products of a flat-flame burner has been pursued. The boric acid fluctuation bands were identified spectroscopically, and conditions for their flame occurrence measured. The work progresses toward establishment of ignition conditions and combustion times of 0.1 to 5 micronboron particles. GRA

N87-16898# Argonne National Lab., Ill.
SUPPORTED LIQUID MEMBRANES IN 1986: NEW TECHNOLOGY OR SCIENTIFIC CURIOSITY
P. R. Danesi 1986 11 p Presented at the International Solvent Extraction Conference, Munich, West Germany, 11 Sep. 1986
(Contract W-31-109-eng-38)
(DE86-007504; CONF-860921-1) Avail: NTIS HC A02/MF A01

Thin layers of organic solutions of solvent extraction reagents (membrane carriers), immobilized on microporous inert supports and interposed between two aqueous solutions (feed and strip), were first proposed more than two decades ago as a new and promising technique for separating and concentrating metal species. Such immobilized layers, representing supported liquid membranes (SLM), have been extensively studied during the last six years mainly for their ability to separate and concentrate metal ions of critical and strategic importance and of relevance to the nuclear industry. In this presentation the major results obtained up to 1986 in the field of SLM's are summarized. A brief indication of the major problems to be addressed to implement SLM's as a new separation technology is also given. DOE

26 METALLIC MATERIALS

Includes physical, chemical, and mechanical properties of metals, e.g., corrosion; and metallurgy.

N87-16899 Virginia Univ. Hospital, Charlottesville.
MECHANISMS OF HELIUM EMBRITTLEMENT Ph.D. Thesis
Robert David Gerke 1985 180 p
Avail: Univ. Microfilms Order No. DA8608542

In an attempt to clarify the role of helium in promoting high temperature intergranular failure, in-situ tensile experiments have been conducted in a high voltage electron microscope (HVEM) attached to a linear ion accelerator used at 80 keV. Two types of experiments were performed on 14 MeV neutron and helium irradiated 40 micron thick foil stainless steel specimens using a heating quantitative load-elongation tensile stage between 25 C and 700 C. A graph of cumulative crack length plotted against total specimen elongation exhibits a slope, S, which increases as specimen ductility (reduction of area, ROA) decreased. It was found that ROA squared x S = 0.4 for all cases studied. High temperature helium embrittlement occurs only at slow strain rates. Dislocations

dragging helium bubbles to grain boundaries is commonly thought to cause the embrittlement. Specimens tensile tested under dual tensile test temperatures exhibited intergranular failure at 700 C and after the tensile test was resumed at 550 C changed to a transgranular failure mode, suggesting that the conditions for intergranular failure cannot be set up under stress and at elevated temperature and continue at a lower temperature. When specimens containing tiny bubbles were tensile tested at 250 and 450 C under rapid and slow strain rates, mixed mode failure (I + T) occurred under all conditions suggesting strain rate insensitive microstructures are possible. Dissert. Abstr.

N87-16900*# National Aeronautics and Space Administration. Marshall Space Flight Center, Huntsville, Ala.
ELECTRICAL PROPERTIES OF Al-In-Sn ALLOYS DIRECTIONALLY SOLIDIFIED IN HIGH AND LOW GRAVITATIONAL FIELDS Center Director's Discretionary Fund Final Report
P. A. Curreri, M. K. Wu (Alabama Univ., Huntsville), J. R. Ashburn, and W. F. Kaukler Oct. 1986 21 p
(NASA-TM-86569; NAS 1.15:86569) Avail: NTIS HC A02/MF A01 CSCL 11F

The Al-In-Sn alloys were directionally solidified in the NASA KC-135 aircraft which flies a series of parabolas to generate high (high-g) and low (low-g) gravity forces parallel to the longitudinal growth axis. Thus, for a given sample, successive sections can be identified which were solidified in high-g and low-g. Measurements of the electronic properties of the samples reveal that: the resistivity of the low-g sections is larger (about a factor of 10) than that of the high-g sections; the low-g sections behave conductively like a semi-metal, while the high-g sections are essentially metallic; and both high-g and low-g sections are superconducting but the superconducting transition temperature of the low-g sections is 1 K higher than that of the high-g sections. Author

N87-16901*# National Aeronautics and Space Administration. Marshall Space Flight Center, Huntsville, Ala.
THE EFFECTS OF GRAVITY LEVEL DURING DIRECTIONAL SOLIDIFICATION ON THE MICROSTRUCTURE OF HYPERMONOTECTIC Al-In-Sn ALLOYS
P. A. Curreri and W. F. Kaukler (Alabama Univ., Huntsville) Nov. 1986 41 p
(NASA-TM-86573; NAS 1.15:86573) Avail: NTIS HC A03/MF A01 CSCL 11F

Five hypermonotectic Al-In-Sn compositions were directionally solidified in a Bridgman-type furnace at normal gravity and during aircraft low-gravity maneuvers. The tendency of the Al-30In alloy to form an indium-rich band at the start of unidirectional growth (SUG) made it difficult to study the integration of L sub 2 into the solidification interface. Hypermonotectic compositions closer to monotectic slightly hypermonotectic caused only a partial band on L sub 2 to form at SUG and allowed the study of such variables as gravity, composition, and monotectic dome height on integration of excess L sub 2 into the solid plus L sub 2 interface. It was found that formation of aligned composite structures for the Al-In-Sn system is not only a function of G and R but also of the degree to which the composition varies from monotectic. Most of the aligned fibrous structures formed from hypermonotectic Al-In-Sn had spacings that were of the order of irregular fibrous structures reported for on monotectic Al-In-Sn. The spacings for the large fibers and aligned globules found for ground and low-gravity processed Al-In-18-Sn-22, respectively, were significantly larger than the others measured and were of the order expected for cell spacings under the growth conditions utilized. It was found that the integration into the solidification front of excess L sub 2 in low gravity was a function of the Sn composition of the alloy. Author

N87-16902*# National Aeronautics and Space Administration. Lewis Research Center, Cleveland, Ohio.
CONVENTIONALLY CAST AND FORGED COPPER ALLOY FOR HIGH-HEAT-FLUX THRUST CHAMBERS
John M. Kazaroff and George A. Repas Feb. 1987 12 p
(NASA-TP-2694; E-3304; NAS 1.60:2694) Avail: NTIS HC A02/MF A01 CSCL 11F

The combustion chamber liner of the space shuttle main engine is made of NARloy-Z; a copper-silver-zirconium alloy. This alloy was produced by vacuum melting and vacuum centrifugal casting; a production method that is currently now available. Using conventional melting, casting, and forging methods, NASA has produced an alloy of the same composition called NASA-Z. This report compares the composition, microstructure, tensile properties, low-cycle fatigue life, and hot-firing life of these two materials. The results show that the materials have similar characteristics. Author

N87-16903# Department of the Navy, Washington, D. C.
FABRICATION OF HOLLOW, CORED, AND COMPOSITE SHAPED PARTS FROM SELECTED ALLOY POWDERS Patent Application
David Goldstein, inventor (to Navy) Filed 2 Jul. 1986 14 p
(AD-D012489; US-Patent-Appl-SN-887407) Avail: NTIS HC A02/MF A01 CSCL 11/6

Alloy powder is packed into a mold which comprises a complex-shaped solid graphic inner core and a similarly complex-shaped thin glass outer wall. The mold is evacuated, sealed, and then heated to the alloy sintering temperature. The glass softens and applies an isostatic pressure on the alloy as the alloy particles consolidate. After the consolidation step, the mold and its contents are cooled and the glass and graphite materials are removed from the alloy object. This method is particularly useful for preparing complex fittings of Nitinol shape memory alloys. GRA

N87-16904# Ames Lab., Iowa.
PREPARATIONS OF RARE EARTH-IRON ALLOYS BY THERMITE REDUCTION Patent Application
F. A. Schmidt, inventor (to DOE), D. T. Peterson, inventor (to DOE), and J. T. Wheelock, inventor (to DOE) Filed 28 Oct. 1985 15 p
(Contract W-7405-eng-82)
(DE86-013753; US-Patent-Appl-SN-791972) Avail: NTIS HC A02/MF A01

Disclosed is an improved method for the preparation of high-purity rare earth-iron alloys by the aluminothermic reduction of a mixture of rare earth and iron fluorides. DOE

N87-16905# Rolls-Royce Ltd., Derby (England).
CORROSION/OXIDATION PROTECTION OF HIGH TEMPERATURE MATERIAL
G. W. Meetham 2 Apr. 1986 22 p Presented at the Materials in Aerospace Conference, England, 2-4 Apr. 1986; sponsored by RAE
(PNR90355; ETN-87-98787) Avail: NTIS HC A02/MF A01

Corrosion resistant coatings of gas turbine blades are discussed. Thermal barrier coatings are described. Applications in aircraft engines are recalled. ESA

27 NONMETALLIC MATERIALS

Includes physical, chemical, and mechanical properties of plastics, elastomers, lubricants, polymers, textiles, adhesives, and ceramic materials.

For composite materials see *24 Composite Materials.*

N87-16906 Materials Quality Assurance Directorate, London (England). Materials Center.
A COMPARISON OF TWO BRITISH STANDARD TEST METHODS FOR THE DETERMINATION OF RESISTANCE TO HUMIDITY OF PAINT FILMS
A. E. Morris Mar. 1986 13 p
(MQAD-TP-918; BR99119; ETN-87-98916) Copyright. Avail: NTIS

British Standard (BS) 3900, Part F2 and BS 3900, Part F9 methods for the determination of resistance to humidity of paint

films were compared. An apparatus operated in accordance with Part F9 but not complying fully with the instrumental design requirements of the method was tested. Exposure of a series of paints of known differing performance shows the methods to be comparable at the extremes of the corrosion assessment scale, and Part F9 test conditions to be less severe in the middle of the scale. Results of panels exposed in the nonstandard F9 apparatus compare favorably with those from the standard apparatus. ESA

N87-16907*# National Aeronautics and Space Administration. Langley Research Center, Hampton, Va.
ETHYNYL TERMINATED ESTER OLIGOMERS AND POLYMERS THEREFROM Patent
Paul M. Hergenrother, inventor (to NASA) and Stephen J. Havens, inventor (to NASA) (Kentron International, Inc., Hampton, Va.) Issued 20 Jan. 1987 7 p
(NASA-Case-LAR-13118-2; US-Patent-4,638,083; US-Patent-Appl-SN-760797; US-Patent-Class-560-104) Avail: U.S. Patent and Trademark Office CSCL 11B

A new class of ethynyl-terminated oligomers and the process for preparing same are disclosed. Upon the application of heat, with or without a catalyst, the ethynyl groups react to provide crosslinking and chain extension to increase the polymer use temperature and improve the polymer solvent resistance. These improved polyesters are potentially useful in packaging, magnetic tapes, capacitors, industrial belting, protective coatings, structural adhesives and composite matrices. NASA

N87-16908*# National Aeronautics and Space Administration. Ames Research Center, Moffett Field, Calif.
VINYL STILBAZOLES Patent
John A. Parker, inventor (to NASA), Alvin H. Heimbuch, inventor (to NASA), Ming-Ta S. Hsu, inventor (to NASA) (San Jose State Univ., Calif.), and Timothy S. Chen, inventor (to NASA) Issued 2 Dec. 1986 9 p Division of US-Patent-4,526,925, US-Patent-Appl-SN-553339, dated 18 Nov. 1983
(NASA-Case-ARC-11429-3CU; US-Patent-4,626,593; US-Patent-Appl-SN-725725; US-Patent-Class-546-339; US-Patent-Class-546-346; US-Patent-Class-546-350) Avail: US Patent and Trademark Office CSCL 11B

Vinyl pyridines including vinyl stilbazole materials and vinyl styrylpyridine oligomer materials are disclosed. These vinylpyridines form copolymers with bismaleimides which copolymers have good fire retardancy and decreased brittleness. The cure temperatures of the copolymers are substantially below the cure temperatures of the bismaleimides alone. Reinforced composites made from the cured copolymers are disclosed as well. NASA

N87-16909*# National Aeronautics and Space Administration. Ames Research Center, Moffett Field, Calif.
FIRE AND HEAT RESISTANT LAMINATING RESINS BASED ON MALEIMIDO SUBSTITUTED AROMATIC CYCLOTRIPHOSPHAZENE POLYMER Patent
Devendra Kumar, inventor (to NASA) (National Academy of Sciences - National Research Council, Washington, D. C.), George M. Fohlen, inventor (to NASA), and John A. Parker, inventor (to NASA) Issued 6 Jan. 1987 20 p Division of US-Patent-4,550,177; US-Patent-Appl-SN-599126, dated 14 Apr. 1984
(NASA-Case-ARC-11428-2; US-Patent-4,634,759; US-Patent-Appl-SN-760374; US-Patent-Class-528-321; US-Patent-Class-528-168; US-Patent-Class-528-322; US-Patent-Class-428-421; US-Patent-Class-428-473.5; US-Patent-Class-428-500; US-Patent-Class-428-704) Avail: US Patent and Trademark Office CSCL 11B

4-Aminophenoxy cyclotriphosphazenes are reacted with maleic anhydride to produce maleamic acids which are converted to the maleimides. The maleimides are polymerized. By selection of starting materials (e.g., hexakis amino or trisaminophenoxy trisphenoxy cyclotriphosphazenes), selection of molar proportions of reactants, use of mixtures of anhydrides and use of dianhydrides as bridging groups a variety of maleimides and polymers are produced. The polymers have high limiting oxygen indices, high char yields and other useful heat and fire resistant properties making them useful as, for example, impregnants of fabrics. NASA

N87-16910*# National Aeronautics and Space Administration. Marshall Space Flight Center, Huntsville, Ala.
THE NON-METALLIC MATERIALS SAMPLE ARRAY
H. M. King, D. D. Webb, and B. E. Goldberg Dec. 1986 20 p
(NASA-TM-86578; NAS 1.15:86578) Avail: NTIS HC A02/MF A01 CSCL 11B

The Non-Metallic Materials Sample Array (MSA) was flown as verification flight instrumentation (VFI) on both Spacelab 1 (SL-1) and Spacelab 2 (SL-2). The basis for materials selection was either previous flight history or probable flight suitability based upon analysis. The observed changes in the optical properties of the exposed materials are, in general, quite minimal; however, this data represents the short exposure of two Space Shuttle missions, and no attempt should be made to extrapolate the long-term exposure. The MSA was in orbit for 10 days at approximately 240 km on SL-1 and for 7 days at approximately 315 km on SL-2. The array was exposed to the solar flux for only a portion of the time in orbit. Author

N87-16911*# National Aeronautics and Space Administration. Langley Research Center, Hampton, Va.
SOLUBLE AROMATIC POLYIMIDES FOR FILM AND COATING APPLICATIONS
Anne K. St.Clair and Terry L. St.Clair Sep. 1986 11 p Presented at the Symposium on High Temperature Polymers for Electronic Applications, Meeting of the American Chemical Society, Anaheim, Calif., 7-12 Sep. 1986
(NASA-TM-89016; NAS 1.15:89016) Avail: NTIS HC A02/MF A01 CSCL 11B

Linear all-aromatic polyimides have been synthesized and characterized which show much potential as films and coatings for electronic applications. Structure-property relations with regard to methods for obtaining solubility of fully imidized polymers will be discussed. Methods used to obtain solubility include variation of polymer molecular structure, variation of isomerism of the diamine monomer, modification of cure time/temperature and atmosphere. Other properties of soluble polyimides will be presented which include glass transition temperatures, thermooxidative stabilities, UV-visible spectra, and refractive indices. Author

N87-16912# Department of the Navy, Washington, D. C.
INTERPENETRATING-NETWORK POLYMERIC ELECTROLYTES Patent Application
Barry J. Bauer, inventor (to Navy), Chwan-Kang Chiang, inventor (to Navy), and George T. Davis, inventor (to Navy) Filed 10 Jul. 1986 13 p
(AD-D012485; US-Patent-Appl-SN-884143) Avail: NTIS HC A02/MF A01 CSCL 07/4

It is an object of this invention to provide new solid electrolytes. Another object of this invention is to provide new polymeric electrolytes. A further object of this invention is to provide polymeric electrolytes that have high conductivities at room temperature and which have good mechanical strength. These and other objects of this invention are accomplished by providing: a solid polymeric electrolyte comprising a two phase interpenetrating polymer network of: (1) a mechanically supporting phase of a continuous network of a crosslinked polymer selected from the group consisting of epoxies, polyurethanes, polymethacrylates, polyacrylates, polyacrylonitriles, and polystyrenes; and (2) an ionic conducting phase comprising: (a) a metal salt complexing liquid polymer selected from the group consisting of poly(ethylene oxide), poly(propylene oxide), poly(ethylene imine), and mixtures, complexed with (b) a metal salt selected from the group consisting of LiI, LiBr, LiClO4, CsClO4, NaI, NaBr, CsI, CsBr, KI, KBr, LiCF3SO3, LiSCN, CsSCN, NaSCN, KSCN, AgNO3, CuCl2, CoCl2, Mg(ClO4)2, PbBr2, MgCl2, and mixtures thereof wherein from more than zero to 0.50 moles of metal salt are added per mole of monomer repeat unit of the metal salt complexing liquid polymer. The mechanically supporting phase comprises from 20 to 55 weight

percent of the solid polymer electrolyte with the ion conducting phase being essentially the remainder. GRA

N87-16913# Midwest Research Inst., Golden, Colo.
EFFECT OF THE SIZE OF STRUCTURAL BULK INHOMOGENEITIES ON THE SPECULAR TRANSMITTANCE OF POLYMER FILMS
H. H. Neidlinger Jul. 1986 8 p Presented at the 30th SPIE Technical Symposium on Optics and Optoelectronic Engineering, San Diego, Calif., 17 Aug. 1986
(Contract DE-AC02-83CH-10093)
(DE86-010727; SERI/TP-255-2995; CONF-860880-19) Avail: NTIS HC A02/MF A01

This paper will be confined to the effect of optical inhomogeneities in polymer films on the scattering or specular transmittance of light. Potential causes for the presence of scattering entities in the bulk phase of polymers will be discussed. It will be shown that practical transmittance measurements are greatly influenced by the angular width of the instrument receptor aperture. The choice of large receptor apertures will tend to include some of the scattering at small angles due to large inhomogeneities in the measurement of specular transmittance. As a consequence, the transmittance measured is not necessarily increased by reducing the size of the inhomogeneities in the polymer films, but there is a critical size when the specular transmittance is a minimum. DOE

28 PROPELLANTS AND FUELS

Includes rocket propellants, igniters, and oxidizers; their storage and handling procedures; and aircraft fuels.

For related information see also *07 Aircraft Propulsion and Power, 20 Spacecraft Propulsion and Power,* and *44 Energy Production and Conversion.*

N87-16914# Rhode Island Univ., Kingston. Dept. of Mechanical Engineering and Applied Mechanics.
A STUDY OF EXPLOSIVE WAVE PROPAGATION IN GRANULAR MATERIALS WITH MICROSTRUCTURE Technical Report, Jun. 1985 - Sep. 1986
Martin H. Sadd, Mohammad Hossain, and Behzad Rohani Sep. 1986 135 p
(Contracts DACA39-85-C-0023; DA Proj. 4A1-61101-A-91-D)
(AD-A173015; WES-TR-SL-86-35) Avail: NTIS HC A07/MF A01 CSCL 19/4

This report describes an investigation into one-dimensional stress wave propagation in granular materials with microstructure. The study employs the distributed body concept advanced by Goodman and the associated wave propagation studies conducted by Nuniziato, Walsh, et al. A one-dimensional computer program, referred to as MIC1D, has been developed for studying wave propagation in granular materials due to airblast loading. This program allows for: (1) arbitrary surface airblast loading, (2) depth-dependent volume distribution function simulating gravity effects in a granular mass, and (3) treatment of grain size and local porosity as random variables. It incorporates three forms of depth-dependent volume distribution functions, i.e., a periodic form, and exponential form, and a combined periodic-exponential formulation. The user can select any of these forms for the particular application at hand. The probabilistic treatment of grain size and local porosity is accomplished by using a moment-generating procedure due to Rosenblueth. The computer program calculates the expected value and the variance of the output quantities, such as stress and particle motion, due to the randomness in these variables. Application of the computer program is demonstrated by presenting the results of a series of parametric calculations dealing with propagation of acceleration waves in granular media. Documentation of MIC1D is provided in an Appendix. GRA

N87-16915# Ballistic Research Labs., Aberdeen Proving Ground, Md.
ATMOSPHERIC PRESSURE STUDIES OF LIQUID PROPELLANT DROPS IN HOT FLOWS Final Report, Feb. - Oct. 1985
Richard A. Beyer Oct. 1986 25 p
(AD-A174639; BRL-TR-2768) Avail: NTIS HC A02/MF A01 CSCL 19/1

Single drops of 13 M aqueous Hydroxyl Ammonium Nitrate (HAN) and a liquid monopropellant (LP 1845) have been studied in hot flows from 700 to 950 C at ambient pressure. Measurements of drop diameter rate behavior show no effect of oxidizer presence and little temperature dependence. This report includes the first known observations of microexplosions of these liquid monopropellants. Drops are seen to explode from internal pressure after typically 25% of the volume has been consumed. These explosions do not appear to consume a substantial portion of the drop material, but they do result in the formation of many small drops, and hence, greatly increased surface areas. Arguments are presented that this effect is due to superheating of the water component. GRA

29 MATERIALS PROCESSING

Includes space-based development of products and processes for commercial applications.

For biological materials see *55 Space Biology.*

N87-16916*# Astro Aerospace Corp., Carpinteria, Calif.
BATTEN AUGMENTED TRIANGULAR BEAM Final Report
Louis R. Adams and John M. Hedgepeth Feb. 1986 58 p
(Contract NAS1-17536)
(NASA-CR-172461; NAS 1.26:172461; AAC-TN-1130-Rev-A) Avail: NTIS HC A04/MF A01 CSCL 22A

The BAT (Batten-Augmented Triangular) BEAM is characterized by battens which are buckled in the deployed state, thus preloading the truss. The preload distribution is determined, and the effects of various external loading conditions are investigated. The conceptual design of a deployer is described and loads are predicted. The influence of joint imperfections on effective member stiffness is investigated. The beam is assessed structurally. Author

N87-16917*# National Aeronautics and Space Administration. Lewis Research Center, Cleveland, Ohio.
RESEARCH OPPORTUNITIES IN MICROGRAVITY SCIENCE AND APPLICATIONS DURING SHUTTLE HIATUS
Bruce N. Rosenthal, Thomas K. Glasgow, Richard E. Black (National Aeronautics and Space Administration. Marshall Space Flight Center, Huntsville, Ala.), and Daniel D. Elleman (Jet Propulsion Lab., California Inst. of Tech., Pasadena) 1987 10 p Proposed for presentation at the 32nd International SAMPE Symposium and Exhibition, Anaheim, Calif., 6-9 Apr. 1987
(NASA-TM-88964; E-3420; NAS 1.15:88964) Avail: NTIS HC A02/MF A01 CSCL 22A

The opportunity to conduct microgravity and related research still exists, even with the temporary delay in the U.S. Space Shuttle program. Several ground-based facilities are available and use of these facilities is highly recommended for the preparation of near and far term shuttle or space station experiments. Drop tubes, drop towers, aircraft, sounding rockets and a wide variety of other ground-based equipment can be used to simulate microgravity. This paper concentrates on the materials processing capabilities available at NASA Lewis Research Cente (NASA Lewis), Marshall Space Flight Center (MSFC), and the California Institute of Technology Jet Propulsion Laboratory (JPL). Also included is information on gaining access to these facilities. Author

31 ENGINEERING (GENERAL)

Includes vacuum technology; control engineering; display engineering; cryogenics; and fire prevention.

N87-16918*# National Aeronautics and Space Administration. Ames Research Center, Moffett Field, Calif.

ELEVATED WATERPROOF ACCESS FLOOR SYSTEM AND METHOD OF MAKING THE SAME Patent
Marc M. Cohen, inventor (to NASA) Issued 20 Jan. 1987 9 p Filed 1 Jun. 1983 Supersedes N83-28281 (21 - 17, p 2736)
(NASA-Case-ARC-11363-1; US-Patent-4,637,181; US-Patent-Appl-SN-500046; US-Patent-Class-52-126.5; US-Patent-Class-52-309.15; US-Patent-Class-52-391; US-Patent-Class-52-511; US-Patent-Class-52-814) Avail: U.S. Patent and Trademark Office CSCL 13B

An elevated waterproof access floor system having subfloor channels or compartments for power lines, gas lines or the like is adapted such that it can be opened and subsequently resealed without destroying the waterproofing and without destroying its aesthetic appearance. A multiplicity of tiles are supported on a support grid, and a flooring sheet is supported on the tiles. Attachment means are provided to prevent lateral but not vertical movement of the flooring sheet with respect to the tiles so that the flooring sheet can be lifted off the tiles, but when the flooring sheet is supported on the tiles, no lateral slipping will occur. The flooring sheet is made of a heat resealable material, so that it can be cut away in sections, and the tiles therebelow lifted off, to provide access to subfloor compartments. NASA

N87-16919*# National Aeronautics and Space Administration. Marshall Space Flight Center, Huntsville, Ala.
THE 5000 GPM FIREFIGHTING MODULE EVALUATION TEST
Ralph A. Burns Nov. 1986 45 p
(NASA-TM-86560; NAS 1.15:86560) Avail: NTIS HC A03/MF A01 CSCL 13B

The 5000 GPM Firefighting Module development was sponsored and shared by the Navy Facilities Engineering Command. It is a lightweight, compact, self-contained, helicopter-transportable unit for fighting harbor and other specialty fires as well as for use in emergency and shipboard water pumping applications. This unit is a more advanced model of the original 1500 GPM module developed for the U.S. Coast Guard. The module and an evaluation test program conducted at the North Island Naval Air Station, San Diego, California, by NASA and the U.S. Navy, are described. Author

N87-16920# Department of the Air Force, Washington, D.C.
METHOD AND APPARATUS FOR DIE FORMING METAL SHEETS AND EXTRUSIONS Patent Application
John L. Darter, inventor (to Air Force) Filed 30 Jun. 1986 13 p
(AD-D012512; US-Patent-Appl-SN-880246) Avail: NTIS HC A02/MF A01 CSCL 13/8

The invention comprises an apparatus for die forming metal sheets and extrusions which utilizes die blocks of low melting temperature metallic material. The die blocks are formed in an adjustable mold which comprises a mold box, a pivotable dam within the mold box and blocking means for locking the pivotable dam member in a desired angular position. Once a desired die block angle is ascertained for a particular joggle, the pivotable member of the mold box is adjusted to produce the desired angle in the die casting made in the mold box. GRA

32 COMMUNICATIONS AND RADAR

Includes radar; land and global communications; communications theory; and optical communications.

For related information see also *04 Aircraft Communications and Navigation* and *17 Space Communications, Spacecraft Communications, Command and Tracking.* For search and rescue see *03 Air Transportation and Safety,* and *16 Space Transportation.*

N87-16921*# Jet Propulsion Lab., California Inst. of Tech., Pasadena.
MULTIPLE TRELLIS CODED MODULATION (MTCM): AN MSAT-X REPORT
D. Divsalar and M. K. Simon 15 Nov. 1986 52 p
(Contract NAS7-918)
(NASA-CR-180134; JPL-Pub-86-44; MSAT-X-141; NAS 1.26:180134) Avail: NTIS HC A04/MF A01 CSCL 17B

Conventional trellis coding outputs one channel symbol per trellis branch. The notion of multiple trellis coding is introduced wherein more than one channel symbol per trellis branch is transmitted. It is shown that the combination of multiple trellis coding with M-ary modulation yields a performance gain with symmetric signal set comparable to that previously achieved only with signal constellation asymmetry. The advantage of multiple trellis coding over the conventional trellis coded asymmetric modulation technique is that the potential for code catastrophe associated with the latter has been eliminated with no additional cost in complexity (as measured by the number of states in the trellis diagram). Author

N87-16922*# Jet Propulsion Lab., California Inst. of Tech., Pasadena.
COHERENT VERSUS NONCOHERENT SIGNALING FOR SATELLITE-AIDED MOBILE COMMUNICATIONS
F. Davarian and J. Sumida 15 Oct. 1986 25 p
(Contract NAS7-918)
(NASA-CR-180133; JPL-Pub-86-43; MSAT-X-140; NAS 1.26:180133) Avail: NTIS HC A02/MF A01 CSCL 17B

The use of coherent versus noncoherent communications is an unresolved issue for the mobile satellite community. Should one select the more robust but less efficient noncoherent strategy for communications over satellite-aided mobile channels, or does the introduction of a space platform in the mobile link improve signal stability (both amplitude and phase) such that conventional coherent schemes become attractive? This publication tries to answer some of the questions by discussing the results from experiments using a coherent QPSK receiver. The issues discussed include items such as the measured performance in Rician fading, the link error floor in a fading environment, etc. The results are compared and contrasted with that of a noncoherent limiter/discriminator FM receiver. Author

N87-16923# European Space Agency, Paris (France).
PROCEEDINGS OF THE SECOND ESA WORKSHOP ON MECHANICAL TECHNOLOGY FOR ANTENNAS
E. J. Rolfe, ed. Noordwijk, Netherlands Aug. 1986 271 p Workshop held in Noordwijk, Netherlands, 20-22 May 1986
(ESA-SP-261; ISSN-0379-6566; ETN-87-98835) Avail: NTIS HC A12/MF A01

Deployable spacecraft antennas; antenna design; mechanical/electrical design verification; antenna components; and structure-attitude and orbit control system interactions were discussed. For individual titles, see N87-16924 through N87-16952.

N87-16924# European Space Agency. European Space Research and Technology Center, ESTEC, Noordwijk (Netherlands). Structures and Configurations Section.
ANTENNA MECHANICAL TECHNOLOGIES WITHIN ESA
G. G. Reibaldi *In its* Proceedings of the Second ESA Workshop on Mechanical Technology for Antennas Aug. 1986 p 5-13 (For primary document see N87-16923 09-32)
Avail: NTIS HC A12/MF A01

Antenna concepts under development within ESA, including solid, depolyable, unfurlables, and inflatable reflectors are surveyed. Technologies needed to support such antenna concepts in the area of materials, analysis, testing, manufacturing, mechanisms, and attitude and orbit control systems/structures coupling are presented. The need to have technology commonality between different requirements is emphasized. ESA

N87-16925# Messerschmitt-Boelkow-Blohm G.m.b.H., Munich (West Germany).
EXPERIENCE GAINED BY SECTOR MODEL TESTING OF AN UNFURLABLE MESH/RIB ANTENNA c37
H. Heinze, H. Herbig, and H. Vorbrugg *In* ESA Proceedings of

the Second ESA Workhop on Mechanical Technology for Antennas Aug. 1986 p 17-22 (For primary document see N87-16923 09-32)
(Contract ESTEC-5206/82-NL-PB(SC))
Avail: NTIS HC A12/MF A01

An unfurlable offset mesh antenna for communication satellite applications in the range 850 MHz to 12 GHz was designed. The reflector design concept should cover aperture diameters from 3.2 (12 GHz) to 12 m (850 MHz) with surface errors between 0.1 mm and 1.4 mm RMS. This versatility is met by a radial rib concept where foldable main ribs and intermediate ribs tension a gold plated molybdenum mesh to the required surface contour. The accuracy is varied by applying a different number of ribs (e.g., 16 for 850 MHz or 30 for 12 GHz) and mesh fastening points (so-called stand-offs). Tests with a two rib test model prove that the deployment and retraction system is reliable and that the mesh provides the required reflector surface. The configuration of the mesh is suitable in a range of frequencies up to 12 GHz. With the right mesh tension there are no passive intermodulation products. ESA

N87-16926# Societe Nationale Industrielle Aerospatiale, Les Mureaux (France). Space and Ballistics Systems.
MECHANICAL AND CONTROL STUDY OF A 7 m OFFSET UNFURLABLE TRACKING ANTENNA **c37**
G. Labruyere, L. Passeron, M. Pastorino, and E. Schaffar *In* ESA Proceedings of the Second ESA Workshop on Mechanical Technology for Antennas Aug. 1986 p 23-30 (For primary document see N87-16923 09-32)
Avail: NTIS HC A12/MF A01

An antenna module for a tracking S-band satellite antenna mechanical concept is presented. The offset unfurlable reflector, the 15 deg antenna pointing mechanism, and the feed system support are described. Antenna pointing control, in presence of multiple flexible structures, is analyzed. ESA

N87-16927# Contraves Corp., Zurich (Switzerland). Space Dept.
DEVELOPMENT OF A 2.8 m OFFSET ANTENNA REFLECTOR USING INFLATABLE, SPACE-RIGIDIZED STRUCTURES TECHNOLOGY
M. C. Bernasconi *In* ESA Proceedings of the Second ESA Workshop on Mechanical Technology for Antennas Aug. 1986 p 31-37 (For primary document see N87-16923 09-32)
Avail: NTIS HC A12/MF A01

Results of the mechanical tests of an offset reflector structure, based on the technology of chemically-rigidized membranes are presented. Folding, stowage, and deployment tests confirm the high packaging efficiency, as well as the controllability of the inflation process. Geometric measurements at different manufacturing stages were used to assess the quality of the surface; the typical surface deviation obtained is 0.9 mm rms. Folding and cure processes have a negligible impact on reflector quality. The packaging and deployment procedures were verified by a depolyment test in vacuum. ESA

N87-16928# Toshiba Research and Development Center, Kawasaki (Japan). Space Program Div.
STUDY ON SOLID SURFACE, DEPLOYABLE ANTENNA REFLECTOR
Y. Tsutsumi, A. Kasahara, Y. Hisada (National Space Development Agency, Ibaraki, Japan), and Y. Itoh *In* ESA Proceedings of the Second ESA Workshop on Mechanical Technology for Antennas Aug. 1986 p 41-45 (For primary document see N87-16923 09-32)
Avail: NTIS HC A12/MF A01

A study was carried out on the precision-contour solid surface, deployable reflector in the 20 to 30 GHz, center-fed Cassegrain antenna to be mounted on data relay and tracking satellites. Reflector sizes are 1.8 m stowed diameter and 5 m deployed diameter. As a solid surface deployable reflector to satisfy the above requirements, two kinds of deployment concepts were developed. Based on the kinematic analysis results, preliminary design was carried out and a partial model was built to confirm the deployment kinematics. Deployment test results, using a partial model, show that two deployment concepts can be applied to the solid surface deployable reflector satisfying the requirements of a large ratio of deployed/stowed dimensions. ESA

N87-16929# Dornier-Werke G.m.b.H., Friedrichshafen (West Germany).
ANALYSIS OF HIGH PRECISION COMPOSITE SANDWICH ANTENNAS
G. Helwig *In* ESA Proceedings of the Second ESA Workshop on Mechanical Technology for Antennas Aug. 1986 p 51-55 (For primary document see N87-16923 09-32)
Avail: NTIS HC A12/MF A01

A data base for all common types of spacecraft antenna skin and core materials was established. Based on these material properties, it is possible to predict accurately the performance of high precision antennas, and there is good agreement between analyses and tests. The orthotropic behavior of the sandwich should be improved by developments of skin and core materials. The research should be directed to a composite sandwich with an overall coefficient of expansion close to zero, giving composite sandwich panels with accuracies better than 1 micron rms for most kinds of temperature loads. ESA

N87-16930# Rome Univ. (Italy). Dept. of Aerospace.
EFFECTS OF CURING STRESSES ON COMPOSITE STRUCTURES **c39**
M. Marchetti, F. Morganti (Selenia S.p.A., Rome, Italy), and S. Tizzi *In* ESA Proceedings of the Second ESA Workshop on Mechanical Technology for Antennas Aug. 1986 p 57-62 Sponsored by Max-Planck Inst. (For primary document see N87-16923 09-32)
Avail: NTIS HC A12/MF A01

The effects of the residual stresses which arise during the manufacturing of laminates constituting the skins of high stability telecommunications antennas for space applications are discussed. A dedicated software to simulate the behavior of a composite structure from the curing temperature to the room condition was developed. The numerical simulation method takes into account all the nonlinearity effects which influence the final results, like viscoelastic properties of the material (creep) and the dependance of the mechanical properties on temperature. ESA

N87-16931# Turin Univ. (Italy). Dipt. di Elettronica.
DIELECTRIC SUPPORT STRUCTURES FOR SPACECRAFT ANTENNA FEEDS **c33**
R. D. Graglia, M. Orefice, U. Ponzi (Rome Univ., Italy), and S. Sgubini *In* ESA Proceedings of the Second ESA Workshop on Mechanical Technology for Antennas Aug. 1986 p 63-71 (For primary document see N87-16923 09-32)
Avail: NTIS HC A12/MF A01

Analysis and design criteria for radio frequency transparent towers, to be used as support structures of feeds or subreflector in spacecraft reflector antennas are discussed. Candidate materials are fiber reinforced plastics, in particular those with good mechanical and dielectric properties, as aramid fiber (Kevlar). The electromagnetic analysis is performed by subdividing the structure in simple members (planes, cylinders, etc.) and considering each individual contribution to the scattering. Typical structures for offset and symmetrical configurations were considered, and design criteria are given. ESA

N87-16932# Messerschmitt-Boelkow-Blohm G.m.b.H., Munich (West Germany).
QUALIFICATION OF GRIDDING PROCESS FOR A POLARIZATION SENSITIVE REFLECTOR (PSR)
R. Leitner, N. Nathrath, and W. Schaefer *In* ESA Proceedings of the Second ESA Workshop on Mechanical Technology for Antennas Aug. 1986 p 73-79 (For primary document see N87-16923 09-32)
(Contract ESTEC-5494/84-NL-GM)
Avail: NTIS HC A12/MF A01

A polarization sensitive satellite reflector configuration for frequency reuse was developed. It consists of two Kevlar fiber

sandwich shells oriented one behind the other and joined along the rim by a Kevlar fiber support ring. For electrical separation of the two systems, the reflector shell surfaces are covered with conductive strip grids which are oriented perpendicular with respect to each other. The gridding process allows direct application of the conductive strips on the prefabricated Kevlar sandwich dishes. Thermal cycling tests show that Tedlar is the most suitable polymeric film to cover the Kevlar surface. ESA

N87-16933# Nippon Telegraph and Telephone Public Corp., Yokosuka (Japan).
DEVELOPMENT OF 30/20 GHz SATELLITE ANTENNA STRUCTURES
M. Minomo and T. Yasaka *In* ESA Proceedings of the Second ESA Workshop on Mechanical Technology for Antennas Aug. 1986 p 85-90 (For primary document see N87-16923 09-32)
Avail: NTIS HC A12/MF A01

An antenna structural design for a large capacity communication satellite using 13 beams in the 30/20GHz frequency bands is discussed. This design is to be utilized in developing a more cost effective domestic satellite communication system for Japan. This system requires 2 high precision deployable antennas with projected aperture diameters of 3.5m at 20GHz and 2.5m at 30GHz. The in-orbit demonstration will use the ETS-6 satellite. Based on experience in the development of spaceborne antennas for 30/20GHz bands (e.g., for the CS-2 and CS-3 satellites) activities in structural design of high precision deployable antennas show the truss reflector structure is promising for achieving required structural properties. ESA

N87-16934# Spar Aerospace Ltd., Ste-Anne-de-Bellevue (Quebec).
DESIGN OF A LOW DISTORTION SHARED APERTURE REFLECTOR
L. Donato and V. K. Jha *In* ESA Proceedings of the Second ESA Workhop on Mechanical Technology for Antennas Aug. 1986 p 91-96 (For primary document see N87-16923 09-32)
(Contract CAN-Dept-Comm-21st-36100-3-031)
Avail: NTIS HC A12/MF A01

A design concept for a low thermal distortion dual gridded shared aperture reflector for satellite antennas is proposed. Low distortion characteristics result in improved on-orbit gain performance of the antenna system. The absence of an intercostal structure between reflectors improves electrical cross polar and gain performance. A finite difference model to predict temperatures of the reflector assembly was generated. From the temperature profiles a finite element model was used to evaluate the distortions of the parabolic surfaces. From the distorted best fit surfaces, pointing errors, defocussing, and rms deviation from the best fit parabola were evaluated and compared to thermal distortions of previous designs. The results show a significant improvement. ESA

N87-16935# Construcciones Aeronauticas S.A., Madrid (Spain). Space Div.
CONSTRUCCIONES AERONAUTICAS S.A. (CASA) LARGE REFLECTOR ANTENNA
J. Escobar *In* ESA Proceedings of the Second ESA Workhop on Mechanical Technology for Antennas Aug. 1986 p 97-102 (For primary document see N87-16923 09-32)
(Contract ESA-5277/82-NL-PP)
Avail: NTIS HC A12/MF A01

The development of a 11/14 GHz large reflector assembly is reviewed. Investigations on CFRP properties, their design and calculation methods, the development of the associated software, the gathering of a data base from tests at component level, and basic studies on the general configuration of antennas are outlined. A demonstration model to resolve the technological problems related with the design, manufacture and test of a large reflector was built. ESA

N87-16936# Selenia S.p.A., Rome (Italy).
DEVELOPMENT OF LIGHTWEIGHT DIMENSIONALLY STABLE CARBON FIBER COMPOSITE ANTENNA REFLECTORS FOR THE INSAT-1 SATELLITE
A. Pace, I. LaRosa, and R. Stonier *In* ESA Proceedings of the Second ESA Workshop on Mechanical Technology for Antennas Aug. 1986 p 103-110 (For primary document see N87-16923 09-32)
Avail: NTIS HC A12/MF A01

A lightweight dimensionally stable carbon fiber composite deployable antenna reflector structure utilizing a rib stiffened thin shell design was developed. Reflectors based on this design were manufactured and tested for the INSAT-1 satellites, and the same technology was used for the reflectors for the ARABSAT satellites. Structural materials were qualified and used on antenna reflector structures. The outstanding in-orbit performance of eight antennas on two INSAT-1 and two ARABSAT satellites, clearly demonstrates the technical success of the program. Three additional satellites with six more antennas/reflectors will be launched. ESA

N87-16937# Societe Nationale Industrielle Aerospatiale, Les Mureaux (France). Div. des Systems Balistiques et Spatiaux.
STRUCTURAL ANALYSIS, MANUFACTURING AND DEVELOPMENT STATUS OF LARGE POLARIZATION SENSITIVE DUAL-GRIDDED REFLECTORS c39
J. D. Lefebvre *In* ESA Proceedings of the Second ESA Workshop on Mechanical Technology for Antennas Aug. 1986 p 111-121 (For primary document see N87-16923 09-32)
Avail: NTIS HC A12/MF A01

The design of a 2.5 m diameter dual-gridded reflector assembly including the dynamic, static, thermal, and thermoelastic analyses is presented. The reflectors consist of two Kevlar sandwich shells, each being fitted with a grid of copper wires, and stiffened on the back by a system of Kevlar webs and struts. Mechanical and RF test results, performed on earlier developed reflector assemblies (1.4 m and 1.8 m) demonstrate the validity of the design. ESA

N87-16938# European Space Agency. European Space Research and Technology Center, ESTEC, Noordwijk (Netherlands).
GIOTTO SPACECRAFT HIGH GAIN ANTENNA MECHANICAL DESIGN AND DEVELOPMENT c37
R. Halm, F. Felici, H. J. Schoedel (Dornier-Werke G.m.b.H., Friedrichshafen, West Germany), and H. Raupp *In its* Proceedings of the Second ESA Workshop on Mechanical Technology for Antennas (date) p 123-126 (For primary document see N87-16923 09-32)
Avail: NTIS HC A12/MF A01

The development approach of the Giotto spacecraft high gain antenna structure is presented. The antenna structure consists of a dynamically and statically balanced offset parabolic reflector and a tripod support structure for the S/X-band feed. The reflector dish is a sandwich construction having CFRP face sheets employing ultra high module fibers bonded to an aluminum honeycomb core. The tripod is designed to provide the required eigenfrequencies by stiff profiles made of CFRP. ESA

N87-16939# Dornier-Werke G.m.b.H., Friedrichshafen (West Germany).
DEVELOPMENT STATUS OF THE ERS-1 SAR ANTENNA
R. Wagner, H. J. Luhmann, R. Sippel, and M. Westphal *In* ESA Proceedings of the Second ESA Workshop on Mechanical Technology for Antennas Aug. 1986 p 131-137 (For primary document see N87-16923 09-32)
Avail: NTIS HC A12/MF A01

A 10 m x 1 m planar array antenna for the ERS-1 satellite is described. It features metallized CFRP waveguides as radiating elements and feeding network components, CFRP sandwich reinforcements of the mechanical panels, a deployable truss structure, and mechanism for launch fixation, release, and deployment. Mechanical design of the antenna structure towards satisfactory dynamic properties in launch configuration within the narrow constraints of mass, volume, and mechanical loads; structural analysis of the stowed and deployment antenna, to determine dynamic properties, internal loads, and deformations; and design of the hold down and release mechanism arrangement

of six hinged clamps for launch fixation, to be released via a system of springs and cables by a pyrotechnic device, are reviewed. ESA

N87-16940# Construcciones Aeronauticas S.A., Madrid (Spain). Space and Systems Div.
ERS-1 WIND SCATTEROMETER ANTENNA: MECHANICAL ASPECTS c37
J. Garcia SanMartin *In* ESA Proceedings of the Second ESA Workshop on Mechanical Technology for Antennas Aug. 1986 p 139-149 (For primary document see N87-16923 09-32)
Avail: NTIS HC A12/MF A01

The ERS-1 wind scatterometer antenna function, general configuration and interfaces; mechanical requirements and constraints; thermostructural design philosophy; mechanism design; and manufacturing are reviewed. The selection process of the thermostructural philosophy and the mechanism design is explained, comparing the retained solutions with alternatives studied, and explaining the reasons for the final selection in each case. ESA

N87-16941# Construcciones Aeronauticas S.A., Madrid (Spain). Space and Systems Div.
DEVELOPMENT OF mm-WAVE RADIOMETER ANTENNA REFLECTOR
P. Cordero, G. Lopez, and R. Garcia *In* ESA Proceedings of the Second ESA Workshop on Mechanical Technology for Antennas Aug. 1986 p 151-159 (For primary docum... see N87-16923 09-32)
(Contract ESA-5263/82-NL-GM)
Avail: NTIS HC A12/MF A01

The development of an antenna for a passive microwave radiometer for the 90 to 300 GHz frequency range is discussed. The operating frequency-range imposes ultrahigh surface accuracy and stability, and electrical reflectivity close to that of the best conductive metals. Critical design areas and technological problems (e.g., CFRP metallizing) are reviewed. ESA

N87-16942# TICRA A/S, Copenhagen (Denmark).
SIMPLE APPROACH FOR EVALUATING MECHANICAL REFLECTOR ANTENNA DISTORTIONS
Knud Pontoppidan *In* ESA Proceedings of the Second ESA Workshop on Mechanical Technology for Antennas Aug. 1986 p 165-170 (For primary document see N87-16923 09-32)
Avail: NTIS HC A12/MF A01

Satellite reflector surface degradations originating from relatively slowly varying distortions, such as thermal deformations and creep are discussed. These surface errors scatter the field from the main beam into the region of the first few sidelobes, thereby deteriorating the isolation between frequency reuse beams. To investigate these errors, the concepts of Zernike modes are introduced. It is demonstrated how this method facilitates the insight and understanding of the physical phenomena occurring when a reflector surface is deformed. An inflatable antenna is used as a test example. ESA

N87-16943# Centro Studi e Laboratori Telecomunicazioni, Turin (Italy).
PREDICTION OF THE ELECTRICAL PERFORMANCE OF INFLATABLE SPACE RIGIDIZED STRUCTURE (ISRS) OFFSET ANTENNA REFLECTORS AND CORRELATION WITH RF MEASUREMENTS
E. Pagana and M. C. Bernasconi (Contraves Corp., Zurich, Switzerland) *In* ESA Proceedings of the Second ESA Workshop on Mechanical Technology for Antennas Aug. 1986 p 171-177 (For primary document see N87-16923 09-32)
Avail: NTIS HC A12/MF A01

The electrical design and testing at microwave frequencies (3 to 22 GHz) on the first Large Offset Antenna Demonstrator (LOAD) breadboard are summarized. The electrical analysis shows the quality of mock-up reflector and contributes to an electrical antenna model. The performance of a large inflatable antenna can be predicted, with good accuracy, only on the basis of the mechanical measurements of a proper set of reflector surface points. ESA

N87-16944# Contraves Italiana, Rome.
CONTRAVES' ANTENNA TIP HINGE MECHANISM FOR SELENIA SPAZIO'S 20/30 GHz ANTENNA c37
D. Stella, F. Morganti (Selenia S.p.A., Rome, Italy), and G. Nielsen (European Space Agency. European Space Research and Technology Center, ESTEC, Noordwijk (Netherlands) *In* ESA Proceedings of the Second ESA Workshop on Mechanical Technology for Antennas Aug. 1986 p 185-194 (For primary document see N87-16923 09-32)
Avail: NTIS HC A12/MF A01

A mechanism which can deploy a folded tip of an antenna in orbit, the Antenna Tip Hinge Mechanism (ATHM) was developed. The ATHM consists of two hinges, each near the edge of the antenna main body and tip interface. Following a command, the antenna tip is released and spiral springs drive the antenna tip to its end position, where latches secure the tip in place. No damping or any form of energy dissipation is provided for, other than that which is caused by friction within the system. Two ATHM's, one at each end of the antenna, enable a 20/30 GHz multibeam antenna to fit in the Ariane 4 shroud. This mechanism can, with minor modifications, be used to deploy a multitude of different systems, provided that they are not too fragile to withstand the deceleration loads that occur at the end of deployment. ESA

N87-16945# Construcciones Aeronauticas S.A., Madrid (Spain). Space and Systems Div.
WIND SCATTEROMETER ANTENNA (WSA) RELEASE SHOCK LOADS c39
P. Luengo and C. Huerta *In* ESA Proceedings of the Second ESA Workshop on Mechanical Technology for Antennas Aug. 1986 p 195-203 (For primary document see N87-16923 09-32)
Avail: NTIS HC A12/MF A01

The shock loads induced on ERS-1 during the release of the side wind scatterometer antenna (WSA-side) were studied on a simplified finite element model applying a transient analysis with a nonlinear force. If the ratio of frequencies between global and local systems is large, the influence of the latter on the shock loads can be neglected when the associated mass is small. For WSA-side, the global mode is 51 Hz and the local mode is greater than 392 Hz. The ratio between frequencies is 8 and the mass associated with the transversal vibration is smaller than the mass associated with the longitudinal. Thus the transversal vibration can be neglected. ESA

N87-16946# Sener, S.A., Madrid (Spain).
A SENER MECHANISM: FINE ADJUSTMENT MECHANISM FOR THE FAR INFRARED AND SUBMILLIMETER SPACE TELESCOPE (FIRST) (F f F) c37
F. delCampo, J. delToro, and J. Rivacoba *In* ESA Proceedings of the Second ESA Workshop on Mechanical Technology for Antennas Aug. 1986 p 205-210 (For primary document see N87-16923 09-32)
Avail: NTIS HC A12/MF A01

A mechanism for obtaining very fine variations of the relative angular position of two surfaces having a common hinge axis is presented. The mechanism introduces no backlash, by using flexing elements for articulations. It can be designed for very high torsional stiffness. Applications include controlling the final angular aperture of deployable antennas, e.g., the petals of the FIRST antenna. For this case, main requirements are: minimum angular step 0.001 arc min; total angular range 2.6 arc min; torsional stiffness 900,000 Nm/rad. ESA

N87-16947# Ricerche e Progetti s.r.l., Turin (Italy).
DYNAMICS AND CONTROL ANALYSIS PACKAGE (DCAP): AN AUTOMATED ANALYSIS AND DESIGN TOOL FOR STRUCTURAL CONTROL OF SPACE STRUCTURES c37
R. P. Singh, R. J. VanderVoort, C. Arduini, A. Festa (Aeritalia S.p.A., Torino, Italy), C. Maccone, and D. Sciacovelli (European Space Agency. European Space Research and Technology Center,

ESTEC, Noordwijk, Netherlands) *In* ESA Proceedings of the Second ESA Workshop on Mechanical Technology for Antennas Aug. 1986 p 211-218 (For primary document see N87-16923 09-32)
Avail: NTIS HC A12/MF A01

The Dynamics and Control Analysis Package (DCAP) automated design and checking tool for the dynamics and control of large flexible structures is described. The DCAP includes programs for nonlinear simulation of multibody systems dynamics; linear or linearized system analysis with frequency and time domain response, stability and sensitivity analysis; modal analysis and order reduction; and control design. It is presently being endowed with a user friendly interactive preprocessor, higher speed capabilities, and an LQG package providing for both analog and digital controls. ESA

N87-16948# European Space Agency. European Space Research and Technology Center, ESTEC, Noordwijk (Netherlands). Mechanical Systems Div.
ENGINEERING AND SOFTWARE INTERFACING FOR THERMAL, STRUCTURAL AND DYNAMIC CONTROL RELATED WITH SPACECRAFT ACTIVITIES **c61**
C. Stavrinidis, M. Klein, and J. Wijker (Royal Netherlands Aircraft Factories Fokker, Schiphol-Oost) *In its* Proceedings of the Second ESA Workshop on Mechanical Technology for Antennas Aug. 1986 p 219-225 (For primary document see N87-16923 09-32)
(Contract ESTEC-5158/82-NL-PB(SC))
Avail: NTIS HC A12/MF A01

Engineering practices and information needed by the different spacecraft disciplines, and the possibilities of coupling thermal, structural, and attitude control analysis programs are discussed. Implementation of identified and developed methods for specific interfaces is described. Engineering and software interfaces between the finite element package ASKA and the dynamic control analysis package DCAP, and between the thermal analysis program SINDA and the finite element package ASKA are presented. The software for the corresponding interface programs are identified as IFDCAP and SINAS. ESA

N87-16949# Liege Univ. (Belgium).
THE EXTENDABLE REFRACTABLE MAST (ERM) THERMAL ANALYSIS: A HEAT RADIATION CASE STUDY VIA THE FINITE ELEMENT METHOD **c34**
M. Hogge, J. P. Cobut, J. Fagnoul, E. Stenne, and P. M. Leonard *In* ESA Proceedings of the Second ESA Workshop on Mechanical Technology for Antennas Aug. 1986 p 227-235 (For primary document see N87-16923 09-32)
Avail: NTIS HC A12/MF A01

A heat radiation finite element procedure was developed for the thermal analysis of an extendable retractable mast (ERM) for space shuttle solar arrays and antennas. Thermal loading of the mast is mainly by radiation, and such heat inputs are barely treated in a comprehensive way in finite element computer programs: radiative heat exchanges are defined in terms of surfaces whereas finite element models deal with nodal unknowns located at the boundary of the radiant areas. A procedure which enables an automatic translation of surface data into nodal inputs via specialized surface elements was developed and may be used along with standard codes for angle factors determination. The effectiveness of the method is demonstrated on ERM thermal models. ESA

N87-16950# Selenia S.p.A., Rome (Italy).
DESIGN AND TECHNOLOGY OF FEED ARRAY AND BEAM FORMING NETWORK FOR CONTOURED BEAM ANTENNAS
F. Aristei, V. Costabile, and V. Menichini *In* ESA Proceedings of the Second ESA Workshop on Mechanical Technology for Antennas Aug. 1986 p 241-248 (For primary document see N87-16923 09-32)
Avail: NTIS HC A12/MF A01

A beam forming network feed array for contoured beam antennas was designed. A modal survey was made by a modal analyzer to elaborate the experimental data acquired on the manufactured hardware. Resonance frequencies and mode shapes were obtained. A simplified thermal analysis, performed by the SINDA program, indicates temperature ranges, thermal gradients, and heat fluxes well within specifications. ESA

N87-16951# European Space Agency. European Space Research and Technology Center, ESTEC, Noordwijk (Netherlands).
BEAM FORMING NETWORK TECHNOLOGIES AND RELATED MANUFACTURING PROCESSES
M. Lisi *In its* Proceedings of the Second ESA Workshop on Mechanical Technology for Antennas Aug. 1986 p 249-254 (For primary document see N87-16923 09-32)
Avail: NTIS HC A12/MF A01

Basic concepts and technologies of beam forming networks (BFN) for satellite multibeam antennas are reviewed. The extensive use of CAD/CAM techniques is shown to be essential for an accurate design of large, complex BFN's. Optical distribution techniques are also discussed. Their possible application in multibeam antenna systems is likely to greatly improve performances and capabilities of BFN designs. ESA

N87-16952# Rome Univ. (Italy). Dipt. Aerospaziale.
THERMOMECHANICAL CHARACTERISTICS OF DICHROIC SUBREFLECTORS **c37**
C. Arduini, R. Barboni, A. Castellani, U. Ponzi, and S. Sgubini *In* ESA Proceedings of the Second ESA Workshop on Mechanical Technology for Antennas Aug. 1986 p 255-260 (For primary document see N87-16923 09-32)
Avail: NTIS HC A12/MF A01

Temperature, stress, and deformation aspects of Kevlar composite dichroic reflectors were studied. Criteria to guarantee that thermal displacements do not exceed any maximum value in the direction normal to the middle surface were derived. The skin of the sandwich was checked for thermal buckling to find a criterion for safe sizing. Different cases of Sun illumination and transient conditions were analyzed to determine the maximum gradient inside the structure. The structural analysis was carried out via finite elements. The type of finite element and the number of grid nodes were a compromise between the modeling requirements and the large number of cases which result from the structural concepts, design requirements, heating conditions, type of constraints, and materials properties. Thermostructural results are presented. ESA

N87-16953*# Case Western Reserve Univ., Cleveland, Ohio. Dept. of Electrical Engineering and Applied Physics.
INVESTIGATION OF A GaAlAs MACH-ZEHNDER ELECTRO-OPTIC MODULATOR M.S. Thesis. Final Contractor Report
David M. Materna Jan. 1987 168 p
(Contract NCC3-54)
(NASA-CR-179573; NAS 1.26:179573) Avail: NTIS HC A08/MF A01 CSCL 09C

A GaAs modulator operating at 0.78 to 0.88 micron wavelength has the potential to be integrated with a GaAs/GaAlAs laser diode for an integrated fiber-optic transmitter. A travelling-wave Mach-Zehnder modulator using the electro-optic effect of GaAs and operating at a wavelength of 0.82 microns has been investigated for the first time. A four layer Strip-loaded ridge optical waveguide has been analyzed using the effective index method and single mode waveguides have been designed. The electro-optic effect of GaAs has also been analyzed and a modulator using the geometry producing the maximum phase shift has been designed. A coplanar transmission line structure is used in an effort to tap the potentially higher bandwidth of travelling-wave electrodes. The modulator bandwidth has been calculated at 11.95 GHz with a required drive power of 2.335 Watts for full intensity modulation. Finally, some preliminary experiments were performed to characterize a fabrication process for the modulator. Author

N87-16954*# Ford Aerospace and Communications Corp., Palo Alto, Calif. Western Development Lab. Div.
APPLICATION OF ADAPTIVE ANTENNA TECHNIQUES TO

FUTURE COMMERCIAL SATELLITE COMMUNICATION Final Report, Apr. 1986 - Jan. 1987
L. Ersoy, E. A. Lee, and E. W. Matthews Jan. 1987 125 p
(Contract NAS3-24892)
(NASA-CR-179566; NAS 1.26:179566; WDL-TR-10941) Avail: NTIS HC A06/MF A01 CSCL 17B

The purpose of this contract was to identify the application of adaptive antenna technique in future operational commercial satellite communication systems and to quantify potential benefits. The contract consisted of two major subtasks. Task 1, Assessment of Future Commercial Satellite System Requirements, was generally referred to as the Adaptive section. Task 2 dealt with Pointing Error Compensation Study for a Multiple Scanning/Fixed Spot Beam Reflector Antenna System and was referred to as the reconfigurable system. Each of these tasks was further sub-divided into smaller subtasks. It should also be noted that the reconfigurable system is usually defined as an open-loop system while the adaptive system is a closed-loop system. The differences between the open- and closed-loop systems were defined. Both the adaptive and reconfigurable systems were explained and the potential applications of such systems were presented in the context of commercial communication satellite systems. Author

N87-16955*# Ford Aerospace and Communications Corp., Palo Alto, Calif. Western Development Lab. Div.
APPLICATION OF ADAPTIVE ANTENNA TECHNIQUES TO FUTURE COMMERCIAL SATELLITE COMMUNICATION Final Report, Apr. 1986 - Jan. 1987
L. Ersoy, E. A. Lee, and E. W. Matthews Jan. 1987 17 p
(Contract NAS3-24892)
(NASA-CR-179566; NAS 1.26:179566; WDL-TR-10941) Avail: NTIS HC A02/MF A01 CSCL 17B

The purpose of this contract was to identify the application of adaptive antenna technique in future operational commercial satellite communication systems and to quantify potential benefits. The contract consisted of two major subtasks. Task 1, Assessment of Future Commercial Satellite System Requirements, was generally referred to as the Adaptive section. Task 2 dealt with Pointing Error Compensation Study for a Multiple Scanning/Fixed Spot Beam Reflector Antenna System and was referred to as the reconfigurable system. Each of these tasks was further subdivided into smaller subtasks. It should also be noted that the reconfigurable system is usually defined as an open-loop system while the adaptive system is a closed-loop system. The differences between the open- and closed-loop systems were defined. Both the adaptive and reconfigurable systems were explained and the potential applications of such systems were presented in the context of commercial communication satellite systems. Author

N87-16956*# Smithsonian Astrophysical Observatory, Cambridge, Mass.
SYSTEM ENGINEERING STUDY OF ELECTRODYNAMIC TETHER AS A SPACEBORNE GENERATOR AND RADIATOR OF ELECTROMAGNETIC WAVES IN THE ULF/ELF FREQUENCY BAND Final Report
Robert D. Estes Feb. 1987 117 p
(Grant NAG8-551)
(NASA-CR-180156; NAS 1.26:180156) Avail: NTIS HC A06/MF A01 CSCL 20N

An electrodynamic tether deployed from a satellite in low-Earth orbit can perform, if properly instrumented, as a partially self-powered generator of electromagnetic waves in the ULF/ELF band, potentially at power levels high enough to be of practical use. Two basic problems are examined. The first is that of the level of wave power that the system can be expected to generate in the ULF/ELF radiation band. The second major question is whether an electrodynamic tethered satellite system for transmitting waves can be made partially self-powering so that power requirements for drag compensation can be met within economical constraints of mass, cost, and complexity. The theoretical developments and the system applications study are presented. The basic design criteria, the drag-compensation method, the effects on the propagation paths from orbit to Earth surface of high-altitude nuclear debris patches, and the estimate of masses and sizes are covered. An outline of recommended analytical work, to be performed as a follow-on to the present study, is contained. B.G.

N87-16957*# National Aeronautics and Space Administration. Ames Research Center, Moffett Field, Calif.
DATA COMMUNICATION REQUIREMENTS FOR THE ADVANCED NAS NETWORK
Eugene Levin, C. K. Eaton (General Electric Co., San Jose, Calif.), and Bruce Young Nov. 1986 26 p
(Contract NCC2-387)
(NASA-TM-89315; RIACS-TR-86.22; NAS 1.15:89315) Avail: NTIS HC A03/MF A01 CSCL 17B

The goal of the Numerical Aerodynamic Simulation (NAS) Program is to provide a powerful computational environment for advanced research and development in aeronautics and related disciplines. The present NAS system consists of a Cray 2 supercomputer connected by a data network to a large mass storage system, to sophisticated local graphics workstations, and by remote communications to researchers throughout the United States. The program plan is to continue acquiring the most powerful supercomputers as they become available. In the 1987/1988 time period it is anticipated that a computer with 4 times the processing speed of a Cray 2 will be obtained and by 1990 an additional supercomputer with 16 times the speed of the Cray 2. The implications of this 20-fold increase in processing power on the data communications requirements are described. The analysis was based on models of the projected workload and system architecture. The results are presented together with the estimates of their sensitivity to assumptions inherent in the models. Author

N87-16958*# National Aeronautics and Space Administration. Lewis Research Center, Cleveland, Ohio.
A NEW MODEL FOR BROADBAND WAVEGUIDE TO MICROSTRIP TRANSITION DESIGN
George E. Ponchak and Alan N. Downey Dec. 1986 18 p
(NASA-TM-88905; E-2935; NAS 1.15:88905) Avail: NTIS HC A02/MF A01 CSCL 17B

A new model is presented which permits the prediction of the resonant frequencies created by antipodal finline waveguide to microstrip transitions. The transition is modeled as a tapered transmission line in series with an infinite set of coupled resonant circuits. The resonant circuits are modeled as simple microwave resonant cavities of which the resonant frequencies are easily determined. The model is developed and the resonant frequencies determined for several different transitions. Experimental results are given to confirm the models. Author

N87-16959# Department of the Air Force, Washington, D.C.
ECM (ELECTRONIC COUNTERMEASURES) PREPROCESSOR OR TRACKER USING MULTI-PROCESSOR MODULES Patent Application
Timothy Dunne, inventor (to Air Force) Filed 30 Jun. 1986 51 p
(AD-D012513; US-Patent-Appl-SN-880242) Avail: NTIS HC A04/MF A01 CSCL 17/4

The tracking apparatus uses multi-processor modules for predicting in real time the parametric behavior of radar signals to be jammed, as part of an electronic countermeasures system. The tracker system is partitioned into three broad (module) types: (1) a subsystem request handler, which transfers data from system buses to the tracker system, (2) one or more multi-processor modules (each including a parameter memory and three arithmetic units with micro-sequencers) which does the actual track operation yielding the prediction data, and (3) a vector buffer module, which transfers the completed prediction data onto the buses for the receiver and transmitter. The system computer transfers to the tracker the necessary parameter information (latest time of arrival, threat type (stable, stagger, agile, etc.), angle of arrival, etc.) and initiates a track loop. Central to the operation of the trackers is the parameter memory which is divided conceptually into two main parts: pattern and parameters. The parameter portion of the memory is subdivided into blocks, each dedicated to a particular

threat. The defining parameters for that threat are passed from the CPU just before a tracker is started. Author (GRA)

N87-16960# Communications Research Centre, Ottawa (Ontario).
COMPARISONS OF THE DETECTION PERFORMANCE OF A SPACE-BASED RADAR SYSTEM USING DIFFERENT ANTENNA SYSTEMS AND APERTURE ILLUMINATIONS
B. J. Rook May 1986 45 p
(AD-A173094; CRC-1401) Avail: NTIS HC A03/MF A01 CSCL 17/9

Comparisons have been made of the results of the detection performance of a space-based radar (SBR) system using uniformly-illuminated circular apertures, and the same apertures with Taylor weighting applied. From the studies, it is shown that the detection performance of an SBR system can be greatly improved with the application of the latter form of weighting. For the comparative studies, two antenna systems with the same physical dimensions were used: (1) a Taylor-weighted circular aperture for transmitting and receiving, and (2) a uniformly-illuminated circular aperture for transmitting, and the same aperture but with Taylor weighting applied for receiving. These comparative studies show that when antenna system (1) was used, 45.0 dB Taylor weighting was required in order to achieve the optimum SBR detection performance whereas for antenna system (2), 55.0 dB was required to give the same detection performance. GRA

N87-16961# Bolt, Beranek, and Newman, Inc., Cambridge, Mass.
NOISE-IMMUNE MULTISENSOR TRANSDUCTION OF SPEECH Final Technical Report, May 1984 - Dec. 1985
Vishu R. Viswanathan, Claudia M. Henry, Alan G. Derr, Salim Roucos, and Richard M. Schwartz Aug. 1986 127 p
(Contract F30602-84-C-0088)
(AD-A174693; BBN-6114; RADC-TR-86-87) Avail: NTIS HC A07/MF A01 CSCL 09/1

Two types of configurations of multiple sensors were developed, tested and evaluated in speech recognition application for robust performance in high levels of acoustic background noise: One type combines the individual sensor signals to provide a single speech signal input, and the other provides several parallel inputs. For single-input systems, several configurations of multiple sensors were developed and tested. Results from formal speech intelligibility and quality tests in simulated fighter aircraft cockpit noise show that each of the two-sensor configurations tested outperforms the constituent individual sensors in high noise. Also presented are results comparing the performance of two-sensor configurations and individual sensors in speaker-dependent, isolated-word speech recognition tests performed using a commercial recognizer (Verbex 4000) in simulated fighter aircraft cockpit noise. GRA

N87-16962# Georgia Tech Research Inst., Atlanta. Electronics and Computer Systems Lab.
IN-BAND ANTENNA COUPLING RESEARCH Final Report, 29 Mar. 1982 - 31 Dec. 1984
Barry J. Cown, C. D. Papanicolopolus, and R. W. Cravey Jun. 1986 86 p
(Contract DAAB07-82-C-J069)
(AD-A175093; GIT-A-3213; CECOM-TR-82-J069-F) Avail: NTIS HC A05/MF A01 CSCL 09/5

Theoretical and numerical analyses were performed to develop a computer algorithm for computing antenna mutual gain for arbitrary arrangements and orientations of antennas located in the near-field of each other and operating in the presence of near-field scattering obstacles. The mathematical expressions and algorithm were developed based on the use of the complex far-field electric field data for each antenna. The algorithm, designated as GTSAF, has been implemented and employed to generate coupling data for directive aperture antennas operating: (1) on a clear site, and (2) in the presence of a scattering obstacle. Coupling data for a pair of soft dipoles has also been generated via GTSAF, and compared with numerical data obtained via the Method of Moments (MOM). GRA

N87-16963# Centre National d'Etudes Spatiales, Toulouse (France). Radar Dept.
VARAN-S RADAR IMAGE INTERPRETATION
N. Lannelongue 30 Aug. 1986 8 p
(CNES-CT/DRT/TIT/RL-54-T; ETN-87-98806) Avail: NTIS HC A02/MF A01

Images taken by the VARAN-S side-looking airborne radar were interpreted. During an Arctic campaign a set of data was collected using the VARAN-S. An image covering a 15 km x 24 km zone is presented with a classification of 6 classes. The interpretation is preliminary but seems very promising to obtain quantitative data in an operational way with ERS. ESA

N87-16964# Centre National d'Etudes Spatiales, Toulouse (France). Radar Dept.
MIZEX VARAN-S RADAR IMAGE CHARACTERISTICS
N. Lannelongue 30 Aug. 1985 6 p
(CNES-CT/DRT/TIT/RL-55-T; ETN-87-98807) Avail: NTIS HC A02/MF A01

The data collected by the side-looking airborne radar (X-band) VARAN-S during the MIZEX experiment (1984) are described. The radar characteristics are given. Digital processing was performed in order to improve geometry and radiometry accuracy. The image restitution is explained. ESA

N87-16965# Research Inst. of National Defence, Linkoeping (Sweden). Dept. 3.
VEGETATION INFLUENCE ON WAVE PROPAGATION
Boerje Asp Sep. 1986 15 p Presented at the Nordic Radio Symposium 86, NRS 86 on Aspects of Wave Propagation on Mobile Radio and Broadband Communications, Saltsjoebaden, Sweden, 15-17 Apr. 1986
(FOA-B-30097-3.3; ISBN-91-7056-072-2; ISSN-0281-0263; ETN-87-98908) Avail: NTIS HC A02/MF A01

Vegetation influence on wave propagation at VHF-UHF was studied in forests, mainly fir, with transmitter and receiver antennas below the tree-tops. A theoretical model was compared with results from experimental studies of wave propagation in forest environments. The lateral wave model provides a consistent physical description of the wave propagation mechanism in forest environments. It gives a fairly good agreement between calculations and measured values, and it may explain the polarization differences found during field trials. ESA

N87-16966# Research Inst. of National Defence, Linkoeping (Sweden). Dept. 3.
TRANSMISSION LOSS MEASUREMENTS IN MOBILE RADIO NETS
Stellan Nilsson Sep. 1986 14 p Presented at the Nordic Radio Symposium, NRS 86 on Aspects of Wave Propagation on Mobile Radio and Broadband Communications, Saltjoebaden, Sweden, 15-27 Apr. 1986
(FOA-B-30098-3.3; ISBN-91-7056-072-2; ISSN-0281-0263; ETN-87-98909) Avail: NTIS HC A02/MF A01

A method to measure the transmission loss and its variability in the service area of a mobile radio network was developed. Results from propagation measurements at 390 MHz in an urban environment are compared with two prediction models. A semiempirical model gives a fairly good prediction of median transmission loss. ESA

N87-16967# Loughborough Univ. of Technology (England). Dept. of Electrical and Electronic Engineering.
A STUDY OF ANOMALOUS PROPAGATION AT RADAR FREQUENCIES AND A PROPOSAL FOR A RADAR COVERAGE FORECASTING MODEL, BOOK 2 OF 2 M.S. Thesis
D. J. Palmer 1986 181 p
(ETN-87-98938) Avail: NTIS HC A09/MF A01

Tropospheric refractive effects on ground-based surveillance and height-finding radars in the frequency range 500 MHz to 4 GHz were investigated. A model to forecast the radar coverage for such radars was derived. Figures and tables from the main report are presented. ESA

N87-17154*# MacDonald, Dettwiler and Associates Ltd., Richmond (British Columbia).
RADARSAT HIGH THROUGHPUT SAR PROCESSOR DEVELOPMENT
P. George *In* JPL The Second Spaceborne Imaging Radar Symposium 1 Dec. 1986 p 142-148 (For primary document see N87-17135 09-43)
Avail: NTIS HC A10/MF A01 CSCL 17I

N87-17158*# Jet Propulsion Lab., California Inst. of Tech., Pasadena.
IMAGING RADAR POLARIMETRY FROM WAVE SYNTHESIS
Howard A. Zebker, Jacob J. VanZyl, and Daniel N. Held *In its* The Second Spaceborne Imaging Radar Symposium 1 Dec. 1986 p 174-184 (For primary document see N87-17135 09-43)
Avail: NTIS HC A10/MF A01 CSCL 17I

N87-17159*# New South Wales Univ., Kensington (Australia). Centre for Remote Sensing.
RADAR SIGNATURE DETERMINATION: TRENDS AND LIMITATIONS
J. A. Richards *In* JPL The Second Spaceborne Imaging Radar Symposium 1 Dec. 1986 p 184-190 (For primary document see N87-17135 09-43)
Avail: NTIS HC A10/MF A01 CSCL 17I

N87-17180*# Texas Univ., Arlington. Wave Scattering Research Center.
EFFECTIVE MEDIUM APPROXIMATION FOR EFFECTIVE PROPAGATION CONSTANT CALCULATION IN A DENSE RANDOM MEDIUM
P. Y. Zhu and A. K. Fung *In* ESA Proceedings of the 1986 International Geoscience and Remote Sensing Symposium (IGARSS '86) on Remote Sensing: Today's Solutions for Tomorrow's Information Needs, Volume 1 Aug. 1986 p 93-97 (For primary document see N87-17163 09-43)
(Grant NAG5-486)
Avail: NTIS HC A99/MF E03; ESA, Paris, France, 3 volume set $90 Member States, AU, CN, and NO (+20% others) CSCL 20N

N87-17199# Dornier-Werke G.m.b.H., Friedrichshafen (West Germany).
NUMERICAL MODELING OF TWO-DIMENSIONAL TIME DOMAIN ELECTROMAGNETIC SCATTERING BY UNDERGROUND INHOMOGENEITIES
C. C. Lin and K. K. Mei (California Univ., Berkeley) *In* ESA Proceedings of the 1986 International Geoscience and Remote Sensing Symposium (IGARSS '86) on Remote Sensing: Today's Solutions for Tomorrow's Information Needs, Volume 1 Aug. 1986 p 211-216 (For primary document see N87-17163 09-43)
Avail: NTIS HC A99/MF E03; ESA, Paris, France, 3 volume set $90 Member States, AU, CN, and NO (+20% others)

N87-17228# MacDonald, Dettwiler and Associates Ltd., Richmond (British Columbia).
ERS-1 SYNTHETIC APERTURE RADAR FST DELIVERY PROCESSOR
P. George and J.-P. Guignard (European Space Agency. European Space Research and Technology Center, ESTEC, Noordwijk, Netherlands) *In* ESA Proceedings of the 1986 International Geoscience and Remote Sensing Symposium (IGARSS '86) on Remote Sensing: Today's Solutions for Tomorrow's Information Needs, Volume 1 Aug. 1986 p 399-403 (For primary document see N87-17163 09-43)
Avail: NTIS HC A99/MF E03; ESA, Paris, France, 3 volume set $90 Member States, AU, CN, and NO (+20% others)

N87-17229# Canada Centre for Remote Sensing, Ottawa (Ontario).
CANADIAN PLANS FOR OPERATIONAL DEMONSTRATIONS OF SATELLITE IMAGING RADAR APPLICATIONS
E. Langham, S. Parashar, N. Denyer, L. McNutt, V. R. Slaney, R. Brown, N. Freeman, and T. Mullane (Atmospheric Environment Service, Ottawa, Ontario) *In* ESA Proceedings of the 1986 International Geoscience and Remote Sensing Symposium (IGARSS '86) on Remote Sensing: Today's Solutions for Tomorrow's Information Needs, Volume 1 Aug. 1986 p 405-409 (For primary document see N87-17163 09-43)
Avail: NTIS HC A99/MF E03; ESA, Paris, France, 3 volume set $90 Member States, AU, CN, and NO (+20% others)

N87-17237# Freiburg Univ. (West Germany). Inst. of Geography.
RADAR IMAGERY OF THE EUROPEAN CITY INFLUENCED BY VARIATIONS IN DEPRESSION ANGLE AND LOOK DIRECTION
W. Geile *In* ESA Proceedings of the 1986 International Geoscience and Remote Sensing Symposium (IGARSS '86) on Remote Sensing: Today's Solutions for Tomorrow's Information Needs, Volume 1 Aug. 1986 p 455-461 (For primary document see N87-17163 09-43)
Avail: NTIS HC A99/MF E03; ESA, Paris, France, 3 volume set $90 Member States, AU, CN, and NO (+20% others)

N87-17239# Vexcell Corp., Boulder, Colo.
USING SECONDARY IMAGE PRODUCTS TO AID IN UNDERSTANDING AND INTERPRETATION OF RADAR IMAGERY
G. Domik and F. Leberl *In* ESA Proceedings of the 1986 International Geoscience and Remote Sensing Symposium (IGARSS '86) on Remote Sensing: Today's Solutions for Tomorrow's Information Needs, Volume 1 Aug. 1986 p 467-468 Sponsored by ESA (For primary document see N87-17163 09-43)
Avail: NTIS HC A99/MF E03; ESA, Paris, France, 3 volume set $90 Member States, AU, CN, and NO (+20% others)

N87-17241# Arkansas Univ., Fayetteville.
INTERFEROMETER APPLICATIONS FOR THE RECTIFICATION OF RADAR IMAGES
J. F. Hug, V. H. Kaupp, W. P. Waite, and H. C. MacDonald *In* ESA Proceedings of the 1986 International Geoscience and Remote Sensing Symposium (IGARSS '86) on Remote Sensing: Today's Solutions for Tomorrow's Information Needs, Volume 1 Aug. 1986 p 473-477 (For primary document see N87-17163 09-43)
Avail: NTIS HC A99/MF E03; ESA, Paris, France, 3 volume set $90 Member States, AU, CN, and NO (+20% others)

N87-17258*# Jet Propulsion Lab., California Inst. of Tech., Pasadena.
ROUNDOFF NOISE ANALYSIS FOR DIGITAL DOPPLER PROCESSORS IN RADAR SCATTEROMETERS
Chong-Yung Chi, D. Long, and K. Li Fuk *In* ESA Proceedings of the 1986 International Geoscience and Remote Sensing Symposium (IGARSS '86) on Remote Sensing: Today's Solutions for Tomorrow's Information Needs, Volume 1 Aug. 1986 p 579-584 (For primary document see N87-17163 09-43)
Avail: NTIS HC A99/MF E03; ESA, Paris, France, 3 volume set $90 Member States, AU, CN, and NO (+20% others) CSCL 17I

N87-17261# Rome Univ. (Italy). Dipt. di Ingegneria Elettronica.
ANTENNA PATTERN CORRECTION IN SCANNING RADIOMETRY: A SINGULAR SYSTEM ANALYSIS
F. Bardati, M. Mongiardo, and D. Solimini *In* ESA Proceedings of the 1986 International Geoscience and Remote Sensing Symposium (IGARSS '86) on Remote Sensing: Today's Solutions for Tomorrow's Information Needs, Volume 1 Aug. 1986 p 595-598 Sponsored by Elettronica S.p.A., Max-Planck Inst., and CNR (For primary document see N87-17163 09-43)
Avail: NTIS HC A99/MF E03; ESA, Paris, France, 3 volume set $90 Member States, AU, CN, and NO (+20% others)

N87-17262# Bern Univ. (Switzerland). Inst. of Applied Physics.
DIELECTRIC AND SURFACE PARAMETERS RELATED TO MICROWAVE SCATTER AND EMISSION PROPERTIES
E. Stotzer, U. Wegmueller, R. Hueppi, and C. Maetzer *In* ESA Proceedings of the 1986 International Geoscience and Remote Sensing Symposium (IGARSS '86) on Remote Sensing: Today's Solutions for Tomorrow's Information Needs, Volume 1 Aug. 1986 p 599-603 (For primary document see N87-17163 09-43)

Avail: NTIS HC A99/MF E03; ESA, Paris, France, 3 volume set $90 Member States, AU, CN, and NO (+20% others)

N87-17278# Kansas Univ. Center for Research, Inc., Lawrence. Radar Systems and Remote Sensing Lab.
SOME TRADE-OFFS IN MODEST-RESOLUTION RADARS FOR SPACE
R. K. Moore *In* ESA Proceedings of the 1986 International Geoscience and Remote Sensing Symposium (IGARSS '86) on Remote Sensing: Today's Solutions for Tomorrow's Information Needs, Volume 1 Aug. 1986 p 703-708 (For primary document see N87-17163 09-43)
Avail: NTIS HC A99/MF E03; ESA, Paris, France, 3 volume set $90 Member States, AU, CN, and NO (+20% others)

N87-17279# Jet Propulsion Lab., California Inst. of Tech., Pasadena.
IMAGING RADAR POLARIMETRY FROM WAVE SYNTHESIS
H. A. Zebker, J. J. VanZyl, and D. N. Held *In* ESA Proceedings of the 1986 International Geoscience and Remote Sensing Symposium (IGARSS '86) on Remote Sensing: Today's Solutions for Tomorrow's Information Needs, Volume 1 Aug. 1986 p 709-713 (For primary document see N87-17163 09-43)
Avail: NTIS HC A99/MF E03; ESA, Paris, France, 3 volume set $90 Member States, AU, CN, and NO (+20% others)

N87-17280# Environmental Research Inst. of Michigan, Ann Arbor.
MULTIFREQUENCY-POLARIMETRIC SAR FOR REMOTE SENSING
A. Kozma, A. D. Nichols, R. F. Rawson, S. J. Shackman, C. W. Haney (Naval Air Development Center, Warminster, Pa.), and J. J. Shanne, Jr. *In* ESA Proceedings of the 1986 International Geoscience and Remote Sensing Symposium (IGARSS '86) on Remote Sensing: Today's Solutions for Tomorrow's Information Needs, Volume 1 Aug. 1986 p 715-719 (For primary document see N87-17163 09-43)
Avail: NTIS HC A99/MF E03; ESA, Paris, France, 3 volume set $90 Member States, AU, CN, and NO (+20% others)

N87-17281# Michigan Univ., Ann Arbor. Radiation Lab.
MILLIMETER-WAVE NETWORK ANALYZER-BASED SCATTEROMETER
F. T. Ulaby, T. F. Haddock, J. East, and V. Liepa *In* ESA Proceedings of the 1986 International Geoscience and Remote Sensing Symposium (IGARSS '86) on Remote Sensing: Today's Solutions for Tomorrow's Information Needs, Volume 1 Aug. 1986 p 721-724 (For primary document see N87-17163 09-43)
Avail: NTIS HC A99/MF E03; ESA, Paris, France, 3 volume set $90 Member States, AU, CN, and NO (+20% others)

N87-17282# Technical Univ. of Budapest (Hungary). Dept. of Microwave Techniques.
A SCATTEROMETER OPERATING AT 10 GHz
I. Bozsoki and S. Mihaly *In* ESA Proceedings of the 1986 International Geoscience and Remote Sensing Symposium (IGARSS '86) on Remote Sensing: Today's Solutions for Tomorrow's Information Needs, Volume 1 Aug. 1986 p 725-729 (For primary document see N87-17163 09-43)
Avail: NTIS HC A99/MF E03; ESA, Paris, France, 3 volume set $90 Member States, AU, CN, and NO (+20% others)

N87-17306*# Texas Univ., Austin.
REMOTE SENSING OF TREE ATTENUATION AT 870 MHz ALONG SIMULATED EARTH-SATELLITE PATHS
W. J. Vogel, G. W. Torrence, J. Goldhirsh (Johns Hopkins Univ., Laurel, Md.), and J. R. Rowland *In* ESA Proceedings of the 1986 International Geoscience and Remote Sensing Symposium (IGARSS '86) on Remote Sensing: Today's Solutions for Tomorrow's Information Needs, Volume 2 Aug. 1986 p 861-866 Prepared for JPL (For primary document see N87-17283 09-43)
(Contracts JPL-956520; N00024-85-C-5301)
Avail: NTIS HC A17/MF A01; ESA, Paris, France, 3 volume set $90 Member States, AU, CN, and NO (+20% others) CSCL 20N

N87-17307# Massachusetts Univ., Amherst. Dept. of Electrical and Computer Engineering.
A BACKSCATTERING MODEL FOR VARIOUS FOLIATED DECIDUOUS TREE TYPES AT MILLIMETER WAVELENGTHS
C. C. Borel and R. E. McIntosh *In* ESA Proceedings of the 1986 International Geoscience and Remote Sensing Symposium (IGARSS '86) on Remote Sensing: Today's Solutions for Tomorrow's Information Needs, Volume 2 Aug. 1986 p 867-872 (For primary document see N87-17283 09-43)
Avail: NTIS HC A17/MF A01; ESA, Paris, France, 3 volume set $90 Member States, AU, CN, and NO (+20% others)

N87-17308# Deutsche Forschungs- und Versuchsanstalt fuer Luft- und Raumfahrt, Oberpfaffenhofen (West Germany). Inst. fuer Hochfrequenztechnik.
THE SIGNIFICANCE OF RADAR CROSS SECTION (RCS) POLARIZATION MEASUREMENTS FOR TREE SIGNATURES
A. J. Sieber *In* ESA Proceedings of the 1986 International Geoscience and Remote Sensing Symposium (IGARSS '86) on Remote Sensing: Today's Solutions for Tomorrow's Information Needs, Volume 2 Aug. 1986 p 873-878 (For primary document see N87-17283 09-43)
Avail: NTIS HC A17/MF A01; ESA, Paris, France, 3 volume set $90 Member States, AU, CN, and NO (+20% others)

N87-17309*# Texas Univ., Arlington. College of Engineering.
A SCATTERING MODEL FOR DEFOLIATED VEGETATION
M. A. Karam and A. K. Fung *In* ESA Proceedings of the 1986 International Geoscience and Remote Sensing Symposium (IGARSS '86) on Remote Sensing: Today's Solutions for Tomorrow's Information Needs, Volume 2 Aug. 1986 p 879-881 (For primary document see N87-17283 09-43)
(Grant NAG5-486)
Avail: NTIS HC A17/MF A01; ESA, Paris, France, 3 volume set $90 Member States, AU, CN, and NO (+20% others) CSCL 20N

N87-17310# Karlsruhe Univ. (West Germany).
COHERENT POLARIMETRIC RADAR CROSS SECTION (RCS) MEASUREMENTS ON TREES
S. Riegger and W. Wiesbeck *In* ESA Proceedings of the 1986 International Geoscience and Remote Sensing Symposium (IGARSS '86) on Remote Sensing: Today's Solutions for Tomorrow's Information Needs, Volume 2 Aug. 1986 p 883-887 (For primary document see N87-17283 09-43)
Avail: NTIS HC A17/MF A01; ESA, Paris, France, 3 volume set $90 Member States, AU, CN, and NO (+20% others)

N87-17311# Stuttgart Univ. (West Germany). Inst. of Navigation.
X AND L-BAND BACKSCATTERING MEASUREMENTS OF AGRICULTURAL CROPS, FOREST STANDS AND SINGLE TREES
Ph. Hartl, M. Reich, and S. Bhagavathula *In* ESA Proceedings of the 1986 International Geoscience and Remote Sensing Symposium (IGARSS '86) on Remote Sensing: Today's Solutions for Tomorrow's Information Needs, Volume 2 Aug. 1986 p 889-894 (For primary document see N87-17283 09-43)
Avail: NTIS HC A17/MF A01; ESA, Paris, France, 3 volume set $90 Member States, AU, CN, and NO (+20% others)

N87-17312# Environmental Research Inst. of Michigan, Ann Arbor. Radar Science Lab.
CALIBRATED X AND L-BAND SCATTERING COEFFICIENTS FROM A SOUTHERN US FOREST
E. S. Kasischke and R. W. Larson *In* ESA Proceedings of the 1986 International Geoscience and Remote Sensing Symposium (IGARSS '86) on Remote Sensing: Today's Solutions for Tomorrow's Information Needs, Volume 2 Aug. 1986 p 895-900 (For primary document see N87-17283 09-43)
(Contracts F19628-84-C-0081; DI-14-08-0001-21748)
Avail: NTIS HC A17/MF A01; ESA, Paris, France, 3 volume set $90 Member States, AU, CN, and NO (+20% others)

N87-17313# INTERA Environmental Consultants Ltd., Ottawa (Ontario).
SAR IMAGERY FOR FOREST MANAGEMENT
R. T. Lowry, P. Vaneck, and R. V. Dams *In* ESA Proceedings of the 1986 International Geoscience and Remote Sensing Symposium (IGARSS '86) on Remote Sensing: Today's Solutions for Tomorrow's Information Needs, Volume 2 Aug. 1986 p 901-906 (For primary document see N87-17283 09-43)
Avail: NTIS HC A17/MF A01; ESA, Paris, France, 3 volume set $90 Member States, AU, CN, and NO (+20% others)

N87-17320# Stuttgart Univ. (West Germany). Inst. fuer Navigation.
FUTURE USER REQUIREMENTS AND REQUIRED TECHNOLOGICAL DEVELOPMENTS OF SPACEBORNE SYNTHETIC APERTURE RADARS
Ph. Hartl and H. M. Braun (Dornier-Werke G.m.b.H., Friedrichshafen, West Germany) *In* ESA Proceedings of the 1986 International Geoscience and Remote Sensing Symposium (IGARSS '86) on Remote Sensing: Today's Solutions for Tomorrow's Information Needs, Volume 2 Aug. 1986 p 941-946 (For primary document see N87-17283 09-43)
Avail: NTIS HC A17/MF A01; ESA, Paris, France, 3 volume set $90 Member States, AU, CN, and NO (+20% others)

N87-17321# Dornier-Werke G.m.b.H., Friedrichshafen (West Germany).
THE X-BAND SAR IN A JOINT MISSION WITH THE SHUTTLE IMAGING RADAR
W. Gils and H. Hoelzl *In* ESA Proceedings of the 1986 International Geoscience and Remote Sensing Symposium (IGARSS '86) on Remote Sensing: Today's Solutions for Tomorrow's Information Needs, Volume 2 Aug. 1986 p 947-951 (For primary document see N87-17283 09-43)
Avail: NTIS HC A17/MF A01; ESA, Paris, France, 3 volume set $90 Member States, AU, CN, and NO (+20% others)

N87-17322# Marconi Space and Defence Systems Ltd., Portsmouth (England).
AN ADVANCED SAR DESIGN FOR FUTURE LAND MISSIONS
F. G. Sawyer and M. A. Brown *In* ESA Proceedings of the 1986 International Geoscience and Remote Sensing Symposium (IGARSS '86) on Remote Sensing: Today's Solutions for Tomorrow's Information Needs, Volume 2 Aug. 1986 p 953-958 Sponsored by ESA/ESTEC (For primary document see N87-17283 09-43)
Avail: NTIS HC A17/MF A01; ESA, Paris, France, 3 volume set $90 Member States, AU, CN, and NO (+20% others)

N87-17323# Deutsche Forschungs- und Versuchsanstalt fuer Luft- und Raumfahrt, Oberpfaffenhofen (West Germany). Inst. fuer Hochfrequenztechnik.
RADAR CROSS SECTION (RCS) DATA BASE DEDUCED FROM RADAR IMAGES
A. J. Sieber *In* ESA Proceedings of the 1986 International Geoscience and Remote Sensing Symposium (IGARSS '86) on Remote Sensing: Today's Solutions for Tomorrow's Information Needs, Volume 2 Aug. 1986 p 959-964 (For primary document see N87-17283 09-43)
Avail: NTIS HC A17/MF A01; ESA, Paris, France, 3 volume set $90 Member States, AU, CN, and NO (+20% others)

N87-17344*# National Aeronautics and Space Administration. Goddard Space Flight Center, Greenbelt, Md.
EVALUATING ROUGHNESS MODELS OF RADAR BACKSCATTER
E. T. Engmann (Agricultural Research Service, Beltsville, Md.) and J. R. Wang *In* ESA Proceedings of the 1986 International Geoscience and Remote Sensing Symposium (IGARSS '86) on Remote Sensing: Today's Solutions for Tomorrow's Information Needs, Volume 2 Aug. 1986 p 1097-1101 (For primary document see N87-17283 09-43)
Avail: NTIS HC A17/MF A01; ESA, Paris, France, 3 volume set $90 Member States, AU, CN, and NO (+20% others) CSCL 17I

N87-17346*# National Aeronautics and Space Administration. Goddard Space Flight Center, Greenbelt, Md.
MICROWAVE BACKSCATTERING FROM AN ANISOTROPIC SOYBEAN CANOPY
R. H. Lang (George Washington Univ., Washington, D.C.), S. Saatchi, and D. M. LeVine *In* ESA Proceedings of the 1986 International Geoscience and Remote Sensing Symposium (IGARSS '86) on Remote Sensing: Today's Solutions for Tomorrow's Information Needs, Volume 2 Aug. 1986 p 1107-1112 (For primary document see N87-17283 09-43)
Avail: NTIS HC A17/MF A01; ESA, Paris, France, 3 volume set $90 Member States, AU, CN, and NO (+20% others) CSCL 20N

N87-17347# Bern Univ. (Switzerland). Inst. of Applied Physics.
L TO X-BAND SCATTER AND EMISSION MEASUREMENTS OF VEGETATION
R. Hueppi and E. Schanda *In* ESA Proceedings of the 1986 International Geoscience and Remote Sensing Symposium (IGARSS '86) on Remote Sensing: Today's Solutions for Tomorrow's Information Needs, Volume 2 Aug. 1986 p 1113-1118 (For primary document see N87-17283 09-43)
Avail: NTIS HC A17/MF A01; ESA, Paris, France, 3 volume set $90 Member States, AU, CN, and NO (+20% others)

N87-17348*# Jet Propulsion Lab., California Inst. of Tech., Pasadena.
ON THE RELATIONSHIP BETWEEN AGE OF LAVA FLOWS AND RADAR BACKSCATTERING
R. G. Blom, P. Cooley, and L. R. Schenck *In* ESA Proceedings of the 1986 International Geoscience and Remote Sensing Symposium (IGARSS '86) on Remote Sensing: Today's Solutions for Tomorrow's Information Needs, Volume 2 Aug. 1986 p 1119-1127 (For primary document see N87-17283 09-43)
Avail: NTIS HC A17/MF A01; ESA, Paris, France, 3 volume set $90 Member States, AU, CN, and NO (+20% others) CSCL 20N

N87-17349# China Research Inst. of Radiowave Propagation, Xinxiang.
BACKSCATTERING POWER SPECTRUM FOR RANDOMLY MOVING VEGETATION
J. Jiankang, Z. Zhongzhi, and S. Zhong *In* ESA Proceedings of the 1986 International Geoscience and Remote Sensing Symposium (IGARSS '86) on Remote Sensing: Today's Solutions for Tomorrow's Information Needs, Volume 2 Aug. 1986 p 1129-1132 (For primary document see N87-17283 09-43)
Avail: NTIS HC A17/MF A01; ESA, Paris, France, 3 volume set $90 Member States, AU, CN, and NO (+20% others)

N87-17354# Rome Univ. (Italy). Dipt. di Ingegneria Elettronica.
EFFECTS OF RAIN CELLS ON SAR PERFORMANCE
P. Ferrazzoli and G. Schiavon *In* ESA Proceedings of the 1986 International Geoscience and Remote Sensing Symposium (IGARSS '86) on Remote Sensing: Today's Solutions for Tomorrow's Information Needs, Volume 2 Aug. 1986 p 1163-1168 (For primary document see N87-17283 09-43)
Avail: NTIS HC A17/MF A01; ESA, Paris, France, 3 volume set $90 Member States, AU, CN, and NO (+20% others)

N87-17355# Deutsche Forschungs- und Versuchsanstalt fuer Luft- und Raumfahrt, Oberpfaffenhofen (West Germany). Inst. fuer Hochfrequenztechnik.
ANTENNA AMBIGUITY INVESTIGATIONS FOR X-SAR
G. Waller *In* ESA Proceedings of the 1986 International Geoscience and Remote Sensing Symposium (IGARSS '86) on Remote Sensing: Today's Solutions for Tomorrow's Information Needs, Volume 2 Aug. 1986 p 1169-1173 (For primary document see N87-17283 09-43)
Avail: NTIS HC A17/MF A01; ESA, Paris, France, 3 volume set $90 Member States, AU, CN, and NO (+20% others)

N87-17356# Canada Centre for Remote Sensing, Ottawa (Ontario).
RECONSIDERATION OF AZIMUTH AMBIGUITIES IN SAR
R. K. Raney and J. Princz *In* ESA Proceedings of the 1986 International Geoscience and Remote Sensing Symposium (IGARSS '86) on Remote Sensing: Today's Solutions for Tomorrow's Information Needs, Volume 2 Aug. 1986 p 1175-1179 (For primary document see N87-17283 09-43)
Avail: NTIS HC A17/MF A01; ESA, Paris, France, 3 volume set $90 Member States, AU, CN, and NO (+20% others)

N87-17357# Dornier-Werke G.m.b.H., Friedrichshafen (West Germany).
PLANAR ARRAY ANTENNA FOR ERS-1 SYNTHETIC APERTURE RADAR
R. Wagner *In* ESA Proceedings of the 1986 International Geoscience and Remote Sensing Symposium (IGARSS '86) on Remote Sensing: Today's Solutions for Tomorrow's Information Needs, Volume 2 Aug. 1986 p 1181-1186 (For primary document see N87-17283 09-43)
Avail: NTIS HC A17/MF A01; ESA, Paris, France, 3 volume set $90 Member States, AU, CN, and NO (+20% others)

N87-17358# National Space Development Agency, Ibaraki (Japan).
A SATELLITE-BORNE SAR TRANSMITTER AND RECEIVER
M. Fukai, K. Nishikawa, I. Izumi, T. Tsuji, H. Kondo, H. Kashihara, H. Nishino, K. Tanaka, Y. Hisada, and Y. Itoh *In* ESA Proceedings of the 1986 International Geoscience and Remote Sensing Symposium (IGARSS '86) on Remote Sensing: Today's Solutions for Tomorrow's Information Needs, Volume 2 Aug. 1986 p 1187-1192 (For primary document see N87-17283 09-43)
Avail: NTIS HC A17/MF A01; ESA, Paris, France, 3 volume set $90 Member States, AU, CN, and NO (+20% others)

N87-17359# Deutsche Forschungs- und Versuchsanstalt fuer Luft- und Raumfahrt, Oberpfaffenhofen (West Germany). Inst. fuer Hochfrequenztechnik.
ANALYSIS OF AMPLITUDE NONLINEARITIES IN THE ERS-1 SAR RECEIVER SYSTEM
T. K. Pike and E. Sappl *In* ESA Proceedings of the 1986 International Geoscience and Remote Sensing Symposium (IGARSS '86) on Remote Sensing: Today's Solutions for Tomorrow's Information Needs, Volume 2 Aug. 1986 p 1193-1194 (For primary document see N87-17283 09-43)
Avail: NTIS HC A17/MF A01; ESA, Paris, France, 3 volume set $90 Member States, AU, CN, and NO (+20% others)

N87-17360# National Space Development Agency, Ibaraki (Japan). Tsukuba Space Center.
PULSE COMPRESSION TEST RESULTS OF THE SAR TRANSMITTER AND RECEIVER
K. Tanaka, H. Shinohara, H. Nishino, H. Kashihara, K. Nishikawa, Y. Hisada, and Y. Itoh *In* ESA Proceedings of the 1986 International Geoscience and Remote Sensing Symposium (IGARSS '86) on Remote Sensing: Today's Solutions for Tomorrow's Information Needs, Volume 2 Aug. 1986 p 1195-1200 (For primary document see N87-17283 09-43)
Avail: NTIS HC A17/MF A01; ESA, Paris, France, 3 volume set $90 Member States, AU, CN, and NO (+20% others)

N87-17361# Marconi Space Systems Ltd., Portsmouth (England).
A POWERFUL UTILITY FOR ASSESSING THE PERFORMANCE OF THE ERS-1 SYNTHETIC APERTURE RADAR
R. J. Blissett, F. G. Sawyer, M. A. Brown, and D. Smith *In* ESA Proceedings of the 1986 International Geoscience and Remote Sensing Symposium (IGARSS '86) on Remote Sensing: Today's Solutions for Tomorrow's Information Needs, Volume 2 Aug. 1986 p 1201-1205 (For primary document see N87-17283 09-43)
Avail: NTIS HC A17/MF A01; ESA, Paris, France, 3 volume set $90 Member States, AU, CN, and NO (+20% others)

N87-17362# Deutsche Forschungs- und Versuchsanstalt fuer Luft- und Raumfahrt, Oberpfaffenhofen (West Germany). Inst. fuer Hochfrequenztechnik.
X-SAR EXTENDS THE FREQUENCY RANGE OF SHUTTLE IMAGING RADAR
W. Keydel *In* ESA Proceedings of the 1986 International Geoscience and Remote Sensing Symposium (IGARSS '86) on Remote Sensing: Today's Solutions for Tomorrow's Information Needs, Volume 2 Aug. 1986 p 1207-1212 (For primary document see N87-17283 09-43)
Avail: NTIS HC A17/MF A01; ESA, Paris, France, 3 volume set $90 Member States, AU, CN, and NO (+20% others)

N87-17370# Centre Oceanologique de Bretagne, Brest (France). Antenne CREO.
EVALUATION OF THE DIFFERENT PARAMETERS IN LONG'S C-BAND MODEL
Alain Cavanie, Joelle Demurger, and Pascal Lecomte *In* ESA Proceedings of an ESA Workshop on ERS-1 Wind and Wave Calibration Sep. 1986 p 47-51 (For primary document see N87-17363 09-43)
Avail: NTIS HC A11/MF A01

N87-17391# Marconi Co. Ltd., Chelmsford (England). Remote Sensing Group.
A SCATTEROMETER RESEARCH PROGRAM
Ian A. Ward *In* ESA Proceedings of an ESA Workshop on ERS-1 Wind and Wave Calibration Sep. 1986 p 181-185 (For primary document see N87-17363 09-43)
Avail: NTIS HC A11/MF A01

N87-17572*# Chalmers Univ. of Technology, Goeteborg (Sweden). Dept. of Physics.
ON THE FEASIBILITY OF CONSTRUCTING AN IMAGING ARRAY OF SLOT-ANTENNAS INTEGRATED WITH SIS MIXERS
D. Winker, W. R. McGrath, B. Nilsson, T. Claeson, J. Johansson, E. Kollberg, K. S. Yngvesson (Massachusetts Univ., Amherst), and S. Rudner (Research Inst. of National Defence, Linkoeping, Sweden) *In* ESA Proceedings of an ESA Workshop on a Spaceborne Submillimeter Astronomy Mission. A Cornerstone of the ESA Long Term Science Program Aug. 1986 p 277-283 Sponsored by NASA Langley Research Center, the Swedish Board for Technical Development, and the Swedish Board for Space Activities (For primary document see N87-17535 09-88)
Avail: NTIS HC A14/MF A01 CSCL 20N

33 ELECTRONICS AND ELECTRICAL ENGINEERING

Includes test equipment and maintainability; components, e.g., tunnel diodes and transistors; microminiaturization; and integrated circuitry.

For related information see also *60 Computer Operations and Hardware* and *76 Solid-State Physics.*

N87-16968*# National Aeronautics and Space Administration. Lewis Research Center, Cleveland, Ohio.
ABSOLUTE GAIN MEASUREMENT BY THE IMAGE METHOD UNDER MISMATCHED CONDITION
Richard Q. Lee and Maurice F. Baddour 1987 6 p Presented at the International AP-S Symposium, Blacksburg, Va., 15-19 Jun. 1987; sponsored by IEEE
(NASA-TM-88924; E-3359; NAS 1.15:88924) Avail: NTIS HC A02/MF A01 CSCL 09C

Purcell's image method for measuring the absolute gain of an antenna is particularly attractive for small test antennas. The method is simple to use and utilizes only one antenna with a reflecting plane to provide an image for the receiving antenna. However, the method provides accurate results only if the antenna is matched to its waveguide. In this paper, a waveguide junction analysis is developed to determine the gain of an antenna under mismatched condition. Absolute gain measurements for two

standard gain horn antennas have been carried out. Experimental results agree closely with published data. Author

N87-16969# Polish Academy of Sciences, Warsaw. Dept. of Mechanical Systems.
ON ROUTES TO CHAOTIC MOTION IN OSCILLATORS WITH UNSYMMETRIC AND SYMMETRIC ELASTIC NONLINEARITY
Wanda Szemplinska-Stupnicka 1986 37 p
(ISSN-0208-5658) Avail: NTIS HC A03/MF A01

In two types of nonlinear oscillators with single equilibrium positions the question of transition to chaos is investigated by making use of computer simulation and approximate analytical methods to study periodic solutions and their stability. The zone of chaotic motion is found as a transition zone between qT-periodic /sub- or subultraharmonic/ solution and the T-periodic solution, thus replacing the classical jump phenomenon. Two routes to chaos are studied: the gentle route via a cascade of period doubling bifurcations which appears to be characteristic in unsymmetrical oscillator, and a sharp route, which proves to accompany a stability limit of symmetrical periodic solutions. An approximate mathematical model of pre-chaotic motion in the sharp transition to chaos is proposed. Author

N87-16970*# National Aeronautics and Space Administration. Marshall Space Flight Center, Huntsville, Ala.
SMALL COMPUTER INTERFACE TO A STEPPER MOTOR
Fred A. Berry, Jr. Dec. 1986 13 p
(NASA-TM-86574; NAS 1.15:86574) Avail: NTIS HC A02/MF A01 CSCL 09C

A Commodore VIC-20 computer has been interfaced with a stepper motor to provide an inexpensive stepper motor controller. Only eight transistors and two integrated circuits compose the interface. The software controls the parallel interface of the computer and provides the four phase drive signals for the motor. Optical sensors control the zeroing of the 12-inch turntable positioned by the controller. The computer calculates the position information and movement of the table and may be programmed in BASIC to execute automatic sequences. Author

N87-16971*# Colby Coll., Waterville, Maine. Dept. of Physics and Astronomy.
LEO HIGH VOLTAGE SOLAR ARRAY ARCING RESPONSE MODEL Interim Report, Feb. 1987
Roger N. Metz Feb. 1987 32 p
(Grant NAG3-576)
(NASA-CR-180073; NAS 1.26:180073) Avail: NTIS HC A03/MF A01 CSCL 09A

A series of mathematical models were developed that describe the electrical behavior of a large solar cell array floating electrically in the low Earth orbit (LEO) space plasma and struck by an arc at a point of negative bias. There are now three models in this series: ARCII, which is a fully analytical, linearized model; ARCIII, which is an extension of ARCIII that includes solar cell inductance as well as load reactance; Nonlinear ARC, which is a numerical model able to treat effects such as non-linearized, i.e., logarithmic solar cell I/V characteristics, conductance switching as a solar cell crosses plasma ground on a voltage excursion and non-ohmic plasma leakage current collection. Author

N87-16972*# TRW Electronic Systems Group, Redondo Beach, Calif.
THE 20 GHz POWER GaAs FET DEVELOPMENT Final Report
M. Crandell Sep. 1986 52 p
(Contract NAS3-22503)
(NASA-CR-179546; NAS 1.26:179546; S/N-36778) Avail: NTIS HC A04/MF A01 CSCL 09A

The development of power Field Effect Transistors (FET) operating in the 20 GHz frequency band is described. The major efforts include GaAs FET device development (both 1 W and 2 W devices), and the development of an amplifier module using these devices. Author

N87-16973 Department of the Air Force, Washington, D.C.
A pi-SECTION DIGITAL PHASE SHIFTER APPARATUS Patent
Binboga S. Yarman, inventor (to Air Force) Issued 5 Aug. 1986 5 p Supersedes US-Patent-Appl-SN-767455
(AD-D012495; US-Patent-4,604,593; US-Patent-Appl-SN-767455; US-Patent-Class-333-139) Avail: US Patent and Trademark Office CSCL 09/5

An extra high frequency pi-section digital phase shifter apparatus having a diode connected between two identical parallel shunt circuits is detailed. The parallel shunt circuits connect to the series inductor/diode circuit at both the input and output and each parallel shunt circuit has an inductor connected in parallel with a capacitor and a diode to provide balanced insertion loss at each diode switching state. When the diodes of the circuit are in the forward-biased state they act as closed short circuit switches. When the diodes are reverse-biased, the inductance in the shunt circuit resonates with the diode capacitance to provide a short circuit path to the RF signal at the center frequency of the RF signal at the desired phase. GRA

N87-16974# Department of the Air Force, Washington, D.C.
HIGH-VOLTAGE MILBERGER SLIP SLIDE POWER CONDITIONER Patent Application
Franklin B. Jones, inventor (to Air Force) Filed 1 Aug. 1986 30 p
(AD-D012504; US-Patent-Appl-SN-891821) Avail: NTIS HC A03/MF A01 CSCL 10/2

A high-voltage converter circuit uses a slip slide power conditioner to reduce non-monotonic non-linearities in the converter output signal is disclosed. The slip slide power conditioner includes: a choke feed dc circulator; two radio frequency (RF) power pumps; a phase detector; a phase controller; and a combiner. The choke feed dc circulator receives the dc input signal and produces therefrom two voltage output signals which are each sent to one of the two RF power pumps. The two RF power pumps produce two out-of-phase square wave output signals which are algebraically combined in the combiner to form an output signal whose amplitude is a function of phase difference. The phase detector and phase controller sample this output signal and adjust the phase of the two power pumps to remove non-linearities due to secondary ranging (resonance) that beats with harmonics of their square wave signals. Author (GRA)

N87-16975# Department of the Army, Washington, D. C.
FREE ELECTRON DIODE OSCILLATOR Patent Application
Brett David vandeSande, inventor (to Army) Filed 19 Aug. 1986 18 p
(AD-D012519; US-Patent-Appl-SN-897692) Avail: NTIS HC A02/MF A01 CSCL 09/1

This invention relates to a crossed-field microwave power tube. Electrons are emitted from a tubular electrode at ground potential. The electrons are accelerated by an electric field toward a high voltage anode located within the tubular electrode. A magnetic field is oriented along the axis of the tube; the magnetic field is perpendicular to the electric field. The electrons follow curved paths in the space between the tubular electrode and the anode, while producing electromagnetic radiation in a transverse electromagnetic mode (TEM). The TEM radiation is easily coupled from the tube. GRA

N87-16976# California Univ., Los Angeles. Dept. of Electrical Engineering.
MICROSTRIP DIPOLES FOR EHF AND MILLIMETER WAVE APPLICATIONS Final Report, 28 Mar. - 31 May 1986
N. G. Alexopoulos 26 Aug. 1986 27 p
(Contract DAAG29-83-K-0067)
(AD-A173025; ARO-19778.10-EL) Avail: NTIS HC A03/MF A01 CSCL 09/5

This is the final report for research performed under DAAG29-83-K-0067. The research performed during the duration of this grant has made an impact in the areas of: (1) Substrate-superstrate effects on printed circuit antennas (2) Modeling electromagnetically coupled microstrip dipoles in a substrate-superstrate configuration

(3) Modeling Microstrip Discontinuities and (4) Investigating substrate anisotropy effects on a variety of integrated circuit structures. During the period of research, very sophisticated algorithms were developed on Green's function methods and integral equation solutions based on a variety of numerical procedures. GRA

N87-16977# General Electric Co., Philadelphia, Pa. Space Systems Div.
HIGH ENERGY SURGE ARRESTER TECHNOLOGY DEVELOPMENT, PART 2 Final Technical Report, 30 Jun. 1982 - 28 Feb. 1986
Danta M. Tasca 28 Feb. 1986 130 p
(Contract DNA001-82-C-0241; DNA Proj. X99-QAXV)
(AD-A173086; Rept-86SDS4239-Pt-2; DNA-TR-86-85-Pt-2) Avail: NTIS HC A07/MF A01 CSCL 09/1

The objective of this program was the development of improved high energy surge arresters (HESAs) to protect installations from EMP induced on extended networks. This phase is associated with the development of a HESA for an RF/C3 transmitter antenna. A unique and innovative all solid state, self recovery HESA design concept was developed using existing metal oxide varistor and saturable magnetic device technologies. This design concept, which is based on a two element hybrid protective device approach, has the dual capability to provide high voltage/fast rise time and long pulse/high current threat protection. The first element provides delay free protection against the fast risetime HEMP threat and was implemented using our metal oxide power varistor product line technology which General Electric developed. The second element provides the high energy relief for the first element, and was implemented using saturable magnetics. Detailed analytical design equations were derived and extensive material characteristics were experimentally obtained in support of this development. Much of this work involved the generation of singular information which was required to support the solutions to the design problems encountered in meeting the design challenge using realistic hardware. Two proof of principle prototype units were designed and fabricated using the technology established in the program. GRA

N87-16978# Sandia National Labs., Albuquerque, N. Mex.
MONITORING TRANSIENTS IN LOW INDUCTANCE CIRCUITS Patent Application
R. P. Guilford, inventor (to DOE) and J. R. Rosborough, inventor (to DOE) Filed 21 Oct. 1985 16 p
(Contract DE-AC04-76DP-00789)
(DE86-013756; US-Patent-Appl-SN-789892) Avail: NTIS HC A02/MF A01

The instant invention relates to methods of and apparatus for monitoring transients in low inductance circuits and to a probe utilized to practice said method and apparatus. More particularly, the instant invention relates to methods of and apparatus for monitoring low inductance circuits, wherein the low inductance circuits include a pair of flat cable transmission lines. The instant invention is further directed to a probe for use in monitoring pairs of flat cable transmission lines. DOE

N87-16931# Turin Univ. (Italy). Dipt. di Elettronica.
DIELECTRIC SUPPORT STRUCTURES FOR SPACECRAFT ANTENNA FEEDS
R. D. Graglia, M. Orefice, U. Ponzi (Rome Univ., Italy), and S. Sgubini *In* ESA Proceedings of the Second ESA Workshop on Mechanical Technology for Antennas Aug. 1986 p 63-71 (For primary document see N87-16923 09-32)
Avail: NTIS HC A12/MF A01

N87-17152*# Dornier-Werke G.m.b.H., Friedrichshafen (West Germany).
FEATURES AND TECHNOLOGIES OF ERS-1 (ESA) AND X-SAR ANTENNAS
R. Schuessler and R. Wagner *In* JPL The Second Spaceborne Imaging Radar Symposium 1 Dec. 1986 p 125-129 (For primary document see N87-17135 09-43)
Avail: NTIS HC A10/MF A01 CSCL 09C

N87-17161*# Jet Propulsion Lab., California Inst. of Tech., Pasadena.
SIR-C, THE NEXT GENERATION SPACEBORNE SAR
E. R. Caro *In its* The Second Spaceborne Imaging Radar Symposium 1 Dec. 1986 p 203-217 (For primary document see N87-17135 09-43)
Avail: NTIS HC A10/MF A01 CSCL 09C

N87-17162*# Deutsche Forschungs- und Versuchsanstalt fuer Luft- und Raumfahrt, Oberpfaffenhofen (West Germany). Inst. fuer Hochfrequenztechnik.
THE X-SAR SYSTEM
Herwig Oettl *In* JPL The Second Spaceborne Imaging Radar Symposium 1 Dec. 1986 p 218-223 (For primary document see N87-17135 09-43)
Avail: NTIS HC A10/MF A01 CSCL 09C

N87-17197# Alfateh Univ., Tripoli (Libya). Dept. of Electrical and Electronics Engineering.
THE INDUCED CURRENT ON A LONG WIRE DUE TO A VERTICAL ELECTRIC DIPOLE ABOVE DISSIPATIVE GROUND
A. A. Aburwein *In* ESA Proceedings of the 1986 International Geoscience and Remote Sensing Symposium (IGARSS '86) on Remote Sensing: Today's Solutions for Tomorrow's Information Needs, Volume 1 Aug. 1986 p 199-203 (For primary document see N87-17163 09-43)
Avail: NTIS HC A99/MF E03; ESA, Paris, France, 3 volume set $90 Member States, AU, CN, and NO (+20% others)

N87-17328# Consiglio Nazionale delle Ricerche, Florence (Italy).
DIGITAL TECHNIQUES FOR NOISE REDUCTION IN AUTOMATIC PICTURE TRANSMISSION (APT) NOAA SATELLITE IMAGES
R. Carla, V. M. Sacco, and S. Baronti *In* ESA Proceedings of the 1986 International Geoscience and Remote Sensing Symposium (IGARSS '86) on Remote Sensing: Today's Solutions for Tomorrow's Information Needs, Volume 2 Aug. 1986 p 995-1000 (For primary document see N87-17283 09-43)
Avail: NTIS HC A17/MF A01; ESA, Paris, France, 3 volume set $90 Member States, AU, CN, and NO (+20% others)

N87-17570# California Univ., Berkeley. Dept. of Physics.
LOW NOISE SIS MIXER WITH GAIN FOR 80-115 GHz
A. V. Raeisaenen (Helsinki Univ. of Technology, Espoo, Finland), D. G. Crete (Ecole Normale Superieure, Paris, France), P. L. Richards, and F. L. Lloyd (National Bureau of Standards, Gaithersburg, Md.) *In* ESA Proceedings of an ESA Workshop on a Spaceborne Submillimeter Astronomy Mission. A Cornerstone of the ESA Long Term Science Program Aug. 1986 p 255-258 (For primary document see N87-17535 09-88)
(Grant AFOSR-85-0230)
Avail: NTIS HC A14/MF A01

34 FLUID MECHANICS AND HEAT TRANSFER

Includes boundary layers; hydrodynamics; fluidics; mass transfer; and ablation cooling.

For related information see also *02 Aerodynamics* and *77 Thermodynamics and Statistical Physics.*

N87-16979 Cincinnati Univ., Ohio.
LASER DOPPLER VELOCIMETER MEASUREMENTS AND THEORETICAL INVESTIGATION OF THREE DIMENSIONAL SCROLL FLOW Ph.D. Thesis
Malak F. Malak 1986 181 p
Avail: Univ. Microfilms Order No. DA8622295

The results of an experimental study of the three-dimensional flow field in a radial inflow turbine scroll are presented. A two color LDV system was used in the measurement of three orthogonal

velocity components at 758 points located throughout the scroll and the unvaned portion of the nozzle. The cold flow experimental results are presented for the three components of the mean velocity throughout the scroll and for the velocity fluctuations and the turbulence parameters at four cross sections. The experimental results of the static pressure measurements over the scroll surfaces are also presented. The measurements of mean velocity components are compared with a numerical solution of the potential flow field using the finite element technique. The experimental results show a variation of the flow exit angle, and the theoretical solution predicted the same variation along the scroll exit peripheral. Combining the cross-flow obtained from experimental measurements with the potential flow theoretical solution results in the secondary flow in the eight cross-sections. Dissert. Abstr.

N87-16980# Illinois Univ., Urbana. Dept. of Chemical Engineering.
PRESSURE GRADIENT EFFECTS IN THE VISCOUS WALL REGION OF A TURBULENT FLOW
Douglas Scott Finnicum Jan. 1987 288 p
(Contract N00014-82-K-0324; NR Proj. 657-728)
(Rept-7) Avail: NTIS HC A13/MF A01

The results of a study investigating the effects of an imposed pressure gradient on the viscous wall region of a turbulent flow are presented. Only imposed pressure gradients homogeneous in the streamwise direction are considered. A computational model that neglects streamwise derivatives is used to study imposed pressure gradients that are constant in time. The shear stress at the edge of the viscous wall region, and not the wall shear stress, is shown to be the proper shear stress to use in scaling the coherent eddy structures responsible for the production of the turbulent kinetic in the viscous wall region. Arguments are presented that show the minimum P sub e+ value at the edge of the viscous wall region, where P sub e+ is defined by tau + = 1 + P sub e+ y+, corresponds to the point of imminent relaminarization of a turbulent flow. It is suggested that the logarithmic region disappears at this minimum value. Author

N87-16981*# Nielsen Engineering and Research, Inc., Mountain View, Calif.
PREDICTION OF VORTEX SHEDDING FROM CIRCULAR AND NONCIRCULAR BODIES IN SUBSONIC FLOW
Michael R. Mendenhall and Daniel J. Lesieutre Washington NASA Jan. 1987 168 p
(Contract NAS1-17962)
(NASA-CR-4037; NAS 1.26:4037) Avail: NTIS HC A08/MF A01 CSCL 20D

An engineering prediction method and associated computer code VTXCLD are presented which predict nose vortex shedding from circular and noncircular bodies in subsonic flow at angles of attack and roll. The axisymmetric body is represented by point sources and doublets, and noncircular cross sections are transformed to a circle by either analytical or numerical conformal transformations. The leeward vortices are modeled by discrete vortices in crossflow planes along the body; thus, the three-dimensional steady flow problem is reduced to a two-dimensional, unsteady, separated flow problem for solution. Comparison of measured and predicted surface pressure distributions, flowfield surveys, and aerodynamic characteristics are presented for bodies with circular and noncircular cross sectional shapes. Author

N87-16982*# Universities Space Research Association, Columbia, Md.
COMPUTATION OF TURBULENT BOUNDARY LAYER FLOWS WITH AN ALGEBRAIC STRESS TURBULENCE MODEL
Sang-Wook Kim and Yen-Sen Chen Nov. 1986 25 p
(Contract NAS8-35918)
(NASA-CR-178967; NAS 1.26:178967) Avail: NTIS HC A02/MF A01 CSCL 20D

An algebraic stress turbulence model is presented, characterized by the following: (1) the eddy viscosity expression is derived from the Reynolds stress turbulence model; (2) the turbulent kinetic energy dissipation rate equation is improved by including a production range time scale; and (3) the diffusion coefficients for turbulence equations are adjusted so that the kinetic energy profile extends further into the free stream region found in most experimental data. The turbulent flow equations were solved using a finite element method. Examples include: fully developed channel flow, fully developed pipe flow, flat plate boundary layer flow, plane jet exhausting into a moving stream, circular jet exhausting into a moving stream, and wall jet flow. Computational results compare favorably with experimental data for most of the examples considered. Significantly improved results were obtained for the plane jet flow, the circular jet flow, and the wall jet flow; whereas the remainder are comparable to those obtained by finite difference methods using the standard kappa-epsilon turbulence model. The latter seems to be promising with further improvement of the expression for the eddy viscosity coefficient. Author

N87-16983*# National Aeronautics and Space Administration, Washington, D.C.
TRANSITIONAL BOUNDARY LAYERS UNDER THE INFLUENCE OF HIGH FREE STREAM TURBULENCE, INTENSIVE WALL COOLING AND HIGH PRESSURE GRADIENTS IN HOT GAS CIRCULATION Ph.D. Thesis - Technische Hochschule, Karlsruhe, 1985
Klaus Rued Feb. 1987 239 p Transl. into ENGLISH of Thesis, "Transitionale Grenzschichten unter dem Einfluss hoher Freistromturbulenz, Intensiver Wandkuehlung und Starken Druckgradienten in Heissgasstroenmungen", Karlsruhe, West Germany, 1985 p 1-191 Transl. by SCITRAN, Inc., Santa Barbara, Calif.
(Contract NASw-4004)
(NASA-TM-88524; NAS 1.15:88524) Avail: NTIS HC A11/MF A01 CSCL 20D

The requirements for fundamental experimental studies of the influence of free stream turbulence, pressure gradients and wall cooling are discussed. Under turbine-like free stream conditions, comprehensive tests of transitional boundary layers with laminar, reversing and turbulent flow increments were performed to decouple the effects of the parameters and to determine the effects during mutual interaction. Author

N87-16984# Von Karman Inst. for Fluid Dynamics, Rhode-Saint-Genese (Belgium).
TWO-PHASE FLOWS IN MAJOR TECHNOLOGICAL HAZARDS, VOLUME 3
1986 312 p Lecture held in Rhode-Saint-Genese, Belgium, 24-28 Mar. 1986
(VKI-LS-1986-03-Vol-3; ETN-87-98843) Avail: NTIS HC A14/MF A01

A general classification of two-phase flow codes and present approachs to two-phase flow problems are outlined. The safety problems in nuclear power plants are particularly referred to. For individual titles, see N87-16985 through N87-16986.

N87-16985# Battelle Inst., Frankfurt am Main (West Germany).
GENERAL CLASSIFICATION OF TWO-PHASE FLOW CODES
L. Wolf *In* Von Karman Inst. for Fluid Dynamics Two-Phase Flows in Major Technological Hazards, Volume 3 1986 147 p (For primary document see N87-16984 09-34)
Avail: NTIS HC A14/MF A01

Possible characteristics for the classification of two-phase flow codes are located in the space formed by the criteria: dimensionality, spatial averaging approach, and two-phase flow representation. Evaluation model codes for licensing evaluation and best estimate codes for realistic predictions are compared. The complementary character of global and local empiricisms required for implementation into the codes using different dimensionality and number of field equations to simulate the two phase flow is qualitatively shown. The optimal decision basis relates the choice of computer code to the risk involved. It would be wrong to apply the software used to analyze large LOCA to the whole spectrum of pipe breaks. ESA

N87-16986# Battelle Inst., Frankfurt am Main (West Germany).
REVIEW OF PRESENT APPROACHES TO TWO-PHASE FLOW PROBLEMS

L. Wolf *In* Von Karman Inst. for Fluid Dynamics Two-Phase Flows in Major Technological Hazards, Volume 3 1986 162 p (For primary document see N87-16984 09-34)
Avail: NTIS HC A14/MF A01

Experimental data and computational results of interest in the context of major technological hazards are reviewed. The discussed areas of two-phase flow include pipe break flow, vessel depressurization, flow through safety relief valves, and two-phase flow jet formation and impingement. Although most data stems from nuclear reactor safety research, important conclusions may be drawn for other technical areas. Data and simulations from models of different sophistication are shown. The applicability of the individual two-phase models and associated codes are discussed. ESA

N87-16987# Von Karman Inst. for Fluid Dynamics, Rhode-Saint-Genese (Belgium).
INTRODUCTION TO NUMERICAL SOLUTION OF INDUSTRIAL FLOWS, VOLUME 1
1986 317 p Lecture held in Rhode-Saint-Genese, Belgium, 12-16 May 1986
(VKI-LS-1986-07-Vol-1; ETN-87-98844) Avail: NTIS HC A14/MF A01

Industrial flow problem flow equations and the steps to be followed in the selection and implementation of a solution technique are discussed. Heat transfer, flow around bluff bodies, dispersion in atmospheric flows, and mass and heat transfer in particulate beds are discussed. For individual titles, see N87-16988 through N87-16993.

N87-16988# Vrije Universiteit, Brussels (Belgium). Dept. of Fluid Dynamics.
AN ANALYSIS OF FLOW MODELS: FROM NAVIER-STOKES TO POTENTIAL FLOW EQUATIONS
Ch. Hirsch *In* Von Karman Inst. for Fluid Dynamics Introduction to Numerical Solution of Industrial Flows, Volume 1 1986 28 p (For primary document see N87-16987 09-34)
Avail: NTIS HC A14/MF A01

Approximation levels to simplify the full system of Reynolds averaged Navier-Stokes equations are presented. The latter are considered as the highest level model of flow description and depend heavily on the turbulence models. Viscous approximations such as the thin shear layer and the parabolized Navier-Stokes models are discussed. The disturbed loss model, applied in turbomachinery, is intermediate between viscous and inviscid approximations. The Euler equations, rotational flow models, and the simplest potential flow are discussed, and their limitations are pointed out. ESA

N87-16989# Vrije Universiteit, Brussels (Belgium). Dept. of Fluid Mechanics.
THE SPATIAL LEVELS OF APPROXIMATION FROM THREE-DIMENSIONAL TO QUASI ONE-DIMENSIONAL REPRESENTATION
Ch. Hirsch *In* Von Karman Inst. for Fluid Dynamics Introduction to Numerical Solution of Industrial Flows, Volume 1 1986 32 p (For primary document see N87-16987 09-34)
Avail: NTIS HC A14/MF A01

The averaging method is presented as an alternative to the stream or pseudo-stream surface methods. This approach consists of averaging out the conservation equations with respect to a chosen coordinate, obtaining equations with the remaining variables as independent variables. Limits of integration have to be defined and hence this procedure is best suited for internal flows with streamwise varying cross sections. The procedure can also be extended to an averaging over a two dimensional region such as the cross section of a channel, leading to a quasi two dimensional flow description. Interest lies mainly in the field of bounded or internal flows. ESA

N87-16990# Vrije Universiteit, Brussels (Belgium). Dept. of Fluid Mechanics.
REVIEW OF DISCRETIZATION TECHNIQUES AND NUMERICAL RESOLUTION METHODS **c64**
Ch. Hirsch *In* Von Karman Inst. for Fluid Dynamics Introduction to Numerical Solution of Industrial Flows, Volume 1 1986 56 p (For primary document see N87-16987 09-34)
Avail: NTIS HC A14/MF A01

Explicit and implicit flow analysis methods, direct and iterative methods, and preconditioning and multigrid convergence acceleration methods are discussed. It is shown that in setting up a numerical scheme the decision steps include a selection of the discretization methods, a selection of the resolution method, and an analysis of the selected numerical algorithm. The finite difference method, the finite element method, and variational methods are described and illustrated. ESA

N87-16991# Vrije Universiteit, Brussels (Belgium). Dept. of Fluid Mechanics.
THE ANALYSIS AND RESOLUTION OF NUMERICAL SCHEMES **c64**
Ch. Hirsch *In* Von Karman Inst. for Fluid Dynamics Introduction to Numerical Solution of Industrial Flows, Volume 1 1986 27 p (For primary document see N87-16987 09-34)
Avail: NTIS HC A14/MF A01

Stability, convergence, and consistency are defined in order to analyze the properties of numerical schemes derived from equations in mathematical flow models. It is shown that for a well posed initial value problem and a consistent discretization scheme, stability is the necessary and sufficient condition for convergence. The von Neumann method for stability analysis, based on the analysis of the Fourier transforms, is described. This method is the most widely applied technique and the amplification factor is easily obtained. The stability conditions cannot always be derived analytically, but one could, if necessary, analyze the properties of the amplification matrix numerically. ESA

N87-16992# Surrey Univ., Guildford (England). Dept. of Mechanical Engineering.
AN INTRODUCTION TO NUMERICAL METHODS FOR FLOW AROUND BLUFF BODIES
I. P. Castro *In* Von Karman Inst. for Fluid Dynamics Introduction to Numerical Solution to Industrial Flows, Volume 1 1986 83 p (For primary document see N87-16987 09-34)
Avail: NTIS HC A14/MF A01

Bluff body flow is presented, emphasizing aspects of particular significance for numerical prediction. The major approaches to numerical prediction of bluff body flows are outlined, including the discrete vortex method and the more conventional turbulence modeling techniques. Finite difference versions are discussed. ESA

N87-16993# Central Electricity Research Labs., Leatherhead (England). Technical Planning and Research Div.
AN INTRODUCTION TO THE NUMERICAL MODELLING OF DISPERSION IN THE ATMOSPHERIC BOUNDARY LAYER **c45**
A. G. Robins *In* Von Karman Inst. for Fluid Dynamics Introduction to Numerical Solution to Industrial Flows, Volume 1 1986 82 p (For primary document see N87-16987 09-34)
Avail: NTIS HC A14/MF A01

The numerical treatment of passive contaminant dispersion is considered, starting from diffusivity theory and leading to second order closure techniques, and including the prediction of both mean and fluctuating concentration levels. Lagrangian statistical models are also discussed. Building-affected dispersion and buoyant plume behavior are treated. Mesoscale and dense gas dispersion modeling are considered. The restrictions imposed by natural variability are commented and a preference for simple models is sustained. ESA

N87-16994# Von Karman Inst. for Fluid Dynamics, Rhode-Saint-Genese (Belgium).
INTRODUCTION TO NUMERICAL SOLUTION OF INDUSTRIAL FLOWS, VOLUME 2
1986 237 p Lecture held in Rhode-Saint-Genese, Belgium, 12-16 May 1986

(VKI-LS-1986-07-Vol-2; ETN-87-98845) Avail: NTIS HC A11/MF A01

Flow equations and the steps to be followed in the selection and implementation of a solution technique are discussed. Heat transfer, flow around bluff bodies, dispersion in atmospheric flows, and mass and heat transfer in particulate beds are considered. For individual titles, see N87-16995 through N87-16999.

N87-16995# Ecole Centrale de Lyon (France). Lab. de Mecanique des Fluides.

NUMERICAL METHODS FOR TWO-DIMENSIONAL AND THREE-DIMENSIONAL HEAT TRANSFER CALCULATIONS

D. Jeandel, M. Buffat, and Philippe Carriere *In* Von Karman Inst. for Fluid Dynamics Introduction to Numerical Solution of Industrial Flows, Volume 2 1986 98 p (For primary document see N87-16994 09-34)

Avail: NTIS HC A11/MF A01

The numerical simulation of two and three dimensional natural convection is studied, including the basic equations, the fractional step method, a discrete formulation of the convection step, the discretization of the Stokes solver, and examples. Direct and iterative methods for solving large scale systems are described. The numerical simulation of turbulent variable density fluid flows is discussed, including time discretization Urzawa method, approximations, Urzawa algorithm with conjugate gradient method, balancing tensor diffusivity for convection dominated flow, and applications to strongly heated axisymmetric systems. ESA

N87-16996# Flow Science, Inc., Los Alamos, N. Mex.

SOLA: A BASIC SOLUTION ALGORITHM FOR FLOW ANALYSIS **c64**

C. W. Hirt *In* Von Karman Inst. for Fluid Dynamics Introduction to Numerical Solution of Industrial Flows, Volume 2 1986 21 p (For primary document see N87-16994 09-34)

Avail: NTIS HC A11/MF A01

A finite difference numerical method for the time dependent, two-dimensional Navier-Stokes equation is outlined. The steps to make one complete time-step advancement of the iterative procedure are summarized. The boundary conditions options included in the computer code are described. A compressible flow extension is discussed. ESA

N87-16997# Flow Science, Inc., Los Alamos, N. Mex.

APPLICATIONS OF SOLA TO CONFINED FLOWS **c64**

C. W. Hirt *In* Von Karman Inst. for Fluid Dynamics Introduction to Numerical Solution of Industrial Flows, Volume 2 1986 25 p (For primary document see N87-16994 09-34)

Avail: NTIS HC A11/MF A01

The applications of a simplified finite difference flow computing method are discussed. The algorithm is based on the marker and cell method. The adaptation of the method to various geometric configurations is studied, discussing pipe expansions, free-slip versus non-slip boundaries, and curved boundaries. Time scale considerations are made referring to a one dimensional acoustic wave example. It is shown that an easily modifiable algorithm such as the one discussed is a powerful tool for a much wider range of applications than intended in its original formulation. Air pollution, stratified flow, and swirl studies are described. ESA

N87-16998# Flow Science, Inc., Los Alamos, N. Mex.

APPLICATIONS OF SOLA TO FREE SURFACE FLOWS **c64**

C. W. Hirt *In* Von Karman Inst. for Fluid Dynamics Introduction to Numerical Solution of Industrial Flows, Volume 2 1986 22 p (For primary document see N87-16994 09-34)

Avail: NTIS HC A11/MF A01

The applications of a finite difference flow algorithm are described. Free boundary cases are presented. For a restricted class of problems, the simple height function method used in the SOLA-SURF computer program can be very efficient. For more general free surface problems the fractional volume-of-fluid (VOF) method used in the SOLA-VOF program is necessary. The treated cases include wave forces on submerged bodies, fluid-structure impacts, ship hydrodynamics, suppression pool surge, bubble collapse, and oil/water flow. ESA

N87-16999# Von Karman Inst. for Fluid Dynamics, Rhode-Saint-Genese (Belgium).

PREDICTION OF HEAT AND MASS TRANSFER IN PARTICULATE BEDS

J.-M. Buchlin *In its* Introduction for Numerical Solution of Industrial Flows, Volume 2 1986 68 p (For primary document see N87-16994 09-34)

Avail: NTIS HC A11/MF A01

Numerical prediction methods are discussed and shown for two deterministic models, used to simulate the thermal behavior of particulate beds. The general two phase (fluid-solid) model is applied to determine the temperature field in a bed reactor cooled by a forced flow of gas. The formation of hot spots due to possible nonuniformities of the solid occupancy is emphasized. A homogeneous model to predict the thermohydraulic behavior of a liquid saturated and self heated particulate bed experiencing boiling process is presented. For the two cases, numerical methods relying upon finite difference techniques are described. ESA

N87-17000*# National Aeronautics and Space Administration. Marshall Space Flight Center, Huntsville, Ala.

SPACE SHUTTLE MAIN ENGINE HIGH PRESSURE FUEL PUMP AFT PLATFORM SEAL CAVITY FLOW ANALYSIS

S. A. Lowry and L. W. Keeton (CHAM of North America, Inc., Huntsville, Ala.) Jan. 1987 134 p

(NASA-TP-2685; NAS 1.60:2685) Avail: NTIS HC A07/MF A01 CSCL 20D

A general purpose, three-dimensional computational fluid dynamics code named PHOENICS, developed by CHAM Inc., is used to model the flow in the aft-platform seal cavity in the high pressure fuel pump of the space shuttle main engine. The model is used to predict the temperatures, velocities, and pressures in the cavity for six different sets of boundary conditions. The results are presented as input for further analysis of two known problems in the region, specifically: erratic pressures and temperatures in the adjacent coolant liner cavity and cracks in the blade shanks near the outer diameter of the aft-platform seal. Author

N87-17001*# National Aeronautics and Space Administration. Lewis Research Center, Cleveland, Ohio.

ANALYSIS OF VISCOUS TRANSONIC FLOW OVER AIRFOIL SECTIONS

Dennis L. Huff, Jiunn-Chi Wu (Georgia Inst. of Tech., Atlanta), and L. N. Sankar Jan. 1987 32 p Presented at the 25th Aerospace Sciences Meeting, Reno, Nev., 12-15 Jan. 1987; sponsored by AIAA

(NASA-TM-88912; E-3340; NAS 1.15:88912; AIAA-87-0420) Avail: NTIS HC A03/MF A01 CSCL 20D

A full Navier-Stokes solver has been used to model transonic flow over three airfoil sections. The method uses a two-dimensional, implicit, conservative finite difference scheme for solving the compressible Navier-Stokes equations. Results are presented as prescribed for the Viscous Transonic Airfoil Workshop to be held at the AIAA 25th Aerospace Sciences Meeting. The NACA 0012, RAE 2822 and Jones airfoils have been investigated for both attached and separated transonic flows. Predictions for pressure distributions, loads, skin friction coefficients, boundary layer displacement thickness and velocity profiles are included and compared with experimental data when possible. Overall, the results are in good agreement with experimental data. Author

N87-17002*# National Aeronautics and Space Administration. Lewis Research Center, Cleveland, Ohio.

A GENERAL METHOD FOR UNSTEADY STAGNATION REGION HEAT TRANSFER AND RESULTS FOR MODEL TURBINE FLOWS

Tuncer Cebeci (California State Univ., Long Beach), Andreas Krainer (Naval Postgraduate School, Monterey, Calif.), Robert J. Simoneau, and Max F. Platzer 1987 8 p Proposed for presentation at the 2nd Thermal Engineering Conference, Honolulu, Hawaii,

22-27 Mar. 1987; sponsored by the ASME and JSME
(NASA-TM-88903; E-3329; NAS 1.15:88903) Avail: NTIS HC A02/MF A01 CSCL 20D

Recent experiments suggest that the heat-transfer characteristics of stator blades are influenced by the frequency of passing of upstream rotor blades. The calculation of these effects requires that the movement of the stagnation point with variations in freestream velocity is properly represented together with the possible effects of turbulence characteristics on the thin leading-edge boundary layer. A procedure to permit the achievement of these purposes is described for laminar flows in this paper together with results of its application to two model problems which demonstrate its abilities and quantify the influence of wake characteristics on fluid-dynamic and heat-transfer properties of the flow and their effects on surface heat transfer. Author

N87-17003*# Texas A&M Univ., College Station. Turbomachinery Labs.
MEASUREMENT OF HEAT TRANSFER AND PRESSURE DROP IN RECTANGULAR CHANNELS WITH TURBULENCE PROMOTERS Final Report
J. C. Han, J. S. Park, and M. Y. Ibrahim Washington NASA Sep. 1986 203 p
(Contract NAS3-24227; DA Proj. 1L1-62209-AH-76)
(NASA-CR-4015; E-3164; NAS 1.26:4015; AVSCOM-TR-86-C-25) Avail: NTIS HC A10/MF A01 CSCL 20D

Periodic rib turbulators were used in advanced turbine cooling designs to enhance the internal heat transfer. The objective of the present project was to investigate the combined effects of the rib angle of attack and the channel aspect ratio on the local heat transfer and pressure drop in rectangular channels with two opposite ribbed walls for Reynolds number varied from 10,000 to 60,000. The channel aspect ratio (W/H) was varied from 1 to 2 to 4. The rib angle of attack (alpha) was varied from 90 to 60 to 45 to 30 degree. The highly detailed heat transfer coefficient distribution on both the smooth side and the ribbed side walls from the channel sharp entrance to the downstream region were measured. The results showed that, in the square channel, the heat transfer for the slant ribs (alpha = 30 -45 deg) was about 30% higher that of the transverse ribs (alpha = 90 deg) for a constant pumping power. However, in the rectangular channels (W/H = 2 and 4, ribs on W side), the heat transfer at alpha = 30 -45 deg was only about 5% higher than 90 deg. The average heat transfer and friction correlations were developed to account for rib spacing, rib angle, and channel aspect ratio over the range of roughness Reynolds number. GRA

N87-17004*# Colorado Univ., Boulder. Dept. of Mathematics
SELECTION PRINCIPLES AND PATTERN FORMATION IN FLUID MECHANICS AND NONLINEAR SHELL THEORY Semiannual Progress Report, 1 Sep. 1986 - 28 Feb. 1987
Duane P. Sather Feb. 1987 6 p
(Grant NAG2-278)
(NASA-CR-180159; NAS 1.26:180159) Avail: NTIS HC A02/MF A01 CSCL 20D

Wave theories of vortex breakdown were studied. A setting which involved dynamical systems and bifurcations of homoclinic and heteroclinic orbits in infinite-dimensional spaces was investigated. The determination of axisymmetric inviscid flows bifurcating from the primary flow lead to the study of a system of ordinary differential equations. The problem of rotating plane Couette flow was solved by means of the structure parameter approach. B.G.

N87-17005# Department of the Air Force, Washington, D.C.
EXPANDABLE PULSE POWER SPACECRAFT RADIATOR Patent Application
Edward T. Mahefkey, inventor (to Air Force) 18 Jun. 1986 23 p
(AD-D012498; US-Patent-Appl-SN-875808) Avail: NTIS HC A02/MF A01 CSCL 20/13

An expandable heat rejection system for radiating heat generated by a source of heat on a spacecraft or like vehicle is described and comprises a fluid heat exchange medium in operative heat exchange contact with the source for absorbing heat by evaporation of liquid phase of the medium, a thin flexible wall structure having an inlet and an outlet and defining a volume expandable and collapsible between preselected limits and defining an inner condensation surface and an outer heat radiating surface, a multiplicity of capillary grooves on the condensation surface for promoting condensation of vaporous medium and for facilitating flow of condensate along the condensation surface toward the outlet, and a pump circulating the medium through the system. GRA

N87-17006# Stanford Univ., Calif.
PROCEEDINGS OF THE 15TH INTERNATIONAL SYMPOSIUM ON SHOCK WAVES AND SHOCK TUBES Final Report, 1 Feb. 1985 - 31 Jan. 1986
Daniel Bershader and Ronald Hanson Sep. 1986 881 p Proceedings held in Berkeley, Calif., 28 Jul. - 2 Aug. 1985
(Grant DAAG29-85-G-0079)
(AD-A173026; ARO-22564.1-EG) Avail: NTIS HC A99/MF A02 CSCL 19/4

One hundred ten papers were presented in 32 sessions. Topics included: The application of Hook-method spectroscopy to the diagnosis of shock-heated gases. The nonintrusive destruction of kidney stones by underwater focused shock waves. Several of the papers reflect the recent and continuing interest in shock wave phenomena in dusty gases and other multiphase and heterogeneous systems, including chemically reactive configurations. The major subject areas were: shock propagation and interactions; shock-general chemical kinetics; shock computation, modeling, and stability problems; shock wave aerodynamics; experimental methods; shocks in multiphase and heterogeneous media; high energy gas excitation and wave phenomena; and technical applications and shocks in condensed matter. GRA

N87-17007# Michigan State Univ., East Lansing. Turbulence Structure Lab.
EXPERIMENTAL INVESTIGATION OF THE TURBULENCE PRODUCTION MECHANISM IN BOUNDARY LAYERS Annual Report, 1 Oct. 1984 - 30 Sep. 1985
R. E. Falco Aug. 1986 41 p
(Contract F49620-85-C-0002)
(AD-A173091; TSL-85-3; AFOSR-86-0942TR) Avail: NTIS HC A03/MF A01 CSCL 20/4

The mechanism of production of the long streaks and a mechanism for creation of vortex ring-like typical eddies are described, and the occurrence of both within a real turbulent boundary layer demonstrated. These aspects were the missing links needed to complete the conceptual structural model. This model de-emphasizes the importance of hairpin vortices in wall layer transport. However, experimental determination of the relative importance of each of the elements of the model in low Reynolds number layers is far from complete, and we know very little of the Reynolds number dependence or pressure gradient dependence of the model. What has been learned so far suggests several critical parameters that can be manipulated to control the production of turbulence and hence reduce drag. In the proposed research the focus is on acquiring additional data to support the rational theory that has been formed so as to provide the basis for determining how much leverage there is to control boundary layer turbulence. GRA

N87-17008# Princeton Univ., N. J. Dept. of Mechanical and Aerospace Engineering.
THE STUDY OF SHOCK WAVE AND TURBULENT BOUNDARY LAYER INTERACTIONS Final Report, 1 Aug. 1984 - 31 Jul. 1986
Seymour M. Bogdonoff Nov. 1986 43 p
(Contract F49620-84-C-0086)
(AD-A175033; Rept-1767-MAE; AFOSR-86-2175TR) Avail: NTIS HC A03/MF A01 CSCL 20/4

The three dimensional shock wave turbulent boundary layer interaction generated by several shock generators defined solely by angles has been carried out at a Mach number of 3. Interactions with thin boundary layers were used to obtain overall characteristics,

while interactions with thick boundary layers permitted detailed high resolution surveys. Investigations of the interactions were carried out by mean and high frequency surface pressure distribution measurements, surface flow visualization, and mean total head, yaw, and static pressure distributions through the flowfield. Major new data sets were obtained for the interaction of the shock wave generated by a 20 deg fin, and by a 24 deg wedge swept at 60 deg to the incoming flow. A series of tests were carried out to examine new concepts of three-dimensional interactions and extensive non-steady results were obtained from the high frequency surface pressure distributions. Close coordination of the experiments with major computational efforts, support new concepts of flow structure and physics for these complex interactions. GRA

N87-17009# Lawrence Livermore National Lab., Calif.
DIRECT COMPUTATION OF WALL BOUNDED AEROSOL TURBULENT FLOW INTERACTIONS
A. C. Buckingham 1986 16 p Presented at the 3rd International Conference on Numerical Methods for Non-Linear Problems, Dubrovnik, Yugoslavia, 15 Sep. 1986
(Contract W-7405-eng-48)
(DE86-013221; UCRL-94800; CONF-8609116-1) Avail: NTIS HC A02/MF A01

A method is described for direct numerical simulations of the statistical interactions between spherical solid particles and a turbulent carrier gas that entrains them. At the present stage of method development, the emphasis is on analysis of wall bounded turbulent, two phase, compressible flow. The bounding geometry described here is a two dimensional channel. The numerical procedure is designed to resolve statistical flow features of both dispersed and continuous phases. The numerical simulations combine a truncated spectral transform collocation procedure for the continuous phase with a Monte Carlo Lagrangian procedure for the dispersed phase. The continuous phase is iteratively matched at discrete time intervals to a random-walk Lagrangian statistical sampling procedure for the dispersed phase momenta and position expectancies. Ensemble averaging produces statistical velocity moments for both dispersed and continuous phases. DOE

N87-17010# Rolls-Royce Ltd., Derby (England).
OBSERVATIONS ON THE TURBULENT STRUCTURE IN AN UNSTEADY, NORMAL SHOCK/BOUNDARY-LAYER INTERACTION
L. C. Squire (Cambridge Univ., England) and J. A. Edwards 24 Sep. 1986 8 p Repr. from ICAS
(PNR90361; ICAS-86-1.2.2; ETN-87-98791) Avail: NTIS HC A02/MF A01

The turbulence structure in an interaction between an oscillating normal shock and a thick turbulent boundary layer was studied using optical methods. The results from the optical studies, together with mean and fluctuating surface pressures are used to illuminate the effects of unsteadiness on the interaction. Failure of the main tunnel window interrupted the tests, but the Schlieren and shadowgraph photography, holographic interferometry, and dynamic Schlieren methods are shown to be valuable. ESA

N87-17011# Institut Franco-Allemand de Recherches, St. Louis (France).
AFTERBODY SHAPE EFFECTS ON THE NEAR-WAKE VELOCITY CHARACTERISTICS AT MACH NUMBERS BETWEEN 0.35 AND 0.92
C. Berner 18 Feb. 1986 12 p Presented at the 38th Annual Meeting of the American Physical Society Div. of Fluid Dynamics, Tucson, Ariz., 24-27 Nov. 1985 Original contains color illustrations
(ISL-CO-205/86; ETN-87-98801) Avail: NTIS HC A02/MF A01

The effect of changing base geometry on near-wake velocity characteristics was studied in an annular nozzle facility whose Mach number ranged between M = 0.2 and 0.93. The models were axisymmetric and consisted of a cylindrical afterbody and several conical boattails. Centerline distribution of the axial and radial components of the mean velocity and corresponding fluctuations such as turbulent intensities and turbulent kinetic energy were obtained by a two-dimensional laser Doppler velocimeter. At constant Mach number, the length of the recirculating region is reduced when increasing the angle and the length of the boattail. This influence is more important when increasing the angle than the length. The same effects can be observed for the turbulent quantities. ESA

N87-17012# Institut Franco-Allemand de Recherches, St. Louis (France).
EXPERIMENTAL INVESTIGATION IN TURBULENT FLOW SEPARATION
C. Berner 30 Apr. 1986 29 p Presented at Wright-Patterson AFB Conference, Dayton, Ohio, 19 Nov. 1985
(ISL-CO-208/86; ETN-87-98803) Avail: NTIS HC A03/MF A01

Laser Doppler velocimeter measurements of the flow field around an airfoil equipped with a spoiler and of the flow field in the near wake of blunt bodies are presented. The results are used in studies of control surfaces and to test turbulence models and the effect of base geometry on near wake velocity. ESA

N87-17013# Office National d'Etudes et de Recherches Aerospatiales, Paris (France). Direction de l'Aerodynamique.
THREE-DIMENSIONAL SEPARATION ON A CYLINDRICAL ELLIPSOID. RESULTS OF THE FIRST TEST CAMPAIGN ON THE F2 WIND TUNNEL [DECOLLEMENT TRIDIMENSIONNEL SUR UN ELLIPSOIDE-CYLINDRE DE REVOLUTION. RESULTATS DE LA PREMIERE CAMPAGNE D'ESSAIS A F2]
B. Chanetz Feb. 1986 144 p In FRENCH
(ONERA-RT-16/7252-AN; ETN-87-98811) Avail: NTIS HC A07/MF A01

Wind tunnel tests were performed on an ellipsoidal cylinder of revolution (ECR) in order to study the three-dimensional flow separation on obstacles with a simple form and to verify theoretical models. The first results allow to give a precise description of the wall flow for upstream velocities between 10 and 90 m/sec and angles of incidence between 0 and 40 deg. The formation of two layers with vortex flow is clearly shown from an angle of incidence of 20 deg on. The flow structure shows to be perfectly symmetrical with respect to the vertical symmetry plane, even for the highest angles of incidences. A laminar separation a little downstream of the models nose is also observed; it induces the boundary layer transition, and is followed by a turbulent reconnection leading to a flattened bulb structure. ESA

N87-17014# Technische Hogeschool Twente, Enschede (Netherlands). Dept. of Applied Mathematics.
ON VARIATIONAL CHARACTERIZATIONS OF STEADY VORTEX RINGS
E. vanGroesen and C. vanderBeek (Technische Hogeschool, Delft (Netherlands).) Jul. 1986 12 p
(MEMO-577; ISSN-0169-2690; ETN-87-99056) Avail: NTIS HC A02/MF A01

Variational formulations that describe a single, steadily propagating, axially symmetric vortex ring in an ideal fluid are considered. It is shown that the two apparently different formulations proposed by Fraenkel and Berger (1974) and by Friedman (1982) are related to one another by a Legendre transform. Variational principles that describe vortex rings of prescribed total energy are presented. ESA

N87-17015# Technische Hogeschool Twente, Enschede (Netherlands). Dept. of Applied Mathematics.
EFFECTIVE PERMEABILITY AND MACRODISPERSION IN LOCALLY HETEROGENEOUS AQUIFERS
Adriaan D. Poley Aug. 1986 18 p
(MEMO-585; ISSN-0169-2690; ETN-87-99064) Avail: NTIS HC A02/MF A01

The global effective permeability and hydrodynamic dispersion tensors due to flow in locally heterogeneous and statistically anisotropic aquifers are analyzed using the self-consistent approximation. For small perturbations the results for the statistically anisotropic case are shown to be consistent with those derived using stochastic continuum theory. However, for larger perturba-

tions the stochastic continuum theory does not produce rigorous results for comparison. The theory indicates that a classical gradient transport (Fickian) relationship is valid for large-scale displacements. ESA

N87-16949# Liege Univ. (Belgium).
THE EXTENDABLE REFRACTABLE MAST (ERM) THERMAL ANALYSIS: A HEAT RADIATION CASE STUDY VIA THE FINITE ELEMENT METHOD
M. Hogge, J. P. Cobut, J. Fagnoul, E. Stenne, and P. M. Leonard *In* ESA Proceedings of the Second ESA Workshop on Mechanical Technology for Antennas Aug. 1986 p 227-235 (For primary document see N87-16923 09-32)
Avail: NTIS HC A12/MF A01

35 INSTRUMENTATION AND PHOTOGRAPHY

Includes remote sensors; measuring instruments and gages; detectors; cameras and photographic supplies; and holography.

For aerial photography see *43 Earth Resources and Remote Sensing.* For related information see also *06 Aircraft Instrumentation,* and *19 Spacecraft Instrumentation.*

N87-17016*# National Aeronautics and Space Administration. Marshall Space Flight Center, Huntsville, Ala.
INTERFACE CIRCUITRY FOR SUPERCONDUCTING BOLOMETER
P. J. Nelson Jan. 1987 11 p
(NASA-TM-86581; NAS 1.15:86581) Avail: NTIS HC A02/MF A01 CSCL 14B

The interface circuitry described links the computer with the superconducting bolometer array. This helps demonstrate the feasibility of the array. Using the circuitry and the array, imaging will be made possible. Initial imaging will be done on laboratory objects, and the pixel characteristics will be investigated experimentally. Author

N87-17017*# National Aeronautics and Space Administration. Marshall Space Flight Center, Huntsville, Ala.
LOW-g MEASUREMENTS BY NASA
Roger P. Chassay and Arthur J. Schwaniger, Jr. Dec. 1986 46 p
(NASA-TM-86585; NAS 1.15:86585) Avail: NTIS HC A03/MF A01 CSCL 14B

Low-g accelerometers were used by NASA on a variety of flights for over 12 years. These flights have included aircraft parabolas, suborbital trajectories, and orbital missions. This large quantity of data has undergone only limited in-depth analyses. Examples of data in many forms and results of analyses such as power spectral densities and shock spectra are given for a wide variety of missions. Accelerometers used to acquire the data are also identified. Author

N87-17018*# National Aeronautics and Space Administration. Langley Research Center, Hampton, Va.
A PRELIMINARY STUDY OF FACTORS AFFECTING THE CALIBRATION STABILITY OF THE IRIDIUM VERSUS IRIDIUM-40 PERCENT RHODIUM THERMOCOUPLE
Shaffiq Ahmed (Youngstown Univ., Ohio), Edward F. Germain, Kamran Daryabeigi, David W. Alderfer, and Robert E. Wright Jan. 1987 20 p
(NASA-TM-89086; NAS 1.15:89086) Avail: NTIS HC A02/MF A01 CSCL 14B

An iridium versus iridium-40% rhodium thermocouple was studied. Problems associated with the use of this thermocouple for high temperature applications (up to 2000 C) were investigated. The metallurgical studies included X-ray, macroscopic, resistance, and metallographic studies. The thermocouples in the as-received condition from the manufacturer revealed large amounts of internal stress caused by cold working during manufacturing. The thermocouples also contained a large amount of inhomogeneities and segregations. No phase transformations were observed in the alloy up to 1100 C. It was found that annealing the thermocouple at 1800 C for two hours, and then at 1400 C for 2 to 3 hours yielded a fine grain structure, relieving some of the strains, and making the wire more ductile. It was also found that the above annealing procedure stabilized the thermal emf behavior of the thermocouple for application below 1800 C (an improvement from + or - 1% to + or - 0.02% within the range of the test parameters used). Author

N87-17019# Department of the Air Force, Washington, D.C.
UNIVERSAL PRESSURE TRANSDUCER Patent Application
Robert E. Olson, inventor (to Air Force) Filed 30 Jun. 1986 15 p
(AD-D012499; US-Patent-Appl-SN-880245) Avail: NTIS HC A02/MF A01 CSCL 09/5

A pressure transducer system, which uses a Wheatstone bridge circuit to produce an electrical signal which is proportional to the amount of pressure exerted on it by gas or liquids, is disclosed. The Wheatstone bridge circuit is thermally isolated from the external environment using two diaphragms which are separated by a reservoir of silicone oil. This allows pressure to be hydraulically conveyed to the Wheatstone bridge circuit while preventing thermal contamination of the electrical signals produced by the Wheatstone bridge circuit. The pressure transducer also contains support circuitry which allows adjustment of the signals to and from the Wheatstone bridge circuit to enable the pressure transducer to be used with various electrical measuring equipment which has different operational ranges. Author (GRA)

N87-17020# Department of the Air Force, Washington, D.C.
UNITIZED HIGH TEMPERATURE PROBES Patent Application
Frederick J. Komanetsky, inventor (to Air Force) Filed 3 Jul. 1986 16 p
(AD-D012508; US-Patent-Appl-SN-882101) Avail: NTIS HC A02/MF A01 CSCL 14/2

The invention comprises a single piece metallic probe manufactured from high temperature material. The probe has integral kiel heads for static instrumentation and is formed in an airfoil shape that minimizes its negative effects on the engine flow stream. In the preferred embodiment of the invention the probe is manufactured by electrical discharge machining from a single piece of stock material. Other aspects of the preferred embodiment of the invention comprise an integral platform for attachment of the probe to an engine housing and static sensors mounted in integral kiel heads positioned on the leading edge of the probe airfoil. It is also preferred that the probe be manufactured from a high temperature material such as an Inconel nickel alloy. In an alternate embodiment of the invention the probe body may be manufactured by a casting method such as powdered metallurgy and finished machined by electrical discharge machining. GRA

N87-17021# Department of the Air Force, Washington, D.C.
INTERFEROMETRIC LOAD SENSOR AND STRAIN GAGE patent Application
William P. Dixon, inventor (to Air Force) 3 Jul. 1986 26 p
(AD-D012509; US-Patent-Appl-SN-882059) Avail: NTIS HC A03/MF A01 CSCL 14/2

The invention comprises a load sensor, or force balance, which utilizes an interferometer in place of conventional wire strain gages. A first etalon plate is positioned on a rigid fixture while the second etalon plate is positioned on a load sensitive fixture that is subject to flexure. The plates each have partially reflecting surfaces that are positioned opposite each other. It is preferred that the adjacent partially reflective surfaces of the two etalon plates are parallel within a few seconds. In a preferred embodiment of the load sensor, the air wedge gap between the two etalon plates is less than 5 seconds. When a monochromatic collimated light source is transmitted through the etalons, light fringes are produced between the two plates. The light fringes are very sensitive to the wedge angle but rather insensitive to the beam angle. Therefore,

flexing of the load sensitive fixture moves the second etalon plate and results in a fringe shift. Detector means are provided for detecting shifts in the light fringes between the etalons. GRA

N87-17022# Department of the Air Force, Washington, D.C.
SWITCHING NETWORK FOR MONITORING STATIONS Patent Application
Michael J. Gauder, inventor (to Air Force) Filed 24 Jun. 1986 46 p
(AD-D012514; US-Patent-Appl-SN-877926) Avail: NTIS HC A03/MF A01 CSCL 17/2

An engineer, who is monitoring signals on oscilloscopes, can use one of a set of pushbuttons to select a specific channel for future monitoring on one or more instruments. The switching network is controlled by a microprocessor and is designed to route any one of N (36) incoming analog signals to one of M (3) instrumentation inputs. The switching network is essentially M independent N-to-1 analog signal at a time can be selected for a single instrumentation channel, while pemitting a signal to be simultaneously used on any or all of the remaining instrumentation channels. A second contact on each relay provides means to tell if the selected relay is energized. Author (GRA)

N87-17023# Washington State Univ., Pullman. Shock Dynamics Lab.
DETERMINING AND MODELING THE RESPONSE OF YTERBIUM PIEZORESISTANCE TRNSDUCERS Final Report, Apr. 1982 - Mar. 1986
Yogendra M. Gupta May 1986 87 p
(Grant AF-AFOSR-0132-82)
(AD-A173085; AFOSR-86-0864TR) Avail: NTIS HC A05/MF A01 CSCL 09/1

The objectives and results of a research effort undertaken to understand the response of ytterbium stress transducers under shock loading are presented. Plate impact experiments, using matrix materials that covered a wide range of mechanical impedances, were performed to determine the gauge response under well characterized conditions. Experiments were designed to conform closely to the requirements of the theoretical analysis. Residual resistance measurements, loading rate effects, and effect of matrix property variations were examined in detail. Quasi-static experimental methods and related analysis were developed to determine the complete set of electro-mechanical constants for the foils of interest. The phenomenological model developed earlier was extended to include strain-hardening in a consistent manner. The model predictions, using the appropriate material constants, agreed very well with the shock wave measurements. Using the analytic model a good understanding of ytterbium stress transducers was achieved. GRA

N87-17024# Rolls-Royce Ltd., Derby (England). Advanced Research Lab.
INDUSTRIAL HOLOGRAPHY: THE ROLLS-ROYCE EXPERIENCE
R. J. Parker and D. G. Jones 29 Jul. 1986 45 p Presented at The International Seminar on Laser and Optoelectronic Technology in Industry: A State of the Art Review, Xiamen, China, 25-27 Jun. 1986 Submitted for publication
(PNR90351; RR(OH)925; ETN-87-98786) Avail: NTIS HC A03/MF A01

Holographic interferometry applications to flow visualization, nondestructive testing, vibration analysis, and holographic contouring are described. Problems encountered and overcome in applying these techniques in a demanding, at times hostile, environment away from the laboratory are discussed. Holography for routine vibration analysis; pulsed holography of large, vibrating assemblies; holographic vibrometry on rotating components; holographic flow visualization in wind tunnels; and pulsed holography in rotating, transonic flow are illustrated. ESA

N87-17025# Institut Franco-Allemand de Recherches, St. Louis (France).
A NEW METHOD FOR COMPENSATING AND MEASURING ANY MOTION OF 3D-OBJECTS IN HOLOGRAPHIC INTERFEROMETRY: RECENT DEVELOPMENTS
A. Stimpfling and P. Smigielski (Strasbourg Univ., France) 19 Dec. 1985 9 p Presented at the 2nd International Technical Symposium on Optical and Electro-optical Applied Science and Engineering. Progress in Holographic Applications, Cannes, France, 2-6 Dec. 1985
(ISL-CO-242/85; ETN-87-98798) Avail: NTIS HC A02/MF A01

A method allowing the compensation and the measurement of the complex motion of an object, the amplitude of which can be greater than the coherence length of the laser used for the holographic recording, is proposed. The method, called Complete Motion Compensation, can be used for real-time, time-average, and double-exposure holographic interferometry even in the case of high-speed phenomena. The rigid block composed by the holographic image and by illuminating object beam is moved to exactly superimpose the object and its holographic image (infinite fringe, i.e., exact compensation of the optical path variations). A perfect optical path compensation only occurs for rigid body motion. In the case of the deformation of an object, the compensation can be done only for a small area. The whole object surface deformation can be studied spot by spot. Rigid displacements and deformations can be quantified by measuring the displacements of the whole rigid block without taking account of the fringe spacing or localization distances. ESA

N87-17112*# Daedalus Enterprises, Inc., Ann Arbor, Mich.
THE TIMS INSTRUMENT
Chuck Stanich *In* JPL, California Inst. of Technology The TIMS Data User's Workshop 1 Nov. 1986 p 5-7 (For primary document see N87-17111 09-43)
Avail: NTIS HC A05/MF A01 CSCL 14B

N87-17113*# Jet Propulsion Lab., California Inst. of Tech., Pasadena.
THE TIMS INVESTIGATOR'S GUIDE
Frank D. Palluconi *In its* The TIMS Data User's Workshop 1 Nov. 1986 p 8 (For primary document see N87-17111 09-43)
Avail: NTIS HC A05/MF A01 CSCL 14B

N87-17115*# National Aeronautics and Space Administration. Earth Resources Lab., Bay St. Louis, Miss.
ATMOSPHERIC CORRECTION OF TIMS DATA
Doug Rickman *In* JPL, California Inst. of Technology The TIMS Data User's Workshop 1 Nov. 1986 p 11 (For primary document see N87-17111 09-43)
Avail: NTIS HC A05/MF A01 CSCL 14B

N87-17200# Tokyo Gas Co. Ltd. (Japan).
DEVELOPMENT OF INTELLIGENT PIPE LOCATOR
Y. Miyamoto and Y. Wasa (Nippon Electric Co. Ltd., Tokyo, Japan) *In* ESA Proceedings of the 1986 International Geoscience and Remote Sensing Symposium (IGARSS '86) on Remote Sensing: Today's Solutions for Tomorrow's Information Needs, Volume 1 Aug. 1986 p 217-222 (For primary document see N87-17163 09-43)
Avail: NTIS HC A99/MF E03; ESA, Paris, France, 3 volume set $90 Member States, AU, CN, and NO (+20% others)

N87-17256# Dornier-Werke G.m.b.H., Friedrichshafen (West Germany).
RECENT PROGRESS IN ERS-1 WIND SCATTEROMETER DESIGN
R. W. Zahn, D. Miller, A. Koppe, C. C. Lin (Marconi Space and Defence Systems Ltd., Portsmouth, England), and D. J. Carter *In* ESA Proceedings of the 1986 International Geoscience and Renote Sensing Symposium (IGARSS '86) on Remote Sensing: Today's Solutions for Tomorrow's Information Needs, Volume 1 Aug. 1986 p 567-572 (For primary document see N87-17163 09-43)
Avail: NTIS HC A99/MF E03; ESA, Paris, France, 3 volume set $90 Member States, AU, CN, and NO (+20% others)

N87-17257# Dornier-Werke G.m.b.H., Friedrichshafen (West Germany).

THE ERS-1 SCATTEROMETER SYSTEM SIMULATOR AND ITS RELEVANCE FOR GROUND PROCESSING DESIGN
H. Munz and P. Hans *In* ESA Proceedings of the 1986 International Geoscience and Remote Sensing Symposium (IGARSS '86) on Remote Sensing: Today's Solutions for Tomorrow's Information Needs, Volume 1 Aug. 1986 p 573-577 (For primary document see N87-17163 09-43)
Avail: NTIS HC A99/MF E03; ESA, Paris, France, 3 volume set $90 Member States, AU, CN, and NO (+20% others)

N87-17260*# National Aeronautics and Space Administration. Goddard Space Flight Center, Greenbelt, Md.
THE ELECTRONICALLY STEERED THINNED ARRAY RADIOMETER (ESTAR)
C. T. Swift (Massachusetts Univ., Amherst), C. Ruf, A. Tanner, and D. Levine *In* ESA Proceedings of the 1986 International Geoscience and Remote Sensing Symposium (IGARSS '86) on Remote Sensing: Today's Solutions for Tomorrow's Information Needs, Volume 1 Aug. 1986 p 591-593 (For primary document see N87-17163 09-43)
Avail: NTIS HC A99/MF E03; ESA, Paris, France, 3 volume set $90 Member States, AU, CN, and NO (+20% others) CSCL 14B

N87-17565# University Coll., London (England). Dept. of Physics.
THE INFLUENCE OF BACKGROUND POWER ON THE PERFORMANCE OF AN IDEAL BOLOMETER
M. J. Griffin *In* ESA Proceedings of an ESA Workshop on a Spaceborne Submillimeter Astronomy Mission. A Cornerstone of the ESA Long Term Science Program Aug. 1986 p 225-229 (For primary document see N87-17535 09-88)
Avail: NTIS HC A14/MF A01

N87-17567# Helsinki Univ. of Technology, Espoo (Finland).
AN 800 MHz BANDWIDTH ACOUSTO-OPTICAL SPECTROMETER AT HELSINKI OBSERVATORY
L. J. Malkamaeki *In* ESA Proceedings of an ESA Workshop on a Spaceborne Submillimeter Astronomy Mission. A Cornerstone of the ESA Long Term Science Program Aug. 1986 p 243-245 (For primary document see N87-17535 09-88)
Avail: NTIS HC A14/MF A01

N87-17569# Science Research Council, Chilton (England).
A 186 GHz RADIOMETER FOR THE MICROWAVE LIMB SOUNDER
P. D. Curtis, D. N. Matheson, D. R. Vizard, and G. E. Peckham (Heriot-Watt Univ., Edinburgh (Scotland).) *In* ESA Proceedings of an ESA Workshop on a Spaceborne Submillimeter Astronomy Mission. A Cornerstone of the ESA Long Term Science Program Aug. 1986 p 251-254 (For primary document see N87-17535 09-88)
Avail: NTIS HC A14/MF A01

36 LASERS AND MASERS

Includes parametric amplifiers.
For related information see also *76 Solid-State Physics.*

N87-17026*# National Aeronautics and Space Administration. Ames Research Center, Moffett Field, Calif.
PROJECTION LENS SCANNING LASER VELOCIMETER SYSTEM Patent
William D. Gunter, Jr., inventor (to NASA) and Anemarie DeYoung, inventor (to NASA) Issued 30 Dec. 1986 7 p Filed 18 Jan. 1985 Supersedes N85-20320 (23 - 11, p 1638)
(NASA-Case-ARC-11547-1; US-Patent-4,632,548; US-Patent-Appl-SN-692745; US-Patent-Class-356-28.5; US-Patent-Class-356-28) Avail: U.S. Patent and Trademark Office CSCL 20E

A laser Doppler velocimeter system is disclosed that has a laser, a waist position adjusting lens, and a beam splitter which direct laser beams parallel to the optical axis of the negative lens. The negative lens is fixed relative to an afocal lens pair. A pair of planar mirrors intersect at right angles and respectively intersect the optical axis and the optical axis of the afocal lens pair. Mirrors are movable along the optical axis toward and away from the afocal lens pair to focus the laser beams in focus area while maintaining a constant beam waist, crossing angle, and intersection with other laser beams. This produces a constant sensitive volume as the focus is changed. NASA

N87-17027# Lawrence Livermore National Lab., Calif.
OPTICAL MODELING OF INDUCTION-LINAC DRIVEN FREE-ELECTRON LASERS
E. T. Scharlemann and W. M. Fawley 31 Mar. 1986 26 p Presented at the SPIE Technical Symposium on Applications of Artificial Intelligence, Orlando, Fla., 31 Mar. 1986
(Contract W-7405-eng-48)
(DE87-001432; UCRL-94258; CONF-860366-12) Avail: NTIS HC A03/MF A01

The free-electron laser (FEL) simulation code FRED, developed at Lawrence Livermore National Laboratory (LLNL) primarily to model single-pass FEL amplifiers driven by induction linear accelerators, is described. The main emphasis is on the modeling of optical propagation in the laser and on the differences between the requirements for modeling RF-linac-driven vs. induction-linac-driven FELs. Examples of optical guiding and mode cleanup are presented for a 50 m FEL. DOE

37 MECHANICAL ENGINEERING

Includes auxiliary systems (nonpower); machine elements and processes; and mechanical equipment.

N87-17028 Alabama Univ., Birmingham.
DYNAMICS AND CONTROL OF FLEXIBLE MANIPULATORS Ph.D. Thesis
Jeries Jacob Abou-Hanna 1986 234 p
Avail: Univ. Microfilms Order No. DA8620097

Modeling and control of manipulator arms possessing structural flexibility and structural damping are examined. A modal approach is used throughout the work to obtain the mathematical model. The arm model is represented mathematically by a state space description defined from truncation on the distributed system. The model describes flexible perturbations superposed onto a prescribed rigid motion of the arm. The rigid motion is spatial and described in terms of the three joint angles of the arm. The actuators and load are represented by lump masses at respective positions along the arm. Structural damping is represented by equivalent viscous damping coefficients corresponding to each flexible mode. The researcher examines the problem of system control via the linearized model using a regulator type of control. The feedback gains are obtained from the equivalent rigid system with interjoint feedbacks and applied to the nonlinear flexible model. Structural damping allows a better control performance; it increases the damping ratio of the dominant poles of the flexible system at high speeds when compared to the undamped case. Some geometric parameters are optimized in order to maximize bandwidth for various payload sizes and programmed tasks. The study examines the controlled system under constant gains using the nonlinear model for simulations following a time varying state trajectory. Dissert. Abstr.

N87-17029 California Univ., Los Angeles.
A MODIFIED LOOP TRANSFER RECOVERY APPROACH FOR ROBUST CONTROL OF FLEXIBLE STRUCTURES Ph.D. Thesis
Paul Andrew Blelloch 1986 214 p
Avail: Univ. Microfilms Order No. DA8621022

A procedure is developed for dealing with performance and robustness issues in the design of multi-input multi-output compensators for lightly damped flexible structures. The procedure is based upon representing errors in the plant design model as structured

uncertainties, and applying a modified version of the Loop Transfer Recovery (LTR) design method. Real parameter errors such as frequency errors, damping errors or modal displacement errors can be treated. The modified method may be implemented in either of two slightly different forms, both of which permit a controlled tradeoff between performance and robustness. The first approach is the main focus. It involves adjusting the cost function in the regulator problem and the process noise model in the estimator problem in a particular manner which reflects the assumed structure of the modeling errors. Numerical examples dealing with the control of a large flexible space antenna with uncertain frequencies demonstrate that this approach represents a considerable improvement over standard LTR methods. Convenient design parameters can be varied until a satisfactory compromise is achieved between performance and robustness. The second approach is a variation on the first in that it uses a similar procedure for adjusting the cost function in the (full-state feedback) regulator problem. Instead of implementing the controller with an estimator, an algebraic procedure is used to achieve loop recovery with a compensator whose poles can be placed at arbitrary locations. Dissert. Abstr.

N87-17030 California Univ., Los Angeles.
LATTICE FILTERS AND ADAPTIVE IDENTIFICATION OF FLEXIBLE STRUCTURES Ph.D. Thesis
Faryar Jabbari 1986 179 p
Avail: Univ. Microfilms Order No. DA8621081

Lattice filters and their applications to parameter identification of flexible structures are studied. Input-output relationships, in the form of Auto Regressive Moving Averages (ARMA), are used to address several issues relevant to modeling and discrete-time control of distributed systems. The ARMA models are studied and methods to obtain them, by projection onto the finite dimensional framework, are developed. It is shown that for a large class of distributed systems, these ARMA models have attractive characteristics which serve as motivation for the study of parameter identification methods. The uncertainty regarding the system order is a major problem in the identification of these systems. Lattice filters, due to their order determination capability, are the primary tool for identification in this dissertation. The new derivation presented here results in a generalization of regular lattices to the case of vector channel lattice forms. This novel approach makes it possible to have all measurements of the system obey the same Auto Regressive model. The advantages of this input-output structure are also discussed. Numerical results are presented to support the arguments regarding the vector channel lattices. It is shown that many important parameters, such as damping, natural frequency and the excitation level, can be estimated for flexible structures even when the system ARMA models can not be successfully identified. Dissert. Abstr.

N87-17031 California Univ., Los Angeles.
POSITION CONTROL OF MECHANICAL MANIPULATORS BY USING NONLINEAR ADAPTIVE CONTROL ALGORITHM Ph.D. Thesis
Shiuh-Jer Huang 1986 235 p
Avail: Univ. Microfilms Order No. DA8621079

The manipulator is a complicated nonlinear coupling system whose dynamics is influenced by the coriolis effect and the gravity effect of the configuration change. Conventional robot control methods which are designed based on linear systems are only applicable to slow moving conditions because at higher speeds the nonlinear effects will deteriorate the performance of the control system. This is one of the industrial robots limitations. Furthermore the payload capacity of industrial robots are very small compared to its arms weight. With growing demand on manipulator performance there is an increasing need for improved dynamic modeling and control technique of manipulators. Two nonlinear adaptive control algorithms are developed for manipulator systems to solve these two problems. The first scheme is designed for the rigid arm robot systems (deterministic), and the second one is designed for the flexible beam manipulator systems (stochastic). These algorithms directly use nonlinear dynamic model in controller design to account for the nonlinear effects of the system. The least-square time varying parameter identification scheme has been used to identify the changes in configuration and payload of the system. Dissert. Abstr.

N87-17032# Royal Aircraft Establishment, Farnborough (England).
DIFFUSION WELDING OF COMPONENT PARTS IN THE AVIATION AND SPACE INDUSTRIES
J. Disam and D. Mietrach Apr. 1986 12 p Transl. into ENGLISH of conference paper "Diffusionsschweissen von Bauteilen in der Luft-und Raumfahrt" presented at the International Conference on Brazing, High-Temperature Brazing and Diffusion Welding, 1981 Conference held in Duesseldorf, West Germany, 21-22 Sep. 1981; sponsored by German Welding Society
(RAE-Trans-2147) Avail: NTIS HC A02/MF A01

Investigations were performed and successfully completed on the materials combinations titanium/titanium, steel/steel, titanium/aluminum, titanium/permenorm, and aluminum/aluminum. Experience gained during the ZKP flap-track program, as well as during the manufacturing of heat pipes for space technology, was used for diffusion bonding of further components such as titanium/steel connections for TV-satellites. Superplastically formed/diffusion bonded titanium components, as well as different material combinations will be used to an increasing extent for civil and military aircraft in the future. In this context, examples are given from civil and military programs. Comments are made on materials and materials combinations. Costs are compared with costs for components manufactured by conventional methods. Trends in the USA show that in the future increasing emphasis will be laid on the joining of semi-finished products having quasi-final contours such as titanium castings and powder-metallurgical parts by, for example, diffusion bonding in order to cut the structural costs in airframe construction drastically. Author

N87-17033*# National Aeronautics and Space Administration. Lewis Research Center, Cleveland, Ohio.
COMMON PROBLEMS AND PITFALLS IN GEAR DESIGN
Dennis P. Townsend Dec. 1986 18 p Presented at the Original Equipment Manufacturing Design Conference, New York, N.Y., 9-11 Dec. 1986
(NASA-TM-88858; E-3223; NAS 1.15:88858) Avail: NTIS HC A02/MF A01 CSCL 13I

There are several pitfalls and problems associated with the successful design of a new gear transmission. A new design will require the knowledge and experience of several technical areas of engineering. Most of the pitfalls and problems associated with a new design are related to an inadequate evaluation of several areas, such as, the lubrication and cooling requirements, complete static and dynamic load analysis, evaluation of materials and heat treatment and the latest manufacturing technology. Some of the common problems of the gear design process are discussed with recommendations made for avoiding these conditions. Author

N87-17034*# National Aeronautics and Space Administration. Pasadena Office, Calif.
TANK TREAD ASSEMBLIES WITH TRACK-LINKING MECHANISM Patent
Earl R. Collins, Jr., inventor (to NASA) (Jet Propulsion Lab., California Inst. of Tech., Pasadena) Issued 2 Dec. 1986 8 p Filed 18 Jan. 1985 Supersedes N85-29291 (23 - 18, p 3117)
(NASA-Case-NPO-16321-1CU; US-Patent-4,626,046;
US-Patent-Appl-SN-692802; US-Patent-Class-305-36;
US-Patent-Class-305-58PC; US-Patent-Class-305-51;
US-Patent-Class-305-58R; US-Patent-Class-474-220) Avail: U.S. Patent and Trademark Office CSCL 13F

The proposed tank tread assembly has adjacent tank tread segments joined by a link bearing tapered pins retained by clips inserted through the tread shells perpendicular to the axes of the pin. It also has highway pads attached by a release rod bearing tapered, grooved cams which interlockingly engage tabs inserted into the tread shells. NASA

N87-17035*# National Aeronautics and Space Administration. Lyndon B. Johnson Space Center, Houston, Tex.
SELF-CONTAINED, SINGLE-USE HOSE AND TUBING CLEANING MODULE Patent
Fred P. Rollins, inventor (to NASA) (Lockheed Engineering and Management Services Co., Inc., Houston, Tex.) and James S. Glass, inventor (to NASA) Issued 13 Jan. 1987 5 p Filed 3 Oct. 1985 Supersedes N86-20807 (24 - 11, p 1784)
(NASA-Case-MSC-20857-1; US-Patent-4,635,663; US-Patent-Appl-SN-783886; US-Patent-Class-134-93; US-Patent-Class-134-166C; US-Patent-Class-210-282) Avail: U.S. Patent and Trademark Office CSCL 13I

A self contained, single use hose and tubing cleaning module which utilizes available water supplies without requiring access to precision cleaning facilities is presented. The module is attached to the water source at the inlet side and to the hose or tubing to be cleaned at the outlet side. The water flows through a water purification zone, a detergent dispensing zone, a filtration zone before the detergent laden water flows into the tubing to clean the tubing walls. The module contains an embedded pad which is impregnated with a pH indicator to indicate to the user when the detergent has dissolved and rinsing of the tubing begins. NASA

N87-17036*# National Aeronautics and Space Administration. Lyndon B. Johnson Space Center, Houston, Tex.
SUN SHIELD Patent
Arthur M. Frank, inventor (to NASA), Silvio F. DeRespinis, inventor (to NASA), and John Mockovciak, Jr., inventor (to NASA) Issued 20 Jan. 1987 8 p Filed 12 Aug. 1985 Supersedes N86-20803 (24 - 11, p 1783)
(NASA-Case-MSC-20162-1; US-Patent-4,637,447; US-Patent-Appl-SN-764805; US-Patent-Class-160-265; US-Patent-Class-160-23R; US-Patent-Class-244-121; US-Patent-Class-244-158R; US-Patent-Class-135-903; US-Patent-Class-296-100) Avail: US Patent and Trademark Office CSCL 13I

A shading device which is capable of compactly storing a flexible shade on a biased, window shade type spring roller is disclosed. It is controlled to deliver the shade selectively to either its operative shading or compact storage orientation. NASA

N87-17037*# National Aeronautics and Space Administration. Marshall Space Flight Center, Huntsville, Ala.
NON-BACKDRIVEABLE FREE WHEELING COUPLING Patent
William R. Llewellin, inventor (to NASA) (Martin Marietta Corp., Bethesda, Md.) Issued 13 Jan. 1987 7 p Filed 22 Apr. 1985 Supersedes N85-29290 (23 - 18, p 3116)
(NASA-Case-MSC-20475-1; US-Patent-4,635,773; US-Patent-Appl-SN-725689; US-Patent-Class-192-46; US-Patent-Class-192-67R) Avail: U.S. Patent and Trademark Office CSCL 13I

A rotary coupling for connecting a driven part to a source of rotary force is described. This device transmits rotary force in one direction only and disengages to permit the driven part to free wheel when the input member is stopped and precludes the backdriving of rotary force from output member to input member. The coupling includes an input member having a splined shaft, a coupling member connected to the splined shaft, and a coaxial output member. The coupling member and the output member having complementary sets of axially facing clutch teeth. Guides in the form of helical grooves on the coupling member and spring loaded followers acting with the guides affect the engagement and disengagement of the clutch teeth by moving the coupling member toward and away from output member, the followers and guides themselves disengaging to permit free wheeling of output member when input member is stopped. NASA

N87-17038*# National Aeronautics and Space Administration. Goddard Space Flight Center, Greenbelt, Md.
RADIAL AND TORSIONALLY CONTROLLED MAGNETIC BEARING Patent
Philip A. Studer, inventor (to NASA) Issued 6 Jan. 1987 13 p Filed 21 Nov. 1985 Supersedes N86-20804 (24 -11, p 1784)
(NASA-Case-GSC-12957-1; US-Patent-4,634,191; US-Patent-Appl-SN-800193; US-Patent-Class-310-90.5) Avail: U.S. Patent and Trademark Office CSCL 13I

A magnetic bearing including a circular stator member with a plurality of circumferential pole faces and a suspended annular ring member with corresponding number of inward facing circumferential pole faces separated by respective air gaps is presented. A source of dc magnetic flux circulates flux between the circumferential pole faces of the stator and the ring to provide axial stability along a central longitudinal axis. Flux coil means are included on the stator member to provide variable flux density along predetermined radial paths to provide active radial stabilization. Flux coil means are included on the stator to actively modulate the magnitude of the magnetic forces as well as their direction by differential flux control involving the dc magnetic flux to produce torquing moments about a pair of mutually orthogonal axes which are perpendicular to the central axis. NASA

N87-17039*# National Aeronautics and Space Administration. Marshall Space Flight Center, Huntsville, Ala.
SOLID ROCKET BOOSTER JOINT SEAL ANALYSES
Carleton J. Moore Jan. 1987 18 p
(NASA-TM-86580; NAS 1.15:86580) Avail: NTIS HC A02/MF A01 CSCL 11B

O-ring response and sealing in pressurized shell structures is examined. The study found that the key elements in the failure of the seal to be joint opening and rotation, assembly out of roundness, and O-ring seal response. Author

N87-17040*# National Aeronautics and Space Administration. Marshall Space Flight Center, Huntsville, Ala.
SRB O-RING FREE RESPONSE ANALYSIS
Carleton J. Moore Dec. 1986 22 p
(NASA-TM-86582; NAS 1.15:86582) Avail: NTIS HC A03/MF A01 CSCL 11A

The free response of viton O-rings were investigated. Two different response mechanisms of viton O-rings are identified and a theoretical representation of the two mechanisms is compared with experimental results for various temperatures. Author

N87-17041*# CHAM of North America, Inc., Huntsville, Ala.
DISCRETE ELEMENT WELD MODEL, PHASE 2 Final Report
C. Prakash, M. Samonds, and A. K. Singhal Jan. 1987 122 p
(Contract NAS8-36716)
(NASA-CR-179009; NAS 1.26:179009; Rept-4036/6) Avail: NTIS HC A06/MF A01 CSCL 13H

A numerical method was developed for analyzing the tungsten inert gas (TIG) welding process. The phenomena being modeled include melting under the arc and the flow in the melt under the action of buoyancy, surface tension, and electromagnetic forces. The latter entails the calculation of the electric potential and the computation of electric current and magnetic field therefrom. Melting may occur at a single temperature or over a temperature range, and the electrical and thermal conductivities can be a function of temperature. Results of sample calculations are presented and discussed at length. A major research contribution has been the development of numerical methodology for the calculation of phase change problems in a fixed grid framework. The model has been implemented on CHAM's general purpose computer code PHOENICS. The inputs to the computer model include: geometric parameters, material properties, and weld process parameters. Author

N87-17042# Royal Aircraft Establishment, Farnborough (England).
THE POSSIBILITY OF REDUCING THE CYCLIC TORQUE FLUCTUATIONS PRODUCED BY TWO-STROKE ENGINES USING THE STORAGE OF MAGNETOSTATIC ENERGY
J. W. R. Cox Apr. 1985 22 p
(RAE-TM-RAD-NAV-265; BR99145; ETN-87-98914) Avail: NTIS

The storage and recovery of magnetostatic energy were considered as a means of reducing the cyclic torque fluctuations of a power source. Approximate figures for the torques attainable for a given size of device were derived assuming utilization of the

Nd-B-Fe system of permanent magnet material. Calculations indicate that, alone, the device would incur a mass penalty of 6 kg, but benefits to UMAs might be attainable by its incorporation with an alternator (possibly leading to the elimination of batteries) and by the reduction of vibrations caused by the power source. ESA

N87-17043# Department of the Navy, Washington, D. C.
ROBOTIC VISION SYSTEM Patent Application
Norman W. Witriol, inventor (to Navy) and William H. Brumage, inventor (to Navy) Filed 9 Jul. 1986 19 p
(AD-D012481; US-Patent-Appl-SN-883249) Avail: NTIS HC A02/MF A01 CSCL 09/2

This patent application discloses a robotic vision system for real time operation based on a luminous fiduciary code located upon a robot and an object the robot is to operate on. The luminescent code, when irradiated, locates the position of the object relative to the robot thus allowing placement of the fiduciary codes, on the object and the robot, into a predetermined desired position and orientation. GRA

N87-17044# Department of the Navy, Washington, D. C.
METALLIZATION FOR HERMETIC SEALING OF CERAMIC MODULES Patent Application
Hayden Morris, inventor (to Navy), Henry W. Rhodes, inventor (to Navy), and Margaret C. Marlow, inventor (to Navy) Filed 1 Jul. 1986 11 p
(AD-D012483; US-Patent-Appl-SN-887166) Avail: NTIS HC A02/MF A01 CSCL 11/1

A superior hermetic seal for ceramic modules is presented. The case base member is provided with metallization around the periphery of the cavity. The case cover is provided with metallization not only to mate with the metallization of the base, but the cover metallization extends onto the thickness edge. The dimensions of the cover are less than the corresponding metallization dimensions of the base member. In this manner the solder bead formed about the periphery will wet the exposed metallization surfaces and form a visually inspectable bead. GRA

N87-17045# Department of the Navy, Washington, D. C.
TEST APPARATUS FOR UNIFORM TENSIONING OF LONG LENGTHS OF SMALL CABLES IN SIMULATED ENVIRONMENTS Patent Application
Alan T. Inouye, inventor (to Navy), Jeffrey V. Wilson, inventor (to Navy), and Mark L. Baker, inventor (to Navy) Filed 20 Jun. 1986 15 p
(AD-D012487; US-Patent-Appl-SN-876618) Avail: NTIS HC A02/MF A01 CSCL 13/9

This invention relates to test apparatus, and more particularly to a system for uniformly tensioning long lengths of small diameter cables, up to several kilometers in length, while simultaneously exposed to simulated environments such as deep ocean conditions. An exemplary embodiment of the invention provides for wrapping long lengths of small cable about a thin bladder which is sealed to the outside of a stiff cylinder within a pressure vessel and pressurizing the bladder to uniformly tension the cable length while undergoing simulated deep ocean environment with the pressure vessel. GRA

N87-17046# Department of the Air Force, Washington, D.C.
DIRECT CABLE ATTACH METHOD Patent Application
Barbara L. Clark, inventor (to Air Force) Filed 14 Jul. 1986 13 p
(AD-D012505; US-Patent-Appl-SN-885116) Avail: NTIS HC A02/MF A01 CSCL 13/5

A direct cable attachment method for directly connecting a flat ribbon cable to a stack of integrated circuit units by pre-tinning the leads of both the ribbon cable and the wiring board with solder is described. The ribbon cable is positioned on the wiring board and sufficient heat is applied to the combination to achieve a physical and electrical connection. Adding epoxy to the assembly structure provides additional strength. GRA

N87-17047# Department of the Air Force, Washington, D.C.
ANTI-ROTATION GUIDE VANE BUSHING Patent Application
George Bonner, inventor (to Air Force) Filed 3 Jul. 1986 14 p
(AD-D012510; US-Patent-Appl-SN-881741) Avail: NTIS HC A02/MF A01 CSCL 13/9

The invention comprises a variable guide vane bushing assembly which includes a bushing, a lock washer and a retainer. The bushing preferably has a sleeve and collar portion. The sleeve portion slides onto a vane stem and the collar portion is positioned adjacent to the vane. In the preferred embodiment of the invention two flat portions are formed on the sleeve of the bushing where it projects from the compressor casing. The lock washer has two race track shaped openings that mate with the sleeves of adjacent bushings where they project from the compressor casing. The flat portions of the race track shaped openings align with the flat portions of the bushing sleeves and prevent bushing rotation. The retainer is substantially square shaped and fits within prebent tabs formed on the lock washer. Thus the retainer is prevented from rotation by the tabs of the lock washer. In the preferred embodiment of the invention an interference fit is formed between the retainer and the sleeve of the bushing. This helps ensure a tight air seal across the engine case. GRA

N87-17048# Materials Research Labs., Ascot Vale (Australia).
GRINDING OF STEEL: A CASE STUDY
G. R. Wilms and R. L. Aghan Aug. 1986 14 p
(AD-A174649; MRL-TN-504) Avail: NTIS HC A02/MF A01 CSCL 13/8

A description is given of grinding studies aimed at overcoming a production problem on the dry grinding of hardened steel gears for aircraft gas turbine engines, in which grinding abuse in the form of both a softening and hardening of the steel led to high rejection rates. By using a combination of reduced grinding wheel speed and graded finishing cuts, gears could be produced without showing any signs of grinding abuse. A feature of the grinding was the occurrence of redeposition, and the extent of the microstructural changes in relation to redeposition under different grinding conditions is discussed. GRA

N87-17049# Oak Ridge National Lab., Tenn. Metals and Ceramics Div.
MICROSTRUCTURAL MODIFICATIONS DURING LASER AND ELECTRON BEAM WELDING
S. A. David and J. M. Vitek 1986 16 p Presented at the International Conference on Power Beam Technology, Brighton, England, 10 Sep. 1986
(Contract DE-AC05-84OR-21400)
(DE86-011076; CONF-8609101-1) Avail: NTIS HC A02/MF A01

Extensive microstructural modifications occur during laser and electron beam welding of various alloys. For austenitic stainless steels, most welds that do not hot crack contain a duplex austenite plus ferrite microstructure when welded by conventional welding processes. However, during laser welding at high speeds, fully austenitic or ferritic microstructures can be obtained in this class of material. The observed modifications in microstructures will be explained in terms of changes in the mode of solidification and also a retardation of solid state transformation. Laser and electron beam welding processes have been successfully used to weld iridium alloys, which are difficult to weld by conventional welding processes. During welding, these alloys have been found to be prone to severe hot cracking. The cracking is influenced to a great extent by the fusion zone microstructure and composition. The successful laser and electron beam welding of these alloys is attributable to the highly concentrated heat source available, precise control of the heat input, and the refinement in fusion -zone microstructure obtained. The refinement in the fusion-zone microstructure and hence the reduction in hot-cracking tendency of these alloys are discussed in terms of the puddle shapes and grain growth during laser or electron beam welding. DOE

N87-17050# Edgerton, Germeshausen and Grier, Inc., Idaho Falls, Idaho.
HEAT TRANSFER IN GAS TUNGSTEN ARC WELDING

H. B. Smartt, J. A. Stewart, and C. J. Einerson May 1986 14 p Presented at the ASM Metals Congress/TMS-AIME Fall Meeting, Toronto, Ontario, 13 Oct. 1985
(Contract DE-AC07-76ID-01570)
(DE86-013457; EGG-J-01586; CONF-8510160-19) Avail: NTIS HC A02/MF A01

The heat transferred from an electrode negative, argon gas tungsten arc to an anode has been measured for a wide range of conditions suitable for mechanized welding applications. The results are given as: (1) the arc efficiency; and (2) the anode heat and current input distribution functional shapes and radii for various anode materials and groove shapes over a wide range of current and voltage, using different electrode geometries, as well as both He and Ar-He shielding gases. The nominal arc is Gaussian with a diameter of about 4 mm and a heat transfer efficiency to the anode of about 75%. Variations from these values are discussed in terms of current knowledge of the electrical and thermal energy transport mechanisms. A new method of measuring the heat transferred from the arc to the anode, using a boiling liquid nitrogen calorimeter, has been developed which gives rapid, accurate values. DOE

N87-17051# Advisory Group for Aerospace Research and Development, Neuilly-Sur-Seine (France). Structures and Materials Panel.
ADVANCED JOINING OF AEROSPACE METALLIC MATERIALS
Loughton, England Jul. 1986 270 p In ENGLISH and FRENCH Meeting held in Oberammergau, West Germany, 11-13 Sep. 1985
(AGARD-CP-398; ISBN-92-835-0397-X) Avail: NTIS HC A12/MF A01

The papers contained in this report provide a review of the state-of-the-art of advanced joining techniques currently available to the manufacturers of aerospace equipment and identify newly emerging techniques and joining problems. Computational weld mechanics, diffusion bonding and superplastic forming, electron-beam welding, tungsten inert gas welding, inspection methods, and repair techniques are addressed. For individual titles, see N87-17052 through N87-17071.

N87-17052# Carleton Univ., Ottawa (Ontario). Dept. of Mechanical and Aeronautical Engineering.
COMPUTATIONAL WELD MECHANICS
John Goldak, Balvantrai Patel (Engineering Mechanics Research, Inc., Troy, Mich.), Malcolm Bibby, and James Moore *In* AGARD Advanced Joining of Aerospace Metallic Materials Jul. 1986 32 p (For primary document see N87-17051 09-37)
Avail: NTIS HC A12/MF A01

An overview of the aims and methods of computational weld mechanics is presented. In particular, relevant literature and recent developments in the authors' laboratory are described. The presentation emphasizes an exposition of the computational principles and the application of computational weld mechanics to practice. In fact, the primary aim of the work is to transfer this technology from the research specialists who are developing it to the engineers who must apply it in the design and production of welded structures. The numerical methods, algorithms, software and computer hardware needed for computing the temperature, displacement, strain and stress fields associated with the welding process are described. While computer methods are widely applied in the engineering community, thermal strain-stress transients are rarely calculated in welding because of the complexity of the problem. Finite element analysis (FEA) together with the equations of continuum mechanics and irreversible thermodynamics forms the basis for a successful analysis of welding processes. The special problems encountered when FEA is used for weld analysis are discussed in detail. Particular attention is focussed on transient temperature field computations. Modelling heat sources, nonlinear thermal properties, the heats of fusion and transformation, and workpiece geometry and boundary conditions are discussed. Predicting relevant properties (strength, hardness, etc.) of weld joints from computed temperatures is included. In addition, thermo-elasto-plastic analysis for calculating residual strain, stresses and workpiece deformation is described. Measured thermal and distortion changes are compared to computed values as a means of verifying the accuracy of the computational methods. Finally, the computing environment (hardware and software) for computational weld mechanics is discussed at some length. Author

N87-17053# Societe Nationale d'Etude et de Construction de Moteurs d'Aviation, Paris (France). Lab. Assemblage Metallurgique.
STUDY OF THE ELECTRON BEAM WELDABILITY OF SUPERALLOYS THROUGH THE ANALYSIS OF MELT ZONE MORPHOLOGY
F. Pierquin and J. Lesgourges *In* AGARD Advanced Joining of Aerospace Metallic Materials Jul. 1986 22 p In FRENCH; ENGLISH summary (For primary document see N87-17051 09-37)
Avail: NTIS HC A12/MF A01

Characterized by high specific energy, the electron beam allows a high welding velocity. The melted zones and heat affected zones are narrow and the thermal cycles involved are short, and therefore, the weld joints are submitted to high stresses. Thus, welding of high strength superalloys raises hot cracking problems, due to their low ductility. The configuration of the melted pond is logically recognized as an important factor in the generation of defects and on their type: vertical cracks, horizontal cracks, axial cracks, spike cracks, etc. To extend the applications of the process, a technique was developed to investigate the melted pond morphology and establish a correlation with the type of defects observed. The process, based on the pollution of the melted pond at a given time during welding, reveals, through micrographic examination, the solidification front configuration. Author

N87-17054# Welding Inst., Cambridge (England). Solid Phase Welding Group.
THE APPLICATION OF DIFFUSION BONDING AND LASER WELDING IN THE FABRICATION OF AEROSPACE STRUCTURES
S. B. Dunkerton and C. J. Dawes *In* AGARD Advanced Joining of Aerospace Metallic Materials Jul. 1986 12 p (For primary document see N87-17051 09-37)
Avail: NTIS HC A12/MF A01

A review is given of work undertaken in both diffusion bonding and laser welding which is relevant to the aerospace industry. The wide use of superplastic forming/diffusion bonding of titanium alloys is mentioned with reference to particular applications. This is extended to include the newly developed superplastic aluminum alloys and data are presented on the diffusion bonding of conventional aluminum materials. The laser welding of aluminum, steel, nickel alloys and titanium alloys is covered with detail given on mechanical properties such as tensile and fatigue. The weld quality is shown to be tolerant to changes in process parameters by means of weldability lobes while dimensional tolerances such as beam/joint alignment and component fit-up can be critical. Finally, the development of laser beam spinning is mentioned with data on the increased tolerance to joint mismatch. Author

N87-17055# Messerschmitt-Boelkow-Blohm G.m.b.H., Augsburg (West Germany). Materials and Technologies.
ECONOMICAL MANUFACTURING AND INSPECTION OF THE ELECTRON-BEAM-WELDED TORNADO WING BOX
Juergen Berggreen *In* AGARD Advanced Joining of Aerospace Metallic Materials Jul. 1986 7 p (For primary document see N87-17051 09-37)
Avail: NTIS HC A12/MF A01

The Tornado wing box is an extensively electron-beam-welded titanium 6Al4V-alloy component. The design and the manufacturing steps are described with emphasis on joining and inspection techniques. As EB-welding requires expensive investments and operations the manufacturing costs have been cut by several means which are shown. The advantages of EB-welding on the material's side and the experience gained with this technique meanwhile allow the use of EB-welding for major titanium structures

even with thick cross sections as a well-known and established and no longer uneconomic advanced joining method. Author

N87-17056# Aeritalia S.p.A., Torino (Italy). Space System Div.
THE WELDING OF ALUMINUM ALLOYS: A NEW TECHNOLOGY IN SPACE APPLICATION
P. Marchese and G. Baning *In* AGARD Advanced Joining of Aerospace Metallic Materials Jul. 1986 11 p (For primary document see N87-17051 09-37)
Avail: NTIS HC A12/MF A01

The optimization of the structural weight of the Spacelab structure, the first European manned laboratory designed according to shuttle requirements, led to the choice of 2219-T851 aluminum alloy, T.I.G. welded with the process completely developed and qualified from Aeritalia as briefly described is this paper. To demonstrate the high quality and reliability of the welded primary structure, new inspection techniques, many different tests on the welded joint, and expensive fracture mechanics analysis were applied. The main assumptions and results are presented. The main efforts were concentrated on the reduction of number and size of welding defects, improving, on the one side, the welding technique and on the otherside, inspecting single defects after fracture mechanics analysis based on sophisticated measurement of their dimensions, on the schematization of embedded flaw in tension and bending, and on carefull measurement of material properties. Possible improvements of T.I.G. application for future space programs (space station) or its substitution with plasma welding processes are also mentioned. Author

N87-17057# British Aerospace Aircraft Group, Bristol (England). Civil Aircraft Div.
DIFFUSION BONDING IN THE MANUFACTURE OF AIRCRAFT STRUCTURE
D. Stephen and S. J. Swadling *In* AGARD Advanced Joining of Aerospace Metallic Materials Jul. 1986 17 p (For primary document see N87-17051 09-37)
Avail: NTIS HC A12/MF A01

Over the last twenty years, considerable aerospace research and development effort has been directed to the development of the diffusion bonding (DB) process as a means of manufacture of low cost structures. To date the main thrust of these developments have been associated with titanium which has inherent metallurgical characteristics which make this material ideally suited for joining by this technique. For these titanium alloys which exhibit superplastic properties, the combined processes of superplastic forming (SPF) and DB considerably extend the range of low cost and structurally efficient titanium aerospace components which can be manufactured; even as replacements for conventionally fabricated aluminum alloy components. Recent developments in the SPF of high strength aluminums and metal matrix composites has stimulated work in the field of DB of aluminum. It is thought that in the longer term this field of DB could have the highest levels of application. This paper details the range of aerospace structural forms which can and are currently being manufactured using the diffusion bonding process. The process options, bond integrity, and nondestructive test (NDT) aspects are discussed. Author

N87-17058# Royal Aircraft Establishment, Farnborough (England). Materials and Structures Dept.
DIFFUSION BONDING OF Al-ALLOYS IN THE SOLID STATE
P. G. Partridge, J. Harvey, and D. V. Dunford *In* AGARD Advanced Joining of Aerospace Metallic Materials Jul. 1986 23 p (For primary document see N87-17051 09-37)
Avail: NTIS HC A12/MF A01

Solid state diffusion bonds have been produced between clad Al-alloy sheets in alloys 7010, 2024, SUPRAL 220 and LITAL A. The sheet surface was first ion plated with a 1 micron layer of silver before bonding at 280 C or 450 C under 130 MPa or 7 MPa pressure. Lap shear strengths were in the range 140 MPa to 180 MPa and peel strengths were more than 40 N/mm. The effects of test piece design, surface finish, clad layer thickness and of oxide films on diffusion bond strengths are described. The results suggest that a combination of thin silver coating and a clad layer should enable any Al-alloy to be diffusion bonded. Author

N87-17059# Technische Univ., Munich (West Germany).
BONDING OF SUPERALLOYS BY DIFFUSION WELDING AND DIFFUSION BRAZING
P. Adam and L. Steinhauser *In* AGARD Advanced Joining of Aerospace Metallic Materials Jul. 1986 6 p (For primary document see N87-17051 09-37)
Avail: NTIS HC A12/MF A01

Several developments of diffusion welded and diffusion bonded superalloy turbine engine parts, blades, vanes, and bliscs, are summarized. The description of results comprises nondestructive testing of parts and mechanical testing of material samples. Results are mainly presented as conclusions on the expense of detailed test results which would require individual parts/material problem presentations. Author

N87-17060# Societe Nationale Industrielle Aerospatiale, Suresnes (France). Dept. Production-Recherches.
APPLICATION OF DIFFUSION BONDING COMBINED WITH SUPERPLASTIC FORMING (SPF/DB) TO THE FABRICATION OF TAGV METAL SHEET STRUCTURES [APPLICATION DU SOUDAGE PAR DIFFUSION ASSOCIE AU FORMAGE SUPERPLASTIQUE (SPF/DB) A LA REALISATION DE STRUCTURES EN TOLES MINCES DE TA6V]
M. Boire and P. Jolys *In* AGARD Advanced Joining of Aerospace Metallic Materials Jul. 1986 14 p In FRENCH (For primary document see N87-17051 09-37)
Avail: NTIS HC A12/MF A01

The potential applications of combined superplastic forming and diffusion bonding (SPF/DB) technology to the fabrication of TA6V titanium alloy structures are discussed. The conditions for the application of this technology are summarized as well as the impacts of certain material properties. Examples of structural fabrication processes are presented and an economical technique is suggested. Finally, the main problems which need to be resolved for a fully-developed industrial process are examined. M.G.

N87-17061# Messerschmitt-Boelkow-Blohm G.m.b.H., Lemwerder (West Germany).
ULTRASONIC TESTING TECHNIQUES FOR DIFFUSION-BONDED TITANIUM COMPONENTS c38
Gustav Tober and Stefan Elze *In* AGARD Advanced Joining of Aerospace Metallic Materials Jul. 1986 10 p (For primary document see N87-17051 09-37)
Avail: NTIS HC A12/MF A01

Diffusion-bonded titanium specimens with bonding defects were tested by ultrasonic techniques. In order to improve the defect detectability, high-frequency ultrasound was applied; the echo signals were analyzed in both the time and frequency domains. Author

N87-17062# Army Construction Engineering Research Lab., Champaign, Ill.
WELD QUALITY MONITOR AND CONTROL SYSTEM c38
F. Kearney, Dawn White, and William Ricci (Army Materials and Mechanics Research Center, Watertown, Mass.) *In* AGARD Advanced Joining of Aerospace Metallic Materials Jul. 1986 8 p (For primary document see N87-17051 09-37)
Avail: NTIS HC A12/MF A01

A non-contact weld quality monitor (WQM) system is being developed to detect, identify, and correct for deviations from established welding procedures and conditions which lead to weld defects in real time. The WQM continually measures with conventional transducers all primary process parameters such as current, voltage, and travel speed, and computes weld quality parameters such as heat input and weld bead geometry. In addition, the WQM monitors the spectral signature of the welding arc by means of a high resolution microprocessor controlled spectrograph. Here, the presence of weld pool and arc atmosphere contaminants, flux and shield gas effectiveness, arc energy input, and penetration/dilution into the base material can be determined. The spectral

response from the welding arc and measurements of process parameters are then normalized, compared to preset operating limits, and processed in real time. Necessary adjustments to primary process parameters are made by automated compensation devices to eliminate weld defects in real time. When necessary, the specific location of discontinuities are provided to facilitate further inspection. Author

N87-17063# Rolls-Royce Ltd., Derby (England).
NDT OF ELECTRON BEAM WELDED JOINTS (MICRO-FOCUS AND REAL TIME X-RAY) c38
R. G. Taylor *In* AGARD Advanced Joining of Aerospace Metallic Materials Jul. 1986 4 p (For primary document see N87-17051 09-37)
Avail: NTIS HC A12/MF A01

The introduction of electron beam welding (EBW) into the aero engine industry in the early 1960's has presented many new problems for non-destructive testing (NDT). Highlighted among these are the following particular problems: (1) accessibility the use of EBW has resulted in the design of many box-like components which makes it difficult, or impossible, to apply conventional NDT methods satisfactorily; (2) center-line defect orientation; and (3) extremely narrow welds which makes the detection of defects by normal radiography very unreliable. The traditional NDT methods such as conventional X-ray, fluorescent penetrant, magnetic particle, together with the occasional use of eddy current and, where accessibility permits, ultrasonics, have been extensively used for the inspection of EBW fabrications. However, the use of these methods has created considerable limitations in defect detection where extremely small defects (under 1mm) must be detected to quarantee a successful life cycle. Initially, these limitations only applied to parts manufactured by EBW, but during recent years, EBW has been increasingly used during the repair and overhaul of aero engine engine components and the NDT limitations now extend into these areas. Recently, significant developments have taken place which has enabled micro-focus X-ray techniques to be used in place of conventional X-ray on EBW and this has resulted in a considerable improvement in defect detection capabilities. An additional bonus has been the reduction in inspection costs and an improvement in productivity. Author

N87-17064# National Research Council of Canada, Boucherville (Quebec).
THERMOELASTIC TESTING OF STRATIFIED MATERIALS c38
Paolo Cielo and Marc Dufour *In* AGARD Advanced Joining of Aerospace Metallic Materials Jul. 1986 15 p (For primary document see N87-17051 09-37)
Avail: NTIS HC A12/MF A01

A non-contact thermoelastic technique for the non-destructive testing of layered materials such as aluminum-epoxy laminates or metallurgical coatings is described. A pulsed laser beam heats a small area on the surface of the layer to be tested, and the thermoelastic deformation of the layer is monitored by a sensitive optical probe. Unbonded areas can be recognized from the abnormally high deformation of the unbonded layer. Localized pulsed heating is shown to be far superior than the extended heating approach which is followed in holographic thermal stressing. The possibility to detect cohesive and adhesive defects by this technique is discussed. Two experimental configurations are described: in the first configuration the probing beam directly monitors the thermoelastic displacement of the heated area, while in the second a thermoelastically-generated annular stress wave converges towards the central probed point. Author

N87-17065# Industrieanlagen-Betriebsgesellschaft m.b.H., Ottobrunn (West Germany).
INFLUENCE OF WELDING FLAWS ON THE FATIGUE STRENGTH OF ELECTRON BEAM WELDMENTS IN Ti Al6 V4 c39
Walter Schuetz and Wolfram Oberparleiter *In* AGARD Advanced Joining of Aerospace Metallic Materials Jul. 1986 11 p (For primary document see N87-17051 09-37)
Avail: NTIS HC A12/MF A01

Electron beam (EB) welding is a well known joining method in aircraft construction. Although a lot of data is available on the fatigue behavior of EB-welded Ti Al6 V4 alloy, only a few data on the effect of flaws in these weldments exist. Therefore artificial flaws of different size were produced in EB-weldments and the effect of these flaws on static strength, fatigue, fracture toughness and crack propagation was studied. Experience has shown, that existing flaws may be not found or heavily underestimated by non-destructive inspection (NDI). Also NDI cannot distinguish between sharp-edged flaws (which may behave like cracks) and spherical cavities. In the present investigation they reduced the static strength up to 35%, the fatigue strength up to 50% (at N = 10(5) cycles), and the fracture toughness up to 10%. Such reductions therefore must be accounted for in the design phase of Ti A16 V4 components containing EB-welds. Author

N87-17066# National Research Council of Canada, Boucherville (Quebec).
A REAL TIME VISION SYSTEM FOR ROBOTIC ARC WELDING
M. Dufour, P. Cielo, and F. Nadeau *In* AGARD Advanced Joining of Aerospace Metallic Materials Jul. 1986 14 p (For primary document see N87-17051 09-37)
Avail: NTIS HC A12/MF A01

Fast real-time vision systems for robotic arc welding have been developed and successfully implemented for seam tracking and adaptive welding functions (mass and heat balance). Typical seam tracking errors of 0.3 mm were achieved for single pass type joints (lap, butt, fillet). In one system the weld preparation profile is first enhanced by a projected laser target formed by a line and dots. A standard TV camera is used to observe the target image at an angle. The rapid preprocessor developed by NRCC and Leigh Instruments Inc as part of the visual aid system of the space shuttle arm is then used to analyse the video signal in real time. Another active vision system was developed in order to process more complex types of joints. It is based on laser flying spot scanning with a mechanically synchronized scanning system for projection and range finding. With a passive system the weld preparation temperature is mapped in front of the arc using a fiber optic bundle. The temperature profile of the joint is then analysed by a microcomputer. Because no single sensor is universal, the combination of active and passive systems on the same robot arm allows the arc welding robot to perform complex tasks. Furthermore, the use of an off-line programming system greatly simplifies the programming task of an arc welding robotic workcell equipped with vision sensors. Author

N87-17067# Hughes Helicopters, Culver City, Calif. Materials, Processes and Standards Dept.
INERTIA WELDING OF NITRALLOY N AND 18 NICKEL MARAGING 250 GRADE STEELS FOR UTILIZATION IN THE MAIN ROTOR DRIVE SHAFT FOR THE AR-64 MILITARY HELICOPTER PROGRAM
A. G. Hirko and L. L. Soffa *In* AGARD Advanced Joining of Aerospace Metallic Materials Jul. 1986 9 p (For primary document see N87-17051 09-37)
Avail: NTIS HC A12/MF A01

Preproduction feasibility studies were performed on laboratory type inertia welded specimens of Nitralloy N and 18 Nickel Maraging 250 Grade Steel prior to a full-scale engineering development program. The full-scale program consisted of producing scaled down drive shaft components to produce engineering test parts and to develop process control parameters for guide lines in the production program. Initial studies consisted of a metallurgical development program to arrive at a satisfactory post aging cycle for the composite or dual alloy drive shaft. In addition, metallurgical and static and dynamic tests were made from coupons excised from inertia-welded assemblies to establish structural behavior. Several sub-scale inertia-welded test specimens were tested in torsion loading to develop flight structural performance. Torsion tests showed the inertia weld exhibited strength characteristics equal or better than the parent metal for the Nitralloy N alloy component. The improved two-alloy, inertia-welded components show an approximate weight saving of 10 to 15 pounds over a drive shaft produced from Nitralloy N. This is due to a higher

strength/weight ratio of 18 Nickel Maraging 250 Grade Steel as compared to Nitralloy N. M.G.

N87-17068# Swiss Aluminum Ltd., Neuhausen am Rheinfall. Materials Technology Dept.
WELDING OF ALUMINUM CASTINGS
J. Leupp, A. Maitland, and K. Schellenberg *In* AGARD Advanced Joining of Aerospace Metallic Materials Jul. 1986 8 p (For primary document see N87-17051 09-37)
Avail: NTIS HC A12/MF A01

Developments in the field of electronics have recently made available new methods and power sources which enable even the most difficult aluminium casting alloys to be welded economically. Each method has specific applications where it is optimally employed. The best results in fabrication welding are obtained with the TIG-PLASMA-KEYHOLE process. With this method the normal classification of casting alloys into those which weld easily and those which weld badly no longer applies. Excellent welds can be obtained for example with the high strength AlCu alloys. The flawless, fine grained weld bead provides mechanical properties equivalent to those of the parent metal - both under static and fatigue loading conditions. The best results in finish and repair welding have been obtained using TIG welding with variable polarity. If due care is taken, this method also enables excellent results to be achieved under all types of loading conditions. Examples where the described methods are successfully employed include not only aircraft constructions but also parts for railway vehicles and electrical switch-gear. Author

N87-17069# Societe Nationale d'Etude et de Construction de Moteurs d'Aviation, Paris (France). Lab. Assemblages Metallurgiques.
THE APPLICATION OF THE RBD PROCESS TO THE DEPOSITION OF ANTI-WEAR ALLOYS
J. Lesgourgues *In* AGARD Advanced Joining of Aerospace Metallic Materials Jul. 1986 11 p (For primary document see N87-17051 09-37)
Avail: NTIS HC A12/MF A01

Initially, the rechargement-brasage-diffusion (RBD) was developed by SNECMA to solve problems occurring during assembly and repair of cast superalloy turbine parts. Beyond the metallurgical possibilities it offers, this process has proved to be economical. Subsequent developments in this field have shown it was possible to apply alloys with specific characteristics, e.g., antiwear properties. This paper presents various applications of The RBD process, mainly in the field of wear protection. Author

N87-17070# National Aerospace Lab., Amsterdam (Netherlands).
EVALUATION OF DDH AND WELD REPAIRED F100 TURBINE VANES UNDER SIMULATED SERVICE CONDITIONS c38
A. J. A. Mom, N. M. Madhava (Chromalloy Div.-Oklahoma, Midwest City), G. A. Kool, and M. Dean (Turbine Support Europa, Tilburg, Netherlands) *In* AGARD Advanced Joining of Aerospace Metallic Materials Jul. 1986 9 p Previously announced as N86-32762 (For primary document see N87-17051 09-37)
Avail: NTIS HC A12/MF A01

Cost and delivery times of high technology turbine components are a strong impetus for the development of advanced repair processes with the ability of complete restoration of unserviceable components. One of such advanced processes, diffusion densification healing (DDH), was applied for repair of cracked and unserviceable F100 turbine vanes. The DDH process was evaluated under simulated service test conditions with respect to the conventional weld/patch coat repair procedure. The evaluation shows that the DDH process is a remarkably effective restoration process, resulting in strongly improved test behavior in relation to the original weld/patch coat procedure. Additional advantages are that scrap rates during repair are likely to be considerably reduced and that for the future some relaxation of current repair limits might even be considered. Author

N87-17071# Liburdi Engineering Ltd., Burlington (Ontario).
REPAIR TECHNIQUES FOR GAS TURBINE COMPONENTS
J. Liburdi and P. Lowden *In* AGARD Advanced Joining of Aerospace Metallic Materials Jul. 1986 12 p (For primary document see N87-17051 09-37)
Avail: NTIS HC A12/MF A01

Areas in which the state of the art in gas turbine repair technology needs to be advanced are discussed. A large part of the discussion deals with current inadequacies of weld repair techniques for high strength superalloys and with possible areas for improvement. In particular, the problems of poor weldability and the low strength of conventional weld repairs are examined, with emphasis on areas for further development including; welding with matching filler metals, pre-weld heat treatment and preparation, modification of welding techniques and post-weld hot isostatic pressing (HIPing) and heat treatment. Another area of discussion is the need for improved techniques for resurfacing and repair of airfoil damage. Two techniques appear to be promising for this application; diffusion brazing and vacuum plasma spraying. The importance of NDT limitations and mechanical analysis with regard to the development and implementation of novel repair techniques is emphasized. Disregard of these factors can lead to repairs which are substantially cosmetic in nature. Author

N87-16925# Messerschmitt-Boelkow-Blohm G.m.b.H., Munich (West Germany).
EXPERIENCE GAINED BY SECTOR MODEL TESTING OF AN UNFURLABLE MESH/RIB ANTENNA
H. Heinze, H. Herbig, and H. Vorbrugg *In* ESA Proceedings of the Second ESA Workhop on Mechanical Technology for Antennas Aug. 1986 p 17-22 (For primary document see N87-16923 09-32) (Contract ESTEC-5206/82-NL-PB(SC))
Avail: NTIS HC A12/MF A01

N87-16926# Societe Nationale Industrielle Aerospatiale, Les Mureaux (France). Space and Ballistics Systems.
MECHANICAL AND CONTROL STUDY OF A 7 m OFFSET UNFURLABLE TRACKING ANTENNA
G. Labruyere, L. Passeron, M. Pastorino, and E. Schaffar *In* ESA Proceedings of the Second ESA Workshop on Mechanical Technology for Antennas Aug. 1986 p 23-30 (For primary document see N87-16923 09-32)
Avail: NTIS HC A12/MF A01

N87-16938# European Space Agency. European Space Research and Technology Center, ESTEC, Noordwijk (Netherlands).
GIOTTO SPACECRAFT HIGH GAIN ANTENNA MECHANICAL DESIGN AND DEVELOPMENT
R. Halm, F. Felici, H. J. Schoedel (Dornier-Werke G.m.b.H., Friedrichshafen, West Germany), and H. Raupp *In its* Proceedings of the Second ESA Workshop on Mechanical Technology for Antennas (date) p 123-126 (For primary document see N87-16923 09-32)
Avail: NTIS HC A12/MF A01

N87-16940# Construcciones Aeronauticas S.A., Madrid (Spain). Space and Systems Div.
ERS-1 WIND SCATTEROMETER ANTENNA: MECHANICAL ASPECTS
J. Garcia SanMartin *In* ESA Proceedings of the Second ESA Workshop on Mechanical Technology for Antennas Aug. 1986 p 139-149 (For primary document see N87-16923 09-32)
Avail: NTIS HC A12/MF A01

N87-16944# Contraves Italiana, Rome.
CONTRAVES' ANTENNA TIP HINGE MECHANISM FOR SELENIA SPAZIO'S 20/30 GHz ANTENNA
D. Stella, F. Morganti (Selenia S.p.A., Rome, Italy), and G. Nielsen (European Space Agency. European Space Research and Technology Center, ESTEC, Noordwijk (Netherlands) *In* ESA Proceedings of the Second ESA Workshop on Mechanical Technology for Antennas Aug. 1986 p 185-194 (For primary document see N87-16923 09-32)
Avail: NTIS HC A12/MF A01

N87-16946# Sener, S.A., Madrid (Spain).
A SENER MECHANISM: FINE ADJUSTMENT MECHANISM FOR THE FAR INFRARED AND SUBMILLIMETER SPACE TELESCOPE (FIRST) (F f F)
F. delCampo, J. delToro, and J. Rivacoba *In* ESA Proceedings of the Second ESA Workshop on Mechanical Technology for Antennas Aug. 1986 p 205-210 (For primary document see N87-16923 09-32)
Avail: NTIS HC A12/MF A01

N87-16947# Ricerche e Progetti s.r.l., Turin (Italy).
DYNAMICS AND CONTROL ANALYSIS PACKAGE (DCAP): AN AUTOMATED ANALYSIS AND DESIGN TOOL FOR STRUCTURAL CONTROL OF SPACE STRUCTURES
R. P. Singh, R. J. VanderVoort, C. Arduini, A. Festa (Aeritalia S.p.A., Torino, Italy), C. Maccone, and D. Sciacovelli (European Space Agency. European Space Research and Technology Center, ESTEC, Noordwijk, Netherlands) *In* ESA Proceedings of the Second ESA Workshop on Mechanical Technology for Antennas Aug. 1986 p 211-218 (For primary document see N87-16923 09-32)
Avail: NTIS HC A12/MF A01

N87-16952# Rome Univ. (Italy). Dipt. Aerospaziale.
THERMOMECHANICAL CHARACTERISTICS OF DICHROIC SUBREFLECTORS
C. Arduini, R. Barboni, A. Castellani, U. Ponzi, and S. Sgubini *In* ESA Proceedings of the Second ESA Workshop on Mechanical Technology for Antennas Aug. 1986 p 255-260 (For primary document see N87-16923 09-32)
Avail: NTIS HC A12/MF A01

38 QUALITY ASSURANCE AND RELIABILITY

Includes product sampling procedures and techniques; and quality control.

N87-17072# Royal Armament Research and Development Establishment, Fort Halstead (England).
APPLICATION OF MODIFIED THREE PARAMETER WEIBULL DISTRIBUTIONS TO BRITTLE MATERIAL DESIGN
J. Margetson and N. E. Cooper Feb. 1986 22 p
(RARDE-16/84; BR99178; ETN-87-98912) Avail: NTIS

A technique for evaluating the parameters of a Weibull distribution from a set of uniaxial fracture data is described. An extension to this technique allows characterization of a brittle material from flexural tests on beams in which the stress field is uniaxial but nonuniform. The characteristic Weibull parameters for surface and volume defects can be obtained. In order that multiaxial stress states can be analyzed, the theory of independent action is invoked. This failure theory uses surface or volume defect Weibull parameters in the failure probability calculation. The method of characterization and failure prediction using the theory of independent action are verified experimentally. ESA

N87-17073# Ames Lab., Iowa.
ABSTRACTS: REVIEW OF PROGRESS IN QUANTITATIVE NDE
1986 480 p Presented at the Review of Progress in Quantitative NDE, Williamsburg, Va., 23 Jun. 1985
(Contract W-7405-eng-82)
(DE87-000769; IS-4879; CONF-8506110-Absts) Avail: NTIS HC A21/MF A01

The conference was organized into the following sessions: introductory; process control for composites; composite materials; NDE of electronic materials and devices; acoustoelasticity and stress; new sensors; composite materials; material properties; composites, NDE applications and reliability; reliability; material properties of surfaces and interfaces; federal policies and strategies; weldments; scattering methodology; acoustic emission; retirement-for-cause (update); inverse scattering; eddy current models and probes; composites-acoustic measurements; deformation and fatigue; porosity in materials; imaging and reconstruction; transducers and transducer materials; eddy currents, ultrasonics, probes, and systems; eddy current inversion; ferromagnetic materials; transition and transfer of NDE technology; survey of imaging techniques; signal processing; and new NDE systems. Brief abstracts of the papers are given. DOE

N87-17061# Messerschmitt-Boelkow-Blohm G.m.b.H., Lemwerder (West Germany).
ULTRASONIC TESTING TECHNIQUES FOR DIFFUSION-BONDED TITANIUM COMPONENTS
Gustav Tober and Stefan Elze *In* AGARD Advanced Joining of Aerospace Metallic Materials Jul. 1986 10 p (For primary document see N87-17051 09-37)
Avail: NTIS HC A12/MF A01

N87-17062# Army Construction Engineering Research Lab., Champaign, Ill.
WELD QUALITY MONITOR AND CONTROL SYSTEM
F. Kearney, Dawn White, and William Ricci (Army Materials and Mechanics Research Center, Watertown, Mass.) *In* AGARD Advanced Joining of Aerospace Metallic Materials Jul. 1986 8 p (For primary document see N87-17051 09-37)
Avail: NTIS HC A12/MF A01

N87-17063# Rolls-Royce Ltd., Derby (England).
NDT OF ELECTRON BEAM WELDED JOINTS (MICRO-FOCUS AND REAL TIME X-RAY)
R. G. Taylor *In* AGARD Advanced Joining of Aerospace Metallic Materials Jul. 1986 4 p (For primary document see N87-17051 09-37)
Avail: NTIS HC A12/MF A01

N87-17064# National Research Council of Canada, Boucherville (Quebec).
THERMOELASTIC TESTING OF STRATIFIED MATERIALS
Paolo Cielo and Marc Dufour *In* AGARD Advanced Joining of Aerospace Metallic Materials Jul. 1986 15 p (For primary document see N87-17051 09-37)
Avail: NTIS HC A12/MF A01

N87-17070# National Aerospace Lab., Amsterdam (Netherlands).
EVALUATION OF DDH AND WELD REPAIRED F100 TURBINE VANES UNDER SIMULATED SERVICE CONDITIONS
A. J. A. Mom, N. M. Madhava (Chromalloy Div.-Oklahoma, Midwest City), G. A. Kool, and M. Dean (Turbine Support Europa, Tilburg, Netherlands) *In* AGARD Advanced Joining of Aerospace Metallic Materials Jul. 1986 9 p Previously announced as N86-32762 (For primary document see N87-17051 09-37)
Avail: NTIS HC A12/MF A01

39 STRUCTURAL MECHANICS

Includes structural element design and weight analysis; fatigue; and thermal stress.

For applications see *05 Aircraft Design, Testing and Performance* and *18 Spacecraft Design, Testing and Performance.*

N87-17074 Rensselaer Polytechnic Inst., Troy, N.Y.
THE THEORY OF FINITE ELASTIC-PLASTIC DEFORMATION WITH INDUCED ANISOTROPY MODELLED AS COMBINED ISOTROPIC-KINEMATIC HARDENING Ph.D. Thesis
Abdolreza Agah-Tehrani 1986 78 p
Avail: Univ. Microfilms Order No. DA8619960

The kinematics of finite elastic plastic deformation in the presence of strain induced anisotropy modeled by the shift of the yield surface in stress space is developed. By using representation theorems for symmetric and anti-symmetric tensor functions of the back stress and rate of the effective plastic strain an evolution law for anisotropy is proposed which includes general expressions

for both the terms expressing the direct effect of current plastic strain rate and also the component associated with the rotation of the anisotropy embedded in the material due to the plastic deformation. The analysis is developed to provide an expression for the total strain rate as the sum of an elastic term, linear in the Jaumann derivative of Kirchoff stress and the strain rate term, which for materials satisfying the normality condition, lead to the appropriate symmetries of the instantaneous elastic plastic moduli and hence the existence of a rate potential function. This makes the field equations self-adjoint, so that all solutions to inhomogenous self-adjoint boundary value problems can be characterized by a variational principle. Dissert. Abstr.

N87-17075 Purdue Univ., West Lafayette, Ind.
STRESS INTENSITY FACTORS FOR FATIGUE CRACKS AT HOLES UNDER CYCLIC STRESS GRADIENTS Ph.D. Thesis
Rigoberto Perez 1986 185 p
Avail: Univ. Microfilms Order No. DA8622207

The objective is to determine stress intensity factors (K) which may be used to predict the fatigue lives of part-through cracks loaded with variable stress gradients. The two types of cracks considered are surface and corner flaws located at holes in plates subjected to various stress distributions. The approach employs the weight function method which uses information from a reference load case to compute the stress intensity factor for a new load situation of interest. Results obtained for a number of crack sizes and load conditions are tabulated to serve as a data source. A second approach for calculating K by direct interpolation of data is also described. The simplicity of this latter technique makes it ideal for use in fatigue predictions where repetitive determination of K is required. Results are incorporated in a fatigue crack growth algorithm, which is used to perform specimen life predictions. The crack growth calculations are compared with experiments to test the validity of stress intensity factors from weight functions. The comparisons obtained are satisfactory. Dissert. Abstr.

N87-17076 Georgia Inst. of Tech., Atlanta.
QUANTITATIVE ANALYSIS OF FRACTURE SURFACES USING COMPUTER AIDED FRACTOGRAPHY Ph.D. Thesis
Kingshuk Banerji 1986 214 p
Avail: Univ. Microfilms Order No. DA8621574

The topography and features of fracture surfaces are the ultimate manifestations of the microfracture processes in materials. The quantitative analysis of fracture surface is of paramount importance in understanding the precise synergism of the microstructure, stresses and the environment that causes material fracture. Several analytical and experimental issues regarding the geometric quantification of fracture surfaces are investigated. The basic topographical parameters are evaluated from the digitized vertical section profiles through the fracture surface. Digitization is accomplished by using a microprocessor-based image analysis system. Physically meaningful parameters relevant to fracture mechanisms are introduced. The concept of fractals is adapted to accurately describe the variation of the profile and surface parameters with the size of the measuring unit of digitization. Procedures to obtain the surface roughness parameter from the profile roughness parameter using stereological considerations are presented. The quantitative fractographic methods developed here are applied to a study of the resulting fracture surfaces. With the 4340 steels, various ramifications of the dimpled rupture process, particularly with regard to the temper embrittlement phenomenon, are revealed. With the aged Al-4% Cu alloys, the influence of grain boundary embrittlement and deformation character on progressive intergranular fracture is deduced on the basis of quantitative parameters. Dissert. Abstr.

N87-17077# European Space Agency, Paris (France).
STRUCTURAL ANALYSIS
Jun. 1986 384 p Transl. into ENGLISH of "Strukturberechnung", DFVLR, Brunswick, West Germany, rept. DFVLR-Mitt-84-21, Nov. 1984 365 p Presented at Conference on Structural Mechanics, Brunswick, West Germany, 7 Jun. 1984 Original language document was announced as N86-71570 (ESA-TT-917; DFVLR-Mitt-84-21; ETN-87-98814) Avail: NTIS HC A17/MF A01; original German version available from DFVLR, Cologne, West Germany DM 95

Coupling of tension and torsion in rods; field consistency in finite element analysis, bucking and post-buckling behavior of small shells; optimization of axially compressed carbon fiber reinforced plastic cylinders; a substructure technique applied to fracture mechanics of composites; stress intensity factors as indicators of crack propagation in unidirectional laminates; and static aeroelastic phenomena of composite wings are discussed. For individual titles, see N87-17078 through N87-17085.

N87-17078# Deutsche Forschungs- und Versuchsanstalt fuer Luft- und Raumfahrt, Brunswick (West Germany). Inst. fuer Strukturmechanik.
RESEARCH ON STRUCTURAL ANALYSIS AT THE DFVLR, BRUNSWICK
Bodo Geier (Deutsche Forschungs- und Versuchsanstalt fuer Luft- und Raumfahrt, Brunswick, West Germany) *In its* Structural Analysis Jun. 1986 p 7-42 Transl. into ENGLISH of "Strukturberechnung", DFVLR, Brunswick, West Germany, Nov. 1984 p 9-40 Original language document was announced as N85-29314 (For primary document see N87-17077 09-39)
Avail: NTIS HC A17/MF A01; original German version available from DFVLR, Cologne, West Germany DM 95

The science of structural mechanics is reviewed, emphasizing computational problems in aerospace research. Light weight construction with composite materials is defined as the central topic. In an assessment of the present state of the art, it is concluded that a very satisfactory situation is achieved in the analysis of linear problems, but not in the solution of nonlinear problems and in structural optimization. ESA

N87-17079# Deutsche Forschungs- und Versuchsanstalt fuer Luft- und Raumfahrt, Brunswick (West Germany). Inst. fuer Strukturmechanik.
TORSION-TENSION COUPLING IN RODS
Dieter Petersen *In its* Structural Analysis Jun. 1986 p 43-76 Transl. into ENGLISH of "Strukturberechnung", DFVLR, Brunswick, West Germany, Nov. 1986 p 41-72 Original language document was announced as N85-29315 (For primary document see N87-17077 09-39)
Avail: NTIS HC A17/MF A01; original German version available from DFVLR, Cologne, West Germany DM 95

The treatment of torsion-tension coupling in rods under finite deformations is discussed. Analyses containing higher order terms due to geometric nonlinearities show inconsistency. The differences of three analyses are discussed via numerical examples. Extremely light constructions in aviation and astronautics can neither abandon rod structures nor give up the demand for a precise analysis. ESA

N87-17080# Deutsche Forschungs- und Versuchsanstalt fuer Luft- und Raumfahrt, Brunswick (West Germany). Inst. fuer Struukturmechanik.
FIELD CONSISTENCY AND FINITE ELEMENT ANALYSIS OF MULTIFIELD STRUCTURAL PROBLEMS
Gangan Prathap *In its* Structural Analysis Jun. 1986 p 77-143 Transl. into ENGLISH of "Strukturberechnung", DFVLR, Brunswick, West Germany, Nov. 1984 p 73-139 Previously announced as N85-29316 (For primary document see N87-17077 09-39)
Avail: NTIS HC A17/MF A01; original German version available from DFVLR, Cologne, West Germany DM 95

A terminology for errors resulting from finite element analysis in structural analysis is introduced. The problem area continuum field problems requiring a multifield characterization in which some field functions are constrained - is identified and defined. The requirement of field consistency is introduced and joins the principles used in the construction of efficient finite element methods. The concept of errors of the second kind delineating a special form of discretization error, and the additional stiffness parameter help to make a posteriori evaluations of such finite elements - with or without locking. Theory and analysis of physical examples, namely the poor bending response of plane stress

elements, shear-flexible beam/plates (shear locking), and curved elements (membrane locking); and incompressible elasticity and fluid flow are given. Techniques to introduce field consistency are explained: unequal order interpolation, reduced integration, reduced interpolation, and addition of incompatible modes. ESA

N87-17081# Deutsche Forschungs- und Versuchsanstalt fuer Luft- und Raumfahrt, Brunswick (West Germany). Inst. fuer Strukturmechanik.

BUCKLING AND POSTBUCKLING BEHAVIOR OF SHALLOW SHELLS

Klaus Rohwer *In its* Structural Analysis Jun. 1986 p 145-207 Transl. into ENGLISH of "Strukturberechnung", DFVLR, Brunswick, West Germany, Nov. 1984 p 141-197 Original language document was announced as N85-29317 (For primary document see N87-17077 09-39)

Avail: NTIS HC A17/MF A01; original German version available from DFVLR, Cologne, West Germany DM 95

Computer programs to study the buckling and postbuckling behavior of shallow shells were developed. Meshwise bicubic interpolation is used to discretize the total potential energy. The minima of the resulting polynomial of fourth order, determined by the computer program NOLIN, specify stable equilibrium states in the geometric nonlinear range. The program BEOS determines bifurcation buckling loads, and from a perturbation analysis finds an approximate initial postbuckling behavior. Comparing the results of the two programs shows that this approximation is not in all cases sufficient to describe the nonlinear behavior. ESA

N87-17082# Deutsche Forschungs- und Versuchsanstalt fuer Luft- und Raumfahrt, Brunswick (West Germany). Inst. fuer Strukturmechanik.

OPTIMIZATION OF AXIALLY COMPRESSED CARBON FIBER REINFORCED PLASTIC (CFRP) CYLINDERS

Rolf Zimmermann *In its* Structural Analysis Jun. 1986 p 208-236 Transl. into ENGLISH of "Strukturberechnung", DFVLR, Brunswick, West Germany, Nov. 1984 p 199-225 Original language document was announced as N85-29318 (For primary document see N87-17077 09-39)

Avail: NTIS HC A17/MF A01; original German version available from DFVLR, Cologne, West Germany DM 95

The numerical optimization of axial compressed CFRP cylinders was investigated. The mass minimization of axially compressed CFRP cylindrical shells which may fail due to buckling or loss of material strength, is replaced by a sequence of buckling load maximizations. The layer orientations are used as variables to be changed continuously and directly. The results show that the optimal orientations are independent of the parameters describing the cylinder. Findings concerning sensitivity and numerical and experimental studies of validity limits are given. ESA

N87-17083# Deutsche Forschungs- und Versuchsanstalt fuer Luft- und Raumfahrt, Brunswick (West Germany).

AN EFFECTIVE SUBSTRUCTURE TECHNIQUE APPLIED TO CRACK PROBLEMS

Hans Eggers *In its* Structural Analysis Jun. 1986 p 237-310 Transl. into ENGLISH of "Strukturberechnung", DFVLR, Brunswick, West Germany, Nov. 1984 p 227-294 Original language document was announced was N85-29319 (For primary document see N87-17077 09-39)

Avail: NTIS HC A17/MF A01; original German version available from DFVLR, Cologne, West Germany DM 95

A specialized substructure technique was developed to solve crack problems, whereby the linearly elastic uncracked structure is limited by conditions describing the cracking. The common methods to determine the stress intensity factors in cracked structures and their accuracy are discussed. The treatment of the material and structural nonlinearity by scalar conditions, which constrains a functional for the linearly elastic structure, is introduced. The finite transformation of the constrained functional yields the usual equations for the linearly elastic structure, as well as equations for the constraints. With increasing damage only the newly added equations for the constraints must be solved. The substructure technique determines the reduced element matrices and the load cracks directly in solving the equations. ESA

N87-17084# Deutsche Forschungs- und Versuchsanstalt fuer Luft- und Raumfahrt, Brunswick (West Germany). Inst. fuer Strukturmechanik.

CRACK PROPAGATION IN UD (UNIDIRECTIONAL) LAMINATES BY THE STRESS INTENSITY FACTORS

Rolf Zick *In its* Structural Analysis Jun. 1986 p 311-334 Transl. into ENGLISH of "Strukturberechnung", DFVLR, Brunswick, West Germany, Nov. 1986 p 295-318 Original language document was announced as N85-29320 (For primary document see N87-17077 09-39)

Avail: NTIS HC A17/MF A01; original German version available from DFVLR, Cologne, West Germany DM 95

Based on test results with notched unidirectional laminates, critical values of the stress intensity factors K1 and K2 were determined. They represent characteristic values for the material properties and form an envelope f(K1, K2) = 0. Any stress state with f(K1, K2) greater than or = 0 leads to further crack propagation. Methods to determine the stress intensity factors from the stress and displacement field, which are computed using finite element methods, are indicated. ESA

N87-17085# Deutsche Forschungs- und Versuchsanstalt fuer Luft- und Raumfahrt, Brunswick (West Germany). Inst. fuer Strukturmechanik.

THE STATIC AEROELASTICITY OF A COMPOSITE WING

Matthias Piening *In its* Structural Analysis Jun. 1986 p 335-383 Transl. into ENGLISH of "Strukturberechnung", DFVLR, Brunswick, West Germany, Nov. 1984 p 319-364 Original language document was announced as N85-29321 (For primary document see N87-17077 09-39)

Avail: NTIS HC A17/MF A01; original German version available from DFVLR, Cologne, West Germany DM 95

A procedure for parametric investigations of the static-aeroelastic behavior of anisotropic wings with average to large aspect ratio was developed. By exploiting the directional stiffness properties of a composite material, coupling of bending and torsional deformations can be achieved. This can be used to influence the spanwise lift distribution, the internal structural forces, and the permissible flying speeds limited by the aeroelastic behavior of the wing. Static divergence can be avoided and forward wing sweep can be realized. The differential equations describing the aeroelastic behavior of a beamlike wing structure are solved by applying the multiple shooting method. Examples show the effects of fiber orientations on lift distributions of a composite wing. ESA

N87-17086*# National Aeronautics and Space Administration. Langley Research Center, Hampton, Va.

A PARALLEL SOLUTION FOR THE SYMMETRIC EIGENPROBLEM

Gaylen A. Thurston Jan. 1987 14 p (NASA-TM-89082; NAS 1.15:89082) Avail: NTIS HC A02/MF A01 CSCL 20K

A completely parallel algorithm for the symmetric eigenproblem AX = Lambda BX is outlined. The algorithm is parallel in the sense that the numerical operations do not occur in a fixed sequence. Therefore, a large number of operations can be programmed to be performed concurrently on a computer with multiple central processing units. The standard symmetric eigenvalue problem AX = Lambda X has the property that the n eigenvalues of the principal submatrix of A of order n are separated by the (n-1) eignvalues of the principal submatrix of order (n-1). The separation property delineated n intervals containing one eigenvalue. Each eigenvalue and corresponding eigenvector can be computed independently. The n eigenproblem calculations can be divided among multiple processing units. Author

N87-17087*# National Aeronautics and Space Administration. Lewis Research Center, Cleveland, Ohio.

SURFACE FLAW RELIABILITY ANALYSIS OF CERAMIC COMONENTS WITH THE SCARE FINITE ELEMENT POSTPRO-

CESSOR PROGRAM

John P. Gyekenyesi and Noel N. Nemeth (WLT Corp., Cleveland, Ohio) 1987 17 p Proposed for presentation at the 32nd International Gas Turbine Conference and Exhibit, Anaheim, Calif., 31 May - 4 Jun. 1987; sponsored by ASME

(NASA-TM-88901; E-3229; NAS 1.15:88901) Avail: NTIS HC A02/MF A01 CSCL 20K

The SCARE (Structural Ceramics Analysis and Reliability Evaluation) computer program on statistical fast fracture reliability analysis with quadratic elements for volume distributed imperfections is enhanced to include the use of linear finite elements and the capability of designing against concurrent surface flaw induced ceramic component failure. The SCARE code is presently coupled as a postprocessor to the MSC/NASTRAN general purpose, finite element analysis program. The improved version now includes the Weibull and Batdorf statistical failure theories for both surface and volume flaw based reliability analysis. The program uses the two-parameter Weibull fracture strength cumulative failure probability distribution model with the principle of independent action for poly-axial stress states, and Batdorf's shear-sensitive as well as shear-insensitive statistical theories. The shear-sensitive surface crack configurations include the Griffith crack and Griffith notch geometries, using the total critical coplanar strain energy release rate criterion to predict mixed-mode fracture. Weibull material parameters based on both surface and volume flaw induced fracture can also be calculated from modulus of rupture bar tests, using the least squares method with known specimen geometry and grouped fracture data. The statistical fast fracture theories for surface flaw induced failure, along with selected input and output formats and options, are summarized. An example problem to demonstrate various features of the program is included. Author

N87-17088*# National Aeronautics and Space Administration. Langley Research Center, Hampton, Va.

A THREE DIMENSIONAL CALCULATION OF ELASTIC EQUILIBRIUM FOR COMPOSITE MATERIALS Final Report

Liviu R. Lustman and Milton E. Rose Jul. 1986 29 p

(Contracts NAS1-17070; NAS1-18107)

(NASA-CR-178158; ICASE-86-51; NAS 1.26:178158) Avail: NTIS HC A03/MF A01 CSCL 20K

A compact scheme is applied to three-dimensional elasticity problems for composite materials, involving simple geometries. The mathematical aspects of this approach are discussed, in particular the iteration method. A vector processor code implementing the compact scheme is presented, and several numerical experiments are summarized. Author

N87-17089*# National Aeronautics and Space Administration, Washington, D.C.

DESIGN OF SOFTWARE FOR DESIGN OF FINITE ELEMENT FOR STRUCTURAL ANALYSIS Ph.D. Thesis - Stuttgart Univ., 22 Nov. 1983

Reinhard Helfrich Feb. 1987 216 p Transl. into ENGLISH of German Thesis p 1-192 Transl. by SCITRAN, Inc., Santa Barbara, Calif.

(Contract NASw-4004)

(NASA-TM-88528; NAS 1.15:88528) Avail: NTIS HC A10/MF A01 CSCL 20K

The concepts of software engineering which allow a user of the finite element method to describe a model, to collect and to check the model data in a data base as well as to form the matrices required for a finite element calculation are examined. Next the components of the model description are conceived including the mesh tree, the topology, the configuration, the kinematic boundary conditions, the data for each element, and the loads. The possibilities for description and review of the data are considered. The concept of the segments for the modularization of the programs follows the components of the model description. The significance of the mesh tree as a globular guiding structure will be understood in view of the principle of the unity of the model, the mesh tree, and the data base. The user-friendly aspects of the software system will be summarized: the principle of language communication, the data generators, error processing, and data security. Author

N87-17090*# National Aeronautics and Space Administration. Langley Research Center, Hampton, Va.

ENERGY DISSIPATION ASSOCIATED WITH CRACK EXTENSION IN AN ELASTIC-PLASTIC MATERIAL

K. N. Shivakumar (Analytical Services and Materials, Inc., Hampton, Va.) and J. H. Crews, Jr. Jan. 1987 36 p

(NASA-TM-89032; NAS 1.15:89032) Avail: NTIS HC A03/MF A01 CSCL 20K

Crack extension in elastic-plastic material involves energy dissipation through the creation of new crack surfaces and additional yielding around the crack front. An analytical procedure, using a two-dimensional elastic-plastic finite element method, was developed to calculate the energy dissipation components during a quasi-static crack extension. The fracture of an isotropic compact specimen was numerically simulated using the critical crack-tip-opening-displacement (CTOD) growth criterion. Two specimen sizes were analyzed for three values of critical CTOD. Results from the analyses showed that the total energy dissipation rate consisted of three components: the crack separation energy rate, the plastic energy dissipation rate, and the residual strain energy rate. All three energy dissipation components and the total energy dissipation rate initially increased with crack extension and finally reached constant values. Author

N87-17091# Pennsylvania State Univ., University Park. Dept. of Materials Science and Engineering.

ON THE INFLUENCE OF STRAIN-PATH CHANGES ON FRACTURE

S. C. Kestner and D. A. Koss Aug. 1986 14 p

(Contract N00014-86-K-0381)

(AD-A172535; TR-1) Avail: NTIS HC A02/MF A01 CSCL 20/11

Abrupt changes in strain path between uniaxial and equibiaxial tension are shown to have a large effect on plane-strain ductility. Data for titanium sheets, both with and without hydrides, show that a significant ductility enhancement occurs at a final strain state of plane-strain tension following multi-stage deformation sequences comprised of uniaxial and equibiaxial tension. While the dependence of ductile fracture on both accumulated damage and strain hardening suggests that failure strains should be sensitive to a nonproportional strain-path history, the detailed cause(s) of the present effect is not known. GRA

N87-17092# California Inst. of Tech., Pasadena. Graduate Aeronautical Labs.

DYNAMIC FRACTURE INITIATION AND PROPAGATION IN 4340 STEEL UNDER IMPACT LOADING

Alan T. Zehnder and Ares J. Rosakis 1986 31 p

(Contract N00014-85-K-0596)

(AD-A173084; GALCIT-SM-86-6) Avail: NTIS HC A03/MF A01 CSCL 11/6

Dynamic fracture initiation and propagation in 4340 steel was investigated experimentally using the optical method of reflected caustics combined with high speed photography. A new crack propagation testing configuration consisting of a three point bend specimen loaded in a drop weight tower was used. It was found that prior to crack initiation the stress intensity factor time record calculated using the dynamic tip load and a static formula disagrees with the actual stress intensity factor measured by caustics. During crack propagation, the crack tip velocity and stress intensity factor time records varied smoothly and repeatably allowing for a straightforward interpretation of the data. The experiments show that for the particular heat treatment of 4340 steel used, the dynamic fracture propagation toughness depends on crack tip velocity through a relation that is a material property. GRA

N87-17093# Edgerton, Germeshausen and Grier, Inc., Idaho Falls, Idaho.

THREE DIMENSIONAL CTOD MEASUREMENTS OF ELASTIC-PLASTIC SURFACE FLAWS

W. G. Reuter and J. S. Epstein 1986 7 p Presented at the

SEM Spring Conference on Experimental Mechanics, New Orleans, La., 8 Jun. 1986
(Contract DE-AC07-76ID-01570)
(DE86-013454; EGG-M-18785; CONF-860682-4) Avail: NTIS HC A02/MF A01

Proven analytical solutions are not available for predicting the conditions for crack initiation and growth of a surface crack in a material with elastic-plastic behavior. An approach based on the relationship between the crack tip opening displacement and J-integral could provide useful insight into applicability of J. This paper presents results of metallographic examinations of the crack tip region of elastic-plastic and fully plastic specimens containing surface cracks. DOE

N87-17094# Aeronautical Research Inst. of Sweden, Stockholm. Structures Dept.
FATIGUE LIFE AND FASTENER FLEXIBILITY OF SINGLE SHEAR RIVETED AND BOLTED JOINTS
Bjoern Palmberg Jun. 1986 50 p
(Contract FMV-FFL-82250-85-076-73-001)
(FFA-TN-1986-35; ETN-87-98905) Avail: NTIS HC A03/MF A01

Fatigue life and fastener flexibility were investigated using open hole specimens, no load transfer specimens, and double row, four columns, single shear joints (S50) made from a 2 mm thick sheet of the aluminum alloy 7475-T761 fastened with rivets and Hi-lok. Computerized flight simulations show that fatigue lives of specimens with Hi-lok fasteners are much longer than for riveted specimens. The fastener flexibilities of riveted joints (S50) are much higher than for joints with Hi-lok fasteners. Fastener flexibility seems to depend on the stress level, the size of individual load cycles, the peak and the trough in a load cycle, and the number of applied flights. ESA

N87-17095# Sheffield Univ. (England). Dept. of Control Engineering.
MODEL SELECTION AND VALIDATION METHODS FOR NON-LINEAR SYSTEMS
I. J. Leontaritis and S. A. Billings Mar. 1986 38 p Sponsored by UK Science and Engineering Research Council
(RR-292; ETN-87-98931) Avail: NTIS HC A03/MF A01

The theory of hypothesis testing is used to select a model with the correct structure. The relation of such a method to the AIC and FPE criteria is investigated. Parametric validation and correlation validation methods for nonlinear difference equation models are developed. Shortcomings of traditional methods, especially when applied to nonlinear systems are described. ESA

N87-16930# Rome Univ. (Italy). Dept. of Aerospace.
EFFECTS OF CURING STRESSES ON COMPOSITE STRUCTURES
M. Marchetti, F. Morganti (Selenia S.p.A., Rome, Italy), and S. Tizzi *In* ESA Proceedings of the Second ESA Workshop on Mechanical Technology for Antennas Aug. 1986 p 57-62 Sponsored by Max-Planck Inst. (For primary document see N87-16923 09-32)
Avail: NTIS HC A12/MF A01

N87-16937# Societe Nationale Industrielle Aerospatiale, Les Mureaux (France). Div. des Systems Balistiques et Spatiaux.
STRUCTURAL ANALYSIS, MANUFACTURING AND DEVELOPMENT STATUS OF LARGE POLARIZATION SENSITIVE DUAL-GRIDDED REFLECTORS
J. D. Lefebvre *In* ESA Proceedings of the Second ESA Workshop on Mechanical Technology for Antennas Aug. 1986 p 111-121 (For primary document see N87-16923 09-32)
Avail: NTIS HC A12/MF A01

N87-16945# Construcciones Aeronauticas S.A., Madrid (Spain). Space and Systems Div.
WIND SCATTEROMETER ANTENNA (WSA) RELEASE SHOCK LOADS
P. Luengo and C. Huerta *In* ESA Proceedings of the Second ESA Workshop on Mechanical Technology for Antennas Aug. 1986 p 195-203 (For primary document see N87-16923 09-32)
Avail: NTIS HC A12/MF A01

N87-17065# Industrieanlagen-Betriebsgesellschaft m.b.H., Ottobrunn (West Germany).
INFLUENCE OF WELDING FLAWS ON THE FATIGUE STRENGTH OF ELECTRON BEAM WELDMENTS IN TI AI6 V4
Walter Schuetz and Wolfram Oberparleiter *In* AGARD Advanced Joining of Aerospace Metallic Materials Jul. 1986 11 p (For primary document see N87-17051 09-37)
Avail: NTIS HC A12/MF A01

42 GEOSCIENCES (GENERAL)

N87-17096# Joint Publications Research Service, Arlington, Va.
USSR REPORT: EARTH SCIENCES
7 May 1986 78 p Transl. into ENGLISH from various Russian articles
(JPRS-UES-86-005) Avail: NTIS HC A05/MF A01

Various topics related to U.S.S.R. research in Earth sciences are discussed. Meteorology, oceanography, terrestrial geophysics, atmospheric physics, and arctic and antarctic research are among the areas covered. For individual titles, see N87-17097 through N87-17108.

N87-17097# Joint Publications Research Service, Arlington, Va.
GEOPHYSICIST COMMENTS ON HOW SOLAR ACTIVITY MAY AFFECT WEATHER **c47**
In its USSR Report: Earth Sciences (JPRS-UES-86-005) 7 May 1986 p 1-2 Transl. into ENGLISH from Gudok (Moscow, USSR), no. 50(18385), 28 Feb. 1986 p 4, cols. 4-8 (For primary document see N87-17096 09-42)
Avail: NTIS HC A05/MF A01

The ways in which solar activity influence Earth weather are discussed in general terms. The solar wind is described as a bridge between the Sun and Earth. The magnetosphere resists penetration of solar particles to Earth-it pulsates, contracts and breathes. Scientists call this process geomagnetic disturbance. The solar wind nevertheless penetrates into the magnetosphere, sharply raising the temperature of the particles. But how can it reach the atmosphere itself, unless easier and well-trod paths exist somewhere? It turns out that they do exist-over the Earth's south and north magnetic poles. The lines of force of the planet's magnetic field converge there, forming shapes like funnels. It is through these funnels that particles of the solar wind seep into layers of the atmosphere, giving rise to polar auroras and magnetic storms that cause of many stresses on Earth. A hypothesis which has become more and more popular lately is that the atmosphere's layers-the ionosphere, the mesostratosphere and the troposphere-form a kind of dynamic unity, and that changes in the upper layers undoubtedly affect the lower ones. Even if particles of the solar wind remain in the ionosphere, pulses generated through their action will release an accumulated reserve of energy in the lower atmosphere. As soon as this happens, meteorologists will record the beginning of climatic fluctuations. Author

N87-17098# Joint Publications Research Service, Arlington, Va.
THERMODYNAMIC ESTIMATE OF CLIMATIC SYSTEM EFFICIENCY Abstract Only **c47**
A. S. Ginzburg *In its* USSR Report: Earth Sciences (JPRS-UES-86-005) 7 May 1986 p 3 Transl. into ENGLISH from Izvestiya Akademii Nauk SSSR: Fizika Atmosfery i Okeana (Moscow, USSR), v. 21, no. 10, Oct. 1985 p 1020-1025 Original language document was announced in IAA as A86-18140 (For primary document see N87-17096 09-42)
Avail: NTIS HC A05/MF A01

Estimates are presented of the maximum useful work which can be performed by the Earth's climatic system assuming average insolation. In the lower latitudes the flux of incoming radiation is greater than the flux of departing thermal radiation.

The relationship is opposite in the higher latitudes. The efficiency is defined as the maximum useful work which can be performed by the system. The maximum possible efficiency of the Martian atmosphere under year-round average conditions is also studied. The estimates obtained demonstrate both common features and basic differences in the climatic systems of the Earth and Mars. The efficiency of the atmosphere and entire climatic system of both planets is near the maximum and simultaneously close to the quantity of generation of kinetic energy in the atmosphere. However, on Earth equalization of temperature occurs not only due to generation and dissipation of kinetic energy, but also due to transfer of other types of energy from warmer to cooler areas, particularly due to evaporation and condensation of water vapor. On Mars, the thin atmosphere of the planet is incapable of transferring large quantities of heat, resulting in great temperature contrasts, attributable to nonuniform heating of the planet by the sun. Author

N87-17099# Joint Publications Research Service, Arlington, Va.
CONTEMPORARY CHANGES IN CLIMATE AND PALEOCLIMATE Abstract Only c47
M. I. Budyko *In its* USSR Report: Earth Sciences (JPRS-UES-86-005) 7 May 1986 p 3-4 Transl. into ENGLISH from Izvestiya Akademii Nauk SSSR: Seriya Geograficheskaya (Moscow, USSR), no. 6, Nov. - Dec. 1985 p 36-42 (For primary document see N87-17096 09-42)
Avail: NTIS HC A05/MF A01

Previous studies by the authors have indicated that the world temperature will increase by 2.50 C between 1970 and 2070. Conferences since the mid-1970s have confirmed the probable increase in world temperature due to anthropogenic effects. Since the 1970s, new approaches have been developed in which the sensitivity of the climatic system to anthropogenic effects is studied based on empirical materials concerning contemporary changes in climate and data on the climate in the geological past. Here, the possibilities afforded for studying anthropogenic change by the use of paleoclimatic material are discussed. Extensive paleoclimatic and paleogeographic materials are summarized. Author

N87-17100# Joint Publications Research Service, Arlington, Va.
DETERMINATION OF NONGLOBAL COMPONENT AGAINST BACKGROUND OF GLOBAL RADIOACTIVE POLLUTION OF ATMOSPHERIC AEROSOLS Abstract Only c45
Z. G. Gritchenko, V. M. Flegontov, and K. Sinkko *In its* USSR Report: Earth Sciences (JPRS-UES-86-005) 7 May 1986 p 4 Transl. into ENGLISH from Radiokhimiya (Leningrad, USSR), v. 27, no. 5, 1985 p 669-673 (For primary document see N87-17096 09-42)
Avail: NTIS HC A05/MF A01

An attempt is made to determine the nonglobal component in global radioactive pollution of atmospheric aerosols, made possible by the advent of precision semiconductor gamma spectrometry. A figure illustrates the main changes in global 137 sub Cs pollution at low altitudes in the middle latitudes of the Northern Hemisphere, 1975 to 1982, based on determination of the ratio of 137 sub Cs to 7Be observed at 11 points in the Northern Hemisphere. Variations in data normalized on the basic of this assumption were plotted. As an example, the data for a location in Sweden indicate elevated concentrations of 137 sub Cs at low altitudes. If there were not methodological errors in the measurements of 7Be and 137 sub Cs in the area, there is probably a source of 137 sub Cs pollution nearby, causing its level to exceed the global pollution level. Author

N87-17101# Joint Publications Research Service, Arlington, Va.
ASSESSMENT OF CONTEMPORARY CHANGES IN GLOBAL CLIMATE c47
K. Ya. Vinnikov *In its* USSR Report: Earth Sciences (JPRS-UES-86-005) 7 May 1986 p 4-5 Transl. into ENGLISH from Gidrometeorologiya: Seriya Meteorologiya (Obninsk, USSR), no. 8, 1985 p 1-52 (For primary document see N87-17096 09-42)
Avail: NTIS HC A05/MF A01

On the basis of empirical data relating to change in the global thermal regime during the period of instrumental meteorological observations, the observed trends in mean air temperature and their causes, as well as the patterns of regional changes in climate associated with change in the global thermal regime are reviewed. It was concluded that the mean annual air surface temperature, averaged for individual hemispheres or the entire Earth, is one of the most important characteristics of contemporaneous climatic changes. Quite reliable data on change in mean temperature during the last century are now available. During the course of this period there was a predominance of a tendency on an increase in air temperature, as a result of which during the last century the mean temperature in the Northern Hemisphere has increased by approximately 0.5 C. This almost precisely coincides with the temperature change which according to the theory of climate should occur as a result of an increase in carbon dioxide content. This is indicative of a decisive influence of anthropogenic factors on the mean trend of air temperature during the last century. It appears possible to give a quantitative description of the main features of change in mean temperature with time with allowance for the influence of variations in atmospheric transparency and increase in CO2. The influence of anthropogenic factors on the contemporaneous change in climate can be considered demonstrated. Author

N87-17102# Joint Publications Research Service, Arlington, Va.
METAL CONTENT OF OCEAN WATER STUDIED WITH RADIO SPECTROMETER c48
In its USSR Report: Earth Sciences (JPRS-UES-86-005) 7 May 1986 p 8 Transl. into ENGLISH from Kazakhstanskaya Pravda (Alma-Ata, USSR), 29 Jan. 1986 p 3 (For primary document see N87-17096 09-42)
Avail: NTIS HC A05/MF A01

A new step toward the extraction of metals from ocean water has been taken by associates of the Tajik Academy of Sciences' Institut of Chemistry. They have developed methods for determining the presence of copper and other elements in equeous solutions, with the aid of radio spectrometers. An interest in the Tajik scientists' work was taken by associates of the Pacific Oceanology Institute of the USSR Academy of Sciences' Far East Research Center. In line with a joint agreement between these institutes, a specialist from the Tajik chemistry institute was included in the crew of the scientific vessel Akademik Aleksandr Vinogradov by the Far East scientists. A field radio spectrometer was taken on board this vessel. Information on the concentration of metals in water was obtained with the aid of this instrument. Author

N87-17103# Joint Publications Research Service, Arlington, Va.
STOCHASTIC MODEL OF TIDAL EVOLUTION OF EARTH-MOON SYSTEM WITH CYCLIC CHANGE IN RESONANT FREQUENCY OF OCEAN Abstract Only c48
B. A. Kagan and N. B. Maslova *In its* USSR Report: Earth Sciences (JPRS-UES-86-005) 7 May 1986 p 14 Transl. into ENGLISH from Doklady Akademii Nauk SSSR (Moscow, USSR), v. 285, no. 5, 1985 p 1082-1086 Original language document was announced in IAA as A86-24303 (For primary document see N87-17096 09-42)
Avail: NTIS HC A05/MF A01

Previous studies attributing tidal evolution in the Earth-Moon system to the resonant properties of the ocean which change under the influence of continental drift have not considered the possibility of cyclical restructuring of the resonant properties of the ocean. This restructuring should be accompanied by weakening of semidiurnal and strengthening of diurnal natural oscillations as the continents converge, with the opposite effect as they drift apart. This should lead to a change in the dissipation of tidal energy in the paleoocean. The effects of this change are discussed. It is limited to a study of the case in which the Moon revolves around the earth in a circular equatorial orbit and the ocean tides are described by a single-mode approximation. Author

N87-17104# Joint Publications Research Service, Arlington, Va.
OCEAN SURFACE TEMPERATURE FIELD VARIABILITY

Abstract Only **c48**
S. A. Molchanov, L. I. Piterbarg, A. A. Ruzmaykin, and D. D. Sokolov *In its* USSR Report: Earth Sciences (JPRS-UES-86-005) 7 May 1986 p 21 Transl. into ENGLISH from Doklady Akademii Nauk SSSR (Moscow, USSR), v. 286, no. 4, Feb. 1986 p 969-972 (For primary document see N87-17096 09-42)
Avail: NTIS HC A05/MF A01

This is essentially a continuation of research published earlier by the authors (S. A. Molchanov, et al., GEOPHYS. ASTROPHYS. FLUID DYNAMICS, Vol. 30, pp 242-259, 1984) on development of a more accurate representation of ocean surface temperature field variability. Equations are derived and analyzed for the annual variation of the ocean surface temperature field and a more precise correlation function for the field of deviations and the possibility of the presence of well-expressed anomalies or intermittence in temperature distribution is evaluated. The heat budget equation vertically integrated in the upper quasihomogeneous layer of the ocean is used as a point of departure. It was found on the basis of the derived equations that synoptic wind fluctuations exert a significant influence on advection of the climatic field of ocean surface temperature and on the feedback factor in the ocean-atmosphere system and generate an additional heat flow. In most middle-latitude ocean regions horizontal heat exchange in the ocean surface temperature field can be attributed to anomalous drift currents and not the macroscale turbulence associated with synoptic eddies. Author

N87-17105# Joint Publications Research Service, Arlington, Va.
SOLUTION OF DIRECT GRAVIMETRY PROBLEMS FOR VERTICAL CYLINDRICAL BODIES Abstract Only **c46**
A. V. Kudrya *In its* USSR Report: Earth Sciences (JPRS-UES-86-005) 7 May 1986 p 35 Transl. into ENGLISH from Geologiya i Geofizika (Novosibirsk, USSR), no. 10, Oct. 1985 p 94-100 (For primary document see N87-17096 09-42)
Avail: NTIS HC A05/MF A01

A new method is presented for calculating the delta g generated by a rectangular prism, the density of which changes exponentially with the vertical coordinate. Analytic and approximate solutions of the direct problem in gravimetry are presented. Author

N87-17106# Joint Publications Research Service, Arlington, Va.
DEVELOPMENT OF NEW AVIATION TECHNOLOGY FOR GRAVIMETRIC SURVEYING Abstract Only **c43**
K. Ye. Besyelov, P. D. Bagdatlishvili, and V. O. Bagramyants *In its* USSR Report: Earth Sciences (JPRS-UES-86-005) 7 May 1986 p 38-39 Transl. into ENGLISH from Ekspress Informatsiya: Morskaya Geologiya i Geofizika (Moscow, USSR), no. 11, 1985 p 1-5 (For primary document see N87-17096 09-42)
Avail: NTIS HC A05/MF A01

In a standard cardan mounting, a gravimetric instrument requires 4 to 6 minutes to settle before measurements can be performed. This makes gravimetric surveying from helicopters quite difficult and reduces the accuracy of the surveys. A restraining device has been suggested for use with the new technology of airborne gravimetric surveying to fix the instrument in position and protect it from contact with the walls and to allow readings to be made 15 to 20 seconds after the restraining system is released. Tests have shown the success of this instrument when used in combination with a winch, which is necessary to create safer conditions for application of the new technology. When the winch is used, the time required to place the gravimetric instrument on the ground is reduced, the amplitude of rocking of the instrument as the observation point is approached through the air is greatly reduced and the quality of observations is improved, since they can be made at heights greater than 30 meters. When observations are made over the shelf, a float on a 2- to 3-meter cable some 15 to 17 meters from the gravimeter can be used as a reference point and the helicopter can be placed in a position such that the float is within view of the pilot, making it easier to maintain the helicopter hovering above the observation point. Author

N87-17107# Joint Publications Research Service, Arlington, Va.
MODELING OF NONLINEAR EFFECTS OF PLASMA WAVE BEAMS ON IONOSPHERIC PLASMA Abstract Only **c75**
G. A. Markov, L. L. Popova, and Yu. V. Chugnov *In its* USSR Report: Earth Sciences (JPRS-UES-86-005) 7 May 1986 p 42-43 Transl. into ENGLISH from Pisma v Zhurnal Tekhnicheskoy Fiziki (Leningrad, USSR), v. 11, no. 23, Dec. 1985 p 1465-1469 (For primary document see N87-17096 09-42)
Avail: NTIS HC A05/MF A01

Results are presented from laboratory modeling of the effect of a field of intensive plasma waves excited by bipole sources on the local parameters of the lower ionosphere. The purpose of the modeling was to determine the effectiveness of this method of action which is related to excitation in the lower layers of the ionosphere of an HF discharge in the form of a self-similar plasma-wave channel extending from the source along the geomagnetic field. The experimental data and theoretical estimates demonstrate the possibility of excitation of columns of hot, dense plasma in the lower ionosphere, which can be used to study nonlinear ionospheric phenomena. The local changes in plasma density are several orders of magnitude greater than the corresponding disturbances in ionospheric parameters observable with traditional methods of acting on the ionosphere using terrestrial radiation sources. Author

N87-17108# Joint Publications Research Service, Arlington, Va.
JOINT INFLUENCE OF TURBULENCE AND WIND ON SIGNAL POWER IN RADIOACOUSTIC SOUNDING OF ATMOSPHERE Abstract Only **c46**
A. I. Kon *In its* USSR Report: Earth Sciences (JPRS-UES-86-005) 7 May 1986 p 47 Transl. into ENGLISH from Izvestiya Akademii Nauk SSSR: Fizika Atmosfery i Okeana (Moscow, USSR), v. 21, no. 12, Dec. 1985 p 1242-1251 (For primary document see N87-17096 09-42)
Avail: NTIS HC A05/MF A01

The joint effect of atmospheric turbulence and wind drift on radio-acoustic sounding signals was studied in an effort to improve sounding method accuracy. A bistatic sounding system was used with the spaced radar transmitting and receiving antennas symmetrically arranged relative to the acoustic source and with the axes of all three antennas parallel; the emitted radio wave is scattered by the structure of permittivity induced in the atmosphere by an acoustic beam. The frequency of the scattered field carrying information on local temperature was investigated. A formula for the strength of the radio-acoustic signal in the absence of turbulence, but in the presence of wind drift, was derived first, followed by a similar derivation for the joint effect of these two factors. This provided basis for an expression describing mean signal strength in a turbulent moving medium. This expression is applicable for virtually any type of radioacoustic apparatus and any sounding ranges. Allowance for these two key factors cannot be made separately because atmospheric turbulence lessens the wind drift influence. The maximum effect on sounding range is governed by turbulence, provided that the transverse wind is not too strong, which can cause the signal-to-noise ratio to drop off sharply even at low altitudes. This impediment can be overcome using adequately high radar potentials. Author

43 EARTH RESOURCES AND REMOTE SENSING

Includes remote sensing of earth resources by aircraft and spacecraft; photogrammetry; and aerial photography.

For instrumentation see *35 Instrumentation and Photography.*

N87-17109 Stanford Univ., Calif.
MICROWAVE SCATTERING FROM THE OCEAN SURFACE Ph.D. Thesis
Stephen Loren Durden 1986 205 p
Avail: Univ. Microfilms Order No. DA8619741

Knowledge of microwave scattering from the ocean surface is necessary for remote sensing of ocean surface winds, waves,

and other ocean surface phenomena. Here, the physics of microwave scattering from the ocean for its own sake are investigated to understand the limitations of empirical models. The physics of scattering from rough surfaces such as the ocean has been analyzed using the small perturbation, physical optics, and two-scale approximations, although their ranges of valid application have not been well established. The best previous calculations of scattering from the ocean were achieved using the two-scale approximation and an ocean surface described by a modified Pierson-Moskowitz spectrum at small wavenumbers and a spectrum found from wave tank observations at large wavenumbers. Agreement of calculated and observed cross sections is good, but surface slope variances calculated from the spectrum are much smaller than independently measured slope variances. In this work researchers examine the validity of the aforementioned scattering approximations by comparing their predictions with calculations done using the method of moments, which is an exact numerical method. Next, a new large wavenumber spectrum for the ocean is proposed. Our moment method calculations show that the two-scale approximation should be accurate for an ocean described by this spectrum, and, in fact, cross section calculations do compare well with observations. Dissert. Abstr.

N87-17110*# Jet Propulsion Lab., California Inst. of Tech., Pasadena.

EVALUATION OF GEOPHYSICAL PARAMETERS MEASURED BY THE NIMBUS-7 MICROWAVE RADIOMETER FOR THE TOGA HEAT EXCHANGE PROJECT

W. Timothy Liu and Donald R. Mock 1 Dec. 1986 26 p (Contract NAS7-918)

(NASA-CR-180151; JPL-Pub-86-50; NAS 1.26:180151) Avail: NTIS HC A03/MF A01 CSCL 08E

The data distributed by the National Space Science Data Center on the Geophysical parameters of precipitable water, sea surface temperature, and surface-level wind speed, measured by the Scanning Multichannel Microwave Radiometer (SMMR) on Nimbus-7, are evaluated with in situ measurements between Jan. 1980 and Oct. 1983 over the tropical oceans. In tracking annual cycles and the 1982-83 E1 Nino/Southern Oscillation episode, the radiometer measurements are coherent with sea surface temperatures and surface-level wind speeds measured at equatorial buoys and with precipitable water derived from radiosonde soundings at tropical island stations. However, there are differences between SMMR and in situ measurements. Corrections based on radiosonde and ship data were derived supplementing correction formulae suggested in the databook. This study is the initial evaluation of the data for quantitative description of the 1982-83 E1 Nino/Southern Oscillation episode. It paves the way for determination of the ocean-atmosphere moisture and latent heat exchanges, a priority of the Tropical Ocean and Global Atmosphere (TOGA) Heat Exchange Program. Author

N87-17111*# Jet Propulsion Lab., California Inst. of Tech., Pasadena.

THE TIMS DATA USER'S WORKSHOP

Anne B. Kahle, ed. and Elsa Abbott, ed. 1 Nov. 1986 96 p Workshop held in Bay Saint Louis, Miss., 18-19 Jun. 1985; sponsored by NASA NSTL Original contains color illustrations (Contract NAS7-918)

(NASA-CR-180130; JPL-Pub-86-38; NAS 1.26:180130) Avail: NTIS HC A05/MF A01 CSCL 08E

A workshop was held to bring together all users of data from NASA's airborne Thermal Infrared Multispectral Scanner (TIMS). The purpose was to allow users to compare results, data processing algorithms, and problems encountered; to update the users on the latest instrument changes and idiosyncracies, including distribution of the TIMS investigation guide; to inform the users of the wide range of problems that are currently being tackled by other TIMS investigators; to explore ways to expand the user community; to discuss current areas where more basic research is required; and to discuss the future directions of NASA's thermal infrared remote sensing programs. Also discussed were: geology, land use, archeology; and data processing and noise research. For individual titles, see N87-17112 through N87-17134.

N87-17112*# Daedalus Enterprises, Inc., Ann Arbor, Mich.

THE TIMS INSTRUMENT **c35**

Chuck Stanich *In* JPL, California Inst. of Technology The TIMS Data User's Workshop 1 Nov. 1986 p 5-7 (For primary document see N87-17111 09-43)

Avail: NTIS HC A05/MF A01 CSCL 14B

The scan head and spectrometer of the Thermal Infrared Multispectral Scanner (TIMS) are mounted in the unpressurized tail cone of a NASA/NSTL Learjet and operated through a hole cut through the skin. Design criteria are discussed. The digitized field of view is described. The functions of the scan head and spectrometer are examined. B.G.

N87-17113*# Jet Propulsion Lab., California Inst. of Tech., Pasadena.

THE TIMS INVESTIGATOR'S GUIDE **c35**

Frank D. Palluconi *In its* The TIMS Data User's Workshop 1 Nov. 1986 p 8 (For primary document see N87-17111 09-43)

Avail: NTIS HC A05/MF A01 CSCL 14B

The Thermal Infrared Multispectral Scanner (TIMS) is a NASA aircraft scanner providing six-channel spectral capability in the thermal infrared region of the electromagnetic spectrum. Operating in the thermal infrared atmospheric window region (8 to 12 microns) with a sensitivity of approximately 0.1 C, TIMS may be used whenever an accurate measurement of spectral radiance or brightness temperature is needed. The purpose of the TIMS Investigator's Guide is to provide in one location, enough information about TIMS that potential investigators can decide whether or not it would provide measurements useful in their research program and to provide a new user of TIMS data sufficient information to begin analysis. B.G.

N87-17114*# National Aeronautics and Space Administration. Earth Resources Lab., Bay St. Louis, Miss.

ESTIMATION OF ABSOLUTE WATER SURFACE TEMPERATURE BASED ON ATMOSPHERICALLY CORRECTED THERMAL INFRARED MULTISPECTRAL SCANNER DIGITAL DATA

James E. Anderson *In* JPL, California Inst. of Technology The TIMS Data User's Workshop 1 Nov. 1986 p 9-10 (For primary document see N87-17111 09-43)

Avail: NTIS HC A05/MF A01 CSCL 05B

Airborne remote sensing systems, as well as those on board Earth orbiting satellites, sample electromagnetic energy in discrete wavelength regions and convert the total energy sampled into data suitable for processing by digital computers. In general, however, the total amount of energy reaching a sensor system located at some distance from the target is composed not only of target related energy, but, in addition, contains a contribution originating from the atmosphere itself. Thus, some method must be devised for removing or at least minimizing the effects of the atmosphere. The LOWTRAN-6 Program was designed to estimate atmospheric transmittance and radiance for a given atmospheric path at moderate spectral resolution over an operational wavelength region from 0.25 to 28.5 microns. In order to compute the Thermal Infrared Multispectral Scanner (TIMS) digital values which were recorded in the absence of the atmosphere, the parameters derived from LOWTRAN-6 are used in a correction equation. The TIMS data were collected at 1:00 a.m. local time on November 21, 1983, over a recirculating cooling pond for a power plant in southeastern Mississippi. The TIMS data were analyzed before and after atmospheric corrections were applied using a band ratioing model to compute the absolute surface temperature of various points on the power plant cooling pond. The summarized results clearly demonstrate the desirability of applying atmospheric corrections. B.G.

N87-17115*# National Aeronautics and Space Administration. Earth Resources Lab., Bay St. Louis, Miss.

ATMOSPHERIC CORRECTION OF TIMS DATA **c35**

Doug Rickman *In* JPL, California Inst. of Technology The TIMS

Data User's Workshop 1 Nov. 1986 p 11 (For primary document see N87-17111 09-43)
Avail: NTIS HC A05/MF A01 CSCL 14B

The Thermal Infrared Multispectral Scanner (TIMS) is a unique sensor for two reasons, it is multispectral in the thermal-infrared and it has on board, active calibration sources. The existence of the calibration permits the recorded DNs to be converted unambiguously to absolute energy units. However, to relate the data to energy originating from a target on the ground it is necessary to remove the atmospheric contribution to the signal, specifically its transmittance and emittance. These can be obtained fairly easily by use of the atmospheric model provided by LOWTRAN-6 and the data from the U.S. Weather Service network of bidaily radiosondes. Using these data with the TIMS responsivity curves an equation can be obtained which permits the unambiguous correction of the TIMS data for the atmosphere. Author

N87-17116*# Jet Propulsion Lab., California Inst. of Tech., Pasadena. Geology Group.
ENHANCEMENT OF TIME IMAGES FOR PHOTOINTERPRETATION
A. R. Gillespie *In its* The TIMS Data User's Workshop 1 Nov. 1986 p 12-24 (For primary document see N87-17111 09-43)
Avail: NTIS HC A05/MF A01 CSCL 14E

The Thermal Infrared Multispectral Scanner (TIMS) images consist of six channels of data acquired in bands between 8 and 12 microns, thus they contain information about both temperature and emittance. Scene temperatures are controlled by reflectivity of the surface, but also by its geometry with respect to the Sun, time of day, and other factors unrelated to composition. Emittance is dependent upon composition alone. Thus the photointerpreter may wish to enhance emittance information selectively. Because thermal emittances in real scenes vary but little, image data tend to be highly correlated along channels. Special image processing is required to make this information available for the photointerpreter. Processing includes noise removal, construction of model emittance images, and construction of false-color pictures enhanced by decorrelation techniques. Author

N87-17117*# Arizona State Univ., Tempe. Dept. of Geology.
THERMAL IMAGING SPECTROSCOPY IN THE KELSO-BAKER REGION, CALIFORNIA
Philip R. Christensen, Michael C. Malin, Donald L. Anderson, and Linda L. Jaramillo *In* JPL, California Inst. of Technology The TIMS Data User's Workshop 1 Nov. 1986 p 25-28 (For primary document see N87-17111 09-43)
Avail: NTIS HC A05/MF A01 CSCL 14E

The ability of the Thermal Infrared Multispectral Scanner (TIMS) data to identify rock composition using thermal-infrared spectroscopy was assessed. A region was selected with a wide range of rock and soil types in an arid environment, and the spectra acquired by TIMS was compared to laboratory spectra of collected samples. A TIMS image was acquired of the Kelso-Baker region in the Mojave desert of California at a surface resolution of approximately 7 m. This image was then used to map the areal extent of each geologic component. The TIMS data provided an excellent means for discriminating and mapping rocks of very similar mineralogy. These findings suggest that thermal-infrared spectroscopy can provide a powerful tool for identifying and mapping rock composition on the Earth and other terrestrial planets. B.G.

N87-17118*# Jet Propulsion Lab., California Inst. of Tech., Pasadena. Geology Group.
LITHOLOGIC MAPPING OF SILICATE ROCKS USING TIMS
A. R. Gillespie *In its* The TIMS Data User's Workshop 1 Nov. 1986 p 29-44 (For primary document see N87-17111 09-43)
Avail: NTIS HC A05/MF A01 CSCL 08B

Common rock-forming minerals have thermal infrared spectral features that are measured in the laboratory to infer composition. An airborne Daedalus scanner (TIMS) that collects six channels of thermal infrared radiance data (8 to 12 microns), may be used to measure these same features for rock identification. Previously, false-color composite pictures made from channels 1, 3, and 5 and emittance spectra for small areas on these images were used to make lithologic maps. Central wavelength, standard deviation, and amplitude of normal curves regressed on the emittance spectra are related to compositional information for crystalline igneous silicate rocks. As expected, the central wavelength varies systematically with silica content and with modal quartz content. Standard deviation is less sensitive to compositional changes, but large values may result from mixed admixture of vegetation. Compression of the six TIMS channels to three image channels made from the regressed parameters may be effective in improving geologic mapping from TIMS data, and these synthetic images may form a basis for the remote assessment of rock composition. Author

N87-17119*# Nevada Univ., Reno. Dept. of Geological Sciences.
DETECTION AND MAPPING OF VOLCANIC ROCK ASSEMBLAGES AND ASSOCIATED HYDROTHERMAL ALTERATION WITH THERMAL INFRARED MULTIBAND SCANNER (TIMS) DATA COMSTOCK LODE MINING DISTRICT, VIRGINIA CITY, NEVADA
James V. Taranik, Amy Hutsinpiller, and Marcus Borengasser *In* JPL, California Inst. of Technology The TIMS Data User's Workshop 1 Nov. 1986 p 45-47 (For primary document see N87-17111 09-43)
Avail: NTIS HC A05/MF A01 CSCL 08K

Thermal infrared Multispectral Scanner (TIMS) data were acquired over the Virginia City area on September 12, 1984. The data were acquired at approximately 1130 hours local time (1723 IRIG). The TIMS data were analyzed using both photointerpretation and digital processing techniques. Karhuen-Loeve transformations were utilized to display variations in radiant spectral emittance. The TIMS image data were compared with color infrared metric camera photography, LANDSAT Thematic Mapper (TM) data, and key areas were photographed in the field. B.G.

N87-17120*# Geological Survey, Denver, Colo.
SIMULATION MODELING AND PRELIMINARY ANALYSIS OF TIMS DATA FROM THE CARLIN AREA AND THE NORTHERN GRAPEVINE MOUNTAINS, NEVADA
Ken Watson, Susanne Hummer-Miller, and Fred A. Kruse *In* JPL, California Inst. of Technoiogy The TIMS Data User's Workshop 1 Nov. 1986 p 48-49 (For primary document see N87-17111 09-43)
Avail: NTIS HC A05/MF A01 CSCL 08B

A theoretical radiance model was employed together with laboratory data on a suite of igneous rock to evaluate various algorithms for processing Thermal Infrared Multispectral Scanner (TIMS) data. Two aspects of the general problem were examined: extraction of emissivity information from the observed TIMS radiance data, and how to use emissivity data in a way that is geologically meaningful. The four algorithms were evaluated for appropriate band combinations of TIMS data acquired on both day and night overflights of the Tuscarora Mountains, including the Carlin gold deposit, in north-central Nevada. Analysis of a color composited PC decorrelated image (Bands 3, 4, 5--blue/green/red) of the Northern Grapevine Mountains, Nevada, area showed some useful correlation with the regional geology. The thermal infrared region provides fundamental spectral information that can be used to discriminate the major rock types occurring on the Earth's surface. B.G.

N87-17121*# Jet Propulsion Lab., California Inst. of Tech., Pasadena.
APPLICATION OF TIMS DATA IN STRATIGRAPHIC ANALYSIS
H. R. Lang *In its* The TIMS Data User's Workshop 1 Nov. 1986 p 50-52 (For primary document see N87-17111 09-43)
Avail: NTIS HC A05/MF A01 CSCL 08B

An in-progress study demonstrates the utility of Thermal Infrared Multispectral Scanner (TIMS) data for unraveling the stratigraphic sequence of a western interior, North American foreland basin. The TIMS data can be used to determine the stratigraphic distribution of minerals that are diagnostic of specific depositional distribution. The thematic mapper (TM) and TIMS data

were acquired in the Wind River/Bighorn area of central Wyoming in November 1982, and July 1983, respectively. Combined image processing, photogeologic, and spectral analysis methods were used to: map strata; construct stratigraphic columns; correlate data; and identify mineralogical facies. Author

N87-17122*# National Aeronautics and Space Administration. Earth Resources Lab., Bay St. Louis, Miss.

MONITORING VEGETATION RECOVERY PATTERNS ON MOUNT ST. HELENS USING THERMAL INFRARED MULTISPECTRAL DATA

Kenneth J. Langran *In* JPL, California Inst. of Technology The TIMS Data User's Workshop 1 Nov. 1986 p 53-54 Previously announced in IAA as A86-46106 (For primary document see N87-17111 09-43)

Avail: NTIS HC A05/MF A01 CSCL 02C

The Mount St. Helens 1980 eruption offers an opportunity to study vegetation recovery rates and patterns in a perturbed ecosystem. The eruptions of Mount St. Helens created new surfaces by stripping and implacing large volumes of eroded material and depositing tephra in the blast area and on the flanks of the mountain. Areas of major disturbance are those in the blast zone that were subject to debris avalanche, pyroclastic flows, mudflows, and blowdown and scorched timber; and those outside the blast zone that received extensive tephra deposits. It was observed that during maximum daytime solar heating, surface temperatures of vegetated areas are cooler than surrounding nonvegetated areas, and that surface temperature varies with percent vegetation cover. A method of measuring the relationship between effective radiant temperature (ERT) and percent vegetation cover in the thermal infrared (8 to 12 microns) region of the electromagnetic spectrum was investigated. Author

N87-17123*# National Aeronautics and Space Administration. Earth Resources Lab., Bay St. Louis, Miss.

INVESTIGATION OF FOREST CANOPY TEMPERATURES RECORDED BY THE THERMAL INFRARED MULTISPECTRAL SCANNER AT H. J. ANDREWS EXPERIMENTAL FOREST

Steven A. Sader *In* JPL, California Inst. of Technology The TIMS Data User's Workshop 1 Nov. 1986 p 55-57 (For primary document see N87-17111 09-43)

Avail: NTIS HC A05/MF A01 CSCL 02F

Thermal Infrared Multispectral Scanner (TIMS) data were collected over the H. J. Andrews Experimental Forest in Western Oregon on July 29, 1983 at approximately 1:30 p.m., Pacific Standard Time. The relation of changes in canopy temperature to green leaf biomass levels in reforested clearcuts and old-growth forest was investigated. A digital data base was generated in order to isolate that portion of the thermal emission that could be attributed to surface properties other than the vegetation biomass component. The TIMS appears to be capable of detecting subtle differences in ERT as related to canopy closure and green lead biomass, however calibration techniques are needed to correct for emissivity and atmospheric effects. B.G.

N87-17124*# National Aeronautics and Space Administration. Earth Resources Lab., Bay St. Louis, Miss.

APPLICATIONS OF TIMS DATA IN AGRICULTURAL AREAS AND RELATED ATMOSPHERIC CONSIDERATIONS

R. E. Pelletier and M. C. Ochoa *In* JPL, California Inst. of Technology The TIMS Data User's Workshop 1 Nov. 1986 p 57-58 Prepared in cooperation with Auburn Univ., Ala. (For primary document see N87-17111 09-43)

Avail: NTIS HC A05/MF A01 CSCL 02C

While much of traditional remote sensing in agricultural research was limited to the visible and reflective infrared, advances in thermal infrared remote sensing technology are adding a dimension to digital image analysis of agricultural areas. The Thermal Infrared Multispectral Scanner (TIMS) an airborne sensor having six bands over the nominal 8.2 to 12.2 m range, offers the ability to calculate land surface emissivities unlike most previous singular broadband sensors. Preliminary findings on the utility of the TIMS for several agricultural applications and related atmospheric considerations are discussed. Author

N87-17125*# Forest Service, Atlanta, Ga.

LOCATING SUBSURFACE GRAVEL WITH THERMAL IMAGERY

Douglas E. Scholen, William H. Clerke, and Douglas E. Luepke *In* JPL, California Inst. of Technology The TIMS Data User's Workshop 1 Nov. 1986 p 59 (For primary document see N87-17111 09-43)

Avail: NTIS HC A05/MF A01 CSCL 08G

A method was discussed for using 6 band thermal imagery to locate subsurface gravel deposits in vegetated areas. Geologic history is reviewed to select potential areas of study. An overflight was made using a thermal scanner. The data were processed with a computerized system to delineate areas showing a quartz signature radiated by a gravel deposit. The method was developed during a search for gravel on National Forest land in Louisiana. Processed data from thermal imagery was compared with known gravel deposits and exploratory drill hole logs. A high correlation was noted for a wide range of deposits, from commercial pits to trace deposits only a foot thick. Overburden at these sites varied from zero to sixty feet, near the maximum annual penetration by the thermal wave. It was concluded that the method can be used to locate buried gravel deposits and that more time and effort are needed to verify the usefulness for developing gravel pits adjacent to proposed construction sites. Author

N87-17126*# Nebraska Univ., Lincoln. Inst. of Agriculture and Natural Resources.

TIMS DATA APPLICATIONS IN NEBRASKA

Lloyd Queen and Gene Murray *In* JPL, California Inst. of Technology The TIMS Data User's Workshop (date) p 60 (For primary document see N87-17111 09-43)

Avail: NTIS HC A05/MF A01 CSCL 08B

A total of 172 flight-line miles of Thermal Infrared Multispectral Scanner (TIMS) data were acquired in the state of Nebraska; and an additional mission is planned for August of this year. Data collected by the scanner were generally applied to investigations in four general areas: hydrology, geology, soils, and vegetation analysis. Relatively simple manipulations of these thermal-emittance data led to excellent classifications of vegetation communities established along topographic gradients in the Nebraska Sandhills. Similar procedures were used to study variations in soil parameters along those same routes. Proposed geologic applications include mapping of the surficial geology along a portion of the Platte River and the delineation of a segment of the Cambridge Arch, a structural feature in central Nebraska. Author

N87-17127*# Pennsylvania State Univ., University Park. Dept. of Agronomy.

THE APPLICATION OF REMOTELY SENSED DATA TO PEDOLOGIC AND GEOMORPHIC MAPPING ON ALLUVIAL FAN AND PLAYA SURFACES IN SALINE VALLEY, CALIFORNIA

D. A. Miller, G. W. Petersen, and A. B. Kahle *In* JPL, California Inst. of Technology The TIMS Data User's Workshop 1 Nov. 1986 p 61 (For primary document see N87-17111 09-43)

Avail: NTIS HC A05/MF A01 CSCL 08G

Arid and semiarid regions yield excellent opportunities for the study of pedologic and geomorphic processes. The dominance of rock and soil exposure over vegetation not only provides the ground observer with observational possibilities but also affords good opportunities for measurement by aircraft and satellite remote sensor devices. Previous studies conducted in the area of pedologic and geomorphic mapping in arid regions with remotely sensed data have utilized information obtained in the visible to near-infrared portion of the spectrum. Thermal Infrared Multispectral Scanner (TIMS) and Thematic Mapping (TM) data collected in 1984 are being used in comjunction with maps compiled during a Bureau of Land Management (BLM) soil survey to aid in a detailed mapping of alluvial fan and playa surfaces within the valley. The results from this study may yield valuable information concerning the

application of thermal data and thermal/visible data combinations to the problem of dating pedologic and geomorphic features in arid regions. Author

N87-17128*# Army Engineer Waterways Experiment Station, Vicksburg, Miss. Geotechnical Lab.
THE RED RIVER VALLEY ARCHEOLOGICAL PROJECT Abstract Only
Jack Bennett, Lawson Smith, and Mark Laustrup (Nebraska Univ., Omaha) *In* JPL, California Inst. of Technology The TIMS Data User's Workshop 1 Nov. 1986 p 62 (For primary document see N87-17111 09-43)
Avail: NTIS HC A05/MF A01 CSCL 08H

The Red River Valley Archeology Project is a long-term effort involving numerous individuals and institutions engaged in archeological investigations in the Texas and Oklahoma portions of the Red River Valley. To date the focus of the project was on site location. The project acquired both Thermal Infrared Multispectral Scanner (TIMS), TMS, and color infrared photographs over a significant portion of the project area in an effort to define signatures for archeological sites and to assist in the detailed geomorphological mapping of the flood plain. Preliminary analysis of acquired data indicates that both the TIMS and TMS can make a substantial contribution to landform definition, the identification of cultural resources, and to the clarification of site-landform correlations in this riverine environment. Author

N87-17129*# National Aeronautics and Space Administration. Goddard Space Flight Center, Greenbelt, Md.
THE PHYSICAL BASIS FOR SPECTRAL VARIATIONS IN THERMAL INFRARED EMITTANCE OF SILICATES AND APPLICATION TO REMOTE SENSING
Louis S. Walter *In* JPL, California Inst. of Technology The TIMS Data User's Workshop 1 Nov. 1986 p 63-64 (For primary document see N87-17111 09-43)
Avail: NTIS HC A05/MF A01 CSCL 08G

The use of infrared spectroscopy for the remote characterization of planetary surfaces has received attention due to efforts in the investigation of these bodies from space. In the 8 to 14 micron region, a depression in the emittance spectra of rocks (sometimes called reststrahlen) is related to the fundamental stretching vibrations of Si-O bonds and shifts in the locations of this feature are ascribed to variations in rock composition. Thus, it should be possible to investigate, quantify, and model the relationships of reststrahlen spectral band location through silicate mineralogical composition to rock classification. This concept will be tested first through the use of laboratory-acquired data on the infrared spectra and mineralogy of selected mineral and rock samples. As a suitable classification model is developed, it will be tested through overflights of appropriate rock outcrops using the Thermal Infrared Multispectral Scanner (TIMS). B.G.

N87-17130*# Jet Propulsion Lab., California Inst. of Tech., Pasadena.
INFRARED SPECTROSCOPY FOR GEOLOGIC INTERPRETATION OF TIMS DATA
Mary Jane Bartholomew *In its* The TIMS Data User's Workshop 1 Nov. 1986 p 65-66 (For primary document see N87-17111 09-43)
Avail: NTIS HC A05/MF A01 CSCL 08G

The Portable Field Emission Spectrometer (PFES) was designed to collect meaningful spectra in the field under climatic, thermal, and sky conditions that approximate those at the time of the overflight. The specifications and procedures of PFES are discussed. Laboratory reflectance measurements of rocks and minerals were examined for the purpose of interpreting Thermal Infrared Multispectral Scanner (TIMS) data. The capability is currently being developed to perform direct laboratory measurement of the normal spectral radiance of Earth surface materials at low temperatures (20 to 30 C) at the Jet Propulsion Laboratory. B.G.

N87-17131*# Jet Propulsion Lab., California Inst. of Tech., Pasadena.
CALCULATION OF DAY AND NIGHT EMITTANCE VALUES
Anne B. Kahle *In its* The TIMS Data User's Workshop 1 Nov. 1986 p 67-70 (For primary document see N87-17111 09-43)
Avail: NTIS HC A05/MF A01 CSCL 04A

In July 1983, the Thermal Infrared Multispectral Scanner (TIMS) was flown over Death Valley, California on both a midday and predawn flight within a two-day period. The availability of calibrated digital data permitted the calculation of day and night surface temperature and surface spectral emittance. Image processing of the data included panorama correction and calibration to radiance using the on-board black bodies and the measured spectral response of each channel. Scene-dependent isolated-point noise due to bit drops, was located by its relatively discontinuous values and replaced by the average of the surrounding data values. A method was developed in order to separate the spectral and temperature information contained in the TIMS data. Night and day data sets were processed. The TIMS is unique in allowing collection of both spectral emittance and thermal information in digital format with the same airborne scanner. For the first time it was possible to produce day and night emittance images of the same area, coregistered. These data add to an understanding of the physical basis for the discrimination of difference in surface materials afforded by TIMS. Author

N87-17132*# Nevada Univ., Reno. Dept. of Geological Sciences.
APPLICATION OF THERMAL INFRARED MULTIBAND SCANNER (TIMS) DATA TO MAPPING OF PLUTONIC AND STRATIFIED ROCK AND ASSEMBLAGES IN ACCRETED TERRAINS OF THE NORTHERN SIERRA, CALIFORNIA
James V. Taranik, David Davis, and Marcus Borengasser *In* JPL, California Inst. of Technology The TIMS Data User's Workshop 1 Nov. 1986 p 71-73 (For primary document see N87-17111 09-43)
Avail: NTIS HC A05/MF A01 CSCL 08B

The Thermal Infrared Multispectral Scanner (TIMS) data were acquired over the Donner Pass area in California on September 12, 1985. The higher peaks in the area approach 9,200 feet in elevation, while the canyon of the north fork of the American River is only 3000 feet in elevation. The vegetation is dominated by conifers, although manzanita and other shrubs are present in areas where soils have developed. The data contain noise patterns which cut across scan lines diagonally. The TIMS data were analyzed using both photointerpretative and digital processing techniques. Preliminary image interpretation and field analysis confirmed that TIMS image data displays the chert units and silicic volcanics as bright red. The imagery appears to display zoning in the batholithic and hypabyssal intrusive rocks, although this was not field checked at this time. Rocks which appear to be more dioritic in composition appear purple on the imagery, while rocks more granitic in composition appear shades of red and pink. Areas that have more than 40% vegetative cover appear green on the imagery. Author

N87-17133*# Jet Propulsion Lab., California Inst. of Tech., Pasadena.
A GEOLOGIC ATLAS OF TIMS DATA
Elsa Abbott *In its* The TIMS Data User's Workshop 1 Nov. 1986 p 74-75 (For primary document see N87-17111 09-43)
Avail: NTIS HC A05/MF A01 CSCL 05B

In the three years since the first data were taken, it was well demonstrated that the Thermal Infrared Multispectral Scanner (TIMS), properly used, can be a most valuable tool for the geologist. Compilation of the TIMS data into a geological atlas was felt to be useful. Several data sets were extensively studied to establish TIMS as a geologic tool and to explore the optimum enhancement techniques. It was found that a decorrelation stretch of bands 1, 3, and 5 enhance the data to a form that is very useful and this enhancement will be used in the geologic atlas along with an accompanying geologic map and description. Many data sets are well published and familiar to TIMS users, but there are some sets that, for lack of time and funds, were not thoroughly studied or published. A short description of these least studied sets of

data is presented. The images presented along with the many previously studied and published TIMS images constitute an enormously useful set of information for the geologist in the 8 to 10 micron range. B.G.

N87-17134*# Geological Survey, Reston, Va.
AIRBORNE THERMAL INFRARED MULTISPECTRAL SCANNER (TIMS) IMAGES OVER DISSEMINATED GOLD DEPOSITS, OSGOOD MOUNTAINS, HUMBOLDT COUNTY, NEVADA
M. Dennis Krohn *In* JPL, California Inst. of Technology The TIMS Data User's Workshop (date) p 76-78 (For primary document see N87-17111 09-43)
Avail: NTIS HC A05/MF A01 CSCL 08G

The U.S. Geological Survey (USGS) acquired airborne Thermal Infrared Multispectral Scanner (TIMS) images over several disseminated gold deposits in northern Nevada in 1983. The aerial surveys were flown to determine whether TIMS data could depict jasperoids (siliceous replacement bodies) associated with the gold deposits. The TIMS data were collected over the Pinson and Getchell Mines in the Osgood Mountains, the Carlin, Maggie Creek, Bootstrap, and other mines in the Tuscarora Mountains, and the Jerritt Canyon Mine in the Independence Mountains. The TIMS data seem to be a useful supplement to conventional geochemical exploration for disseminated gold deposits in the western United States. Siliceous outcrops are readily separable in the TIMS image from other types of host rocks. Different forms of silicification are not readily separable, yet, due to limitations of spatial resolution and spectral dynamic range. Features associated with the disseminated gold deposits, such as the large intrusive bodies and fault structures, are also resolvable on TIMS data. Inclusion of high-resolution thermal inertia data would be a useful supplement to the TIMS data. B.G.

N87-17135*# Jet Propulsion Lab., California Inst. of Tech., Pasadena.
THE SECOND SPACEBORNE IMAGING RADAR SYMPOSIUM
1 Dec. 1986 223 p Symposium held in Pasadena, Calif., 28-30 Apr. 1986
(Contract NAS7-918)
(NASA-CR-180131; JPL-Pub-86-26; NAS 1.26:180131) Avail: NTIS HC A10/MF A01 CSCL 05B

Summaries of the papers presented at the Second Spaceborne Imaging Radar Symposium are presented. The purpose of the symposium was to present an overwiew of recent developments in the different scientific and technological fields related to spaceborne imaging radars and to present future international plans. For individual titles, see N87-17136 through N87-17162.

N87-17136*# Cornell Univ., Ithaca, N.Y. Dept. of Geological Sciences.
TECTONIC GEOMORPHOLOGY OF THE ANDES WITH SIR-A AND SIR-B
Arthur L. Bloom and Eric J. Fielding *In* JPL The Second Spaceborne Imaging Radar Symposium 1 Dec. 1986 p 5-10 (For primary document see N87-17135 09-43)
Avail: NTIS HC A10/MF A01 CSCL 08G

Data takes from SIR-A and SIR-B (Shuttle Imaging Radar) crossed all of the principal geomorphic provinces of the central Andes between 17 and 34 S latitude. In conjunction with Thematic Mapping images and photographs from hand-held cameras as well as from the Large Format Camera that was flown with SIR-B, the radar images give an excellent sampling of Andean geomorphology. In particular, the radar images show new details of volcanic rocks and landforms of late Cenozoic age in the Puna, and the exhumed surfaces of tilted blocks of Precambrian crystalline basement in the Sierras Pampeanas. E.R.

N87-17137*# Chevron Oil Field Research Co., La Habra, Calif.
SPACE SHUTTLE RADAR IMAGES OF INDONESIA
Floyd F. Sabins and John P. Ford (Jet Propulsion Lab., California Inst. of Tech., Pasadena) *In* JPL The Second Spaceborne Imaging Radar Symposium 1 Dec. 1986 p 11-16 (For primary document see N87-17135 09-43)
Avail: NTIS HC A10/MF A01 CSCL 17I

Sabins (1983) interpreted Shuttle imaging Radar (SIR)-A images of Indonesia; Sabins and Ford (1985) interpreted SIR-B images. These investigations had the following major results: (1) major lithologic assemblages are recognizable by their terrain characteristics in the SIR images, and (2) both local and regional geologic structures are mappable. These results are summarized. Author

N87-17138*# Massachusetts Inst. of Tech., Cambridge. Earth Resources Lab.
DELINEATION OF FAULT ZONES USING IMAGING RADAR
M. N. Toksoz, L. Gulen, M. Prange, J. Matarese, G. H. Pettengill, and P. G. Ford *In* JPL The Second Spaceborne Imaging Radar Symposium 1 Dec. 1986 p 17-24 (For primary document see N87-17135 09-43)
Avail: NTIS HC A10/MF A01 CSCL 08G

The assessment of earthquake hazards and mineral and oil potential of a given region requires a detailed knowledge of geological structure, including the configuration of faults. Delineation of faults is traditionally based on three types of data: (1) seismicity data, which shows the location and magnitude of earthquake activity; (2) field mapping, which in remote areas is typically incomplete and of insufficient accuracy; and (3) remote sensing, including LANDSAT images and high altitude photography. Recently, high resolution radar images of tectonically active regions have been obtained by SEASAT and Shuttle Imaging Radar (SIR-A and SIR-B) systems. These radar images are sensitive to terrain slope variations and emphasize the topographic signatures of fault zones. Techniques were developed for using the radar data in conjunction with the traditional types of data to delineate major faults in well-known test sites, and to extend interpretation techniques to remote areas. Author

N87-17139*# Geological Survey, Flagstaff, Ariz.
THE MEGAGEOMORPHOLOGY OF THE RADAR RIVERS OF THE EASTERN SAHARA
John F. McCauley, Carol S. Breed, and Gerald G. Schaber *In* JPL The Second Spaceborne Imaging Radar Symposium 1 Dec. 1986 p 25-36 (For primary document see N87-17135 09-43)
Avail: NTIS HC A10/MF A01 CSCL 08H

The Eastern Sahara is devoid of surface drainage; this unusual characteristic distinguishes its morphology from that of most other desert regions where running water dominates landscape development. A map derived from SIR-A/B and LANDSAT images and the literature, shows the major presently known paleodrainages in the Eastern Sahara. This compilation permits consideration of the key questions: Where did the radar rivers come from and where did they go? Analysis of SIR-A data led McCauley et al. to suggest that the radar rivers, because of their southwestward trends, once flowed into the Chad basin. This key North African feature is a regional structural low formed in the Early Cretaceous in response to initial opening of the South Atlantic. The problem of the origin of headwaters for the radar rivers was less tractable. The idea that the source areas of the radar rivers might originally have been the same as those later captured by the Nile was proposed tentatively. A more extensive review of the Cenozoic tectonic history of North Africa reveals no reason now to suppose that the Central African tributaries of the present Nile were ever connected to the large alluvial valleys in southwestern Egypt and northwestern Sudan. formed in the Early Cretaceous in response to initial opening of the South Atlantic. The problem of the origin of headwaters for the radar rivers was less tractable. The idea that the source areas of the radar rivers might originally have been the same as those (The Ethiopian Highlands) later captured by the Nile was proposed tentatively. A more extensive review of the Cenozoic tectonic history of North Africa reveals no reason now to support that the Central African tributaries of the present Nile were ever connected to the large alluvial valleys in southwestern Egypt and northwestern Sudan. E.R.

N87-17140*# Jet Propulsion Lab., California Inst. of Tech., Pasadena.
GEOLOGICAL APPLICATIONS OF MULTIPOLARIZATION SAR DATA

Diane L. Evans *In its* The Second Spaceborne Imaging Radar Symposium 1 Dec. 1986 p 36-41 (For primary document see N87-17135 09-43)
Avail: NTIS HC A10/MF A01 CSCL 08G

Spaceborne Synthetic Aperture Radar (SAR) data acquired by SEASAT and the Shuttle Imaging Radar (SIR-A/B) operating at L-band with HH polarization were found to be useful in conjunction with other sensors for lithologic discrimination in arid environments with limited vegetation cover. In order to assess the utility of more advanced sensors for geologic research and define the unique contributions each sensor makes, remote sensing data were collected over the Deadman Butte area of the Wind River Basin, Wyoming. The Wind River Basin is an asymmetric sedimentary basin in central Wyoming created during the early Eocene Laramide orogeny. The stratigraphic section of the Deadman Butte study area, which was measured by Woodward is made up of Paleozoic and Mesozoic marine shales, siltstones, limestones, and sandstones. Sensor systems included LANDSAT 4 Thematic Mapper (TM), Thermal Infrared Multispectral Scanner (TIMS) and the Multipolarization, L-band airborne SAR, a prototype for the next Shuttle Imaging Radar (SIR-C). Sensor parameters are given.
Author

N87-17141*# Jet Propulsion Lab., California Inst. of Tech., Pasadena.
SPACEBORNE IMAGING RADAR RESEARCH IN THE 90's
Charles Elachi *In its* The Second Spaceborne Imaging Radar Symposium 1 Dec. 1986 p 45-55 (For primary document see N87-17135 09-43)
Avail: NTIS HC A10/MF A01 CSCL 17I

The imaging radar experiments on SEASAT and on the space shuttle (SIR-A and SIR-B) have led to a wide interest in the use of spaceborne imaging radars in Earth and planetary sciences. The radar sensors provide unique and complimentary information to what is acquired with visible and infrared imagers. This includes subsurface imaging in arid regions, all weather observation of ocean surface dynamic phenomena, structural mapping, soil moisture mapping, stereo imaging and resulting topographic mapping. However, experiments up to now have exploited only a very limited range of the generic capability of radar sensors. With planned sensor developments in the late 80's and early 90's, a quantum jump will be made in our ability to fully exploit the potential of these sensors. These developments include: multiparameter research sensors such as SIR-C and X-SAR, long-term and global monitoring sensors such as ERS-1, JERS-1, EOS, Radarsat, GLORI and the spaceborne sounder, planetary mapping sensors such as the Magellan and Cassini/Titan mappers, topographic three-dimensional imagers such as the scanning radar altimeter and three-dimensional rain mapping. These sensors and their associated research are briefly described.
Author

N87-17142*# Jet Propulsion Lab., California Inst. of Tech., Pasadena.
VENUS RADAR MAPPER (VRM): MULTIMODE RADAR SYSTEM DESIGN **c91**
William T. K. Johnson and Alvin T. Edgerton (Hughes Aircraft Co., El Segundo, Calif.) *In its* The Second Spaceborne Imaging Radar Symposium 1 Dec. 1986 p 56-66 (For primary document see N87-17135 09-43)
Avail: NTIS HC A10/MF A01 CSCL 03B

The surface of Venus has remained a relative mystery because of the very dense atmosphere that is opaque to visible radiation and, thus, normal photographic techniques used to explore the other terrestrial objects in the solar system are useless. The atmosphere is, however, almost transparent to radar waves and images of the surface have been produced via Earth-based and orbital radars. The technique of obtaining radar images of a surface is variously called side looking radar, imaging radar, or synthetic aperture radar (SAR). The radar requires a moving platform in which the antenna is side looking. High resolution is obtained in the cross-track or range direction by conventional radar pulse encoding. In the along-track or azimuth direction, the resolution would normally be the antenna beam width, but for the SAR case, a much longer antenna (or much sharper beam) is obtained by moving past a surface target as shown, and then combining the echoes from many pulses, by using the Doppler data, to obtain the images. The radar design of the Venus Radar Mapper (VRM) is discussed. It will acquire global radar imagery and altimetry data of the surface of Venus.
Author

N87-17143*# Jet Propulsion Lab., California Inst. of Tech., Pasadena.
SPACEBORNE IMAGING RADAR PROJECT
Neil Herman *In its* The Second Spaceborne Imaging Radar Symposium 1 Dec. 1986 p 67-73 (For primary document see N87-17135 09-43)
Avail: NTIS HC A10/MF A01 CSCL 17I

In June of 1985 the Project Initiation Agreement was signed by the Jet Propulsion Laboratory and the NASA Office of Space Science and Applications for the Spaceborne Imaging Radar Project (SIR). The thrust of the Spaceborne Imaging Radar Project is to continue the evolution of synthetic aperture radar (SAR) science and technology developed during SEASAT, SIR-A and SIR-B missions to meet the needs of the Earth Observing System (EOS) in the mid 1990's. As originally formulated, the Project plans were for a reflight of the SIR-B in 1987, the development of a new SAR, SIR-C, for missions in mid 1989 and early 1990, and the upgrade of SIR-C to EOS configuration with a qualification flight aboard the shuttle in the 1993 time frame (SIR-D). However, the loss of the shuttle Challenger has delayed the first manifest for SIR to early 1990. This delay prompted the decision to drop SIR-B reflight plans and move ahead with SIR-C to more effectively utilize this first mission opportunity. The planning for this project is discussed.
Author

N87-17144*# Canada Centre for Remote Sensing, Ottawa (Ontario). RADARSAT Project Office.
AN ALTERNATIVE MULTI-MODE SAR FOR RADARSAT
R. K. Raney *In* JPL The Second Spaceborne Imaging Radar Symposium 1 Dec. 1986 p 74-78 (For primary document see N87-17135 09-43)
Avail: NTIS HC A10/MF A01 CSCL 17I

The RADARSAT project was asked by the Canadian government in the spring of 1986 to design for reduced costs and increased radar performance as compared to the well-known baseline design. Both the Project Office and Canadian industry (lead by SPAR Aerospace of Montreal) have undertaken to meet this request, with a proposal to cabinet to be submitted in the fall of 1986. One alternative SAR concept is outlined which is under consideration for a revised RADARSAT configuration. The radar system described uses two frequencies (C&L band) over four possible modes: near range swath; far range swath; wide swath; and high resolution. Good sensitivity, resolution, and coverage are obtained with modest power and data rates. The antenna systems are relatively simple. Indeed, no break-through technological developments are needed. The design allows several mode combinations for simultaneous data collection or performance enhancement. The principal parameters are described. A nominal mean altitude of 700 km is assumed.
Author

N87-17145*# Jet Propulsion Lab., California Inst. of Tech., Pasadena.
PRESENT STATUE OF JAPANESE ERS-1 PROJECT **c18**
Yasufumi Ishiwada and Yoshiaki Nemoto *In its* The Second Spaceborne Imaging Radar Symposium 1 Dec. 1986 p 79-83 (For primary document see N87-17135 09-43)
Avail: NTIS HC A10/MF A01 CSCL 22B

Earth Resources Satellite 1 (ERS-1) will be launched in the FY 1990 with the H-1 rocket from Tanegashima Space Center. ERS-1 will seek to firmly establish remote sensing technologies from space by using synthetic aperture radar and optical sensors, as well as primarily exploring for non-renewable resources and also monitoring for land use, agriculture, forestry, fishery, conservation of environment, prevention of disasters, and surveillance of coastal regions. ERS-1 is a joint project in which the main

responsibility for the development of the mission equipment is assumed by the Agency of Industrial Science and Technology, MITI, and the Technology Research Association of Resources Remote Sensing System, while that for the satellite itself and launching rocket is assumed by the Science and Technology Agency (STA) and the National Space Development Agency (NASDA). In relation to this project, users have maintained a close working relationship with the manufacturers after submitting their requirements in 1984 on the specifications of the mission equipments. This missions parameters are outlined. Author

N87-17146*# Jet Propulsion Lab., California Inst. of Tech., Pasadena.

A SCANNING RADAR ALTIMETER FOR MAPPING CONTINENTAL TOPOGRAPHY

T. H. Dixon *In its* The Second Spaceborne Imaging Radar Symposium 1 Dec. 1986 p 84-88 (For primary document see N87-17135 09-43)

Avail: NTIS HC A10/MF A01 CSCL 08B

Topographic information constitutes a fundamental data set for the Earth sciences. In the geological and geophysical sciences, topography combined with gravitational information provides an important constraint on tne structure and rheologic properties of the crust and lithosphere. Detailed topography data can also be used to map offsets associated with faulting and to reveal the effects of tectonic deformation. In the polar regions, elevation data form a crucial but as yet largely unavailable resource for studying ice sheet mass balance and ice flow dynamics. The vast Antarctic ice sheet is the largest fresh water reservoir on Earth and is an important influence on ocean circulation and global climate. However, our knowledge of its stability is so limited that we cannot even specify whether the Antarctic ice sheet is growing or shrinking. It is clear that there is need for high quality global topography data. A summary of potential applications with their resolution requirements is shown. Author

N87-17147*# Johns Hopkins Univ., Laurel, Md. Applied Physics Lab.

HYDRODYNAMICS OF INTERNAL SOLITONS AND A COMPARISON OF SIR-A AND SIR-B DATA WITH OCEAN MEASUREMENTS

J. R. Apel, R. F. Gasparovic, and D. R. Thompson *In* JPL The Second Spaceborne Imaging Radar Symposium 1 Dec. 1986 p 91-102 (For primary document see N87-17135 09-43)

Avail: NTIS HC A10/MF A01 CSCL 08H

Large internal solitary waves have been observed by Shuttle SIR-A and SIR-B at locations in the Andaman Sea and the New York Bight. Satellite imagery and oceanographic measurements are used in conjunction with hydrodynamic interaction and electromagnetic scattering models to estimate the expected SAR image intensity modulations associated with the internal waves. There is reasonable agreement between the predicted and observed internal wave signatures. Author

N87-17148*# Jet Propulsion Lab., California Inst. of Tech., Pasadena.

OCEAN WAVES NEAR HURRICANE JOSEPHINE FROM SIR-B **c48**

Benjamin Holt and F. I. Gonzalez (National Oceanic and Atmospheric Administration, Seattle, Wash.) *In its* The Second Spaceborne Imaging Radar Symposium 1 Dec. 1986 p 103-106 Previously announced in IAA as A86-49688 (For primary document see N87-17135 09-43)

Avail: NTIS HC A10/MF A01 CSCL 08C

Radar images of ocean surface waves near hurricane Josephine were acquired with the Shuttle Imaging Radar-B (SIR-B) system on October 12, 1984. Fast Fourier transform analyses of the images were performed along most of the 600-km image track. These data reveal the presence of at least two dominant wave systems which undergo significant spatial variations in wavelength and direction. Author

N87-17149*# Johns Hopkins Univ., Laurel, Md. Applied Physics Lab.

OPERATIONAL WAVE FORECASTING WITH SPACEBORNE SAR: PROSPECTS AND PITFALLS **c48**

R. C. Beal *In* JPL The Second Spaceborne Imaging Radar Symposium 1 Dec. 1986 p 107-113 (For primary document see N87-17135 09-43)

Avail: NTIS HC A10/MF A01 CSCL 08C

Measurements collected in the Shuttle Imaging Radar (SIR-B) Extreme Waves Experiment confirm the ability of Synthetic Aperture Radar (SAR) to yield useful estimates of wave directional energy spectra over global scales, at least for shuttle altitudes. However, azimuth fall-off effects tend to become severe for wavelengths shorter than about 100 m in most sea states. Moreover, the azimuth fall-off problem becomes increasingly severe as the platform altitude increases beyond 300 km. The most viable solution to the global wave measurements problem may be a low altitude spacecraft containing a combination of both the SAR and the Radar Ocean Wave Spectrometry (ROWS). Such a combination could have a synergy which yield global spectral estimates superior to those of either instrument singly employed. Author

N87-17150*# Environmental Research Inst. of Michigan, Ann Arbor. Radar Science Lab.

IMAGING RADAR CONTRIBUTIONS TO A MAJOR AIR-SEA-ICE INTERACTION STUDY IN THE GREENLAND SEA **c48**

Robert A. Shuchman *In* JPL The Second Spaceborne Imaging Radar Symposium 1 Dec. 1986 p 114-118 (For primary document see N87-17135 09-43)

Avail: NTIS HC A10/MF A01 CSCL 08C

By virtue of the Synthetic Aperture Radar (SAR's) imaging capabilities, such as all-weather imaging, relatively high resolution, and large dynamic range of backscatter from SAR ice and open ocean, information on the important marginal ice zone (MIZ) parameters can be derived from the SAR data. Information on ice edge location and location of ice-edge eddies, for example, can be obtained directly from examination of the imagery as can detection of ocean fronts and internal waves. With machine-assisted manual image analysis, estimates of ice concentration, floe size distributions, and ice field motion can also be derived. Full digital analysis, however, is required to obtain gravity wave spectral information and backscatter statistics for ice type discrimination and automated ice concentration algorithms. Author

N87-17151*# Washington Univ., Seattle. Applied Physics Lab.

OBSERVING THE POLAR OCEANS WITH SPACEBORNE RADAR **c48**

Drew Rothrock *In* JPL The Second Spaceborne Imaging Radar Symposium 1 Dec. 1986 p 119-122 (For primary document see N87-17135 09-43)

Avail: NTIS HC A10/MF A01 CSCL 08C

The application of spaceborne imaging radar data to polar oceanography and sea ice is explored. Several problems come to mind which are presently ripe with ideas and models, but are in need of new data, SAR data, for any progress to be made. These are the study of the ice mass balance, the ice momentum balance, and the circulation of the Arctic Ocean. These problems are described along with the data which is applicable to them and can be extracted from SAR imagery. Some uses are discussed of these data to explore mesoscale processes which affect the oceans and ice cover. Author

N87-17152*# Dornier-Werke G.m.b.H., Friedrichshafen (West Germany).

FEATURES AND TECHNOLOGIES OF ERS-1 (ESA) AND X-SAR ANTENNAS **c33**

R. Schuessler and R. Wagner *In* JPL The Second Spaceborne Imaging Radar Symposium 1 Dec. 1986 p 125-129 (For primary document see N87-17135 09-43)

Avail: NTIS HC A10/MF A01 CSCL 09C

Features and technologies of planar waveguide array antennas developed for spaceborne microwave sensors are described. Such antennas are made from carbon fiber reinforced plastic

(CFRP) employing special manufacturing and metallization techniques to achieve satisfactory electrical properties. Mechanical design enables deployable antenna structures necessary for satellite applications (e.g., ESA ERS-1). The slotted waveguide concept provides high aperture efficiency, good beamshaping capabilities, and low losses. These CFRP waveguide antennas feature low mass, high accuracy and stiffness, and can be operated within wide temperature ranges. Author

N87-17153*# Deutsche Forschungs- und Versuchsanstalt fuer Luft- und Raumfahrt, Porz (West Germany).

OFF-LINE PROCESSING OF ERS-1 SYNTHETIC APERTURE RADAR DATA WITH HIGH PRECISION AND HIGH THROUGHPUT

J. Gredel, W. Markwitz, W. Noack, and G. Schreier *In* JPL The Second Spaceborne Imaging Radar Symposium 1 Dec. 1986 p 130-142 (For primary document see N87-17135 09-43)

Avail: NTIS HC A10/MF A01 CSCL 05B

The first European remote sensing satellite ERS-1 will be launched by the European Space Agency (ESA) in 1989. The expected lifetime is two to three years. The spacecraft sensors will primarily support ocean investigations and to a limited extent also land applications. Prime sensor is the Active Microwave Instrumentation (AMI) operating in C-Band either as Synthetic Aperture Radar (SAR) or as Wave-Scatterometer and simultaneously as Wind-Scatterometer. In Europe there will be two distinct types of processing for ERS-1 SAR data, Fast Delivery Processing and Precision Processing. Fast Delivery Proceessing will be carried out at the ground stations and up to three Fast Delivery products per pass will be delivered to end users via satellite within three hours after data acquisition. Precision Processing will be carried out in delayed time and products will not be generated until several days or weeks after data acquisition. However, a wide range of products will be generated by several Processing and Archiving Facilities (PAF) in a joint effort coordinated by ESA. The German Remote Sensing Data Center (Deutsches Fernerkundungsdatenzentrum DFD) will develop and operate one of these facilities. The related activities include the acquisition, processing and evaluation of such data for scientific, public and commercial users. Based on this experience the German Remote Sensing Data Center is presently performing a Phase-B study regarding the development of a SAR processor for ERS-1. The conceptual design of this processing facility is briefly outlined. E.R.

N87-17154*# MacDonald, Dettwiler and Associates Ltd., Richmond (British Columbia).

RADARSAT HIGH THROUGHPUT SAR PROCESSOR DEVELOPMENT **c32**

P. George *In* JPL The Second Spaceborne Imaging Radar Symposium 1 Dec. 1986 p 142-148 (For primary document see N87-17135 09-43)

Avail: NTIS HC A10/MF A01 CSCL 17I

MacDonald Dettwiler & Associates has been involved with the Canadian Radarsat (RSAT) project for a number of years. This included Phase A definition studies and for the past two years, Phase B ground station design and processor prototyping efforts. The current baseline design for the SAR processing facility (SARDPF) is described along with its requirements and functional decomposition. This forms the context for then discussing the prototype SAR processor and extensions necessary to meet current ground station processing requirements. Author

N87-17155*# Jet Propulsion Lab., California Inst. of Tech., Pasadena.

THE SIR-C GROUND DATA SYSTEM: DIGITAL PROCESSOR, DATA PRODUCTS, INFORMATION FLOW

John C. Curlander *In its* The Second Spaceborne Imaging Radar Symposium 1 Dec. 1986 p 149-156 (For primary document see N87-17135 09-43)

Avail: NTIS HC A10/MF A01 CSCL 05B

The SIR-C (Shuttle Imaging Radar) instrument will collect both C-Band and L-Band data with each frequency band consisting of direct (HH or VV) and cross-polarized (HV or VH) data. Considering all possible combinations as many as eight different data channels will be available for any given target area. This data will be digitized and formatted on-board for direct downlink via the Tracking and Data Relay Satellite System (TDRSS), or it will be buffered through on-board high density digital recorders for storage or transmission when TDRSS is available. The data is received by the TDRSS ground station at White Sands and is nominally relayed via DOMSAT to the high data rate recording facility at GSFC. The tapes are then shipped to JPL for processing into imagery and eventual distribution to the SIR-C investigators. Author

N87-17156*# Purdue Univ., West Lafayette, Ind. Dept. of Forestry and Natural Resources.

ANALYSIS OF MULTIPLE INCIDENCE ANGLE SIR-B DATA FOR DETERMINING FOREST STAND CHARACTERISTICS

R. M. Hoffer, D. F. Lozano-Garcia, D. D. Gillespie, P. W. Mueller, and M. J. Ruzek (Jet Propulsion Lab., California Inst. of Tech., Pasadena) *In* JPL The Second Spaceborne Imaging Radar Symposium 1 Dec. 1986 p 159-164 (For primary document see N87-17135 09-43)

Avail: NTIS HC A10/MF A01 CSCL 02F

For the first time in the U.S. space program, digital synthetic aperture radar (SR) data were obtained from different incidence angles during Space Shuttle Mission 41-G. Shuttle Imaging Radar-B (SIR-B) data were obtained at incidence angles of 58 deg., 45 deg., and 28 deg., on October 9, 10, and 11, 1984, respectively, for a predominantly forested study area in northern Florida. Cloud-free LANDSAT Thematic Mapper (T.M.) data were obtained over the same area on October 12. The SIR-B data were processed and then digitally registered to the LANDSAT T.M. data by scientists at the Jet Propulsion Laboratory. This is the only known digitally registered SIR-B and T.M. data set for which the data were obtained nearly simultaneously. The data analysis of this information is discussed. Author

N87-17157*# Jet Propulsion Lab., California Inst. of Tech., Pasadena.

MULTIPLE INCIDENCE ANGLE SIR-B EXPERIMENT OVER ARGENTINA

JoBea Cimino, Daren Casey, Stephen Wall, Aldo Brandani (Consejo Nacional de Investigaciones Cientificas y Tecnicas, Mar del Plata, Argentina), Gitta Domik (Vexcell Corp., Boulder, Colo.), and Franz Leberl *In its* The Second Spaceborne Imaging Radar Symposium 1 Dec. 1986 p 165-173 (For primary document see N87-17135 09-43)

Avail: NTIS HC A10/MF A01 CSCL 08B

The Shuttle Imaging Radar (SIR-B), the second synthetic aperture radar (SAR) to fly aboard a shuttle, was launched on October 5, 1984. One of the primary goals of the SIR-B experiment was to use multiple incidence angle radar images to distinguish different terrain types through the use of their characteristic backscatter curves. This goal was accomplished in several locations including the Chubut Province of southern Argentina. Four descending image acquisitions were collected providing a multiple incidence angle image set. The data were first used to assess stereo-radargrammetric techniques. A digital elevation model was produced using the optimum pair of multiple incidence angle images. This model was then used to determine the local incidence angle of each picture element to generate curves of relative brightness vs. incidence angle. Secondary image products were also generated using the multi-angle data. The results of this work indicate that: (1) various forest species and various structures of a single species may be discriminated using multiple incidence angle radar imagery, and (2) it is essential to consider the variation in backscatter due to a variable incidence angle when analyzing and comparing data collected at varying frequencies and polarizations. Author

N87-17158*# Jet Propulsion Lab., California Inst. of Tech., Pasadena.

IMAGING RADAR POLARIMETRY FROM WAVE SYNTHESIS **c32**

Howard A. Zebker, Jacob J. VanZyl, and Daniel N. Held *In its*

The Second Spaceborne Imaging Radar Symposium 1 Dec. 1986 p 174-184 (For primary document see N87-17135 09-43)
Avail: NTIS HC A10/MF A01 CSCL 17I

It was shown that it is possible to measure the complete scattering matrix of an object using data acquired on a single aircraft pass, and can combine the signals later in the data processor to generate radar images corresponding to any desired combination of transmit and receive polarization. Various scattering models predict different dependence on polarization state of received power from an object. The imaging polarimeter permits determination of this dependence, which is called the polarization signature, of each point in a radar image. Comparison of the theoretical predictions and observational data yield identification of possible scattering mechanisms for each area of interest. It was found that backscatter from the ocean is highly polarized and well-modeled by Bragg scattering, while scattering from trees in a city park possesses a considerable unpolarized component. Urban regions exhibit the characteristics expected from dihedral corner reflectors and their polarization signatures are quite different from the one-bounce Bragg model. Author

N87-17159*# New South Wales Univ., Kensington (Australia). Centre for Remote Sensing.
RADAR SIGNATURE DETERMINATION: TRENDS AND LIMITATIONS **c32**
J. A. Richards *In* JPL The Second Spaceborne Imaging Radar Symposium 1 Dec. 1986 p 184-190 (For primary document see N87-17135 09-43)
Avail: NTIS HC A10/MF A01 CSCL 17I

Modelling studies, as means for assessing what could be called radar signatures, are a part of two radar remote sensing research programs with which the author is affiliated. First, at the University of New South Wales, assessment of SIR-B data is being undertaken for a number of purposes including its value in arid land geomorphological and geological studies, forest and crop assessment, and mapping. A number of early results have been reported, however modelling aspects are still at an early stage. Secondly, the author recently spent 6 months working on SIR-B invertible forest canopy modelling in the Department of Geography at the University of California, Santa Barbara. Results from this work are outlined. Author

N87-17160*# Michigan Univ., Ann Arbor.
SIR-B MEASUREMENTS AND MODELING OF VEGETATION
Fawwaz T. Ulaby and M. Craig Dobson *In* JPL The Second Spaceborne Imaging Radar Symposium 1 Dec. 1986 p 191-200 (For primary document see N87-17135 09-43)
Avail: NTIS HC A10/MF A01 CSCL 02C

A summary is presented of the results derived from analysis of six SIR-B data takes over an agricultural test site in west central Illinois. The first part describes the procedure used to calibrate the SIR-B imagery, the second part pertains to the observed radar response to soil moisture content, and the last part examines the information derivable from multiangle observations. Author

N87-17161*# Jet Propulsion Lab., California Inst. of Tech., Pasadena.
SIR-C, THE NEXT GENERATION SPACEBORNE SAR **c33**
E. R. Caro *In its* The Second Spaceborne Imaging Radar Symposium 1 Dec. 1986 p 203-217 (For primary document see N87-17135 09-43)
Avail: NTIS HC A10/MF A01 CSCL 09C

SIR-C represents a significant advance in spaceborne SAR system capabilities. The design approach is responsive to the requirements identified by the Science Steering Committee. This multimode feature of the sensor will provide science investigators with new dimensions in acquiring and interpreting scientific data. The flexibility of the SIR-C design will provide a core instrument which will meet the needs of SAR data users into the 1990's and serve as a foundation for ultimate incorporation into the EOS platform. Author

N87-17162*# Deutsche Forschungs- und Versuchsanstalt fuer Luft- und Raumfahrt, Oberpfaffenhofen (West Germany). Inst. fuer Hochfrequenztechnik.
THE X-SAR SYSTEM **c33**
Herwig Oettl *In* JPL The Second Spaceborne Imaging Radar Symposium 1 Dec. 1986 p 218-223 (For primary document see N87-17135 09-43)
Avail: NTIS HC A10/MF A01 CSCL 09C

During the past few years, there has been significant progress made in the planning for an X-band SAR, designed to fly in the shuttle together with the SIR-C system of NASA/JPL. New work and studies have been initiated to enable the goal of two missions in 1990 to be met. The antennas of X-SAR and SIR-C will be placed side-by-side on a pivoted steerable foldable structure, which will allow antenna movement without changing the attitude of the shuttle. This figure also shows the pallet, underneath the antenna structure, which houses the electronic sub-systems of both radars. Although the two radar systems, X-band SAR and the L- and C-band SAR of SIR-C, have different technical designs, their overall system performance, in terms of image quality, is expected to be similar. The current predicted performance of the X-SAR system based on results of the continuing Phase B studies is detailed. Differences between the performance parameters of X-SAR and those of SIR-C are only detailed in as far as they affect planning decisions to be made by experimenters. E.R.

N87-17163# European Space Agency, Paris (France).
PROCEEDINGS OF THE 1986 INTERNATIONAL GEOSCIENCE AND REMOTE SENSING SYMPOSIUM (IGA 'S '86) ON REMOTE SENSING: TODAY'S SOLUTIONS FOR TOMORROW'S INFORMATION NEEDS, VOLUME 1
T. D. Guyenne, ed. and J. J. Hunt, ed. Aug. 1986 752 p Symposium held in Zurich, Switzerland, 8-11 Sep. 1986; sponsored by NASA, IEEE Geoscience and Remote Sensing Society, ESA, EARSeL, NOAA, CNES, DFVLR, Swiss Academy of Sciences, the Swiss Association for Space Technology, Contraves Ltd., et al. (ESA-SP-254-Vol-1; IEEE-86CH2268-1-Vol-1; LC-86-80109-Vol-1; ISSN-0379-6566; ETN-87-98535) Avail: NTIS HC A99/MF E03; ESA, Paris, France, 3 volume set $90 Member States, AU, CN, and NO (+20% others)

New instruments with enormous information gathering abilities are being planned to provide data from all parts of the spectrum. New data processing and storage hardware, combined with fundamental advances in information systems concepts and algorithms are awaiting the research efforts to mold them for special use. Some topics covered in the proceedings are: Optical and infrared remote sensing systems; information transfer and Third World development; wave target interaction mechanisms; microwave remote sensing of sea ice; ERS-1 sensor performance, calibration, and data validation; geophysics; imaging spectrometry; image analysis systems; ocean radar scattering; marginal ice zone remote sensing; geomorphology; SAR applications; geology; multispectral image analysis; ocean wind scatterometry; passive microwave sensing; radar mapping and land use; meteorology and atmospheric sounding; and radar instrumentation. For individual titles, see N87-17164 through N87-17282.

N87-17164# Michigan Univ., Ann Arbor. Inst. of Environmental Research.
COMPONENTS AND COMPARISONS OF POTENTIAL INFORMATION FROM SEVERAL IMAGING SATELLITES
A. Malila *In* ESA Proceedings of the 1986 International Geoscience and Remote Sensing Symposium (IGARSS '86) on Remote Sensing: Today's Solutions for Tomorrow's Information Needs, Volume 1 Aug. 1986 p 3-8 (For primary document see N87-17163 09-43)
Avail: NTIS HC A99/MF E03; ESA, Paris, France, 3 volume set $90 Member States, AU, CN, and NO (+20% others)

An approach for measuring and comparing the potential information content of multispectral image data, based on sensor system specifications is developed. The method extends beyond the spectral and spatial domains to include the temporal domain, and adds a measure of the information in spatial registration. The

total potential information of LANDSAT Thematic Mapper data is found to be the greatest of the systems analyzed, and that of the geostationary Visible Infrared Spin Scan Radiometer (VISSR) the least. Polar-orbiting Advanced Very High Resolution Radiometer (AVHRR) and Coastal Zone Color Scanner (CZCS) meteorological systems with wide-angle coverage, moderate spatial resolution, and five or six spectral bands rank below the TM but above the LANDSAT MSS and SPOT HRV which are comparable to each other. ESA

N87-17165# Freiburg Univ. (West Germany).
COMPARISON OF THEMATIC MAPPER (TM) AND SPOT SIMULATION DATA FOR AGRICULTURAL APPLICATIONS IN SOUTH WEST GERMANY
W. Mauser, H.-J. Stibig, and W. Kirchhof (Deutsche Forschungs- und Versuchsanstalt fuer Luft- und Raumfahrt, Oberpfaffenhofen, West Germany) *In* ESA Proceedings of the 1986 International Geoscience and Remote Sensing Symposium (IGARSS '86) on Remote Sensing: Today's Solutions for Tomorrow's Information Needs, Volume 1 Aug. 1986 p 9-13 (For primary document see N87-17163 09-43)
Avail: NTIS HC A99/MF E03; ESA, Paris, France, 3 volume set $90 Member States, AU, CN, and NO (+20% others)

Data sets of pixel-sizes of 10, 20, 30, 50, and 80m created from data of a LANDSAT Thematic Mapper (TM) simulation were used for a comparative analysis between TM and SPOT-data of the information content in agricultural and forestry applications. The discrimination of objects depending on pixel-size and spectral bands was investigated. The TM-bands together with the improved resolution brought strong improvements in the separation of vegetated and built-up areas as well as growth stages of vegetation in comparison to MSS. The TM is found to be well suited for application in areas with average field sizes of 1.5 ha. The information content of the SPOT-multiband data-set is found to not essentially differ from that of TM. The results of a classification of the SPOT-multiband data are slightly less accurate than those using the TM-data. ESA

N87-17166# National Space Development Agency, Tokyo (Japan). Earth Observation Center.
SOME RESULTS OF MARINE OBSERVATION SATELLITE (MOS-1) AIRBORNE VERIFICATION EXPERIMENT MULTISPECTRAL ELECTRONIC SELF SCANNING RADIOMETER (MESSR)
K. Maeda, M. Kojima, and Y. Azuma *In* ESA Proceedings of the 1986 International Geoscience and Remote Sensing Symposium (IGARSS '86) on Remote Sensing: Today's Solutions for Tomorrow's Information Needs, Volume 1 Aug. 1986 p 15-20 (For primary document see N87-17163 09-43)
Avail: NTIS HC A99/MF E03; ESA, Paris, France, 3 volume set $90 Member States, AU, CN, and NO (+20% others)

In order to develop distortion correction methods for Marine Observation Satellite-1 (MOS-1) data and the evaluation methods for Earth observation system, airborne verification experiments using three airborne sensors equivalent in performance to MOS-1 sensors were conducted. A multispectral electronic self-scanning radiometer (MESSR) developed by modifying the engineering model of MOS-1 MESSR, which is capable of observing in visible and near-infrared wavelengths with CCD detector elements was tested in an airborne configuration. Results will be used in the spaceborne verification. ESA

N87-17167# Messerschmitt-Boelkow-Blohm G.m.b.H., Munich (West Germany).
THE STEREO-PUSHBROOM SCANNER SYSTEM DIGITAL PHOTOGRAMMETRY SYSTEM (DPS) AND ITS ACCURACY
O. Hofmann *In* ESA Proceedings of the 1986 International Geoscience and Remote Sensing Symposium (IGARSS '86) on Remote Sensing: Today's Solutions for Tomorrow's Information Needs, Volume 1 Aug. 1986 p 21-28 (For primary document see N87-17163 09-43)
Avail: NTIS HC A99/MF E03; ESA, Paris, France, 3 volume set $90 Member States, AU, CN, and NO (+20% others)

A digital stereo-scanner with three line sensor arrays working on the pushbroom principle and a suitable, rigorous compilation process was developed. It delivers the orientation data of the camera in selectable update points along the flight path of aircraft, spacecraft, or missiles, the three-dimensional coordinates of the digital elevation model, ortho and stereo-orthophotos, digital elements for line maps, and rectified multispectral images. By computer simulated operational models, the influence of the camera and flight parameters on the accuracy of the models were tested. Results show high stability and nearly constant accuracy over an entire strip model. ESA

N87-17168# Deutsche Forschungs- und Versuchsanstalt fuer Luft- und Raumfahrt, Oberpfaffenhofen (West Germany).
STEREO LINE SCANNER (SLS): SYSTEM CONSIDERATIONS ON AN OPERATIONAL INSTRUMENT FOR METEOROLOGY AND WEATHER FORECASTS **c47**
A. Drescher *In* ESA Proceedings of the 1986 International Geoscience and Remote Sensing Symposium (IGARSS '86) on Remote Sensing: Today's Solutions for Tomorrow's Information Needs, Volume 1 Aug. 1986 p 29-32 (For primary document see N87-17163 09-43)
Avail: NTIS HC A99/MF E03; ESA, Paris, France, 3 volume set $90 Member States, AU, CN, and NO (+20% others)

A Stereo Line Scanner (SLS) supplemented by a scanning Laser Ranger (LAR) to be flown on a polar orbiting satellite was designed. The mission aim is to provide three dimensional images of the cloud distribution and horizontal wind vectors from cloud displacements with true height assignment two times per day (at day and night time). Envisaged accuracies are + or - 1 m/sec for wind velocity and + or - 150 m for height. The along track wind component is derived from the difference between apparent stereoscopic height of SLS and true height from LAR. The main application areas are weather forecasts, meteorology, and climatology. ESA

N87-17169# European Space Agency. European Space Research and Technology Center, ESTEC, Noordwijk (Netherlands).
CONCEPT OF A FUTURE MULTISPECTRAL THERMAL INFRARED (TIR) PUSHBROOM MISSION FOR EARTH OBSERVATION FROM SPACE
M. Rast and M. L. Reynolds *In its* Proceedings of the 1986 International Geoscience and Remote Sensing Symposium (IGARSS '86) on Remote Sensing: Today's Solutions for Tomorrow's Information Needs, Volume 1 Aug. 1986 p 33-37 (For primary document see N87-17163 09-43)
Avail: NTIS HC A99/MF E03; ESA, Paris, France, 3 volume set $90 Member States, AU, CN, and NO (+20% others)

Mission requirements and instrument specifications for a multispectral thermal infrared pushbroom imager for land observation and coastal and inland water applications are outlined. Applications to vegetation, agriculture, and forestry; water resources; geosciences; and environmental monitoring are described. ESA

N87-17170# Florida International Univ., Miami. Dept. of International Business.
THE TRANSFER OF REMOTE SENSING TECHNOLOGY TO DEVELOPING COUNTRIES: A SURVEY OF EXPERTS IN THE FIELD **c85**
C. Specter *In* ESA Proceedings of the 1986 International Geoscience and Remote Sensing Symposium (IGARSS '86) on Remote Sensing: Today's Solutions for Tomorrow's Information Needs, Volume 1 Aug. 1986 p 41-44 (For primary document see N87-17163 09-43)
Avail: NTIS HC A99/MF E03; ESA, Paris, France, 3 volume set $90 Member States, AU, CN, and NO (+20% others)

The transfer of LANDSAT-related remote sensing technology from the United States to developing countries was examined. A questionnaire was sent to experts in the field of remote sensing technology to determine what they perceived as the major barriers to remote sensing technology transfer (RSTT). Useable questionnaire responses were received from 618 professionals in

63 countries. Responses of participants representing developed countries, developing countries, and international organizations were compared in order to identify similarities and differences in their perceptions of the RSTT barriers. Of the eight major barriers identified, five are related to economics. Participants tend to perceive the withdrawal of the U.S. government from management of the LANDSAT system, the lack of knowledge about application of remote sensing technology among government decision-makers in developing countries, and the lack of personnel experienced in using computer compatible tapes as major RSTT barriers. ESA

N87-17171# Indian Inst. of Tech., Bombay. Center of Studies in Resources Engineering.
IN SERVICE TRAINING OF SCIENTISTS AND ENGINEERS: AN IMPORTANT METHOD OF INFORMATION TRANSFER IN THE AREA OF SATELLITE REMOTE SENSING AND ITS APPLICATIONS
T. V. Pavate *In* ESA Proceedings of the 1986 International Geoscience and Remote Sensing Symposium (IGARSS '86) on Remote Sensing: Today's Solutions for Tomorrow's Information Needs, Volume 1 Aug. 1986 p 45-48 (For primary document see N87-17163 09-43)
Avail: NTIS HC A99/MF E03; ESA, Paris, France, 3 volume set $90 Member States, AU, CN, and NO (+20% others)

Space technology and its spin offs have resulted into various uses on the Earth surface. Satellite remote sensing or teledetection is an emerging area and its applications in identification, exploitation and management of natural resources on global basis demands priority with respect to information transfer. Training of inservice engineers and scientists has assumed a new dimension in veiw of continuous and repetitive sensor data which needs to be transferred to user agencies for operational and quantitative remote sensing. To overcome shortcomings of trained manpower, it is felt especially in developing countries that stress has to be laid on training inservice engineers and scientists from various user agencies. Various aspects of the problem is considered in light of experience gained by various training programs conducted in the area of application of satellite remote sensing for inservice engineers and scientists. ESA

N87-17172# Institut Geographique National, Paris (France).
MONITORING OF LARGE PHENOMENA IN DEVELOPING COUNTRIES THROUGH SATELLITE IMAGERY
L. Guyot *In* ESA Proceedings of the 1986 International Geoscience and Remote Sensing Symposium (IGARSS '86) on Remote Sensing: Today's Solutions for Tomorrow's Information Needs, Volume 1 Aug. 1986 p 49-51 (For primary document see N87-17163 09-43)
Avail: NTIS HC A99/MF E03; ESA, Paris, France, 3 volume set $90 Member States, AU, CN, and NO (+20% others)

Inter-annual comparisons between satellite images showing the effects of slowly evolving phenomena such as forest degradation or desert spreading, and intra-annual comparisons between images showing the flooding conditions over large areas are discussed. Trampling and overgrazing around a borehole, and monitoring of Niger river throughout a flooding season are described. ESA

N87-17173# Stanford Univ., Calif.
SPATIAL ANALYSIS OF THE DYNAMICS OF AN ECOSYSTEM BY MULTISTAGE REMOTE SENSING IN KENYA
H. R. Goetting and R. Maeckel (Freiburg Univ., West Germany) *In* ESA Proceedings of the 1986 International Geoscience and Remote Sensing Symposium (IGARSS '86) on Remote Sensing: Today's Solutions for Tomorrow's Information Needs, Volume 1 Aug. 1986 p 53-56 (For primary document see N87-17163 09-43)
Avail: NTIS HC A99/MF E03; ESA, Paris, France, 3 volume set $90 Member States, AU, CN, and NO (+20% others)

Satellite data, an aerial survey, and ground reference data were used as a database for the analysis of the carrying capacity and the desertification process in the Uaso Nyiro River Basin of Northern Kenya. The carrying capacity in terms of the population density of the semi-arid Leroghi Plateau is 7 P/sqkm. But there are 14.5 P/sqkm currently living there and the population is growing. Due to the desertification process, the vegetation to support the livestock decreased by 11% in the last 16 yr. In the arid river basin the calculated carrying capacity is 2 P/sqkm. If one assumes that this calculation is still up to date, then the area south of the river is overpopulated by 275%. The overpopulation in the area north of the river reaches 490%. Due to the desertification process and the shrinking grazing land, todays carrying capacity of the river basin is a mere 1 P/sqkm. The dangerous overpopulation points toward a human tragedy in the near future in the arid lands of Northern Kenya. ESA

N87-17174# Zurich Univ. (Switzerland). Dept. of Geography.
SRI LANKA'S SOLUTION TO LAND USE MAPPING AND MONITORING FOR THIRD WORLD COUNTRIES DEVELOPMENT
K. I. Itten, S. D. F. C. Nanayakkara (Center for Remote Sensing, Colombo, Sri Lanka), H. S. Jayatilaka, M. Bichsel, G. Schneider, and R. Heumbel *In* ESA Proceedings of the 1986 International Geoscience and Remote Sensing Symposium (IGARSS '86) on Remote Sensing: Today's Solutions for Tomorrow's Information Needs, Volume 1 Aug. 1986 p 57-61 (For primary document see N87-17163 09-43)
Avail: NTIS HC A99/MF E03; ESA, Paris, France, 3 volume set $90 Member States, AU, CN, and NO (+20% others)

Airphoto interpretation with digitally corrected and enhanced LANDSAT MSS imagery was used for land use mapping in Sri Lanka in the scale of 1:1,000,000. Thematic masking procedures starting from the single classes from the land use map, result in an easy assessment of per class changes, with newly acquired satellite imagery. Thus inventorying the land use and monitoring its changes have become an operational national task of the Center for Remote Sensing of the Sri Lanka Survey Department. ESA

N87-17175# Instituto de Pesquisas Espaciais, Sao Paulo (Brazil).
ENVIRONMENTAL MODIFICATION OF METROPOLITAN AREAS THROUGH SATELLITE IMAGES: STUDY OF URBAN DESIGN IN THE TROPICS **c85**
M. A. Lombardo *In* ESA Proceedings of the 1986 International Geoscience and Remote Sensing Symposium (IGARSS '86) on Remote Sensing: Today's Solutions for Tomorrow's Information Needs, Volume 1 Aug. 1986 p 63-65 (For primary document see N87-17163 09-43)
Avail: NTIS HC A99/MF E03; ESA, Paris, France, 3 volume set $90 Member States, AU, CN, and NO (+20% others)

The application of remote sensing to identification of Sao Paulo's urban land use patterns, and the relationships between these uses and urban heat island effects, including air pollution, is described. Results show a pattern of temperature according to urban land use class. Highest temperatures are registered where the concentration of industries and buildings is heaviest. Conversely, municipalities, large green areas, and water reservoirs register the lowest readings. The horizontal thermal gradient in Sao Paulo, in stable atmospheric conditions, shows the greatest gradients in temperature. The thermal gradient intensity in the heat island is over 10 C, far surpassing measurements taken among cities in midlatitudes. ESA

N87-17176# Software Sciences Ltd., Farnborough (England).
THE DESIGN OF AN INTERNATIONAL DATA CENTRE FOR REMOTE SENSING **c82**
D. R. Sloggett *In* ESA Proceedings of the 1986 International Geoscience and Remote Sensing Symposium (IGARSS '86) on Remote Sensing: Today's Solutions for Tomorrow's Information Needs, Volume 1 Aug. 1986 p 67-71 (For primary document see N87-17163 09-43)
Avail: NTIS HC A99/MF E03; ESA, Paris, France, 3 volume set $90 Member States, AU, CN, and NO (+20% others)

An architecure for a worldwide infrastructure to enable effective research, commercial, and national exploitation of remote sensing data is presented. A modula approach that caters to the needs of many different countries and application areas relevant to those countries is envisaged. The work being conducted in the UK to set up a national infrastructure forms a useful basis for other countries to work from as a baseline. The concept requires work

to provide a worldwide infrastructure for monitoring all aspects of the environment, and the effects of mankind and nature upon our world. ESA

N87-17177# Earth Observation Satellite Co., Va.
COMMERCIAL OPPORTUNITIES IN EARTH OBSERVATION FROM SPACE
C. P. Williams *In* ESA Proceedings of the 1986 International Geoscience and Remote Sensing Symposium (IGARSS '86) on Remote Sensing: Today's Solutions for Tomorrow's Information Needs, Volume 1 Aug. 1986 p 73-76 (For primary document see N87-17163 09-43)
Avail: NTIS HC A99/MF E03; ESA, Paris, France, 3 volume set $90 Member States, AU, CN, and NO (+20% others)

Land and ocean remote sensing programs are listed. The LANDSAT and SPOT instruments are described. Commercial prospects for the 21st century are considered. ESA

N87-17178# Bern Univ. (Switzerland). Inst. of Applied Physics.
ON MICROWAVE SCATTERING PROPERTIES OF HETEROGENEOUS TWO-COMPONENT MIXTURES
E. Schanda *In* ESA Proceedings of the 1986 International Geoscience and Remote Sensing Symposium (IGARSS '86) on Remote Sensing: Today's Solutions for Tomorrow's Information Needs, Volume 1 Aug. 1986 p 79-84 (For primary document see N87-17163 09-43)
Avail: NTIS HC A99/MF E03; ESA, Paris, France, 3 volume set $90 Member States, AU, CN, and NO (+20% others)

For randomly distributed scattering centers within a background medium, two concepts for modeling the scatter behavior are discussed. In most practical cases these mixed media can be regarded as composed of two components with isotropic, random distribution in space. For the simple case of a dry (refrozen) snow crust the first order Born approximation yields surprisingly good results. For water inclusions in snow and soil the strong fluctuation of permittivity concept is applied. Various, strongly simplifying assumptions are made (their validity still to be proven) when the relative contribution of volume scattering by these mixtures is computed. ESA

N87-17179# Helsinki Univ. of Technology, Espoo (Finland).
DIELECTRIC AND SCATTERING BEHAVIOR OF SNOW AT MICROWAVE FREQUENCIES
M. Hallikainen and F. T. Ulaby (Michigan Univ., Ann Arbor) *In* ESA Proceedings of the 1986 International Geoscience and Remote Sensing Symposium (IGARSS '86) on Remote Sensing: Today's Solutions for Tomorrow's Information Needs, Volume 1 Aug. 1986 p 87-91 (For primary document see N87-17163 09-43)
Avail: NTIS HC A99/MF E03; ESA, Paris, France, 3 volume set $90 Member States, AU, CN, and NO (+20% others)

The interaction of microwaves with snow for dry and wet conditions is examined. The dielectric permittivity of dry snow is governed by the snow density, and its dielectric loss factor is governed by the density, frequency, and temperature. At frequencies above 15 GHz, volume scattering is the dominant loss mechanism in dry snow. Experimental data between 10 and 90 GHz show that the extinction coefficient of dry snow depends strongly on frequency and snow particle size. The surface scattering loss is determined by frequency and surface roughness. The dielectric properties of wet snow are dominated by those of liquid water at 0 C. ESA

N87-17180*# Texas Univ., Arlington. Wave Scattering Research Center.
EFFECTIVE MEDIUM APPROXIMATION FOR EFFECTIVE PROPAGATION CONSTANT CALCULATION IN A DENSE RANDOM MEDIUM **c32**
P. Y. Zhu and A. K. Fung *In* ESA Proceedings of the 1986 International Geoscience and Remote Sensing Symposium (IGARSS '86) on Remote Sensing: Today's Solutions for Tomorrow's Information Needs, Volume 1 Aug. 1986 p 93-97 (For primary document see N87-17163 09-43)
(Grant NAG5-486)
Avail: NTIS HC A99/MF E03; ESA, Paris, France, 3 volume set $90 Member States, AU, CN, and NO (+20% others) CSCL 20N

The effective medium approximation (EMA) formalism developed for scalar wave calculations in solid state physics is generalized to electromagnetic wave scattering in a dense random medium. Results are applied to compute the effective propagation constant in a dense medium involving discrete spherical scatterers. When compared with a common quasicrystalline approximation (QCA), it is found that EMA accounts for backward scattering and the effect of correlation among three scatterers which are not available in QCA. It is also found that there is not much difference in the calculated normalized phase velocity between the use of these two approximations. However, there is a significant difference in the computed effective loss tangent in a nonabsorptive random medium. The computed effective loss tangent using EMA and measurements from a snow medium are compared, showing good agreement. ESA

N87-17181# Hokkaido Univ., Sapporo (Japan). Inst. of Low Temperature Sciences.
SNOW STRATIGRAPHY OBSERVED BY AN FM-CW MICROWAVE SYSTEM
K. Fujino, G. Wakahama, M. Suzuku, and T. Matsumoto *In* ESA Proceedings of the 1986 International Geoscience and Remote Sensing Symposium (IGARSS '86) on Remote Sensing: Today's Solutions for Tomorrow's Information Needs, Volume 1 Aug. 1986 p 99-102 (For primary document see N87-17163 09-43)
Avail: NTIS HC A99/MF E03; ESA, Paris, France, 3 volume set $90 Member States, AU, CN, and NO (+20% others)

Snow stratigraphy was determined in the field by an Frequency Modulation-Continuous Wave (FM-CW) active microwave system at frequencies ranging from 6 to 12 GHz and 2 to 8 GHz. Physical properties of the snowpack were measured by digging a snow pit near the site. The dielectric constant of each layer was determined from the density of the layer, using a revised mixing formula for the dry snowpack. The frequencies of each spectrum obtained by the system agree with those determined from the density profile of the snowpack. ESA

N87-17182*# Johns Hopkins Univ., Laurel, Md. Applied Physics Lab.
RAIN MEASUREMENT RESULTS DERIVED FROM A TWO POLARIZATION S-BAND RADAR EMPLOYING FREQUENCY DIVERSITY AT WALLOPS ISLAND, VIRGINIA **c47**
J. Goldhirsh, J. Rowland, and B. Musiani *In* ESA Proceedings of the 1986 International Geoscience and Remote Sensing Symposium (IGARSS '86) on Remote Sensing: Today's Solutions for Tomorrow's Information Needs, Volume 1 Aug. 1986 p 103-108 Sponsored by NASA Goddard Space Flight Center and NASA, Washington (For primary document see N87-17163 09-43)
(Contract N00024-85-C-5301)
Avail: NTIS HC A99/MF E03; ESA, Paris, France, 3 volume set $90 Member States, AU, CN, and NO (+20% others) CSCL 04B

A dual polarization meteorological radar is described. It operates with a slow switch having a cycle time of 0.7 sec and incorporates a frequency diversity technique to achieve independent sampling over short intervals of time. Rain rate measurements derived from the dual polarization radar and low and high resolution rain gages located at a remote site are compared. Average percent differences in rainfall of $< 5\%$ and 16% are demonstrated when comparing the dual polarization radar measurements with the low and high resolution rain gages, respectively. Striking correlations of the rain rates are present during one rain day. The rain measurement cases examined were limited to only light rain rates (<7 mm/hr). ESA

N87-17183# China Research Inst. of Radiowave Propagation, Xinxiang.
A SPATIALLY HOMOGENEOUS ANISOTROPIC SURFACE MODEL WITH VARIABLE PARAMETERS FOR SCATTERING FROM BARE SOIL
J. Zeming *In* ESA Proceedings of the 1986 International Geoscience and Remote Sensing Symposium (IGARSS '86) on Remote

Sensing: Today's Solutions for Tomorrow's Information Needs, Volume 1 Aug. 1986 p 109-113 (For primary document see N87-17163 09-43)
Avail: NTIS HC A99/MF E03; ESA, Paris, France, 3 volume set $90 Member States, AU, CN, and NO (+20% others)

An irregular surface model for microwave remote sensing of bare soil moisture was developed. The heights of bare soil surfaces are assumed to be of two-dimensional normal or Gamma distributions containing statistical parameters dependent on angle of illumination and moisture, and autocorrelative functions of elliptic contours. Two-dimensional Gamma probability density and characteristic functions in closed form are derived, with which, under the Kirchhoff approximation, the expressions for backward scattering coefficients and for optimal angle of incidence for remote sensing of soil moisture are presented. The results are supported by experiments and published results in isotropic cases. ESA

N87-17184*# Environmental Research Inst. of Michigan, Ann Arbor. Radar Science Lab.
AN INTER-SENSOR COMPARISON OF THE MICROWAVE SIGNATURES OF ARCTIC SEA ICE
R. G. Onstott *In* ESA Proceedings of the 1986 International Geoscience and Remote Sensing Symposium (IGARSS '86) on Remote Sensing: Today's Solutions for Tomorrow's Information Needs, Volume 1 Aug. 1986 p 117-120 (For primary document see N87-17163 09-43)
(Grant NAGw-334; Contract N00014-81-C-0295; Grants N00014-83-C-0404; N00014-85-K-0200)
Avail: NTIS HC A99/MF E03; ESA, Paris, France, 3 volume set $90 Member States, AU, CN, and NO (+20% others) CSCL 08L

Active and passive microwave and physical properties of Arctic sea ice in the marginal ice zone were measured during the summer. Results of an intercomparison of data acquired by an aircraft synthetic aperture radar, a passive microwave imager and a helicopter-mounted scatterometer indicate that early-to-mid summer sea ice microwave signatures are dominated by snowpack characteristics. Measurements show that the greatest contrast between thin first-year and multiyear sea ice occurs when operating actively between 5 and 10 GHz. Significant information about the state of melt of snow and ice is contained in the active and passive microwave signatures. ESA

N87-17185*# National Aeronautics and Space Administration. Goddard Space Flight Center, Greenbelt, Md.
ACTIVE/PASSIVE MICROWAVE SENSOR COMPARISON OF MIZ-ICE CONCENTRATION ESTIMATES
B. A. Burns (Environmental Research Inst. of Michigan, Ann Arbor), D. J. Cavalieri, and M. R. Keller (Naval Research Lab., Washington, D. C.) *In* ESA Proceedings of the 1986 International Geoscience and Remote Sensing Symposium (IGARSS '86) on Remote Sensing: Today's Solutions for Tomorrow's Information Needs, Volume 1 Aug. 1986 p 121-125 (For primary document see N87-17163 09-43)
Avail: NTIS HC A99/MF E03; ESA, Paris, France, 3 volume set $90 Member States, AU, CN, and NO (+20% others) CSCL 08L

Active and passive microwave data collected during the 1984 summer Marginal Ice Zone Experiment in the Fram Strait (MIZEX 84) are used to compare ice concentration estimates derived from synthetic aperture radar (SAR) data to those obtained from passive microwave imagery at several frequencies. The comparison is carried out to evaluate SAR performance against the more established passive microwave technique, and to investigate discrepancies in terms of how ice surface conditions, imaging geometry, and choice of algorithm parameters affect each sensor. Active and passive estimates of ice concentration agree on average to within 12%. Estimates from the multichannel passive microwave data show best agreement with the SAR estimates because the multichannel algorithm effectively accounts for the range in ice floe brightness temperatures observed in the MIZ. ESA

N87-17186*# Stanford Univ., Calif. STAR Lab.
AUTOMATED REMOTE SENSING OF SEA ICE USING SYNTHETIC APERTURE RADAR c48
J. F. Vesecky, R. Samadani, M. P. Smith, J. M. Daida, and R. N. Bracewell *In* ESA Proceedings of the 1986 International Geoscience and Remote Sensing Symposium (IGARSS '86) on Remote Sensing: Today's Solutions for Tomorrow's Information Needs, Volume 1 Aug. 1986 p 127-132 Sponsored by NASA and ONR (For primary document see N87-17163 09-43)
Avail: NTIS HC A99/MF E03; ESA, Paris, France, 3 volume set $90 Member States, AU, CN, and NO (+20% others) CSCL 08J

Two techniques for automated sea ice tracking: image pyramids (hierarchical correlation) and feature tracking were applied to a pair of SEASAT SAR sea ice images. The results compare well with each other and manually tracked estimates of the ice velocity field. Refinement of the image pyramid technique should include removal of a small number of erroneous velocity vectors using constraints dependent on correlation coefficient, near neighbor velocities, and velocity gradients. Estimates of sea ice velocity are successfully obtained over limited areas using the boundary segment tracking technique. Refinement of the feature tracking technique should include use of pressure ridge features, constrained search, and relaxation techniques. ESA

N87-17187*# Massachusetts Inst. of Tech., Cambridge. Dept. of Electrical Engineering and Computer Science.
MICROWAVE REMOTE SENSING OF SNOW-COVERED SEA ICE c48
M. Borgeaud, J. A. Kong, and F. C. Lin *In* ESA Proceedings of the 1986 International Geoscience and Remote Sensing Symposium (IGARSS '86) on Remote Sensing: Today's Solutions for Tomorrow's Information Needs, Volume 1 Aug. 1986 p 133-138 (For primary document see N87-17163 09-43)
(Contracts NAG5-270; N00014-83-K-0525; Grant NSF ECS-85-04381)
Avail: NTIS HC A99/MF E03; ESA, Paris, France, 3 volume set $90 Member States, AU, CN, and NO (+20% others) CSCL 08J

Snow and ice are modeled as random media characterized by different dielectric constants and correlation functions. In order to model the brine inclusions of sea ice, the random medium is assumed to be anisotropic. A three-layer model is used to simulate a snow-covered ice field with the top layer being snow, the middle layer being ice, and the bottom layer being sea water. The theoretical results are illustrated for thick first-year sea ice covered by dry snow, and for artificial, thin first-year sea ice covered by wet snow as measured in controlled model tank experiments. The radar backscattering cross sections are seen to increase with snow cover for snow-covered sea ice owing to large volume scattering effects of snow. ESA

N87-17188*# Kansas Univ. Center for Research, Inc., Lawrence. Radar Systems and Remote Sensing Lab.
MICROWAVE BACKSCATTER COEFFICIENTS OF ARTIFICIALLY GROWN FIRST-YEAR SEA ICE c48
D. Xue, R. K. Moore, T. H. Lee Williams, and R. Onstott *In* ESA Proceedings of the 1986 International Geoscience and Remote Sensing Symposium (IGARSS '86) on Remote Sensing: Today's Solutions for Tomorrow's Information Needs, Volume 1 Aug. 1986 p 139-146 Sponsored by NASA (For primary document see N87-17163 09-43)
(Contract N00014-85-K-0200)
Avail: NTIS HC A99/MF E03; ESA, Paris, France, 3 volume set $90 Member States, AU, CN, and NO (+20% others) CSCL 08J

The radar backscattering coefficient of simulated first year sea ice was measured at 5.2, 9.6, 13.6, and 16.6 GHz, using a dual-antenna FM-CW scatterometer. The measurements were corrected for antenna separation and beamwidth, to obtain true values of scattering coefficient. Above 15 deg, snow-covered and rough gray ice have similar angular responses, while the decrease in scattering coefficient with incidence angle is more rapid for smoother surfaces. True scattering coefficients and surface roughness data estimated with an antenna-beamwidth correction based on a physical-optics model give values close to those measured. ESA

N87-17189# Canada Centre for Remote Sensing, Ottawa (Ontario). RADARSAT Project Office.
AN OVERVIEW OF OPERATIONAL SAR DATA COLLECTION AND DISSEMINATION PLANS FOR ERS-1 ICE DATA IN CANADA **c48**
L. McNutt and T. Mullane (Atmospheric Environment Service, Ottawa, Ontario) *In* ESA Proceedings of the 1986 International Geoscience and Remote Sensing Symposium (IGARSS '86) on Remote Sensing: Today's Solutions for Tomorrow's Information Needs, Volume 1 Aug. 1986 p 147-152 (For primary document see N87-17163 09-43)
Avail: NTIS HC A99/MF E03; ESA, Paris, France, 3 volume set $90 Member States, AU, CN, and NO (+20% others)

The ERS-1 and RADARSAT automated ice information system is described. This Ice Data Integration and Analysis System (IDIAS) will receive data from several sources, including satellite, aircraft, and ship reports, and integrate these onto a standard base map for production of ice forecast products. The satellite data will be received via the station in Gatineau, Quebec and the aircraft data will be downlinked to line-of-sight stations in the Arctic and retransmitted to Ottawa via the Anik-D satellite. The plans for ERS-1 data reception at Gatineau, data integration and product generation from the IDIAS system, and Canadian plans for operational demonstrations of the end-to-end information system within the ERS-1 timeframe are discussed. ESA

N87-17190# European Space Agency, Paris (France).
OVERVIEW AND STATUS OF THE ERS-1 PROGRAM
G. Duchossois *In its* Proceedings of the 1986 International Geoscience and Remote Sensing Symposium (IGARSS '86) on Remote Sensing: Today's Solutions for Tomorrow's Information Needs, Volume 1 Aug. 1986 p 155-159 (For primary document see N87-17163 09-43)
Avail: NTIS HC A99/MF E03; ESA, Paris, France, 3 volume set $90 Member States, AU, CN, and NO (+20% others)

The ERS-1 satellite system, and the ground segment configuration selected to allow global oceanic mission and delivery of standard products to users within 3 hr from observation are presented. Key features of the ERS-1 program, and information on the Announcement of Opportunity issued to sollicit proposals for science investigations and application demonstrations are outlined. ESA

N87-17191# Dornier-Werke G.m.b.H., Friedrichshafen (West Germany).
DEVELOPMENT STATUS OF THE ERS-1 PAYLOAD INSTRUMENTS **c19**
E. H. Velten and G. H. Dieterle (European Space Agency. European Space Research and Technology Center, ESTEC, Noordwijk, Netherlands) *In* ESA Proceedings of the 1986 International Geoscience and Remote Sensing Symposium (IGARSS '86) on Remote Sensing: Today's Solutions for Tomorrow's Information Needs, Volume 1 Aug. 1986 p 161-166 (For primary document see N87-17163 09-43)
Avail: NTIS HC A99/MF E03; ESA, Paris, France, 3 volume set $90 Member States, AU, CN, and NO (+20% others)

The ERS-1 Active Microwave Instrumentation containing a synthetic aperture radar and a microwave scatterometer, and a Radar Altimeter are presented. Supplementary instruments are an along track scanning radiometer, a microwave sounder, a precise range and range rate experiment and a laser retroreflector. Breadboard models and demonstration models were successfully tested. ESA

N87-17192# European Space Agency. European Space Research and Technology Center, ESTEC, Noordwijk (Netherlands).
THE ESA APPROACH FOR ERS-1 SENSOR CALIBRATION AND PERFORMANCE VERIFICATION **c19**
J. Louet *In its* Proceedings of the 1986 International Geoscience and Remote Sensing Symposium (IGARSS '86) on Remote Sensing: Today's Solutions for Tomorrow's Information Needs, Volume 1 Aug. 1986 p 167-174 (For primary document see N87-17163 09-43)
Avail: NTIS HC A99/MF E03; ESA, Paris, France, 3 volume set $90 Member States, AU, CN, and NO (+20% others)

The approach taken for validation and calibration of the ERS-1 mission is outlined. A clear distinction is made between the engineering and geophysical performances of the mission. The pre and post-launch activities required to calibrate the ERS-1 system and validate the geophysical performances are described. ESA

N87-17193# Marconi Space and Defence Systems Ltd., Portsmouth (England).
ON-GROUND VERIFICATION AND IN-ORBIT PERFORMANCE PREDICTION OF THE ERS-1 WIND SCATTEROMETER **c19**
D. J. Q. Carter *In* ESA Proceedings of the 1986 International Geoscience and Remote Sensing Symposium (IGARSS '86) on Remote Sensing: Today's Solutions for Tomorrow's Information Needs, Volume 1 Aug. 1986 p 175-180 (For primary document see N87-17163 09-43)
Avail: NTIS HC A99/MF E03; ESA, Paris, France, 3 volume set $90 Member States, AU, CN, and NO (+20% others)

The ERS-1 single polarization wind scatterometer (SCATT) major top level requirements and the relationships with lower level parameters used for the space segment hardware design are discussed. Areas impacted by interaction with the SAR are mentioned. The mechanisms by which the top level performance parameters are intended to be verified by use of lower level testing and verification are described, along with the subsequent prediction of the top level requirements. Performance predictions for the SCATT are included. ESA

N87-17194# European Space Agency. European Space Research and Technology Center, ESTEC, Noordwijk (Netherlands).
ERS-1 RADAR ALTIMETER: PERFORMANCE, CALIBRATION AND DATA VALIDATION **c19**
C. R. Francis *In its* Proceedings of the 1986 International Geoscience and Remote Sensing Symposium (IGARSS '86) on Remote Sensing: Today's Solutions for Tomorrow's Information Needs, Volume 1 Aug. 1986 p 181-184 (For primary document see N87-17163 09-43)
Avail: NTIS HC A99/MF E03; ESA, Paris, France, 3 volume set $90 Member States, AU, CN, and NO (+20% others)

Key characteristics of the ERS-1 radar altimeter and of the overall measurement system are described. Operating modes include ocean and ice. Calibration is based on ground test and simulation data and onboard, independent measures. Performance will be established once the hardware implementation is complete. The altimeter is not sensitive to yaw, but a roll tilt mode used when calibrating the wind scatterometer leads to loss of altimeter data. Science data are tape recorded and telemetered in a high speed dump in real time to ground stations. ESA

N87-17195# Mullard Space Science Lab., Dorking (England).
AN AUTOMATIC TRACKING MODE SWITCHING ALGORITHM FOR THE ERS-1 ALTIMETER **c19**
D. J. Wingham *In* ESA Proceedings of the 1986 International Geoscience and Remote Sensing Symposium (IGARSS '86) on Remote Sensing: Today's Solutions for Tomorrow's Information Needs, Volume 1 Aug. 1986 p 185-190 (For primary document see N87-17163 09-43)
(Contract ESTEC-6375/85-NL-BI)
Avail: NTIS HC A99/MF E03; ESA, Paris, France, 3 volume set $90 Member States, AU, CN, and NO (+20% others)

A tracking system which switches automatically the ERS-1 radio altimeter tracking mode and the range window width is described. The system estimates the shape of the return, which may be used to control the instrument gain and determine if the return is sufficiently ocean-like for the use of an ocean specific error algorithm; and it provides a linear height error algorithm for a wide variety of return shapes, which permits the height error to be open or close the range window. The linear height error substantially improves the tracking performance in areas where the range to the surface is varying rapidly. Simulated performance over a variety of geographical surfaces, in particular the ocean,

sea ice and ice shelves, and simulations of the altimeter and of the normal incidence radar returns from these surfaces are described. By combining these two, it is possible to assess the performance of the control system over these surfaces. The examples are deliberately chosen as worst case possibilities, and it is clear that the system offers a great increase in coverage over any previous system. ESA

N87-17196# Duisburg Univ. (West Germany). Dept. of Electrical Engineering.

THEORETICAL CONSIDERATION ON RESISTANCE GEOELECTRICS **c64**

A. Beyer *In* ESA Proceedings of the 1986 International Geoscience and Remote Sensing Symposium (IGARSS '86) on Remote Sensing: Today's Solutions for Tomorrow's Information Needs, Volume 1 Aug. 1986 p 193-197 (For primary document see N87-17163 09-43)

Avail: NTIS HC A99/MF E03; ESA, Paris, France, 3 volume set $90 Member States, AU, CN, and NO (+20% others)

A field problem of geoelectrics in which the knowledge of the electric field in the infinite half space with finite conductivity is needed to reflect on the field which is disturbed by a general ellipsoid is described. Using an elliptical coordinate system, the field problem is solved in terms of Lame's functions. The analyses include the determination of electric potentials and the electric field strengths for the infinite half space considered. Numerical results of sounding measurement models show the applicability of the method. ESA

N87-17197# Alfateh Univ., Tripoli (Libya). Dept. of Electrical and Electronics Engineering.

THE INDUCED CURRENT ON A LONG WIRE DUE TO A VERTICAL ELECTRIC DIPOLE ABOVE DISSIPATIVE GROUND **c33**

A. A. Aburwein *In* ESA Proceedings of the 1986 International Geoscience and Remote Sensing Symposium (IGARSS '86) on Remote Sensing: Today's Solutions for Tomorrow's Information Needs, Volume 1 Aug. 1986 p 199-203 (For primary document see N87-17163 09-43)

Avail: NTIS HC A99/MF E03; ESA, Paris, France, 3 volume set $90 Member States, AU, CN, and NO (+20% others)

A closed form expression for the induced current along an infinitely long wire due to a distant vertical electric dipole is found. The dipole and the wire are situated above but near a dissipative ground half space. The wire is assumed to be thin but of finite radius. The solution of this problem is important if the setup is used as an intrusion sensing system. The intruding object can be anywhere between the dipole and the wire. The sensing can be done remotely by monitoring the changes in the induced current along the wire. ESA

N87-17198# Cairo Univ. (Egypt). Dept. of Electronic Engineering.

DETERMINATION OF RESISTIVITY AND PERMITTIVITY PROFILES OF A LAYERED EARTH **c46**

H. M. Assal and S. F. Mahmoud *In* ESA Proceedings of the 1986 International Geoscience and Remote Sensing Symposium (IGARSS '86) on Remote Sensing: Today's Solutions for Tomorrow's Information Needs, Volume 1 Aug. 1986 p 205-209 (For primary document see N87-17163 09-43)

(Grant FRCU-842019)

Avail: NTIS HC A99/MF E03; ESA, Paris, France, 3 volume set $90 Member States, AU, CN, and NO (+20% others)

An algorithm for determination of depth profiles of resistivity and permittivity of a layered Earth is presented. The algorithm uses wide-band measurements of the Earth surface impedance, at low frequencies or at high frequencies. An Earth model which consists of a large number of thin layers is adopted. The layer thickness is taken constant relative to the local skin depth in the low frequency case. In the high frequency case, the time delay through each layer is the constant parameter. The surface reflection coefficient of the adopted model is expressed as a ratio of two polynomials in a normalized frequency parameter. The model parameters are estimated by fitting the surface measurements to the model theoretical response. Results show that the method can predict profiles even in cases of very sharp changes of resistivity. ESA

N87-17199# Dornier-Werke G.m.b.H., Friedrichshafen (West Germany).

NUMERICAL MODELING OF TWO-DIMENSIONAL TIME DOMAIN ELECTROMAGNETIC SCATTERING BY UNDERGROUND INHOMOGENEITIES **c32**

C. C. Lin and K. K. Mei (California Univ., Berkeley) *In* ESA Proceedings of the 1986 International Geoscience and Remote Sensing Symposium (IGARSS '86) on Remote Sensing: Today's Solutions for Tomorrow's Information Needs, Volume 1 Aug. 1986 p 211-216 (For primary document see N87-17163 09-43)

Avail: NTIS HC A99/MF E03; ESA, Paris, France, 3 volume set $90 Member States, AU, CN, and NO (+20% others)

Time domain electromagnetic scattering by elongated subsurface structures was analyzed. The numerical modelings of the responses from two-dimensional inhomogeneities buried in the homogeneous Earth are performed in the presence of an impulsive wave excitation where the spatial width of the pulse is comparable to the target cross-section. The point-matched finite element method enables the direct numerical solution of Maxwell's differential equations in the time domain. The radiation condition at the numerical boundary is satisfied by an extension of the free space radiation boundary condition to the case of lossy layered media. Results for various scatterer properties and configurations are presented. The time histories of the scattered fields along the ground surface are shown. ESA

N87-17200# Tokyo Gas Co. Ltd. (Japan).

DEVELOPMENT OF INTELLIGENT PIPE LOCATOR **c35**

Y. Miyamoto and Y. Wasa (Nippon Electric Co. Ltd., Tokyo, Japan) *In* ESA Proceedings of the 1986 International Geoscience and Remote Sensing Symposium (IGARSS '86) on Remote Sensing: Today's Solutions for Tomorrow's Information Needs, Volume 1 Aug. 1986 p 217-222 (For primary document see N87-17163 09-43)

Avail: NTIS HC A99/MF E03; ESA, Paris, France, 3 volume set $90 Member States, AU, CN, and NO (+20% others)

An inductive pipe locator was developed, so that the position and depth of an underground gas pipe can be accurately located by passing an ac current to the pipe and measuring the generated magnetic field. An ac current (several to 100 kHz) of several tens of mA is transmitted to the underground pipe, and a magnetic sensor above the ground catches the induced magnetic field to estimate the position and depth of the pipe. ESA

N87-17201# Arizona State Univ., Tempe. Dept. of Electrical and Computer Engineering.

GRADIENT METHODS FOR GEOPHYSICAL IMAGE INVERSIONS **c46**

M. S. Frank and C. A. Balanis *In* ESA Proceedings of the 1986 International Geoscience and Remote Sensing Symposium (IGARSS '86) on Remote Sensing: Today's Solutions for Tomorrow's Information Needs, Volume 1 Aug. 1986 p 223-227 (For primary document see N87-17163 09-43)

(Contract DAAG29-85-K-0045)

Avail: NTIS HC A99/MF E03; ESA, Paris, France, 3 volume set $90 Member States, AU, CN, and NO (+20% others)

A conjugate gradient algorithm was adapted to solve the linear equations arising from simulated electromagnetic geophysical data. The reconstruction of a circular cylinder buried in a homogeneous medium was achieved with good results for three of four test cases considered. The conjugate gradient algorithm gives a more accurate reconstruction, compared to the algebraic reconstruction technique, at the cost of additional computation and computer memory requirements. ESA

N87-17202*# Jet Propulsion Lab., California Inst. of Tech., Pasadena.

IMAGING SPECTROMETRY: AIRCRAFT AND SPACE PROGRAM

M. J. Abrams *In* ESA Proceedings of the 1986 International Geoscience and Remote Sensing Symposium (IGARSS '86) on Remote Sensing: Today's Solutions for Tomorrow's Information Needs, Volume 1 Aug. 1986 p 231-234 (For primary document see N87-17163 09-43)
Avail: NTIS HC A99/MF E03; ESA, Paris, France, 3 volume set $90 Member States, AU, CN, and NO (+20% others) CSCL 08B

Imaging spectrometry for the remote sensing of the Earth is introduced. Reflected solar energy from the surface is dispersed in a spectrometer and used to form up to 200 registered spectral images. Each pixel has associated with it sufficient information for the reconstruction of a complete reflectance spectrum. The technique allows the diagnostic narrow band spectral features that are characteristic of many surface materials to be used to identify those materials. These spectral features are typically 20 to 40 nm wide; spectral imaging systems which acquire data in contiguous 10 nm bands therefore have sufficient resolution for direct identification of those materials with diagnostic spectral bands. ESA

N87-17203# Stanford Univ., Calif. Dept. of Applied Earth Science.
A KNOWLEDGE-BASED SOFTWARE ENVIRONMENT FOR THE ANALYSIS OF SPECTRORADIOMETER DATA c60
H. R. Goetting and R. J. P. Lyon *In* ESA Proceedings of the 1986 International Geoscience and Remote Sensing Symposium (IGARSS '86) on Remote Sensing: Today's Solutions for Tomorrow's Information Needs, Volume 1 Aug. 1986 p 235-238 (For primary document see N87-17163 09-43)
Avail: NTIS HC A99/MF E03; ESA, Paris, France, 3 volume set $90 Member States, AU, CN, and NO (+20% others)

A mineral identification expert system for the interpretation of symbolic features extracted from numerical data by sequential heuristic classification is described. Solutions for a given classification become data for the next classification step. In this way the expert system is used to merge numerical data with (symbolic) knowledge. The prototype expert system distinguishes between various spectral features in mineral samples by interpreting waveforms from a spectroradiometer. ESA

N87-17204*# Jet Propulsion Lab., California Inst. of Tech., Pasadena.
ANALYSIS OF AIS RADIOMETRY AT MONO LAKE, CALIFORNIA
J. E. Conel, S. L. Adams, R. E. Alley, G. L. Hoover, and S. Schultz *In* ESA Proceedings of the 1986 International Geoscience and Remote Sensing Symposium (IGARSS '86) on Remote Sensing: Today's Solutions for Tomorrow's Information Needs, Volume 1 Aug. 1986 p 239-244 (For primary document see N87-17163 09-43)
Avail: NTIS HC A99/MF E03; ESA, Paris, France, 3 volume set $90 Member States, AU, CN, and NO (+20% others) CSCL 08B

Airborne imaging spectrometer (AIS) data were studied to establish absolute instrumental calibration and to provide atmospheric corrections. Good agreement is found between calculated and measured radiances for uniform surface targets (beaches), but simulations of atmospheric properties with LOWTRAN lead to unreasonably low values of atmospheric precipitable water. Absorptions from CO2 are not detected in the AIS data, but are strongly present in the LOWTRAN model. The apparent low contrast of all atmospheric absorption bands leads to a study of contamination from overlapping spectral orders in the AIS data. The suspected contamination is shown unambiguously to be present beyond 1500 nm. The magnitude remains uncertain. Spectral band filling at 1400 nm cannot be accounted for by order mixing because of the 800 nm blocking filter used. Rough corrections for short wavelength mode observations might be possible if an after-the-fact radiometric calibration of the instrument can be developed. ESA

N87-17205*# Operations Research, Inc., Rockville, Md.
THE SEQUENTIAL FILTER IMAGING RADIOMETER (SFIR), A NEW INSTRUMENT CONFIGURATION FOR EARTH OBSERVATIONS c19
M. S. Maxwell *In* ESA Proceedings of the 1986 International Geoscience and Remote Sensing Symposium (IGARSS '86) on Remote Sensing: Today's Solutions for Tomorrow's Information Needs, Volume 1 Aug. 1986 p 245-250 (For primary document see N87-17163 09-43)
(Contract NAS5-28057)
Avail: NTIS HC A99/MF E03; ESA, Paris, France, 3 volume set $90 Member States, AU, CN, and NO (+20% others) CSCL 14B

The sequential filter imaging radiometer (SFIR) concept is presented, contrasted with other sensor configurations, and its strengths and weaknesses discussed. In a pushbroom SFIR the optics images the scene onto a long, narrow area array. The length of the array defines the field of view. The spectral defining filters are sequentially placed over the full array, a sample of data for that band taken, and then the next filter placed in front of the array. All of the filters are placed over the array in the time that it takes the image of the scene to advance the array width. Thus the entire scene is observed in each band. Advantages of the SFIR are: spectral bands can be broad, narrow or overlap; it is easy to improve signal to noise ratio; and it is simple to make bands polarized. Its main disadvantage is that it requires more detectors than other instrument configurations. ESA

N87-17206# Flinders Univ., Bedford Park (Australia). Dept. of Environment and Planning.
THE FRS-68010: A NEW CONCEPT FOR THE ACQUISITION AND ANALYSIS OF NOAA HRPT DATA c14
M. Wegener *In* ESA Proceedings of the 1986 International Geoscience and Remote Sensing Symposium (IGARSS '86) on Remote Sensing: Today's Solutions for Tomorrow's Information Needs, Volume 1 Aug. 1986 p 253-258 (For primary document see N87-17163 09-43)
Avail: NTIS HC A99/MF E03; ESA, Paris, France, 3 volume set $90 Member States, AU, CN, and NO (+20% others)

A concept for a NOAA ground station using an array of yagis instead of tracking antennas is presented. This inexpensive antenna configuration guarantees a sufficient signal to noise ratio for the reliable acquisition of HRPT data of the South Australian coastal waters between 32-36 S and 134-141 E. Data processing is performed by a microprocessor system based on the Motorola 68010. Due to the software being written in C and assembly language, basic image processing operations can be performed in 1 sec. Part of the FRS-68010 is a video display processor storing 4 images of 576 by 448 pixels. The image format is reconfigurable by software yielding up to 64 smaller images which can be represented as a loop movie. ESA

N87-17207# Instituto Nacional de Meteorologia e Geofisica, Lisbon (Portugal).
DIGITAL SATELLITE IMAGERY ACQUISITION AND PROCESSING
R. Almeida, I. Gomes, L. Pessanha, and C. Tavares *In* ESA Proceedings of the 1986 International Geoscience and Remote Sensing Symposium (IGARSS '86) on Remote Sensing: Today's Solutions for Tomorrow's Information Needs, Volume 1 Aug. 1986 p 259-263 (For primary document see N87-17163 09-43)
Avail: NTIS HC A99/MF E03; ESA, Paris, France, 3 volume set $90 Member States, AU, CN, and NO (+20% others)

The equipment and organization of a satellite imagery ground station are described. Research concerning calibration, IR radiance to temperature conversion, normalization of VIS image data, geometric corrections, pseudocolor table generation, image enhancement, and classification is summarized. ESA

N87-17208*# National Aeronautics and Space Administration. Ames Research Center, Moffett Field, Calif.
PORTABLE EDITOR (PEDITOR): A PORTABLE IMAGE PROCESSING SYSTEM
G. Angelici, R. Slye, M. Ozga (Department of Agriculture, Washington, D.C.), and P. Ritter (California Univ., Berkeley.) *In* ESA Proceedings of the 1986 International Geoscience and Remote

Sensing Symposium (IGARSS '86) on Remote Sensing: Today's Solutions for Tomorrow's Information Needs, Volume 1 Aug. 1986 p 265-269 (For primary document see N87-17163 09-43)
Avail: NTIS HC A99/MF E03; ESA, Paris, France, 3 volume set $90 Member States, AU, CN, and NO (+20% others)

The PEDITOR image processing system was created to be readily transferable from one type of computer system to another. While nearly identical in function and operation to its predecessor, EDITOR, PEDITOR employs additional techniques which greatly enhance its portability. These cover system structure and processing. In order to confirm the portability of the software system, two different types of computer systems running greatly differing operating systems were used as target machines. A DEC-20 computer running the TOPS-20 operating system and using a Pascal Compiler was utilized for initial code development. The remaining programmers used a Motorola Corporation 68000-based Forward Technology FT-3000 supermicrocomputer running the UNIX-based XENIX operating system and using the Silicon Valley Software Pascal compiler and the XENIX C compiler for their initial code development. ESA

N87-17209# California Univ., Santa Barbara. Dept. of Geography.
THE IMAGE PROCESSING WORKBENCH - PORTABLE SOFTWARE FOR REMOTE SENSING INSTRUCTION AND RESEARCH c61
J. Frew and J. Dozier *In* ESA Proceedings of the 1986 International Geoscience and Remote Sensing Symposium (IGARSS '86) on Remote Sensing: Today's Solutions for Tomorrow's Information Needs, Volume 1 Aug. 1986 p 271-276 (For primary document see N87-17163 09-43)
Avail: NTIS HC A99/MF E03; ESA, Paris, France, 3 volume set $90 Member States, AU, CN, and NO (+20% others)

The Image Processing Workbench (IPW) UNIX-based image processing software system oriented towards algorithm development and applications prototyping is presented. The IPW user interface has a simple, uniform command syntax, and a single image data format. Most IPW commands have a single input and a single output data stream, and can be sequentially connected using UNIX pipes. The fundamental IPW commands were selected to be of maximum utility in constructing more complicated processing pipelines. The IPW is coded with an emphasis on portability and ease of maintenance. It runs on DEC VAX-11 minicomputers, SUN workstations, and IBM PC/AT microcomputers. ESA

N87-17210# Tohoku Univ., Sendai (Japan). Dept. of Information Engineering.
KNOWLEDGE-BASED AERIAL IMAGE UNDERSTANDING SYSTEMS
T. Matsuyama *In* ESA Proceedings of the 1986 International Geoscience and Remote Sensing Symposium (IGARSS '86) on Remote Sensing: Today's Solutions for Tomorrow's Information Needs, Volume 1 Aug. 1986 p 277-282 (For primary document see N87-17163 09-43)
Avail: NTIS HC A99/MF E03; ESA, Paris, France, 3 volume set $90 Member States, AU, CN, and NO (+20% others)

Application of artificial intelligence techniques to automatic photointerpretation is discussed. Knowledge representation and control structure for aerial image understanding are considered. A model of expert systems for image processing is introduced. This model can be used to develop consultation systems for remote sensing. The importance of the integration of image understanding and geographic information systems is emphasized. ESA

N87-17211# Analytic Sciences Corp., Reading, Mass.
EXTRACTING SURFACE FEATURES IN MULTISPECTRAL IMAGERY
M. J. Carlotto *In* ESA Proceedings of the 1986 International Geoscience and Remote Sensing Symposium (IGARSS '86) on Remote Sensing: Today's Solutions for Tomorrow's Information Needs, Volume 1 Aug. 1986 p 283-288 (For primary document see N87-17163 09-43)
Avail: NTIS HC A99/MF E03; ESA, Paris, France, 3 volume set $90 Member States, AU, CN, and NO (+20% others)

A method for recognizing surface features in multispectral imagery is described. First, the surface material composition (SMC) is inferred using a combination of spectral shape and histogram analysis techniques. A symbolic description is then computed in which each connected area in the SMC map is represented by a node in a graph structure. Surface features are represented by a set of constraints over groupings of connected areas (nodes in the graph structure) in the form of rules. Examples illustrating the extraction of selected surface feature classes from LANDSAT Thematic Mapper imagery are included. ESA

N87-17212*# National Water Research Inst., Burlington (Ontario).
A TWO-SCALE BRAGG SCATTERING MODEL FOR MICROWAVE BACKSCATTER FROM WIND GENERATED WAVES c48
M. A. Donelan and W. J. Pierson, Jr. (City Coll. of the City Univ. of New York.) *In* ESA Proceedings of the 1986 International Geoscience and Remote Sensing Symposium (IGARSS '86) on Remote Sensing: Today's Solutions for Tomorrow's Information Needs, Volume 1 Aug. 1986 p 291-296 (For primary document see N87-17163 09-43)
(Grant NAGw-690)
Avail: NTIS HC A99/MF E03; ESA, Paris, France, 3 volume set $90 Member States, AU, CN, and NO (+20% others) CSCL 08C

A model for the wavenumber spectrum for fully developed seas is derived as a function of the mean wind gradient. The high wavenumber part of the spectrum, which defines the Bragg wavenumbers, is an equilibrium spectrum in balance by a wind forcing term determined by viscous dissipation, which is a strong function of water temperature, and dissipation by breaking and microbreaking. The low wavenumber spectrum, constructed from surface elevation observations of gravity waves, is merged with the high wavenumber spectrum. Parameters are adjusted to fit circle flight data for Ku-band. The full spectrum is used in the two-scale Bragg scattering theory, plus specular reflection, to compute backscatter as a function of wind speed, direction, incidence angle, and water temperature (which determines viscosity) for Ku-band. ESA

N87-17213*# City Coll. of the City Univ. of New York.
VERIFICATION RESULTS FOR A TWO-SCALE MODEL OF MICROWAVE BACKSCATTER FROM THE SEA SURFACE c48
W. J. Pierson, Jr. and M. A. Donelan (National Water Research Inst., Burlington, Ontario) *In* ESA Proceedings of the 1986 International Geoscience and Remote Sensing Symposium (IGARSS '86) on Remote Sensing: Today's Solutions for Tomorrow's Information Needs, Volume 1 Aug. 1986 p 297-302 (For primary document see N87-17163 09-43)
(Grant NAGW-690)
Avail: NTIS HC A99/MF E03; ESA, Paris, France, 3 volume set $90 Member States, AU, CN, and NO (+20% others) CSCL 08C

The backscatter model of Donelan and Pierson (1986) was adjusted to fit Ku-Band at 13.9 GHz. Data from L to Ka-band are used to test the model. In general, there is no power law. When the wind drops below certain threshold speeds there may be no detectable Bragg backscatter. Saturation may occur at high winds. Results from the Seasat-SASS are used to substantiate the predictions of the model. Suggestions for experiments for determining the overall validity of the model are made. ESA

N87-17214# Universite Catholique de Louvain (Belgium). Lab. de Telecommunications et d'Hyperfrequences.
A MODIFIED BOUNDARY PERTURBATION APPROACH TO MICROWAVE SCATTERING AND EMISSION BY THE OCEAN SURFACE c48
A. Guissard, P. Sobieski, and D. Vanhoenacker *In* ESA Proceedings of the 1986 International Geoscience and Remote Sensing Symposium (IGARSS '86) on Remote Sensing: Today's Solutions for Tomorrow's Information Needs, Volume 1 Aug. 1986 p 303-309 (For primary document see N87-17163 09-43)
(Contract ESA-5285/82)

Avail: NTIS HC A99/MF E03; ESA, Paris, France, 3 volume set $90 Member States, AU, CN, and NO (+20% others)

A modified two-scale model for scattering and emissivity calculations for random rough surfaces is proposed. It is based on an approach by Borrows and Brown (1973, 1981) extended to bistatic scattering by lossy dielectric surfaces, and it incorporates modified Fresnel reflection coefficients and a simple correction for multiple scattering effects. This leads to a method that could be both simple and accurate enough for realtime inversion algorithms in microwave remote sensing. The method is shown to be applicable to the ocean surface for light and moderate winds. Examples of backscattering and emissivity results are given. ESA

N87-17215# Physics and Electronics Lab. TNO, The Hague (Netherlands).

C AND Ku-BAND SCATTEROMETER RESULTS FROM THE SCATTMOD INTERNAL WAVE EXPERIMENT c48

D. vanHalsema, A. L. Gray (Canada Centre for Remote Sensing, Ottawa, Ontario) 03(Defence Research Establishment Pacific, Victoria, British Columbia), S. J. Hughes, and B. A. Hughes *In* ESA Proceedings of the 1986 International Geoscience and Remote Sensing Symposium (IGARSS '86) on Remote Sensing: Today's Solutions for Tomorrows's Information Needs, Volume 1 Aug. 1986 p 311-317 Sponsored by a Canadian Defence Research Fellowship (For primary document see N87-17163 09-43)

Avail: NTIS HC A99/MF E03; ESA, Paris, France, 3 volume set $90 Member States, AU, CN, and NO (+20% others)

Microwave backscatter values were obtained every 12.5 m by aircraft for incidence angles between 17 and 53 deg for 10 internal wave groups in Georgia Strait. Simultaneously, surface measurements (wave slopes, surface current, position, wind) were made. Under all conditions encountered during the 6 day experiment, internal-wave-induced backscatter modulations were measured. The magnitude of the modulations depends strongly on the wind speed. At low wind speed (1.5 to 2 m/sec) high contrasts (20 dB) are observed. At intermediate higher wind speed (6 m/sec) the modulations are much smaller (2 dB) and only weakly dependent on incidence angle. The average contrast in the Ku-band is 1 dB larger than in the C-band. When the magnitude of the modulations is plotted against the first order Bragg wavenumber, a distinct discontinuity occurs at the transition point between C and Ku-band. ESA

N87-17216# TRW Space Technology Labs., Redondo Beach, Calif. Fluid Mechanics Dept.

IDENTIFICATION OF THE CONTRIBUTION OF BRAGG SCATTERING AND SPECULAR REFLECTION TO X-BAND MICROWAVE BACKSCATTERING IN AN OCEAN EXPERIMENT c48

D. S. W. Kwoh, B. M. Lake, and H. Rungaldier *In* ESA Proceedings of the 1986 International Geoscience and Remote Sensing Symposium (IGARSS '86) on Remote Sensing: Today's Solutions for Tomorrow's Information Needs, Volume 1 Aug. 1986 p 319-325 Sponsored by DARPA (For primary document see N87-17163 09-43)

Avail: NTIS HC A99/MF E03; ESA, Paris, France, 3 volume set $90 Member States, AU, CN, and NO (+20% others)

A shipboard ocean experiment was carried out to study the significance of specular reflection relative to Bragg scattering in X-band microwave backscattering. The surface slope was measured by a laser slope gage. The modulation of Bragg wave (at X-band) is deduced. A shipboard focused X-band radar measured backscattering at 20 and 40 deg incidence angles. A video system was deployed to detect specular points. Specular reflection is important at 20 deg incidence angle and remains significant at 40 deg under a wide range of conditions. The shipboard radar measures a background modulation which agrees well with the Bragg wave modulation as measured by the slope gage. However, there is an additional source of modulation, highly spiky, which comes from specular reflection. ESA

N87-17217# Kansas Univ. Center for Research, Inc., Lawrence. Radar Systems and Remote Sensing Lab.

TOWER-BASED BROADBAND BACKSCATTERING MEASUREMENTS FROM THE OCEAN SURFACE IN THE NORTH SEA c48

A. H. Chaudry, S. P. Gogineni, and R. K. Moore *In* ESA Proceedings of the 1986 International Geoscience and Remote Sensing Symposium (IGARSS '86) on Remote Sensing: Today's Solutions for Tomorrow's Information Needs, Volume 1 Aug. 1986 p 327-335 (For primary document see N87-17163 09-43)

Avail: NTIS HC A99/MF E03; ESA, Paris, France, 3 volume set $90 Member States, AU, CN, and NO (+20% others)

Broadband radar backscatter measurements were made in the North Sea, from aircraft and from a tower. Vertically and horizontally polarized radar backscattering measurements from the tower at C, X and Ku-bands, for the incidence angle range of 18 to 70 deg, wind speed range of 3 to 25 m/sec, and antenna look directions of upwind, downwind, and crosswind were made. Wind scatterometry and modulation-transfer-function (MTF) results are compared with those obtained from aircraft measurements and previous observations. Tower measurements compare well with the aircraft measurements in contradiction to results that showed higher scattering coefficient for the tower than for the aircraft. The magnitude of the crosswind MTF is higher than that for upwind. Location of the maximum scattering on the long ocean wave is obtained by the phase of the MTF and by the cross correlation lag of the radar power return and the long wave height. ESA

N87-17218# Bulgarian Academy of Science, Sofia. Inst. of Electronics.

SPATIAL DEPENDENCE ON SEA SPIKES c48

D. V. Stoyanov and V. L. Vasilev *In* ESA Proceedings of the 1986 International Geoscience and Remote Sensing Symposium (IGARSS '86) on Remote Sensing: Today's Solutions for Tomorrow's Information Needs, Volume 1 Aug. 1986 p 337-341 (For primary document see N87-17163 09-43)

Avail: NTIS HC A99/MF E03; ESA, Paris, France, 3 volume set $90 Member States, AU, CN, and NO (+20% others)

The spatial dependence of spikes above the threshold at horizontal and circular radar polarizations is investigated. It is shown that the correlation interval of spikes along the wave direction is commensurable to the coherency length of sea motion. The estimated mean number of correlated spikes is two. The shadowing between the coherent wave crests is therefore relatively weak. The shadowing between the different wave packets of the sea motion is more substantial for the spiky structure. A formula for the mean spike density in dependence on the distance, suitable for comparison with the experiment, is given. ESA

N87-17219# Environmental Research Inst. of Michigan, Ann Arbor. Radar Science Lab.

GEOPHYSICS OF THE MARGINAL ICE ZONE FROM SAR c48

R. A. Schuchman, B. A. Burns, C. G. Caruthers, J. D. Lyden, E. Svendsen (Bergen Univ., Norway), O. M. Johannessen, T. Olaussen, and J. A. Johannessen *In* ESA Proceedings of the 1986 International Geoscience and Remote Sensing Symposium (IGARSS '86) on Remote Sensing: Today's Solutions for Tomorrow's Information Needs, Volume 1 Aug. 1986 p 345-351 (For primary document see N87-17163 09-43)

(Contracts N00014-81-C-0295; N00014-83-C-0404)

Avail: NTIS HC A99/MF E03; ESA, Paris, France, 3 volume set $90 Member States, AU, CN, and NO (+20% others)

Marginal Ice Zone (MIZ) sequential high resolution aircraft Synthetic Aperture Radar (SAR) images from a region in the Fram Strait north of 78 N were analyzed. Changes in ice concentration, floe size distribution, and ice edge position, as well as eddy location and floe motion derived from multitemporal SAR images are investigated in terms of ocean surface current, wind fields and the bathymetry of the region. The SAR observations show that the MIZ ice cover is highly variable and exhibits rapid dynamic and thermodynamic responses. At the ice edge, during light to moderate wind conditions, the ice drift mirrors the ocean circulation. Radar derived ice kinematics also provide information on ocean eddies beneath the ice in the interior of the MIZ. ESA

N87-17220*# Environmental Research Inst. of Michigan, Ann Arbor. Radar Science Lab.

MICROWAVE PROPERTIES OF SEA ICE IN THE MARGINAL ICE ZONE c48

R. G. Onstott and R. W. Larson *In* ESA Proceedings of the 1986 International Geoscience and Remote Sensing Symposium (IGARSS '86) on Remote Sensing: Today's Solutions for Tomorrow's Information Needs, Volume 1 Aug. 1986 p 353-356 (For primary document see N87-17163 09-43)

(Grant NAGw-334; Contract N00014-85-K-0200)

Avail: NTIS HC A99/MF E03; ESA, Paris, France, 3 volume set $90 Member States, AU, CN, and NO (+20% others) CSCL 08C

Active microwave properties of summer sea ice were measured. Backscatter data were acquired at frequencies from 1 to 17 GHz, at angles from 0 to 70 deg from vertical, and with like and cross antenna polarizations. Results show that melt-water, snow thickness, snowpack morphology, snow surface roughness, ice surface roughness, and deformation characteristics are the fundamental scene parameters which govern the summer sea ice backscatter response. A thick, wet snow cover dominates the backscatter response and masks any ice sheet features below. However, snow and melt-water are not distributed uniformly and the stage of melt may also be quite variable. These nonuniformities related to ice type are not necessarily well understood and produce unique microwave signature characteristics. ESA

N87-17221# Technical Univ. of Denmark, Lyngby. Inst. of Electromagnetics.

SEA ICE IN THE GREENLAND SEA OBSERVED BY THE NIMBUS-7 SCANNING MULTICHANNEL MICROWAVE RADIOMETER (SMMR) c48

P. Sloth and L. T. Pedersen *In* ESA Proceedings of the 1986 International Geoscience and Remote Sensing Symposium (IGARSS '86) on Remote Sensing: Today's Solutions for Tomorrow's Information Needs, Volume 1 Aug. 1986 p 357-361 Sponsored by the Technical Univ. of Denmark, the Danish Space Research Committee, the Commission for Scientific Research, Greenland, and IBM Denmark (For primary document see N87-17163 09-43)

Avail: NTIS HC A99/MF E03; ESA, Paris, France, 3 volume set $90 Member States, AU, CN, and NO (+20% others)

Using a simple model for the relation between microwave radiances and sea ice concentration, the ice cover in the Greenland Sea was investigated. Analysis of a time series of data from the NIMBUS-7 Scanning Microwave Radiometer suggests a theory for the formation of the ice cover phenomenon Odden, a large tongue of ice in the Greenland Sea. A cellular circulation on the shelf driven by strong winds from the north is proposed as the driving mechanism behind the melting of ice along the shelf slope. ESA

N87-17222# Columbia Univ., Palisades, N.Y. Lamont-Doherty Geological Observatory.

SAR ICE FLOE KINEMATICS AND CORRELATION WITH MESOSCALE OCEANIC STRUCTURE WITHIN THE MARGINAL ICE ZONE c48

T. O. Manley, R. A. Shuchman (Environmental Research Inst. of Michigan, Ann Arbor.), and B. A. Burns *In* ESA Proceeding of the 1986 International Geoscience and Remote Sensing Symposium (IGARSS '86) on Remote Sensing: Today's Solutions for Tomorrow's Information Needs, Volume 1 Aug. 1986 p 363-366 (For primary document see N87-17163 09-43)

(Contracts N00014-85-C-0132; N00014-81-C-0259; N00014-83-C-0404)

Avail: NTIS HC A99/MF E03; ESA, Paris, France, 3 volume set $90 Member States, AU, CN, and NO (+20% others)

Synthetic aperture radar images collected over the same geographic area and over fairly short periods of time were used to prepare ice floe kinematic (floe trajectory) diagrams which show a positive correlation with a subice mesoscale frontal feature. The subice mesoscale feature is confirmed using helicopter-based oceanographic conductivity, temperature, density profiles and neutrally-buoyant sofar drifting floats. ESA

N87-17223# Environmental Research Inst. of Michigan, Ann Arbor.

ANALYSIS OF MULTICHANNEL SAR DATA OF SPITSBERGEN

B. A. Burns, R. Shuchman, C. Matzler (Bern Univ., Switzerland), and J. Dowdeswell (Scott Polar Research Inst., Cambridge, England) *In* ESA Proceedings of the 1986 International Geoscience and Remote Sensing Symposium (IGARSS '86) on Remote Sensing: Today's Solutions for Tomorrow's Information Needs, Volume 1 Aug. 1986 p 367-371 (For primary document see N87-17163 09-43)

Avail: NTIS HC A99/MF E03; ESA, Paris, France, 3 volume set $90 Member States, AU, CN, and NO (+20% others)

Multitemporal aircraft SAR images obtained over Spitsbergen in summer are used to illustrate the application of SAR data to identification and monitoring of features of glaciological interest. Snow cover on bare ground, on glaciers, and on moraines, as well as ice cover on lakes, can be clearly identified. Monitoring the up-glacier retreat of the snowline is also possible. This discrimination is based on relative backscatter signatures, and is shown to depend on the frequency and polarization of the radar wave. Other features such as terminal moraines are discriminated on the basis of topographic expression, which is enhanced with stereo images. ESA

N87-17224# European Space Agency. European Space Research and Technology Center, ESTEC, Noordwijk (Netherlands).

ERS-1 FAST DELIVERY PROCESSING AND PRODUCTS

J. P. Guignard *In its* Proceedings of the 1986 International Geoscience and Remote Sensing Symposium (IGARSS '86) on Remote Sensing: Today's Solutions for Tomorrow's Information Needs, Volume 1 Aug. 1986 p 375-379 (For primary document see N87-17163 09-43)

Avail: NTIS HC A99/MF E03; ESA, Paris, France, 3 volume set $90 Member States, AU, CN, and NO (+20% others)

The ERS-1 satellite SAR image mode and wave mode products, scatterometer products, and altimeter products are listed. Ground station organization and facilities are described. ESA

N87-17225# European Space Agency. European Space Research and Technology Center, ESTEC, Noordwijk (Netherlands).

RESULTS OF THE ESA AIRBORNE C-BAND SCATTEROMETER CAMPAIGNS

E. P. W. Attema, A. E. Long, and A. L. Gray (Canada Centre for Remote Sensing, Ottawa, Ontario) *In its* Proceedings of the 1986 International Geoscience and Remote Sensing Symposium (IGARSS '86) on Remote Sensing: Today's Solutions for Tomorrow's Information Needs, Volume 1 Aug. 1986 p 381-387 (For primary document see N87-17163 09-43)

Avail: NTIS HC A99/MF E03; ESA, Paris, France, 3 volume set $90 Member States, AU, CN, and NO (+20% others)

A V-polarization radar echo model relating the normalized surface scattering cross-section sigma zero to radar beam incidence angle, wind speed, and direction was derived from C-band airborne scatterometer measurements. Simultaneous C-band and Ku-band measurements are presented to compare the estimated ERS-1 performance with the results from the Seasat scatterometer. The comparison reveals significantly larger changes in Ku backscatter than at C-band for the same change in wind speed. For the more important moderate to high wind speed regime, however, the advantage Ku-band data has over C-band decreases and, on the basis of backscatter sensitivity and azimuthal modulation, satisfactory performance can be expected from the ERS-1 wind scatterometer. ESA

N87-17226# Dornier-Werke G.m.b.H., Friedrichshafen (West Germany). ERS-1 Project Team.

QUASI REAL TIME CONVERSION OF ERS-1 SCATTEROMETER RAW DATA TO SIGMA ZERO TRIPLETS

P. Hans, H. Munz, and R. Kremer *In* ESA Proceedings of the 1986 International Geoscience and Remote Sensing Symposium (IGARSS '86) on Remote Sensing: Today's Solutions for Tomorrow's Information Needs, Volume 1 Aug. 1986 p 389-394 (For primary document see N87-17163 09-43)

Avail: NTIS HC A99/MF E03; ESA, Paris, France, 3 volume set

$90 Member States, AU, CN, and NO (+20% others)

The ground processing flow for the conversion of ERS-1 scatterometer wind mode raw data into scattering coefficient triplets is outlined. It will be implemented on a Norsk Data ND 550 connected to an array processor FPS 5305 as part of the fast delivery ground processing station at Kiruna. Processing of scatterometer raw data during a time period after raw data transmission during Kiruna coverage, which corresponds to the raw data generation time, is discussed. In order to meet the requirement with the hardware configuration, orbit time dependent parameters, used in the ground processing chain, are derived from look-up tables generated by a separate software package derived from the Scatterometer System Simulator. ESA

N87-17227# Institut Francais de Recherche pour l'Exploitation de la Mer, Brest (France). Antenné CREO.

ERS-1 WIND SCATTEROMETER: WIND EXTRACTION AND AMBIGUITY REMOVAL c47

A. G. Cavanie and D. Offiler (Meteorological Office, Bracknell, England) *In* ESA Proceedings of the 1986 International Geoscience and Remote Sensing Symposium (IGARSS '86) on Remote Sensing: Today's Solutions for Tomorrow's Information Needs, Volume 1 Aug. 1986 p 395-398 Sponsored by ESA (For primary document see N87-17163 09-43)

Avail: NTIS HC A99/MF E03; ESA, Paris, France, 3 volume set $90 Member States, AU, CN, and NO (+20% others)

Algorithms for the extraction and dealiasing of wind solutions from the ERS-1 scatterometer are presented. They are considerably simplified, compared to Seasat, by the use of data from three antennas. The wind extraction algorithms all achieve wind extraction rms accuracies (assuming the ambiguity can be correctly chosen) of under 1m/sec and 10 deg. The general routines are too slow for fast delivery (FD) processing, but the more specialized algorithms are capable of a much higher throughput. None of the ambiguity removal methods is fully satisfactory and all fail in specific cases: regions of two antenna data, short antenna swath lengths (limited by land or zones of calm), or imperfect knowledge of the sigma-zero relationship to wind vector. For FD processing, a background meteorological wind field has to be a forecast, which itself contains uncertainties. ESA

N87-17228# MacDonald, Dettwiler and Associates Ltd., Richmond (British Columbia).

ERS-1 SYNTHETIC APERTURE RADAR FAST DELIVERY PROCESSOR c32

P. George and J.-P. Guignard (European Space Agency. European Space Research and Technology Center, ESTEC, Noordwijk, Netherlands) *In* ESA Proceedings of the 1986 International Geoscience and Remote Sensing Symposium (IGARSS '86) on Remote Sensing: Today's Solutions for Tomorrow's Information Needs, Volume 1 Aug. 1986 p 399-403 (For primary document see N87-17163 09-43)

Avail: NTIS HC A99/MF E03; ESA, Paris, France, 3 volume set $90 Member States, AU, CN, and NO (+20% others)

The ESA ground station facility at Kiruna, Sweden, responsible for the reception of ERS-1 data and its processing into fast delivery products is presented. Due to its high latitude, Kiruna can receive data from 10 of 14 passes per day, making its processing throughput requirements among the highest in the ERS-1 network. The SAR processor system responsible for part of this product generation is described with the ground station environment. The processor requirements, hardware, and software are considered. ESA

N87-17229# Canada Centre for Remote Sensing, Ottawa (Ontario).

CANADIAN PLANS FOR OPERATIONAL DEMONSTRATIONS OF SATELLITE IMAGING RADAR APPLICATIONS c32

E. Langham, S. Parashar, N. Denyer, L. McNutt, V. R. Slaney, R. Brown, N. Freeman, and T. Mullane (Atmospheric Environment Service, Ottawa, Ontario) *In* ESA Proceedings of the 1986 International Geoscience and Remote Sensing Symposium (IGARSS '86) on Remote Sensing: Today's Solutions for Tomorrow's Information Needs, Volume 1 Aug. 1986 p 405-409 (For primary document see N87-17163 09-43)

Avail: NTIS HC A99/MF E03; ESA, Paris, France, 3 volume set $90 Member States, AU, CN, and NO (+20% others)

Canadian objectives for the utilization of data from ERS-1, particularly SAR image data, for ocean, ice, and land and resources monitoring are presented. The ERS-1 data will allow suitable preparations and readiness of data handling systems and user capability for exploiting data from Canadian RADARSAT satellite. These efforts will receive support from a radar program based on ground-based and airborne scattterometers, airborne SAR, and data processing and analysis systems. ESA

N87-17230# Marconi Co. Ltd., Chelmsford (England).

THE UK ERS DATA CENTRE, AN OFFLINE PROCESSING AND ARCHIVING FACILITY c82

N. J. Veck, P. N. Churchill (Hunting Technical Services Ltd., Borehamwood, England), S. Campbell (Software Sciences Ltd., Farnborough, England), and C. Evans (Smith Associates Ltd., Guildford, England) *In* ESA Proceedings of the 1986 International Geoscience and Remote Sensing Symposium (IGARSS '86) on Remote Sensing: Today's Solutions for Tomorrow's Information Needs, Volume 1 Aug. 1986 p 411-415 Sponsored by RAE (For primary document see N87-17163 09-43)

Avail: NTIS HC A99/MF E03; ESA, Paris, France, 3 volume set $90 Member States, AU, CN, and NO (+20% others)

A facility for the off-line processing and archiving of ERS-1 data is presented. The processing tasks to be performed at the Data Center facility range from the quality checking of raw data to the generation of single pass, single sensor precision products. Substantial user liaison services on a comprehensive research and development facility will be incorporated. The Center will provide a service to users of remotely sensed data by taking raw data from the ERS-1 satellite via Kiruna or the proposed UK receiving station and generating a range of products. Such products will be made available for use by commercial, industrial, academic, and government bodies within the UK and internationally. ESA

N87-17231# Deutsche Forschungs- und Versuchsanstalt fuer Luft- und Raumfahrt, Oberpfaffenhofen (West Germany).

THE GERMAN ERS-1 SAR POSTPROCESSING SYSTEM PLANS AND CONCEPTS c60

G. Schreier and R. Winter *In* ESA Proceedings of the 1986 International Geoscience and Remote Sensing Symposium (iGARSS '86) on Remote Sensing: Today's Solutions for Tomorrow's Information Needs, Volume 1 Aug. 1986 p 417-422 (For primary document see N87-17163 09-43)

Avail: NTIS HC A99/MF E03; ESA, Paris, France, 3 volume set $90 Member States, AU, CN, and NO (+20% others)

Activities to build up an operational high throughput system for the rectification and geocoding of ERS-1 SAR images are described. Problem areas, algorithmic approaches, and design of this geocoding system are outlined, emphasizing a UNIX workstation network concept and adapted image processing software. Proposed products are listed. The best location accuracy of the products is in the range of a pixel diameter. ESA

N87-17232# Centre for Earth Science Studies, Trivandrum (India).

SIGNIFICANCE OF SPACE IMAGE, AIR PHOTO AND DRAINAGE LINEARS IN RELATION TO WEST COAST TECTONICS, INDIA

V. Raghavan and D. Chandrasekharam (Centre for Water Resources Development and Management, Calicut, India) *In* ESA Proceedings of the 1986 International Geoscience and Remote Sensing Symposium (IGARSS '86) on Remote Sensing: Today's Solutions for Tomorrow's Information Needs, Volume 1 Aug. 1986 p 425-429 (For primary document see N87-17163 09-43)

Avail: NTIS HC A99/MF E03; ESA, Paris, France, 3 volume set $90 Member States, AU, CN, and NO (+20% others)

Lineament patterns over northern Kerala along the western continental margin of India (WCMI) were analyzed in conjunction with the structural, geochronological, and geological data to understand the structural and geomorphic evolution of WCMI. The NNW and ENE sets are subparallel to the basic dyke swarms

in the region. Regional structural framework reveals that N-S compressive stresses produced the NNW lineaments whereas the ENE trends represent younger tensional fractures developed due to near E-W compression. These fractures were periodically reactivated. Predominant air photo linears represent joints developed due to neotectonic stresses. Drainage development in the region is structurally controlled. Neotectonism involving vertical upliftment is suggested. ESA

N87-17233# University of North-Eastern Hill, Shillong (India). School of Environmental Sciences.
STRUCTURAL AND GEOMORPHIC EVOLUTION OF MEGHALAYA PLATEAU, INDIA ON LANDSAT IMAGERY
R. K. Rai *In* ESA Proceedings of the 1986 International Geoscience and Remote Sensing Symposium (IGARSS '86) on Remote Sensing: Today's Solutions for Tomorrow's Information Needs, Volume 1 Aug. 1986 p 431-435 (For primary document see N87-17163 09-43)
Avail: NTIS HC A99/MF E03; ESA, Paris, France, 3 volume set $90 Member States, AU, CN, and NO (+20% others)

The remote areas of North East Region of India were studied by LANDSAT imagery to analyze geological, structural, and geomorphological characteristics. The potential of LANDSAT imagery for structural and geomorphic evolution studies of Meghalaya Plateau is shown. Results indicate that rivers adapted their courses to regional structure and lineaments. All the major lineaments run in SW-NE direction. Field evidence such as deep gorges, wateralls, river terraces, and breaks in slopes indicate that the plateau presents multicyclic surfaces at different altitudes. ESA

N87-17234# Karlsruhe Univ. (West Germany). Inst. fuer Photogrammetrie und Topographie.
HYDROGEOLOGICAL RESEARCH IN PELOPONNESUS (GREECE) KARST AREA BY SUPPORT AND COMPLETION OF LANDSAT-THEMATIC DATA
H. Kaufmann, B. Reichart, and H. Hoetzl *In* ESA Proceedings of the 1986 International Geoscience and Remote Sensing Symposium (IGARSS '86) on Remote Sensing: Today's Solutions for Tomorrow's Information Needs, Volume 1 Aug. 1986 p 437-441 (For primary document see N87-17163 09-43)
Avail: NTIS HC A99/MF E03; ESA, Paris, France, 3 volume set $90 Member States, AU, CN, and NO (+20% others)

Karst drainage from Pelopennesian catchment areas to springs at the coast, and possible pathways to win the fresh water before its submarine discharge were investigated, using high resolution satellite data to support and complement hydrogeological research. The derived fracture pattern, separated into strike-slip faults and joints by field check, and combined with known karst cavities and tracer experiments, gives results for possible underground pathways of the water. By use of a special band combination of the reflective data, the recharge area is subdivided into several categories. Several submarine springs near the coast are detected by the thermal band of the LANDSAT Thematic Mapper. ESA

N87-17235# Centre for Earth Science Studies, Trivandrum (India).
COMPUTER-AIDED ANALYSIS OF LANDSAT DATA FOR MAPPING GEOLOGIC AND GEOMORPHIC FEATURES, NORTH BOMBAY, INDIA
V. Raghavan, S. M. Tarique (Aligarh Muslim Univ., India), and A. T. PedroFernandes (Directorate of Mines and Industries, Panjim, India) *In* ESA Proceedings of the 1986 International Geoscience and Remote Sensing Symposium (IGARSS '86) on Remote Sensing: Today's Solutions for Tomorrow's Information Needs, Volume 1 Aug. 1986 p 443-447 (For primary document see N87-17163 09-43)
Avail: NTIS HC A99/MF E03; ESA, Paris, France, 3 volume set $90 Member States, AU, CN, and NO (+20% others)

Geologic and geomorphic information extraction from remotely sensed data using visual and computer aided techniques were attempted for a test area in North Bombay. Visual interpretations of LANDSAT images offer a limited possibility to demarcate terrain units. Computer aided analysis discriminates nine distinct spectral classes that correpond to various geomorphic/geologic units in the area. A combination of visual and computer aided techniques in addition to field data enables the preparation of thematic maps. ESA

N87-17236# Geological Survey of India, Jaipur. Photogeology and Remote Sensing Div.
COMPARATIVE STUDY OF LANDSAT MSS, SALYUT-7 (TERRA) AND RADAR (SIR-A) IMAGES FOR GEOLOGICAL AND GEOMORPHOLOGICAL APPLICATIONS: A CASE STUDY FROM RAJASTHAN AND GUJARAT, INDIA
P. C. Bakliwal *In* ESA Proceedings of the 1986 International Geoscience and Remote Sensing Symposium (IGARSS '86) on Remote Sensing: Today's Solutions for Tomorrow's Information Needs, Volume 1 Aug. 1986 p 449-452 (For primary document see N87-17163 09-43)
Avail: NTIS HC A99/MF E03; ESA, Paris, France, 3 volume set $90 Member States, AU, CN, and NO (+20% others)

Rajasthan and Gujarat provinces of India were surveyed using the MKF-6 multispectral and KATE-140 stereo space photographs collected during TERRA experiment and SIR-A radar data acquired during the flight of Columbia Space Shuttle on Nov. 12, 1981. A comparative evaluation of these data for geological applications indicates that lithological discrimination is possible from SIR-A due to differential surface roughness and from KATE-140 due to stereo vision. Structural elements on SIR-A and KATE-140 are better interpreted. Radar data is most suitable for different surface covers and thus provides better details for geomorphic mapping. It is also found that MKF-6 and LANDSAT MSS data provide better data on geomorphology in decreasing order; KATE-140 provides altitude variations and is, therefore, most helpful in pediplain areas. ESA

N87-17237# Freiburg Univ. (West Germany). Inst. of Geography.
RADAR IMAGERY OF THE EUROPEAN CITY INFLUENCED BY VARIATIONS IN DEPRESSION ANGLE AND LOOK DIRECTION **c32**
W. Geile *In* ESA Proceedings of the 1986 International Geoscience and Remote Sensing Symposium (IGARSS '86) on Remote Sensing: Today's Solutions for Tomorrow's Information Needs, Volume 1 Aug. 1986 p 455-461 (For primary document see N87-17163 09-43)
Avail: NTIS HC A99/MF E03; ESA, Paris, France, 3 volume set $90 Member States, AU, CN, and NO (+20% others)

By means of depression angle and look direction as variables in optically processed X-band SAR images, the different building structures of the heterogeneously composed architecture of a city were differentiated by visual image analysis. The shape of the individual radar returns and the texture of the spaces between returns served as interpretation criteria. The signal pattern changed with alternations of look direction, in a way specific for each type of building structure. By superimposing a negative and a positive transparency of the same image, a pseudo-stereo-effect was achieved to filter sharply bordered returns, and thus saperate strong building signatures and eliminate possible confusion from weak and unsharp targets. ESA

N87-17238# Florence Univ. (Italy). Dipt. di Ingegneria Elettronica.
MULTISPECTRAL CLASSIFICATION OF MICROWAVE REMOTE SENSING IMAGES
G. Benelli, V. Cappellini, E. DelRe, and L. Nigro *In* ESA Proceedings of the 1986 International Geoscience and Remote Sensing Symposium (IGARSS '86) on Remote Sensing: Today's Solutions for Tomorrow's Information Needs, Volume 1 Aug. 1986 p 463-466 (For primary document see N87-17163 09-43)
Avail: NTIS HC A99/MF E03; ESA, Paris, France, 3 volume set $90 Member States, AU, CN, and NO (+20% others)

Methods for the automatic classification and discrimination of crops are described. Microwave images in bands X and C collected during the European SAR 580 compaign are used. One and two dimensional classification algorithms using Bayes rule or the block

distance are analysed. The probability of correct classification for different crops is presented. ESA

N87-17239# Vexcell Corp., Boulder, Colo.
USING SECONDARY IMAGE PRODUCTS TO AID IN UNDERSTANDING AND INTERPRETATION OF RADAR IMAGERY **c32**

G. Domik and F. Leberl *In* ESA Proceedings of the 1986 International Geoscience and Remote Sensing Symposium (IGARSS '86) on Remote Sensing: Today's Solutions for Tomorrow's Information Needs, Volume 1 Aug. 1986 p 467-468 Sponsored by ESA (For primary document see N87-17163 09-43)
Avail: NTIS HC A99/MF E03; ESA, Paris, France, 3 volume set $90 Member States, AU, CN, and NO (+20% others)

Radar grammetric exploitation of radar images as single images, stereo pairs, images combined with collateral data to from multisensor data sets, and as time series was reviewed. Secondary image products (ortho images, stereo ortho images, slope-effect reduced images, simulated radar images, and false color presentations using image products and synergetic data sets) were designed to satisfy the needs to analyze, predict, and extract information from radar images by bringing the original image closer to the investigator. ESA

N87-17240# Kansas Univ. Center for Research, Inc., Lawrence. Radar Systems and Remote Sensing Lab.
DETERMINING THE VERTICAL PATTERN OF A SPACEBORNE SAR BY OBSERVATION OF UNIFORM TARGETS

R. K. Moore, V. S. Frost, H. Westmoreland, D. Frank, and M. Hemmat *In* ESA Proceedings of the 1986 International Geoscience and Remote Sensing Symposium (IGARSS '86) on Remote Sensing: Today's Solutions for Tomorrow's Information Needs, Volume 1 Aug. 1986 p 469-472 (For primary document see N87-17163 09-43)
Avail: NTIS HC A99/MF E03; ESA, Paris, France, 3 volume set $90 Member States, AU, CN, and NO (+20% others)

Pattern measurements were made for SIR-B antenna while it was in space by use of ground receivers. The measurements were supplemented by using the radar signal returned from large homogeneous areas of the surface. Results indicate that the beam is slightly wider than the theoretical pattern used in producing the corrected images, but final conclusions await receipt of more uncorrected data tapes. ESA

N87-17241# Arkansas Univ., Fayetteville.
INTERFEROMETER APPLICATIONS FOR THE RECTIFICATION OF RADAR IMAGES **c32**

J. F. Hug, V. H. Kaupp, W. P. Waite, and H. C. MacDonald *In* ESA Proceedings of the 1986 International Geoscience and Remote Sensing Symposium (IGARSS '86) on Remote Sensing: Today's Solutions for Tomorrow's Information Needs, Volume 1 Aug. 1986 p 473-477 (For primary document see N87-17163 09-43)
Avail: NTIS HC A99/MF E03; ESA, Paris, France, 3 volume set $90 Member States, AU, CN, and NO (+20% others)

Information contained in radar interferometric signals was used to estimate the height of terrain points and to perform a point-by-point rectification of the image. The algorithm requires no human intervention and is not computationally intensive. The approach also produces topographic data which could be useful for purposes other than image rectification. In virtually all of the instances tested, excellent results are obtained by at least one combination of system parameters. In every instance where the rectification algorithm performs poorly, the problem is directly attributable to a misestimate of the integer number of wavelengths in the path difference (N). Since a very simple approach was used to estimate N, considerable improvements could be made without greatly increasing the complexity of the process. ESA

N87-17242# Stanford Univ., Calif. Dept. of Applied Sciences.
INTERRELATIONSHIP BETWEEN FIELD SPECTRA AND AIRBORNE MSS SYSTEMS IN THE SINGATSE RANGE, (YERINGTON) NEVADA

R. J. P. Lyon *In* ESA Proceedings of the 1986 International Geoscience and Remote Sensing Symposium (IGARSS '86) on Remote Sensing: Today's Solutions for Tomorrow's Information Needs, Volume 1 Aug. 1986 p 481-484 (For primary document see N87-17163 09-43)
Avail: NTIS HC A99/MF E03; ESA, Paris, France, 3 volume set $90 Member States, AU, CN, and NO (+20% others)

Two stages of Singatse Range (Nevada) classical hydrothermal alterations of the felsic rock minerals to clays and other hydrous-bearing materials were mapped: early hypogene were associated with the Jurassic porphyry dike intrusion, and later geothermal (Jurassic/Cretaceous), associated with the circulation of meteoritic waters beneath the cogenetic volcanic pile. The whole rock mass of the Singatse Range was rotated 70 degW, so that what was once vertical is now flat-lying exposed over the 6Km of outcrop trending 290 deg (ESE-WNW) across the range. Due to the long thin nature of the economically-interesting target (hydrothermal alteration) aircraft flights were flown as parallel lines with this 290 deg trend. Spectral absorptions due to clay minerals in the hydrothermally-altered rocks can be seen readily in band-ratio imagery, from LANDSAT TM, TMS, and AIS digital data sets. Comparable spectral evidence can be seen in data from repeated flights over the same terrain, ground spectral measurements confirm the types of O-H bearing minerals seen in the flight data. ESA

N87-17243# Consiglio Nazionale delle Ricerche, Frascati (Italy). Ist. Astrofisica.
INTEGRATED ANALYSIS OF GEOLOGICAL AND REMOTE SENSING DATA AIMED AT MINERAL DEPOSITS DETECTION IN THE MONAPO AREA (NORTHERN MOZAMBIQUE)

M. Poscolieri, M. Lorenzini, G. Onorati, and S. Salvi *In* ESA Proceedings of the 1986 International Geoscience and Remote Sensing Symposium (IGARSS '86) on Remote Sensing: Today's Solutions for Tomorrow's Information Needs, Volume 1 Aug. 1986 p 485-490 (For primary document see N87-17163 09-43)
Avail: NTIS HC A99/MF E03; ESA, Paris, France, 3 volume set $90 Member States, AU, CN, and NO (+20% others)

Geophysical, geological, geomorphological, and LANDSAT spectral data, concerning the Monapo Klippe area (Northern Mozambique) were retrieved for ore bodies research. Variables were analyzed through an approach that allows the user to integrate different sources of digital data and to infer the relationships among them, using display, mapping, and statistical analysis. On the basis of the interpretation of the relationships among multisource data, geological strutures indicating mineral interest zones were sought. The importance of circular structures and lineaments swarms for the emplacement of pegmatites and mineralized bodies was assessed. A hypothesis concerning mutual relationships among late Precambrian tectonic episodes was formulated for the study area. ESA

N87-17244# Stockholm Univ. (Sweden). Dept. of Physical Geography.
A STATISTICAL APPROACH TO SELECT THE OPTIMAL WAVELENGTH BANDS FOR SEPARATING ROCKS IN THE WAVELENGTH REGION 0.4 TO 2.3 MICRONS

K. Wester and B. Lunden *In* ESA Proceedings of the 1986 International Geoscience and Remote Sensing Symposium (IGARSS '86) on Remote Sensing: Today's Solutions for Tomorrow's Information Needs, Volume 1 Aug. 1986 p 491-494 (For primary document see N87-17163 09-43)
Avail: NTIS HC A99/MF E03; ESA, Paris, France, 3 volume set $90 Member States, AU, CN, and NO (+20% others)

The use of laboratory measured spectral signatures for separation of rock types is considered. Spectral reflectances of different rock types (acid, semiacid, and basic) were measured in the laboratory using a reflectometer. The laboratory measured spectra provide a useful basis for determining the separability and the best wavelength regions for discrimination of the rock types. For the analysis, eight bands were used, LANSAT Thematic Mapper bands plus two more bands in the near infrared. The used algorithm, a discriminant analysis for computer based comparisons of the

different rock types, is described. The spectral signatures, the ranking for the best bands, combinations of bands, and the classification accuracy are discussed. ESA

N87-17245# Arkansas Univ., Fayetteville. Dept. of Electrical Engineering.

HAWAIIAN LAVA FLOWS AND SIR-B RESULTS c46

B. A. Derryberry, W. P. Waite, V. H. Kaupp, H. C. MacDonald, L. R. Gaddis (Hawaii Inst. of Geophysics, Honolulu.), and P. Mouginis-Mark *In* ESA Proceedings of the 1986 International Geoscience and Remote Sensing Symposium (IGARSS '86) on Remote Sensing: Today's Solutions for Tomorrow's Information Needs, Volume 1 Aug. 1986 p 497-501 (For primary document see N87-17163 09-43)

Avail: NTIS HC A99/MF E03; ESA, Paris, France, 3 volume set $90 Member States, AU, CN, and NO (+20% others)

Analysis of SIR-B data is applied to the estimation of sigma zero for basaltic lava flows, the sea, and tropical rain forest. Aerial photo data, ground truth observations, and surface roughness measurements are included. Empirical and theoretical electromagnetic scattering models for sigma zero are considered, allowing that the radar return may not be limited to a simple surface scattering problem. A relative calibration model for the SIR-B data based upon ancillary information about the sea state around Hawaii is proposed. ESA

N87-17246*# Dartmouth Coll., Hanover, N.H. Dept. of Earth Sciences.

DISCRIMINATION OF LITHOLOGIC UNITS USING GEOBOTANICAL AND LANDSAT TM SPECTRAL DATA

R. W. Birnie and N. J. DeFeo *In* ESA Proceedings of the 1986 International Geoscience and Remote Sensing Symposium (IGARSS '86) on Remote Sensing: Today's Solutions for Tomorrow's Information Needs, Volume 1 Aug. 1986 p 503-506 (For primary document see N87-17163 09-43)

(Contracts NASw-4049; JPL-956937)

Avail: NTIS HC A99/MF E03; ESA, Paris, France, 3 volume set $90 Member States, AU, CN, and NO (+20% others) CSCL 08B

Thematic Mapper (TM) spectral data were correlated with lithologic units, geobotanical forest associations, and geomorphic site parameters in the Ridge and Valley Province of Pennsylvania. Both the TM and forest association data can be divided into four groups based on their lithology (sandstone or shale) and geomorphic aspect (north or south facing). In this clastic sedimentary terrane, geobotanical associations are useful indicators of lithology and these different geobotanical associations are detectable in LANDSAT TM data. ESA

N87-17247# Karlsruhe Univ. (West Germany). Inst. fuer Photogrammetrie und Topographie.

RESULTS OF TECTONIC AND SPECTRAL INVESTIGATIONS ALONG THE WADI ARABA FAULT IN JORDAN USING SPECIAL PROCESSED THEMATIC MAPPING (TM) DATA

H. Kaufman *In* ESA Proceedings of the 1986 International Geoscience and Remote Sensing Symposium (IGARSS '86) on Remote Sensing: Today's Solutions for Tomorrow's Information Needs, Volume 1 Aug. 1986 p 507-512 (For primary document see N87-17163 09-43)

Avail: NTIS HC A99/MF E03; ESA, Paris, France, 3 volume set $90 Member States, AU, CN, and NO (+20% others)

Tectonic and lithological investigations carried out in the Wadi Araba-Jordan graben area were supported by use of LANDSAT/Thematic Mapper data. A processing concept was developed to satisfy the requirements for several user groups. Use of the data sets to complete supraregional tectonic research is discussed. The applicability of the processed data for registration of hydrothermal alteration minerals is demonstrated. The detection of an Fe-deposit is illustrated. ESA

N87-17248# Geological Survey of Canada, Ottawa (Ontario). Mineral Resources Div.

INTEGRATION OF SURFICIAL GEOCHEMISTRY AND LANDSAT IMAGERY TO DISCOVER SKARN TUNGSTEN DEPOSITS USING IMAGE ANALYSIS TECHNIQUES

S. Aranoff (Dipix Systems Ltd., Ottawa, Ontario), W. Goodfellow, G. F. Bonham-Carter, and D. J. Ellwood *In* ESA Proceedings of the 1986 International Geoscience and Remote Sensing Symposium (IGARSS '86) on Remote Sensing: Todays Solutions for Tomorrow's Information Needs, Volume 1 Aug. 1986 p 513-520 (For primary document see N87-17163 09-43)

(Contrib-19586) Avail: NTIS HC A99/MF E03; ESA, Paris, France, 3 volume set $90 Member States, AU, CN, and NO (+20% others)

A deposit model, LANDSAT imagery, and surficial geochemistry were used to develop a procedure for locating tungsten mineralization associated with shallowly buried intrusions. Image analysis techniques were used to develop a co-occurrence index, which was used to identify promising exploration targets. ESA

N87-17249# Kanazawa Inst. of Tech. (Japan).

BITEMPORAL ANALYSIS OF THEMATIC MAPPER DATA FOR LAND COVER CLASSIFICATION

S. Ueno, T. Kusaka, and Y. Kawata *In* ESA Proceedings of the 1986 International Geoscience and Remote Sensing Symposium (IGARSS '86) on Remote Sensing: Today's Solutions for Tomorrow's Information Needs, Volume 1 Aug. 1986 p 523-528 (For primary document see N87-17163 09-43)

(Grant Jap-Min-of-Ed-60129032)

Avail: NTIS HC A99/MF E03; ESA, Paris, France, 3 volume set $90 Member States, AU, CN, and NO (+20% others)

Time-sequential analysis of LANDSAT-5 Thematic Mapper (TM) data was performed for diverse land-cover types in Kanazawa area, Takayama district, Japan. The subscene of TM data in the study site covering 800x800 pixels of 25 m span was extracted from the full scene data. After preprocessing, the gray levels in TM data were classified by the Gaussian Maximum Likelihood classifier, allowing for feature selection. The classification procedure was compared for two seasons, i.e., August and October, in terms of the atmospheric reflectance, and the statistical quantities of the gray levels. Results show that atmospheric reflectance is effective for the bitemporal analysis of TM data for land cover classification. ESA

N87-17250# Cranfield Inst. of Tech., Bedford (England). Silsoe Coll.

THE INFLUENCE OF RESAMPLING METHOD AND MULTITEMPORAL LANDSAT IMAGERY ON CROP CLASSIFICATION ACCURACY IN THE UNITED KINGDOM

A. S. Belward and J. C. Taylor *In* ESA Proceedings of the 1986 International Geoscience and Remote Sensing Symposium (IGARSS '86) on Remote Sensing: Today's Solutions for Tomorrow's Information Needs, Volume 1 Aug. 1986 p 529-534 (For primary document see N87-17163 09-43)

Avail: NTIS HC A99/MF E03; ESA, Paris, France, 3 volume set $90 Member States, AU, CN, and NO (+20% others)

Six sequential LANDSAT MSS scenes for a test site were geometrically corrected. Resampling to 50m pixel size was carried out with bilinear interpolation and nearest neighbor. Spectral coincident plots and decision boundaries were used for feature selection, and supervised maximum likelihood classification used for crop classification. Bilinear interpolation gives a mean increase in classification accuracy of 1.95% over nearest neighbor. Multitemporal data give better overall classification accuracies than single date images. A spring/early summer combination gives a mean classification purity of 70%, a 6% increase over the best single date classification from May, and 46% better than the worst from February. ESA

N87-17251# IBM Japan. Tokyo Scientific Center.

EVALUATION OF LANDSAT 5 THEMATIC MAPPING (TM) DATA FOR IMAGE CLUSTERING AND CLASSIFICATION

M. Ioka and M. Koda *In* ESA Proceedings of the 1986 International Geoscience and Remote Sensing Symposium (IGARSS '86) on Remote Sensing: Today's Solutions for Tomorrow's Information Needs, Volume 1 Aug. 1986 p 535-540 (For primary document see N87-17163 09-43)

Avail: NTIS HC A99/MF E03; ESA, Paris, France, 3 volume set $90 Member States, AU, CN, and NO (+20% others)

Analysis and evaluation on the quality of the LANDSAT-5 Thematic Mapper (TM) data for multisprectral image clustering and classification are performed. Data used is the TM test data of Tokyo metropolitan area (Path-107; Row-035) dated November 4, 1984. Map-precision geometric correction is performed and the TM data are resampled to 30 m pixel spacing. Statistical characteristics of seven TM bands are analyzed, then information content is evaluated based on the clustering and supervised image classification. For routine land-cover classification, a concept of training data file is proposed and generated to assure the stability of the classification processes. The results are quantitatively compared with the ground truth data with 10 m spatial accuracy. Results confirm that the classification accuracy can be increased with the improvement of ground resolution of the satellite image data in general. ESA

N87-17252# Norwegian Computing Center, Oslo (Norway).
A SIMULATION STUDY OF SOME CONTEXTUAL CLASSIFICATION METHODS FOR REMOTELY SENSED DATA
N. L. Hjort, E. Mohn, and G. Storvik *In* ESA Proceedings of the 1986 International Geoscience and Remote Sensing Symposium (IGARSS '86) on Remote Sensing: Today's Solutions for Tomorrow's Information Needs, Volume 1 Aug. 1986 p 541-545 (For primary document see N87-17163 09-43)
Avail: NTIS HC A99/MF E03; ESA, Paris, France, 3 volume set $90 Member States, AU, CN, and NO (+20% others)

Methods for contextual classification of multispectral scanner data using ordinary noncontextual rules based on transformed data; classification based on stochastic models for the classes over the scene and for the vectors given the classes; and simultaneous classification of all pixels, using, e.g., Markov random field models, were compared via Monte Carlo simulation. Contextual methods usually reduce the error rates considerably compared to noncontextual rules. Strong spatial dependency in the noise term of the data increases the error rate of contextual methods, but not so much for methods designed to handle this difficulty. Contextual methods seen to work particularly well in homogeneous areas and on borders with a simple structure. ESA

N87-17253# Centre d'Etude Spatiale des Rayonnements, Toulouse (France).
A NONPARAMETRIC SUPERVISED MULTISPRECTRAL CLASSIFICATION METHOD USING BINARY MORPHOLOGICAL OPERATORS
J. P. Madier, G. Flouzat, and M. Jourlin (Laboratoire Traitement du Signal et Instrumentation, Saint-Etienne, France) *In* ESA Proceedings of the 1986 International Geoscience and Remote Sensing Symposium (IGARSS '86) on Remote Sensing: Todays's Solutions for Tomorrow's Information Needs, Volume 1 Aug. 1986 p 547-552 (For primary document see N87-17163 09-43)
Avail: NTIS HC A99/MF E03; ESA, Paris, France, 3 volume set $90 Member States, AU, CN, and NO (+20% others)

Binary mathematical morphology was applied to a nonparametric supervised segmentation method in a 2-D pattern space. The method is divided into modeling of clusters hulls of maining samples; hull superposition and overlapping region processing; and 2-D pattern space partition. Remote sensing image classification is presented as an application of this method. ESA

N87-17254# Centre d'Etude Spatiale des Rayonnements, Toulouse (France).
SEGMENTATION BY MATHEMATICAL MORPHOLOGY PROCESSING HAND ON THE IMAGE UNDERSTANDING MODEL IN REMOTE SENSING
P. Bousquet and G. Flouzat *In* ESA Proceedings of the 1986 International Geoscience and Remote Sensing Symposium (IGARSS '86) on Remote Sensing: Today's Solutions for Tomorrow's Information Needs, Volume 1 Aug. 1986 p 553-557 (For primary document see N87-17163 09-43)
Avail: NTIS HC A99/MF E03; ESA, Paris, France, 3 volume set $90 Member States, AU, CN, and NO (+20% others)

Image segmentation based on edge detection using geometrical operators of mathematical morphology is outlined. The process consists of improvement of the image by extraction of the textured regions and by filtering of the untextured regions; edge element extraction by gradient operator using local maximum and local minimum; thinning, and false edge element elimination and gap closing. ESA

N87-17255# Analytic Sciences Corp., Reading, Mass.
A SYNERGISTIC APPROACH FOR MULTISPECTRAL IMAGE RESTORATION USING REFERENCE IMAGERY
V. T. Tom *In* ESA Proceedings of the 1986 International Geoscience and Remote Sensing Symposium (IGARSS '86) on Remote Sensing: Today's Solutions for Tomorrow's Information Needs, Volume 1 Aug. 1986 p 559-564 (For primary document see N87-17163 09-43)
Avail: NTIS HC A99/MF E03; ESA, Paris, France, 3 volume set $90 Member States, AU, CN, and NO (+20% others)

A synergistic image restoration approach, based on a local multichannel least-squares (LS) modeling technique, is demonstrated on multispectral satellite imagery. This approach differs from more traditional global enhancement techniques by effectively exploiting the local correlation properties of multispectral imagery in order to spatially enhance or reduce noise in individual component images. The LS technique optimally estimates the input image using other spectral bands or image sources as local reference data. The procedure is applied to spatially enhance LANDSAT-D MSS and SPOT multispectral data and to reduce noise levels in LANDSAT-D TM data. ESA

N87-17256# Dornier-Werke G.m.b.H., Friedrichshafen (West Germany).
RECENT PROGRESS IN ERS-1 WIND SCATTEROMETER DESIGN **c35**
R. W. Zahn, D. Miller, A. Koppe, C. C. Lin (Marconi Space and Defence Systems Ltd., Portsmouth, England), and D. J. Carter *In* ESA Proceedings of the 1986 International Geoscience and Renote Sensing Symposium (IGARSS '86) on Remote Sensing: Today's Solutions for Tomorrow's Information Needs, Volume 1 Aug. 1986 p 567-572 (For primary document see N87-17163 09-43)
Avail: NTIS HC A99/MF E03; ESA, Paris, France, 3 volume set $90 Member States, AU, CN, and NO (+20% others)

A model to determine the ERS-1 scatterometer impulse response function and modulation transfer function is presented. These two-dimensional functions are the basis for further calculations of the system properties. System design aspects for the scatterometer are discussed, using results from the simulation model. Although simplifications are introduced, the design model is a valuable tool to support the scatterometer design. ESA

N87-17257# Dornier-Werke G.m.b.H., Friedrichshafen (West Germany).
THE ERS-1 SCATTEROMETER SYSTEM SIMULATOR AND ITS RELEVANCE FOR GROUND PROCESSING DESIGN **c35**
H. Munz and P. Hans *In* ESA Proceedings of the 1986 International Geoscience and Remote Sensing Symposium (IGARSS '86) on Remote Sensing: Today's Solutions for Tomorrow's Information Needs, Volume 1 Aug. 1986 p 573-577 (For primary document see N87-17163 09-43)
Avail: NTIS HC A99/MF E03; ESA, Paris, France, 3 volume set $90 Member States, AU, CN, and NO (+20% others)

Simulation capability, models for principal system components, and basic software structure of the ERS-1 Wind Scatterometer System Simulator (SSS) are outlined. Its use for ground processing design and ground segment development is described. Relevance of various parts of the SSS software package for the operational Active Microwave Instrument Wind Scaterometer System is discussed. ESA

N87-17258*# Jet Propulsion Lab., California Inst. of Tech., Pasadena.
ROUNDOFF NOISE ANALYSIS FOR DIGITAL DOPPLER PROCESSORS IN RADAR SCATTEROMETERS **c32**

Chong-Yung Chi, D. Long, and K. Li Fuk *In* ESA Proceedings of the 1986 International Geoscience and Remote Sensing Symposium (IGARSS '86) on Remote Sensing: Today's Solutions for Tomorrow's Information Needs, Volume 1 Aug. 1986 p 579-584 (For primary document see N87-17163 09-43)
Avail: NTIS HC A99/MF E03; ESA, Paris, France, 3 volume set $90 Member States, AU, CN, and NO (+20% others) CSCL 17I

The noise due to finite word length effects for digital Doppler processors (DPP) in radar scatterometers, is analyzed. The roundoff noise-to-signal ratio in the measurement of the radar return signal power is derived. Computer simulations which validate the analytical results are presented. The results can be used in tradeoff studies of hardware design such as number of bits required at each processing stage. The results are used in the design of a DPP for the NASA scatterometer planned to be launched in 1990. ESA

N87-17259# Atmospheric Environment Service, Downsview (Ontario).
APPLICATION OF THE SEASAT SCATTEROMETER TO OBSERVATIONS OF WIND SPEED AND DIRECTION AND ARCTIC ICE/WATER BOUNDARIES
S. Peterherych, A. F. Davies, and G. Muttit *In* ESA Proceedings of the 1986 International Geoscience and Remote Sensing Symposium (IGARSS '86) on Remote Sensing: Today's Solutions for Tomorrow's Information Needs, Volume 1 Aug. 1986 p 585-588 (For primary document see N87-17163 09-43)
Avail: NTIS HC A99/MF E03; ESA, Paris, France, 3 volume set $90 Member States, AU, CN, and NO (+20% others)

Using conventional marine, land, and undealiased scatterometer data, a streamline analysis, a surface pressure analysis, and an Arctic ice-water boundary analysis were prepared. A low pressure center located near the coast in the Gulf of Alaska produced high winds as far west as the Chukchi Sea (70 N, 180 W) northward to 75 N and eastward to Victoria Island (110 W). Surface ship and land data is used to assist the selection of the correct wind direction. A streamline and MSL pressure analysis are prepared. Undealiased Seasat data are used to identify the ice/water boundary. ESA

N87-17260*# National Aeronautics and Space Administration. Goddard Space Flight Center, Greenbelt, Md.
THE ELECTRONICALLY STEERED THINNED ARRAY RADIOMETER (ESTAR) c35
C. T. Swift (Massachusetts Univ., Amherst), C. Ruf, A. Tanner, and D. Levine *In* ESA Proceedings of the 1986 International Geoscience and Remote Sensing Symposium (IGARSS '86) on Remote Sensing: Today's Solutions for Tomorrow's Information Needs, Volume 1 Aug. 1986 p 591-593 (For primary document see N87-17163 09-43)
Avail: NTIS HC A99/MF E03; ESA, Paris, France, 3 volume set $90 Member States, AU, CN, and NO (+20% others) CSCL 14B

The concept of a thinned array radiometer is described as an alternate to large filled apertures to achieve high resolution imaging from space. The serious limitations of conventional mechanical scanning systems and the practical problems associated with a multiple receiver pushbroom system that utilizes a large antenna are discussed. The thinned array is developed in terms of aperture synthesis techniques used in radio astronomy. Examples of thinned array configurations are presented, and future directions are discussed. ESA

N87-17261# Rome Univ. (Italy). Dipt. di Ingegneria Elettronica.
ANTENNA PATTERN CORRECTION IN SCANNING RADIOMETRY: A SINGULAR SYSTEM ANALYSIS c32
F. Bardati, M. Mongiardo, and D. Solimini *In* ESA Proceedings of the 1986 International Geoscience and Remote Sensing Symposium (IGARSS '86) on Remote Sensing: Today's Solutions for Tomorrow's Information Needs, Volume 1 Aug. 1986 p 595-598 Sponsored by Elettronica S.p.A., Max-Planck Inst., and CNR (For primary document see N87-17163 09-43)
Avail: NTIS HC A99/MF E03; ESA, Paris, France, 3 volume set $90 Member States, AU, CN, and NO (+20% others)

The singular system method for antenna pattern correction is considered. This technique allows a direct estimate of the achievable spatial resolution and of the accuracy of retrievals. The performance of the method is discussed by means of a numerical simulation of the reconstruction for one-dimensional brightness scenery. Isolated high emission spots are identified with appreciably high resolution, while the restoration of continuously distributed sceneries is more difficult, especially when a high radiometric accuracy is required. ESA

N87-17262# Bern Univ. (Switzerland). Inst. of Applied Physics.
DIELECTRIC AND SURFACE PARAMETERS RELATED TO MICROWAVE SCATTER AND EMISSION PROPERTIES c32
E. Stotzer, U. Wegmueller, R. Hueppi, and C. Maetzer *In* ESA Proceedings of the 1986 International Geoscience and Remote Sensing Symposium (IGARSS '86) on Remote Sensing: Today's Solutions for Tomorrow's Information Needs, Volume 1 Aug. 1986 p 599-603 (For primary document see N87-17163 09-43)
Avail: NTIS HC A99/MF E03; ESA, Paris, France, 3 volume set $90 Member States, AU, CN, and NO (+20% others)

A correlated study of the dielectric properties, surface roughness, and the backscatter and emission behavior of bare soil is presented. For the measurement of the permittivity of the soil field proof dielectric sensors at frequencies between 0.5 and 1 GHz were developed. A surface sensor measures the dielectric constant of a top 1 cm layer and a volume sensor averages over a depth of 15 cm. For the measurement of surface roughness, a laser distance measurement system was designed. It measures a 1 m long surface height profile. Quantities like distribution and standard deviation of heights and slopes, or the autocorrelation function are computed and used in scattering models. Temperature profiles, soil moisture, and texture are determined. Together with the soil parameters, the microwave signatures are measured with an L to X-band radiometer-scatterometer. Emissivities and backscattering coefficients are related to the soil parameters, and compared with model calculations. ESA

N87-17263# Rome Univ. (Italy). Dipt. di Ingegneria Elettronica.
EFFECT OF ELECTRICAL AND THERMAL PROPERTIES OF MATERIALS ON MICROWAVE BRIGHTNESS TEMPERATURE OF THE TERRESTRIAL CRUST
F. Bardati, D. Solimini, and P. Tognolatti *In* ESA Proceedings of the 1986 International Geoscience and Remote Sensing Symposium (IGARSS '86) on Remote Sensing: Today's Solutions for Tomorrow's Information Needs, Volume 1 Aug. 1986 p 605-609 Sponsored by Max-Planck Inst. and CNR (For primary document see N87-17163 09-43)
Avail: NTIS HC A99/MF E03; ESA, Paris, France, 3 volume set $90 Member States, AU, CN, and NO (+20% others)

The influence on the daily range of the brightness temperature, and of the dielectric and thermal parameters of the terrestrial crust was investigated. A numerical analysis was carried out for the case of a terrain layer over a semi-infinite solid. The influence of thermal parameters of the buried medium on the daily range of the brightness is recovered even if the layer masks the corresponding influence on the daily range of the surface temperature. ESA

N87-17264# Helsinki Univ. of Technology, Espoo (Finland). Radio Lab.
DEVELOPPEMENT OF ALGORITHMS TO RETRIEVE THE WATER EQUIVALENT OF SNOW COVER FROM SATELLITE MICROWAVE RADIOMETER DATA
M. Hallikainen and P. Jolma *In* ESA Proceedings of the 1986 International Geoscience and Remote Sensing Symposium (IGARSS '86) on Remote Sensing: Today's Solutions for Tomorrow's Information Needs, Volume 1 Aug. 1986 p 611-616 (For primary document see N87-17163 09-43)
Avail: NTIS HC A99/MF E03; ESA, Paris, France, 3 volume set $90 Member States, AU, CN, and NO (+20% others)

Algorithms to retrieve the water equivalent of snow cover from NIMBUS-7 scanning Multichannel Microwave Radiometer for winters 1978-79 through 1981-82 were tested. Using the best algorithm, the microwave response to snow water equivalent was examined. Substantial short-term and long-term (annual) variations

are observed in the response, due to the thermal history of snow. First-order regression lines were fitted to each winter's data. ESA

N87-17265# Centre d'Etude Spatiale des Rayonnements, Toulouse (France).
EXTRACTION OF THE BACKSCATTER COEFFICIENT OF AGRICULTURAL FIELDS FROM AN AIRBORNE SAR IMAGE
A. Lopes and R. Touzi *In* ESA Proceedings of the 1986 International Geoscience and Remote Sensing Symposium (IGARSS '86) on Remote Sensing: Today's Solutions for Tomorrow's Information Needs, Volume 1 Aug. 1986 p 621-628 (For primary document see N87-17163 09-43)
(Contract ESA-6153/WI-MS)
Avail: NTIS HC A99/MF E03; ESA, Paris, France, 3 volume set $90 Member States, AU, CN, and NO (+20% others)

Relative and absolute calibration was performed on an X-band SAR image of an agricultural area. The image presented distortions due mainly to aircraft motions and to the antenna gain function. Distortions due to aircraft motions, resulting in dark rays perpendicular to the flight direction, are corrected by a spectral filtering method. The thermal noise is estimated and substracted from the image. The antenna gain is evaluated by using a distributed target of a priori known angular variation. A correction taking into account the antenna gain and the range is applied to the image. The scattering coefficient is estimated using a Luneberg lens located in the scene. Errors in this estimation are assessed. ESA

N87-17266# Freiburg Univ. (West Germany). Abt. Luftbildmessung und Fernerkunde.
MICROWAVE REMOTE SENSING: ITS APPLICATIONS AND LIMITATIONS IN OPERATIONAL TASKS OF LAND USE INVENTORY AND FOREST MANAGEMENT
R. Kessler *In* ESA Proceedings of the 1986 International Geoscience and Remote Sensing Symposium (IGARSS' 86) on Remote Sensing: Today's Solutions for Tomorrow's Information Needs, Volume 1 Aug. 1986 p 629-631 (For primary document see N87-17163 09-43)
Avail: NTIS HC A99/MF E03; ESA, Paris, France, 3 volume set $90 Member States, AU, CN, and NO (+20% others)

Woodland and agricultural aspects of land use, based on experience with Seasat-SAR, SAR-580 and SIR-B imagery are reviewed. Potential applications and the limitations of microwave remote sensing sensors for operational tasks of land use inventory are described. ESA

N87-17267# Zurich Univ. (Switzerland). Dept. of Geography.
MERGING SPACEBORNE IMAGE DATA OF OPTICAL AND MICROWAVE SENSORS
D. R. Nuesch, E. H. Meier, D. K. Blaettler, K. Ch. Graf, and F. M. Holecz *In* ESA Proceedings of the 1986 International Geoscience and Remote Sensing Symposium (IGARSS '86) on Remote Sensing: Today's Solutions for Tomorrow's Information Needs, Volume 1 Aug. 1986 p 633-637 (For primary document see N87-17163 09-43)
Avail: NTIS HC A99/MF E03; ESA, Paris, France, 3 volume set $90 Member States, AU, CN, and NO (+20% others)

Seasat SAR images and LANDSAT TM images were merged with high accuracy by a pixel-to-map transformation. The spatial resolution of 1 pixel was limited to 100 m, due to the grid size of the digital terrain model (DTM) required for the SAR image rectification. Accuracy depends on the grid size of the DTM which should be as fine meshed as possible, preferably on the order of the spatial resolution capability of the sensor being used. Results demonstrate that missing information or incomplete data from optical sensors, due for instance to clouds during the overflight, can be completed by data from microwave sensors. It is suggested that images with clouds taken by photographic cameras could be restored after being scanned by a raster device scanner. The procedure could also be applied to meteorological satellite images. ESA

N87-17268# Arkansas Univ., Fayetteville.
COMPUTER-DERIVED HEIGHT FROM SIR-B STEREO RADAR IMAGES
J. K. Thomas, V. H. Kaupp, W. P. Waite, and H. C. MacDonald *In* ESA Proceedings of the 1986 International Geoscience and Remote Sensing Symposium (IGARSS '86) on Remote Sensing: Today's Solutions for Tomorrow's Information Needs, Volume 1 Aug. 1986 p 639-643 (For primary document see N87-17163 09-43)
Avail: NTIS HC A99/MF E03; ESA, Paris, France, 3 volume set $90 Member States, AU, CN, and NO (+20% others)

An unguided computer algorithm was used to generate a digital elevation model (DEM) from an overlapping image pair. The DEM was used to study the topography of a region and to map the images into a desired projection. The first processing step low-pass filters the images to suppress the effects of noise. In the second step, an unguided computer algorithm finds match points. In the final step, terrain elevation (DEM) is computed from the match points and the radar's imaging geometry. ESA

N87-17269# INTERA Environmental Consultants Ltd., Calgary (Alberta).
DIGITAL TERRAIN MAPPING WITH STAR-1 SAR DATA
J. B. Mercer, R. T. Lowry, F. Leberl (Vexcell Corp., Boulder, Colo.), and G. Domik *In* ESA Processings of the 1986 International Geoscience and Remote Sensing Symposium (IGARSS' 86) on Remote Sensing: Today's Solutions for Tomorrow's Information Needs, Volume 1 Aug. 1986 p 645-650 (For primary document see N87-17163 09-43)
Avail: NTIS HC A99/MF E03; ESA, Paris, France, 3 volume set $90 Member States, AU, CN, and NO (+20% others)

A program to assess the capability of deriving Digital Terrain Mapping (DTM) products from STAR-1 data, an airborne, digital SAR is outlined. A 500 sq km area was flown over varied terrain, and the resultant stereo images were analyzed on an analytical plotter. The DTM thus derived was used to rectify the imagery. Contour plots and an ortho-photo-like radar image were derived at a scale of 1:50,000. An error analysis was performed indicating that rms elevation errors less than 30 m can be achieved in a production environment. ESA

N87-17270*# Arizona Univ., Tucson.
EXTRAPOLATION OF EARTH-BASED SOLAR IRRADIANCE MEASUREMENTS TO EXOATMOSPHERIC LEVELS FOR BROAD-BAND AND SELECTED ABSORPTION-BAND OBSERVATIONS c46
J. A. Reagan, P. A. Pilewskie, I. C. Scott-Fleming, and B. M. Herrmann *In* ESA Proceedings of the 1986 International Geoscience and Remote Sensing Symposium (IGARSS '86) on Remote Sensing: Today's Solutions for Tomorrow's Information Needs, Volume 1 Aug. 1986 p 653-659 (For primary document see N87-17163 09-43)
(NASA Order L-83161-B; NASA Order A-32033-C; Contract NOAA-NA-80RAD00065)
Avail: NTIS HC A99/MF E03; ESA, Paris, France, 3 volume set $90 Member States, AU, CN, and NO (+20% others) CSCL 04A

Techniques for extrapolating Earth-based spectral band measurements of directly transmitted solar irradiance to equivalent exoatmospheric signal levels were used to aid in determining system gain settings of the Halogen Occultation Experiment (HALOE) sunsensor system being developed for the NASA Upper Atmosphere Research Satellite and for the Stratospheric Aerosol and Gas (SAGE) 2 instrument on the Earth Radiation Budget Satellite. A band transmittance approach was employed for the HALOE sunsensor which has a broad-band channel determined by the spectral responsivity of a silicon detector. A modified Langley plot approach, assuming a square-root law behavior for the water vapor transmittance, was used for the SAGE-2 940 nm water vapor channel. ESA

N87-17271# National Severe Storms Lab., Norman, Okla.
APPLICATION OF DOPPLER RADAR AND LIDAR TO DIAGNOSE ATMOSPHERIC PHENOMENA c46
R. J. Doviak, M. Eilts, V. Mazur, M. Sachidananda, and D. S. Zrnic *In* ESA Proceedings of the 1986 International Geoscience

and Remote Sensing Symposium (IGARSS '86) on Remote Sensing: Today's Solutions for Tomorrow's Information Needs, Volume 1 Aug. 1986 p 661-666 (For primary document see N87-17163 09-43)
Avail: NTIS HC A99/MF E03; ESA, Paris, France, 3 volume set $90 Member States, AU, CN, and NO (+20% others)

Observations and comparison of measurements of wind, waves, and turbulence, made with Doppler radar, lidar, and in-situ sensors, are presented. Applications to the detection of weather hazards to safe flight are discussed. A method to estimate rainfall with a polarization diversity Doppler radar is shown to be less sensitive to drop size distribution variations than commonly used Z-R relations. The Doppler radar is also used to observe characteristics of lightning produced plasma channels which exhibit vertical accelerations caused by buoyancy acting on the hot plasma and interaction with Earth's magnetic field. ESA

N87-17272# National Oceanic and Atmospheric Administration, Boulder, Colo. Wave Propagation Lab.
REMOTE PROBING OF WIND AND REFRACTIVE-INDEX STRUCTURE USING OPTICAL SCINTILLATION TECHNIQUES c47
G. R. Ochs and S. F. Clifford *In* ESA Proceedings of the 1986 International Geoscience and Remote Sensing Symposium (IGARSS '86) on Remote Sensing: Today's Solutions for Tomorrow's Information Needs, Volume 1 Aug. 1986 p 667-670 Sponsored by US Army Dugway Proving Ground, and US Army Atmospheric Sciences Lab. (For primary document see N87-17163 09-43)
Avail: NTIS HC A99/MF E03; ESA, Paris, France, 3 volume set $90 Member States, AU, CN, and NO (+20% others)

A wind-profiling system to measure crosswinds simultaneously at 5 locations along an optical path 200 m to 1 km long, using optics of modest size, and a profiling system to measure the refractive index structure parameter, Cn sq, simultaneously at 6 locations along the same optical path are discussed. The wind profiler employs transmitting and receiving spatial filters arranged to form a filter in space, sensitive to irregularities moving across the light path, and matched to a specific spatial wavelength at a specific location along the optical path. The Cn sq measurement employs single incoherent transmitting and receiving apertures, much larger in diameter than the Fresnel zone size for the path. It can be shown that the location of the peak of the weighting function for Cn measurement is a function of the ratio of the transmitting and receiving aperture diameters. ESA

N87-17273# Zurich Univ. (Switzerland). Remote Sensing Labs.
VIEWING ANGLE CORRECTIONS OF AIRBORNE MULTISPECTRAL SCANNER DATA ACQUIRED OVER FORESTED SURFACES
K. Staenz, P. Meyer, K. I. Itten, D. G. Goodenough (Canada Centre for Remote Sensing, Ottawa (Ontario).), and P. M. Teillet *In* ESA Proceedings ot the 1986 International Geoscience and Remote Sensing Symposium (IGARSS '86) on Remote Sensing: Today's Solutions for Tomorrow's Information Needs, Volume 1 Aug. 1986 p 671-676 (For primary document see N87-17163 09-43)
Avail: NTIS HC A99/MF E03; ESA, Paris, France, 3 volume set $90 Member States, AU, CN, and NO (+20% others)

Airborne MSS BENDIX M2S Scanner data obtained over a forested area were analyzed in order to assess the viewing angle effect. All of the bands situated within 0.4 to 1.1 microns are affected by the viewing angle. The magnitude of this effect results in a gray level difference of up to 35% within a viewing angle range from 0 (nadir) to 40 deg. In order to remove this radiometric distortion due to off-nadir viewing, two correction procedures, the additive adjustment technique and different band transformations (NIR-red ratio, NIR-red difference, vegetation and biomass index) were applied to the image data. The additive adjustment technique gives the best result. Due to the viewing angle correction, a significant improvement of the classification accuracy is achieved. ESA

N87-17274# Bern Univ. (Switzerland). Inst. of Geography.
ATMOSPHERIC CORRECTIONS OF NOAA-AVHRR DATA VERIFICATION OF DIFFERENT METHODS BY GROUND TRUTH MEASUREMENTS
G. Nejedly *In* ESA Proceedings of the 1986 International Geoscience and Remote Sensing Symposium (IGARSS '86) on Remote Sensing: Today's Solutions for Tomorrow's Information Needs, Volume 1 Aug. 1986 p 677-682 Sponsored by the Swiss National Science Foundation (For primary document see N87-17163 09-43)
Avail: NTIS HC A99/MF E03; ESA, Paris, France, 3 volume set $90 Member States, AU, CN, and NO (+20% others)

Satellite data and precision radiation thermometer radiation temperature measurements carried out from low-altitude airplanes over land and water surfaces were compared. The WINDOW radiation transfer model and several split-window algorithms are tested for their suitability to eliminate the atmospheric effect. It is shown that, if meteorological soundings are available, the influence of the atmosphere can be minimized by using the WINDOW model. For water temperature retrievals over Switzerland, a split-window algorithm is computed using satellite data and compared to published algorithms. ESA

N87-17275# Swiss Inst. of Meteorology, Zurich.
FORECASTER'S NEED IN METEOROLOGY FOR THE NEXT GENERATION OF SATELLITES c47
C. H. Fourcy *In* ESA Proceedings of the 1986 International Geoscience and Remote Sensing Symposium (IGARSS '86) on Remote Sensing: Today's Solutions for Tomorrow's Information Needs, Volume 1 Aug. 1986 p 683-685 (For primary document see N87-17163 09-43)
Avail: NTIS HC A99/MF E03; ESA, Paris, France, 3 volume set $90 Member States, AU, CN, and NO (+20% others)

Weather forecaster's needs for the next 10 to 20 years in the conception of the observation, its transmission, and the forecast are discussed. This conception will include automatic stations, profilers, and satellite sounding, the fine mesh numerical forecast, and satellite images. ESA

N87-17276# Swiss Inst. of Meteorology, Zurich.
REAL-TIME APPLICATION OF REMOTELY SENSED DATA
P. Binder and G. Galli (Osservatorio Ticinese, Locarno-Monti (Switzerland).) *In* ESA Proceedings of the 1986 International Geoscience and Remote Senting Symposium (IGARSS '86) on Remote Sensing: Today's Solutions for Tomorrow's Information Needs, Volume 1 Aug. 1986 p 687-693 (For primary document see N87-17163 09-43)
Avail: NTIS HC A99/MF E03; ESA, Paris, France, 3 volume set $90 Member States, AU, CN, and NO (+20% others)

The way the Swiss meteorological Institute provides forecasters with satellite and radar information in quasi real-time is explained. The configuration of the processing system is described. User facilities to display and inspect data are presented. Two pictorial products are explained: the Swiss Radar Composite, and the Normalized Meteosat Visible Imagery. The physical model that defines the normalization algorithm together with related operational aspects for its implementation are outlined. ESA

N87-17277# Naval Research Lab., Washington, D. C. Space Systems and Technology Div.
APPLICATION OF SPACEBORNE DISTRIBUTED APERTURE/COHERENT ARRAY PROCESSING (SDA/CAP) TECHNOLOGY TO ACTIVE AND PASSIVE MICROWAVE REMOTE SENSING
M. S. Kaplan *In* ESA Proceedings of the 1986 International Geoscience and Remote Sensing Symposium (IGARSS '86) on Remote Sensing: Today's Solutions for Tomorrow's Information Needs, Volume 1 Aug. 1986 p 697-701 (For primary document see N87-17163 09-43)
Avail: NTIS HC A99/MF E03; ESA, Paris, France, 3 volume set $90 Member States, AU, CN, and NO (+20% others)

Application of spaceborne distributed aperture/coherent array processing (SDA/CAP) to environmental remote sensing missions is discussed. This technology differs from conventional monostatic

remote sensing approaches in that sensor elements are distributed among many space platforms. It is possible to coherently combine the inputs from many receiving spacecraft in order to form a very large distributed aperture, thousands of kilometers in size. This enormous effective aperture size can provide nanoradian resolution in the microwave region of the spectrum. Relative spacecraft phase measurement accuracies on the order of a fraction of a wavelength are required to support the technology. Spacecraft relative position and time measurement via hydrogen maser time references on each spacecraft and laser ranging between spacecraft is proposed. Intersatellite laser ranging technology needs to be developed to support the application of SDA/CAP techniques for advanced space environmental remote sensor systems. ESA

N87-17278# Kansas Univ. Center for Research, Inc., Lawrence. Radar Systems and Remote Sensing Lab.

SOME TRADE-OFFS IN MODEST-RESOLUTION RADARS FOR SPACE **c32**

R. K. Moore *In* ESA Proceedings of the 1986 International Geoscience and Remote Sensing Symposium (IGARSS '86) on Remote Sensing: Today's Solutions for Tomorrow's Information Needs, Volume 1 Aug. 1986 p 703-708 (For primary document see N87-17163 09-43)

Avail: NTIS HC A99/MF E03; ESA, Paris, France, 3 volume set $90 Member States, AU, CN, and NO (+20% others)

It is argued that radars may be added easily to radiometers to provide a synergistic capability, while providing improved resolution within the radiometer footprint with little additional power. Modest-resolution radars without radiometers are so much simpler than focussed SARs that they can provide useful alternatives where image resolution need not be fine, such as geologic exploration, soil-moisture measurement, and mapping ocean features other than wave spectra. Modest-resolution radar systems often require transmitter power of only milliwatts; under some conditions the power required is less than that of the local oscillator of the acompanying radiometer receiver. The lowest power requirement is for forward-looking radars that achieve modest resolution in the along-track direction by Doppler filtering. ESA

N87-17279# Jet Propulsion Lab., California Inst. of Tech., Pasadena.

IMAGING RADAR POLARIMETRY FROM WAVE SYNTHESIS **c32**

H. A. Zebker, J. J. VanZyl, and D. N. Held *In* ESA Proceedings of the 1986 International Geoscience and Remote Sensing Symposium (IGARSS '86) on Remote Sensing: Today's Solutions for Tomorrow's Information Needs, Volume 1 Aug. 1986 p 709-713 (For primary document see N87-17163 09-43)

Avail: NTIS HC A99/MF E03; ESA, Paris, France, 3 volume set $90 Member States, AU, CN, and NO (+20% others)

It is shown that it is possible to measure the complete scattering matrix of an object using data acquired on a single aircraft pass, and combine the signals later in the data processor to generate radar images corresponding to any desired combination of transmit and receive polarization. Various scattering models predict different dependence on polarization state of received power from an object. The imaging polarimeter permits determination of this dependence, the polarization signature, of each point in a radar image. Comparison of predictions and observational data reveals scattering mechanisms for each area of interest. Backscatter from the ocean is highly polarized and well-modeled by Bragg scattering, while scattering from trees in a city park possesses a considerable unpolarized component. Urban regions exhibit the characteristics expected from dihedral corner reflectors, and their polarization signatures are quite different from the on-bounce Bragg model. ESA

N87-17280# Environmental Research Inst. of Michigan, Ann Arbor.

MULTIFREQUENCY-POLARIMETRIC SAR FOR REMOTE SENSING **c32**

A. Kozma, A. D. Nichols, R. F. Rawson, S. J. Shackman, C. W. Haney (Naval Air Development Center, Warminster, Pa.), and J. J. Shanne, Jr. *In* ESA Proceedings of the 1986 International Geoscience and Remote Sensing Symposium (IGARSS '86) on Remote Sensing: Today's Solutions for Tomorrow's Information Needs, Volume 1 Aug. 1986 p 715-719 (For primary document see N87-17163 09-43)

Avail: NTIS HC A99/MF E03; ESA, Paris, France, 3 volume set $90 Member States, AU, CN, and NO (+20% others)

A multifrequency-polarimetric airborne SAR for remote sensing applications at a range resolution of 1.6 m and an azimuth resolution of 2.2 m in the fine resolution mode and at twice the range resolution in the coarse resolution mode is presented. Three frequencies are used: X-band, C-band, and L-band. The mapping modes and control system are described. ESA

N87-17281# Michigan Univ., Ann Arbor. Radiation Lab.

MILLIMETER-WAVE NETWORK ANALYZER-BASED SCATTEROMETER **c32**

F. T. Ulaby, T. F. Haddock, J. East, and V. Liepa *In* ESA Proceedings of the 1986 International Geoscience and Remote Sensing Symposium (IGARSS '86) on Remote Sensing: Today's Solutions for Tomorrow's Information Needs, Volume 1 Aug. 1986 p 721-724 (For primary document see N87-17163 09-43)

Avail: NTIS HC A99/MF E03; ESA, Paris, France, 3 volume set $90 Member States, AU, CN, and NO (+20% others)

The Millimeter Polarimeter (MMP) network-analyzer based scatterometer and reflectometer system was developed in a program to characterize radar clutter at 35, 94, and 140 GHz. An HP 8510A network analyzer is employed in the MMP system as a signal conditioner and processor to facilitate real-time data reduction, to reduce the short time-delay leakage noise inherent in traditional FM/CW radar, and to enhance the signal-to-noise ratio of the system through signal processing techniques. Operation of the system at millimeter wavelengths is achieved with upconversion and harmonic downconversion. The use of harmonic downconverters permits low-frequency signal connections between components of the system and allows easy reconfiguration in either scatterometer, bistatic, or reflection/transmission modes. ESA

N87-17282# Technical Univ. of Budapest (Hungary). Dept. of Microwave Techniques.

A SCATTEROMETER OPERATING AT 10 GHz **c32**

I. Bozsoki and S. Mihaly *In* ESA Proceedings of the 1986 International Geoscience and Remote Sensing Symposium (IGARSS '86) on Remote Sensing: Today's Solutions for Tomorrow's Information Needs, Volume 1 Aug. 1986 p 725-729 (For primary document see N87-17163 09-43)

Avail: NTIS HC A99/MF E03; ESA, Paris, France, 3 volume set $90 Member States, AU, CN, and NO (+20% others)

An FM/CW microwave scatterometer operating in the X-band was developed for truck-mounted field measurements to investigate scatterometry and the application of scattering data for modeling the scattering properties of agricultural areas, vegetation covered soils. Data correction techniques and results of field experiments are presented. It is shown that if the signal processing can be made under laboratory conditions, the drawbacks of the direct-mixing system can be eliminated saving its advantages. ESA

N87-17283# European Space Agency, Paris (France).

PROCEEDINGS OF THE 1986 INTERNATIONAL GEOSCIENCE AND REMOTE SENSING SYMPOSIUM (IGARSS' 86) ON REMOTE SENSING: TODAY'S SOLUTIONS FOR TOMORROW'S INFORMATION NEEDS, VOLUME 2

T. D. Guyenne, ed. and J. J. Hunt, ed. Aug. 1986 388 p Symposium held in Zurich, Switzerland, 8-11 Sep. 1986; sponsored by NASA, ESA, EARSeL NOAA, CNES, DFVLR, Swiss Academy of Sciences, Swiss Association for Space Technology, Contraves Ltd., Dornier-Werke GmbH, Intern. Union of Radio Science, et al. (ESA-SP-254-Vol-2; IEEE-86CH2268-1-Vol-2; LC-86-80109-Vol-2; ISSN-0379-6566; ETN-87-98536) Avail: NTIS HC A17/MF A01; ESA, Paris, France, 3 volume set $90 Member States, AU, CN, and NO (+20% others)

Remote sensing applications to agriculture; image processing methodology; active microwave sensing of the ocean; passive microwave sensing of vegetation and soils; radar forestry; hydrol-

ogy; imaging radar missions; SAR observation of ocean waves; land analysis with optical sensors; and SAR system considerations were discussed. For individual titles, see N87-17284 through N87-17362.

N87-17284# Canada Centre for Remote Sensing, Ottawa (Ontario).
AN OVERVIEW OF REMOTE SENSING AGRICULTURAL APBAD CAPS LANGUAGE[-[pli[-]CATIONS IN NORTH AMERICA: PAST, PRESENT AND FUTURE
R. J. Brown *In* ESA Proceedings of the 1986 International Geoscience and Remote Sensing Symposium (IGARSS' 86) on Remote Sensing: Today's Solutions for Tomorrow's Information Needs, Volume 2 Aug. 1986 p 733-737 (For primary document see N87-17283 09-43)
Avail: NTIS HC A17/MF A01; ESA, Paris, France, 3 volume set $90 Member States, AU, CN, and NO (+20% others)

The use of remote sensing for crop condition monitoring and crop area determination is reviewed. The Large Area Crop Inventory Experiment and the AGRISTARS project are recalled. The LANDSAT and NOAA satellite instruments used in agricultural remote sensing are described. ESA

N87-17285# Agricultural Research Service, Beltsville, Md.
APPLICATIONS OF REMOTE SENSING IN THE US DEPARTMENT OF AGRICULTURE
J. C. Price *In* ESA Proceedings of the 1986 International Geoscience and Remote Sensing Symposium (IGARSS '86) on Remote Sensing: Today's Solutions for Tomorrow's Information Needs, Volume 2 Aug. 1986 p 739-742 (For primary document see N87-17283 09-43)
Avail: NTIS HC A17/MF A01; ESA, Paris, France, 3 volume set $90 Member States, AU, CN, and NO (+20% others)

The U.S. Department of Agriculture uses remote sensing to monitor and assess crop conditions and to manage renewable resources. The Foreign Agriculture Service uses meteorological satellite data and LANDSAT data to monitor the status of crops in major agricultural regions of the world. The National Agricultural Statistics Service uses LANDSAT data to improve estimates of crop acreage in the central U.S. The Soil Conservation Service will use aircraft data to aid in the inventory of U.S agricultural lands. Research to improve agency procedures is described. ESA

N87-17286# Kansas State Univ., Manhattan. E.T. Lab.
ASSESSING GRASS CANOPY CONDITION AND GROWTH FROM COMBINED OPTICAL-MICROWAVE MEASUREMENTS
G. Asrar, E. T. Kanemasu, and R. D. Martin *In* ESA Proceedings of the 1986 International Geoscience and Remote Sensing Symposium (IGARSS '86) on Remote Sensing: Today's Solutions for Tomorrow's Information Needs, Volume 2 Aug. 1986 p 743-744 (For primary document see N87-17283 09-43)
Avail: NTIS HC A17/MF A01; ESA, Paris, France, 3 volume set $90 Member States, AU, CN, and NO (+20% others)

The potential of a combined optical-microwave sensor system for monitoring canopy condition and development in a natural tallgrass prairie was assessed. A set of linear classification functions was derived for distinguishing among tallgrass prairie surface cover types based on their spectral characteristics. An indirect procedure for estimating green leaf area index and phytomass for measurements of red and near infrared canopy reflectance was developed. Microwave (C-band) scatterometer measurements are found to strongly correlate with near-surface soil water content of the grassland. ESA

N87-17287# Laval Univ. (Quebec).
ANALYSIS OF THE SPATIAL STRUCTURE OF SYNTHETIC APERTURE RADAR (SAR) IMAGERY FOR A BETTER SEPARABILITY OF CEREAL CROPS, WHEAT AND BARLEY
C. Dube, H. Proulx, and K. P. B. Thompson *In* ESA Proceedings of the 1986 International Geoscience and Remote Sensing Symposium (IGARSS '86) on Remote Sensing: Today's Solutions for Tomorrow's Information Needs, Volume 2 Aug. 1986 p 745-750 (For primary document see N87-17283 09-43)
Avail: NTIS HC A17/MF A01; ESA, Paris, France, 3 volume set $90 Member States, AU, CN, and NO (+20% others)

The analysis of the statistical characteristics of radar data for wheat and barley is discussed. The SAR data set is of good quality and comprises two depression angles, two row directions for each field, and three flight dates. A methodology of image processing which concerns the examination of structure and texture in image data is outlined. Results reveal two important characteristics in separating wheat from barley: the degree of homogeneity and the row effect. The texture analysis can be used to separate wheat and barley. ESA

N87-17288# Centre National d'Etudes des Telecommunications, Issy-les-Moulineaux (France).
TOWARD A SATELLITE SYSTEM TO MONITOR THE SPATIAL AND TEMPORAL BEHAVIOR OF SOIL WATER CONTENT
R. Bernard, O. Taconet, and D. Vidal-Madjar *In* ESA Proceedings of the 1986 International Geoscience and Remote Sensing Symposium (IGARSS '86) on Remote Sensing: Today's Solutions for Tomorrow's Information Needs, Volume 2 Aug. 1986 p 751-753 (For primary document see N87-17283 09-43)
Avail: NTIS HC A17/MF A01; ESA, Paris, France, 3 volume set $90 Member States, AU, CN, and NO (+20% others)

It is shown that using proper simple parameterizations of the soil/vegetation/atmosphere system it is possible to derive soil water content and surface atmospheric fluxes at satellite pixels scale. Though the algorithms must be further tested, it is anticipated that a future space system (geostationary satellites and polar platforms) using visible, thermal infrared, and microwave remote sensing may be used on an operational basis as a hydrologic observatory. ESA

N87-17289# California Univ., Berkeley. 260 Space Sciences Lab.
UTILITY OF REMOTE SENSING DATA IN RENEWABLE RESOURCE SAMPLE SURVEY
R. W. Thomas *In* ESA Proceedings of the 1986 International Geoscience and Remote Sensing Symposium (IGARSS '86) on Remote Sensing: Today's Solutions for Tomorrow's Information Needs, Volume 2 Aug. 1986 p 755-758 (For primary document see N87-17283 09-43)
Avail: NTIS HC A17/MF A01; ESA, Paris, France, 3 volume set $90 Member States, AU, CN, and NO (+20% others)

It is shown how remote sensing technology offers possibilities for sample-based estimation of renewable resource means and totals. Studies show that significant improvements in estimate precision, cost, or timeliness are available for estimation of crop and irrigated area, forest wood volume and growth, and useable livestock forage when satellite data and/or aerial photography are included as sample stages. Land satellite data often provide a highly cost-effective, rapid alternative for stratifying a region into strata having a smaller range of variation in the ground parameters(s) of interest. Satellite and aircraft data can provide sample unit-specific measurements, correlated to corresponding ground measurements, reducing required ground sample size and inventory time. ESA

N87-17290# Saskatchewan Univ., Saskatoon. Dept. of Electrical Engineering.
IMAGE REPRESENTATION VIA ITS SYMMETRICAL COMPONENTS
A. G. Wacker and G. Lohar *In* ESA Proceedings of the 1986 International Geoscience and Remote Sensing Symposium (IGARSS '86) on Remote Sensing: Today's Solutions for Tomorrow's Information Needs, Volume 2 Aug. 1986 p 761-766 Sponsored by Canadian Natural Sciences and Engineering Research Council (For primary document see N87-17283 09-43)
Avail: NTIS HC A17/MF A01; ESA, Paris, France, 3 volume set $90 Member States, AU, CN, and NO (+20% others)

It is shown that a sampled and quantized (monochrome) image represented by a pxp matrix can be decomposed into a combination of circulant subimages. This decomposition is based on the result: A pxp matrix (H) can be expressed as (H) = Sigma

sup rho-1 sub i = 0 (AT(i))(Hc(i)) where (Hc(i)) is a circulant matrix and the diagonal matrix (AT(i)) = diag(T*i) with T*i denoting the complex conjugate of the i-th column of a pxp DFT matrix (T). The matrix decomposition is interpreted as a two-dimensional symmetrical component decomposition of (H). A relationship between the symmetrical components and the Fourier coefficients of an image is indicated. ESA

N87-17291# South Carolina Univ., Columbia. Dept. of Media Arts.

ADVANCED ALTERNATING FRAME TECHNOLOGY (VISIDEP (TM)) AND THREE-DIMENSIONAL REMOTE SENSING

A. P. McLaurin, E. R. Jones, and L. Cathey *In* ESA Proceedings of the 1986 International Geoscience and Remote Sensing Symposium (IGARSS '86) on Remote Sensing: Today's Solutions for Tomorrow's Information Needs, Volume 2 Aug. 1986 p 767-770 (For primary document see N87-17283 09-43)

Avail: NTIS HC A17/MF A01; ESA, Paris, France, 3 volume set $90 Member States, AU, CN, and NO (+20% others)

The theoretical requirements for real-time, full color, three-dimensional display and for single source, processed full color display systems are discussed. Both are based, in part, on research evolving from three-dimensional video technology and can be applied to any platform for sensing, whether submarine, aerial, or terrestrial. Due to the requirements established, system size is not a limitation, and any imaging which can be displayed on a flat surface can be represented to the unaided eye with controllable depth illusions which can generate measurable relationships for the viewer. All such data can be recorded using standard equipment and replayed, manipulated, and processed on standard equipment once produced. Replays retain full color and dimensionality just as the original information, and can be viewed with the unaided eye. Applications reviewed include X-ray, infrared, and standard video. ESA

N87-17292# Jet Propulsion Lab., California Inst. of Tech., Pasadena.

IMAGE PROCESSING METHODS IN TWO AND THREE DIMENSIONS USED TO ANIMATE REMOTELY SENSED DATA

K. J. Hussey, J. R. Hall, and R. A. Mortensen *In* ESA Proceedings of the 1986 International Geoscience and Remote Sensing Symposium (IGARSS '86) on Remote Sensing: Today's Solutions for Tomorrow's Information Needs, Volume 2 Aug. 1986 p 771-776 (For primary document see N87-17283 09-43)

Avail: NTIS HC A17/MF A01; ESA, Paris, France, 3 volume set $90 Member States, AU, CN, and NO (+20% others)

Image processing methods and software used to animate nonimaging remotely sensed data on cloud cover are described. Three FORTRAN programs were written in the VICAR2/TAE image processing domain to perform 3D perspective rendering, to interactively select parameters controlling the projection, and to interpolate parameter sets for animation images between key frames. Operation of the 3D programs and transferring the images to film is automated using executive control language and custom hardware to link the computer and camera. ESA

N87-17293# Manitoba Univ., Winnipeg. Dept. of Geophysics.

APPLICATION OF 2-D HILBERT TRANSFORM IN THE INTERPRETATION OF REMOTELY SENSED POTENTIAL FIELD DATA

W. Moon and A. Ushah *In* ESA Proceedings of the 1986 International Geoscience and Remote Sensing Symposium (IGARSS '86) on Remote Sensing: Today's Solutions for Tomorrow's Information Needs, Volume 2 Aug. 1986 p 777-781 (For primary document see N87-17283 09-43)

(Grant NSERC-A-7400)

Avail: NTIS HC A17/MF A01; ESA, Paris, France, 3 volume set $90 Member States, AU, CN, and NO (+20% others)

The relationships between the 2-D Hilbert transform and 3-D potential field data are studied and the application of these relations in geological remote sensing is investigated. In the overburden covered area, direct mapping of geological formations using LANDSAT or other short wavelength remote sensing data are not possible and it becomes necessary to use other available data sets. The most readily available geophysical data are the potential field data sets and the 2-D Hilbert transform method was tested and applied to digital potential field data sets to compute the first and second vertical derivatives. Results show that the method speeds up the processing, and that the vertical derivatives convincingly identify the subsurface geological boundaries. ESA

N87-17294# Centre d'Etude Spatiale des Rayonnements, Toulouse (France).

COMPUTER-AIDED INTERPRETATION OF COMPLEX GEOLOGICAL PATTERNS IN REMOTE SENSING **c61**

G. Flouzat and K. Moueddene *In* ESA Proceedings of the 1986 International Geoscience and Remote Sensing Symposium (IGARSS '86) on Remote Sensing: Today's Solutions for Tomorrow's Information Needs, Volume 2 Aug. 1986 p 783-786 (For primary document see N87-17283 09-43)

Avail: NTIS HC A17/MF A01; ESA, Paris, France, 3 volume set $90 Member States, AU, CN, and NO (+20% others) CSCL 09B

A framework for aiding geological interpretation of remote sensing imagery, based on mathematical morphology for analyzing classified images is outlined. The case of a geologic fold is used to show ensemblist and structuring methodologies. In the first case, the direction anticline is known. The extraction of the connected components representing the folding uses this hypothesis. In the second case, the searched information is the main direction. The phenomenon characterization must be protected from the disturbance caused by the orientation of other relief elements. The entities which indicate the complex form studied are the sites of relatively strong slope. They correspond to forests and umbra areas. Therefore, the processing begins by searching the low reflectance pixels. A radiometric treatment based on a classification is the first step of the sequence. But artificial textures can be generated and then must be eliminated. Morphologic filtering is applied at the different channels before classification, to increase compactness of the obtained connected components. ESA

N87-17295# Defence Research Establishment Pacific, Victoria (British Columbia).

ESTIMATION OF INTERNAL WAVE CURRENTS FROM SAR AND INFRARED SCATTEROMETER IMAGERY **c48**

S. J. Hughes and B. A. Hughes *In* ESA Proceedings of the 1986 International Geoscience and Remote Sensing Symposium IGARSS '86) on Remote Sensing: Today's Solutions for Tomorrow's Information Needs, Volume 2 Aug. 1986 p 789-794 (For primary document see N87-17283 09-43)

Avail: NTIS HC A17/MF A01; ESA, Paris, France, 3 volume set $90 Member States, AU, CN, and NO (+20% others)

Models for estimating internal-wave surface currents from SAR and infrared scatterometer images of the ocean surface are presented. Selected SAR images were analyzed using linear hydrodynamic interaction theory and first-order hydrodynamic interaction theory and first-order Bragg scattering, and one IR scatterometer image was analyzed using a semi empirical slope-probability-density model. It is shown that surface features evident in the remote imagery correspond to fluctuations in the measured internal-wave surface current. For both models, it is assumed that the internal-wave current amplitude is much smaller than the propagation speed. Although the wave fields presented have current amplitudes which may be too large for a rigorous application of this linear approximation, the estimated currents compare well with the surface-truth measurements. ESA

N87-17296# Naval Ocean Research and Development Activity, Bay St. Louis, Miss.

OBSERVATIONS OF SURFACE CURRENTS AT NANTUCKET SHOALS AND IMPLICATIONS FOR RADAR IMAGING OF THE BOTTOM **c48**

P. Smith *In* ESA Proceedings of the 1986 International Geoscience and Remote Sensing Symposium (IGARSS '86) on Remote Sensing: Today's Solutions for Tomorrow's Information Needs, Volume 2 Aug. 1986 p 795-800 (For primary document see N87-17283 09-43)

Avail: NTIS HC A17/MF A01; ESA, Paris, France, 3 volume set $90 Member States, AU, CN, and NO (+20% others)

Measurements of surface current over a submerged ridge on the Nantucket Shoals and implications for the straining of surface waves are discussed. A photogrammetric analysis of the waves over the ridges is compared with predicted wavelengths. Aerial photos of surface roughness reveal a transition in roughness congruent with a lineal light streak. Ship drift across the ridge crest discloses a rapid drop in surface velocity at the crest. The measured strain rate disagrees, substantially, with the predicted strain rate, assuming barotropic flow and employing 2-D mass conservation. Wave blocking and refraction is consistent with the observed surface current and roughness distributions. ESA

N87-17297# Environmental Research Inst. of Michigan, Ann Arbor. Radar Science Lab.

ANALYSIS OF SYNTHETIC APERTURE RADAR IMAGERY OF SURFACE SHIP WAKES **c48**

J. D. Lyden, D. R. Lyzenga, and R. A. Schuchman *In* ESA Proceedings of the 1986 International Geoscience and Remote Sensing Symposium (IGARSS '86) on Remote Sensing: Today's Solutions for Tomorrow's Information Needs, Volume 2 Aug. 1986 p 801-805 (For primary document see N87-17283 09-43)
(Contract N00014-81-C-0692)
Avail: NTIS HC A17/MF A01; ESA, Paris, France, 3 volume set $90 Member States, AU, CN, and NO (+20% others)

Understanding of the phenomena involved in the SAR imaging of ship wakes is summarized. Wakes caused by ship-generated surface waves (including narrow wakes and classical Kelvin wakes) are relatively well understood, although the dependence on environmental conditions and radar parameters is not resolved. Turbulent wakes are the least understood. Although initial modeling results appear encouraging, additional data collected over a broader range of environmental conditions with more detailed surface measurements need to be studied to validate these models. Ship-generated internal waves are at an intermediate level of understanding. Detailed models exist for these phenomena which appear to yield reasonable results, at least at L-band, but which need to be further evaluated by detailed comparison with actual SAR images. ESA

N87-17298# TRW Space Technology Labs., Redondo Beach, Calif.

SAR IMAGING OF BOTTOM TOPOGRAPHY IN THE OCEAN: RESULTS FROM AN IMPROVED MODEL **c48**

H. C. Yuen, D. R. Crawford (Jet Propulsion Lab., California Inst. of Tech., Pasadena.), and P. G. Saffman *In* ESA Proceedings of the 1986 International Geoscience and Remote Sensing Symposium (IGARSS '86) on Remote Sensing: Today's Solutions for Tomorrow's Information Needs, Volume 2 Aug. 1986 p 807-815 (For primary document see N87-17283 09-43)
Avail: NTIS HC A17/MF A01; ESA, Paris, France, 3 volume set $90 Member States, AU, CN, and NO (+20% others)

A two-space dimensional model, which is applicable to arbitrary bottom topography and wind, is applied to Seasat Revs. 762, 957, 1430, and 1473. The model includes the additional modulational effects of a long-wave field on the short Bragg waves, both in the presence of a variable current field and results compared to data. Modulations associated with other radar frequencies are also calculated under Rev. 762 conditions. It is shown that when the long-wave field effects are included, signature strength does not decrease with increasing radar frequency. The percentage enhancement due to long waves ranges from 7% for L band to 850% for K band. ESA

N87-17299# Environmental Research Inst. of Michigan, Ann Arbor. Radar Science Lab.

AN IMPROVED METHOD FOR THE DETERMINATION OF WATER DEPTH FROM SURFACE WAVE REFRACTION PATTERNS **c48**

J. R. Bennett *In* ESA Proceedings of the 1986 International Geoscience and Remote Sensing Symposium (IGARSS '86) on Remote Sensing: Today's Solutions for Tomorrow's Information Needs, Volume 2 Aug. 1986 p 813-817 (For primary document see N87-17283 09-43)
(Contract N00014-84-C-2312)
Avail: NTIS HC A17/MF A01; ESA, Paris, France, 3 volume set $90 Member States, AU, CN, and NO (+20% others)

A mathematical model for using wave refraction observations to determine water depth from a synthetic aperture radar is presented. The model assumes that the waves are long-crested and obey linear theory, that the currents are negligible, and that there is a single dominant frequency. In principle, under these assumptions, the wavenumber magnitude alone is sufficient to determine the depth using the dispersion relation. However, observations of wavelength and direction do not necessarily obey the basic assumptions which lead to this relation. Therefore, before determining the depth from the dispersion relation, the model filters the data so that it is consistent with the theory. The method is tested against Seasat data. Results include the analysis of the expected error in mapping the depth for a given error in wavelength and the development of an algorithm for objectively analyzing an observed field of wavelength and direction data. This analysis provides a physically consistent field of wavenumber components which is close to the original data but which also obeys the law of conservation of waves and Snell's law. ESA

N87-17300# Physics and Electronics Lab. TNO, The Hague (Netherlands).

SEA WAVE MEASUREMENTS USING A SHIP'S RADAR **c48**

P. Hoogeboom, J. C. M. Kleijweg, and D. vanHalsema *In* ESA Proceedings of the 1986 International Geoscience and Remote Sensing Symposium (IGARSS '86) on Remote Sensing: Today's Solutions for Tomorrow's Information Needs, Volume 2 Aug. 1986 p 819-823 (For primary document see N87-17283 09-43)
Avail: NTIS HC A17/MF A01; ESA, Paris, France, 3 volume set $90 Member States, AU, CN, and NO (+20% others)

The capabilities of a shore based ship radar as an ocean wave sensor for short ranges up to 5 km were assessed. Radar data was recorded from a number of fixed points at the sea surface along the line of sight, during a certain time, giving a two dimensional dataset in time and place. By applying a spectral filter to the Fourier transformed data it is possible to improve the useful measurement range of the radar. The resulting spectra fit better to a traditional determined waveheight spectrum. This fit is further improved by multiplying the spectrum by f sq. The data sets were used to determine average water depth and water current in the direction of the radar by fitting the dispersion relation to the data. Only the water depth could be checked. A correlation coefficient of 0.96 is found. ESA

N87-17301# Ministry of Posts and Telecommunications, Ibaraki (Japan). Radio Research Labs.

MEASUREMENT OF SEA BACKSCATTER AT EXTREMELY LOW GRAZING ANGLE BY C-BAND DOPPLER RADAR **c48**

T. Iguchi, K. Nakamura, H. Fukuchi, T. Okuyama, K. Okamoto, and H. Mineno *In* ESA Proceedings of the 1986 International Geoscience and Remote Sensing Symposium (IGARSS '86) on Remote Sensing: Today's Solutions for Tomorrow's Information Needs, Volume 2 Aug. 1986 p 825-830 (For primary document see N87-17283 09-43)
Avail: NTIS HC A17/MF A01; ESA, Paris, France, 3 volume set $90 Member States, AU, CN, and NO (+20% others)

Backscattering from the sea surface of ground based C-band Doppler radar was measured over a 1 month period with horizontal polarization at grazing angle less than 0.5 deg. Characteristics of the received signal, such as the dependence of the received power on the distance, are discussed. The received powers are compared with the wave heights and the wind speeds. Doppler spectra were also calculated. The Doppler shift varies with the wind speed and its variation depends on the azimuth angle of radar and the wind direction. The Doppler bandwidth also depends on the wind speed but shows no dependence on the azimuth angle of the radar. ESA

N87-17302*# National Aeronautics and Space Administration. Goddard Space Flight Center, Greenbelt, Md.

EFFECTS OF SALINITY ON THE MICROWAVE EMISSION OF SOILS

T. J. Jackson (Agricultural Research Service, Beltsville, Md.) and P. E. ONeill *In* ESA Proceedings of the 1986 International Geoscience and Remote Sensing Symposium (IGARSS '86) on Remote Sensing: Today's Solutions for Tomorrow's Information Needs, Volume 2 Aug. 1986 p 833-837 (For primary document see N87-17283 09-43)

Avail: NTIS HC A17/MF A01; ESA, Paris, France, 3 volume set $90 Member States, AU, CN, and NO (+20% others) CSCL 08M

Controlled plot experiments were conducted to collect L and C band passive microwave data concurrent with ground observations of salinity and soil moisture. Two dielectric mixing models were used with an emission model to predict the emissivity from a bare smooth uniform profile. The models produce nearly identical results when near zero salinity is involved and reproduce the observed data at L band extremely well. Discrepancies at C band are attributed to sampling depth problems. Comparisons of predicted emissivities at various salinities with observed values indicate that the dynamic range of the emissivities can be explained using either of the dielectric mixing models. Evaluation of the entire data set, which included four salinity levels, indicates that for general application the effects of soil salinity can be ignored in interpreting microwave data for estimating soil moisture under most agricultural conditions. ESA

N87-17303*# National Aeronautics and Space Administration. Goddard Space Flight Center, Greenbelt, Md.

DISCRIMINATION OF SOIL HYDRAULIC PROPERTIES BY COMBINED THERMAL INFRARED AND MICROWAVE REMOTE SENSING

A. A. vandeGriend and P. E. ONeill *In* ESA Proceedings of the 1986 International Geoscience and Remote Sensing Symposium (IGARSS '86) on Remote Sensing: Today's Solutions for Tomorrow's Information Needs, Volume 2 Aug. 1986 p 839-845 Sponsored by the National Research Council (For primary document see N87-17283 09-43)

Avail: NTIS HC A17/MF A01; ESA, Paris, France, 3 volume set $90 Member States, AU, CN, and NO (+20% others) CSCL 08H

Using the De Vries models for thermal conductivity and heat capacity, thermal inertia was determined as a function of soil moisture for 12 classes of soil types ranging from sand to clay. A coupled heat and moisture balance model was used to describe the thermal behavior of the top soil, while microwave remote sensing was used to estimate the soil moisture content of the same top soil. Soil hydraulic parameters are found to be very highly correlated with the combination of soil moisture content and thermal inertia at the same moisture content. Therefore, a remotely sensed estimate of the thermal behavior of the soil from diurnal soil temperature observations and an independent remotely sensed estimate of soil moisture content gives the possibility of estimating soil hydraulic properties by remote sensing. ESA

N87-17304# Texas Instruments, Inc., Dallas.

THE EFFECT OF MEASUREMENT ERROR AND CONFUSION FROM VEGETATION ON PASSIVE MICROWAVE ESTIMATES OF SOIL MOISTURE

S. W. Theis and A. J. Blanchard *In* ESA Proceedings of the 1986 International Geoscience and Remote Sensing Symposium (IGARSS '86) on Remote Sensing: Today's Solutions for Tomorrow's Information Needs, Volume 2 Aug. 1986 p 847-851 (For primary document see N87-17283 09-43)

Avail: NTIS HC A17/MF A01; ESA, Paris, France, 3 volume set $90 Member States, AU, CN, and NO (+20% others)

The sensitivity of error in soil moisture estimates to passive microwave measurement error as a function of vegetation was studied using a simple model and measurements. Roughness confusion is not considered. The direct problem is defined as investigating the sensor response as the dependent variable to the parameter of interest while the inverse problem uses the parameter of interest as the dependent variable. The inverse method must be used for operational remote sensing applications. It is shown that this difference becomes very important when both confusion and measurement error are considered. A methodology whereby the sensitivity to measurement error attributed to vegetation can be estimated from the perpendicular vegetation index is presented. ESA

N87-17305# Helsinki Univ. of Technology, Espoo (Finland). Radio Lab.

CLASSIFICATION OF FOREST AND SURFACE TYPES BY SATELLITE MICROWAVE RADIOMETRY

M. Hallikainen and P. Jolma *In* ESA Proceedings of the 1986 International Geoscience and Remote Sensing Symposium (IGARSS '86) on Remote Sensing: Today's Solutions for Tomorrow's Information Needs, Volume 2 Aug. 1986 p 853-858 (For primary document see N87-17283 09-43)

Avail: NTIS HC A17/MF A01; ESA, Paris, France, 3 volume set $90 Member States, AU, CN, and NO (+20% others)

Scanning Multichannel Microwave Radiometer 10-GHz and 18-GHz data from Nimbus-7 were employed to investigate the classification of forest and surface types. Data for Falls 1978 and 1979 were compared against a digital map that shows 7 different forest and surface types for Southern Finland. The results indicate that four different categories can be discriminated: pine-dominant forest, other forest types (spruce-dominant and deciduous) and bogs, farmland, and water. ESA

N87-17306*# Texas Univ., Austin.

REMOTE SENSING OF TREE ATTENUATION AT 870 MHz ALONG SIMULATED EARTH-SATELLITE PATHS c32

W. J. Vogel, G. W. Torrence, J. Goldhirsh (Johns Hopkins Univ., Laurel, Md.), and J. R. Rowland *In* ESA Proceedings of the 1986 International Geoscience and Remote Sensing Symposium (IGARSS '86) on Remote Sensing: Today's Solutions for Tomorrow's Information Needs, Volume 2 Aug. 1986 p 861-866 Prepared for JPL (For primary document see N87-17283 09-43)

(Contracts JPL-956520; N00024-85-C-5301)

Avail: NTIS HC A17/MF A01; ESA, Paris, France, 3 volume set $90 Member States, AU, CN, and NO (+20% others) CSCL 20N

Tree attenuation at 870 MHz was studied using a helicopter as a source platform and a van with receiver and data acquisition instrumentation. Tree attenuation results were obtained with the van stationary and in motion to determine land mobile satellite systems link parameter requirements (expected fading due to roadside trees for mobile and stationary vehicles). Single tree attenuation results give worst case median fades as high as 15 dB although roadside tree values produce fades greater than 20 dB for small percentages of time. The cumulative fade distributions and their relative contributions as a function of path elevation angle, right side versus left side driving, and different road types are derived from the field measurements. ESA

N87-17307# Massachusetts Univ., Amherst. Dept. of Electrical and Computer Engineering.

A BACKSCATTERING MODEL FOR VARIOUS FOLIATED DECIDUOUS TREE TYPES AT MILLIMETER WAVELENGTHS c32

C. C. Borel and R. E. McIntosh *In* ESA Proceedings of the 1986 International Geoscience and Remote Sensing Symposium (IGARSS '86) on Remote Sensing: Today's Solutions for Tomorrow's Information Needs, Volume 2 Aug. 1986 p 867-872 (For primary document see N87-17283 09-43)

Avail: NTIS HC A17/MF A01; ESA, Paris, France, 3 volume set $90 Member States, AU, CN, and NO (+20% others)

A model for microwave backscatter from foliage in the frequency range from 35 to 215 GHz was developed using geometrical optics. The leaf is modeled as a segment of a thin spherical shell of dielectric material, made of a mixture of water and solid material. The normalized radar cross section is computed using probability density functions for the radius of curvature of the leaves. The position of the leaves is computed using fractal theory for the tree structure. The probabilistic leaf inclination angle distribution is assumed as one of five different types. A computer

simulation computes the normalized radar cross section (NRCS) for a small area of the tree viewed from an arbitrary point. The NRCS-pixels form a picture of the tree and indicate how the scattering intensity is a function of the position. The computations take shadowing and absorption into account. ESA

N87-17308# Deutsche Forschungs- und Versuchsanstalt fuer Luft- und Raumfahrt, Oberpfaffenhofen (West Germany). Inst. fuer Hochfrequenztechnik.

THE SIGNIFICANCE OF RADAR CROSS SECTION (RCS) POLARIZATION MEASUREMENTS FOR TREE SIGNATURES **c32**

A. J. Sieber *In* ESA Proceedings of the 1986 International Geoscience and Remote Sensing Symposium (IGARSS '86) on Remote Sensing: Today's Solutions for Tomorrow's Information Needs, Volume 2 Aug. 1986 p 873-878 (For primary document see N87-17283 09-43)

Avail: NTIS HC A17/MF A01; ESA, Paris, France, 3 volume set $90 Member States, AU, CN, and NO (+20% others)

Radar cross section L and X-band polarization measurements were used to evaluate the structure of tree crowns and to detect the nature of such types of volume scatterers. Further measurements are needed to analyze the various scatterers of trees, e.g., needles and branches. ESA

N87-17309*# Texas Univ., Arlington. College of Engineering.

A SCATTERING MODEL FOR DEFOLIATED VEGETATION **c32**

M. A. Karam and A. K. Fung *In* ESA Proceedings of the 1986 International Geoscience and Remote Sensing Symposium (IGARSS '86) on Remote Sensing: Today's Solutions for Tomorrow's Information Needs, Volume 2 Aug. 1986 p 879-881 (For primary document see N87-17283 09-43)

(Grant NAG5-486)

Avail: NTIS HC A17/MF A01; ESA, Paris, France, 3 volume set $90 Member States, AU, CN, and NO (+20% others) CSCL 20N

A scattering model for defoliated vegetation is conceived as a layer of dielectric, finite-length cylinders with specified size and orientation distributions above an irregular ground surface. The scattering phase matrix of a single cylinder is computed, then the radiative transfer technique is applied to link volume scattering from vegetation to surface scattering from the soil surface. Polarized and depolarized scattering are computed and the effects of the cylinder size and orientation distributions are illustrated. It is found that size and orientation distributions have significant effects on the backscattered signal. The model is compared with scattering from defoliated trees and agricultural crops. ESA

N87-17310# Karlsruhe Univ. (West Germany).

COHERENT POLARIMETRIC RADAR CROSS SECTION (RCS) MEASUREMENTS ON TREES **c32**

S. Riegger and W. Wiesbeck *In* ESA Proceedings of the 1986 International Geoscience and Remote Sensing Symposium (IGARSS '86) on Remote Sensing: Today's Solutions for Tomorrow's Information Needs, Volume 2 Aug. 1986 p 883-887 (For primary document see N87-17283 09-43)

Avail: NTIS HC A17/MF A01; ESA, Paris, France, 3 volume set $90 Member States, AU, CN, and NO (+20% others)

Measurement procedures and equipment to determine by a coherent measurement the radar cross section of details of forest plants, i.e., leaves and needles are shown. Measurements show that the frequency dependence of phase and amplitude of radar cross section (RCS) does not agree with most theoretical models. Investigations on picea abies branches demonstrate clearly the need for new theoretical models to establish significant RCS signature catalogs. ESA

N87-17311# Stuttgart Univ. (West Germany). Inst. of Navigation.

X AND L-BAND BACKSCATTERING MEASUREMENTS OF AGRICULTURAL CROPS, FOREST STANDS AND SINGLE TREES **c32**

Ph. Hartl, M. Reich, and S. Bhagavathula *In* ESA Proceedings of the 1986 International Geoscience and Remote Sensing Symposium (IGARSS '86) on Remote Sensing: Today's Solutions for Tomorrow's Information Needs, Volume 2 Aug. 1986 p 889-894 (For primary document see N87-17283 09-43)

Avail: NTIS HC A17/MF A01; ESA, Paris, France, 3 volume set $90 Member States, AU, CN, and NO (+20% others)

System configuration and operation of two scatterometers used for ground based measurements of trees and agricultural targets are outlined. Data acquisition procedures used in different campaigns, and calibrating are described. The flexibility of operating these systems with high data acquisition rates is emphasized. ESA

N87-17312# Environmental Research Inst. of Michigan, Ann Arbor. Radar Science Lab.

CALIBRATED X AND L-BAND SCATTERING COEFFICIENTS FROM A SOUTHERN US FOREST **c32**

E. S. Kasischke and R. W. Larson *In* ESA Proceedings of the 1986 International Geoscience and Remote Sensing Symposium (IGARSS '86) on Remote Sensing: Today's Solutions for Tomorrow's Information Needs, Volume 2 Aug. 1986 p 895-900 (For primary document see N87-17283 09-43)

(Contracts F19628-84-C-0081; DI-14-08-0001-21748)

Avail: NTIS HC A17/MF A01; ESA, Paris, France, 3 volume set $90 Member States, AU, CN, and NO (+20% others)

Calibrated X and L-band (VV) SAR radar scattering coefficients (sigma zero) from 23 test sites located in a forest are presented. The scattering coefficients are correlated to forest/tree parameters. Correlations between L-band sigma zero and tree height for the pine stands, L-band sigma zero and stems/acre for the deciduous stands, and X-band sigma zero and basal area for the deciduous stands are found. ESA

N87-17313# INTERA Environmental Consultants Ltd., Ottawa (Ontario).

SAR IMAGERY FOR FOREST MANAGEMENT **c32**

R. T. Lowry, P. Vaneck, and R. V. Dams *In* ESA Proceedings of the 1986 International Geoscience and Remote Sensing Symposium (IGARSS '86) on Remote Sensing: Today's Solutions for Tomorrow's Information Needs, Volume 2 Aug. 1986 p 901-906 (For primary document see N87-17283 09-43)

Avail: NTIS HC A17/MF A01; ESA, Paris, France, 3 volume set $90 Member States, AU, CN, and NO (+20% others)

A high resolution, digital, airborne, HH polarized, X-band SAR was tested for forest management. The SAR was compared with conventional panchromatic aerial photography in terms of information content, aerial coverage and costs; and with existing forest cover-type maps in which vegetation types, tree density, and height classes are provided. The evaluation of clearcut areas and other types of forestry and industry environmental effects (e.g., loss of timber volume through extensive seismic line clearing activities) was also assessed. Results show that if suitable base maps do not exist, they can be derived from SAR imagery; broad forestry inventories can be developed; and changing land use patterns can be mapped and existing inventories updated. The SAR is inferior to photography for classifications, but is not weather dependent. ESA

N87-17314# Toba Merchant Marine Coll. (Japan).

ESTIMATION OF MAXIMUM SNOW VOLUME DISTRIBUTION USING NOAA-AVHRR DATA

S. Takeuchi, K. Takeda, H. Ochiai, and T. Seki *In* ESA Proceedings of the 1986 International Geoscience and Remote Sensing Symposium (IGARSS '86) on Remote Sensing: Today's Solutions for Tomorrow's Information Needs, Volume 2 Aug. 1986 p 909-914 (For primary document see N87-17283 09-43)

Avail: NTIS HC A17/MF A01; ESA, Paris, France, 3 volume set $90 Member States, AU, CN, and NO (+20% others)

Snow volume was represented as snow water equivalent value at the maximum stage obtained by combining the extraction of snow-nonsnow boundary mesh from AVHRR images and the degree day method. The maximum snow water equivalent at a certain snow boundary mesh is calculated by the degree day method using daily average air temperature data of the nearest neighbor weather station. The estimated snow water equivalent

values are extended to maps covering the whole area of north-east Japan. Case studies show the usefulness of satellite data for yearly monitoring of snow volume distribution which extends over several tens of thousands of square kilometers. ESA

N87-17315*# National Aeronautics and Space Administration. Goddard Space Flight Center, Greenbelt, Md.
SNOW PROPERTY MEASUREMENTS CORRELATIVE TO MICROWAVE EMISSION AT 35 GHz
R. E. Davis (California Univ., Santa Barbara.), J. Dozier, and A. T. C. Chang *In* ESA Proceedings of the 1986 International Geoscience and Remote Sensing Symposium (IGARSS '86) on Remote Sensing: Today's Solutions for Tomorrow's Information Needs, Volume 2 Aug. 1986 p 915-920 (For primary document see N87-17283 09-43)
Avail: NTIS HC A17/MF A01; ESA, Paris, France, 3 volume set $90 Member States, AU, CN, and NO (+20% others) CSCL 08L

Snow microstructure, measured by plane section analysis, and snow wetness, measured by the dilution method, are used to calculate input parameters for a microwave emission model that uses the radiative transfer method. The scattering and absorbing properties are calculated by Mie theory. The effects of different equivalent sphere conversions, adjustments for near-field interference, and different snow wetness characterizations are compared for various snow conditions. The concentric shell geometry of liquid water in snow yields higher emissivities and better model results than the separate-sphere configuration for liquid water contents greater than 0.05, while at lower liquid water contents the separate-sphere treatment gives better results. ESA

N87-17316# Zurich Univ. (Switzerland). Dept. of Geography.
SNOW COVER RECESSION IN AN ALPINE ECOLOGICAL SYSTEM
M. Keller and K. Seidel (Eidgenoessische Technische Hochschule, Zurich, Switzerland) *In* ESA Proceedings of the 1986 International Geoscience and Remote Sensing Symposium (IGARSS '86) on Remote Sensing: Today's Solutions for Tomorrow's Information Needs, Volume 2 Aug. 1986 p 921-924 (For primary document see N87-17283 09-43)
Avail: NTIS HC A17/MF A01; ESA, Paris, France, 3 volume set $90 Member States, AU, CN, and NO (+20% others)

In the Man and Biosphere project, an ecological survey in a high Alpine valley was carried out. Data from climatology, forestry, game biology, land use history, pedology, and vegetation were assembled into a Geographic Information System. A LANDSAT based snow cover recession map is found to be a fundamental variable influencing a number of layers within the ecological data set. It is shown quantitatively, for example, how snow cover recession and floral associations are related. This assists in vegetation mapping and can be used to simulate vegetation. ESA

N87-17317# Zurich Univ. (Switzerland). Dept. of Geography.
TOWARDS SNOWMELT RUNOFF FORECAST USING LANDSAT-MSS AND NOAA/AVHRR DATA
M. F. Baumgartner, K. Seidel (Eidgenoessische Technische Hochschule, Zurich, Switzerland), and J. Martinec (Eidgenoessisches Inst. fuer Schnee- und Lawinenforschung, Weissfluhjoch/Davos, Switzerland) *In* ESA Proceedings of the 1986 International Geoscience and Remote Sensing Symposium (IGARSS '86) on Remote Sensing: Today's Solutions for Tomorrow's Information Needs, Volume 2 Aug. 1986 p 925-928 (For primary document see N87-17283 09-43)
Avail: NTIS HC A17/MF A01; ESA, Paris, France, 3 volume set $90 Member States, AU, CN, and NO (+20% others)

Digital snow cover mapping by NOAA/AVHRR to assist snowmelt runoff forecasting from LANDSAT MSS data is discussed. It is shown how remote sensing information from LANDSAT-MSS and NOAA/AVHRR supplement each other. When using coarse spatial sensor resolution, special attention to the area, topography, and amount of snow coverage must be paid. ESA

N87-17318*# National Aeronautics and Space Administration. Goddard Space Flight Center, Greenbelt, Md.
DEPENDENCE OF SNOW MELTING AND SURFACE-ATMOSPHERE INTERACTIONS ON THE FOREST STRUCTURE
J. Ottermann (Tel-Aviv Univ, Israel), K. Staenz (Zurich Univ., Switzerland), K. I. Itten, and G. Kukla (Lamont-Doherty Geological Inst., Palisades, N.Y.) *In* ESA Proceedings of the 1986 International Geoscience and Remote Sensing Symposium (IGARSS '86) on Remote Sensing: Today's Solutions for Tomorrow's Information Needs, Volume 2 Aug. 1986 p 929-932 (For primary document see N87-17283 09-43)
(Grant NSF ATM-85-05558)
Avail: NTIS HC A17/MF A01; ESA, Paris, France, 3 volume set $90 Member States, AU, CN, and NO (+20% others) CSCL 02F

The surface albedo and the surface roughness for forested areas with snow on the ground are expressed in terms of the tree silhouette parameter, the projection on the vertical plane of trees per unit area. The absorption of insolation (direct solar beam) is quantitatively described for a horizontal snow surface with vertical tree trunks, stressing the role of the bark at snow level as triggering the snowmelt. ESA

N87-17319# Oslo Univ. (Norway). Dept. of Geography.
A CLIMATOLOGICAL-HYDROLOGICAL STUDY OF LAKE ICE IN THE SOUTHWESTERN MOUNTAIN AREA IN NORWAY BY USE OF SATELLITE SENSING
J. E. Skorve *In* ESA Proceedings of the 1986 International Geoscience and Remote Sensing Symposium (IGARSS '86) on Remote Sensing: Today's Solutions for Tomorrow's Information Needs, Volume 2 Aug. 1986 p 933-938 (For primary document see N87-17283 09-43)
Avail: NTIS HC A17/MF A01; ESA, Paris, France, 3 volume set $90 Member States, AU, CN, and NO (+20% others)

Snow and lake ice melting in a 63,000 sqkm area of the southwestern mountains in Norway was studied by use of cloud-free LANDSAT imagery obtained during the period 1975-83. Results confirm the utility of satellite imagery for water management in remote areas, and confirm that snow cover is the single most important parameter in lake ice melting. ESA

N87-17320# Stuttgart Univ. (West Germany). Inst. fuer Navigation.
FUTURE USER REQUIREMENTS AND REQUIRED TECHNOLOGICAL DEVELOPMENTS OF SPACEBORNE SYNTHETIC APERTURE RADARS c32
Ph. Hartl and H. M. Braun (Dornier-Werke G.m.b.H., Friedrichshafen, West Germany) *In* ESA Proceedings of the 1986 International Geoscience and Remote Sensing Symposium (IGARSS '86) on Remote Sensing: Today's Solutions for Tomorrow's Information Needs, Volume 2 Aug. 1986 p 941-946 (For primary document see N87-17283 09-43)
Avail: NTIS HC A17/MF A01; ESA, Paris, France, 3 volume set $90 Member States, AU, CN, and NO (+20% others)

The ERS-1 and SIR-C SAR systems are introduced. Attempts to meet future user requirements by developing a long antenna, wide swath SAR and a multimode SAR are reviewed. Trends in SAR antennas, high power amplifiers, and real time SAR processing are discussed. ESA

N87-17321# Dornier-Werke G.m.b.H., Friedrichshafen (West Germany).
THE X-BAND SAR IN A JOINT MISSION WITH THE SHUTTLE IMAGING RADAR c32
W. Gils and H. Hoelzl *In* ESA Proceedings of the 1986 International Geoscience and Remote Sensing Symposium (IGARSS '86) on Remote Sensing: Today's Solutions for Tomorrow's Information Needs, Volume 2 Aug. 1986 p 947-951 (For primary document see N87-17283 09-43)
Avail: NTIS HC A17/MF A01; ESA, Paris, France, 3 volume set $90 Member States, AU, CN, and NO (+20% others)

The Shuttle-borne X-band synthetic aperture radar (X-SAR) is described. It will operate together with NASA radars working at L and C-band. Simultaneous operation gives experimenters the opportunity to investigate the spectral reflectivity of different objects at 3 frequencies (1.3 GHz, 5.3 GHz, and 9.6 GHz). Many combina-

tions of polarization and incidence angle are available. Nominal orbit altitude for operation is 255 km. The X-SAR will provide geometrical resolution of 30 m and a swath of 15 to 35 km. Constraints result mainly from the 45 Mbps maximum data rate transmittable by the orbiter. The analogous video signals will be 4+4 or 6+6 bit quantized with a 20 dB adjustable dynamic range. To adapt the instrument to different geometrical conditions, the system bandwith is switchable. The X-SAR and SIR have different ground segments. ESA

N87-17322# Marconi Space and Defence Systems Ltd., Portsmouth (England).
AN ADVANCED SAR DESIGN FOR FUTURE LAND MISSIONS c32
F. G. Sawyer and M. A. Brown *In* ESA Proceedings of the 1986 International Geoscience and Remote Sensing Symposium (IGARSS '86) on Remote Sensing: Today's Solutions for Tomorrow's Information Needs, Volume 2 Aug. 1986 p 953-958 Sponsored by ESA/ESTEC (For primary document see N87-17283 09-43)
Avail: NTIS HC A17/MF A01; ESA, Paris, France, 3 volume set $90 Member States, AU, CN, and NO (+20% others)

A multiple swath C-band SAR with swath width greater than 350 km is proposed. Swaths are contiguous across the coverage region and it is possible to realise coverage of 20 to 45 deg by the use of two swaths. Operation may be on either or both of these swaths. Platform resource limitations restrict the overall performance envelope and hence it is possible to select the particular mode of operation to optimize against the selected performance criteria. Means of extending the design to provide dual frequency operation are discussed. ESA

N87-17323# Deutsche Forschungs- und Versuchsanstalt fuer Luft- und Raumfahrt, Oberpfaffenhofen (West Germany). Inst. fuer Hochfrequenztechnik.
RADAR CROSS SECTION (RCS) DATA BASE DEDUCED FROM RADAR IMAGES c32
A. J. Sieber *In* ESA Proceedings of the 1986 International Geoscience and Remote Sensing Symposium (IGARSS '86) on Remote Sensing: Today's Solutions for Tomorrow's Information Needs, Volume 2 Aug. 1986 p 959-964 (For primary document see N87-17283 09-43)
Avail: NTIS HC A17/MF A01; ESA, Paris, France, 3 volume set $90 Member States, AU, CN, and NO (+20% others)

The creation of radar cross section (RCS) catalogs using existing radar images is discussed. Analysis of SIR-B images shows that spatial resolution has a significant impact on the radar data information content. Interpretation of radar data must be based on physical reasonable models, which are not just mean RCS models. Therefore, for an RCS data catalog model assumptions, e.g., expressed by parameterized distribution functions, are to be included. Such parameterized distributions could belong to the group of K-distributions which would provide not only the mean-value and the variance of the distribution function but moreover a parameter, characterizing the shape of the function. This parameter can be directly explained by a physical scattering process. ESA

N87-17324# INTERA Environmental Consultants Ltd., Ottawa (Ontario).
THERMAL INFRARED REMOTE SENSING: ONE OF TODAY'S SOLUTIONS
J. P. Tracey and G. R. Lawrence *In* ESA Proceedings of the 1986 International Geoscience and Remote Sensing Symposium (IGARSS '86) on Remote Sensing: Today's Solutions for Tomorrow's Information Needs, Volume 2 Aug. 1986 p 967-973 (For primary document see N87-17283 09-43)
Avail: NTIS HC A17/MF A01; ESA, Paris, France, 3 volume set $90 Member States, AU, CN, and NO (+20% others)

Airborne thermal infrared linescanning programs for environmental and engineering applications are summarized. Individual airborne thermal surveys are discussed with pertinent logistics described for each. Thermal infrared imagery for specific applications is included. It is shown how operational thermal imaging linescanning programs are utilized to satisfy the requirements of resource and utility managers. ESA

N87-17325# Tokyo Univ. (Japan).
MODELS FOR TEMPERATURE ESTIMATION FROM REMOTELY SENSED THERMAL IR DATA
S. Fujimura and T. Yokota *In* ESA Proceedings of the 1986 International Geoscience and Remote Sensing Symposium (IGARSS '86) on Remote Sensing: Today's Solutions for Tomorrow's Information Needs, Volume 2 Aug. 1986 p 975-980 (For primary document see N87-17283 09-43)
Avail: NTIS HC A17/MF A01; ESA, Paris, France, 3 volume set $90 Member States, AU, CN, and NO (+20% others)

The accuracy of the temperatures estimated from remotely sensed thermal IR data was evaluated by comparison with ground measurements. A relation between them is derived from a simple physical model, on which the evaluation should be based. The atmosphere is represented by a thin layer with a transmittance and an effective temperature. Four kinds of models slightly modified from one to another are considered. The regression coefficients obtained through regression analysis by taking the estimated temperature as dependent variable, and the measured one as independent variable are discussed. It is shown for all the models that the regression coefficient should be less than 1. Most of actual data taken over the sea satisfy this relation. ESA

N87-17326# Catania Univ. (Italy). Dept. of Engineering.
THERMAL INFRARED IMAGERY FROM HELICOPTER FOR HEAT LOSS CALCULATIONS IN INDUSTRIAL PLANTS
A. L. Geraci and S. Crimi *In* ESA Proceedings of the 1986 International Geoscience and Remote Sensing Symposium (IGARSS '86) on Remote Sensing: Today's Solutions for Tomorrow's Information Needs, Volume 2 Aug. 1986 p 981-986 (For primary document see N87-17283 09-43)
Avail: NTIS HC A17/MF A01; ESA, Paris, France, 3 volume set $90 Member States, AU, CN, and NO (+20% others)

An airborne maritime surveillance system was flown on a helicopter over an industrial plant to demonstrate its usefulness for energy conservation. More than 600 thermal infrared images, acquired in 3 different periods of time, were used for the mosaic of the study area. Data were analyzed using computer-assisted interpretation of digitized aerial imagery. The results prove the usefulness of the system used for calculating the heat losses and the energy distribution of the plant. ESA

N87-17327# Purdue Univ., West Lafayette, Ind. School of Electrical Engineering.
PARAMETER SPACE TECHNIQUES FOR IMAGE REGISTRATION
P. Anuta and C. McGillem *In* ESA Proceedings of the 1986 International Geoscience and Remote Sensing Symposium (IGARSS '86) on Remote Sensing: Today's Solutions for Tomorrow's Information Needs, Volume 2 Aug. 1986 p 989-994 (For primary document see N87-17283 09-43)
(Grant NSF ECS-82-15539)
Avail: NTIS HC A17/MF A01; ESA, Paris, France, 3 volume set $90 Member States, AU, CN, and NO (+20% others)

Three methods using parameter space analysis for image registration are compared. The first is a direct correlation of gray tone image patches. The second is a correlation of edge images derived from the image pair to be registered. The third is the parameter space method in which intersecting line segments are located in the two images. The methods are also tested on LANDSAT multispectral scanner and thematic mapper imagery. It is shown that the performance of the three methods is roughly equivalent for high signal-to-noise ratios but that the parameter space method is more robust at low ratios. ESA

N87-17328# Consiglio Nazionale delle Ricerche, Florence (Italy).
DIGITAL TECHNIQUES FOR NOISE REDUCTION IN AUTOMATIC PICTURE TRANSMISSION (APT) NOAA SATELLITE IMAGES c33
R. Carla, V. M. Sacco, and S. Baronti *In* ESA Proceedings of the

1986 International Geoscience and Remote Sensing Symposium (IGARSS '86) on Remote Sensing: Today's Solutions for Tomorrow's Information Needs, Volume 2 Aug. 1986 p 995-1000 (For primary document see N87-17283 09-43)
Avail: NTIS HC A17/MF A01; ESA, Paris, France, 3 volume set $90 Member States, AU, CN, and NO (+20% others)

Noise reduction filters were tested using NOAA satellite images. The best results, in terms of noise suppression and blur attenuation are obtained by two kinds of digital filtering techniques: weighted median filter with central pixel weight = 3 and decision threshold = 12; and extremal filter with maximum number of extremal pixels=3. The other kinds of techniques show a nonuniform behavior, mainly in terms of noise pixel leaving. Both the filters were used in iterative mode: the weighted median filter needs fewer iterations to reach a stable condition than the extremal filter. However the mean computing time per iteration of the extremal filter is 30% less than the weighted filter time. ESA

N87-17329# Kanazawa Univ. (Japan).
RADIOMETRIC CORRECTION METHOD WHICH REMOVES BOTH ATMOSPHERIC AND TOPOGRAPHIC EFFECTS FROM THE LANDSAT-MSS DATA
Y. Kawata, S. Ueno, and T. Kusaka *In* ESA Proceedings of the 1986 International Geoscience and Remote Sensing Symposium (IGARSS '86) on Remote Sensing: Today's Solutions for Tomorrow's Information Needs, Volume 2 Aug. 1986 p 1001-1004 (For primary document see N87-17283 09-43)
Avail: NTIS HC A17/MF A01; ESA, Paris, France, 3 volume set $90 Member States, AU, CN, and NO (+20% others)

A radiometric correction method which can remove atmospheric and topographic effects from rugged terrain image data remotely sensed by LANDSAT was applied to a mountainous test site where digital terrain data is available. The values of necessary atmospheric parameters, such as the optical thickness, the single scattering albedo, and the turbidity factor of the atmosphere were derived from LOWTRAN 5 Code in the evaluation of scattering and transmission functions. Lambert's law of reflection on the ground surface is assumed. Results are satisfactory. ESA

N87-17330# European Space Agency, Paris (France).
SHAPE SIMILARITY IN REMOTE SENSING IMAGES USING GRAPH MATCHING TECHNIQUES
S. Fernandez *In its* Proceedings of the 1986 International Geoscience and Remote Sensing Symposium (IGARSS '86) on Remote Sensing: Today's Solutions for Tomorrow's Information Needs, Volume 2 Aug. 1986 p 1005-1009 (For primary document see N87-17283 09-43)
Avail: NTIS HC A17/MF A01; ESA, Paris, France, 3 volume set $90 Member States, AU, CN, and NO (+20% others)

A method to detect loosely defined objects in a remotely sensed image is described. The objects are two dimensional in nature and have a graph structure given by the linear features found in most of the available images. The procedure extracts a condensed description of the image in terms of graphs through edge detection, edge thinning, and edge following to detect points of intersection and of maximal curvature. Given a similar description of an object, a graph matching algorithm with forward checking and backtracking is used to find the matching subgraph, based on the accumulated error in the angles between adjacent nodes as a measure of dissimilarity. ESA

N87-17331# Massachusetts Inst. of Tech., Cambridge.
AN ITERATIVE MULTI-RESOLUTION SHAPE-FROM-SHADING ALGORITHM AND ITS APPLICATION TO PLANETARY MAPPING
P. L. VanHove and M. J. Carlotto (Analytic Sciences Corp., Reading, Mass.) *In* ESA Proceedings of the 1986 International Geoscience and Remote Sensing Symposium (IGARSS '86) on Remote Sensing: Today's Solutions for Tomorrow's Information Needs, Volume 2 Aug. 1986 p 1011-1016 (For primary document see N87-17283 09-43)
Avail: NTIS HC A17/MF A01; ESA, Paris, France, 3 volume set $90 Member States, AU, CN, and NO (+20% others)

Experimentation with an algorithm for reconstructing the 3-D structure of a scene from a single image is reported. The algorithm is the synthesis of a two-step reconstruction of elevation maps with multiresolution iterative algorithms. Performance of the algorithm is assessed on synthetic test imagery. Convergence to metric accuracy is obtained only after large numbers of iterations, and is affected by image size and illumination conditions. Initial reconstructions for an impact crater and a mesa on Mars from Viking orbiter imaging are presented. ESA

N87-17332# Indiana State Univ., Terre Haute.
IRSAP: AN IMPROVED APPROACH IN PROCESSING REMOTELY SENSED DATA
M. P. Bishop, K. Lulla, and P. Mausel *In* ESA Proceedings of the 1986 International Geoscience and Remote Sensing Symposium (IGARSS '86) on Remote Sensing: Today's Solutions for Tomorrow's Information Needs, Volume 2 Aug. 1986 p 1017-1021 (For primary document see N87-17283 09-43)
Avail: NTIS HC A17/MF A01; ESA, Paris, France, 3 volume set $90 Member States, AU, CN, and NO (+20% others)

A software accessing package named Interactive Remote Sensing Applications Package (IRSAP) was developed to rectify lack of interaction between software which when used together promotes synergism, flexibility, and efficiency for complex analyses in remote sensing/geographical information systems applications. The IRSAP software system is modular in design with menu driven architecture. The software system allows for easy integration of new application programs and software modules with existing system software. Its implementation allows users to process remotely sensed data in one processing environment even when accessing other software packages. Consequently, users need not contact programming staff in order to access other software packages, or have previous computer science background in order to process remotely sensed data. ESA

N87-17333# Johns Hopkins Univ., Laurel, Md. Applied Physics Lab.
CHARACTERISTICS OF A VERY LOW ALTITUDE SPACECRAFT FOR COLLECTING GLOBAL DIRECTIONAL WAVE SPECTRA WITH SPACEBORNE SYNTHETIC APERTURE RADAR **c48**
R. C. Beal *In* ESA Proceedings of the 1986 International Geoscience and Remote Sensing Symposium (IGARSS '86) on Remote Sensing: Today's Solutions for Tomorrow's Information Needs, Volume 2 Aug. 1986 p 1025-1029 (For primary document see N87-17283 09-43)
Avail: NTIS HC A17/MF A01; ESA, Paris, France, 3 volume set $90 Member States, AU, CN, and NO (+20% others)

To assess the importance of spacecraft altitude on SAR azimuth wave detectability in realistic seas, an empirically determined azimuth wavenumber limit was combined with typical winter wave climatological data. A cumulative probability of azimuth wave attenuation as a function of spacecraft altitude indicates that, for the winter North Atlantic, azimuth wave detection begins to degrade for a spacecraft altitude as low as 200 km. The degradation becomes substantial (greater than 30% probability) around 300 km, and is essentially complete (greater than 95% probability) at 600 km altitude and higher. The results indicate that spaceborne SAR's should be placed in orbits no higher than 275 km to yield useful directional wave spectra, and probably should be combined with a radar ocean wave spectrometer to be most effective. ESA

N87-17334# Johns Hopkins Univ., Laurel, Md. Applied Physics Lab.
THE SAR IMAGE MODULATION TRANSFER FUNCTION DERIVED FROM SIR-B IMAGE SPECTRA AND AIRBORNE MEASUREMENTS OF OCEAN WAVE HEIGHT SPECTRA **c48**
F. Monaldo *In* ESA Proceedings of the 1986 International Geoscience and Remote Sensing Symposium (IGARSS '86) on Remote Sensing: Today's Solutions for Tomorrow's Information Needs, Volume 2 Aug. 1986 p 1031-1035 (For primary document see N87-17283 09-43)
Avail: NTIS HC A17/MF A01; ESA, Paris, France, 3 volume set $90 Member States, AU, CN, and NO (+20% others)

Using a procedure to estimate ocean height-variance spectra from SAR imagery, imagery from the SIR-B experiment is used to estimate directional ocean wave spectra. Comparison of these spectra with independent airborne wave spectra estimates indicate that a SAR is capable of producing relative height-variance spectra. It is also capable of producing height-variance spectra in absolute units. ESA

N87-17335# Marconi Co. Ltd., Chelmsford (England).
SIR-B OBSERVATIONS OF OCEAN WAVES IN THE NE ATLANTIC **c48**
J. T. Macklin, R. A. Cordey, and G. E. Keyte *In* ESA Proceedings of the 1986 International Geoscience and Remote Sensing Symposium (IGARSS '86) on Remote Sensing: Today's Solutions for Tomorrow's Information Needs, Volume 2 Aug. 1986 p 1037-1041 (For primary document see N87-17283 09-43)
Avail: NTIS HC A17/MF A01; ESA, Paris, France, 3 volume set $90 Member States, AU, CN, and NO (+20% others)

Synthetic-aperture radar (SAR) imagery from Shuttle Imaging Radar was obtained over a deep-water site in the NE Atlantic Ocean. Wave spectra derived from 2 almost orthogonal passes, separated by 6 hr, were compared with simultaneous wave-buoy observations in order to test the predictions of wave-imaging theories. Although azimuth-traveling waves were detected in the second pass, the discrepancy between the SAR and buoy wave spectra is almost an order of magnitude. It is suggested that the velocity-bunching mechanism predicted for azimuth-traveling waves is incorrectly described by the theories. ESA

N87-17336*# Johns Hopkins Univ., Laurel, Md. Applied Physics Lab.
DERIVING TWO-DIMENSIONAL OCEAN WAVE SPECTRA AND SURFACE HEIGHT MAPS FROM THE SHUTTEL IMAGING RADAR (SIR-B) **c48**
D. G. Tilley *In* ESA Proceedings of the 1986 International Geoscience and Remote Sensing Symposium (IGARSS '86) on Remote Sensing: Today's Solutions for Tomorrow's Information Needs, Volume 2 Aug. 1986 p 1043-1049 Sponsored by NASA (For primary document see N87-17283 09-43)
Avail: NTIS HC A17/MF A01; ESA, Paris, France, 3 volume set $90 Member States, AU, CN, and NO (+20% others) CSCL 08C

Directional ocean wave spectra were derived from Shuttle Imaging Radar (SIR-B) imagery in regions where nearly simultaneous aircraft-based measurements of the wave spectra were also available as part of the NASA Shuttle Mission 41G experiments. The SIR-B response to a coherently speckled scene is used to estimate the stationary system transfer function in the 15 even terms of an eighth-order two-dimensional polynomial. Surface elevation contours are assigned to SIR-B ocean scenes Fourier filtered using a empirical model of the modulation transfer function calibrated with independent measurements of wave height. The empirical measurements of the wave height distribution are illustrated for a variety of sea states. ESA

N87-17337# Johns Hopkins Univ., Laurel, Md. Applied Physics Lab.
SPATIAL EVOLUTION OF WAVE SPECTRA IN THE VICINITY OF THE AGULHAS CURRENT FROM SIR-B **c48**
D. E. Irvine *In* ESA Proceedings of the 1986 International Geoscience and Remote Sensing Symposium (IGARSS '86) on Remote Sensing: Today's Solutions for Tomorrow's Information Needs, Volume 2 Aug. 1986 p 1051-1053 (For primary document see N87-17283 09-43)
Avail: NTIS HC A17/MF A01; ESA, Paris, France, 3 volume set $90 Member States, AU, CN, and NO (+20% others)

The SIR-B Agulhas (Southern Africa) experiment studied the propagation of swell across a major current as a test of technique and to understand the swell-related background to the Giant Wave problem. Image spectra, interpreted as wave spectra, show two distinct wave systems. One, evidently heading upstream, is tentatively identified as a trapped wave. ESA

N87-17338# Environmental Research Inst. of Michigan, Ann Arbor. Radar Science Lab.
CHARACTERISATION OF INTERNAL WAVE SURFACE PATTERNS ON AIRBORNE SAR IMAGERY **c48**
E. S. Kasischke *In* ESA Proceedings of the 1986 International Geoscience and Remote Sensing Symposium (IGARSS '86) on Remote Sensing: Today's Solutions for Tomorrow's Information Needs, Volume 2 Aug. 1986 p 1055-1060 (For primary document see N87-17283 09-43)
(Contract N00014-81-C-0692)
Avail: NTIS HC A17/MF A01; ESA, Paris, France, 3 volume set $90 Member States, AU, CN, and NO (+20% others)

Techniques to characterize the signatures of surface patterns associated with oceanic international waves which appear on X and L-band, airborne SAR imagery collected during the SAR international wave imaging experiment (SARSEX) are presented. This data set shows that commonly-held conceptions concerning SAR detection of internal waves may need reevaluation. The SAR clearly images azimuth-traveling waves during SARSEX, and in some cases the X-band internal wave signature was stronger than the L-band signature. ESA

N87-17339# National Oceanic and Atmospheric Administration, Boulder, Colo. Wave Propagation Lab.
GROUND-BASED MICROWAVE RADIOMETRIC OBSERVATIONS OF ATMOSPHERIC GEOPOTENTIAL HEIGHT FLUCTUATIONS **c46**
E. R. Westwater, A. J. Bedard, P. Ciotti (Rome Univ., Italy), and M. T. Decker (Colorado Univ., Boulder) *In* ESA Proceedings of the 1986 International Geoscience and Remote Sensing Symposium (IGARSS '86) on Remote Sensing: Today's Solutions for Tomorrow's Information Needs, Volume 2 Aug. 1986 p 1063-1068 (For primary document see N87-17283 09-43)
Avail: NTIS HC A17/MF A01; ESA, Paris, France, 3 volume set $90 Member States, AU, CN, and NO (+20% others)

A ground-based, zenith viewing microwave radiometer was designed to measure precipitable water vapor, cloud liquid, and temperature profiles. It has two moisture-sensing channels and four temperature-sounding channels. Data are used to derive geopotential heights and thicknesses from the surface (830 mb) to 300 mb. Time series and spectra of directly measured and inferred quantities are analyzed for three meteorological situations: a period of unusual calm, a frontal passage, and a wave event. Comparisons of these data with various sources of ground truth, including radiosondes, aircraft, satellite cloud observations, and arrays of microbarographs, show excellent agreement. ESA

N87-17340*# Minnesota Univ., Minneapolis. Dept. of Physics and Astronomy.
MICROWAVE RADIANCES FROM HORIZONTALLY FINITE PRECIPITATING CLOUDS CONTAINING ICE AND LIQUID HYDROMETEORS **c47**
C. Kummerow and J. A. Weinman (Wisconsin Univ., Madison) *In* ESA Proceedings of the 1986 International Geoscience and Remote Sensing Symposium (IGARSS '86) on Remote Sensing: Today's Solutions for Tomorrow's Information Needs, Volume 2 Aug. 1986 p 1069-1075 (For primary document see N87-17283 09-43)
(Grants NAG5-580; N00014-86-K-2001)
Avail: NTIS HC A17/MF A01; ESA, Paris, France, 3 volume set $90 Member States, AU, CN, and NO (+20% others) CSCL 04B

Microwave radiances that would be measured from satellite borne radiometers were computed as a function of rainfall rates from horizontally finite precipitating clouds containing ice and liquid hydrometeors capped by a layer of nonprecipitating ice that covers the remainder of the footprint. Ice at the top of the precipitating clouds depresses the brightness temperatures which depend on rainfall rates because the ice hydrometeor concentrations are assumed to be related to the rainfall rates at the cloud base. It is also found that the brightness temperatures of footprints partially covered by precipitation cells are a nonlinear function of the rainfall rate averaged over the footprint. Thus the average brightness

temperatures depend on the peak rainfall rates and the size of the precipitating cloud. ESA

N87-17341# Universite Catholique de Louvain (Belgium). Lab. de Telecommunications et d'Hyperfrequences.
A TWO-STEP ALGORITHM FOR THE SEPARATE RETRIEVAL OF OCEAN SURFACE AND ATMOSPHERIC PARAMETERS FROM MICROWAVE RADIOMETERS c61
A. Guissard, P. Sobieski, and A. M. Guillaume *In* ESA Proceedings of the 1986 International Geoscience and Remote Sensing Symposium (IGARSS '86) on Remote Sensing: Today's Solutions for Tomorrow's Information Needs, Volume 2 Aug. 1986 p 1077-1082 (For primary document see N87-17283 09-43)
Avail: NTIS HC A17/MF A01; ESA, Paris, France, 3 volume set $90 Member States, AU, CN, and NO (+20% others)

An algorithm for passive microwave remote sensing of the ocean through the atmosphere is proposed. It is based on a contracted form of the radiative transfer equation and on an iterative two-step procedure, such that the extraction of the sea surface parameters and of the atmospheric parameters can be performed separately to a first approximation. Tests on synthetic measurements show that the algorithm is stable, converges rapidly, is independent of the first guess, and works properly in the presence of realistic instrumental errors. The method applies to a rough open sea and will be extended to include foam effects. ESA

N87-17342# Helsinki Univ. of Technology, Espoo (Finland). Radio Lab.
RETRIEVAL OF NEAR-SURFACE WIND SPEED IN THE BALTIC SEA FROM NIMBUS-7 SCANNING MULTICHANNEL MICROWAVE RADIOMETER (SMMR) OBSERVATIONS c47
M. Hallikainen, T. Tolmunen, and P. Talmola *In* ESA Proceedings of the 1986 International Geoscience and Remote Sensing Symposium (IGARSS '86) on Remote Sensing: Today's Solutions for Tomorrow's Information Needs, Volume 2 Aug. 1986 p 1083-1088 (For primary document see N87-17283 09-43)
Avail: NTIS HC A17/MF A01; ESA, Paris, France, 3 volume set $90 Member States, AU, CN, and NO (+20% others)

Retrieval of near-surface wind speed in semienclosed seas from NIMBUS-7 Scanning Multichannel Microwave Radiometer (SMMR) data was investigated. The effects of antenna sidelobes over land and those of wind direction were assessed. The feasibility of all SMMR frequencies and polarizations to wind speed retrieval was tested. The effect of daily precipitation and integrated water vapor to the retrieval accuracy was studied. Based on the least squares method, a first-order polynomial was formed to calculate the brightness temperature from the wind speed at each SMMR frequency and polarization. The correlation coefficient between the brightness temperature and wind speed was calculated in each case. ESA

N87-17343# Helsinki Univ. of Technology, Espoo (Finland). Radio Lab.
SEA ICE STUDIES IN THE BALTIC SEA USING SATELLITE MICROWAVE RADIOMETER DATA c48
M. Hallikainen and P.-V. Mikkola *In* ESA Proceedings of the 1986 International Geoscience and Remote Sensing Symposium (IGARSS '86) on Remote Sensing: Today's Solutions for Tomorrow's Information Needs, Volume 2 Aug. 1986 p 1089-1094 (For primary document see N87-17283 09-43)
Avail: NTIS HC A17/MF A01; ESA, Paris, France, 3 volume set $90 Member States, AU, CN, and NO (+20% others)

Data from NIMBUS-7 Scanning Multichannel Microwave Radiometer for Winter 1978 to 1979 were used to develop algorithms for retrieval of sea-ice concentration. Due to the small width of the Baltic Sea, only 18 GHz and 37 GHz data could be employed. Comparison of the algorithms indicates that the 37-GHz algorithm is much more sensitive to the properties of the snow cover upon the ice, including the liquid water content, snow depth, and snow grain size. ESA

N87-17344*# National Aeronautics and Space Administration. Goddard Space Flight Center, Greenbelt, Md.
EVALUATING ROUGHNESS MODELS OF RADAR BACKSCATTER c32
E. T. Engmann (Agricultural Research Service, Beltsville, Md.) and J. R. Wang *In* ESA Proceedings of the 1986 International Geoscience and Remote Sensing Symposium (IGARSS '86) on Remote Sensing: Today's Solutions for Tomorrow's Information Needs, Volume 2 Aug. 1986 p 1097-1101 (For primary document see N87-17283 09-43)
Avail: NTIS HC A17/MF A01; ESA, Paris, France, 3 volume set $90 Member States, AU, CN, and NO (+20% others) CSCL 17I

Three radar backscatter roughness models were assessed using soil moisture data collected by the Space Shuttle flight 41G SIR-B SAR in an intensively farmed area. The SIR-B data swath included a large number of bare, dry fields with a large variety of surface roughnesses. The small perturbation model gives the best results, particularly when fields with a definite periodic row structure were omitted. The standard deviation of surface heights appears to be a good measure of relative roughness conditions, but the correlation length is not a good descriptor of the surface, and does not seem to be related in any way to the measured backscatter. ESA

N87-17345# Michigan Univ., Ann Arbor.
MICROWAVE DIELECTRIC SPECTRUM OF VEGETATION MATERIAL
F. T. Ulaby and M. El-Rayes *In* ESA Proceedings of the 1986 International Geoscience and Remote Sensing Symposium (IGARSS '86) on Remote Sensing: Today's Solutions for Tomorrow's Information Needs, Volume 2 Aug. 1986 p 1103-1106 (For primary document see N87-17283 09-43)
Avail: NTIS HC A17/MF A01; ESA, Paris, France, 3 volume set $90 Member States, AU, CN, and NO (+20% others)

A network analyzer connected to a coaxial probe through a directional coupler was developed to measure the dielectric constant of vegetation material accurately, rapidly, and nondestructively. The probe was used to measure dielectric spectra from 0.1 GHz to 20 GHz for many types of vegetation material over a wide range of moisture content. The data were used to guide the development of a double-dispersion model that incorporates separate relaxation spectra for bound water and free water. ESA

N87-17346*# National Aeronautics and Space Administration. Goddard Space Flight Center, Greenbelt, Md.
MICROWAVE BACKSCATTERING FROM AN ANISOTROPIC SOYBEAN CANOPY c32
R. H. Lang (George Washington Univ., Washington, D.C.), S. Saatchi, and D. M. LeVine *In* ESA Proceedings of the 1986 International Geoscience and Remote Sensing Symposium (IGARSS '86) on Remote Sensing: Today's Solutions for Tomorrow's Information Needs, Volume 2 Aug. 1986 p 1107-1112 (For primary document see N87-17283 09-43)
Avail: NTIS HC A17/MF A01; ESA, Paris, France, 3 volume set $90 Member States, AU, CN, and NO (+20% others) CSCL 20N

Electromagnetic backscattering from a soybean canopy is modeled in the L band region of the spectrum. Mature soybean plants are taken as an ensemble of leaves and stems which are represented by lossy dielectric disks and rods respectively. Field data indicated that leaves and stems are not distributed uniformly in the azimuth coordinate. The plant has a tendency to grow out into the area between the rows. The effects on backscattered radar waves was computed by the distorted Born approximation. Results for look directions along the rows and perpendicular to the rows show that only a modest difference occurs in the L band frequency range. The use of another nonuniform distribution, different from those observed experimentally, results in a significant effect due to vegetation asymmetry. ESA

N87-17347# Bern Univ. (Switzerland). Inst. of Applied Physics.
L TO X-BAND SCATTER AND EMISSION MEASUREMENTS OF VEGETATION c32
R. Hueppi and E. Schanda *In* ESA Proceedings of the 1986 International Geoscience and Remote Sensing Symposium (IGARSS '86) on Remote Sensing: Today's Solutions for Tomor-

row's Information Needs, Volume 2 Aug. 1986 p 1113-1118 (For primary document see N87-17283 09-43)
Avail: NTIS HC A17/MF A01; ESA, Paris, France, 3 volume set $90 Member States, AU, CN, and NO (+20% others)

A broad-band H and V polarization radiometer was combined with a noise transmitter to an instrument for measuring active and passive microwave signatures at seven frequencies between L and X band. This radiometer-scatterometer is operated from a cherry picker over agricultural fields. During the growing seasons the development of sugar-beet, wheat, and corn was measured. The geometrical structure of the vegetation cover was described by recording the crop type, the distances between the plants, and the canopy height. The soil underneath was characterized by moisture, temperature profile, and dielectric constant. Another variable was the seasonal change in water content of the plants. Relating these parameters to the microwave signatures reveals the interaction of scatter and emission processes between soil and vegetation. Significant differences of the emission and scattering behavior for the measured crops are found. ESA

N87-17348*# Jet Propulsion Lab., California Inst. of Tech., Pasadena.
ON THE RELATIONSHIP BETWEEN AGE OF LAVA FLOWS AND RADAR BACKSCATTERING **c32**
R. G. Blom, P. Cooley, and L. R. Schenck *In* ESA Proceedings of the 1986 International Geoscience and Remote Sensing Symposium (IGARSS '86) on Remote Sensing: Today's Solutions for Tomorrow's Information Needs, Volume 2 Aug. 1986 p 1119-1127 (For primary document see N87-17283 09-43)
Avail: NTIS HC A17/MF A01; ESA, Paris, France, 3 volume set $90 Member States, AU, CN, and NO (+20% others) CSCL 20N

The observation that older lava flows have lower backscatter in radar images is assessed with multiwavelength/polarization scatterometer data with incidence angles from 15 to 50 deg. Backscatter decreases over time because surface roughness decreases due to infilling with dust and mechanical weathering of the rocks. Pahoehoe lavas in the Snake River Plain with ages of 2.1, 7,4, and 12.0 K yr are best separated with 2.25 cm wavelength data. Blocky obsidian flows at Medicine Lake Highland and Newberry Volcano with ages of 0.9, 1.1 and 1.4 K yr are best separated with 6.3 cm wavelength data. Two Pleistocene flows at the Snake River Plain are best separated with 19.0 cm wavelength data. Incidence angles from 20 to 35 deg are best. These data indicate it may be possible to separate lava flows into eruptive periods using calibrated multiwavelength radar backscatter data. ESA

N87-17349# China Research Inst. of Radiowave Propagation, Xinxiang.
BACKSCATTERING POWER SPECTRUM FOR RANDOMLY MOVING VEGETATION **c32**
J. Jiankang, Z. Zhongzhi, and S. Zhong *In* ESA Proceedings of the 1986 International Geoscience and Remote Sensing Symposium (IGARSS '86) on Remote Sensing: Today's Solutions for Tomorrow's Information Needs, Volume 2 Aug. 1986 p 1129-1132 (For primary document see N87-17283 09-43)
Avail: NTIS HC A17/MF A01; ESA, Paris, France, 3 volume set $90 Member States, AU, CN, and NO (+20% others)

The vegetation backscattering power spectrum in the presence of winds is derived. The physical process of the action of stems and leaves of the vegetation is analyzed. A statistical distribution of the random velocity of stems and leaves is obtained, and the vegetation backscattering power spectral density which is dependent on the wind speed and direction as well as the incident wave parameters is given. In the case of uniform notion of vegetation in the direction of winds, the results provide a good interpretation of Fishbein's empirical model. The determination of the values of the equivalent parameters in the spectrum is discussed, and comparisons are made between the derived spectrum and measured published spectra with satisfactory consistence. ESA

N87-17350# Joint Research Centre of the European Communities, Ispra (Italy).
RURAL LAND USE INVENTORY AND MAPPING IN THE ARDECHE AREA (FRANCE) USING MULTITEMPORAL THEMATIC MAPPING (TM) DATA
J. Hill and J. Megier *In* ESA Proceedings of the 1986 International Geoscience and Remote Sensing Symposium (IGARSS '86) on Remote Sensing: Today's Solutions for Tomorrow's Information Needs, Volume 2 Aug. 1986 p 1135-1141 (For primary document see N87-17283 09-43)
Avail: NTIS HC A17/MF A01; ESA, Paris, France, 3 volume set $90 Member States, AU, CN, and NO (+20% others)

A set of 4 Thematic Mapper scenes (LANDSAT-5) covering the Ardeche region (Southern France) was examined. Image rectification was performed by least squares solution of polynomial equations using 39 to 45 GCP per TM half frame. Since a digital terrain model was not available, image registration was performed for restricted subimages (600 x 600 pixel) which were mosaiced with reference to one master scene. Problems result from relief dependent dislocations which affect the superposition of images, especially from different orbits and in mountaineous areas. Further image analysis included the generation of multitemporal normalized vegetation index, image enhancement by edge preserving smoothing, verification and refinement of ground truth information, and supervised classification (maximum likelihood). ESA

N87-17351# Istanbul Univ. (Turkey). Faculty of Forestry.
LANDSAT-5 THEMATIC MAPPING (TM) DATA APPLICATIONS TO LAND USE CLASSIFICATION ON AROUND THE BOSPHORUS AREA, TURKEY
K. Eidin, A. Hizal, and E. Ataman *In* ESA Proceedings of the 1986 International Geoscience and Remote Sensing Symposium (IGARSS '86) on Remote Sensing: Today's Solutions for Tomorrow's Information Needs, Volume 2 Aug. 1986 p 1143-1148 (For primary document see N87-17283 09-43)
Avail: NTIS HC A17/MF A01; ESA, Paris, France, 3 volume set $90 Member States, AU, CN, and NO (+20% others)

Data from LANDSAT-5 TM were evaluated to delineate forest land use classifications by means of computer assisted techniques. The land use map was checked in the field. Results show that LANDSAT-5 TM Band 5/4 combination is the most convenient to classify forest land use types. ESA

N87-17352# Aston Univ., Birmingham (England). Dept. of Civil Engineering.
DISCRIMATION OF LAND FEATURES USING LANDSAT FALSE COLOUR COMPOSITE IN N IRAN
H. Takerkia and W. G. Collins *In* ESA Proceedings of the 1986 International Geoscience and Remote Sensing Symposium (IGARSS '86) on Remote Sensing: Today's Solutions for Tomorrow's Information Needs, Volume 2 Aug. 1986 p 1149-1153 (For primary document see N87-17283 09-43)
Avail: NTIS HC A17/MF A01; ESA, Paris, France, 3 volume set $90 Member States, AU, CN, and NO (+20% others)

Multispectral LANDSAT data was studied as a source of information for land and water resources (inventories). Two false color composite images, scale 1:250,000, were used as the data source. Forestry, rice cultivation, and drainage networks were mapped and the results compared with data from published 1:250,000 topographic maps. The results show that LANDSAT provides an acceptable degree of accuracy to permit first order mapping of surface drainage, forestry, and rice fields in Iran, where there is an acute shortage of information relating to the land and water resources. ESA

N87-17353# Kombinet VEB Carl Zeiss, Jena (East Germany).
OPTICAL VISUAL EVALUATION AND INTERPRETATION OF REMOTE SENSING DATA
W. Marckwardt *In* ESA Proceedings of the 1986 International Geoscience and Remote Sensing Symposium (IGARSS '86) on Remote Sensing: Today's Solutions for Tomorrow's Information Needs, Volume 2 Aug. 1986 p 1155-1159 (For primary document see N87-17283 09-43)

Avail: NTIS HC A17/MF A01; ESA, Paris, France, 3 volume set $90 Member States, AU, CN, and NO (+20% others)

A photographic system for satellite-borne remote sensing is described. The multispectral camera operates with 6 parallelly aligned normal-angle lenses of 125 mm focal length and 6 separate cassettes for 70 mm film. The film frames have the format 81 mm x 56 mm with the longer side being transverse to the flight direction. A narrow-band interference filter is attached to each lens (centroid wavelengths 480, 540, 600, 660, 720, 840 nm). At 250 km altitude, the camera supplies photographs at the scale 1:2,000,000 covering an area of 160 km x 110 km and allowing a detail recognizability of 10 to 25 m. Ground processing is achieved by instruments for multispectral projection, stereoscopic viewing and superposition, and optical-mechanical rectification. ESA

N87-17354# Rome Univ. (Italy). Dipt. di Ingegneria Elettronica.
EFFECTS OF RAIN CELLS ON SAR PERFORMANCE c32
P. Ferrazzoli and G. Schiavon *In* ESA Proceedings of the 1986 International Geoscience and Remote Sensing Symposium (IGARSS '86) on Remote Sensing: Today's Solutions for Tomorrow's Information Needs, Volume 2 Aug. 1986 p 1163-1168 (For primary document see N87-17283 09-43)
Avail: NTIS HC A17/MF A01; ESA, Paris, France, 3 volume set $90 Member States, AU, CN, and NO (+20% others)

A method to estimate the performance degradation suffered by a microwave remote sensing SAR system due to the presence of rain is proposed. Models already implemented for telecommunication systems are extended. The average swath ratio between the interfering radar response and the useful radar response is assumed to be the parameter which statistically quantifies the degradation. The method is applied to numerical calculations for typical SAR configurations at 5, 10, and 15 GHz, and for 3 different climatic zones. Results show that, although a microwave system is more protected from weather conditions variability than an infrared or optical one, rain may produce degradation effects which cannot be neglected, especially in the worst climatic zones. ESA

N87-17355# Deutsche Forschungs- und Versuchsanstalt fuer Luft- und Raumfahrt, Oberpfaffenhofen (West Germany). Inst. fuer Hochfrequenztechnik.
ANTENNA AMBIGUITY INVESTIGATIONS FOR X-SAR c32
G. Waller *In* ESA Proceedings of the 1986 International Geoscience and Remote Sensing Symposium (IGARSS '86) on Remote Sensing: Today's Solutions for Tomorrow's Information Needs, Volume 2 Aug. 1986 p 1169-1173 (For primary document see N87-17283 09-43)
Avail: NTIS HC A17/MF A01; ESA, Paris, France, 3 volume set $90 Member States, AU, CN, and NO (+20% others)

The effects of range and azimuth ambiguities of distributed and point targets on X-SAR sensor, which is being designed for a joint shuttle mission with SIR-C to provide simultaneous spaceborne SAR experiments in L, C and X-band, were investigated. Results show that ambiguity suppressions greater than 20 dB can be achieved unless contributing scatterers are located at higher gain levels within the antenna mainlobe. Simulations confirm the potential of coherent processing for additional ambiguity reduction in the case of point targets. Due to the very small quadratic range migration component and the low time-bandwidth-product of the azimuth waveforms, only the range ambiguities are additionally reduced by 6 dB, at X-SAR. The interdependence of azimuth ambiguity effects and the applied correlation procedures is indicated. ESA

N87-17356# Canada Centre for Remote Sensing, Ottawa (Ontario).
RECONSIDERATION OF AZIMUTH AMBIGUITIES IN SAR c32
R. K. Raney and J. Princz *In* ESA Proceedings of the 1986 International Geoscience and Remote Sensing Symposium (IGARSS '86) on Remote Sensing: Today's Solutions for Tomorrow's Information Needs, Volume 2 Aug. 1986 p 1175-1179 (For primary document see N87-17283 09-43)
Avail: NTIS HC A17/MF A01; ESA, Paris, France, 3 volume set $90 Member States, AU, CN, and NO (+20% others)

The dependence of SAR azimuth ambiguities arising from ensembles of strong point reflectors in the principal sidelobes of the antenna, which in turn are aliased into the processed Doppler bandwith by the radar pulse repetition frequency (PRF) on radar wavelength and PRF was investigated. It is shown that such ambiguous image elements are strengthened in proportion to lambda sup -2, and PRF sup -1. The theoretical structure is based on orbital SAR geometry, including Earth rotation. The work is applied to a SIR-B L-band radar scene in which azimuth ambiguities are clearly observed. The level and spatial position of these ambiguities are measured in the digital image. The results are extrapolated to higher frequency radars such as ERS-1 and RADARSAT. It is concluded that for these C-band radars the point azimuth ambiguity restraint is more relevant (and more binding) than the traditional energy balance method. ESA

N87-17357# Dornier-Werke G.m.b.H., Friedrichshafen (West Germany).
PLANAR ARRAY ANTENNA FOR ERS-1 SYNTHETIC APERTURE RADAR c32
R. Wagner *In* ESA Proceedings of the 1986 International Geoscience and Remote Sensing Symposium (IGARSS '86) on Remote Sensing: Today's Solutions for Tomorrow's Information Needs, Volume 2 Aug. 1986 p 1181-1186 (For primary document see N87-17283 09-43)
Avail: NTIS HC A17/MF A01; ESA, Paris, France, 3 volume set $90 Member States, AU, CN, and NO (+20% others)

To meet ERS-1 SAR specifications as to high gain, very narrow beamwidth in azimuth, and a slightly tapered shaped beam in elevation, a long narrow antenna was designed. At 5.3 GHz center frequency, the slotted waveguide antenna concept was selected over the reflector or the microstrip principles. Reasons are the low losses, good beamshaping capability, and mechanical compactness. A resonant array is chosen. All waveguides are made from metallized CFRP for reasons of low mass. The mechanical antenna system features a deployable configuration, plus the associated mechanisms. The performance verification concept, through analyses, and tests at different levels, is described. ESA

N87-17358# National Space Development Agency, Ibaraki (Japan).
A SATELLITE-BORNE SAR TRANSMITTER AND RECEIVER c32
M. Fukai, K. Nishikawa, I. Izumi, T. Tsuji, H. Kondo, H. Kashihara, H. Nishino, K. Tanaka, Y. Hisada, and Y. Itoh *In* ESA Proceedings of the 1986 International Geoscience and Remote Sensing Symposium (IGARSS '86) on Remote Sensing: Today's Solutions for Tomorrow's Information Needs, Volume 2 Aug. 1986 p 1187-1192 (For primary document see N87-17283 09-43)
Avail: NTIS HC A17/MF A01; ESA, Paris, France, 3 volume set $90 Member States, AU, CN, and NO (+20% others)

A SAR transmitter-receiver for Earth observations from space was designed for the Japanese Earth Resources Satellite-1. Thermal vacuum and vibration tests were executed on critical components, i.e., the oscillator, the high power amplifier, the power supply for the high power amplifier, and the chirp pulse generator. Results prove that the thermal and structural design is satisfactory. Subsystem designs were verified by evaluating the SAR R and D model. ESA

N87-17359# Deutsche Forschungs- und Versuchsanstalt fuer Luft- und Raumfahrt, Oberpfaffenhofen (West Germany). Inst. fuer Hochfrequenztechnik.
ANALYSIS OF AMPLITUDE NONLINEARITIES IN THE ERS-1 SAR RECEIVER SYSTEM c32
T. K. Pike and E. Sappl *In* ESA Proceedings of the 1986 International Geoscience and Remote Sensing Symposium (IGARSS '86) on Remote Sensing: Today's Solutions for Tomorrow's Information Needs, Volume 2 Aug. 1986 p 1193-1194 (For primary document see N87-17283 09-43)
Avail: NTIS HC A17/MF A01; ESA, Paris, France, 3 volume set $90 Member States, AU, CN, and NO (+20% others)

The effect of amplitude nonlinearities in the ERS-1 SAR receiver

chain on the image quality is used as an illustration of how analytical and computational methods can be applied to such a problem. Results from both methods indicate that so long as ERS-1 remains within specification, image distortions due to amplitude nonlinearities should be minimal, for standard targets. ESA

N87-17360# National Space Development Agency, Ibaraki (Japan). Tsukuba Space Center.
PULSE COMPRESSION TEST RESULTS OF THE SAR TRANSMITTER AND RECEIVER c32
K. Tanaka, H. Shinohara, H. Nishino, H. Kashihara, K. Nishikawa, Y. Hisada, and Y. Itoh *In* ESA Proceedings of the 1986 International Geoscience and Remote Sensing Symposium (IGARSS '86) on Remote Sensing: Today's Solutions for Tomorrow's Information Needs, Volume 2 Aug. 1986 p 1195-1200 (For primary document see N87-17283 09-43)
Avail: NTIS HC A17/MF A01; ESA, Paris, France, 3 volume set $90 Member States, AU, CN, and NO (+20% others)

The pulse compression test principle and the test results on the breadboard model of the spaceborne SAR for the Japanese Earth Resources Satellite 1 are summarized. Using their own transmitter chirp pulse as the test signal for the transitter-receiver, the resultant receiver output pulses are digitized and recorded by high density digital tape recorder then processed by the ideal matched-filter. The usefulness of the pulse compression test method for evaluation of the SAR transmitter-receiver in view of range focusing capability is emphasized. A pulse compression ratio greater than 392 is obtained. ESA

N87-17361# Marconi Space Systems Ltd., Portsmouth (England).
A POWERFUL UTILITY FOR ASSESSING THE PERFORMANCE OF THE ERS-1 SYNTHETIC APERTURE RADAR c32
R. J. Blissett, F. G. Sawyer, M. A. Brown, and D. Smith *In* ESA Proceedings of the 1986 International Geoscience and Remote Sensing Symposium (IGARSS '86) on Remote Sensing: Today's Solutions for Tomorrow's Information Needs, Volume 2 Aug. 1986 p 1201-1205 (For primary document see N87-17283 09-43)
Avail: NTIS HC A17/MF A01; ESA, Paris, France, 3 volume set $90 Member States, AU, CN, and NO (+20% others)

A suite of software programs, which enables the in-flight performance of ERS-1 SAR to be assessed from the results of measurements made on the instrument before launch, was developed. The individual parameters characterizing the performance models are discussed. The performance assessment models are described with reference to specific algorithms for the SAR image quality parameters. The expected in-flight SAR performance is assessed based on hardware data. ESA

N87-17362# Deutsche Forschungs- und Versuchsanstalt fuer Luft- und Raumfahrt, Oberpfaffenhofen (West Germany). Inst. fuer Hochfrequenztechnik.
X-SAR EXTENDS THE FREQUENCY RANGE OF SHUTTLE IMAGING RADAR c32
W. Keydel *In* ESA Proceedings of the 1986 International Geoscience and Remote Sensing Symposium (IGARSS '86) on Remote Sensing: Today's Solutions for Tomorrow's Information Needs, Volume 2 Aug. 1986 p 1207-1212 (For primary document see N87-17283 09-43)
Avail: NTIS HC A17/MF A01; ESA, Paris, France, 3 volume set $90 Member States, AU, CN, and NO (+20% others)

The X-SAR/SIR-C mission is introduced. The mission will be a multifrequency SAR with multipolarization capability. The X-SAR to SIR-C addition extends the frequency range of the whole mission to the upper frequency limit existing today due to physical and technological limits. The experiments cover worldwide very many test areas under the same geometrical, atmospheric and radar technical conditions. The X-SAR development and its application together with SIR-C will strongly impact the future of microwave sensing development with respect to planned future activities like polar platforms, the advanced ERS-1, and the space station. ESA

N87-17363# European Space Agency, Paris (France).
PROCEEDINGS OF AN ESA WORKSHOP ON ERS-1 WIND AND WAVE CALIBRATION
J. J. Hunt, ed. Noordwijk, Netherlands Sep. 1986 240 p Workshop held in Schliersee, West Germany, 2-6 Jun. 1986; sponsored by ESA
(ESA-SP-262; ISSN-0072-6566; ETN-87-98836) Avail: NTIS HC A11/MF A01

Classification of ERS-1 wind and wave measurements; wind and wave models; surface and airborne measurements to calibrate the ERS-1 instruments; and planned and on-going climate and oceanographic programs were discussed. For individual titles, see N87-17364 through N87-17392.

N87-17364# European Space Agency. European Space Research and Technology Center, ESTEC, Noordwijk (Netherlands).
ERS-1 MISSION CONSTRAINTS RELATED TO WIND AND WAVE CALIBRATION
Jacques Louet *In its* Proceedings of an ESA Workshop on ERS-1 Wind and Wave Calibration Sep. 1986 p 3-10 (For primary document see N87-17363 09-43)
Avail: NTIS HC A11/MF A01

The approach taken for validation and calibration of the ERS-1 mission is outlined. A clear distinction is made between the engineering and geophysical performances of the mission. The pre and post-launch activities required to calibrate the ERS-1 system and validate the geophysical performance are described. ESA

N87-17365# Institute of Oceanographic Sciences, Wormley (England).
THE INFLUENCE OF SPATIAL AND TEMPORAL SCALES ON CALIBRATION/VALIDATION
Peter G. Challenor, Trevor H. Guymer, and Meric A. Srokosz *In* ESA Proceedings of an ESA Workshop on ERS-1 Wind and Wave Calibration Sep. 1986 p 11-16 (For primary document see N87-17363 09-43)
Avail: NTIS HC A11/MF A01

Calibration of the ERS-1 wind/wave sensors is discussed. It is necessary to include data not coincident with the sensor footprint. A knowledge of the space and time scales of the wind and wave fields is needed to decide whether to include or exclude data from the calibration. It is shown that the significant wave height variation, in space and time, can be split into two signals: a low frequency scale, corresponding to depressions, and a high frequency noise signal. Results for wind speed suggest a similar division of scales. ESA

N87-17366*# Jet Propulsion Lab., California Inst. of Tech., Pasadena. Radar Science and Engineering Section.
NASA SCATTEROMETER DATA PROCESSING SYSTEM: FEATURES FOR VALIDATION
Philip S. Callahan and J. R. Benada *In* ESA Proceedings of an ESA Workshop on ERS-1 Wind and Wave Calibration Sep. 1986 p 17-25 (For primary document see N87-17363 09-43)
Avail: NTIS HC A11/MF A01 CSCL 05B

The design of the N-ROSS scatterometer data system and the development of key processing algorithms are described. The data products and parts of the data system to be directly validated are listed. The main features of the Data Management Subsystem, which delivers data to science users and supports system validation are outlined. ESA

N87-17367# Science Research Council, Chilton (England). Rutherford Appleton Lab.
GATHERING AND PROCESSING A COMPARATIVE DATA SET FOR THE CALIBRATION AND VALIDATION OF ERS-1 DATA PRODUCTS; PREPARATORY WORK AT THE UK-ERS-DC
Redvers John Powell *In* ESA Proceedings of an ESA Workshop on ERS-1 Wind and Wave Calibration Sep. 1986 p 27-30 (For primary document see N87-17363 09-43)
Avail: NTIS HC A11/MF A01

It is suggested that the main European effort to validate the wind and wave data products of ERS-1 should be concentrated in the North-East Atlantic and Norwegian sea. Also, that conven-

tional oceanographic data gathering techniques using ships and buoys should be augmented with permanently deployed and well validated master stations and airborne instrumentation. The need to site such stations and altimeter transponders on the ground track argues strongly for the early selection of the location of the ground tracks associated with the initial three-day repeat orbit and for ensuring that any higher repeat cycle is a multiple of three. Work on this subject at the UK-ERS data center is described. ESA

N87-17368# National Environmental Satellite Service, Washington, D. C.
VALIDATION OF WIND SPEED AND SIGNIFICANT WAVE HEIGHT FROM GEOSAT
John Wilkerson *In* ESA Proceedings of an ESA Workship on ERS-1 Wind and Wave Calibration Sep. 1986 p 31-36 (For primary document see N87-17363 09-43)
Avail: NTIS HC A11/MF A01

Validation of Geosat wind and wave data used for operational warnings and weather forecasts is discussed. Geosat ground tracks come within 150 km or less of NOAA moored buoys on the average of 25 times each 3 months. Of these, 10 are within 50 km or less. If only ground tracks within 50 km of buoys are used for validation comparison, the network yields in 1 yr 1600 data pairs for wind speed and 1400 comparison pairs for wave height evaluation. These numbers increase to 4400 and 4000 if the range is extended to 150 km. Error budgets are estimated to account for uncertainties in Geosat and in situ measurements due to time and space variability, instrument measurement accuracies, and averaging times for buoy measurements, particularly for winds. ESA

N87-17369# Institute of Oceanographic Sciences, Wormley (England).
REQUIREMENTS AND CONSTRAINTS IN THE CALIBRATION AND VALIDATION OF ERS-1 WIND AND WAVE PARAMETERS c48
Trevor H. Guymer *In* ESA Proceedings of an ESA Workshop on ERS-1 Wind and Wave Calibration Sep. 1986 p 37-43 (For primary document see N87-17363 09-43)
Avail: NTIS HC A11/MF A01

Calibration and validation of ERS-1 wind and wave parameters are discussed using the experience of other oceanographic satellite missions. Major limitations of past efforts appear to be: the limited number of comparisons with near-coincident in-situ platforms, the small dynamic ranges encountered, and the introduction of regional biases by calibrations that were heavily weighted to midlatitude, summertime conditions. On the basis of a study of climatological statistics, suitable locations for measuring high wind and wave conditions are suggested. ESA

N87-17370# Centre Oceanologique de Bretagne, Brest (France). Antenne CREO.
EVALUATION OF THE DIFFERENT PARAMETERS IN LONG'S C-BAND MODEL c32
Alain Cavanie, Joelle Demurger, and Pascal Lecomte *In* ESA Proceedings of an ESA Workshop on ERS-1 Wind and Wave Calibration Sep. 1986 p 47-51 (For primary document see N87-17363 09-43)
Avail: NTIS HC A11/MF A01

Scatterometer measurements over the ocean were analyzed and a model for sigma-zero (S) as a function of wind speed, wind direction relative to the beam direction, and incidence angle was derived for ERS-1. Because ERS-1 is yaw-steered: in the space of 00 values of the forward, rear, and central, antennas (S1, S2, S3), the surface of solutions is symmetric with respect to the plan S1 = S2. The ratios S1/S2 or S2/S1 reach 2 distinct maxima for a given wind speed. Two independent methods of calibration of parameters in the C-Band model, using only the wind speed furnished by meteorological fields are obtained. Such methods could be applied to pretune the scatterometer in its first months of flight, investigate regional variations, and monitor possible evolutions in the instrument's behavior. ESA

N87-17371# Meteorological Office, Bracknell (England).
THE USE OF NUMERICAL WIND AND WAVE MODELS TO PROVIDE AREAL AND TEMPORAL EXTENSION TO INSTRUMENT CALIBRATION AND VALIDATION OF REMOTELY SENSED DATA
Peter E. Francis *In* ESA Proceedings of an ESA Workshop on ERS-1 Wind and Wave Calibration Sep. 1986 p 53-55 (For primary document see N87-17363 09-43)
Avail: NTIS HC A11/MF A01

A scheme to use satellite derived ocean surface data in environmental sciences is outlined. The scheme involves comparisons between satellite data and ground based measurements, between ground based measurements and numerical models, and between numerical models and satellite data. Each comparison yields vital information, e.g., primary retrieval algorithms, model validation, extension of satellite data validation beyond the regions of surface based networks. Examples of performance characteristics and output products of the UK Meteorological Office global atmospheric and sea state models are given. ESA

N87-17372*# Jet Propulsion Lab., California Inst. of Tech., Pasadena. NASA Scatterometer Project.
SATELLITE SCATTEROMETER COMPARISONS WITH SURFACE MEASUREMENTS: TECHNIQUES AND SEASAT RESULTS
Michael H. Freilich *In* ESA Proceedings of an ESA Workshop on ERS-1 Wind and Wave Calibration Sep. 1986 p 57-62 Sponsored by NASA (For primary document see N87-17363 09-43)
Avail: NTIS HC A11/MF A01 CSCL 08C

A method by which satellite and surface measurements can be compared in order to validate satellite wind observations is presented. The regression method requires knowledge of the expected differences (due to atmospheric variability and differing averaging) between perfect satellite and perfect buoy measurements. A model for estimating these differences is described. The regression method is applied to comparisons between Seasat Scatterometer (SASS) and U.S. National Data Buoy Office buoy data. Comparisons indicating a dependence of SASS accuracy on sea-surface temperature are summarized. ESA

N87-17373# GKSS-Forschungszentrum Geesthacht (West Germany).
COMPARISON CONCEPT OF SATELLITE DERIVED WIND AND WAVE DATA WITH GROUND TRUTH
Wolfgang Koch and R. Ramseier *In* ESA Proceedings of an ESA Workshop on ERS-1 Wind and Wave Calibration Sep. 1986 p 63-68 (For primary document see N87-17363 09-43)
Avail: NTIS HC A11/MF A01

To demonstrate the capabilities of numerical models for the calibration of satellite derived pressure, wind, and wave-fields, results from numerical simulations are shown and compared to measurements and SMMR-data from NIMBUS 7. The proposed calibration procedure relies on numerical simulation models which themselves are quantitatively calibrated with regionally representative measurements. ESA

N87-17374# Institute of Oceanographic Sciences, Wormley (England).
VALIDATION OF ERS-1 WIND DATA USING OBSERVATIONS FROM RESEARCH AND VOLUNTARY OBSERVING SHIPS c48
Peter K. Taylor *In* ESA Proceedings of an ESA Workshop on ERS-1 Wind and Wave Calibration Sep. 1986 p 69-75 (For primary document see N87-17363 09-43)
Avail: NTIS HC A11/MF A01

A method for validation of ERS-1 wind measurements using observations from the Voluntary Observing Ships (VOS) is proposed. The data are available from most ocean regions allowing validation over a wide range of conditions. Although the observations are individually of poor quality, data from the North Sea is used to demonstrate that, where sufficient observations exist, a mean value averaged over 1 month and a few hundred kilometers should be accurate to 1m/sec or better. For absolute calibration a subset of the VOS would be used. For these ships,

the wind errors due to poor anemometer exposure must be determined. Results obtained by mounting a high mast in ships' bows are encouraging. ESA

N87-17375# National Environmental Satellite Service, Washington, D. C.
ACCURACY ESTIMATES OF WIND AND WAVE OBSERVATIONS FROM SHIPS OF OPPORTUNITY IN THE WMO VOLUNTARY OBSERVING SHIP PROGRAM **c48**
John Wilkerson *In* ESA Proceedings of an ESA Workshop on ERS-1 Wind and Wave Calibration Sep. 1986 p 77-84 (For primary document see N87-17363 09-43)
Avail: NTIS HC A11/MF A01

Wind and wave reports from ships of opportunity are compared with each other and with reports from 47 moored buoys when the ships were within 100 km of the buoys or each other at the same reporting times. Analyses were performed on greater than 113,000 paired reports dating from 1973 to 1983. Standard deviations of differences for winds are of the order of 5 to 8 knots and 40 to 50 deg with means of 2 to 4 knots and 10 deg. Poor agreement is the result of systematic errors shown to be in part the preference for reporting speed in multiples of 5 knots and directions near 8 points of the compass. Differences in significant wave heights reported by ships and buoys have a mean of 0.5 m with standard deviations of 1.5 to 2.5 m. ESA

N87-17376# Royal Netherlands Meteorological Inst., De Bilt.
THE ACCURACY AND AVAILABILITY OF OPERATIONAL MARINE SURFACE WIND DATA FOR ERS-1 SENSOR CALIBRATION AND VALIDATION FROM FIXED PLATFORMS AND FREE DRIFTING BUOYS **c48**
Wiebe A. Oost *In* ESA Proceedings of an ESA Workshop on ERS-1 Wind and Wave Calibration Sep. 1986 p 85-86 (For primary document see N87-17363 09-43)
Avail: NTIS HC A11/MF A01

Problems when using wind data from oil or gas production platforms and a proposal for a calibration experiment, using drifting buoys are outlined. The problems with platforms are discussed on the basis of studies on the K13-A platform in the southern North Sea. Drifting buoys being the most cost-effective platforms to obtain data from the high seas, a suggestion is made to deploy a group of drifters measuring wind and, possibly, waves. This could be done by cooperation with the COST-43 organization, which maintains drifting buoy programs in 2 areas. ESA

N87-17377# Centre Oceanologique de Bretagne, Brest (France).
USING BUOYS AND SHIPS TO CALIBRATE ERS-1 ALTIMETER AND SCATTEROMETER **c48**
Robert Ezraty *In* ESA Proceedings of an ESA Workshop on ERS-1 Wind and Wave Calibration Sep. 1986 p 91-97 (For primary document see N87-17363 09-43)
Avail: NTIS HC A11/MF A01

Given the stated accuracy of ERS-1 sensors, the constraints to be dealt with using ships and buoys for a dedicated calibration experiment are discussed. Wave measuring buoys giving directional and non directional information are available to be used remotely in the open ocean. Wind measurements from ships can be considered as a reference, if ship effects are properly taken into account. Sea tests of a spar buoy, measuring the wind vector at 4 m are being conducted. The importance of the continuity of wind data is stressed and has to be accounted for to plan the on-board electronics. The geometry of wave and wind buoy networks are different since the altimeter and scatterometer do not scan the same area. Network configurations are presented. ESA

N87-17378# Deutsche Forschungs- und Versuchsanstalt fuer Luft- und Raumfahrt, Oberpfaffenhofen (West Germany).
DFVLR FLIGHT OPERATION ACTING AS A USEFUL SERVICE UNIT FOR ERS-1
Heinz Finkenzeller *In* ESA Proceedings of an ESA Workshop on ERS-1 Wind and Wave Calibration Sep. 1986 p 99-100 (For primary document see N87-17363 09-43)
Avail: NTIS HC A11/MF A01

Preparation for ERS-1 scatterometer campaigns on Dornier 228.101 aircraft are summarized. Flight tests of payloads and the flexibility of the aircraft are described. ESA

N87-17379# Canada Centre for Remote Sensing, Ottawa (Ontario).
CANADA CENTER FOR REMOTE SENSING (CCRS) CONVAIR 580 RESULTS RELEVANT TO ERS-1 WIND AND WAVE CALIBRATION
Nelson G. Freeman, A. L. Gray, R. K. Hawkins, and C. E. Livingstone *In* ESA Proceedings of an ESA Workshop on ERS-1 Wind and Wave Calibration Sep. 1986 p 101-109 (For primary document see N87-17363 09-43)
Avail: NTIS HC A11/MF A01

Results from Convair 580 wind and wave measurement campaigns are presented to demonstrate the usefulness of such an airborne microwave research facility for ERS-1 dedicated calibration and validation experiments. Scatterometer measurements from the PROMESS campaigns show that C-band sensitivity for wind speeds (2 to 12 m/sec) is 70% to 80% of the Ku-band sensitivity. It is also shown that the ERS-1 active microwave image mode should be able to detect surface oil as a 5 to 7 dB drop in scattering cross section when observed at 23 deg incidence angle. Ship targets, however, may be lost in the sea clutter for wind speeds greater than 8m/sec. Results from the Cape Sable SAR wave imaging experiments indicate that airborne SAR can be used to investigate the effect of R/V scaling and look direction on azimuthal falloff in SAR derived directional wave spectra. ESA

N87-17380*# National Aeronautics and Space Administration. Goddard Space Flight Center, Greenbelt, Md.
OCEANOGRAPHIC MEASUREMENT CAPABILITIES OF THE NASA P-3 AIRCRAFT
Erik Mollo-Christensen, F. C. Jackson, E. J. Walsh, and F. Hoge *In* ESA Proceedings of an ESA Workshop on ERS-1 Wind and Wave Calibration Sep. 1986 p 111-121 (For primary document see N87-17363 09-43)
Avail: NTIS HC A11/MF A01 CSCL 04B

Instrumentation on NASA P3 aircraft available to provide ground truth for ERS-1 is described. The wave sensors include the 36 GHz Surface Contour Radar (SCR), the Ku-band Radar Ocean Wave Spectrometer (ROWS), and the Airborne Oceanographic Lidar. The other sensors include a C-band scatterometer, video camera, radiation thermometer, and AXRTs. The SCR and ROWS directional spectrum measurements are discussed. When planning for an underflight mission, the limited endurance of the aircraft (6 hr) and flight cost (2.7 K$/hr) must be considered. The advantage of the redundancy afforded by the several wave instruments is another important consideration. ESA

N87-17381# Johns Hopkins Univ., Laurel, Md. Applied Physics Lab.
A PROCEDURE FOR ESTIMATION OF TWO-DIMENSIONAL OCEAN HEIGHT-VARIANCE SPECTRA FROM SAR IMAGERY **c48**
Frank Monaldo *In* ESA Proceedings of an ESA Workshop on ERS-1 Wind and Wave Calibration Sep. 1986 p 123-129 (For primary document see N87-17363 09-43)
Avail: NTIS HC A11/MF A01

A step-by-step procedure to convert synthetic aperture radar (SAR) imagery into estimates of the ocean surface wave spectra is outlined. The procedure is based on a linearized version of a model to convert SAR image intensity spectra into either wave slope or height-variance spectra. The procedure is applied to SAR imagery from the SIR-B mission and shown to produce spectra which are highly correlated to two-dimensional spectra measured independently. ESA

N87-17382# Meteorological Office, Bracknell (England).
THE USE OF AIRCRAFT FOR WIND SCATTEROMETER CALIBRATION **c47**
David Offiler *In* ESA Proceedings of an ESA Workshop on ERS-1

Wind and Wave Calibration Sep. 1986 p 131-134 (For primary document see N87-17363 09-43)
Avail: NTIS HC A11/MF A01

The use of a Hercules aircraft to assist in the calibration and verification of ERS wind scatterometer products is proposed. The capabilities of this aircraft and its advantages are described, and compared to other sources of calibration data. ESA

N87-17383# Science Research Council, Chilton (England). Rutherford Appleton Lab.
MEASUREMENT OF THE DIRECTIONAL SPECTRUM OF OCEAN WAVES USING A CONICALLY-SCANNING RADAR c48
Andrew Robert Birks *In* ESA Proceedings of an ESA Workshop on ERS-1 Wind and Wave Calibration Sep. 1986 p 135-138 (For primary document see N87-17363 09-43)
Avail: NTIS HC A11/MF A01

It is proposed to use a short-pulse radar altimeter, modified by the addition of a steerable antenna which can scan a cone about nadir, to measure the directional spectrum of ocean waves. The method can be used from either a satellite or aircraft; application from an aircraft is described, having in mind its use in the validation of satellite instruments. Near simultaneous measurements of significant wave height and of the directional wave spectrum are possible with the same instrument, enhancing the value of both measurements. Airborne measurements were made using a 13GHz radar during a campaign with the NASA CV-900 aircraft. ESA

N87-17384*# Jet Propulsion Lab., California Inst. of Tech., Pasadena.
AN OVERVIEW OF THE NSCAT/N-ROSS PROGRAM
B. D. Martin, Michael H. Freilich, F. K. Li, and Phillip S. Callahan *In* ESA Proceedings of an ESA Workshop on ERS-1 Wind and Wave Calibration Sep. 1986 p 143-149 Sponsored by NASA (For primary document see N87-17363 09-43)
Avail: NTIS HC A11/MF A01 CSCL 14B

The NASA Scatterometer (NSCAT) to fly on the U.S. Navy Remote Ocean Sensing System (N-ROSS) mission is presented. The overall N-ROSS mission, the NSCAT flight instrument and groundbased data processing/distribution system, and NASA-supported science and verification activities are described. The N-ROSS system is designed to provide measurements of near-surface wind, ocean topography, wave height, sea-surface temperature, and atmospheric water content over the global oceans. The NSCAT is an improved version of the Seasat scatterometer. It will measure near surface vector winds. ESA

N87-17385# Naval Ocean Research and Development Activity, Bay St. Louis, Miss.
N-ROSS VALIDATION c48
D. R. Johnson *In* ESA Proceedings of an ESA Workshop on ERS-1 Wind and Wave Calibration Sep. 1986 p 151-156 (For primary document see N87-17363 09-43)
Avail: NTIS HC A11/MF A01

Validation of the N-ROSS geophysical parameters, validation of the data base synthesis and geophysical model products, and determination of the usefulness of NROSS as an operational system are discussed. Since its mission time frame, orbital characteristics, and sensor packages are similar to those of ERS-1, collaboration of efforts to validate the satellites makes sense, both from the points of view of sharing resources and experience, as well as from the potential dividends from enhanced coverage and performance comparisons of intercalibrated systems. ESA

N87-17386# Massachusetts Univ., Amherst.
INTERSENSOR COMPARISONS FOR VALIDATION OF WIND SPEED MEASUREMENTS FROM ERS-1 ALTIMETER AND SCATTEROMETER c47
Calvin Swift and N. M. Mognard *In* ESA Proceedings of an ESA Workshop on ERS-1 Wind and Wave Calibration Sep. 1986 p 157-164 (For primary document see N87-17363 09-43)
Avail: NTIS HC A11/MF A01

Discrepancies in wind magnitude data from the three wind sensors on board Seasat, namely the radar altimeter, the scatterometer, and the scanning microwave multifrequency radiometer were analyzed on a global and regional scale for time periods varying from the entire 3-month Seasat period, to a monthly, and a 3-day time scale. The data are analyzed in the Southern Oceans where, during the Seasat lifetime, the highest sea state conditions were found. The algorithms used to process each data set are the official JPL Seasat algorithms. The results point to a more detailed verification activity for future satellite systems such as the SSM/I, NSCATT and the ERS-1 scatterometer. ESA

N87-17387# Commonwealth Scientific and Industrial Research Organization, Aspendale (Australia). Div. of Atmospheric Research.
AUSTRALIAN VALIDATION PLANS FOR ERS-1
Ian J. Barton *In* ESA Proceedings of an ESA Workshop on ERS-1 Wind and Wave Calibration Sep. 1986 p 165-168 (For primary document see N87-17363 09-43)
Avail: NTIS HC A11/MF A01

Australian calibration/validation plans for the instruments carried on the ERS-1 satellite are described. A large experiment is planned for 1990 in the tropical waters to the north-east of the continent. Although the prime concern of this experiment is the validation of the along track scanning radiometer in tropical areas there will be side programs involving the validation of the products from the microwave instrumentation. Extended comparison between measurements from two HF radars (one ground-wave and one sky-wave) and the ERS-1 data will also be attempted. Other studies planned relate to the calibration and general use of data both over land and ocean surfaces and in Antarctica. ESA

N87-17388# World Meteorological Organization, Geneva (Switzerland).
AN OVERVIEW OF THE IMPLEMENTATION OF THE WORLD CLIMATE RESEARCH PROGRAM
Thomas Kaneshige *In* ESA Proceedings of an ESA Workshop on ERS-1 Wind and Wave Calibration Sep. 1986 p 169-172 (For primary document see N87-17363 09-43)
Avail: NTIS HC A11/MF A01

The meteorological, oceanic, satellite observation, data management, and global environmental monitoring aspects of the World Climate Research Program (WCRP) are outlined. The WCRP was established to study climate variability and its causes, of natural or human origin. The research strategy is formulated in terms of three specific objectives or streams. Each objective is a stepping stone for the next, which encompasses a wider range of interactions between the atmosphere, ocean, ice, and land surface, and calls for a more refined treatment of energy sources and sinks. ESA

N87-17389# Max-Planck-Inst. fuer Meteorologie, Hamburg (West Germany).
WAVE MODELING ACTIVITIES OF THE WAVE MODELING (WAM) GROUP RELEVANT TO ERS-1 c48
Klaus Hasselmann *In* ESA Proceedings of an ESA Workshop on ERS-1 Wind and Wave Calibration Sep. 1986 p 173-175 (For primary document see N87-17363 09-43)
Avail: NTIS HC A11/MF A01

A third generation wave model was developed and successfully tested in hindcast studies, in global and regional, deep and shallow water versions. The model will be applied to assimilate wind and wave data from ERS-1. The model will be embedded in a data assimilation system based on a global atmospheric circulation model together with the wave model. The availability of such an operational system at the time of the ERS-1 commissioning phase would greatly assist the calibration and validation of the ERS-1 wind and wave sensors. ESA

N87-17390# Ministerio de Obras Publicas, Madrid (Spain). Direccion General de Puertos y Costas.
MARINE CLIMATE PROGRAM c47
Juan Jose Conde, Josie Enrique Luis, and Adolfo Maron *In* ESA Proceedings of an ESA Workshop on ERS-1 Wind and Wave Calibration Sep. 1986 p 177-179 (For primary document see

N87-17363 09-43)
Avail: NTIS HC A11/MF A01

Research on ocean wave forecasting, wave time series analysis, and flow propagation is summarized. A buoy network for the Spanish littoral is described. ESA

N87-17391# Marconi Co. Ltd., Chelmsford (England). Remote Sensing Group.
A SCATTEROMETER RESEARCH PROGRAM c32
Ian A. Ward *In* ESA Proceedings of an ESA Workshop on ERS-1 Wind and Wave Calibration Sep. 1986 p 181-185 (For primary document see N87-17363 09-43)
Avail: NTIS HC A11/MF A01

A research program on SAR ocean surface scattering and imaging is outlined. It covers Bragg scattering, specular reflection, and wedge diffraction. Speckle statistics; bias to longer wavelengths in azimuthaliy traveling-waves; orbital and phase-velocities of swell waves; velocity-bunching; the degradation of azimuthal resolution; information from nonlinear imaging situations; and imaging theory to incorporate breaking-waves are covered. ESA

N87-17392# Turin Univ. (Italy). Ist. di Fisica Generale.
BULK RICHARDSON'S NUMBER ISOGRAMS DEDUCED FROM SAR DATA c48
B. Fiscella, P. P. Lombardini, Paolo Trivero, and C. Cappa *In* ESA Proceedings of an ESA Workshop on ERS-1 Wind and Wave Calibration Sep. 1986 p 187-190 (For primary document see N87-17363 09-43)
Avail: NTIS HC A11/MF A01

Elaborating SAR data taken by Seasat-A over the Ligurian Sea, it is shown that when sufficient information on wind and surface sea current are available, Richardson bulk number and air-sea temperature difference may be mapped on the basis of SAR observation from space of a marine area. ESA

N87-17393*# Michigan Univ., Ann Arbor. Dept. of Electrical and Computer Engineering.
MICROWAVE DIELECTRIC BEHAVIOR OF VEGETATION MATERIAL
Mohamed A. ElRayes and Fawwaz T. Ulaby Jan. 1987 445 p (Grant NAG5-480)
(NASA-CR-180096; NAS 1.26:180096) Avail: NTIS HC A19/MF A01 CSCL 20N

The microwave dielectric behavior of vegetation was examined through the development of theoretical models involving dielectric dispersion by both bound and free water and supported by extensive dielectric measurements conducted over a wide range of conditions. The experimental data were acquired using an open-ended coaxial probe that was developed for sensing the dielectric constant of thin layers of materials, such as leaves, from measurements of the complex reflection coefficient using a network analyzer. The probe system was successfully used to record the spectral variation of the dielectric constant over a wide frequency range extending from 0.5 to 20.4 GHz at numerous temperatures between -40 to +40 C. The vegetation samples were measured over a wide range of moisture conditions. To model the dielectric spectrum of the bound water component of the water included in vegetation, dielectric measurements were made for several sucrose-water solutions as analogs for the situation in vegetation. The results were used in conjunction with the experimental data for leaves to determine some of the constant coefficients in the theoretical models. Two models, both of which provide good fit to the data, are proposed. Author

N87-17394*# National Aeronautics and Space Administration, Washington, D.C.
TRAINING PROGRAMS IN REMOTE SENSING FOR PROFESSIONALS, STUDENTS AND THE GENERAL PUBLIC
R. Galeano Jan. 1987 24 p Transl. into ENGLISH of conference paper presented at the Reunion de Expertos en Ciencia y Tecnologia Espaciales y sus Aplicaciones, 1986 p 1-23 Meeting held in Mexico City, Mex., 13-17 Oct. 1986; sponsored by Marco de Sistemas Educacionales Transl. by The Corporate Word, Inc., Pittsburgh, Pa.
(Contract NASw-4006)
(NASA-TM-88541; NAS 1.15:88541) Avail: NTIS HC A02/MF A01 CSCL 05C

What remote sensing is, how and why it is used, and why more people should be trained in the field is discussed. Suggestions are offered concerning differences in teaching technicians, the general public, and children in schools. Author

N87-17395# Los Alamos National Lab., N. Mex. Theoretical Div.
CANOPY HOT-SPOT AS CROP IDENTIFIER
S. A. W. Gerstl, C. Simmer, and B. J. Powers May 1986 10 p Presented at the 12th International Conference on Very Large Databases, Kyoto, Japan, 25 Aug. 1986
(Contract W-7405-eng-36)
(DE86-011258; LA-UR-86-1596; CONF-860888-1) Avail: NTIS HC A02/MF A01

Illuminating any reflective rough or structured surface by a directional light source results in an angular reflectance distribution that shows a narrow peak in the direction of retro-reflection. This is called the Heiligenschein or hot-spot of vegetation canopies and is caused by mutual shading of leaves. The angular intensity distribution of the hot-spot, its brightness and slope, are therefore indicators of the plant's geometry. We propose the use of hot-spot characteristics as crop identifiers in satellite remote sensing because the canopy hot-spot carries information about plant stand architecture that is more distinctive for different plant species than, for instance, their spectral reflectance characteristics. A simple three-dimensional Monte Carlo/ray tracing model and an analytic two-dimensional model are developed to estimate the angular distribution of the hot-spot as a function of the size of the plant leaves. The results show that the brightness-distribution and slope of the hot-spot change distinctively for different leaf sizes indicating a much more peaked maximum for the smaller leaves. DOE

N87-17106# Joint Publications Research Service, Arlington, Va.
DEVELOPMENT OF NEW AVIATION TECHNOLOGY FOR GRAVIMETRIC SURVEYING Abstract Only
K. Ye. Besyelov, P. D. Bagdatlishvili, and V. O. Bagramyants *In its* USSR Report: Earth Sciences (JPRS-UES-86-005) 7 May 1986 p 38-39 Transl. into ENGLISH from Ekspress Informatsiya: Morskaya Geologiya i Geofizika (Moscow, USSR), no. 11, 1985 p 1-5 (For primary document see N87-17096 09-42)
Avail: NTIS HC A05/MF A01

44 ENERGY PRODUCTION AND CONVERSION

Includes specific energy conversion systems, e.g., fuel cells; global sources of energy; geophysical conversion; and windpower.

For related information see also *07 Aircraft Propulsion and Power, 20 Spacecraft Propulsion and Power,* and *28 Propellants and Fuels.*

N87-17396*# Jet Propulsion Lab., California Inst. of Tech., Pasadena.
SAFETY CONSIDERATIONS OF LITHIUM-THIONYL CHLORIDE CELLS
Surampudi Subbarao, Gerald Halpert, and Irving Stein 1 Jun. 1986 85 p
(Contract NAS7-918)
(NASA-CR-180129; JPL-Pub-86-015; NAS 1.26:180129) Avail: NTIS HC A05/MF A01 CSCL 10B

The use of spirally wound lithium-thionyl chloride (Li-SOCl2) cells is currently limited because of their hazardous behavior. Safety hazards have ranged from mild venting of toxic materials to violent explosions and fires. These incidents may be related to both user- and manufacturer-induced causes. Many explanations have been offered to explain the unsafe behavior of the cells under operating

and abuse conditions. Explanations fall into two categories: (1) thermal mechanisms, and (2) chemical mechanisms. However, it is quite difficult to separate the two. Both may be responsible for cell venting or explosion. Some safety problems encountered with these cells also may be due to design deficiencies and ineffective quality control during cell fabrication. A well-coordinated basic and applied research program is needed to develop safe Li-SOCl2 cells. Recommendations include: (1) learnig more about Li-SOL2 cell chemistry; (2) modeling cell and battery behavior; (3) optimizing cell design for safety and performance, (4) implementing quality control procedures; and (5) educating users. Author

N87-17397*# Jet Propulsion Lab., California Inst. of Tech., Pasadena.
THE NASA AEROSPACE BATTERY SAFETY HANDBOOK
Gerald Halpert, Surampudi Subbarao, and John J. Rowlette 15 Jul. 1986 99 p
(Contract NAS7-918)
(NASA-CR-180127; JPL-Pub-86-14; NAS 1.26:180127) Avail: NTIS HC A05/MF A01 CSCL 10B

This handbook has been written for the purpose of acquainting those involved with batteries with the information necessary for the safe handling, storage, and disposal of these energy storage devices. Included in the document is a discussion of the cell and battery design considerations and the role of the components within a cell. The cell and battery hazards are related to user- and/or manufacturer-induced causes. The Johnson Space Center (JSC) Payload Safety Guidelines for battery use in Shuttle applications are also provided. The electrochemical systems are divided into zinc anode and lithium anode primaries, secondary cells, and fuel cells. Each system is briefly described, typical applications are given, advantages and disadvantages are tabulated, and most importantly, safety hazards associated with its use are given. Author

N87-17398*# System Development Corp., Camarillo, Calif.
LUNAR POWER SYSTEMS Final Report
12 Dec. 1986 324 p
(Contract NAS9-17359)
(NASA-CR-171956; NAS 1.26:171956) Avail: NTIS HC A14/MF A01 CSCL 10B

The findings of a study on the feasibility of several methods of providing electrical power for a permanently manned lunar base are provided. Two fundamentally different methods for lunar electrical power generation are considered. One is the use of a small nuclear reactor and the other is the conversion of solar energy to electricity. The baseline goal was to initially provide 300 kW of power with growth capability to one megawatt and eventually to 10 megawatts. A detailed, day by day scenario for the establishment, build-up, and operational activity of the lunar base is presented. Also presented is a conceptual approach to a supporting transportation system which identifies the number, type, and deployment of transportation vehicles required to support the base. An approach to the use of solar cells in the lunar environment was developed. There are a number of heat engines which are applicable to solar/electric conversions, and these are examined. Several approaches to energy storage which were used by the electric power utilities were examined and those which could be used at a lunar base were identified. B.G.

N87-17399*# National Aeronautics and Space Administration. Pasadena Office, Calif.
HIGH BAND GAP 2-6 AND 3-5 TUNNELING JUNCTIONS FOR SILICON MULTIJUNCTION SOLAR CELLS Patent
Taher Daud, inventor (to NASA) (Jet Propulsion Lab., California Inst. of Tech., Pasadena) and Akaram H. Kachare, inventor (to NASA) Issued 23 Dec. 1986 5 p
(NASA-Case-NPO-16526-1CU; US-Patent-4,631,352; US-Patent-Appl-SN-809975; US-Patent-Class-136-249) Avail: U.S. Patent and Trademark Office CSCL 10A

A multijunction silicon solar cell of high efficiency is provided by providing a tunnel junction between the solar cell junctions to connect them in series. The tunnel junction is comprised of p+ and n+ layers of high band gap 3-5 or 2-6 semiconductor materials that match the lattice structure of silicon, such as GaP (band gap 2.24 eV) or ZnS (band gap 3.6 eV). Each of which has a perfect lattice match with silicon to avoid defects normally associated with lattice mismatch. NASA

N87-17400*# Electrotek Concepts, Inc., Knoxville, Tenn.
UTILITY INTERCONNECTION ISSUES FOR WIND POWER GENERATION Status Report
J. I. Herrera, J. S. Lawler, T. W. Reddoch, and R. L. Sullivan Jun. 1986 45 p
(Contracts NAS3-24105; DE-AI01-76ET-20320)
(NASA-CR-175056; DOE/NASA/4105-2; NAS 1.26:175056) Avail: NTIS HC A03/MF A01 CSCL 10B

This document organizes the total range of utility related issues, reviews wind turbine control and dynamic characteristics, identifies the interaction of wind turbines to electric utility systems, and identifies areas for future research. The material is organized at three levels: the wind turbine, its controls and characteristics; connection strategies as dispersed or WPSs; and the composite issue of planning and operating the electric power system with wind generated electricity. Author

N87-17401*# Cleveland State Univ., Ohio.
DESIGN AND DYNAMIC SIMULATION OF A FIXED PITCH 56 kW WIND TURBINE DRIVE TRAIN WITH A CONTINUOUSLY VARIABLE TRANSMISSION Final Report
C. Gallo, R. Kasuba, A. Pintz, and J. Spring Mar. 1986 45 p
(Contracts NCC3-6; DE-AI01-76ET-20320)
(NASA-CR-179543; DOE/NASA/0006-3; NAS 1.26:179543) Avail: NTIS HC A03/MF A01 CSCL 10B

The dynamic analysis of a horizontal axis fixed pitch wind turbine generator (WTG) rated at 56 kW is discussed. A mechanical Continuously Variable Transmission (CVT) was incorporated in the drive train to provide variable speed operation capability. One goal of the dynamic analysis was to determine if variable speed operation, by means of a mechanical CVT, is capable of capturing the transient power in the WTG/wind environment. Another goal was to determine the extent of power regulation possible with CVT operation. Author

N87-17402# AeroVironment, Inc., Monrovia, Calif.
HAWT PERFORMANCE WITH DYNAMIC STALL
B. D. Hibbs Feb. 1986 88 p
(Contract DE-AC02-83CH-10093)
(DE86-004428; SERI/STR-217-2732) Avail: NTIS HC A05/MF A01

The effects of flow nonuniformities (wing shear, tower wake, yaw, and large-scale turbulence) on the performance of a horizontal axis wind turbine are calculated, accounting for dynamic stall. The PROP program was modified to incorporate and compare these effects with the uniform flow case. The MIT model, which predicts dynamic lift coefficients substantially higher than the static maximum values and includes a crude model of the vortex roll-off phenomenon, represented dynamic stall. As associated model for drag was also used. The dynamic stall model was tested against experimental data for three typical reduced frequencies. Good instantaneous correlation was obtained. The effects of nonuniformities with and without the dynamic stall were calculated using the Westinghouse Mod O and Enertech 44/25 turbines. Modeling the dynamic stall has little effect on performance. Furthermore, the performance with nonuniform flow differed only slightly from the uniform flow case. Thus the new PROP model provides a powerful general capability to handle nonuniform flows. DOE

N87-17403# Midwest Research Inst., Golden, Colo. Solar Energy Research Inst.
FEASIBILITY OF USING WIND POWER FOR AN AEROSTAT-BORNE RADAR SYSTEM
H. Sklar May 1986 41 p
(Contract DE-AC02-83CH-10093)
(DE86-004461; SERI/STR-217-2899) Avail: NTIS HC A03/MF A01

The feasibility of using a wind power system on an aerostat (tethered balloon) was studied. The system would be used by the US Air Force North Warning Program to provide power for a radar carried on the aerostat. Upper atmosphere wind data for a potential site were collected and probability functions for wind speed and wind power density calculated. Information was collected on aerostats, tethers, telemetry transmitters, and auxiliary equipment. Important design considerations were identified and useful mathematical expressions, e.g., wind reliability, derived. A first-cut wind power system was designed and system performance and aerodynamic loads were calculated. The benefits and risks of a wind power system were enumerated. The study concluded that a wind system is feasible for this application. DOE

N87-17404# Midwest Research Inst., Golden, Colo. Solar Energy Research Inst.
WIND ENERGY TECHNICAL READING LIST
1986 20 p
(Contract DE-AC02-83CH-10093)
(DE86-010704; SERI/SP-273-2911) Avail: NTIS HC A02/MF A01

The Wind Energy Technical Reading List provides a short bibliography of recent technical publications by the US Department of Energy's National Laboratories and their subcontractors and other organizations doing wind energy research and development. The list was prepared by the Technical Information Branch and the Wind Energy Research Center at the Solar Energy Research Institute (SERI). It includes journal articles, papers presented in conference proceedings, and technical reports. DOE

N87-17405# Rensselaer Polytechnic Inst., Troy, N.Y.
RESEARCH ON SINGLE-CRYSTAL CdTe SOLAR CELLS Annual Subcontract Report, 1 Feb. 1985 - 1 Feb. 1986
J. M. Borrego and S. K. Ghandhi Jun. 1986 17 p
(Contract DE-AC02-83CH-10093)
(DE86-010719; SERI/STR-211-2962) Avail: NTIS HC A02/MF A01

This report outlines work carried out during Phase 1 of growth and characterization of single-crystal CdTe layers to explore their potential in high-efficiency solar cells. High-quality InSb layers can be grown by organometallic vapor phase epitaxy (OMVPE). Layers have been grown whose photoluminescence peak has a full width half maximum of 5.8 MeV, the lowest value achieved to date in epitaxial layers of this compound semiconductor. CdTe layers with featureless morphology were grown at 350 to 420 C. All layers are n-type. A hole lifetime of 1.5 micrometers was measured by optical techniques and corroborated by DLTS measurements. Both Schottky and p-n junction cells have been made on these layers. Device characteristics are contained in the report. DOE

N87-17406# Pacific Northwest Labs., Richland, Wash.
MODEL FOR SIMULATING ROTATIONAL DATA FOR WIND TURBINE APPLICATIONS
D. C. Powell and J. R. Connell Apr. 1986 114 p
(Contract DE-AC06-76RL-01830)
(DE86-010784; PNL-5857) Avail: NTIS HC A06/MF A01

This document describes a wind simulation model to be used in relation to wind turbine operations. The model is a computer code written in FORTRAN 77. The model simulates turbulence and mean wind effects as they are experienced at a rotating point on the blade of either a horizontal-axis wind turbine (HAWT) or a vertical-axis wind turbine (VAWT). The model is fast, requiring 15 to 120 seconds of VAX execution time to produce a simulation and related statistics. The model allows the user to set a number of wind parameters so that he may evaluate the uncertainty of model results as well as their typical values. When this capability is combined with short execution time, the user can quickly produce a number of simulations based on reasonable variation of input parameters and can use these simulations to obtain a range of wind turbine responses to the turbulence. This ability is important because some of the wind parameters that cannot be precisely evaluated should be prescribed over a range of values. This document is essentially a user's guide. Its features include theoretical derivations, samples of output, comparisons of measured and modeled results, a listing of the FORTRAN code, a glossary for the code, and the input and output of a sample run. DOE

N87-17407# Pacific Northwest Labs., Richland, Wash.
REVIEW OF WIND SIMULATION METHODS FOR HORIZONTAL-AXIS WIND TURBINE ANALYSIS
D. C. Powell and J. R. Connell Jun. 1986 45 p
(Contract DE-AC06-76RL-01830)
(DE86-012223; PNL-5903) Avail: NTIS HC A03/MF A01

This report reviews three reports on simulation of winds for use in wind turbine fatigue analysis. The three reports are presumed to represent the state of the art. The Purdue and Sandia methods simulate correlated wind data at two points rotating as on the rotor of a horizontal-axis wind turbine. The PNL method at present simulates only one point, which rotates either as on a horizontal-axis wind turbine blade or as on a vertical-axis wind turbine blade. The spectra of simulated data are presented from the Sandia and PNL models under comparable input conditions, and the energy calculated in the rotational spikes in the spectra by the two models is compared. Although agreement between the two methods is not impressive at this time, improvement of the Sandia and PNL methods is recommended as the best way to advance the state of the art. Physical deficiencies of the models are cited in the report and technical recommendations are made for improvement. The report also reviews two general methods for simulating single-point data, called the harmonic method and the white noise method. The harmonic method, which is the basis of all three specific methods reviewed, is recommended over the white noise method in simulating winds for wind turbine analysis. DOE

N87-17408*# Pennsylvania State Univ., University Park.
USE OF LOW ENERGY ION IMPLANTS IN HIGH EFFICIENCY CRYSTALLINE SILICON SOLAR CELLS Final Report
S. J. Fonash, Rambir Singh, and X. C. Mu 1986 60 p
(Contracts NAS-7-100; JPL-957126)
(NASA-CR-179971; NAS 1.26:179971; DE86-012364; DOE/NBM-6012364) Avail: NTIS HC A04/MF A01 CSCL 10A

This program explored the use of low energy hydrogen ion implants in the fabrication of high efficiency crystalline silicon solar cells. The work established that low energy hydrogen ion implants can result in hydrogen - caused effects in all three regions of a solar cell; viz, emitter, space charge region, and base. In web, Cz, and Fz material low energy hydrogen ion implantation can reduce surface recombination velocity. In web, Cz, and Fz material hydrogen implants were found to passivate space charge region recombination centers. In web cells, hydrogen implants were found also to passivate the base region. However, similar improvement was not seen for the base region of Cz or Fz cells. In the case of web material, hydrogen is believed to be able to diffuse into the base region where it can passivate structural defects present in web in the base. DOE

45 ENVIRONMENT POLLUTION

Includes atmospheric, noise, thermal, and water pollution.

N87-16993# Central Electricity Research Labs., Leatherhead (England). Technical Planning and Research Div.
AN INTRODUCTION TO THE NUMERICAL MODELLING OF DISPERSION IN THE ATMOSPHERIC BOUNDARY LAYER
A. G. Robins *In* Von Karman Inst. for Fluid Dynamics Introduction to Numerical Solution to Industrial Flows, Volume 1 1986 82 p
(For primary document see N87-16987 09-34)
Avail: NTIS HC A14/MF A01

N87-17100# Joint Publications Research Service, Arlington, Va.
DETERMINATION OF NONGLOBAL COMPONENT AGAINST BACKGROUND OF GLOBAL RADIOACTIVE POLLUTION OF ATMOSPHERIC AEROSOLS Abstract Only
Z. G. Gritchenko, V. M. Flegontov, and K. Sinkko *In its* USSR

Report: Earth Sciences (JPRS-UES-86-005) 7 May 1986 p 4 Transl. into ENGLISH from Radiokhimiya (Leningrad, USSR), v. 27, no. 5, 1985 p 669-673 (For primary document see N87-17096 09-42)
Avail: NTIS HC A05/MF A01

46 GEOPHYSICS

Includes aeronomy; upper and lower atmosphere studies; ionospheric and magnetospheric physics; and geomagnetism.

For space radiation see *93 Space Radiation.*

N87-17409 California Inst. of Tech., Pasadena.
DYNAMICAL MODELS FOR THE EARTH'S GEOID Ph.D. Thesis
Mark Alan Richards 1986 329 p
Avail: Univ. Microfilms Order No. DA8620947

The Earth's largest geoid anomalies occur at the lowest spherical harmonic degrees, or longest wavelengths, and are primarily the result of mantle convection. Thermal density contrasts due to convection are partially compensated by boundary deformations due to viscous flow whose effects must be included in order to obtain a dynamically consistent model for geoids. These deformations occur rapidly with respect to the timescale for convection, and geoids response kernels were calculated for steady-state, viscous, incompressible, self-gravitating, layered-Earth models which include the deformation of boundaries due to internal loads. Both the sign and magnitude of geoid anomalies depend strongly upon the viscosity structure of the mantle as well as the possible presence of chemical layering. Correlations of various global geophysical data sets with the observed geoid can be used to construct theoretical geoid models which constrain the dynamics of mantle convection. Recent models for seismic heterogeneity in the mantle provide additional constraints. Dissert. Abstr.

N87-17410 Florida State Univ., Tallahassee.
VARIABILITY IN THE EARTH RADIATION BUDGET AS DETERMINED FROM THE NIMBUS ERB EXPERIMENTS Ph.D. Thesis
Philip Edward Ardanuy 1986 344 p
Avail: Univ. Microfilms Order No. DA8619135

Data taken by the Earth Radiation Budget (ERB) experiment on board the Nimbus-6 and Nimbus-7 satellites is examined. The goal is an understanding of the bounds of variability of the radiation budget components. This variability is examined on daily, monthly, and annual time scales. An in-flight characterization of the instrument was performed, and a set of calibration adjustments for the Nimbus-7 ERB was developed that enabled interannual climate studies to be made. A technique for the transfer of this calibration to the Nimbus-6 ERB experiment was derived that enables the creation of a decadal joint ERB data set. Error bars for the data set were established. The radiation budget component (albedo and longwave emission) responses to the 1982 eruptions of the El Chichon volcano were examined. Based on the observations, an understanding of the global distribution, evolution, and persistence of the resultant aerosol cloud was achieved. The evolution of the major 1982/1983 ENSO event was monitored for the first time by broadband radiometers. Quasi-stationary, planetary-scale tropical and midlatitude teleconnection patterns are shown to emerge as the event reaches its peak intensity. The onset, intensification, and withdrawal of drought over Indonesia, Australia, the Pacific Ocean island chains, and the Amazon River Valley was monitored based on inferred irrotational, three-dimensional flow fields. Anomalous subsidence, forced by the ENSO episode was noted over all drought regions.
Dissert. Abstr.

N87-17411 Utah State Univ., Logan.
MODEL STUDY OF THE MID-LATITUDE ATMOSPHERIC INTERACTION WITH ENERGETIC O+ AND He+ (> 20 keV) PRECIPITATION DURING A STORM Ph.D. Thesis
Michi Ishimoto 1985 213 p
Avail: Univ. Microfilms Order No. DA8619402

Satellite observations since 1969 have measured energetic oxygen ion precipitation equatorward of the auroral zone. The measured energy fluxes of particles with kinetic energy from 0.7 to 12 keV were found to be as high as 0.4 erg/sq cm/s/sr. Satellite data have shown that there is also some He ion precipitation. Ground based spectrometric observations indicate that energetic O(+) precipitation causes the low-latitude auroral emissions. A model computation was used to investigate the midlatitude atmospheric interaction with energetic O(+) and He(+) precipitation during a storm. The steady state continuity equations for the fluxes are formulated as a system of first order ordinary differential equations. The model, consisting of three components, O, N2, and He, computes the upward and downward fluxes resulting from energetic ion precipitation by solving sets of this system of equations. The model computes the heating, the ion production, the N2(+) first negative (O-O) band and N2 second positive (O-O) band emission intensities in the atmosphere, and the escape fluxes to the magnetosphere. Dissert. Abstr.

N87-17412 California Univ., Los Angeles.
TRANSMISSION OF ATMOSPHERIC INTERNAL GRAVITY WAVES INTO THE STRATOSPHERE Ph.D. Thesis
Teddie Lee Keller 1986 167 p
Avail: Univ. Microfilms Order No. DA8621090

Atmospheric internal gravity waves are often produced when air flows over mountainous terrain. Associated with these waves is a transport of horizontal momentum from the surface of the Earth to the upper atmosphere. This momentum flux is considered to be a major source of drag in the middle atmosphere. The transmission of mountain induced internal gravity waves through the troposphere and into the stratosphere is investigated. To capture the essential dynamical features, an atmospheric structure was chosen in which the wind increases linearly with height to the tropospause, above which it remains constant, and the stability is constant in the troposphere and constant in the stratosphere. Both linear analytic techniques and a nonlinear numerical model were used. With computer aided analysis analytic solutions were obtained to the problem of this representative troposphere stratosphere model which has remained intractable until now. The nonlinear numerical model developed has the unique feature that it incorporates a conformal terrain following coordinate system, allowing for arbitrary mountain profiles. Results from both the linear analysis and the nonlinear numerical model are given.
Dissert. Abstr.

N87-17413*# Polytechnic Inst. of Brooklyn, Farmingdale, N. Y. Research Inst.
A STUDY OF LARGE, MEDIUM AND SMALL SCALE STRUCTURES IN THE TOPSIDE IONOSPHERE Final Technical Report
Stanley H. Gross, Spencer P. Kuo, and Jerry Shmoys Dec. 1986 7 p
(Grant NAGw-284)
(NASA-CR-180068; NAS 1.26:180068; POLY-MRI-1454-86) Avail: NTIS HC A02/MF A01 CSCL 04A

Alouette and ISIS data were studied for large, medium, and small scale structures in the ionosphere. Correlation was also sought with measurements by other satellites, such as the Atmosphere Explorer C and E and the Dynamic Explorer 2 satellites, of both neutrals and ionization, and with measurements by ground facilities, such as the incoherent scatter radars. Large scale coherent wavelike structures were found from ISIS 2 electron density contours from above the F peak to nearly the satellite altitude. Such structures were also found to correlate with the observation by AE-C below the F peak during a conjunction of the two satellites. Vertical wavefronts found in the upper F region suggest the dominance of diffusion along field lines as well. Also discovered were multiple, evenly spaced field-aligned ducts in the F region that, at low latitudes, extended to the other hemisphere and were in the form of field-aligned sheets in the east-west

direction. Low latitude heating events were discovered that could serve as sources for waves in the ionosphere. B.G.

N87-17414*# International Council of Scientific Unions, Urbana, Ill.
MIDDLE ATMOSPHERE PROGRAM. HANDBOOK FOR MAP, VOLUME 22
James M. Russell, III, ed. Sep. 1986 308 p Sponsored by NASA
(NASA-CR-180128; NAS 1.26:180128) Avail: NTIS HC A14/MF A01 CSCL 04A

A series of plots are presented that describe the state of the stratosphere and to some degree, the mesosphere as revealed by satellite observations. The pertinent instrument features, spatial and temporal coverage, and details of accuracy and precision for the experiments providing the data are described. The main features of zonal mean cross sections and polar stereographic projections are noted and intercomparisons are discussed where a parameter was measured by more than one experiment. It was not the attempt to be exhaustive in this or to present detailed results of scientific investigations. The main purpose was to collect the available data in one place and provide enough information on limitations or cautions about the data so that they could be used in model comparisons and science studies. Without a doubt, when these are used, numerous questions will arise that were not addressed here. In such cases, the reader is encouraged to contact the experimenters for proper clarification. Author

N87-17415*# Ohio State Univ., Columbus. Dept. of Geodetic Science and Surveying.
BASIC RESEARCH FOR THE GEODYNAMICS PROGRAM Semi-annual Status Report, Jul. - Dec. 1986
Dec. 1986 20 p
(Grant NsG-5265; OSURF Proj. 711055)
(NASA-CR-180137; NAS 1.26:180137; SASR-17) Avail: NTIS HC A02/MF A01 CSCL 08G

Further development of utility program software for analyzing final results of Earth rotation parameter determination from different space geodetic systems was completed. Main simulation experiments were performed. Results and conclusions were compiled. The utilization of range-difference observations in geodynamics is also examined. A method based on the Bayesian philosophy and entropy measure of information is given for the elucidation of time-dependent models of crustal motions as part of a proposed algorithm. The strategy of model discrimination and design of measurements is illustrated in an example for the case of crustal deformation models. B.G.

N87-17416*# Ohio State Univ., Columbus. Dept. of Geodetic Science and Surveying.
IMPROVEMENT OF THE EARTH'S GRAVITY FIELD FROM TERRESTRIAL AND SATELLITE DATA Status Report, 1 Nov. 1984 - 31 Dec. 1986
Jan. 1987 9 p
(Grant NGR-36-008-161; OSURF Proj. 783210)
(NASA-CR-180139; NAS 1.26:180139; SR-42) Avail: NTIS HC A02/MF A01 CSCL 08G

The terrestrial gravity data base was updated. Studies related to the Geopotential Research Mission (GRM) have primarily considered the local recovery of gravity anomalies on the surface of the Earth based on satellite to satellite tracking or gradiometer data. A simulation study was used to estimate the accuracy of 1 degree-mean anomalies which could be recovered from the GRM data. Numerous procedures were developed for the intent of performing computations at the laser stations in the SL6 system to improve geoid undulation calculations. B.G.

N87-17417*# National Aeronautics and Space Administration. Langley Research Center, Hampton, Va.
SAGE AEROSOL MEASUREMENTS. VOLUME 3: JANUARY 1, 1981 TO NOVEMBER 18, 1981
M. Patrick McCormick Feb. 1987 274 p
(NASA-RP-1173; L-16177; NAS 1.61:1173) Avail: NTIS HC A12/MF A01 CSCL 04A

The Stratospheric Aerosol and Gas Experiment (SAGE) satellite system, launched February 18, 1979, obtained profiles of aerosol extinction at 1.00 micron and 0.45 micron ozone concentration, and nitrogen dioxide concentration. Data taken during sunset events are presented in the form of zonal and seasonal averages of aerosol extinction of 1.00 micron and 0.45 micron, ratios of aerosol extinction to molecular extinction at 1.00 micron and ratios of aerosol extinction at 0.45 micron to aerosol extinction at 1.00 micron. Averages for 1981 are shown in tables, and in profile and contour plots (as a function of altitude and latitude). In addition, temperature data provided by NOAA for the time and location of each SAGE measurement are averaged and shown in a similar format. The stratospheric aerosol distribution for 1981 shows effects of volcanically injected material from eruptions of Ulawun, Alaid, and Pagan. Peak values of aerosol extinction at 0.45 micron and 1.00 micron were 2 to 4 times higher than typical peak values observed during near background conditions. Stratospheric aerosol optical depth values at 1.00 microns increased by a factor of about 2 from near background levels in regions of volcanic activity. During the year, these values ranged from between 0.001 and 0.006. The largest were near the location of a recent eruption. The distribution of the ratio of aerosol to molecular extinction at 1.00 microns also showed that maximum values are found in the vicinity of an eruption. These maximums varied in altitude, but remained below a height of about 25 km. No attempt has been made to give detailed explanations or interpretations of these data. The intent is to provide, in a ready-to-use visual format, representative zonal and seasonal averages of aerosol extinction data for the third calendar year of the SAGE data set to facilitate atmospheric and climatic studies. Author

N87-17418*# Purdue Univ., West Lafayette, Ind. Dept. of Earth and Atmospheric Sciences.
IMPROVING THE GEOLOGICAL INTERPRETATION OF MAGNETIC AND GRAVITY SATELLITE ANOMALIES Final Report, 1 Apr. 1985 - 31 Nov. 1986
William J. Hinze, Lawrence W. Braile, and Ralph R. B. vonFrese (Ohio State Univ., Columbus) Jan. 1987 124 p
(Grant NAGw-736)
(NASA-CR-180149; NAS 1.26:180149) Avail: NTIS HC A06/MF A01 CSCL 08G

Quantitative analysis of the geologic component of observed satellite magnetic and gravity fields requires accurate isolation of the geologic component of the observations, theoretically sound and viable inversion techniques, and integration of collateral, constraining geologic and geophysical data. A number of significant contributions were made which make quantitative analysis more accurate. These include procedures for: screening and processing orbital data for lithospheric signals based on signal repeatability and wavelength analysis; producing accurate gridded anomaly values at constant elevations from the orbital data by three-dimensional least squares collocation; increasing the stability of equivalent point source inversion and criteria for the selection of the optimum damping parameter; enhancing inversion techniques through an iterative procedure based on the superposition theorem of potential fields; and modeling efficiently regional-scale lithospheric sources of satellite magnetic anomalies. In addition, these techniques were utilized to investigate regional anomaly sources of North and South America and India and to provide constraints to continental reconstruction. Since the inception of this research study, eleven papers were presented with associated published abstracts, three theses were completed, four papers were published or accepted for publication, and an additional manuscript was submitted for publication. Author

N87-17419# Slovak Academy of Sciences, Bratislava (Czechoslovakia). Geomagnetic Observatory.
RESULTS OF GEOMAGNETIC OBSERVATIONS AT THE HURBANOVO GEOMAGNETIC OBSERVATORY IN 1985
1986 75 p In CZECHOSLOVAKIAN, RUSSIAN and ENGLISH
Avail: NTIS HC A04/MF A01

The absolute observations were made at regular intervals of

7 days, activity of the geomagnetic field permitting. Some observations with the proton magnetometer, however, were made more frequently, i.e., twice a week. Declination, horizontal component, vertical component, and total field measurements were taken.B.G.

N87-17420*# Saint Louis Univ., Mo. Dept. of Earth and Atmospheric Sciences.
A DIAGNOSTIC APPROACH TO OBTAINING PLANETARY BOUNDARY LAYER WINDS USING SATELLITE-DERIVED THERMAL DATA Final Report
Carol L. Belt and Henry E. Fuelberg Mar. 1984 173 p Previously announced as N85-14330
(Contract NAS8-33370)
(NASA-CR-178972; NAS 1.26:178972) Avail: NTIS HC A08/MF A01 CSCL 04A

The feasibility of using satellite derived thermal data to generate realistic synoptic scale winds within the planetary boundary layer (PBL) is examined. Diagnostic modified Ekman wind equations from the Air Force Global Weather Central (AFGWC) Boundary Layer Model are used to compute winds at seven levels within the PBL transition layer (50 m to 1600 m AGL). Satellite derived winds based on 62 predawn TIROS-N soundings are compared to similarly derived wind fields based on 39 AVE-SESAME II rawinsonde (RAOB) soundings taken 2 h later. Actual wind fields are also used as a basis for comparison. Qualitative and statistical comparisons show that the Ekman winds from both sources are in very close agreement, with an average vector correlation coefficient of 0.815. Best results are obtained at 300 m AGL. Satellite winds tend to be slightly weaker than their RAOB counterparts and exhibit a greater degree of cross-isobaric flow. The modified Ekman winds show a significant improvement over geostrophic values at levels nearest the surface. Author

N87-17421# Institut d'Aeronomie Spatiale de Belgique, Brussels.
A MODEL FOR AN ELECTROMOTIVE FORCE GENERATOR IN THE MAGNETOSPHERE: A SOURCE OF DISCRETE AURORAL ARCS
M. Roth, D. S. Evans (National Oceanic and Atmospheric Administration, Boulder, Colo.), and J. Lemaire 1986 25 p Presented at the Agard Meeting on The Aerospace Environment at High Altitudes and its Implications for Spacecraft Charging and Communications, The Hague, Netherlands, 2-7 Jun. 1986
(Aeronomica-Acta-A-309-1986; ISSN-0065-3713; ETN-87-98838)
Avail: NTIS HC A02/MF A01

Results obtained from solving Maxwell's and Vlasov's equations to obtain the electrical structure of the sheath which separates magnetospheric particle populations of different densities and temperatures are presented. It is shown that for reasonable magnetospheric plasma populations, an electric potential difference of several kilovolts exists across such a boundary. This potential can serve as the necessary electromotive force for the auroral current circuit. The colocation between a magnetospheric plasma boundary and a discrete aurora is a natural consequence of this picture. ESA

N87-17422# Instituto Nacional de Tecnica Aeroespacial, Madrid (Spain). Dept. de Estructuras y Materiales Estructurales.
GROUND VIBRATION TESTS [ENSAYO DE VIBRACION EN TIERRA]
Rafael Gonzalo Ugartel 1986 13 p In SPANISH; ENGLISH summary
(ETN-87-98847) Avail: NTIS HC A02/MF A01

Ground vibration tests are used to improve and to ratify the dynamic model of aircraft prototypes. The goal is to verify the absence of flutter. The basic dynamic equations and the basis of the semiautomatic procedure developed to isolate resonance modes and to determine all modal parameters are shown. All necessary equipment and their layouts are exposed. The tests performed on the Attas aircraft are commented upon. ESA

N87-17105# Joint Publications Research Service, Arlington, Va.
SOLUTION OF DIRECT GRAVIMETRY PROBLEMS FOR VERTICAL CYLINDRICAL BODIES Abstract Only
A. V. Kudrya *In its* USSR Report: Earth Sciences (JPRS-UES-86-005) 7 May 1986 p 35 Transl. into ENGLISH from Geologiya i Geofizika (Novosibirsk, USSR), no. 10, Oct. 1985 p 94-100 (For primary document see N87-17096 09-42)
Avail: NTIS HC A05/MF A01

N87-17108# Joint Publications Research Service, Arlington, Va.
JOINT INFLUENCE OF TURBULENCE AND WIND ON SIGNAL POWER IN RADIOACOUSTIC SOUNDING OF ATMOSPHERE Abstract Only
A. I. Kon *In its* USSR Report: Earth Sciences (JPRS-UES-86-005) 7 May 1986 p 47 Transl. into ENGLISH from Izvestiya Akademii Nauk SSSR: Fizika Atmosfery i Okeana (Moscow, USSR), v. 21, no. 12, Dec. 1985 p 1242-1251 (For primary document see N87-17096 09-42)
Avail: NTIS HC A05/MF A01

N87-17198# Cairo Univ. (Egypt). Dept. of Electronic Engineering.
DETERMINATION OF RESISTIVITY AND PERMITTIVITY PROFILES OF A LAYERED EARTH
H. M. Assal and S. F. Mahmoud *In* ESA Proceedings of the 1986 International Geoscience and Remote Sensing Symposium (IGARSS '86) on Remote Sensing: Today's Solutions for Tomorrow's Information Needs, Volume 1 Aug. 1986 p 205-209 (For primary document see N87-17163 09-43)
(Grant FRCU-842019)
Avail: NTIS HC A99/MF E03; ESA, Paris, France, 3 volume set $90 Member States, AU, CN, and NO (+20% others)

N87-17201# Arizona State Univ., Tempe. Dept. of Electrical and Computer Engineering.
GRADIENT METHODS FOR GEOPHYSICAL IMAGE INVERSIONS
M. S. Frank and C. A. Balanis *In* ESA Proceedings of the 1986 International Geoscience and Remote Sensing Symposium (IGARSS '86) on Remote Sensing: Today's Solutions for Tomorrow's Information Needs, Volume 1 Aug. 1986 p 223-227 (For primary document see N87-17163 09-43)
(Contract DAAG29-85-K-0045)
Avail: NTIS HC A99/MF E03; ESA, Paris, France, 3 volume set $90 Member States, AU, CN, and NO (+20% others)

N87-17245# Arkansas Univ., Fayetteville. Dept. of Electrical Engineering.
HAWAIIAN LAVA FLOWS AND SIR-B RESULTS
B. A. Derryberry, W. P. Waite, V. H. Kaupp, H. C. MacDonald, L. R. Gaddis (Hawaii Inst. of Geophysics, Honolulu.), and P. Mouginis-Mark *In* ESA Proceedings of the 1986 International Geoscience and Remote Sensing Symposium (IGARSS '86) on Remote Sensing: Today's Solutions for Tomorrow's Information Needs, Volume 1 Aug. 1986 p 497-501 (For primary document see N87-17163 09-43)
Avail: NTIS HC A99/MF E03; ESA, Paris, France, 3 volume set $90 Member States, AU, CN, and NO (+20% others)

N87-17270*# Arizona Univ., Tucson.
EXTRAPOLATION OF EARTH-BASED SOLAR IRRADIANCE MEASUREMENTS TO EXOATMOSPHERIC LEVELS FOR BROAD-BAND AND SELECTED ABSORPTION-BAND OBSERVATIONS
J. A. Reagan, P. A. Pilewskie, I. C. Scott-Fleming, and B. M. Hermann *In* ESA Proceedings of the 1986 International Geoscience and Remote Sensing Symposium (IGARSS '86) on Remote Sensing: Today's Solutions for Tomorrow's Information Needs, Volume 1 Aug. 1986 p 653-659 (For primary document see N87-17163 09-43)
(NASA Order L-83161-B; NASA Order A-32033-C; Contract NOAA-NA-80RAD00065)
Avail: NTIS HC A99/MF E03; ESA, Paris, France, 3 volume set $90 Member States, AU, CN, and NO (+20% others) CSCL 04A

N87-17271# National Severe Storms Lab., Norman, Okla.
APPLICATION OF DOPPLER RADAR AND LIDAR TO DI-

AGNOSE ATMOSPHERIC PHENOMENA
R. J. Doviak, M. Eilts, V. Mazur, M. Sachidananda, and D. S. Zrnic *In* ESA Proceedings of the 1986 International Geoscience and Remote Sensing Symposium (IGARSS '86) on Remote Sensing: Today's Solutions for Tomorrow's Information Needs, Volume 1 Aug. 1986 p 661-666 (For primary document see N87-17163 09-43)
Avail: NTIS HC A99/MF E03; ESA, Paris, France, 3 volume set $90 Member States, AU, CN, and NO (+20% others)

N87-17339# National Oceanic and Atmospheric Administration, Boulder, Colo. Wave Propagation Lab.
GROUND-BASED MICROWAVE RADIOMETRIC OBSERVATIONS OF ATMOSPHERIC GEOPOTENTIAL HEIGHT FLUCTUATIONS
E. R. Westwater, A. J. Bedard, P. Ciotti (Rome Univ., Italy), and M. T. Decker (Colorado Univ., Boulder) *In* ESA Proceedings of the 1986 International Geoscience and Remote Sensing Symposium (IGARSS '86) on Remote Sensing: Today's Solutions for Tomorrow's Information Needs, Volume 2 Aug. 1986 p 1063-1068 (For primary document see N87-17283 09-43)
Avail: NTIS HC A17/MF A01; ESA, Paris, France, 3 volume set $90 Member States, AU, CN, and NO (+20% others)

47 METEOROLOGY AND CLIMATOLOGY

Includes weather forecasting and modification.

N87-17423 Purdue Univ., West Lafayette, Ind.
A LABORATORY INVESTIGATION OF TWO-CELLED VORTEX FLOWS Ph.D. Thesis
Randal Lee Pauley 1986 147 p
Avail: Univ. Microfilms Order No. DA8622206

An experimental study of the steady-state kinematics, dynamics, and morphology of two-celled vortex flows has been conducted in the Ward-type tornado vortex chamber (TVC) at Purdue University, with emphasis on exploring the vertical momentum balance in the vortex core and better defining the flow near the external boundaries of the TVC. Results show that in the Purdue TVC the flow downstream of the vortex breakdown is everywhere two-celled, with the strongest axial downflow occurring at middle levels. The pressure on the axis in the two-celled vortices increases with height immediately downstream of the breakdown, with the axial pressure gradient tending toward zero farther downstream. Analysis of the laboratory findings within the context of the vertical momentum equation shows that the vertical shear stress can play an important role in the axial momentum balance of two-celled vortices by opposing the filling of the vortex core from aloft and so helping to maintain low pressure and high velocities near the surface. The numerical model of Rotunno (1984) is successful in qualitatively replicating several of the flow characteristics in the TVC, including two-cell flow, multiple subsidiary vortices, strongest downflow at middle levels, axial pressure increasing with height, and the role of vertical shear stress in the axial momentum balance. Dissert. Abstr.

N87-17424 California Inst. of Tech., Pasadena.
EMPIRICAL RELATIONS BETWEEN THE EARTH'S RADIATION BUDGET, CLOUDINESS, AND VARIOUS METEOROLOGICAL PARAMETERS Ph.D. Thesis
Daniel Wenkert 1986 202 p
Avail: Univ. Microfilms Order No. DA8620954

The effect of variation of meteorological variables, cloudiness, and surface variables (such as albedo and continentality) on the reflected solar and emitted terrestrial radiation leaving the top of the atmosphere was investigated. Radiometric data from the scanner channels of the Earth Radiation Budget (ERB) instrument on Nimbus-7; cloudiness variables from analysis done on data from the Temperature and Humidity Infrared Radiometer (THIR) on Nimbus-7; and meteorological data from the FGGE (First Garp Global Experiment) Level 3-b global weather analyses were investigated. The data were analyzed on time scales of one day and spatial scales of about 450 km. The effect of cloudiness on the net radiation was determined for various surface and atmospheric conditions. It was determined whether or not this type of linear analysis on a data set of synoptic time and space scales could be used for a resonable and empirically accurate parameterization of radiation to be used in simple energy balance climate models. The regressions determined from this data set between radiation, cloudiness, and weather were compared with the internal statistics developed in a Global Circulation Model (GCM), with the idea that eventually this type of linear analysis could be used as a constraint on the GCMs used by the atmospheric science community. Dissert. Abstr.

N87-17425*# Universities Space Research Association, Boulder, Colo.
RESULTS FROM 1984 AIRBORNE DOPPLER LIDAR WIND MEASUREMENT PROGRAM. FLIGHT 6: ANALYSIS OF LINE-OF-SIGHT ELEVATION ANGLE ERRORS AND APPARENT DOPPLER VELOCITIES Interim Report
Jeffry Rothermel Jan. 1987 18 p
(Contract NAS8-34010)
(NASA-CR-178994; NAS 1.26:178994) Avail: NTIS HC A02/MF A01 CSCL 04B

During the summer of 1984 the Marshall Space Flight Center's Airborne Doppler Lidar System (ADLS) made a series of wind measurements in the California Central Valley. This study quantifies the lidar beam angle errors and velocity errors through analysis of ground return signals. Line-of-sight elevation (LOSE) angle errors are under 1 deg. Apparent Doppler ground velocities, as large as 2m/s, are considerably less than in a previous flight experiment in 1981. No evidence was found of a Schuler resonance phenomenon common to inertial navigation systems (INS), however the aperiodic nature of the apparent velocities implies an error in the INS-derived ground speeds. Certain features and subtleties in the ground returns are explained in terms of atmospheric structure and characteristics of the ADLS hardware and software. Finally, least squares and low-pass filtering techniques are suggested for eliminating errors during post-processing. Author

N87-17426*# South Dakota School of Mines and Technology, Rapid City. Inst. of Atmospheric Sciences.
T-28 DATA ACQUISITION DURING COHMEX 1986 Final Report
Dennis J. Musil and Paul L. Smith Dec. 1986 24 p
(Contract NAS8-36489)
(NASA-CR-179001; NAS 1.26:179001; SDSMT/IAS/R-86/08)
Avail: NTIS HC A02/MF A01 CSCL 04B

As part of the 1986 Cooperative Huntsville Meteorological Experiment (COHMEX) a cloud physics instrumented T-28 aircraft was used in conjunction with multiple ground based Doppler radars to characterize hydrometeors and updraft structure within developing summertime cumulus and cumulonimbus cloud systems near Huntsville, Alabama. Instrumentation aboard the aircraft included a Particle Measuring Systems (PMS) Forward Scattering Spectrometer Probe (FSSP), a PMS 2D Cloud Probe and a PMS 2D Precipitation Probe, as well as a hail spectrometer and a foil impactor. Hydrometeor spectra were obtained in the interior of mature thunderstorms over the size range from cloud droplets through hailstones. In addition, vertical wind speed, temperature, Johnson-Williams (JW) liquid water content and electric field measurements were made. Significant microphysical differences exist between these clouds and summertime cumulonimbus clouds which develop over the Central Plains. One notable difference in clouds displaying similar radar reflectivities is that COHMEX hydrometeors are typically smaller and more numerous than those observed in the Central Plains. The COHMEX cloud microphysical measurements represent ground truth values for the remote sensing instrumentation which was flown over the cloud tops at altitudes between 60,000 and 70,000 ft aboard NASA U-2 and ER-2 aircraft. They are also being used jointly with a numerical cloud model to assist in understanding the development of summertime subtropical clouds. Author

N87-17427# European Office of Aerospace Research and Development, FPO New York 09510.
HOMOGENIZING SURFACE AND SATELLITE OBSERVATIONS OF CLOUD Interim Report, 1 Oct. 1985 - 30 Sep. 1986
Ann Henderson-Sellers and Alan Goodman 28 Nov. 1986 89 p (Grant AF-AFOSR-0299-85)
(AD-A174691; EOARD-TR-87-01) Avail: NTIS HC A05/MF A01 CSCL 04/1

The major types of cloud retrieval algorithms are reviewed with special emphasis being placed upon recent developments and novel techniques. Satellite based retrieval algorithms can be grouped into three classes: threshold methods, statistical procedures and radiative transfer techniques although each algorithm depends upon implicit, if not overt, inversion of the radiative transfer equation. The fourth type of retrieval differs very considerably from the satellite based techniques as it depends upon surface based measurements which are generally, but not always, human rather than computer based. There is a tendency to assume that surface based observations, especially of total cloud, are correct but that they may differ from satellite based retrievals because of the differences in viewing geometry. Actually the literature reveals surprisingly few intercomparison studies. None of the satellite based techniques have yet been well validated in a variety of situations while surface based observations are made in all terrain and climate regimes. Overall there seems to be good reason to believe that surface based observations of cloud amount and especially of low cloud amount, character and base height can add significantly to satellite based retrieval algorithms. GRA

N87-17097# Joint Publications Research Service, Arlington, Va.
GEOPHYSICIST COMMENTS ON HOW SOLAR ACTIVITY MAY AFFECT WEATHER
In its USSR Report: Earth Sciences (JPRS-UES-86-005) 7 May 1986 p 1-2 Transl. into ENGLISH from Gudok (Moscow, USSR), no. 50(18385), 28 Feb. 1986 p 4, cols. 4-8 (For primary document see N87-17096 09-42)
Avail: NTIS HC A05/MF A01

N87-17098# Joint Publications Research Service, Arlington, Va.
THERMODYNAMIC ESTIMATE OF CLIMATIC SYSTEM EFFICIENCY Abstract Only
A. S. Ginzburg *In its* USSR Report: Earth Sciences (JPRS-UES-86-005) 7 May 1986 p 3 Transl. into ENGLISH from Izvestiya Akademii Nauk SSSR: Fizika Atmosfery i Okeana (Moscow, USSR), v. 21, no. 10, Oct. 1985 p 1020-1025 Original language document was announced in IAA as A86-18140 (For primary document see N87-17096 09-42)
Avail: NTIS HC A05/MF A01

N87-17099# Joint Publications Research Service, Arlington, Va.
CONTEMPORARY CHANGES IN CLIMATE AND PALEOCLIMATE Abstract Only
M. I. Budyko *In its* USSR Report: Earth Sciences (JPRS-UES-86-005) 7 May 1986 p 3-4 Transl. into ENGLISH from Izvestiya Akademii Nauk SSSR: Seriya Geograficheskaya (Moscow, USSR), no. 6, Nov. - Dec. 1985 p 36-42 (For primary document see N87-17096 09-42)
Avail: NTIS HC A05/MF A01

N87-17101# Joint Publications Research Service, Arlington, Va.
ASSESSMENT OF CONTEMPORARY CHANGES IN GLOBAL CLIMATE
K. Ya. Vinnikov *In its* USSR Report: Earth Sciences (JPRS-UES-86-005) 7 May 1986 p 4-5 Transl. into ENGLISH from Gidrometeorologiya: Seriya Meteorologiya (Obninsk, USSR), no. 8, 1985 p 1-52 (For primary document see N87-17096 09-42)
Avail: NTIS HC A05/MF A01

N87-17168# Deutsche Forschungs- und Versuchsanstalt fuer Luft- und Raumfahrt, Oberpfaffenhofen (West Germany).
STEREO LINE SCANNER (SLS): SYSTEM CONSIDERATIONS ON AN OPERATIONAL INSTRUMENT FOR METEOROLOGY AND WEATHER FORECASTS
A. Drescher *In* ESA Proceedings of the 1986 International Geoscience and Remote Sensing Symposium (IGARSS '86) on Remote Sensing: Today's Solutions for Tomorrow's Information Needs, Volume 1 Aug. 1986 p 29-32 (For primary document see N87-17163 09-43)
Avail: NTIS HC A99/MF E03; ESA, Paris, France, 3 volume set $90 Member States, AU, CN, and NO (+20% others)

N87-17182*# Johns Hopkins Univ., Laurel, Md. Applied Physics Lab.
RAIN MEASUREMENT RESULTS DERIVED FROM A TWO POLARIZATION S-BAND RADAR EMPLOYING FREQUENCY DIVERSITY AT WALLOPS ISLAND, VIRGINIA
J. Goldhirsh, J. Rowland, and B. Musiani *In* ESA Proceedings of the 1986 International Geoscience and Remote Sensing Symposium (IGARSS '86) on Remote Sensing: Today's Solutions for Tomorrow's Information Needs, Volume 1 Aug. 1986 p 103-108 Sponsored by NASA Goddard Space Flight Center and NASA, Washington (For primary document see N87-17163 09-43)
(Contract N000024-85-C-5301)
Avail: NTIS HC A99/MF E03; ESA, Paris, France, 3 volume set $90 Member States, AU, CN, and NO (+20% others) CSCL 04B

N87-17227# Institut Francais de Recherche pour l'Exploitation de la Mer, Brest (France). Antenne CREO.
ERS-1 WIND SCATTEROMETER: WIND EXTRACTION AND AMBIGUITY REMOVAL
A. G. Cavanie and D. Offiler (Meteorological Office, Bracknell, England) *In* ESA Proceedings of the 1986 International Geoscience and Remote Sensing Symposium (IGARSS '86) on Remote Sensing: Today's Solutions for Tomorrow's Information Needs, Volume 1 Aug. 1986 p 395-398 Sponsored by ESA (For primary document see N87-17163 09-43)
Avail: NTIS HC A99/MF E03; ESA, Paris, France, 3 volume set $90 Member States, AU, CN, and NO (+20% others)

N87-17272# National Oceanic and Atmospheric Administration, Boulder, Colo. Wave Propagation Lab.
REMOTE PROBING OF WIND AND REFRACTIVE-INDEX STRUCTURE USING OPTICAL SCINTILLATION TECHNIQUES
G. R. Ochs and S. F. Clifford *In* ESA Proceedings of the 1986 International Geoscience and Remote Sensing Symposium (IGARSS '86) on Remote Sensing: Today's Solutions for Tomorrow's Information Needs, Volume 1 Aug. 1986 p 667-670 Sponsored by US Army Dugway Proving Ground, and US Army Atmospheric Sciences Lab. (For primary document see N87-17163 09-43)
Avail: NTIS HC A99/MF E03; ESA, Paris, France, 3 volume set $90 Member States, AU, CN, and NO (+20% others)

N87-17275# Swiss Inst. of Meteorology, Zurich.
FORECASTER'S NEED IN METEOROLOGY FOR THE NEXT GENERATION OF SATELLITES
C. H. Fourcy *In* ESA Proceedings of the 1986 International Geoscience and Remote Sensing Symposium (IGARSS '86) on Remote Sensing: Today's Solutions for Tomorrow's Information Needs, Volume 1 Aug. 1986 p 683-685 (For primary document see N87-17163 09-43)
Avail: NTIS HC A99/MF E03; ESA, Paris, France, 3 volume set $90 Member States, AU, CN, and NO (+20% others)

N87-17340*# Minnesota Univ., Minneapolis. Dept. of Physics and Astronomy.
MICROWAVE RADIANCES FROM HORIZONTALLY FINITE PRECIPITATING CLOUDS CONTAINING ICE AND LIQUID HYDROMETEORS
C. Kummerow and J. A. Weinman (Wisconsin Univ., Madison) *In* ESA Proceedings of the 1986 International Geoscience and Remote Sensing Symposium (IGARSS '86) on Remote Sensing: Today's Solutions for Tomorrow's Information Needs, Volume 2 Aug. 1986 p 1069-1075 (For primary document see N87-17283 09-43)
(Grants NAG5-580; N00014-86-K-2001)

Avail: NTIS HC A17/MF A01; ESA, Paris, France, 3 volume set $90 Member States, AU, CN, and NO (+20% others) CSCL 04B

N87-17342# Helsinki Univ. of Technology, Espoo (Finland). Radio Lab.
RETRIEVAL OF NEAR-SURFACE WIND SPEED IN THE BALTIC SEA FROM NIMBUS-7 SCANNING MULTICHANNEL MICROWAVE RADIOMETER (SMMR) OBSERVATIONS
M. Hallikainen, T. Tolmunen, and P. Talmola *In* ESA Proceedings of the 1986 International Geoscience and Remote Sensing Symposium (IGARSS '86) on Remote Sensing: Today's Solutions for Tomorrow's Information Needs, Volume 2 Aug. 1986 p 1083-1088 (For primary document see N87-17283 09-43)
Avail: NTIS HC A17/MF A01; ESA, Paris, France, 3 volume set $90 Member States, AU, CN, and NO (+20% others)

N87-17382# Meteorological Office, Bracknell (England).
THE USE OF AIRCRAFT FOR WIND SCATTEROMETER CALIBRATION
David Offiler *In* ESA Proceedings of an ESA Workshop on ERS-1 Wind and Wave Calibration Sep. 1986 p 131-134 (For primary document see N87-17363 09-43)
Avail: NTIS HC A11/MF A01

N87-17386# Massachusetts Univ., Amherst.
INTERSENSOR COMPARISONS FOR VALIDATION OF WIND SPEED MEASUREMENTS FROM ERS-1 ALTIMETER AND SCATTEROMETER
Calvin Swift and N. M. Mognard *In* ESA Proceedings of an ESA Workshop on ERS-1 Wind and Wave Calibration Sep. 1986 p 157-164 (For primary document see N87-17363 09-43)
Avail: NTIS HC A11/MF A01

N87-17390# Ministerio de Obras Publicas, Madrid (Spain). Direccion General de Puertos y Costas.
MARINE CLIMATE PROGRAM
Juan Jose Conde, Josie Enrique Luis, and Adolfo Maron *In* ESA Proceedings of an ESA Workshop on ERS-1 Wind and Wave Calibration Sep. 1986 p 177-179 (For primary document see N87-17363 09-43)
Avail: NTIS HC A11/MF A01

48 OCEANOGRAPHY

Includes biological, dynamic, and physical oceanography; and marine resources.

For related information see also *43 Earth Resources and Remote Sensing.*

N87-17428# Danish Meteorological Inst., Copenhagen.
THE ICE CONDITIONS IN THE GREENLAND WATERS, 1980
Jens S. Fabricius 1986 167 p
(Rept-551.467.3.068(988); ISBN-87-7478-275-4) Avail: NTIS HC A08/MF A01

During the period July to September 1980, the Danish Hydraulic Institute (DHI) made a series of special ice reconnaissances off East Greenland for the Greenland Geological Survey (GGU). Twelve monthly compiled charts followed by an annes (A through F) containing copies of all Danish ice reconnaissance charts, regionally arranged. The Danish Meteorological Institute (DMI) interpreted a series of satellite images. The charts from DHI/GGU and the satellite interpretations from DMI are added to this annual as appendix I and II. B.G.

N87-17429*# Lamont-Doherty Geological Observatory, Palisades, N.Y.
MAGNETIZATION OF THE OCEANIC CRUST: TRM OR CRM?
C. A. Raymond and J. L. LaBrecque 1987 50 p
(Grant NAG5-598)
(NASA-CR-179896; NAS 1.26:179896) Avail: NTIS HC A03/MF A01 CSCL 08C

A model was proposed in which chemical remanent magnetization (CRM) acquired within the first 20 Ma of crustal evolution may account for 80% of the bulk natural remanent magnetization (NRM) of older basalts. The CRM of the crust is acquired as the original thermoremanent magnetization (TRM) is lost through low temperature alteration. The CRM intensity and direction are controlled by the post-emplacement polarity history. This model explains several independent observations concerning the magnetization of the oceanic crust. The model accounts for amplitude and skewness discrepancies observed in both the intermediate wavelength satellite field and the short wavelength sea surface magnetic anomaly pattern. It also explains the decay of magnetization away from the spreading axis, and the enhanced magnetization of the Cretaceous Quiet Zones while predicting other systematic variations with age in the bulk magnetization of the oceanic crust. The model also explains discrepancies in the anomaly skewness parameter observed for anomalies of Cretaceous age. Further studies indicate varying rates of TRM decay in very young crust which depicts the advance of low temperature alteration through the magnetized layer. Author

N87-17102# Joint Publications Research Service, Arlington, Va.
METAL CONTENT OF OCEAN WATER STUDIED WITH RADIO SPECTROMETER
In its USSR Report: Earth Sciences (JPRS-UES-86-005) 7 May 1986 p 8 Transl. into ENGLISH from Kazakhstanskaya Pravda (Alma-Ata, USSR), 29 Jan. 1986 p 3 (For primary document see N87-17096 09-42)
Avail: NTIS HC A05/MF A01

N87-17103# Joint Publications Research Service, Arlington, Va.
STOCHASTIC MODEL OF TIDAL EVOLUTION OF EARTH-MOON SYSTEM WITH CYCLIC CHANGE IN RESONANT FREQUENCY OF OCEAN Abstract Only
B. A. Kagan and N. B. Maslova *In its* USSR Report: Earth Sciences (JPRS-UES-86-005) 7 May 1986 p 14 Transl. into ENGLISH from Doklady Akademii Nauk SSSR (Moscow, USSR), v. 285, no. 5, 1985 p 1082-1086 Original language document was announced in IAA as A86-24303 (For primary document see N87-17096 09-42)
Avail: NTIS HC A05/MF A01

N87-17104# Joint Publications Research Service, Arlington, Va.
OCEAN SURFACE TEMPERATURE FIELD VARIABILITY Abstract Only
S. A. Molchanov, L. I. Piterbarg, A. A. Ruzmaykin, and D. D. Sokolov *In its* USSR Report: Earth Sciences (JPRS-UES-86-005) 7 May 1986 p 21 Transl. into ENGLISH from Doklady Akademii Nauk SSSR (Moscow, USSR), v. 286, no. 4, Feb. 1986 p 969-972 (For primary document see N87-17096 09-42)
Avail: NTIS HC A05/MF A01

N87-17148*# Jet Propulsion Lab., California Inst. of Tech., Pasadena.
OCEAN WAVES NEAR HURRICANE JOSEPHINE FROM SIR-B
Benjamin Holt and F. I. Gonzalez (National Oceanic and Atmospheric Administration, Seattle, Wash.) *In its* The Second Spaceborne Imaging Radar Symposium 1 Dec. 1986 p 103-106 Previously announced in IAA as A86-49688 (For primary document see N87-17135 09-43)
Avail: NTIS HC A10/MF A01 CSCL 08C

N87-17149*# Johns Hopkins Univ., Laurel, Md. Applied Physics Lab.
OPERATIONAL WAVE FORECASTING WITH SPACEBORNE SAR: PROSPECTS AND PITFALLS
R. C. Beal *In* JPL The Second Spaceborne Imaging Radar Symposium 1 Dec. 1986 p 107-113 (For primary document see N87-17135 09-43)
Avail: NTIS HC A10/MF A01 CSCL 08C

N87-17150*# Environmental Research Inst. of Michigan, Ann Arbor. Radar Science Lab.
IMAGING RADAR CONTRIBUTIONS TO A MAJOR AIR-SEA-ICE INTERACTION STUDY IN THE GREENLAND SEA

Robert A. Shuchman *In* JPL The Second Spaceborne Imaging Radar Symposium 1 Dec. 1986 p 114-118 (For primary document see N87-17135 09-43)
Avail: NTIS HC A10/MF A01 CSCL 08C

N87-17151*# Washington Univ., Seattle. Applied Physics Lab.
OBSERVING THE POLAR OCEANS WITH SPACEBORNE RADAR
Drew Rothrock *In* JPL The Second Spaceborne Imaging Radar Symposium 1 Dec. 1986 p 119-122 (For primary document see N87-17135 09-43)
Avail: NTIS HC A10/MF A01 CSCL 08C

N87-17186*# Stanford Univ., Calif. STAR Lab.
AUTOMATED REMOTE SENSING OF SEA ICE USING SYNTHETIC APERTURE RADAR
J. F. Vesecky, R. Samadani, M. P. Smith, J. M. Daida, and R. N. Bracewell *In* ESA Proceedings of the 1986 International Geoscience and Remote Sensing Symposium (IGARSS '86) on Remote Sensing: Today's Solutions for Tomorrow's Information Needs, Volume 1 Aug. 1986 p 127-132 Sponsored by NASA and ONR (For primary document see N87-17163 09-43)
Avail: NTIS HC A99/MF E03; ESA, Paris, France, 3 volume set $90 Member States, AU, CN, and NO (+20% others) CSCL 08J

N87-17187*# Massachusetts Inst. of Tech., Cambridge. Dept. of Electrical Engineering and Computer Science.
MICROWAVE REMOTE SENSING OF SNOW-COVERED SEA ICE
M. Borgeaud, J. A. Kong, and F. C. Lin *In* ESA Proceedings of the 1986 International Geoscience and Remote Sensing Symposium (IGARSS '86) on Remote Sensing: Today's Solutions for Tomorrow's Information Needs, Volume 1 Aug. 1986 p 133-138 (For primary document see N87-17163 09-43)
(Contracts NAG5-270; N00014-83-K-0525; Grant NSF ECS-85-04381)
Avail: NTIS HC A99/MF E03; ESA, Paris, France, 3 volume set $90 Member States, AU, CN, and NO (+20% others) CSCL 08J

N87-17188*# Kansas Univ. Center for Research, Inc., Lawrence. Radar Systems and Remote Sensing Lab.
MICROWAVE BACKSCATTER COEFFICIENTS OF ARTIFICIALLY GROWN FIRST-YEAR SEA ICE
D. Xue, R. K. Moore, T. H. Lee Williams, and R. Onstott *In* ESA Proceedings of the 1986 International Geoscience and Remote Sensing Symposium (IGARSS '86) on Remote Sensing: Today's Solutions for Tomorrow's Information Needs, Volume 1 Aug. 1986 p 139-146 Sponsored by NASA (For primary document see N87-17163 09-43)
(Contract N00014-85-K-0200)
Avail: NTIS HC A99/MF E03; ESA, Paris, France, 3 volume set $90 Member States, AU, CN, and NO (+20% others) CSCL 08J

N87-17189# Canada Centre for Remote Sensing, Ottawa (Ontario). RADARSAT Project Office.
AN OVERVIEW OF OPERATIONAL SAR DATA COLLECTION AND DISSEMINATION PLANS FOR ERS-1 ICE DATA IN CANADA
L. McNutt and T. Mullane (Atmospheric Environment Service, Ottawa, Ontario) *In* ESA Proceedings of the 1986 International Geoscience and Remote Sensing Symposium (IGARSS '86) on Remote Sensing: Today's Solutions for Tomorrow's Information Needs, Volume 1 Aug. 1986 p 147-152 (For primary document see N87-17163 09-43)
Avail: NTIS HC A99/MF E03; ESA, Paris, France, 3 volume set $90 Member States, AU, CN, and NO (+20% others)

N87-17212*# National Water Research Inst., Burlington (Ontario).
A TWO-SCALE BRAGG SCATTERING MODEL FOR MICROWAVE BACKSCATTER FROM WIND GENERATED WAVES
M. A. Donelan and W. J. Pierson, Jr. (City Coll. of the City Univ. of New York.) *In* ESA Proceedings of the 1986 International Geoscience and Remote Sensing Symposium (IGARSS '86) on Remote Sensing: Today's Solutions for Tomorrow's Information Needs, Volume 1 Aug. 1986 p 291-296 (For primary document see N87-17163 09-43)
(Grant NAGw-690)
Avail: NTIS HC A99/MF E03; ESA, Paris, France, 3 volume set $90 Member States, AU, CN, and NO (+20% others) CSCL 08C

N87-17213*# City Coll. of the City Univ. of New York.
VERIFICATION RESULTS FOR A TWO-SCALE MODEL OF MICROWAVE BACKSCATTER FROM THE SEA SURFACE
W. J. Pierson, Jr. and M. A. Donelan (National Water Research Inst., Burlington, Ontario) *In* ESA Proceedings of the 1986 International Geoscience and Remote Sensing Symposium (IGARSS '86) on Remote Sensing: Today's Solutions for Tomorrow's Information Needs, Volume 1 Aug. 1986 p 297-302 (For primary document see N87-17163 09-43)
(Grant NAGW-690)
Avail: NTIS HC A99/MF E03; ESA, Paris, France, 3 volume set $90 Member States, AU, CN, and NO (+20% others) CSCL 08C

N87-17214# Universite Catholique de Louvain (Belgium). Lab. de Telecommunications et d'Hyperfrequences.
A MODIFIED BOUNDARY PERTURBATION APPROACH TO MICROWAVE SCATTERING AND EMISSION BY THE OCEAN SURFACE
A. Guissard, P. Sobieski, and D. Vanhoenacker *In* ESA Proceedings of the 1986 International Geoscience and Remote Sensing Symposium (IGARSS '86) on Remote Sensing: Today's Solutions for Tomorrow's Information Needs, Volume 1 Aug. 1986 p 303-309 (For primary document see N87-17163 09-43)
(Contract ESA-5285/82)
Avail: NTIS HC A99/MF E03; ESA, Paris, France, 3 volume set $90 Member States, AU, CN, and NO (+20% others)

N87-17215# Physics and Electronics Lab. TNO, The Hague (Netherlands).
C AND Ku-BAND SCATTEROMETER RESULTS FROM THE SCATTMOD INTERNAL WAVE EXPERIMENT
D. vanHalsema, A. L. Gray (Canada Centre for Remote Sensing, Ottawa, Ontario) 03(Defence Research Establishment Pacific, Victoria, British Columbia), S. J. Hughes, and B. A. Hughes *In* ESA Proceedings of the 1986 International Geoscience and Remote Sensing Symposium (IGARSS '86) on Remote Sensing: Today's Solutions for Tomorrows's Information Needs, Volume 1 Aug. 1986 p 311-317 Sponsored by a Canadian Defence Research Fellowship (For primary document see N87-17163 09-43)
Avail: NTIS HC A99/MF E03; ESA, Paris, France, 3 volume set $90 Member States, AU, CN, and NO (+20% others)

N87-17216# TRW Space Technology Labs., Redondo Beach, Calif. Fluid Mechanics Dept.
IDENTIFICATION OF THE CONTRIBUTION OF BRAGG SCATTERING AND SPECULAR REFLECTION TO X-BAND MICROWAVE BACKSCATTERING IN AN OCEAN EXPERIMENT
D. S. W. Kwoh, B. M. Lake, and H. Rungaldier *In* ESA Proceedings of the 1986 International Geoscience and Remote Sensing Symposium (IGARSS '86) on Remote Sensing: Today's Solutions for Tomorrow's Information Needs, Volume 1 Aug. 1986 p 319-325 Sponsored by DARPA (For primary document see N87-17163 09-43)
Avail: NTIS HC A99/MF E03; ESA, Paris, France, 3 volume set $90 Member States, AU, CN, and NO (+20% others)

N87-17217# Kansas Univ. Center for Research, Inc., Lawrence. Radar Systems and Remote Sensing Lab.
TOWER-BASED BROADBAND BACKSCATTERING MEASUREMENTS FROM THE OCEAN SURFACE IN THE NORTH SEA
A. H. Chaudry, S. P. Gogineni, and R. K. Moore *In* ESA Proceedings of the 1986 International Geoscience and Remote Sensing Symposium (IGARSS '86) on Remote Sensing: Today's Solutions for Tomorrow's Information Needs, Volume 1 Aug. 1986 p 327-335 (For primary document see N87-17163 09-43)

Avail: NTIS HC A99/MF E03; ESA, Paris, France, 3 volume set $90 Member States, AU, CN, and NO (+20% others)

N87-17218# Bulgarian Academy of Science, Sofia. Inst. of Electronics.
SPATIAL DEPENDENCE ON SEA SPIKES
D. V. Stoyanov and V. L. Vasilev *In* ESA Proceedings of the 1986 International Geoscience and Remote Sensing Symposium (IGARSS '86) on Remote Sensing: Today's Solutions for Tomorrow's Information Needs, Volume 1 Aug. 1986 p 337-341 (For primary document see N87-17163 09-43)
Avail: NTIS HC A99/MF E03; ESA, Paris, France, 3 volume set $90 Member States, AU, CN, and NO (+20% others)

N87-17219# Environmental Research Inst. of Michigan, Ann Arbor. Radar Science Lab.
GEOPHYSICS OF THE MARGINAL ICE ZONE FROM SAR
R. A. Schuchman, B. A. Burns, C. G. Caruthers, J. D. Lyden, E. Svendsen (Bergen Univ., Norway), O. M. Johannessen, T. Olaussen, and J. A. Johannessen *In* ESA Proceedings of the 1986 International Geoscience and Remote Sensing Symposium (IGARSS '86) on Remote Sensing: Today's Solutions for Tomorrow's Information Needs, Volume 1 Aug. 1986 p 345-351 (For primary document see N87-17163 09-43)
(Contracts N00014-81-C-0295; N00014-83-C-0404)
Avail: NTIS HC A99/MF E03; ESA, Paris, France, 3 volume set $90 Member States, AU, CN, and NO (+20% others)

N87-17220*# Environmental Research Inst. of Michigan, Ann Arbor. Radar Science Lab.
MICROWAVE PROPERTIES OF SEA ICE IN THE MARGINAL ICE ZONE
R. G. Onstott and R. W. Larson *In* ESA Proceedings of the 1986 International Geoscience and Remote Sensing Symposium (IGARSS '86) on Remote Sensing: Today's Solutions for Tomorrow's Information Needs, Volume 1 Aug. 1986 p 353-356 (For primary document see N87-17163 09-43)
(Grant NAGw-334; Contract N000-14-85-K-0200)
Avail: NTIS HC A99/MF E03; ESA, Paris, France, 3 volume set $90 Member States, AU, CN, and NO (+20% others) CSCL 08C

N87-17221# Technical Univ. of Denmark, Lyngby. Inst. of Electromagnetics.
SEA ICE IN THE GREENLAND SEA OBSERVED BY THE NIMBUS-7 SCANNING MULTICHANNEL MICROWAVE RADIOMETER (SMMR)
P. Sloth and L. T. Pedersen *In* ESA Proceedings of the 1986 International Geoscience and Remote Sensing Symposium (IGARSS '86) on Remote Sensing: Today's Solutions for Tomorrow's Information Needs, Volume 1 Aug. 1986 p 357-361 Sponsored by the Technical Univ. of Denmark, the Danish Space Research Committee, the Commission for Scientific Research, Greenland, and IBM Denmark (For primary document see N87-17163 09-43)
Avail: NTIS HC A99/MF E03; ESA, Paris, France, 3 volume set $90 Member States, AU, CN, and NO (+20% others)

N87-17222# Columbia Univ., Palisades, N.Y. Lamont-Doherty Geological Observatory.
SAR ICE FLOE KINEMATICS AND CORRELATION WITH MESOSCALE OCEANIC STRUCTURE WITHIN THE MARGINAL ICE ZONE
T. O. Manley, R. A. Shuchman (Environmental Research Inst. of Michigan, Ann Arbor.), and B. A. Burns *In* ESA Proceeding of the 1986 International Geoscience and Remote Sensing Symposium (IGARSS '86) on Remote Sensing: Today's Solutions for Tomorrow's Information Needs, Volume 1 Aug. 1986 p 363-366 (For primary document see N87-17163 09-43)
(Contracts N00014-85-C-0132; N00014-81-C-0259; N00014-83-C-0404)
Avail: NTIS HC A99/MF E03; ESA, Paris, France, 3 volume set $90 Member States, AU, CN, and NO (+20% others)

N87-17295# Defence Research Establishment Pacific, Victoria (British Columbia).
ESTIMATION OF INTERNAL WAVE CURRENTS FROM SAR AND INFRARED SCATTEROMETER IMAGERY
S. J. Hughes and B. A. Hughes *In* ESA Proceedings of the 1986 International Geoscience and Remote Sensing Symposium IGARSS '86) on Remote Sensing: Today's Solutions for Tomorrow's Information Needs, Volume 2 Aug. 1986 p 789-794 (For primary document see N87-17283 09-43)
Avail: NTIS HC A17/MF A01; ESA, Paris, France, 3 volume set $90 Member States, AU, CN, and NO (+20% others)

N87-17296# Naval Ocean Research and Development Activity, Bay St. Louis, Miss.
OBSERVATIONS OF SURFACE CURRENTS AT NANTUCKET SHOALS AND IMPLICATIONS FOR RADAR IMAGING OF THE BOTTOM
P. Smith *In* ESA Proceedings of the 1986 International Geoscience and Remote Sensing Symposium (IGARSS '86) on Remote Sensing: Today's Solutions for Tomorrow's Information Needs, Volume 2 Aug. 1986 p 795-800 (For primary document see N87-17283 09-43)
Avail: NTIS HC A17/MF A01; ESA, Paris, France, 3 volume set $90 Member States, AU, CN, and NO (+20% others)

N87-17297# Environmental Research Inst. of Michigan, Ann Arbor. Radar Science Lab.
ANALYSIS OF SYNTHETIC APERTURE RADAR IMAGERY OF SURFACE SHIP WAKES
J. D. Lyden, D. R. Lyzenga, and R. A. Schuchman *In* ESA Proceedings of the 1986 International Geoscience and Remote Sensing Symposium (IGARSS '86) on Remote Sensing: Today's Solutions for Tomorrow's Information Needs, Volume 2 Aug. 1986 p 801-805 (For primary document see N87-17283 09-43)
(Contract N00014-81-C-0692)
Avail: NTIS HC A17/MF A01; ESA, Paris, France, 3 volume set $90 Member States, AU, CN, and NO (+20% others)

N87-17298# TRW Space Technology Labs., Redondo Beach, Calif.
SAR IMAGING OF BOTTOM TOPOGRAPHY IN THE OCEAN: RESULTS FROM AN IMPROVED MODEL
H. C. Yuen, D. R. Crawford (Jet Propulsion Lab., California Inst. of Tech., Pasadena.), and P. G. Saffman *In* ESA Proceedings of the 1986 International Geoscience and Remote Sensing Symposium (IGARSS '86) on Remote Sensing: Today's Solutions for Tomorrow's Information Needs, Volume 2 Aug. 1986 p 807-815 (For primary document see N87-17283 09-43)
Avail: NTIS HC A17/MF A01; ESA, Paris, France, 3 volume set $90 Member States, AU, CN, and NO (+20% others)

N87-17299# Environmental Research Inst. of Michigan, Ann Arbor. Radar Science Lab.
AN IMPROVED METHOD FOR THE DETERMINATION OF WATER DEPTH FROM SURFACE WAVE REFRACTION PATTERNS
J. R. Bennett *In* ESA Proceedings of the 1986 International Geoscience and Remote Sensing Symposium (IGARSS '86) on Remote Sensing: Today's Solutions for Tomorrow's Information Needs, Volume 2 Aug. 1986 p 813-817 (For primary document see N87-17283 09-43)
(Contract N00014-84-C-2312)
Avail: NTIS HC A17/MF A01; ESA, Paris, France, 3 volume set $90 Member States, AU, CN, and NO (+20% others)

N87-17300# Physics and Electronics Lab. TNO, The Hague (Netherlands).
SEA WAVE MEASUREMENTS USING A SHIP'S RADAR
P. Hoogeboom, J. C. M. Kleijweg, and D. vanHalsema *In* ESA Proceedings of the 1986 International Geoscience and Remote Sensing Symposium (IGARSS '86) on Remote Sensing: Today's Solutions for Tomorrow's Information Needs, Volume 2 Aug. 1986 p 819-823 (For primary document see N87-17283 09-43)
Avail: NTIS HC A17/MF A01; ESA, Paris, France, 3 volume set $90 Member States, AU, CN, and NO (+20% others)

N87-17301# Ministry of Posts and Telecommunications, Ibaraki (Japan). Radio Research Labs.
MEASUREMENT OF SEA BACKSCATTER AT EXTREMELY LOW GRAZING ANGLE BY C-BAND DOPPLER RADAR
T. Iguchi, K. Nakamura, H. Fukuchi, T. Okuyama, K. Okamoto, and H. Mineno *In* ESA Proceedings of the 1986 International Geoscience and Remote Sensing Symposium (IGARSS '86) on Remote Sensing: Today's Solutions for Tomorrow's Information Needs, Volume 2 Aug. 1986 p 825-830 (For primary document see N87-17283 09-43)
Avail: NTIS HC A17/MF A01; ESA, Paris, France, 3 volume set $90 Member States, AU, CN, and NO (+20% others)

N87-17333# Johns Hopkins Univ., Laurel, Md. Applied Physics Lab.
CHARACTERISTICS OF A VERY LOW ALTITUDE SPACECRAFT FOR COLLECTING GLOBAL DIRECTIONAL WAVE SPECTRA WITH SPACEBORNE SYNTHETIC APERTURE RADAR
R. C. Beal *In* ESA Proceedings of the 1986 International Geoscience and Remote Sensing Symposium (IGARSS '86) on Remote Sensing: Today's Solutions for Tomorrow's Information Needs, Volume 2 Aug. 1986 p 1025-1029 (For primary document see N87-17283 09-43)
Avail: NTIS HC A17/MF A01; ESA, Paris, France, 3 volume set $90 Member States, AU, CN, and NO (+20% others)

N87-17334# Johns Hopkins Univ., Laurel, Md. Applied Physics Lab.
THE SAR IMAGE MODULATION TRANSFER FUNCTION DERIVED FROM SIR-B IMAGE SPECTRA AND AIRBORNE MEASUREMENTS OF OCEAN WAVE HEIGHT SPECTRA
F. Monaldo *In* ESA Proceedings of the 1986 International Geoscience and Remote Sensing Symposium (IGARSS '86) on Remote Sensing: Today's Solutions for Tomorrow's Information Needs, Volume 2 Aug. 1986 p 1031-1035 (For primary document see N87-17283 09-43)
Avail: NTIS HC A17/MF A01; ESA, Paris, France, 3 volume set $90 Member States, AU, CN, and NO (+20% others)

N87-17335# Marconi Co. Ltd., Chelmsford (England).
SIR-B OBSERVATIONS OF OCEAN WAVES IN THE NE ATLANTIC
J. T. Macklin, R. A. Cordey, and G. E. Keyte *In* ESA Proceedings of the 1986 International Geoscience and Remote Sensing Symposium (IGARSS '86) on Remote Sensing: Today's Solutions for Tomorrow's Information Needs, Volume 2 Aug. 1986 p 1037-1041 (For primary document see N87-17283 09-43)
Avail: NTIS HC A17/MF A01; ESA, Paris, France, 3 volume set $90 Member States, AU, CN, and NO (+20% others)

N87-17336*# Johns Hopkins Univ., Laurel, Md. Applied Physics Lab.
DERIVING TWO-DIMENSIONAL OCEAN WAVE SPECTRA AND SURFACE HEIGHT MAPS FROM THE SHUTTEL IMAGING RADAR (SIR-B)
D. G. Tilley *In* ESA Proceedings of the 1986 International Geoscience and Remote Sensing Symposium (IGARSS '86) on Remote Sensing: Today's Solutions for Tomorrow's Information Needs, Volume 2 Aug. 1986 p 1043-1049 Sponsored by NASA (For primary document see N87-17283 09-43)
Avail: NTIS HC A17/MF A01; ESA, Paris, France, 3 volume set $90 Member States, AU, CN, and NO (+20% others) CSCL 08C

N87-17337# Johns Hopkins Univ., Laurel, Md. Applied Physics Lab.
SPATIAL EVOLUTION OF WAVE SPECTRA IN THE VICINITY OF THE AGULHAS CURRENT FROM SIR-B
D. E. Irvine *In* ESA Proceedings of the 1986 International Geoscience and Remote Sensing Symposium (IGARSS '86) on Remote Sensing: Today's Solutions for Tomorrow's Information Needs, Volume 2 Aug. 1986 p 1051-1053 (For primary document see N87-17283 09-43)
Avail: NTIS HC A17/MF A01; ESA, Paris, France, 3 volume set $90 Member States, AU, CN, and NO (+20% others)

N87-17338# Environmental Research Inst. of Michigan, Ann Arbor. Radar Science Lab.
CHARACTERISATION OF INTERNAL WAVE SURFACE PATTERNS ON AIRBORNE SAR IMAGERY
E. S. Kasischke *In* ESA Proceedings of the 1986 International Geoscience and Remote Sensing Symposium (IGARSS '86) on Remote Sensing: Today's Solutions for Tomorrow's Information Needs, Volume 2 Aug. 1986 p 1055-1060 (For primary document see N87-17283 09-43)
(Contract N00014-81-C-0692)
Avail: NTIS HC A17/MF A01; ESA, Paris, France, 3 volume set $90 Member States, AU, CN, and NO (+20% others)

N87-17343# Helsinki Univ. of Technology, Espoo (Finland). Radio Lab.
SEA ICE STUDIES IN THE BALTIC SEA USING SATELLITE MICROWAVE RADIOMETER DATA
M. Hallikainen and P.-V. Mikkola *In* ESA Proceedings of the 1986 International Geoscience and Remote Sensing Symposium (IGARSS '86) on Remote Sensing: Today's Solutions for Tomorrow's Information Needs, Volume 2 Aug. 1986 p 1089-1094 (For primary document see N87-17283 09-43)
Avail: NTIS HC A17/MF A01; ESA, Paris, France, 3 volume set $90 Member States, AU, CN, and NO (+20% others)

N87-17369# Institute of Oceanographic Sciences, Wormley (England).
REQUIREMENTS AND CONSTRAINTS IN THE CALIBRATION AND VALIDATION OF ERS-1 WIND AND WAVE PARAMETERS
Trevor H. Guymer *In* ESA Proceedings of an ESA Workshop on ERS-1 Wind and Wave Calibration Sep. 1986 p 37-43 (For primary document see N87-17363 09-43)
Avail: NTIS HC A11/MF A01

N87-17374# Institute of Oceanographic Sciences, Wormley (England).
VALIDATION OF ERS-1 WIND DATA USING OBSERVATIONS FROM RESEARCH AND VOLUNTARY OBSERVING SHIPS
Peter K. Taylor *In* ESA Proceedings of an ESA Workshop on ERS-1 Wind and Wave Calibration Sep. 1986 p 69-75 (For primary document see N87-17363 09-43)
Avail: NTIS HC A11/MF A01

N87-17375# National Environmental Satellite Service, Washington, D. C.
ACCURACY ESTIMATES OF WIND AND WAVE OBSERVATIONS FROM SHIPS OF OPPORTUNITY IN THE WMO VOLUNTARY OBSERVING SHIP PROGRAM
John Wilkerson *In* ESA Proceedings of an ESA Workshop on ERS-1 Wind and Wave Calibration Sep. 1986 p 77-84 (For primary document see N87-17363 09-43)
Avail: NTIS HC A11/MF A01

N87-17376# Royal Netherlands Meteorological Inst., De Bilt.
THE ACCURACY AND AVAILABILITY OF OPERATIONAL MARINE SURFACE WIND DATA FOR ERS-1 SENSOR CALIBRATION AND VALIDATION FROM FIXED PLATFORMS AND FREE DRIFTING BUOYS
Wiebe A. Oost *In* ESA Proceedings of an ESA Workshop on ERS-1 Wind and Wave Calibration Sep. 1986 p 85-86 (For primary document see N87-17363 09-43)
Avail: NTIS HC A11/MF A01

N87-17377# Centre Oceanologique de Bretagne, Brest (France).
USING BUOYS AND SHIPS TO CALIBRATE ERS-1 ALTIMETER AND SCATTEROMETER
Robert Ezraty *In* ESA Proceedings of an ESA Workshop on ERS-1 Wind and Wave Calibration Sep. 1986 p 91-97 (For primary document see N87-17363 09-43)
Avail: NTIS HC A11/MF A01

N87-17381# Johns Hopkins Univ., Laurel, Md. Applied Physics Lab.
A PROCEDURE FOR ESTIMATION OF TWO-DIMENSIONAL OCEAN HEIGHT-VARIANCE SPECTRA FROM SAR IMAGERY
Frank Monaldo *In* ESA Proceedings of an ESA Workshop on ERS-1 Wind and Wave Calibration Sep. 1986 p 123-129 (For primary document see N87-17363 09-43)
Avail: NTIS HC A11/MF A01

N87-17383# Science Research Council, Chilton (England). Rutherford Appleton Lab.
MEASUREMENT OF THE DIRECTIONAL SPECTRUM OF OCEAN WAVES USING A CONICALLY-SCANNING RADAR
Andrew Robert Birks *In* ESA Proceedings of an ESA Workshop on ERS-1 Wind and Wave Calibration Sep. 1986 p 135-138 (For primary document see N87-17363 09-43)
Avail: NTIS HC A11/MF A01

N87-17385# Naval Ocean Research and Development Activity, Bay St. Louis, Miss.
N-ROSS VALIDATION
D. R. Johnson *In* ESA Proceedings of an ESA Workshop on ERS-1 Wind and Wave Calibration Sep. 1986 p 151-156 (For primary document see N87-17363 09-43)
Avail: NTIS HC A11/MF A01

N87-17389# Max-Planck-Inst. fuer Meteorologie, Hamburg (West Germany).
WAVE MODELING ACTIVITIES OF THE WAVE MODELING (WAM) GROUP RELEVANT TO ERS-1
Klaus Hasselmann *In* ESA Proceedings of an ESA Workshop on ERS-1 Wind and Wave Calibration Sep. 1986 p 173-175 (For primary document see N87-17363 09-43)
Avail: NTIS HC A11/MF A01

N87-17392# Turin Univ. (Italy). Ist. di Fisica Generale.
BULK RICHARDSON'S NUMBER ISOGRAMS DEDUCED FROM SAR DATA
B. Fiscella, P. P. Lombardini, Paolo Trivero, and C. Cappa *In* ESA Proceedings of an ESA Workshop on ERS-1 Wind and Wave Calibration Sep. 1986 p 187-190 (For primary document see N87-17363 09-43)
Avail: NTIS HC A11/MF A01

51 LIFE SCIENCES (GENERAL)

No abstracts in this category.

52 AEROSPACE MEDICINE

Includes physiological factors; biological effects of radiation; and effects of weightlessness on man and animals.

N87-17430*# Massachusetts Inst. of Tech., Cambridge. Dept. of Chemical Engineering.
SUPERCRITICAL WATER OXIDATION OF PRODUCTS OF HUMAN METABOLISM Final Report
Jefferson W. Tester, George A. Huff, Richard K. Helling, T. B. Thomasson (Modar, Inc., Natick, Mass.), and K. C. Swallow [1986] 36 p
(Grants NAG2-224; NsG-2403)
(NASA-CR-180144; NAS 1.26:180144) Avail: NTIS HC A03/MF A01 CSCL 06P

Although the efficient destruction of organic material was demonstrated in the supercritical water oxidation process, the reaction kinetics and mechanisms are unknown. The kinetics and mechanisms of carbon monoxide and ammonia oxidation in and reaction with supercritical water were studied experimentally. Experimental oxidation of urine and feces in a microprocessor controlled system was performed. A minaturized supercritical water oxidation process for space applications was design, including preliminary mass and energy balances, power, space and weight requirements. B.G.

N87-17431*# Good Samaritan Hospital and Medical Center, Portland, Oreg. Neurological Sciences Inst.
ROLE OF ORIENTATION REFERENCE SELECTION IN MOTION SICKNESS Semiannual Status Report
Robert J. Peterka and F. Owen Black Feb. 1987 10 p
(Grant NAG9-117)
(NASA-CR-180161; NAS 1.26:180161) Avail: NTIS HC A02/MF A01 CSCL 06S

The objectives of this proposal were developed to further explore and quantify the orientation reference selection abilities of subjects and the relation, if any, between motion sickness and orientation reference selection. The overall objectives of this proposal are to determine (1) if motion sickness susceptibility is related to sensory orientation reference selection abilities of subjects, (2) if abnormal vertical canal-otolith function is the source of these abnormal posture control strategies and if it can be quantified by vestibular and oculomotor reflex measurements, and (3) if quantifiable measures of perception of vestibular and visual motion cues can be related to motion sickness susceptibility and to orientation reference selection ability demonstrated by tests which systematically control the sensory imformation available for orientation. Author

N87-17432# Institut Franco-Allemand de Recherches, St. Louis (France).
BIOLOGICAL EFFECTS OF AERIAL SHOCK WAVES: REVIEW OF WORK TO DATE [EFFETS BIOLOGIQUES DES ONDES DE CHOC AERIENNES: SYNTHESE DES TRAVAUX REALISES A CE JOUR]
P. Vassout 20 May 1985 68 p In FRENCH; GERMAN summary
(ISL-NB-402/85; ETN-87-98805) Avail: NTIS HC A04/MF A01

The effects of aerial shock waves on living beings are reviewed. The biological effects of shock waves were studied on several animal species, and extrapolated to human beings. The most strongly affected organs are the eardrum, the respiratory system, and the gastrointestinal system. The effects of shock waves were investigated in the free field and in a reflecting environment, and compared with the effects of strong noise. Protection possibilities were examined. The harmful effects, as well as propagation models for shock waves in a biological medium are reported on. ESA

53 BEHAVIORAL SCIENCES

Includes psychological factors; individual and group behavior; crew training and evaluation; and psychiatric research.

No abstracts in this category.

54 MAN/SYSTEM TECHNOLOGY AND LIFE SUPPORT

Includes human engineering; biotechnology; and space suits and protective clothing.

For related information see also *16 Space Transportation.*

N87-17433# Drexel Univ., Philadelphia, Pa. Biomedical Engineering and Science Inst.
AN EXPERIMENTAL MICROCOMPUTER CONTROLLED SYS-

TEM FOR SYNCHRONIZED PULSATING ANTI-GRAVITY SUIT Interim Report
Thomas Moore, Joanne Foley, B. R. Reddy, Frank Kepics, and Don Jaron Jul. 1986 22 p
(Contract N00014-85-K-0566)
(AD-A174640; NADC-86119-60) Avail: NTIS HC A02/MF A01 CSCL 06/17

This report describes an experimental system to deliver Synchronized External Pressure Pulsations (SEP) to the lower body. The system is designed using a micro-computer with a realtime interface and an electro-pneumatic subsystem capable of delivering pressure pulses to a modified anti-G suit at a fast rate. It is versatile, containing many options for synchronizing, phasing and sequencing of the pressure pulsations. Details of its software and hardware are described along with the results of initial testing in a Dynamic Flight Simulator on human volunteers. GRA

N87-17434# Virginia Polytechnic Inst. and State Univ., Blacksburg. Human Factors Lab.
UNITARY SUPRATHRESHOLD COLOR-DIFFERENCE METRICES OF LEGIBILITY FOR CRT RASTER IMAGERY Technical Report, 1982 - 1985
Thomas M. Lippert and Harry L. Snyder Sep. 1986 107 p
(Contract N00014-78-Ck-0238)
(AD-A175062; HFL/ONR-86-3) Avail: NTIS HC A06/MF A01 CSCL 05/10

This research examined the relationships between color contrast and legibility for digital raster video imagery. CIE colorimetric components were combined into three-dimensional color coordinate systems whose coordinates map one-to-one with the physical energy parameters of all colors. The distance between any two colors' coordinates in these 3-spaces is termed Color-Difference (Delta E). Delta A was hypothesized as a metric of the speed (RS) with which observers possessing normal vision could accurately read random numeral strings on one color displayed against backgrounds of another color. Two studies totalling 32064 practice and experimental trials were conducted. The first study determined that the CIE Uniform Color Spaces are inappropriate for the modelling of RS. Subsequently, a different 3-space geometry and colorimetric component scaling were empirically derived from the Study 1 data to produce a one-dimensional Delta E scale which approximates an interval scale of RS. This Delta E scale and others were then applied to the different stimulus conditions in Study 2 to determine the generalizability of such Delta E metrics. GRA

N87-17435# Technische Hogeschool Twente, Enschede (Netherlands). Dept. of Applied Mathematics.
MODEL OF THE HUMAN CONTROLLER OF A DYNAMIC SYSTEM
P. H. Wewerinke Aug. 1986 25 p
(MEMO-580; ISSN-0169-2690; ETN-87-99059) Avail: NTIS HC A02/MF A01

A model of the human controller of a dynamic system involving regulating and tracking a desired finite trajectory in an optimal sense is presented. The latter concerns control behavior at a higher mental level involving planning (finite time, open loop control) and decision making (control intermittency). It is assumed that the human operator derives information about the system from instruments and/or the visual scene. This complex visual information process and the control and decision making behavior is described in terms of stochastic optimal estimation control and decision theory. ESA

55 SPACE BIOLOGY

Includes exobiology; planetary biology; and extraterrestrial life.

No abstracts in this category.

59 MATHEMATICAL AND COMPUTER SCIENCES (GENERAL)

N87-17436*# National Aeronautics and Space Administration. Langley Research Center, Hampton, Va.
EVOLUTION OF A LOCALIZED THERMAL EXPLOSION IN A REACTIVE GAS Final Report
T. L. Jackson, A. K. Kapila, and D. S. Stewart Jan. 1987 63 p Submitted for publication
(Contract NAS1-18107)
(NASA-CR-178231; ICASE-87-2; NAS 1.26:178231) Avail: NTIS HC A04/MF A01 CSCL 12A

Experimental observations of ignition in premixed gaseous reactants indicate that perfectly homogeneous initiation is practically unrealizable. Instead, combustion first sets in, as a rule, at small, discrete sites where inherent inhomogeneities cause chemical activity to proceed preferentially and lead to localized explosions. Combustion waves propagating away from these hot spots or reaction centers eventually envelop the remaining bulk. This study examines the spatial structure and temporal evolution of a hot spot for a model involving Arrhenius kinetics. The hot spot, characterized by peaks in pressure and temperature with little diminution in local density, is shown to have one of two possible self-similar structures. The analysis employs a combination of asymptotics and numerics, and terminates when pressure and temperature in the explosion have peaked. Author

60 COMPUTER OPERATIONS AND HARDWARE

Includes hardware for computer graphics, firmware, and data processing.

For components see *33 Electronics and Electrical Engineering.*

N87-17437# California Univ., Berkeley.
THE DESIGN AND EVALUATION OF A HIGH PERFORMANCE SMALLTALK SYSTEM Ph.D. Thesis
David M. Ungar Feb. 1986 239 p
(Contracts N00039-84-C-0089; ARPA Order 4871)
(AD-A173022) Avail: NTIS HC A11/MF A01 CSCL 09/2

The Smalltalk-80 sub TM system makes it possible to write programs quickly by providing object-oriented programming, incremental complication, run-time type checking, use-extensible data types and control structures, and an interactive graphical interface. However, the potential savings in programming effort have been curtailed by poor performance in widely available computers or high processor cost. Smalltalk-80 systems pose tough challenges for implementors: dynamic data typing, a high-level instruction set, frequent and expensive procedure calls, and object-oriented storage management. The dissertation documents two results that run counter to conventional wisdom: that a reduced instruction set computer can offer excellent performance of a system with dynamic data typing such as Smalltalk-80, and that automatic storage reclamation need not be time-consuming. GRA

N87-17203# Stanford Univ., Calif. Dept. of Applied Earth Science.
A KNOWLEDGE-BASED SOFTWARE ENVIRONMENT FOR THE ANALYSIS OF SPECTRORADIOMETER DATA
H. R. Goetting and R. J. P. Lyon *In* ESA Proceedings of the 1986 International Geoscience and Remote Sensing Symposium (IGARSS '86) on Remote Sensing: Today's Solutions for Tomorrow's Information Needs, Volume 1 Aug. 1986 p 235-238 (For primary document see N87-17163 09-43)
Avail: NTIS HC A99/MF E03; ESA, Paris, France, 3 volume set $90 Member States, AU, CN, and NO (+20% others)

N87-17231# Deutsche Forschungs- und Versuchsanstalt fuer Luft- und Raumfahrt, Oberpfaffenhofen (West Germany).
THE GERMAN ERS-1 SAR POSTPROCESSING SYSTEM PLANS AND CONCEPTS
G. Schreier and R. Winter *In* ESA Proceedings of the 1986 International Geoscience and Remote Sensing Symposium (IGARSS '86) on Remote Sensing: Today's Solutions for Tomorrow's Information Needs, Volume 1 Aug. 1986 p 417-422 (For primary document see N87-17163 09-43)
Avail: NTIS HC A99/MF E03; ESA, Paris, France, 3 volume set $90 Member States, AU, CN, and NO (+20% others)

61 COMPUTER PROGRAMMING AND SOFTWARE

Includes computer programs, routines, algorithms, and specific applications, e.g., CAD/CAM.

N87-17438 National Physical Lab., Teddington (England). Div. of Information Technology and Computing.
AN IMPLEMENTATION OF THE HOUGH TRANSFORM USING A LINEAR ARRAY PROCESSOR IN CONJUNCTION WITH A PDP/11MICROPROCESSOR
V. F. Leavers (Kings Coll., London, England) and J. F. Boyce Oct. 1986 19 p
(Contract EMRM-82-0437)
(NPL-DITC-74/86; ISSN-0262-5369; ETN-87-98917) Copyright. Avail: Issuing Activity

The Hough transform was implemented using a linear array processor in conjunction with a PDP/11 microcomputer in a computer vision arrangement. The image framestore is used as a 256 x 256 accumulator table. The need for a substantial core memory normally associated with the generation of Hough accumulators is precluded. The fine resolution available in Hough space makes it possible to identify the shape of the maxima which correspond to straight line segments in image space. Theoretical considerations led to the exploitation of this characteristic shape, that of a butterfly, to construct a filter capable of automatically locating the maxima corresponding to straight line segments. It is shown that the binary relations of connectedness and parallelism may be extracted and used to formulate a two dimensional model of an object. It is suggested that an extension of the treatment to a pair of stereo images provides sufficient information with which to formulate a three dimensional model of an object. ESA

N87-17439 Virginia Polytechnic Inst. and State Univ., Blacksburg.
COMPARATIVE ADVANTAGES OF GRAPHIC VERSUS NUMERIC REPRESENTATION OF QUANTITATIVE DATA Ph.D. Thesis
Fred W. Lacerda, Jr. 1986 267 p
Avail: Univ. Microfilms Order No. DA8620635

It was proposed in the context of preliminary data analysis, to determine whether one can generate more insights (meaningful or possibly relevant relationships suggested by the data), by looking at a graphic (multiple bar chart) representation, as opposed to numeric table, of a large multivariate quantitative dataset (twenty variables with twenty-four observations each), displayed and manipulated interactively in a personal computer-based system. The major issue involved is not how to communicate more effectively information to a large audience; it is rather what would stimulate deeper, sharper, and more expeditious analysis of a problem. A methodology was developed for objective scoring of the raw data (written notes with requested observations and inferences). Observations were eliminated on the basis of repetition, incompleteness, and lack of validation from the underlying dataset. Dissert. Abstr.

N87-17440*# Cornell Univ., Ithaca, N.Y. School of Electrical Engineering.
ALGORITHMS AND PROGRAMMING TOOLS FOR IMAGE PROCESSING ON THE MPP, PART 2 Report, Aug. 1985 - Mar. 1986
Anthony P. Reeves 1986 65 p
(Grant NAG5-403)
(NASA-CR-180146; NAS 1.26:180146) Avail: NTIS HC A04/MF A01 CSCL 09B

A number of algorithms were developed for image warping and pyramid image filtering. Techniques were investigated for the parallel processing of a large number of independent irregular shaped regions on the MPP. In addition some utilities for dealing with very long vectors and for sorting were developed. Documentation pages for the algorithms which are available for distribution are given. The performance of the MPP for a number of basic data manipulations was determined. From these results it is possible to predict the efficiency of the MPP for a number of algorithms and applications. The Parallel Pascal development system, which is a portable programming environment for the MPP, was improved and better documentation including a tutorial was written. This environment allows programs for the MPP to be developed on any conventional computer system; it consists of a set of system programs and a library of general purpose Parallel Pascal functions. The algorithms were tested on the MPP and a presentation on the development system was made to the MPP users group. The UNIX version of the Parallel Pascal System was distributed to a number of new sites. B.G.

N87-17441*# National Aeronautics and Space Administration. Lewis Research Center, Cleveland, Ohio.
A COMPARISON OF FIVE BENCHMARKS
Janice E. Huss and James A. Pennline Feb. 1987 15 p
(NASA-TM-88956; E-3411; NAS 1.15:88956) Avail: NTIS HC A02/MF A01 CSCL 09B

Five benchmark programs were obtained and run on the NASA Lewis CRAY X-MP/24. A comparison was made between the programs codes and between the methods for calculating performance figures. Several multitasking jobs were run to gain experience in how parallel performance is measured. Author

N87-17442*# National Aeronautics and Space Administration. Langley Research Center, Hampton, Va.
LINE PLOTTING PROGRAM USING DI-3000/GRAFMAKER ROUTINES
William A. Poppen, Jr. (Tennessee Univ., Knoxville.) and Rudeen Smith-Taylor Sep. 1986 46 p
(NASA-TM-89010; NAS 1.15:89010) Avail: NTIS HC A03/MF A01 CSCL 09B

A line plotting program has been developed using the DI-3000 graphics libraries and incorporates Grafmaker subroutines. The program allows multiple lines on a frame and multiple frames per run. Options such as automatic scaling, linear or single-cycle log graphs, and plot text such as titles, legends and axis labels are incorporated in the program. Greek and other fonts can be used in the plot text as well as upper and lower case text. Plot inputs are specified through a control file. The program also allows display of multiple independent data sets on a single graph. Author

N87-17443*# National Aeronautics and Space Administration. Ames Research Center, Moffett Field, Calif.
PROFILING UNDER UNIX BY PATCHING
Matt Bishop Oct. 1986 17 p
(NASA-TM-89316; RIACS-TR-86.24; NAS 1.15:89316) Avail: NTIS HC A02/MF A01 CSCL 09B

Profiling under UNIX is done by inserting counters into programs either before or during the compilation or assembly phases. A fourth type of profiling involves monitoring the execution of a program, and gathering relevant statistics during the run. This method and an implementation of this method are examined, and its advantages and disadvantages are discussed. Author

N87-17444*# National Aeronautics and Space Administration. Langley Research Center, Hampton, Va.
MULTIGRID APPLIED TO SINGULAR PERTURBATION PROB-

LEMS Final Report
David Kamowitz Jan. 1987 28 p Submitted for publication
(Contract NAS1-18107)
(NASA-CR-178230; ICASE-87-1; NAS 1.26:178230) Avail: NTIS HC A03/MF A01 CSCL 09B

The solution of the singular perturbation problem by a multigrid algorithm is considered. Theoretical and experimental results for a number of different discretizations are presented. The theoretical and observed rates agree with the results developed in an earlier work of Kamowitz and Parter. In addition, the rate of convergence of the algorithm when the coarse grid operator is the natural finite difference analog of the fine grid operator is presented. This is in contrast to the case in the previous work where the Galerkin choice (I sup H sub h L sub h,I sup h sub H) was used for the coarse grid operators. Author

N87-17445# Oak Ridge National Lab., Tenn. Center for Engineering Systems Advanced Research.
PROGRAMMING ROBOTICS APPLICATIONS ON AN ADVANCED HYPERCUBE MULTIPROCESSOR
J. Barhen 1986 7 p Presented at the International NATO Workshop on Languages for Sensor-based Control in Robotics, Castelvecchio Pascoli, Italy, 1 Sep. 1986
(Contract DE-AC05-84OR-21400)
(DE86-008895; CONF-860963-1) Avail: NTIS HC A02/MF A01

Specialized computer architectures for advanced robotics applications at ORNL/CESAR are based on the hypercube ensemble concept. The current status of algorithm development is summarized and results for robot dynamics and navigation problems are presented. DOE

N87-17446# Lawrence Livermore National Lab., Calif.
INTERACTIVE WRAPPER TOOL FOR MAPPING OBJECTS TO FORTRAN LIBRARY FUNCTIONS
B. S. Lawver 1 Apr. 1986 11 p Presented at the ACM Conference on Object Oriented Programming Systems, Languages, and Applications, Portland, Ore., 29 Sep. 1986
(Contract W-7405-eng-48)
(DE86-009686; UCRL-94377; CONF-860967-1) Avail: NTIS HC A02/MF A01

A wrapper serves as a software interface between non-object-oriented software and software that must be used but exists in a form that is not object-oriented. A tool designed to accomplish the wrapping function for a library of Fortran routines used by the Electrical Engineering Department at Lawrence Livermore National Laboratory is described. DOE

N87-17209# California Univ., Santa Barbara. Dept. of Geography.
THE IMAGE PROCESSING WORKBENCH - PORTABLE SOFTWARE FOR REMOTE SENSING INSTRUCTION AND RESEARCH
J. Frew and J. Dozier *In* ESA Proceedings of the 1986 International Geoscience and Remote Sensing Symposium (IGARSS '86) on Remote Sensing: Today's Solutions for Tomorrow's Information Needs, Volume 1 Aug. 1986 p 271-276 (For primary document see N87-17163 09-43)
Avail: NTIS HC A99/MF E03; ESA, Paris, France, 3 volume set $90 Member States, AU, CN, and NO (+20% others)

N87-17294# Centre d'Etude Spatiale des Rayonnements, Toulouse (France).
COMPUTER-AIDED INTERPRETATION OF COMPLEX GEOLOGICAL PATTERNS IN REMOTE SENSING
G. Flouzat and K. Moueddene *In* ESA Proceedings of the 1986 International Geoscience and Remote Sensing Symposium (IGARSS '86) on Remote Sensing: Today's Solutions for Tomorrow's Information Needs, Volume 2 Aug. 1986 p 783-786 (For primary document see N87-17283 09-43)
Avail: NTIS HC A17/MF A01; ESA, Paris, France, 3 volume set $90 Member States, AU, CN, and NO (+20% others) CSCL 09B

N87-17341# Universite Catholique de Louvain (Belgium). Lab. de Telecommunications et d'Hyperfrequences.
A TWO-STEP ALGORITHM FOR THE SEPARATE RETRIEVAL OF OCEAN SURFACE AND ATMOSPHERIC PARAMETERS FROM MICROWAVE RADIOMETERS
A. Guissard, P. Sobieski, and A. M. Guillaume *In* ESA Proceedings of the 1986 International Geoscience and Remote Sensing Symposium (IGARSS '86) on Remote Sensing: Today's Solutions for Tomorrow's Information Needs, Volume 2 Aug. 1986 p 1077-1082 (For primary document see N87-17283 09-43)
Avail: NTIS HC A17/MF A01; ESA, Paris, France, 3 volume set $90 Member States, AU, CN, and NO (+20% others)

N87-16948# European Space Agency. European Space Research and Technology Center, ESTEC, Noordwijk (Netherlands). Mechanical Systems Div.
ENGINEERING AND SOFTWARE INTERFACING FOR THERMAL, STRUCTURAL AND DYNAMIC CONTROL RELATED WITH SPACECRAFT ACTIVITIES
C. Stavrinidis, M. Klein, and J. Wijker (Royal Netherlands Aircraft Factories Fokker, Schiphol-Oost) *In its* Proceedings of the Second ESA Workshop on Mechanical Technology for Antennas Aug. 1986 p 219-225 (For primary document see N87-16923 09-32)
(Contract ESTEC-5158/82-NL-PB(SC))
Avail: NTIS HC A12/MF A01

62 COMPUTER SYSTEMS

Includes computer networks and special application computer systems.

N87-17447 Rensselaer Polytechnic Inst., Troy, N.Y.
A STUDY OF SPATIAL MODELS AND HUMAN NAVIGATION WITHIN COMPLEX COMPUTER INTERFACES Ph.D. Thesis
Candace Soderston 1986 285 p
Avail: Univ. Microfilms Order No. DA8619997

The process of building a conceptual model of the layout of information within a computer system was examined. An experiment was performed in which eighty people (with five different types of background) had to search for sixteen pieces of information within each of two computer interfaces. Four interface designs were tested, varying on underlying structure and access method. Exploration, retrieval, and error recovery tasks were examined and data were collected on subject performance, preference, and cognitive model. It was concluded that systems should provide survey access to all functions, however, learning aids should include an emphasis upon building up route knowledge of the system. Furthermore, on-line information should be structured hierarchically. Dissert. Abstr.

N87-17448*# Carnegie-Mellon Univ., Pittsburgh, Pa. Dept. of Electrical and Computer Engineering.
FAULT-FREE PERFORMANCE VALIDATION OF FAULT-TOLERANT MULTIPROCESSORS
Edward W. Czeck, Frank E. Feather, Ann Marie Grizzaffi, Zary Z. Segall, and Daniel P. Siewiorek Jan. 1987 68 p
(Grant NAG1-190)
(NASA-CR-178236; NAS 1.26:178236) Avail: NTIS HC A04/MF A01 CSCL 09B

A validation methodology for testing the performance of fault-tolerant computer systems was developed and applied to the Fault-Tolerant Multiprocessor (FTMP) at NASA-Langley's AIRLAB facility. This methodology was claimed to be general enough to apply to any ultrareliable computer system. The goal of this research was to extend the validation methodology and to demonstrate the robustness of the validation methodology by its more extensive application to NASA's Fault-Tolerant Multiprocessor System (FTMP) and to the Software Implemented Fault-Tolerance (SIFT) Computer System. Furthermore, the performance of these two multiprocessors was compared by conducting similar experiments. An analysis of the results shows high level language

instruction execution times for both SIFT and FTMP were consistent and predictable, with SIFT having greater throughput. At the operating system level, FTMP consumes 60% of the throughput for its real-time dispatcher and 5% on fault-handling tasks. In contrast, SIFT consumes 16% of its throughput for the dispatcher, but consumes 66% in fault-handling software overhead. Author

63 CYBERNETICS

Includes feedback and control theory, artificial intelligence, robotics and expert systems.

For related information see also *54 Man/System Technology and Life Support.*

N87-17449 Stanford Univ., Calif.
ADAPTIVE CONTROL OF A FLEXIBLE STRUCTURE Ph.D. Thesis
Michael David Sidman 1986 205 p
Avail: Univ. Microfilms Order No. DA8619822

The demonstration of a high-performance adaptive control system for a lightly-damped flexible mechanical structure, such as found in large space structures, lightweight robots, and computer peripherals, is discussed. The system accurately identifies the frequencies of three resonances and one anti-resonance, as well as the overall gain of the experimental plant, the Stanford Four Disk System. The robustness and reliability of the system were demonstrated in the presence of large, sudden changes in plant dynamics that include a complex pole-zero flip and near pole-zero cancellation that occur as payload mass is added to the system. Fixed-gain robust control performance, both colocated and noncolocated, are compared to noncolocated adaptive control performance. A new method of pole-placement ensures excellent reference-command step responses, substantial active damping of modeled modes, modest amount of control effort and low computational intensity despite major changes in plant dynamics. Techniques ensure stable control, at least a minimum level of performance at all times and fast recovery after large sudden changes in plant parameters that occur even while the plant is in a quiescent state. Dissert. Abstr.

N87-17450 Stanford Univ., Calif.
ADAPTIVE CONTROL OF MECHANICAL MANIPULATORS Ph.D. Thesis
John James Craig 1986 164 p
Avail: Univ. Microfilms Order No. DA8619733

When an accurate dynamic model of a mechanical manipulator is available, it may be used in a non-linear model-based scheme to control the manipulator. Such a control formulation yields a controller which suppresses disturbances and tracks desired trajectories uniformly in all configurations of the manipulator. However, use of a poor dynamic model in this kind of model-based decoupling and linearizing scheme may result in performance which is inferior to a much simpler fixed gain scheme. Nonlinear control of mechanical manipulators in those cases where the physical models which describe the manipulators are not well known are addressed. The robustness of the model-based servo in the presence of poorly known parameters is investigated. A sufficient condition for stability of the overall system in the presence of parameter errors is developed. A parameter-adaptive control scheme is developed in the form of a set of adaptive laws that can be added to the non-linear model-based controller. The scheme is unique in that it is designed specifically for this model-based controller, and is rigorously proven stable in the full non-linear setting. The issues of sufficient excitation and the effect of disturbances are also discussed. A learning control scheme is developed which can be added to the model-based controller in order to learn compensation for friction and other effects which are difficult to model parametrically. Dissert. Abstr.

N87-17451*# Jet Propulsion Lab., California Inst. of Tech., Pasadena.
KALMAN FILTERING, SMOOTHING AND RECURSIVE ROBOT ARM FORWARD AND INVERSE DYNAMICS
G. Rodriguez 1 Dec. 1986 47 p
(Contract NAS7-918)
(NASA-CR-180135; JPL-Pub-86-48; NAS 1.26:180135) Avail: NTIS HC A03/MF A01 CSCL 09B

The inverse and forward dynamics problems for multi-link serial manipulators are solved by using recursive techniques from linear filtering and smoothing theory. The pivotal step is to cast the system dynamics and kinematics as a two-point boundary-value problem. Solution of this problem leads to filtering and smoothing techniques identical to the equations of Kalman filtering and Bryson-Frazier fixed time-interval smoothing. The solutions prescribe an inward filtering recursion to compute a sequence of constraint moments and forces followed by an outward recursion to determine a corresponding sequence of angular and linear accelerations. In addition to providing techniques to compute joint accelerations from applied joint moments (and vice versa), the report provides an approach to evaluate recursively the composite multi-link system inertia matrix and its inverse. The report lays the foundation for the potential use of filtering and smoothing techniques in robot inverse and forward dynamics and in robot control design. Author

N87-17452# Technische Hogeschool Twente, Enschede (Netherlands). Dept. of Applied Mathematics.
DYNAMIC INPUT-OUTPUT DECOUPLING OF NONLINEAR CONTROL SYSTEMS
Henk Nijmeijer and Witold Respondek (Polish Academy of Sciences, Warsaw.) Jul. 1986 29 p
(MEMO-575; ISSN-0169-2690; ETN-87-99054) Avail: NTIS HC A03/MF A01

Dynamic input-output decoupling of nonlinear control systems is solved using an analytic algorithm to obtain necessary and sufficient conditions for the solvability of this problem. The solution of the problems is constructive by applying, iteratively, feedback and precompensation. Interesting connections with other approaches in nonlinear control theory are discussed. ESA

64 NUMERICAL ANALYSIS

Includes iteration, difference equations, and numerical approximation.

N87-17453*# National Aeronautics and Space Administration. Langley Research Center, Hampton, Va.
CONVENIENT TOTAL VARIATION DIMINISHING CONDITIONS FOR NONLINEAR DIFFERENCE SCHEMES Final Report
Eitan Tadmor (Tel-Aviv Univ. (Israel).) Nov. 1986 33 p Submitted for publication
(Contract NAS1-18107)
(NASA-CR-178209; ICASE-86-74; NAS 1.26:178209) Avail: NTIS HC A03/MF A01 CSCL 12A

Convenient conditions for nonlinear difference schemes to be total-variation diminishing (TVD) are reviewed. It is shown that such schemes share the TVD property, provided their numerical fluxes meet a certain positivity condition at extrema values but can be arbitrary otherwise. The conditions are invariant under different incremental representations of the nonlinear schemes, and thus provide a simplified generalization of the TVD conditions due to Harten and others. Author

N87-17454# Loughborough Univ. of Technology (England). Dept. of Mathematics.
GLOBALLY CONVERGENT HYBRID CONJUGATE GRADIENT METHODS
D. Touati-Ahmed and C. Storey Nov. 1986 109 p
(MR-196) Avail: NTIS HC A06/MF A01

Two hybrid conjugate gradient methods are presented. The first hybrid, Hybrid 1, uses the Polak-Ribiere beta as long as it is positive and less than or equal to that of Fletcher-Reeves and

uses the Fletcher-Reeves beta instead, otherwise. This condition ensures that every time a Polak-Ribiere beta is used, the angle between the search direction and the negative gradient is smaller than that between the Fletcher-Reeves direction and the negative gradient. The second hybrid, Hybrid 2, on the other hand, is an extension of Hybrid 1 in the sense that for every Polak-Ribiere beta that is greater than that of Fletcher-Reeves, an angle test is performed to check whether the cosine of the angle between the search direction and the negative gradient is within a constant multiple of the cosine of the angle between the Fletcher-Reeves direction and the negative gradient. If this is the case, the Polak-Ribiere beta is used, otherwise the Fletcher-Reeves beta is used instead. Descent property and global convergence proofs are given for both method when exact and inexact line searches are performed. Computational results show that Hybrid 1 outperforms the Fletcher-Reeves method and performs about as well as the Polak-Ribiere method with the advantage of being globally convergent, whereas Hybrid 2 outperforms both the Fletcher-Reeves and the Polak-Ribiere methods on a wide class of problems. Author

N87-17455*# National Aeronautics and Space Administration. Marshall Space Flight Center, Huntsville, Ala.
ON THE ANALYTICAL DETERMINATION OF RELAXATION MODULUS OF VISCOELASTIC MATERIALS BY PRONY'S INTERPOLATION METHOD
Pedro I. Rodriguez Dec. 1986 31 p
(NASA-TM-86579; NAS 1.15:86579) Avail: NTIS HC A03/MF A01 CSCL 12A

A computer implementation to Prony's curve fitting by exponential functions is presented. The method, although more than one hundred years old, has not been utilized to its fullest capabilities due to the restriction that the time range must be given in equal increments in order to obtain the best curve fit for a given set of data. The procedure used in this paper utilizes the 3-dimensional capabilities of the Interactive Graphics Design System (I.G.D.S.) in order to obtain the equal time increments. The resultant information is then input into a computer program that solves directly for the exponential constants yielding the best curve fit. Once the exponential constants are known, a simple least squares solution can be applied to obtain the final form of the equation. Author

N87-17456*# National Aeronautics and Space Administration. Langley Research Center, Hampton, Va.
SURVEY OF THE STATUS OF FINITE ELEMENT METHODS FOR PARTIAL DIFFERENTIAL EQUATIONS Final Report
Roger Temam Nov. 1986 64 p
(Contract NAS1-18107)
(NASA-CR-178222; ICASE-86-77; NAS 1.26:178222) Avail: NTIS HC A04/MF A01 CSCL 12A

The finite element methods (FEM) have proved to be a powerful technique for the solution of boundary value problems associated with partial differential equations of either elliptic, parabolic, or hyperbolic type. They also have a good potential for utilization on parallel computers particularly in relation to the concept of domain decomposition. This report is intended as an introduction to the FEM for the nonspecialist. It contains a survey which is totally nonexhaustive, and it also contains as an illustration, a report on some new results concerning two specific applications, namely a free boundary fluid-structure interaction problem and the Euler equations for inviscid flows. Author

N87-17457*# Hawaii Univ., Honolulu. Dept. of Electrical Engineering.
CYCLIC UNEQUAL ERROR PROTECTION CODES CONSTRUCTED FROM CYCLIC CODES OF COMPOSITE LENGTH Technical Report, 1 Jul. 1985 - 30 Jun. 1986
Shu Lin 1 Mar. 1987 47 p
(Grant NAG5-407)
(NASA-CR-180165; NAS 1.26:180165) Avail: NTIS HC A03/MF A01 CSCL 12A

The distance structure of cyclic codes of composite length was investigated. A lower bound on the minimum distance for this class of codes is derived. In many cases, the lower bound gives the true minimum distance of a code. Then the distance structure of the direct sum of two cyclic codes of composite length were investigated. It was shown that, under certain conditions, the direct-sum code provides two levels of error correcting capability, and hence is a two-level unequal error protection (UEP) code. Finally, a class of two-level UEP cyclic direct-sum codes and a decoding algorithm for a subclass of these codes are presented. Author

N87-17458*# Hawaii Univ., Honolulu. Dept. of Electrical Engineering.
ON CODES WITH MULTI-LEVEL ERROR-CORRECTION CAPABILITIES Technical Report, 1 Jul. 1985 - 30 Jun. 1986
Shu Lin 1 Mar. 1987 63 p
(Grant NAG5-407)
(NASA-CR-180166; NAS 1.26:180166) Avail: NTIS HC A04/MF A01 CSCL 12A

In conventional coding for error control, all the information symbols of a message are regarded equally significant, and hence codes are devised to provide equal protection for each information symbol against channel errors. However, in some occasions, some information symbols in a message are more significant than the other symbols. As a result, it is desired to devise codes with multilevel error-correcting capabilities. Another situation where codes with multi-level error-correcting capabilities are desired is in broadcast communication systems. An m-user broadcast channel has one input and m outputs. The single input and each output form a component channel. The component channels may have different noise levels, and hence the messages transmitted over the component channels require different levels of protection against errors. Block codes with multi-level error-correcting capabilities are also known as unequal error protection (UEP) codes. Structural properties of these codes are derived. Based on these structural properties, two classes of UEP codes are constructed. Author

N87-17459# Arizona State Univ., Tempe. Dept. of Mathematics.
A PSEUDO-ARCLENGTH CONTINUATION METHOD FOR NONLINEAR EIGENVALUE PROBLEMS
Hans D. Mittelmann Oct. 1985 32 p
(Grant AF-AFOSR-0315-84)
(AD-A173019; TR-88) Avail: NTIS HC A03/MF A01 CSCL 12/1

A variant of the classical pseudo-arclength continuation method is proposed. Basically, the method can be viewed as pseudo-arclength continuation in (r, lambda) space where r is a functional of the solution. Another difference is a three-parameter predictor instead of the standard Euler step. This predictor, as well as the Newton corrector iteration, are justified and some numerical results for reaction-diffusion equations are presented. The method provides a simple algebraic check for symmetry breaking bifurcation, the most common type of secondary bifurcation in physical examples. GRA

N87-17460# Johns Hopkins Univ., Baltimore, Md. Dept. of Electrical Engineering and Computer Science.
RECURSIVE LINEAR SMOOTHING FOR DISSIPATIVE HYPERBOLIC SYSTEMS Interim Report, 1 May 1985 - 22 Sep. 1986
Laurence R. Riddle and Howard L. Weinert 25 Sep. 1986 41 p
(Contract N00014-85-K-0255)
(AD-A173020; JHU/EE-86/19) Avail: NTIS HC A03/MF A01 CSCL 09/3

This paper presents an efficient method of smoothing steady-state, dissipative hyperbolic systems with one spatial dimension. The observations are from point sensors placed on the system. Using this characterization, one develops a smoothing algorithm that is recursive with respect to the sensors, resulting in a significant decrease in computational complexity relative to other methods. The algorithm's performance is illustrated by studying the smoothing problem for sound waves in an air filled pipe. GRA

N87-17461# Clarkson Coll. of Technology, Potsdam, N.Y. Dept. of Mathematics and Computer Science.
NONLINEAR WAVE PROPAGATION Progress Report, 1 Oct. 1985 - 28 Apr. 1986
Mark J. Ablowitz 8 Apr. 1986 4 p
(Grant AF-AFOSR-0005-84)
(AD-A175073; AFOSR-86-2192TR) Avail: NTIS HC A02/MF A01 CSCL 12/1

The central theme involved in this work is the continuing study of certain fundamental features associated with the nonlinear wave propagation arising in and motivated by physical problems. The usefulness of the work is attested to by the varied applications, and wide areas of interest in physics, engineering and mathematics. The work accomplished involves wave propagation in a number of areas including fluid mechanics, plasma physics, theoretical physics, statistical mechanics, nonlinear optics, multidimensional solitons, multidimensional inverse problems, Painleve equations, direct linearizations of certain nonlinear wave equations, DBAR problems, Riemann-Hilbert boundary value problems, differential geometry, etc. GRA

N87-17462# Oxford Univ. (England). Dept. of Engineering Science.
RECURSIVE TECHNIQUES IN IDENTIFICATION
K. Warwick 1986 31 p Presented at the IEE Colloquium on System Identification for Control, Durham, England, 26 Sep. 1986
(OUEL-1644/86; ETN-87-98930) Avail: NTIS HC A03/MF A01

Recursive parameter estimation scheme structure and implementation are discussed. Problems with parameter drift, algorithm convergence, and numerical stability are considered. It is shown how estimation equations can be modified in order to account for time varying systems. ESA

N87-17463# Technische Hogeschool Twente, Enschede (Netherlands). Dept. of Applied Mathematics.
A TRANSPORTATION QUEUEING MODEL, SOLVED AS A RIEMANN BOUNDARY VALUE PROBLEM
W. M. Najwijn Jun. 1986 18 p
(MEMO-573; ISSN-0169-2690; ETN-87-99052) Avail: NTIS HC A02/MF A01

A queueing model that can be solved as a Riemann boundary value problem on the circle is applied to jobs arriving according to a homogeneous Poisson process at a loading station then queueing for loading into a carrier. Two carriers move along a closed chain with constant speed, so that loading takes place at discrete timepoints. Since the carriers have infinite capacity all waiting jobs are loaded into a carrier upon its arrival at the loading station. Jobs are unloaded and taken into service by a single server situated along the chain, one at a time since there is no waiting room in front of the server. Service times are negative exponential and handling times are negligible. The mean number of jobs in the system and the probability generating function of the number of jobs in the loading station, in the carriers and at the server are derived. ESA

N87-17464# Technische Hogeschool Twente, Enschede (Netherlands). Dept. of Applied Mathematics.
A REPRESENTATION FOR PIECEWISE CUBIC C SUP 1-SPLINES ON ARBITRARY TRIANGULATIONS
R. H. J. GmeligMeyling Jul. 1986 32 p
(MEMO-574; ISSN-0169-2690; ETN-87-99053) Avail: NTIS HC A03/MF A01

An efficient representation for bivariate cubic C sup 1-splines on arbitrary triangulations is presented. A numerical method for computing the dimension of the space S (sup 1 sub 3) (Delta) of these splines is discussed. Subspaces satisfying certain boundary conditions are considered. Applications are given where piecewise cubic C sup 1-functions are used to solve interpolation problems and least squares approximation problems are given. ESA

N87-17465# Technische Hogeschool Twente, Enschede (Netherlands). Dept. of Applied Mathematics.
A NOTE ON BRANIN'S METHOD FOR FINDING THE CRITICAL POINTS OF SMOOTH FUNCTIONS
Hubertus Th. Jongen, Peter Jonker, and Frank Twilt Jul. 1986 23 p
(MEMO-576; ISSN-0169-2690; ETN-87-99055) Avail: NTIS HC A02/MF A01

For a generic subclass of smooth functions f on R sup n, a globally defined autonomous differential equation on R sup n underlying the Newton-iteration method for finding critical points of f is studied. The set of all equilibria of the differential equation is described, and the local phase portraits around these points is discussed. ESA

N87-17466# Technische Hogeschool Twente, Enschede (Netherlands). Dept. of Applied Mathematics.
PERTURBATION THEORY FOR UNBOUNDED MARKOV PROCESSES WITH APPLICATIONS TO QUEUEING
N. M. vanDijk Aug. 1986 21 p
(MEMO-579; ISSN-0169-2690; ETN-87-99058) Avail: NTIS HC A02/MF A01

A perturbation in the one-step transition probabilities and rewards of a discrete-time Markov reward process with a possibly unbounded one-step reward function is considered. A perturbation estimate for the finite horizon and average reward function is derived. Existing results are extended to the unbounded case. The analysis is illustrated for one and two-dimensional queueing processes by an M/M/1-queue and an overflow queueing model with an error bound in the arrival rate. ESA

N87-17467# Technische Hogeschool Twente, Enschede (Netherlands). Dept. of Applied Mathematics.
SIMPLE AND INSENSITIVE BOUNDS FOR A GRADING AND AN OVERFLOW MODEL
N. M. vanDijk Aug. 1986 12 p
(MEMO-581; ISSN-0169-2690; ETN-87-99060) Avail: NTIS HC A02/MF A01

Simple and intuitively obvious lower and upper bounds for a grading and an overflow model are suggested. The bounds are based on product type modifications and are insensitive. Numerical support indicates a potential usefulness for quick engineering purposes. ESA

N87-17468# Technische Hogeschool Twente, Enschede (Netherlands). Dept. of Applied Mathematics.
A FORMAL PROOF FOR THE INSENSIBILITY OF SIMPLE BOUNDS FOR FINITE MULTISERVER NONEXPONENTIAL TANDEM QUEUES
N. M. vanDijk Aug. 1986 27 p
(MEMO-582; ISSN-0169-2690; ETN-87-99061) Avail: NTIS HC A03/MF A01

It is proved that for multiserver disciplines, bounds for finite tandem queues in the exponential case are insensitive, that is remain valid for the nonexponential case. The technique applied extends standard monotonicity techniques and seems promising for further application. ESA

N87-16990# Vrije Universiteit, Brussels (Belgium). Dept. of Fluid Mechanics.
REVIEW OF DISCRETIZATION TECHNIQUES AND NUMERICAL RESOLUTION METHODS
Ch. Hirsch *In* Von Karman Inst. for Fluid Dynamics Introduction to Numerical Solution of Industrial Flows, Volume 1 1986 56 p
(For primary document see N87-16987 09-34)
Avail: NTIS HC A14/MF A01

N87-16991# Vrije Universiteit, Brussels (Belgium). Dept. of Fluid Mechanics.
THE ANALYSIS AND RESOLUTION OF NUMERICAL SCHEMES
Ch. Hirsch *In* Von Karman Inst. for Fluid Dynamics Introduction to Numerical Solution of Industrial Flows, Volume 1 1986 27 p
(For primary document see N87-16987 09-34)
Avail: NTIS HC A14/MF A01

N87-16996# Flow Science, Inc., Los Alamos, N. Mex.
SOLA: A BASIC SOLUTION ALGORITHM FOR FLOW ANALYSIS
C. W. Hirt *In* Von Karman Inst. for Fluid Dynamics Introduction to Numerical Solution of Industrial Flows, Volume 2 1986 21 p (For primary document see N87-16994 09-34)
Avail: NTIS HC A11/MF A01

N87-16997# Flow Science, Inc., Los Alamos, N. Mex.
APPLICATIONS OF SOLA TO CONFINED FLOWS
C. W. Hirt *In* Von Karman Inst. for Fluid Dynamics Introduction to Numerical Solution of Industrial Flows, Volume 2 1986 25 p (For primary document see N87-16994 09-34)
Avail: NTIS HC A11/MF A01

N87-16998# Flow Science, Inc., Los Alamos, N. Mex.
APPLICATIONS OF SOLA TO FREE SURFACE FLOWS
C. W. Hirt *In* Von Karman Inst. for Fluid Dynamics Introduction to Numerical Solution of Industrial Flows, Volume 2 1986 22 p (For primary document see N87-16994 09-34)
Avail: NTIS HC A11/MF A01

N87-17196# Duisburg Univ. (West Germany). Dept. of Electrical Engineering.
THEORETICAL CONSIDERATION ON RESISTANCE GEOELECTRICS
A. Beyer *In* ESA Proceedings of the 1986 International Geoscience and Remote Sensing Symposium (IGARSS '86) on Remote Sensing: Today's Solutions for Tomorrow's Information Needs, Volume 1 Aug. 1986 p 193-197 (For primary document see N87-17163 09-43)
Avail: NTIS HC A99/MF E03; ESA, Paris, France, 3 volume set $90 Member States, AU, CN, and NO (+20% others)

65 STATISTICS AND PROBABILITY

Includes data sampling and smoothing; Monte Carlo method; and stochastic processes.

N87-17469*# Research Triangle Inst., Research Triangle Park, N.C.
ON THE STOCHASTIC DISSEMINATION OF FAULTS IN AN ADMISSIBLE NETWORK
A. Kyrala Jan. 1987 36 p
(Contract NAS1-17964)
(NASA-CR-178238; NAS 1.26:178238) Avail: NTIS HC A03/MF A01 CSCL 12A

The dynamic distribution of faults in a general type network is discussed. The starting point is a uniquely branched network in which each pair of nodes is connected by a single branch. Mathematical expressions for the uniquely branched network transition matrix are derived to show that sufficient stationarity exists to ensure the validity of the use of the Markov Chain model to analyze networks. In addition the conditions for the use of Semi-Markov models are discussed. General mathematical expressions are derived in an examination of branch redundancy techniques commonly used to increase reliability. Author

N87-17470# Ford Aerospace and Communications Corp., Palo Alto, Calif.
ON FIRST PASSAGE TIMES AND DIFFERENTIAL EQUATIONS
Michael L. Wenocur 1986 25 p
(Contract F49620-86-C-0022)
(AD-A174648; AFOSR-86-0478TR) Avail: NTIS HC A02/MF A01 CSCL 12/1

Practical and theoretical considerations in computing first passage time statistics are considered. We are motivated by first passage times as models of failure times. In Section 1, the relevance of first passage time distributions as failure time models is indicated. Also, the spectral series expansion solution to the backward equation is introduced. In Section 2, algorithms for approximating w(x,t) are obtained. In particular, the infinite spectral expansion of rw(x,t) is approximated by an n-term sub-expansion which matches the first n-1 moments. Proofs validating the spectral expansion and the related approximation scheme are given in the Appendix. In Sections 3 and 4, methods are given for obtaining the eigenvalues and first passage moments, necessary for computing approximations to w(x,t). In Section 5, computational issues related to calculating the moment generating function are considered. Sections 6 and 7 include theoretical complements about first passage times. In particular, the moment generating function is shown to possess an interesting representation having exponential form (cf equations (7.1)). This exponential representation is related to asymptotic expansions used in analyzing perturbations of certain second-order differential equations. GRA

N87-17471# Sheffield Univ. (England). Dept. of Control Engineering.
A PREDICTION ERROR ESTIMATE FOR NONLINEAR STOCHASTIC SYSTEMS
I. J. Leontaritis and S. A. Billings Mar. 1986 28 p Sponsored by UK Science and Engineering Research Council
(RR-295; ETN-87-98932) Avail: NTIS HC A03/MF A01

A prediction error estimation algorithm incorporating model selection and validation techniques for a class of multivariable discrete time stochastic nonlinear systems which can be represented by the Nonlinear Auto Regressive Moving Average Model with exogenous inputs model was developed. The square root method of decomposing a positive definite symmetric matrix was used to ensure an efficient numerical minimization of the loss function. Two methods of selecting the correct model were used, the model expansion and the model reduction methods. The Householder orthogonal transformation was employed to evaluate the criterion the selected model must minimize. ESA

66 SYSTEMS ANALYSIS

Includes mathematical modeling; network analysis; and operations research.

N87-17472*# Ford Aerospace and Communications Corp., Palo Alto, Calif.
COMMUNICATIONS SATELLITE SYSTEMS OPERATIONS WITH THE SPACE STATION. VOLUME 1: EXECUTIVE SUMMARY Final Report, Jul. 1985 - Sep. 1986
K. Price, J. Dixon, and C. Weyandt Feb. 1987 17 p
(Contract NAS3-24253)
(NASA-CR-179526; NAS 1.26:179526) Avail: NTIS HC A02/MF A01 CSCL 12B

The benefits of new space-based activities are quantified and the impacts on the satellite design and the space station are assessed. B.G.

N87-17473*# Ford Aerospace and Communications Corp., Palo Alto, Calif.
COMMUNICATIONS SATELLITE SYSTEMS OPERATIONS WITH THE SPACE STATION, VOLUME 2 Final Report, Jul. 1985 - Sep. 1986
K. Price, J. Dixon, and C. Weyandt Feb. 1987 190 p
(Contract NAS3-24253)
(NASA-CR-179527; NAS 1.26:179527) Avail: NTIS HC A09/MF A01 CSCL 12B

A financial model was developed which described quantitatively the economics of the space segment of communication satellite systems. The model describes the economics of the space system throughout the lifetime of the satellite. The expected state-of-the-art status of communications satellite systems and operations beginning service in 1995 were assessed and described. New or enhanced space-based activities and associated satellite system designs that have the potential to achieve future communications satellite operations in geostationary orbit with improved economic performance were postulated and defined. Three scenarios using combinations of space-based activities were analyzed: a spin

stabilized satellite, a three axis satellite, and assembly at the Space Station and GEO servicing. Functional and technical requirements placed on the Space Station by the scenarios were detailed. Requirements on the satellite were also listed. B.G.

N87-17474*# National Aeronautics and Space Administration, Washington, D.C.
DECENTRALIZED CONTROL OF LARGE-SCALE SYSTEMS: FIXED MODES, SENSITIVITY AND PARAMETRIC ROBUSTNESS Ph.D. Thesis - Universite Paul Sabatier, 1985
A. Tarras Feb. 1987 273 p Transl. into ENGLISH of French Thesis p 1-242 Transl. by Kanner (Leo) Associates, Redwood City, Calif.
(Contract NASw-4005)
(NASA-TM-88537; NAS 1.15:88537) Avail: NTIS HC A12/MF A01 CSCL 12B

The problem of stabilization/pole placement under structural constraints of large scale linear systems is discussed. The existence of a solution to this problem is expressed in terms of fixed modes. The aim is to provide a bibliographic survey of the available results concerning the fixed modes (characterization, elimination, control structure selection to avoid them, control design in their absence) and to present the author's contribution to this problem which can be summarized by the use of the mode sensitivity concept to detect or to avoid them, the use of vibrational control to stabilize them, and the addition of parametric robustness considerations to design an optimal decentralized robust control. Author

N87-17475# Technische Hogeschool Twente, Enschede (Netherlands). Dept. of Applied Mathematics.
A NOTE ON A CORE CATCHER OF A COOPERATIVE GAME
T. S. H. Driessen Jun. 1986 7 p
(MEMO-572; ISSN-0169-2690; ETN-87-99051) Avail: NTIS HC A02/MF A01

In Driessen (1986) it is shown that for games satisfying a certain condition the core of the game is included in the convex hull of the set of certain marginal worth vectors of the game, while it is conjectured that the inclusion holds without any conditin on the game. In this note it is proven that the inclusion holds for all games. Author (ESA)

67 THEORETICAL MATHEMATICS

Includes topology and number theory.

N87-17476# Technische Hogeschool Twente, Enschede (Netherlands). Dept. of Applied Mathematics.
A CONSTRUCTION OF SOLUTIONS OF THE MULTICOMPONENT KP-HIERARCHY
G. F. Helminck Sep. 1986 13 p
(MEMO-584; ISSN-0169-2690; ETN-87-99063) Avail: NTIS HC A02/MF A01

The multicomponent KP-hierarchy is introduced, showing that in order to obtain solutions of this collection of nonlinear partial differential equations it suffices to solve a set of linear equations. The Grassmann manifold of a certain Banach space is the basic object from where the construction starts. The scheme to obtain solutions of the multicomponent KP-hierarchy is the same as that used in Segal and Wilson (1985) and Helminck (no date) to construct solutions of the KP-hierarchy. ESA

70 PHYSICS (GENERAL)

For precision time and time interval (PTTI) see *35 Instrumentation and Photography;* for geophysics, astrophysics or solar physics see *46 Geophysics, 90 Astrophysics,* or *92 Solar Physics.*

N87-17477# Department of the Navy, Washington, D. C.
APPARATUS AND METHOD FOR STIRRING FLUID BORNE PARTICLES Patent Application
Earl F. Skelton, inventor (to Navy), William T. Elam, inventor (to Navy), and Alan W. Webb, inventor (to Navy) Filed 2 Jul. 1986 17 p
(AD-D012486; US-Patent-Appl-SN-890201) Avail: NTIS HC A02/MF A01 CSCL 13/9

Specimen particles in pressurized liquid sea are reoriented by magnetic stirring as a magnetic field surrounding the particles changes direction and the particles reorient themselves to respond to the change. Nonmagnetic particles as well as magnetic particles can be reoriented by simply including magnetic particles along with the nonmagnetic particles in the sea so that the magnetic particles collide with the nonmagnetic particles or attach to them so as to reorient them (individual particles) as they themselves reorient in response to change in direction of the magnetic field. GRA

71 ACOUSTICS

Includes sound generation, transmission and attenuation. For noise pollution see *45 Environment Pollution.*

N87-17478 California Univ., Los Angeles.
SOUND PROPAGATION IN A SUPERFLUID HELIUM FILLED POROUS SOLID: THEORY AND EXPERIMENT Ph.D. Thesis
Steven Richard Baker 1986 392 p
Avail: Univ Microfilms Order No. DA8621018

The propagation of sound in a superfluid helium filled solid was investigated theoretically and experimentally. Motivated by the Biot theory for the propagation of elastic waves in a fluid saturated porous solid, a set of linearized two fluid equations, averaged over the fine structure of the solid, was developed. From these were derived dispersion relations for the transitions from first sound to fourth sound (c sub 1 yields c sub 4) and from second sound to diffusion (c sub 2 yields diffusion) in a superfluid helium filled porous solid as the viscous drag on the normal component varies from zero to infinity. The theory also predicts a transition from second sound to fifth sound under pressure release boundary conditions. The description of each mode is formally identical to a simple viscoelastic transition characterized by a single relaxation time. The values of the three Biot parameters which depend only on the microscopic pore geometry, the tortuosity, the permeability, and the structural factor, can be extracted from measurements of the speed and attenuation of these modes. Dissert. Abstr.

N87-17479*# National Aeronautics and Space Administration. Langley Research Center, Hampton, Va.
POWER CEPSTRUM TECHNIQUE WITH APPLICATION TO MODEL HELICOPTER ACOUSTIC DATA
R. M. Martin and C. L. Burley Washington Jun. 1986 68 p
(NASA-TP-2586; L-16070; NAS 1.60:2586) Avail: NTIS HC A04/MF A01 CSCL 20A

The application of the power cepstrum to measured helicopter-rotor acoustic data is investigated. A previously applied correction to the reconstructed spectrum is shown to be incorrect. For an exact echoed signal, the amplitude of the cepstrum echo spike at the delay time is linearly related to the echo relative amplitude in the time domain. If the measured spectrum is not entirely from the source signal, the cepstrum will not yield the desired echo characteristics and a cepstral aliasing may occur because of the effective sample rate in the frequency domain. The spectral analysis bandwidth must be less than one-half the echo ripple frequency or cepstral aliasing can occur. The power cepstrum editing technique is a useful tool for removing some of the contamination because of acoustic reflections from measured rotor acoustic spectra. The cepstrum editing yields an improved estimate of the free field spectrum, but the correction process is limited by the lack of accurate knowledge of the echo transfer function. An alternate procedure, which does not require cepstral editing, is proposed which allows the complete correction of a contaminated

spectrum through use of both the transfer function and delay time of the echo process. Author

N87-17480*# National Aeronautics and Space Administration. Lewis Research Center, Cleveland, Ohio.
COMBUSTION NOISE FROM GAS TURBINE AIRCRAFT ENGINES MEASUREMENT OF FAR-FIELD LEVELS
Eugene A. Krejsa 1987 8 p Proposed for presentation at the 1987 National Conference on Noise Control Engineering, University Park, Pa., 8-10 Jun. 1987
(NASA-TM-88971; E-3407; NAS 1.15:88971) Avail: NTIS HC A02/MF A01 CSCL 20A

Combustion noise can be a significant contributor to total aircraft noise. Measurement of combustion noise is made difficult by the fact that both jet noise and combustion noise exhibit broadband spectra and peak in the same frequency range. Since in-flight reduction of jet noise is greater than that of combustion noise, the latter can be a major contributor to the in-flight noise of an aircraft but will be less evident, and more difficult to measure, under static conditions. Several methods for measuring the far-field combustion noise of aircraft engines are discussed in this paper. These methods make it possible to measure combustion noise levels even in situations where other noise sources, such as jet noise, dominate. Measured far-field combustion noise levels for several turbofan engines are presented. These levels were obtained using a method referred to as three-signal coherence, requiring that fluctuating pressures be measured at two locations within the engine core in addition to the far-field noise measurement. Cross-spectra are used to separate the far-field combustion noise from far-field noise due to other sources. Spectra and directivities are presented. Comparisons with existing combustion noise predictions are made. Author

N87-17481*# General Electric Co., Cincinnati, Ohio. Aircraft Engine Business Group.
SIMULATED FLIGHT ACOUSTIC INVESTIGATION OF TREATED EJECTOR EFFECTIVENESS ON ADVANCED MECHANICAL SUPPRESORS FOR HIGH VELOCITY JET NOISE REDUCTION Final Contractor Report
J. F. Brausch, R. E. Motsinger, and D. J. Hoerst Washington NASA Nov. 1986 413 p
(Contract NAS3-23275)
(NASA-CR-4019; E-3134; NAS 1.26:4019; R85AEB518) Avail: NTIS HC A18/MF A01 CSCL 20A

Ten scale-model nozzles were tested in an anechoic free-jet facility to evaluate the acoustic characteristics of a mechanically suppressed inverted-velocity-profile coannular nozzle with an accoustically treated ejector system. The nozzle system used was developed from aerodynamic flow lines evolved in a previous contract, defined to incorporate the restraints imposed by the aerodynamic performance requirements of an Advanced Supersonic Technology/Variable Cycle Engine system through all its mission phases. Accoustic data of 188 test points were obtained, 87 under static and 101 under simulated flight conditions. The tests investigated variables of hardwall ejector application to a coannular nozzle with 20-chute outer annular suppressor, ejector axial positioning, treatment application to ejector and plug surfaces, and treatment design. Laser velocimeter, shadowgraph photograph, aerodynamic static pressure, and temperature measurement were acquired on select models to yield diagnositc information regarding the flow field and aerodynamic performance characteristics of the nozzles. Author

N87-17482*# National Aeronautics and Space Administration. Langley Research Center, Hampton, Va.
NOISE PROPAGATION FROM A FOUR-ENGINE, PROPELLER-DRIVEN AIRPLANE
William L. Willshire, Jr. Feb. 1987 41 p
(NASA-TM-89035; L-16179; NAS 1.15:89035) Avail: NTIS HC A03/MF A01 CSCL 20A

A flight experiment was conducted to investigate the propagation of periodic low-frequency noise from a propeller-driven airplane. The test airplane was a large four-engine, propeller-driven airplane flown at altitudes from 15 to 500 m over the end of an 1800-m-long, 22-element microphone array. The acoustic data were reduced by a one-third octave-band analysis. The primary propagation quantities computed were lateral attenuation and ground effects, both of which become significant at shallow elevation angles. Scatter in the measured results largely obscured the physics of the low-frequency noise propagation. Variability of the noise source, up to 9.5 dB over a 2-sec interval, was the major contributor to the data scatter. The microphones mounted at ground level produced more consistent results with less scatter than those mounted 1.2 m above ground. The ground noise levels were found to be greater on the port side than on the starboard side. Author

N87-17483*# National Aeronautics and Space Administration. Langley Research Center, Hampton, Va.
AIRCRAFT NOISE SYNTHESIS SYSTEM
David A. McCurdy and Robert E. Grandle Feb. 1987 43 p
(NASA-TM-89040; L-16140; NAS 1.15:89040) Avail: NTIS HC A03/MF A01 CSCL 20A

A second-generation Aircraft Noise Synthesis System has been developed to provide test stimuli for studies of community annoyance to aircraft flyover noise. The computer-based system generates realistic, time-varying, audio simulations of aircraft flyover noise at a specified observer location on the ground. The synthesis takes into account the time-varying aircraft position relative to the observer; specified reference spectra consisting of broadband, narrowband, and pure-tone components; directivity patterns; Doppler shift; atmospheric effects; and ground effects. These parameters can be specified and controlled in such a way as to generate stimuli in which certain noise characteristics, such as duration or tonal content, are independently varied, while the remaining characteristics, such as broadband content, are held constant. The system can also generate simulations of the predicted noise characteristics of future aircraft. A description of the synthesis system and a discussion of the algorithms and methods used to generate the simulations are provided. An appendix describing the input data and providing user instructions is also included. Author

N87-17484*# Syracuse Univ., N. Y. Dept. of Mechanical and Aerospace Engineering.
AEROACOUSTICS OF SUPERSONIC JET FLOWS FROM CONTOURED AND SOLID/POROUS CONICAL PLUG-NOZZLES Final Report
Darshan S. Dosanjh and Indu S. Das Jan. 1987 187 p
(Grant NAG1-129)
(NASA-CR-178095; NAS 1.26:178095) Avail: NTIS HC A09/MF A01 CSCL 20A

The results of an experimental study of the acoustic far-field, the shock associated noise, and the nature of the repetitive shock structure of supersonic jet flows issuing from plug-nozzles having externally-expanded plugs with pointed termination operated at a range of supercritical pressure ratios Xi approaching 2 to 4.5 are reported. The plug of one of these plug-nozzles was contoured. The other plug-nozzles had short conical plugs with either a solid surface or a combination of solid/porous surface of different porosities. The contoured and the uncontoured plug-nozzles had the same throat area and the same annulus-radius ratio K = R sub p/R sub N = 0.43. As the result of modifications of the shock structure, the acoustic performance of improperly expanded jet flows of an externally-expanded short uncontoured plug of an appropriate geometry with suitably perforated plug and a pointed termination, is shown to approach the acoustic performance of a shock-free supersonic jet issuing from an equivalent externally-expanded contoured plug-nozzle. Author

72 ATOMIC AND MOLECULAR PHYSICS

Includes atomic structure, electron properties, and molecular spectra.

N87-17485# Los Alamos National Lab., N. Mex. Applied Theoretical Physics Div.

RECENT DEVELOPMENTS IN DISCRETE-ORDINATES ELECTRON TRANSPORT
J. E. Morel and L. J. Lorence, Jr. (Sandia National Labs., Albuquerque, N. Mex.) 1986 6 p Presented at the American Nuclear Society Annual Meeting, Reno, Nev., 15 Jun. 1986 Prepared in cooperation with Sandia National Labs., Albuquerque, NM.
(Contract DE-AC04-76DP-00789)
(DE86-007827; SAND-86-0335C; CONF-860610-24) Avail: NTIS HC A02/MF A01

The computational state-of-the-art for coupled electron-photon transport (CEPT) calculations is not as developed as that for neutron transport calculations. The only production codes currently available for CEPT calculations are condensed-history Monte Carlo codes such as ETRAN and the ITS codes. A deterministic capability for production calculations is clearly needed. In response to this need, the development of a production discrete-ordinates code for CEPT calculations is described. The purpose of this paper is to describe the basic approach which is being taken, discuss the current status of the project, and present some new computational results. DOE

N87-17486# Stockholm Univ. (Sweden). Inst. of Physics.
THE A-X AND B-X BAND SYSTEMS OF SrH: WAVENUMBERS AND MOLECULAR CONSTANTS
O. Appelblad, L. Klynning, and J. W. C. Johns (National Research Council of Canada, Ottawa, Ontario) Apr. 1986 24 p
(USIP-86-04; ETN-87-98904) Avail: NTIS HC A02/MF A01

Investigations of the A-X and B-X band systems of SrH were completed by Fourier transform spectroscopy. The wavenumbers of all the analyzed rotational lines of these systems are collected, and effective as well as deperturbed rotational constants are given. Since the ground state shows no irregularities, it can be represented by a simple energy expression. Under these circumstances it is advantageous to calculate the term values of the excited states simultaneously with the molecular constants of the ground state. The molecular constants obtained for the ground state using this method are given. ESA

73 NUCLEAR AND HIGH-ENERGY PHYSICS

Includes elementary and nuclear particles; and reactor theory.

For space radiation see *93 Space Radiation.*

N87-17487*# National Aeronautics and Space Administration. Langley Research Center, Hampton, Va.
DOUBLY DIFFERENTIAL CROSS SECTIONS FOR GALACTIC HEAVY-ION FRAGMENTATION
Francis A. Cucinotta (Old Dominion Univ., Norfolk, Va.), John W. Norbury, Govind S. Khandelwal, and Lawrence W. Townsend Feb. 1987 23 p
(NASA-TP-2659; L-16187; NAS 1.60:2659) Avail: NTIS HC A02/MF A01 CSCL 20H

An abrasion-ablation T-matrix formulation is applied to the calculation of double differential-cross sections in projectile fragmentation of 2.1 GeV/nucleon O-16 on Be-9 and 86 MeV/nucleon C-12 on C-12 and Ag-108. An exponential parameterization of the ablation T-matrix is used and the total width of the intermediate states is taken as a parameter. Fitted values of the total width to experimental results are used to predict the lifetime of the ablation stage and indicate a decay time on the order of 10 to the -19th power sec. Author

N87-17488# California Univ., Berkeley. Lawrence Berkeley Lab. Accelerator and Fusion Research Div.
FUTURE ACCELERATOR TECHNOLOGY
A. M. Sessler May 1986 10 p Presented at the 2nd Conference on Particle and Nuclear Physics, Lake Louise, Canada, 26 May 1986
(Contract DE-AC03-76SF-00098)
(DE86-013190; LBL-21536; CONF-860575-17) Avail: NTIS HC A02/MF A01

A general discussion is presented of the acceleration of particles. Upon this foundation is built a categorization scheme into which all accelerators can be placed. Special attention is devoted to accelerators which employ a wake-field mechanism and a restricting theorem is examined. It is shown how the theorem may be circumvented. Comments are made on various acceleration schemes. DOE

N87-17489# Lawrence Livermore National Lab., Calif.
EMPIRICAL CONSIDERATIONS FOR LASER GUIDED ELECTRON BEAMS IN THE ADVANCED TEST ACCELERATOR
F. Rainer, G. J. Caporaso, Y. P. Chong, E. J. Lauer, D. S. Prono, K. W. Struve, and J. T. Weir 1986 6 p Presented at the 6th International Conference on High Power Particle Beams, Kobe, Japan, 9 Jun. 1986
(Contract W-7405-eng-48)
(DE86-013218; UCRL-93752; CONF-860665-12) Avail: NTIS HC A02/MF A01

Relativistic electron beam currents in excess of 10 kA have been propagated successfully for 64 m through the Advanced Test Accelerator (ATA), and up to 31 m beyond that, by means of an electro-static column of benzene ions generated by a KrF laser pulse. The immediate consequence was a dramatic reduction in transverse rf beam displacements to less than 0.1 mm. The absence of any magnetic focusing or steering necessitated stringent controls on the pointing, focusing, spatial uniformity and temporal stability of the ionizing laser. The control and monitoring of a benzene pressure profile in a hostile radiation environment have been addressed but still require constant attention. The subtleties of matching the electron beam between ion columns and magnetic transport out of the injector, at bends in the beam line, and at other transition zones are not yet fully understood. The consequences of temporal, spatial, and angular mismatch impact the electron beam output rise time, pulse shape, pulse length, total current, energy spread and emittance. DOE

N87-17490# Brown Univ., Providence, R. I. Dept. of Physics.
RESEARCH PROGRAM IN THEORETICAL HIGH-ENERGY PHYSICS Task A Progress Report, Jan. 1 - 31 Dec. 1986
D. Feldman, H. M. Fried, A. Jevicki, K. Kang, and C. I. Tan 30 Jun. 1986 17 p
(Contract DE-AC02-76ER-03130)
(DE86-013326; DOE/ER-03130/379; BROWN/HET-586; COO-3130TA-379) Avail: NTIS HC A02/MF A01

This year's research has dealt with a side range of theoretical optics of current interest. New results include: an operator formulation of the covariant interacting string field theory of Witten the string and nonlinear sigma model connection; Kac-Moody and Virasoro algebras and their applications to string theories; compactified strings on group manifold as non-linear sigma models with Wess-Zumino terms and BRST quantization simplicial lattice formulation of gravity and strings; numerical studies of Polyakov strings and their Hausdorff dimensions; stability of vacuum energies for strings compactified on various tori; tests for topological features of string interactions for hadronic processes. Studies in strong coupling phenomena and the continuum description by the technique of infrared extraction, the structure of non-semisimple gauge theories and contracted gauge theories have been continued. Problems associated with the family structure of quarks and leptons, and the interface between cosmology and the grand unification of particle interactions have also been addressed: predictions on the fourth generation quarks; gauge model of fermion flavors and breaking patterns at axion scale; massive neutrinos and oscillations calculability problem in flavor mixings; axion emission for representative types of stars. DOE

N87-17491# Stanford Linear Accelerator Center, Calif.
UNIFIED FORMULATION FOR LINEAR ACCELERATOR DESIGN
Z. D. Farkas May 1986 7 p Presented at the Linear Accelerator Conference, Stanford, Calif., 2 Jun. 1986
(Contract DE-AC03-76SF-00515)
(DE86-013441; SLAC-PUB-3981; CONF-860629-25) Avail: NTIS HC A02/MF A01

Expressions for peak and average powers required to produce a given average gradient in an accelerator section are given. They are valid for both lossy and lossless (superconducting) sections, for both traveling wave and standing wave sections, and for pulsed or continuous wave rf input. The expressions are given in terms of structure parameters that are equally applicable to traveling wave or standing wave. These parameters delineate the effect of wall losses and energy required to build up the field. For both traveling wave and standing wave sections it is possible to make the rf pulse length short enough to make the wall losses negligible at the expense of increased peak power requirement. Therefore the expressions will include the effects of pulse compression. DOE

N87-17492# Edgerton, Germeshausen and Grier, Inc., Idaho Falls, Idaho.
ATHENA CODE MANUAL. VOLUME 1: CODE STRUCTURE, SYSTEM MODELS, AND SOLUTION METHODS
K. E. Carlson, P. A. Roth, and V. H. Ransom Sep. 1986 338 p
(Contract DE-AC07-76ID-01570)
(DE87-001430; EGG-RTH-7397-Vol-1) Avail: NTIS HC A15/MF A01

The ATHENA (Advanced Thermal Hydraulic Energy Network Analyzer) code has been developed to perform transient simulation of the thermal hydraulic systems which may be found in fusion reactors, space reactors, and other advanced systems. A generic modeling approach is utilized which permits as much of a particular system to be modeled as necessary. Control system and secondary system components are included to permit modeling of a complete facility. Several working fluids are available to be used in one or more interacting loops. Different loops may have different fluids with thermal connections between loops. The modeling theory and associated numerical schemes are documented in Volume 1 in order to acquaint the user with the modeling base and thus aid effective use of the code. The second volume contains detailed instructions for input data preparation. DOE

74 OPTICS

N87-17493*# National Aeronautics and Space Administration. Marshall Space Flight Center, Huntsville, Ala.
WELDING TORCH WITH ARC LIGHT REFLECTOR Patent
Stephen S. Gordon, inventor (to NASA) (Rockwell International Corp., Canoga Park, Calif.) Issued 30 Dec. 1986 5 p Filed 3 Oct. 1985 Supersedes N86-20130 (24 - 10, p 1670)
(NASA-Case-MFS-29134-1; US-Patent-4,633,060; US-Patent-Appl-SN-783890; US-Patent-Class-219-130.01; US-Patent-Class-219-124.34) Avail: U.S. Patent and Trademark Office CSCL 20F

A welding torch arc light reflector is disclosed for welding torches having optical viewing systems. A schematic of a welding torch having an internal coaxial viewing system consisting of a lens which focuses the field of view of the weld scene of the workpiece onto the end of the fiberoptic bundle is provided. The transmitted image of the fiberoptic bundle is provided to a camera lens which focuses it onto a TV sensor array for transmission. To improve the parity of the image of the monitoring system, an arc light reflector is shown fitted to the end of the torch housing or gas cup. The arc light reflector has an internal conical section portion which is polished to serve as a mirror which reflects the bright arc light back onto the darker areas of the weld area and thereby provides a more detailed image for the monitoring system. The novelty of the invention lies in the use of an arc light reflector on welding torches having optical viewing systems. NASA

N87-17494*# Arizona Univ., Tucson. Optical Sciences Center.
DYNAMIC ANALYSIS AND DESIGN OF THE SIRTF PRIMARY MIRROR MOUNT Final Report, Jun. 1985 - Sep. 1986
Ralph M. Richard, Daniel Vukobratovich, and L. Wayne Pollard 4 Mar. 1987 55 p
(Grant NAG2-220)
(NASA-CR-180158; NAS 1.26:180158) Avail: NTIS HC A04/MF A01 CSCL 20F

The criteria and considerations for the design of the support system for the Space Infrared Telescope Facility (SIRTF) primary mirror are presented. A flexural-gimbal-baseplate design for the 0.5 m primary mirror was developed. Preliminary studies have indicated that this design may be further improved by replacing the flexures by a post-gimbal system wherein the gimbal design accomodates both the cryogenic cool down effects, the dynamic launch loads, and manufacturing tolerance effects. Additionally, a prestressed baseplate concept had evolved and was presented for the full scale 1.0 m mirror. However, preliminary design studies indicate that this concept will not be required, and the post-gimbal-baseplate design similar to the 0.5 m alternate support system will meet the cryogenic cool down, dynamic launch load criteria, and manufacturing tolerance effects. Author

N87-17495# Department of the Air Force, Washington, D.C.
METAL FILM LIGHT MODULATOR Patent Application
Dietrich W. Langer, inventor (to Air Force) Filed 14 Jul. 1986 12 p
(AD-D012506; US-Patent-Appl-SN-885103) Avail: NTIS HC A02/MF A01 CSCL 20/6

An improved device for modulating the intensity of a light beam is described which comprises a first isoceles optical prism: a first dielectric layer, a thin metallic layer, and a second dielectric layer substantially identical in composition and thickness to the first dielectric layer deposited successively on the base of the first prism: a second isoceles optical prism disposed with the base thereof contacting the last deposited layer: and a controllable source of electrical current connected to the metallic layer for establishing and modulating an electromagnetic field at the respective surfaces of the metallic layer. GRA

N87-17496# Department of the Air Force, Washington, D.C.
HIGH INTENSITY SELECTABLE POLY OR MONOCHROMATIC SLIT LIGHT SOURCE APPARATUS FOR OPTICAL INSTRUMENTS Patent Application
Radames K. Gebel, inventor (to Air Force) Filed 8 Jul. 1986 16 p
(AD-D012507; US-Patent-Appl-SN-883222) Avail: NTIS HC A02/MF A01 CSCL 20/6

This patent application discloses an optical fiber apparatus for providing light to optical and other instruments from an auxiliary light source which may include a laser. The disclosed apparatus is a light source optically connected to a fiber optic bundle having its individual fibers aligned in the shape of a circle at its input end and in the shape of a rectangle at its output end. Ferrules hold, align and shape the optical fibers at both ends. The light source may be a pulsed or a continuous wave laser producing substantially monochromatic light. Another embodiment incorporates the new light source apparatus in a retinascope having a holder for supporting the output ferrule and the fiber optic bundle output. The holder may include means for adjusting both the linear and rotational position of the fiber optic bundle output end in relation to the retinascope head. The retinascope may include a filterholder for using narrow bandwidth filters, or filters selecting from a polychromatic light source any desired light color, to increase detail contrast when used with suitable broad spectrum bright light sources. Author (GRA)

N87-17497# University of Southern California, Los Angeles. Signal and Image Processing Inst.

NONLINEAR REAL-TIME OPTICAL SIGNAL PROCESSING
Annual Report, 1 Jul. 1984 - 30 Jun. 1985
A. A. Sawchuk and B. J. Jenkins 10 Jul. 1986 27 p
(Grant AF-AFOSR-0181-84)
(AD-A173119; AFOSR-86-0903TR) Avail: NTIS HC A03/MF A01 CSCL 20/6

During the period 1 July 1984 - 30 June 1985, the research under Grant AFOSR-84-0181 has concentrated on four major areas. First, work has continued on an experimental sequential optical binary parallel architecture that is constructed from an array of binary optical switching elements (NOR gates) with interconnections done by a computer-generated hologram. We are examining new binary array SLM's, high efficiency, high space-bandwidth product (SBWP) interconnection holograms, and compact reflection versions of the general architecture with the intent of building a larger demonstration system with great capabilities. Next, we have studied improved methods of providing the interconnections in these systems by the use of hybrid digital/analog (facet) holograms. We have examined analytical techniques for mapping circuit diagrams into gate locations and hologram arrays, and optimization procedures to determine the minimum set of necessary space-invariant basis functions and minimum set of space-variant indexing holograms. Another area of study has been the evaluation of devices and materials for high speed optical switching and bistability. Switching energies of 1 to 10 pJ and response times of 10 ns have been experimentally demonstrated at the University of Arizona for devices consisting of an array of Fabry-Perot cavities filled with a nonlinear material. We have begun to use the specifications of these devices and other high speed switching technologies in order to determine better designs and fundamental limits of the binary optical computing architectures under consideration. GRA

N87-17498# Washington State Univ., Pullman. Dept. of Physics.
LIGHT SCATTERING THEORY FOR BUBBLES IN WATER: INVERSE SCATTERING, COATED BUBBLES AND STATISTICS
Final Report, 1 Feb. - 30 Sep. 1986
Philip L. Marston 17 Nov. 1986 57 p
(Contract N00014-86-K-0242)
(AD-A174997) Avail: NTIS HC A04/MF A01 CSCL 20/6

Light scattering theory was applied to practical problems related to the detection and sizing of bubbles in ocean water. The emphasis of these calculations was on scattering from microbubbles illuminated by a Gaussian beam into angles close to the critical scattering angle (approximately 83 deg). This emphasis is appropriate for applications to an instrument being developed by NORDA. The specific problems include: (1) Computational analysis of the effects of surface films on the optical scattering properties of bubbles in water; (2) Physical optics approximation for the scattering from a coated bubble--explanation of the shift in the coarse structure and polarization effects; (3) Brewster-angle scattering from coated and uncoated bubbles: applications to measurement of film thickness and to the discrimination of bubbles from particles; (4) Detector placement and inversion of scattering data to obtain the bubble size on an event-by-event basis; and (5) Statistical properties of the photodetector voltages and a possible alternative to event-by-event data inversion. The event-by-event inversion procedure for obtaining the size of each bubble is discussed in an Appendix. Author (GRA)

N87-17499# Lawrence Livermore National Lab., Calif.
NANOSECOND TWO-DIMENSIONAL IMAGING USING TOMOGRAPHIC TECHNIQUES
H. A. Koehler and B. A. Jacoby 1986 20 p Presented at the 17th International Congress on High Speed Photography and Photonics, Pretoria, South Africa, 1 Sep. 1986
(Contract W-7405-eng-48)
(DE86-008164; UCRL-93185; CONF-860950-1) Avail: NTIS HC A02/MF A01

Several fast, single transient data imaging systems have been developed for time-resolved imaging of pulsed radiation sources. Both MCP intensified solid-state, two-dimensional framing cameras and streak cameras/solid-state camera systems are used. The streak camera system yields small, two-dimensional images with limited spatial resolution (less than or equal to 150 spatial points) and less than or equal to 0.5 nsec exposure. It is those streak camera systems developed at Lawrence Livermore National Laboratory that are used for obtaining time-resolved, tomographically reconstructed, two-dimensional images of electron and x-ray beams. DOE

N87-17500# California Univ., Berkeley. Lawrence Berkeley Lab.
REFLECTION GRATING SPECTROMETER FOR THE X-RAY MULTI-MIRROR (XMM) SPACE OBSERVATORY: DESIGN AND CALCULATED PERFORMANCE
M. C. Hettrick and S. M. Kahn Oct. 1985 14 p Presented at the 2nd International Technical Symposium on Optical and Electro-optical Applied Science and Engineering, Cannes, France, 25 Nov., 1985
(Contract DE-AC03-76SF-00098)
(DE86-013485; LBL-20466; CONF-8511123-5) Avail: NTIS HC A02/MF A01

A spectrometer design candidate is presented for the X-ray Multi-Mirror (XMM) observatory, being planned by the European Space Agency (ESA) as a long-lived large-area of telescopes. The science requirement of moderate resolution (E/E approx. 100) spectroscopy in a two octave region (0.5 to 2 keV) with extremely high throughput (effective area greater than 500 cm) results in the use of grazing incidence reflection gratings. Due to the low image quality of the telescopes (approx. 1 minute of arc), the grating dispersion must be maximized by use of the classical grating mount in which the spectrum is dispersed within the plane of incident radiation. Due to the small field of view by the x-ray telescopes, the gratings must be situated in the converging beam at the exit of the telescope. A spectrometer module consists of a thin-foil conical mirror telescope, a stack of plane varied-space reflection gratings and an imaging proportional counter. This system is analyzed on the basis of dispersion, geometric aberrations and efficiency. At a spectral resolution of 0.15 A, a twenty module XMM would attain an average effective area of approx. 900 cm, reaching twice this value at the peak wavelength (15 A). Similar throughput is obtained in second order centered at 7.5 A, the two spectral orders separated by the non-dispersive energy resolution of the proportional counter. DOE

N87-17501# Lawrence Livermore National Lab., Calif. Chemistry and Materials Science Dept.
OPTICAL THIN FILM MONITORING USING OPTICAL FIBERS
N. L. Thomas Oct. 1986 8 p Presented at the 30th SPIE Technical Symposium on Optics and Optoelectronic Engineering, San Diego, Calif., 17 Aug. 1986
(Contract W-7405-eng-48)
(DE87-001355; UCRL-94970; CONF-860880-34) Avail: NTIS HC A02/MF A01

A technique for monitoring optical thin film thickness by direct evaporation onto the end of an optical fiber is described. The optical fiber is suspended inside a coating chamber so that the fiber distal end faces the evaporation source and is illuminated with a chopped light source. The light which is reflected from the fiber end is returned through the fiber and is collected by a 45° mirror with a hole in it. The signal is detected and displayed on led displays and a chart recorder. Multiple fibers are used to monitor individual layers in a stack, or a single fiber is used after cleaving the end with a tool to produce a clean, flat, uncoated surface without breaking the vacuum. DOE

N87-17566# Paris VII Univ. (France).
ACTIVE OPTICS FOR THE FAR INFRARED SUBMILLIMETER WAVE SPACE TELESCOPE (FIRST): A HIGH ANGULAR RESOLUTION MODE
Pierre Lena *In* ESA Proceedings of an ESA Workshop on a Spaceborne Submillimeter Astronomy Mission. A Cornerstone of the ESA Long Term Science Program Aug. 1986 p 239-242
(For primary document see N87-17535 09-88)
Avail: NTIS HC A14/MF A01

75 PLASMA PHYSICS

Includes magnetohydrodynamics and plasma fusion.

For ionospheric plasmas see *46 Geophysics*. For space plasmas see *90 Astrophysics*.

N87-17502*# Smithsonian Astrophysical Observatory, Cambridge, Mass.
INVESTIGATION OF PLASMA CONTACTORS FOR USE WITH ORBITING WIRES Semiannual Report, 1 Jan. - 30 Jun. 1986
Robert D. Estes Feb. 1987 33 p
(Grant NAG9-126)
(NASA-CR-180154; NAS 1.26:180154; SAR-1) Avail: NTIS HC A03/MF A01 CSCL 20I

The results of a number of orbital simulations for a 300km orbital height and 28 degrees orbital inclination are included to emphasize the importance of the choice of the timing of the experiments. The bulk of the effort has gone into trying to determine the shape, size, and other optical properties of the plasma clouds that will be emitted by the hollow cathodes. B.G.

N87-17503# Nagoya Univ. (Japan). Inst. of Plasma Physics.
ANNUAL REVIEW, APRIL 1985 - MARCH 1986
[1986] 75 p
(ISSN-0547-1567) Avail: NTIS HC A04/MF A01

Topics addressed include: current systems; high energy beam experiment (SPAC-VII); Nagoya Bumpy Torus; radio frequency containment; inertial confinement; fusion engineering; basic studies; theory and computation; research information center; and the fusion and plasma diagnostic center. B.G.

N87-17504# Ceskoslovenska Akademie Ved, Prague. Inst. of Plasma Physics.
ON THE POSSIBLE ROLE OF THE BOOTSTRAP EFFECT IN THE RF CURRENT DRIVE EXPERIMENTS, PART 2
R. Klima and V. A. Petrzilka Dec. 1985 28 p
(IPPCZ-263) Avail: NTIS HC A03/MF A01

Conditions of existence of the bootstrap effect at anomalous diffusion in Tokamaks are dismissed. Assuming that these conditions are fulfilled at lower hybrid current drive, various models of anomalous diffusion and of temperature profiles are considered. Toroidal current density profiles and related quantities are calculated, demonstrating strong dependences on the electron temperature profiles and on the effective ion charge. Recommendations for experimental revealing the bootstrap current are presented. Author

N87-17505# Institute of Plasma Physics, Prague (Czechoslovakia).
INITIAL-VALUE PROBLEM FOR THE 1-D WAVE EQUATION IN AN INHOMOGENEOUS MEDIUM
Z. Sedlacek, J. A. Adam (Old Dominion Univ., Norfolk, Va.), and B. Roberts (Saint Andrew's Univ., Scotland) Mar. 1986 57 p Sponsored in part by the Science and Engineering Research Council of the United Kingdom
(IPPCZ-268) Avail: NTIS HC A04/MF A01

A complete mathematical analysis of oscillations of an inhomogeneous medium described by a wave equation with a space-dependent coefficient is given. The initial-value problem is solved both by the Laplace transform and by the normal-mode analysis and the equivalency of both approaches is demonstrated. The Green's function of the problem is a double-valued function of the complex frequency, analytic in the upper and lower halves of the complex frequency plane with a discontinuity on the whole real axis, corresponding to the continuous frequency spectrum of the physical system in question. The Green's function has complex poles on analytic continuation onto the unphysical sheet of its Riemann surface. This makes it possible, by inverting the Laplace transform, to interpret the solution of the initial value problem in terms of damped eigen modes. The continuum eigenmodes can be constructed directly and are also recovered by integrating the Green's function in the complex frequency plane along a closed contour enclosing the spectrum. The orthogonality and completeness is proved. The solution of the initial-value problem synthesized from the continuum eigenmodes can be interpreted in terms of travelling disturbances scattered by the inhomogeneity. B.G.

N87-17506# Institute of Plasma Physics, Prague (Czechoslovakia). Inst. of Plasma Physics.
PLASMA FORMATION AND SUSTAINMENT BY A MULTIJUNCTION GRILL ON THE CASTOR TOKAMAK
S. Nanobashvili, J. Datlov, J. Stoeckel, and F. Zacek Nov. 1985 19 p
(IPPCZ-255) Avail: NTIS HC A02/MF A01

Radio frequency (RF) power up to 40 kW, injected into the vacuum chamber of the CASTOR Tokamak by a multijunction grill, was used for plasma formation during the rampup phase of the toroidal magnetic field. When electron cyclotron resonance (ECR) appears inside the Tokamak chamber for given pumping frequency (f = 1.25 GHz) a plasma with density greater than 2 x 10 to the 18th power/cu m and temperature T sub e = 10 to 40 eV is produced. Plasma is sustained at some lower value of the density during the whole RF pulse. Simultaneously, a toroidal current up to approximately or equal to 0.2 kA is generated. The energy confinement time is estimated to be about 30 microsec during the ECR breakdown. Author

N87-17507# Nagoya Univ. (Japan). Inst. of Plasma Physics.
THE OPTIMUM CONDITION OF TPD-1 RECOMBINING HELIUM PLASMA FOR VUV COHERENT LASING ACTION
Utaro Furukane, Yasumasa Tsuji (Ehime Univ., Matsuyama, Japan), and Toshiatsu Oda (Hiroshima Univ., Japan) Nov. 1986 33 p
(IPPJ-798; ISSN-0469-4732) Avail: NTIS HC A03/MF A01

The optimum conditions of initial electron density and temperature, decay time, flow velocity, and plasma shape for the continuous VUV coherent laser oscillation are presented together with an explanation of the population inversion mechanism in the recombining plasma of TPD-1, which consists basically of two parts: the discharge region and the plasma column region with the axial magnetic field. According to calculations, the initial plasma of the extremely high temperature and density is not necessarily required for the continuous coherent VUV wavelength laser oscillation. The continuous coherent laser of wavelength 164 nm which corresponds to the transistion n = 3 yields 2 in H(+)(sub e) ion will be oscillated if the initial steady state extremely thin sheet plasma flow with the electron density of 1.28 x 10 to the 15th power to 1.25 to the 16th power/cu cm and with high speed of 2,000,000 cm/sec are cooled down to 0.2 eV with the decay time of 10 to the minus 7th to 10 to the minus 8th power sec. Author

N87-17508# Nagoya Univ. (Japan). Inst. of Plasma Physics.
RF PLUGGING AND TANDEM MIRROR EXPERIMENTS IN A CUSP-ANCHORED MIRROR DEVICE
T. Sato, R. Kumazawa, S. Okamura, K. Adati, T. Aoki, H. Fujita, S. Hidekuma, T. Kawamoto, H. Masumoto, K. Nishimura et al Nov. 1986 18 p Prepared in cooperation with Tokai Univ., Hiratsuka, Japan, Physics International Corp., San Francisco, Calif. and GA Technologies, Inc., San Diego, Calif.
(Contract DE-AT03-83SF-11713)
(IPPJ-800; ISSN-0469-4732) Avail: NTIS HC A02/MF A01

Three experimental topics are covered: an empirical scaling relation for the radio frequency (RF) plug potential (ponderomotive potential) is obtained and the maximum plug potential measured is 1kV; a negative potential mode produced with ICRF power only was discovered and its equilibrium was investigated; and the magnetohydrodynamic (MHD) stability condition in a cusp-anchored mirror plasma was obtained experimentally. Author

N87-17509# Nagoya Univ. (Japan). Inst. of Plasma Physics.
IMPLICIT PARTICLE SIMULATION OF ELECTROMAGNETIC PLASMA PHENOMENA
T. Kamimura, E. Montalvo (Texas Univ., Austin.), D. C. Barnes (Science Applications International Corp., Austin, Tex.), J. N. Leboeuf (Texas Univ., Austin.), and T. Tajima Nov. 1986 40 p
(IPPJ-799; ISSN-0469-4732) Avail: NTIS HC A03/MF A01

A direct method for the implicit particle simulation of electro-

magnetic phenomena in magnetized, multi-dimensional plasmas is developed. The method is second-order accurate for omega delta t is less than one, with omega a characteristic frequency and time step delta t. Direct time integration of the implicit equations with simplified space differencing allows the consistent inclusion of finite particle size. Decentered time differencing of the Lorentz force permits the efficient simulation of strongly magnetized plasmas. A Fourier-space iterative technique for solving the implicit field corrector equation, based on the separation of plasma responses perpendicular and parallel to the magnetic field and longitudinal and transverse to the wavevector, is described. Wave propagation properties in a uniform plasma are in excellent agreement with theoretical expectations. Applications to collisionless tearing and coalescence instabilities further demonstrate the usefullness of the algorithm. Author

N87-17510# Nagoya Univ. (Japan). Inst. of Plasma Physics.
TILT STABILITY OF FIELD-REVERSED CONFIGURATIONS
Akio Ishida (Niigata Univ., Japan) and Hiromu Momota Nov. 1986 19 p Sponsored by the Japanese Ministry of Education
(IPPJ-802; ISSN-0469-4732) Avail: NTIS HC A02/MF A01

By means of the two-fluid model in which the ion fluid is rigidly rotating with finite temperature and the electron fluid is at rest in equilibrium, the internal tilt stability of a field-reversed configuration (FRC) is studied theoretically. In contrast with previous theoretical studies, it is found that the elongated FRCs can be stabilized when both the elongation and scale factors are suitably chosen. Comparison of the present results with the experiments is made. Author

N87-17511# Nagoya Univ. (Japan). Inst. of Plasma Physics.
A SELF-CONSISTENT MODELING OF A QUASI-STEADY STATE COMPACT TORUS EVOLVING TO IGNITION
K. Hirano Nov. 1986 102 p
(IPPJ-801; ISSN-0469-4732) Avail: NTIS HC A06/MF A01

Self-consistent modeling shows Field-Reversed Configuration (FRC) has a strong possibility to be evolved into ignited state of advanced fuel cycle. Analyses were pursured using general basic equation sets describing an axisymmetric toroidal system under quasi-steady state, which were derived from moments of the Boltzmann equation to be applied to FRC and spheromak. Transient behaviors are studied by similarity solutions existing if plasma is heated up exclusively by injected beams. The key idea leading to simplify the analysis is in beam injection of different charge state in a counter way in order to cancel out the net beam current keeping the beam generated emf finite. Using the similarity solutions, we studied scenarios and requirements for FRC and spheromak to be evolved into ignited state. Author

N87-17512# Nagoya Univ. (Japan). Inst. of Plasma Physics.
ADVANCED FUELS IN A FIELD-REVERSED CONFIGURATION
Hiromu Momota, Masao Okamoto, Yasuyuki Nomura, Masami Ohnishi (Kyoto Univ., Japan),, Kiyoshi Yoshikawa, Herbert L. Berk (Texas Univ., Austin), Toshiki Tajima, Akio Ishida (Niigata Univ., Japan), Kunihiro Sato (Himeji Inst. of Tech., Japan), Shoichi Ohi (Osaka Univ., Japan) et al Nov. 1986 53 p Submitted for publication
(IPPJ-804; ISSN-0469-4732) Avail: NTIS HC A04/MF A01

The characteristics of fusion reactors using advanced fuel cycles are discussed. Among various deuteron-based fuel cycles, the importance of D-(sup 3)He is emphasized as the most efficient cycle with the least neutron fraction. In order to develop the D-(sup 3)He fusion reactor in a field-reversed configuration (FRC), some physics problems are considered in respect to FRC equilibrium, stability, steady maintenance, heating method, and physics of open plasmas. The feasibility and effectiveness of the plasma direct energy converters are also examined. Author

N87-17513# Nagoya Univ. (Japan). Inst. of Plasma Physics.
PHYSICS CONSIDERATIONS ON A FUSION PLASMA IN A FIELD-REVERSED CONFIGURATION
Hiromu Momota, Masao Okamoto, Yasuyuki Nomura, Kiyoshi Yoshikawa (Kyoto Univ., Japan), Masami Ohnishi, Akio Ishida (Niigata Univ., Japan), Kunihiro Sato (Himeji Inst. of Tech. (Japan).), Shoichi Ohi (Osaka Univ. (Japan).), Herbert L. Berk (Texas Univ., Austin), and Toshiki Tajima Nov. 1986 18 p
(IPPJ-803; ISSN-0469-4732) Avail: NTIS HC A02/MF A01

A Field-Reversed Configuration (FRC)/DD-(He-3) fusion device has the advantages of less neutron fraction and higher overall plant efficiency. Physics issues inherent in the FRC-DD-(He-3) fusion reactors are discussed, particularly, the achievement of ignited plasmas, current sustainment by fusion produced protons, and the stabilization of tilt modes by means of the plasma rotation. Author

N87-17514# Oxford Univ. (England). Dept. of Engineering Science.
AN ELECTROSTATIC PROBE TECHNIQUE FOR R.F. PLASMA
N. St. J. Braithwaite, N. M. P. Benjamin, and J. E. Allen 1986 13 p Sponsored by the Alvey Directorate (VLSI)
(OUEL-1637/86; ETN-87-98929) Avail: NTIS HC A02/MF A01

A technique in which the RF potential difference between probe and plasma is nulled out by externally driving the probe with synchronous RF of suitable phase and amplitude is demonstrated. An application of this technique to the measurement of electrical structure within a 13.56 MHz argon discharge is demonstrated. ESA

N87-17107# Joint Publications Research Service, Arlington, Va.
MODELING OF NONLINEAR EFFECTS OF PLASMA WAVE BEAMS ON IONOSPHERIC PLASMA Abstract Only
G. A. Markov, L. L. Popova, and Yu. V. Chugnov *In its* USSR Report: Earth Sciences (JPRS-UES-86-005) 7 May 1986 p 42-43 Transl. into ENGLISH from Pisma v Zhurnal Tekhnicheskoy Fiziki (Leningrad, USSR), v. 11, no. 23, Dec. 1985 p 1465-1469 (For primary document see N87-17096 09-42)
Avail: NTIS HC A05/MF A01

76 SOLID-STATE PHYSICS

Includes superconductivity.

For related information, see also *33 Electronics and Electrical Engineering* and *36 Lasers and Masers.*

N87-17515*# M/A-COM, Inc., Burlington, Mass.
THE 60 GHz IMPATT DIODE DEVELOPMENT Final Report, Mar. 1982 - Jul. 1986
Rovindra Dat, Murthy Ayyagari, David Hoag, David Sloat, Yogi Anand, and Stan Whitely Jul. 1986 174 p
(Contract NAS3-23339)
(NASA-CR-179536; NAS 1.26:179536) Avail: NTIS HC A08/MF A01 CSCL 20L

The objective is to develop 60 GHz IMPATT diodes suitable for communications applications. The performance goals of the 60 GHz IMPATT is 1W CW output power with a conversion efficiency of 15 percent and 10-year lifetime. The final design of the 60 GHz IMPATT structure evolved from computer simulations performed at the University of Michigan. The initial doping profile, involving a hybrid double-drift (HDD) design, was derived from a drift-diffusion model that used the static velocity-field characteristics for GaAs. Unfortunately, the model did not consider the effects of velocity undershoot and delay of the avalanche process due to energy relaxation. Consequently, the initial devices were oscillating at a much lower frequency than anticipated. With a revised simulation program that included the two effects given above, a second HDD profile was generated and was used as a basis for fabrication efforts. In the area of device fabrication, significant progress was made in epitaxial growth and characterization, wafer processing, and die assembly. The organo-metallic chemical vapor deposition (OMCVD) was used. Starting with a baseline X-Band IMPATT technology, appropriate processing steps were modified to satisfy the device requirements at V-Band. In terms of efficiency and reliability, the device requirements dictate a reduction in its series resistance and thermal resistance values. Qualitatively,

researchers were able to reduce the diodes' series resistance by reducing the thickness of the N+ GaAs substrate used in its fabrication. Author

N87-17516*# Continuum, Inc., Huntsville, Ala.
CRYSTAL GROWTH AND FURNACE ANALYSIS Final Report
Youssef M. Dakhoul 30 Jun. 1986 32 p
(Contract NAS8-35331)
(NASA-CR-178998; NAS 1.26:178998; CI-FR-0094) Avail: NTIS HC A03/MF A01 CSCL 20L

A thermal analysis of Hg/Cd/Te solidification in a Bridgman cell is made using Continuum's VAST code. The energy equation is solved in an axisymmetric, quasi-steady domain for both the molten and solid alloy regions. Alloy composition is calculated by a simplified one-dimensional model to estimate its effect on melt thermal conductivity and, consequently, on the temperature field within the cell. Solidification is assumed to occur at a fixed temperature of 979 K. Simplified boundary conditions are included to model both the radiant and conductive heat exchange between the furnace walls and the alloy. Calculations are performed to show how the steady-state isotherms are affected by: the hot and cold furnace temperatures, boundary condition parameters, and the growth rate which affects the calculated alloy's composition. The Advanced Automatic Directional Solidification Furnace (AADSF), developed by NASA, is also thermally analyzed using the CINDA code. The objective is to determine the performance and the overall power requirements for different furnace designs. Author

N87-17517# Royal Signals and Radar Establishment, Malvern (England).
APPLICATIONS OF FOCUSED ION BEAMS IN MICROELECTRONICS
C. Broughton, M. I. J. Beale, and V. G. I. Deshmukh Apr. 1986 49 p
(RSRE-MEMO-3948; BR100130; ETN-87-98911) Avail: NTIS

The design and performance of focused beam implanters and the viability of their application to semiconductor device fabrication are discussed. Applications in lithography, direct implantation, and micromachining are compared with existing techniques, emphasizing the relative throughputs. Results on a spot size measurement technique and the effect of beam heating on resist; and the results of studies into implantation passivation of resist to oxygen plasma attack as basis for a dry development lithography scheme are presented. A lithography system employing flood electron exposure from a photocathode which is patterned by a focused ion beam which can also be used to repair mask defects is described. ESA

N87-17518# Department of the Army, Washington, D. C.
DUAL CHANNEL HIGH ELECTRON MOBILITY FIELD EFFECT TRANSISTOR Patent Application
Gerald J. Iafrate, Louis E. Poli, Thomas R. AuCoin, and Linda S. Heath, inventors (to Army) Filed 18 Aug. 1986 42 p
(AD-D012474; US-Patent-Appl-SN-900128) Avail: NTIS HC A03/MF A01 CSCL 09/5

A multi-terminal Group III-V semiconductor high electron mobility field effect transistor comprised of a sandwich of molecular beam epitaxially grown layers and including two high mobility charge flow channels in respective two dimensional electron gas regions implemented, for example, by at least one doped layer of aluminum gallium arsenide adjacent an undoped gallium arsenide, layer separated by a heterojunctions. A pair of opposing two dimensional electron gas (2DEG) regions are generated in the layer of undoped gallium arsenide by the bending of the energy levels of the semiconductor materials. Charge flow occurs in a unidirectional fashion from one channel to the other in the common undoped gallium arsenide layer under the control of an electric field applied transversely through the structure by means of a top gate electrode and a bottom field plate electrode. Alternatively, the source voltage can be increased until the requisite amount of energy has been provided for the electrons to become hot enough to transfer from one channel to the other, in which cases a lower biasing contact is not required. GRA

N87-17519 Department of the Air Force, Washington, D.C.
TECHNIQUE FOR THE GROWTH OF COMPOSITIONALLY UNGRADED SINGLE CRYSTALS OF SOLID SOLUTIONS Patent
Robert C. Marshall, inventor (to Air Force), John K. Kennedy, inventor (to Air Force), and Charles S. Sahagian, inventor (to Air Force) 29 Jul. 1986 7 p Supersedes US-Patent-Appl-SN-731744
(AD-D012488; US-Patent-4,602,979; US-Patent-Appl-SN-731744; US-Patent-Class-156-617) Avail: US Patent and Trademark Office CSCL 20/2

This invention describes a modified method of growing high purity, compositionally ungraded, single crystals of multicomponent solid solutions by the Czochralski, Kyropoulos, Bridgman or other related melt growth techniques. In the method of this invention, the container or crucible used to contain the multicomponent crystal growing melt is fabricated from the higher melting point component of the multicomponent melt while lower melting point components are positioned within the crucible. The temperature of the crucible is then raised beyond the melting point of the lower melting point component to a temperature which is the exact melting point of the solid solution, or crystal alloy desired. This will dissolve an amount of the crucible material (higher melting point compenent) equal to the exact amount required to produce a solid solution having the desired composition. A seed is then introduced into the melt and normal crystal pulling is initiated resulting in the growth of a compositionally ungraded crystal having a uniform compositional content throughout its structure. Author (GRA)

N87-17520 Department of the Air Force, Washington, D.C.
LOW NOISE POLYCRYSTALLINE SEMICONDUCTOR RESISTORS BY HYDROGEN PASSIVATION Patent
Joseph Y. Lee, inventor (to Air Force), Michael H. Kriegel, inventor (to Air Force), and Thomas Y. Chuh, inventor (to Air Force) Issued 29 Jul. 1986 4 p Supersedes US-Patent-Appl-SN-726558
(AD-D012492; US-Patent-4,602,421; US-Patent-Appl-SN-726558; US-Patent-Class-29-576) Avail: US Patent and Trademark Office CSCL 20/12

The present invention is a process of fabricating low noise polycrystalline silicon resistors. This process includes steps to passivate the resistors to reduce the I/f noise which is routinely observed in prior art devices. As mentioned above, most theories suggest that the I/f noise originates in the interfaces where there are carrier traps. The process of the present invention includes a step to passivate these interfaces with hydrogen in a unique treatment which serves to demonstratably improve the I/f noise characteristics of polysilicon resistors. The low noise crystalline silicon resistors are fabricated in the following sequence: (1) deposit an appropriate thickness of polysilicon film on an oxidized wafer, (2) resistor doping of the polysilicon film by ion implantation, (3) heavy doping of the end-contact regions of the polysilicon film by high-dose ion implantation, (4) patterning the polysilicon resistor, (5) oxidation/annealing of the polysilicon resistor, (6) open contacts to the polysilicon resistor, (7) aluminum metallization to form ohmic contacts, and (8) a long (e.g., 3 hours) low temperature (e.g., at 375 C) pure hydrogen annealing to passivate the interface states in polysilicon resistors. GRA

N87-17521# Rockwell International Science Center, Thousand Oaks, Calif.
RESEARCH ON MILLIMETER WAVE DIELECTRIC MATERIALS Annual Report, 1 Mar. 1985 - 28 Feb. 1986
J. R. Oliver and R. R. Neurgaonkar Aug. 1986 79 p
(Contract N00014-81-C-0463)
(AD-A173017; SC5345.AR) Avail: NTIS HC A05/MF A01 CSCL 20/2

Much of the early effort in this program was devoted to single crystal strontium barium niobate (SBN), a tungsten bronze with an unusually large room-temperature dielectric response. More recently, other tungsten bronzes such as potassium lithium niobate (KLN) and barium strontium potassium sodium niobate (BSKNN) have been prepared and studied to elucidate the role of unfilled crystallographic sites in influencing dielectric loss. Currently, we

are developing preparation techniques for morphotropic phase boundary (MPB) bronzes, such as lead barium niobate (PBN), which should exhibit exceptionally large nonlinear electrical and optical response for a Pb:Ba ratio of 60:40, where it undergoes a transition from tetragonal to orthorhombic form. Large, high quality BSKNN single crystals have now been developed for free-space millimeter wave measurements. Measurements on BSKNN and SBN at room and cryogenic temperatures are reported, and a theoretical model has been successfully formulated for the dielectric response. Low frequency data are also presented for a new orthorhombic bronze, SCNN, which shows high suitability for millimeter wave development. GRA

N87-17522# Air Force Weapons Lab., Kirtland AFB, N. Mex.
THE EFFECT OF OPERATING FREQUENCY IN THE RADIATION INDUCED BUILDUP OF TRAPPED HOLES AND INTERFACE STATES IN MOS DEVICES Final Report, 3 Jul. 1984 - 15 Jun. 1985
Timothy D. Stanley Jul. 1986 110 p
(AD-A173097; AFWL-TR-86-12) Avail: NTIS HC A06/MF A01 CSCL 20/12

The threshold voltage shift in MOS devices caused by ionizing radiation is strongly dependent on the bias voltage applied to the gate of the MOS device both during and after the radiation. Past attempts found that n-channel MOSFETs alternately biased off and on did not have a threshold voltage shift that corresponded to the average bias, but the observed shift was more positive than the shift for either the continuously on or off bias conditions. Over 200 test transistors, built in a radiation hardened 4/3 micron process, were irradiated at various operating frequencies, temperatures and bias voltages in an effort to understand if the observed threshold voltage shifts were determined through subthreshold current measurements. The source of this anomalous alternating bias effect on the radiation response of MOS devices is reduced hole trapping and increased interface state buildup in n-channel MOS devices. In p-channel devices, reduced hole trapping is the primary source of this effect which results when holes, trapped at the oxide-silicon interface during the on half of the cycle, are annihilated by radiation-produced electrons pulled into the trapped hole space charged during the off bias portion of the cycle. GRA

N87-17523# Aerospace Corp., El Segundo, Calif. Chemistry and Physics Lab.
INTERFACIAL STRUCTURE OF In/Pt/GaAs HETEROJUNCTION OHMIC CONTACTS
Dean C. Marvin, Neil A. Ives, and Martin S. Leung 30 Sep. 1986 18 p
(Contract F04701-85-C-0086)
(AD-A175102; TR-0086(6945-09)-2; SD-TR-86-59) Avail: NTIS HC A02/MF A01 CSCL 20/12

Graded heterojunction InGaAs ohmic contracts to n-GaAs have been prepared which show improved electrical and morphological properties compared with other diffused contacts. The improvements result primarily from the use of a thin (400 A) Pt layer between the 4000-A In layer and the substrate to control the reaction of the In and the GaAs. A study of chemically etched samples using energy dispersive X-ray (EDX) analysis has revealed the formation of a smooth In(x)Ga(1-x)As heterojunction interface. GRA

N87-17524# Sandia National Labs., Albuquerque, N. Mex.
PERFORMANCE OF POLYSILICON GATE CMOS DEVICES IN SPACE AND SDI ENVIRONMENTS
J. R. Schwank, F. W. Sexton, P. S. Winokur, D. M. Fleetwood, and P. V. Dressendorfer Apr. 1986 3 p Presented at the Space Electronics Conference, Albuquerque, N. Mex., 9 Sep. 1986
(Contract DE-AC04-76DP-00789)
(DE86-009025; SAND-86-0845C; CONF-860966-1) Avail: NTIS HC A02/MF A01

The purpose of this work is to investigate the radiation response of state-of-the-art hardened polysilicon gate CMOS devices in space and SDI environments. To simulate the different radiation evnironments both very high and very low dose rate sources will be used. The results will be examined from the basic mechanisms involved which will be correlated to device functionality. In addition, we also will examine the radiation responses of devices exposed to large, short duration pulses after having been previously irradiated at much lower dose rates. DOE

N87-17525# Societe de Fabrication d'Instruments de Mesure, Massy (France).
HIGH VOLTAGE SEMICONDUCTORS FOR INERTIAL SENSORS Final Report [SEMI-CONDUCTEURS HAUTE TENSION POUR SENSEURS INERTIELS]
23 Dec. 1985 18 p In FRENCH
(Contract DRET-84-411)
(SFIM-13293-CP/LS; ETN-87-98810) Avail: NTIS HC A02/MF A01

High voltage, low current MOS transistors (channel N and channel P) were designed in order to realize high voltage amplifiers with low consumption for the control of electrostatic gyroscope motors. The characteristics of the realized amplifiers are very close to the desired ones; the feasibility of a pair of MOS transistors to obtain this result is demonstrated. Three points remain to be improved, the drain-source breakdown voltage, the drain-source leakage current, and the transconductance. The reasons for these deficiencies are known, and proposals for improvements are given. ESA

77 THERMODYNAMICS AND STATISTICAL PHYSICS

Includes quantum mechanics; theoretical physics; and Bose and Fermi statistics.

For related information see also *25 Inorganic and Physical Chemistry* and *34 Fluid Mechanics and Heat Transfer.*

No abstracts in this category.

80 SOCIAL SCIENCES (GENERAL)

Includes educational matters.

N87-17526*# George Washington Univ., Hampton, Va. Joint Inst. for Advancement of Flight Sciences.
FLIGHT-VEHICLE STRUCTURES EDUCATION IN THE US: ASSESSMENT AND RECOMMENDATIONS
Ahmed K. Noor Washington NASA Feb. 1987 89 p
(Grant NGR09-010-078)
(NASA-CR-4048; NAS 1.26:4048) Avail: NTIS HC A05/MF A01 CSCL 05I

An assessment is made of the technical contents of flight-vehicle structures curricula at 41 U.S. universities with accredited aerospace engineering programs. The assessment is based on the technical needs for new and projected aeronautical and space systems as well as on the likely characteristics of the aerospace engineering work environment. A number of deficiencies and areas of concern are identified and recommendations are presented for enhancing the effectiveness of flight-vehicle structures education. A number of government supported programs that can help aerospace engineering education are listed in the appendix. Author

81 ADMINISTRATION AND MANAGEMENT

Includes management planning and research.

N87-17527# Army Engineer School, Fort Belvoir, Va. Inst. for Water Resources.

COLLABORATIVE PROBLEM SOLVING FOR INSTALLATION PLANNING AND DECISION MAKING
C. M. Dunning Sep. 1986 90 p
(AD-A174611; IWR-86-R-6) Avail: NTIS HC A05/MF A01 CSCL 05/1

This manual introduces collaborative problem solving (CPS) as a method of accomplishing installation planning tasks. CPS is a process in which those with a stake in the outcome of a decision participate in a search for solutions which all can support. The manual describes the general principles involved in CPS, and presents the steps involved in designing and conducting the CPS meetings at installations. GRA

82 DOCUMENTATION AND INFORMATION SCIENCE

Includes information management; information storage and retrieval technology; technical writing; graphic arts; and micrography.

For computer documentation see *61 Computer Programming and Software.*

N87-17528*# Jet Propulsion Lab., California Inst. of Tech., Pasadena.
VIBROACOUSTIC PAYLOAD ENVIRONMENT PREDICTION SYSTEM (VAPEPS): DATA BASE MANAGEMENT CENTER REMOTE ACCESS GUIDE
V. C. Thomas 15 Sep. 1986 50 p
(Contract NAS7-918)
(NASA-CR-180132; JPL-Pub-86-39; NAS 1.26:180132) Avail: NTIS HC A03/MF A01 CSCL 05B

A Vibroacoustic Data Base Management Center has been established at the Jet Propulsion Laboratory (JPL). The center utilizes the Vibroacoustic Payload Environment Prediction System (VAPEPS) software package to manage a data base of shuttle and expendable launch vehicle flight and ground test data. Remote terminal access over telephone lines to a dedicated VAPEPS computer system has been established to provide the payload community a convenient means of querying the global VAPEPS data base. This guide describes the functions of the JPL Data Base Management Center and contains instructions for utilizing the resources of the center. Author

N87-17529*# Massachusetts Inst. of Tech., Cambridge. Dept. of Aeronautics and Astronautics.
A RESEARCH PROGRAM IN ADVANCED INFORMATION SYSTEMS Final Report
Wallace E. VanderVelde 12 Feb. 1987 22 p
(Grant NAGw-448)
(NASA-CR-180150; NAS 1.26:180150) Avail: NTIS HC A02/MF A01 CSCL 05B

Topics addressed cover: identification of large space structure dynamics; special-purpose architectures for computational fluid dynamics; fault-tolerant processor architectures; data flow techniques; software specification and verification tools; management of software development; software environment for concurrent computing; and parallel algorithms and architectures for the solution of partial differential equations. B.G.

N87-17530*# National Aeronautics and Space Administration, Washington, D.C.
NASA THESAURUS SUPPLEMENT (SUPPLEMENT 2)
Jan. 1987 186 p
(NASA-SP-7053(Supp-2); NAS 1.21:7053(Supp-2)) Avail: NTIS HC A09 CSCL 05B

The four part cumulative NASA Thesaurus Supplement to the 1985 edition of the NASA Thesaurus includes Part 1, Hierarchical Listing, Part 2, Access Vocabulary, Part 3, NASA Thesaurus Definitions, and Part 4, Changes. The semiannual supplement gives complete hierarchies for new terms. Author

N87-17531*# National Aeronautics and Space Administration. Langley Research Center, Hampton, Va.
SCIENTIFIC AND TECHNICAL INFORMATION OUTPUT OF THE LANGLEY RESEARCH CENTER FOR CALENDAR YEAR 1986
Jan. 1987 265 p
(NASA-TM-89065; NAS 1.15:89065) Avail: NTIS HC A12/MF A01 CSCL 05B

This document is a compilation of the scientific and technical information that the Langley Research Center has produced during the calendar year 1986. Included are citations for Formal Reports, Quick-Release Technical Memorandums, Contractor Reports, Journal Articles and Other Publications, Meeting Presentations, Technical Talks, Computer Programs, Tech Briefs, and Patents. Author

N87-17532*# National Aeronautics and Space Administration. Marshall Space Flight Center, Huntsville, Ala.
FY 1986 SCIENTIFIC AND TECHNICAL REPORTS, ARTICLES, PAPERS AND PRESENTATIONS
Joyce E. Turner, comp. Oct. 1986 72 p
(NASA-TM-86575; NAS 1.15:86575) Avail: NTIS HC A04/MF A01 CSCL 05B

Formal NASA technical reports, papers published in technical journals, and presentations by Marshall Space Flight Center (MSFC) personnel in FY-86 are presented. Also included are papers of MSFC contractors. Author

N87-17533# Carnegie-Mellon Univ., Pittsburgh, Pa. Dept. of Computer Science.
INFORMATION PROCESSING RESEARCH Final Report, Jan. 1981 - Dec. 1984
Eugene Ball, Jon Bentley, Nico Habermann, Peter Hibbard, and Takeo Kanade Sep. 1986 135 p
(Contract F33615-81-K-1539)
(AD-A173028; AFWAL-TR-86-1011) Avail: NTIS HC A07/MF A01 CSCL 09/2

This report documents DARPA-supported basic research in Carnegie-Mellon University's Computer Science Department during the period 1 January 1981 through December 1983, extended to 31 December 1984. Each chapter discusses one of seven major research areas. Sections within a chapter present the area's general context, the specific problems addressed, our contributions and their significance, and an annotated bibliography. GRA

N87-17176# Software Sciences Ltd., Farnborough (England).
THE DESIGN OF AN INTERNATIONAL DATA CENTRE FOR REMOTE SENSING
D. R. Sloggett *In* ESA Proceedings of the 1986 International Geoscience and Remote Sensing Symposium (IGARSS '86) on Remote Sensing: Today's Solutions for Tomorrow's Information Needs, Volume 1 Aug. 1986 p 67-71 (For primary document see N87-17163 09-43)
Avail: NTIS HC A99/MF E03; ESA, Paris, France, 3 volume set $90 Member States, AU, CN, and NO (+20% others)

N87-17230# Marconi Co. Ltd., Chelmsford (England).
THE UK ERS DATA CENTRE, AN OFFLINE PROCESSING AND ARCHIVING FACILITY
N. J. Veck, P. N. Churchill (Hunting Technical Services Ltd., Borehamwood, England), S. Campbell (Software Sciences Ltd., Farnborough, England), and C. Evans (Smith Associates Ltd., Guildford, England) *In* ESA Proceedings of the 1986 International Geoscience and Remote Sensing Symposium (IGARSS '86) on Remote Sensing: Today's Solutions for Tomorrow's Information Needs, Volume 1 Aug. 1986 p 411-415 Sponsored by RAE (For primary document see N87-17163 09-43)
Avail: NTIS HC A99/MF E03; ESA, Paris, France, 3 volume set $90 Member States, AU, CN, and NO (+20% others)

83 ECONOMICS AND COST ANALYSIS

Includes cost effectiveness studies.

N87-17534# Technische Hogeschool Twente, Enschede (Netherlands). Dept. of Applied Mathematics.
ADVANTAGEOUS SYNDICATES IN A BILATERAL MARKET GAME: THE CASE OF THE tau-VALUE
T. S. H. Driessen Aug. 1986 18 p
(MEMO-583; ISSN-0169-2690; ETN-87-99062) Avail: NTIS HC A02/MF A01

An exchange economy consisting of five traders of two types and of two completely complementary commodities is modelled as a bilateral market game. The behavior of the solution tau-value for this market game, when a syndicate is formed by some traders is studied. It is shown that the involved syndications lead to a higher payoff for the syndicated traders according to the tau-value. A comparison with results according to the nucleolus and the Shapley value is also given. ESA

84 LAW, POLITICAL SCIENCE AND SPACE POLICY

Includes NASA appropriation hearings; aviation law; space law and policy; international law; international cooperation; and patent policy.

No abstracts in this category.

85 URBAN TECHNOLOGY AND TRANSPORTATION

Includes applications of space technology to urban problems; technology transfer; technology assessment; and surface and mass transportation.

For related information see also *03 Air Transportation and Safety, 16 Space Transportation,* and *44 Energy Production and Conversion.*

N87-17170# Florida International Univ., Miami. Dept. of International Business.
THE TRANSFER OF REMOTE SENSING TECHNOLOGY TO DEVELOPING COUNTRIES: A SURVEY OF EXPERTS IN THE FIELD
C. Specter *In* ESA Proceedings of the 1986 International Geoscience and Remote Sensing Symposium (IGARSS '86) on Remote Sensing: Today's Solutions for Tomorrow's Information Needs, Volume 1 Aug. 1986 p 41-44 (For primary document see N87-17163 09-43)
Avail: NTIS HC A99/MF E03; ESA, Paris, France, 3 volume set $90 Member States, AU, CN, and NO (+20% others)

N87-17175# Instituto de Pesquisas Espaciais, Sao Paulo (Brazil).
ENVIRONMENTAL MODIFICATION OF METROPOLITAN AREAS THROUGH SATELLITE IMAGES: STUDY OF URBAN DESIGN IN THE TROPICS
M. A. Lombardo *In* ESA Proceedings of the 1986 International Geoscience and Remote Sensing Symposium (IGARSS '86) on Remote Sensing: Today's Solutions for Tomorrow's Information Needs, Volume 1 Aug. 1986 p 63-65 (For primary document see N87-17163 09-43)
Avail: NTIS HC A99/MF E03; ESA, Paris, France, 3 volume set $90 Member States, AU, CN, and NO (+20% others)

88 SPACE SCIENCES (GENERAL)

N87-17535# European Space Agency, Paris (France).
PROCEEDINGS OF AN ESA WORKSHOP ON A SPACEBORNE SUBMILLIMETER ASTRONOMY MISSION. A CORNERSTONE OF THE ESA LONG TERM SCIENCE PROGRAM
Norman Longdon, ed. Aug. 1986 315 p Workshop held in Segovia, Spain, 4-7 Jun. 1986
(ESA-SP-260; ISSN-0379-6566; ETN-87-98834) Avail: NTIS HC A14/MF A01

The concept of a submillimeter space observatory for spectroscopy, imaging, and photometry was discussed. The physics of the interstellar medium; star formation; cosmology; and properties of the primitive solar system revealed through molecular studies of comets were considered. Scientific and technological aspects of the mission were addressed. For individual titles, see N87-17536 through N87-17574.

N87-17536# Royal Observatory, Edinburgh (Scotland).
STATUS OF OBSERVATIONAL ASTRONOMY IN THE 1990'S: POSITION OF SUBMILLIMETRE ASTRONOMY **c89**
M. S. Longair *In* ESA Proceedings of an ESA Workshop on a Spaceborne Submillimeter Astronomy Mission. A Cornerstone of the ESA Long Term Science Program Aug. 1986 p 7-14 (For primary document see N87-17535 09-88)
Avail: NTIS HC A14/MF A01

The status of observational astronomy in the 1990s is surveyed on the basis of the proposed programs of national and international agencies. The multidisciplinary nature of all contemporary astronomy is emphasised. The unique features of submillimeter astronomy from space are described, and examples of important programs are outlined. ESA

N87-17537# Groningen Rijksuniversiteit (Netherlands). Lab. for Space Research.
REVIEW OF COHERENT AND INCOHERENT DETECTION TECHNIQUES: OUTLOOK AND LIMITATION **c89**
Thijs deGraauw *In* ESA Proceedings of an ESA Workshop on a Spaceborne Submillimeter Astronomy Mission. A Cornerstone of the ESA Long Term Science Program Aug. 1986 p 15-24 (For primary document see N87-17535 09-88)
Avail: NTIS HC A14/MF A01

The ESA Far Infrared and Submillimeter Space Telescope (FIRST) model payload is described. The frequency/wavelength coverage versus spectral resolution capabilities of FIRST submillimeter heterodyne receivers, a short wavelength spectrometer, and multiband array photometer are shown. At 1hr intervals, photometric and infrared spectroscopic sensitivities are 1mJy and 100 mJy respectively. For heterodyne spectroscopy, Tsyst = (Frequency in Ghz) x K. ESA

N87-17538# United Kingdom Infrared Telescope Unit, Hilo, Hawaii.
OBSERVATIONS OF ACTIVE GALACTIC NUCLEI WITH FIRST **c89**
Malcom G. Smith *In* ESA Proceedings of an ESA Workshop on a Spaceborne Submillimeter Astronomy Mission. A Cornerstone of the ESA Long Term Science Program Aug. 1986 p 25-31 (For primary document see N87-17535 09-88)
Avail: NTIS HC A14/MF A01

Research on active galaxies, quasars, and BL Lac objects is reviewed. Areas where the high sensitivity and spatial resolution offered by the submillimeter astronomy satellite, FIRST, will be of particular advantage are highlighted. ESA

N87-17539# Rome Univ. (Italy). Dipt. di Fisica.
THE EARLY UNIVERSE **c90**
Franchesco Melchiorri, G. DallOglio, P. deBernardis, N. Mandolesi, Silvia Masi, G. Moreno, B. Olivo, and G. Pucacco *In* ESA Proceedings of an ESA Workshop on a Spaceborne Submillimeter Astronomy Mission. A Cornerstone of the ESA Long Term Science Program Aug. 1986 p 33-52 (For primary document see N87-17535

09-88)
Avail: NTIS HC A14/MF A01

Theories concerning the birth and the evolution of the Universe and its structures are reviewed. Relations between the properties of the 2.7 K blackbody radiation and the structures of the early Universe are discussed. The possibility of observing the 2.7 K anisotropies by ground based, balloon-borne, and satellite experiments is considered. ESA

N87-17540# Observatoire de Paris-Meudon (France).
A STUDY OF PLANETARY ATMOSPHERES IN THE SUBMILLIMETRIC RANGE **c91**
Emmanuel Lellouch and Therese Encrenaz *In* ESA Proceedings of an ESA Workshop on a Spaceborne Submillimeter Astronomy Mission. A Cornerstone of the ESA Long Term Science Program Aug. 1986 p 53-55 (For primary document see N87-17535 09-88)
Avail: NTIS HC A14/MF A01

The submillimeter spectra of planetary atmospheres are reviewed to define atmospheric parameters that could be extracted from observations with the ESA Far Infrared Submillimeter Space Telescope (FIRST) facility. A feasibility study shows that each of the three focal instruments planned on FIRST could provide useful information: the imaging photometer could allow measurements of He/H2 ratio in the 4 giant planets, the high resolution spectrometer could give access to vertical distribution of a number of minor atmospheric species and allow detection of new molecules in the atmosphere of the giant planets. The superheterodyne instrument would be of great interest for the study of Titan's atmosphere. ESA

N87-17541# Observatoire de Paris-Meudon (France).
SUBMILLIMETER COMETARY SPECTROSCOPY **c90**
J. Crovisier *In* ESA Proceedings of an ESA Workshop on a Spaceborne Submillimeter Astronomy Mission. A Cornerstone of the ESA Long Term Science Program Aug. 1986 p 57-65 (For primary document see N87-17535 09-88)
Avail: NTIS HC A14/MF A01

Observations and theoretical works concerning cometary molecules relevant to submillimeter spectroscopy are reviewed. The study of the rotational lines of water, the prevailing cometary volatile molecule is discussed. Its I10-I01 line at 557 GHz may be observable even in small comets. It is shown that the high spectroscopic resolution achieved by heterodyne techniques is adequate to the study of the kinematics of cometary atmosphere. ESA

N87-17542# Air Force Geophysics Lab., Hanscom AFB, Mass.
INTERPLANETARY DUST **c90**
Stephen D. Price *In* ESA Proceedings of an ESA Workshop on a Spaceborne Submillimeter Astronomy Mission. A Cornerstone of the ESA Long Term Science Program Aug. 1986 p 67-72 (For primary document see N87-17535 09-88)
Avail: NTIS HC A14/MF A01

Visual and infrared observations which reveal the complex geometry of the zodiacal dust cloud are reviewed. The plane of symmetry is probably warped and coincides with neither the ecliptic nor invariable plane. The albedo of the dust particles is small, 0.1, although the dust responsible for reflected sunlight may have different properties from that giving rise to the infrared. Infrared observations which support both an asteroidal and cometary origin for the dust are discussed, and observations to resolve this issue by large telescopes in space are suggested. ESA

N87-17543# Observatoire de Marseille (France).
THE INTERSTELLAR MEDIUM AT SUBMM WAVELENGTHS **c90**
James Lequeux *In* ESA Proceedings of an ESA Workshop on a Spaceborne Submillimeter Astronomy Mission. A Cornerstone of the ESA Long Term Science Program Aug. 1986 p 73-78 (For primary document see N87-17535 09-88)
Avail: NTIS HC A14/MF A01

The components of emission/absorption of the interstellar medium at submillimeter wavelengths: dust, lines from HII regions, and molecular and atomic lines from HI regions are discussed. The use of the fine-structure lines to study the cold interstellar clouds is reviewed. ESA

N87-17544# University Coll., London (England). Dept. of Physics.
SUBMILLIMETRE WAVELENGTH STUDIES OF PROTOSTARS: THE ROLE OF FIRST **c89**
Glenn J. White *In* ESA Proceedings of an ESA Workshop on a Spaceborne Submillimeter Astronomy Mission. A Cornerstone of the ESA Long Term Science Program Aug. 1986 p 79-91 (For primary document see N87-17535 09-88)
Avail: NTIS HC A14/MF A01

The characteristics of protostellar forming regions are examined based on millimeter and submillimeter wavelength observational studies. From consideration of the likely excitation conditions of the material in these regions, the role which FIRST will play in the characterization of their physical environment is discussed. Constraints on the design of the FIRST payload based on the astrophysical objectives envisaged for studies of protostellar forming regions are suggested. ESA

N87-17545# Max-Planck-Inst. fuer Radioastronomie, Bonn (West Germany).
INTERSTELLAR DUST **c90**
E. Kruegel *In* ESA Proceedings of an ESA Workshop on a Spaceborne Submillimeter Astronomy Mission. A Cornerstone of the ESA Long Term Science Program Aug. 1986 p 93-99 (For primary document see N87-17535 09-88)
Avail: NTIS HC A14/MF A01

Interstellar dust models are reviewed, emphasizing inadequate knowledge of grain properties at submillimeter wavelengths. The relevance of submillimeter continuum measurements is illustrated by discussing the determination of cloud masses, the derivation of matter distribution in star forming regions, and the search for protostars. The benefits excepted from measurements with the ESA Far Infrared Submillimeter Space Telescope are indicated. Ways in which continuum data can complement the analysis of spectroscopic measurements are considered. ESA

N87-17546# California Inst. of Tech., Pasadena.
EXCITATION AND TRANSFER OF SUBMILLIMETER MOLECULAR TRANSITIONS **c90**
T. G. Philips *In* ESA Proceedings of an ESA Workshop on a Spaceborne Submillimeter Astronomy Mission. A Cornerstone of the ESA Long Term Science Program Aug. 1986 p 101-106 (For primary document see N87-17535 09-88)
Avail: NTIS HC A14/MF A01

Excitation and radiation transport processes for typical observing situations in the submillimeter astronomy of molecules are discussed. Examples of linear molecules, such as Co and HD and more complex molecules, H2O and CH3CN are used. The increased interaction between dust and molecular excitation as compared with the situation in the millimeter band is emphasized. ESA

N87-17547# Harvard-Smithsonian Center for Astrophysics, Cambridge, Mass.
INTERSTELLAR CHEMISTRY AND SUBMILLIMETER OBSERVATIONS **c90**
Ewine F. vanDishoeck *In* ESA Proceedings of an ESA Workshop on a Spaceborne Submillimeter Astronomy Mission. A Cornerstone of the ESA Long Term Science Program Aug. 1986 p 107-117 (For primary document see N87-17535 09-88)
Avail: NTIS HC A14/MF A01

The study of diffuse, dense and shocked interstellar cloud chemical processes is discussed. Observational and theoretical developments are described. Important future observations, in particular those at submillimeter wavelengths, are pointed out. ESA

N87-17548# Chalmers Univ. of Technology, Goeteborg (Sweden). Astrophysics Section.

CIRCUMSTELLAR ENVELOPES AROUND EVOLVED STARS c90

Peter Wannier *In* ESA Proceedings of an ESA Workshop on a Spaceborne Submillimeter Astronomy Mission. A Cornerstone of the ESA Long Term Science Program Aug. 1986 p 119-127 (For primary document see N87-17535 09-88)
Avail: NTIS HC A14/MF A01

The composition of circumstellar envelopes, and their observation by the ESA Far Infrared Submillimeter Wave Space Telescope (FIRST) are discussed. Circumstellar shells are ideally suited to submillimeter or far infrared wavelengths, where emission lines and dust emission are very strong. With FIRST, spatial mapping should be possible in many objects, providing information complementary to that available from existing techniques. It will probe radii of 10 to the 15th to 17th power cm, distant for near infrared techniques but close for millimeter observations. Requirements placed on the FIRST mission by such observations include high spectral resolution, large aperture size and long mission duration. Examples of infrared and (sub)millimeter results which demonstrate convincingly the potential for such observations are reviewed. ESA

N87-17549# Grenoble Univ. (France).
MOLECULAR ABUNDANCES IN CIRCUMSTELLAR ENVELOPES c90

A. Omont *In* ESA Proceedings of an ESA Workshop on a Spaceborne Submillimeter Astronomy Mission. A Cornerstone of the ESA Long Term Science Program Aug. 1986 p 129-133 (For primary document see N87-17535 09-88)
Avail: NTIS HC A14/MF A01

About 30 molecules were identified in extended massive circumstellar envelopes of late type stars from millimeter and infrared observations. Their abundances contain important clues on nucleosynthesis and evolution of the stars, and physical and chemical conditions in different types of envelopes. The main chemical processes are reviewed. Submillimeter astronomy will explore the unknown behavior of basic species throughout the whole envelopes, as well as the detailed composition of the relatively warm intermediate layers. ESA

N87-17550# European Space Agency. European Space Research and Technology Center, ESTEC, Noordwijk (Netherlands). Space Science Div.
FAR INFRARED SUBMILLIMETER WAVE SPACE TELESCOPE (FIRST) OBSERVATIONS OF STARS WITH LARGE MASS LOSS RATES c89

J. Herman *In its* Proceedings of an ESA Workshop on a Spaceborne Submillimeter Astronomy Mission. A Cornerstone of the ESA Long Term Science Program Aug. 1986 p 135-138 (For primary document see N87-17535 09-88)
Avail: NTIS HC A14/MF A01

Continuum observations by FIRST of stars in the far infrared and submillimeter region to determine dust properties and mass loss rates are discussed. The possibilities of FIRST to observe stars which lose mass at a high rate are limited to galactic distances, and to asymptotic giant branch stars in the thermal pulse phase mainly. The large collecting area is essential for the sensitivity, but of no great use when it comes to mapping the circumstellar shells. Continuum observations of the thermal dust emission will, even when only a coherent detector system is available, yield a large enough sample of oxygen-rich as well as carbon-rich stars to determine the emissivity and the average size of the particles. Observations of molecular line emission will give mass loss rates and temperatures in the optically thick case, and column densities and relative abundances in the optically thin case. Both types of observations give the stellar velocity and the expansion velocity of the envelope. ESA

N87-17551# Lecce Univ. (Italy). Dept. of Physics.
SOME RESULTS ABOUT LABORATORY DUST ANALYSIS IN THE FIR RANGE c90

A. Blanco, A. Borghesi, E. Bussoletti, L. Colangeli, S. Fonti, and V. Orofino *In* ESA Proceedings of an ESA Workshop on a Spaceborne Submillimeter Astronomy Mission. A Cornerstone of the ESA Long Term Science Program Aug. 1986 p 141-146 (For primary document see N87-17535 09-88)
Avail: NTIS HC A14/MF A01

Amorphous carbon and silicon carbide submicron grains were produced under experimental conditions and analyzed to measure properties of interstellar and/or circumstellar solid matter. Morphological and optical properties of the grains were determined. Far infrared (FIR) extinction measurements were performed to determine the spectral trend, a critical parameter in models of the diffuse galactic FIR emission from the cosmic dust and the distortion of the cosmic background radiation. The measurements can be used to study the early history of the Universe. ESA

N87-17552# Consiglio Nazionale delle Ricerche, Bologna (Italy).
ON THE IDENTIFICATION OF IRAS DEEP FIELD SOURCES: THE RADIO COUNTERPARTS c93

L. Bassani, M. J. Coe, N. Mandolesi, B. Partridge, and L. Spinoglio *In* ESA Proceedings of an ESA Workshop on a Spaceborne Submillimeter Astronomy Mission. A Cornerstone of the ESA Long Term Science Program Aug. 1986 p 151-155 (For primary document see N87-17535 09-88)
Avail: NTIS HC A14/MF A01

Six IRAS deep fields containing serendipitous infrared sources were observed at 6 and 20 cm using the NRAO Very Large Array (VLA) in its C configuration in order to identify possible radio counterparts. Each IRAS map of 0.5x1.5 deg contains an average of 10 objects and is reasonably well covered by a limited number of VLA observations. The positional accuracies of the IRAS and VLA instruments are typically of the order of 1 arcmin and few arcsecs respectively. Results concerning source coincidences are presented and infrared and 6 cm radio data on these objects are compared. The combination of detectable emission at far infrared and cm frequencies as well as the shape of the spectral distribution over this bandwidth make these objects interesting for millimeter and submillimeter observations. ESA

N87-17553# Observatorio Astromico Nacional, Guadalajara (Spain). Centro Astronomico de Yebes.
MASER AND THERMAL SiO EMISSION IN EVOLVED STARS c93

V. Bujarrabal, A. Barcia, P. Planesas, J. Gomez-Gonzalez, J. Martin-Pintado, and J. D. Gallego *In* ESA Proceedings of an ESA Workshop on a Spaceborne Submillimeter Astronomy Mission. A Cornerstone of the ESA Long Term Science Program Aug. 1986 p 157-160 (For primary document see N87-17535 09-88)
(Contract CAICYT-477/84)
Avail: NTIS HC A14/MF A01

Evolved star SiO maser emission at 43 GHz was observed by a 14m radio telescope, and SiO thermal emission at 87 GHz with a 30 m radio telescope. As a reference, the 115 GHz line of CO, a good tracer of circumstellar matter, was also observed. The observations suggest that maser and thermal SiO emission in M-type stars are probably generated in an extended inner region (less than 10 solar radii) in which the grains are still not completely formed. Physical conditions for this inner envelope are derived. ESA

N87-17554# Centre d'Etude Spatiale des Rayonnements, Toulouse (France).
NEW RESULTS ABOUT DIFFUSE GALACTIC EMISSION AT 380 MICRONS c93

E. Caux and Guy Serra *In* ESA Proceedings of an ESA Workshop on a Spaceborne Submillimeter Astronomy Mission. A Cornerstone of the ESA Long Term Science Program Aug. 1986 p 161-164 (For primary document see N87-17535 09-88)
Avail: NTIS HC A14/MF A01

Observations in the submillimeter range of the galactic disk from l=-150 to l=82deg were made with a balloon-borne instrument. In-flight calibration of the instrument was made using Jupiter. The longitude profile obtained exhibits diffuse emission all along the disk with bright peaks associated with resolved sources. The averaged galactic spectrum agrees with a temperature distribution of the interstellar cold dust. ESA

N87-17555# Imperial Coll. of Science and Technology, London (England).
OPPORTUNITIES AND POTENTIAL FOR A MILLIMETRE WAVELENGTH SEARCH FOR THE SUNYAEV-ZELDOVICH EFFECT **c93**
Simon T. Chase, R. D. Joseph, N. A. Robertson, and P. A. R. Ade *In* ESA Proceedings of an ESA Workshop on a Spaceborne Submillimeter Astronomy Mission. A Cornerstone of the ESA Long Term Science Program Aug. 1986 p 165-171 (For primary document see N87-17535 09-88)
Avail: NTIS HC A14/MF A01

A ground-based attempt to measure the Sunyaev-Zeldovich (S-Z) effect at 1.15 mm wavelength is discussed. The relative advantages and the problems and limitations of such attempts in comparison to ground-based radio methods and to space-based millimeter-wave observation are assessed. It is concluded that, while millimeter-wave techniques in general have significant advantages over radio observations, the full exploitation of the S-Z effect as an observational tool demands space-based broadband millimeter-wave detectors. ESA

N87-17556# Groningen Rijksuniversiteit (Netherlands). Lab. for Space Research.
INFRARED RADIATION FROM INTERFACE REGIONS IN MOLECULAR CLOUDS: L1551 AND THE SERPENS NEBULA **c93**
F. O. Clark, Rene J. Laureijs, G. Chlewicki, C. Y. Zhang, W. vanOosterom, and D. Kester *In* ESA Proceedings of an ESA Workshop on a Spaceborne Submillimeter Astronomy Mission. A Cornerstone of the ESA Long Term Science Program Aug. 1986 p 173-176 (For primary document see N87-17535 09-88)
Avail: NTIS HC A14/MF A01

The extended infrared emission from dust around the L1551 flow and the extended and small scale infrared emission from the Serpens nebula are analyzed using IRAS data. The extended infrared emission from the L1551 flow has an infrared bolometric luminosity greater than 20 Lo. Ultraviolet radiation appears to heat the dust surrounding the flow. The infrared emission raises the total energy requirement over a 100,000 yr lifetime by 2 orders of magnitude to 10 to the 46 to 47th ergs. In all four IRAS bands the Serpens nebula exhibits infrared emission over a scale of a degree around three stars of spectral class B and A. The stars appear to lie near an interface region. The infrared emission from the central 12 arcmin portion of the nebula correlates well with ammonia. ESA

N87-17557# Max-Planck-Inst. fuer Radioastronomie, Bonn (West Germany).
IRAS OBSERVATIONS OF THE PLEIADES **c89**
P. Cox and A. Leene (Kapteyn Astronomical Lab., Groningen (Netherlands).) *In* ESA Proceedings of an ESA Workshop on a Spaceborne Submillimeter Astronomy Mission. A Cornerstone of the ESA Long Term Science Program Aug. 1986 p 177-180 (For primary document see N87-17535 09-88)
Avail: NTIS HC A14/MF A01

The Pleiades dust was examined using IRAS data. The data show large flux densities at 12 and 25 microns extended over the optical nebulosity. This strong excess emission, implying temperatures of a few hundred degrees Kelvin, indicates a population of very small grains in the Pleiades. It is suggested that these grains are similar to the small grains needed to explain the surface brightness measurements made in the ultraviolet. ESA

N87-17558# Lanchester Polytechnic, Coventry (England).
SUBMILLIMETRE CONTINUUM OBSERVATIONS OF ACTIVE GALACTIC NUCLEI **c89**
Walter K. Gear, E. I. Robson, and L. M. J. Brown *In* ESA Proceedings of an ESA Workshop of a Spaceborne Submillimeter Astronomy Mission. A Cornerstone of the ESA Long Term Science Program Aug. 1986 p 181-184 (For primary document see N87-17535 09-88)
Avail: NTIS HC A14/MF A01

It is shown how submillimeter continuum observations may be used to investigate the physical conditions in thermal and nonthermal extragalactic sources. Observations of a flare in 3C273 led to the development of a model of compact radio sources. A luminous thermal component in the far infrared spectrum of NGC1275 which is attributed to star formation fed by a cooling accretion flow, was discovered. ESA

N87-17559# Kapteyn Astronomical Lab., Groningen (Netherlands). Lab. for Space Research.
FAR INFRARED AND OPTICAL STUDY OF THE HIGH LATITUDE CLOUD L1642 **c89**
Rene J. Laureijs, K. Mattila, and G. Schnur *In* ESA Proceedings of an ESA Workshop on a Spaceborne Submillimeter Astronomy Mission. A Cornerstone of the ESA Long Term Science Program Aug. 1986 p 185-188 (For primary document see N87-17535 09-88)
Avail: NTIS HC A14/MF A01

Optical surface brightnesses and extinction data, and IRAS infrared maps at 60 and 100 microns for the high galactic latitude cloud L1642 are compared. The optical albedo of the grains and the ratio of 100 micron and optical opacities are derived. The albedo does not depend strongly on wavelength; on average the albedo is 0.5 between 3450 and 5500 A. L1642 is detected also at 12 and 25 microns, where the morphology of the brightness distribution supports an explanation in terms of nonequilibrium emission for small grains and/or large aromatic molecules. ESA

N87-17560# Centre National de la Recherche Scientifique, Verrieres-Le Buisson (France).
SUBMILLIMETER OBSERVATION OF THE INTEGRATED GALACTIC EMISSION FROM THE SOUTH POLE **c89**
F. Pajot, R. Gispert, J. M. Lamarre, R. Peyturaux (Institut d'Astrophysique, Paris, France), M. A. Pomerantz (Delaware Univ., Newark), J.-L. Puget (Ecole Normale Superieure, Paris, France)* 07(Centre d'Etude Spatiale des Rayonnements, Toulouse, France), and Guy Serra *In* ESA Proceedings of an ESA Workshop on a Spaceborne Submillimeter Astronomy Mission. A Cornerstone of the ESA Long Term Science Program Aug. 1986 p 189-190 (For primary document see N87-17535 09-88)
Avail: NTIS HC A14/MF A01

The EMILIE experiment allowed ground based photometry of the galactic diffuse emission in the submillimeter range during a first campaign in Hawaii. A second campaign at the geographic South Pole observed the regions of the galaxy visible only from the Southern Hemisphere. The quality of this site for submillimeter astronomy is confirmed. A better reference level for the emission was determined, leading to a width at half maximum of the latitude profile close to 1 deg. ESA

N87-17561# Observatorio Astromico Nacional, Guadalajara (Spain). Centro Astronomico de Yebes.
VIBRATIONALLY EXCITED CYANOACETYLENE IN REGIONS OF MASSIVE STAR FORMATION **c90**
J. Martin-Pintado, J. Gomez-Gonzalez, A. delRomero, P. Planesas, and V. Bujarrabal *In* ESA Proceedings of an ESA Workshop on a Spaceborne Submillimeter Astronomy Mission. A Cornerstone of the ESA Long Term Science Program Aug. 1986 p 191-194 (For primary document see N87-17535 09-88)
(Contract CAYCYT-477/84)
Avail: NTIS HC A14/MF A01

Observations of the J=2-11 and J=10-9 transitions of cyanoacetylene in the ground and the V7=1 vibrationally excited state towards Orion/IRc2, W51A, and Sgr B2 are presented. In W51A, 2 sources of vibrationally excited emission at the positions of the H2O masers, IRS2 and W51e are detected. The vibrationally excited emission in Orion peaks within 2' of IRC2. Excitation temperatures greater than 150 K, in agreement with determinations of kinetic temperatures are obtained. The vibrationally excited emission in Orion and Sgr B2 are 12'x = or less than 10' and 14x = or less than 10' respectively. The excitation temperatures and sizes can be explained by radiative pumping. ESA

N87-17562# University Coll., London (England). Dept. of Physics.

SUBMILLIMETER HCO+ OBSERVATIONS OF DENSE CLOUD CORES **c89**

K. J. Richardson and Glenn J. White *In* ESA Proceedings of an ESA Workshop on a Spaceborne Submillimeter Astronomy Mission. A Cornerstone of the ESA Long Term Science Program Aug. 1986 p 195-199 (For primary document see N87-17535 09-88)
Avail: NTIS HC A14/MF A01

Submillimeter wavelength observations of the cores of the molecular clouds S255, DR21, DR21 (OH), OMC2, and Mon R2, in the J = 4-3 transitions of HCO(+) and H13CO(+) were made. The line profiles suggest the presence of small scale clumping in the densest regions. The data are analyzed with continuum measurements at 370 microns, which are used to estimate average gas densities. Hence, constraints are placed on the relative abundance of HCO(+), and dilution factors derived. Such submillimeter observations of dense and inhomogeneous cloud cores have the advantage of not being contaminated by emission and absorption in any less dense interclump medium or foreground material. ESA

N87-17563# Radio Sterrenwacht, Dwingeloo (Netherlands).
CO OBSERVATIONS OF THE OUTFLOW SOURCE NGC 7023 **c89**

Graeme D. Watt *In* ESA Proceedings of an ESA Workshop on a Spaceborne Submillimeter Astronomy Mission. A Cornerstone of the ESA Long Term Science Program Aug. 1986 p 207-214 (For primary document see N87-17535 09-88)
(Grant NSF AST-79-21812)
Avail: NTIS HC A14/MF A01

Maps for C12Q and C13Q J=1 - greater than 0 rotational transitions of the region surrounding the nebula NGC 7023 are presented. Features which are characteristic of embedded objects undergoing mass outflow are evident. There is little indication from the spectra of high-velocity wings arising from material accelerated within the lobes, but dense CO clumps are located at the extremities of these lobes, suggesting that compression and heating of the cloud occurred there. Optical depths, excitation temperatures, and column densities are derived from the data, and a geometric model is constructed to fit the observed and derived parameters. A disk structure, which surrounds the central sources and lies along the major axis of the cloud, is interpreted as the heated inner surface of the cavity created by the expanding shell. ESA

N87-17564# European Space Agency. European Space Research and Technology Center, ESTEC, Noordwijk (Netherlands).
A PROPOSED CORNERSTONE MISSION: FAR INFRARED SUBMILLIMETER WAVE TELESCOPE (FIRST) **c89**

Nigel G. Douglas and U. O. Frisk *In its* Proceedings of an ESA Workshop on a Spaceborne Submillimeter Astronomy Mission. A Cornerstone of the ESA Long Term Science Program Aug. 1986 p 219-224 (For primary document see N87-17535 09-88)
Avail: NTIS HC A14/MF A01.

The reasons ESA chose a submillimeter observatory (FIRST) as a cornestone mission are summarized. Many key problems in astrophysics, such as the chemistry and dynamics of molecular clouds, the mechanisms of star formation, and cosmology, may be addressed with such an observatory. Ground-based astronomy is virtually impossible at these wavelengths due to the extreme opacity of the Earth's atmosphere. The availability of heterodyne techniques permits observations of enormous spectral resolving power. Velocity information can be extracted to below the level of 1 km/sec. This distinguishes FIRST markedly from infrared missions such as IRAS and ISO. Instrument specifications are outlined.ESA

N87-17565# University Coll., London (England). Dept. of Physics.
THE INFLUENCE OF BACKGROUND POWER ON THE PERFORMANCE OF AN IDEAL BOLOMETER **c35**

M. J. Griffin *In* ESA Proceedings of an ESA Workshop on a Spaceborne Submillimeter Astronomy Mission. A Cornerstone of the ESA Long Term Science Program Aug. 1986 p 225-229 (For primary document see N87-17535 09-88)
Avail: NTIS HC A14/MF A01

The effects of radiant power loading on the performance of an ideal bolometer are analyzed. The operation of the bolometer is characterized in terms of dimensionless parameters which correspond to the temperature sensitivity of the thermometric material, the electrical bias point, and the amount of optical power loading. Expressions for the zero frequency noise equivalent power and responsivity are derived. Examples for the case of a typical 3He3 cooled detector used for far infrared or submillimeter photometry are given. ESA

N87-17566# Paris VII Univ. (France).
ACTIVE OPTICS FOR THE FAR INFRARED SUBMILLIMETER WAVE SPACE TELESCOPE (FIRST): A HIGH ANGULAR RESOLUTION MODE **c74**

Pierre Lena *In* ESA Proceedings of an ESA Workshop on a Spaceborne Submillimeter Astronomy Mission. A Cornerstone of the ESA Long Term Science Program Aug. 1986 p 239-242 (For primary document see N87-17535 09-88)
Avail: NTIS HC A14/MF A01

It is proposed to equip the focal plane of the Far Infrared Submillimeter Wave Space Telescope (FIRST) with an active-adaptive optics system, which could provide diffraction limited images at wavelengths leas than 100 microns, possibly as short as 10 microns. This considerably broadens the spectral range covered by FIRST and provides at shorter wavelengths a spatial resolution larger than ever obtained in space. Such a high angular resolution mode (0.2 arcsec at 8 microns) would match the highest resolution obtainable with the next generation ground-based telescopes and extend it at all infrared wavelengths. ESA

N87-17567# Helsinki Univ. of Technology, Espoo (Finland).
AN 800 MHz BANDWIDTH ACOUSTO-OPTICAL SPECTROMETER AT HELSINKI OBSERVATORY **c35**

L. J. Malkamaeki *In* ESA Proceedings of an ESA Workshop on a Spaceborne Submillimeter Astronomy Mission. A Cornerstone of the ESA Long Term Science Program Aug. 1986 p 243-245 (For primary document see N87-17535 09-88)
Avail: NTIS HC A14/MF A01

An 800 MHz bandwidth acousto-optical spectrometer with 1800 resolution spots is described. With active stabilization exceptionally good frequency stability is achieved. This along with very low background light level allows the use of long on-off integration times. ESA

N87-17568# Max-Planck-Inst. fuer Radioastronomie, Bonn (West Germany).
THE SUBMILLIMETER TELESCOPE (SMT) PROJECT **c89**

J. W. M. Baars and R. N. Martin (Arizona Univ., Tucson) *In* ESA Proceedings of an ESA Workshop on a Spaceborne Submillimeter Astronomy Mission. A Cornerstone of the ESA Long Term Science Program Aug. 1986 p 247-250 Sponsored by the Alfried Krupp von Bohlen und Halbach Stiftung (For primary document see N87-17535 09-88)
Avail: NTIS HC A14/MF A01

A 10 m diameter submillimeter-telescope to be located at 3230 m on Mount Graham (NE-Arizona) is described. Reflector accuracy (15 microns and pointing stability (1') will provide excellent performance at 350 micron wavelength. Extensive use of carbon fiber reinforced plastic for reflector panels and structural members minimizes thermal deformations and allows operation of the telescope exposed to the environment. During poor weather the telescope will be protected by a corotating enclosure. The reflector panels are replicated from molds made of pyrex-glass. These are ground to 3 micron accuracy. ESA

N87-17569# Science Research Council, Chilton (England).
A 186 GHz RADIOMETER FOR THE MICROWAVE LIMB SOUNDER **c35**

P. D. Curtis, D. N. Matheson, D. R. Vizard, and G. E. Peckham (Heriot-Watt Univ., Edinburgh (Scotland).) *In* ESA Proceedings of an ESA Workshop on a Spaceborne Submillimeter Astronomy Mission. A Cornerstone of the ESA Long Term Science Program

Aug. 1986 p 251-254 (For primary document see N87-17535 09-88)
Avail: NTIS HC A14/MF A01

A 183 GHz heterodyne radiometer was built for the Microwave Limb Sounder experiment, designed to measure atmospheric thermal emission from selected molecular species at millimeter wavelengths on the Upper Atmosphere Research Satellite. The radiometer includes a broad band quasioptical coupler, a solid state local oscillator, and a whisker contacted varistor diode single-ended waveguide mixer. ESA

N87-17570# California Univ., Berkeley. Dept. of Physics.
LOW NOISE SIS MIXER WITH GAIN FOR 80-115 GHz c33
A. V. Raeisaenen (Helsinki Univ. of Technology, Espoo, Finland), D. G. Crete (Ecole Normale Superieure, Paris, France), P. L. Richards, and F. L. Lloyd (National Bureau of Standards, Gaithersburg, Md.) *In* ESA Proceedings of an ESA Workshop on a Spaceborne Submillimeter Astronomy Mission. A Cornerstone of the ESA Long Term Science Program Aug. 1986 p 255-258 (For primary document see N87-17535 09-88)
(Grant AFOSR-85-0230)
Avail: NTIS HC A14/MF A01

Superconductor-insulator-superconductor quasiparticle mixers were designed and tested for the frequency range from 80 to 115 GHz. The sliding backshort is the only adjustable RF-tuning element. The RF-filter reactance is used as a fixed RF-matching element. A mixer which uses a single 2 sq micron Pb-alloy junction in a 1/4-height waveguide mount has a coupled conversion gain of GM(DSB) = 2.6 + or - 0.5 dB with an associated noise temperature of TM(DSB) = 16.4 + or - 1.8 K at the best DSB operation point. The receiver noise temperature TR(DSB) is 27.5 + or - 0.8 K. This mixer provides a SSB receiver noise temperature below 50 K over the frequency range from 91 to 96 GHz, the minimum being TR(SSB) = 44 + or - 4 K. ESA

N87-17571*# Jet Propulsion Lab., California Inst. of Tech., Pasadena.
THE LARGE DEPLOYABLE REFLECTOR: A NASA SUBMILLIMETER-INFRARED ORBITING OBSERVATORY
Paul N. Swanson *In* ESA Proceedings of an ESA Workshop on a Spaceborne Submillimeter Astronomy Mission. A Cornerstone of the ESA Long Term Science Program Aug. 1986 p 265-276 (For primary document see N87-17535 09-88)
Avail: NTIS HC A14/MF A01

The Large Deployable Reflector (LDR) concept is outlined. The LDR telescope is based on a 20-m diameter reflector. The primary mirror is a filled aperture made up of 84 hexagonal panels, each 2 m edge-to-edge. The panels are based on lightweight structural composite materials. The optical configuration is a four mirror two stage system. The primary mirror is passive. The active optical elements for figure control are at the quaternary mirror. The primary mirror panels are supported by a deployable PAC truss backup structure at the vertices of each hexagon. The four focal plane instruments covering the range of 30 to 1000 microns are located near the vertex of the primary mirror. Some instruments will be cooled with stored cryogens to liquid helium temperatures, others to liquid nitrogen temperatures. The spacecraft functions will be located in a resource module behind the primary mirror. The LDR will be transferred to orbit by the space transportation system and assembled and tested at the space station. It will then be boosted to an orbit of greater than or = 700 km as a free flyer. ESA

N87-17572*# Chalmers Univ. of Technology, Goeteborg (Sweden). Dept. of Physics.
ON THE FEASIBILITY OF CONSTRUCTING AN IMAGING ARRAY OF SLOT-ANTENNAS INTEGRATED WITH SIS MIXERS c32
D. Winkler, W. R. McGrath, B. Nilsson, T. Claeson, J. Johansson, E. Kollberg, K. S. Yngvesson (Massachusetts Univ., Amherst), and S. Rudner (Research Inst. of National Defence, Linkoeping, Sweden) *In* ESA Proceedings of an ESA Workshop on a Spaceborne Submillimeter Astronomy Mission. A Cornerstone of the ESA Long Term Science Program Aug. 1986 p 277-283 Sponsored by NASA Langley Research Center, the Swedish Board for Technical Development, and the Swedish Board for Space Activities (For primary document see N87-17535 09-88)
Avail: NTIS HC A14/MF A01 CSCL 20N

A prototype 700 GHz subharmonically pumped superconductor-insulator-superconductor (SIS) mixer integrated with a tapered slot antenna on a silicon substrate is described. Imaging using integrated SIS-mixer-antenna chips is discussed. ESA

N87-17573# Cologne Univ. (West Germany). Inst. fuer Physik.
OBSERVATIONS FROM THE GORNERGRAT OBSERVATORY (SWITZERLAND) WITH THE UNIVERSITY OF COLOGNE 3-m RADIO TELESCOPE c89
G. Winnewisser, M. Bester, R. Ewald, W. Hilberath, K. Jacobs, M. Miller, T. Pauls, A. Piciorgros, G. Rau, M. Reich et al *In* ESA Proceedings of an ESA Workshop on a Spaceborne Submillimeter Astronomy Mission. A Cornerstone of the ESA Long Term Science Program Aug. 1986 p 285-292 (For primary document see N87-17535 09-88)
(Grant DFG-SFB-301)
Avail: NTIS HC A14/MF A01

The technical status of the Gornergrat Observatory (Switzerland), performance tests, and molecular observations of the galactic center region are summarized. The surface accuracy of the reflector is 30 microns. Receivers comprise a cooled GaAs Schottky-barrier mixer for the 70 to 116 GHz band, an SIS mixer covering the 140 to 150 GHz range, and a 345 GHz cooled GaAs-Schottky-Barrier mixer will be added. Backends include a filter bank, three acousto-optical spectrometers with different bandwidths and resolutions, and a 500 MHz bandwidth continuum system. ESA

N87-17574# Space Telescope Science Inst., Baltimore, Md.
STRUCTURE OF MOLECULAR CLOUDS AND SPACE-BASED SUB-MILLIMETER TELESCOPES, FOR EXAMPLE FIRST c89
Colin A. Norman *In* ESA Proceedings of an ESA Workshop on a Spaceborne Submillimeter Astronomy Mission. A Cornerstone of the ESA Long Term Science Program Aug. 1986 p 295-297 (For primary document see N87-17535 09-88)
Avail: NTIS HC A14/MF A01

Aspects of molecular cloud physics and their associated star forming regions that could be very significantly elucidated by a spaceborne mission such as the ESA Far Infrared Submillimeter Wave Space Telescope (FIRST) are discussed. These include the distribution in external galaxies, cloud substructure, circumstellar disks, bipolar flows, masers, Herbig-Haro objects, and molecular clouds in the Galactic Center. It is emphasized that the highest possible spatial and/or spectral resolution and wavelength coverage are necessary to actually observationally solve these questions and that FIRST has this capability. ESA

89 ASTRONOMY

Includes radio, gamma-ray, and infrared astronomy, and astrometry.

N87-17575 Max-Planck-Inst. fuer Physik und Astrophysik, Garching (West Germany). Inst. fuer Extraterrestrische Physik.
A SOFT X-RAY OBSERVATION OF OMEGA CENTAURI WITH EXOSAT
F. Verbunt, R. A. Shafer (European Space Agency. European Space Operations Center, Darmstadt West Germany), F. Jansen (Leiden Univ., Netherlands) 05Amsterdam Univ., (Netherlands), K. A. Arnaud, and J. vanParadijs Jul. 1986 15 p Submitted for publication
(MPE-Preprint-60; ETN-87-98966) Copyright. Avail: Issuing Activity

In an observation with the LE1 CMA detector of the EXOSAT observatory, two X-ray sources previously discovered in the globular cluster omega Cen with the IPC detector on board the Einstein satellite were detected. Improved positions for these two sources

are given. Comparison of the EXOSAT and Einstein count rates indicates that these two sources are either very soft (kT = 40 eV) or highly variable. If they are very soft, previous estimates of their X-ray luminosity can be too high by an order of magnitude. ESA

N87-17576 Max-Planck-Inst. fuer Physik und Astrophysik, Garching (West Germany). Inst. fuer Extraterrestrische Physik.
OBSERVATIONS OF QUASI-PERIODIC OSCILLATIONS IN CYG X-2
Guenter Hasinger Jul. 1986 15 p Presented at the IAU Symposium 125 on the Origin and Evolution of Neutron Stars, Nanjing, China, 23-30 May 1986 Submitted for publication
(MPE-Preprint-61; ETN-87-98967) Copyright. Avail: Issuing Activity

The EXOSAT observations of Cyg X-2, which reveal two types of periodic oscillations (QPO) associated with different spectral behavior are discussed. The QPO in the range 18 to 55 Hz with a hard spectrum are found in all observations where the source is on the horizontal branch in a hardness-versus-intensity diagram. On the vertical branch, however, QPO's with a soft spectrum are found at a stable frequency of 5.6 Hz. A multitude of QPO frequency-intensity relations, found in different horizontal branch observations, coalesce to an almost unique relation when the QPO frequency is correlated with spectral hardness. A cross-correlation analysis of the rapid variability reveals a time lag of hard photons by 1.5 to 3.8 ms; the lag being smaller when the QPO frequency is larger. Results are consistent with a model where QPO's represent the Kepler frequency at the edge of the neutron star magnetosphere. The data do not require the assumption of a beat frequency. The derived surface magnetic field strength is of the order of 10 billion G. ESA

N87-17577 Stanford Univ., Calif.
FAR INFRARED SPECTROSCOPY OF GALAXIES FROM THE KUIPER AIRBORNE OBSERVATORY Ph.D. Thesis
Philip Bliss Duffy 1986 152 p
Avail: Univ. Microfilms Order No. DA8619740

One possible energy source for infrared emitting galaxies is many newly formed stars. This idea is tested by observing far infrared emission lines of interstellar oxygen and nitrogen gas in the galaxy M82 and the colliding galaxy system Arp 299. Observed fluxes in 4 lines in M82 roughly match those calculated from existing models of M82 which predict active massive star formation. In Arp 299, an upper limit was measured on the flux in one line of doubly ionized oxygen (O++), also consistent with fluxes predicted. These arguments support the picture that M82 and Arp 299 are powered by many newly formed high mass stars. Other results are briefly discussed. Average electron densities were found in M82 which are 10 to 100 times lower than in typically observed HII regions in this galaxy. Lower densities may result from winds from frequent supernovae in M82. Dissert. Abstr.

N87-17578 Stanford Univ., Calif.
SPECTRAL FLUX FROM LOW-DENSITY PHOTOSPHERES Ph.D. Thesis
Stephen Jeffrey Hershkowitz 1986 208 p
Avail: Univ. Microfilms Order No. DA8619758

Radiative transfer through sharp, quasi-static atmospheres whose opacity is dominated by hydrogen is considered at densities low enough that scattering usually dominates absorption and radiative excitations usually dominate collisional excitations. It is found that the balance between photoionization and radiative recombination which governs the atomic level populations greatly reduces the effective absorptive opacity. Numerical and approximate analytical results for the emergent continuum spectral flux are obtained for effective temperatures 4000 to 16,000 K. Calculations incorporate the constraint of statistical equilibrium directly into the transfer equation. This equation is then solved subject to the constraint of radiative equilibrium. Comparison with observations of Type II supernovae, which lack a Balmer jump, (and in particular detail for supernova 1980k for which there are the most complete observations) implies that the flux is diluted below that of a blackbody at the same color temperature, which tends to increase the value of the Hubble constant previously obtained by the Baade method. Dissert. Abstr.

N87-17579 New Mexico Univ., Albuquerque.
POLARIMETRY AND PHOTOMETRY OF ACTIVE QUASARS AT VISUAL AND NEAR-INFRARED WAVELENGTHS Ph.D. Thesis
Paul Sidney Smith 1986 342 p
Avail: Univ. Microfilms Order No. DA8620994

The optical and near infrared continua of highly luminous BL Lacertae (BL Lac) objects and optically violent variable (OVV) quasars are studied through simultaneous broad band photometry and linear polarimetry. Nineteen BL Lacs and OVVs were monitored during an approx. 1 1/2 year period, with the major aim of characterizing the wavelength dependent polarization exhibited by these objects. Optical (UBVR) observations were conducted at the UCSD/U. Minn. 1.5 m telescope. Simultaneous near infrared measurements were made using the KPNO 2.1 m telescope. Most of the BL Lac objects exhibit large variations in polarization and brightness on a time scale of less than a week. The degree of fractional linear polarization is not observed to be related to brightness or optical spectral index. Most BL Lacs did not show a preferred polarization position angle. Wavelength dependent polarization and position angle are observed in almost all BL Lacs, but not always simultaneously. Wavelength dependence is transient, and for most objects, rarely observed. Linear polarization is almost always observed to increase toward shorter wavelengths in the 0.36 to 2.2 mm spectral region when wavelength dependent polarization is observed. Dissert. Abstr.

N87-17580 Maryland Univ., College Park.
THE DEVELOPMENT OF THE GODDARD COMPTON GAMMA-RAY TELESCOPE AND NEUTRAL HYDROGEN Ph.D. Thesis
John Gregory Stacy 1985 343 p
Avail: Univ. Microfilms Order No. DA8614291

The development of an instrument designed to conduct balloon-borne observations in the medium energy gamma-ray region is described. Based on the Compton coincidence principle, the NASA/Goddard Advanced Compton Telescope (ACT), is intended for the study of point sources of cosmic gamma-rays in the energy range from approximately 0.5 to 30 MeV. The value of the results anticipated from the experiment are summarized in terms of constraints which may be imposed on currently viable models of gamma-ray emission from Seyfert galaxies. The results of a 21 cm neutral hydrogen survey, performed in a region of the galactic disk known as the Puppis Window, are reported. Observations were conducted on the NRAO 43 m radio telescope on an area of the Milky Way which contains much less absorbing interstellar dust and associated gas than is found in more typical regions of the Galaxy. Reports of optical spiral tracers at distances up to 8 kcp from the Sun make this area of the galactic disk ideal for the comparison of optical and radio data. Correlations of specific HI features with optical spiral tracers are discussed, along with the corresponding implications regarding the spiral structure in this quadrant of the Galaxy. Finally, the association of the young pulsar PSRO740-28 with an HI shell in Puppis is established, and evidence pointing towards its possible origin in a second-generation supernova event is discussed. Dissert. Abstr.

N87-17581*# Wheaton Coll., Norton, Mass. Dept. of Physics and Astronomy.
THE IONIZATION STRUCTURE OF PLANETARY NEBULAE. 8: NGC 6826
Timothy Barker [1987] 34 p
(Grant NsG-5376)
(NASA-CR-180142; NAS 1.26:180142) Avail: NTIS HC A03/MF A01 CSCL 03A

Spectrophotometric observations of emission-line intensities over the spectral range 1400 to 1700 A were made in seven positions in the planetary nebulae NCG 6826. The O(++) electron temperature varies little from 8900 K throughout the nebula; the Balmer continuum electron temperature averages 1500 K higher. The wavelength 4267 C II line intensities imply C(++) abundances that are systematically higher than those

determined from the wavelength 1906, 1909 C III lines, but because of uncertainties in the intensities of the ultraviolet lines relative to the optical ones, this discrepancy is less conclusively demonstrated in NGC 6826 than in other planetaries in this series. Standard equations used to correct for the existence of elements in other than the optically observable ionization stages give results that are consistent and also in approximate agreement with abundances calculated using ultraviolet lines in the few cases where the relevant ultraviolet lines are measurable. The results of the logarithmic abundances differ somewhat from the recent study by Aller and Czyzak, in part because their measured electron temperatures are somewhat higher. The Ar, Ne, and, to some extent, O and S abundances appear to be somewhat low, suggesting that the progenitor to NGC 6826 like that to NGC 7662, may have formed out of somewhat metal-poor material. Author

N87-17582*# Wheaton Coll., Norton, Mass. Dept. of Physics and Astronomy.
THE IONIZATION STRUCTURE OF PLANETARY NEBULAE. PART 7: NEW OBSERVATIONS IN THE RING NEBULA
Timothy Barker 1986 36 p Sponsored in part by NSF (Grant NsG-5376)
(NASA-CR-180141; NAS 1.26:180141) Avail: NTIS HC A03/MF A01 CSCL 03A

New optical spectrophotometric observations of emission-line intensities have been made in eight positions in the Ring Nebula corresponding to those observed previously with the Ultraviolet Explorer satellite; the total coverage is therefore 1400 to 7200 A. The intensities are in generally good agreement with those found previously in corresponding positions. The 0(++) and Balmer continuum electron temperatures agree well on the average and, like the N(+) electron temperatures, decrease with increasing distance from the central star. As found previously for the Ring Nebula and for other planetaries in this series, the lambda 4267 C 2 line intensity near the central star implies a C(++) abundance that is higher than that determined from the lambda 1906, 1909 C 3 lines. The discrepancy again decreases with increasing distance from the central star and vanishes from the outermost positions, again suggesting that the excitation mechanism from the lambda 4267 line is not understood. Standard equations used to correct for the existence of elements in other than the optically observable ionization stages give results that are consistent and in appropriate agreement with abundances calculated using UV lines. The rather high abundances of O, N, and C, and, to some extent N, indicate that some mixing of CNO processed material into the nebular shell may have occurred in the Ring Nebula. Author

N87-17583*# Smithsonian Astrophysical Observatory, Cambridge, Mass.
OBSERVATIONS OF YOUNG LOW-MASS STARS IN DENSE CORES Semiannual Status Report, 1 Oct. 1985 - 31 Mar. 1986
Philip C. Myers Feb. 1987 3 p
(Grant NAG2-374)
(NASA-CR-180152; NAS 1.26:180152; SASR-1) Avail: NTIS HC A02/MF A01 CSCL 03A

In this period the first maps were made during two flights of the Kuipper Airborne Observatory (KAO) in January 1986. One of these shows extended emission at 100 and 160 microns from the dense core B35 containing the IRAS point source 05417+0907. The 160 micron emission has approximately the same extent as the NH3 (1,1) line emission at 1.4 cm, indicating close correspondence between the warm dust and the dense gas. The 160 micron map shows a previously unknown secondary maximum about 90 arcsec north of the IRAS source. Author

N87-17584*# Columbia Univ., New York.
INTERNATIONAL ULTRAVIOLET EXPLORER OBSERVING PROGRAM: ULTRAVIOLET OBSERVATIONS OF SELECTED ASTRONOMICAL SOURCES Semiannual Status Report, 7 Jul. - 31 Dec. 1986
Jules Halpern Feb. 1987 5 p
(Grant NAG5-823)
(NASA-CR-180155; NAS 1.26:180155; Episode-9; CAL-1638) Avail: NTIS HC A02/MF A01 CSCL 03A

Progress is described for the following topics: rapid variations in the far ultraviolet spectrum of the cool Ap star 21 Com; elliptical Seyfert galaxies; variations of cool Ap stars with strong magnetic fields; and X-ray selected BL Lac Objects. B.G.

N87-17585# Geneva Observatory (Switzerland).
REDISTRIBUTION OF ANGULAR MOMENTUM BY NONAXISYMMETRIC INSTABILITIES IN A THICK ACCRETION DISK
W. H. Zurek and W. Benz 1986 17 p Submitted for publication Sponsored in part by the Swiss National Science Foundation
(Publ-Ser-C-Fasc-4; LA-UR-85-39-53; ETN-87-98900) Avail: NTIS HC A02/MF A01

The evolution of thick accretion tori around black holes was investigated. Using three-dimensional computer models, it is shown that isentropic, pressure supported tori with constant specific angular momentum (Omega = r sup - 2) are unstable. Nonaxisymmetric instabilities grow and lead to the redistribution of specific angular momentum l on a short, dynamical timescale from the initial l = const to l = r sup qc, where qc = 0.25. Significance of these results for the models of active galactic nuclei and other jet-producing astrophysical sources is discussed. ESA

N87-17536# Royal Observatory, Edinburgh (Scotland).
STATUS OF OBSERVATIONAL ASTRONOMY IN THE 1990'S: POSITION OF SUBMILLIMETRE ASTRONOMY
M. S. Longair *In* ESA Proceedings of an ESA Workshop on a Spaceborne Submillimeter Astronomy Mission. A Cornerstone of the ESA Long Term Science Program Aug. 1986 p 7-14 (For primary document see N87-17535 09-88)
Avail: NTIS HC A14/MF A01

N87-17537# Groningen Rijksuniversiteit (Netherlands). Lab. for Space Research.
REVIEW OF COHERENT AND INCOHERENT DETECTION TECHNIQUES: OUTLOOK AND LIMITATION
Thijs deGraauw *In* ESA Proceedings of an ESA Workshop on a Spaceborne Submillimeter Astronomy Mission. A Cornerstone of the ESA Long Term Science Program Aug. 1986 p 15-24 (For primary document see N87-17535 09-88)
Avail: NTIS HC A14/MF A01

N87-17538# United Kingdom Infrared Telescope Unit, Hilo, Hawaii.
OBSERVATIONS OF ACTIVE GALACTIC NUCLEI WITH FIRST
Malcom G. Smith *In* ESA Proceedings of an ESA Workshop on a Spaceborne Submillimeter Astronomy Mission. A Cornerstone of the ESA Long Term Science Program Aug. 1986 p 25-31 (For primary document see N87-17535 09-88)
Avail: NTIS HC A14/MF A01

N87-17544# University Coll., London (England). Dept. of Physics.
SUBMILLIMETRE WAVELENGTH STUDIES OF PROTOSTARS: THE ROLE OF FIRST
Glenn J. White *In* ESA Proceedings of an ESA Workshop on a Spaceborne Submillimeter Astronomy Mission. A Cornerstone of the ESA Long Term Science Program Aug. 1986 p 79-91 (For primary document see N87-17535 09-88)
Avail: NTIS HC A14/MF A01

N87-17550# European Space Agency. European Space Research and Technology Center, ESTEC, Noordwijk (Netherlands). Space Science Div.
FAR INFRARED SUBMILLIMETER WAVE SPACE TELESCOPE (FIRST) OBSERVATIONS OF STARS WITH LARGE MASS LOSS RATES
J. Herman *In its* Proceedings of an ESA Workshop on a Spaceborne Submillimeter Astronomy Mission. A Cornerstone of the ESA Long Term Science Program Aug. 1986 p 135-138 (For primary document see N87-17535 09-88)
Avail: NTIS HC A14/MF A01

N87-17557# Max-Planck-Inst. fuer Radioastronomie, Bonn (West Germany).
IRAS OBSERVATIONS OF THE PLEIADES
P. Cox and A. Leene (Kapteyn Astronomical Lab., Groningen (Netherlands).) *In* ESA Proceedings of an ESA Workshop on a Spaceborne Submillimeter Astronomy Mission. A Cornerstone of the ESA Long Term Science Program Aug. 1986 p 177-180 (For primary document see N87-17535 09-88)
Avail: NTIS HC A14/MF A01

N87-17558# Lanchester Polytechnic, Coventry (England).
SUBMILLIMETRE CONTINUUM OBSERVATIONS OF ACTIVE GALACTIC NUCLEI
Walter K. Gear, E. I. Robson, and L. M. J. Brown *In* ESA Proceedings of an ESA Workshop of a Spaceborne Submillimeter Astronomy Mission. A Cornerstone of the ESA Long Term Science Program Aug. 1986 p 181-184 (For primary document see N87-17535 09-88)
Avail: NTIS HC A14/MF A01

N87-17559# Kapteyn Astronomical Lab., Groningen (Netherlands). Lab. for Space Research.
FAR INFRARED AND OPTICAL STUDY OF THE HIGH LATITUDE CLOUD L1642
Rene J. Laureijs, K. Mattila, and G. Schnur *In* ESA Proceedings of an ESA Workshop on a Spaceborne Submillimeter Astronomy Mission. A Cornerstone of the ESA Long Term Science Program Aug. 1986 p 185-188 (For primary document see N87-17535 09-88)
Avail: NTIS HC A14/MF A01

N87-17560# Centre National de la Recherche Scientifique, Verrieres-Le Buisson (France).
SUBMILLIMETER OBSERVATION OF THE INTEGRATED GALACTIC EMISSION FROM THE SOUTH POLE
F. Pajot, R. Gispert, J. M. Lamarre, R. Peyturaux (Institut d'Astrophysique, Paris, France), M. A. Pomerantz (Delaware Univ., Newark), J.-L. Puget (Ecole Normale Superieure, Paris, France)* 07(Centre d'Etude Spatiale des Rayonnements, Toulouse, France), and Guy Serra *In* ESA Proceedings of an ESA Workshop on a Spaceborne Submillimeter Astronomy Mission. A Cornerstone of the ESA Long Term Science Program Aug. 1986 p 189-190 (For primary document see N87-17535 09-88)
Avail: NTIS HC A14/MF A01

N87-17562# University Coll., London (England). Dept. of Physics.
SUBMILLIMETER HCO+ OBSERVATIONS OF DENSE CLOUD CORES
K. J. Richardson and Glenn J. White *In* ESA Proceedings of an ESA Workshop on a Spaceborne Submillimeter Astronomy Mission. A Cornerstone of the ESA Long Term Science Program Aug. 1986 p 195-199 (For primary document see N87-17535 09-88)
Avail: NTIS HC A14/MF A01

N87-17563# Radio Sterrenwacht, Dwingeloo (Netherlands).
CO OBSERVATIONS OF THE OUTFLOW SOURCE NGC 7023
Graeme D. Watt *In* ESA Proceedings of an ESA Workshop on a Spaceborne Submillimeter Astronomy Mission. A Cornerstone of the ESA Long Term Science Program Aug. 1986 p 207-214 (For primary document see N87-17535 09-88)
(Grant NSF AST-79-21812)
Avail: NTIS HC A14/MF A01

N87-17564# European Space Agency. European Space Research and Technology Center, ESTEC, Noordwijk (Netherlands).
A PROPOSED CORNERSTONE MISSION: FAR INFRARED SUBMILLIMETER WAVE TELESCOPE (FIRST)
Nigel G. Douglas and U. O. Frisk *In its* Proceedings of an ESA Workshop on a Spaceborne Submillimeter Astronomy Mission. A Cornerstone of the ESA Long Term Science Program Aug. 1986 p 219-224 (For primary document see N87-17535 09-88)
Avail: NTIS HC A14/MF A01

N87-17568# Max-Planck-Inst. fuer Radioastronomie, Bonn (West Germany).
THE SUBMILLIMETER TELESCOPE (SMT) PROJECT
J. W. M. Baars and R. N. Martin (Arizona Univ., Tucson) *In* ESA Proceedings of an ESA Workshop on a Spaceborne Submillimeter Astronomy Mission. A Cornerstone of the ESA Long Term Science Program Aug. 1986 p 247-250 Sponsored by the Alfried Krupp von Bohlen und Halbach Stiftung (For primary document see N87-17535 09-88)
Avail: NTIS HC A14/MF A01

N87-17573# Cologne Univ. (West Germany). Inst. fuer Physik.
OBSERVATIONS FROM THE GORNERGRAT OBSERVATORY (SWITZERLAND) WITH THE UNIVERSITY OF COLOGNE 3-m RADIO TELESCOPE
G. Winnewisser, M. Bester, R. Ewald, W. Hilberath, K. Jacobs, M. Miller, T. Pauls, A. Piciorgros, G. Rau, M. Reich et al *In* ESA Proceedings of an ESA Workshop on a Spaceborne Submillimeter Astronomy Mission. A Cornerstone of the ESA Long Term Science Program Aug. 1986 p 285-292 (For primary document see N87-17535 09-88)
(Grant DFG-SFB-301)
Avail: NTIS HC A14/MF A01

N87-17574# Space Telescope Science Inst., Baltimore, Md.
STRUCTURE OF MOLECULAR CLOUDS AND SPACE-BASED SUB-MILLIMETER TELESCOPES, FOR EXAMPLE FIRST
Colin A. Norman *In* ESA Proceedings of an ESA Workshop on a Spaceborne Submillimeter Astronomy Mission. A Cornerstone of the ESA Long Term Science Program Aug. 1986 p 295-297 (For primary document see N87-17535 09-88)
Avail: NTIS HC A14/MF A01

90 ASTROPHYSICS

Includes cosmology; celestial mechanics; space plasmas; and interstellar and interplanetary gases and dust.
For related information see also *75 Plasma Physics.*

N87-17586 California Univ., Los Angeles.
A NUMERICAL STUDY OF JET PRODUCTION AND ACCRETION DISK STRUCTURE IN SUPER-EDDINGTON BLACK HOLE ACCRETION Ph.D. Thesis
Gordon Eric Eggum 1986 480 p
Avail: Univ. Microfilms Order No. DA8621057

The analysis of thick, radiation pressure dominated (super Eddington) accretion disks has proven to be difficult. Purely analytical methods have not yet been adequate to determine the structure of the disk and associated jet. The analytical problems are circumvented by using a numerical method; the results are based on a series of numerical simulations of disk accretion onto a three solar mass black hole. The computer code used in the analysis solves the coupled radiation gas dynamic equations for axisymmetric accretion onto a black hole. Newtonian mechanics is used, since relativistic corrections are essential only very near the black hole. The accretion is assumed to be driven by a macroscopic viscous stress tensor. The range of parameters used in the analysis was chosen to conform to expectations for a realistic disk. The conclusions are valid for disks in which the viscous stress magnitude is a significant fraction of the disk pressure, and for accretion rates M similar to or $<$ 10 times the Eddington rate. The primary conclusions are given and briefly discussed. Dissert. Abstr.

N87-17587 State Univ. of New York, Stony Brook.
DARK MATTER AND THE DYNAMICS OF GALAXY CLUSTERING Ph.D. Thesis
August E. Evrard 1986 187 p
Avail: Univ. Microfilms Order No. DA8619528

The dynamics of galaxy clustering is investigated in simulations of the large scale structure of the universe. Emphasis is placed on determining the accuracy of virial mass estimates, and therefore

of the mean mass density in the universe. For galaxies modelled as point masses, the virial theorem yields mass estimates accurate to within a factor of 2 for a wide range of clustered systems. The point mass approximation, however, is incapable of reproducing observed small scale clustering behavior and is unrealistic in view of the observational and theoretical evidence for dominant amounts of dark matter around individual galaxies and in clusters. Simulations of the large scale clustering of galaxies with massive dark halos are then performed for both a critically dense and open universe. The extended mass distribution and dynamical friction, both absent in the point mass models, conspire to reduce galactic peculiar velocities on clustered scales and enhance galaxy correlations at small separations. The median virial mass estimates of galaxy groups systematically underestimate the total mass present by at least a factor of 3. Dissert. Abstr.

N87-17588 California Inst. of Tech., Pasadena.
PARSEC-SCALE STRUCTURE IN THE NUCLEI OF DOUBLE LOBED RADIO QUASARS Ph.D. Thesis
David Hans Hough 1986 225 p
Avail: Univ. Microfilms Order No. DA8620939

A complete sample of double lobed quasars is defined, which is believed to be randomly oriented and which contains many objects with central components accessible to very long baseline interferometry (VLBI). The purpose of defining the sample in this way is to facilitate tests of physical models proposed to explain both the compact and extended structures in extragalactic radio sources. Statistical studies of the properties of these objects on the > approx. kiloparsec scale are consistent with the assumption of random orientations and the simple relativistic beaming theory. The central components of six double lobed quasars were mapped at high resolution and high sensitivity with VLBI. Each object exhibits a double or extended structure on the approx. parsec scale. This structure can be interpreted as a core jet, the same morphology found in the dominant cores of powerful flat spectrum sources, thus indicating a relation between the two classes of compact radio source. The presumed VLBI jets are all fairly well aligned with > approx. kiloparsec scale, one sided jets. The fact that the VLBI and large scale jets always lie on the same side of the compact core suggests the same cause for the assymmetric structure on both scales. Dissert. Abstr.

N87-17589 Michigan Univ., Ann Arbor.
SCALE-FREE MODELS OF HIGHLY FLATTENED ELLIPTICAL GALAXIES Ph.D. Thesis
Harold F. Levison 1986 99 p
Avail: Univ. Microfilms Order No. DA8621327

Three surveys (one oblate and two triaxial) of dynamical models of E6 elliptical galaxies were constructed in a flattened isothermal gravitational potential. These models represent a complete survey of all three dimensional shapes possible for these galaxies that are consistent with observations. Observational properties of the models compared with observations of E6 ellipticals in order to constrain the shape of the galaxies. The models were built using Schwarzschild's method of linear programming. The most surprising result is that in most models, the position angle of maximum observed rotation is not orthogonal to the position angle of zero rotation. Only one galaxy (NGC 4261) is known to have minor axis rotation. This indicated that either most elliptical galaxies are oblate or some process in their formation prohibits minor axis rotation. Dissert. Abstr.

N87-17590 Michigan Univ., Ann Arbor.
YELLOW SUPERGIANTS IN OPEN CLUSTERS Ph.D. Thesis
James Robert Sowell 1986 159 p
Avail: Univ. Microfilms Order No. DA8621383

Superluminous giant stars (SLGs) have been reported in young globular clusters in the Large Magellanic Cloud (LMC). These stars appear to be in the post asymptotic giant branch phase of evolution. This program was an investigation of galactis SLG candidates in open clusters, which are more like the LMC young globular clusters. These were chosen because luminosity, mass, and age determination can be made for members since cluster distances and interstellar reddenings are known. Color magnitude diagrams were searched for candidates, using the same selection criteria as for SLGs in the LMC. Classification spectra were obtained of 115 program stars from McGraw-Hill Observatory and of 68 stars from Cerro Tololo Inter-American Observatory in Chile. These stars were visually classified on the MK system using spectral scans of standard stars taken at the respective observations. A total of 62 objects were found to be of high luminosity and to warrant further investigations. Seven stars were monitored over a 90 day period for luminosity variations. These observations were analyzed to measure radial velocities and to detect emission features. Dissert. Abstr.

N87-17591 Rensselaer Polytechnic Inst., Troy, N.Y.
NUMERICAL CALCULATIONS OF RADIATION TRANSPORT IN A DUSTY MEDIUM IN DISK GEOMETRY Ph.D. Thesis
George F. Spagna, Jr. 1986 124 p
Avail: Univ. Microfilms Order No. DA8619998

Both theoretical and observational evidence suggest that nonspherical geometries should be invoked to describe many astrophysical sources. Geometries dominated by considerations of angular momentum are favored by current models of the star formation process. Radiation transport in the two-dimensional coordinates appropriate to disk geometry was studied. The approach used is to recast the transport equation in second-order form by using a series of angular momentums of the radiation field, and by the introduction of a set of auxillary functions dependent on the geometry and on the anisctropy of the radiation field. The resulting system of equations is solved by Newton-Raphson iteration to yield a self-consistent temperature and mean intensity for each point in the disk, under the assumptions of radiative equilibrium and complete isotropy of the radiation field. Detailed angular variations of the local radiation field, and of the emergent intensity are recovered by tracing a set of rays through the disk. This technique was applied to model a set of disk-shaped, quiescent dust clouds, using realistic optical properties for the assumed grain mixture, and using an ambient external radiation field consistent with that observed in the solar neighborhood. Dissert. Abstr.

N87-17592 Harvard Univ., Cambridge, Mass.
THE ASTROPHYSICAL IMPLICATIONS OF WEAKLY INTERACTING, MASSIVE PARTICLES Ph.D. Thesis
David Nathaniel Spergel 1986 201 p
Avail: Univ. Microfilms Order No. DA8620537

The possibility is explored that most of the universe is composed of weakly interacting non-baryonic particles. These particles comprise most of the mass of the galaxy's halo. Some of these particles were captured by the Sun in elastic scattering off of nuclei of the Sun. Once inside the Sun, they are very effective at energy transport. They alter the thermal profile of the Sun, thus reconciling the predicted solar neutrino flux with observations. If they exist, these particles could be detected by low temperature detectors. Dissert. Abstr.

N87-17593*# Stanford Univ., Calif. Dept. of Physics.
A SEARCH FOR RAPIDLY MODULATED EMISSION IN BRIGHT X-RAY SOURCES USING THE HEAO A-1 DATA BASE Final Report
William M. Fairbank 18 Feb. 1987 7 p
(Grant NAG8-490)
(NASA-CR-180148; NAS 1.26:180148) Avail: NTIS HC A02/MF A01 CSCL 03B

A search was performed in the HEAO A-1 Data Base (located at the Naval Research Laboratory in Washington, D.C.) for evidence of rapidly-rotating neutron stars that could be sources of coherent gravitational radiation. A new data analysis algorithm, which was developed, is described. The algorithm was applied to data from observations of Cyg X-2, Cyg X-3, and 1820-30. Upper limits on pulse fraction were derived and reported. Author

N87-17594*# Smithsonian Astrophysical Observatory, Cambridge, Mass.

THE STUDY OF THE PHYSICS OF COMETARY NUCLEI Semiannual Progress Report, 1 Apr. 1985 - 30 Sep. 1986
Fred L. Whipple Feb. 1987 34 p
(Grant NsG-7082)
(NASA-CR-180153; NAS 1.26:180153; SAPR-22; SAPR-23; SAPR-24) Avail: NTIS HC A03/MF A01 CSCL 03B

The numerical calculations of stability for many possible orbits of the double nucleus for P/Holmes showed that the likelihood of such a precollision history was quite high. A number of investigations were made of hypothetical orbits for particles about the asteroid Amphitrite to test for stability. The purpose was to establish more favorable fly-by orbits close to the asteroid for the Galileo missions en-route to Jupiter, reducing the collisional hazards. A statistical study was made of the orbits of long-period comets with small original semi-major axes recently perturbed from the great Opik-Oort Cloud. The results from the space missions to Halley's comet are partially reported in the two papers in the appendices. B.G.

N87-17595*# National Aeronautics and Space Administration, Washington, D.C.
ZHAMANSHIN METEOR CRATER
P. V. Florenskiy and A. I. Dabizha Jan. 1987 136 p Transl. into ENGLISH of the book "Meteoritniy Krater Zhamanshin" Moscow, USSR, Nauka, 1980 p 1-127 Transl. by Kanner (Leo) Associates, Redwood City, Calif.
(Contract NASw-4005)
(NASA-TM-88531; NAS 1.15:88531) Avail: NTIS HC A07/MF A01 CSCL 03B

A historical survey and geographic, geologic and geophysical characteristics, the results of many years of study of the Zhamanshin meteor crater in the Northern Aral region, are reported. From this data the likely initial configuration and cause of formation of the crater are reconstructed. Petrographic and mineralogical analyses are given of the brecciated and remelted rocks, of the zhamanshinites and irgizite tektites in particular. The impact melting, dispersion and quenching processes resulting in tektite formation are discussed. Author

N87-17596*# Smithsonian Astrophysical Observatory, Cambridge, Mass.
THE DYNAMICS AND EVOLUTION OF CLUSTERS OF GALAXIES Semiannual Report, 1 Jul. - 31 Dec. 1986
Margaret Geller and John P. Huchra Jan. 1987 13 p
(Grant NAGw-201)
(NASA-CR-180169; NAS 1.26:180169; SAR-11) Avail: NTIS HC A02/MF A01 CSCL 03B

Research was undertaken to produce a coherent picture of the formation and evolution of large-scale structures in the universe. The program is divided into projects which examine four areas: the relationship between individual galaxies and their environment; the structure and evolution of individual rich clusters of galaxies; the nature of superclusters; and the large-scale distribution of individual galaxies. A brief review of results in each area is provided. B.G.

N87-17539# Rome Univ. (Italy). Dipt. di Fisica.
THE EARLY UNIVERSE
Franchesco Melchiorri, G. DallOglio, P. deBernardis, N. Mandolesi, Silvia Masi, G. Moreno, B. Olivo, and G. Pucacco *In* ESA Proceedings of an ESA Workshop on a Spaceborne Submillimeter Astronomy Mission. A Cornerstone of the ESA Long Term Science Program Aug. 1986 p 33-52 (For primary document see N87-17535 09-88)
Avail: NTIS HC A14/MF A01

N87-17541# Observatoire de Paris-Meudon (France).
SUBMILLIMETER COMETARY SPECTROSCOPY
J. Crovisier *In* ESA Proceedings of an ESA Workshop on a Spaceborne Submillimeter Astronomy Mission. A Cornerstone of the ESA Long Term Science Program Aug. 1986 p 57-65 (For primary document see N87-17535 09-88)
Avail: NTIS HC A14/MF A01

N87-17542# Air Force Geophysics Lab., Hanscom AFB, Mass.
INTERPLANETARY DUST
Stephen D. Price *In* ESA Proceedings of an ESA Workshop on a Spaceborne Submillimeter Astronomy Mission. A Cornerstone of the ESA Long Term Science Program Aug. 1986 p 67-72 (For primary document see N87-17535 09-88)
Avail: NTIS HC A14/MF A01

N87-17543# Observatoire de Marseille (France).
THE INTERSTELLAR MEDIUM AT SUBMM WAVELENGTHS
James Lequeux *In* ESA Proceedings of an ESA Workshop on a Spaceborne Submillimeter Astronomy Mission. A Cornerstone of the ESA Long Term Science Program Aug. 1986 p 73-78 (For primary document see N87-17535 09-88)
Avail: NTIS HC A14/MF A01

N87-17545# Max-Planck-Inst. fuer Radioastronomie, Bonn (West Germany).
INTERSTELLAR DUST
E. Kruegel *In* ESA Proceedings of an ESA Workshop on a Spaceborne Submillimeter Astronomy Mission. A Cornerstone of the ESA Long Term Science Program Aug. 1986 p 93-99 (For primary document see N87-17535 09-88)
Avail: NTIS HC A14/MF A01

N87-17546# California Inst. of Tech., Pasadena.
EXCITATION AND TRANSFER OF SUBMILLIMETER MOLECULAR TRANSITIONS
T. G. Philips *In* ESA Proceedings of an ESA Workshop on a Spaceborne Submillimeter Astronomy Mission. A Cornerstone of the ESA Long Term Science Program Aug. 1986 p 101-106 (For primary document see N87-17535 09-88)
Avail: NTIS HC A14/MF A01

N87-17547# Harvard-Smithsonian Center for Astrophysics, Cambridge, Mass.
INTERSTELLAR CHEMISTRY AND SUBMILLIMETER OBSERVATIONS
Ewine F. vanDishoeck *In* ESA Proceedings of an ESA Workshop on a Spaceborne Submillimeter Astronomy Mission. A Cornerstone of the ESA Long Term Science Program Aug. 1986 p 107-117 (For primary document see N87-17535 09-88)
Avail: NTIS HC A14/MF A01

N87-17548# Chalmers Univ. of Technology, Goeteborg (Sweden). Astrophysics Section.
CIRCUMSTELLAR ENVELOPES AROUND EVOLVED STARS
Peter Wannier *In* ESA Proceedings of an ESA Workshop on a Spaceborne Submillimeter Astronomy Mission. A Cornerstone of the ESA Long Term Science Program Aug. 1986 p 119-127 (For primary document see N87-17535 09-88)
Avail: NTIS HC A14/MF A01

N87-17549# Grenoble Univ. (France).
MOLECULAR ABUNDANCES IN CIRCUMSTELLAR ENVELOPES
A. Omont *In* ESA Proceedings of an ESA Workshop on a Spaceborne Submillimeter Astronomy Mission. A Cornerstone of the ESA Long Term Science Program Aug. 1986 p 129-133 (For primary document see N87-17535 09-88)
Avail: NTIS HC A14/MF A01

N87-17551# Lecce Univ. (Italy). Dept. of Physics.
SOME RESULTS ABOUT LABORATORY DUST ANALYSIS IN THE FIR RANGE
A. Blanco, A. Borghesi, E. Bussoletti, L. Colangeli, S. Fonti, and V. Orofino *In* ESA Proceedings of an ESA Workshop on a Spaceborne Submillimeter Astronomy Mission. A Cornerstone of the ESA Long Term Science Program Aug. 1986 p 141-146 (For primary document see N87-17535 09-88)
Avail: NTIS HC A14/MF A01

N87-17561# Observatorio Astromico Nacional, Guadalajara (Spain). Centro Astronomico de Yebes.

VIBRATIONALLY EXCITED CYANOACETYLENE IN REGIONS OF MASSIVE STAR FORMATION
J. Martin-Pintado, J. Gomez-Gonzalez, A. delRomero, P. Planesas, and V. Bujarrabal *In* ESA Proceedings of an ESA Workshop on a Spaceborne Submillimeter Astronomy Mission. A Cornerstone of the ESA Long Term Science Program Aug. 1986 p 191-194 (For primary document see N87-17535 09-88)
(Contract CAYCYT-477/84)
Avail: NTIS HC A14/MF A01

91 LUNAR AND PLANETARY EXPLORATION

Includes planetology; and manned and unmanned flights. For spacecraft design or space stations see *18 Spacecraft Design, Testing and Performance.*

N87-17597 California Univ., Los Angeles.
MAGMATIC DIFFERENTIATION IN PARTIALLY MOLTEN SYSTEMS: APPLICATIONS TO THE MOON AND THE PALISADES SILL Ph.D. Thesis
David Noyes Shirley 1986 202 p
Avail: Univ. Microfilms Order No. DA8621134

The primary mechanism by which igneous systems differentiate is through partitioning of elements between liquid and solid phases and the subsequent separation of those phases. Many physical processes that produce this type of differentiation are understood in only a qualitative manner, especially in systems that are mostly solid rather than liquid. This work quantitatively models differentiation in partially molten systems and compares the results to experimental data. Such comparisons provide quantitative constraints on the natural differentiation processes and in some cases provide estimates of physical parameters that operated in the natural systems. The first problem covered is the early global differentiation of the Moon. The other topic covered is the process of compaction of partially molten igneous cumulates driven by the density difference between the liquid and solid phases. A theoretical examination of the physical process of compaction is studied, and a detailed geochemical study of the Palisades Sill was performed. Comparisons between the results of the modeling and the observations on the sill are then used to constrain the differentiation process. Dissert. Abstr.

N87-17598*# National Aeronautics and Space Administration. Goddard Inst. for Space Studies, New York, N.Y.
THE JOVIAN ATMOSPHERES
Michael Allison, ed. and Larry D. Travis, ed. Oct. 1986 129 p Conference held in New York, N.Y., 6-8 May 1985 Submitted for publication
(NASA-CP-2441; NAS 1.55:2441) Avail: NTIS HC A07/MF A01 CSCL 84B

A conference on the atmosphere of Jupiter produced papers in the areas of thermal and ortho-para hydrogen structure, clouds and chemistry, atmospheric structure, global dynamics, synoptic features and processes, atmospheric dynamics, and future spaceflight opportunities. A session on the atmospheres of Uranus and Neptune was included, and the atmosphere of Saturn was discussed in several papers. For individual titles, see N87-17599 through N87-17647.

N87-17599*# National Aeronautics and Space Administration. Goddard Space Flight Center, Greenbelt, Md.
PARA HYDROGEN EQUILIBRATION IN THE ATMOSPHERES OF THE OUTER PLANETS
Barney J. Conrath *In* NASA. Goddard Inst. for Space Studies The Jovian Atmospheres Oct. 1986 p 5-18 (For primary document see N87-17598 09-91)
Avail: NTIS HC A07/MF A01 CSCL 84B

The thermodynamic behavior of the atmospheres of the Jovian planets is strongly dependent on the extent to which local thermal equilibration of the ortho and para states of molecular hydrogen is achieved. Voyager IRIS data from Jupiter imply substantial departures of the para hydrogen fraction from equilibrium in the upper troposphere at low latitudes, but with values approaching equilibrium at higher latitudes. Data from Saturn are less sensitive to the orth-para ratio, but suggest para hydrogen fractions near the equilibrium value. Above approximately the 200 K temperature level, para hydrogen conversion can enhance the efficiency of convection, resulting in a substantial increase in overturning times on all of the outer planets. Currently available data cannot definitively establish the ortho-para ratios in the atmospheres of Uranus and Neptune, but suggest values closer to local equilibrium than to the 3.1 normal ratio. Modeling of sub-millimeter wavelength measurements of these planets suggest thermal structures with frozen equilibrium lapse rates in their convective regions. Author

N87-17600*# Jet Propulsion Lab., California Inst. of Tech., Pasadena.
SPATIAL AND TEMPORAL VARIABILITY OF INFRARED-OBSERVABLE PROPERTIES OF THE JOVIAN ATMOSPHERE: A PARTIAL SURVEY
Glenn S. Orton *In* NASA. Goddard Inst. for Space Studies The Jovian Atmospheres Oct. 1986 p 19-25 (For primary document see N87-17598 09-91)
Avail: NTIS HC A07/MF A01 CSCL 84B

Examination of infrared characteristics of the Jovian atmosphere are made using Voyager IRIS mapping from 1979, groud based scanning from 1979-1983, and ground based mapping from 1983 to the present. In general, there is a strong correlation between tropospheric thermal properties and the visual cloud albedo for all observations. The Voyager IRIS maps show no strong evidence for day/night differences. Temperature differences diminish with depth in the troposphere. Temporal changes over several weeks indicate a high correlation between thermal and visual properties, although no changes in the distribution of para H2 and ortho H2 are seen. Stratospheric banded organization is different from the troposphere, and there is a temperature enhancement near the north magnetic pole. The spatial distributions of ammonia gas and ammonia ice absorption are different. Stratospheric temperatures exhibit seasonal hemispheric asymmetry. Other temperature changes at and below the 150-mb level correlate with changes in the Jovian visual structure. The stratospheric temperature field is uncorrelated with visual features or temperatures below the 150-mb level. Elevated temperatures are observed near both north and south magnetic pole positions. Both the meridional positions and the relative intensities of stratospheric banded organization change significantly, especially after 1982. Ground based mapping confirms a correlation between temperatures and various measures of cloud distribution. Complex and unexpected characteristics are observed in the stratospheric temperature field; these include dramatic temporal changes on short time scales. Author

N87-17601*# Arizona Univ., Tucson.
MODELING THE TEMPORAL AND SPATIAL VARIATIONS OF THE VERTICAL STRUCTURE OF JUPITER'S ATMOSPHERE USING OBSERVATIONS OF THE 3-0 HYDROGEN QUADRUPOLE LINES Abstract Only
C. C. Cunningham, D. M. Hunten, and M. G. Tomasko *In* NASA. Goddard Inst. for Space Studies The Jovian Atmospheres Oct. 1986 p 26-28 Submitted for publication (For primary document see N87-17598 09-91)
Avail: NTIS HC A07/MF A01 CSCL 84B

An observational program was established in 1983 to monitor the spatial and temporal variations in the Jovian atmosphere over short and long time scales. The program involves tracking several different longitudes as they rotate around the planet from one limb to another. This tracking experiment was done at many different wavelengths including the 3-0 S(1) and S(0) hydrogen quadrupole lines as well as several broad band methane absorptions. The June 1983 hydrogen quadrupole data was reduced and equivalent widths were measured for approximately 25 east-west positions across the planet at 7 different latitudes for both

wavelengths. The data for the South Tropical Zone (20 deg. S) was modeled extensively and the effects of the various model parameters on the value of the calculated equivalent widths of both lines was measured as a longitude rotated from the east (or morning) limb to the west (or evening) limb. The value of the equivalent width is also quite sensitive to the height of the NH3 cloud top and to the value used for the single scattering albedo. A combination of these parameters changing on a diurnal time scale could also explain these observations. This gradual increase from one limb to the other appears in the data for both the North and South Equatorial Belts as well as the equatorial region and the North Tropical Zone. Models that used only normal hydrogen and models that used only equilibrium hydrogen were studied.
Author

N87-17602*# Texas Univ., Austin.
CHANGES IN SATURN'S SOUTH-TEMPERATE HAZE DISTRIBUTION DURING THE SUMMER OF 1973-1980 Abstract Only
L. Trafton *In* NASA. Goddard Inst. for Space Studies The Jovian Atmospheres Oct. 1986 p 29-31 Full version announced in IAA as A86-15594 (For primary document see N87-17598 09-91)
Avail: NTIS HC A07/MF A01 CSCL 84B

Attention is given to the results of a long term monitoring study of Saturn's H2 quadrupole and CH4 band absorptions outside the equatorial zone, over an interval of half a Saturn year that covers most of the perihelion half of Saturn's elliptical orbit (which is approximately bounded by the equinoxes). Marked long term changes are noted in the CH4 absorption, accompanied by weakly opposite changes in the H2 absorption. Seasonal changes are inferred on the basis of temporal variations in absorption. Spatial measurements have also been made in the 6450 A NH3 band since the 1980 equinox.
Author

N87-17603*# New Mexico State Univ., Las Cruces.
SEASONAL NORTH-SOUTH ASYMMETRY IN SOLAR RADIATION AT THE TOP OF JUPITER'S ATMOSPHERE
R. Beebe and R. Suggs *In* NASA. Goddard Inst. for Space Studies The Jovian Atmospheres Oct. 1986 p 32-33 Full version announced in IAA as A86-45889 (For primary document see N87-17598 09-91)
Avail: NTIS HC A07/MF A01 CSCL 84B

A selected set of planetocentric latitudes is used in calculations of the seasonal solar radiation pattern incident on top of the Jovian atmosphere, thereby demonstrating the combined effect of solar distance and declination. Attention is given to hemispheric asymmetries in the Jovian atmosphere's average zonal winds and cloud system morphologies. Marked hemispheric asymmetries are noted in the cloud morphology and in the magnitude and latitudinal position of eastward and westward maxima in the average zonal winds, suggesting seasonal forcing on the order of magnitude presently considered. Supporting observations by Voyagers 1 and 2 are cited.
Author

N87-17604*# California Inst. of Tech., Pasadena.
THERMAL BALANCE OF THE ATMOSPHERES OF JUPITER AND URANUS
A. J. Friedson and A. P. Ingersoll *In* NASA. Goddard Inst. for Space Studies The Jovian Atmospheres Oct. 1986 p 34-40 (For primary document see N87-17598 09-91)
Avail: NTIS HC A07/MF A01 CSCL 84B

Two-dimensional, radiative-convective-dynamical models of the visible atmospheres of Jupiter and Uranus are presented. Zonally-averaged temperatures and heat fluxes are calculated numerically as functions of pressure and latitude. In addition to radiative heat fluxes, the dynamical heat flux due to large-scale baroclinic eddies is included and is parametrized using a mixing length theory which gives heat fluxes similar to those of Stone. The results for Jupiter indicate that the internal heat flow is non-uniform in latitude and nearly balances the net radiative flux leaving the atmosphere. The thermal emission is found to be uniform in latitude in agreement with Pioneer and Voyager observations. Baroclinic eddies are calculated to transport only a small amount of the meridional heat flow necessary to account for the uniformity of thermal emission with latitude. The bulk of the meridional heat transfer is found to occur very deep in the stable interior of Jupiter as originally proposed by Ingersoll and Porco. The relative importance of baroclinic eddies vs. internal heat flow in the thermal balance of Uranus depends on the ratio of emitted thermal power to absorbed solar power. The thermal balance of Uranus is compared to that of Jupiter for different values of this ratio.
Author

N87-17605*# National Aeronautics and Space Administration. Goddard Space Flight Center, Greenbelt, Md.
WATER VAPOR IN JUPITER'S ATMOSPHERE
G. L. Bjoraker (Arizona Univ., Tucson), H. P. Larson, and V. G. Kunde *In* NASA. Goddard Inst. for Space Studies The Jovian Atmospheres Oct. 1986 p 48-52 (For primary document see N87-17598 09-91)
Avail: NTIS HC A07/MF A01 CSCL 84B

High spectral resolution observations of Jupiter at 2.7 and 5 microns acquired from the Kuiper Airborne Observatory were used to infer the vertical distribution of H2O between 0.7 and 6 bars. The H2O mole fraction, qH2O, is saturated for $P<2$ bars, qH2O = 4x.000001 in the 2 to 4 bar range and it increases to 3x.00001 at 6 bars where $T = 288$ K. The base of the 5 micron line formation region is determined by pressure-induced H2 opacity. At this deepest accessible level, the O/H ratio in Jupiter is depleted by a factor of 50 with respect to the solar atmosphere. High spatial resolution Voyager IRIS spectra of Jupiter's North Tropical Zone, Equatorial Zone, and Hot Spots in the North and South Equatorial Belt were analyzed to determine the spatial variation of H2O across the planet. The column abundance of H2O above the 4 bar level is the same in the zones as in the SEB Hot Spots, about 20 cm-amgt. A cloud model for Jupiter's belts and zones was developed in order to fit the IRIS 5 micron spectra. An absorbing cloud located at 2 bars whose 5 micron optical thickness varies between 1 in the Hot Spots and 4 in the coldest zones satisfactorily matches the IRIS data.
Author

N87-17606*# California Univ., Berkeley.
VLA OBSERVATIONS OF JUPITER AT 1.3 - 20 cm WAVELENGTHS
Imke dePater *In* NASA. Goddard Inst. for Space Studies The Jovian Atmospheres Oct. 1986 p 53-55 (For primary document see N87-17598 09-91)
Avail: NTIS HC A07/MF A01 CSCL 84B

In order to study the vertical distribution of ammonia as a function of Jovian latitude, high resolution images were obtained with the VLA at 1.3, 2, 6 and 20 cm wavelengths. Although the interpretation of the data is quite complicated due to Jupiter's synchrotron radiation, which in fact is the dominant source of radiation at 29 cm, the belt-zone structure is clearly present at 2 and 6 cm wavelengths. At 1.3 cm near the center of the ammonia band, the structure is less pronounced, and at 20 cm it is absent. The data is currently being fitted with model atmosphere calculations. Since one probes in and through the visible cloud layers at these wavelengths (temperatures of 135 to 400 K), and the opacity is likely all provided by ammonia gas, a detailed vertical distribution of this gas can be obtained as a function of Jovian latitude. This ought to give insight in the formation processes of the white cloud layers in the zones and their absence above the belts.
Author

N87-17607*# Arizona Univ., Tucson.
THE VERTICAL STRUCTURE OF JUPITER'S EQUATORIAL AND TROPICAL REGIONS Abstract Only
P. H. Smith *In* NASA. Goddard Inst. for Space Studies The Jovian Atmospheres Oct. 1986 p 56-57 Full version announced in IAA as A86-37281 (For primary document see N87-17598 09-91)
Avail: NTIS HC A07/MF A01 CSCL 84B

The equatorial and tropical regions of Jupiter are presently treated in light of an inhomogeneous atmospheric model that encompasses both polarizing aerosols and methane gas, in keeping with Pioneer polarimetry and photometry data as well as the methane band data obtained by West (1979). The relative strengths of weak and strong methane bands are addressed by a

two-cloud model with overlying stratospheric haze. For all the regions considered, the best fit for polarization measurements is a negatively polarizing ammonia cloud beneath a positively polarizing haze. Unlike the nearby features, the equatorial region and the Great Red Spot have a negative polarization at 80-deg phase angle, implying less gas above the clouds in these regions. Author

N87-17608*# National Aeronautics and Space Administration. Goddard Inst. for Space Studies, New York, N.Y.
VERTICAL CLOUD STRUCTURE MODELS FOR THE NTRZ EQZ, SEB AND STRZ OF JUPITER
B. E. Carlson and R. D. Cess (State Univ. of New York, Stony Brook) *In its* The Jovian Atmospheres Oct. 1986 p 58-63 (For primary document see N87-17598 09-91)
Avail: NTIS HC A07/MF A01 CSCL 84B

Latitude-dependent models of the vertically inhomogeneous Jovian cloud structure are presented. The models assume an atmospheric composition with (CH4)/(H2) = 2.0 x .003, (He)/(H2) = 0.11 and (NH3)/(H2) = 2.0 x .0004 consistent with the Voyager IRIS measurements and employ refractive indices appropriate for ammonia ice particles and a photochemical stratospheric aerosol layer. The free parameters of the models are determined by fitting the results of multiple, scratching calculations to the near-infrared center and limb spectra of Clark and McCord and the center-to-limb 6190, 6350, 7250, 7500, 8900 and 9500 A photometric measurements of West. The resulting synthetic center-to-limb profiles are in excellent agreement with the observations. Of the regions studied the tropical zones are the most similar, with the observed differences explained by variations in the vertical extent of the cloudy layers. The Equatorial Zone is a unique region with denser NH3 clouds than either of the tropical zones. At visible and near-infrared wavelengths the belt-zone contrasts can be explained by opacity differences. The optical depth of the stratospheric aerosol layer is larger in a belt, while the tropospheric clouds are deeper and thinner. Author

N87-17609*# National Aeronautics and Space Administration. Goddard Space Flight Center, Greenbelt, Md.
STUDY OF THE AMMONIA ICE CLOUD LAYER IN THE NORTH TROPICAL ZONE OF JUPITER FROM THE INFRARED INTERFEROMETRIC EXPERIMENT ON VOYAGER
William A. Shaffer, Robert E. Samuelson, and Barney J. Conrath *In* NASA. Goddard Inst. for Space Studies The Jovian Atmospheres Oct. 1986 p 64-70 (For primary document see N87-17598 09-91)
Avail: NTIS HC A07/MF A01 CSCL 84B

An average of 51 Voyager 1 IRIS spectra of Jupiter's North Tropical Zone was analyzed to infer the abundance, vertical extent, and size distribution of the particles making up the ammonia cloud in this region. It is assumed that the cloud base coincides with the level at which 100% saturation of ammonia vapor occurs. The vertical distribution of particulates above this level is determined by assuming a constant total ammonia mixing ratio and adjusting the two phases so that the vapor is saturated throughout the cloud. A constant scaling factor then adjusts the base number density. A radiative transfer program is used that includes the effects of absorption and emission of all relevant gases as well as anisotropic scattering by cloud particles. Mie scattering from a gaussian particle size distribution is assumed. The vertical thermal structure is inferred from a temperature retrieval program that utilizes the collision induced S(0) and S(1) molecular hydrogen lines between 300 and 700.cm, and the 1304.cm methane band. Author

N87-17610*# Arizona Univ., Tucson.
CONSTRAINTS ON THE COMPOSITION OF JUPITER'S STRATOSPHERIC AEROSOLS FROM ULTRAVIOLET PHOTOMETRY Abstract Only
M. G. Tomasko, E. Karkoschka, and S. Martinek (Pacific-Sierra Research Corp., Los Angeles, Calif.) *In* NASA. Goddard Inst. for Space Studies The Jovian Atmospheres Oct. 1986 p 71-72 Full version announced in IAA as A86-37278 (For primary document see N87-17598 09-91)
Avail: NTIS HC A07/MF A01 CSCL 84B

The absolute reflectivity of Jupiter has been obtained in 50 A-wide regions centering on 0.221, 0.233, 0.252, and 0.330 microns from three series of IUE satellite spectra taken in November 1979. The data indicate a strong decrease in reflectivity for latitudes greater than about 30 deg, in keeping with Voyager measurements. An additional 24 spectra were also obtained in a west-east series along the equator, as well as near 40 deg N latitude. These data favor models in which the haze particles have effective radii within a factor of 2 of 0.2 microns. Near the equator, the haze aerosols produce much less absorption than near 40 deg N; the aerosol distributions and optical properties derived are noted to be more dependent on the assumed location and reflectivity of the top of the tropospheric cloud. Author

N87-17611*# Rice Univ., Houston, Tex.
THE DISTRIBUTION OF ATOMIC HYDROGEN IN THE JOVIAN ATMOSPHERE
R. M. Killen and J. W. Chamberlain *In* NASA. Goddard Inst. for Space Studies The Jovian Atmospheres Oct. 1986 p 73-76 (For primary document see N87-17598 09-91)
Avail: NTIS HC A07/MF A01 CSCL 84B

An analysis is presented of the Voyager and IUE lyman alpha spectra of the Jovian equatorial emission in which was derived a zonal asymmetry in the hydrogen column abundance. Using two estimates of the fraction of Lyman alpha which is due to direct excitation by charged particle precipitation from the ionosphere, upper and lower limits were derived to the H column abundance within and without the perturbed region. That the asymmetry in H abundance may be due to localized heating near the homopause with a consequent rise in scale height is shown. The derived exospheric temperature remains fairly constant with longitude. The required additional heat input over the bulge region, 0.02 erg/cm/s, is supplied by an additional flux of magnetospheric electrons due to Jupiter's magnetic anomaly. Author

N87-17612*# Centre National de la Recherche Scientifique, Meudon-Bellevue (France).
SPATIAL VARIATION OF THE THERMAL STRUCTURE OF JUPITER'S ATMOSPHERE
C. Bezanger, B. Bezard, and D. Gautier *In* NASA. Goddard Inst. for Space Studies The Jovian Atmospheres Oct. 1986 p 79-82 (For primary document see N87-17598 09-91)
Avail: NTIS HC A07/MF A01 CSCL 84B

The radiative seasonal model described by Bezard and Gautier for the case of Saturn was adapted to Jupiter. That the atmosphere is radiatively controlled above the 500 mb pressure level and that the temperature at the radiative-convective boundary level is constant for all latitudes is assumed. An internal heat source and absorption by methane and aerosols contribute to atmospheric heating. Absorption by aerosols was adjusted to give a planetary Bond albedo equal to 0.343. Despite Jupiter's low obliquity, the model predicts seasonal variations of temperature of several degrees for the 1 mb pressure level at mid-latitude regions. Author

N87-17613*# Arizona Univ., Tucson. Lunar and Planetary Lab.
THE SINGLE SCATTERING PHASE FUNCTIONS OF JUPITER'S CLOUDS
L. R. Doose, M. G. Tomasko, and N. D. Castillo *In* NASA. Goddard Inst. for Space Studies The Jovian Atmospheres Oct. 1986 p 83-93 (For primary document see N87-17598 09-91)
Avail: NTIS HC A07/MF A01 CSCL 84B

The determination of the single scattering phase functions of Jupiter's clouds and a thin upper haze by Tomasko et al. was refined and extended to seven latitudes in blue and red light. The phase function is well-constrained by the Pioneer 10 and 11 photometric data sets. Multiple scattering models were computed to match the limb darkening at each latitude at up to 15 phase angles from 12 deg to 151 deg. Ground-based observations were used for absolute calibration and to extend the data to lower phase angles. The phase functions were parameterized using the double Henyey-Greenstein function. The three Henyey-Greenstein

parameters and the single scattering albedo were determined using a non-linear least squares method for the haze and the clouds below. The phase functions derived for the northen zone and belt are remarkably similar to the phase functions of the corresponding regions in the south, with most of the differences in brightness of the northern and southern features resulting from minor differences in single scattering albedo. Analysis of the Equatorial Region is complicated by the presence of numerous small features, but the phase function required is generally similar to that seen in the more homogeneous regions. Details of the phase functions of the haze and clouds are presented, and the differences between the cloud phase functions at low and high latitudes in red and blue light are discussed. Author

N87-17614*# Observatoire de Paris-Meudon (France).
ENHANCED ACETYLENE EMISSION NEAR THE NORTH POLE OF JUPITER Abstract Only
Pierre Drossart, Bruno Bezard, Therese Encrenaz, Sushil Atreya (Michigan Univ., Ann Arbor), John Lacy (Texas Univ., Austin), Eugene Serabyn (California Univ., Berkeley), and Alan Tokunaga (Hawaii Univ., Honolulu) *In* NASA. Goddard Inst. for Space Studies The Jovian Atmospheres Oct. 1986 p 94 Full version announced in IAA as A86-47864 (For primary document see N87-17598 09-91)
Avail: NTIS HC A07/MF A01 CSCL 84B

The present paper is concerned with observations of acetylene fundamental and hot band vibrational emission lines from the planet Jupiter. It is pointed out that the observation of a polar bright spot in the atmosphere of Jupiter is characterized by an enhancement in the individual lines of C2H2 which can be interpreted as an enhancement in the acetylene abundance. However, a purely thermal effect, on non-LTE phenomena cannot be excluded. The intensity of the observed hot band lines is also consistent with either hypothesis. The reported observations were performed with a cooled Fabry-Perot Grating Spectrometer (FPGS). Observations and instrumentation are considered in detail along with the calculation of synthetic spectra on the basis of a line-by-line computation, and the interpretation of the obtained data. Author

N87-17615*# National Aeronautics and Space Administration. Goddard Space Flight Center, Greenbelt, Md.
TWO MICRON QUADRUPOLE LINE EMISSION OF H2 FROM THE JOVIAN AURORAL ZONE
S. Kim and W. Maguire *In* NASA. Goddard Inst. for Space Studies The Jovian Atmospheres Oct. 1986 p 95-98 (For primary document see N87-17598 09-91)
Avail: NTIS HC A07/MF A01 CSCL 84B

Energetic electron bombardment of the H2 atmosphere in the Jovian auroral zone was studied using a theoretical model for the vibrational-ratational excitation processes. A non-relativistic electron energy deposition program originally developed by Peterson et al. was used. Assuming an incident energy electron spectrum from IUE observations, the calculated intensities of the two micron quadrupole lines from the Jovian auroral zone are shown to be comparable to the intensities of infrared objects in the Orion nebula. Jupiter is fairly dark in the 2 to 2.5 micron spectral range because of strong absorption of cH4 and NH3 vibrational-rotational bands. Consequently, assuming no significant decrease in Jovian auroral activity since the Voyager encounter with Jupiter in 1979, the two micron quadrupole emission of H2 may be observable by ground-based telescope through the two micron atmospheric window. Author

N87-17616*# Arizona Univ., Tucson. Lunar and Planetary Lab.
BROWN DWARFS AND JOVIAN PLANETS: A COMPARISON Abstract Only
J. I. Lunine, W. B. Hubbard, and M. Marley *In* NASA. Goddard Inst. for Space Studies The Jovian Atmospheres Oct. 1986 p 99-101 (For primary document see N87-17598 09-91)
Avail: NTIS HC A07/MF A01 CSCL 84B

The recent detection of a subluminous companion to the M dwarf star VB8 has renewed interest in the characteristics of objects spanning the mass range from Jupiter to hydrogen burning stars. Atmospheric and interior models were constructed for objects in this mass regime, up to 30 Jupiter masses, with emphasis on understanding the relationship of brown dwarfs such as the VB8 companion to the better-studied Jovian planets. The atmospheric model solves the equation of radiative transfer assuming frequency dependent molecular opacity sources H2, He, H2O, CO, and CH4 which are important by virtue of the high cosmic abundance of their constituent atoms. Condensation of cosmochemically important materials, iron and silicates, in the atmosphere is possible, and the effect of such grains as opacity sources is assessed. The luminosity of the object is presumed due to degenerate cooling following a collapse phase and possibly deuterium burning and an interior model is constructed using as an outer boundary condition the temperature and pressure level at which the atmosphere becomes convective. The interior model is analogous to Jupiter, with a large liquid metallic-hydrogen core and a thinner molecular-hydrogen envelope. The oxidation state of carbon in the outer envelope of a brown dwarf of similar age to Jupiter is a function of the object's mass. This makes the wavelength dependence of the atmospheric opacity sensitive to the carbon to oxygen ratio, since the abundance of the primary source of molecular opacity, H2O, decreases as more oxygen is tied up as CO. Author

N87-17617*# Lowell Observatory, Flagstaff, Ariz.
A POSSIBLE DEUTERIUM ANOMALY: IMPLICATIONS OF THE CH3D/CH4 MIXING RATIOS IN THE ATMOSPHERES OF JUPITER, SATURN, AND URANUS
Barry L. Lutz, Catherine deBergh (Centre National de la Recherche Scientifique, Marseilles, France), and Tobias Owen (State Univ. of New York, Stony Brook) *In* NASA. Goddard Inst. for Space Studies The Jovian Atmospheres Oct. 1986 p 102-108 (For primary document see N87-17598 09-91)
Avail: NTIS HC A07/MF A01 CSCL 84B

Observations of CH3D in the atmospheres of the outer planets provide a test of the theory of deuterium fractionation equilibrium in the formation and evolution of these planets. Recent measurements of the CH3D/CH4 mixing ratios made for Saturn and Uranus are presented and intercompared with current values of Jupiter, illustrating large differences between the planets. Their implied D/H ratios are compared to D/H ratios derived from measurements of HD/H2; and, in the cases of Jupiter and Saturn, they may be incompatible. Implications of these comparisons are discussed in terms of the deuterium fractionation chemistry and possible enrichments of deuterium in the core ices of the planets. Author

N87-17618*# State Univ. of New York, Stony Brook.
THE ABUNDANCES OF ETHANE TO ACETYLENE IN THE ATMOSPHERES OF JUPITER AND SATURN Abstract Only
K. S. Noll, R. F. Knacke, A. T. Tokunaga (Hawaii Univ., Honolulu), J. H. Lacy (Texas Univ., Austin), S. Beck (Northeastern Univ., Boston, Mass.), and E. Serabyn (California Univ., Berkeley) *In* NASA. Goddard Inst. for Space Studies The Jovian Atmospheres Oct. 1986 p 109 Full version announced in IAA as A86-37280 (For primary document see N87-17598 09-91)
Avail: NTIS HC A07/MF A01 CSCL 84B

The present determination of the stratospheric abundances of ethane and acetylene on Jupiter and Saturn on the basis of IR spectra near 780/cm uses atmospheric models whose thermal and density profiles have constant mixing ratios. The ratio of ethane to acetylene is noted to be insensitive to model atmosphere assumptions; it is 55 + or - 31 for Jupiter and 23 + or - 12 where model mixing ratios are uniform. Atmospheric model density profiles adapted from theoretical photochemical models are noted to also yield a higher ethane/acetylene ratios for Jupiter. Author

N87-17619*# Washington Univ., St. Louis, Mo.
A DETECTED FEATURE AT THE EXPECTED WAVELENGTH FOR THE HD R5(0) LINE IN JUPITER'S AND URANUS' ATMOSPHERES Abstract Only
Wm. Hayden Smith, William Schempp, and William Macy (Lockheed Missiles and Space Co., Palo Alto, Calif.) *In* NASA. Goddard Inst. for Space Studies The Jovian Atmospheres Oct. 1986 p 110

(For primary document see N87-17598 09-91)
(Grants NsG-7334; NSF 83-03108)
Avail: NTIS HC A07/MF A01 CSCL 84B

A feature was detected at the expected wavelength for the HD R5(0) line in Jupiter's and Uranus' atmospheres. An upper limit for Neptune was also found. Added to the earlier detection of a similar feature for Saturn, it is proposed that all evidence from this type of measurement can be interpreted as arising from a D/H ratio of about .0004 for all the major planets. This value is not in agreement with measurements from CH3D transitions, and is at least fifty times the accepted interstellar medium value of 5 x .000001, implying deuterium enhancement in the solar system via fractionation in the proto-solar nebula. Author

N87-17620*# Georgia Inst. of Tech., Atlanta.
LABORATORY MEASUREMENTS OF MICROWAVE ABSORPTION FROM GASEOUS ATMOSPHERIC CONSTITUENTS UNDER CONDITIONS FOR THE OUTER PLANETS
Paul G. Steffes *In* NASA. Goddard Inst. for Space Studies The Jovian Atmospheres Oct. 1986 p 111-116 (For primary document see N87-17598 09-91)
Avail: NTIS HC A07/MF A01 CSCL 84B

Quite often the interpretive work on the microwave and millimeter-wave absorption profiles, which are inferred from radio occultation measurements or radio astronomical observations of the outer planets, employs theoretically-derived absorption coefficients to account for contributions to the observed opacity from gaseous constituents. Variations of the actual absorption coefficients from those which are theoretically derived, especially under the environmental conditions characteristic of the outer planets, can result in significant errors in the inferred abundances of the absorbing constituents. The recognition of the need to make laboratory measurements of the absorptivity of gases such as NH3, CH4, and H2O in a predominantly H2 atmosphere, under temperature and pressure conditions simulating the outer planets' atmospheres, and at wavelengths corresponding to both radio occultation and radio astronomical observations, has led to the development of a facility capable of making such measurements at Georgia Tech. The laboratory measurement system, the measurement techniques, and the proposed experimental regimen for Winter 1985 are described. Author

N87-17621*# National Aeronautics and Space Administration. Goddard Space Flight Center, Greenbelt, Md.
GLOBAL DYNAMICS AND THERMAL STRUCTURE OF JUPITER'S ATMOSPHERE Abstract Only
F. M. Flasar *In* NASA. Goddard Inst. for Space Studies The Jovian Atmospheres Oct. 1986 p 119-123 Full version announced in IAA as A86-37282 (For primary document see N87-17598 09-91)
Avail: NTIS HC A07/MF A01 CSCL 84B

Voyager flyby observations have yielded the first detailed maps of wind and temperature fields in the Jupiter atmosphere; these data indicate that Jupiter's zonal currents violate the barotropic instability criterion if they extend only a few scale heights below the cloud tops. Microwave observations at mm and cm wavelengths have probed the atmosphere down to a level of about 7 bars, thereby constraining horizontal and vertical thermal structure in a region of the atmosphere about which little was known. Temporal variations in the temperature field suggest that dynamical processes may be important in the establishment of tropopause structure on short time scales. Ground-based and Voyager observations have also indicated a hemispheric asymmetry in temperature in the upper stratosphere. Author

N87-17622*# Wisconsin Univ., Madison.
JUPITER: NEW ESTIMATES OF MEAN ZONAL FLOW AT THE CLOUD LEVEL Abstract Only
Sanjay S. Limaye *In* NASA. Goddard Inst. for Space Studies The Jovian Atmospheres Oct. 1986 p 124-128 Full version announced in IAA as A86-37284 (For primary document see N87-17598 09-91)
Avail: NTIS HC A07/MF A01 CSCL 84B

In order to reexamine the magnitude differences of the Jovian atmosphere's jets, as determined by Voyager 1 and 2 images, a novel approach is used to ascertain the zonal mean east-west component of motion. This technique is based on digital pattern matching, and is applied on pairs of mapped images to yield a profile of the mean zonal component that reproduces the exact locations of the easterly and westerly jets between + and 60 deg latitude. Results were obtained for all of the Voyager 1 and 2 cylindrical mosaics; the correlation coefficient between Voyagers 1 and 2 in mean zonal flow between + and - 60 deg latitude, determined from violet filter mosaics, is 0.998. Author

N87-17623*# Wisconsin Univ., Madison.
CLOUD-TOP MERIDIONAL MOMENTUM TRANSPORTS ON SATURN AND JUPITER
L. A. Sromovsky, H. E. Revercomb, and R. J. Krauss *In* NASA. Goddard Inst. for Space Studies The Jovian Atmospheres Oct. 1986 p 129-143 (For primary document see N87-17598 09-91)
Avail: NTIS HC A07/MF A01 CSCL 84B

Cloud-tracked wind measurements reported by Sromovsky et al. were analyzed to determine meridional momentum transports in Saturn's northern middle latitudes. Results are expressed in terms of eastward and northward velocity components (u and v), and eddy components u and v. At most latitudes between 13 and 44 deg N (planetocentric), the transport by the mean flow ($\langle u \rangle \langle v \rangle$) is measurably southward, tending to support Saturn's large equatorial jet, and completely dominating the eddy transport. Meridional velocities are near zero at the peak of the relatively weak westward jet; along the flanks of that jet, measurements indicate divergent flow out of the jet. In this region the dominant eddy transport ($\langle u'v' \rangle$) is northward on the north side of the jet, but not resolvable on the south side. Eddy transports at most other latitudes are not significantly different from measurement error. The conversion of eddy kinetic energy to mean kinetic energy, indicated by the correlation between $\langle u'v' \rangle$ and $d\langle y \rangle / dy$ (where y is meridional distance) is clearly smaller than various values reported for Jupiter, and not significantly different from zero. Both Jovian and Saturnian results may be biased by the tendency for cloud tracking to favor high contrast features, and thus may not be entirely representative of the cloud level motions as a whole. Author

N87-17624*# National Aeronautics and Space Administration. Marshall Space Flight Center, Huntsville, Ala.
CONVECTIVE FORCING OF GLOBAL CIRCULATIONS ON THE JOVIAN PLANETS
David H. Hathaway *In* NASA. Goddard Inst. for Space Studies The Jovian Atmospheres Oct. 1986 p 144-155 (For primary document see N87-17598 09-91)
Avail: NTIS HC A07/MF A01 CSCL 84B

Examples of convection in rotating layers are presented to illustrate how convection can drive global circulations on the Jovian planets. For rapid rotation the convective motions become largely two-dimensional and produce Reynold stresses which drive large scale flows. The initial tendency is to produce a prograde equatorial jet and a meridional circulation which is directed toward the poles in the surface layers. Fully nonlinear numerical simulations for the slowly rotating solar convection zone show that the meridional circulation does not reach the poles. Instead a multicellular meridional circulation is produced which has a downward flowing branch in the mid-latitudes. For more rapidly rotating objects such as Jupiter and Saturn this meridional circulation may consist of a larger number of cells. Axisymmetric convective models then show that prograde jets form at the downflow latitudes. A nonlinear numerical simulation of convection in a prograde jet is presented to illustrate the interactions which occur between convection and these jets. Without rotation the convection removes energy and momentum from the jet. With rotation the convection feeds energy and momentum into the jet. Author

N87-17625*# California Inst. of Tech., Pasadena.
CONVECTION WITHOUT EDDY VISCOSITY: AN ATTEMPT TO MODEL THE INTERIORS OF GIANT PLANETS
A. P. Ingersoll *In* NASA. Goddard Inst. for Space Studies The Jovian Atmospheres Oct. 1986 p 156-162 (For primary document

see N87-17598 09-91)
Avail: NTIS HC A07/MF A01 CSCL 84B

In the theory of hydrostatic quasi-geostrophic flow in the Earth's atmosphere the principal results do not depend on the eddy viscosity. This contrasts with published theories of convection in deep rotating fluid spheres, where the wavelength of the fastest growing disturbance varies as E sup 1/3, where E, the Ekman number, is proportional to the eddy viscosity. A new theory of quasi-columnar motions in stably stratified fluid spheres attempts to capture the luck of the meteorologists. The theory allows one to investigate the stability of barotropic and baroclinic zonal flows that extend into the planetary interior. It is hypothesized that the internal heat Jupiter and Saturn comes out not radially but on sloping surfaces defined by the internal entropy distribution. To test the hypothesis one searches for basic states in which the wavelength of the fastest-growing disturbance remains finite as E tends to zero, and is which the heat flux vector is radially outward and poleward. Author

N87-17626*# Massachusetts Inst. of Tech., Cambridge.
CONVECTIVE ADJUSTMENT IN BAROCLINIC ATMOSPHERES
Kerry A. Emanuel *In* NASA. Goddard Inst. for Space Studies The Jovian Atmospheres Oct. 1986 p 163-174 (For primary document see N87-17598 09-91)
Avail: NTIS HC A07/MF A01 CSCL 84B

Local convection in planetary atmospheres is generally considered to result from the action of gravity on small regions of anomalous density. That in rotating baroclinic fluids the total potential energy for small scale convection contains a centrifugal as well as a gravitational contribution is shown. Convective adjustment in such an atmosphere results in the establishment of near adiabatic lapse rates of temperature along suitably defined surfaces of constant angular momentum, rather than in the vertical. This leads in general to sub-adiabatic vertical lapse rates. That such an adjustment actually occurs in the earth's atmosphere is shown by example and the magnitude of the effect for several other planetary atmospheres is estimated. Author

N87-17627*# Washington Univ., Seattle.
EDDY PROCESSES IN THE GENERAL CIRCULATION OF THE JOVIAN ATMOSPHERES
Conway Leovy *In* NASA. Goddard Inst. for Space Studies The Jovian Atmospheres Oct. 1986 p 177-192 (For primary document see N87-17598 09-91)
Avail: NTIS HC A07/MF A01 CSCL 84B

Two fundamentally different views of the general circulation of Jovian atmospheres have emerged. According to one view, the observed jet streams at the cloud tops are controlled by the vorticity transfers of small scale eddies generated by planetary wave instabilities within a shallow atmospheric layer. According to the alternate point of view, the zonal jets are surface manifestations of deep interior convection organized into cylindrical motion with axes parallel to the planetary rotation axis. Both approaches may be considered in the context of the very different roles assumed by the potential vorticity. A possible reconciliation of the two kinds of dynamical systems is considered in which the interior motion is overlaid with a statically stable cappling layer driven by turbulent energy injection from below. A simple model for the eddy driving of quasi-geostrophic dynamics in the capping layer is presented which is consistent with the tentative evidence for up-gradient momentum flux on Jupiter and IRIS observations of thermal contrast correlations with cyclonic and anticyclonic shear zones. Certain synoptic-scale cloud features in Jupiter's atmosphere are interpreted as breaking waves, which may also influence the lateral mixing of tracers such as the ortho-para hydrogen ratio. Author

N87-17628*# National Aeronautics and Space Administration. Goddard Space Flight Center, Greenbelt, Md.
MESOSCALE WAVES AS A PROBE OF JUPITER'S DEEP ATMOSPHERE Abstract Only
F. M. Flaser and P. J. Gierasch (Cornell Univ., Ithaca, N.Y.) *In* NASA. Goddard Inst. for Space Studies The Jovian Atmospheres Oct. 1986 p 193-194 Submitted for publication (For primary document see N87-17598 09-91)
Avail: NTIS HC A07/MF A01 CSCL 84B

Images from the Voyager north/south mapping sequences were searched for waves. A remarkable class of mesoscale waves was identified, with the following features: (1) the wavetrains are usually aligned zonally, i.e., wavecrests are north-south; (2) the average wavelength is 300 km with a standard deviation of only 20%; (3) the wavetrains are long; (4) the waves occur within 25 degrees of the equator, the bulk being at the equator itself; (5) the waves are centered at the extrema (in latitude) of the zonal flow; and (6) the meridional extent of the waves is typically 1 degree of latitude. These observations are interpreted as evidence of gravity waves propagating vertically within a leaky duct. A three-level model is assumed composed of a stable duct which extends up to the base of the NH3 cloud deck near 600 mb. Above this is a thin wave-trapping region characterized by a Richardson number Ri less than 1/4 and containing a critical level, where the local value of the zonal flow velocity equals the phase speed of the wave. This in turn is overlain by a stable region, representing the tropopause region and stratosphere. Author

N87-17629*# Imperial Coll. of Science and Technology, London (England).
THE SATURNIAN RIBBON FEATURE: A BAROCLINICALLY UNSTABLE MODEL Abstract Only
D. Godfrey *In* NASA. Goddard Inst. for Space Studies The Jovian Atmospheres Oct. 1986 p 195 Submitted for publication (For primary document see N87-17598 09-91)
Avail: NTIS HC A07/MF A01 CSCL 84B

Using measurements made by the Voyager spacecraft, an oscillatory feature in the northern midlatitudes of Saturn is examined. Measurements made by the imaging and infrared instruments are used to estimate its horizontal wavelength and vertical extent. Some of these characteristics suggest that the feature could be due to baroclinic instability. A numerical model is described of such an instability with parameters based upon the Voyager observations, and using the lower boundary condition developed by Gierasch et al for the Jovian planets. Author

N87-17630*# Meteorological Office, London (England).
QUASI-GEOSTROPHIC FREE MODE MODELS OF LONG-LIVED JOVIAN EDDIES: FORCING MECHANISMS AND CRUCIAL OBSERVATIONAL TESTS Abstract Only
P. L. Read *In* NASA. Goddard Inst. for Space Studies The Jovian Atmospheres Oct. 1986 p 196-197 Full version announced in IAA as A86-37283 (For primary document see N87-17598 09-91)
Avail: NTIS HC A07/MF A01 CSCL 84B

Observations of Jupiter and Saturn long-lived eddies, such as Jupiter's Great Red Spot and White Ovals, are presently compared with laboratory experiments and corresponding numerical simulations for free thermal convection in a rotating fluid that is subject to horizontal differential heating and cooling. Difficulties in determining the essential processes maintaining and dissipating stable eddies, on the basis of global energy budget studies, are discussed; such difficulties do not arise in considerations of the flow's potential vorticity budget. On Jupiter, diabatically forced and transient eddy-driven flows primarily differ in the implied role of transient eddies in transporting potential vorticity across closed geostrophic streamlines in the time mean. Author

N87-17631*# National Center for Atmospheric Research, Boulder, Colo.
MOISTURE DRIVEN CONVECTION ON JUPITER: A MECHANISM TO PRODUCE THE EQUATORIAL PLUMES Abstract Only
C. Stoker *In* NASA. Goddard Inst. for Space Studies The Jovian Atmospheres Oct. 1986 p 198-200 Full version announced in IAA as A87-10085 (For primary document see N87-17598 09-91)
Avail: NTIS HC A07/MF A01 CSCL 84B

Possible roles are explored for moist convection in the production of bright plume features in the Jupiter atmosphere. The features have been observed at least since 1881. A one-dimensional model is developed for a Jovian cloud and the conditions necessary for convection to occur on Jupiter are defined.

The model is used to predict the vertical velocity and maximum altitude of moist clouds that are convected over a vertical extent of 100, 10 and 1 km. Convection within the ammonia layer would not produce sufficient buoyancy to sublime from the rising air parcel. Water rising from the 5 bar to 1 bar level could carry enough ammonia to the cooler region to form plume anvils in the stable layer above 700 mbar. If unpolluted during the convection, the water could be the source of high altitude haze above the entire equatorial zone. Author

N87-17632*# New Mexico State Univ., Las Cruces.
A PROPOSAL FOR ADOPTING A STANDARD COORDINATE SYSTEM FOR DEFINING ATMOSPHERIC NOMENCLATURE FOR THE GIANT PLANETS Abstract Only
R. Beebe *In* NASA. Goddard Inst. for Space Studies The Jovian Atmospheres Oct. 1986 p 203 (For primary document see N87-17598 09-91)
Avail: NTIS HC A07/MF A01 CSCL 84B

Although the albedo of specific belts and zones varies as a function of time, there is evidence that wind maxima may be fixed in latitude. Before considering a standard notation for wind jets, it is necessary to establish a coordinate system within which the nomenclature would be defined. Traditionally, the BAA has used planetographic latitudes; however, this system is based not only on an accurate determination of the polar diameter but also on the assumption that the equipotential surfaces can be represented by biaxial ellipsoids. The International Astronomical Union strives to adopt unambiguous nomenclature that will be universally acceptable. It is proposed that planetocentric coordinates be utilized and that a standardized value of the ratio of the polar diameter to the equatorial diameter be established for each planet to facilitate transformation into planetographic coordinates. Author

N87-17633*# Oxford Univ. (England).
INVESTIGATION OF LONG-LIVED EDDIES ON JUPITER
S. R. Lewis, S. B. Calcutt, F. W. Taylor, and P. L. Read (Meteorological Office, London, England) *In* NASA. Goddard Inst. for Space Studies The Jovian Atmospheres Oct. 1986 p 204-206 (For primary document see N87-17598 09-91)
Avail: NTIS HC A07/MF A01 CSCL 84B

Quasi-geostrophic, two layer models of the Jovian atmosphere are under development; these may be used to simulate eddy phemonena in the atmosphere and include tracer dynamics explicitly. The models permit the investigation of the dynamics of quasi-geostrophic eddies under more controlled conditions than are possible in the laboratory. They can also be used to predict the distribution and behavior of tracer species, and hence to discriminate between different models of the mechanisms forcing the eddies, provided suitable observations can be obtained. At the same time, observational strategies are being developed for the Near Infrared Mapping Spectrometer on the Galileo Orbiter, with the objective of obtaining composition measurements for comparison with the models. Maps of features at thermal infrared wavelengths near 5 micron and reflected sunlight maps as a function of wavelength and phase angle will be obtained. These should provide further useful information on the morphology, composition and microstructure of clouds within eddy features. Equilibrium chemistry models which incorporate advection may then be used to relate these results of the dynamical models and provide addtional means of classifying different types of eddies. Author

N87-17634*# National Aeronautics and Space Administration. Goddard Space Flight Center, Greenbelt, Md.
CHAOTIC MOTION IN THE JOVIAN ATMOSPHERE
Joseph Pirraglia *In* NASA. Goddard Inst. for Space Studies The Jovian Atmospheres Oct. 1986 p 207-209 (For primary document see N87-17598 09-91)
Avail: NTIS HC A07/MF A01 CSCL 84B

Strong nonlinear interactions among unstable waves and the mean flow occur in a simplified quasigeostrophic spectral model of the upper troposphere of Jupiter. The upper boundary of the layer inhibits vertical motion while at the lower boundary perturbations of the potential temperature are not permitted. On an infinite beta plane the forced flow of alternating zones of prograde and retrograde zonal winds, decreasing with height, are linearly unstable and it is shown that the nonlinear terms stabilize the flow by bounding the growth of the eddies. Explicit viscosity terms are not needed. This does not imply that energy would not cascade to the small scale flow but suggests that the nature of the large scale flow is independent of the viscosity at small scales. Numerical time integration shows the flow to be chaotic but, in some cases, with transient propagating features and meandering zonal flow. Author

N87-17635*# Meteorological Office, London (England).
TRANSPORT OF ABSOLUTE ANGULAR MOMENTUM IN QUASI-AXISYMMETRIC EQUATORIAL JET STREAMS
P. L. Read *In* NASA. Goddard Inst. for Space Studies The Jovian Atmospheres Oct. 1986 p 210-220 (For primary document see N87-17598 09-91)
Avail: NTIS HC A07/MF A01 CSCL 84B

It is well known that prograde equatorial jet stresses cannot occur in an axisymmetric inviscid fluid, owing to the constraints of local angular momentum conservation. For a viscous fluid, the constraints of mass conservation prevent the formation of any local maximum of absolute angular momentum (m) without a means of transferring m against its gradient (delta m) in the meridional plane. The circumstances under which m can be diffused up-gradient by normal molecular viscosity are derived, and illustrated with reference to numerical simulations of axisymmetric flows in a cylindrical annulus. Viscosity is shown to act so as to tend to expel m from the interior outwards from the rotation axis. Such an effect can produce local super-rotation even in a mechanically isolated fluid. The tendency of viscosity to result in the expulsion of m is shown to be analogous in certain respects to a vorticity-mixing hypothesis for the effects of non-axisymmetric eddies of the zonally-averaged flow. It is shown how the advective and diffusive transport of m by non-axisymmetric eddies can be represented by the Transformed Eulerian Mean meridional circulation and the Eliassen-Palm (EP) flux of Andrews and McIntyre respectively, in the zonal mean. Constraints on the form and direction of the EP flux in an advective/diffusive flow for such eddies are derived, by analogy with similar constraints on the diffusive flux of m due to viscosity. Author

N87-17636*# Jet Propulsion Lab., California Inst. of Tech., Pasadena.
AN UPDATED HYDROCARBON PHOTOCHEMICAL MODEL FOR THE JOVIAN ATMOSPHERE FROM THE TROPOSPHERE THROUGH THE HOMOPAUSE: A PRELUDE TO GALILEO
M. Allen, G. R. Gladstone (California Inst. of Tech., Pasadena), and Y. L. Yung *In* NASA. Goddard Inst. for Space Studies The Jovian Atmospheres Oct. 1986 p 224-227 Full version announced in IAA as A85-40425 (For primary document see N87-17598 09-91)
Avail: NTIS HC A07/MF A01 CSCL 84B

A photochemical model for the atmosphere of Jupiter, including 1-D vertical eddy diffusive transport, was developed. It extends from the upper troposphere through the homopause. The hydrocarbon chemistry involves species containing up to four carbon atoms (and polyynes through C8H2). The calculations show that a large fraction of photochemical carbon may be contained in molecules with more than two carbon atoms. At the tropopause, C2H6 is the major photochemical species and C2H2, C3H8, and C4H10 are of comparable abundance and down from C2H6 by a factor of ten. These species may be detectable with the mass spectrometer of the Galileo Probe. The vertical distributions of the photochemical species are sensitive to the magnitude of eddy diffusive mixing in the troposphere and stratosphere and the details of the interface region. Author

N87-17637*# Arizona Univ., Tucson.
NON-SOLAR NOBLE GAS ABUNDANCES IN THE ATMOSPHERE OF JUPITER Abstract Only
Jonathan I. Lunine and David J. Stevenson (California Inst. of Tech., Pasadena) *In* NASA. Goddard Inst. for Space Studies The

Jovian Atmospheres Oct. 1986 p 228-230 Full version announced in IAA as A85-40425 (For primary document see N87-17598 09-91)
(Grant NAGw-185)
Avail: NTIS HC A07/MF A01 CSCL 84B

The thermodynamic stability of clathrate hydrate is calculated to predict the formation conditions corresponding to a range of solar system parameters. The calculations were performed using the statistical mechanical theory developed by van der Waals and Platteeuw (1959) and existing experimental data concerning clathrate hydrate and its components. Dissociation pressures and partition functions (Langmuir constants) are predicted at low pressure for CO clathrate (hydrate) using the properties of chemicals similar to CO. It is argued that nonsolar but well constrained noble gas abundances may be measurable by the Galileo spacecraft in the Jovian atmosphere if the observed carbon enhancement is due to bombardment of the atmosphere by clathrate-bearing planetesimals sometime after planetary formation. The noble gas abundances of the Jovian satellite Titan are predicted, assuming that most of the methane in Titan is accreted as clathrate. It is suggested that under thermodynamically appropriate conditions, complete clathration of water ice could have occurred in high-pressure nebulas around giant planets, but probably not in the outer solar nebula. The stability of clathrate in other pressure ranges is also discussed. Author

N87-17638*# State Univ. of New York, Stony Brook.
THE CASSINI MISSION
Tobias Owen *In* NASA. Goddard Inst. for Space Studies The Jovian Atmospheres Oct. 1986 p 231-237 (For primary document see N87-17598 09-91)
Avail: NTIS HC A07/MF A01 CSCL 84B

An assessment study of a Saturn-Orbiter plus Titan-probe mission was made. The NASA Solar System Exploration Committee (SSEC) had recommended two separate missions to the Saturn system, in keeping with its charter to design low-cost, dedicated planetary missions. These were a Titan probe, to be carried by a small spacecraft that would include some type of radar mapping device, and a Saturn Orbiter that would be a more sophisticated spacecraft, to be launched separately. A Saturn orbiter and a Titan probe are combined in a single mission that would be carried out in collaboration with NASA. It is this proposal, called the Cassini Project, which was approved by NASA and ESA for an assessment study to be carried out over the next year and a half. Details of the Cassini mission are discussed. E.R.

N87-17639*# Jet Propulsion Lab., California Inst. of Tech., Pasadena.
THE VOYAGER ENCOUNTER WITH URANUS AND NEPTUNE
Ellis D. Miner *In* NASA. Goddard Inst. for Space Studies The Jovian Atmospheres Oct. 1986 p 238-246 (For primary document see N87-17598 09-91)
Avail: NTIS HC A07/MF A01 CSCL 84B

Voyager 2 approaches Uranus at a relative low phase angle and high southerly latitude. Only when the spacecraft is very close to Uranus does the geometry change appreciably. Most of the important observations occur within six hours of closest approach. Voyager flies through an Earth and solar occulation zone and leaves Uranus at a relatively high phase angle of about 145 degrees. There isn't much of an opportunity to look at the equatorial region of the planet. At Neptune, on the other hand, the approach is more nearly equatorial (about 35 deg S lat). Voyager 2 will come much closer to Nepture than to any of the other gas giants as it skims within about 2000 km of Neptune's cloudtops. It will pass through earth and solar occultation zones at both Neptune and its satellite, Triton. Again, Voyager 2 will leave Neptune at about 35 deg S latitude. Voyager operational instrument, interplanetary trajectories and planetary encounters are briefly discussed. E.R.

N87-17640*# Jet Propulsion Lab., California Inst. of Tech., Pasadena.
THE ORTHO-PARA H2 DISTRIBUTION ON URANUS: CONSTRAINTS FROM THE COLLISION-INDUCED 3-0 DIPOLE BAND AND 4-0 S(0) AND S(1) QUADRUPOLE LINE PROFILES Abstract Only
K. H. Baines and J. T. Bergstralh *In* NASA. Goddard Inst. for Space Studies The Jovian Atmospheres Oct. 1986 p 249-251 Full version announced in IAA as A86-37288 (For primary document see N87-17598 09-91)
Avail: NTIS HC A07/MF A01 CSCL 84B

Recent high quality spectral observations have allowed the derivation of constraints on the atmospheric structure of Uranus. The present analysis, which is based on the detailed modeling of a broadband geometric albedo spectrum and high resolution observations of the H2 4-0 quadrupole and 6818.9-A CH4 features, yields (1) a family of models which parameterize an upper tropospheric haze layer, (2) a lower, optically infinite cloud at a given pressure level, (3) the cloud-level methane molar fraction, and (4) the mean ortho/para ratio in the visible atmosphere. The single scattering albedo of atmospheric aerosols exhibits a steep darkening between 5890 and 6040 A. Author

N87-17641*# Jet Propulsion Lab., California Inst. of Tech., Pasadena.
RADIATIVE-CONVECTIVE EQUILIBRIUM MODELS OF URANUS AND NEPTUNE Abstract Only
J. F. Appleby *In* NASA. Goddard Inst. for Space Studies The Jovian Atmospheres Oct. 1986 p 252-253 Full version announced in IAA as A86-37287 (For primary document see N87-17598 09-91)
Avail: NTIS HC A07/MF A01 CSCL 84B

The present study of Uranus and Neptune radiative-convective equilibrium models gives emphasis to such aspects of the stratospheric energy balance as the influence of aerosol heating and convective penetration. The results obtained for Uranus imply that a continuum absorber may be a significant factor in the stratosphere despite the great distance from the sun. The results obtained for Neptune show that such a continuum absorber could significantly contribute to the energy balance within a localized stratospheric region, although it probably cannot furnish sufficient power to account for the observed IR spectrum irrespective of its vertical distribution. Attention is accordingly given to the convective penetration that could arise under such rapid vertical mixing that CH4's condensation cannot occur before the gas is carried above the condensation region. Author

N87-17642*# Centre National de la Recherche Scientifique, Meudon-Bellevue (France).
A MODEL OF THE SPATIAL AND TEMPORAL VARIATION OF THE URANUS THERMAL STRUCTURE
B. Bezard and D. Gautier *In* NASA. Goddard Inst. for Space Studies The Jovian Atmospheres Oct. 1986 p 254-260 (For primary document see N87-17598 09-91)
Avail: NTIS HC A07/MF A01 CSCL 84B

Seasonal variability of the temperature structure of Uranus is modeled for all latitudes in the .0004 to 2 bar pressure range in anticipation of the Voyager encounter in January 1986. Atmospheric heating in the model results on the one hand from an internal heat source and, on the other hand, from absorption of solar energy by methane and by non-conservative aerosols located between the 0.5 and 2 bar levels. Various cases for the behavior of the internal heat flux are investigated, such as constant with latitude or constrained to yield a time-averaged thermal emission independent of latitude. Meridional transport of heat in the stably stratified atmosphere is not taken into account. The results indicate that the Voyager encounter time, very small north-south temperature asymmetry should be expected. Moreover, the northern hemisphere, although not illuminated, should emit as much energy (within one percent) as the southern hemisphere at this date. At a given latitude, extreme temperatures are reached at the equinoxes. At the poles, seasonal amplitudes of about 10 K in the upper stratosphere and 6 K at the 0.6 bar level are predicted, and the variation with time of the emission to space is found to be at most 20 percent. The atmosphere of Uranus appears to be characterized by very long radiative response times (mainly due to its cold temperature) which inhibit the large seasonal variations

that one could otherwise expect in view of the high obliquity of the planet and its long orbital period. Author

N87-17643*# National Aeronautics and Space Administration. Ames Research Center, Moffett Field, Calif.
VERTICAL STRUCTURE OF AEROSOLS AND CLOUDS IN THE ATMOSPHERES OF URANUS AND NEPTUNE: IMPLICATIONS FOR THEIR HEAT BUDGETS Abstract Only
James B. Pollack, Kathy Rages, Jay Bergstralh (Jet Propulsion Lab., California Inst. of Tech., Pasadena), Kevin Baines, Daniel Wenkert, and G. Edward Danielson (California Inst. of Tech., Pasadena) *In* NASA. Goddard Inst. for Space Studies The Jovian Atmospheres Oct. 1986 p 261-263 Full version announced in IAA as A86-37289 (For primary document see N87-17598 09-91)
Avail: NTIS HC A07/MF A01 CSCL 84B

Models possessing an upper haze layer of finite optical depth and a lower cloud layer of infinite optical depth at discrete altitudes are used to bound the wavelength-averaged phase integrals and bolometric albedos of Uranus and Neptune. The models differ in the assumed value of the particles single scattering phase function and the wavelength dependence of the haze optical depth. A range of phase functions, from the isotropic to those characterizing Titan, Jupiter, and Saturn atmosphere particles, are discussed. The results obtained imply that the meteorological regimes in the observable atmospheres of Uranus and Neptune may differ considerably; internal heat flux could play a much more important role for Neptune than for Uranus. E.R.

N87-17644*# Arizona Univ., Tucson. Lunar and Planetary Lab.
ON THE OBLATENESS AND ROTATION RATE OF NEPTUNE'S ATMOSPHERE
W. B. Hubbard *In* NASA. Goddard Inst. for Space Studies The Jovian Atmospheres Oct. 1986 p 264-270 (For primary document see N87-17598 09-91)
Avail: NTIS HC A07/MF A01 CSCL 84B

Recent observations of a stellar occultation by Neptune give an oblateness of 0.022 + or - 0.004 for Neptune's atmosphere at the 1-microbar pressure level. This results is consistent with hydrostatic equilibrium at a uniform atmospheric rotation period of 15 hours, although the error bars on quantities used in the calculation are such that an 18-hour period is not excluded. The oblateness of a planetary atmosphere is determined from stellar occultations by measuring the times at which a specified point on immersion or emersion occultation profiles is reached. Whether this standard procedure for deriving the shape of the atmosphere is consistent with what is known about vertical and horizontal temperature gradients in Neptune's atmosphere is evaluated. The nature of the constraint placed on the interior mass distribution by an oblateness determined in this manner is consided, as is the effects of possible differential rotation. A 15-hour Neptune internal mass distribution is approximately homologous to Uranus', but an 18-hour period is not. The implications for Neptune's interior structure if its body rotation period is actually 18 hours are discussed. Author

N87-17645*# National Aeronautics and Space Administration. Ames Research Center, Moffett Field, Calif.
ARE THE AEROSOLS ON URANUS AND NEPTUNE COMPOSED OF METHANE PHOTOPOLYMERS? Abstract Only
M. Podolak, L. Giver, and D. Goorvitch *In* NASA. Goddard Inst. for Space Studies The Jovian Atmospheres Oct. 1986 p 273 (For primary document see N87-17598 09-91)
Avail: NTIS HC A07/MF A01 CSCL 84B

The measured optical properties of photochemically produced aerosols in an adding-doubling radiative transfer code were used to match various points in the spectra of Uranus and Neptune. How well these points are fit are shown by different assumptions regarding the size and distribution of these aerosols in the Uranus and Neptune atmospheres. The consistency of these derived distributions with those expected from computations of the sedimentation rate of such aerosols is discussed. Author

N87-17646*# Jet Propulsion Lab., California Inst. of Tech., Pasadena.
THE HD/H2 RATIO IN THE ATMOSPHERE OF URANUS Abstract Only
J. T. Trauger *In* NASA. Goddard Inst. for Space Studies The Jovian Atmospheres Oct. 1986 p 274 (For primary document see N87-17598 09-91)
Avail: NTIS HC A07/MF A01 CSCL 84B

High resolution spectra of HD and H2 were brought together to derive the D/H ratio for Uranus. The deuterium concentration in the dominant molecular hydrogen phase is least susceptible to the effects of isotope fractionation in the planetary atmosphere, and the determination of relative abundances of HD and H2 is unambiguous due to nearness and relative weakness of the chosen spectral lines. The HD 5-0 R(0) and R(1) dipole lines and the H2 4-0 S(0), S(1), and S(2) quadrupole lines were obtained with a PEPSIOS instrument at the Palomar 5-meter telescope. The H2 spectra, which resolve the asymmetric line profiles resulting from pressure shifts in the deep stratified Uranus atmosphere, unambiguously define the line-of-sight hydrogen abundance for comparison with the HD spectra. The 5-0 band of HD was chosen to minimize interference from blended CH4 lines. However, weak interfering lines were found in the 5-0 bands from Uranus as well, and some uncertainties remain regarding the intrinsic line strengths in molecular hydrogen, complicating the analysis of the HD/H2 data. Nevertheless, it is established that the D/H ratio in the atmosphere of Uranus is smaller than the Jovian value, and is significantly smaller than recent theoretical predictions for Uranus based on estimates of isotope fractionation in the pre-planetary solar nebulae. Author

N87-17647*# National Aeronautics and Space Administration. Goddard Inst. for Space Studies, New York, N.Y.
ASTRONOMICAL, PHYSICAL, AND METEOROLOGICAL PARAMETERS FOR PLANETARY ATMOSPHERES
Michael Allison and Larry D. Travis *In its* The Jovian Atmospheres Oct. 1986 p 293-319 (For primary document see N87-17598 09-91)
Avail: NTIS HC A07/MF A01 CSCL 84B

A newly compiled table of astronomical, physical, and meteorological parameters for planetary atmospheres is presented. Formulae and explanatory notes for their application and a complete listing of sources are also given. Author

N87-17648*# Woods Hole Oceanographic Institution, Mass.
ANALYSIS OF HARMONIC SPLINE GRAVITY MODELS FOR VENUS AND MARS Final Report, 15 May 1985 - 31 Dec. 1986
Carl Bowin Dec. 1986 12 p
(Grant NAGw-792)
(NASA-CR-180147; NAS 1.26:180147) Avail: NTIS HC A02/MF A01 CSCL 03B

Methodology utilizing harmonic splines for determining the true gravity field from Line-Of-Sight (LOS) acceleration data from planetary spacecraft missions was tested. As is well known, the LOS data incorporate errors in the zero reference level that appear to be inherent in the processing procedure used to obtain the LOS vectors. The proposed method offers a solution to this problem. The harmonic spline program was converted from the VAX 11/780 to the Ridge 32C computer. The problem with the matrix inversion routine that improved inversion of the data matrices used in the Optimum Estimate program for global Earth studies was solved. The problem of obtaining a successful matrix inversion for a single rev supplemented by data for the two adjacent revs still remains. B.G.

N87-17649*# University of Northern Arizona, Flagstaff. Dept. of Geology.
INVESTIGATION OF THE MODE OF COMPENSATION OF VENUS TOPOGRAPHY Final Technical Report, 1 Jan. 1985 - 1 Jan. 1986
Paul Morgan 1986 17 p
(Grant NAG2-330)
(NASA-CR-180145; NAS 1.26:180145) Avail: NTIS

HC A02/MF A01 CSCL 03B

The Venus gravity data derived from the Pioneer Venus Orbiter indicates a strong correlation of gravity to topography at all resolvable wavelengths. Focus was on an analysis in the spatial domain, using a geophysical model of topographic compensation together with the topography data to compute gravity vectors corresponding to the observed data and comparison of the calculated and observed gravity vectors. B.G.

N87-17650# Institut d'Aeronomie Spatiale de Belgique, Brussels.
THE EFFECT OF SATURN'S RINGS ON THE UPPER-BOUNDARY INSOLATION OF ITS ATMOSPHERE
E. VanHemelrijck 1986 40 p Submitted for publication
(Aeronomica-Acta-A-308-1986; ISSN-0065-3713; ETN-87-98840)
Avail: NTIS HC A03/MF A01

The daily solar radiation incident at the top of Saturn's atmosphere is calculated taking into account the oblateness of the planet and the shadow of the ring system. It is found that the decrease of the daily insolation in winter is important near the solstices up to midlatitudes and in the neighborhood of the equinoxes for equatorial and low latitudes. The combined effect of Saturn's rings and its flattening on the mean winter and annual daily insolations is also studied. Numerical results show that the mean wintertime insolation falls gradually in the 0 to 20 deg latitude region to a peak value of 50%. Beyond 20 deg the loss of insolation decreases, and from 45 deg up to polar region latitudes, the decrease reaches a constant level of 35%. The mean annual daily insolation is maximally reduced by 20% at localities of 20 deg. ESA

N87-17142*# Jet Propulsion Lab., California Inst. of Tech., Pasadena.
VENUS RADAR MAPPER (VRM): MULTIMODE RADAR SYSTEM DESIGN
William T. K. Johnson and Alvin T. Edgerton (Hughes Aircraft Co., El Segundo, Calif.) *In its* The Second Spaceborne Imaging Radar Symposium 1 Dec. 1986 p 56-66 (For primary document see N87-17135 09-43)
Avail: NTIS HC A10/MF A01 CSCL 03B

N87-17540# Observatoire de Paris-Meudon (France).
A STUDY OF PLANETARY ATMOSPHERES IN THE SUBMILLIMETRIC RANGE
Emmanuel Lellouch and Therese Encrenaz *In* ESA Proceedings of an ESA Workshop on a Spaceborne Submillimeter Astronomy Mission. A Cornerstone of the ESA Long Term Science Program Aug. 1986 p 53-55 (For primary document see N87-17535 09-88)
Avail: NTIS HC A14/MF A01

92 SOLAR PHYSICS

Includes solar activity, solar flares, solar radiation and sunspots.

For related information see *93 Space Radiation.*

N87-17651 Michigan Univ., Ann Arbor.
THE HYDROGEN GEOCORONA: SIMULTANEOUS OPTICAL AND RADAR OBSERVATIONS AT ARECIBO Ph.D. Thesis
Robert Bruce Kerr 1986 255 p
Avail: Univ. Microfilms Order No. DA8621311

Observations of the geocoronal H sub alpha emission with a high resolution Fabry-Perot interferometer have been made simultaneously with observations of the topside F region using the incoherent scatter radar at Arecibo, for the purpose of monitoring the exobase temperature and the hydrogen velocity distribution over half of a solar cycle. The variation of H density with solar activity agrees with that of previous observations. These observations have shown that the charge exchange reaction of H with H+ perturbs the ballistic hydrogen velocity distribution above the exobase in the fall and winter months at Arecibo. The exobase temperature is hotter than would be expected for winter solar minimum conditions due to a drop of the protonosphere base during these periods. A multi-constituent analysis of the radar data places the base of the protonosphere near 550 km in the early morning hours of the late fall and early winter. A maximum in downward ion velocities is also observed during these times. For observations near the vernal equinox, the charge exchange reaction does not significantly perturb the neutral hydrogen velocity distribution. Fourier analysis of the H sub alpha spectral profile shows that H cools with increasing geocentric distance during these periods, in a manner consistent with the diminishing energy required for escape with increasing distance from the Earth.
Dissert. Abstr.

N87-17652# Pacific Northwest Labs., Richland, Wash.
ULTRALOW BACKGROUND SEARCHES FOR BETA BETA-DECAY, COLD DARK MATTER AND SOLAR AXIONS
F. T. Avignone (South Carolina Univ., Columbia), S. P. Ahlen (Boston Univ., Mass.), R. L. Brodzinski, S. Dimopolous (Stanford Univ., Calif.), A. K. Drukier (Harvard-Smithsonian Center for Astrophysics, Cambridge, Mass.), G. Gelmini (Harvard Univ., Cambridge, Mass.), B. W. Lynn (Stanford Linear Accelerator Center, Calif.), H. S. Miley (South Carolina Univ., Columbia), J. H. Reeves, D. N. Spergel (Harvard Univ., Cambridge, Mass.) et al Jul. 1986 6 p Presented at the International Symposium on Weak and Electromagnetic Interactions in Nuclei, Heidelberg, West Germany, 1 Jul. 1986 Prepared in cooperation with South Carolina Univ., Columbia.; Boston Univ., MA.; Stanford Univ., CA.; Harvard-Smithsonian Center for Astrophysics, Cambridge, MA.; Harvard Univ., Cambridge, MA.
(Contract DE-AC06-76RL-01830; Grant NSF PHY-84-095654)
(DE86-013592; PNL-SA-14160; CONF-860741-9) Avail: NTIS HC A02/MF A01

An ultralow background Ge detector in the Homestake gold mine is applied to searches for 0 nu Beta-Beta-decay, cold dark matter candidates and invisible axions from the sun. A large body of low background Ge data imply (m sub nu) is less than or approximate to 2.3 eV. Particles with spin independent Z^0 exchange interactions and masses between 20 GeV and 5 TeV are excluded as dominant in the galactic halo. Finally, axions with F(2x' sub e) is less than or approximate to 0.5 x 10 to the 7th power GeV are also ruled out. DOE

N87-17653# Institut d'Aeronomie Spatiale de Belgique, Brussels.
THE INTERACTION BETWEEN THE SOLAR WIND AND THE COMETS [L'INTERACTION DU VENT SOLAIRE AVEC LES COMETES]
M. Roth 1986 34 p In FRENCH; ENGLISH summary Presented at a conference, Brussels, Belgium, 17 Apr. 1986 Submitted for publication
(Aeronomica-Acta-A-306-1986; ISSN-0065-3713; ETN-87-98839)
Avail: NTIS HC A03/MF A01

The macroscopic aspect of the interaction between the solar wind and a comet close to the Sun is described. The history of the discovery of the solar wind is depicted. The formation of comet tails is explained. The large scale structure of the solar wind and the interplanetary magnetic field are given. The Alfven model for the interaction between the cometary ionosphere and the interplanetary magnetic field, and the magnetohydrodynamic model for the interaction between the solar wind and a comet are presented. Results obtained by the Interplanetary Cometary Explorer and in experiments in laboratory and space are presented. Recently, microscopic aspects of the interaction were revealed by in situ measurements onboard space probes. ESA

93 SPACE RADIATION

Includes cosmic radiation; and inner and outer earth's radiation belts.

For biological effects of radiation see *52 Aerospace Medicine.* For theory see *73 Nuclear and High-Energy Physics.*

N87-17654 New Hampshire Univ., Durham.
ON THE SPECTRA OF GAMMA-RAY BURSTS AT HIGH ENER-

GIES Ph.D. Thesis
Steven Michael Matz 1986 148 p
Avail: Univ. Microfilms Order No. DA8621607

Between 1980 February and 1983 August the Gamma Ray Spectrometer (GRS) on the Solar Maximum Mission satellite (SMM) observed 71 gamma ray bursts. These events form a representative subset of the class of classical gamma ray bursts. Since their discovery more than 15 years ago, hundreds of gamma ray bursts have been detected; however most observations have been limited to an energy range of roughly 30 keV to 1 MeV. The large sensitive area and spectral range of the GRS allow, for the first time, and investigation of high energy (>1MeV) behavior of a substantial number of gamma ray bursts. It is found that high energy emission is seen in a large fraction of all events and that the data are consistent with all bursts emitting to at least 5 MeV with no cut offs. Further, no burst spectrum measured by GRS has a clear high energy cut off. The high energy emission can be a significant part of the total burst energy; on the average about 30% of the observed energy above 30 keV is contained in the > 1 MeV photons. Tests of spectral models yield mixed results. Neither a power law nor a thermal model can adequately explain all of the observed spectra. Dissert. Abstr.

N87-17655 Harvard Univ., Cambridge, Mass.
RADIATIVE PROCESSES UNDERLYING THE X-RAY AND GAMMA-RAY CONTINUA OF ACTIVE GALACTIC NUCLEI AND GAMMA-RAY BURSTS Ph.D. Thesis
Andrzej Antoni Zdziarski 1986 151 p
Avail: Univ. Microfilms Order No. DA8620559

Steady relativistic plasmas are studied. Compton scattering, electron-positron pair production and annihilation, and bremsstrahlung and synchrotron emission are considered. In the steady state, the pair production rate equals the pair annihilation rate, and the energy production rate equals the electron cooling rate. Two kinds of plasmas are studied: purely thermal plasmas, and two-component ones containing nonthermal as well as thermal electrons. The results are applied to two classes of cosmic X-ray and gamma-ray radiation: active galactic nuclei and gamma-ray bursts. The onset, intensification, and withdrawal of drought over Indonesia, Austrailia, the Pacific Ocean island chains, and the Amazon River Valley is monitored based on inferred irrotational, three-dimensional flow fields. Anomalous subsidence, forced by the ENSO episode is noted over all drought regions.
Dissert. Abstr.

N87-17552# Consiglio Nazionale delle Ricerche, Bologna (Italy).
ON THE IDENTIFICATION OF IRAS DEEP FIELD SOURCES: THE RADIO COUNTERPARTS
L. Bassani, M. J. Coe, N. Mandolesi, B. Partridge, and L. Spinoglio *In* ESA Proceedings of an ESA Workshop on a Spaceborne Submillimeter Astronomy Mission. A Cornerstone of the ESA Long Term Science Program Aug. 1986 p 151-155 (For primary document see N87-17535 09-88)
Avail: NTIS HC A14/MF A01

N87-17553# Observatorio Astromico Nacional, Guadalajara (Spain). Centro Astronomico de Yebes.
MASER AND THERMAL SiO EMISSION IN EVOLVED STARS
V. Bujarrabal, A. Barcia, P. Planesas, J. Gomez-Gonzalez, J. Martin-Pintado, and J. D. Gallego *In* ESA Proceedings of an ESA Workshop on a Spaceborne Submillimeter Astronomy Mission. A Cornerstone of the ESA Long Term Science Program Aug. 1986 p 157-160 (For primary document see N87-17535 09-88)
(Contract CAICYT-477/84)
Avail: NTIS HC A14/MF A01

N87-17554# Centre d'Etude Spatiale des Rayonnements, Toulouse (France).
NEW RESULTS ABOUT DIFFUSE GALACTIC EMISSION AT 380 MICRONS
E. Caux and Guy Serra *In* ESA Proceedings of an ESA Workshop on a Spaceborne Submillimeter Astronomy Mission. A Cornerstone of the ESA Long Term Science Program Aug. 1986 p 161-164 (For primary document see N87-17535 09-88)
Avail: NTIS HC A14/MF A01

N87-17555# Imperial Coll. of Science and Technology, London (England).
OPPORTUNITIES AND POTENTIAL FOR A MILLIMETRE WAVELENGTH SEARCH FOR THE SUNYAEV-ZELDOVICH EFFECT
Simon T. Chase, R. D. Joseph, N. A. Robertson, and P. A. R. Ade *In* ESA Proceedings of an ESA Workshop on a Spaceborne Submillimeter Astronomy Mission. A Cornerstone of the ESA Long Term Science Program Aug. 1986 p 165-171 (For primary document see N87-17535 09-88)
Avail: NTIS HC A14/MF A01

N87-17556# Groningen Rijksuniversiteit (Netherlands). Lab. for Space Research.
INFRARED RADIATION FROM INTERFACE REGIONS IN MOLECULAR CLOUDS: L1551 AND THE SERPENS NEBULA
F. O. Clark, Rene J. Laureijs, G. Chlewicki, C. Y. Zhang, W. vanOosterom, and D. Kester *In* ESA Proceedings of an ESA Workshop on a Spaceborne Submillimeter Astronomy Mission. A Cornerstone of the ESA Long Term Science Program Aug. 1986 p 173-176 (For primary document see N87-17535 09-88)
Avail: NTIS HC A14/MF A01

99 GENERAL

N87-17656*# National Aeronautics and Space Administration. Lewis Research Center, Cleveland, Ohio.
RESEARCH AND TECHNOLOGY Annual Report, 1986
1986 103 p
(NASA-TM-88868; NAS 1.15:88868) Avail: NTIS HC A06/MF A01 CSCL 05A

The research and technology accomplishments of the NASA Lewis Research Center are summarized for the fiscal year 1986, the 45th anniversary year of the Center. Five major sections are presented covering: aeronautics, aerospace technology, space communications, space station systems, and computational technology support. A table of contents by subjects was developed to assist the reader in finding articles of special interest.
Author

Typical Subject Index Listing

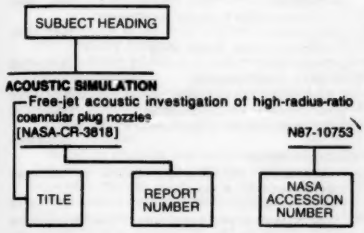

The subject heading is the key to the subject content of the document. Titles, report numbers, and accession numbers of pertinent documents are provided under each subject heading. When the title is insufficiently descriptive of the document content, a title extension has been added, separated from the title by three hyphens. The report number helps to indicate the type of document cited (e.g., NASA report, NASA translation, NASA contractor report). The NASA accession number is the number by which the document abstracts are arranged in this journal and by which the document is sold or requested. The titles, with title extensions if present, are arranged under each subject heading in ascending accession number order. The subject headings have been selected from the latest revision of the *NASA Thesaurus* (NASA SP-7053).

A

ABLATION
Hypersonic nonequilibrium flow over an ablating teflon surface N87-16787

ABSORPTION SPECTRA
Interrelationship between field spectra and airborne MSS systems in the Singatse range, (Yerington) Nevada --- multispectral scanner (MSS) mineral exploration N87-17242

ABSORPTIVITY
Heat exchanger for electrothermal devices [NASA-CASE-LEW-14037-1] N87-16875
Laboratory measurements of microwave absorption from gaseous atmospheric constituents under conditions for the outer planets N87-17620

ABSTRACTS
Compendium of NASA Langley reports on hypersonic aerodynamics [NASA-TM-87760] N87-16802
Abstracts: Review of progress in quantitative NDE [DE87-000769] N87-17073

ABUNDANCE
Molecular abundances in circumstellar envelopes N87-17549
The ionization structure of planetary nebulae. 8: NGC 6826 [NASA-CR-180142] N87-17581
Enhanced acetylene emission near the north pole of Jupiter N87-17614
The abundances of ethane to acetylene in the atmospheres of Jupiter and Saturn N87-17618

ACCELERATION (PHYSICS)
A study of explosive wave propagation in granular materials with microstructure [AD-A173015] N87-16914

ACCELERATION PROTECTION
An experimental microcomputer controlled system for synchronized pulsating anti-gravity suit [AD-A174640] N87-17433

ACCELERATION TOLERANCE
An experimental microcomputer controlled system for synchronized pulsating anti-gravity suit [AD-A174640] N87-17433

ACCELEROMETERS
Low-g measurements by NASA [NASA-TM-86585] N87-17017

ACCESS CONTROL
A study of spatial models and human navigation within complex computer interfaces N87-17447

ACCESSORIES
Flameholder with removable flameholder attachments [AD-D012466] N87-16893

ACCIDENT PREVENTION
Two-Phase Flows in Major Technological Hazards, volume 3 [VKI-LS-1986-03-VOL-3] N87-16984

ACCIDENTS
A new day: Challenger and space flight thereafter [NASA-TM-77717] N87-16856
General classification of two-phase flow codes N87-16985
Review of present approaches to two-phase flow problems N87-16986

ACCRETION DISKS
Redistribution of angular momentum by nonaxisymmetric instabilities in a thick accretion disk [PUBL-SER-C-FASC-4] N87-17585
A numerical study of jet production and accretion disk structure in super-Eddington black hole accretion N87-17586

ACETYLENE
Ethynyl terminated ester oligomers and polymers therefrom [NASA-CASE-LAR-13118-2] N87-16907
Enhanced acetylene emission near the north pole of Jupiter N87-17614
The abundances of ethane to acetylene in the atmospheres of Jupiter and Saturn N87-17618

ACOUSTIC EMISSION
An approach to AE monitoring during the rig shop testing of large CFRP aero-engine components — acoustic emission (AE) [PNR90350] N87-16841
Vibroacoustic payload environment prediction system (VAPEPS): Data base management center remote access guide [NASA-CR-180132] N87-17528

ACOUSTIC MEASUREMENT
Power cepstrum technique with application to model helicopter acoustic data [NASA-TP-2586] N87-17479
Combustion noise from gas turbine aircraft engines measurement of far-field levels [NASA-TM-88971] N87-17480
Noise propagation from a four-engine, propeller-driven airplane [NASA-TM-89035] N87-17482

ACOUSTIC SCATTERING
Noise propagation from a four-engine, propeller-driven airplane [NASA-TM-89035] N87-17482

ACOUSTIC SOUNDING
Joint influence of turbulence and wind on signal power in radioacoustic sounding of atmosphere N87-17108

ACOUSTO-OPTICS
An 800 MHz bandwidth acousto-optical spectrometer at Helsinki Observatory N87-17567

ACTUATORS
Dynamics and control of flexible manipulators N87-17028

ADAPTIVE CONTROL
Adaptive control techniques for large space structures [AD-A173083] N87-16871
Application of adaptive antenna techniques to future commercial satellite communication [NASA-CR-179566] N87-16954
Application of adaptive antenna techniques to future commercial satellite communication [NASA-CR-179566] N87-16955
Position control of mechanical manipulators by using nonlinear adaptive control algorithm N87-17031
Adaptive control of a flexible structure N87-17449
Adaptive control of mechanical manipulators N87-17450

ADAPTIVE OPTICS
Active optics for the far infrared submillimeter wave space telescope (FIRST): A high angular resolution mode N87-17566

ADHESIVE BONDING
Effect of adherend thickness and mixed mode loading on debond growth in adhesively bonded composite joints [NASA-TM-88992] N87-16882
Thermoelastic testing of stratified materials N87-17064

ADIABATIC FLOW
Convective adjustment in baroclinic atmospheres N87-17626

AERIAL PHOTOGRAPHY
Knowledge-based aerial image understanding systems N87-17210
Significance of space image, air photo and drainage linears in relation to west coast tectonics, India N87-17232
Thermal infrared imagery from helicopter for heat loss calculations in industrial plants N87-17326

AERIAL RECONNAISSANCE
The ice conditions in the Greenland waters, 1980 [REPT-551.467.3.068(988)] N87-17428

AEROACOUSTICS
The aerodynamics and aeroacoustics of rotating transonic disturbances N87-16786

AEROASSIST
Aeroassisted coplanar orbital transfer of flight vehicles using the sequential gradient restoration algorithm N87-16857

AERODYNAMIC CHARACTERISTICS
The effects of heavy rain on profile aerodynamics [ETN-87-98848] N87-16809
Unsteady aerodynamics of a rotating compressor blade row in incompressible flow. Volume 1: Experimental facilities, procedures and sample data [AD-A173043] N87-16831
Unsteady aerodynamics of a rotating compressor blade row at low Mach number. Volume 2: Analysis of experimental results and comparison with theory [AD-A173044] N87-16832

AERODYNAMIC CONFIGURATIONS
A comparison of single-block and multi-block grids around wing-fuselage configurations [FFA-TN-1986-42] N87-16811
Flight investigation of the effect of tail configuration on stall, spin, and recovery characteristics of a low-wing general aviation research airplane [NASA-TP-2644] N87-16815

AERODYNAMIC DRAG
The contraction of satellite orbits under the influence of air drag. Part 7: Orbits of high eccentricity, with scale height dependent on altitude [RAE-TR-86013] N87-16859

AERODYNAMIC INTERFERENCE
Over-the-wing propeller [NASA-CASE-LAR-13134-2] N87-16828

AERODYNAMIC LOADS
Over-the-wing propeller [NASA-CASE-LAR-13134-2] N87-16828

AERODYNAMIC STABILITY
Linearised theory of stability and resonance for projectiles with aerodynamically induced roll variations [WSRL-0449-TR] N87-16795
Over-the-wing propeller [NASA-CASE-LAR-13134-2] N87-16828
Development of a sensitivity analysis technique for multiloop flight control systems N87-16847

AERODYNAMIC STALLING
Flight investigation of the effect of tail configuration on stall, spin, and recovery characteristics of a low-wing general aviation research airplane [NASA-TP-2644] N87-16815
HAWT performance with dynamic stall [DE86-004426] N87-17402

AERODYNAMICS
The aerodynamics and aeroacoustics of rotating transonic disturbances N87-16786
Euler analysis of the three dimensional flow field of a high-speed propeller: Boundary condition effects [NASA-TM-88955] N87-16796
Computational, unsteady transonic aerodynamics and aeroelasticity about airfoils and wings [NASA-TM-89414] N87-16801
Compendium of NASA Langley reports on hypersonic aerodynamics [NASA-TM-87760] N87-16802
Unsteady aerodynamics of a rotating compressor blade row in incompressible flow. Volume 1: Experimental facilities, procedures and sample data [AD-A173043] N87-16831
Proceedings of the 15th International Symposium on Shock Waves and Shock Tubes [AD-A173026] N87-17006
Model for simulating rotational data for wind turbine applications [DE86-010784] N87-17406

AEROELASTICITY
Loads and Aeroelasticity Division research and technology accomplishments for FY 1986 and plans for FY 1987 [NASA-TM-89084] N87-16796
Computational, unsteady transonic aerodynamics and aeroelasticity about airfoils and wings [NASA-TM-89414] N87-16801
The static aeroelasticity of a composite wing N87-17085

AERONAUTICAL ENGINEERING
A distributed data acquisition system for aeronautics test facilities [NASA-TM-88961] N87-16851
Data communication requirements for the advanced NAS network [NASA-TM-89315] N87-16957
FY 1986 scientific and technical reports, articles, papers and presentations [NASA-TM-86575] N87-17532
Research and technology [NASA-TM-88868] N87-17656

AEROSOLS
Representation of the vaporization behavior of turbulent polydisperse sprays by equivalent monodisperse sprays [NASA-TM-88906] N87-16827
Droplet sizing research program [AD-A173100] N87-16895
Direct computation of wall bounded aerosol turbulent flow interactions [DE86-013221] N87-17009
Determination of nonglobal component against background of global radioactive pollution of atmospheric aerosols N87-17100
Variability in the Earth radiation budget as determined from the Nimbus ERB experiments N87-17410
SAGE aerosol measurements. Volume 3: January 1, 1981 to November 18, 1981 [NASA-RP-1173] N87-17417
Constraints on the composition of Jupiter's stratospheric aerosols from ultraviolet photometry N87-17610
Are the aerosols on Uranus and Neptune composed of methane photopolymers? N87-17645

AEROSPACE ENGINEERING
Adaptive control techniques for large space structures [AD-A173083] N87-16871
Diffusion welding of component parts in the aviation and space industries [RAE-TRANS-2147] N87-17032
Advanced Joining of Aerospace Metallic Materials — conference proceedings [AGARD-CP-398] N87-17051
The application of diffusion bonding and laser welding in the fabrication of aerospace structures N87-17054
Research on structural analysis at the DFVLR, Brunswick N87-17078
Flight-vehicle structures education in the US: Assessment and recommendations [NASA-CR-4048] N87-17526

AEROSPACE ENVIRONMENTS
The non-metallic materials sample array [NASA-TM-86578] N87-16910
The NASA Aerospace Battery Safety Handbook [NASA-CR-180127] N87-17397

AEROSPACE TECHNOLOGY TRANSFER
Aircraft derivative gas turbine development in China [PNR90359] N87-16844

AFTERBODIES
Afterbody shape effects on the near-wake velocity characteristics at Mach numbers between 0.35 and 0.92 [ISL-CO-205/86] N87-17011

AFTERBURNING
Flameholder with removable flameholder attachments [AD-D012466] N87-16893

AGRICULTURE
Applications of TIMS data in agricultural areas and related atmospheric considerations N87-17124
Comparison of Thematic Mapper (TM) and SPOT simulation data for agricultural applications in south west Germany N87-17165
Extraction of the backscatter coefficient of agricultural fields from an airborne SAR image N87-17265
Applications of remote sensing in the US Department of Agriculture N87-17285
X and L-band backscattering measurements of agricultural crops, forest stands and single trees N87-17311

AGRISTARS PROJECT
An overview of remote sensing agricultural apcations in North America: Past, present and future N87-17284

AH-64 HELICOPTER
Inertia welding of nitralloy N and 18 nickel maraging 250 grade steels for utilization in the main rotor drive shaft for the AR-64 military helicopter program N87-17067

AILERONS
Flight service evaluation of advanced composite ailerons on the L-1011 transport aircraft [NASA-CR-178170] N87-16883

AIR
Hypersonic nonequilibrium flow over an ablating teflon surface N87-16787

AIR LAND INTERACTIONS
Dependence of snow melting and surface-atmosphere interactions on the forest structure N87-17318
Transmission of atmospheric internal gravity waves into the stratosphere N87-17412

AIR POLLUTION
An introduction to the numerical modelling of dispersion in the atmospheric boundary layer N87-16993
Determination of nonglobal component against background of global radioactive pollution of atmospheric aerosols N87-17100
SAGE aerosol measurements. Volume 3: January 1, 1981 to November 18, 1981 [NASA-RP-1173] N87-17417

AIR SEA ICE INTERACTIONS
Imaging radar contributions to a major air-sea-ice interaction study in the Greenland Sea N87-17150
Application of the Seasat scatterometer to observations of wind speed and direction and Arctic ice/water boundaries N87-17259

AIR TRAFFIC CONTROL
Air traffic control radar beacon system transponder performance study and analysis. Volume 2: Appendixes [DOT/FAA/FS-86/1-VOL-2] N87-16812

AIR WATER INTERACTIONS
Ocean surface temperature field variability N87-17104
Ocean waves near Hurricane Josephine from SIR-B N87-17148

AIRBORNE EQUIPMENT
Development of new aviation technology for gravimetric surveying N87-17106
Multifrequency-polarimetric SAR for remote sensing N87-17280
Thermal infrared remote sensing: One of today's solutions N87-17324
Characterisation of internal wave surface patterns on airborne SAR imagery N87-17338
Results from 1984 airborne Doppler lidar wind measurement program. Flight 6: Analysis of line-of-sight elevation angle errors and apparent Doppler velocities [NASA-CR-178994] N87-17425

AIRCRAFT ACCIDENTS
The effects of heavy rain on profile aerodynamics [ETN-87-98848] N87-16809

AIRCRAFT CONSTRUCTION MATERIALS
Fatigue life and fastener flexibility of single shear riveted and bolted joints [FFA-TN-1986-35] N87-17094

AIRCRAFT CONTROL
Optimal turning at high angle of attack of supersonic and hypersonic vehicles N87-16814

AIRCRAFT DESIGN
Geometries for roughness shapes in laminar flow [NASA-CASE-LAR-13255-1] N87-16793
Performance data Aeroc 8.2.AC.20(300), issue 1 N87-16818
Flight-vehicle structures education in the US: Assessment and recommendations [NASA-CR-4048] N87-17526

AIRCRAFT ENGINES
Reducing the cost of aero engine research and development [PNR90341] N87-16836
Component lifing — aircraft engines [PNR90346] N87-16838
Observation of ice/water formations on a model intake section subjected to simulated cloud conditions — aircraft engine [PNR90347] N87-16839
Future trends in propulsion — aircraft [PNR90349] N87-16840
An approach to AE monitoring during the rig shop testing of large CFRP aero-engine components — acoustic emission (AE) [PNR90350] N87-16841
The technology of advanced prop-fan transmissions [PNR90357] N87-16843
Aircraft derivative gas turbine development in China [PNR90359] N87-16844
Operational aids to engine development [PNR90362] N87-16845
Grinding of steel: A case study [AD-A174649] N87-17048

AIRCRAFT MAINTENANCE
Evaluation of DDH and weld repaired F100 turbine vanes under simulated service conditions N87-17070
Repair techniques for gas turbine components N87-17071

AIRCRAFT NOISE
Identification and proposed control of helicopter transmission noise at the source [NASA-TM-89312] N87-16816
The influence of wind-tunnel walls on discrete frequency noise N87-16850
Combustion noise from gas turbine aircraft engines measurement of far-field levels [NASA-TM-88971] N87-17480
Aircraft noise synthesis system [NASA-TM-89040] N87-17483

AIRCRAFT PERFORMANCE
Performance data Aeroc 8.2.AC.20, issue 5, Dash 8, series 100 N87-16817

AIRCRAFT PRODUCTION
Method and apparatus for die forming metal sheets and extrusions [AD-D012512] N87-16920
Economical manufacturing and inspection of the electron-beam-welded Tornado wing box N87-17055
Diffusion bonding in the manufacture of aircraft structure N87-17057
Inertia welding of nitralloy N and 18 nickel maraging 250 grade steels for utilization in the main rotor drive shaft for the AR-64 military helicopter program N87-17067

AIRCRAFT SPIN
Flight investigation of the effect of tail configuration on stall, spin, and recovery characteristics of a low-wing general aviation research airplane [NASA-TP-2644] N87-16815

AIRCRAFT STRUCTURES
Diffusion welding of component parts in the aviation and space industries [RAE-TRANS-2147] N87-17032
Economical manufacturing and inspection of the electron-beam-welded Tornado wing box N87-17055
Diffusion bonding in the manufacture of aircraft structure N87-17057
Structural Analysis [ESA-TT-917] N87-17077
Research on structural analysis at the DFVLR, Brunswick N87-17078
Torsion-tension coupling in rods N87-17079
Ground vibration tests [ETN-87-98847] N87-17422
Flight-vehicle structures education in the US: Assessment and recommendations [NASA-CR-4048] N87-17526

AIRFOILS
Measurement of the three-dimensional aerodynamics of an annular cascade airfoil row N87-16788
Euler solutions using an implicit multigrid technique [NASA-TM-58276] N87-16792
Navier-Stokes solution for laminar transonic flow over a NACA0012 airfoil [FAA-140] N87-16794
Computational, unsteady transonic aerodynamics and aeroelasticity about airfoils and wings [NASA-TM-89414] N87-16801
Profile design in transonic regime [ETN-87-98849] N87-16810
Analysis of viscous transonic flow over airfoil sections [NASA-TM-88912] N87-17001
Unitized high temperature probes [AD-D012508] N87-17020

AIRFRAMES
Assessment of damage tolerance requirements and analysis. Volume 1: Executive summary [AD-A175110] N87-16822

AIRPORTS
Frost action predictive techniques for roads and airfields: A comprehensive survey of research findings [DOT/FAA/PM-85/23] N87-16853

AIRSPEED
Digital program for calculating static pressure position error
[NASA-TM-86726] N87-16821
ALBEDO
Vertical structure of aerosols and clouds in the atmospheres of Uranus and Neptune: Implications for their heat budgets N87-17643
ALGEBRA
Computation of turbulent boundary layer flows with an algebraic stress turbulence model
[NASA-CR-178967] N87-16982
ALGORITHMS
SOLA: A basic solution algorithm for flow analysis N87-16996
Applications of SOLA to confined flows — numerical flow computing methods N87-16997
Applications of SOLA to free surface flows — flow computing method N87-16998
Position control of mechanical manipulators by using nonlinear adaptive control algorithm N87-17031
A parallel solution for the symmetric Eigenproblem
[NASA-TM-89082] N87-17086
Simulation modeling and preliminary analysis of TIMS data from the Carlin area and the northern Grapevine Mountains, Nevada N87-17120
An automatic tracking mode switching algorithm for the ERS-1 altimeter N87-17195
Determination of resistivity and permittivity profiles of a layered Earth N87-17198
ERS-1 wind scatterometer: Wind extraction and ambiguity removal N87-17227
Developpement of algorithms to retrieve the water equivalent of snow cover from satellite microwave radiometer data N87-17264
An iterative multi-resolution shape-from-shading algorithm and its application to planetary mapping N87-17331
A two-step algorithm for the separate retrieval of ocean surface and atmospheric parameters from microwave radiometers N87-17341
Basic research for the geodynamics program
[NASA-CR-180137] N87-17415
Homogenizing surface and satellite observations of cloud
[AD-A174691] N87-17427
Algorithms and programming tools for image processing on the MPP, part 2
[NASA-CR-180146] N87-17440
Globally convergent hybrid conjugate gradient methods
[MR-196] N87-17454
Recursive linear smoothing for dissipative hyperbolic systems
[AD-A173020] N87-17460
On first passage times and differential equations
[AD-A174648] N87-17470
Implicit particle simulation of electromagnetic plasma phenomena
[IPPJ-799] N87-17509
A search for rapidly modulated emission in bright X-ray sources using the HEAO A-1 data base
[NASA-CR-180148] N87-17593
ALPS MOUNTAINS (EUROPE)
Snow cover recession in an Alpine ecological system N87-17316
ALTITUDE
The contraction of satellite orbits under the influence of air drag. Part 7: Orbits of high eccentricity, with scale height dependent on altitude
[RAE-TR-86013] N87-16859
ALUMINUM
A composite aluminum conductor for pulsed power applications at cryogenic temperatures and method of its manufacture
[AD-D012501] N87-16885
Investigation of a GaAlAs Mach-Zehnder electro-optic modulator
[NASA-CR-179573] N87-16953
ALUMINUM ALLOYS
The application of diffusion bonding and laser welding in the fabrication of aerospace structures N87-17054
The welding of aluminum alloys: A new technology in space application N87-17056
Diffusion bonding in the manufacture of aircraft structure N87-17057
Diffusion bonding of Al-alloys in the solid state N87-17058
Welding of aluminum castings N87-17068
ALUMINUM COATINGS
Burner rig and engine test experience of platinum aluminide coatings
[PNR90342] N87-16837
AMBIGUITY
Antenna ambiguity investigations for X-SAR — shuttle-borne radar N87-17355
Reconsideration of azimuth ambiguities in SAR N87-17356
AMMONIA
VLA observations of Jupiter at 1.3 - 20 cm wavelengths N87-17606
Study of the ammonia ice cloud layer in the north tropical zone of Jupiter from the infrared interferometric experiment on Voyager N87-17609
AMMONIUM NITRATES
Atmospheric pressure studies of liquid propellant drops in hot flows
[AD-A174639] N87-16915
ANALYSIS (MATHEMATICS)
A three dimensional calculation of elastic equilibrium for composite materials
[NASA-CR-178158] N87-17088
On the analytical determination of relaxation modulus of viscoelastic materials by Prony's interpolation method
[NASA-TM-86579] N87-17455
ANDES MOUNTAINS (SOUTH AMERICA)
Tectonic geomorphology of the Andes with SIR-A and SIR-B N87-17136
ANGLE OF ATTACK
Optimal turning at high angle of attack of supersonic and hypersonic vehicles N87-16814
ANGULAR MOMENTUM
Spacecraft attitude control momentum requirements analysis
[NASA-CR-178219] N87-16864
Redistribution of angular momentum by nonaxisymmetric instabilities in a thick accretion disk
[PUBL-SER-C-FASC-4] N87-17585
Numerical calculations of radiation transport in a dusty medium in disk geometry N87-17591
Transport of absolute angular momentum in quasi-axisymmetric equatorial jet streams N87-17635
ANGULAR RESOLUTION
Active optics for the far infrared submillimeter wave space telescope (FIRST): A high angular resolution mode N87-17566
ANISOTROPIC MEDIA
Effective permeability and macrodispersion in locally heterogeneous aquifers
[MEMO-585] N87-17015
ANISOTROPY
Microstrip dipoles for EHF and millimeter wave applications
[AD-A173025] N87-16976
A spatially homogeneous anisotropic surface model with variable parameters for scattering from bare soil N87-17183
ANNEALING
Low noise polycrystalline semiconductor resistors by hydrogen passivation
[AD-D012492] N87-17520
ANNIHILATION REACTIONS
Radiative processes underlying the X-ray and gamma-ray continua of active galactic nuclei and gamma-ray bursts N87-17655
ANNUAL VARIATIONS
Ocean surface temperature field variability N87-17104
Monitoring of large phenomena in developing countries through satellite imagery N87-17172
A model of the spatial and temporal variation of the Uranus thermal structure N87-17642
ANNULAR FLOW
Measurement of the three-dimensional aerodynamics of an annular cascade airfoil row N87-16788
ANNULAR NOZZLES
Afterbody shape effects on the near-wake velocity characteristics at Mach numbers between 0.35 and 0.92
[ISL-CO-205/86] N87-17011
ANOMALIES
Dynamical models for the Earth's geoid N87-17409
Improvement of the Earth's gravity field from terrestrial and satellite data
[NASA-CR-180139] N87-17416
ANTARCTIC REGIONS
USSR report: Earth sciences
[JPRS-UES-86-005] N87-17096
ANTENNA ARRAYS
The Electronically Steered Thinned Array Radiometer (ESTAR) N87-17260
Planar array antenna for ERS-1 synthetic aperture radar N87-17357
ANTENNA COMPONENTS
Composite space antenna structures: Properties and environmental effects
[NASA-TM-88859] N87-16880
ANTENNA COUPLERS
In-band antenna coupling research
[AD-A175093] N87-16962
ANTENNA DESIGN
Proceedings of the Second ESA Workshop on Mechanical Technology for Antennas
[ESA-SP-261] N87-16923
Antenna mechanical technologies within ESA N87-16924
Mechanical and control study of a 7 m offset unfurlable tracking antenna N87-16926
Development of a 2.8 m offset antenna reflector using inflatable, space-rigidized structures technology N87-16927
Study on solid surface, deployable antenna reflector — satellite antenna N87-16928
Analysis of high precision composite sandwich antennas — spacecraft antennas N87-16929
Dielectric support structures for spacecraft antenna feeds N87-16931
Qualification of gridding process for a Polarization Sensitive Reflector (PSR) — satellite antenna N87-16932
Design of a low distortion shared aperture reflector — satellite antenna N87-16934
Development of lightweight dimensionally stable carbon fiber composite antenna reflectors for the INSAT-1 satellite N87-16936
Giotto spacecraft high gain antenna mechanical design and development N87-16938
Development status of the ERS-1 SAR antenna N87-16939
ERS-1 wind scatterometer antenna: Mechanical aspects N87-16940
Design and technology of feed array and beam forming network for contoured beam antennas — satellite antennas N87-16950
Beam forming network technologies and related manufacturing processes — satellite antennas N87-16951
Application of adaptive antenna techniques to future commercial satellite communication
[NASA-CR-179566] N87-16954
Comparisons of the detection performance of a space-based radar system using different antenna systems and aperture illuminations
[AD-A173094] N87-16960
The FRS-66010: A new concept for the acquisition and analysis of NOAA HRPT data N87-17206
The Electronically Steered Thinned Array Radiometer (ESTAR) N87-17260
Planar array antenna for ERS-1 synthetic aperture radar N87-17357
ANTENNA FEEDS
Dielectric support structures for spacecraft antenna feeds N87-16931
Design and technology of feed array and beam forming network for contoured beam antennas — satellite antennas N87-16950
ANTENNA RADIATION PATTERNS
Design and technology of feed array and beam forming network for contoured beam antennas — satellite antennas N87-16950
In-band antenna coupling research
[AD-A175093] N87-16962
Absolute gain measurement by the image method under mismatched condition
[NASA-TM-88924] N87-16968
Determining the vertical pattern of a spaceborne SAR by observation of uniform targets — SIR-B N87-17240
Antenna pattern correction in scanning radiometry: A singular system analysis N87-17261
Antenna ambiguity investigations for X-SAR — shuttle-borne radar N87-17355
ANTENNAS
ICNIA (Integrated Communications Navigation Identification Avionics) HF transmitter system preliminary study
[AD-A173013] N87-16823
In-band antenna coupling research
[AD-A175093] N87-16962
High energy surge arrester technology development, part 2
[AD-A173086] N87-16977
APERTURES
Effect of the size of structural bulk inhomogeneities on the specular transmittance of polymer films
[DE86-010727] N87-16913
Comparisons of the detection performance of a space-based radar system using different antenna systems and aperture illuminations
[AD-A173094] N87-16960
In-band antenna coupling research
[AD-A175093] N87-16962
APPLICATIONS PROGRAMS (COMPUTERS)
Calculation of sidewall boundary-layer parameters from rake measurements for the Langley 0.3-meter transonic cryogenic tunnel
[NASA-CR-178241] N87-16807

Digital program for calculating static pressure position error
[NASA-TM-86726] N87-16821
IRSAP: An improved approach in processing remotely sensed data — Interactive Remote Sensing Applications Package (IRSAP) N87-17332

APPROXIMATION
A multigrid LU-SSOR scheme for approximate Newton iteration applied to the Euler equations
[NASA-CR-179524] N87-16803
Introduction to Numerical Solution of Industrial Flows, volume 1 — conference
[VKI-LS-1986-07-VOL-1] N87-16987
An analysis of flow models: From Navier-Stokes to potential flow equations N87-16988
The spatial levels of approximation from three-dimensional to quasi one-dimensional representation — averaging procedure (flow computation) N87-16989
Introduction to Numerical Solution of Industrial Flows, volume 2 — conference
[VKI-LS-1986-07-VOL-2] N87-16994

AQUIFERS
Effective permeability and macrodispersion in locally heterogeneous aquifers
[MEMO-585] N87-17015

ARC WELDING
Weld quality monitor and control system N87-17062
A real time vision system for robotic arc welding N87-17066

ARCHAEOLOGY
The Red River Valley archeological project N87-17128

ARCHITECTURE (COMPUTERS)
Data communication requirements for the advanced NAS network
[NASA-TM-89315] N87-16957
The design and evaluation of a high performance smalltalk system
[AD-A173022] N87-17437
Algorithms and programming tools for image processing on the MPP, part 2
[NASA-CR-180146] N87-17440
Programming robotics applications on an advanced hypercube multiprocessor
[DE86-008895] N87-17445
Information processing research
[AD-A173028] N87-17533

ARCTIC OCEAN
Observing the polar oceans with spaceborne radar N87-17151
An inter-sensor comparison of the microwave signatures of Arctic sea ice N87-17184
Active/passive microwave sensor comparison of MIZ-ice concentration estimates — Marginal Ice Zone (MIZ) N87-17185
Sea ice in the Greenland sea observed by the Nimbus-7 Scanning Multichannel Microwave Radiometer (SMMR) N87-17221
Application of the Seasat scatterometer to observations of wind speed and direction and Arctic ice/water boundaries N87-17259

ARCTIC REGIONS
USSR report: Earth sciences
[JPRS-UES-86-005] N87-17096

ARGENTINA
Multiple incidence angle SIR-B experiment over Argentina N87-17157

ARID LANDS
Spatial analysis of the dynamics of an ecosystem by multistage remote sensing in Kenya N87-17173

ARTIFICIAL INTELLIGENCE
Knowledge-based aerial image understanding systems N87-17210
Programming robotics applications on an advanced hypercube multiprocessor
[DE86-008895] N87-17445

ASTEROIDS
The study of the physics of cometary nuclei
[NASA-CR-180153] N87-17594

ASTROMETRY
Parsec-scale structure in the nuclei of double lobed radio quasars N87-17588

ASTRONOMICAL MODELS
Interstellar dust N87-17545
Scale-free models of highly flattened elliptical galaxies N87-17589
Numerical calculations of radiation transport in a dusty medium in disk geometry N87-17591
The dynamics and evolution of clusters of galaxies
[NASA-CR-180169] N87-17596

ASTRONOMICAL OBSERVATORIES
Observations from the Gornergrat Observatory (Switzerland) with the University of Cologne 3-m radio telescope N87-17573

ASTRONOMICAL PHOTOMETRY
Submillimeter observation of the integrated galactic emission from the South Pole N87-17560

ASTRONOMICAL SATELLITES
Far infrared submillimeter wave space telescope (FIRST) observations of stars with large mass loss rates N87-17550
A proposed cornerstone mission: Far infrared submillimeter wave telescope (FIRST) N87-17564
Structure of molecular clouds and space-based sub-millimeter telescopes, for example FIRST — Far Infrared Submillimeter Wave Space Telescope (FIRST) N87-17574

ASTRONOMICAL SPECTROSCOPY
Submillimeter cometary spectroscopy N87-17541
An 800 MHz bandwidth acousto-optical spectrometer at Helsinki Observatory N87-17567
Changes in Saturn's south-temperate haze distribution during the summer of 1973-1980 N87-17602

ASTRONOMY
International ultraviolet explorer observing program: Ultraviolet observations of selected astronomical sources
[NASA-CR-180155] N87-17584

ASTROPHYSICS
FY 1986 scientific and technical reports, articles, papers and presentations
[NASA-TM-86575] N87-17532

ATMOSPHERIC ATTENUATION
Analysis of AIS radiometry at Mono Lake, California — Airborne Imaging Spectrometer (AIS) N87-17204
Extrapolation of Earth-based solar irradiance measurements to exoatmospheric levels for broad-band and selected absorption-band observations N87-17270
Effects of rain cells on SAR performance N87-17354

ATMOSPHERIC BOUNDARY LAYER
An introduction to the numerical modelling of dispersion in the atmospheric boundary layer N87-16993

ATMOSPHERIC CHEMISTRY
The Jovian Atmospheres
[NASA-CP-2441] N87-17598

ATMOSPHERIC CIRCULATION
Global dynamics and thermal structure of Jupiter's atmosphere N87-17621
Jupiter: New estimates of mean zonal flow at the cloud level N87-17622
Convective forcing of global circulations on the Jovian planets N87-17624
Eddy processes in the general circulation of the Jovian atmospheres N87-17627
The Saturnian ribbon feature: A baroclinically unstable model N87-17629
Quasi-geostrophic free mode models of long-lived Jovian eddies: Forcing mechanisms and crucial observational tests N87-17630
A proposal for adopting a standard coordinate system for defining atmospheric nomenclature for the giant planets N87-17632
Astronomical, physical, and meteorological parameters for planetary atmospheres N87-17647

ATMOSPHERIC COMPOSITION
Determination of nonglobal component against background of global radioactive pollution of atmospheric aerosols N87-17100
Middle Atmosphere Program. Handbook for MAP, volume 22
[NASA-CR-180128] N87-17414
SAGE aerosol measurements. Volume 3: January 1, 1981 to November 18, 1981
[NASA-RP-1173] N87-17417
Water vapor in Jupiter's atmosphere N87-17605
Vertical cloud structure models for the NTRZ EQZ, SEB and STRZ of Jupiter N87-17608
Enhanced acetylene emission near the north pole of Jupiter N87-17614
Brown dwarfs and Jovian planets: A comparison N87-17616
The abundances of ethane to acetylene in the atmospheres of Jupiter and Saturn N87-17618
Laboratory measurements of microwave absorption from gaseous atmospheric constituents under conditions for the outer planets N87-17620
The HD/H2 ratio in the atmosphere of Uranus N87-17646

ATMOSPHERIC CORRECTION
Estimation of absolute water surface temperature based on atmospherically corrected thermal infrared multispectral scanner digital data N87-17114
Atmospheric correction of TIMS data N87-17115

ATMOSPHERIC DIFFUSION
An introduction to the numerical modelling of dispersion in the atmospheric boundary layer N87-16993

ATMOSPHERIC EFFECTS
The contraction of satellite orbits under the influence of air drag. Part 7: Orbits of high eccentricity, with scale height dependent on altitude
[RAE-TR-86013] N87-16859
A study of anomalous propagation at radar frequencies and a proposal for a radar coverage forecasting model, book 2 of 2
[ETN-87-98938] N87-16967
Applications of TIMS data in agricultural areas and related atmospheric considerations N87-17124
Atmospheric corrections of NOAA-AVHRR data verification of different methods by ground truth measurements N87-17274
Radiometric correction method which removes both atmospheric and topographic effects from the LANDSAT-MSS data N87-17329
A two-step algorithm for the separate retrieval of ocean surface and atmospheric parameters from microwave radiometers N87-17341

ATMOSPHERIC HEAT BUDGET
Evaluation of geophysical parameters measured by the Nimbus-7 microwave radiometer for the TOGA Heat Exchange Project
[NASA-CR-180151] N87-17110

ATMOSPHERIC HEATING
Spatial variation of the thermal structure of Jupiter's atmosphere N87-17612
A model of the spatial and temporal variation of the Uranus thermal structure N87-17642

ATMOSPHERIC MODELS
An introduction to the numerical modelling of dispersion in the atmospheric boundary layer N87-16993
Atmospheric correction of TIMS data N87-17115
Applications of TIMS data in agricultural areas and related atmospheric considerations N87-17124
Model study of the mid-latitude atmospheric interaction with energetic O+ and He+ (20 keV) precipitation during a storm N87-17411
Empirical relations between the Earth's radiation budget, cloudiness, and various meteorological parameters N87-17424
Modeling the temporal and spatial variations of the vertical structure of Jupiter's atmosphere using observations of the 3-0 hydrogen quadrupole lines N87-17601
Thermal balance of the atmospheres of Jupiter and Uranus N87-17604
Water vapor in Jupiter's atmosphere N87-17605
The vertical structure of Jupiter's equatorial and tropical regions N87-17607
The single scattering phase functions of Jupiter's clouds N87-17613
Brown dwarfs and Jovian planets: A comparison N87-17616
The ortho-para H2 distribution on Uranus: Constraints from the collision-induced 3-0 dipole band and 4-0 S(0) and S(1) quadrupole line profiles N87-17640

ATMOSPHERIC MOISTURE
Ground-based microwave radiometric observations of atmospheric geopotential height fluctuations N87-17339
A diagnostic approach to obtaining planetary boundary layer winds using satellite-derived thermal data
[NASA-CR-178972] N87-17420
Moisture driven convection on Jupiter: A mechanism to produce the equatorial plumes N87-17631

ATMOSPHERIC OPTICS
A study of anomalous propagation at radar frequencies and a proposal for a radar coverage forecasting model, book 2 of 2
[ETN-87-98938] N87-16967
Analysis of AIS radiometry at Mono Lake, California — Airborne Imaging Spectrometer (AIS) N87-17204

ATMOSPHERIC PHYSICS
USSR report: Earth sciences
[JPRS-UES-86-005] N87-17096
FY 1986 scientific and technical reports, articles, papers and presentations
[NASA-TM-86575] N87-17532

ATMOSPHERIC PRESSURE
Spatial variation of the thermal structure of Jupiter's atmosphere N87-17612

ATMOSPHERIC RADIATION
VLA observations of Jupiter at 1.3 - 20 cm wavelengths N87-17606

ATMOSPHERIC SCATTERING
The single scattering phase functions of Jupiter's clouds N87-17613

ATMOSPHERIC SOUNDING
Joint influence of turbulence and wind on signal power in radioacoustic sounding of atmosphere N87-17108

Proceedings of the 1986 International Geoscience and Remote Sensing Symposium (IGARSS '86) on Remote Sensing: Today's Solutions for Tomorrow's Information Needs, volume 1
[ESA-SP-254-VOL-1] N87-17163
Application of Doppler radar and lidar to diagnose atmospheric phenomena N87-17271
Proceedings of the 1986 International Geoscience and Remote Sensing Symposium (IGARSS' 86) on Remote Sensing: Today's Solutions for Tomorrow's Information Needs, volume 2
[ESA-SP-254-VOL-2] N87-17283
Ground-based microwave radiometric observations of atmospheric geopotential height fluctuations N87-17339
A study of planetary atmospheres in the submillimetric range N87-17540
A 186 GHz radiometer for the microwave limb sounder N87-17589

ATMOSPHERIC STRATIFICATION
Modeling the temporal and spatial variations of the vertical structure of Jupiter's atmosphere using observations of the 3-0 hydrogen quadrupole lines N87-17601

ATMOSPHERIC TEMPERATURE
Contemporary changes in climate and paleoclimate N87-17099
Assessment of contemporary changes in global climate N87-17101
Spatial variation of the thermal structure of Jupiter's atmosphere N87-17612
Global dynamics and thermal structure of Jupiter's atmosphere N87-17621
Convective adjustment in baroclinic atmospheres N87-17626
Chaotic motion in the Jovian atmosphere N87-17634
Radiative-convective equilibrium models of Uranus and Neptune N87-17641

ATMOSPHERIC TURBULENCE
Joint influence of turbulence and wind on signal power in radioacoustic sounding of atmosphere N87-17108
Application of Doppler radar and lidar to diagnose atmospheric phenomena N87-17271

ATTITUDE CONTROL
Structural dynamics and attitude control study of early manned capability space station configurations
[NASA-TM-89078] N87-16861
Spacecraft attitude control momentum requirements analysis
[NASA-CR-178219] N87-16864

AUGMENTATION
Batten augmented triangular beam
[NASA-CR-172461] N87-16916

AURORAL ARCS
A model for an electromotive force generator in the magnetosphere: A source of discrete auroral arcs
[AERONOMICA-ACTA-A-309-1986] N87-17421

AURORAL ZONES
Two micron quadrupole line emission of H2 from the Jovian auroral zone N87-17615

AURORAS
Model study of the mid-latitude atmospheric interaction with energetic O+ and He+ (20 keV) precipitation during a storm N87-17411

AUSTENITIC STAINLESS STEELS
Microstructural modifications during laser and electron beam welding
[DE86-011076] N87-17049

AUTOMATIC CONTROL
Weld quality monitor and control system N87-17062

AUTOREGRESSIVE PROCESSES
A prediction error estimate for nonlinear stochastic systems
[RR-295] N87-17471

AVALANCHE DIODES
The 60 GHz IMPATT diode development
[NASA-CR-179536] N87-17515

AVERAGE
The spatial levels of approximation from three-dimensional to quasi one-dimensional representation — averaging procedure (flow computation) N87-16989

AVIONICS
ICNIA (Integrated Communications Navigation Identification Avionics) HF transmitter system preliminary study
[AD-A173013] N87-16823

AXIAL COMPRESSION LOADS
Optimization of axially compressed Carbon Fiber Reinforced Plastic (CFRP) cylinders N87-17082

AXIAL FLOW
Measurements of the unsteady flow field within the stator row of a transonic axial-flow fan. 1: Measurement and analysis technique
[NASA-TM-88945] N87-16789

AXIAL FLOW TURBINES
Measurements of the unsteady flow field within the stator row of a transonic axial-flow fan. Part 2: Results and discussion
[NASA-TM-88946] N87-16790
Unsteady flows in a single-stage transonic axial-flow fan stator row
[NASA-TM-88929] N87-16805
Application of flow calculation methods to transonic and supersonic axial turbomachines
[ONERA-RTS-80/7103-EY] N87-16846

AXIAL STRAIN
On the influence of strain-path changes on fracture
[AD-A172535] N87-17091

AZIMUTH
Reconsideration of azimuth ambiguities in SAR N87-17356

AZOLES
Vinyl stilbazoles
[NASA-CASE-ARC-11429-3CU] N87-16908

B

BACKGROUND NOISE
Noise-immune multisensor transduction of speech
[AD-A174693] N87-16961
The influence of background power on the performance of an ideal bolometer N87-17585

BACKGROUND RADIATION
Opportunities and potential for a millimetre wavelength search for the Sunyaev-Zeldovich effect N87-17555
Ultralow background searches for beta beta-decay, cold dark matter and solar axions
[DE86-013592] N87-17652

BACKSCATTERING
Imaging radar polarimetry from wave synthesis N87-17158
Radar signature determination: Trends and limitations N87-17159
A spatially homogeneous anisotropic surface model with variable parameters for scattering from bare soil N87-17183
Microwave backscatter coefficients of artificially grown first-year sea ice N87-17188
Verification results for a two-scale model of microwave backscatter from the sea surface N87-17213
Tower-based broadband backscattering measurements from the ocean surface in the North Sea N87-17217
Extraction of the backscatter coefficient of agricultural fields from an airborne SAR image N87-17265
Measurement of sea backscatter at extremely low grazing angle by C-band Doppler radar N87-17301
A backscattering model for various foliated deciduous tree types at millimeter wavelengths N87-17307
A scattering model for defoliated vegetation N87-17309
Evaluating roughness models of radar backscatter N87-17344
Microwave backscattering from an anisotropic soybean canopy N87-17346
On the relationship between age of lava flows and radar backscattering N87-17348
Backscattering power spectrum for randomly moving vegetation N87-17349

BALANCE
Interferometric load sensor and strain gage
[AD-D012509] N87-17021

BALL BEARINGS
Oil film thickness measurement and analysis for an angular contact ball bearing operating in parched elastohydrodynamic lubrication
[NASA-CR-179506] N87-16879

BALLOON-BORNE INSTRUMENTS
New results about diffuse galactic emission at 380 microns N87-17554

BALMER SERIES
International ultraviolet explorer observing program: Ultraviolet observations of selected astronomical sources
[NASA-CR-180155] N87-17584

BALTIC SEA
Retrieval of near-surface wind speed in the Baltic Sea from NIMBUS-7 Scanning Multichannel Microwave Radiometer (SMMR) observations N87-17342
Sea ice studies in the Baltic Sea using satellite microwave radiometer data N87-17343

BANACH SPACE
A construction of solutions of the multicomponent KP-hierarchy
[MEMO-584] N87-17476

BARIUM COMPOUNDS
Research on millimeter wave dielectric materials
[AD-A173017] N87-17521

BARLEY
Analysis of the spatial structure of Synthetic Aperture Radar (SAR) imagery for a better separability of cereal crops, wheat and barley N87-17287

BAROCLINIC INSTABILITY
The Saturnian ribbon feature: A baroclinically unstable model N87-17629
Quasi-geostrophic free mode models of long-lived Jovian eddies: Forcing mechanisms and crucial observational tests N87-17630

BAROCLINIC WAVES
Convective adjustment in baroclinic atmospheres N87-17626

BAROCLINITY
Convection without eddy viscosity: An attempt to model the interiors of giant planets N87-17625

BAROTROPIC FLOW
Convection without eddy viscosity: An attempt to model the interiors of giant planets N87-17625

BATHYMETERS
Observations of surface currents at Nantucket Shoals and implications for radar imaging of the bottom N87-17296

BEAM INJECTION
A self-consistent modeling of a quasi-steady state compact torus evolving to ignition
[IPPJ-801] N87-17511

BEAM SPLITTERS
Projection lens scanning laser velocimeter system
[NASA-CASE-ARC-11547-1] N87-17026

BEAMS (RADIATION)
Modeling of nonlinear effects of plasma wave beams on ionospheric plasma N87-17107
Nanosecond two-dimensional imaging using tomographic techniques
[DE86-008164] N87-17499

BEAMS (SUPPORTS)
Estimation and control of distributed models for certain elastic systems arising in large space structures
[AD-A175019] N87-16872
Comparison of composite rotor blade models: A coupled-beam analysis and an MSC/NASTRAN finite-element model
[NASA-TM-89024] N87-16884
Batten augmented triangular beam
[NASA-CR-172461] N87-16916

BEARING (DIRECTION)
Measurement of the directional spectrum of ocean waves using a conically-scanning radar N87-17383

BEDS (PROCESS ENGINEERING)
Prediction of heat and mass transfer in particulate beds N87-16999

BENDING
Reducing shuttle-payload dynamic interaction with notch filters
[NASA-CR-171958] N87-16862

BENZENE
Empirical considerations for laser guided electron beams in the advanced test accelerator
[DE86-013218] N87-17489

BETA PARTICLES
Ultralow background searches for beta beta-decay, cold dark matter and solar axions
[DE86-013592] N87-17652

BIBLIOGRAPHIES
Compendium of NASA Langley reports on hypersonic aerodynamics
[NASA-TM-87760] N87-16802
Wind energy technical reading list
[DE86-010704] N87-17404
Scientific and technical information output of the Langley Research Center for calendar year 1986
[NASA-TM-89065] N87-17531

BIG BANG COSMOLOGY
The early universe N87-17539

BIOLOGICAL EFFECTS
Biological effects of aerial shock waves: Review of work to date
[ISL-NB-402/85] N87-17432

BIOT METHOD
Sound propagation in a superfluid helium filled porous solid: Theory and experiment N87-17478

BISMALEIMIDE
Vinyl stilbazoles
[NASA-CASE-ARC-11429-3CU] N87-16908

BLACK BODY RADIATION
The early universe N87-17539

BLACK HOLES (ASTRONOMY)
Redistribution of angular momentum by nonaxisymmetric instabilities in a thick accretion disk
[PUBL-SER-C-FASC-4] N87-17585
A numerical study of jet production and accretion disk structure in super-Eddington black hole accretion N87-17586

BLAST LOADS
Development of a drag measurement system for the CERF 6-foot shock tube
[AD-A173087] N87-16854
A study of explosive wave propagation in granular materials with microstructure
[AD-A173015] N87-16914
BLUFF BODIES
An introduction to numerical methods for flow around bluff bodies N87-16992
BLUNT BODIES
Computation of separation ahead of blunt fin in supersonic turbulent flow
[NASA-TM-89416] N87-16791
BOLOMETERS
The influence of background power on the performance of an ideal bolometer N87-17565
BOLTS
Fatigue life and fastener flexibility of single shear riveted and bolted joints
[FFA-TN-1986-35] N87-17094
BOUNDARY LAYER CONTROL
Experimental investigation of the turbulence production mechanism in boundary layers
[AD-A173091] N87-17007
BOUNDARY LAYER FLOW
Computation of turbulent boundary layer flows with an algebraic stress turbulence model
[NASA-CR-178967] N87-16982
BOUNDARY LAYER SEPARATION
Experimental investigation in turbulent flow separation
[ISL-CO-208/86] N87-17012
Three-dimensional separation on a cylindrical ellipsoid. Results of the first test campaign on the F2 wind tunnel
[ONERA-RT-16/7252-AN] N87-17013
BOUNDARY LAYER STABILITY
Stability characteristics of a supersonic boundary layer and their relation to the position of the laminar-turbulent transition point
[NASA-TM-88533] N87-16797
BOUNDARY LAYER TRANSITION
Transitional boundary layers under the influence of high free stream turbulence, intensive wall cooling and high pressure gradients in hot gas circulation
[NASA-TM-88524] N87-16983
BOUNDARY LAYERS
A general method for unsteady stagnation region heat transfer and results for model turbine flows
[NASA-TM-88903] N87-17002
BOUNDARY VALUE PROBLEMS
Design of software for design of finite element for structural analysis
[NASA-TM-88528] N87-17089
Theoretical consideration on resistance geoelectrics N87-17196
Survey of the status of finite element methods for partial differential equations
[NASA-CR-178222] N87-17456
A pseudo-arclength continuation method for nonlinear Eigenvalue problems
[AD-A173019] N87-17459
A transportation queueing model, solved as a Riemann boundary value problem
[MEMO-573] N87-17463
Simple and insensitive bounds for a grading and an overflow model
[MEMO-581] N87-17467
A formal proof for the insensibility of simple bounds for finite multiserver nonexponential tandem queues
[MEMO-582] N87-17468
Initial-value problem for the 1-D wave equation in an inhomogeneous medium
[IPPCZ-266] N87-17505
Crystal growth and furnace analysis
[NASA-CR-178998] N87-17516
BRAGG ANGLE
A two-scale Bragg scattering model for microwave backscatter from wind generated waves N87-17212
Identification of the contribution of Bragg scattering and specular reflection to X-band microwave backscattering in an ocean experiment N87-17216
BRANCHING (MATHEMATICS)
On routes to chaotic motion in oscillators with unsymmetric and symmetric elastic nonlinearity
[ISSN-0208-5658] N87-16969
Selection principles and pattern formation in fluid mechanics and nonlinear shell theory
[NASA-CR-180159] N87-17004
On the stochastic dissemination of faults in an admissible network
[NASA-CR-178238] N87-17469
BRAZING
Bonding of superalloys by diffusion welding and diffusion brazing N87-17059
The application of the RBD process to the deposition of anti-wear alloys N87-17069
Repair techniques for gas turbine components N87-17071
BREMSSTRAHLUNG
Radiative processes underlying the X-ray and gamma-ray continua of active galactic nuclei and gamma-ray bursts N87-17655
BRIDGMAN METHOD
Crystal growth and furnace analysis
[NASA-CR-178998] N87-17516
BRIGHTNESS TEMPERATURE
The TIMS investigator's guide N87-17113
Effect of electrical and thermal properties of materials on microwave brightness temperature of the terrestrial crust N87-17263
Microwave radiances from horizontally finite precipitating clouds containing ice and liquid hydrometeors N87-17340
BRITTLE MATERIALS
Application of modified three parameter Weibull distributions to brittle material design
[RARDE-16/84] N87-17072
BROADBAND
A new model for broadband waveguide to microstrip transition design
[NASA-TM-88905] N87-16958
Extrapolation of Earth-based solar irradiance measurements to exoatmospheric levels for broad-band and selected absorption-band observations N87-17270
BROADCASTING
On codes with multi-level error-correction capabilities
[NASA-CR-180166] N87-17458
BROKEN SYMMETRY
Research program in theoretical high-energy physics
[DE86-013326] N87-17490
BUBBLES
Light scattering theory for bubbles in water: Inverse scattering, coated bubbles and statistics
[AD-A174997] N87-17498
BUCKLING
Buckling and postbuckling behavior of shallow shells N87-17081
BUILDINGS
Radar imagery of the European city influenced by variations in depression angle and look direction N87-17237
BUOYS
The accuracy and availability of operational marine surface wind data for ERS-1 sensor calibration and validation from fixed platforms and free drifting buoys N87-17376
Using buoys and ships to calibrate ERS-1 altimeter and scatterometer N87-17377
BYPASSES
A pi-section digital phase shifter apparatus
[AD-D012495] N87-16973

C

C BAND
C and Ku-band scatterometer results from the SCATTMOD internal wave experiment N87-17215
Results of the ESA airborne C-band scatterometer campaigns — ERS-1 N87-17225
Measurement of sea backscatter at extremely low grazing angle by C-band Doppler radar N87-17301
An advanced SAR design for future land missions N87-17322
Evaluation of the different parameters in Long's C-band model — for ERS-1 scatterometer N87-17370
C-130 AIRCRAFT
The use of aircraft for wind scatterometer calibration — ERS-1 scatterometer N87-17382
C-135 AIRCRAFT
The effects of gravity level during directional solidification on the microstructure of hypermonotectic Al-In-Sn alloys
[NASA-TM-86573] N87-16801
CABLES (ROPES)
Test apparatus for uniform tensioning of long lengths of small cables in simulated environments
[AD-D012487] N87-17045
CADMIUM TELLURIDES
Research on single-crystal CdTe solar cells
[DE86-010719] N87-17405
CALIBRATING
Low-g measurements by NASA
[NASA-TM-86585] N87-17017
A preliminary study of factors affecting the calibration stability of the iridium versus iridium-40 percent rhodium thermocouple
[NASA-TM-89086] N87-17018
Atmospheric correction of TIMS data N87-17115
SIR-B measurements and modeling of vegetation N87-17160
The ESA approach for ERS-1 sensor calibration and performance verification N87-17192
ERS-1 radar altimeter: Performance, calibration and data validation N87-17194
Analysis of AIS radiometry at Mono Lake, California — Airborne Imaging Spectrometer (AIS) N87-17204
Extraction of the backscatter coefficient of agricultural fields from an airborne SAR image N87-17265
Calibrated X and L-band scattering coefficients from a southern US forest N87-17312
Proceedings of an ESA Workshop on ERS-1 Wind and Wave Calibration
[ESA-SP-262] N87-17363
ERS-1 mission constraints related to wind and wave calibration N87-17364
The influence of spatial and temporal scales on calibration/validation — ERS-1 sensors N87-17365
Gathering and processing a comparative data set for the calibration and validation of ERS-1 data products; preparatory work at the UK-ERS-DC — Data Center (DC) N87-17367
Requirements and constraints in the calibration and validation of ERS-1 wind and wave parameters N87-17369
The use of numerical wind and wave models to provide areal and temporal extension to instrument calibration and validation of remotely sensed data — satellite data N87-17371
The accuracy and availability of operational marine surface wind data for ERS-1 sensor calibration and validation from fixed platforms and free drifting buoys N87-17376
Using buoys and ships to calibrate ERS-1 altimeter and scatterometer N87-17377
Canada Center for Remote Sensing (CCRS) Convair 580 results relevant to ERS-1 wind and wave calibration N87-17379
The use of aircraft for wind scatterometer calibration — ERS-1 scatterometer N87-17382
Australian validation plans for ERS-1 N87-17387
Variability in the Earth radiation budget as determined from the Nimbus ERB experiments N87-17410
CALIFORNIA
Thermal imaging spectroscopy in the Kelso-Baker Region, California N87-17117
The application of remotely sensed data to pedologic and geomorphic mapping on alluvial fan and playa surfaces in Saline Valley, California N87-17127
Application of Thermal Infrared Multiband Scanner (TIMS) data to mapping of Plutonic and stratified rock and assemblages in accreted terrains of the Northern Sierra, California N87-17132
CANADIAN SPACE PROGRAM
Canadian plans for operational demonstrations of satellite imaging radar applications — ERS-1 N87-17229
CANOPIES (VEGETATION)
Investigation of forest canopy temperatures recorded by the thermal infrared multispectral scanner at H. J. Andrews Experimental Forest N87-17123
Applications of TIMS data in agricultural areas and related atmospheric considerations N87-17124
TIMS data applications in Nebraska N87-17126
Analysis of multiple incidence angle SIR-B data for determining forest stand characteristics N87-17156
Assessing grass canopy condition and growth from combined optical-microwave measurements N87-17286
Microwave backscattering from an anisotropic soybean canopy N87-17346
L to X-band scatter and emission measurements of vegetation N87-17347
Canopy hot-spot as crop identifier
[DE86-011258] N87-17395
CANTILEVER PLATES
Estimation and control of distributed models for certain elastic systems arising in large space structures
[AD-A175019] N87-16872
CAPACITANCE
Oil film thickness measurement and analysis for an angular contact ball bearing operating in parched elastohydrodynamic lubrication
[NASA-CR-179506] N87-16879
Unified formulation for linear accelerator design
[DE86-013441] N87-17491
CAPILLARY TUBES
Expandable pulse power spacecraft radiator
[AD-D012498] N87-17005
CARBON DIOXIDE CONCENTRATION
Assessment of contemporary changes in global climate N87-17101
CARBON FIBER REINFORCED PLASTICS
An approach to AE monitoring during the rig shop testing of large CFRP aero-engine components — acoustic emission (AE)
[PNR90350] N87-16841
Optimization of axially compressed Carbon Fiber Reinforced Plastic (CFRP) cylinders N87-17082

CARBON FIBERS
Carbon fibre composite coupons: Static and fatigue behaviour after impact damage
[ARL-STRUC-R-422] N87-16861
CARBON MONOXIDE
Lumped model generation and evaluation: Sensitivity and lie algebraic techniques with applications to combustion
[AD-A174984] N87-16896
CO observations of the outflow source NGC 7023 N87-17563
CASCADE FLOW
Measurement of the three-dimensional aerodynamics of an annular cascade airfoil row N87-16788
CASSEGRAIN ANTENNAS
Study on solid surface, deployable antenna reflector — satellite antenna N87-16928
CASTING
Method and apparatus for die forming metal sheets and extrusions
[AD-D012512] N87-16920
Unitized high temperature probes
[AD-D012508] N87-17020
CASTINGS
Welding of aluminum castings N87-17068
CATALOGS (PUBLICATIONS)
Radar Cross Section (RCS) data base deduced from radar images N87-17323
CATALYSIS
Transient catalytic combustion
[AD-A173098] N87-16894
CATHODE RAY TUBES
Unitary suprathreshold color-difference metrices of legibility for CRT raster imagery
[AD-A175062] N87-17434
CAVITIES
Space shuttle main engine high pressure fuel pump aft platform seal cavity flow analysis
[NASA-TP-2685] N87-17000
CEPSTRAL ANALYSIS
Power cepstrum technique with application to model helicopter acoustic data
[NASA-TP-2586] N87-17479
CERAMIC COATINGS
Metallization for hermetic sealing of ceramic modules
[AD-D012483] N87-17044
CERAMICS
Surface flaw reliability analysis of ceramic comonents with the SCARE finite element postprocessor program
[NASA-TM-88901] N87-17067
CH-47 HELICOPTER
Identification of a dynamic model of a helicopter from flight tests N87-16813
CHALLENGER (ORBITER)
A new day: Challenger and space flight thereafter
[NASA-TM-77717] N87-16856
CHANNEL FLOW
Measurement of heat transfer and pressure drop in rectangular channels with turbulence promoters
[NASA-CR-4015] N87-17003
CHAOS
On routes to chaotic motion in oscillators with unsymmetric and symmetric elastic nonlinearity
[ISSN-0208-5658] N87-16969
CHARACTERIZATION
On variational characterizations of steady vortex rings
[MEMO-577] N87-17014
Crack propagation in UD (Unidirectional) laminates by the stress intensity factors N87-17084
CHARGE TRANSFER
Dual channel high electron mobility field effect transistor
[AD-D012474] N87-17518
CHARGED PARTICLES
Enhanced acetylene emission near the north pole of Jupiter N87-17614
CHEMICAL ANALYSIS
Metal content of ocean water studied with radio spectrometer N87-17102
CHEMICAL CLOUDS
Study of the ammonia ice cloud layer in the north tropical zone of Jupiter from the infrared interferometric experiment on Voyager N87-17609
CHEMICAL COMPOSITION
Metal content of ocean water studied with radio spectrometer N87-17102
Lithologic mapping of silicate rocks using TIMS N87-17118
The physical basis for spectral variations in thermal infrared emittance of silicates and application to remote sensing N87-17129
CHEMICAL FRACTIONATION
A detected feature at the expected wavelength for the HD R5(0) line in Jupiter's and Uranus' atmospheres N87-17619
CHEMICAL FUELS
Fuels combustion research
[AD-A175040] N87-16897
CHEMICAL INDICATORS
Self-contained, single-use hose and tubing cleaning module
[NASA-CASE-MSC-20857-1] N87-17035
CHEMICAL REACTIONS
Hypersonic nonequilibrium flow over an ablating teflon surface N87-16787
Evolution of a localized thermal explosion in a reactive gas
[NASA-CR-178231] N87-17436
CHLOROCARBONS
CF2 and CFCl fluorescence from VUV excitation of C2F3Cl N87-16891
CIRCUITS
High-voltage Milberger slip slide power conditioner
[AD-D012504] N87-16974
Monitoring transients in low inductance circuits
[DE86-013756] N87-16978
Universal pressure transducer
[AD-D012499] N87-17019
CIRCULAR CYLINDERS
Prediction of vortex shedding from circular and noncircular bodies in subsonic flow
[NASA-CR-4037] N87-16961
CIRCULAR POLARIZATION
Spatial dependence on sea spikes N87-17218
CITIES
Radar imagery of the European city influenced by variations in depression angle and look direction N87-17237
CLASSIFICATIONS
General classification of two-phase flow codes N87-16985
The physical basis for spectral variations in thermal infrared emittance of silicates and application to remote sensing N87-17129
Multispectral classification of microwave remote sensing images — SAR crop identification N87-17238
A statistical approach to select the optimal wavelength bands for separating rocks in the wavelength region 0.4 to 2.3 microns N87-17244
Evaluation of LANDSAT 5 Thematic Mapping (TM) data for image clustering and classification N87-17251
A simulation study of some contextual classification methods for remotely sensed data N87-17252
Classification of forest and surface types by satellite microwave radiometry N87-17305
CLATHRATES
Non-solar noble gas abundances in the atmosphere of Jupiter N87-17637
CLEANING
Self-contained, single-use hose and tubing cleaning module
[NASA-CASE-MSC-20857-1] N87-17035
CLIMATE
Geophysicist comments on how solar activity may affect weather N87-17097
Thermodynamic estimate of climatic system efficiency N87-17098
Contemporary changes in climate and paleoclimate N87-17099
Assessment of contemporary changes in global climate N87-17101
An overview of the implementation of the World Climate Research program N87-17388
CLIMATOLOGY
Contemporary changes in climate and paleoclimate N87-17099
Assessment of contemporary changes in global climate N87-17101
Imaging radar contributions to a major air-sea-ice interaction study in the Greenland Sea N87-17150
Wind energy technical reading list
[DE86-010704] N87-17404
CLOSED ECOLOGICAL SYSTEMS
Snow cover recession in an Alpine ecological system N87-17316
Supercritical water oxidation of products of human metabolism
[NASA-CR-180144] N87-17430
CLOUD COVER
Image processing methods in two and three dimensions used to animate remotely sensed data — cloud cover N87-17292
Vertical cloud structure models for the NTRZ EQZ, SEB and STRZ of Jupiter N87-17608
CLOUD GLACIATION
Microwave radiances from horizontally finite precipitating clouds containing ice and ..quid hydrometeors N87-17340
CLOUD PHOTOGRAPHY
Stereo Line Scanner (SLS): System considerations on an operational instrument for meteorology and weather forecasts N87-17168
Image processing methods in two and three dimensions used to animate remotely sensed data — cloud cover N87-17292
CLOUD PHYSICS
T-28 data acquisition during COHMEX 1986
[NASA-CR-179001] N87-17426
CLOUDS
Homogenizing surface and satellite observations of cloud
[AD-A174691] N87-17427
The vertical structure of Jupiter's equatorial and tropical regions N87-17607
Jupiter: New estimates of mean zonal flow at the cloud level N87-17622
CLOUDS (METEOROLOGY)
Microwave radiances from horizontally finite precipitating clouds containing ice and liquid hydrometeors N87-17340
The Jovian Atmospheres
[NASA-CP-2441] N87-17598
Cloud-top meridional momentum transports on Saturn and Jupiter N87-17623
Investigation of long-lived eddies on Jupiter N87-17633
CLUSTER ANALYSIS
Evaluation of LANDSAT 5 Thematic Mapping (TM) data for image clustering and classification N87-17251
A nonparametric supervised multiaprectral classification method using binary morphological operators N87-17253
CLUTCHES
Non-backdriveable free wheeling coupling
[NASA-CASE-MSC-20475-1] N87-17037
CMOS
Performance of polysilicon gate CMOS devices in space and SDI environments
[DE86-009025] N87-17524
COASTS
The ice conditions in the Greenland waters, 1980
[REPT-551.467.3.068(988)] N87-17428
COATING
The application of the RBD process to the deposition of anti-wear alloys N87-17069
COATINGS
The non-metallic materials sample array
[NASA-TM-88578] N87-16910
COCKPITS
Noise-immune multisensor transduction of speech
[AD-A174693] N87-16961
CODING
Multiple Trellis Coded Modulation (MTCM): An MSAT-X report
[NASA-CR-180134] N87-16921
Robotic vision system
[AD-D012481] N87-17043
Cyclic unequal error protection codes constructed from cyclic codes of composite length
[NASA-CR-180165] N87-17457
COHERENT ELECTROMAGNETIC RADIATION
Coherent versus noncoherent signaling for satellite-aided mobile communications
[NASA-CR-180133] N87-16922
COHERENT RADAR
Application of Spaceborne Distributed Aperture/Coherent Array Processing (SDA/CAP) technology to active and passive microwave remote sensing N87-17277
Coherent polarimetric Radar Cross Section (RCS) measurements on trees N87-17310
COHERENT RADIATION
A search for rapidly modulated emission in bright X-ray sources using the HEAO A-1 data base
[NASA-CR-180148] N87-17593
COLD TRAPS
Low noise polycrystalline semiconductor resistors by hydrogen passivation
[AD-D012492] N87-17520
COLLISION PARAMETERS
Doubly differential cross sections for galactic heavy-ion fragmentation
[NASA-TP-2659] N87-17487
COLLOCATION
Adaptive control of a flexible structure N87-17449
COLOR
Unitary suprathreshold color-difference metrices of legibility for CRT raster imagery
[AD-A175062] N87-17434
COLORIMETRY
Unitary suprathreshold color-difference metrices of legibility for CRT raster imagery
[AD-A175062] N87-17434

COMBUSTION
Lumped model generation and evaluation: Sensitivity and lie algebraic techniques with applications to combustion
[AD-A174984] N87-16896
Evolution of a localized thermal explosion in a reactive gas
[NASA-CR-178231] N87-17436
Combustion noise from gas turbine aircraft engines measurement of far-field levels
[NASA-TM-88971] N87-17480

COMBUSTION CHAMBERS
Transition mixing study
[NASA-CR-175062] N87-16830
Developments in data acquisition and processing using an advanced combustion research facility — gas turbine engines
[RAE-TM-P1089] N87-16852
Space station auxiliary thrust chamber technology
[NASA-CR-179552] N87-16874
Transient catalytic combustion
[AD-A173098] N87-16894
Lumped model generation and evaluation: Sensitivity and lie algebraic techniques with applications to combustion
[AD-A174984] N87-16896
Conventionally cast and forged copper alloy for high-heat-flux thrust chambers
[NASA-TP-2694] N87-16902

COMET NUCLEI
The study of the physics of cometary nuclei
[NASA-CR-180153] N87-17594

COMETS
Submillimeter cometary spectroscopy N87-17541
The interaction between the solar wind and the comets
[AERONOMICA-ACTA-A-306-1986] N87-17653

COMMERCE
Advantageous syndicates in a bilateral market game: The case of the tau-value
[MEMO-583] N87-17534

COMMUNICATION
Research and technology
[NASA-TM-88868] N87-17656

COMMUNICATION NETWORKS
Application of adaptive antenna techniques to future commercial satellite communication
[NASA-CR-179566] N87-16954
Application of adaptive antenna techniques to future commercial satellite communication
[NASA-CR-179566] N87-16955
Transmission loss measurements in mobile radio nets
[FOA-B-30098-3.3] N87-16966

COMMUNICATION SATELLITES
Communications satellite systems operations with the space station. Volume 1: Executive summary
[NASA-CR-179526] N87-17472
Communications satellite systems operations with the space station, volume 2
[NASA-CR-179527] N87-17473

COMPARISON
Comparison of three explicit multigrid methods for the Euler and Navier-Stokes equations
[NASA-TM-88878] N87-16784
Comparisons of the detection performance of a space-based radar system using different antenna systems and aperture illuminations
[AD-A173094] N87-16960

COMPILERS
Information processing research
[AD-A173028] N87-17533

COMPLEX SYSTEMS
Decentralized control of large-scale systems: Fixed modes, sensitivity and parametric robustness
[NASA-TM-86537] N87-17474

COMPOSITE MATERIALS
Effect of adherend thickness and mixed mode loading on debond growth in adhesively bonded composite joints
[NASA-TM-88992] N87-16882
Structural Analysis
[ESA-TT-917] N87-17077
A three dimensional calculation of elastic equilibrium for composite materials
[NASA-CR-178158] N87-17088

COMPOSITE STRUCTURES
Composite space antenna structures: Properties and environmental effects
[NASA-TM-88859] N87-16880
Flight service evaluation of advanced composite ailerons on the L-1011 transport aircraft
[NASA-CR-178170] N87-16883
Comparison of composite rotor blade models: A coupled-beam analysis and an MSC/NASTRAN finite-element model
[NASA-TM-89024] N87-16884
Analysis of high precision composite sandwich antennas — spacecraft antennas N87-16929
Effects of curing stresses on composite structures N87-16930

COMPRESSIBLE FLOW
Calculation of supersonic flow over a compression corner N87-16785
Direct computation of wall bounded aerosol turbulent flow interactions
[DE86-013221] N87-17009

COMPRESSOR BLADES
Unsteady aerodynamics of a rotating compressor blade row in incompressible flow. Volume 1: Experimental facilities, procedures and sample data
[AD-A173043] N87-16831
Unsteady aerodynamics of a rotating compressor blade row at low Mach number. Volume 2: Analysis of experimental results and comparison with theory
[AD-A173044] N87-16832
Unsteady aerodynamics of a rotating compressor blade row at low mach number. Volume 3: Experimental data base and users manual
[AD-A173045] N87-16833

COMPRESSOR ROTORS
Unsteady aerodynamics of a rotating compressor blade row in incompressible flow. Volume 1: Experimental facilities, procedures and sample data
[AD-A173043] N87-16831
Unsteady aerodynamics of a rotating compressor blade row at low Mach number. Volume 2: Analysis of experimental results and comparison with theory
[AD-A173044] N87-16832
Unsteady aerodynamics of a rotating compressor blade row at low mach number. Volume 3: Experimental data base and users manual
[AD-A173045] N87-16833

COMPTON EFFECT
Opportunities and potential for a millimetre wavelength search for the Sunyaev-Zeldovich effect N87-17555
The development of the Goddard Compton gamma-ray telescope and neutral hydrogen N87-17580
Radiative processes underlying the X-ray and gamma-ray continua of active galactic nuclei and gamma-ray bursts N87-17655

COMPUTATION
Computation of separation ahead of blunt fin in supersonic turbulent flow
[NASA-TM-89416] N87-16791
Computational weld mechanics N87-17052

COMPUTATIONAL FLUID DYNAMICS
Comparison of three explicit multigrid methods for the Euler and Navier-Stokes equations
[NASA-TM-88878] N87-16784
Euler analysis of the three dimensional flow field of a high-speed propeller: Boundary condition effects
[NASA-TM-88955] N87-16798
Transonic unsteady aerodynamic and aeroelastic calculations about airfoils and wings
[NASA-TM-89417] N87-16800
Computational, unsteady transonic aerodynamics and aeroelasticity about airfoils and wings
[NASA-TM-89414] N87-16801
A high resolution shock capturing scheme for high Mach number internal flow
[NASA-CR-179523] N87-16804
An LU-SSOR scheme for the Euler and Navier-Stokes equations
[NASA-CR-179556] N87-16806
Profile design in transonic regime
[ETN-87-98849] N87-16810
Advanced 3-D viscous SSME turbine rotor stator CFD algorithms
[NASA-CR-178997] N87-16829
Application of flow calculation methods to transonic and supersonic axial turbomachines
[ONERA-RTS-80/7103-EY] N87-16846
Data communication requirements for the advanced NAS network
[NASA-TM-89315] N87-16957
Computation of turbulent boundary layer flows with an algebraic stress turbulence model
[NASA-CR-178967] N87-16982
Introduction to Numerical Solution of Industrial Flows, volume 1 — conference
[VKI-LS-1986-07-VOL-1] N87-16987
An analysis of flow models: From Navier-Stokes to potential flow equations N87-16988
The spatial levels of approximation from three-dimensional to quasi one-dimensional representation — averaging procedure (flow computation) N87-16989
Review of discretization techniques and numerical resolution methods N87-16990
The analysis and resolution of numerical schemes — flow problems N87-16991
An introduction to numerical methods for flow around bluff bodies N87-16992
An introduction to the numerical modelling of dispersion in the atmospheric boundary layer N87-16993
Introduction to Numerical Solution of Industrial Flows, volume 2 — conference
[VKI-LS-1986-07-VOL-2] N87-16994
Numerical methods for two-dimensional and three-dimensional heat transfer calculations N87-16995
SOLA: A basic solution algorithm for flow analysis N87-16996
Applications of SOLA to confined flows — numerical flow computing methods N87-16997
Applications of SOLA to free surface flows — flow computing method N87-16998
Prediction of heat and mass transfer in particulate beds N87-16999
Analysis of viscous transonic flow over airfoil sections
[NASA-TM-88912] N87-17001
FY 1986 scientific and technical reports, articles, papers and presentations
[NASA-TM-86575] N87-17532

COMPUTATIONAL GRIDS
Comparison of three explicit multigrid methods for the Euler and Navier-Stokes equations
[NASA-TM-88878] N87-16784
Euler solutions using an implicit multigrid technique
[NASA-TM-58276] N87-16792
A multigrid LU-SSOR scheme for approximate Newton iteration applied to the Euler equations
[NASA-CR-179524] N87-16803
A comparison of single-block and multi-block grids around wing-fuselage configurations
[FFA-TN-1986-42] N87-16811
Multigrid applied to singular perturbation problems
[NASA-CR-178230] N87-17444

COMPUTER AIDED DESIGN
Low aspect ratio turbine design at Rolls-Royce
[PNR90338] N87-16824
Operational aids to engine development
[PNR90362] N87-16845
The 60 GHz IMPATT diode development
[NASA-CR-179536] N87-17515

COMPUTER AIDED MANUFACTURING
Manufacturing cell for the V2500 variable vanes
[PNR90330] N87-16835

COMPUTER AIDED MAPPING
Computer-aided analysis of LANDSAT data for mapping geologic and geomorphic features, North Bombay, India N87-17235
Computer-derived height from SIR-B stereo radar images N87-17268
Image processing methods in two and three dimensions used to animate remotely sensed data — cloud cover N87-17292
Computer-aided interpretation of complex geological patterns in remote sensing N87-17294

COMPUTER GRAPHICS
The design and evaluation of a high performance smalltalk system
[AD-A173022] N87-17437
Comparative advantages of graphic versus numeric representation of quantitative data N87-17439
Line plotting program using DI-3000/Grafmaker routines
[NASA-TM-89010] N87-17442

COMPUTER PROGRAMMING
Profile design in transonic regime
[ETN-87-98849] N87-16810
General classification of two-phase flow codes N87-16985
The design and evaluation of a high performance smalltalk system
[AD-A173022] N87-17437
Profiling under UNIX by patching
[NASA-TM-89316] N87-17443
Multigrid applied to singular perturbation problems
[NASA-CR-178230] N87-17444
Vibroacoustic payload environment prediction system (VAPEPS): Data base management center remote access guide
[NASA-CR-180132] N87-17528

COMPUTER PROGRAMS
Transonic unsteady aerodynamic and aeroelastic calculations about airfoils and wings
[NASA-TM-89417] N87-16800
Discrete element weld model, phase 2
[NASA-CR-179009] N87-17041
Buckling and postbuckling behavior of shallow shells N87-17081
Surface flaw reliability analysis of ceramic comonents with the SCARE finite element postprocessor program
[NASA-TM-88901] N87-17087
HAWT performance with dynamic stall
[DE86-004428] N87-17402

COMPUTER SYSTEMS DESIGN
Design of software for design of finite element for structural analysis
[NASA-TM-88528] N87-17089
The design of an international data centre for remote sensing N87-17176
A knowledge-based software environment for the analysis of spectroradiometer data — mineral identification N87-17203
Portable EDITOR (PEDITOR): A portable image processing system — satellite images N87-17208
The ERS-1 scatterometer system simulator and its relevance for ground processing design N87-17257
COMPUTER SYSTEMS PERFORMANCE
A comparison of five benchmarks
[NASA-TM-88956] N87-17441
Fault-free performance validation of fault-tolerant multiprocessors
[NASA-CR-178236] N87-17448
COMPUTER SYSTEMS PROGRAMS
Dynamics and Control Analysis Package (DCAP): An automated analysis and design tool for structural control of space structures N87-16947
Engineering and software interfacing for thermal, structural and dynamic control related with spacecraft activities N87-16948
The image processing workbench - portable software for remote sensing instruction and research N87-17209
Interactive wrapper tool for mapping objects to Fortran library functions
[DE86-009686] N87-17446
COMPUTER TECHNIQUES
In-band antenna coupling research
[AD-A175093] N87-16962
Robotic vision system
[AD-D012481] N87-17043
RADARSAT high throughput SAR processor development N87-17154
COMPUTER VISION
A real time vision system for robotic arc welding N87-17066
An implementation of the Hough transform using a linear array processor in conjunction with a PDP/11microprocessor — computer vision
[NPL-DITC-74/86] N87-17438
COMPUTERIZED SIMULATION
The effects of heavy rain on profile aerodynamics
[ETN-87-98848] N87-16809
Direct computation of wall bounded aerosol turbulent flow interactions
[DE86-013221] N87-17009
Optical modeling of induction-linac driven free-electron lasers
[DE87-001432] N87-17027
Model for simulating rotational data for wind turbine applications
[DE86-010784] N87-17406
CONDENSERS (LIQUEFIERS)
Expandable pulse power spacecraft radiator
[AD-D012498] N87-17005
CONDUCTIVITY
Oil film thickness measurement and analysis for an angular contact ball bearing operating in parched elastohydrodynamic lubrication
[NASA-CR-179506] N87-16879
CONDUCTORS
A composite aluminum conductor for pulsed power applications at cryogenic temperatures and method of its manufacture
[AD-D012501] N87-16885
CONFERENCES
Proceedings of the Second ESA Workshop on Mechanical Technology for Antennas
[ESA-SP-261] N87-16923
Introduction to Numerical Solution of Industrial Flows, volume 1 — conference
[VKI-LS-1986-07-VOL-1] N87-16987
Introduction to Numerical Solution of Industrial Flows, volume 2 — conference
[VKI-LS-1986-07-VOL-2] N87-16994
Proceedings of the 15th International Symposium on Shock Waves and Shock Tubes
[AD-A173026] N87-17006
Advanced Joining of Aerospace Metallic Materials — conference proceedings
[AGARD-CP-398] N87-17051
Abstracts: Review of progress in quantitative NDE
[DE87-000769] N87-17073
The TIMS Data User's Workshop
[NASA-CR-180130] N87-17111
Proceedings of the 1986 International Geoscience and Remote Sensing Symposium (IGARSS '86) on Remote Sensing: Today's Solutions for Tomorrow's Information Needs, volume 1
[ESA-SP-254-VOL-1] N87-17163
Proceedings of the 1986 International Geoscience and Remote Sensing Symposium (IGARSS' 86) on Remote Sensing: Today's Solutions for Tomorrow's Information Needs, volume 2
[ESA-SP-254-VOL-2] N87-17283
Proceedings of an ESA Workshop on ERS-1 Wind and Wave Calibration
[ESA-SP-262] N87-17383
Proceedings of an ESA Workshop on a Spaceborne Submillimeter Astronomy Mission. A Cornerstone of the ESA Long Term Science Program
[ESA-SP-260] N87-17535
CONICAL SCANNING
Measurement of the directional spectrum of ocean waves using a conically-scanning radar N87-17383
CONJUGATE GRADIENT METHOD
Gradient methods for geophysical image inversions N87-17201
Globally convergent hybrid conjugate gradient methods
[MR-196] N87-17454
CONSERVATION EQUATIONS
Hypersonic nonequilibrium flow over an ablating teflon surface N87-16787
CONTINUITY (MATHEMATICS)
A pseudo-arclength continuation method for nonlinear Eigenvalue problems
[AD-A173019] N87-17459
CONTINUOUS RADIATION
Submillimetre continuum observations of active galactic nuclei N87-17558
CONTINUOUS WAVE LASERS
High intensity selectable poly or monochromatic slit light source apparatus for optical instruments
[AD-D012507] N87-17496
The optimum condition of TPD-1 recombining helium plasma for VUV coherent lasing action
[IPPJ-798] N87-17507
CONTINUOUS WAVE RADAR
Snow stratigraphy observed by an FM-CW microwave system N87-17181
A scatterometer operating at 10 GHz N87-17282
CONTROL SYSTEMS DESIGN
Piloted simulator study of allowable time delays in large-airplane response
[NASA-TP-2652] N87-16849
Adaptive control techniques for large space structures
[AD-A173083] N87-16871
Adaptive control of a flexible structure N87-17449
CONTROL THEORY
Dynamics and control of flexible manipulators N87-17028
Lattice filters and adaptive identification of flexible structures N87-17030
Model of the human controller of a dynamic system
[MEMO-580] N87-17435
Dynamic input-output decoupling of nonlinear control systems
[MEMO-575] N87-17452
Decentralized control of large-scale systems: Fixed modes, sensitivity and parametric robustness
[NASA-TM-88537] N87-17474
CONTROLLERS
Development of a sensitivity analysis technique for multiloop flight control systems N87-16847
Small computer interface to a stepper motor
[NASA-TM-86574] N87-16970
Dynamics and control of flexible manipulators N87-17028
A modified loop transfer recovery approach for robust control of flexible structures N87-17029
Position control of mechanical manipulators by using nonlinear adaptive control algorithm N87-17031
Adaptive control of mechanical manipulators N87-17450
CONVECTION CLOUDS
Moisture driven convection on Jupiter: A mechanism to produce the equatorial plumes N87-17631
CONVECTIVE FLOW
Numerical methods for two-dimensional and three-dimensional heat transfer calculations N87-16995
Brown dwarfs and Jovian planets: A comparison N87-17616
Convective forcing of global circulations on the Jovian planets N87-17624
Convection without eddy viscosity: An attempt to model the interiors of giant planets N87-17625
Convective adjustment in baroclinic atmospheres N87-17626
CONVECTIVE HEAT TRANSFER
Transient catalytic combustion
[AD-A173098] N87-16894
CONVERGENCE
The analysis and resolution of numerical schemes — flow problems N87-16991
COOPERATION
A note on a core catcher of a cooperative game
[MEMO-572] N87-17475
COPPER
Metal content of ocean water studied with radio spectrometer N87-17102
COPPER ALLOYS
Conventionally cast and forged copper alloy for high-heat-flux thrust chambers
[NASA-TP-2694] N87-16902
CORROSION PREVENTION
Corrosion/oxidation protection of high temperature material — gas turbine engines
[PNR90355] N87-16905
COSMIC DUST
Some results about laboratory dust analysis in the FIR range — cosmic dust simulation N87-17551
COSMOCHEMISTRY
Non-solar noble gas abundances in the atmosphere of Jupiter N87-17637
COSMOLOGY
Research program in theoretical high-energy physics
[DE86-013326] N87-17490
COST ANALYSIS
Performance data Aeroc 8.2.AC.20(300), issue 1 N87-16818
An alternative multi-mode SAR for RADARSAT N87-17144
COST EFFECTIVENESS
Diffusion welding of component parts in the aviation and space industries
[RAE-TRANS-2147] N87-17032
Utility of remote sensing data in renewable resource sample survey N87-17289
COST REDUCTION
Reducing the cost of aero engine research and development
[PNR90341] N87-16836
COUETTE FLOW
Selection principles and pattern formation in fluid mechanics and nonlinear shell theory
[NASA-CR-180159] N87-17004
COUNTING
Profiling under UNIX by patching
[NASA-TM-89316] N87-17443
COUPLERS
ICNIA (Integrated Communications Navigation Identification Avionics) HF transmitter system preliminary study
[AD-A173013] N87-16823
COUPLING
Microstrip dipoles for EHF and millimeter wave applications
[AD-A173025] N87-16976
Torsion-tension coupling in rods N87-17079
Dynamic input-output decoupling of nonlinear control systems
[MEMO-575] N87-17452
COUPLINGS
Comparison of composite rotor blade models: A coupled-beam analysis and an MSC/NASTRAN finite-element model
[NASA-TM-89024] N87-16884
Non-backdriveable free wheeling coupling
[NASA-CASE-MSC-20475-1] N87-17037
CRACK INITIATION
Preliminary investigations into the microcracking of PMR-15/graphite composites. Part 1: Effect of cure temperature
[PNR90348] N87-16887
An effective substructure technique applied to crack problems N87-17083
Dynamic fracture initiation and propagation in 4340 steel under impact loading
[AD-A173084] N87-17092
Three dimensional CTOD measurements of elastic-plastic surface flaws
[DE86-013454] N87-17093
CRACK PROPAGATION
Assessment of damage tolerance requirements and analysis. Volume 1: Executive summary
[AD-A175110] N87-16822
Stress intensity factors for fatigue cracks at holes under cyclic stress gradients N87-17075
Structural Analysis
[ESA-TT-917] N87-17077
An effective substructure technique applied to crack problems N87-17083
Crack propagation in UD (Unidirectional) laminates by the stress intensity factors N87-17084
Energy dissipation associated with crack extension in an elastic-plastic material
[NASA-TM-89032] N87-17090
Dynamic fracture initiation and propagation in 4340 steel under impact loading
[AD-A173084] N87-17092

Three dimensional CTOD measurements of elastic-plastic surface flaws
[DE86-013454] N87-17093

CRACK TIPS
Three dimensional CTOD measurements of elastic-plastic surface flaws
[DE86-013454] N87-17093

CRACKS
Assessment of damage tolerance requirements and analysis. Volume 1: Executive summary
[AD-A175110] N87-16822
Study of the electron beam weldability of superalloys through the analysis of melt zone morphology N87-17053
Stress intensity factors for fatigue cracks at holes under cyclic stress gradients N87-17075
Surface flaw reliability analysis of ceramic components with the SCARE finite element postprocessor program
[NASA-TM-88901] N87-17087

CRATERS
Zhamanshin meteor crater
[NASA-TM-86531] N87-17595

CREEP PROPERTIES
SRB O-ring free response analysis
[NASA-TM-86582] N87-17040

CRITICAL POINT
A note on Branin's method for finding the critical points of smooth functions
[MEMO-578] N87-17465

CROP GROWTH
Assessing grass canopy condition and growth from combined optical-microwave measurements N87-17286
L to X-band scatter and emission measurements of vegetation N87-17347

CROP IDENTIFICATION
Multispectral classification of microwave remote sensing images — SAR crop identification N87-17238
The influence of resampling method and multitemporal LANDSAT imagery on crop classification accuracy in the United Kingdom N87-17250

CROP INVENTORIES
Rural land use inventory and mapping in the Ardeche area (France) using multitemporal Thematic Mapping (TM) data N87-17350

CROPS
A scatterometer operating at 10 GHz N87-17282

CROSS FLOW
Laser Doppler velocimeter measurements and theoretical investigation of three dimensional scroll flow N87-16979

CROSSED FIELD AMPLIFIERS
Free electron diode oscillator
[AD-D012519] N87-16975

CROSSLINKING
Interpenetrating-network polymeric electrolytes
[AD-D012485] N87-16912

CRUISING FLIGHT
Optimal turning at high angle of attack of supersonic and hypersonic vehicles N87-16814

CRUSTAL FRACTURES
Basic research for the geodynamics program
[NASA-CR-180137] N87-17415

CRYOGENIC FLUID STORAGE
Tethered orbital refueling study
[NASA-CR-171953] N87-16855

CRYOGENICS
A composite aluminum conductor for pulsed power applications at cryogenic temperatures and method of its manufacture
[AD-D012501] N87-16885

CRYSTAL GROWTH
Research on single-crystal CdTe solar cells
[DE86-010719] N87-17405

CUMULONIMBUS CLOUDS
T-28 data acquisition during COHMEX 1986
[NASA-CR-179001] N87-17426

CUMULUS CLOUDS
Moisture driven convection on Jupiter: A mechanism to produce the equatorial plumes N87-17631

CURING
Preliminary investigations into the microcracking of PMR-15/graphite composites. Part 1: Effect of cure temperature
[PNR90348] N87-16887
Effects of curing stresses on composite structures N87-16930

CYANO COMPOUNDS
Vibrationally excited cyanoacetylene in regions of massive star formation N87-17561

CYCLIC LOADS
Effect of adherend thickness and mixed mode loading on debond growth in adhesively bonded composite joints
[NASA-TM-88992] N87-16882
Stress intensity factors for fatigue cracks at holes under cyclic stress gradients N87-17075

CYLINDRICAL BODIES
Solution of direct gravimetry problems for vertical cylindrical bodies N87-17105

CYLINDRICAL SHELLS
Optimization of axially compressed Carbon Fiber Reinforced Plastic (CFRP) cylinders N87-17082

CZECHOSLOVAKIA
Results of geomagnetic observations at the Hurbanovo Geomagnetic Observatory in 1985 N87-17419

D

DAMAGE
Assessment of damage tolerance requirements and analysis. Volume 1: Executive summary
[AD-A175110] N87-16822
Damage and repairing of fiber composites, a summary
[FOA-C-20620-2.5] N87-16888

DARK MATTER
Dark matter and the dynamics of galaxy clustering N87-17587

DATA ACQUISITION
Design and initial application of the extended aircraft interrogation and display system: Multiprocessing ground support equipment for digital flight systems
[NASA-TM-86740] N87-16820
A distributed data acquisition system for aeronautics test facilities
[NASA-TM-88961] N87-16851
Developments in data acquisition and processing using an advanced combustion research facility — gas turbine engines
[RAE-TM-P1089] N87-16852
Atmospheric correction of TIMS data N87-17115
Detection and mapping of volcanic rock assemblages and associated hydrothermal alteration with Thermal Infrared Multiband Scanner (TIMS) data Comstock Lode Mining District, Virginia City, Nevada N87-17119
Investigation of forest canopy temperatures recorded by the thermal infrared multispectral scanner at H. J. Andrews Experimental Forest N87-17123
TIMS data applications in Nebraska N87-17126
A geologic atlas of TIMS data N87-17133
The FRS-68010: A new concept for the acquisition and analysis of NOAA HRPT data N87-17206
Digital satellite imagery acquisition and processing N87-17207

DATA BASE MANAGEMENT SYSTEMS
Vibroacoustic payload environment prediction system (VAPEPS): Data base management center remote access guide
[NASA-CR-180132] N87-17528

DATA BASES
Unsteady aerodynamics of a rotating compressor blade row at low mach number. Volume 3: Experimental data base and users manual
[AD-A173045] N87-16833
Space shuttle main engine vibration data base
[NASA-TM-86576] N87-16876
A geologic atlas of TIMS data N87-17133
The design of an international data centre for remote sensing N87-17176
The UK ERS Data Centre, an offline processing and archiving facility N87-17230
Radar Cross Section (RCS) data base deduced from radar images N87-17323
Gathering and processing a comparative data set for the calibration and validation of ERS-1 data products; preparatory work at the UK-ERS-DC — Data Center (DC) N87-17367
Improvement of the Earth's gravity field from terrestrial and satellite data
[NASA-CR-180139] N87-17416

DATA CONVERSION ROUTINES
Quasi real time conversion of ERS-1 scatterometer raw data to sigma zero triplets N87-17226

DATA MANAGEMENT
Initial utilization of the CVIRB video production facility
[NASA-TM-89036] N87-16873
An overview of operational SAR data collection and dissemination plans for ERS-1 ice data in Canada N87-17189

DATA PROCESSING
Developments in data acquisition and processing using an advanced combustion research facility — gas turbine engines
[RAE-TM-P1089] N87-16852
Data communication requirements for the advanced NAS network
[NASA-TM-89315] N87-16957
Off-line processing of ERS-1 synthetic aperture radar data with high precision and high throughput N87-17153
RADARSAT high throughput SAR processor development N87-17154
ERS-1 synthetic aperture radar fast delivery processor N87-17228
IRSAP: An improved approach in processing remotely sensed data — Interactive Remote Sensing Applications Package (IRSAP) N87-17332
NASA scatterometer data processing system: Features for validation N87-17366
Comparative advantages of graphic versus numeric representation of quantitative data N87-17439

DATA REDUCTION
Unsteady aerodynamics of a rotating compressor blade row at low mach number. Volume 3: Experimental data base and users manual
[AD-A173045] N87-16833
Comparative advantages of graphic versus numeric representation of quantitative data N87-17439

DATA SAMPLING
The influence of resampling method and multitemporal LANDSAT imagery on crop classification accuracy in the United Kingdom N87-17250
Utility of remote sensing data in renewable resource sample survey N87-17289

DATA STORAGE
Unsteady aerodynamics of a rotating compressor blade row at low mach number. Volume 3: Experimental data base and users manual
[AD-A173045] N87-16833

DATA SYSTEMS
NASA scatterometer data processing system: Features for validation N87-17366
Gathering and processing a comparative data set for the calibration and validation of ERS-1 data products; preparatory work at the UK-ERS-DC — Data Center (DC) N87-17367

DATA TRANSMISSION
Single frequency multitransmitter telemetry
[NASA-CASE-LAR-13006-1] N87-16863

DE HAVILLAND AIRCRAFT
Performance data Aeroc 8.2.AC.20, issue 5, Dash 8, series 100 N87-16817

DECIDUOUS TREES
A backscattering model for various foliated deciduous tree types at millimeter wavelengths N87-17307

DECISION MAKING
Collaborative problem solving for installation planning and decision making
[AD-A174611] N87-17527

DECOUPLING
Dynamic input-output decoupling of nonlinear control systems
[MEMO-575] N87-17452

DEEP SPACE
On the identification of IRAS deep field sources: The radio counterparts N87-17552

DEFECTS
Study of the electron beam weldability of superalloys through the analysis of melt zone morphology N87-17053
Influence of welding flaws on the fatigue strength of electron beam weldments in Ti Al6 V4 N87-17065

DEFOLIATION
A scattering model for defoliated vegetation N87-17309

DEFORESTATION
Monitoring of large phenomena in developing countries through satellite imagery N87-17172

DEFORMATION
Dynamical models for the Earth's geoid N87-17409

DEICERS
Performance data Aeroc 8.2.AC.20, issue 5, Dash 8, series 100 N87-16817

DELAMINATING
Carbon fibre composite coupons: Static and fatigue behaviour after impact damage
[ARL-STRUC-R-422] N87-16881
Effect of adherend thickness and mixed mode loading on debond growth in adhesively bonded composite joints
[NASA-TM-88992] N87-16882

DENSE PLASMAS
Modeling of nonlinear effects of plasma wave beams on ionospheric plasma N87-17107

DENSITY MEASUREMENT
Simultaneous density velocity measurements in premixed turbulent flames to assess a theoretical model N87-16889

DEPLOYMENT
Wind Scatterometer Antenna (WSA) release shock loads — ERS-1 N87-16945

DEPTH
Determination of resistivity and permittivity profiles of a layered Earth N87-17198

DEPTH MEASUREMENT
An improved method for the determination of water depth from surface wave refraction patterns — SAR imagery N87-17299
DESCRIPTIONS
Performance data Aeroc 8.2.AC.20, issue 5, Dash 8, series 100 N87-16817
DESERTIFICATION
Monitoring of large phenomena in developing countries through satellite imagery N87-17172
Spatial analysis of the dynamics of an ecosystem by multistage remote sensing in Kenya N87-17173
DESIGN ANALYSIS
Common problems and pitfalls in gear design [NASA-TM-88858] N87-17033
N-ROSS validation N87-17385
Design and dynamic simulation of a fixed pitch 56 kW wind turbine drive train with a continuously variable transmission [NASA-CR-179543] N87-17401
Physics considerations on a fusion plasma in a field-reversed configuration [IPPJ-803] N87-17513
DETECTION
Comparisons of the detection performance of a space-based radar system using different antenna systems and aperture illuminations [AD-A173094] N87-16960
Light scattering theory for bubbles in water: Inverse scattering, coated bubbles and statistics [AD-A174997] N87-17498
DETERGENTS
Self-contained, single-use hose and tubing cleaning module [NASA-CASE-MSC-20857-1] N87-17035
DEUTERIUM
Physics considerations on a fusion plasma in a field-reversed configuration [IPPJ-803] N87-17513
A detected feature at the expected wavelength for the HD R5(0) line in Jupiter's and Uranus' atmospheres N87-17619
The HD/H2 ratio in the atmosphere of Uranus N87-17646
DEUTERIUM COMPOUNDS
A possible deuterium anomaly: Implications of the CH3D/CH4 mixing ratios in the atmospheres of Jupiter, Saturn, and Uranus N87-17617
DEUTERONS
Advanced fuels in a field-reversed configuration [IPPJ-804] N87-17512
DEVELOPING NATIONS
Sri Lanka's solution to land use mapping and monitoring for Third World countries development N87-17174
DICHROISM
Thermomechanical characteristics of dichroic subreflectors — satellite antennas N87-16952
DICTIONARIES
NASA thesaurus supplement (supplement 2) [NASA-SP-7053(SUPP-2)] N87-17530
DIELECTRIC PROPERTIES
Effect of electrical and thermal properties of materials on microwave brightness temperature of the terrestrial crust N87-17263
Research on millimeter wave dielectric materials [AD-A173017] N87-17521
DIELECTRICS
Microwave dielectric spectrum of vegetation material N87-17345
Metal film light modulator [AD-D012506] N87-17495
Research on millimeter wave dielectric materials [AD-A173017] N87-17521
DIES
Method and apparatus for die forming metal sheets and extrusions [AD-D012512] N87-16920
DIFFERENCE EQUATIONS
Convenient total variation diminishing conditions for nonlinear difference schemes [NASA-CR-178209] N87-17453
DIFFERENTIAL EQUATIONS
On first passage times and differential equations [AD-A174648] N87-17470
DIFFERENTIAL INTERFEROMETRY
Interferometer applications for the rectification of radar images N87-17241
DIFFUSION
On the possible role of the bootstrap effect in the RF current drive experiments, part 2 [IPPCZ-263] N87-17504
DIFFUSION WELDING
Diffusion welding of component parts in the aviation and space industries [RAE-TRANS-2147] N87-17032
Advanced Joining of Aerospace Metallic Materials — conference proceedings [AGARD-CP-398] N87-17051
The application of diffusion bonding and laser welding in the fabrication of aerospace structures N87-17054
Diffusion bonding in the manufacture of aircraft structure N87-17057
Diffusion bonding of Al-alloys in the solid state N87-17058
Bonding of superalloys by diffusion welding and diffusion brazing N87-17059
Application of diffusion bonding combined with superplastic forming (SPF/DB) to the fabrication of TAGV metal sheet structures N87-17060
Ultrasonic testing techniques for diffusion-bonded titanium components N87-17061
The application of the RBD process to the deposition of anti-wear alloys N87-17069
DIGITAL COMMAND SYSTEMS
Design and initial application of the extended aircraft interrogation and display system: Multiprocessing ground support equipment for digital flight systems [NASA-TM-86740] N87-16820
DIGITAL COMPUTERS
Quantitative analysis of fracture surfaces using computer aided fractography N87-17076
DIGITAL DATA
The SIR-C ground data system: Digital processor, data products, information flow N87-17155
Digital satellite imagery acquisition and processing N87-17207
DIGITAL ELECTRONICS
A pi-section digital phase shifter apparatus [AD-D012495] N87-16973
DIGITAL RADAR SYSTEMS
Roundoff noise analysis for digital Doppler processors in radar scatterometers N87-17258
Digital terrain mapping with STAR-1 SAR data N87-17269
DIGITAL SIMULATION
A powerful utility for assessing the performance of the ERS-1 synthetic aperture radar N87-17361
DIGITAL SYSTEMS
The SIR-C ground data system: Digital processor, data products, information flow N87-17155
DIGITAL TECHNIQUES
Detection and mapping of volcanic rock assemblages and associated hydrothermal alteration with Thermal Infrared Multiband Scanner (TIMS) data Comstock Lode Mining District, Virginia City, Nevada N87-17119
Applications of TIMS data in agricultural areas and related atmospheric considerations N87-17124
Calculation of day and night emittance values N87-17131
Application of Thermal Infrared Multiband Scanner (TIMS) data to mapping of Plutonic and stratified rock and assemblages in accreted terrains of the Northern Sierra, California N87-17132
Digital techniques for noise reduction in Automatic Picture Transmission (APT) NOAA satellite images N87-17328
DIMENSIONAL STABILITY
Design of a low distortion shared aperture reflector — satellite antenna N87-16934
Development of lightweight dimensionally stable carbon fiber composite antenna reflectors for the INSAT-1 satellite N87-16936
DIOXIDES
Measurement of HO2 chemical kinetics with a new detection method [NASA-CR-180114] N87-16890
DIRECTIONAL SOLIDIFICATION (CRYSTALS)
Electrical properties of Al-In-Sn alloys directionally solidified in high and low gravitational fields [NASA-TM-86569] N87-16900
The effects of gravity level during directional solidification on the microstructure of hypermonotectic Al-In-Sn alloys [NASA-TM-86573] N87-16901
Crystal growth and furnace analysis [NASA-CR-178998] N87-17516
DISCRETE FUNCTIONS
Recent developments in discrete-ordinates electron transport [DE86-007827] N87-17485
DISCRIMINANT ANALYSIS (STATISTICS)
A statistical approach to select the optimal wavelength bands for separating rocks in the wavelength region 0.4 to 2.3 microns N87-17244
DISPERSING
Effective permeability and macrodispersion in locally heterogeneous aquifers [MEMO-585] N87-17015
DISPERSIONS
Representation of the vaporization behavior of turbulent polydisperse sprays by equivalent monodisperse sprays [NASA-TM-88906] N87-16827
An introduction to the numerical modelling of disperaion in the atmospheric boundary layer N87-16993
Apparatus and method for stirring fluid borne particles [AD-D012486] N87-17477
DISPLACEMENT
Calculation of sidewall boundary-layer parameters from rake measurements for the Langley 0.3-meter transonic cryogenic tunnel [NASA-CR-178241] N87-16807
DISPLAY DEVICES
Design and initial application of the extended aircraft interrogation and display system: Multiprocessing ground support equipment for digital flight systems [NASA-TM-86740] N87-16820
Advanced alternating frame technology (VISIDEP (TM)) and three-dimensional remote sensing N87-17291
Unitary suprathreshold color-difference metrices of legibility for CRT raster imagery [AD-A175062] N87-17434
DISTRIBUTED PROCESSING
A distributed data acquisition system for aeronautics test facilities [NASA-TM-88961] N87-16851
Information processing research [AD-A173028] N87-17533
DISTURBANCES
A study of large, medium and small scale structures in the topside ionosphere [NASA-CR-180068] N87-17413
DIURNAL VARIATIONS
Effect of electrical and thermal properties of materials on microwave brightness temperature of the terrestrial crust N87-17263
DOPPLER RADAR
Roundoff noise analysis for digital Doppler processors in radar scatterometers N87-17258
Application of Doppler radar and lidar to diagnose atmospheric phenomena N87-17271
Measurement of sea backscatter at extremely low grazing angle by C-band Doppler radar N87-17301
Results from 1984 airborne Doppler lidar wind measurement program. Flight 6: Analysis of line-of-sight elevation angle errors and apparent Doppler velocities [NASA-CR-178994] N87-17425
DRAG MEASUREMENT
Development of a drag measurement system for the CERF 6-foot shock tube [AD-A173087] N87-16854
DRAINAGE
Towards snowmelt runoff forecast using LANDSAT-MSS and NOAA/AVHRR data N87-17317
DRAINAGE PATTERNS
The megageomorphology of the radar rivers of the eastern Sahara N87-17139
Significance of space image, air photo and drainage linears in relation to west coast tectonics, India N87-17232
Hydrogeological research in Peloponnesus (Greece) Karst area by support and completion of LANDSAT-thematic data N87-17234
DROP SIZE
Droplet sizing research program [AD-A173100] N87-16895
DROPS (LIQUIDS)
Droplet sizing research program [AD-A173100] N87-16895
Atmospheric pressure studies of liquid propellant drops in hot flows [AD-A174639] N87-16915
DROUGHT
Variability in the Earth radiation budget as determined from the Nimbus ERB experiments N87-17410
DUCTILITY
On the influence of strain-path changes on fracture [AD-A172535] N87-17091
DUCTS
The influence of wind-tunnel walls on discrete frequency noise N87-16850
DUST
Observations of young low-mass stars in dense cores [NASA-CR-180152] N87-17583
DWARF STARS
Brown dwarfs and Jovian planets: A comparison N87-17616
DYNAMIC CONTROL
Estimation and control of distributed models for certain elastic systems arising in large space structures [AD-A175019] N87-16872
Lattice filters and adaptive identification of flexible structures N87-17030
Dynamic input-output decoupling of nonlinear control systems [MEMO-575] N87-17452
DYNAMIC MODELS
Identification of a dynamic model of a helicopter from flight tests N87-16813

DYNAMIC PRESSURE
Development of a drag measurement system for the CERF 6-foot shock tube
[AD-A173087] N87-16854
DYNAMIC RESPONSE
Unsteady aerodynamics of a rotating compressor blade row in incompressible flow. Volume 1: Experimental facilities, procedures and sample data
[AD-A173043] N87-16831
Adaptive control techniques for large space structures
[AD-A173083] N87-16871
SRB O-ring free response analysis
[NASA-TM-86582] N87-17040
DYNAMIC STRUCTURAL ANALYSIS
Structural dynamics and attitude control study of early manned capability space station configurations
[NASA-TM-89078] N87-16861
Comparison of composite rotor blade models: A coupled-beam analysis and an MSC/NASTRAN finite-element model
[NASA-TM-89024] N87-16884
Batten augmented triangular beam
[NASA-CR-172461] N87-16916
Simple approach for evaluating mechanical reflector antenna distortions — satellite antennas N87-16942
Wind Scatterometer Antenna (WSA) release shock loads — ERS-1 N87-16945
Dynamics and Control Analysis Package (DCAP): An automated analysis and design tool for structural control of space structures N87-16947
Engineering and software interfacing for thermal, structural and dynamic control related with spacecraft activities N87-16948
A research program in advanced information systems
[NASA-CR-180150] N87-17529
DYNAMIC TESTS
Dynamic fracture initiation and propagation in 4340 steel under impact loading
[AD-A173084] N87-17092
DYNAMICAL SYSTEMS
Model of the human controller of a dynamic system
[MEMO-580] N87-17435
Kalman filtering, smoothing and recursive robot arm forward and inverse dynamics
[NASA-CR-180135] N87-17451
Dynamic input-output decoupling of nonlinear control systems
[MEMO-575] N87-17452

E

EARTH (PLANET)
Improvement of the Earth's gravity field from terrestrial and satellite data
[NASA-CR-180139] N87-17416
EARTH ALBEDO
Dependence of snow melting and surface-atmosphere interactions on the forest structure N87-17318
EARTH ATMOSPHERE
Geophysicist comments on how solar activity may affect weather N87-17097
Thermodynamic estimate of climatic system efficiency N87-17098
Determination of nonglobal component against background of global radioactive pollution of atmospheric aerosols N87-17100
EARTH CRUST
A scanning radar altimeter for mapping continental topography N87-17146
Effect of electrical and thermal properties of materials on microwave brightness temperature of the terrestrial crust N87-17263
EARTH MANTLE
Dynamical models for the Earth's geoid N87-17409
EARTH OBSERVATIONS (FROM SPACE)
Concept of a future multispectral Thermal Infrared (TIR) pushbroom mission for Earth observation from space N87-17169
Commercial opportunities in Earth observation from space N87-17177
The Sequential Filter Imaging Radiometer (SFIR), a new instrument configuration for Earth observations N87-17205
The Electronically Steered Thinned Array Radiometer (ESTAR) N87-17260
X-SAR extends the frequency range of Shuttle Imaging Radar N87-17362
EARTH OBSERVING SYSTEM (EOS)
SIR-C, the next generation spaceborne SAR N87-17161
Some results of Marine Observation Satellite (MOS-1) airborne verification experiment Multispectral Electronic Self Scanning Radiometer (MESSR) N87-17166
EARTH ORBITS
Characteristics of a very low altitude spacecraft for collecting global directional wave spectra with spaceborne synthetic aperture radar N87-17333
EARTH RADIATION BUDGET
Empirical relations between the Earth's radiation budget, cloudiness, and various meteorological parameters N87-17424
EARTH RADIATION BUDGET EXPERIMENT
Extrapolation of Earth-based solar irradiance measurements to exoatmospheric levels for broad-band and selected absorption-band observations N87-17270
Variability in the Earth radiation budget as determined from the Nimbus ERB experiments N87-17410
EARTH RESOURCES
The Second Spaceborne Imaging Radar Symposium
[NASA-CR-180131] N87-17135
Present statue of Japanese ERS-1 Project N87-17145
An overview of remote sensing agricultural apcations in North America: Past, present and future N87-17284
EARTH RESOURCES PROGRAM
An overview of remote sensing agricultural apcations in North America: Past, present and future N87-17284
EARTH ROTATION
Basic research for the geodynamics program
[NASA-CR-180137] N87-17415
EARTH SURFACE
Infrared spectroscopy for geologic interpretation of TIMS data N87-17130
Extracting surface features in multispectral imagery N87-17211
Dielectric and surface parameters related to microwave scatter and emission properties N87-17262
Classification of forest and surface types by satellite microwave radiometry N87-17305
EARTH-MOON SYSTEM
Stochastic model of tidal evolution of Earth-Moon system with cyclic change in resonant frequency of ocean N87-17103
EARTHQUAKES
Delineation of fault zones using imaging radar N87-17138
ECCENTRIC ORBITS
The contraction of satellite orbits under the influence of air drag. Part 7: Orbits of high eccentricity, with scale height dependent on altitude
[RAE-TR-86013] N87-16859
ECONOMIC FACTORS
Economical manufacturing and inspection of the electron-beam-welded Tornado wing box N87-17055
ECONOMICS
Communications satellite systems operations with the space station. Volume 1: Executive summary
[NASA-CR-179526] N87-17472
Communications satellite systems operations with the space station, volume 2
[NASA-CR-179527] N87-17473
Advantageous syndicates in a bilateral market game: The case of the tau-value
[MEMO-583] N87-17534
ECOSYSTEMS
Monitoring vegetation recovery patterns on Mount St. Helens using thermal infrared multispectral data N87-17122
EDDINGTON APPROXIMATION
A numerical study of jet production and accretion disk structure in super-Eddington black hole accretion N87-17586
EDDY VISCOSITY
Convection without eddy viscosity: An attempt to model the interiors of giant planets N87-17625
Eddy processes in the general circulation of the Jovian atmospheres N87-17627
Investigation of long-lived eddies on Jupiter N87-17633
Chaotic motion in the Jovian atmosphere N87-17634
Transport of absolute angular momentum in quasi-axisymmetric equatorial jet streams N87-17635
An updated hydrocarbon photochemical model for the Jovian atmosphere from the troposphere through the homopause: A prelude to Galileo N87-17636
EDGES
Segmentation by mathematical morphology processing hand on the image understanding model in remote sensing N87-17254
EDITING ROUTINES (COMPUTERS)
Portable EDITOR (PEDITOR): A portable image processing system — satellite images N87-17208
EDUCATION
The transfer of remote sensing technology to developing countries: A survey of experts in the field N87-17170
In service training of scientists and engineers: An important method of information transfer in the area of satellite remote sensing and its applications N87-17171
Training programs in remote sensing for professionals, students and the general public
[NASA-TM-88541] N87-17394
Flight-vehicle structures education in the US: Assessment and recommendations
[NASA-CR-4048] N87-17526
EFFICIENCY
Thermodynamic estimate of climatic system efficiency N87-17098
EIGENVALUES
A parallel solution for the symmetric Eigenproblem
[NASA-TM-89082] N87-17086
A pseudo-arclength continuation method for nonlinear Eigenvalue problems
[AD-A173019] N87-17459
On first passage times and differential equations
[AD-A174648] N87-17470
ELASTIC BENDING
Estimation and control of distributed models for certain elastic systems arising in large space structures
[AD-A175019] N87-16872
ELASTIC DEFORMATION
The theory of finite elastic-plastic deformation with induced anisotropy modelled as combined isotropic-kinematic hardening N87-17074
ELASTIC PROPERTIES
On routes to chaotic motion in oscillators with unsymmetric and symmetric elastic nonlinearity
[ISSN-0208-5658] N87-16969
A three dimensional calculation of elastic equilibrium for composite materials
[NASA-CR-178158] N87-17088
ELASTIC SCATTERING
The astrophysical implications of weakly interacting, massive particles N87-17592
ELASTOHYDRODYNAMICS
Oil film thickness measurement and analysis for an angular contact ball bearing operating in parched elastohydrodynamic lubrication
[NASA-CR-179506] N87-16879
ELASTOPLASTICITY
The theory of finite elastic-plastic deformation with induced anisotropy modelled as combined isotropic-kinematic hardening N87-17074
Energy dissipation associated with crack extension in an elastic-plastic material
[NASA-TM-89032] N87-17090
ELECTRIC ARCS
Heat transfer in gas tungsten arc welding
[DE86-013457] N87-17050
Welding torch with arc light reflector
[NASA-CASE-MFS-29134-1] N87-17493
ELECTRIC BRIDGES
Universal pressure transducer
[AD-D012499] N87-17019
ELECTRIC CONTACTS
Direct cable attach method
[AD-D012505] N87-17046
Low noise polycrystalline semiconductor resistors by hydrogen passivation
[AD-D012492] N87-17520
Interfacial structure of In/Pt/GaAs heterojunction ohmic contacts
[AD-A175102] N87-17523
ELECTRIC DIPOLES
The induced current on a long wire due to a vertical electric dipole above dissipative ground N87-17197
ELECTRIC FIELDS
Theoretical consideration on resistance geoelectrics N87-17196
ELECTRIC POTENTIAL
Dual channel high electron mobility field effect transistor
[AD-D012474] N87-17518
ELECTRIC POWER SUPPLIES
Lunar power systems
[NASA-CR-171956] N87-17398
ELECTRIC POWER TRANSMISSION
Utility interconnection issues for wind power generation
[NASA-CR-175056] N87-17400
ELECTRIC PROPULSION
Investigation of a repetitive pulsed electrothermal thruster
[NASA-CR-179464] N87-16878
ELECTRIC WIRE
Direct cable attach method
[AD-D012505] N87-17046
The induced current on a long wire due to a vertical electric dipole above dissipative ground N87-17197
ELECTRICAL MEASUREMENT
Prediction of the electrical performance of Inflatable Space Rigidized Structure (ISRS) offset antenna reflectors and correlation with RF measurements N87-16943

ELECTRICAL PROPERTIES
Electrical properties of Al-In-Sn alloys directionally solidified in high and low gravitational fields
[NASA-TM-86569] N87-16900
LEO high voltage solar array arcing response model
[NASA-CR-180073] N87-16971
ELECTRICAL RESISTANCE
Theoretical consideration on resistance geoelectrics
N87-17196
ELECTRICAL RESISTIVITY
Determination of resistivity and permittivity profiles of a layered Earth N87-17198
ELECTRICITY
Heat exchanger for electrothermal devices
[NASA-CASE-LEW-14037-1] N87-16875
ELECTRO-OPTICS
Investigation of a GaAlAs Mach-Zehnder electro-optic modulator
[NASA-CR-179573] N87-16953
ELECTROCHEMICAL CELLS
Safety considerations of lithium-thionyl chloride cells
[NASA-CR-180129] N87-17396
The NASA Aerospace Battery Safety Handbook
[NASA-CR-180127] N87-17397
ELECTRODES
Heat transfer in gas tungsten arc welding
[DE86-013457] N87-17050
ELECTRODYNAMICS
System engineering study of electrodynamic tether as a spaceborne generator and radiator of electromagnetic waves in the ULF/ELF frequency band
[NASA-CR-180156] N87-16956
Investigation of plasma contactors for use with orbiting wires
[NASA-CR-180154] N87-17502
ELECTROMAGNETIC INTERACTIONS
The interaction between the solar wind and the comets
[AERONOMICA-ACTA-A-306-1986] N87-17853
ELECTROMAGNETIC SCATTERING
Hydrodynamics of internal solitons and a comparison of SIR-A and SIR-B data with ocean measurements
N87-17147
Effective medium approximation for effective propagation constant calculation in a dense random medium — electromagnetic wave scattering N87-17180
Numerical modeling of two-dimensional time domain electromagnetic scattering by underground inhomogeneities N87-17199
ELECTROMECHANICAL DEVICES
Determining and modeling the response of ytterbium piezoresistance transducers
[AD-A173085] N87-17023
ELECTROMOTIVE FORCES
A model for an electromotive force generator in the magnetosphere: A source of discrete auroral arcs
[AERONOMICA-ACTA-A-309-1986] N87-17421
ELECTRON BEAM WELDING
Microstructural modifications during laser and electron beam welding
[DE86-011076] N87-17049
Advanced Joining of Aerospace Metallic Materials — conference proceedings
[AGARD-CP-398] N87-17051
Study of the electron beam weldability of superalloys through the analysis of melt zone morphology
N87-17053
Economical manufacturing and inspection of the electron-beam-welded Tornado wing box N87-17055
NDT of electron beam welded joints (micro-focus and real time X-ray) N87-17063
Influence of welding flaws on the fatigue strength of electron beam weldments in Ti Al6 V4 N87-17065
ELECTRON BEAMS
Empirical considerations for laser guided electron beams in the advanced test accelerator
[DE86-013218] N87-17489
Nanosecond two-dimensional imaging using tomographic techniques
[DE86-008164] N87-17499
ELECTRON DENSITY (CONCENTRATION)
A study of large, medium and small scale structures in the topside ionosphere
[NASA-CR-180068] N87-17413
Investigation of plasma contactors for use with orbiting wires
[NASA-CR-180154] N87-17502
ELECTRON TRANSFER
Recent developments in discrete-ordinates electron transport
[DE86-007827] N87-17485
ELECTRONIC COUNTERMEASURES
ECM (electronic countermeasures) preprocessor or tracker using multi-processor modules
[AD-D012513] N87-16959
ELECTRONIC EQUIPMENT
Soluble aromatic polyimides for film and coating applications
[NASA-TM-89016] N87-16911
ELECTRONIC MODULES
Metallization for hermetic sealing of ceramic modules
[AD-D012483] N87-17044
ELECTROSTATIC PROBES
An electrostatic probe technique for R.F. plasma
[OUEL-1637/86] N87-17514
ELECTROTHERMAL ENGINES
Heat exchanger for electrothermal devices
[NASA-CASE-LEW-14037-1] N87-16875
Investigation of a repetitive pulsed electrothermal thruster
[NASA-CR-179464] N87-16878
ELEVATION
Elevated waterproof access floor system and method of making the same
[NASA-CASE-ARC-11363-1] N87-16918
ELEVATION ANGLE
Results from 1984 airborne Doppler lidar wind measurement program. Flight 6: Analysis of line-of-sight elevation angle errors and apparent Doppler velocities
[NASA-CR-178994] N87-17425
ELLIPSOIDS
Three-dimensional separation on a cylindrical ellipsoid. Results of the first test campaign on the F2 wind tunnel
[ONERA-RT-16/7252-AN] N87-17013
ELLIPTICAL GALAXIES
Scale-free models of highly flattened elliptical galaxies
N87-17589
ELLIPTICAL ORBITS
Orbit determination for low Earth orbit spacecraft based on satellite to satellite tracking techniques via a unique very high altitude relay constellation N87-16858
EMBRITTLEMENT
Mechanisms of helium embrittlement N87-16899
EMISSION SPECTRA
The ionization structure of planetary nebulae. 8: NGC 6826
[NASA-CR-180142] N87-17581
The ionization structure of planetary nebulae. Part 7: New observations in the ring nebula
[NASA-CR-180141] N87-17582
EMISSIVITY
A modified boundary perturbation approach to microwave scattering and emission by the ocean surface
N87-17214
Effects of salinity on the microwave emission of soils
N87-17302
Snow property measurements correlative to microwave emission at 35 GHz N87-17315
EMITTANCE
Enhancement of time images for photointerpretation
N87-17116
Lithologic mapping of silicate rocks using TIMS
N87-17118
The Red River Valley archeological project
N87-17126
The physical basis for spectral variations in thermal infrared emittance of silicates and application to remote sensing N87-17129
Infrared spectroscopy for geologic interpretation of TIMS data N87-17130
ENERGY CONSERVATION
Use of low energy ion implants in high efficiency crystalline silicon solar cells
[NASA-CR-179971] N87-17408
ENERGY CONVERSION EFFICIENCY
Use of low energy ion implants in high efficiency crystalline silicon solar cells
[NASA-CR-179971] N87-17408
Physics considerations on a fusion plasma in a field-reversed configuration
[IPPJ-803] N87-17513
ENERGY DISSIPATION
Energy dissipation associated with crack extension in an elastic-plastic material
[NASA-TM-89032] N87-17090
ENERGY GAPS (SOLID STATE)
High band gap 2-6 and 3-5 tunneling junctions for silicon multijunction solar cells
[NASA-CASE-NPO-16526-1CU] N87-17399
ENERGY LEVELS
Dual channel high electron mobility field effect transistor
[AD-D012474] N87-17518
ENERGY SPECTRA
Operational wave forecasting with spaceborne SAR: Prospects and pitfalls N87-17149
Review of wind simulation methods for horizontal-axis wind turbine analysis
[DE86-012223] N87-17407
On the spectra of gamma-ray bursts at high energies
N87-17654
ENERGY STORAGE
The possibility of reducing the cyclic torque fluctuations produced by two-stroke engines using the storage of magnetostatic energy
[RAE-TM-RAD-NAV-265] N87-17042
The NASA Aerospace Battery Safety Handbook
[NASA-CR-180127] N87-17397
Lunar power systems
[NASA-CR-171956] N87-17398
ENERGY TRANSFER
Thermodynamic estimate of climatic system efficiency
N87-17098
ENGINE DESIGN
Impact of IPS and IRS configuration on engine installation design — helicopter engines
[PNR90324] N87-16834
Reducing the cost of aero engine research and development
[PNR90341] N87-16836
Future trends in propulsion — aircraft
[PNR90349] N87-16840
Gas turbine materials: A review
[PNR90356] N87-16842
The technology of advanced prop-fan transmissions
[PNR90357] N87-16843
Operational aids to engine development
[PNR90362] N87-16845
Space station auxiliary thrust chamber technology
[NASA-CR-179552] N87-16874
ENGINE INLETS
Observation of ice/water formations on a model intake section subjected to simulated cloud conditions — aircraft engine
[PNR90347] N87-16839
ENGINE PARTS
Component lifing — aircraft engines
[PNR90348] N87-16838
Bonding of superalloys by diffusion welding and diffusion brazing N87-17059
NDT of electron beam welded joints (micro-focus and real time X-ray) N87-17063
Evaluation of DDH and weld repaired F100 turbine vanes under simulated service conditions N87-17070
Repair techniques for gas turbine components
N87-17071
ENGINE TESTING LABORATORIES
Developments in data acquisition and processing using an advanced combustion research facility — gas turbine engines
[RAE-TM-P1089] N87-16852
ENGINE TESTS
Burner rig and engine test experience of platinum aluminide coatings
[PNR90342] N87-16837
Observation of ice/water formations on a model intake section subjected to simulated cloud conditions — aircraft engine
[PNR90347] N87-16839
An approach to AE monitoring during the rig shop testing of large CFRP aero-engine components — acoustic emission (AE)
[PNR90350] N87-16841
ENGINES
Anti-rotation guide vane bushing
[AD-D012510] N87-17047
ENVIRONMENT EFFECTS
Contemporary changes in climate and paleoclimate
N87-17099
Assessment of contemporary changes in global climate N87-17101
Environmental modification of metropolitan areas through satellite images: Study of urban design in the tropics N87-17175
Wind energy technical reading list
[DE86-010704] N87-17404
ENVIRONMENT SIMULATION
Test apparatus for uniform tensioning of long lengths of small cables in simulated environments
[AD-D012487] N87-17045
ENVIRONMENTAL MONITORING
Proceedings of the 1986 International Geoscience and Remote Sensing Symposium (IGARSS '86) on Remote Sensing: Today's Solutions for Tomorrow's Information Needs, volume 1
[ESA-SP-254-VOL-1] N87-17163
Monitoring of large phenomena in developing countries through satellite imagery N87-17172
Sri Lanka's solution to land use mapping and monitoring for Third World countries development N87-17174
The design of an international data centre for remote sensing N87-17176
Application of Spaceborne Distributed Aperture/Coherent Array Processing (SDA/CAP) technology to active and passive microwave remote sensing N87-17277

Proceedings of the 1986 International Geoscience and Remote Sensing Symposium (IGARSS' 86) on Remote Sensing: Today's Solutions for Tomorrow's Information Needs, volume 2
[ESA-SP-254-VOL-2] N87-17283
The use of numerical wind and wave models to provide areal and temporal extension to instrument calibration and validation of remotely sensed data — satellite data N87-17371

EQUATORIAL ATMOSPHERE
The vertical structure of Jupiter's equatorial and tropical regions N87-17607
Moisture driven convection on Jupiter: A mechanism to produce the equatorial plumes N87-17631
Transport of absolute angular momentum in quasi-axisymmetric equatorial jet streams N87-17635

EQUIPMENT SPECIFICATIONS
The TIMS instrument N87-17112

ERROR ANALYSIS
Surface flaw reliability analysis of ceramic components with the SCARE finite element postprocessor program
[NASA-TM-88901] N87-17087
The effect of measurement error and confusion from vegetation on passive microwave estimates of soil moisture N87-17304
Results from 1984 airborne Doppler lidar wind measurement program. Flight 6: Analysis of line-of-sight elevation angle errors and apparent Doppler velocities
[NASA-CR-178994] N87-17425
On the stochastic dissemination of faults in an admissible network
[NASA-CR-176238] N87-17469

ERROR CORRECTING CODES
Cyclic unequal error protection codes constructed from cyclic codes of composite length
[NASA-CR-180165] N87-17457
On codes with multi-level error-correction capabilities
[NASA-CR-180166] N87-17458

ERRORS
Digital program for calculating static pressure position error
[NASA-TM-86726] N87-16821
Variability in the Earth radiation budget as determined from the Nimbus ERB experiments N87-17410
Cyclic unequal error protection codes constructed from cyclic codes of composite length
[NASA-CR-180165] N87-17457
On codes with multi-level error-correction capabilities
[NASA-CR-180166] N87-17458

ERS-1 (ESA SATELLITE)
Development status of the ERS-1 SAR antenna N87-16939
ERS-1 wind scatterometer antenna: Mechanical aspects N87-16940
Wind Scatterometer Antenna (WSA) release shock loads — ERS-1 N87-16945
Features and technologies of ERS-1 (ESA) and X-SAR antennas N87-17152
Off-line processing of ERS-1 synthetic aperture radar data with high precision and high throughput N87-17153
An overview of operational SAR data collection and dissemination plans for ERS-1 ice data in Canada N87-17189
Overview and status of the ERS-1 program N87-17190
Development status of the ERS-1 payload instruments N87-17191
The ESA approach for ERS-1 sensor calibration and performance verification N87-17192
On-ground verification and in-orbit performance prediction of the ERS-1 wind scatterometer N87-17193
ERS-1 radar altimeter: Performance, calibration and data validation N87-17194
An automatic tracking mode switching algorithm for the ERS-1 altimeter N87-17195
ERS-1 fast delivery processing and products N87-17224
Results of the ESA airborne C-band scatterometer campaigns — ERS-1 N87-17225
Quasi real time conversion of ERS-1 scatterometer raw data to sigma zero triplets N87-17226
ERS-1 wind scatterometer: Wind extraction and ambiguity removal N87-17227
ERS-1 synthetic aperture radar fast delivery processor N87-17228
Canadian plans for operational demonstrations of satellite imaging radar applications — ERS-1 N87-17229
The UK ERS Data Centre, an offline processing and archiving facility N87-17230
The German ERS-1 SAR postprocessing system plans and concepts N87-17231
Recent progress in ERS-1 wind scatterometer design N87-17256
The ERS-1 scatterometer system simulator and its relevance for ground processing design N87-17257
Future user requirements and required technological developments of spaceborne synthetic aperture radars N87-17320
Planar array antenna for ERS-1 synthetic aperture radar N87-17357
Analysis of amplitude nonlinearities in the ERS-1 SAR receiver system N87-17359
A powerful utility for assessing the performance of the ERS-1 synthetic aperture radar N87-17361
Proceedings of an ESA Workshop on ERS-1 Wind and Wave Calibration
[ESA-SP-262] N87-17363
ERS-1 mission constraints related to wind and wave calibration N87-17364
The influence of spatial and temporal scales on calibration/validation — ERS-1 sensors N87-17365
Gathering and processing a comparative data set for the calibration and validation of ERS-1 data products; preparatory work at the UK-ERS-DC — Data Center (DC) N87-17367
Requirements and constraints in the calibration and validation of ERS-1 wind and wave parameters N87-17369
Evaluation of the different parameters in Long's C-band model — for ERS-1 scatterometer N87-17370
Validation of ERS-1 wind data using observations from research and voluntary observing ships N87-17374
The accuracy and availability of operational marine surface wind data for ERS-1 sensor calibration and validation from fixed platforms and free drifting buoys N87-17376
Using buoys and ships to calibrate ERS-1 altimeter and scatterometer N87-17377
DFVLR flight operation acting as a useful service unit for ERS-1 N87-17378
Canada Center for Remote Sensing (CCRS) Convair 580 results relevant to ERS-1 wind and wave calibration N87-17379
Oceanographic measurement capabilities of the NASA P-3 aircraft — ERS-1 mission N87-17380
The use of aircraft for wind scatterometer calibration — ERS-1 scatterometer N87-17382
Intersensor comparisons for validation of wind speed measurements from ERS-1 altimeter and scatterometer — Seasat N87-17386
Australian validation plans for ERS-1 N87-17387
Wave modeling activities of the Wave Modeling (WAM) group relevant to ERS-1 N87-17389

ESA SATELLITES
Review of coherent and incoherent detection techniques: Outlook and limitation — spaceborne submillimeter astronomy N87-17537
A study of planetary atmospheres in the submillimetric range N87-17540
Submillimetre wavelength studies of protostars: The role of FIRST — Far Infrared Submillimeter Space Telescope (FIRST) N87-17544
Far infrared submillimeter wave space telescope (FIRST) observations of stars with large mass loss rates N87-17550
A proposed cornerstone mission: Far infrared submillimeter wave telescope (FIRST) N87-17564
Active optics for the far infrared submillimeter wave space telescope (FIRST): A high angular resolution mode N87-17566
Structure of molecular clouds and space-based sub-millimeter telescopes, for example FIRST — Far Infrared Submillimeter Wave Space Telescope (FIRST) N87-17574

ESA SPACECRAFT
Antenna mechanical technologies within ESA N87-16924

ETHANE
The abundances of ethane to acetylene in the atmospheres of Jupiter and Saturn N87-17618

EULER EQUATIONS OF MOTION
Comparison of three explicit multigrid methods for the Euler and Navier-Stokes equations
[NASA-TM-88878] N87-16784
Euler solutions using an implicit multigrid technique
[NASA-TM-58276] N87-16792
Euler analysis of the three dimensional flow field of a high-speed propeller: Boundary condition effects
[NASA-TM-88955] N87-16798
A multigrid LU-SSOR scheme for approximate Newton iteration applied to the Euler equations
[NASA-CR-179524] N87-16803
An LU-SSOR scheme for the Euler and Navier-Stokes equations
[NASA-CR-179556] N87-16806

EUROPEAN SPACE PROGRAMS
Proceedings of an ESA Workshop on a Spaceborne Submillimeter Astronomy Mission. A Cornerstone of the ESA Long Term Science Program
[ESA-SP-260] N87-17535
A proposed cornerstone mission: Far infrared submillimeter wave telescope (FIRST) N87-17564

EVAPORATION
Optical thin film monitoring using optical fibers
[DE87-001355] N87-17501

EVOLUTION (DEVELOPMENT)
Stochastic model of tidal evolution of Earth-Moon system with cyclic change in resonant frequency of ocean N87-17103

EXCITATION
Modeling of nonlinear effects of plasma wave beams on ionospheric plasma N87-17107

EXPANDABLE STRUCTURES
Evaluation of Pactruss design characteristics critical to space station primary structure
[NASA-CR-178171] N87-16870

EXPERIMENT DESIGN
Concept definition for space station technology development experiments. Experiment definition, task 2
[NASA-CR-178153] N87-16860
A comparison of two British standard test methods for the determination of resistance to humidity of paint films
[MOAD-TP-918] N87-16906
X-SAR extends the frequency range of Shuttle Imaging Radar N87-17362

EXPERT SYSTEMS
A knowledge-based software environment for the analysis of spectroradiometer data — mineral identification N87-17203

EXPLOSIONS
Evolution of a localized thermal explosion in a reactive gas
[NASA-CR-178231] N87-17436

EXPLOSIVES
A study of explosive wave propagation in granular materials with microstructure
[AD-A173015] N87-16914

EXTRAPOLATION
Extrapolation of Earth-based solar irradiance measurements to exoatmospheric levels for broad-band and selected absorption-band observations N87-17270

EXTREMELY HIGH FREQUENCIES
Microstrip dipoles for EHF and millimeter wave applications
[AD-A173025] N87-16976
Calibrated X and L-band scattering coefficients from a southern US forest N87-17312
Snow property measurements correlative to microwave emission at 35 GHz N87-17315

F

F REGION
A study of large, medium and small scale structures in the topside ionosphere
[NASA-CR-180068] N87-17413
The hydrogen geocorona: Simultaneous optical and radar observations at Arecibo N87-17651

F-111 AIRCRAFT
AFTI/F-111 MAW flight control system and redundancy management description
[NASA-TM-88267] N87-16819

FABRICATION
The application of diffusion bonding and laser welding in the fabrication of aerospace structures N87-17054
Use of low energy ion implants in high efficiency crystalline silicon solar cells
[NASA-CR-179971] N87-17408

FAILURE ANALYSIS
An approach to AE monitoring during the rig shop testing of large CFRP aero-engine components — acoustic emission (AE)
[PNR90350] N87-16841
Solid rocket booster joint seal analyses
[NASA-TM-86580] N87-17039
Application of modified three parameter Weibull distributions to brittle material design
[RARDE-16/84] N87-17072

FAILURE MODES
Real time identification of large space structures
[NASA-CR-171957] N87-16867

FAR INFRARED RADIATION
Review of coherent and incoherent detection techniques: Outlook and limitation — spaceborne submillimeter astronomy N87-17537
Observations of active galactic nuclei with FIRST — Far Infrared Submillimeter Space Telescope (FIRST) N87-17538

Far infrared submillimeter wave space telescope (FIRST) observations of stars with large mass loss rates N87-17550
Some results about laboratory dust analysis in the FIR range --- cosmic dust simulation N87-17551
Far infrared and optical study of the high latitude cloud L1642 N87-17559
A proposed cornerstone mission: Far infrared submillimeter wave telescope (FIRST) N87-17564
Active optics for the far infrared submillimeter wave space telescope (FIRST): A high angular resolution mode N87-17566
Far infrared spectroscopy of galaxies from the Kuiper Airborne Observatory N87-17577

FARM CROPS
Canopy hot-spot as crop identifier
[DE86-011258] N87-17395

FARMLANDS
Evaluating roughness models of radar backscatter N87-17344

FASTENERS
Flameholder with removable flameholder attachments
[AD-D012466] N87-16893

FATIGUE (MATERIALS)
Carbon fibre composite coupons: Static and fatigue behaviour after impact damage
[ARL-STRUC-R-422] N87-16881
Stress intensity factors for fatigue cracks at holes under cyclic stress gradients N87-17075
Review of wind simulation methods for horizontal-axis wind turbine analysis
[DE86-012223] N87-17407

FATIGUE LIFE
Component lifing --- aircraft engines
[PNR90346] N87-16838
Influence of welding flaws on the fatigue strength of electron beam weldments in Ti Al6 V4 N87-17065
Fatigue life and fastener flexibility of single shear riveted and bolted joints
[FFA-TN-1986-35] N87-17094

FATIGUE TESTS
Inertia welding of nitralloy N and 18 nickel maraging 250 grade steels for utilization in the main rotor drive shaft for the AR-64 military helicopter program N87-17067

FAULT TOLERANCE
Fault-free performance validation of fault-tolerant multiprocessors
[NASA-CR-178236] N87-17448

FEASIBILITY ANALYSIS
Feasibility of using wind power for an aerostat-borne radar system
[DE86-004461] N87-17403

FEEDBACK CONTROL
Development of a sensitivity analysis technique for multiloop flight control systems N87-16847
Reducing shuttle-payload dynamic interaction with notch filters
[NASA-CR-171958] N87-16862
Application of adaptive antenna techniques to future commercial satellite communication
[NASA-CR-179566] N87-16955
A modified loop transfer recovery approach for robust control of flexible structures N87-17029
Investigation of plasma contactors for use with orbiting wires
[NASA-CR-180154] N87-17502

FERROELECTRICITY
Research on millimeter wave dielectric materials
[AD-A173017] N87-17521

FIBER OPTICS
Test apparatus for uniform tensioning of long lengths of small cables in simulated environments
[AD-D012487] N87-17045
High intensity selectable poly or monochromatic slit light source apparatus for optical instruments
[AD-D012507] N87-17496
Optical thin film monitoring using optical fibers
[DE87-001355] N87-17501

FIBER REINFORCED COMPOSITES
Carbon fibre composite coupons: Static and fatigue behaviour after impact damage
[ARL-STRUC-R-422] N87-16881
Damage and repairing of fiber composites, a summary
[FOA-C-20620-2.5] N87-16888

FIBERS
Mechanical properties of graphite epoxy used for Zero CTE Program
[DE86-013227] N87-16886

FIELD EFFECT TRANSISTORS
The 20 GHz power GaAs FET development
[NASA-CR-179546] N87-16972

FIGHTER AIRCRAFT
Assessment of damage tolerance requirements and analysis. Volume 1: Executive summary
[AD-A175110] N87-16822
Noise-immune multisensor transduction of speech
[AD-A174693] N87-16961

FILTER WHEEL INFRARED SPECTROMETERS
The Sequential Filter Imaging Radiometer (SFIR), a new instrument configuration for Earth observations N87-17205

FINITE DIFFERENCE THEORY
Review of discretization techniques and numerical resolution methods N87-16990
An introduction to numerical methods for flow around bluff bodies N87-16992
SOLA: A basic solution algorithm for flow analysis N87-16996
Applications of SOLA to free surface flows --- flow computing method N87-16998
Implicit particle simulation of electromagnetic plasma phenomena
[IPPJ-799] N87-17509

FINITE ELEMENT METHOD
The Extendable Refractable Mast (ERM) thermal analysis: A heat radiation case study via the finite element method N87-16949
Review of discretization techniques and numerical resolution methods N87-16990
Structural Analysis
[ESA-TT-917] N87-17077
Field consistency and finite element analysis of multifield structural problems N87-17080
Surface flaw reliability analysis of ceramic comonents with the SCARE finite element postprocessor program
[NASA-TM-88901] N87-17087
Design of software for design of finite element for structural analysis
[NASA-TM-88528] N87-17089
Energy dissipation associated with crack extension in an elastic-plastic material
[NASA-TM-89032] N87-17090
Survey of the status of finite element methods for partial differential equations
[NASA-CR-178222] N87-17456
Dynamic analysis and design of the SIRTF primary mirror mount
[NASA-CR-180158] N87-17494

FINS
Computation of separation ahead of blunt fin in supersonic turbulent flow
[NASA-TM-89416] N87-16791

FIRE FIGHTING
The 5000 GPM firefighting module evaluation test
[NASA-TM-86560] N87-16919

FLAME HOLDERS
Flameholder with removable flameholder attachments
[AD-D012466] N87-16893

FLAME PROPAGATION
Transient catalytic combustion
[AD-A173098] N87-16894
Lumped model generation and evaluation: Sensitivity and lie algebraic techniques with applications to combustion
[AD-A174984] N87-16896

FLAMMABILITY
Fire and heat resistant laminating resins based on maleimido substituted aromatic cyclotriphosphazene polymer
[NASA-CASE-ARC-11428-2] N87-16909

FLAPS (CONTROL SURFACES)
AFTI/F-111 MAW flight control system and redundancy management description
[NASA-TM-88267] N87-16819

FLAT PLATES
Development of a drag measurement system for the CERF 6-foot shock tube
[AD-A173087] N87-16854

FLEXIBILITY
Reducing shuttle-payload dynamic interaction with notch filters
[NASA-CR-171958] N87-16862
interferometric load sensor and strain gage
[AD-D012509] N87-17021
Sun shield
[NASA-CASE-MSC-20162-1] N87-17036
Fatigue life and fastener flexibility of single shear riveted and bolted joints
[FFA-TN-1986-35] N87-17094

FLEXIBLE BODIES
Dynamics and control of flexible manipulators N87-17028
Lattice filters and adaptive identification of flexible structures N87-17030
Adaptive control of a flexible structure N87-17449

FLEXIBLE SPACECRAFT
Description of the Spacecraft Control Laboratory Experiment (SCOLE) facility
[NASA-TM-89057] N87-16848
Dynamics and Control Analysis Package (DCAP): An automated analysis and design tool for structural control of space structures N87-16947
A modified loop transfer recovery approach for robust control of flexible structures N87-17029

FLIGHT CHARACTERISTICS
Piloted simulator study of allowable time delays in large-airplane response
[NASA-TP-2652] N87-16849

FLIGHT CONTROL
AFTI/F-111 MAW flight control system and redundancy management description
[NASA-TM-88267] N87-16819
Development of a sensitivity analysis technique for multiloop flight control systems N87-16847

FLIGHT SIMULATION
Design and initial application of the extended aircraft interrogation and display system: Multiprocessing ground support equipment for digital flight systems
[NASA-TM-86740] N87-16820
Observation of ice/water formations on a model intake section subjected to simulated cloud conditions --- aircraft engine
[PNR90347] N87-16839
Simulated flight acoustic investigation of treated ejector effectiveness on advanced mechanical suppresors for high velocity jet noise reduction
[NASA-CR-4019] N87-17481

FLIGHT SIMULATORS
Piloted simulator study of allowable time delays in large-airplane response
[NASA-TP-2652] N87-16849

FLIGHT TESTS
Design and initial application of the extended aircraft interrogation and display system: Multiprocessing ground support equipment for digital flight systems
[NASA-TM-86740] N87-16820
Flight service evaluation of advanced composite ailerons on the L-1011 transport aircraft
[NASA-CR-178170] N87-16883
Some results of Marine Observation Satellite (MOS-1) airborne verification experiment Multispectral Electronic Self Scanning Radiometer (MESSR) N87-17166
DFVLR flight operation acting as a useful service unit for ERS-1 N87-17378
Canada Center for Remote Sensing (CCRS) Convair 580 results relevant to ERS-1 wind and wave calibration N87-17379
Noise propagation from a four-engine, propeller-driven airplane
[NASA-TM-89035] N87-17482

FLOOD CONTROL
The 5000 GPM firefighting module evaluation test
[NASA-TM-86560] N87-16919

FLOORS
Elevated waterproof access floor system and method of making the same
[NASA-CASE-ARC-11363-1] N87-16918

FLOW CHARACTERISTICS
Direct computation of wall bounded aerosol turbulent flow interactions
[DE86-013221] N87-17009

FLOW DISTRIBUTION
The aerodynamics and aeroacoustics of rotating transonic disturbances N87-16786
Measurement of the three-dimensional aerodynamics of an annular cascade airfoil row N87-16788
Measurements of the unsteady flow field within the stator row of a transonic axial-flow fan. 1: Measurement and analysis technique
[NASA-TM-88945] N87-16789
Measurements of the unsteady flow field within the stator row of a transonic axial-flow fan. Part 2: Results and discussion
[NASA-TM-88946] N87-16790
Euler analysis of the three dimensional flow field of a high-speed propeller: Boundary condition effects
[NASA-TM-88955] N87-16798
Advanced 3-D viscous SSME turbine rotor stator CFD algorithms
[NASA-CR-178997] N87-16829
Transition mixing study
[NASA-CR-175062] N87-16830
Laser Doppler velocimeter measurements and theoretical investigation of three dimensional scroll flow N87-16979
The study of shock wave and turbulent boundary layer interactions
[AD-A175033] N87-17008
Observations on the turbulent structure in an unsteady, normal shock/boundary-layer interaction --- blowdown supersonic tunnel
[PNR90361] N87-17010

FLOW EQUATIONS
Introduction to Numerical Solution of Industrial Flows, volume 1 — conference [VKI-LS-1986-07-VOL-1] N87-16987
An analysis of flow models: From Navier-Stokes to potential flow equations N87-16988
The spatial levels of approximation from three-dimensional to quasi one-dimensional representation — averaging procedure (flow computation) N87-16989
Review of discretization techniques and numerical resolution methods N87-16990
The analysis and resolution of numerical schemes — flow problems N87-16991
An introduction to numerical methods for flow around bluff bodies N87-16992
Introduction to Numerical Solution of Industrial Flows, volume 2 — conference [VKI-LS-1986-07-VOL-2] N87-16994
Numerical methods for two-dimensional and three-dimensional heat transfer calculations N87-16995
SOLA: A basic solution algorithm for flow analysis N87-16996
Applications of SOLA to confined flows — numerical flow computing methods N87-16997
Applications of SOLA to free surface flows — flow computing method N87-16998

FLOW GEOMETRY
Applications of SOLA to confined flows — numerical flow computing methods N87-16997

FLOW MEASUREMENT
Calculation of supersonic flow over a compression corner N87-16785
Measurement of the three-dimensional aerodynamics of an annular cascade airfoil row N87-16788
Experimental investigation in turbulent flow separation [ISL-CO-208/86] N87-17012

FLOW STABILITY
A laboratory investigation of two-celled vortex flows N87-17423

FLOW THEORY
On variational characterizations of steady vortex rings [MEMO-577] N87-17014
Effective permeability and macrodispersion in locally heterogeneous aquifers [MEMO-585] N87-17015

FLOW VELOCITY
Transient catalytic combustion [AD-A173098] N87-16894

FLOW VISUALIZATION
The study of shock wave and turbulent boundary layer interactions [AD-A175033] N87-17008
Observations on the turbulent structure in an unsteady, normal shock/boundary-layer interaction — blowdown supersonic tunnel [PNR90361] N87-17010
Industrial holography: The Rolls-Royce experience [PNR90351] N87-17024

FLUID DYNAMICS
A laboratory investigation of two-celled vortex flows N87-17423

FLUID FLOW
ATHENA code manual. Volume 1: Code structure, system models, and solution methods [DE87-001430] N87-17492

FLUID MECHANICS
Selection principles and pattern formation in fluid mechanics and nonlinear shell theory [NASA-CR-180159] N87-17004
Nonlinear wave propagation [AD-A175073] N87-17461

FLUORESCENCE
CF2 and CFCl fluorescence from VUV excitation of C2F3Cl N87-16891

FLUORIDES
Preparations of rare earth-iron alloys by thermite reduction [DE86-013753] N87-16904

FLUOROCARBONS
CF2 and CFCl fluorescence from VUV excitation of C2F3Cl N87-16891

FLUTTER
Ground vibration tests [ETN-87-98647] N87-17422

FLYING SPOT SCANNERS
A real time vision system for robotic arc welding N87-17066

FOCAL PLANE DEVICES
Projection lens scanning laser velocimeter system [NASA-CASE-ARC-11547-1] N87-17026

FOLDING STRUCTURES
Study on solid surface, deployable antenna reflector — satellite antenna N87-16928
Contraves' antenna tip hinge mechanism for Selenia Spazio's 20/30 GHz antenna — satellite antenna N87-16944
Sun shield [NASA-CASE-MSC-20162-1] N87-17036

FOREST MANAGEMENT
Microwave remote sensing: Its applications and limitations in operational tasks of land use inventory and forest management N87-17266
Classification of forest and surface types by satellite microwave radiometry N87-17305
SAR imagery for forest management N87-17313

FORESTS
Investigation of forest canopy temperatures recorded by the thermal infrared multispectral scanner at H. J. Andrews Experimental Forest N87-17123
Locating subsurface gravel with thermal imagery N87-17125
Analysis of multiple incidence angle SIR-B data for determining forest stand characteristics N87-17156
Multiple incidence angle SIR-B experiment over Argentina N87-17157
Comparison of Thematic Mapper (TM) and SPOT simulation data for agricultural applications in south west Germany N87-17165
Viewing angle corrections of airborne multispectral scanner data acquired over forested surfaces N87-17273
Classification of forest and surface types by satellite microwave radiometry N87-17305
X and L-band backscattering measurements of agricultural crops, forest stands and single trees N87-17311
Calibrated X and L-band scattering coefficients from a southern US forest N87-17312
Dependence of snow melting and surface-atmosphere interactions on the forest structure N87-17318
LANDSAT-5 Thematic Mapping (TM) data applications to land use classification on around the Bosphorus area, Turkey N87-17351

FORMALISM
Effective medium approximation for effective propagation constant calculation in a dense random medium — electromagnetic wave scattering N87-17180

FORMING TECHNIQUES
Fabrication of hollow, cored, and composite shaped parts from selected alloy powders [AD-D012489] N87-16903
Application of diffusion bonding combined with superplastic forming (SPF/DB) to the fabrication of TAGV metal sheet structures N87-17060

FOURIER ANALYSIS
The analysis and resolution of numerical schemes — flow problems N87-16991

FOURIER TRANSFORMATION
Image representation via its symmetrical components N87-17290

FRACTOGRAPHY
Quantitative analysis of fracture surfaces using computer aided fractography N87-17076

FRACTURE MECHANICS
An effective substructure technique applied to crack problems N87-17083
Energy dissipation associated with crack extension in an elastic-plastic material [NASA-TM-89032] N87-17090
On the influence of strain-path changes on fracture [AD-A172535] N87-17091
Dynamic fracture initiation and propagation in 4340 steel under impact loading [AD-A173084] N87-17092

FRACTURE STRENGTH
Influence of welding flaws on the fatigue strength of electron beam weldments in Ti Al6 V4 N87-17065
Welding of aluminum castings N87-17068

FRACTURING
On the influence of strain-path changes on fracture [AD-A172535] N87-17091

FRANCE
Rural land use inventory and mapping in the Ardeche area (France) using multitemporal Thematic Mapping (TM) data N87-17350

FREE ELECTRON LASERS
Optical modeling of induction-linac driven free-electron lasers [DE87-001432] N87-17027
Future accelerator technology [DE86-013190] N87-17488

FREE FLOW
Transitional boundary layers under the influence of high free stream turbulence, intensive wall cooling and high pressure gradients in hot gas circulation [NASA-TM-88524] N87-16983

FREE JETS
Combined density and velocity measurements. Application to the investigation of a free jet [ISL-CO-206/86] N87-16808
Particle-laden swirling free jets: Measurements and predictions [NASA-TM-88904] N87-16826

FREQUENCIES
The effect of operating frequency in the radiation induced buildup of trapped holes and interface states in MOS devices [AD-A173097] N87-17522

FREQUENCY MODULATION
Snow stratigraphy observed by an FM-CW microwave system N87-17181
A scatterometer operating at 10 GHz N87-17282

FREQUENCY REUSE
Qualification of gridding process for a Polarization Sensitive Reflector (PSR) — satellite antenna N87-16932

FREQUENCY SHIFT KEYING
Single frequency multitransmitter telemetry [NASA-CASE-LAR-13006-1] N87-16863

FREQUENCY SYNTHESIZERS
Aircraft noise synthesis system [NASA-TM-89040] N87-17483

FRICTION MEASUREMENT
Oil film thickness measurement and analysis for an angular contact ball bearing operating in parched elastohydrodynamic lubrication [NASA-CR-179506] N87-16879

FRICTION WELDING
Inertia welding of nitralloy N and 18 nickel maraging 250 grade steels for utilization in the main rotor drive shaft for the AR-64 military helicopter program N87-17067

FROST
Frost action predictive techniques for roads and airfields: A comprehensive survey of research findings [DOT/FAA/PM-85/23] N87-16853

FUEL CELLS
The NASA Aerospace Battery Safety Handbook [NASA-CR-180127] N87-17397

FUEL COMBUSTION
Transient catalytic combustion [AD-A173098] N87-16894
Fuels combustion research [AD-A175040] N87-16897

FUEL CONSUMPTION
Performance data Aeroc 8.2.AC.20, issue 5, Dash 8, series 100 N87-16817
Performance data Aeroc 8.2.AC.20(300), issue 1 N87-16818

FUEL PUMPS
Space shuttle main engine high pressure fuel pump aft platform seal cavity flow analysis [NASA-TP-2685] N87-17000

FUELS
Advanced fuels in a field-reversed configuration [IPPJ-804] N87-17512

FUNCTIONAL ANALYSIS
A pseudo-arclength continuation method for nonlinear Eigenvalue problems [AD-A173019] N87-17459

FURLABLE ANTENNAS
Experience gained by sector model testing of an unfurlable mesh/rib antenna N87-16925
Mechanical and control study of a 7 m offset unfurlable tracking antenna N87-16926

FUSELAGES
A comparison of single-block and multi-block grids around wing-fuselage configurations [FFA-TN-1986-42] N87-16811

G

GALACTIC CLUSTERS
Far infrared spectroscopy of galaxies from the Kuiper Airborne Observatory N87-17577
Dark matter and the dynamics of galaxy clustering N87-17587
The dynamics and evolution of clusters of galaxies [NASA-CR-180169] N87-17596

GALACTIC EVOLUTION
The dynamics and evolution of clusters of galaxies [NASA-CR-180169] N87-17596

GALACTIC NUCLEI
Observations of active galactic nuclei with FIRST — Far Infrared Submillimeter Space Telescope (FIRST) N87-17538
Submillimetre continuum observations of active galactic nuclei N87-17558
Radiative processes underlying the X-ray and gamma-ray continua of active galactic nuclei and gamma-ray bursts N87-17655

GALACTIC RADIATION
Submillimeter observation of the integrated galactic emission from the South Pole N87-17560
Far infrared spectroscopy of galaxies from the Kuiper Airborne Observatory N87-17577

GALACTIC RADIO WAVES
New results about diffuse galactic emission at 380 microns N87-17554
GALACTIC STRUCTURE
The development of the Goddard Compton gamma-ray telescope and neutral hydrogen N87-17580
Scale-free models of highly flattened elliptical galaxies N87-17589
The dynamics and evolution of clusters of galaxies [NASA-CR-180169] N87-17596
GALAXIES
Doubly differential cross sections for galactic heavy-ion fragmentation [NASA-TP-2659] N87-17487
GALLIUM ARSENIDES
Investigation of a GaAlAs Mach-Zehnder electro-optic modulator [NASA-CR-179573] N87-16953
The 20 GHz power GaAs FET development [NASA-CR-179546] N87-16972
The 60 GHz IMPATT diode development [NASA-CR-179536] N87-17515
Interfacial structure of In/Pt/GaAs heterojunction ohmic contacts [AD-A175102] N87-17523
GAME THEORY
A note on a core catcher of a cooperative game [MEMO-572] N87-17475
Advantageous syndicates in a bilateral market game: The case of the tau-value [MEMO-583] N87-17534
GAMMA RAY BURSTS
On the spectra of gamma-ray bursts at high energies N87-17654
GAMMA RAY SPECTROMETERS
Determination of nonglobal component against background of global radioactive pollution of atmospheric aerosols N87-17100
GAMMA RAY TELESCOPES
The development of the Goddard Compton gamma-ray telescope and neutral hydrogen N87-17580
GAS DYNAMICS
Proceedings of the 15th International Symposium on Shock Waves and Shock Tubes [AD-A173026] N87-17006
Evolution of a localized thermal explosion in a reactive gas [NASA-CR-178231] N87-17436
The Jovian Atmospheres [NASA-CP-2441] N87-17598
GAS FLOW
Atmospheric pressure studies of liquid propellant drops in hot flows [AD-A174839] N87-16915
Transitional boundary layers under the influence of high free stream turbulence, intensive wall cooling and high pressure gradients in hot gas circulation [NASA-TM-88524] N87-16983
GAS GIANT PLANETS
The Jovian Atmospheres [NASA-CP-2441] N87-17598
GAS JETS
A numerical study of jet production and accretion disk structure in super-Eddington black hole accretion N87-17586
GAS PIPES
Development of intelligent pipe locator N87-17200
GAS TUNGSTEN ARC WELDING
Discrete element weld model, phase 2 [NASA-CR-179009] N87-17041
Heat transfer in gas tungsten arc welding [DE86-013457] N87-17050
Advanced Joining of Aerospace Metallic Materials --- conference proceedings [AGARD-CP-398] N87-17051
The welding of aluminum alloys: A new technology in space application N87-17056
Welding of aluminum castings N87-17068
GAS TURBINE ENGINES
Transition mixing study [NASA-CR-175062] N87-16830
Gas turbine materials: A review [PNR90358] N87-16842
Aircraft derivative gas turbine development in China [PNR90359] N87-16844
Developments in data acquisition and processing using an advanced combustion research facility --- gas turbine engines [RAE-TM-P1089] N87-16852
Corrosion/oxidation protection of high temperature material --- gas turbine engines [PNR90355] N87-16905
Bonding of superalloys by diffusion welding and diffusion brazing N87-17059
Repair techniques for gas turbine components N87-17071
Combustion noise from gas turbine aircraft engines measurement of far-field levels [NASA-TM-88971] N87-17480
GAS TURBINES
Flameholder with removable flameholder attachments [AD-D012466] N87-16893
Measurement of heat transfer and pressure drop in rectangular channels with turbulence promoters [NASA-CR-4015] N87-17003
GAS-GAS INTERACTIONS
Proceedings of the 15th International Symposium on Shock Waves and Shock Tubes [AD-A173026] N87-17006
GASES
Observations of young low-mass stars in dense cores [NASA-CR-180152] N87-17583
GATES (CIRCUITS)
The 20 GHz power GaAs FET development [NASA-CR-179546] N87-16972
Dual channel high electron mobility field effect transistor [AD-D012474] N87-17518
GAUGE THEORY
Research program in theoretical high-energy physics [DE86-013326] N87-17490
GEARS
Common problems and pitfalls in gear design [NASA-TM-88858] N87-17033
Grinding of steel: A case study [AD-A174649] N87-17048
GENERAL AVIATION AIRCRAFT
Flight investigation of the effect of tail configuration on stall, spin, and recovery characteristics of a low-wing general aviation research airplane [NASA-TP-2644] N87-16815
GEOBOTANY
Discrimination of lithologic units using geobotanical and LANDSAT TM spectral data N87-17246
GEOCHEMISTRY
Integration of surficial geochemistry and LANDSAT imagery to discover skarn tungsten deposits using image analysis techniques [CONTRIB-19586] N87-17248
GEOCHRONOLOGY
On the relationship between age of lava flows and radar backscattering N87-17348
GEOCORONAL EMISSIONS
The hydrogen geocorona: Simultaneous optical and radar observations at Arecibo N87-17651
GEODESY
An iterative multi-resolution shape-from-shading algorithm and its application to planetary mapping N87-17331
GEODYNAMICS
Basic research for the geodynamics program [NASA-CR-180137] N87-17415
GEOELECTRICITY
Theoretical consideration on resistance geoelectrics N87-17196
Gradient methods for geophysical image inversions N87-17201
GEOIDS
Dynamical models for the Earth's geoid N87-17409
Improvement of the Earth's gravity field from terrestrial and satellite data [NASA-CR-180139] N87-17416
GEOLOGICAL FAULTS
Delineation of fault zones using imaging radar N87-17138
The megageomorphology of the radar rivers of the eastern Sahara N87-17139
A scanning radar altimeter for mapping continental topography N87-17146
GEOLOGICAL SURVEYS
Structural and geomorphic evolution of Meghalaya plateau, India on LANDSAT imagery N87-17233
Hydrogeological research in Peloponnesus (Greece) Karst area by support and completion of LANDSAT-thematic data N87-17234
Computer-aided analysis of LANDSAT data for mapping geologic and geomorphic features, North Bombay, India N87-17235
Comparative study of LANDSAT MSS, Salyut-7 (TERRA) and radar (SIR-A) images for geological and geomorphological applications: A case study from Rajasthan and Gujarat, India N87-17236
Interrelationship between field spectra and airborne MSS systems in the Singatse range, (Yerington) Nevada --- multispectral scanner (MSS) mineral exploration N87-17242
Integrated analysis of geological and remote sensing data aimed at mineral deposits detection in the Monapo area (northern Mozambique) N87-17243
Application of 2-D Hilbert transform in the interpretation of remotely sensed potential field data --- geology N87-17293
Computer-aided interpretation of complex geological patterns in remote sensing N87-17294
GEOLOGY
Infrared spectroscopy for geologic interpretation of TIMS data N87-17130
A geologic atlas of TIMS data N87-17133
GEOMETRIC RECTIFICATION (IMAGERY)
Interferometer applications for the rectification of radar images N87-17241
GEOMETRICAL OPTICS
A backscattering model for various foliated deciduous tree types at millimeter wavelengths N87-17307
GEOMORPHOLOGY
The application of remotely sensed data to pedologic and geomorphic mapping on alluvial fan and playa surfaces in Saline Valley, California N87-17127
The Red River Valley archeological project N87-17128
Tectonic geomorphology of the Andes with SIR-A and SIR-B N87-17136
Space shuttle radar images of Indonesia N87-17137
Delineation of fault zones using imaging radar N87-17138
The megageomorphology of the radar rivers of the eastern Sahara N87-17139
Structural and geomorphic evolution of Meghalaya plateau, India on LANDSAT imagery N87-17233
Computer-aided analysis of LANDSAT data for mapping geologic and geomorphic features, North Bombay, India N87-17235
Comparative study of LANDSAT MSS, Salyut-7 (TERRA) and radar (SIR-A) images for geological and geomorphological applications: A case study from Rajasthan and Gujarat, India N87-17236
GEOPHYSICAL OBSERVATORIES
Results of geomagnetic observations at the Hurbanovo Geomagnetic Observatory in 1985 N87-17419
GEOPHYSICAL SATELLITES
Evaluation of geophysical parameters measured by the Nimbus-7 microwave radiometer for the TOGA Heat Exchange Project [NASA-CR-180151] N87-17110
GEOPHYSICS
USSR report: Earth sciences [JPRS-UES-86-005] N87-17096
Improving the geological interpretation of magnetic and gravity satellite anomalies [NASA-CR-180149] N87-17418
Magnetization of the oceanic crust: TRM or CRM? [NASA-CR-179896] N87-17429
Zhamanshin meteor crater [NASA-TM-88531] N87-17595
GEOPOTENTIAL HEIGHT
Ground-based microwave radiometric observations of atmospheric geopotential height fluctuations N87-17339
GEOSTROPHIC WIND
Eddy processes in the general circulation of the Jovian atmospheres N87-17627
Investigation of long-lived eddies on Jupiter N87-17633
Chaotic motion in the Jovian atmosphere N87-17634
GIOTTO MISSION
Giotto spacecraft high gain antenna mechanical design and development N87-16938
GLACIOLOGY
Analysis of multichannel SAR data of Spitsbergen --- glaciology N87-17223
GLOBULAR CLUSTERS
A soft X-ray observation of omega Centauri with EXOSAT [MPE-PREPRINT-60] N87-17575
GOLD
Airborne Thermal Infrared Multispectral Scanner (TIMS) images over disseminated gold deposits, Osgood Mountains, Humboldt County, Nevada N87-17134
GRAND UNIFIED THEORY
Research program in theoretical high-energy physics [DE86-013326] N87-17490
GRANULAR MATERIALS
A study of explosive wave propagation in granular materials with microstructure [AD-A173015] N87-16914
GRAPH THEORY
Shape similarity in remote sensing images using graph matching techniques N87-17330
GRAPHITE-EPOXY COMPOSITES
Flight service evaluation of advanced composite ailerons on the L-1011 transport aircraft [NASA-CR-178170] N87-16883
Mechanical properties of graphite epoxy used for Zero CTE Program [DE86-013227] N87-16886

Preliminary investigations into the microcracking of PMR-15/graphite composites. Part 1: Effect of cure temperature
[PNR90348] N87-16887
Development of lightweight dimensionally stable carbon fiber composite antenna reflectors for the INSAT-1 satellite N87-16936

GRAPHITIZATION
Fabrication of hollow, cored, and composite shaped parts from selected alloy powders
[AD-D012489] N87-16903

GRAPHS (CHARTS)
A study of anomalous propagation at radar frequencies and a proposal for a radar coverage forecasting model, book 2 of 2
[ETN-87-98938] N87-16967

GRASSLANDS
Assessing grass canopy condition and growth from combined optical-microwave measurements N87-17286

GRAVELS
Locating subsurface gravel with thermal imagery N87-17125

GRAVIMETERS
Development of new aviation technology for gravimetric surveying N87-17106

GRAVIMETRY
Solution of direct gravimetry problems for vertical cylindrical bodies N87-17105
Development of new aviation technology for gravimetric surveying N87-17106

GRAVITATIONAL EFFECTS
Electrical properties of Al-In-Sn alloys directionally solidified in high and low gravitational fields
[NASA-TM-86569] N87-16900
The effects of gravity level during directional solidification on the microstructure of hypermonotectic Al-In-Sn alloys
[NASA-TM-86573] N87-16901

GRAVITATIONAL FIELDS
Solution of direct gravimetry problems for vertical cylindrical bodies N87-17105
Improvement of the Earth's gravity field from terrestrial and satellite data
[NASA-CR-180139] N87-17416

GRAVITATIONAL WAVES
Transmission of atmospheric internal gravity waves into the stratosphere N87-17412
A search for rapidly modulated emission in bright X-ray sources using the HEAO A-1 data base
[NASA-CR-180148] N87-17593

GRAVITY ANOMALIES
Improving the geological interpretation of magnetic and gravity satellite anomalies
[NASA-CR-180149] N87-17418
Analysis of harmonic spline gravity models for Venus and Mars
[NASA-CR-180147] N87-17648

GRAVITY WAVES
A study of large, medium and small scale structures in the topside ionosphere
[NASA-CR-180068] N87-17413
Mesoscale waves as a probe of Jupiter's deep atmosphere N87-17628
Investigation of the mode of compensation of Venus topography
[NASA-CR-180145] N87-17649

GRAZING
Spatial analysis of the dynamics of an ecosystem by multistage remote sensing in Kenya N87-17173

GRAZING INCIDENCE
Measurement of sea backscatter at extremely low grazing angle by C-band Doppler radar N87-17301

GREECE
Hydrogeological research in Peloponnesus (Greece) Karst area by support and completion of LANDSAT-thematic data N87-17234

GREENLAND
The ice conditions in the Greenland waters, 1980
[REPT-551.467.3.068(988)] N87-17428

GRINDING MACHINES
Grinding of steel: A case study
[AD-A174649] N87-17048

GROUND STATIONS
RADARSAT high throughput SAR processor development N87-17154
The SIR-C ground data system: Digital processor, data products, information flow N87-17155
The FRS-68010: A new concept for the acquisition and analysis of NOAA HRPT data N87-17206
Digital satellite imagery acquisition and processing N87-17207

GROUND TESTS
Outdoor test stand performance of a convertible engine with variable inlet guide vanes for advanced rotorcraft propulsion
[NASA-TM-88939] N87-16825
Research opportunities in microgravity science and applications during shuttle hiatus
[NASA-TM-88964] N87-16917
Ground vibration tests
[ETN-87-98847] N87-17422

GROUND TRUTH
Atmospheric corrections of NOAA-AVHRR data verification of different methods by ground truth measurements N87-17274
Comparison concept of satellite derived wind and wave data with ground truth N87-17373
Oceanographic measurement capabilities of the NASA P-3 aircraft — ERS-1 mission N87-17380

GROWTH
Spatially growing disturbances in a two-stream, coplanar jet
[NASA-TM-88949] N87-16799

GUIDE VANES
Anti-rotation guide vane bushing
[AD-D012510] N87-17047

GYROSCOPES
High voltage semiconductors for inertial sensors
[SFIM-13293-CP/LS] N87-17525

H

HALLEY'S COMET
The study of the physics of cometary nuclei
[NASA-CR-180153] N87-17584

HALOS
The astrophysical implications of weakly interacting, massive particles N87-17592

HARDENING (MATERIALS)
The theory of finite elastic-plastic deformation with induced anisotropy modelled as combined isotropic-kinematic hardening N87-17074

HARMONIC OSCILLATORS
On routes to chaotic motion in oscillators with unsymmetric and symmetric elastic nonlinearity
[ISSN-0208-5658] N87-16969

HARMONICS
Review of wind simulation methods for horizontal-axis wind turbine analysis
[DE86-012223] N87-17407

HAWAII
Hawaiian lava flows and SIR-B results N87-17245

HAZARDS
Two-Phase Flows in Major Technological Hazards, volume 3
[VKI-LS-1986-03-VOL-3] N87-16984

HEAT EXCHANGERS
Heat exchanger for electrothermal devices
[NASA-CASE-LEW-14037-1] N87-16875

HEAT FLUX
Conventionally cast and forged copper alloy for high-heat-flux thrust chambers
[NASA-TP-2694] N87-16902
Thermal balance of the atmospheres of Jupiter and Uranus N87-17604
Convection without eddy viscosity: An attempt to model the interiors of giant planets N87-17625

HEAT ISLANDS
Environmental modification of metropolitan areas through satellite images: Study of urban design in the tropics N87-17175

HEAT MEASUREMENT
Heat transfer in gas tungsten arc welding
[DE86-013457] N87-17050
Thermal infrared imagery from helicopter for heat loss calculations in industrial plants N87-17326

HEAT RADIATORS
Measurement of heat transfer and pressure drop in rectangular channels with turbulence promoters
[NASA-CR-4015] N87-17003

HEAT RESISTANT ALLOYS
A composite aluminum conductor for pulsed power applications at cryogenic temperatures and method of its manufacture
[AD-D012501] N87-16885
Corrosion/oxidation protection of high temperature material — gas turbine engines
[PNR90355] N87-16905
Study of the electron beam weldability of superalloys through the analysis of melt zone morphology N87-17053
Bonding of superalloys by diffusion welding and diffusion brazing N87-17059
The application of the RBD process to the deposition of anti-wear alloys N87-17069
Repair techniques for gas turbine components N87-17071
Technique for the growth of compositionally ungraded single crystals of solid solutions
[AD-D012488] N87-17519

HEAT TRANSFER
Numerical methods for two-dimensional and three-dimensional heat transfer calculations N87-16995
Prediction of heat and mass transfer in particulate beds N87-16999
A general method for unsteady stagnation region heat transfer and results for model turbine flows
[NASA-TM-88903] N87-17002
Measurement of heat transfer and pressure drop in rectangular channels with turbulence promoters
[NASA-CR-4015] N87-17003
Heat transfer in gas tungsten arc welding
[DE86-013457] N87-17050
Effect of electrical and thermal properties of materials on microwave brightness temperature of the terrestrial crust N87-17263
ATHENA code manual. Volume 1: Code structure, system models, and solution methods
[DE87-001430] N87-17492

HEAT TREATMENT
A preliminary study of factors affecting the calibration stability of the iridium versus iridium-40 percent rhodium thermocouple
[NASA-TM-89086] N87-17018
Dynamic fracture initiation and propagation in 4340 steel under impact loading
[AD-A173084] N87-17092

HEAVY IONS
Doubly differential cross sections for galactic heavy-ion fragmentation
[NASA-TP-2659] N87-17487

HEIGHT
Computer-derived height from SIR-B stereo radar images N87-17268
Validation of wind speed and significant wave height from Geosat N87-17368

HELICOPTER ENGINES
Impact of IPS and IRS configuration on engine installation design — helicopter engines
[PNR90324] N87-16834

HELICOPTER PROPELLER DRIVE
Inertia welding of nitralloy N and 18 nickel maraging 250 grade steels for utilization in the main rotor drive shaft for the AR-64 military helicopter program N87-17067

HELICOPTERS
Development of new aviation technology for gravimetric surveying N87-17106
Power cepstrum technique with application to model helicopter acoustic data
[NASA-TP-2586] N87-17479

HELIUM
Mechanisms of helium embrittlement N87-16899
The optimum condition of TPD-1 recombining helium plasma for VUV coherent lasing action
[IPPJ-798] N87-17507

HERMETIC SEALS
Metallization for hermetic sealing of ceramic modules
[AD-D012483] N87-17044

HETEROJUNCTIONS
Interfacial structure of In/Pt/GaAs heterojunction ohmic contacts
[AD-A175102] N87-17523

HIERARCHIES
A study of spatial models and human navigation within complex computer interfaces N87-17447
A construction of solutions of the multicomponent KP-hierarchy
[MEMO-584] N87-17476

HIGH ELECTRON MOBILITY TRANSISTORS
Dual channel high electron mobility field effect transistor
[AD-D012474] N87-17518

HIGH ENERGY INTERACTIONS
Research program in theoretical high-energy physics
[DE86-013326] N87-17490
On the spectra of gamma-ray bursts at high energies N87-17654

HIGH GAIN
Absolute gain measurement by the image method under mismatched condition
[NASA-TM-88924] N87-16968

HIGH POWER LASERS
High intensity selectable poly or monochromatic slit light source apparatus for optical instruments
[AD-D012507] N87-17496

HIGH PRESSURE
Space shuttle main engine high pressure fuel pump aft platform seal cavity flow analysis
[NASA-TP-2685] N87-17000

HIGH RESOLUTION
A high resolution shock capturing scheme for high Mach number internal flow
[NASA-CR-179523] N87-16804

HIGH SPEED
Euler analysis of the three dimensional flow field of a high-speed propeller: Boundary condition effects [NASA-TM-88955] N87-16798
HIGH STRENGTH ALLOYS
Welding of aluminum castings N87-17068
Repair techniques for gas turbine components N87-17071
HIGH TEMPERATURE
Conventionally cast and forged copper alloy for high-heat-flux thrust chambers [NASA-TP-2694] N87-16902
Unitized high temperature probes [AD-D012508] N87-17020
HIGH TEMPERATURE PLASMAS
Modeling of nonlinear effects of plasma wave beams on ionospheric plasma N87-17107
HIGH VOLTAGES
High-voltage Milberger slip slide power conditioner [AD-D012504] N87-16974
High voltage semiconductors for inertial sensors [SFIM-13293-CP/LS] N87-17525
HILBERT TRANSFORMATION
Application of 2-D Hilbert transform in the interpretation of remotely sensed potential field data — geology N87-17293
HINGES
Contraves' antenna tip hinge mechanism for Selenia Spazio's 20/30 GHz antenna — satellite antenna N87-16944
HOLES (ELECTRON DEFICIENCIES)
The effect of operating frequency in the radiation induced buildup of trapped holes and interface states in MOS devices [AD-A173097] N87-17522
HOLLOW CATHODES
Investigation of plasma contactors for use with orbiting wires [NASA-CR-180154] N87-17502
HOLOGRAPHIC INTERFEROMETRY
Industrial holography: The Rolls-Royce experience [PNR90351] N87-17024
A new method for compensating and measuring any motion of 3D-objects in holographic interferometry: Recent developments [ISL-CO-242/85] N87-17025
Thermoelastic testing of stratified materials N87-17064
HOMOSPHERE
An updated hydrocarbon photochemical model for the Jovian atmosphere from the troposphere through the homopause: A prelude to Galileo N87-17636
HOSES
Self-contained, single-use hose and tubing cleaning module [NASA-CASE-MSC-20857-1] N87-17035
HOT ISOSTATIC PRESSING
Evaluation of DDH and weld repaired F100 turbine vanes under simulated service conditions N87-17070
HOT MACHINING
Unitized high temperature probes [AD-D012508] N87-17020
HOUSINGS
Development of new aviation technology for gravimetric surveying N87-17106
HOVERING
Identification of a dynamic model of a helicopter from flight tests N87-16813
HUMAN BEHAVIOR
Space station human productivity study, volume 1 [NASA-CR-171961] N87-16869
HUMAN BEINGS
An experimental microcomputer controlled system for synchronized pulsating anti-gravity suit [AD-A174640] N87-17433
HUMAN FACTORS ENGINEERING
Space station human productivity study. Volume 4: Issues [NASA-CR-171963] N87-16865
Space station human productivity study. Volume 5: Management plans [NASA-CR-171964] N87-16866
Space station human productivity study. Volume 2: Executive summary and oral review presentation [NASA-CR-171962] N87-16868
HUMAN PERFORMANCE
Model of the human controller of a dynamic system [MEMO-580] N87-17435
HUMAN WASTES
Supercritical water oxidation of products of human metabolism [NASA-CR-180144] N87-17430
HUMIDITY
A comparison of two British standard test methods for the determination of resistance to humidity of paint films [MOAD-TP-918] N87-16906
HURRICANES
Ocean waves near Hurricane Josephine from SIR-B N87-17148
HYDROCARBONS
An updated hydrocarbon photochemical model for the Jovian atmosphere from the troposphere through the homopause: A prelude to Galileo N87-17636
HYDRODYNAMICS
Hydrodynamics of internal solitons and a comparison of SIR-A and SIR-B data with ocean measurements N87-17147
HYDROGEN
Low noise polycrystalline semiconductor resistors by hydrogen passivation [AD-D012492] N87-17520
The development of the Goddard Compton gamma-ray telescope and neutral hydrogen N87-17560
The Jovian Atmospheres [NASA-CP-2441] N87-17598
Modeling the temporal and spatial variations of the vertical structure of Jupiter's atmosphere using observations of the 3-0 hydrogen quadrupole lines N87-17601
The ortho-para H2 distribution on Uranus: Constraints from the collision-induced 3-0 dipole band and 4-0 S(0) and S(1) quadrupole line profiles N87-17640
The hydrogen geocorona: Simultaneous optical and radar observations at Arecibo N87-17651
HYDROGEN ATOMS
The distribution of atomic hydrogen in the Jovian atmosphere N87-17611
Two micron quadrupole line emission of H2 from the Jovian auroral zone N87-17615
The HD/H2 ratio in the atmosphere of Uranus N87-17646
HYDROGEN COMPOUNDS
The A-X and B-X band systems of SrH: Wavenumbers and molecular constants [USIP-86-04] N87-17486
Submillimeter HCO+ observations of dense cloud cores — interstellar clouds N87-17562
HYDROGEOLOGY
Hydrogeological research in Peloponnesus (Greece) Karst area by support and completion of LANDSAT-thematic data N87-17234
HYDROMETEOROLOGY
Microwave radiances from horizontally finite precipitating clouds containing ice and liquid hydrometeors N87-17340
HYDROXYL EMISSION
Measurement of HO2 chemical kinetics with a new detection method [NASA-CR-180114] N87-16890
HYDROXYL RADICALS
Measurement of HO2 chemical kinetics with a new detection method [NASA-CR-180114] N87-16890
Atmospheric pressure studies of liquid propellant drops in hot flows [AD-A174639] N87-16915
HYPERBOLIC DIFFERENTIAL EQUATIONS
Recursive linear smoothing for dissipative hyperbolic systems [AD-A173020] N87-17460
HYPERSONIC AIRCRAFT
Compendium of NASA Langley reports on hypersonic aerodynamics [NASA-TM-87760] N87-16802
Optimal turning at high angle of attack of supersonic and hypersonic vehicles N87-16814
HYPERSONIC FLOW
Hypersonic nonequilibrium flow over an ablating teflon surface N87-16787
A high resolution shock capturing scheme for high Mach number internal flow [NASA-CR-179523] N87-16804

I

ICE
The ice conditions in the Greenland waters, 1980 [REPT-551.467.3.068(988)] N87-17428
ICE ENVIRONMENTS
Imaging radar contributions to a major air-sea-ice interaction study in the Greenland Sea N87-17150
Observing the polar oceans with spaceborne radar N87-17151
ICE FLOES
SAR ice floe kinematics and correlation with mesoscale oceanic structure within the marginal ice zone N87-17222
ICE FORMATION
Observation of ice/water formations on a model intake section subjected to simulated cloud conditions — aircraft engine [PNR90347] N87-16839
ICE MAPPING
Automated remote sensing of sea ice using synthetic aperture radar N87-17186
An overview of operational SAR data collection and dissemination plans for ERS-1 ice data in Canada N87-17189
Geophysics of the marginal ice zone from SAR N87-17219
ICE NUCLEI
Microwave radiances from horizontally finite precipitating clouds containing ice and liquid hydrometeors N87-17340
IDEAL FLUIDS
On variational characterizations of steady vortex rings [MEMO-577] N87-17014
IDENTIFYING
A knowledge-based software environment for the analysis of spectroradiometer data — mineral identification N87-17203
IGNITION
Evolution of a localized thermal explosion in a reactive gas [NASA-CR-178231] N87-17436
IGNITION TEMPERATURE
Transient catalytic combustion [AD-A173098] N87-16894
IMAGE ANALYSIS
Quantitative analysis of fracture surfaces using computer aided fractography N87-17076
Comparison of Thematic Mapper (TM) and SPOT simulation data for agricultural applications in south west Germany N87-17165
Extracting surface features in multispectral imagery N87-17211
Using secondary image products to aid in understanding and interpretation of radar imagery N87-17239
Integration of surficial geochemistry and LANDSAT imagery to discover skarn tungsten deposits using image analysis techniques [CONTRIB-19586] N87-17248
The influence of resampling method and multitemporal LANDSAT imagery on crop classification accuracy in the United Kingdom N87-17250
A nonparametric supervised multispectral classification method using binary morphological operators N87-17253
Analysis of the spatial structure of Synthetic Aperture Radar (SAR) imagery for a better separability of cereal crops, wheat and barley N87-17287
Computer-aided interpretation of complex geological patterns in remote sensing N87-17294
Analysis of synthetic aperture radar imagery of surface ship wakes N87-17297
Parameter space techniques for image registration N87-17327
Shape similarity in remote sensing images using graph matching techniques N87-17330
IMAGE CONTRAST
Unitary suprathreshold color-difference metrices of legibility for CRT raster imagery [AD-A175062] N87-17434
IMAGE ENHANCEMENT
A synergistic approach for multispectral image restoration using reference imagery N87-17255
Merging spaceborne image data of optical and microwave sensors N87-17267
IMAGE FILTERS
Algorithms and programming tools for image processing on the MPP, part 2 [NASA-CR-180146] N87-17440
IMAGE MOTION COMPENSATION
A new method for compensating and measuring any motion of 3D-objects in holographic interferometry: Recent developments [ISL-CO-242/85] N87-17025
IMAGE PROCESSING
Enhancement of time images for photointerpretation N87-17116
Detection and mapping of volcanic rock assemblages and associated hydrothermal alteration with Thermal Infrared Multiband Scanner (TIMS) data Comstock Lode Mining District, Virginia City, Nevada N87-17119
Application of TIMS data in stratigraphic analysis N87-17121
Calculation of day and night emittance values N87-17131
The SIR-C ground data system: Digital processor, data products, information flow N87-17155
SIR-B measurements and modeling of vegetation N87-17160

Gradient methods for geophysical image inversions N87-17201
Digital satellite imagery acquisition and processing N87-17207
Portable EDITOR (PEDITOR): A portable image processing system — satellite images N87-17208
The image processing workbench - portable software for remote sensing instruction and research N87-17209
Extracting surface features in multispectral imagery N87-17211
ERS-1 fast delivery processing and products N87-17224
The German ERS-1 SAR postprocessing system plans and concepts N87-17231
Multispectral classification of microwave remote sensing images — SAR crop identification N87-17238
Using secondary image products to aid in understanding and interpretation of radar imagery N87-17239
A simulation study of some contextual classification methods for remotely sensed data N87-17252
Segmentation by mathematical morphology processing hand on the image understanding model in remote sensing N87-17254
The ERS-1 scatterometer system simulator and its relevance for ground processing design N87-17257
Image representation via its symmetrical components N87-17290
Advanced alternating frame technology (VISIDEP (TM)) and three-dimensional remote sensing N87-17291
Image processing methods in two and three dimensions used to animate remotely sensed data — cloud cover N87-17292
Application of 2-D Hilbert transform in the interpretation of remotely sensed potential field data — geology N87-17293
Computer-aided interpretation of complex geological patterns in remote sensing N87-17294
Parameter space techniques for image registration N87-17327
An iterative multi-resolution shape-from-shading algorithm and its application to planetary mapping N87-17331
Optical visual evaluation and interpretation of remote sensing data N87-17353
A procedure for estimation of two-dimensional ocean height-variance spectra from SAR imagery N87-17361
Unitary suprathreshold color-difference metrices of legibility for CRT raster imagery [AD-A175062] N87-17434
Algorithms and programming tools for image processing on the MPP, part 2 [NASA-CR-180146] N87-17440
Recursive linear smoothing for dissipative hyperbolic systems [AD-A173020] N87-17460
Nanosecond two-dimensional imaging using tomographic techniques [DE86-008164] N87-17499

IMAGE RECONSTRUCTION
Gradient methods for geophysical image inversions N87-17201
A synergistic approach for multispectral image restoration using reference imagery N87-17255
Merging spaceborne image data of optical and microwave sensors N87-17267
An iterative multi-resolution shape-from-shading algorithm and its application to planetary mapping N87-17331

IMAGERY
Absolute gain measurement by the image method under mismatched condition [NASA-TM-88924] N87-16968

IMAGES
VARAN-S radar image interpretation [CNES-CT/DRT/TIT/RL-54-T] N87-16963
MIZEX VARAN-S radar image characteristics [CNES-CT/DRT/TIT/RL-55-T] N87-16964
Unitary suprathreshold color-difference metrices of legibility for CRT raster imagery [AD-A175062] N87-17434

IMAGING RADAR
The Second Spaceborne Imaging Radar Symposium [NASA-CR-180131] N87-17135
Delineation of fault zones using imaging radar N87-17138
Spaceborne imaging radar research in the 90's N87-17141
Spaceborne Imaging Radar Project N87-17143
Imaging radar contributions to a major air-sea-ice interaction study in the Greenland Sea N87-17150
Observing the polar oceans with spaceborne radar N87-17151
Imaging radar polarimetry from wave synthesis N87-17158
Imaging radar polarimetry from wave synthesis N87-17279

IMAGING TECHNIQUES
Interface circuitry for superconducting bolometer [NASA-TM-86581] N87-17016
Locating subsurface gravel with thermal imagery N87-17125
Imaging spectrometry: Aircraft and space program N87-17202
The Sequential Filter Imaging Radiometer (SFIR), a new instrument configuration for Earth observations N87-17205
Advanced alternating frame technology (VISIDEP (TM)) and three-dimensional remote sensing N87-17291
Nanosecond two-dimensional imaging using tomographic techniques [DE86-008164] N87-17499

IMIDES
Fire and heat resistant laminating resins based on maleimido substituted aromatic cyclotriphosphazene polymer [NASA-CASE-ARC-11426-2] N87-16909

IMPACT LOADS
Dynamic fracture initiation and propagation in 4340 steel under impact loading [AD-A173084] N87-17092

IMPACT TESTS
Dynamic fracture initiation and propagation in 4340 steel under impact loading [AD-A173084] N87-17092

INCIDENCE
Multiple incidence angle SIR-B experiment over Argentina N87-17157

INCIDENT RADIATION
Seasonal north-south asymmetry in solar radiation at the top of Jupiter's atmosphere N87-17603

INCOMPRESSIBLE FLOW
Unsteady aerodynamics of a rotating compressor blade row in incompressible flow. Volume 1: Experimental facilities, procedures and sample data [AD-A173043] N87-16831

INDEXES (DOCUMENTATION)
NASA thesaurus supplement (supplement 2) [NASA-SP-7053(SUPP-2)] N87-17530
Scientific and technical information output of the Langley Research Center for calendar year 1986 [NASA-TM-89065] N87-17531

INDIA
Significance of space image, air photo and drainage linears in relation to west coast tectonics, India N87-17232
Structural and geomorphic evolution of Meghalaya plateau, India on LANDSAT imagery N87-17233

INDIAN OCEAN
Spatial evolution of wave spectra in the vicinity of the Agulhas current from SIR-B N87-17337

INDIUM ARSENIDES
Interfacial structure of In/Pt/GaAs heterojunction ohmic contacts [AD-A175102] N87-17523

INDONESIA
Space shuttle radar images of Indonesia N87-17137

INDUCTANCE
Monitoring transients in low inductance circuits [DE86-013756] N87-16978
The induced current on a long wire due to a vertical electric dipole above dissipative ground N87-17197

INDUSTRIAL PLANTS
Thermal infrared imagery from helicopter for heat loss calculations in industrial plants N87-17326

INDUSTRIAL SAFETY
Review of present approaches to two-phase flow problems N87-16986

INERTIAL CONFINEMENT FUSION
Annual review, April 1985 - March 1986 [ISSN-0547-1567] N87-17503

INFLATABLE SPACECRAFT
Expandable pulse power spacecraft radiator [AD-D012498] N87-17005

INFLATABLE STRUCTURES
Development of a 2.8 m offset antenna reflector using inflatable, space-rigidized structures technology N87-16927

INFORMATION RETRIEVAL
Homogenizing surface and satellite observations of cloud [AD-A174691] N87-17427
A study of spatial models and human navigation within complex computer interfaces N87-17447
NASA thesaurus supplement (supplement 2) [NASA-SP-7053(SUPP-2)] N87-17530

INFORMATION THEORY
Components and comparisons of potential information from several imaging satellites N87-17164

INFRARED ASTRONOMY
Interface circuitry for superconducting bolometer [NASA-TM-86581] N87-17016
Review of coherent and incoherent detection techniques: Outlook and limitation — spaceborne submillimeter astronomy N87-17537
Observations of active galactic nuclei with FIRST — Far Infrared Submillimeter Space Telescope (FIRST) N87-17538
Interplanetary dust N87-17542
Submillimetre wavelength studies of protostars: The role of FIRST — Far Infrared Submillimeter Space Telescope (FIRST) N87-17544
Circumstellar envelopes around evolved stars N87-17548
Far infrared submillimeter wave space telescope (FIRST) observations of stars with large mass loss rates N87-17550
Observations of young low-mass stars in dense cores [NASA-CR-180152] N87-17583

INFRARED ASTRONOMY SATELLITE
On the identification of IRAS deep field sources: The radio counterparts N87-17552
IRAS observations of the Pleiades N87-17557

INFRARED DETECTORS
The influence of background power on the performance of an ideal bolometer N87-17565

INFRARED IMAGERY
Concept of a future multispectral Thermal Infrared (TIR) pushbroom mission for Earth observation from space N87-17169
Estimation of internal wave currents from SAR and infrared scatterometer imagery N87-17295
Thermal infrared remote sensing: One of today's solutions N87-17324
Thermal infrared imagery from helicopter for heat loss calculations in industrial plants N87-17326

INFRARED INTERFEROMETERS
Study of the ammonia ice cloud layer in the north tropical zone of Jupiter from the infrared interferometric experiment on Voyager N87-17609

INFRARED PHOTOGRAPHY
Thermal infrared imagery from helicopter for heat loss calculations in industrial plants N87-17326

INFRARED PHOTOMETRY
Polarimetry and photometry of active quasars at visual and near-infrared wavelengths N87-17579

INFRARED RADAR
Spaceborne imaging radar research in the 90's N87-17141

INFRARED RADIATION
Infrared radiation from interface regions in molecular clouds: L1551 and the Serpens nebula N87-17556
Spatial and temporal variability of infrared-observable properties of the Jovian atmosphere: A partial survey N87-17600

INFRARED RADIOMETERS
Discrimination of soil hydraulic properties by combined thermal infrared and microwave remote sensing N87-17303

INFRARED SCANNERS
The TIMS Data User's Workshop [NASA-CR-180130] N87-17111
The TIMS instrument N87-17112
Models for temperature estimation from remotely sensed thermal IR data N87-17325

INFRARED SPECTRA
IRAS observations of the Pleiades N87-17557
Vibrationally excited cyanoacetylene in regions of massive star formation N87-17561
Study of the ammonia ice cloud layer in the north tropical zone of Jupiter from the infrared interferometric experiment on Voyager N87-17609

INFRARED SPECTROSCOPY
Far infrared spectroscopy of galaxies from the Kuiper Airborne Observatory N87-17577

INFRARED TELESCOPES
A Sener mechanism: Fine adjustment mechanism for the Far Infrared and Submillimeter Space Telescope (FIRST) (F f F) N87-16946
Observations of active galactic nuclei with FIRST — Far Infrared Submillimeter Space Telescope (FIRST) N87-17538
Submillimetre wavelength studies of protostars: The role of FIRST — Far Infrared Submillimeter Space Telescope (FIRST) N87-17544
Far infrared submillimeter wave space telescope (FIRST) observations of stars with large mass loss rates N87-17550
A proposed cornerstone mission: Far infrared submillimeter wave telescope (FIRST) N87-17564
Active optics for the far infrared submillimeter wave space telescope (FIRST): A high angular resolution mode N87-17566
The large deployable reflector: A NASA submillimeter-infrared orbiting observatory N87-17571

Structure of molecular clouds and space-based sub-millimeter telescopes, for example FIRST — Far Infrared Submillimeter Wave Space Telescope (FIRST) N87-17574

INHOMOGENEITY
Effect of the size of structural bulk inhomogeneities on the specular transmittance of polymer films [DE86-010727] N87-16913
Numerical modeling of two-dimensional time domain electromagnetic scattering by underground inhomogeneities N87-17199

INLET FLOW
Laser Doppler velocimeter measurements and theoretical investigation of three dimensional scroll flow N87-16979

INSOLATION
The effect of Saturn's rings on the upper-boundary insolation of its atmosphere [AERONOMICA-ACTA-A-308-1986] N87-17650

INSPECTION
Economical manufacturing and inspection of the electron-beam-welded Tornado wing box N87-17055
The welding of aluminum alloys: A new technology in space application N87-17056
Thermoelastic testing of stratified materials N87-17064

INSTALLING
Collaborative problem solving for installation planning and decision making [AD-A174611] N87-17527

INTAKE SYSTEMS
Unsteady aerodynamics of a rotating compressor blade row in incompressible flow. Volume 1: Experimental facilities, procedures and sample data [AD-A173043] N87-16831

INTEGRATED CIRCUITS
Microstrip dipoles for EHF and millimeter wave applications [AD-A173025] N87-16976

INTELLIGIBILITY
Noise-immune multisensor transduction of speech [AD-A174693] N87-16961

INTERFACES
Geometries for roughness shapes in laminar flow [NASA-CASE-LAR-13255-1] N87-16793
Small computer interface to a stepper motor [NASA-TM-86574] N87-16970
The effect of operating frequency in the radiation induced buildup of trapped holes and interface states in MOS devices [AD-A173097] N87-17522

INTERFACIAL ENERGY
Interfacial structure of In/Pt/GaAs heterojunction ohmic contacts [AD-A175102] N87-17523

INTERFEROMETERS
Interferometric load sensor and strain gage [AD-D012509] N87-17021

INTERFEROMETRY
Interferometric load sensor and strain gage [AD-D012509] N87-17021

INTERNAL WAVES
Hydrodynamics of internal solitons and a comparison of SIR-A and SIR-B data with ocean measurements N87-17147
C and Ku-band scatterometer results from the SCATTMOD internal wave experiment N87-17215
Estimation of internal wave currents from SAR and infrared scatterometer imagery N87-17295
Characterisation of internal wave surface patterns on airborne SAR imagery N87-17338
Transmission of atmospheric internal gravity waves into the stratosphere N87-17412

INTERNATIONAL COOPERATION
A new day: Challenger and space flight thereafter [NASA-TM-77717] N87-16856

INTERPLANETARY DUST
Interplanetary dust N87-17542

INTERROGATION
Design and initial application of the extended aircraft interrogation and display system: Multiprocessing ground support equipment for digital flight systems [NASA-TM-86740] N87-16820

INTERSTELLAR CHEMISTRY
Excitation and transfer of submillimeter molecular transitions — interstellar chemistry N87-17546
Interstellar chemistry and submillimeter observations N87-17547
Far infrared and optical study of the high latitude cloud L1642 N87-17559
Vibrationally excited cyanoacetylene in regions of massive star formation N87-17561
Submillimeter HCO+ observations of dense cloud cores — interstellar clouds N87-17562
CO observations of the outflow source NGC 7023 N87-17563

INTERSTELLAR EXTINCTION
The interstellar medium at submm wavelengths N87-17543
Far infrared and optical study of the high latitude cloud L1642 N87-17559

INTERSTELLAR GAS
Far infrared spectroscopy of galaxies from the Kuiper Airborne Observatory N87-17577

INTERSTELLAR MASERS
Maser and thermal SiO emission in evolved stars N87-17553

INTERSTELLAR MATTER
The interstellar medium at submm wavelengths N87-17543
Interstellar dust N87-17545
Some results about laboratory dust analysis in the FIR range — cosmic dust simulation N87-17551
IRAS observations of the Pleiades N87-17557

INTERSTELLAR RADIATION
The interstellar medium at submm wavelengths N87-17543
Interstellar dust N87-17545
Excitation and transfer of submillimeter molecular transitions — interstellar chemistry N87-17546

INTERSTELLAR SPACE
The interstellar medium at submm wavelengths N87-17543

INVENTORIES
Microwave remote sensing: Its applications and limitations in operational tasks of land use inventory and forest management N87-17266

INVERSE SCATTERING
Light scattering theory for bubbles in water: Inverse scattering, coated bubbles and statistics [AD-A174997] N87-17498

INVERSIONS
Gradient methods for geophysical image inversions N87-17201
Improving the geological interpretation of magnetic and gravity satellite anomalies [NASA-CR-180149] N87-17418

ION BEAMS
Heat exchanger for electrothermal devices [NASA-CASE-LEW-14037-1] N87-16875
Applications of focused ion beams in microelectronics [RSRE-MEMO-3948] N87-17517

ION CURRENTS
Interpenetrating-network polymeric electrolytes [AD-D012485] N87-16912

ION IMPLANTATION
Use of low energy ion implants in high efficiency crystalline silicon solar cells [NASA-CR-179971] N87-17408
Applications of focused ion beams in microelectronics [RSRE-MEMO-3948] N87-17517
Low noise polycrystalline semiconductor resistors by hydrogen passivation [AD-D012492] N87-17520

IONIZATION
The ionization structure of planetary nebulae. 8: NGC 6826 [NASA-CR-180142] N87-17581
The ionization structure of planetary nebulae. Part 7: New observations in the ring nebula [NASA-CR-180141] N87-17582

IONIZING RADIATION
The effect of operating frequency in the radiation induced buildup of trapped holes and interface states in MOS devices [AD-A173097] N87-17522

IONOSPHERES
Modeling of nonlinear effects of plasma wave beams on ionospheric plasma N87-17107

IONOSPHERIC DISTURBANCES
Modeling of nonlinear effects of plasma wave beams on ionospheric plasma N87-17107

IONOSPHERIC ION DENSITY
Model study of the mid-latitude atmospheric interaction with energetic O+ and He+ (20 keV) precipitation during a storm N87-17411

IONS
Total and dissociative photoionization cross sections of N2 from threshold to 107 eV [NASA-CR-180172] N87-16892

IRAN
Discrimination of land features using LANDSAT false colour composite in N Iran N87-17352

IRON ALLOYS
Preparations of rare earth-iron alloys by thermite reduction [DE86-013753] N87-16904

IRRADIANCE
Extrapolation of Earth-based solar irradiance measurements to exoatmospheric levels for broad-band and selected absorption-band observations N87-17270

IRRADIATION
Mechanisms of helium embrittlement N87-16899

ITERATION
A multigrid LU-SSOR scheme for approximate Newton iteration applied to the Euler equations [NASA-CR-179524] N87-16803
An iterative multi-resolution shape-from-shading algorithm and its application to planetary mapping N87-17331
A note on Branin's method for finding the critical points of smooth functions [MEMO-576] N87-17465

ITERATIVE SOLUTION
Globally convergent hybrid conjugate gradient methods [MR-196] N87-17454

J

JAMMING
ECM (electronic countermeasures) preprocessor or tracker using multi-processor modules [AD-D012513] N87-16959

JAPANESE SPACE PROGRAM
Present statue of Japanese ERS-1 Project N87-17145
A satellite-borne SAR transmitter and receiver N87-17358
Pulse compression test results of the SAR transmitter and receiver — satellite-borne SAR N87-17360

JET ENGINE FUELS
Fuels combustion research [AD-A175040] N87-16897

JET ENGINES
Low aspect ratio turbine design at Rolls-Royce [PNR90338] N87-16824

JET FLOW
Spatially growing disturbances in a two-stream, coplanar jet [NASA-TM-88949] N87-16799
Aeroacoustics of supersonic jet flows from contoured and solid/porous conical plug-nozzles [NASA-CR-178095] N87-17484

JET STREAMS (METEOROLOGY)
Convective forcing of global circulations on the Jovian planets N87-17624
Eddy processes in the general circulation of the Jovian atmospheres N87-17627
A proposal for adopting a standard coordinate system for defining atmospheric nomenclature for the giant planets N87-17632
Transport of absolute angular momentum in quasi-axisymmetric equatorial jet streams N87-17635

JOINTS (JUNCTIONS)
Effect of adherend thickness and mixed mode loading on debond growth in adhesively bonded composite joints [NASA-TM-88992] N87-16882
Solid rocket booster joint seal analyses [NASA-TM-86580] N87-17039

JORDAN
Results of tectonic and spectral investigations along the Wadi Araba fault in Jordan using special processed Thematic Mapping (TM) data N87-17247

JUNCTION DIODES
High band gap 2-6 and 3-5 tunneling junctions for silicon multijunction solar cells [NASA-CASE-NPO-16526-1CU] N87-17399

JUPITER (PLANET)
Para hydrogen equilibration in the atmospheres of the outer planets N87-17599

JUPITER ATMOSPHERE
The Jovian Atmospheres [NASA-CP-2441] N87-17598
Modeling the temporal and spatial variations of the vertical structure of Jupiter's atmosphere using observations of the 3-0 hydrogen quadrupole lines N87-17601
Seasonal north-south asymmetry in solar radiation at the top of Jupiter's atmosphere N87-17603
Thermal balance of the atmospheres of Jupiter and Uranus N87-17604
Water vapor in Jupiter's atmosphere N87-17605
VLA observations of Jupiter at 1.3 - 20 cm wavelengths N87-17606
The vertical structure of Jupiter's equatorial and tropical regions N87-17607
Vertical cloud structure models for the NTRZ EQZ, SEB and STRZ of Jupiter N87-17608
Study of the ammonia ice cloud layer in the north tropical zone of Jupiter from the infrared interferometric experiment on Voyager N87-17609
Constraints on the composition of Jupiter's stratospheric aerosols from ultraviolet photometry N87-17610

The distribution of atomic hydrogen in the Jovian atmosphere N87-17611
Spatial variation of the thermal structure of Jupiter's atmosphere N87-17612
The single scattering phase functions of Jupiter's clouds N87-17613
Enhanced acetylene emission near the north pole of Jupiter N87-17614
Two micron quadrupole line emission of H2 from the Jovian auroral zone N87-17615
Brown dwarfs and Jovian planets: A comparison N87-17616
A possible deuterium anomaly: Implications of the CH3D/CH4 mixing ratios in the atmospheres of Jupiter, Saturn, and Uranus N87-17617
The abundances of ethane to acetylene in the atmospheres of Jupiter and Saturn N87-17618
A detected feature at the expected wavelength for the HD R5(0) line in Jupiter's and Uranus' atmospheres N87-17619
Global dynamics and thermal structure of Jupiter's atmosphere N87-17621
Jupiter: New estimates of mean zonal flow at the cloud level N87-17622
Cloud-top meridional momentum transports on Saturn and Jupiter N87-17623
Eddy processes in the general circulation of the Jovian atmospheres N87-17627
Mesoscale waves as a probe of Jupiter's deep atmosphere N87-17628
Quasi-geostrophic free mode models of long-lived Jovian eddies: Forcing mechanisms and crucial observational tests N87-17630
Moisture driven convection on Jupiter: A mechanism to produce the equatorial plumes N87-17631
Investigation of long-lived eddies on Jupiter N87-17633
Chaotic motion in the Jovian atmosphere N87-17634
Transport of absolute angular momentum in quasi-axisymmetric equatorial jet streams N87-17635
An updated hydrocarbon photochemical model for the Jovian atmosphere from the troposphere through the homopause: A prelude to Galileo N87-17636

K

KALMAN FILTERS
Kalman filtering, smoothing and recursive robot arm forward and inverse dynamics [NASA-CR-180135] N87-17451
KARST
Hydrogeological research in Peloponnesus (Greece) Karst area by support and completion of LANDSAT-thematic data N87-17234
KEVLAR (TRADEMARK)
Qualification of gridding process for a Polarization Sensitive Reflector (PSR) — satellite antenna N87-16932
KINEMATICS
SAR ice floe kinematics and correlation with mesoscale oceanic structure within the marginal ice zone N87-17222
A laboratory investigation of two-celled vortex flows N87-17423
KINETIC ENERGY
Thermodynamic estimate of climatic system efficiency N87-17098
KINETICS
Lumped model generation and evaluation: Sensitivity and lie algebraic techniques with applications to combustion [AD-A174984] N87-16896
KNOWLEDGE
Training programs in remote sensing for professionals, students and the general public [NASA-TM-88541] N87-17394

L

LABORATORIES
Description of the Spacecraft Control Laboratory Experiment (SCOLE) facility [NASA-TM-89057] N87-16848
Research opportunities in microgravity science and applications during shuttle hiatus [NASA-TM-88964] N87-16917
LAKE ICE
A climatological-hydrological study of lake ice in the southwestern mountain area in Norway by use of satellite sensing N87-17319
LAKES
Analysis of AIS radiometry at Mono Lake, California — Airborne Imaging Spectrometer (AIS) N87-17204
LAMINAR BOUNDARY LAYER
Stability characteristics of a supersonic boundary layer and their relation to the position of the laminar-turbulent transition point [NASA-TM-88533] N87-16797
LAMINAR FLOW
Navier-Stokes solution for laminar transonic flow over a NACA0012 airfoil [FAA-140] N87-16794
A general method for unsteady stagnation region heat transfer and results for model turbine flows [NASA-TM-88903] N87-17002
LAMINAR FLOW AIRFOILS
Geometries for roughness shapes in laminar flow [NASA-CASE-LAR-13255-1] N87-16793
LAMINATES
Thermoelastic testing of stratified materials N87-17064
Crack propagation in UD (Unidirectional) laminates by the stress intensity factors N87-17084
A three dimensional calculation of elastic equilibrium for composite materials [NASA-CR-178158] N87-17088
LAND ICE
Sea ice in the Greenland sea observed by the Nimbus-7 Scanning Multichannel Microwave Radiometer (SMMR) N87-17221
LAND MOBILE SATELLITE SERVICE
Coherent versus noncoherent signaling for satellite-aided mobile communications [NASA-CR-180133] N87-16922
Application of adaptive antenna techniques to future commercial satellite communication [NASA-CR-179566] N87-16955
Remote sensing of tree attenuation at 870 MHz along simulated Earth-satellite paths N87-17306
LAND USE
Sri Lanka's solution to land use mapping and monitoring for Third World countries development N87-17174
Bitemporal analysis of Thematic Mapper data for land cover classification N87-17249
LANDSAT SATELLITES
Comparison of Thematic Mapper (TM) and SPOT simulation data for agricultural applications in south west Germany N87-17165
The transfer of remote sensing technology to developing countries: A survey of experts in the field N87-17170
Structural and geomorphic evolution of Meghalaya plateau, India on LANDSAT imagery N87-17233
Hydrogeological research in Peloponnesus (Greece) Karst area by support and completion of LANDSAT-thematic data N87-17234
Computer-aided analysis of LANDSAT data for mapping geologic and geomorphic features, North Bombay, India N87-17235
Comparative study of LANDSAT MSS, Salyut-7 (TERRA) and radar (SIR-A) images for geological and geomorphological applications: A case study from Rajasthan and Gujarat, India N87-17236
Discrimination of lithologic units using geobotanical and LANDSAT TM spectral data N87-17246
Results of tectonic and spectral investigations along the Wadi Araba fault in Jordan using special processed Thematic Mapping (TM) data N87-17247
Integration of surficial geochemistry and LANDSAT imagery to discover skarn tungsten deposits using image analysis techniques [CONTRIB-19586] N87-17248
The influence of resampling method and multitemporal LANDSAT imagery on crop classification accuracy in the United Kingdom N87-17250
Towards snowmelt runoff forecast using LANDSAT-MSS and NOAA/AVHRR data N87-17317
Radiometric correction method which removes both atmospheric and topographic effects from the LANDSAT-MSS data N87-17329
Discrimination of land features using LANDSAT false colour composite in N Iran N87-17352
LANDSAT 5
Bitemporal analysis of Thematic Mapper data for land cover classification N87-17249
Evaluation of LANDSAT 5 Thematic Mapping (TM) data for image clustering and classification N87-17251
Rural land use inventory and mapping in the Ardeche area (France) using multitemporal Thematic Mapping (TM) data N87-17350
LANDSAT-5 Thematic Mapping (TM) data applications to land use classification on around the Bosphorus area, Turkey N87-17351
LAP JOINTS
Diffusion bonding of Al-alloys in the solid state N87-17058
LARGE AREA CROP INVENTORY EXPERIMENT
An overview of remote sensing agricultural apcations in North America: Past, present and future N87-17284
LARGE SPACE STRUCTURES
Description of the Spacecraft Control Laboratory Experiment (SCOLE) facility [NASA-TM-89057] N87-16848
Real time identification of large space structures [NASA-CR-171957] N87-16867
Evaluation of Pactruss design characteristics critical to space station primary structure [NASA-CR-178171] N87-16870
Adaptive control techniques for large space structures [AD-A173063] N87-16871
Estimation and control of distributed models for certain elastic systems arising in large space structures [AD-A175019] N87-16872
Dynamics and Control Analysis Package (DCAP): An automated analysis and design tool for structural control of space structures N87-16947
A modified loop transfer recovery approach for robust control of flexible structures N87-17029
A research program in advanced information systems [NASA-CR-180150] N87-17529
LASER APPLICATIONS
Droplet sizing research program [AD-A173100] N87-16895
Thermoelastic testing of stratified materials N87-17064
A real time vision system for robotic arc welding N87-17066
LASER DOPPLER VELOCIMETERS
Combined density and velocity measurements. Application to the investigation of a free jet [ISL-CO-206/86] N87-16808
Laser Doppler velocimeter measurements and theoretical investigation of three dimensional scroll flow N87-16979
Experimental investigation in turbulent flow separation [ISL-CO-208/86] N87-17012
Projection lens scanning laser velocimeter system [NASA-CASE-ARC-11547-1] N87-17026
LASER GUIDANCE
Empirical considerations for laser guided electron beams in the advanced test accelerator [DE86-013218] N87-17489
LASER OUTPUTS
Projection lens scanning laser velocimeter system [NASA-CASE-ARC-11547-1] N87-17026
LASER WELDING
Microstructural modifications during laser and electron beam welding [DE86-011076] N87-17049
The application of diffusion bonding and laser welding in the fabrication of aerospace structures N87-17054
LASING
The optimum condition of TPD-1 recombining helium plasma for VUV coherent lasing action [IPPJ-798] N87-17507
LATE STARS
Molecular abundances in circumstellar envelopes N87-17549
LATTICES (MATHEMATICS)
Lattice filters and adaptive identification of flexible structures N87-17030
LAUNCH VEHICLES
Vibroacoustic payload environment prediction system (VAPEPS): Data base management center remote access guide [NASA-CR-180132] N87-17528
LAVA
Hawaiian lava flows and SIR-B results N87-17245
On the relationship between age of lava flows and radar backscattering N87-17348
LEAD COMPOUNDS
Research on millimeter wave dielectric materials [AD-A173017] N87-17521
LEADING EDGES
Geometries for roughness shapes in laminar flow [NASA-CASE-LAR-13255-1] N87-16793
Unitized high temperature probes [AD-D012508] N87-17020
LEARNING
Training programs in remote sensing for professionals, students and the general public [NASA-TM-88541] N87-17394
LEAST SQUARES METHOD
Real time identification of large space structures [NASA-CR-171957] N87-16867
A synergistic approach for multispectral image restoration using reference imagery N87-17255
LEAVES
A backscattering model for various foliated deciduous tree types at millimeter wavelengths N87-17307
LENSES
Projection lens scanning laser velocimeter system [NASA-CASE-ARC-11547-1] N87-17026

LIBRARIES
Interactive wrapper tool for mapping objects to Fortran library functions
[DE86-009686] N87-17446
LIE GROUPS
Lumped model generation and evaluation: Sensitivity and lie algebraic techniques with applications to combustion
[AD-A174984] N87-16896
LIFT DRAG RATIO
Over-the-wing propeller
[NASA-CASE-LAR-13134-2] N87-16828
LIGHT MODULATION
Metal film light modulator
[AD-D012506] N87-17495
LIGHT SCATTERING
Droplet sizing research program
[AD-A173100] N87-16895
Imaging radar polarimetry from wave synthesis N87-17158
Radar signature determination: Trends and limitations N87-17159
Light scattering theory for bubbles in water: Inverse scattering, coated bubbles and statistics
[AD-A174997] N87-17498
The single scattering phase functions of Jupiter's clouds N87-17613
LIGHT SOURCES
Interferometric load sensor and strain gage
[AD-D012509] N87-17021
High intensity selectable poly or monochromatic slit light source apparatus for optical instruments
[AD-D012507] N87-17496
LIGHT TRANSMISSION
Effect of the size of structural bulk inhomogeneities on the specular transmittance of polymer films
[DE86-010727] N87-16913
LIMB DARKENING
Constraints on the composition of Jupiter's stratospheric aerosols from ultraviolet photometry N87-17610
LIMITER CIRCUITS
High energy surge arrester technology development, part 2
[AD-A173086] N87-16977
LINE CURRENT
The induced current on a long wire due to a vertical electric dipole above dissipative ground N87-17197
LINE OF SIGHT
Results from 1984 airborne Doppler lidar wind measurement program. Flight 6: Analysis of line-of-sight elevation angle errors and apparent Doppler velocities
[NASA-CR-178994] N87-17425
LINE SPECTRA
The ionization structure of planetary nebulae. 8: NGC 6826
[NASA-CR-180142] N87-17581
The ionization structure of planetary nebulae. Part 7: New observations in the ring nebula
[NASA-CR-180141] N87-17582
Modeling the temporal and spatial variations of the vertical structure of Jupiter's atmosphere using observations of the 3-0 hydrogen quadrupole lines N87-17601
Two micron quadrupole line emission of H2 from the Jovian auroral zone N87-17615
A detected feature at the expected wavelength for the HD R5(0) line in Jupiter's and Uranus' atmospheres N87-17619
The ortho-para H2 distribution on Uranus: Constraints from the collision-induced 3-0 dipole band and 4-0 S(0) and S(1) quadrupole line profiles N87-17640
LINEAR ACCELERATORS
Optical modeling of induction-linac driven free-electron lasers
[DE87-001432] N87-17027
Unified formulation for linear accelerator design
[DE86-013441] N87-17491
LINEAR PROGRAMMING
Scale-free models of highly flattened elliptical galaxies N87-17589
LINEAR SYSTEMS
Recursive linear smoothing for dissipative hyperbolic systems
[AD-A173020] N87-17460
Decentralized control of large-scale systems: Fixed modes, sensitivity and parametric robustness
[NASA-TM-88537] N87-17474
LINEAR TRANSFORMATIONS
An implementation of the Hough transform using a linear array processor in conjunction with a PDP/11microprocessor — computer vision
[NPL-DITC-74/86] N87-17438
LINEARITY
Linearised theory of stability and resonance for projectiles with aerodynamically induced roll variations
[WSRL-0449-TR] N87-16795
LININGS
Transition mixing study
[NASA-CR-175062] N87-16830
Conventionally cast and forged copper alloy for high-heat-flux thrust chambers
[NASA-TP-2694] N87-16902
LIPSCHITZ CONDITION
Convenient total variation diminishing conditions for nonlinear difference schemes
[NASA-CR-178209] N87-17453
LIQUID HELIUM
Sound propagation in a superfluid helium filled porous solid: Theory and experiment N87-17478
LIQUID ROCKET PROPELLANTS
Investigation of a repetitive pulsed electrothermal thruster
[NASA-CR-179464] N87-16878
LIQUID-SOLID INTERFACES
Magmatic differentiation in partially molten systems: Applications to the moon and the palisades sill N87-17597
LIQUIDS
Supported liquid membranes in 1986: New technology or scientific curiosity
[DE86-007504] N87-16898
LITHIUM CHLORIDES
Safety considerations of lithium-thionyl chloride cells
[NASA-CR-180129] N87-17396
LITHIUM COMPOUNDS
Research on millimeter wave dielectric materials
[AD-A173017] N87-17521
LITHOLOGY
Lithologic mapping of silicate rocks using TIMS N87-17118
Application of TIMS data in stratigraphic analysis N87-17121
A geologic atlas of TIMS data N87-17133
Space shuttle radar images of Indonesia N87-17137
Geological applications of multipolarization SAR data N87-17140
Discrimination of lithologic units using geobotanical and LANDSAT TM spectral data N87-17246
Results of tectonic and spectral investigations along the Wadi Araba fault in Jordan using special processed Thematic Mapping (TM) data N87-17247
LITHOSPHERE
Improving the geological interpretation of magnetic and gravity satellite anomalies
[NASA-CR-180149] N87-17418
LOADS (FORCES)
Loads and Aeroelasticity Division research and technology accomplishments for FY 1986 and plans for FY 1987
[NASA-TM-89084] N87-16796
Evaluation of Pactruss design characteristics critical to space station primary structure
[NASA-CR-178171] N87-16870
LOGIC CIRCUITS
Nonlinear real-time optical signal processing
[AD-A173119] N87-17497
Performance of polysilicon gate CMOS devices in space and SDI environments
[DE88-009025] N87-17524
LONG TERM EFFECTS
A new day: Challenger and space flight thereafter
[NASA-TM-77717] N87-16856
Changes in Saturn's south-temperate haze distribution during the summer of 1973-1980 N87-17602
LOOK ANGLES (TRACKING)
Radar imagery of the European city influenced by variations in depression angle and look direction N87-17237
LOUISIANA
Locating subsurface gravel with thermal imagery N87-17125
LOW ALTITUDE
Characteristics of a very low altitude spacecraft for collecting global directional wave spectra with spaceborne synthetic aperture radar N87-17333
LOW ASPECT RATIO
Low aspect ratio turbine design at Rolls-Royce
[PNR90336] N87-16824
LOW NOISE
Low noise polycrystalline semiconductor resistors by hydrogen passivation
[AD-D012492] N87-17520
Low noise SIS mixer with gain for 80-115 GHz — superconductor-insulator-superconductor (SIS) radio telescope N87-17570
LOW SPEED
Piloted simulator study of allowable time delays in large-airplane response
[NASA-TP-2652] N87-16849
LOW WEIGHT
Development of lightweight dimensionally stable carbon fiber composite antenna reflectors for the INSAT-1 satellite N87-16936
LUBRICANTS
Oil film thickness measurement and analysis for an angular contact ball bearing operating in parched elastohydrodynamic lubrication
[NASA-CR-179506] N87-16879
LUMINESCENCE
Robotic vision system
[AD-D012481] N87-17043
LUNAR BASES
Lunar power systems
[NASA-CR-171956] N87-17398
LUNAR ENVIRONMENT
Lunar power systems
[NASA-CR-171956] N87-17398
LUNAR ORBITS
Stochastic model of tidal evolution of Earth-Moon system with cyclic change in resonant frequency of ocean N87-17103
LYMAN ALPHA RADIATION
The distribution of atomic hydrogen in the Jovian atmosphere N87-17611
LYMAN SPECTRA
The distribution of atomic hydrogen in the Jovian atmosphere N87-17611

M

M STARS
Maser and thermal SiO emission in evolved stars N87-17553
MACH NUMBER
A high resolution shock capturing scheme for high Mach number internal flow
[NASA-CR-179523] N87-16804
Calculation of sidewall boundary-layer parameters from rake measurements for the Langley 0.3-meter transonic cryogenic tunnel
[NASA-CR-178241] N87-16807
MACH-ZEHNDER INTERFEROMETERS
Investigation of a GaAlAs Mach-Zehnder electro-optic modulator
[NASA-CR-179573] N87-16953
MAGELLAN PROJECT (NASA)
Venus Radar Mapper (VRM): Multimode radar system design N87-17142
MAGNETIC ANOMALIES
Improving the geological interpretation of magnetic and gravity satellite anomalies
[NASA-CR-180149] N87-17418
Magnetization of the oceanic crust: TRM or CRM?
[NASA-CR-179896] N87-17429
MAGNETIC BEARINGS
Radial and torsionally controlled magnetic bearing
[NASA-CASE-GSC-12957-1] N87-17038
MAGNETIC COILS
Radial and torsionally controlled magnetic bearing
[NASA-CASE-GSC-12957-1] N87-17038
MAGNETIC FIELD CONFIGURATIONS
Tilt stability of field-reversed configurations
[IPPJ-802] N87-17510
A self-consistent modeling of a quasi-steady state compact torus evolving to ignition
[IPPJ-801] N87-17511
MAGNETIC FIELDS
Apparatus and method for stirring fluid borne particles
[AD-D012486] N87-17477
International ultraviolet explorer observing program: Ultraviolet observations of selected astronomical sources
[NASA-CR-180155] N87-17584
MAGNETIC FLUX
Radial and torsionally controlled magnetic bearing
[NASA-CASE-GSC-12957-1] N87-17038
MAGNETIC MEASUREMENT
Development of intelligent pipe locator N87-17200
MAGNETIC PERMEABILITY
Magmatic differentiation in partially molten systems: Applications to the moon and the palisades sill N87-17597
MAGNETIC PROPERTIES
Apparatus and method for stirring fluid borne particles
[AD-D012486] N87-17477
MAGNETIC STORMS
Model study of the mid-latitude atmospheric interaction with energetic O+ and He+ (20 keV) precipitation during a storm N87-17411
MAGNETIZATION
Magnetization of the oceanic crust: TRM or CRM?
[NASA-CR-179896] N87-17429

MAGNETOHYDRODYNAMIC STABILITY
RF plugging and tandem mirror experiments in a cusp-anchored mirror device
[IPPJ-800] N87-17508
A self-consistent modeling of a quasi-steady state compact torus evolving to ignition
[IPPJ-801] N87-17511
MAGNETOMETERS
Results of geomagnetic observations at the Hurbanovo Geomagnetic Observatory in 1985 N87-17419
MAGNETOSPHERE
A model for an electromotive force generator in the magnetosphere: A source of discrete auroral arcs
[AERONOMICA-ACTA-A-309-1986] N87-17421
MAGNETOSPHERIC ELECTRON DENSITY
The distribution of atomic hydrogen in the Jovian atmosphere N87-17611
MAGNETOSTATICS
The possibility of reducing the cyclic torque fluctuations produced by two-stroke engines using the storage of magnetostatic energy
[RAE-TM-RAD-NAV-265] N87-17042
MAINTENANCE
Damage and repairing of fiber composites, a summary
[FOA-C-20620-2.5] N87-16888
MALEATES
Fire and heat resistant laminating resins based on maleimido substituted aromatic cyclotriphosphazene polymer
[NASA-CASE-ARC-11428-2] N87-16909
MAN ENVIRONMENT INTERACTIONS
Spatial analysis of the dynamics of an ecosystem by multistage remote sensing in Kenya N87-17173
Environmental modification of metropolitan areas through satellite images: Study of urban design in the tropics N87-17175
MAN MACHINE SYSTEMS
Model of the human controller of a dynamic system
[MEMO-580] N87-17435
MAN-COMPUTER INTERFACE
Initial utilization of the CVIRB video production facility
[NASA-TM-89036] N87-16873
A study of spatial models and human navigation within complex computer interfaces N87-17447
MANAGEMENT PLANNING
Space station human productivity study. Volume 5: Management plans
[NASA-CR-171964] N87-16866
Space station human productivity study. Volume 2: Executive summary and oral review presentation
[NASA-CR-171962] N87-16868
Space station human productivity study, volume 1
[NASA-CR-171961] N87-16869
Collaborative problem solving for installation planning and decision making
[AD-A174611] N87-17527
MANIFOLDS (MATHEMATICS)
A construction of solutions of the multicomponent KP-hierarchy
[MEMO-584] N87-17476
MANIPULATORS
Dynamics and control of flexible manipulators N87-17028
Position control of mechanical manipulators by using nonlinear adaptive control algorithm N87-17031
Adaptive control of mechanical manipulators N87-17450
Kalman filtering, smoothing and recursive robot arm forward and inverse dynamics
[NASA-CR-180135] N87-17451
MANNED SPACE FLIGHT
Concept definition for space station technology development experiments. Experiment definition, task 2
[NASA-CR-178153] N87-16860
MANNED SPACECRAFT
Structural dynamics and attitude control study of early manned capability space station configurations
[NASA-TM-89078] N87-16861
MANUALS
Collaborative problem solving for installation planning and decision making
[AD-A174611] N87-17527
MANUFACTURING
Economical manufacturing and inspection of the electron-beam-welded Tornado wing box N87-17055
Diffusion bonding in the manufacture of aircraft structure N87-17057
MAPPING
Microwave remote sensing: Its applications and limitations in operational tasks of land use inventory and forest management N87-17266
Computer-derived height from SIR-B stereo radar images N87-17268
Digital terrain mapping with STAR-1 SAR data N87-17269
The ice conditions in the Greenland waters, 1980
[REPT-551.467.3.068(988)] N87-17428
Observations of young low-mass stars in dense cores
[NASA-CR-180152] N87-17583
Investigation of the mode of compensation of Venus topography
[NASA-CR-180145] N87-17649
MARAGING STEELS
Inertia welding of nitralloy N and 18 nickel maraging 250 grade steels for utilization in the main rotor drive shaft for the AR-64 military helicopter program N87-17067
MARINE METEOROLOGY
Marine climate program N87-17390
MARITIME SATELLITES
Some results of Marine Observation Satellite (MOS-1) airborne verification experiment Multispectral Electronic Self Scanning Radiometer (MESSR) N87-17166
NASA scatterometer data processing system: Features for validation N87-17366
N-ROSS validation N87-17385
MARKOV PROCESSES
Perturbation theory for unbounded Markov processes with applications to queueing
[MEMO-579] N87-17466
MARS (PLANET)
Analysis of harmonic spline gravity models for Venus and Mars
[NASA-CR-180147] N87-17648
MARS ATMOSPHERE
Thermodynamic estimate of climatic system efficiency N87-17098
MASS DISTRIBUTION
Dark matter and the dynamics of galaxy clustering N87-17587
On the oblateness and rotation rate of Neptune's atmosphere N87-17644
MASS TRANSFER
Prediction of heat and mass transfer in particulate beds N87-16999
MATERIALS RECOVERY
Supported liquid membranes in 1986: New technology or scientific curiosity
[DE86-007504] N87-16898
MATHEMATICAL MODELS
A study of anomalous propagation at radar frequencies and a proposal for a radar coverage forecasting model, book 2 of 2
[ETN-87-98938] N87-16967
LEO high voltage solar array arcing response model
[NASA-CR-180073] N87-16971
Two-Phase Flows in Major Technological Hazards, volume 3
[VKI-LS-1986-03-VOL-3] N87-16984
Review of present approaches to two-phase flow problems N87-16986
Introduction to Numerical Solution of Industrial Flows, volume 1 --- conference
[VKI-LS-1986-07-VOL-1] N87-16987
An analysis of flow models: From Navier-Stokes to potential flow equations N87-16988
Introduction to Numerical Solution of Industrial Flows, volume 2 --- conference
[VKI-LS-1986-07-VOL-2] N87-16994
SRB O-ring free response analysis
[NASA-TM-86582] N87-17040
Discrete element weld model, phase 2
[NASA-CR-179009] N87-17041
Computational weld mechanics N87-17052
Model selection and validation methods for nonlinear systems
[RR-292] N87-17095
Estimation of absolute water surface temperature based on atmospherically corrected thermal infrared multispectral scanner digital data N87-17114
Simulation modeling and preliminary analysis of TIMS data from the Carlin area and the northern Grapevine Mountains, Nevada N87-17120
On microwave scattering properties of heterogeneous two-component mixtures --- soil/snow N87-17178
Microwave remote sensing of snow-covered sea ice N87-17187
Numerical modeling of two-dimensional time domain electromagnetic scattering by underground inhomogeneities N87-17199
Verification results for a two-scale model of microwave backscatter from the sea surface N87-17213
A modified boundary perturbation approach to microwave scattering and emission by the ocean surface N87-17214
Recent progress in ERS-1 wind scatterometer design N87-17256
SAR imaging of bottom topography in the ocean: Results from an improved model N87-17298
A backscattering model for various foliated deciduous tree types at millimeter wavelengths N87-17307
A scattering model for defoliated vegetation N87-17309
Evaluating roughness models of radar backscatter N87-17344
Microwave dielectric behavior of vegetation material
[NASA-CR-180096] N87-17393
Canopy hot-spot as crop identifier
[DE86-011258] N87-17395
Dynamical models for the Earth's geoid N87-17409
Improving the geological interpretation of magnetic and gravity satellite anomalies
[NASA-CR-180149] N87-17418
Dynamic analysis and design of the SIRTF primary mirror mount
[NASA-CR-180158] N87-17494
The Saturnian ribbon feature: A baroclinically unstable model N87-17629
MATRICES (MATHEMATICS)
Image representation via its symmetrical components N87-17290
MATRIX MATERIALS
Determining and modeling the response of ytterbium piezoresistance transducers
[AD-A173085] N87-17023
MATTER (PHYSICS)
Ultralow background searches for beta beta-decay, cold dark matter and solar axions
[DE86-013592] N87-17652
MAXIMUM LIKELIHOOD ESTIMATES
Identification of a dynamic model of a helicopter from flight tests N87-16813
MAXWELL EQUATION
Numerical modeling of two-dimensional time domain electromagnetic scattering by underground inhomogeneities N87-17199
MEASURING INSTRUMENTS
Universal pressure transducer
[AD-D012499] N87-17019
Determining and modeling the response of ytterbium piezoresistance transducers
[AD-A173085] N87-17023
Optical thin film monitoring using optical fibers
[DE87-001355] N87-17501
MECHANICAL ENGINEERING
Proceedings of the Second ESA Workshop on Mechanical Technology for Antennas
[ESA-SP-261] N87-16923
Antenna mechanical technologies within ESA N87-16924
ERS-1 wind scatterometer antenna: Mechanical aspects N87-16940
MECHANICAL PROPERTIES
Composite space antenna structures: Properties and environmental effects
[NASA-TM-88859] N87-16880
Interpenetrating-network polymeric electrolytes
[AD-D012485] N87-16912
Diffusion welding of component parts in the aviation and space industries
[RAE-TRANS-2147] N87-17032
MEGALOPOLISES
Environmental modification of metropolitan areas through satellite images: Study of urban design in the tropics N87-17175
MELTING
Snow cover recession in an Alpine ecological system N87-17316
Towards snowmelt runoff forecast using LANDSAT-MSS and NOAA/AVHRR data N87-17317
Dependence of snow melting and surface-atmosphere interactions on the forest structure N87-17318
A climatological-hydrological study of lake ice in the southwestern mountain area in Norway by use of satellite sensing N87-17319
MELTING POINTS
Technique for the growth of compositionally ungraded single crystals of solid solutions
[AD-D012488] N87-17519
MELTS (CRYSTAL GROWTH)
Study of the electron beam weldability of superalloys through the analysis of melt zone morphology N87-17053
Technique for the growth of compositionally ungraded single crystals of solid solutions
[AD-D012488] N87-17519
MEMBRANES
Supported liquid membranes in 1986: New technology or scientific curiosity
[DE86-007504] N87-16898
MERIDIONAL FLOW
Cloud-top meridional momentum transports on Saturn and Jupiter N87-17623
Convective forcing of global circulations on the Jovian planets N87-17624

MESOSCALE PHENOMENA
SAR ice floe kinematics and correlation with mesoscale oceanic structure within the marginal ice zone N87-17222
Mesoscale waves as a probe of Jupiter's deep atmosphere N87-17628
MESSAGE PROCESSING
Cyclic unequal error protection codes constructed from cyclic codes of composite length [NASA-CR-180165] N87-17457
On codes with multi-level error-correction capabilities [NASA-CR-180166] N87-17458
METAL COATINGS
Diffusion bonding of Al-alloys in the solid state N87-17058
The application of the RBD process to the deposition of anti-wear alloys N87-17069
METAL FATIGUE
Assessment of damage tolerance requirements and analysis. Volume 1: Executive summary [AD-A175110] N87-16822
METAL FILMS
Metal film light modulator [AD-D012506] N87-17495
METAL OXIDE SEMICONDUCTORS
The effect of operating frequency in the radiation induced buildup of trapped holes and interface states in MOS devices [AD-A173097] N87-17522
High voltage semiconductors for inertial sensors [SFIM-13293-CP/LS] N87-17525
METAL POWDER
Fabrication of hollow, cored, and composite shaped parts from selected alloy powders [AD-D012489] N87-16903
The application of the RBD process to the deposition of anti-wear alloys N87-17069
METAL SHEETS
Method and apparatus for die forming metal sheets and extrusions [AD-D012512] N87-16920
Diffusion bonding of Al-alloys in the solid state N87-17058
Application of diffusion bonding combined with superplastic forming (SPF/DB) to the fabrication of TAGV metal sheet structures N87-17060
METAL-METAL BONDING
Advanced Joining of Aerospace Metallic Materials — conference proceedings [AGARD-CP-398] N87-17051
Computational weld mechanics N87-17052
Study of the electron beam weldability of superalloys through the analysis of melt zone morphology N87-17053
Diffusion bonding in the manufacture of aircraft structure N87-17057
Diffusion bonding of Al-alloys in the solid state N87-17058
Bonding of superalloys by diffusion welding and diffusion brazing N87-17059
Application of diffusion bonding combined with superplastic forming (SPF/DB) to the fabrication of TAGV metal sheet structures N87-17060
Thermoelastic testing of stratified materials N87-17064
Welding of aluminum castings N87-17068
The application of the RBD process to the deposition of anti-wear alloys N87-17069
Evaluation of DDH and weld repaired F100 turbine vanes under simulated service conditions N87-17070
Repair techniques for gas turbine components N87-17071
METALLIZING
Metallization for hermetic sealing of ceramic modules [AD-D012483] N87-17044
METALLURGY
A preliminary study of factors affecting the calibration stability of the iridium versus iridium-40 percent rhodium thermocouple [NASA-TM-89086] N87-17018
METEOROLOGICAL FLIGHT
DFVLR flight operation acting as a useful service unit for ERS-1 N87-17378
Canada Center for Remote Sensing (CCRS) Convair 580 results relevant to ERS-1 wind and wave calibration N87-17379
Oceanographic measurement capabilities of the NASA P-3 aircraft — ERS-1 mission N87-17380
The use of aircraft for wind scatterometer calibration — ERS-1 scatterometer N87-17382
METEOROLOGICAL PARAMETERS
A two-step algorithm for the separate retrieval of ocean surface and atmospheric parameters from microwave radiometers N87-17341
Empirical relations between the Earth's radiation budget, cloudiness, and various meteorological parameters N87-17424
Astronomical, physical, and meteorological parameters for planetary atmospheres N87-17647
METEOROLOGICAL RADAR
Imaging radar contributions to a major air-sea-ice interaction study in the Greenland Sea N87-17150
Rain measurement results derived from a two polarization S-band radar employing frequency diversity at Wallops Island, Virginia N87-17182
METEOROLOGICAL RESEARCH AIRCRAFT
T-28 data acquisition during COHMEX 1986 [NASA-CR-179001] N87-17426
METEOROLOGICAL SATELLITES
Stereo Line Scanner (SLS): System considerations on an operational instrument for meteorology and weather forecasts N87-17168
Forecaster's need in meteorology for the next generation of satellites N87-17275
METEOROLOGICAL SERVICES
Real-time application of remotely sensed data — meteorology N87-17276
METEOROLOGY
USSR report: Earth sciences [JPRS-UES-86-005] N87-17096
METHANE
A possible deuterium anomaly: Implications of the CH3D/CH4 mixing ratios in the atmospheres of Jupiter, Saturn, and Uranus N87-17617
The ortho-para H2 distribution on Uranus: Constraints from the collision-induced 3-0 dipole band and 4-0 S(0) and S(1) quadrupole line profiles N87-17640
Are the aerosols on Uranus and Neptune composed of methane photopolymers? N87-17645
MICROCOMPUTERS
Small computer interface to a stepper motor [NASA-TM-86574] N87-16970
MICROCRACKS
Preliminary investigations into the microcracking of PMR-15/graphite composites. Part 1: Effect of cure temperature [PNR90348] N87-16887
MICROELECTRONICS
Applications of focused ion beams in microelectronics [RSRE-MEMO-3948] N87-17517
MICROPROCESSORS
Switching network for monitoring stations [AD-D012514] N87-17022
The design and evaluation of a high performance smalltalk system [AD-A173022] N87-17437
MICROSTRIP TRANSMISSION LINES
A new model for broadband waveguide to microstrip transition design [NASA-TM-88905] N87-16958
MICROSTRUCTURE
A study of explosive wave propagation in granular materials with microstructure [AD-A173015] N87-16914
Grinding of steel: A case study [AD-A174649] N87-17048
Microstructural modifications during laser and electron beam welding [DE86-011076] N87-17049
Quantitative analysis of fracture surfaces using computer aided fractography N87-17076
Snow property measurements correlative to microwave emission at 35 GHz N87-17315
MICROWAVE EMISSION
A modified boundary perturbation approach to microwave scattering and emission by the ocean surface N87-17214
Dielectric and surface parameters related to microwave scatter and emission properties N87-17262
Effect of electrical and thermal properties of materials on microwave brightness temperature of the terrestrial crust N87-17263
Effects of salinity on the microwave emission of soils N87-17302
Snow property measurements correlative to microwave emission at 35 GHz N87-17315
Microwave radiances from horizontally finite precipitating clouds containing ice and liquid hydrometeors N87-17340
L to X-band scatter and emission measurements of vegetation N87-17347
Laboratory measurements of microwave absorption from gaseous atmospheric constituents under conditions for the outer planets N87-17620
MICROWAVE PROBES
Microwave dielectric spectrum of vegetation material N87-17345
MICROWAVE RADIOMETERS
Development of mm-wave radiometer antenna reflector — satellite antennas N87-16941
Evaluation of geophysical parameters measured by the Nimbus-7 microwave radiometer for the TOGA Heat Exchange Project [NASA-CR-180151] N87-17110
Sea ice in the Greenland sea observed by the Nimbus-7 Scanning Multichannel Microwave Radiometer (SMMR) N87-17221
The Electronically Steered Thinned Array Radiometer (ESTAR) N87-17260
Antenna pattern correction in scanning radiometry: A singular system analysis N87-17261
Effect of electrical and thermal properties of materials on microwave brightness temperature of the terrestrial crust N87-17263
Developpement of algorithms to retrieve the water equivalent of snow cover from satellite microwave radiometer data N87-17264
Atmospheric corrections of NOAA-AVHRR data verificatcn of different methods by ground truth measurements N87-17274
Effects of salinity on the microwave emission of soils N87-17302
Discrimination of soil hydraulic properties by combined thermal infrared and microwave remote sensing N87-17303
Classification of forest and surface types by satellite microwave radiometry N87-17305
Estimation of maximum snow volume distribution using NOAA-AVHRR data N87-17314
Ground-based microwave radiometric observations of atmospheric geopotential height fluctuations N87-17339
A two-step algorithm for the separate retrieval of ocean surface and atmospheric parameters from microwave radiometers N87-17341
Retrieval of near-surface wind speed in the Baltic Sea from NIMBUS-7 Scanning Multichannel Microwave Radiometer (SMMR) observations N87-17342
Sea ice studies in the Baltic Sea using satellite microwave radiometer data N87-17343
Intersensor comparisons for validation of wind speed measurements from ERS-1 altimeter and scatterometer — Seasat N87-17386
A 186 GHz radiometer for the microwave limb sounder N87-17569
MICROWAVE SCATTERING
Microwave scattering from the ocean surface N87-17109
On microwave scattering properties of heterogeneous two-component mixtures — soil/snow N87-17178
Dielectric and scattering behavior of snow at microwave frequencies N87-17179
Snow stratigraphy observed by an FM-CW microwave system N87-17181
Microwave backscatter coefficients of artificially grown first-year sea ice N87-17188
A two-scale Bragg scattering model for microwave backscatter from wind generated waves N87-17212
Verification results for a two-scale model of microwave backscatter from the sea surface N87-17213
A modified boundary perturbation approach to microwave scattering and emission by the ocean surface N87-17214
C and Ku-band scatterometer results from the SCATTMOD internal wave experiment N87-17215
Identification of the contribution of Bragg scattering and specular reflection to X-band microwave backscattering in an ocean experiment N87-17216
Microwave properties of sea ice in the marginal ice zone N87-17220
Dielectric and surface parameters related to microwave scatter and emission properties N87-17262
L to X-band scatter and emission measurements of vegetation N87-17347
MICROWAVE SENSORS
Features and technologies of ERS-1 (ESA) and X-SAR antennas N87-17152
Off-line processing of ERS-1 synthetic aperture radar data with high precision and high throughput N87-17153
Development status of the ERS-1 payload instruments N87-17191
Assessing grass canopy condition and growth from combined optical-microwave measurements N87-17286
Microwave dielectric behavior of vegetation material [NASA-CR-180096] N87-17393
MICROWAVE SOUNDING
An inter-sensor comparison of the microwave signatures of Arctic sea ice N87-17184
Active/passive microwave sensor comparison of MIZ-ice concentration estimates — Marginal Ice Zone (MIZ) N87-17185
Microwave remote sensing of snow-covered sea ice N87-17187

MICROWAVE SPECTRA
Microwave dielectric spectrum of vegetation material N87-17345

MICROWAVE TRANSMISSION
A new model for broadband waveguide to microstrip transition design
[NASA-TM-88905] N87-16958

MICROWAVE TUBES
Free electron diode oscillator
[AD-D012519] N87-16975

MIDDLE ATMOSPHERE
Middle Atmosphere Program. Handbook for MAP, volume 22
[NASA-CR-180126] N87-17414

MIE SCATTERING
Light scattering theory for bubbles in water: Inverse scattering, coated bubbles and statistics
[AD-A174997] N87-17498

MILLIMETER WAVES
Development of mm-wave radiometer antenna reflector — satellite antennas N87-16941
Microstrip dipoles for EHF and millimeter wave applications
[AD-A173025] N87-16976
Millimeter-wave network analyzer-based scatterometer N87-17281
A backscattering model for various foliated deciduous tree types at millimeter wavelengths N87-17307
Opportunities and potential for a millimetre wavelength search for the Sunyaev-Zeldovich effect N87-17555
Low noise SIS mixer with gain for 80-115 GHz — superconductor-insulator-superconductor (SIS) radio telescope N87-17570

MINERAL EXPLORATION
Airborne Thermal Infrared Multispectral Scanner (TIMS) images over disseminated gold deposits, Osgood Mountains, Humboldt County, Nevada N87-17134
Interrelationship between field spectra and airborne MSS systems in the Singatse range, (Yerington) Nevada — multispectral scanner (MSS) mineral exploration N87-17242
Integrated analysis of geological and remote sensing data aimed at mineral deposits detection in the Monapo area (northern Mozambique) N87-17243
Integration of surficial geochemistry and LANDSAT imagery to discover skarn tungsten deposits using image analysis techniques
[CONTRIB-19586] N87-17248

MINERALS
Application of TIMS data in stratigraphic analysis N87-17121
A knowledge-based software environment for the analysis of spectroradiometer data — mineral identification N87-17203

MIRRORS
Dynamic analysis and design of the SIRTF primary mirror mount
[NASA-CR-180158] N87-17494
RF plugging and tandem mirror experiments in a cusp-anchored mirror device
[IPPJ-800] N87-17508

MISMATCH (ELECTRICAL)
Absolute gain measurement by the image method under mismatched condition
[NASA-TM-88924] N87-16968

MISSING MASS (ASTROPHYSICS)
Dark matter and the dynamics of galaxy clustering N87-17587

MISSION ADAPTIVE WINGS
AFTI/F-111 MAW flight control system and redundancy management description
[NASA-TM-88267] N87-16819

MISSION PLANNING
Present statue of Japanese ERS-1 Project N87-17145
The Cassini mission N87-17638

MIXING
Transition mixing study
[NASA-CR-175062] N87-16830

MIXING CIRCUITS
Low noise SIS mixer with gain for 80-115 GHz — superconductor-insulator-superconductor (SIS) radio telescope N87-17570
On the feasibility of constructing an imaging array of slot-antennas integrated with SIS mixers — radio astronomy N87-17572

MOBILE COMMUNICATION SYSTEMS
Multiple Trellis Coded Modulation (MTCM): An MSAT-X report
[NASA-CR-180134] N87-16921
Coherent versus noncoherent signaling for satellite-aided mobile communications
[NASA-CR-180133] N87-16922
Transmission loss measurements in mobile radio nets
[FOA-B-30098-3.3] N87-16966

MODELS
T-28 data acquisition during COHMEX 1986
[NASA-CR-179001] N87-17426
Communications satellite systems operations with the space station, volume 2
[NASA-CR-179527] N87-17473
Power cepstrum technique with application to model helicopter acoustic data
[NASA-TP-2586] N87-17479

MODULATION
Multiple Trellis Coded Modulation (MTCM): An MSAT-X report
[NASA-CR-180134] N87-16921

MODULATION TRANSFER FUNCTION
The SAR image modulation transfer function derived from SIR-B image spectra and airborne measurements of ocean wave height spectra N87-17334

MODULES
The 5000 GPM firefighting module evaluation test
[NASA-TM-88560] N87-16919

MOISTURE CONTENT
Developpement of algorithms to retrieve the water equivalent of snow cover from satellite microwave radiometer data N87-17264
Estimation of maximum snow volume distribution using NOAA-AVHRR data N87-17314

MOISTURE RESISTANCE
A comparison of two British standard test methods for the determination of resistance to humidity of paint films
[MOAD-TP-918] N87-16906

MOLDS
Method and apparatus for die forming metal sheets and extrusions
[AD-D012512] N87-16920

MOLECULAR BEAMS
Dual channel high electron mobility field effect transistor
[AD-D012474] N87-17518

MOLECULAR CLOUDS
Excitation and transfer of submillimeter molecular transitions — interstellar chemistry N87-17546
Interstellar chemistry and submillimeter observations N87-17547
Infrared radiation from interface regions in molecular clouds: L1551 and the Serpens nebula N87-17556
Far infrared and optical study of the high latitude cloud L1642 N87-17559
Vibrationally excited cyanoacetylene in regions of massive star formation N87-17561
Submillimeter HCO+ observations of dense cloud cores — interstellar clouds N87-17562
CO observations of the outflow source NGC 7023 N87-17563
Structure of molecular clouds and space-based sub-millimeter telescopes, for example FIRST — Far Infrared Submillimeter Wave Space Telescope (FIRST) N87-17574

MOLECULAR EXCITATION
CF2 and CFCl fluorescence from VUV excitation of C2F3Cl N87-16891
Excitation and transfer of submillimeter molecular transitions — interstellar chemistry N87-17546

MOLECULAR GASES
Circumstellar envelopes around evolved stars N87-17548
Molecular abundances in circumstellar envelopes N87-17549

MOLECULAR ROTATION
The A-X and B-X band systems of SrH: Wavenumbers and molecular constants
[USIP-86-04] N87-17486

MOLECULAR SPECTRA
Submillimeter cometary spectroscopy N87-17541
Excitation and transfer of submillimeter molecular transitions — interstellar chemistry N87-17546
Submillimeter HCO+ observations of dense cloud cores — interstellar clouds N87-17562
CO observations of the outflow source NGC 7023 N87-17563

MOLECULAR SPECTROSCOPY
The A-X and B-X band systems of SrH: Wavenumbers and molecular constants
[USIP-86-04] N87-17486

MOMENTUM THEORY
Redistribution of angular momentum by nonaxisymmetric instabilities in a thick accretion disk
[PUBL-SER-C-FASC-4] N87-17585

MOMENTUM TRANSFER
Transmission of atmospheric internal gravity waves into the stratosphere N87-17412
Cloud-top meridional momentum transports on Saturn and Jupiter N87-17623

MONITORS
Monitoring transients in low inductance circuits
[DE86-013756] N87-16978
Switching network for monitoring stations
[AD-D012514] N87-17022

MONOMERS
Ethynyl terminated ester oligomers and polymers therefrom
[NASA-CASE-LAR-13118-2] N87-16907

MONOPROPELLANTS
Atmospheric pressure studies of liquid propellant drops in hot flows
[AD-A174639] N87-16915

MONOTECTIC ALLOYS
The effects of gravity level during directional solidification on the microstructure of hypermonotectic Al-In-Sn alloys
[NASA-TM-86573] N87-16901

MONTE CARLO METHOD
Canopy hot-spot as crop identifier
[DE86-011258] N87-17395

MORPHOLOGY
A nonparametric supervised multispectral classification method using binary morphological operators N87-17253
Segmentation by mathematical morphology processing hand on the image understanding model in remote sensing N87-17254
Computer-aided interpretation of complex geological patterns in remote sensing N87-17294

MOTION PICTURES
Image processing methods in two and three dimensions used to animate remotely sensed data — cloud cover N87-17292

MOTION SICKNESS
Role of orientation reference selection in motion sickness
[NASA-CR-180161] N87-17431

MOUNTAINS
Airborne Thermal Infrared Multispectral Scanner (TIMS) images over disseminated gold deposits, Osgood Mountains, Humboldt County, Nevada N87-17134

MOZAMBIQUE
Integrated analysis of geological and remote sensing data aimed at mineral deposits detection in the Monapo area (northern Mozambique) N87-17243

MRCA AIRCRAFT
Economical manufacturing and inspection of the electron-beam-welded Tornado wing box N87-17055

MSAT
Multiple Trellis Coded Modulation (MTCM): An MSAT-X report
[NASA-CR-180134] N87-16921

MULTIPROCESSING (COMPUTERS)
A comparison of five benchmarks
[NASA-TM-88956] N87-17441
Fault-free performance validation of fault-tolerant multiprocessors
[NASA-CR-178236] N87-17448

MULTISENSOR APPLICATIONS
Noise-immune multisensor transduction of speech
[AD-A174693] N87-16961

MULTISPECTRAL BAND CAMERAS
Optical visual evaluation and interpretation of remote sensing data N87-17353

MULTISPECTRAL BAND SCANNERS
The TIMS Data User's Workshop
[NASA-CR-180130] N87-17111
The TIMS instrument N87-17112
Concept of a future multispectral Thermal Infrared (TIR) pushbroom mission for Earth observation from space N87-17169
Imaging spectrometry: Aircraft and space program N87-17202
Extracting surface features in multispectral imagery N87-17211
Comparative study of LANDSAT MSS, Salyut-7 (TERRA) and radar (SIR-A) images for geological and geomorphological applications: A case study from Rajasthan and Gujarat, India N87-17236
Interrelationship between field spectra and airborne MSS systems in the Singatse range, (Yerington) Nevada — multispectral scanner (MSS) mineral exploration N87-17242
The influence of resampling method and multitemporal LANDSAT imagery on crop classification accuracy in the United Kingdom N87-17250
A simulation study of some contextual classification methods for remotely sensed data N87-17252
A nonparametric supervised multispectral classification method using binary morphological operators N87-17253
A synergistic approach for multispectral image restoration using reference imagery N87-17255
Viewing angle corrections of airborne multispectral scanner data acquired over forested surfaces N87-17273
Radiometric correction method which removes both atmospheric and topographic effects from the LANDSAT-MSS data N87-17329

Discrimination of land features using LANDSAT false colour composite in N Iran N87-17352
MULTISPECTRAL PHOTOGRAPHY
Components and comparisons of potential information from several imaging satellites N87-17164

N

NASA PROGRAMS
A new day: Challenger and space flight thereafter [NASA-TM-77717] N87-16856
The large deployable reflector: A NASA submillimeter-infrared orbiting observatory N87-17571
NASA SPACE PROGRAMS
Research opportunities in microgravity science and applications during shuttle hiatus [NASA-TM-88964] N87-16917
NATURAL LANGUAGE (COMPUTERS)
Information processing research [AD-A173028] N87-17533
NATURAL SATELLITES
Non-solar noble gas abundances in the atmosphere of Jupiter N87-17637
NAVIER-STOKES EQUATION
Comparison of three explicit multigrid methods for the Euler and Navier-Stokes equations [NASA-TM-88878] N87-16784
Navier-Stokes solution for laminar transonic flow over a NACA0012 airfoil [FAA-140] N87-16794
An LU-SSOR scheme for the Euler and Navier-Stokes equations [NASA-CR-179556] N87-16806
An analysis of flow models: From Navier-Stokes to potential flow equations N87-16968
SOLA: A basic solution algorithm for flow analysis N87-16996
NAVIGATION
ICNIA (Integrated Communications Navigation Identification Avionics) HF transmitter system preliminary study [AD-A173013] N87-16823
NEAR WAKES
Afterbody shape effects on the near-wake velocity characteristics at Mach numbers between 0.35 and 0.92 [ISL-CO-205/86] N87-17011
NEBULAE
Infrared radiation from interface regions in molecular clouds: L1551 and the Serpens nebula N87-17556
IRAS observations of the Pleiades N87-17557
CO observations of the outflow source NGC 7023 N87-17563
NEPTUNE ATMOSPHERE
The Jovian Atmospheres [NASA-CP-2441] N87-17598
The Voyager encounter with Uranus and Neptune N87-17639
Radiative-convective equilibrium models of Uranus and Neptune N87-17641
Vertical structure of aerosols and clouds in the atmospheres of Uranus and Neptune: Implications for their heat budgets N87-17643
On the oblateness and rotation rate of Neptune's atmosphere N87-17644
Are the aerosols on Uranus and Neptune composed of methane photopolymers? N87-17645
NETWORK ANALYSIS
Millimeter-wave network analyzer-based scatterometer N87-17281
On the stochastic dissemination of faults in an admissible network [NASA-CR-178238] N87-17469
NETWORK CONTROL
Beam forming network technologies and related manufacturing processes --- satellite antennas N87-16951
NEUTRON SCATTERING
Recent developments in discrete-ordinates electron transport [DE86-007827] N87-17485
NEUTRON STARS
Observations of quasi-periodic oscillations in Cyg X-2 [MPE-PREPRINT-61] N87-17576
A search for rapidly modulated emission in bright X-ray sources using the HEAO A-1 data base [NASA-CR-180148] N87-17593
NEVADA
Detection and mapping of volcanic rock assemblages and associated hydrothermal alteration with Thermal Infrared Multiband Scanner (TIMS) data Comstock Lode Mining District, Virginia City, Nevada N87-17119
Simulation modeling and preliminary analysis of TIMS data from the Carlin area and the northern Grapevine Mountains, Nevada N87-17120
TIMS data applications in Nebraska N87-17126
Airborne Thermal Infrared Multispectral Scanner (TIMS) images over disseminated gold deposits, Osgood Mountains, Humboldt County, Nevada N87-17134
Interrelationship between field spectra and airborne MSS systems in the Singatse range, (Yerington) Nevada --- multispectral scanner (MSS) mineral exploration N87-17242
NEWTON THEORY
A multigrid LU-SSOR scheme for approximate Newton iteration applied to the Euler equations [NASA-CR-179524] N87-16803
NEWTON-RAPHSON METHOD
Numerical calculations of radiation transport in a dusty medium in disk geometry N87-17591
NICKEL ALLOYS
Fabrication of hollow, cored, and composite shaped parts from selected alloy powders [AD-D012499] N87-16903
NICKEL STEELS
Inertia welding of nitralloy N and 18 nickel maraging 250 grade steels for utilization in the main rotor drive shaft for the AR-64 military helicopter program N87-17067
NIMBUS 7 SATELLITE
Evaluation of geophysical parameters measured by the Nimbus-7 microwave radiometer for the TOGA Heat Exchange Project [NASA-CR-180151] N87-17110
Developpement of algorithms to retrieve the water equivalent of snow cover from satellite microwave radiometer data N87-17264
Classification of forest and surface types by satellite microwave radiometry N87-17305
Retrieval of near-surface wind speed in the Baltic Sea from NIMBUS-7 Scanning Multichannel Microwave Radiometer (SMMR) observations N87-17342
Sea ice studies in the Baltic Sea using satellite microwave radiometer data N87-17343
NITROGEN
Total and dissociative photoionization cross sections of N2 from threshold to 107 eV [NASA-CR-180172] N87-16892
NITROGEN POLYMERS
Interpenetrating-network polymeric electrolytes [AD-D012485] N87-16912
NOAA SATELLITES
The FRS-68010: A new concept for the acquisition and analysis of NOAA HRPT data N87-17206
Estimation of maximum snow volume distribution using NOAA-AVHRR data N87-17314
Towards snowmelt runoff forecast using LANDSAT-MSS and NOAA/AVHRR data N87-17317
Digital techniques for noise reduction in Automatic Picture Transmission (APT) NOAA satellite images N87-17328
NOISE (SOUND)
Noise-immune multisensor transduction of speech [AD-A174693] N87-16961
NOISE INTENSITY
Aeroacoustics of supersonic jet flows from contoured and solid/porous conical plug-nozzles [NASA-CR-178095] N87-17484
NOISE MEASUREMENT
Identification and proposed control of helicopter transmission noise at the source [NASA-TM-89312] N87-16816
The influence of wind-tunnel walls on discrete frequency noise N87-16850
NOISE PROPAGATION
The influence of wind-tunnel walls on discrete frequency noise N87-16850
Noise propagation from a four-engine, propeller-driven airplane [NASA-TM-89035] N87-17482
Aircraft noise synthesis system [NASA-TM-89040] N87-17483
NOISE REDUCTION
Identification and proposed control of helicopter transmission noise at the source [NASA-TM-89312] N87-16816
Noise-immune multisensor transduction of speech [AD-A174693] N87-16961
Digital techniques for noise reduction in Automatic Picture Transmission (APT) NOAA satellite images N87-17328
Simulated flight acoustic investigation of treated ejector effectiveness on advanced mechanical suppressors for high velocity jet noise reduction [NASA-CR-4019] N87-17481
NOISE SPECTRA
Combustion noise from gas turbine aircraft engines measurement of far-field levels [NASA-TM-88971] N87-17480
NOMENCLATURES
A proposal for adopting a standard coordinate system for defining atmospheric nomenclature for the giant planets N87-17632
NONDESTRUCTIVE TESTS
Industrial holography: The Rolls-Royce experience [PNR90351] N87-17024
Ultrasonic testing techniques for diffusion-bonded titanium components N87-17061
NDT of electron beam welded joints (micro-focus and real time X-ray) N87-17063
Thermoelastic testing of stratified materials N87-17064
Abstracts: Review of progress in quantitative NDE [DE87-000769] N87-17073
NONEQUILIBRIUM FLOW
Hypersonic nonequilibrium flow over an ablating teflon surface N87-16787
NONLINEAR EQUATIONS
A note on Branin's method for finding the critical points of smooth functions [MEMO-576] N87-17485
NONLINEAR OPTICS
Nonlinear wave propagation [AD-A175073] N87-17481
NONLINEAR SYSTEMS
Adaptive control techniques for large space structures [AD-A173083] N87-16871
On routes to chaotic motion in oscillators with unsymmetric and symmetric elastic nonlinearity [ISSN-0206-5658] N87-16969
Model selection and validation methods for nonlinear systems [RR-292] N87-17095
Dynamic input-output decoupling of nonlinear control systems [MEMO-575] N87-17452
A prediction error estimate for nonlinear stochastic systems [RR-295] N87-17471
Nonlinear real-time optical signal processing [AD-A173119] N87-17497
NONLINEARITY
Analysis of amplitude nonlinearities in the ERS-1 SAR receiver system N87-17359
Convenient total variation diminishing conditions for nonlinear difference schemes [NASA-CR-178209] N87-17453
A pseudo-arclength continuation method for nonlinear Eigenvalue problems [AD-A173019] N87-17459
NONPARAMETRIC STATISTICS
A nonparametric supervised multispectral classification method using binary morphological operators N87-17253
NOZZLE GEOMETRY
Aeroacoustics of supersonic jet flows from contoured and solid/porous conical plug-nozzles [NASA-CR-178095] N87-17484
NOZZLES
Simulated flight acoustic investigation of treated ejector effectiveness on advanced mechanical suppressors for high velocity jet noise reduction [NASA-CR-4019] N87-17481
NULL HYPOTHESIS
Model selection and validation methods for nonlinear systems [RR-292] N87-17095
NUMERICAL ANALYSIS
An LU-SSOR scheme for the Euler and Navier-Stokes equations [NASA-CR-179556] N87-16806
Aeroassisted coplanar orbital transfer of flight vehicles using the sequential gradient restoration algorithm N87-16857
Analysis of viscous transonic flow over airfoil sections [NASA-TM-88912] N87-17001
A parallel solution for the symmetric Eigenproblem [NASA-TM-89082] N87-17066
Comparative advantages of graphic versus numeric representation of quantitative data N87-17439
Multigrid applied to singular perturbation problems [NASA-CR-178230] N87-17444
Light scattering theory for bubbles in water: Inverse scattering, coated bubbles and statistics [AD-A174997] N87-17498
Initial-value problem for the 1-D wave equation in an inhomogeneous medium [IPPCZ-268] N87-17505
NUMERICAL CONTROL
Switching network for monitoring stations [AD-D012514] N87-17022

O

O RING SEALS
Solid rocket booster joint seal analyses [NASA-TM-86580] N87-17039

SRB O-ring free response analysis
[NASA-TM-86582] N87-17040

OBLATE SPHEROIDS
On the obliteness and rotation rate of Neptune's atmosphere N87-17644

OBSERVATION
The ionization structure of planetary nebulae. Part 7: New observations in the ring nebula
[NASA-CR-180141] N87-17582

OBSERVATORIES
Reflection grating spectrometer for the X-ray Multi-Mirror (XMM) space observatory: design and calculated performance
[DE86-013485] N87-17500

OCEAN BOTTOM
Observations of surface currents at Nantucket Shoals and implications for radar imaging of the bottom N87-17296
SAR imaging of bottom topography in the ocean: Results from an improved model N87-17298
Magnetization of the oceanic crust: TRM or CRM?
[NASA-CR-179896] N87-17429

OCEAN CURRENTS
Estimation of internal wave currents from SAR and infrared scatterometer imagery N87-17295
Observations of surface currents at Nantucket Shoals and implications for radar imaging of the bottom N87-17296
Spatial evolution of wave spectra in the vicinity of the Agulhas current from SIR-B N87-17337

OCEAN DATA ACQUISITIONS SYSTEMS
Proceedings of the 1986 International Geoscience and Remote Sensing Symposium (IGARSS '86) on Remote Sensing: Today's Solutions for Tomorrow's Information Needs, volume 1
[ESA-SP-254-VOL-1] N87-17163
Proceedings of the 1986 International Geoscience and Remote Sensing Symposium (IGARSS' 86) on Remote Sensing: Today's Solutions for Tomorrow's Information Needs, volume 2
[ESA-SP-254-VOL-2] N87-17283
Characteristics of a very low altitude spacecraft for collecting global directional wave spectra with spaceborne synthetic aperture radar N87-17333
The accuracy and availability of operational marine surface wind data for ERS-1 sensor calibration and validation from fixed platforms and free drifting buoys N87-17376
Oceanographic measurement capabilities of the NASA P-3 aircraft — ERS-1 mission N87-17380

OCEAN DYNAMICS
Ocean waves near Hurricane Josephine from SIR-B N87-17148
Operational wave forecasting with spaceborne SAR: Prospects and pitfalls N87-17149
SAR ice floe kinematics and correlation with mesoscale oceanic structure within the marginal ice zone N87-17222

OCEAN MODELS
Wave modeling activities of the Wave Modeling (WAM) group relevant to ERS-1 N87-17389
Marine climate program N87-17390

OCEAN SURFACE
Ocean surface temperature field variability N87-17104
Microwave scattering from the ocean surface N87-17109
An automatic tracking mode switching algorithm for the ERS-1 altimeter N87-17195
A two-scale Bragg scattering model for microwave backscatter from wind generated waves N87-17212
Verification results for a two-scale model of microwave backscatter from the sea surface N87-17213
A modified boundary perturbation approach to microwave scattering and emission by the ocean surface N87-17214
C and Ku-band scatterometer results from the SCATTMOD internal wave experiment N87-17215
Identification of the contribution of Bragg scattering and specular reflection to X-band microwave backscattering in an ocean experiment N87-17216
Tower-based broadband backscattering measurements from the ocean surface in the North Sea N87-17217
Spatial dependence on sea spikes N87-17218
Estimation of internal wave currents from SAR and infrared scatterometer imagery N87-17295
Observations of surface currents at Nantucket Shoals and implications for radar imaging of the bottom N87-17296
Sea wave measurements using a ship's radar N87-17300
Measurement of sea backscatter at extremely low grazing angle by C-band Doppler radar N87-17301
The SAR image modulation transfer function derived from SIR-B image spectra and airborne measurements of ocean wave height spectra N87-17334
Deriving two-dimensional ocean wave spectra and surface height maps from the Shuttle Imaging Radar (SIR-B) N87-17336
Characterisation of internal wave surface patterns on airborne SAR imagery N87-17338
A two-step algorithm for the separate retrieval of ocean surface and atmospheric parameters from microwave radiometers N87-17341
Retrieval of near-surface wind speed in the Baltic Sea from NIMBUS-7 Scanning Multichannel Microwave Radiometer (SMMR) observations N87-17342
The use of numerical wind and wave models to provide areal and temporal extension to instrument calibration and validation of remotely sensed data — satellite data N87-17371
Satellite scatterometer comparisons with surface measurements: Techniques and Seasat results N87-17372
Validation of ERS-1 wind data using observations from research and voluntary observing ships N87-17374
Accuracy estimates of wind and wave observations from ships of opportunity in the WMO voluntary observing ship program N87-17375
The accuracy and availability of operational marine surface wind data for ERS-1 sensor calibration and validation from fixed platforms and free drifting buoys N87-17376
A procedure for estimation of two-dimensional ocean height-variance spectra from SAR imagery N87-17381
Measurement of the directional spectrum of ocean waves using a conically-scanning radar N87-17383
An overview of the NSCAT/N-ROSS program N87-17384
Intersensor comparisons for validation of wind speed measurements from ERS-1 altimeter and scatterometer — Seasat N87-17386
A scatterometer research program N87-17391
Bulk Richardson's number isograms deduced from SAR data — ocean surface N87-17392

OCEAN TEMPERATURE
Ocean surface temperature field variability N87-17104

OCEANOGRAPHIC PARAMETERS
The Second Spaceborne Imaging Radar Symposium
[NASA-CR-180131] N87-17135
Hydrodynamics of internal solitons and a comparison of SIR-A and SIR-B data with ocean measurements N87-17147
A two-step algorithm for the separate retrieval of ocean surface and atmospheric parameters from microwave radiometers N87-17341
Gathering and processing a comparative data set for the calibration and validation of ERS-1 data products; preparatory work at the UK-ERS-DC — Data Center (DC) N87-17367
Validation of wind speed and significant wave height from Geosat N87-17368
Requirements and constraints in the calibration and validation of ERS-1 wind and wave parameters N87-17369
Evaluation of the different parameters in Long's C-band model — for ERS-1 scatterometer N87-17370

OCEANOGRAPHY
USSR report: Earth sciences
[JPRS-UES-86-005] N87-17096
The TIMS Data User's Workshop
[NASA-CR-180130] N87-17111

OCEANS
Metal content of ocean water studied with radio spectrometer N87-17102
Stochastic model of tidal evolution of Earth-Moon system with cyclic change in resonant frequency of ocean N87-17103
Ocean surface temperature field variability N87-17104
Light scattering theory for bubbles in water: Inverse scattering, coated bubbles and statistics
[AD-A174997] N87-17498

OFFSHORE PLATFORMS
Tower-based broadband backscattering measurements from the ocean surface in the North Sea N87-17217
The accuracy and availability of operational marine surface wind data for ERS-1 sensor calibration and validation from fixed platforms and free drifting buoys N87-17376

OH-58 HELICOPTER
Identification and proposed control of helicopter transmission noise at the source
[NASA-TM-89312] N87-16816

OKLAHOMA
The Red River Valley archeological project N87-17128

ON-LINE SYSTEMS
Adaptive control techniques for large space structures
[AD-A173083] N87-16871

OPERATORS (MATHEMATICS)
A nonparametric supervised multispectral classification method using binary morphological operators N87-17253

OPTICAL DATA PROCESSING
Nonlinear real-time optical signal processing
[AD-A173119] N87-17497

OPTICAL MEASURING INSTRUMENTS
Present statue of Japanese ERS-1 Project N87-17145

OPTICAL PROPERTIES
The non-metallic materials sample array
[NASA-TM-86578] N87-16910

OPTICAL RADAR
Stereo Line Scanner (SLS): System considerations on an operational instrument for meteorology and weather forecasts N87-17168
Application of Doppler radar and lidar to diagnose atmospheric phenomena N87-17271
Results from 1984 airborne Doppler lidar wind measurement program. Flight 6: Analysis of line-of-sight elevation angle errors and apparent Doppler velocities
[NASA-CR-178994] N87-17425

OPTICAL SCANNERS
A real time vision system for robotic arc welding N87-17066
Stereo Line Scanner (SLS): System considerations on an operational instrument for meteorology and weather forecasts N87-17168
Assessing grass canopy condition and growth from combined optical-microwave measurements N87-17286

OPTICAL SWITCHING
Nonlinear real-time optical signal processing
[AD-A173119] N87-17497

OPTICAL WAVEGUIDES
Investigation of a GaAlAs Mach-Zehnder electro-optic modulator
[NASA-CR-179573] N87-16953

OPTIMIZATION
Optimization of axially compressed Carbon Fiber Reinforced Plastic (CFRP) cylinders N87-17082

ORBIT CALCULATION
Orbit determination for low Earth orbit spacecraft based on satellite to satellite tracking techniques via a unique very high altitude relay constellation N87-16858

ORBIT DECAY
The contraction of satellite orbits under the influence of air drag. Part 7: Orbits of high eccentricity, with scale height dependent on altitude
[RAE-TR-86013] N87-16859

ORBITAL MANEUVERING VEHICLES
Communications satellite systems operations with the space station. Volume 1: Executive summary
[NASA-CR-179526] N87-17472

ORBITAL MECHANICS
The contraction of satellite orbits under the influence of air drag. Part 7: Orbits of high eccentricity, with scale height dependent on altitude
[RAE-TR-86013] N87-16859
The study of the physics of cometary nuclei
[NASA-CR-180153] N87-17594

ORBITAL SPACE STATIONS
Tethered orbital refueling study
[NASA-CR-171953] N87-16855
Spacecraft attitude control momentum requirements analysis
[NASA-CR-178219] N87-16864
Space station human productivity study. Volume 4: Issues
[NASA-CR-171963] N87-16865
Space station human productivity study. Volume 5: Management plans
[NASA-CR-171964] N87-16866
Space station human productivity study. Volume 2: Executive summary and oral review presentation
[NASA-CR-171962] N87-16868
Evaluation of Pactruss design characteristics critical to space station primary structure
[NASA-CR-178171] N87-16870
Communications satellite systems operations with the space station. Volume 1: Executive summary
[NASA-CR-179526] N87-17472
Communications satellite systems operations with the space station, volume 2
[NASA-CR-179527] N87-17473
Research and technology
[NASA-TM-88868] N87-17656

OREGON
Investigation of forest canopy temperatures recorded by the thermal infrared multispectral scanner at H. J. Andrews Experimental Forest N87-17123

ORTHOGONALITY
Geometries for roughness shapes in laminar flow
[NASA-CASE-LAR-13255-1] N87-16793

OSCILLATING FLOW
The Saturnian ribbon feature: A baroclinically unstable model N87-17629
OSCILLATIONS
Initial-value problem for the 1-D wave equation in an inhomogeneous medium
[IPPCZ-268] N87-17505
The optimum condition of TPD-1 recombining helium plasma for VUV coherent lasing action
[IPPJ-798] N87-17507
OSCILLOSCOPES
Switching network for monitoring stations
[AD-D012514] N87-17022
OUTPUT
High-voltage Milberger slip slide power conditioner
[AD-D012504] N87-16974
OXIDATION
Supercritical water oxidation of products of human metabolism
[NASA-CR-180144] N87-17430
OXIDATION RESISTANCE
Corrosion/oxidation protection of high temperature material — gas turbine engines
[PNR90355] N87-16905
OZONE
Measurement of HO2 chemical kinetics with a new detection method
[NASA-CR-180114] N87-16890

P

P-3 AIRCRAFT
Oceanographic measurement capabilities of the NASA P-3 aircraft — ERS-1 mission N87-17380
PAINTS
A comparison of two British standard test methods for the determination of resistance to humidity of paint films
[MQAD-TP-918] N87-16906
PAIR PRODUCTION
Radiative processes underlying the X-ray and gamma-ray continua of active galactic nuclei and gamma-ray bursts N87-17655
PARA HYDROGEN
Para hydrogen equilibration in the atmospheres of the outer planets N87-17599
PARABOLIC FLIGHT
The effects of gravity level during directional solidification on the microstructure of hypermonotectic Al-In-Sn alloys
[NASA-TM-86573] N87-16901
PARABOLIC REFLECTORS
Development of a 2.8 m offset antenna reflector using inflatable, space-rigidized structures technology N87-16927
Design of a low distortion shared aperture reflector — satellite antenna N87-16934
Construcciones Aeronauticas S.A. (CASA) large reflector antenna — satellite antenna N87-16935
Structural analysis, manufacturing and development status of large polarization sensitive dual-gridded reflectors — satellite antenna N87-16937
Development of mm-wave radiometer antenna reflector — satellite antennas N87-16941
Simple approach for evaluating mechanical reflector antenna distortions — satellite antennas N87-16942
The large deployable reflector: A NASA submillimeter-infrared orbiting observatory N87-17571
PARALLEL PROCESSING (COMPUTERS)
A parallel solution for the symmetric Eigenproblem
[NASA-TM-89082] N87-17086
Algorithms and programming tools for image processing on the MPP, part 2
[NASA-CR-180146] N87-17440
A comparison of five benchmarks
[NASA-TM-88956] N87-17441
PARAMETER IDENTIFICATION
Real time identification of large space structures
[NASA-CR-171957] N87-16867
Lattice filters and adaptive identification of flexible structures N87-17030
Position control of mechanical manipulators by using nonlinear adaptive control algorithm N87-17031
Application of modified three parameter Weibull distributions to brittle material design
[RARDE-16/84] N87-17072
Model selection and validation methods for nonlinear systems
[RR-292] N87-17095
The effect of measurement error and confusion from vegetation on passive microwave estimates of soil moisture N87-17304
Recursive techniques in identification
[OUEL-1644/86] N87-17462
PARAMETERIZATION
The static aeroelasticity of a composite wing N87-17085
A spatially homogeneous anisotropic surface model with variable parameters for scattering from bare soil N87-17183
Toward a satellite system to monitor the spatial and temporal behavior of soil water content N87-17288
Parameter space techniques for image registration N87-17327
Evaluation of the different parameters in Long's C-band model — for ERS-1 scatterometer N87-17370
PARTIAL DIFFERENTIAL EQUATIONS
Survey of the status of finite element methods for partial differential equations
[NASA-CR-178222] N87-17456
A pseudo-arclength continuation method for nonlinear Eigenvalue problems
[AD-A173019] N87-17459
A research program in advanced information systems
[NASA-CR-180150] N87-17529
PARTICLE COLLISIONS
Doubly differential cross sections for galactic heavy-ion fragmentation
[NASA-TP-2659] N87-17487
PARTICLE INTERACTIONS
Ultralow background searches for beta beta-decay, cold dark matter and solar axions
[DE86-013592] N87-17652
PARTICLE LADEN JETS
Particle-laden swirling free jets: Measurements and predictions
[NASA-TM-88904] N87-16826
PARTICLE SIZE DISTRIBUTION
Representation of the vaporization behavior of turbulent polydisperse sprays by equivalent monodisperse sprays
[NASA-TM-88906] N87-16827
Interstellar dust N87-17545
PARTICLES
Apparatus and method for stirring fluid borne particles
[AD-D012486] N87-17477
PASSIVITY
Low noise polycrystalline semiconductor resistors by hydrogen passivation
[AD-D012492] N87-17520
PATTERN RECOGNITION
Shape similarity in remote sensing images using graph matching techniques N87-17330
An implementation of the Hough transform using a linear array processor in conjunction with a PDP/11microprocessor — computer vision
[NPL-DITC-74/86] N87-17438
Programming robotics applications on an advanced hypercube multiprocessor
[DE86-006895] N87-17445
PATTERN REGISTRATION
Parameter space techniques for image registration N87-17327
PERFORMANCE PREDICTION
Prediction of the electrical performance of inflatable Space Rigidized Structure (ISRS) offset antenna reflectors and correlation with RF measurements N87-16943
On-ground verification and in-orbit performance prediction of the ERS-1 wind scatterometer N87-17193
ERS-1 radar altimeter: Performance, calibration and data validation N87-17194
PERFORMANCE TESTS
Air traffic control radar beacon system transponder performance study and analysis. Volume 2: Appendixes
[DOT/FAA/FS-86/1-VOL-2] N87-16812
Performance data Aeroc 8.2.AC.20(300), issue 1 N87-16818
Outdoor test stand performance of a convertible engine with variable inlet guide vanes for advanced rotorcraft propulsion
[NASA-TM-88939] N87-16825
Experience gained by sector model testing of an unfurlable mesh/rib antenna N87-16925
A satellite-borne SAR transmitter and receiver N87-17358
Pulse compression test results of the SAR transmitter and receiver — satellite-borne SAR N87-17360
A comparison of five benchmarks
[NASA-TM-88956] N87-17441
Observations from the Gornergrat Observatory (Switzerland) with the University of Cologne 3-m radio telescope N87-17573
PERIODIC VARIATIONS
Observations of quasi-periodic oscillations in Cyg X-2
[MPE-PREPRINT-61] N87-17576
PERMEABILITY
Effective permeability and macrodispersion in locally heterogeneous aquifers
[MEMO-585] N87-17015
PERMITTIVITY
Dielectric and scattering behavior of snow at microwave frequencies N87-17179
Determination of resistivity and permittivity profiles of a layered Earth N87-17198
Dielectric and surface parameters related to microwave scatter and emission properties N87-17262
Microwave dielectric behavior of vegetation material
[NASA-CR-180096] N87-17393
PERTURBATION
Spatially growing disturbances in a two-stream, coplanar jet
[NASA-TM-88949] N87-16799
Dynamical models for the Earth's geoid N87-17409
A study of large, medium and small scale structures in the topside ionosphere
[NASA-CR-180068] N87-17413
PERTURBATION THEORY
Multigrid applied to singular perturbation problems
[NASA-CR-178230] N87-17444
Perturbation theory for unbounded Markov processes with applications to queueing
[MEMO-579] N87-17466
PHASE DIAGRAMS
Magmatic differentiation in partially molten systems: Applications to the moon and the palisades sill N87-17597
PHASE SHIFT CIRCUITS
A pi-section digital phase shifter apparatus
[AD-D012495] N87-16973
PHASE TRANSFORMATIONS
Magmatic differentiation in partially molten systems: Applications to the moon and the palisades sill N87-17597
PHENOLIC RESINS
Fire and heat resistant laminating resins based on maleimido substituted aromatic cyclotriphosphazene polymer
[NASA-CASE-ARC-11428-2] N87-16909
PHOSPHAZENE
Fire and heat resistant laminating resins based on maleimido substituted aromatic cyclotriphosphazene polymer
[NASA-CASE-ARC-11428-2] N87-16909
PHOTOABSORPTION
CF2 and CFCl fluorescence from VUV excitation of C2F3Cl N87-16891
Total and dissociative photoionization cross sections of N2 from threshold to 107 eV
[NASA-CR-180172] N87-16892
PHOTOCHEMICAL REACTIONS
An updated hydrocarbon photochemical model for the Jovian atmosphere from the troposphere through the homopause: A prelude to Galileo N87-17636
Are the aerosols on Uranus and Neptune composed of methane photopolymers? N87-17645
PHOTOGRAMMETRY
The stereo-pushbroom scanner system Digital Photogrammetry System (DPS) and its accuracy N87-17167
PHOTOINTERPRETATION
Enhancement of time images for photointerpretation N87-17116
Detection and mapping of volcanic rock assemblages and associated hydrothermal alteration with Thermal Infrared Multiband Scanner (TIMS) data Comstock Lode Mining District, Virginia City, Nevada N87-17119
Application of Thermal Infrared Multiband Scanner (TIMS) data to mapping of Plutonic and stratified rock and assemblages in accreted terrains of the Northern Sierra, California N87-17132
Knowledge-based aerial image understanding systems N87-17210
PHOTOIONIZATION
Total and dissociative photoionization cross sections of N2 from threshold to 107 eV
[NASA-CR-180172] N87-16892
Empirical considerations for laser guided electron beams in the advanced test accelerator
[DE86-013218] N87-17489
Spectral flux from low-density photospheres N87-17578
PHOTOLUMINESCENCE
Research on single-crystal CdTe solar cells
[DE86-010719] N87-17405
PHOTON-ELECTRON INTERACTION
Recent developments in discrete-ordinates electron transport
[DE86-007827] N87-17485
PHOTONS
Opportunities and potential for a millimetre wavelength search for the Sunyaev-Zeldovich effect N87-17555
PHOTOSPHERE
Spectral flux from low-density photospheres N87-17578
PHYSIOLOGICAL EFFECTS
Biological effects of aerial shock waves: Review of work to date
[ISL-NB-402/85] N87-17432

PIEZORESISTIVE TRANSDUCERS
Determining and modeling the response of ytterbium piezoresistance transducers
[AD-A173085] N87-17023
PIPES (TUBES)
Self-contained, single-use hose and tubing cleaning module
[NASA-CASE-MSC-20857-1] N87-17035
Recursive linear smoothing for dissipative hyperbolic systems
[AD-A173020] N87-17460
PITCH (INCLINATION)
Design and dynamic simulation of a fixed pitch 56 kW wind turbine drive train with a continuously variable transmission
[NASA-CR-179543] N87-17401
PLANAR STRUCTURES
Planar array antenna for ERS-1 synthetic aperture radar N87-17357
PLANE WAVES
A study of explosive wave propagation in granular materials with microstructure
[AD-A173015] N87-16914
PLANETARY ATMOSPHERES
A study of planetary atmospheres in the submillimetric range N87-17540
Para hydrogen equilibration in the atmospheres of the outer planets N87-17599
Spatial and temporal variability of infrared-observable properties of the Jovian atmosphere: A partial survey N87-17600
Convective forcing of global circulations on the Jovian planets N87-17624
Convective adjustment in baroclinic atmospheres N87-17626
A proposal for adopting a standard coordinate system for defining atmospheric nomenclature for the giant planets N87-17632
Non-solar noble gas abundances in the atmosphere of Jupiter N87-17637
Astronomical, physical, and meteorological parameters for planetary atmospheres N87-17647
PLANETARY BOUNDARY LAYER
A diagnostic approach to obtaining planetary boundary layer winds using satellite-derived thermal data
[NASA-CR-178972] N87-17420
PLANETARY CORES
Convection without eddy viscosity: An attempt to model the interiors of giant planets N87-17625
On the oblateness and rotation rate of Neptune's atmosphere N87-17644
PLANETARY EVOLUTION
Non-solar noble gas abundances in the atmosphere of Jupiter N87-17637
PLANETARY LIMB
Modeling the temporal and spatial variations of the vertical structure of Jupiter's atmosphere using observations of the 3-0 hydrogen quadrupole lines N87-17601
PLANETARY NEBULAE
The ionization structure of planetary nebulae. 8: NGC 6826
[NASA-CR-180142] N87-17581
The ionization structure of planetary nebulae. Part 7: New observations in the ring nebula
[NASA-CR-180141] N87-17582
PLANETARY RADIATION
Spatial and temporal variability of infrared-observable properties of the Jovian atmosphere: A partial survey N87-17600
Vertical structure of aerosols and clouds in the atmospheres of Uranus and Neptune: Implications for their heat budgets N87-17643
PLANETARY ROTATION
On the oblateness and rotation rate of Neptune's atmosphere N87-17644
PLANETARY STRUCTURE
Astronomical, physical, and meteorological parameters for planetary atmospheres N87-17647
PLANETARY SURFACES
The physical basis for spectral variations in thermal infrared emittance of silicates and application to remote sensing N87-17129
PLANETOCENTRIC COORDINATES
A proposal for adopting a standard coordinate system for defining atmospheric nomenclature for the giant planets N87-17632
PLANETOLOGY
An iterative multi-resolution shape-from-shading algorithm and its application to planetary mapping N87-17331
PLASMA ACCELERATORS
Future accelerator technology
[DE86-013190] N87-17488
PLASMA ARC WELDING
The welding of aluminum alloys: A new technology in space application N87-17056
Welding of aluminum castings N87-17068
PLASMA CONTROL
Plasma formation and sustainment by a multijunction grill on the castor tokamak
[IPPCZ-255] N87-17506
Tilt stability of field-reversed configurations
[IPPJ-802] N87-17510
Advanced fuels in a field-reversed configuration
[IPPJ-804] N87-17512
Physics considerations on a fusion plasma in a field-reversed configuration
[IPPJ-803] N87-17513
PLASMA DIAGNOSTICS
Annual review, April 1985 - March 1986
[ISSN-0547-1567] N87-17503
An electrostatic probe technique for R.F. plasma
[OUEL-1637/86] N87-17514
PLASMA PHYSICS
Annual review, April 1985 - March 1986
[ISSN-0547-1567] N87-17503
PLASMA SPRAYING
Repair techniques for gas turbine components N87-17071
PLASMA WAVES
Modeling of nonlinear effects of plasma wave beams on ionospheric plasma N87-17107
PLASMAS (PHYSICS)
Nonlinear wave propagation
[AD-A175073] N87-17461
Future accelerator technology
[DE86-013190] N87-17488
Investigation of plasma contactors for use with orbiting wires
[NASA-CR-180154] N87-17502
The optimum condition of TPD-1 recombining helium plasma for VUV coherent lasing action
[IPPJ-798] N87-17507
Implicit particle simulation of electromagnetic plasma phenomena
[IPPJ-799] N87-17509
PLASTIC ANISOTROPY
The theory of finite elastic-plastic deformation with induced anisotropy modelled as combined isotropic-kinematic hardening N87-17074
PLASTIC DEFORMATION
The theory of finite elastic-plastic deformation with induced anisotropy modelled as combined isotropic-kinematic hardening N87-17074
PLASTICS
Three dimensional CTOD measurements of elastic-plastic surface flaws
[DE86-013454] N87-17093
PLATINUM ALLOYS
Burner rig and engine test experience of platinum aluminide coatings
[PNR90342] N87-16837
PLOTTERS
Line plotting program using DI-3000/Grafmaker routines
[NASA-TM-89010] N87-17442
PLUG NOZZLES
Aeroacoustics of supersonic jet flows from contoured and solid/porous conical plug-nozzles
[NASA-CR-178095] N87-17484
PLUGGING
RF plugging and tandem mirror experiments in a cusp-anchored mirror device
[IPPJ-800] N87-17508
PLUMES
Moisture driven convection on Jupiter: A mechanism to produce the equatorial plumes N87-17631
POLAR REGIONS
Observing the polar oceans with spaceborne radar N87-17151
POLARIMETRY
Imaging radar polarimetry from wave synthesis N87-17158
Imaging radar polarimetry from wave synthesis N87-17279
Millimeter-wave network analyzer-based scatterometer N87-17281
Coherent polarimetric Radar Cross Section (RCS) measurements on trees N87-17310
Polarimetry and photometry of active quasars at visual and near-infrared wavelengths N87-17579
POLARIZATION (SPIN ALIGNMENT)
Polarimetry and photometry of active quasars at visual and near-infrared wavelengths N87-17579
POLARIZATION (WAVES)
Qualification of gridding process for a Polarization Sensitive Reflector (PSR) — satellite antenna N87-16932
POLES
Radial and torsionally controlled magnetic bearing
[NASA-CASE-GSC-12957-1] N87-17038
POLYCRYSTALS
Low noise polycrystalline semiconductor resistors by hydrogen passivation
[AD-D012492] N87-17520
POLYESTERS
Ethynyl terminated ester oligomers and polymers therefrom
[NASA-CASE-LAR-13118-2] N87-16907
POLYETHER RESINS
Soluble aromatic polyimides for film and coating applications
[NASA-TM-89016] N87-16911
POLYIMIDES
Soluble aromatic polyimides for film and coating applications
[NASA-TM-89016] N87-16911
POLYMERIC FILMS
Effect of the size of structural bulk inhomogeneities on the specular transmittance of polymer films
[DE86-010727] N87-16913
POLYMERIZATION
Ethynyl terminated ester oligomers and polymers therefrom
[NASA-CASE-LAR-13118-2] N87-16907
POLYNOMIALS
Cyclic unequal error protection codes constructed from cyclic codes of composite length
[NASA-CR-180165] N87-17457
A representation for piecewise cubic C sup 1-splines on arbitrary triangulations
[MEMO-574] N87-17464
POPULATIONS
Spatial analysis of the dynamics of an ecosystem by multistage remote sensing in Kenya N87-17173
POROSITY
A study of explosive wave propagation in granular materials with microstructure
[AD-A173015] N87-16914
PORTABLE EQUIPMENT
Portable EDITOR (PEDITOR): A portable image processing system — satellite images N87-17206
The image processing workbench - portable software for remote sensing instruction and research N87-17209
POSITION (LOCATION)
Digital program for calculating static pressure position error
[NASA-TM-86726] N87-16821
Position control of mechanical manipulators by using nonlinear adaptive control algorithm N87-17031
POSITION INDICATORS
Development of intelligent pipe locator N87-17200
POTASSIUM COMPOUNDS
Research on millimeter wave dielectric materials
[AD-A173017] N87-17521
POTENTIAL FIELDS
Application of 2-D Hilbert transform in the interpretation of remotely sensed potential field data — geology N87-17293
POTENTIAL FLOW
Laser Doppler velocimeter measurements and theoretical investigation of three dimensional scroll flow N87-16979
POWDER (PARTICLES)
Sound propagation in a superfluid helium filled porous solid: Theory and experiment N87-17478
POWDER METALLURGY
Fabrication of hollow, cored, and composite shaped parts from selected alloy powders
[AD-D012489] N87-16903
Diffusion welding of component parts in the aviation and space industries
[RAE-TRANS-2147] N87-17032
POWER CONDITIONING
High-voltage Milberger slip slide power conditioner
[AD-D012504] N87-16974
POWER CONVERTERS
High-voltage Milberger slip slide power conditioner
[AD-D012504] N87-16974
POWER EFFICIENCY
Some trade-offs in modest-resolution radars for space N87-17278
POWER SPECTRA
Backscattering power spectrum for randomly moving vegetation N87-17349
PREDICTION ANALYSIS TECHNIQUES
Unsteady aerodynamics of a rotating compressor blade row at low Mach number. Volume 2: Analysis of experimental results and comparison with theory
[AD-A173044] N87-16832
Component lifing — aircraft engines
[PNR90346] N87-16838

Frost action predictive techniques for roads and airfields: A comprehensive survey of research findings
[DOT/FAA/PM-85/23] N87-16853
Simultaneous density velocity measurements in premixed turbulent flames to assess a theoretical model N87-16889
Application of modified three parameter Weibull distributions to brittle material design
[RARDE-16/84] N87-17072
Operational wave forecasting with spaceborne SAR: Prospects and pitfalls N87-17149
A prediction error estimate for nonlinear stochastic systems
[RR-295] N87-17471

PREDICTIONS
Particle-laden swirling free jets: Measurements and predictions
[NASA-TM-88904] N87-16826
Prediction of vortex shedding from circular and noncircular bodies in subsonic flow
[NASA-CR-4037] N87-16981
Prediction of heat and mass transfer in particulate beds N87-16999

PREMIXED FLAMES
Simultaneous density velocity measurements in premixed turbulent flames to assess a theoretical model N87-16889

PREPROCESSING
ECM (electronic countermeasures) preprocessor or tracker using multi-processor modules
[AD-D012513] N87-16959

PRESSURE GRADIENTS
Pressure gradient effects in the viscous wall region of a turbulent flow
[REPT-7] N87-16980
Transitional boundary layers under the influence of high free stream turbulence, intensive wall cooling and high pressure gradients in hot gas circulation
[NASA-TM-88524] N87-16983
Experimental investigation of the turbulence production mechanism in boundary layers
[AD-A173091] N87-17007

PRESSURE MEASUREMENT
Calculation of sidewall boundary-layer parameters from rake measurements for the Langley 0.3-meter transonic cryogenic tunnel
[NASA-CR-178241] N87-16807

PRESSURE PULSES
An experimental microcomputer controlled system for synchronized pulsating anti-gravity suit
[AD-A174640] N87-17433

PRESSURE SENSORS
Universal pressure transducer
[AD-D012499] N87-17019

PRESSURE SUITS
An experimental microcomputer controlled system for synchronized pulsating anti-gravity suit
[AD-A174640] N87-17433

PRINCIPLES
Training programs in remote sensing for professionals, students and the general public
[NASA-TM-88541] N87-17394

PRINTED CIRCUITS
Microstrip dipoles for EHF and millimeter wave applications
[AD-A173025] N87-16976

PRINTING
Line plotting program using DI-3000/Grafmaker routines
[NASA-TM-89010] N87-17442

PRISMS
Metal film light modulator
[AD-D012506] N87-17495

PROBABILITY THEORY
Simple and insensitive bounds for a grading and an overflow model
[MEMO-581] N87-17467

PROBLEM SOLVING
Euler solutions using an implicit multigrid technique
[NASA-TM-58276] N87-16792
Navier-Stokes solution for laminar transonic flow over a NACA0012 airfoil
[FAA-140] N87-16794
Common problems and pitfalls in gear design
[NASA-TM-88858] N87-17033
Collaborative problem solving for installation planning and decision making
[AD-A174611] N87-17527

PROCESS CONTROL (INDUSTRY)
Weld quality monitor and control system N87-17062

PRODUCT DEVELOPMENT
Construcciones Aeronauticas S.A. (CASA) large reflector antenna — satellite antenna N87-16935
Giotto spacecraft high gain antenna mechanical design and development N87-16938

PRODUCTION ENGINEERING
Applications of focused ion beams in microelectronics
[RSRE-MEMO-3948] N87-17517

PRODUCTIVITY
Space station human productivity study. Volume 4: Issues
[NASA-CR-171963] N87-16865
Space station human productivity study. Volume 5: Management plans
[NASA-CR-171964] N87-16866
Space station human productivity study. Volume 2: Executive summary and oral review presentation
[NASA-CR-171962] N87-16868
Space station human productivity study, volume 1
[NASA-CR-171961] N87-16869

PROGRAM VERIFICATION (COMPUTERS)
Profiling under UNIX by patching
[NASA-TM-88316] N87-17443

PROGRESS
Abstracts: Review of progress in quantitative NDE
[DE87-000769] N87-17073

PROJECT MANAGEMENT
Overview and status of the ERS-1 program N87-17190

PROJECT PLANNING
Spaceborne Imaging Radar Project N87-17143

PROJECTILES
Linearised theory of stability and resonance for projectiles with aerodynamically induced roll variations
[WSRL-0449-TR] N87-16795

PRONY SERIES
On the analytical determination of relaxation modulus of viscoelastic materials by Prony's interpolation method
[NASA-TM-86579] N87-17455

PROPELLANT TRANSFER
Tethered orbital refueling study
[NASA-CR-171953] N87-16855

PROPELLER EFFICIENCY
Over-the-wing propeller
[NASA-CASE-LAR-13134-2] N87-16828

PROPELLERS
Euler analysis of the three dimensional flow field of a high-speed propeller: Boundary condition effects
[NASA-TM-88955] N87-16798

PROPULSION SYSTEM CONFIGURATIONS
Over-the-wing propeller
[NASA-CASE-LAR-13134-2] N87-16828
Future trends in propulsion — aircraft
[PNR90349] N87-16840

PROPULSION SYSTEM PERFORMANCE
Future trends in propulsion — aircraft
[PNR90349] N87-16840

PROTECTIVE COATINGS
Soluble aromatic polyimides for film and coating applications
[NASA-TM-89016] N87-16911
The application of the RBD process to the deposition of anti-wear alloys N87-17069

PROTOSTARS
Submillimetre wavelength studies of protostars: The role of FIRST — Far Infrared Submillimeter Space Telescope (FIRST) N87-17544

PROVING
N-ROSS validation N87-17385
Australian validation plans for ERS-1 N87-17387
Fault-free performance validation of fault-tolerant multiprocessors
[NASA-CR-178236] N87-17448

PSYCHOACOUSTICS
Aircraft noise synthesis system
[NASA-TM-89040] N87-17483

PULSE AMPLITUDE
Analysis of amplitude nonlinearities in the ERS-1 SAR receiver system N87-17359

PULSE COMPRESSION
Pulse compression test results of the SAR transmitter and receiver — satellite-borne SAR N87-17360

PULSED JET ENGINES
Investigation of a repetitive pulsed electrothermal thruster
[NASA-CR-179464] N87-16878

PULSED RADIATION
Nanosecond two-dimensional imaging using tomographic techniques
[DE86-008164] N87-17499

PULSES
A composite aluminum conductor for pulsed power applications at cryogenic temperatures and method of its manufacture
[AD-D012501] N87-16885

PUMPS
The 5000 GPM firefighting module evaluation test
[NASA-TM-86560] N87-16919

PURIFICATION
Supported liquid membranes in 1986: New technology or scientific curiosity
[DE86-007504] N87-16898

PUSHBROOM SENSOR MODES
The stereo-pushbroom scanner system Digital Photogrammetry System (DPS) and its accuracy N87-17187
Concept of a future multispectral Thermal Infrared (TIR) pushbroom mission for Earth observation from space N87-17189
The Sequential Filter Imaging Radiometer (SFIR), a new instrument configuration for Earth observations N87-17205

PYRIDINES
Vinyl stilbazoles
[NASA-CASE-ARC-11429-3CU] N87-16908

PYROLYSIS
Atmospheric pressure studies of liquid propellant drops in hot flows
[AD-A174639] N87-16915

Q

QUALITY CONTROL
Economical manufacturing and inspection of the electron-beam-welded Tornado wing box N87-17055
Weld quality monitor and control system N87-17062

QUANTITATIVE ANALYSIS
Abstracts: Review of progress in quantitative NDE
[DE87-000769] N87-17073
Quantitative analysis of fracture surfaces using computer aided fractography N87-17076

QUASARS
Polarimetry and photometry of active quasars at visual and near-infrared wavelengths N87-17579
Parsec-scale structure in the nuclei of double lobed radio quasars N87-17588

QUEUEING THEORY
A transportation queueing model, solved as a Riemann boundary value problem
[MEMO-573] N87-17463
Perturbation theory for unbounded Markov processes with applications to queueing
[MEMO-579] N87-17466
Simple and insensitive bounds for a grading and an overflow model
[MEMO-581] N87-17467
A formal proof for the insensibility of simple bounds for finite multiserver nonexponential tandem queues
[MEMO-582] N87-17468

R

RADAR
Feasibility of using wind power for an aerostat-borne radar system
[DE86-004461] N87-17403

RADAR ANTENNAS
Development status of the ERS-1 SAR antenna N87-16939
Comparisons of the detection performance of a space-based radar system using different antenna systems and aperture illuminations
[AD-A173094] N87-16960
SIR-C, the next generation spaceborne SAR N87-17161
The X-SAR System N87-17162
Antenna ambiguity investigations for X-SAR — shuttle-borne radar N87-17355
Planar array antenna for ERS-1 synthetic aperture radar N87-17357

RADAR ATTENUATION
A study of anomalous propagation at radar frequencies and a proposal for a radar coverage forecasting model, book 2 of 2
[ETN-87-99938] N87-16967

RADAR BEACONS
Air traffic control radar beacon system transponder performance study and analysis. Volume 2: Appendixes
[DOT/FAA/FS-86/1-VOL-2] N87-16812

RADAR CROSS SECTIONS
The significance of Radar Cross Section (RCS) polarization measurements for tree signatures N87-17308
Coherent polarimetric Radar Cross Section (RCS) measurements on trees N87-17310
Radar Cross Section (RCS) data base deduced from radar images N87-17323

RADAR DATA
An overview of operational SAR data collection and dissemination plans for ERS-1 ice data in Canada N87-17189

Analysis of multichannel SAR data of Spitsbergen — glaciology N87-17223
ERS-1 synthetic aperture radar fast delivery processor N87-17228
Sea wave measurements using a ship's radar N87-17300
Bulk Richardson's number isograms deduced from SAR data — ocean surface N87-17392

RADAR GEOLOGY
The Second Spaceborne Imaging Radar Symposium [NASA-CR-180131] N87-17135

RADAR IMAGERY
VARAN-S radar image interpretation [CNES-CT/DRT/TIT/RL-54-T] N87-16963
MIZEX VARAN-S radar image characteristics [CNES-CT/DRT/TIT/RL-55-T] N87-16964
Off-line processing of ERS-1 synthetic aperture radar data with high precision and high throughput N87-17153
Analysis of multiple incidence angle SIR-B data for determining forest stand characteristics N87-17156
Radar signature determination: Trends and limitations N87-17159
SAR ice floe kinematics and correlation with mesoscale oceanic structure within the marginal ice zone N87-17222
Analysis of multichannel SAR data of Spitsbergen — glaciology N87-17223
Canadian plans for operational demonstrations of satellite imaging radar applications — ERS-1 N87-17229
The German ERS-1 SAR postprocessing system plans and concepts N87-17231
Comparative study of LANDSAT MSS, Salyut-7 (TERRA) and radar (SIR-A) images for geological and geomorphological applications: A case study from Rajasthan and Gujarat, India N87-17236
Radar imagery of the European city influenced by variations in depression angle and look direction N87-17237
Multispectral classification of microwave remote sensing images — SAR crop identification N87-17238
Using secondary image products to aid in understanding and interpretation of radar imagery N87-17239
Interferometer applications for the rectification of radar images N87-17241
Extraction of the backscatter coefficient of agricultural fields from an airborne SAR image N87-17265
Microwave remote sensing: Its applications and limitations in operational tasks of land use inventory and forest management N87-17266
Computer-derived height from SIR-B stereo radar images N87-17268
Analysis of the spatial structure of Synthetic Aperture Radar (SAR) imagery for a better separability of cereal crops, wheat and barley N87-17287
Estimation of internal wave currents from SAR and infrared scatterometer imagery N87-17295
Observations of surface currents at Nantucket Shoals and implications for radar imaging of the bottom N87-17296
Analysis of synthetic aperture radar imagery of surface ship wakes N87-17297
SAR imaging of bottom topography in the ocean: Results from an improved model N87-17298
An improved method for the determination of water depth from surface wave refraction patterns — SAR imagery N87-17299
SAR imagery for forest management N87-17313
Radar Cross Section (RCS) data base deduced from radar images N87-17323
The SAR image modulation transfer function derived from SIR-B image spectra and airborne measurements of ocean wave height spectra N87-17334
SIR-B observations of ocean waves in the NE Atlantic N87-17335
Deriving two-dimensional ocean wave spectra and surface height maps from the Shuttel Imaging Radar (SIR-B) N87-17336
Spatial evolution of wave spectra in the vicinity of the Agulhas current from SIR-B N87-17337
Characterisation of internal wave surface patterns on airborne SAR imagery N87-17338
Reconsideration of azimuth ambiguities in SAR N87-17356
X-SAR extends the frequency range of Shuttle Imaging Radar N87-17362
A procedure for estimation of two-dimensional ocean height-variance spectra from SAR imagery N87-17381
A scatterometer research program N87-17391

RADAR MAPS
Venus Radar Mapper (VRM): Multimode radar system design N87-17142
A scanning radar altimeter for mapping continental topography N87-17146
Deriving two-dimensional ocean wave spectra and surface height maps from the Shuttel Imaging Radar (SIR-B) N87-17336

RADAR MEASUREMENT
Rain measurement results derived from a two polarization S-band radar employing frequency diversity at Wallops Island, Virginia N87-17182
Tower-based broadband backscattering measurements from the ocean surface in the North Sea N87-17217
Geophysics of the marginal ice zone from SAR N87-17219
Sea wave measurements using a ship's radar N87-17300
Deriving two-dimensional ocean wave spectra and surface height maps from the Shuttel Imaging Radar (SIR-B) N87-17336
L to X-band scatter and emission measurements of vegetation N87-17347
Validation of wind speed and significant wave height from Geosat N87-17368
Measurement of the directional spectrum of ocean waves using a conically-scanning radar N87-17383

RADAR RECEIVERS
A satellite-borne SAR transmitter and receiver N87-17358
Analysis of amplitude nonlinearities in the ERS-1 SAR receiver system N87-17359
Pulse compression test results of the SAR transmitter and receiver — satellite-borne SAR N87-17360

RADAR RESOLUTION
Some trade-offs in modest-resolution radars for space N87-17276

RADAR SCATTERING
A study of anomalous propagation at radar frequencies and a proposal for a radar coverage forecasting model, book 2 of 2 [ETN-87-98938] N87-16967
Spatial dependence on sea spikes N87-17218
Results of the ESA airborne C-band scatterometer campaigns — ERS-1 N87-17225
Hawaiian lava flows and SIR-B results N87-17245
Roundoff noise analysis for digital Doppler processors in radar scatterometers N87-17258
Extraction of the backscatter coefficient of agricultural fields from an airborne SAR image N87-17265
Imaging radar polarimetry from wave synthesis N87-17279
Measurement of sea backscatter at extremely low grazing angle by C-band Doppler radar N87-17301
X and L-band backscattering measurements of agricultural crops, forest stands and single trees N87-17311
Calibrated X and L-band scattering coefficients from a southern US forest N87-17312
Evaluating roughness models of radar backscatter N87-17344
Microwave backscattering from an anisotropic soybean canopy N87-17348
On the relationship between age of lava flows and radar backscattering N87-17348
Effects of rain cells on SAR performance N87-17354
A scatterometer research program N87-17391

RADAR SIGNATURES
Imaging radar polarimetry from wave synthesis N87-17158
Radar signature determination: Trends and limitations N87-17159
An inter-sensor comparison of the microwave signatures of Arctic sea ice N87-17184
Microwave properties of sea ice in the marginal ice zone N87-17220
The significance of Radar Cross Section (RCS) polarization measurements for tree signatures N87-17308

RADAR TARGETS
Determining the vertical pattern of a spaceborne SAR by observation of uniform targets — SIR-B N87-17240

RADAR TRACKING
Automated remote sensing of sea ice using synthetic aperture radar N87-17186
An automatic tracking mode switching algorithm for the ERS-1 altimeter N87-17195

RADAR TRANSMISSION
ECM (electronic countermeasures) preprocessor or tracker using multi-processor modules [AD-D012513] N87-16959

RADAR TRANSMITTERS
A satellite-borne SAR transmitter and receiver N87-17358
Pulse compression test results of the SAR transmitter and receiver — satellite-borne SAR N87-17360

RADARSAT
An alternative multi-mode SAR for RADARSAT N87-17144
RADARSAT high throughput SAR processor development N87-17154

RADIANCE
The TIMS investigator's guide N87-17113
Simulation modeling and preliminary analysis of TIMS data from the Carlin area and the northern Grapevine Mountains, Nevada N87-17120
Infrared spectroscopy for geologic interpretation of TIMS data N87-17130
Microwave radiances from horizontally finite precipitating clouds containing ice and liquid hydrometeors N87-17340

RADIATION ABSORPTION
Laboratory measurements of microwave absorption from gaseous atmospheric constituents under conditions for the outer planets N87-17620

RADIATION DAMAGE
Mechanisms of helium embrittlement N87-16899

RADIATION DETECTORS
Measurement of HO2 chemical kinetics with a new detection method [NASA-CR-180114] N87-16890
Ultralow background searcher for beta beta-decay, cold dark matter and solar axions [DE86-013592] N87-17852

RADIATION EFFECTS
The non-metallic materials sample array [NASA-TM-86578] N87-16910
The effect of operating frequency in the radiation induced buildup of trapped holes and interface states in MOS devices [AD-A173097] N87-17522
Performance of polysilicon gate CMOS devices in space and SDI environments [DE86-009025] N87-17524

RADIATION HARDENING
Performance of polysilicon gate CMOS devices in space and SDI environments [DE86-009025] N87-17524

RADIATION MEASUREMENT
Extrapolation of Earth-based solar irradiance measurements to exoatmospheric level, for broad-band and selected absorption-band observations N87-17270

RADIATION MEASURING INSTRUMENTS
Variability in the Earth radiation budget as determined from the Nimbus ERB experiments N87-17410

RADIATION PRESSURE
A numerical study of jet production and accretion disk structure in super-Eddington black hole accretion N87-17586

RADIATION PROTECTION
Sun shield [NASA-CASE-MSC-20162-1] N87-17036

RADIATION TRANSPORT
Excitation and transfer of submillimeter molecular transitions — interstellar chemistry N87-17546
Numerical calculations of radiation transport in a dusty medium in disk geometry N87-17591

RADIATIVE HEAT TRANSFER
The Extendable Refractable Mast (ERM) thermal analysis: A heat radiation case study via the finite element method N87-16849

RADIATIVE TRANSFER
Atmospheric corrections of NOAA-AVHRR data verification of different methods by ground truth measurements N87-17274
Homogenizing surface and satellite observations of cloud [AD-A174691] N87-17427
Spectral flux from low-density photospheres N87-17578
Brown dwarfs and Jovian planets: A comparison N87-17616

RADIO ALTIMETERS
Development status of the ERS-1 payload instruments N87-17191
ERS-1 radar altimeter: Performance, calibration and data validation N87-17194
An automatic tracking mode switching algorithm for the ERS-1 altimeter N87-17195
ERS-1 fast delivery processing and products N87-17224
Using buoys and ships to calibrate ERS-1 altimeter and scatterometer N87-17377
Measurement of the directional spectrum of ocean waves using a conically-scanning radar N87-17383
Intersensor comparisons for validation of wind speed measurements from ERS-1 altimeter and scatterometer — Seasat N87-17386

RADIO ASTRONOMY
Review of coherent and incoherent detection techniques: Outlook and limitation — spaceborne submillimeter astronomy N87-17537
Submillimetre wavelength studies of protostars: The role of FIRST — Far Infrared Submillimeter Space Telescope (FIRST) N87-17544
Opportunities and potential for a millimetre wavelength search for the Sunyaev-Zeldovich effect N87-17555

Submillimetre continuum observations of active galactic nuclei N87-17558
Parsec-scale structure in the nuclei of double lobed radio quasars N87-17588

RADIO ATTENUATION
Remote sensing of tree attenuation at 870 MHz along simulated Earth-satellite paths N87-17306

RADIO COMMUNICATION
Transmission loss measurements in mobile radio nets [FOA-B-30098-3.3] N87-16966

RADIO FREQUENCY DISCHARGE
An electrostatic probe technique for R.F. plasma [OUEL-1637/86] N87-17514

RADIO FREQUENCY HEATING
On the possible role of the bootstrap effect in the RF current drive experiments, part 2 [IPPCZ-263] N87-17504
Plasma formation and sustainment by a multijunction grill on the castor tokamak [IPPCZ-255] N87-17506
RF plugging and tandem mirror experiments in a cusp-anchored mirror device [IPPJ-800] N87-17508

RADIO GALAXIES
Parsec-scale structure in the nuclei of double lobed radio quasars N87-17588

RADIO SIGNALS
ECM (electronic countermeasures) preprocessor or tracker using multi-processor modules [AD-D012513] N87-16959

RADIO SOURCES (ASTRONOMY)
On the identification of IRAS deep field sources: The radio counterparts N87-17552

RADIO TELESCOPES
A Sener mechanism: Fine adjustment mechanism for the Far Infrared and Submillimeter Space Telescope (FIRST) (F f F) N87-16948
The submillimeter telescope (SMT) project N87-17568
Low noise SIS mixer with gain for 80-115 GHz --- superconductor-insulator-superconductor (SIS) radio telescope N87-17570
The large deployable reflector: A NASA submillimeter-infrared orbiting observatory N87-17571
On the feasibility of constructing an imaging array of slot-antennas integrated with SIS mixers --- radio astronomy N87-17572
Observations from the Gornergrat Observatory (Switzerland) with the University of Cologne 3-m radio telescope N87-17573
Structure of molecular clouds and space-based sub-millimeter telescopes, for example FIRST --- Far Infrared Submillimeter Wave Space Telescope (FIRST) N87-17574

RADIO TRANSMISSION
Vegetation influence on wave propagation [FOA-B-30097-3.3] N87-16965

RADIO WAVE REFRACTION
A study of anomalous propagation at radar frequencies and a proposal for a radar coverage forecasting model, book 2 of 2 [ETN-87-98938] N87-16967
An improved method for the determination of water depth from surface wave refraction patterns --- SAR imagery N87-17299

RADIO WAVES
Joint influence of turbulence and wind on signal power in radioacoustic sounding of atmosphere N87-17108

RADIOACTIVITY
Determination of nonglobal component against background of global radioactive pollution of atmospheric aerosols N87-17100

RADIOMETERS
Some results of Marine Observation Satellite (MOS-1) airborne verification experiment Multispectral Electronic Self Scanning Radiometer (MESSR) N87-17166
Analysis of AIS radiometry at Mono Lake, California --- Airborne Imaging Spectrometer (AIS) N87-17204
The Sequential Filter Imaging Radiometer (SFIR), a new instrument configuration for Earth observations N87-17205

RADIOMETRIC CORRECTION
Antenna pattern correction in scanning radiometry: A singular system analysis N87-17261
Viewing angle corrections of airborne multispectral scanner data acquired over forested surfaces N87-17273
Atmospheric corrections of NOAA-AVHRR data verification of different methods by ground truth measurements N87-17274
Radiometric correction method which removes both atmospheric and topographic effects from the LANDSAT-MSS data N87-17329

RADIOMETRIC RESOLUTION
Analysis of AIS radiometry at Mono Lake, California --- Airborne Imaging Spectrometer (AIS) N87-17204

RAIN
The effects of heavy rain on profile aerodynamics [ETN-87-98848] N87-16809
Rain measurement results derived from a two polarization S-band radar employing frequency diversity at Wallops Island, Virginia N87-17182
Effects of rain cells on SAR performance N87-17354

RAMAN SPECTROSCOPY
Combined density and velocity measurements. Application to the investigation of a free jet [ISL-CO-206/86] N87-16808

RARE EARTH ALLOYS
Preparations of rare earth-iron alloys by thermite reduction [DE86-013753] N87-16904

REACTION KINETICS
Measurement of HO2 chemical kinetics with a new detection method [NASA-CR-180114] N87-16890
Proceedings of the 15th International Symposium on Shock Waves and Shock Tubes [AD-A173026] N87-17006
Supercritical water oxidation of products of human metabolism [NASA-CR-180144] N87-17430

REACTOR SAFETY
Two-Phase Flows in Major Technological Hazards, volume 3 [VKI-LS-1986-03-VOL-3] N87-16984
Review of present approaches to two-phase flow problems N87-16986
ATHENA code manual. Volume 1: Code structure, system models, and solution methods [DE87-001430] N87-17492

REACTOR TECHNOLOGY
Annual review, April 1985 - March 1986 [ISSN-0547-1567] N87-17503
Advanced fuels in a field-reversed configuration [IPPJ-804] N87-17512
Physics considerations on a fusion plasma in a field-reversed configuration [IPPJ-803] N87-17513

REAL TIME OPERATION
Real time identification of large space structures [NASA-CR-171957] N87-16867
ECM (electronic countermeasures) preprocessor or tracker using multi-processor modules [AD-D012513] N87-16959
Weld quality monitor and control system N87-17062
NDT of electron beam welded joints (micro-focus and real time X-ray) N87-17063
A real time vision system for robotic arc welding N87-17066
Quasi real time conversion of ERS-1 scatterometer raw data to sigma zero triplets N87-17226
ERS-1 synthetic aperture radar fast delivery processor N87-17228
Real-time application of remotely sensed data --- meteorology N87-17276
Nonlinear real-time optical signal processing [AD-A173119] N87-17497

RECOMBINATION REACTIONS
The optimum condition of TPD-1 recombining helium plasma for VUV coherent lasing action [IPPJ-798] N87-17507

RECURSIVE FUNCTIONS
Kalman filtering, smoothing and recursive robot arm forward and inverse dynamics [NASA-CR-180135] N87-17451
Recursive techniques in identification [OUEL-1644/86] N87-17462

REDUCED GRAVITY
The effects of gravity level during directional solidification on the microstructure of hypermonotectic Al-In-Sn alloys [NASA-TM-86573] N87-16901
Research opportunities in microgravity science and applications during shuttle hiatus [NASA-TM-88964] N87-16917
Low-g measurements by NASA [NASA-TM-86585] N87-17017

REDUCTION (CHEMISTRY)
Preparations of rare earth-iron alloys by thermite reduction [DE86-013753] N87-16904

REDUNDANCY
AFTI/F-111 MAW flight control system and redundancy management description [NASA-TM-88267] N87-16819
On codes with multi-level error-correction capabilities [NASA-CR-180166] N87-17458

REENTRY DECOYS
Hypersonic nonequilibrium flow over an ablating teflon surface N87-16787

REFLECTION
Interferometric load sensor and strain gage [AD-D012509] N87-17021

REFLECTORS
Composite space antenna structures: Properties and environmental effects [NASA-TM-86859] N87-16880
Development of lightweight dimensionally stable carbon fiber composite antenna reflectors for the INSAT-1 satellite N87-16936
Thermomechanical characteristics of dichroic subreflectors --- satellite antennas N87-16952
Welding torch with arc light reflector [NASA-CASE-MFS-29134-1] N87-17493

REFRACTIVITY
Remote probing of wind and refractive-index structure using optical scintillation techniques N87-17272

REFRACTORY COATINGS
Corrosion/oxidation protection of high temperature material --- gas turbine engines [PNR90355] N87-16905

REFRACTORY MATERIALS
Gas turbine materials: A review [PNR90356] N87-16842

REFUELING
Tethered orbital refueling study [NASA-CR-171953] N87-16855

REGRESSION ANALYSIS
Estimation of absolute water surface temperature based on atmospherically corrected thermal infrared multispectral scanner digital data N87-17114

RELATIVISTIC PLASMAS
Radiative processes underlying the X-ray and gamma-ray continua of active galactic nuclei and gamma-ray bursts N87-17655

RELAXATION METHOD (MATHEMATICS)
On the analytical determination of relaxation modulus of viscoelastic materials by Prony's interpolation method [NASA-TM-86579] N87-17455

RELIABILITY
Surface flaw reliability analysis of ceramic components with the SCARE finite element postprocessor program [NASA-TM-88901] N87-17087

RELIC RADIATION
The early universe N87-17539

RELIEF MAPS
Digital terrain mapping with STAR-1 SAR data N87-17269

REMOTE CONTROL
Radial and torsionally controlled magnetic bearing [NASA-CASE-GSC-12957-1] N87-17038

REMOTE MANIPULATOR SYSTEM
Reducing shuttle-payload dynamic interaction with notch filters [NASA-CR-171958] N87-16862

REMOTE SENSING
The TIMS investigator's guide N87-17113
Thermal imaging spectroscopy in the Kelso-Baker Region, California N87-17117
Lithologic mapping of silicate rocks using TIMS N87-17118
TIMS data applications in Nebraska N87-17126
The application of remotely sensed data to pedologic and geomorphic mapping on alluvial fan and playa surfaces in Saline Valley, California N87-17127
The Red River Valley archeological project N87-17128
The physical basis for spectral variations in thermal infrared emittance of silicates and application to remote sensing N87-17129
Proceedings of the 1986 International Geoscience and Remote Sensing Symposium (IGARSS '86) on Remote Sensing: Today's Solutions for Tomorrow's Information Needs, volume 1 [ESA-SP-254-VOL-1] N87-17163
The transfer of remote sensing technology to developing countries: A survey of experts in the field N87-17170
In service training of scientists and engineers: An important method of information transfer in the area of satellite remote sensing and its applications N87-17171
The design of an international data centre for remote sensing N87-17176
Commercial opportunities in Earth observation from space N87-17177
An inter-sensor comparison of the microwave signatures of Arctic sea ice N87-17184
Automated remote sensing of sea ice using synthetic aperture radar N87-17186
Microwave remote sensing of snow-covered sea ice N87-17187
Overview and status of the ERS-1 program N87-17190
The image processing workbench - portable software for remote sensing instruction and research N87-17209
Multispectral classification of microwave remote sensing images --- SAR crop identification N87-17236
Integrated analysis of geological and remote sensing data aimed at mineral deposits detection in the Monapo area (northern Mozambique) N87-17243

A simulation study of some contextual classification methods for remotely sensed data N87-17252
Segmentation by mathematical morphology processing hand on the image understanding model in remote s...sing N87-17254
Microwave remote sensing: Its applications and limitations in operational tasks of land use inventory and forest management N87-17266
Remote probing of wind and refractive-index structure using optical scintillation techniques N87-17272
Real-time application of remotely sensed data — meteorology N87-17276
Application of Spaceborne Distributed Aperture/Coherent Array Processing (SDA/CAP) technology to active and passive microwave remote sensing N87-17277
Multifrequency-polarimetric SAR for remote sensing N87-17280
Proceedings of the 1986 International Geoscience and Remote Sensing Symposium (IGARSS' 86) on Remote Sensing: Today's Solutions for Tomorrow's Information Needs, volume 2
[ESA-SP-254-VOL-2] N87-17283
An overview of remote sensing agricultural apcations in North America: Past, present and future N87-17284
Applications of remote sensing in the US Department of Agriculture N87-17285
Assessing grass canopy condition and growth from combined optical-microwave measurements N87-17286
Analysis of the spatial structure of Synthetic Aperture Radar (SAR) imagery for a better separability of cereal crops, wheat and barley N87-17287
Toward a satellite system to monitor the spatial and temporal behavior of soil water content N87-17288
Utility of remote sensing data in renewable resource sample survey N87-17289
Advanced alternating frame technology (VISIDEP (TM)) and three-dimensional remote sensing N87-17291
Image processing methods in two and three dimensions used to animate remotely sensed data — cloud cover N87-17292
Application of 2-D Hilbert transform in the interpretation of remotely sensed potential field data — geology N87-17293
Computer-aided interpretation of complex geological patterns in remote sensing N87-17294
The effect of measurement error and confusion from vegetation on passive microwave estimates of soil moisture N87-17304
Towards snowmelt runoff forecast using LANDSAT-MSS and NOAA/AVHRR data N87-17317
A climatological-hydrological study of lake ice in the southwestern mountain area in Norway by use of satellite sensing N87-17319
Thermal infrared remote sensing: One of today's solutions N87-17324
Models for temperature estimation from remotely sensed thermal IR data N87-17325
Parameter space techniques for image registration N87-17327
Shape similarity in remote sensing images using graph matching techniques N87-17330
IRSAP: An improved approach in processing remotely sensed data — Interactive Remote Sensing Applications Package (IRSAP) N87-17332
Optical visual evaluation and interpretation of remote sensing data N87-17353
The use of numerical wind and wave models to provide areal and temporal extension to instrument calibration and validation of remotely sensed data — satellite data N87-17371
Training programs in remote sensing for professionals, students and the general public
[NASA-TM-88541] N87-17394
SAGE aerosol measurements. Volume 3: January 1, 1981 to November 18, 1981
[NASA-RP-1173] N87-17417
A diagnostic approach to obtaining planetary boundary layer winds using satellite-derived thermal data
[NASA-CR-178972] N87-17420

REMOTE SENSORS
Proceedings of the 1986 International Geoscience and Remote Sensing Symposium (IGARSS '86) on Remote Sensing: Today's Solutions for Tomorrow's Information Needs, volume 1
[ESA-SP-254-VOL-1] N87-17163
Active/passive microwave sensor comparison of MIZ-ice concentration estimates — Marginal Ice Zone (MIZ) N87-17185
The ESA approach for ERS-1 sensor calibration and performance verification N87-17192
Development of intelligent pipe locator N87-17200
Proceedings of the 1986 International Geoscience and Remote Sensing Symposium (IGARSS' 86) on Remote Sensing: Today's Solutions for Tomorrow's Information Needs, volume 2
[ESA-SP-254-VOL-2] N87-17283
ERS-1 mission constraints related to wind and wave calibration N87-17364
The influence of spatial and temporal scales on calibration/validation — ERS-1 sensors N87-17365
Homogenizing surface and satellite observations of cloud
[AD-A174691] N87-17427

REPORTS
Compendium of NASA Langley reports on hypersonic aerodynamics
[NASA-TM-87760] N87-16802
FY 1986 scientific and technical reports, articles, papers and presentations
[NASA-TM-88575] N87-17532

RESEARCH AIRCRAFT
Flight investigation of the effect of tail configuration on stall, spin, and recovery characteristics of a low-wing general aviation research airplane
[NASA-TP-2644] N87-16815
Noise propagation from a four-engine, propeller-driven airplane
[NASA-TM-89035] N87-17482

RESEARCH AND DEVELOPMENT
Reducing the cost of aero engine research and development
[PNR90341] N87-16836
Annual review, April 1985 - March 1986
[ISSN-0547-1567] N87-17503
Research and technology
[NASA-TM-88868] N87-17656

RESEARCH FACILITIES
Research opportunities in microgravity science and applications during shuttle hiatus
[NASA-TM-88964] N87-16917
Noise propagation from a four-engine, propeller-driven airplane
[NASA-TM-89035] N87-17482
Scientific and technical information output of the Langley Research Center for calendar year 1986
[NASA-TM-89065] N87-17531
Laboratory measurements of microwave absorption from gaseous atmospheric constituents under conditions for the outer planets N87-17620

RESEARCH MANAGEMENT
Loads and Aeroelasticity Division research and technology accomplishments for FY 1986 and plans for FY 1987
[NASA-TM-89084] N87-16796
Compendium of NASA Langley reports on hypersonic aerodynamics
[NASA-TM-87760] N87-16802
Research opportunities in microgravity science and applications during shuttle hiatus
[NASA-TM-88964] N87-16917
Research on structural analysis at the DFVLR, Brunswick N87-17078
An overview of the implementation of the World Climate Research program N87-17388

RESIDUAL STRESS
Effects of curing stresses on composite structures N87-16930

RESISTORS
Low noise polycrystalline semiconductor resistors by hydrogen passivation
[AD-D012492] N87-17520

RESONANCE
Linearised theory of stability and resonance for projectiles with aerodynamically induced roll variations
[WSRL-0449-TR] N87-16795

RESONANT FREQUENCIES
Stochastic model of tidal evolution of Earth-Moon system with cyclic change in resonant frequency of ocean N87-17103

RESOURCES MANAGEMENT
Utility of remote sensing data in renewable resource sample survey N87-17289

RETRACTABLE EQUIPMENT
The Extendable Refractable Mast (ERM) thermal analysis: A heat radiation case study via the finite element method N87-16949

REVERSE FIELD PINCH
Tilt stability of field-reversed configurations
[IPPJ-802] N87-17510
Advanced fuels in a field-reversed configuration
[IPPJ-804] N87-17512

RICHARDSON NUMBER
Bulk Richardson's number isograms deduced from SAR data — ocean surface N87-17392

RIEMANN MANIFOLD
A transportation queueing model, solved as a Riemann boundary value problem
[MEMO-573] N87-17463

RIVERS
The megageomorphology of the radar rivers of the eastern Sahara N87-17139

RIVETED JOINTS
Fatigue life and fastener flexibility of single shear riveted and bolted joints
[FFA-TN-1986-35] N87-17094

ROADS
Frost action predictive techniques for roads and airfields: A comprehensive survey of research findings
[DOT/FAA/PM-85/23] N87-16853

ROBOTICS
Robotic vision system
[AD-D012481] N87-17043
A real time vision system for robotic arc welding N87-17066
Programming robotics applications on an advanced hypercube multiprocessor
[DE86-008895] N87-17445
Kalman filtering, smoothing and recursive robot arm forward and inverse dynamics
[NASA-CR-180135] N87-17451

ROBOTS
Position control of mechanical manipulators by using nonlinear adaptive control algorithm N87-17031
Robotic vision system
[AD-D012481] N87-17043
Adaptive control of mechanical manipulators N87-17450

ROBUSTNESS (MATHEMATICS)
A modified loop transfer recovery approach for robust control of flexible structures N87-17029
Decentralized control of large-scale systems: Fixed modes, sensitivity and parametric robustness
[NASA-TM-88537] N87-17474

ROCKET ENGINES
Space station auxiliary thrust chamber technology
[NASA-CR-179552] N87-16874

ROCKS
Thermal imaging spectroscopy in the Kelso-Baker Region, California N87-17117
Lithologic mapping of silicate rocks using TIMS N87-17118
Detection and mapping of volcanic rock assemblages and associated hydrothermal alteration with Thermal Infrared Multiband Scanner (TIMS) data Comstock Lode Mining District, Virginia City, Nevada N87-17119
Simulation modeling and preliminary analysis of TIMS data from the Carlin area and the northern Grapevine Mountains, Nevada N87-17120
Infrared spectroscopy for geologic interpretation of TIMS data N87-17130
Calculation of day and night emittance values N87-17131
Application of Thermal Infrared Multiband Scanner (TIMS) data to mapping of Plutonic and stratified rock and assemblages in accreted terrains of the Northern Sierra, California N87-17132
A geologic atlas of TIMS data N87-17133
Space shuttle radar images of Indonesia N87-17137
A statistical approach to select the optimal wavelength bands for separating rocks in the wavelength region 0.4 to 2.3 microns N87-17244

RODS
Torsion-tension coupling in rods N87-17079

ROLL
Linearised theory of stability and resonance for projectiles with aerodynamically induced roll variations
[WSRL-0449-TR] N87-16795

ROOM TEMPERATURE
Interpenetrating-network polymeric electrolytes
[AD-D012485] N87-16912

ROTARY WING AIRCRAFT
Outdoor test stand performance of a convertible engine with variable inlet guide vanes for advanced rotorcraft propulsion
[NASA-TM-88939] N87-16825

ROTARY WINGS
The aerodynamics and aeroacoustics of rotating transonic disturbances N87-16786

ROTATING CYLINDERS
Non-backdriveable free wheeling coupling
[NASA-CASE-MSC-20475-1] N87-17037

ROTATION
Anti-rotation guide vane bushing
[AD-D012510] N87-17047
Role of orientation reference selection in motion sickness
[NASA-CR-180161] N87-17431

ROTORS
Comparison of composite rotor blade models: A coupled-beam analysis and an MSC/NASTRAN finite-element model
[NASA-TM-89024] N87-16884
Bonding of superalloys by diffusion welding and diffusion brazing N87-17059
RURAL LAND USE
Microwave remote sensing: Its applications and limitations in operational tasks of land use inventory and forest management N87-17266
Classification of forest and surface types by satellite microwave radiometry N87-17305
Rural land use inventory and mapping in the Ardeche area (France) using multitemporal Thematic Mapping (TM) data N87-17350
LANDSAT-5 Thematic Mapping (TM) data applications to land use classification on around the Bosphorus area, Turkey N87-17351
Discrimation of land features using LANDSAT false colour composite in N Iran N87-17352

S

S MATRIX THEORY
Imaging radar polarimetry from wave synthesis N87-17158
Effective medium approximation for effective propagation constant calculation in a dense random medium — electromagnetic wave scattering N87-17180
A two-scale Bragg scattering model for microwave backscatter from wind generated waves N87-17212
Imaging radar polarimetry from wave synthesis N87-17279
A scattering model for defoliated vegetation N87-17309
SAFETY MANAGEMENT
Safety considerations of lithium-thionyl chloride cells
[NASA-CR-180129] N87-17396
The NASA Aerospace Battery Safety Handbook
[NASA-CR-180127] N87-17397
SAGE SATELLITE
SAGE aerosol measurements. Volume 3: January 1, 1981 to November 18, 1981
[NASA-RP-1173] N87-17417
SAHARA DESERT (AFRICA)
The megageomorphology of the radar rivers of the eastern Sahara N87-17139
SALINITY
Effects of salinity on the microwave emission of soils N87-17302
SALYUT SPACE STATION
Comparative study of LANDSAT MSS, Salyut-7 (TERRA) and radar (SIR-A) images for geological and geomorphological applications: A case study from Rajasthan and Gujarat, India N87-17236
SANDWICH STRUCTURES
Analysis of high precision composite sandwich antennas — spacecraft antennas N87-16929
Qualification of gridding process for a Polarization Sensitive Reflector (PSR) — satellite antenna N87-16932
Dual channel high electron mobility field effect transistor
[AD-D012474] N87-17518
SATELLITE ALTIMETRY
A scanning radar altimeter for mapping continental topography N87-17146
SATELLITE ANTENNAS
Antenna mechanical technologies within ESA N87-16924
Experience gained by sector model testing of an unfurlable mesh/rib antenna N87-16925
Mechanical and control study of a 7 m offset unfurlable tracking antenna N87-16926
Study on solid surface, deployable antenna reflector — satellite antenna N87-16928
Qualification of gridding process for a Polarization Sensitive Reflector (PSR) — satellite antenna N87-16932
Development of 30/20 GHz satellite antenna structures N87-16933
Design of a low distortion shared aperture reflector — satellite antenna N87-16934
Construcciones Aeronauticas S.A. (CASA) large reflector antenna — satellite antenna N87-16935
Development of lightweight dimensionally stable carbon fiber composite antenna reflectors for the INSAT-1 satellite N87-16936
Structural analysis, manufacturing and development status of large polarization sensitive dual-gridded reflectors — satellite antenna N87-16937
Development status of the ERS-1 SAR antenna N87-16939
ERS-1 wind scatterometer antenna: Mechanical aspects N87-16940
Development of mm-wave radiometer antenna reflector — satellite antennas N87-16941
Simple approach for evaluating mechanical reflector antenna distortions — satellite antennas N87-16942
Prediction of the electrical performance of Inflatable Space Rigidized Structure (ISRS) offset antenna reflectors and correlation with RF measurements N87-16943
Contraves' antenna tip hinge mechanism for Selenia Spazio's 20/30 GHz antenna — satellite antenna N87-16944
Design and technology of feed array and beam forming network for contoured beam antennas — satellite antennas N87-16950
Beam forming network technologies and related manufacturing processes — satellite antennas N87-16951
Thermomechanical characteristics of dichroic subreflectors — satellite antennas N87-16952
Features and technologies of ERS-1 (ESA) and X-SAR antennas N87-17152
SATELLITE ATMOSPHERES
A study of planetary atmospheres in the submillimetric range N87-17540
SATELLITE COMMUNICATION
Coherent versus noncoherent signaling for satellite-aided mobile communications
[NASA-CR-180133] N87-16922
Application of adaptive antenna techniques to future commercial satellite communication
[NASA-CR-179566] N87-16954
Application of adaptive antenna techniques to future commercial satellite communication
[NASA-CR-179566] N87-16955
SATELLITE CONFIGURATIONS
An alternative multi-mode SAR for RADARSAT N87-17144
SATELLITE DESIGN
Overview and status of the ERS-1 program N87-17190
N-ROSS validation N87-17385
SATELLITE IMAGERY
Proceedings of the 1986 International Geoscience and Remote Sensing Symposium (IGARSS '86) on Remote Sensing: Today's Solutions for Tomorrow's Information Needs, volume 1
[ESA-SP-254-VOL-1] N87-17163
Components and comparisons of potential information from several imaging satellites N87-17164
Comparison of Thematic Mapper (TM) and SPOT simulation data for agricultural applications in south west Germany N87-17165
The stereo-pushbroom scanner system Digital Photogrammetry System (DPS) and its accuracy N87-17167
Concept of a future multispectral Thermal Infrared (TIR) pushbroom mission for Earth observation from space N87-17169
Monitoring of large phenomena in developing countries through satellite imagery N87-17172
Spatial analysis of the dynamics of an ecosystem by multistage remote sensing in Kenya N87-17173
Environmental modification of metropolitan areas through satellite images: Study of urban design in the tropics N87-17175
Digital satellite imagery acquisition and processing N87-17207
Portable EDITOR (PEDITOR): A portable image processing system — satellite images N87-17208
Extracting surface features in multispectral imagery N87-17211
ERS-1 fast delivery processing and products N87-17224
Canadian plans for operational demonstrations of satellite imaging radar applications — ERS-1 N87-17229
Significance of space image, air photo and drainage linears in relation to west coast tectonics, India N87-17232
Structural and geomorphic evolution of Meghalaya plateau, India on LANDSAT imagery N87-17233
Hydrogeological research in Peloponnesus (Greece) Karst area by support and completion of LANDSAT-thematic data N87-17234
Discrimination of lithologic units using geobotanical and LANDSAT TM spectral data N87-17246
The influence of resampling method and multitemporal LANDSAT imagery on crop classification accuracy in the United Kingdom N87-17250
Evaluation of LANDSAT 5 Thematic Mapping (TM) data for image clustering and classification N87-17251
A synergistic approach for multispectral image restoration using reference imagery N87-17255
Merging spaceborne image data of optical and microwave sensors N87-17267
Application of 2-D Hilbert transform in the interpretation of remotely sensed potential field data — geology N87-17293
Estimation of maximum snow volume distribution using NOAA-AVHRR data N87-17314
A climatological-hydrological study of lake ice in the southwestern mountain area in Norway by use of satellite sensing N87-17319
Digital techniques for noise reduction in Automatic Picture Transmission (APT) NOAA satellite images N87-17328
Radiometric correction method which removes both atmospheric and topographic effects from the LANDSAT-MSS data N87-17329
Rural land use inventory and mapping in the Ardeche area (France) using multitemporal Thematic Mapping (TM) data N87-17350
LANDSAT-5 Thematic Mapping (TM) data applications to land use classification on around the Bosphorus area, Turkey N87-17351
Discrimation of land features using LANDSAT false colour composite in N Iran N87-17352
Optical visual evaluation and interpretation of remote sensing data N87-17353
Canada Center for Remote Sensing (CCRS) Convair 580 results relevant to ERS-1 wind and wave calibration N87-17379
Canopy hot-spot as crop identifier
[DE86-011258] N87-17395
The ice conditions in the Greenland waters, 1980
[REPT-551.467.3.068(988)] N87-17428
SATELLITE OBSERVATION
Components and comparisons of potential information from several imaging satellites N87-17164
Sea ice in the Greenland sea observed by the Nimbus-7 Scanning Multichannel Microwave Radiometer (SMMR) N87-17221
An advanced SAR design for future land missions N87-17322
The use of numerical wind and wave models to provide areal and temporal extension to instrument calibration and validation of remotely sensed data — satellite data N87-17371
Satellite scatterometer comparisons with surface measurements: Techniques and Seasat results N87-17372
Comparison concept of satellite derived wind and wave data with ground truth N87-17373
A study of large, medium and small scale structures in the topside ionosphere
[NASA-CR-180068] N87-17413
Middle Atmosphere Program. Handbook for MAP, volume 22
[NASA-CR-180128] N87-17414
A diagnostic approach to obtaining planetary boundary layer winds using satellite-derived thermal data
[NASA-CR-178972] N87-17420
Homogenizing surface and satellite observations of cloud
[AD-A174691] N87-17427
SATELLITE ORBITS
Orbit determination for low Earth orbit spacecraft based on satellite to satellite tracking techniques via a unique very high altitude relay constellation N87-16858
The contraction of satellite orbits under the influence of air drag. Part 7: Orbits of high eccentricity, with scale height dependent on altitude
[RAE-TR-86013] N87-16859
SATELLITE SOUNDING
A study of planetary atmospheres in the submillimetric range N87-17540
SATELLITE TRACKING
Orbit determination for low Earth orbit spacecraft based on satellite to satellite tracking techniques via a unique very high altitude relay constellation N87-16858
Mechanical and control study of a 7 m offset unfurlable tracking antenna N87-16926
Basic research for the geodynamics program
[NASA-CR-180137] N87-17415
Improvement of the Earth's gravity field from terrestrial and satellite data
[NASA-CR-180139] N87-17416
SATELLITE-BORNE INSTRUMENTS
Some results of Marine Observation Satellite (MOS-1) airborne verification experiment Multispectral Electronic Self Scanning Radiometer (MESSR) N87-17166
The stereo-pushbroom scanner system Digital Photogrammetry System (DPS) and its accuracy N87-17167
Stereo Line Scanner (SLS): System considerations on an operational instrument for meteorology and weather forecasts N87-17168
Development status of the ERS-1 payload instruments N87-17191
Evaluation of LANDSAT 5 Thematic Mapping (TM) data for image clustering and classification N87-17251

Extrapolation of Earth-based solar irradiance measurements to exoatmospheric levels for broad-band and selected absorption-band observations N87-17270
Proceedings of an ESA Workshop on ERS-1 Wind and Wave Calibration [ESA-SP-262] N87-17363
The use of numerical wind and wave models to provide areal and temporal extension to instrument calibration and validation of remotely sensed data — satellite data N87-17371
An overview of the NSCAT/N-ROSS program N87-17384
Australian validation plans for ERS-1 N87-17387
Review of coherent and incoherent detection techniques: Outlook and limitation — spaceborne submillimeter astronomy N87-17537
A 186 GHz radiometer for the microwave limb sounder N87-17569

SATELLITE-BORNE PHOTOGRAPHY
Optical visual evaluation and interpretation of remote sensing data N87-17353

SATELLITE-BORNE RADAR
Geological applications of multipolarization SAR data N87-17140
Spaceborne Imaging Radar Project N87-17143
Observing the polar oceans with spaceborne radar N87-17151
Off-line processing of ERS-1 synthetic aperture radar data with high precision and high throughput N87-17153
SIR-C, the next generation spaceborne SAR N87-17161
Some trade-offs in modest-resolution radars for space N87-17278
Future user requirements and required technological developments of spaceborne synthetic aperture radars N87-17320
An advanced SAR design for future land missions N87-17322
Characteristics of a very low altitude spacecraft for collecting global directional wave spectra with spaceborne synthetic aperture radar N87-17333
A satellite-borne SAR transmitter and receiver N87-17358
Analysis of amplitude nonlinearities in the ERS-1 SAR receiver system N87-17359
Pulse compression test results of the SAR transmitter and receiver — satellite-borne SAR N87-17360
Validation of wind speed and significant wave height from Geosat N87-17368
Bulk Richardson's number isograms deduced from SAR data — ocean surface N87-17392

SATURN (PLANET)
Para hydrogen equilibration in the atmospheres of the outer planets N87-17599
The Cassini mission N87-17638

SATURN ATMOSPHERE
The Jovian Atmospheres [NASA-CP-2441] N87-17598
Changes in Saturn's south-temperate haze distribution during the summer of 1973-1980 N87-17602
A possible deuterium anomaly: Implications of the CH3D/CH4 mixing ratios in the atmospheres of Jupiter, Saturn, and Uranus N87-17617
The abundances of ethane to acetylene in the atmospheres of Jupiter and Saturn N87-17618
Cloud-top meridional momentum transports on Saturn and Jupiter N87-17623
The Saturnian ribbon feature: A baroclinically unstable model N87-17629
Quasi-geostrophic free mode models of long-lived Jovian eddies: Forcing mechanisms and crucial observational tests N87-17630
Transport of absolute angular momentum in quasi-axisymmetric equatorial jet streams N87-17635
The effect of Saturn's rings on the upper-boundary insolation of its atmosphere [AERONOMICA-ACTA-A-308-1986] N87-17650

SATURN RINGS
The effect of Saturn's rings on the upper-boundary insolation of its atmosphere [AERONOMICA-ACTA-A-308-1986] N87-17650

SCALE HEIGHT
The contraction of satellite orbits under the influence of air drag. Part 7: Orbits of high eccentricity, with scale height dependent on altitude [RAE-TR-86013] N87-16859

SCALE MODELS
Experience gained by sector model testing of an unfurlable mesh/rib antenna N87-16925

SCANNERS
The stereo-pushbroom scanner system Digital Photogrammetry System (DPS) and its accuracy N87-17167

SCATTER PROPAGATION
Effective medium approximation for effective propagation constant calculation in a dense random medium — electromagnetic wave scattering N87-17180

SCATTERING COEFFICIENTS
Microwave backscatter coefficients of artificially grown first-year sea ice N87-17188
Quasi real time conversion of ERS-1 scatterometer raw data to sigma zero triplets N87-17226
Hawaiian lava flows and SIR-B results N87-17245
Extraction of the backscatter coefficient of agricultural fields from an airborne SAR image N87-17265
Calibrated X and L-band scattering coefficients from a southern US forest N87-17312

SCATTERING CROSS SECTIONS
Doubly differential cross sections for galactic heavy-ion fragmentation [NASA-TP-2659] N87-17487

SCATTEROMETERS
ERS-1 wind scatterometer antenna: Mechanical aspects N87-16940
Wind Scatterometer Antenna (WSA) release shock loads — ERS-1 N87-16945
Development status of the ERS-1 payload instruments N87-17191
On-ground verification and in-orbit performance prediction of the ERS-1 wind scatterometer N87-17193
ERS-1 fast delivery processing and products N87-17224
Results of the ESA airborne C-band scatterometer campaigns — ERS-1 N87-17225
Quasi real time conversion of ERS-1 scatterometer raw data to sigma zero triplets N87-17226
ERS-1 wind scatterometer: Wind extraction and ambiguity removal N87-17227
Recent progress in ERS-1 wind scatterometer design N87-17256
The ERS-1 scatterometer system simulator and its relevance for ground processing design N87-17257
Roundoff noise analysis for digital Doppler processors in radar scatterometers N87-17258
Application of the Seasat scatterometer to observations of wind speed and direction and Arctic ice/water boundaries N87-17259
Millimeter-wave network analyzer-based scatterometer N87-17281
A scatterometer operating at 10 GHz N87-17282
Estimation of internal wave currents from SAR and infrared scatterometer imagery N87-17295
X and L-band backscattering measurements of agricultural crops, forest stands and single trees N87-17311
The influence of spatial and temporal scales on calibration/validation — ERS-1 sensors N87-17365
NASA scatterometer data processing system: Features for validation N87-17366
Evaluation of the different parameters in Long's C-band model — for ERS-1 scatterometer N87-17370
Satellite scatterometer comparisons with surface measurements: Techniques and Seasat results N87-17372
The accuracy and availability of operational marine surface wind data for ERS-1 sensor calibration and validation from fixed platforms and free drifting buoys N87-17376
Using buoys and ships to calibrate ERS-1 altimeter and scatterometer N87-17377
DFVLR flight operation acting as a useful service unit for ERS-1 N87-17378
Canada Center for Remote Sensing (CCRS) Convair 580 results relevant to ERS-1 wind and wave calibration N87-17379
The use of aircraft for wind scatterometer calibration — ERS-1 scatterometer N87-17382
An overview of the NSCAT/N-ROSS program N87-17384
Intersensor comparisons for validation of wind speed measurements from ERS-1 altimeter and scatterometer — Seasat N87-17386
A scatterometer research program N87-17391

SCINTILLATION
Remote probing of wind and refractive-index structure using optical scintillation techniques N87-17272

SEA ICE
Observing the polar oceans with spaceborne radar N87-17151
An inter-sensor comparison of the microwave signatures of Arctic sea ice N87-17184
Active/passive microwave sensor comparison of MIZ-ice concentration estimates — Marginal Ice Zone (MIZ) N87-17185
Automated remote sensing of sea ice using synthetic aperture radar N87-17186
Microwave remote sensing of snow-covered sea ice N87-17187
Microwave backscatter coefficients of artificially grown first-year sea ice N87-17188
Geophysics of the marginal ice zone from SAR N87-17219
Microwave properties of sea ice in the marginal ice zone N87-17220
Sea ice in the Greenland sea observed by the Nimbus-7 Scanning Multichannel Microwave Radiometer (SMMR) N87-17221
Sea ice studies in the Baltic Sea using satellite microwave radiometer data N87-17343

SEA STATES
Microwave scattering from the ocean surface N87-17109

SEA TRUTH
Satellite scatterometer comparisons with surface measurements: Techniques and Seasat results N87-17372
Validation of ERS-1 wind data using observations from research and voluntary observing ships N87-17374

SEA WATER
Metal content of ocean water studied with radio spectrometer N87-17102
Light scattering theory for bubbles in water: Inverse scattering, coated bubbles and statistics [AD-A174997] N87-17498

SEALING
Solid rocket booster joint seal analyses [NASA-TM-86580] N87-17039
Metallization for hermetic sealing of ceramic modules [AD-D012483] N87-17044

SEALS (STOPPERS)
Space shuttle main engine high pressure fuel pump aft platform seal cavity flow analysis [NASA-TP-2685] N87-17000

SEASAT SATELLITES
Geological applications of multipolarization SAR data N87-17140
Application of the Seasat scatterometer to observations of wind speed and direction and Arctic ice/water boundaries N87-17259
Satellite scatterometer comparisons with surface measurements: Techniques and Seasat results N87-17372
Intersensor comparisons for validation of wind speed measurements from ERS-1 altimeter and scatterometer — Seasat N87-17386
Bulk Richardson's number isograms deduced from SAR data — ocean surface N87-17392

SECULAR VARIATIONS
Changes in Saturn's south-temperate haze distribution during the summer of 1973-1980 N87-17602

SEGMENTS
Segmentation by mathematical morphology processing hand on the image understanding model in remote sensing N87-17254

SELF CONSISTENT FIELDS
Field consistency and finite element analysis of multifield structural problems N87-17080

SELF ERECTING DEVICES
Development of a 2.8 m offset antenna reflector using inflatable, space-rigidized structures technology N87-16927

SEMICONDUCTOR DEVICES
Applications of focused ion beams in microelectronics [RSRE-MEMO-3948] N87-17517

SEMICONDUCTORS (MATERIALS)
Dual channel high electron mobility field effect transistor [AD-D012474] N87-17518
Low noise polycrystalline semiconductor resistors by hydrogen passivation [AD-D012492] N87-17520

SEPARATED FLOW
Computation of separation ahead of blunt fin in supersonic turbulent flow [NASA-TM-89416] N87-16791
Experimental investigation in turbulent flow separation [ISL-CO-208/86] N87-17012
Three-dimensional separation on a cylindrical ellipsoid. Results of the first test campaign on the F2 wind tunnel [ONERA-RT-16/7252-AN] N87-17013

SEPARATION
Magmatic differentiation in partially molten systems: Applications to the moon and the palisades sill N87-17597

SERIES EXPANSION
Gradient methods for geophysical image inversions N87-17201
On first passage times and differential equations [AD-A174648] N87-17470

SERVICE LIFE
Component lifing — aircraft engines [PNR90346] N87-16838

SEYFERT GALAXIES
The development of the Goddard Compton gamma-ray telescope and neutral hydrogen N87-17580
SHADES
Sun shield
[NASA-CASE-MSC-20162-1] N87-17036
SHAFTS (MACHINE ELEMENTS)
Non-backdriveable tree wheeling coupling
[NASA-CASE-MSC-20475-1] N87-17037
SHALLOW SHELLS
Buckling and postbuckling behavior of shallow shells N87-17081
SHAPE CONTROL
A modified loop transfer recovery approach for robust control of flexible structures N87-17029
SHAPES
Unitized high temperature probes
[AD-D012508] N87-17020
SHEAR FLOW
Pressure gradient effects in the viscous wall region of a turbulent flow
[REPT-7] N87-16980
SHEAR STRENGTH
Diffusion bonding of Al-alloys in the solid state N87-17058
SHIPS
Analysis of synthetic aperture radar imagery of surface ship wakes N87-17297
Validation of ERS-1 wind data using observations from research and voluntary observing ships N87-17374
Accuracy estimates of wind and wave observations from ships of opportunity in the WMO voluntary observing ship program N87-17375
Using buoys and ships to calibrate ERS-1 altimeter and scatterometer N87-17377
SHOCK LOADS
Determining and modeling the response of ytterbium piezoresistance transducers
[AD-A173085] N87-17023
SHOCK TUBES
Development of a drag measurement system for the CERF 6-foot shock tube
[AD-A173087] N87-16854
Proceedings of the 15th International Symposium on Shock Waves and Shock Tubes
[AD-A173026] N87-17006
SHOCK WAVE INTERACTION
Proceedings of the 15th International Symposium on Shock Waves and Shock Tubes
[AD-A173026] N87-17006
The study of shock wave and turbulent boundary layer interactions
[AD-A175033] N87-17008
Observations on the turbulent structure in an unsteady, normal shock/boundary-layer interaction — blowdown supersonic tunnel
[PNR90361] N87-17010
SHOCK WAVE PROPAGATION
Proceedings of the 15th International Symposium on Shock Waves and Shock Tubes
[AD-A173026] N87-17006
SHOCK WAVES
A high resolution shock capturing scheme for high Mach number internal flow
[NASA-CR-179523] N87-16804
Proceedings of the 15th International Symposium on Shock Waves and Shock Tubes
[AD-A173026] N87-17006
Biological effects of aerial shock waves: Review of work to date
[ISL-NB-402/85] N87-17432
SHORT CIRCUITS
A pi-section digital phase shifter apparatus
[AD-D012495] N87-16973
SHUTTLE IMAGING RADAR
The Second Spaceborne Imaging Radar Symposium
[NASA-CR-180131] N87-17135
Tectonic geomorphology of the Andes with SIR-A and SIR-B N87-17136
Space shuttle radar images of Indonesia N87-17137
Delineation of fault zones using imaging radar N87-17138
The megageomorphology of the radar rivers of the eastern Sahara N87-17139
Geological applications of multipolarization SAR data N87-17140
Spaceborne imaging radar research in the 90's N87-17141
Spaceborne Imaging Radar Project N87-17143
Hydrodynamics of internal solitons and a comparison of SIR-A and SIR-B data with ocean measurements N87-17147
Ocean waves near Hurricane Josephine from SIR-B N87-17148
The SIR-C ground data system: Digital processor, data products, information flow N87-17155
Analysis of multiple incidence angle SIR-B data for determining forest stand characteristics N87-17156
Multiple incidence angle SIR-B experiment over Argentina N87-17157
Radar signature determination: Trends and limitations N87-17159
SIR-B measurements and modeling of vegetation N87-17160
SIR-C, the next generation spaceborne SAR N87-17161
The X-SAR System N87-17162
Comparative study of LANDSAT MSS, Salyut-7 (TERRA) and radar (SIR-A) images for geological and geomorphological applications: A case study from Rajasthan and Gujarat, India N87-17236
Determining the vertical pattern of a spaceborne SAR by observation of uniform targets — SIR-B N87-17240
Hawaiian lava flows and SIR-B results N87-17245
Computer-derived height from SIR-B stereo radar images N87-17268
Future user requirements and required technological developments of spaceborne synthetic aperture radars N87-17320
The X-band SAR in a joint mission with the Shuttle Imaging Radar N87-17321
The SAR image modulation transfer function derived from SIR-B image spectra and airborne measurements of ocean wave height spectra N87-17334
SIR-B observations of ocean waves in the NE Atlantic N87-17335
Deriving two-dimensional ocean wave spectra and surface height maps from the Shuttel Imaging Radar (SIR-B) N87-17336
Spatial evolution of wave spectra in the vicinity of the Agulhas current from SIR-B N87-17337
X-SAR extends the frequency range of Shuttle imaging Radar N87-17362
SIDE-LOOKING RADAR
VARAN-S radar image interpretation
[CNES-CT/DRT/TIT/RL-54-T] N87-16963
MIZEX VARAN-S radar image characteristics
[CNES-CT/DRT/TIT/RL-55-T] N87-16964
SIGNAL ANALYZERS
ECM (electronic countermeasures) preprocessor or tracker using multi-processor modules
[AD-D012513] N87-16959
SIGNAL DETECTORS
Noise-immune multisensor transduction of speech
[AD-A174693] N87-16961
SIGNAL FADING RATE
Remote sensing of tree attenuation at 870 MHz along simulated Earth-satellite paths N87-17306
SIGNAL GENERATORS
System engineering study of electrodynamic tether as a spaceborne generator and radiator of electromagnetic waves in the ULF/ELF frequency band
[NASA-CR-180156] N87-16956
SIGNAL PROCESSING
Multiple Trellis Coded Modulation (MTCM): An MSAT-X report
[NASA-CR-180134] N87-16921
Coherent versus noncoherent signaling for satellite-aided mobile communications
[NASA-CR-180133] N87-16922
ECM (electronic countermeasures) preprocessor or tracker using multi-processor modules
[AD-D012513] N87-16959
Roundoff noise analysis for digital Doppler processors in radar scatterometers N87-17258
Nonlinear real-time optical signal processing
[AD-A173119] N87-17497
SIGNAL RECEPTION
Single frequency multitransmitter telemetry
[NASA-CASE-LAR-13006-1] N87-16863
SIGNAL REFLECTION
Power cepstrum technique with application to model helicopter acoustic data
[NASA-TP-2566] N87-17479
SIGNAL TO NOISE RATIOS
Roundoff noise analysis for digital Doppler processors in radar scatterometers N87-17258
Digital techniques for noise reduction in Automatic Picture Transmission (APT) NOAA satellite images N87-17328
SIGNAL TRANSMISSION
Monitoring transients in low inductance circuits
[DE86-013756] N87-16978
SIGNATURE ANALYSIS
A statistical approach to select the optimal wavelength bands for separating rocks in the wavelength region 0.4 to 2.3 microns N87-17244
SILICATES
Lithologic mapping of silicate rocks using TIMS N87-17118
The Red River Valley archeological project N87-17128
The physical basis for spectral variations in thermal infrared emittance of silicates and application to remote sensing N87-17129
SILICON OXIDES
Maser and thermal SiO emission in evolved stars N87-17553
SILICON POLYMERS
Low noise polycrystalline semiconductor resistors by hydrogen passivation
[AD-D012492] N87-17520
Performance of polysilicon gate CMOS devices in space and SDI environments
[DE86-009025] N87-17524
SIMULATION
Review of wind simulation methods for horizontal-axis wind turbine analysis
[DE86-012223] N87-17407
Aircraft noise synthesis system
[NASA-TM-89040] N87-17483
SINGLE CRYSTALS
Technique for the growth of compositionally ungraded single crystals of solid solutions
[AD-D012488] N87-17519
Research on millimeter wave dielectric materials
[AD-A173017] N87-17521
SINTERING
Fabrication of hollow, cored, and composite shaped parts from selected alloy powders
[AD-D012489] N87-16903
SITE SELECTION
Wind energy technical reading list
[DE86-010704] N87-17404
SIZE DETERMINATION
Droplet sizing research program
[AD-A173100] N87-16895
SLEEVES
Anti-rotation guide vane bushing
[AD-D012510] N87-17047
SLOT ANTENNAS
On the feasibility of constructing an imaging array of slot-antennas integrated with SIS mixers — radio astronomy N87-17572
SLURRY PROPELLANTS
Fuels combustion research
[AD-A175040] N87-16897
SMOOTHING
Kalman filtering, smoothing and recursive robot arm forward and inverse dynamics
[NASA-CR-180135] N87-17451
Recursive linear smoothing for dissipative hyperbolic systems
[AD-A173020] N87-17460
SNOW
On microwave scattering properties of heterogeneous two-component mixtures — soil/snow N87-17178
Dielectric and scattering behavior of snow at microwave frequencies N87-17179
Snow stratigraphy observed by an FM-CW microwave system N87-17181
Snow property measurements correlative to microwave emission at 35 GHz N87-17315
Dependence of snow melting and surface-atmosphere interactions on the forest structure N87-17318
SNOW COVER
Microwave remote sensing of snow-covered sea ice N87-17187
Developpement of algorithms to retrieve the water equivalent of snow cover from satellite microwave radiometer data N87-17264
Estimation of maximum snow volume distribution using NOAA-AVHRR data N87-17314
Snow cover recession in an Alpine ecological system N87-17316
Towards snowmelt runoff forecast using LANDSAT-MSS and NOAA/AVHRR data N87-17317
A climatological-hydrological study of lake ice in the southwestern mountain area in Norway by use of satellite sensing N87-17319
SOFTWARE ENGINEERING
Design of software for design of finite element for structural analysis
[NASA-TM-88528] N87-17089
Basic research for the geodynamics program
[NASA-CR-180137] N87-17415
Interactive wrapper tool for mapping objects to Fortran library functions
[DE86-009686] N87-17446
A research program in advanced information systems
[NASA-CR-180150] N87-17529
SOFTWARE TOOLS
Interactive wrapper tool for mapping objects to Fortran library functions
[DE86-009686] N87-17446

Vibroacoustic payload environment prediction system (VAPEPS): Data base management center remote access guide
[NASA-CR-180132] N87-17528

SOIL MECHANICS
A study of explosive wave propagation in granular materials with microstructure
[AD-A173015] N87-16914

SOIL MOISTURE
SIR-B measurements and modeling of vegetation N87-17160
A spatially homogeneous anisotropic surface model with variable parameters for scattering from bare soil N87-17183
Toward a satellite system to monitor the spatial and temporal behavior of soil water content N87-17288
Effects of salinity on the microwave emission of soils N87-17302
Discrimination of soil hydraulic properties by combined thermal infrared and microwave remote sensing N87-17303
The effect of measurement error and confusion from vegetation on passive microwave estimates of soil moisture N87-17304

SOIL SCIENCE
Frost action predictive techniques for roads and airfields: A comprehensive survey of research findings
[DOT/FAA/PM-85/23] N87-16853
The application of remotely sensed data to pedologic and geomorphic mapping on alluvial fan and playa surfaces in Saline Valley, California N87-17127
Effects of salinity on the microwave emission of soils N87-17302
Discrimination of soil hydraulic properties by combined thermal infrared and microwave remote sensing N87-17303

SOILS
A study of explosive wave propagation in granular materials with microstructure
[AD-A173015] N87-16914
Thermal imaging spectroscopy in the Kelso-Baker Region, California N87-17117
TIMS data applications in Nebraska N87-17126
On microwave scattering properties of heterogeneous two-component mixtures — soil/snow N87-17178
A spatially homogeneous anisotropic surface model with variable parameters for scattering from bare soil N87-17183
Determination of resistivity and permittivity profiles of a layered Earth N87-17198
Dielectric and surface parameters related to microwave scatter and emission properties N87-17262
Effects of salinity on the microwave emission of soils N87-17302

SOLAR ACTIVITY EFFECTS
Geophysicist comments on how solar activity may affect weather N87-17097

SOLAR ARRAYS
The Extendable Refractable Mast (ERM) thermal analysis: A heat radiation case study via the finite element method N87-16949
LEO high voltage solar array arcing response model
[NASA-CR-180073] N87-16971

SOLAR CELLS
LEO high voltage solar array arcing response model
[NASA-CR-180073] N87-16971
High band gap 2-6 and 3-5 tunneling junctions for silicon multijunction solar cells
[NASA-CASE-NPO-16526-1CU] N87-17399
Research on single-crystal CdTe solar cells
[DE86-010719] N87-17405
Use of low energy ion implants in high efficiency crystalline silicon solar cells
[NASA-CR-179971] N87-17408

SOLAR HEATING
Assessment of contemporary changes in global climate N87-17101

SOLAR PLANETARY INTERACTIONS
Seasonal north-south asymmetry in solar radiation at the top of Jupiter's atmosphere N87-17603

SOLAR RADIATION
Seasonal north-south asymmetry in solar radiation at the top of Jupiter's atmosphere N87-17603

SOLAR RADIATION SHIELDING
Sun shield
[NASA-CASE-MSC-20162-1] N87-17036

SOLAR SPECTRA
Extrapolation of Earth-based solar irradiance measurements to exoatmospheric levels for broad-band and selected absorption-band observations N87-17270

SOLAR WIND
Geophysicist comments on how solar activity may affect weather N87-17097
The interaction between the solar wind and the comets
[AERONOMICA-ACTA-A-306-1986] N87-17653

SOLDERING
Direct cable attach method
[AD-D012505] N87-17046

SOLID ELECTROLYTES
Interpenetrating-network polymeric electrolytes
[AD-D012485] N87-16912

SOLID SOLUTIONS
Technique for the growth of compositionally ungraded single crystals of solid solutions
[AD-D012488] N87-17519

SOLID STATE DEVICES
High energy surge arrester technology development, part 2
[AD-A173086] N87-16977

SOLID SURFACES
Study on solid surface, deployable antenna reflector — satellite antenna N87-16928

SOLID SUSPENSIONS
Apparatus and method for stirring fluid borne particles
[AD-D012486] N87-17477

SOLITARY WAVES
Hydrodynamics of internal solitons and a comparison of SIR-A and SIR-B data with ocean measurements N87-17147

SOLUBILITY
Soluble aromatic polyimides for film and coating applications
[NASA-TM-89016] N87-16911

SOLVENT EXTRACTION
Supported liquid membranes in 1986: New technology or scientific curiosity
[DE86-007504] N87-16898

SOOT
Fuels combustion research
[AD-A175040] N87-16897

SOUND PROPAGATION
Sound propagation in a superfluid helium filled porous solid: Theory and experiment N87-17478

SOUND TRANSMISSION
Identification and proposed control of helicopter transmission noise at the source
[NASA-TM-89312] N87-16816

SOUND WAVES
Recursive linear smoothing for dissipative hyperbolic systems
[AD-A173020] N87-17460

SOYBEANS
Microwave backscattering from an anisotropic soybean canopy N87-17346

SPACE BASED RADAR
Comparisons of the detection performance of a space-based radar system using different antenna systems and aperture illuminations
[AD-A173094] N87-16860
Spaceborne imaging radar research in the 90's N87-17141

SPACE COMMERCIALIZATION
Commercial opportunities in Earth observation from space N87-17177
Communications satellite systems operations with the space station, volume 2
[NASA-CR-179527] N87-17473

SPACE ENVIRONMENT SIMULATION
Some results about laboratory dust analysis in the FIR range — cosmic dust simulation N87-17551

SPACE ERECTABLE STRUCTURES
Development of a 2.8 m offset antenna reflector using inflatable, space-rigidized structures technology N87-16927
Prediction of the electrical performance of Inflatable Space Rigidized Structure (ISRS) offset antenna reflectors and correlation with RF measurements N87-16943

SPACE EXPLORATION
The Jovian Atmospheres
[NASA-CP-2441] N87-17598
The Cassini mission N87-17638

SPACE INFRARED TELESCOPE FACILITY
Dynamic analysis and design of the SIRTF primary mirror mount
[NASA-CR-180158] N87-17494

SPACE OBSERVATIONS (FROM EARTH)
Status of observational astronomy in the 1990's: Position of submillimetre astronomy N87-17536

SPACE PLASMAS
LEO high voltage solar array arcing response model
[NASA-CR-180073] N87-16971

SPACE SHUTTLE BOOSTERS
Solid rocket booster joint seal analyses
[NASA-TM-86580] N87-17039
SRB O-ring free response analysis
[NASA-TM-86582] N87-17040

SPACE SHUTTLE MAIN ENGINE
Advanced 3-D viscous SSME turbine rotor stator CFD algorithms
[NASA-CR-178997] N87-16829
Space shuttle main engine vibration data base
[NASA-TM-86576] N87-16876
Statistical analysis of 59 inspected SSME HPFTP turbine blades (uncracked and cracked)
[NASA-TM-86584] N87-16877
Conventionally cast and forged copper alloy for high-heat-flux thrust chambers
[NASA-TP-2694] N87-16902
Space shuttle main engine high pressure fuel pump aft platform seal cavity flow analysis
[NASA-TP-2685] N87-17000

SPACE SHUTTLE MISSION 51-L
A new day: Challenger and space flight thereafter
[NASA-TM-77717] N87-16856

SPACE SHUTTLE PAYLOADS
Reducing shuttle-payload dynamic interaction with notch filters
[NASA-CR-171958] N87-16862
Low-g measurements by NASA
[NASA-TM-86585] N87-17017
Vibroacoustic payload environment prediction system (VAPEPS): Data base management center remote access guide
[NASA-CR-180132] N87-17528

SPACE SHUTTLES
The NASA Aerospace Battery Safety Handbook
[NASA-CR-180127] N87-17397

SPACE STATIONS
Concept definition for space station technology development experiments. Experiment definition, task 2
[NASA-CR-178153] N87-16860
Structural dynamics and attitude control study of early manned capability space station configurations
[NASA-TM-89078] N87-16861
Space station human productivity study, volume 1
[NASA-CR-171961] N87-16869
Initial utilization of the CVIRB video production facility
[NASA-TM-89036] N87-16873
Space station auxiliary thrust chamber technology
[NASA-CR-179552] N87-16874

SPACEBORNE ASTRONOMY
Proceedings of an ESA Workshop on a Spaceborne Submillimeter Astronomy Mission. A Cornerstone of the ESA Long Term Science Program
[ESA-SP-260] N87-17535
Status of observational astronomy in the 1990's: Position of submillimetre astronomy N87-17536
Review of coherent and incoherent detection techniques: Outlook and limitation — spaceborne submillimeter astronomy N87-17537
Observations of active galactic nuclei with FIRST — Far Infrared Submillimeter Space Telescope (FIRST) N87-17538
A study of planetary atmospheres in the submillimetric range N87-17540
Submillimetre wavelength studies of protostars: The role of FIRST — Far Infrared Submillimeter Space Telescope (FIRST) N87-17544
Circumstellar envelopes around evolved stars N87-17548
Far infrared submillimeter wave space telescope (FIRST) observations of stars with large mass loss rates N87-17550

SPACEBORNE EXPERIMENTS
Antenna ambiguity investigations for X-SAR — shuttle-borne radar N87-17355
X-SAR extends the frequency range of Shuttle Imaging Radar N87-17362

SPACEBORNE TELESCOPES
A Sener mechanism: Fine adjustment mechanism for the Far Infrared and Submillimeter Space Telescope (FIRST) (F I F) N87-16946
Observations of active galactic nuclei with FIRST — Far Infrared Submillimeter Space Telescope (FIRST) N87-17538
Far infrared submillimeter wave space telescope (FIRST) observations of stars with large mass loss rates N87-17550
Active optics for the far infrared submillimeter wave space telescope (FIRST): A high angular resolution mode N87-17566
The large deployable reflector: A NASA submillimeter-infrared orbiting observatory N87-17571
Structure of molecular clouds and space-based sub-millimeter telescopes, for example FIRST — Far Infrared Submillimeter Wave Space Telescope (FIRST) N87-17574

SPACECRAFT ANTENNAS
Composite space antenna structures: Properties and environmental effects
[NASA-TM-88859] N87-16880
Proceedings of the Second ESA Workshop on Mechanical Technology for Antennas
[ESA-SP-261] N87-16923

Development of a 2.8 m offset antenna reflector using inflatable, space-rigidized structures technology N87-16927
Analysis of high precision composite sandwich antennas — spacecraft antennas N87-16929
Effects of curing stresses on composite structures N87-16930
Dielectric support structures for spacecraft antenna feeds N87-16931
Giotto spacecraft high gain antenna mechanical design and development N87-16938
A Sener mechanism: Fine adjustment mechanism for the Far Infrared and Submillimeter Space Telescope (FIRST) (F f F) N87-16946
The Extendable Refractable Mast (ERM) thermal analysis: A heat radiation case study via the finite element method N87-16949
Application of adaptive antenna techniques to future commercial satellite communication [NASA-CR-179586] N87-16954

SPACECRAFT CONSTRUCTION MATERIALS
The welding of aluminum alloys: A new technology in space application N87-17056

SPACECRAFT CONTROL
Description of the Spacecraft Control Laboratory Experiment (SCOLE) facility [NASA-TM-89057] N87-16848
Dynamics and Control Analysis Package (DCAP): An automated analysis and design tool for structural control of space structures N87-16947
Engineering and software interfacing for thermal, structural and dynamic control related with spacecraft activities N87-16948

SPACECRAFT DESIGN
Space station human productivity study, volume 1 [NASA-CR-171961] N87-16869

SPACECRAFT INSTRUMENTS
Evaluation of geophysical parameters measured by the Nimbus-7 microwave radiometer for the TOGA Heat Exchange Project [NASA-CR-180151] N87-17110

SPACECRAFT LAUNCHING
Communications satellite systems operations with the space station. Volume 1: Executive summary [NASA-CR-179526] N87-17472

SPACECRAFT MODELS
Estimation and control of distributed models for certain elastic systems arising in large space structures [AD-A175019] N87-16872
Engineering and software interfacing for thermal, structural and dynamic control related with spacecraft activities N87-16948

SPACECRAFT POWER SUPPLIES
Safety considerations of lithium-thionyl chloride cells [NASA-CR-180129] N87-17396

SPACECRAFT PROPULSION
Space station auxiliary thrust chamber technology [NASA-CR-179552] N87-16874

SPACECRAFT RADIATORS
Expendable pulse power spacecraft radiator [AD-D012498] N87-17005

SPACECRAFT STRUCTURES
Engineering and software interfacing for thermal, structural and dynamic control related with spacecraft activities N87-16948
The welding of aluminum alloys: A new technology in space application N87-17056

SPACECREWS
Space station human productivity study. Volume 4: Issues [NASA-CR-171963] N87-16865
Space station human productivity study. Volume 5: Management plans [NASA-CR-171964] N87-16866
Space station human productivity study. Volume 2: Executive summary and oral review presentation [NASA-CR-171962] N87-16868

SPACELAB
The welding of aluminum alloys: A new technology in space application N87-17056

SPACELAB PAYLOADS
The non-metallic materials sample array [NASA-TM-86578] N87-16910

SPACETENNAS
A modified loop transfer recovery approach for robust control of flexible structures N87-17029

SPATIAL DISTRIBUTION
Spatially growing disturbances in a two-stream, coplanar jet [NASA-TM-88949] N87-16799
Spatial and temporal variability of infrared-observable properties of the Jovian atmosphere: A partial survey N87-17600
Water vapor in Jupiter's atmosphere N87-17605
The distribution of atomic hydrogen in the Jovian atmosphere N87-17611
Spatial variation of the thermal structure of Jupiter's atmosphere N87-17612
A model of the spatial and temporal variation of the Uranus thermal structure N87-17642

SPATIAL RESOLUTION
Antenna pattern correction in scanning radiometry: A singular system analysis N87-17281
The influence of spatial and temporal scales on calibration/validation — ERS-1 sensors N87-17365

SPECTRAL EMISSION
Calculation of day and night emittance values N87-17131
Yellow supergiants in open clusters N87-17590
Two micron quadrupole line emission of H2 from the Jovian auroral zone N87-17615
On the spectra of gamma-ray bursts at high energies N87-17654

SPECTRAL REFLECTANCE
Imaging spectrometry: Aircraft and space program N87-17202
A statistical approach to select the optimal wavelength bands for separating rocks in the wavelength region 0.4 to 2.3 microns N87-17244
Results of tectonic and spectral investigations along the Wadi Araba fault in Jordan using special processed Thematic Mapping (TM) data N87-17247

SPECTRAL SIGNATURES
Interrelationship between field spectra and airborne MSS systems in the Singatse range, (Yerington) Nevada — multispectral scanner (MSS) mineral exploration N87-17242
A statistical approach to select the optimal wavelength bands for separating rocks in the wavelength region 0.4 to 2.3 microns N87-17244

SPECTROMETERS
Metal content of ocean water studied with radio spectrometer N87-17102
Imaging spectrometry: Aircraft and space program N87-17202
Reflection grating spectrometer for the X-ray Multi-Mirror (XMM) space observatory: design and calculated performance [DE86-013485] N87-17500
An 800 MHz bandwidth acousto-optical spectrometer at Helsinki Observatory N87-17567

SPECTRORADIOMETERS
A knowledge-based software environment for the analysis of spectroradiometer data — mineral identification N87-17203

SPECTROSCOPY
Proceedings of the 15th International Symposium on Shock Waves and Shock Tubes [AD-A173026] N87-17006

SPECTRUM ANALYSIS
Thermal imaging spectroscopy in the Kelso-Baker Region, California N87-17117
Simulation modeling and preliminary analysis of TIMS data from the Carlin area and the northern Grapevine Mountains, Nevada N87-17120
Application of TIMS data in stratigraphic analysis N87-17121
A statistical approach to select the optimal wavelength bands for separating rocks in the wavelength region 0.4 to 2.3 microns N87-17244

SPECULAR REFLECTION
Identification of the contribution of Bragg scattering and specular reflection to X-band microwave backscattering in an ocean experiment N87-17216

SPEECH RECOGNITION
Noise-immune multisensor transduction of speech [AD-A174693] N87-16961

SPHERICAL HARMONICS
Improvement of the Earth's gravity field from terrestrial and satellite data [NASA-CR-180139] N87-17416

SPLINE FUNCTIONS
A representation for piecewise cubic C sup 1-splines on arbitrary triangulations [MEMO-574] N87-17464
Analysis of harmonic spline gravity models for Venus and Mars [NASA-CR-180147] N87-17648

SPRAY CHARACTERISTICS
Representation of the vaporization behavior of turbulent polydisperse sprays by equivalent monodisperse sprays [NASA-TM-88906] N87-16827

SPRAY NOZZLES
Representation of the vaporization behavior of turbulent polydisperse sprays by equivalent monodisperse sprays [NASA-TM-88906] N87-16827

STABILITY AUGMENTATION
Development of a sensitivity analysis technique for multiloop flight control systems N87-16847

STAGNATION POINT
A general method for unsteady stagnation region heat transfer and results for model turbine flows [NASA-TM-88903] N87-17002

STANDARDS
A comparison of two British standard test methods for the determination of resistance to humidity of paint films [MOAD-TP-918] N87-16906

STANDING WAVES
Unified formulation for linear accelerator design [DE86-013441] N87-17491

STAR CLUSTERS
Yellow supergiants in open clusters N87-17590

STAR FORMATION
Numerical calculations of radiation transport in a dusty medium in disk geometry N87-17591

STATIC DEFORMATION
The static aeroelasticity of a composite wing N87-17065

STATIC PRESSURE
Digital program for calculating static pressure position error [NASA-TM-86726] N87-16821

STATISTICAL ANALYSIS
Space shuttle main engine vibration data base [NASA-TM-86576] N87-16876
Statistical analysis of 59 inspected SSME HPFTP turbine blades (uncracked and cracked) [NASA-TM-86584] N87-16877
Empirical relations between the Earth's radiation budget, cloudiness, and various meteorological parameters N87-17424
Profiling under UNIX by patching [NASA-TM-89316] N87-17443
On first passage times and differential equations [AD-A174848] N87-17470

STATISTICAL MECHANICS
Nonlinear wave propagation [AD-A175073] N87-17461

STATOR BLADES
Unsteady flows in a single-stage transonic axial-flow fan stator row [NASA-TM-88929] N87-16805

STATORS
Measurements of the unsteady flow field within the stator row of a transonic axial-flow fan. 1: Measurement and analysis technique [NASA-TM-88945] N87-16789
Measurements of the unsteady flow field within the stator row of a transonic axial-flow fan. Part 2: Results and discussion [NASA-TM-88946] N87-16790
Manufacturing cell for the V2500 variable vanes [PNR90330] N87-16835
Radial and torsionally controlled magnetic bearing [NASA-CASE-GSC-12957-1] N87-17038

STEELS
Quantitative analysis of fracture surfaces using computer aided fractography N87-17076
Dynamic fracture initiation and propagation in 4340 steel under impact loading [AD-A173064] N87-17092

STELLAR COLOR
Yellow supergiants in open clusters N87-17590

STELLAR COMPOSITION
Circumstellar envelopes around evolved stars N87-17548
Molecular abundances in circumstellar envelopes N87-17549

STELLAR ENVELOPES
Circumstellar envelopes around evolved stars N87-17548
Molecular abundances in circumstellar envelopes N87-17549
Some results about laboratory dust analysis in the FIR range — cosmic dust simulation N87-17551
CO observations of the outflow source NGC 7023 N87-17563

STELLAR EVOLUTION
Vibrationally excited cyanoacetylene in regions of massive star formation N87-17561

STELLAR LUMINOSITY
Yellow supergiants in open clusters N87-17590

STELLAR MASS ACCRETION
Redistribution of angular momentum by nonaxisymmetric instabilities in a thick accretion disk [PUBL-SER-C-FASC-4] N87-17585

STELLAR MASS EJECTION
Far infrared submillimeter wave space telescope (FIRST) observations of stars with large mass loss rates N87-17550

STELLAR OSCILLATIONS
Observations of quasi-periodic oscillations in Cyg X-2 [MPE-PREPRINT-61] N87-17576

STELLAR SPECTRA
Observations of quasi-periodic oscillations in Cyg X-2 [MPE-PREPRINT-61] N87-17576
Spectral flux from low-density photospheres N87-17578
Yellow supergiants in open clusters N87-17590
STEPPING MOTORS
Small computer interface to a stepper motor [NASA-TM-86574] N87-16970
STEREOPHOTOGRAPHY
The stereo-pushbroom scanner system Digital Photogrammetry System (DPS) and its accuracy N87-17167
Stereo Line Scanner (SLS): System considerations on an operational instrument for meteorology and weather forecasts N87-17168
Computer-derived height from SIR-B stereo radar images N87-17268
STEREOSCOPY
Analysis of multichannel SAR data of Spitsbergen — glaciology N87-17223
Advanced alternating frame technology (VISIDEP (TM)) and three-dimensional remote sensing N87-17291
STILBENE
Vinyl stilbazoles [NASA-CASE-ARC-11429-3CU] N87-16908
STIRRING
Apparatus and method for stirring fluid borne particles [AD-D012486] N87-17477
STOCHASTIC PROCESSES
Stochastic model of tidal evolution of Earth-Moon system with cyclic change in resonant frequency of ocean N87-17103
On the stochastic dissemination of faults in an admissible network [NASA-CR-178238] N87-17469
A prediction error estimate for nonlinear stochastic systems [RR-295] N87-17471
STORAGE BATTERIES
Safety considerations of lithium-thionyl chloride cells [NASA-CR-180129] N87-17396
The NASA Aerospace Battery Safety Handbook [NASA-CR-180127] N87-17397
STRAIN GAGES
Interferometric load sensor and strain gage [AD-D012509] N87-17021
STRAIN HARDENING
On the influence of strain-path changes on fracture [AD-A172535] N87-17091
STRANGE ATTRACTORS
On routes to chaotic motion in oscillators with unsymmetric and symmetric elastic nonlinearity [ISSN-0208-5658] N87-16969
STRATA
Numerical modeling of two-dimensional time domain electromagnetic scattering by underground inhomogeneities N87-17199
STRATIGRAPHY
Application of TIMS data in stratigraphic analysis N87-17121
Snow stratigraphy observed by an FM-CW microwave system N87-17181
STRATOSPHERE
SAGE aerosol measurements. Volume 3: January 1, 1981 to November 18, 1981 [NASA-RP-1173] N87-17417
Constraints on the composition of Jupiter's stratospheric aerosols from ultraviolet photometry N87-17610
Radiative-convective equilibrium models of Uranus and Neptune N87-17641
STRESS ANALYSIS
Effects of curing stresses on composite structures N87-16930
The theory of finite elastic-plastic deformation with induced anisotropy modelled as combined isotropic-kinematic hardening N87-17074
STRESS CONCENTRATION
Computation of turbulent boundary layer flows with an algebraic stress turbulence model [NASA-CR-178967] N87-16982
STRESS INTENSITY FACTORS
Stress intensity factors for fatigue cracks at holes under cyclic stress gradients N87-17075
Crack propagation in UD (Unidirectional) laminates by the stress intensity factors N87-17084
STRESS MEASUREMENT
Determining and modeling the response of ytterbium piezoresistance transducers [AD-A173085] N87-17023
STRESS PROPAGATION
Dynamic fracture initiation and propagation in 4340 steel under impact loading [AD-A173084] N87-17092
STRING THEORY
Research program in theoretical high-energy physics [DE86-013326] N87-17490
STRIP TRANSMISSION LINES
Microstrip dipoles for EHF and millimeter wave applications [AD-A173025] N87-16976
STRONTIUM COMPOUNDS
The A-X and B-X band systems of SrH: Wavenumbers and molecular constants [USIP-86-04] N87-17486
Research on millimeter wave dielectric materials [AD-A173017] N87-17521
STRUCTURAL ANALYSIS
Analysis of high precision composite sandwich antennas — spacecraft antennas N87-16929
Structural analysis, manufacturing and development status of large polarization sensitive dual-gridded reflectors — satellite antenna N87-16937
Experimental investigation of the turbulence production mechanism in boundary layers [AD-A173091] N87-17007
Structural Analysis [ESA-TT-917] N87-17077
Research on structural analysis at the DFVLR, Brunswick N87-17078
Field consistency and finite element analysis of multifield structural problems N87-17080
Design of software for design of finite element for structural analysis [NASA-TM-88528] N87-17089
Survey of the status of finite element methods for partial differential equations [NASA-CR-178222] N87-17456
Interfacial structure of In/Pt/GaAs heterojunction ohmic contacts [AD-A175102] N87-17523
STRUCTURAL DESIGN
Dielectric support structures for spacecraft antenna feeds N87-16931
Development of 30/20 GHz satellite antenna structures N87-16933
Diffusion welding of component parts in the aviation and space industries [RAE-TRANS-2147] N87-17032
Wind energy technical reading list [DE86-010704] N87-17404
Dynamic analysis and design of the SIRTF primary mirror mount [NASA-CR-180158] N87-17494
The submillimeter telescope (SMT) project N87-17568
STRUCTURAL DESIGN CRITERIA
Geometries for roughness shapes in laminar flow [NASA-CASE-LAR-13255-1] N87-16793
Tethered orbital refueling study [NASA-CR-171953] N87-16855
Space station human productivity study. Volume 4: Issues [NASA-CR-171963] N87-16865
Space station human productivity study. Volume 2: Executive summary and oral review presentation [NASA-CR-171962] N87-16868
Evaluation of Pactruss design characteristics critical to space station primary structure [NASA-CR-178171] N87-16870
STRUCTURAL ENGINEERING
Research on structural analysis at the DFVLR, Brunswick N87-17078
STRUCTURAL FAILURE
Real time identification of large space structures [NASA-CR-171957] N87-16867
STRUCTURAL PROPERTIES (GEOLOGY)
Airborne Thermal Infrared Multispectral Scanner (TIMS) images over disseminated gold deposits, Osgood Mountains, Humboldt County, Nevada N87-17134
Significance of space image, air photo and drainage linears in relation to west coast tectonics, India N87-17232
Structural and geomorphic evolution of Meghalaya plateau, India on LANDSAT imagery N87-17233
STRUCTURAL STABILITY
Structural dynamics and attitude control study of early manned capability space station configurations [NASA-TM-89078] N87-16861
STRUCTURAL STRAIN
Torsion-tension coupling in rods N87-17079
STRUCTURAL VIBRATION
Decentralized control of large-scale systems: Fixed modes, sensitivity and parametric robustness [NASA-TM-88537] N87-17474
SUBMILLIMETER WAVES
Proceedings of an ESA Workshop on a Spaceborne Submillimeter Astronomy Mission. A Cornerstone of the ESA Long Term Science Program [ESA-SP-260] N87-17535
Status of observational astronomy in the 1990's: Position of submillimetre astronomy N87-17536
Review of coherent and incoherent detection techniques: Outlook and limitation — spaceborne submillimeter astronomy N87-17537
Observations of active galactic nuclei with FIRST — Far Infrared Submillimeter Space Telescope (FIRST) N87-17538
A study of planetary atmospheres in the submillimetric range N87-17540
Submillimeter cometary spectroscopy N87-17541
The interstellar medium at submm wavelengths N87-17543
Submillimetre wavelength studies of protostars: The role of FIRST — Far Infrared Submillimeter Space Telescope (FIRST) N87-17544
Interstellar dust N87-17545
Excitation and transfer of submillimeter molecular transitions — interstellar chemistry N87-17546
Interstellar chemistry and submillimeter observations N87-17547
Circumstellar envelopes around evolved stars N87-17548
Far infrared submillimeter wave space telescope (FIRST) observations of stars with large mass loss rates N87-17550
New results about diffuse galactic emission at 380 microns N87-17554
Submillimetre continuum observations of active galactic nuclei N87-17558
Submillimeter observation of the integrated galactic emission from the South Pole N87-17560
A proposed cornerstone mission: Far infrared submillimeter wave telescope (FIRST) N87-17564
Active optics for the far infrared submillimeter wave space telescope (FIRST): A high angular resolution mode N87-17566
The submillimeter telescope (SMT) project N87-17568
The large deployable reflector: A NASA submillimeter-infrared orbiting observatory N87-17571
Structure of molecular clouds and space-based sub-millimeter telescopes, for example FIRST — Far Infrared Submillimeter Wave Space Telescope (FIRST) N87-17574
SUBSONIC FLOW
Prediction of vortex shedding from circular and noncircular bodies in subsonic flow [NASA-CR-4037] N87-16981
Afterbody shape effects on the near-wake velocity characteristics at Mach numbers between 0.35 and 0.92 [ISL-CO-205/86] N87-17011
SUBSTRATES
Microstrip dipoles for EHF and millimeter wave applications [AD-A173025] N87-16976
SUBSTRUCTURES
Elevated waterproof access floor system and method of making the same [NASA-CASE-ARC-11363-1] N87-16918
An effective substructure technique applied to crack problems N87-17083
SUMMER
An inter-sensor comparison of the microwave signatures of Arctic sea ice N87-17184
Microwave properties of sea ice in the marginal ice zone N87-17220
T-28 data acquisition during COHMEX 1986 [NASA-CR-179001] N87-17426
SUNLIGHT
Sun shield [NASA-CASE-MSC-20162-1] N87-17036
SUPERCOMPUTERS
Data communication requirements for the advanced NAS network [NASA-TM-89315] N87-16957
Programming robotics applications on an advanced hypercube multiprocessor [DE86-008895] N87-17445
SUPERCONDUCTORS
Electrical properties of Al-In-Sn alloys directionally solidified in high and low gravitational fields [NASA-TM-86569] N87-16900
Interface circuitry for superconducting bolometer [NASA-TM-86581] N87-17016
Low noise SIS mixer with gain for 80-115 GHz — superconductor-insulator-superconductor (SIS) radio telescope N87-17570
On the feasibility of constructing an imaging array of slot-antennas integrated with SIS mixers — radio astronomy N87-17572
SUPERCRITICAL FLUIDS
Supercritical water oxidation of products of human metabolism [NASA-CR-180144] N87-17430

SUPERFLUIDITY
Sound propagation in a superfluid helium filled porous solid: Theory and experiment N87-17478
SUPERGIANT STARS
Yellow supergiants in open clusters N87-17590
SUPERHEATING
Atmospheric pressure studies of liquid propellant drops in hot flows
[AD-A174639] N87-16915
SUPERHIGH FREQUENCIES
Development of 30/20 GHz satellite antenna structures N87-16933
Features and technologies of ERS-1 (ESA) and X-SAR antennas N87-17152
The X-SAR System N87-17162
Rain measurement results derived from a two polarization S-band radar employing frequency diversity at Wallops Island, Virginia N87-17182
C and Ku-band scatterometer results from the SCATTMOD internal wave experiment N87-17215
Identification of the contribution of Bragg scattering and specular reflection to X-band microwave backscattering in an ocean experiment N87-17216
A scatterometer operating at 10 GHz N87-17262
Calibrated X and L-band scattering coefficients from a southern US forest N87-17312
The X-band SAR in a joint mission with the Shuttle Imaging Radar N87-17321
L to X-band scatter and emission measurements of vegetation N87-17347
Antenna ambiguity investigations for X-SAR — shuttle-borne radar N87-17355
X-SAR extends the frequency range of Shuttle Imaging Radar N87-17362
SUPERNOVAE
Spectral flux from low-density photospheres N87-17578
SUPERPLASTICITY
Application of diffusion bonding combined with superplastic forming (SPF/DB) to the fabrication of TAGV metal sheet structures N87-17060
SUPERSONIC AIRCRAFT
Computational, unsteady transonic aerodynamics and aeroelasticity about airfoils and wings
[NASA-TM-89414] N87-16801
Optimal turning at high angle of attack of supersonic and hypersonic vehicles N87-16814
AFTI/F-111 MAW flight control system and redundancy management description
[NASA-TM-88267] N87-16819
SUPERSONIC BOUNDARY LAYERS
Stability characteristics of a supersonic boundary layer and their relation to the position of the laminar-turbulent transition point
[NASA-TM-88533] N87-16797
SUPERSONIC FLOW
Calculation of supersonic flow over a compression corner N87-16785
Computation of separation ahead of blunt fin in supersonic turbulent flow
[NASA-TM-89416] N87-16791
Application of flow calculation methods to transonic and supersonic axial turbomachines
[ONERA-RTS-80/7103-EY] N87-16846
Aeroacoustics of supersonic jet flows from contoured and solid/porous conical plug-nozzles
[NASA-CR-178095] N87-17484
SUPERSONIC TRANSPORTS
Simulated flight acoustic investigation of treated ejector effectiveness on advanced mechanical suppressors for high velocity jet noise reduction
[NASA-CR-4019] N87-17481
SUPERSONIC TURBINES
Measurements of the unsteady flow field within the stator row of a transonic axial-flow fan. Part 2: Results and discussion
[NASA-TM-88946] N87-16790
SUPPORTS
Flameholder with removable flameholder attachments
[AD-D012466] N87-16893
Dielectric support structures for spacecraft antenna feeds N87-16931
SURFACE COOLING
Transitional boundary layers under the influence of high free stream turbulence, intensive wall cooling and high pressure gradients in hot gas circulation
[NASA-TM-88524] N87-16983
SURFACE DEFECTS
Three dimensional CTOD measurements of elastic-plastic surface flaws
[DE86-013454] N87-17093
SURFACE DISTORTION
Simple approach for evaluating mechanical reflector antenna distortions — satellite antennas N87-16942
SURFACE PROPERTIES
Surface flaw reliability analysis of ceramic comonents with the SCARE finite element postprocessor program
[NASA-TM-88901] N87-17087
SURFACE ROUGHNESS
Dielectric and surface parameters related to microwave scatter and emission properties N87-17262
Observations of surface currents at Nantucket Shoals and implications for radar imaging of the bottom N87-17296
SURFACE ROUGHNESS EFFECTS
Dependence of snow melting and surface-atmosphere interactions on the forest structure N87-17318
Radiometric correction method which removes both atmospheric and topographic effects from the LANDSAT-MSS data N87-17329
Evaluating roughness models of radar backscatter N87-17344
SURFACE TEMPERATURE
Ocean surface temperature field variability N87-17104
Estimation of absolute water surface temperature based on atmospherically corrected thermal infrared multispectral scanner digital data N87-17114
Enhancement of time images for photointerpretation N87-17116
Calculation of day and night emittance values N87-17131
Discrimination of soil hydraulic properties by combined thermal infrared and microwave remote sensing N87-17303
SURFACE WAVES
Applications of SOLA to free surface flows — flow computing method N87-16998
Observations of surface currents at Nantucket Shoals and implications for radar imaging of the bottom N87-17296
SURGES
High energy surge arrester technology development, part 2
[AD-A173086] N87-16977
Monitoring transients in low inductance circuits
[DE86-013756] N87-16978
SWEPT FORWARD WINGS
The static aeroelasticity of a composite wing N87-17085
SWIRLING
Particle-laden swirling free jets: Measurements and predictions
[NASA-TM-88904] N87-16826
SWITCHING CIRCUITS
A pi-section digital phase shifter apparatus
[AD-D012495] N87-16973
Switching network for monitoring stations
[AD-D012514] N87-17022
SYMMETRY
A parallel solution for the symmetric Eigenproblem
[NASA-TM-89082] N87-17086
SYNCHRONISM
An experimental microcomputer controlled system for synchronized pulsating anti-gravity suit
[AD-A174640] N87-17433
SYNCHROTRON RADIATION
CF2 and CFCl fluorescence from VUV excitation of C2F3Cl N87-16891
SYNOPTIC METEOROLOGY
The Jovian Atmospheres
[NASA-CP-2441] N87-17598
SYNTHESIS (CHEMISTRY)
Ethynyl terminated ester oligomers and polymers therefrom
[NASA-CASE-LAR-13118-2] N87-16907
SYNTHETIC APERTURE RADAR
Development status of the ERS-1 SAR antenna N87-16939
The Second Spaceborne Imaging Radar Symposium
[NASA-CR-180131] N87-17135
Geological applications of multipolarization SAR data N87-17140
Venus Radar Mapper (VRM): Multimode radar system design N87-17142
Spaceborne Imaging Radar Project N87-17143
An alternative multi-mode SAR for RADARSAT N87-17144
Present statue of Japanese ERS-1 Project N87-17145
A scanning radar altimeter for mapping continental topography N87-17146
Operational wave forecasting with spaceborne SAR: Prospects and pitfalls N87-17149
Observing the polar oceans with spaceborne radar N87-17151
Features and technologies of ERS-1 (ESA) and X-SAR antennas N87-17152
Off-line processing of ERS-1 synthetic aperture radar data with high precision and high throughput N87-17153
RADARSAT high throughput SAR processor development N87-17154
Analysis of multiple incidence angle SIR-B data for determining forest stand characteristics N87-17156
Multiple incidence angle SIR-B experiment over Argentina N87-17157
SIR-B measurements and modeling of vegetation N87-17160
SIR-C, the next generation spaceborne SAR N87-17161
The X-SAR System N87-17162
Automated remote sensing of sea ice using synthetic aperture radar N87-17186
An overview of operational SAR data collection and dissemination plans for ERS-1 ice data in Canada N87-17189
Development status of the ERS-1 payload instruments N87-17191
Geophysics of the marginal ice zone from SAR N87-17219
SAR ice floe kinematics and correlation with mesoscale oceanic structure within the marginal ice zone N87-17222
Analysis of multichannel SAR data of Spitsbergen — glaciology N87-17223
ERS-1 synthetic aperture radar fast delivery processor N87-17228
Canadian plans for operational demonstrations of satellite imaging radar applications — ERS-1 N87-17229
The German ERS-1 SAR postprocessing system plans and concepts N87-17231
Radar imagery of the European city influenced by variations in depression angle and look direction N87-17237
Multispectral classification of microwave remote sensing images — SAR crop identification N87-17238
Extraction of the backscatter coefficient of agricultural fields from an airborne SAR image N87-17265
Merging spaceborne image data of optical and microwave sensors N87-17267
Digital terrain mapping with STAR-1 SAR data N87-17269
Multifrequency-polarimetric SAR for remote sensing N87-17280
Analysis of the spatial structure of Synthetic Aperture Radar (SAR) imagery for a better separability of cereal crops, wheat and barley N87-17287
Estimation of internal wave currents from SAR and infrared scatterometer imagery N87-17295
Analysis of synthetic aperture radar imagery of surface ship wakes N87-17297
SAR imaging of bottom topography in the ocean: Results from an improved model N87-17298
An improved method for the determination of water depth from surface wave refraction patterns — SAR imagery N87-17299
SAR imagery for forest management N87-17313
Future user requirements and required technological developments of spaceborne synthetic aperture radars N87-17320
The X-band SAR in a joint mission with the Shuttle Imaging Radar N87-17321
An advanced SAR design for future land missions N87-17322
Characteristics of a very low altitude spacecraft for collecting global directional wave spectra with spaceborne synthetic aperture radar N87-17333
The SAR image modulation transfer function derived from SIR-B image spectra and airborne measurements of ocean wave height spectra N87-17334
SIR-B observations of ocean waves in the NE Atlantic N87-17335
Characterisation of internal wave surface patterns on airborne SAR imagery N87-17338
Effects of rain cells on SAR performance N87-17354
Antenna ambiguity investigations for X-SAR — shuttle-borne radar N87-17355
Reconsideration of azimuth ambiguities in SAR N87-17356
Planar array antenna for ERS-1 synthetic aperture radar N87-17357
A satellite-borne SAR transmitter and receiver N87-17358
Analysis of amplitude nonlinearities in the ERS-1 SAR receiver system N87-17359
Pulse compression test results of the SAR transmitter and receiver — satellite-borne SAR N87-17360
A powerful utility for assessing the performance of the ERS-1 synthetic aperture radar N87-17361
X-SAR extends the frequency range of Shuttle Imaging Radar N87-17362

A procedure for estimation of two-dimensional ocean height-variance spectra from SAR imagery N87-17381
A scatterometer research program N87-17391
Bulk Richardson's number isograms deduced from SAR data — ocean surface N87-17392
SYNTHETIC APERTURES
Application of Spaceborne Distributed Aperture/Coherent Array Processing (SDA/CAP) technology to active and passive microwave remote sensing N87-17277
SYNTHETIC ARRAYS
The Electronically Steered Thinned Array Radiometer (ESTAR) N87-17260
Application of Spaceborne Distributed Aperture/Coherent Array Processing (SDA/CAP) technology to active and passive microwave remote sensing N87-17277
SYSTEM IDENTIFICATION
Identification of a dynamic model of a helicopter from flight tests N87-16813
Recursive techniques in identification [OUEL-1644/86] N87-17462
SYSTEMS ANALYSIS
Air traffic control radar beacon system transponder performance study and analysis. Volume 2: Appendixes [DOT/FAA/FS-86/1-VOL-2] N87-16812
Spacecraft attitude control momentum requirements analysis [NASA-CR-178219] N87-16864
Wind energy technical reading list [DE86-010704] N87-17404
Decentralized control of large-scale systems: Fixed modes, sensitivity and parametric robustness [NASA-TM-88537] N87-17474
SYSTEMS COMPATIBILITY
Portable EDITOR (PEDITOR): A portable image processing system — satellite images N87-17206
The image processing workbench - portable software for remote sensing instruction and research N87-17209
SYSTEMS ENGINEERING
Space station human productivity study, volume 1 [NASA-CR-171961] N87-16869
Venus Radar Mapper (VRM): Multimode radar system design N87-17142
The design and evaluation of a high performance smalltalk system [AD-A173022] N87-17437
SYSTEMS SIMULATION
The ERS-1 scatterometer system simulator and its relevance for ground processing design N87-17257
Remote sensing of tree attenuation at 870 MHz along simulated Earth-satellite paths N87-17306
A powerful utility for assessing the performance of the ERS-1 synthetic aperture radar N87-17361
SYSTEMS STABILITY
The analysis and resolution of numerical schemes — flow problems N87-16991

T

T-28 AIRCRAFT
T-28 data acquisition during COHMEX 1986 [NASA-CR-179001] N87-17426
TABLES (DATA)
A study of anomalous propagation at radar frequencies and a proposal for a radar coverage forecasting model, book 2 of 2 [ETN-87-98938] N87-16967
TAIL ASSEMBLIES
Flight investigation of the effect of tail configuration on stall, spin, and recovery characteristics of a low-wing general aviation research airplane [NASA-TP-2644] N87-16815
TANKS (COMBAT VEHICLES)
Tank tread assemblies with track-linking mechanism [NASA-CASE-NPO-16321-1CU] N87-17034
TECHNICAL WRITING
FY 1986 scientific and technical reports, articles, papers and presentations [NASA-TM-86575] N87-17532
TECHNOLOGICAL FORECASTING
Future trends in propulsion — aircraft [PNR90349] N87-16840
The technology of advanced prop-fan transmissions [PNR90357] N87-16843
TECHNOLOGY ASSESSMENT
Loads and Aeroelasticity Division research and technology accomplishments for FY 1986 and plans for FY 1987 [NASA-TM-89084] N87-16796
Concept definition for space station technology development experiments. Experiment definition, task 2 [NASA-CR-178153] N87-16860
Components and comparisons of potential information from several imaging satellites N87-17164
Comparative study of LANDSAT MSS, Salyut-7 (TERRA) and radar (SIR-A) images for geological and geomorphological applications: A case study from Rajasthan and Gujarat, India N87-17236
Scientific and technical information output of the Langley Research Center for calendar year 1986 [NASA-TM-89065] N87-17531
TECHNOLOGY TRANSFER
The transfer of remote sensing technology to developing countries: A survey of experts in the field N87-17170
Scientific and technical information output of the Langley Research Center for calendar year 1986 [NASA-TM-89065] N87-17531
TECHNOLOGY UTILIZATION
Aircraft derivative gas turbine development in China [PNR90359] N87-16844
Industrial holography: The Rolls-Royce experience [PNR90351] N87-17024
The transfer of remote sensing technology to developing countries: A survey of experts in the field N87-17170
Microwave remote sensing: Its applications and limitations in operational tasks of land use inventory and forest management N87-17266
Applications of remote sensing in the US Department of Agriculture N87-17285
Thermal infrared remote sensing: One of today's solutions N87-17324
Applications of focused ion beams in microelectronics [RSRE-MEMO-3948] N87-17517
TECTONICS
Tectonic geomorphology of the Andes with SIR-A and SIR-B N87-17136
Delineation of fault zones using imaging radar N87-17138
Significance of space image, air photo and drainage linears in relation to west coast tectonics, India N87-17232
Results of tectonic and spectral investigations along the Wadi Araba fault in Jordan using special processed Thematic Mapping (TM) data N87-17247
TEFLON (TRADEMARK)
Hypersonic nonequilibrium flow over an ablating teflon surface N87-16787
TEKTITES
Zhamanshin meteor crater [NASA-TM-88531] N87-17595
TELECOMMUNICATION
ICNIA (Integrated Communications Navigation Identification Avionics) HF transmitter system preliminary study [AD-A173013] N87-16823
TELEMETRY
Single frequency multitransmitter telemetry [NASA-CASE-LAR-13008-1] N87-16863
TEMPERATURE CONTROL
Engineering and software interfacing for thermal, structural and dynamic control related with spacecraft activities N87-16948
TEMPERATURE DISTRIBUTION
Thermal balance of the atmospheres of Jupiter and Uranus N87-17604
Global dynamics and thermal structure of Jupiter's atmosphere N87-17621
A model of the spatial and temporal variation of the Uranus thermal structure N87-17642
TEMPERATURE EFFECTS
Preliminary investigations into the microcracking of PMR-15/graphite composites. Part 1: Effect of cure temperature [PNR90348] N87-16887
A preliminary study of factors affecting the calibration stability of the iridium versus iridium-40 percent rhodium thermocouple [NASA-TM-89086] N87-17018
TEMPERATURE GRADIENTS
Ocean surface temperature field variability N87-17104
On the oblateness and rotation rate of Neptune's atmosphere N87-17644
TEMPERATURE MEASUREMENT
Enhancement of time images for photointerpretation N87-17116
Monitoring vegetation recovery patterns on Mount St. Helens using thermal infrared multispectral data N87-17122
Investigation of forest canopy temperatures recorded by the thermal infrared multispectral scanner at H. J. Andrews Experimental Forest N87-17123
Models for temperature estimation from remotely sensed thermal IR data N87-17325
TEMPERATURE PROBES
Unitized high temperature probes [AD-D012508] N87-17020
TEMPERATURE PROFILES
On the possible role of the bootstrap effect in the RF current drive experiments, part 2 [IPPCZ-263] N87-17504
TEMPORAL DISTRIBUTION
Spatial and temporal variability of infrared-observable properties of the Jovian atmosphere: A partial survey N87-17600
A model of the spatial and temporal variation of the Uranus thermal structure N87-17642
TEMPORAL RESOLUTION
The influence of spatial and temporal scales on calibration/validation — ERS-1 sensors N87-17365
TENSILE DEFORMATION
On the influence of strain-path changes on fracture [AD-A172535] N87-17091
TENSILE STRENGTH
Influence of welding flaws on the fatigue strength of electron beam weldments in Ti Al6 V4 N87-17065
Inertia welding of nitralloy N and 18 nickel maraging 250 grade steels for utilization in the main rotor drive shaft for the AR-64 military helicopter program N87-17067
TENSILE STRESS
Test apparatus for uniform tensioning of long lengths of small cables in simulated environments [AD-D012487] N87-17045
TENSILE TESTS
Mechanisms of helium embrittlement N87-16899
TENSIOMETERS
Test apparatus for uniform tensioning of long lengths of small cables in simulated environments [AD-D012487] N87-17045
TERRAIN
Multiple incidence angle SIR-B experiment over Argentina N87-17157
Interferometer applications for the rectification of radar images N87-17241
Computer-derived height from SIR-B stereo radar images N87-17268
Digital terrain mapping with STAR-1 SAR data N87-17269
TEST FACILITIES
Compendium of NASA Langley reports on hypersonic aerodynamics [NASA-TM-87760] N87-16802
Description of the Spacecraft Control Laboratory Experiment (SCOLE) facility [NASA-TM-89057] N87-16848
A distributed data acquisition system for aeronautics test facilities [NASA-TM-88961] N87-16851
Research opportunities in microgravity science and applications during shuttle hiatus [NASA-TM-88964] N87-16917
TEST STANDS
Outdoor test stand performance of a convertible engine with variable inlet guide vanes for advanced rotorcraft propulsion [NASA-TM-88939] N87-16825
TETHERED SATELLITES
System engineering study of electrodynamic tether as a spaceborne generator and radiator of electromagnetic waves in the ULF/ELF frequency band [NASA-CR-180156] N87-16956
TETHERING
Tethered orbital refueling study [NASA-CR-171953] N87-16855
TETHERLINES
Tethered orbital refueling study [NASA-CR-171953] N87-16855
Non-backdriveable free wheeling coupling [NASA-CASE-MSC-20475-1] N87-17037
TEXAS
The Red River Valley archeological project N87-17128
THEMATIC MAPPING
Application of TIMS data in stratigraphic analysis N87-17121
The application of remotely sensed data to pedologic and geomorphic mapping on alluvial fan and playa surfaces in Saline Valley, California N87-17127
Tectonic geomorphology of the Andes with SIR-A and SIR-B N87-17136
Analysis of multiple incidence angle SIR-B data for determining forest stand characteristics N87-17156
Comparison of Thematic Mapper (TM) and SPOT simulation data for agricultural applications in south west Germany N87-17165
Sri Lanka's solution to land use mapping and monitoring for Third World countries development N87-17174
Hydrogeological research in Peloponnesus (Greece) Karst area by support and completion of LANDSAT-thematic data N87-17234
Computer-aided analysis of LANDSAT data for mapping geologic and geomorphic features, North Bombay, India N87-17235

Discrimination of lithologic units using geobotanical and LANDSAT TM spectral data N87-17246
Results of tectonic and spectral investigations along the Wadi Araba fault in Jordan using special processed Thematic Mapping (TM) data N87-17247
Bitemporal analysis of Thematic Mapper data for land cover classification N87-17249
Evaluation of LANDSAT 5 Thematic Mapping (TM) data for image clustering and classification N87-17251
Merging spaceborne image data of optical and microwave sensors N87-17267
An iterative multi-resolution shape-from-shading algorithm and its application to planetary mapping N87-17331
Rural land use inventory and mapping in the Ardeche area (France) using multitemporal Thematic Mapping (TM) data N87-17350
LANDSAT-5 Thematic Mapping (TM) data applications to land use classification on around the Bosphorus area, Turkey N87-17351
Discrimation of land features using LANDSAT false colour composite in N Iran N87-17352

THEORETICAL PHYSICS
Research program in theoretical high-energy physics [DE86-013326] N87-17490

THERMAL ANALYSIS
The Extendable Refractable Mast (ERM) thermal analysis: A heat radiation case study via the finite element method N87-16949
Thermal infrared imagery from helicopter for heat loss calculations in industrial plants N87-17326
Crystal growth and furnace analysis [NASA-CR-179098] N87-17516

THERMAL EMISSION
Effect of electrical and thermal properties of materials on microwave brightness temperature of the terrestrial crust N87-17263
Maser and thermal SiO emission in evolved stars N87-17553

THERMAL EXPANSION
Composite space antenna structures: Properties and environmental effects [NASA-TM-88859] N87-16880
Mechanical properties of graphite epoxy used for Zero CTE Program [DE86-013227] N87-16886

THERMAL INSULATION
Thermal infrared imagery from helicopter for heat loss calculations in industrial plants N87-17326

THERMAL MAPPING
The TIMS Data User's Workshop [NASA-CR-180130] N87-17111
The TIMS instrument N87-17112
The TIMS investigator's guide N87-17113
Estimation of absolute water surface temperature based on atmospherically corrected thermal infrared multispectral scanner digital data N87-17114
Atmospheric correction of TIMS data N87-17115
Enhancement of time images for photointerpretation N87-17116
Thermal imaging spectroscopy in the Kelso-Baker Region, California N87-17117
Lithologic mapping of silicate rocks using TIMS N87-17118
Detection and mapping of volcanic rock assemblages and associated hydrothermal alteration with Thermal Infrared Multiband Scanner (TIMS) data Comstock Lode Mining District, Virginia City, Nevada N87-17119
Simulation modeling and preliminary analysis of TIMS data from the Carlin area and the northern Grapevine Mountains, Nevada N87-17120
Application of TIMS data in stratigraphic analysis N87-17121
Monitoring vegetation recovery patterns on Mount St. Helens using thermal infrared multispectral data N87-17122
Investigation of forest canopy temperatures recorded by the thermal infrared multispectral scanner at H. J. Andrews Experimental Forest N87-17123
Applications of TIMS data in agricultural areas and related atmospheric considerations N87-17124
Locating subsurface gravel with thermal imagery N87-17125
TIMS data applications in Nebraska N87-17126
The application of remotely sensed data to pedologic and geomorphic mapping on alluvial fan and playa surfaces in Saline Valley, California N87-17127
The physical basis for spectral variations in thermal infrared emittance of silicates and application to remote sensing N87-17129
Infrared spectroscopy for geologic interpretation of TIMS data N87-17130
Calculation of day and night emittance values N87-17131
Application of Thermal Infrared Multiband Scanner (TIMS) data to mapping of Plutonic and stratified rock and assemblages in accreted terrains of the Northern Sierra, California N87-17132
A geologic atlas of TIMS data N87-17133
Airborne Thermal Infrared Multispectral Scanner (TIMS) images over disseminated gold deposits, Osgood Mountains, Humboldt County, Nevada N87-17134
Concept of a future multispectral Thermal Infrared (TIR) pushbroom mission for Earth observation from space N87-17169
Spatial and temporal variability of infrared-observable properties of the Jovian atmosphere: A partial survey N87-17800
Investigation of long-lived eddies on Jupiter N87-17833

THERMAL PLASMAS
The astrophysical implications of weakly interacting, massive particles N87-17592

THERMAL RADIATION
Spatial variation of the thermal structure of Jupiter's atmosphere N87-17612

THERMAL RESISTANCE
Fire and heat resistant laminating resins based on maleimido substituted aromatic cyclotriphosphazene polymer [NASA-CASE-ARC-11428-2] N87-16909

THERMAL STABILITY
Design of a low distortion shared aperture reflector — satellite antenna N87-16934
Non-solar noble gas abundances in the atmosphere of Jupiter N87-17637

THERMITES
Preparations of rare earth-iron alloys by thermite reduction [DE86-013753] N87-16904

THERMOCOUPLES
A preliminary study of factors affecting the calibration stability of the iridium versus iridium-40 percent rhodium thermocouple [NASA-TM-89086] N87-17018

THERMODYNAMIC EQUILIBRIUM
Para hydrogen equilibration in the atmospheres of the outer planets N87-17599
Thermal balance of the atmospheres of Jupiter and Uranus N87-17604
Radiative-convective equilibrium models of Uranus and Neptune N87-17641

THERMODYNAMIC PROPERTIES
Thermomechanical characteristics of dichroic subreflectors — satellite antennas N87-16952

THERMODYNAMICS
Thermodynamic estimate of climatic system efficiency N87-17096
ATHENA code manual. Volume 1: Code structure, system models, and solution methods [DE87-001430] N87-17492
The Jovian Atmospheres [NASA-CP-2441] N87-17598

THERMOELASTICITY
Thermoelastic testing of stratified materials N87-17064

THESAURI
NASA thesaurus supplement (supplement 2) [NASA-SP-7053(SUPP-2)] N87-17530

THICKNESS
Effect of adherend thickness and mixed mode loading on debond growth in adhesively bonded composite joints [NASA-TM-88992] N87-16882

THIN FILMS
Soluble aromatic polyimides for film and coating applications [NASA-TM-89016] N87-16911
Optical thin film monitoring using optical fibers [DE87-001355] N87-17501

THREE DIMENSIONAL BODIES
A three dimensional calculation of elastic equilibrium for composite materials [NASA-CR-178158] N87-17088

THREE DIMENSIONAL BOUNDARY LAYER
The study of shock wave and turbulent boundary layer interactions [AD-A175033] N87-17008

THREE DIMENSIONAL FLOW
Measurement of the three-dimensional aerodynamics of an annular cascade airfoil row N87-16788
Euler analysis of the three dimensional flow field of a high-speed propeller: Boundary condition effects [NASA-TM-88955] N87-16798
Laser Doppler velocimeter measurements and theoretical investigation of three dimensional scroll flow N87-16979
The spatial levels of approximation from three-dimensional to quasi one-dimensional representation — averaging procedure (flow computation) N87-16989
Three-dimensional separation on a cylindrical ellipsoid. Results of the first test campaign on the F2 wind tunnel [ONERA-RT-16/7252-AN] N87-17013

THREE DIMENSIONAL MOTION
A new method for compensating and measuring any motion of 3D-objects in holographic interferometry: Recent developments [ISL-CO-242/85] N87-17025

TIDES
Stochastic model of tidal evolution of Earth-Moon system with cyclic change in resonant frequency of ocean N87-17103

TIME
On first passage times and differential equations [AD-A174648] N87-17470

TIME DEPENDENCE
On the analytical determination of relaxation modulus of viscoelastic materials by Prony's interpolation method [NASA-TM-86579] N87-17455

TIME LAG
Piloted simulator study of allowable time delays in large-airplane response [NASA-TP-2652] N87-16849

TIME MEASUREMENT
Profiling under UNIX by patching [NASA-TM-89316] N87-17443

TIME SERIES ANALYSIS
Bitemporal analysis of Thematic Mapper data for land cover classification N87-17249

TIROS N SERIES SATELLITES
Atmospheric corrections of NOAA-AVHRR data verification of different methods by ground truth measurements N87-17274

TITAN
The Cassini mission N87-17638

TITANIUM ALLOYS
Fabrication of hollow, cored, and composite shaped parts from selected alloy powders [AD-D012489] N87-16903
The application of diffusion bonding and laser welding in the fabrication of aerospace structures N87-17054
Economical manufacturing and inspection of the electron-beam-welded Tornado wing box N87-17055
Diffusion bonding in the manufacture of aircraft structure N87-17057
Application of diffusion bonding combined with superplastic forming (SPF/DB) to the fabrication of TAGV metal sheet structures N87-17060
Ultrasonic testing techniques for diffusion-bonded titanium components N87-17061
Influence of welding flaws on the fatigue strength of electron beam weldments in Ti Al6 V4 N87-17065
On the influence of strain-path changes on fracture [AD-A172535] N87-17091

TOKAMAK DEVICES
On the possible role of the bootstrap effect in the RF current drive experiments, part 2 [IPPCZ-263] N87-17504
Plasma formation and sustainment by a multijunction grill on the castor tokamak [IPPCZ-255] N87-17506

TOPOGRAPHY
Application of Thermal Infrared Multiband Scanner (TIMS) data to mapping of Plutonic and stratified rock and assemblages in accreted terrains of the Northern Sierra, California N87-17132
Spaceborne imaging radar research in the 90's N87-17141
A scanning radar altimeter for mapping continental topography N87-17146
SAR imaging of bottom topography in the ocean: Results from an improved model N87-17298

TORCHES
Welding torch with arc light reflector [NASA-CASE-MFS-29134-1] N87-17493

TOROIDAL PLASMAS
On the possible role of the bootstrap effect in the RF current drive experiments, part 2 [IPPCZ-263] N87-17504
Plasma formation and sustainment by a multijunction grill on the castor tokamak [IPPCZ-255] N87-17506
Tilt stability of field-reversed configurations [IPPJ-802] N87-17510
A self-consistent modeling of a quasi-steady state compact torus evolving to ignition [IPPJ-801] N87-17511

TORQUE
The possibility of reducing the cyclic torque fluctuations produced by two-stroke engines using the storage of magnetostatic energy [RAE-TM-RAD-NAV-265] N87-17042

TORSION
Torsion-tension coupling in rods N87-17079

TOWERS
Tower-based broadband backscattering measurements from the ocean surface in the North Sea N87-17217
TRACKED VEHICLES
Tank tread assemblies with track-linking mechanism [NASA-CASE-NPO-16321-1CU] N87-17034
TRADEOFFS
Some trade-offs in modest-resolution radars for space N87-17278
TRAINING DEVICES
In service training of scientists and engineers: An important method of information transfer in the area of satellite remote sensing and its applications N87-17171
TRANSFER FUNCTIONS
Identification of a dynamic model of a helicopter from flight tests N87-16813
The single scattering phase functions of Jupiter's clouds N87-17613
TRANSFER ORBITS
Aeroassisted coplanar orbital transfer of flight vehicles using the sequential gradient restoration algorithm N87-16857
TRANSFORMATIONS (MATHEMATICS)
An implementation of the Hough transform using a linear array processor in conjunction with a PDP/11microprocessor --- computer vision [NPL-DITC-74/86] N87-17438
TRANSIENT LOADS
Wind Scatterometer Antenna (WSA) release shock loads --- ERS-1 N87-16945
TRANSITION FLOW
Stability characteristics of a supersonic boundary layer and their relation to the position of the laminar-turbulent transition point [NASA-TM-88533] N87-16797
Transition mixing study [NASA-CR-175062] N87-16830
TRANSMISSION LINES
Monitoring transients in low inductance circuits [DE86-013756] N87-16978
TRANSMISSION LOSS
Vegetation influence on wave propagation [FOA-B-30097-3.3] N87-16965
Transmission loss measurements in mobile radio nets [FOA-B-30098-3.3] N87-16966
TRANSMISSIONS (MACHINE ELEMENTS)
The technology of advanced prop-fan transmissions [PNR90357] N87-16843
Common problems and pitfalls in gear design [NASA-TM-88858] N87-17033
Design and dynamic simulation of a fixed pitch 56 kW wind turbine drive train with a continuously variable transmission [NASA-CR-179543] N87-17401
TRANSMITTERS
ICNIA (Integrated Communications Navigation Identification Avionics) HF transmitter system preliminary study [AD-A173013] N87-16823
Single frequency multitransmitter telemetry [NASA-CASE-LAR-13006-1] N87-16863
The 20 GHz power GaAs FET development [NASA-CR-179546] N87-16972
High energy surge arrester technology development, part 2 [AD-A173086] N87-16977
TRANSONIC COMPRESSORS
Measurements of the unsteady flow field within the stator row of a transonic axial-flow fan. 1: Measurement and analysis technique [NASA-TM-88945] N87-16789
TRANSONIC FLIGHT
Computational, unsteady transonic aerodynamics and aeroelasticity about airfoils and wings [NASA-TM-89414] N87-16801
TRANSONIC FLOW
The aerodynamics and aeroacoustics of rotating transonic disturbances N87-16786
Euler solutions using an implicit multigrid technique [NASA-TM-58276] N87-16792
Navier-Stokes solution for laminar transonic flow over a NACA0012 airfoil [FAA-140] N87-16794
Transonic unsteady aerodynamic and aeroelastic calculations about airfoils and wings [NASA-TM-89417] N87-16800
Unsteady flows in a single-stage transonic axial-flow fan stator row [NASA-TM-88929] N87-16805
An LU-SSOR scheme for the Euler and Navier-Stokes equations [NASA-CR-179556] N87-16806
Profile design in transonic regime [ETN-87-98849] N87-16810
Application of flow calculation methods to transonic and supersonic axial turbomachines [ONERA-RTS-80/7103-EY] N87-16846
Analysis of viscous transonic flow over airfoil sections [NASA-TM-88912] N87-17001
TRANSPONDERS
Air traffic control radar beacon system transponder performance study and analysis. Volume 2: Appendixes [DOT/FAA/FS-86/1-VOL-2] N87-16812
TRANSPORT AIRCRAFT
Piloted simulator study of allowable time delays in large-airplane response [NASA-TP-2652] N87-16849
Flight service evaluation of advanced composite ailerons on the L-1011 transport aircraft [NASA-CR-178170] N87-16883
TRANSPORT PROPERTIES
Recent developments in discrete-ordinates electron transport [DE86-007827] N87-17485
TRANSPORT THEORY
A transportation queueing model, solved as a Riemann boundary value problem [MEMO-573] N87-17463
TRANSPORTATION
A transportation queueing model, solved as a Riemann boundary value problem [MEMO-573] N87-17463
TRANSVERSE WAVES
Free electron diode oscillator [AD-D012519] N87-16975
TRAVELING WAVES
Unified formulation for linear accelerator design [DE86-013441] N87-17491
TREADS
Tank tread assemblies with track-linking mechanism [NASA-CASE-NPO-16321-1CU] N87-17034
TREES
Calibrated X and L-band scattering coefficients from a southern US forest N87-17312
TREES (PLANTS)
Remote sensing of tree attenuation at 870 MHz along simulated Earth-satellite paths N87-17306
The significance of Radar Cross Section (RCS) polarization measurements for tree signatures N87-17308
Coherent polarimetric Radar Cross Section (RCS) measurements on trees N87-17310
X and L-band backscattering measurements of agricultural crops, forest stands and single trees N87-17311
TRIANGLES
Batten augmented triangular beam [NASA-CR-172461] N87-16916
TRIANGULATION
A representation for piecewise cubic C sup 1-splines on arbitrary triangulations [MEMO-574] N87-17464
TROPICAL REGIONS
Evaluation of geophysical parameters measured by the Nimbus-7 microwave radiometer for the TOGA Heat Exchange Project [NASA-CR-180151] N87-17110
TROPOSPHERE
Para hydrogen equilibration in the atmospheres of the outer planets N87-17599
Changes in Saturn's south-temperate haze distribution during the summer of 1973-1980 N87-17602
An updated hydrocarbon photochemical model for the Jovian atmosphere from the troposphere through the homopause: A prelude to Galileo N87-17636
TROPOSPHERIC SCATTERING
A study of anomalous propagation at radar frequencies and a proposal for a radar coverage forecasting model, book 2 of 2 [ETN-87-98938] N87-16967
TRUSSES
Structural dynamics and attitude control study of early manned capability space station configurations [NASA-TM-89078] N87-16861
Evaluation of Pactruss design characteristics critical to space station primary structure [NASA-CR-178171] N87-16870
TUNGSTEN
Integration of surficial geochemistry and LANDSAT imagery to discover skarn tungsten deposits using image analysis techniques [CONTRIB-19586] N87-17248
TUNNEL DIODES
High band gap 2-6 and 3-5 tunneling junctions for silicon multijunction solar cells [NASA-CASE-NPO-16526-1CU] N87-17399
TURBINE BLADES
Burner rig and engine test experience of platinum aluminide coatings [PNR90342] N87-16837
Bonding of superalloys by diffusion welding and diffusion brazing N87-17059
HAWT performance with dynamic stall [DE86-004428] N87-17402
TURBINE PUMPS
Advanced 3-D viscous SSME turbine rotor stator CFD algorithms [NASA-CR-178997] N87-16829
Statistical analysis of 59 inspected SSME HPFTP turbine blades (uncracked and cracked) [NASA-TM-86584] N87-16877
Space shuttle main engine high pressure fuel pump aft platform seal cavity flow analysis [NASA-TP-2685] N87-17000
TURBINES
A general method for unsteady stagnation region heat transfer and results for model turbine flows [NASA-TM-88903] N87-17002
TURBOCOMPRESSORS
Unsteady flows in a single-stage transonic axial-flow fan stator row [NASA-TM-88929] N87-16805
TURBOFAN ENGINES
Measurements of the unsteady flow field within the stator row of a transonic axial-flow fan. Part 2: Results and discussion [NASA-TM-88946] N87-16790
Unsteady flows in a single-stage transonic axial-flow fan stator row [NASA-TM-88929] N87-16805
Manufacturing cell for the V2500 variable vanes [PNR90330] N87-16835
The technology of advanced prop-fan transmissions [PNR90357] N87-16843
Evaluation of DDH and weld repaired F100 turbine vanes under simulated service conditions N87-17070
TURBOFANS
Measurements of the unsteady flow field within the stator row of a transonic axial-flow fan. 1: Measurement and analysis technique [NASA-TM-88945] N87-16789
TURBOPROP ENGINES
The technology of advanced prop-fan transmissions [PNR90357] N87-16843
TURBULENCE
Measurement of heat transfer and pressure drop in rectangular channels with turbulence promoters [NASA-CR-4015] N87-17003
TURBULENT BOUNDARY LAYER
Computation of separation ahead of blunt fin in supersonic turbulent flow [NASA-TM-89416] N87-16791
Stability characteristics of a supersonic boundary layer and their relation to the position of the laminar-turbulent transition point [NASA-TM-88533] N87-16797
Calculation of sidewall boundary-layer parameters from rake measurements for the Langley 0.3-meter transonic cryogenic tunnel [NASA-CR-178241] N87-16807
Computation of turbulent boundary layer flows with an algebraic stress turbulence model [NASA-CR-178967] N87-16982
Transitional boundary layers under the influence of high free stream turbulence, intensive wall cooling and high pressure gradients in hot gas circulation [NASA-TM-88524] N87-16983
Experimental investigation of the turbulence production mechanism in boundary layers [AD-A173091] N87-17007
The study of shock wave and turbulent boundary layer interactions [AD-A175033] N87-17008
Observations on the turbulent structure in an unsteady, normal shock/boundary-layer interaction --- blowdown supersonic tunnel [PNR90361] N87-17010
TURBULENT DIFFUSION
An introduction to the numerical modelling of dispersion in the atmospheric boundary layer N87-16993
TURBULENT FLOW
Simultaneous density velocity measurements in premixed turbulent flames to assess a theoretical model N87-16889
Pressure gradient effects in the viscous wall region of a turbulent flow [REPT-7] N87-16980
Direct computation of wall bounded aerosol turbulent flow interactions [DE86-013221] N87-17009
Experimental investigation in turbulent flow separation [ISL-CO-208/86] N87-17012
HAWT performance with dynamic stall [DE86-004428] N87-17402

TURNING FLIGHT
Optimal turning at high angle of attack of supersonic and hypersonic vehicles N87-16814
TWO PHASE FLOW
Two-Phase Flows in Major Technological Hazards, volume 3
[VKI-LS-1986-03-VOL-3] N87-16984
General classification of two-phase flow codes N87-16985
Review of present approaches to two-phase flow problems N87-16986

U

U.S.S.R.
USSR report: Earth sciences
[JPRS-UES-86-005] N87-17096
ULTRAHIGH FREQUENCIES
Vegetation influence on wave propagation
[FOA-B-30097-3.3] N87-16965
Transmission loss measurements in mobile radio nets
[FOA-B-30098-3.3] N87-16966
Rain measurement results derived from a two polarization S-band radar employing frequency diversity at Wallops Island, Virginia N87-17182
Remote sensing of tree attenuation at 870 MHz along simulated Earth satellite paths N87-17306
Microwave backscattering from an anisotropic soybean canopy N87-17346
L to X-band scatter and emission measurements of vegetation N87-17347
An 800 MHz bandwidth acousto-optical spectrometer at Helsinki Observatory N87-17567
ULTRASONIC FLAW DETECTION
Ultrasonic testing techniques for diffusion-bonded titanium components N87-17061
ULTRASONIC TESTS
Ultrasonic testing techniques for diffusion-bonded titanium components N87-17061
ULTRAVIOLET SPECTRA
International ultraviolet explorer observing program: Ultraviolet observations of selected astronomical sources
[NASA-CR-180155] N87-17584
Constraints on the composition of Jupiter's stratospheric aerosols from ultraviolet photometry N87-17610
UNDERGROUND STRUCTURES
Development of intelligent pipe locator N87-17200
UNITED KINGDOM
The UK ERS Data Centre, an offline processing and archiving facility N87-17230
UNITED STATES
Applications of remote sensing in the US Department of Agriculture N87-17285
UNIVERSE
The early universe N87-17539
The dynamics and evolution of clusters of galaxies
[NASA-CR-180169] N87-17596
UNIVERSITIES
Flight-vehicle structures education in the US: Assessment and recommendations
[NASA-CR-4048] N87-17526
UNSTEADY FLOW
Measurements of the unsteady flow field within the stator row of a transonic axial-flow fan. 1: Measurement and analysis technique
[NASA-TM-88945] N87-16789
Measurements of the unsteady flow field within the stator row of a transonic axial-flow fan. Part 2: Results and discussion
[NASA-TM-88946] N87-16790
Unsteady flows in a single-stage transonic axial-flow fan stator row
[NASA-TM-88929] N87-16805
Unsteady aerodynamics of a rotating compressor blade row in incompressible flow. Volume 1: Experimental facilities, procedures and sample data
[AD-A173043] N87-16831
Unsteady aerodynamics of a rotating compressor blade row at low Mach number. Volume 2: Analysis of experimental results and comparison with theory
[AD-A173044] N87-16832
A general method for unsteady stagnation region heat transfer and results for model turbine flows
[NASA-TM-88903] N87-17002
The study of shock wave and turbulent boundary layer interactions
[AD-A175033] N87-17008
URANUS ATMOSPHERE
The Jovian Atmospheres
[NASA-CP-2441] N87-17598
Thermal balance of the atmospheres of Jupiter and Uranus N87-17604
A possible deuterium anomaly: Implications of the CH3D/CH4 mixing ratios in the atmospheres of Jupiter, Saturn, and Uranus N87-17617
A detected feature at the expected wavelength for the HD R5(0) line in Jupiter's and Uranus' atmospheres N87-17619
The Voyager encounter with Uranus and Neptune N87-17639
The ortho-para H2 distribution on Uranus: Constraints from the collision-induced 3-0 dipole band and 4-0 S(0) and S(1) quadrupole line profiles N87-17640
Radiative-convective equilibrium models of Uranus and Neptune N87-17641
A model of the spatial and temporal variation of the Uranus thermal structure N87-17642
Vertical structure of aerosols and clouds in the atmospheres of Uranus and Neptune: Implications for their heat budgets N87-17643
Are the aerosols on Uranus and Neptune composed of methane photopolymers? N87-17645
The HD/H2 ratio in the atmosphere of Uranus N87-17646
URBAN PLANNING
Environmental modification of metropolitan areas through satellite images: Study of urban design in the tropics N87-17175
USER MANUALS (COMPUTER PROGRAMS)
Algorithms and programming tools for image processing on the MPP, part 2
[NASA-CR-180146] N87-17440
USER REQUIREMENTS
Impact of IPS and IRS configuration on engine installation design — helicopter engines
[PNR90324] N87-16834
The TIMS investigator's guide N87-17113
Forecaster's need in meteorology for the next generation of satellites N87-17275
Future user requirements and required technological developments of spaceborne synthetic aperture radars N87-17320

V

VANES
Bonding of superalloys by diffusion welding and diffusion brazing N87-17059
Evaluation of DDH and weld repaired F100 turbine vanes under simulated service conditions N87-17070
VAPOR DEPOSITION
The 60 GHz IMPATT diode development
[NASA-CR-179536] N87-17515
VARIABLE STREAM CONTROL ENGINES
Outdoor test stand performance of a convertible engine with variable inlet guide vanes for advanced rotorcraft propulsion
[NASA-TM-88939] N87-16825
VARIATIONAL PRINCIPLES
Review of discretization techniques and numerical resolution methods N87-16990
On variational characterizations of steady vortex rings
[MEMO-577] N87-17014
VEGETATION
Vegetation influence on wave propagation
[FOA-B-30097-3.3] N87-16965
A scatterometer operating at 10 GHz N87-17282
The effect of measurement error and confusion from vegetation on passive microwave estimates of soil moisture N87-17304
A scattering model for defoliated vegetation N87-17309
Microwave dielectric spectrum of vegetation material N87-17345
Backscattering power spectrum for randomly moving vegetation N87-17349
Microwave dielectric behavior of vegetation material
[NASA-CR-180096] N87-17393
VEGETATION GROWTH
Monitoring vegetation recovery patterns on Mount St. Helens using thermal infrared multispectral data N87-17122
Application of Thermal Infrared Multiband Scanner (TIMS) data to mapping of Plutonic and stratified rock and assemblages in accreted terrains of the Northern Sierra, California N87-17132
VEGETATIVE INDEX
SIR-B measurements and modeling of vegetation N87-17160
VEHICULAR TRACKS
Tank tread assemblies with track-linking mechanism
[NASA-CASE-NPO-16321-1CU] N87-17034
VELOCITY DISTRIBUTION
Afterbody shape effects on the near-wake velocity characteristics at Mach numbers between 0.35 and 0.92
[ISL-CO-205/86] N87-17011
VELOCITY MEASUREMENT
Simultaneous density velocity measurements in premixed turbulent flames to assess a theoretical model N87-16889
Droplet sizing research program
[AD-A173100] N87-16895
VENUS (PLANET)
Analysis of harmonic spline gravity models for Venus and Mars
[NASA-CR-180147] N87-17648
Investigation of the mode of compensation of Venus topography
[NASA-CR-180145] N87-17649
VENUS SURFACE
Venus Radar Mapper (VRM): Multimode radar system design N87-17142
VERTICAL DISTRIBUTION
Water vapor in Jupiter's atmosphere N87-17605
VLA observations of Jupiter at 1.3 - 20 cm wavelengths N87-17606
VERTICAL ORIENTATION
Vertical cloud structure models for the NTRZ EQZ, SEB and STRZ of Jupiter N87-17608
VERY HIGH FREQUENCIES
Vegetation influence on wave propagation
[FOA-B-30097-3.3] N87-16965
VESTIBULAR TESTS
Role of orientation reference selection in motion sickness
[NASA-CR-180161] N87-17431
VIBRATION
Space shuttle main engine vibration data base
[NASA-TM-86576] N87-16876
VIBRATION DAMPING
The possibility of reducing the cyclic torque fluctuations produced by two-stroke engines using the storage of magnetostatic energy
[RAE-TM-RAD-NAV-265] N87-17042
Decentralized control of large-scale systems: Fixed modes, sensitivity and parametric robustness
[NASA-TM-88537] N87-17474
VIBRATION MEASUREMENT
Industrial holography: The Rolls-Royce experience
[PNR90351] N87-17024
VIBRATION TESTS
Ground vibration tests
[ETN-87-98847] N87-17422
VIBRATIONAL SPECTRA
Vibrationally excited cyanoacetylene in regions of massive star formation N87-17561
VIBRATORY LOADS
Vibroacoustic payload environment prediction system (VAPEPS): Data base management center remote access guide
[NASA-CR-180132] N87-17528
VIDEO DATA
Advanced alternating frame technology (VISIDEP (TM)) and three-dimensional remote sensing N87-17291
VIDEO DISKS
Initial utilization of the CVIRB video production facility
[NASA-TM-89036] N87-16873
VIEW EFFECTS
Viewing angle corrections of airborne multispectral scanner data acquired over forested surfaces N87-17273
VINYL COPOLYMERS
Vinyl stilbazoles
[NASA-CASE-ARC-11429-3CU] N87-16908
VIRIAL THEOREM
Dark matter and the dynamics of galaxy clustering N87-17587
VISCOELASTICITY
On the analytical determination of relaxation modulus of viscoelastic materials by Prony's interpolation method
[NASA-TM-86579] N87-17455
Sound propagation in a superfluid helium filled porous solid: Theory and experiment N87-17478
VISCOSITY
Convenient total variation diminishing conditions for nonlinear difference schemes
[NASA-CR-178209] N87-17453
VISCOUS DAMPING
Dynamics and control of flexible manipulators N87-17026
VISCOUS FLOW
Calculation of supersonic flow over a compression corner N87-16785
Pressure gradient effects in the viscous wall region of a turbulent flow
[REPT-7] N87-16980
Analysis of viscous transonic flow over airfoil sections
[NASA-TM-88912] N87-17001
VISION
Robotic vision system
[AD-D012481] N87-17043

VISUAL PERCEPTION
Role of orientation reference selection in motion sickness
[NASA-CR-180161] N87-17431
VISUAL PHOTOMETRY
Polarimetry and photometry of active quasars at visual and near-infrared wavelengths N87-17579
VOLCANOES
Detection and mapping of volcanic rock assemblages and associated hydrothermal alteration with Thermal Infrared Multiband Scanner (TIMS) data Comstock Lode Mining District, Virginia City, Nevada N87-17119
Monitoring vegetation recovery patterns on Mount St. Helens using thermal infrared multispectral data N87-17122
Variability in the Earth radiation budget as determined from the Nimbus ERB experiments N87-17410
VOLCANOLOGY
On the relationship between age of lava flows and radar backscattering N87-17348
VORTEX BREAKDOWN
Selection principles and pattern formation in fluid mechanics and nonlinear shell theory
[NASA-CR-180159] N87-17004
A laboratory investigation of two-celled vortex flows N87-17423
VORTEX RINGS
On variational characterizations of steady vortex rings
[MEMO-577] N87-17014
VORTEX SHEDDING
Prediction of vortex shedding from circular and noncircular bodies in subsonic flow
[NASA-CR-4037] N87-16981
VORTICES
Experimental investigation of the turbulence production mechanism in boundary layers
[AD-A173091] N87-17007
A laboratory investigation of two-celled vortex flows N87-17423
Quasi-geostrophic free mode models of long-lived Jovian eddies: Forcing mechanisms and crucial observational tests N87-17630
VOYAGER PROJECT
The Voyager encounter with Uranus and Neptune N87-17639

W

WADIS
Results of tectonic and spectral investigations along the Wadi Araba fault in Jordan using special processed Thematic Mapping (TM) data N87-17247
WAFERS
The 60 GHz IMPATT diode development
[NASA-CR-179536] N87-17515
WAKES
Analysis of synthetic aperture radar imagery of surface ship wakes N87-17297
WALL FLOW
Pressure gradient effects in the viscous wall region of a turbulent flow
[REPT-7] N87-16980
Direct computation of wall bounded aerosol turbulent flow interactions
[DE86-013221] N87-17009
WASHERS (SPACERS)
Anti-rotation guide vane bushing
[AD-D012510] N87-17047
WASHINGTON
Monitoring vegetation recovery patterns on Mount St. Helens using thermal infrared multispectral data N87-17122
WATER DEPTH
An improved method for the determination of water depth from surface wave refraction patterns --- SAR imagery N87-17299
WATER FLOW
Self-contained, single-use hose and tubing cleaning module
[NASA-CASE-MSC-20857-1] N87-17035
WATER INJECTION
Investigation of a repetitive pulsed electrothermal thruster
[NASA-CR-179464] N87-16878
WATER MANAGEMENT
Towards snowmelt runoff forecast using LANDSAT-MSS and NOAA/AVHRR data N87-17317
A climatological-hydrological study of lake ice in the southwestern mountain area in Norway by use of satellite sensing N87-17319
WATER VAPOR
Water vapor in Jupiter's atmosphere N87-17605
WATER WAVES
Microwave scattering from the ocean surface N87-17109
Ocean waves near Hurricane Josephine from SIR-B N87-17148
Operational wave forecasting with spaceborne SAR: Prospects and pitfalls N87-17149
A two-scale Bragg scattering model for microwave backscatter from wind generated waves N87-17212
C and Ku-band scatterometer results from the SCATTMOD internal wave experiment N87-17215
Estimation of internal wave currents from SAR and infrared scatterometer imagery N87-17295
Observations of surface currents at Nantucket Shoals and implications for radar imaging of the bottom N87-17296
Sea wave measurements using a ship's radar N87-17300
Characteristics of a very low altitude spacecraft for collecting global directional wave spectra with spaceborne synthetic aperture radar N87-17333
The SAR image modulation transfer function derived from SIR-B image spectra and airborne measurements of ocean wave height spectra N87-17334
SIR-B observations of ocean waves in the NE Atlantic N87-17335
Deriving two-dimensional ocean wave spectra and surface height maps from the Shuttle Imaging Radar (SIR-B) N87-17336
Spatial evolution of wave spectra in the vicinity of the Agulhas current from SIR-B N87-17337
Characterisation of internal wave surface patterns on airborne SAR imagery N87-17338
Proceedings of an ESA Workshop on ERS-1 Wind and Wave Calibration
[ESA-SP-262] N87-17363
ERS-1 mission constraints related to wind and wave calibration N87-17364
Gathering and processing a comparative data set for the calibration and validation of ERS-1 data products; preparatory work at the UK-ERS-DC --- Data Center (DC) N87-17367
Validation of wind speed and significant wave height from Geosat N87-17368
Requirements and constraints in the calibration and validation of ERS-1 wind and wave parameters N87-17369
Comparison concept of satellite derived wind and wave data with ground truth N87-17373
Accuracy estimates of wind and wave observations from ships of opportunity in the WMO voluntary observing ship program N87-17375
A procedure for estimation of two-dimensional ocean height-variance spectra from SAR imagery N87-17381
Measurement of the directional spectrum of ocean waves using a conically-scanning radar N87-17383
Wave modeling activities of the Wave Modeling (WAM) group relevant to ERS-1 N87-17389
Marine climate program N87-17390
A scatterometer research program N87-17391
WATERPROOFING
Elevated waterproof access floor system and method of making the same
[NASA-CASE-ARC-11363-1] N87-16918
WAVE EQUATIONS
Initial-value problem for the 1-D wave equation in an inhomogeneous medium
[IPPCZ-268] N87-17505
WAVE PROPAGATION
A study of explosive wave propagation in granular materials with microstructure
[AD-A173015] N87-16914
System engineering study of electrodynamic tether as a spaceborne generator and radiator of electromagnetic waves in the ULF/ELF frequency band
[NASA-CR-180156] N87-16956
Transmission of atmospheric internal gravity waves into the stratosphere N87-17412
Nonlinear wave propagation
[AD-A175073] N87-17461
Unified formulation for linear accelerator design
[DE86-013441] N87-17491
Implicit particle simulation of electromagnetic plasma phenomena
[IPPJ-799] N87-17509
Mesoscale waves as a probe of Jupiter's deep atmosphere N87-17628
WAVEFORMS
Spatial dependence on sea spikes N87-17218
WAVEGUIDE ANTENNAS
Features and technologies of ERS-1 (ESA) and X-SAR antennas N87-17152
WAVEGUIDES
Design and technology of feed array and beam forming network for contoured beam antennas --- satellite antennas N87-16950
A new model for broadband waveguide to microstrip transition design
[NASA-TM-89905] N87-16958
WAVELENGTHS
A statistical approach to select the optimal wavelength bands for separating rocks in the wavelength region 0.4 to 2.3 microns N87-17244
WEAK INTERACTIONS (FIELD THEORY)
The astrophysical implications of weakly interacting, massive particles N87-17592
WEAPON SYSTEMS
Mechanical properties of graphite epoxy used for Zero CTE Program
[DE86-013227] N87-16886
WEAR RESISTANCE
The application of the RBD process to the deposition of anti-wear alloys N87-17069
WEATHER
Geophysicist comments on how solar activity may affect weather N87-17097
WEATHER FORECASTING
Forecaster's need in meteorology for the next generation of satellites N87-17275
Real-time application of remotely sensed data --- meteorology N87-17276
Empirical relations between the Earth's radiation budget, cloudiness, and various meteorological parameters N87-17424
WEBS (SHEETS)
Use of low energy ion implants in high efficiency crystalline silicon solar cells
[NASA-CR-179971] N87-17408
WEDGE FLOW
The study of shock wave and turbulent boundary layer interactions
[AD-A175033] N87-17008
WEIBULL DENSITY FUNCTIONS
Application of modified three parameter Weibull distributions to brittle material design
[RARDE-16/84] N87-17072
WELD STRENGTH
Computational weld mechanics N87-17052
The application of diffusion bonding and laser welding in the fabrication of aerospace structures N87-17054
Diffusion bonding in the manufacture of aircraft structure N87-17057
Diffusion bonding of Al-alloys in the solid state N87-17058
Influence of welding flaws on the fatigue strength of electron beam weldments in Ti Al6 V4 N87-17065
Welding of aluminum castings N87-17068
Repair techniques for gas turbine components N87-17071
WELD TESTS
Advanced Joining of Aerospace Metallic Materials --- conference proceedings
[AGARD-CP-398] N87-17051
The welding of aluminum alloys: A new technology in space application N87-17056
Ultrasonic testing techniques for diffusion-bonded titanium components N87-17061
Weld quality monitor and control system N87-17062
NDT of electron beam welded joints (micro-focus and real time X-ray) N87-17063
Influence of welding flaws on the fatigue strength of electron beam weldments in Ti Al6 V4 N87-17065
Inertia welding of nitralloy N and 18 nickel maraging 250 grade steels for utilization in the main rotor drive shaft for the AR-64 military helicopter program N87-17067
Welding of aluminum castings N87-17068
Evaluation of DDH and weld repaired F100 turbine vanes under simulated service conditions N87-17070
WELDABILITY
Repair techniques for gas turbine components N87-17071
WELDED JOINTS
Advanced Joining of Aerospace Metallic Materials --- conference proceedings
[AGARD-CP-398] N87-17051
Computational weld mechanics N87-17052
Study of the electron beam weldability of superalloys through the analysis of melt zone morphology N87-17053
The application of diffusion bonding and laser welding in the fabrication of aerospace structures N87-17054
Economical manufacturing and inspection of the electron-beam-welded Tornado wing box N87-17055
The welding of aluminum alloys: A new technology in space application N87-17056
Weld quality monitor and control system N87-17062
NDT of electron beam welded joints (micro-focus and real time X-ray) N87-17063
Influence of welding flaws on the fatigue strength of electron beam weldments in Ti Al6 V4 N87-17065
Inertia welding of nitralloy N and 18 nickel maraging 250 grade steels for utilization in the main rotor drive shaft for the AR-64 military helicopter program N87-17067
WELDING
Computational weld mechanics N87-17052

Evaluation of DDH and weld repaired F100 turbine vanes under simulated service conditions N87-17070

WELDING MACHINES
Welding torch with arc light reflector
[NASA-CASE-MFS-29134-1] N87-17493

WEST GERMANY
The German ERS-1 SAR postprocessing system plans and concepts N87-17231

WHEAT
Analysis of the spatial structure of Synthetic Aperture Radar (SAR) imagery for a better separability of cereal crops, wheat and barley N87-17257

WHEATSTONE BRIDGES
Universal pressure transducer
[AD-D012499] N87-17019

WHEELS
Non-backdriveable free wheeling coupling
[NASA-CASE-MSC-20475-1] N87-17037

WIND (METEOROLOGY)
Joint influence of turbulence and wind on signal power in radioacoustic sounding of atmosphere N87-17108
Microwave scattering from the ocean surface N87-17109
Review of wind simulation methods for horizontal-axis wind turbine analysis
[DE86-012223] N87-17407

WIND DIRECTION
Tower-based broadband backscattering measurements from the ocean surface in the North Sea N87-17217
Application of the Seasat scatterometer to observations of wind speed and direction and Arctic ice/water boundaries N87-17259
A diagnostic approach to obtaining planetary boundary layer winds using satellite-derived thermal data
[NASA-CR-178972] N87-17420

WIND EFFECTS
A two-scale Bragg scattering model for microwave backscatter from wind generated waves N87-17212
Backscattering power spectrum for randomly moving vegetation N87-17349

WIND MEASUREMENT
ERS-1 wind scatterometer antenna: Mechanical aspects N87-16940
On-ground verification and in-orbit performance prediction of the ERS-1 wind scatterometer N87-17193
Results of the ESA airborne C-band scatterometer campaigns — ERS-1 N87-17225
ERS-1 wind scatterometer: Wind extraction and ambiguity removal N87-17227
Recent progress in ERS-1 wind scatterometer design N87-17256
Application of the Seasat scatterometer to observations of wind speed and direction and Arctic ice/water boundaries N87-17259
Application of Doppler radar and lidar to diagnose atmospheric phenomena N87-17271
Remote probing of wind and refractive-index structure using optical scintillation techniques N87-17272
Proceedings of an ESA Workshop on ERS-1 Wind and Wave Calibration
[ESA-SP-262] N87-17363
ERS-1 mission constraints related to wind and wave calibration N87-17364
Gathering and processing a comparative data set for the calibration and validation of ERS-1 data products; preparatory work at the UK-ERS-DC — Data Center (DC) N87-17367
Requirements and constraints in the calibration and validation of ERS-1 wind and wave parameters N87-17369
Satellite scatterometer comparisons with surface measurements: Techniques and Seasat results N87-17372
Comparison concept of satellite derived wind and wave data with ground truth N87-17373
Validation of ERS-1 wind data using observations from research and voluntary observing ships N87-17374
Accuracy estimates of wind and wave observations from ships of opportunity in the WMO voluntary observing ship program N87-17375
The accuracy and availability of operational marine surface wind data for ERS-1 sensor calibration and validation from fixed platforms and free drifting buoys N87-17376
An overview of the NSCAT/N-ROSS program N87-17384
Results from 1984 airborne Doppler lidar wind measurement program. Flight 6: Analysis of line-of-sight elevation angle errors and apparent Doppler velocities
[NASA-CR-178934] N87-17425

WIND PROFILES
Remote probing of wind and refractive-index structure using optical scintillation techniques N87-17272
Transmission of atmospheric internal gravity waves into the stratosphere N87-17412

WIND TUNNEL TESTS
Observations on the turbulent structure in an unsteady, normal shock/boundary-layer interaction — blowdown supersonic tunnel
[PNR90361] N87-17010
Three-dimensional separation on a cylindrical ellipsoid. Results of the first test campaign on the F2 wind tunnel
[ONERA-RT-16/7252-AN] N87-17013

WIND TUNNEL WALLS
Calculation of sidewall boundary-layer parameters from rake measurements for the Langley 0.3-meter transonic cryogenic tunnel
[NASA-CR-178241] N87-16807
The influence of wind-tunnel walls on discrete frequency noise N87-16850

WIND TURBINES
Utility interconnection issues for wind power generation
[NASA-CR-175056] N87-17400
Design and dynamic simulation of a fixed pitch 56 kW wind turbine drive train with a continuously variable transmission
[NASA-CR-179543] N87-17401
HAWT performance with dynamic stall
[DE86-004428] N87-17402
Model for simulating rotational data for wind turbine applications
[DE86-010784] N87-17406
Review of wind simulation methods for horizontal-axis wind turbine analysis
[DE86-012223] N87-17407

WIND VELOCITY
Application of the Seasat scatterometer to observations of wind speed and direction and Arctic ice/water boundaries N87-17259
A diagnostic approach to obtaining planetary boundary layer winds using satellite-derived thermal data
[NASA-CR-178972] N87-17420
Cloud-top meridional momentum transports on Saturn and Jupiter N87-17623

WIND VELOCITY MEASUREMENT
Retrieval of near-surface wind speed in the Baltic Sea from NIMBUS-7 Scanning Multichannel Microwave Radiometer (SMMR) observations N87-17342
Validation of wind speed and significant wave height from Geosat N87-17368
Intersensor comparisons for validation of wind speed measurements from ERS-1 altimeter and scatterometer — Seasat N87-17386

WINDPOWER UTILIZATION
Utility interconnection issues for wind power generation
[NASA-CR-175056] N87-17400
Feasibility of using wind power for an aerostat-borne radar system
[DE86-004461] N87-17403
Wind energy technical reading list
[DE86-010704] N87-17404

WINDPOWERED GENERATORS
Utility interconnection issues for wind power generation
[NASA-CR-175056] N87-17400
Design and dynamic simulation of a fixed pitch 56 kW wind turbine drive train with a continuously variable transmission
[NASA-CR-179543] N87-17401

WINGS
Computational, unsteady transonic aerodynamics and aeroelasticity about airfoils and wings
[NASA-TM-89414] N87-16801
A comparison of single-block and multi-block grids around wing-fuselage configurations
[FFA-TN-1985-42] N87-16811
Economical manufacturing and inspection of the electron-beam-welded Tornado wing box N87-17055

WORKLOADS (PSYCHOPHYSIOLOGY)
Identification and proposed control of helicopter transmission noise at the source
[NASA-TM-89312] N87-16816

WORLD DATA CENTERS
The design of an international data centre for remote sensing N87-17176

WORLD METEOROLOGICAL ORGANIZATION
An overview of the implementation of the World Climate Research program N87-17388

WYOMING
Application of TIMS data in stratigraphic analysis N87-17121

X

X RAY INSPECTION
NDT of electron beam welded joints (micro-focus and real time X-ray) N87-17063

X RAY IRRADIATION
Nanosecond two-dimensional imaging using tomographic techniques
[DE86-008164] N87-17499

X RAY SOURCES
A soft X-ray observation of omega Centauri with EXOSAT
[MPE-PREPRINT-60] N87-17575

X RAY SPECTRA
A soft X-ray observation of omega Centauri with EXOSAT
[MPE-PREPRINT-60] N87-17575
Observations of quasi-periodic oscillations in Cyg X-2
[MPE-PREPRINT-61] N87-17576

X RAY TELESCOPES
Reflection grating spectrometer for the X-ray Multi-Mirror (XMM) space observatory: design and calculated performance
[DE86-013485] N87-17500

X RAYS
A search for rapidly modulated emission in bright X-ray sources using the HEAO A-1 data base
[NASA-CR-180148] N87-17593

Y

YAGI ANTENNAS
The FRS-68010: A new concept for the acquisition and analysis of NOAA HRPT data N87-17206

YIELD STRENGTH
Inertia welding of nitralloy N and 18 nickel maraging 250 grade steels for utilization in the main rotor drive shaft for the AR-64 military helicopter program N87-17067

YTTERBIUM
Determining and modeling the response of ytterbium piezoresistance transducers
[AD-A173085] N87-17023

Z

ZODIACAL LIGHT
Interplanetary dust N87-17542

ZONAL FLOW (METEOROLOGY)
Middle Atmosphere Program. Handbook for MAP, volume 22
[NASA-CR-180128] N87-17414
Jupiter: New estimates of mean zonal flow at the cloud level N87-17622
Mesoscale waves as a probe of Jupiter's deep atmosphere N87-17628
Chaotic motion in the Jovian atmosphere N87-17634

Typical Personal Author Index Listing

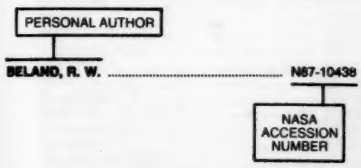

Listings in this index are arranged alphabetically by personal author. The NASA accession number denotes the number by which the citation is identified.

A

ABBOTT, ELSA N87-17111
N87-17133
ABBOTT, PETER W. N87-16855
ABLOWITZ, MARK J. N87-17461
ABOU-HANNA, JERIES JACOB N87-17028
ABRAMS, M. J. N87-17202
ABURWEIN, A. A. N87-17197
ADAM, J. A. N87-17505
ADAM, P. N87-17059
ADAMCZYK, J. J. N87-16789
N87-16790
ADAMS, LOUIS R. N87-16916
ADAMS, S. L. N87-17204
ADATI, K. N87-17508
ADE, P. A. R. N87-17555
AGAH-TEHRANI, ABDOLREZA N87-17074
AGGARWAL, S. K. N87-16827
AGHAN, R. L. N87-17048
AHLEN, S. P. N87-17652
AHMED, SHAFFIQ N87-17018
ALDERFER, DAVID W. N87-17018
ALEXANDER, J. D. N87-16842
ALEXOPOULOS, N. G. N87-16976
ALLEN, J. E. N87-17514
ALLEN, M. N87-17636
ALLEY, R. E. N87-17204
ALLISON, MICHAEL N87-17598
N87-17647
ALMEIDA, R. N87-17207
ANAND, YOGI N87-17515
ANDERSON, DONALD L. N87-17117
ANDERSON, JAMES E. N87-17114
ANGEL, G. C. N87-16892
ANGELICI, G. N87-17208
ANUTA, P. N87-17327
AOKI, T. N87-17508
APEL, J. R. N87-17147
APPELBLAD, O. N87-17486
APPLEBY, BRENT D. N87-16862
APPLEBY, J. F. N87-17641
ARAHOFF, S. N87-17248
ARDANUY, PHILIP EDWARD N87-17410
ARDUINI, C. N87-16947
N87-16952
ARISTEI, F. N87-16950
ARNAUD, K. A. N87-17575
ASHBURN, J. R. N87-16900
ASP, BOERJE N87-16965
ASRAR, G. N87-17286
ASSAL, H. M. N87-17198
ATAMAN, E. N87-17351
ATREYA, SUSHIL N87-17614
ATTEMA, E. P. W. N87-17225
AUCOIN, THOMAS R. N87-17518
AVIGNONE, F. T. N87-17652
AYERS, J. KIRK N87-16861
AYYAGARI, MURTHY N87-17515
AZUMA, Y. N87-17166

B

BAARS, J. W. M. N87-17568
BADDOUR, MAURICE F. N87-16968
BAGDATLISHVILI, P. D. N87-17106
BAGRAMYANTS, V. O. N87-17106
BAINES, K. H. N87-17640
BAINES, KEVIN N87-17643
BAKER, MARK L. N87-17045
BAKER, STEVEN RICHARD N87-17478
BAKLIWAL, P. C. N87-17236
BALANIS, C. A. N87-17201
BALL, EUGENE N87-17533
BALLARD, J. R. N87-16834
BANERJI, KINGSHUK N87-17076
BANING, G. N87-17056
BARBONI, R. N87-16952
BARCIA, A. N87-17553
BARDATI, F. N87-17261
N87-17263
BARHEN, J. N87-17445
BARKER, TIMOTHY N87-17581
N87-17582
BARNES, D. C. N87-17509
BARONTI, S. N87-17328
BARTHOLOMEW, MARY JANE N87-17130
BARTON, IAN J. N87-17387
BASAPUR, VENKATESH K. N87-16857
BASSANI, L. N87-17552
BAUER, BARRY J. N87-16912
BAUMGARTNER, M. F. N87-17317
BEAL, R. C. N87-17149
N87-17333
BEALE, M. I. J. N87-17517
BECK, S. N87-17618
BEDARD, A. J. N87-17339
BEEBE, R. N87-17603
N87-17632
BELT, CAROL L. N87-17420
BELWARD, A. S. N87-17250
BENADA, J. R. N87-17366
BENELLI, G. N87-17238
BENJAMIN, N. M. P. N87-17514
BENNETT, H. W. N87-16840
BENNETT, J. R. N87-17299
BENNETT, JACK N87-17128
BENTLEY, JON N87-17533
BENZ, W. N87-17585
BERG, R. L. N87-16853
BERGGREEN, JUERGEN N87-17055
BERGLIND, TORSTEN N87-16811
BERGSTRALH, J. T. N87-17640
BERGSTRALH, JAY N87-17643
BERK, HERBERT L. N87-17512
N87-17513
BERNARD, R. N87-17288
BERNASCONI, M. C. N87-16927
N87-16943
BERNER, C. N87-17011
N87-17012
BERRY, FRED A., JR. N87-16970
BERSHADER, DANIEL N87-17006
BESTER, M. N87-17573
BESYELOV, K. YE. N87-17106
BETTRIDGE, D. F. N87-16837
BEYER, A. N87-17196
BEYER, RICHARD A. N87-16915
BEZANGER, C. N87-17612
BEZARD, B. N87-17612
N87-17642
BEZARD, BRUNO N87-17614
BHAGAVATHULA, S. N87-17311
BIBBY, MALCOLM N87-17052
BICHSEL, M. N87-17174
BILLINGS, S. A. N87-17095
N87-17471
BINDER, P. N87-17276
BIRKS, ANDREW ROBERT N87-17383
BIRNIE, R. W. N87-17246
BISHOP, M. P. N87-17332
BISHOP, MATT N87-17443
BJORAKER, G. L. N87-17605
BLACK, F. OWEN N87-17431
BLACK, RICHARD E. N87-16917
BLAETTLER, D. K. N87-17267
BLANCHARD, A. J. N87-17304
BLANCO, A. N87-17551
BLELLOCH, PAUL ANDREW N87-17029
BLISSETT, R. J. N87-17361
BLOM, R. G. N87-17348
BLOOM, ARTHUR L. N87-17136
BLUMENTHAL, PHILIP Z. N87-16851
BOBIN, L. N87-16808
BOGDONOFF, SEYMOUR M. N87-17008
BOIRE, M. N87-17060
BONHAM-CARTER, G. F. N87-17248
BONNER, GEORGE N87-17047
BOREL, C. C. N87-17307
BORENGASSER, MARCUS N87-17119
N87-17132
BORGEAUD, M. N87-17187
BORGHESI, A. N87-17551
BORREGO, J. M. N87-17405
BOUSQUET, P. N87-17254
BOWIN, CARL N87-17648
BOYCE, J. F. N87-17438
BOZSOKI, I. N87-17282
BRACEWELL, R. N. N87-17186
BRAILE, LAWRENCE W. N87-17418
BRAITHWAITE, N. ST. J. N87-17514
BRANDANI, ALDO N87-17157
BRAUN, H. M. N87-17320
BRAUSCH, J. F. N87-17481
BREED, CAROL S. N87-17139
BRODZINSKI, R. L. N87-17652
BROUGHTON, C. N87-17517
BROWN, L. M. J. N87-17558
BROWN, M. A. N87-17322
N87-17361
BROWN, R. N87-17229
BROWN, R. J. N87-17284
BRUMAGE, WILLIAM H. N87-17043
BUCHLIN, J.-M. N87-16999
BUCKINGHAM, A. C. N87-17009
BUDYKO, M. I. N87-17099
BUFFAT, M. N87-16995
BUJARRABAL, V. N87-17553
N87-17561
BULLARD, J. B. N87-16852
BULZAN, D. L. N87-16826
BURGHART, GEORGE H. N87-16854
BURLEY, C. L. N87-17479
BURNS, B. A. N87-17185
N87-17219
N87-17222
N87-17223
BURNS, RALPH A. N87-16919
BURTON, R. L. N87-16878
BUSQUETS, ANTHONY M. N87-16873
BUSSOLETTI, E. N87-17551

C

CALCUTT, S. B. N87-17633
CALLAHAN, PHILIP S. N87-17366
CALLAHAN, PHILLIP S. N87-17384
CAMPBELL, S. N87-17230
CAPORASO, G. J. N87-17489
CAPPA, C. N87-17392
CAPPELLINI, V. N87-17238
CARLA, R. N87-17328
CARLOTTO, M. J. N87-17211
N87-17331
CARLSON, B. E. N87-17608
CARLSON, K. E. N87-17492
CARO, E. R. N87-17161
CARRENO, VICTOR A. N87-16863
CARRIERE, PHILIPPE N87-16995
CARTA, FRANKLIN O. N87-16831
N87-16832
N87-16833
CARTER, D. J. N87-17256
CARTER, D. J. Q. N87-17193
CARUTHERS, C. G. N87-17219
CARY, AUBREY M. N87-16802
CASEY, DAREN N87-17157

CASTELLANI, A. N87-16952
CASTILLO, N. D. N87-17613
CASTRO, I. P. N87-16992
CATHEY, L. N87-17291
CAUX, E. N87-17554
CAVALIERI, D. J. N87-17185
CAVANIE, A. G. N87-17227
CAVANIE, ALAIN N87-17370
CEBECI, TUNCER N87-17002
CESS, R. D. N87-17608
CHALLENOR, PETER G. N87-17365
CHAMBERLAIN, E. J. N87-16853
CHAMBERLAIN, J. W. N87-17611
CHANDRASEKHARAM, D. N87-17232
CHANETZ, B. N87-17013
CHANG, A. T. C. N87-17315
CHASE, SIMON T. N87-17555
CHASSAY, ROGER P. N87-17017
CHAUDRY, A. H. N87-17217
CHEN, TIMOTHY S. N87-16908
CHEN, YEN-SEN N87-16982
CHI, CHONG-YUNG N87-17258
CHIANG, CHWAN-KANG N87-16912
CHIMA, RODRICK V. N87-16784
CHLEWICKI, G. N87-17556
CHONG, Y. P. N87-17489
CHRISTENSEN, PHILIP R. N87-17117
CHUGNOV, YU. V. N87-17107
CHUH, THOMAS Y. N87-17520
CHURCHILL, P. N. N87-17230
CIELO, P. N87-17066
CIELO, PAOLO N87-17064
CIMINO, JOBEA N87-17157
CIOTTI, P. N87-17339
CIRILLO, WILLIAM M. N87-16861
CLAESON, T. N87-17572
CLARK, B. J. N87-16798
CLARK, BARBARA L. N87-17046
CLARK, F. O. N87-17556
CLARK, G. N87-16881
CLERKE, WILLIAM H. N87-17125
CLIFFORD, S. F. N87-17272
COBUT, J. P. N87-16949
COE, M. J. N87-17552
COHEN, MARC M. N87-16916
COLANGELI, L. N87-17551
COLE, D. M. N87-16853
COLLINS, EARL R., JR. N87-17034
COLLINS, W. G. N87-17352
CONDE, JUAN JOSE N87-17390
CONEL, J. E. N87-17204
CONNELL, J. R. N87-17406
N87-17407
CONRATH, BARNEY J. N87-17599
N87-17609
COOLEY, P. N87-17348
COOPER, N. E. N87-17072
CORDERO, P. N87-16941
CORDEY, R. A. N87-17335
COSTABILE, V. N87-16950
COWN, BARRY J. N87-16962
COX, J. W. R. N87-17042
COX, P. N87-17557
COX, P. E. N87-16841
COY, JOHN J. N87-16816
CRAIG, JOHN JAMES N87-17450
CRANDELL, M. N87-16972
CRAVEY, R. W. N87-16962
CRAWFORD, D. R. N87-17298
CRETE, D. G. N87-17570
CREWS, J. H., JR. N87-17090
CRIMI, S. N87-17326
CROVISIER, J. N87-17541
CUCINOTTA, FRANCIS A. N87-17487
CUNNINGHAM, C. C. N87-17601
CURLANDER, JOHN C. N87-17155
CURRERI, P. A. N87-16900
N87-16901
CURTIS, P. D. N87-17569
CZECK, EDWARD W. N87-17448

D

DABIZHA, A. I. N87-17595
DAIDA, J. M. N87-17186
DAKHOUL, YOUSSEF M. N87-17516
DALLOGLIO, G. N87-17539
DAMS, R. V. N87-17313
DANESI, P. R. N87-16898
DANIELSON, G. EDWARD N87-17643
DARTER, JOHN L. N87-16920
DARYABEIGI, KAMRAN N87-17018
DAS, INDU S. N87-17484
DAT, ROVINDRA N87-17515
DATLOV, J. N87-17506
DAUD, TAHER N87-17399
DAVARIAN, F. N87-16922
DAVID, S. A. N87-17049
DAVIES, A. F. N87-17259
DAVIS, DAVID N87-17132
DAVIS, GEORGE T. N87-16912
DAVIS, R. E. N87-17315
DAWES, C. J. N87-17054
DEAN, M. N87-17070
DEBERGH, CATHERINE N87-17617
DEBERNARDIS, P. N87-17539
DECKER, M. T. N87-17339
DEFEO, N. J. N87-17246
DEGRAAUW, THIJS N87-17537
DELCAMPO, F. N87-16946
DELRE, E. N87-17238
DELROMERO, A. N87-17561
DELTORO, J. N87-16946
DEMURGER, JOELLE N87-17370
DENYER, N. N87-17229
DEPATER, IMKE N87-17606
DERESPINIS, SILVIO F. N87-17036
DERR, ALAN G. N87-16961
DERRYBERRY, B. A. N87-17245
DESHMUKH, V. G. I. N87-17517
DEYOUNG, ANEMARIE N87-17026
DIETERLE, G. H. N87-17191
DIMOPOLOUS, S. N87-17652
DISAM, J. N87-17032
DIVSALAR, D. N87-16921
DIXON, J. N87-17472
N87-17473
DIXON, S. C. N87-16796
DIXON, T. H. N87-17146
DIXON, WILLIAM P. N87-17021
DOBSON, M. CRAIG N87-17160
DOMACK, CHRISTOPHER S. N87-16793
DOMIK, G. N87-17239
N87-17269
DOMIK, GITTA N87-17157
DOMINY, J. N87-16843
DONATO, L. N87-16934
DONELAN, M. A. N87-17212
N87-17213
DOOSE, L. R. N87-17613
DOSANJH, DARSHAN S. N87-17484
DOUGLAS, NIGEL G. N87-17564
DOVIAK, R. J. N87-17271
DOWDESWELL, J. N87-17223
DOWNEY, ALAN N. N87-16958
DOWNS, S. J. N87-16839
DOZIER, J. N87-17209
N87-17315
DRESCHER, A. N87-17168
DRESSENDORFER, P. V. N87-17524
DRIESSEN, T. S. H. N87-17475
N87-17534
DRIVER, D. N87-16842
DROSSART, PIERRE N87-17614
DRUKIER, A. K. N87-17652
DRYER, F. L. N87-16896
N87-16897
DUBE, C. N87-17287
DUCHOSSOIS, G. N87-17190
DUFFY, PHILIP BLISS N87-17577
DUFOUR, M. N87-17066
DUFOUR, MARC N87-17064
DUNFORD, D. V. N87-17058
DUNKERTON, S. B. N87-17054
DUNNE, TIMOTHY N87-16959
DUNNING, C. M. N87-17527
DURDEN, STEPHEN LOREN N87-17109

E

EAST, J. N87-17261
EATON, C. K. N87-16957
EDGERTON, ALVIN T. N87-17142
EDWARDS, J. A. N87-17010
EGGERS, HANS N87-17083
EGGUM, GORDON ERIC N87-17586
EICHHORN, GUNTHER N87-16893
EILTS, M. N87-17271
EINERSON, C. J. N87-17050
EL-RAYES, M. N87-17345
ELACHI, CHARLES N87-17141
ELAM, WILLIAM T. N87-17477
ELLEMAN, DANIEL D. N87-16917
ELLWOOD, D. J. N87-17248
ELRAYES, MOHAMED A. N87-17393
ELZE, STEFAN N87-17061
EMANUEL, KERRY A. N87-17626
ENCRENAZ, THERESE N87-17540
N87-17614
ENDRES, NED M. N87-16880
ENGMANN, E. T. N87-17344
EPSTEIN, J. S. N87-17093
ERDIN, K. N87-17351
ERSOY, L. N87-16954
N87-16955
ESCOBAR, J. N87-16935
ESTES, ROBERT D. N87-16956
N87-17502
EVANS, C. N87-17230
EVANS, D. S. N87-17421
EVANS, DIANE L. N87-17140
EVERETT, R. A., JR. N87-16882
EVRARD, AUGUST E. N87-17587
EWALD, R. N87-17573
EZRATY, ROBERT N87-17377

F

FABRICIUS, JENS S. N87-17428
FAETH, G. M. N87-16826
FAGNOUL, J. N87-16949
FAIRBANK, WILLIAM M. N87-17593
FALCO, R. E. N87-17007
FARKAS, Z. D. N87-17491
FAWLEY, W. M. N87-17027
FEATHER, FRANK E. N87-17448
FELDMAN, D. N87-17490
FELICI, F. N87-16938
FERNANDEZ, S. N87-17330
FERRAZZOLI, P. N87-17354
FESTA, A. N87-16947
FESTER, DALE A. N87-16855
FICKE, JULES M. N87-16821
FIELDING, ERIC J. N87-17136
FINKENZELLER, HEINZ N87-17378
FINNICUM, DOUGLAS SCOTT N87-16980
FISCELLA, B. N87-17392
FLASAR, F. M. N87-17621
FLASER, F. M. N87-17628
FLEETWOOD, D. M. N87-17524
FLEGONTOV, V. M. N87-17100
FLEISCHER, D. N87-16878
FLORENSKIY, P. V. N87-17595
FLOUZAT, G. N87-17253
N87-17254
N87-17294
FOHLEN, GEORGE M. N87-16909
FOLEY, JOANNE N87-17433
FONASH, S. J. N87-17408
FONTI, S. N87-17551
FORD, JOHN P. N87-17137
FORD, P. G. N87-17138
FOURCY, C. H. N87-17275
FRANCIS, C. R. N87-17194
FRANCIS, PETER E. N87-17371
FRANK, ARTHUR M. N87-17036
FRANK, D. N87-17240
FRANK, M. S. N87-17201
FREEMAN, N. N87-17229
FREEMAN, NELSON G. N87-17379
FREILICH, MICHAEL H. N87-17372
N87-17384
FREW, J. N87-17209
FRIED, H. M. N87-17490
FRIEDSON, A. J. N87-17604
FRISK, U. O. N87-17564
FRONEK, DENNIS L. N87-16851
FROST, V. S. N87-17240
FUELBERG, HENRY E. N87-17420
FUJIMURA, S. N87-17325
FUJINO, K. N87-17181
FUJITA, H. N87-17508
FUK, K. LI N87-17258
FUKAI, M. N87-17358
FUKUCHI, H. N87-17301
FUNG, A. K. N87-17180
N87-17309
FURUKANE, UTARO N87-17507

G

GADDIS, L. R. N87-17245
GALEANO, R. N87-17394
GALLEGO, J. D. N87-17553
GALLI, G. N87-17276
GALLO, C. N87-17401
GARCIA, R. N87-16941
GARDNER, JAMES E. N87-16796
GASPAROVIC, R. F. N87-17147
GAUDER, MICHAEL J. N87-17022
GAUTIER, D. N87-17612
N87-17642
GEAR, WALTER K. N87-17558
GEBEL, RADAMES K. N87-17496

GEIER, BODO N87-17078
GEILE, W. N87-17237
GELLER, MARGARET N87-17596
GELMINI, G. N87-17652
GEORGE, P. N87-17154
N87-17228
GERACI, A. L. N87-17326
GERKE, ROBERT DAVID N87-16899
GERMAIN, EDWARD F. N87-17018
GERSTL, S. A. W. N87-17395
GHANDHI, S. K. N87-17405
GIERASCH, P. J. N87-17628
GIESY, DANIEL P. N87-16861
GILLESPIE, A. R. N87-17116
N87-17118
GILLESPIE, D. D. N87-17156
GILS, W. N87-17321
GINTY, CAROL A. N87-16880
GINZBURG, A. S. N87-17098
GISPERT, R. N87-17560
GIVER, L. N87-17645
GLADSTONE, G. R. N87-17636
GLASGOW, THOMAS K. N87-16917
GLASS, JAMES S. N87-17035
GLASSMAN, I. N87-16897
GLOVER, RICHARD D. N87-16820
GMELIGMEYLING, R. H. J. N87-17464
GODFREY, D. N87-17629
GOETTING, H. R. N87-17173
N87-17203
GOGINENI, S. P. N87-17217
GOLDAK, JOHN N87-17052
GOLDBERG, B. E. N87-16910
GOLDHIRSH, J. N87-17182
N87-17306
GOLDSTEIN, DAVID N87-16903
GOLDSTEIN, S. A. N87-16878
GOMES, I. N87-17207
GOMEZ-GONZALEZ, J. N87-17553
N87-17561
GOMEZ, FERNANDO MONGE N87-16810
GONZALEZ, F. I. N87-17148
GOODENOUGH, D. G. N87-17273
GOODFELLOW, W. N87-17248
GOODMAN, ALAN N87-17427
GOORJIAN, PETER M. N87-16800
N87-16801
GOORVITCH, D. N87-17645
GORDON, STEPHEN S. N87-17493
GRAF, K. CH. N87-17267
GRAGLIA, R. D. N87-16931
GRANDLE, ROBERT E. N87-17483
GRANTHAM, WILLIAM D. N87-16849
GRAY, A. L. N87-17215
N87-17225
N87-17379
GREDEL, J. N87-17153
GRIFFIN, M. J. N87-17565
GRITCHENKO, Z. G. N87-17100
GRIZZAFFI, ANN MARIE N87-17448
GROENEWEG, J. F. N87-16798
GROSS, STANLEY H. N87-17413
GROSSRODE, PAT N87-16855
GUIGNARD, J. P. N87-17224
GUIGNARD, J.-P. N87-17228
GUILFORD, R. P. N87-16978
GUILLAUME, A. M. N87-17341
GUISSARD, A. N87-17214
N87-17341
GULATI, ANIL N87-16889
GULEN, L. N87-17138
GUNTER, WILLIAM D., JR. N87-17026
GUPTA, YOGENDRA M. N87-17023
GURUSWAMY, GURU P. N87-16800
N87-16801
GUYENNE, T. D. N87-17163
N87-17283
GUYMER, TREVOR H. N87-17365
N87-17369
GUYOT, L. N87-17172
GYEKENYESI, JOHN P. N87-17087

H

HABERMANN, NICO N87-17533
HADDOCK, T. F. N87-17281
HALL, J. R. N87-17292
HALLIKAINEN, M. N87-17179
N87-17264
N87-17305
N87-17342
N87-17343
HALM, R. N87-16938
HALPERN, JULES N87-17584
HALPERT, GERALD N87-17396
N87-17397
HAN, J. C. N87-17003
HANDSCHUH, ROBERT F. N87-16816
HANEY, C. W. N87-17280
HANS, P. N87-17226
N87-17257
HANSON, RONALD N87-17006
HARDIN, LARRY W. N87-16831
N87-16832
N87-16833
HARTL, PH. N87-17311
N87-17320
HARVEY, J. N87-17058
HASINGER, GUENTER N87-17576
HASSAN, AHMED A. N87-16793
HASSELMANN, KLAUS N87-17389
HATHAWAY, DAVID H. N87-17624
HATHAWAY, M. D. N87-16789
N87-16790
HATHAWAY, MICHAEL D. N87-16805
HAVENS, STEPHEN J. N87-16907
HAWKINS, R. K. N87-17379
HAY, J. N. N87-16887
HEATH, LINDA S. N87-17518
HECK, MICHAEL L. N87-16864
HEDGEPETH, JOHN M. N87-16870
N87-16916
HEIMBUCH, ALVIN H. N87-16908
HEINZE, H. N87-16925
HELD, D. N. N87-17279
HELD, DANIEL N. N87-17158
HELFRICH, REINHARD N87-17089
HELLING, RICHARD K. N87-17430
HELMINCK, G. F. N87-17476
HELWIG, G. N87-16929
HEMMAT, M. N87-17240
HENDERSON-SELLERS, ANN N87-17427
HENRY, CLAUDIA M. N87-16961
HERBIG, H. N87-16925
HERGENROTHER, PAUL M. N87-16907
HERMAN, J. N87-17550
HERMAN, NEIL N87-17143
HERMANN, B. M. N87-17270
HERRERA-VAILLARD, ALFREDO N87-16847
HERRERA, J. I. N87-17400
HERSHKOWITZ, STEPHEN JEFFREY N87-17578
HESS, CECIL F. N87-16895
HETTRICK, M. C. N87-17500
HEUMBEL, R. N87-17174
HIBBARD, PETER N87-17533
HIBBS, B. D. N87-17402
HIDEKUMA, S. N87-17508
HILBERATH, W. N87-17573
HILL, A. J. N87-16835
HILL, J. N87-17350
HINZE, WILLIAM J. N87-17418
HIRANO, K. N87-17511
HIRKO, A. G. N87-17067
HIROMOTO, D. S. N87-16886
HIRSCH, CH. N87-16988
N87-16989
N87-16990
N87-16991
HIRT, C. W. N87-16996
N87-16997
N87-16998
HISADA, Y. N87-16928
N87-17358
N87-17360
HITCHCOCK, JAY C. N87-16861
HIZAL, A. N87-17351
HJORT, N. L. N87-17252
HOAG, DAVID N87-17515
HODGES, ROBERT V. N87-16884
HOELZL, H. N87-17321
HOERST, D. J. N87-17481
HOETZL, H. N87-17234
HOFFER, R. M. N87-17156
HOFMANN, O. N87-17167
HOGE, F. N87-17380
HOGGE, M. N87-16949
HOGGE, THOMAS W. N87-16873
HOLECZ, F. M. N87-17267
HOLMES, BRUCE J. N87-16793
HOLROYD, T. J. N87-16841
HOLT, BENJAMIN N87-17148
HOOGEBOOM, P. N87-17300
HOOVER, G. L. N87-17204
HOSSAIN, MOHAMMAD N87-16914
HOUGH, DAVID HANS N87-17588
HSU, MING-TA S. N87-16908
HUANG, SHIUH-JER N87-17031
HUBBARD, W. B. N87-17616
N87-17644
HUCHRA, JOHN P. N87-17596
HUEPPI, R. N87-17262
N87-17347
HUERTA, C. N87-16945
HUFF, DENNIS L. N87-17001
HUFF, GEORGE A. N87-17430
HUFF, RONALD G. N87-16816
HUG, J. F. N87-17241
HUGHES, B. A. N87-17215
N87-17295
HUGHES, S. J. N87-17215
N87-17295
HUMMER-MILLER, SUSANNE N87-17120
HUNG, CHING-MAO N87-16791
HUNT, J. J. N87-17163
N87-17283
N87-17363
HUNTEN, D. M. N87-17601
HUNTER, SCOTT D. N87-16879
HUSS, JANICE E. N87-17441
HUSSEY, K. J. N87-17292
HUTSINPILLER, AMY N87-17119

I

IAFRATE, GERALD J. N87-17518
IBRAHIM, M. Y. N87-17003
IGUCHI, T. N87-17301
INGERSOLL, A. P. N87-17604
N87-17625
INOUYE, ALAN T. N87-17045
IOKA, M. N87-17251
IRVINE, D. E. N87-17337
ISHIDA, AKIO N87-17510
N87-17512
N87-17513
ISHIMOTO, MICHI N87-17411
ISHIWADA, YASUFUMI N87-17145
ITOH, Y. N87-16928
N87-17358
N87-17360
ITTEN, K. I. N87-17174
N87-17273
N87-17318
IVES, NEIL A. N87-17523
IZUMI, I. N87-17358

J

JABBARI, FARYAR N87-17030
JACKSON, F. C. N87-17380
JACKSON, T. J. N87-17302
JACKSON, T. L. N87-17436
JACOBS, K. N87-17573
JACOBY, B. A. N87-17499
JAMESON, ANTONY N87-16803
N87-16804
N87-16806
JANSEN, F. N87-17575
JANUS, J. MARK N87-16829
JARAMILLO, LINDA L. N87-17117
JARON, DON N87-17433
JAYATILAKA, H. S. N87-17174
JEANDEL, D. N87-16995
JENKINS, B. J. N87-17497
JEPPS, G. N87-16795
JEVICKI, A. N87-17490
JHA, V. K. N87-16934
JIANKANG, J. N87-17349
JOHANNESSEN, J. A. N87-17219
JOHANNESSEN, O. M. N87-17219
JOHANSSON, J. N87-17572
JOHNS, J. W. C. N87-17486
JOHNSON, D. R. N87-17385
JOHNSON, F. N87-16887
JOHNSON, J. BLAIR N87-16821
JOHNSON, JOSEPH L., JR. N87-16828
JOHNSON, T. C. N87-16853
JOHNSON, W. S. N87-16882
JOHNSON, WILLIAM T. K. N87-17142
JOLMA, P. N87-17264
N87-17305
JOLYS, P. N87-17060
JONES, D. G. N87-17024
JONES, E. R. N87-17291
JONES, FRANKLIN B. N87-16974
JONGEN, HUBERTUS TH. N87-17455
JONKER, PETER N87-17455
JOSEPH, R. D. N87-17555
JOURLIN, M. N87-17253

K

KACHARE, AKARAM H. N87-17399
KAGAN, B. A. N87-17103
KAHLE, A. B. N87-17127
KAHLE, ANNE B. N87-17111
N87-17131

KAHN, S. M. N87-17500
KAMIMURA, T. N87-17509
KAMOWITZ, DAVID N87-17444
KANADE, TAKEO N87-17533
KANEMABU, E. T. N87-17266
KANESHIGE, THOMAS N87-17388
KANG, K. N87-17490
KAPILA, A. K. N87-17436
KAPLAN, M. S. N87-17277
KARAM, M. A. N87-17309
KARCHMER, ALLAN M. N87-16816
KARKOSCHKA, E. N87-17610
KASAHARA, A. N87-16928
KASHIHARA, H. N87-17358
N87-17360
KASISCHKE, E. S. N87-17312
N87-17336
KASUBA, R. N87-17401
KASZUBOWSKI, MARTIN J. N87-16861
KAUFMAN, H. N87-17247
KAUFMANN, H. N87-17234
KAUKLER, W. F. N87-16900
N87-16901
KAUPP, V. H. N87-17241
N87-17245
N87-17268
KAWAMOTO, T. N87-17508
KAWATA, Y. N87-17249
N87-17329
KAZAROFF, JOHN M. N87-16902
KEARNEY, F. N87-17062
KEETON, L. W. N87-17000
KELLER, M. N87-17316
KELLER, M. R. N87-17185
KELLER, TEDDIE LEE N87-17412
KENNEDY, JOHN K. N87-17519
KEPICS, FRANK N87-17433
KERR, ROBERT BRUCE N87-17651
KESSLER, R. N87-17266
KESTER, D. N87-17556
KESTNER, S. C. N87-17091
KEYDEL, W. N87-17362
KEYTE, G. E. N87-17335
KHANDELWAL, GOVIND S. N87-17487
KIEFEL, ERLINDA R. N87-16855
KILLEN, R. M. N87-17611
KIM, S. N87-17615
KIM, SANG-WOOK N87-16982
KING-HELE, D. G. N87-16859
KING, H. M. N87-16910
KIRCHHOF, W. N87-17165
KLEIJWEG, J. C. M. N87-17300
KLEIN, M. N87-16948
KLIMA, R. N87-17504
KLYNNING, L. N87-17486
KNACKE, R. F. N87-17618
KOCH, WOLFGANG N87-17373
KODA, M. N87-17251
KOEHLER, H. A. N87-17499
KOJIMA, M. N87-17166
KOLLBERG, E. N87-17572
KOMANETSKY, FREDERICK J. N87-17020
KON, A. I. N87-17108
KONDO, H. N87-17358
KONG, J. A. N87-17187
KOOL, G. A. N87-17070
KOPPE, A. N87-17256
KOSS, D. A. N87-17091
KOSUT, ROBERT L. N87-16871
KOZMA, A. N87-17280
KRAINER, ANDREAS N87-17002
KRAUSS, R. J. N87-17623
KREJSA, EUGENE A. N87-16816
N87-17480
KREMER, R. N87-17226
KRIEGEL, MICHAEL H. N87-17520
KROHN, M. DENNIS N87-17134
KRUEGEL, E. N87-17545
KRUSE, FRED A. N87-17120
KUDRYA, A. V. N87-17105
KUKLA, G. N87-17318
KUMAR, DEVENDRA N87-16909
KUMAZAWA, R. N87-17508
KUMMEROW, C. N87-17340
KUNDE, V. G. N87-17605
KUO, SPENCER P. N87-17413
KUSAKA, T. N87-17249
N87-17329
KUSHNICK, STEVEN B. N87-16893
KWOH, D. S. W. N87-17216
KYRALA, A. N87-17469

L

LABRECQUE, J. L. N87-17429
LABRUYERE, G. N87-16926
LACERDA, FRED W., JR. N87-17439
LACY, J. H. N87-17618
LACY, JOHN N87-17614
LAKE, B. M. N87-17216
LAMARRE, J. M. N87-17560
LANG, H. R. N87-17121
LANG, R. H. N87-17346
LANGER, DIETRICH W. N87-17495
LANGHAM, E. N87-17229
LANGRAN, KENNETH J. N87-17122
LANNELONGUE, N. N87-16963
N87-16964
LAROSA, I. N87-16936
LARSON, H. P. N87-17605
LARSON, R. W. N87-17220
N87-17312
LARSON, RICHARD R. N87-16819
LARSON, TERRY J. N87-16821
LAUER, E. J. N87-17489
LAUREIJS, RENE J. N87-17556
N87-17559
LAUSTRUP, MARK N87-17128
LAWLER, J. S. N87-17400
LAWRENCE, G. R. N87-17324
LAWSON, SHIRLEY W. N87-16802
LAWVER, B. S. N87-17446
LEAVERS, V. F. N87-17438
LEBERL, F. N87-17239
N87-17269
LEBERL, FRANZ N87-17157
LEBOEUF, J. N. N87-17509
LECOMTE, PASCAL N87-17370
LEE, E. A. N87-16954
N87-16955
LEE, JAEMYONG N87-16814
LEE, JOSEPH Y. N87-17520
LEE, LONG C. N87-16890
N87-16891
LEE, RICHARD Q. N87-16968
LEENE, A. N87-17557
LEFEBVRE, J. D. N87-16937
LEITNER, R. N87-16932
LELLOUCH, EMMANUEL N87-17540
LEMAIRE, J. N87-17421
LENA, PIERRE N87-17566
LEONARD, P. M. N87-16949
LEONTARITIS, I. J. N87-17095
N87-17471
LEOVY, CONWAY N87-17627
LEQUEUX, JAMES N87-17543
LESGOURGES, J. N87-17053
LESGOURGUES, J. N87-17069
LESIEUTRE, DANIEL J. N87-16981
LEUNG, MARTIN S. N87-17523
LEUPP, J. N87-17068
LEVIN, EUGENE N87-16957
LEVINE, D. N87-17260
LEVINE, D. M. N87-17346
LEVISON, HAROLD F. N87-17589
LEVY, MEIR N87-16822
LEWALLEN, PAT N87-16876
LEWICKI, DAVID G. N87-16816
LEWIS, S. R. N87-17633
LI, CHIEN-PENG N87-16792
LI, F. K. N87-17384
LIBURDI, J. N87-17071
LIEPA, V. N87-17281
LIMAYE, SANJAY S. N87-17622
LIN, C. C. N87-17199
N87-17256
LIN, F. C. N87-17187
LIN, SHU N87-17457
N87-17458
LIND, D. N87-16887
LIPPERT, THOMAS M. N87-17434
LISI, M. N87-16951
LIU, W. TIMOTHY N87-17110
LIVINGSTONE, C. E. N87-17379
LLEWELLIN, WILLIAM R. N87-17037
LLOYD, F. L. N87-17570
LOHAR, G. N87-17290
LOMBARDINI, P. P. N87-17392
LOMBARDO, M. A. N87-17175
LONG, A. E. N87-17225
LONG, D. N87-17258
LONGAIR, M. S. N87-17536
LONGDON, NORMAN N87-17535
LOPES, A. N87-17265
LOPEZ, G. N87-16941
LORENCE, L. J., JR. N87-17485
LORENZINI, M. N87-17243
LOUET, J. N87-17192
LOUET, JACQUES N87-17364
LOWDEN, P. N87-17071
LOWRY, R. T. N87-17269
N87-17313
LOWRY, S. A. N87-17000
LOZANO-GARCIA, D. F. N87-17156
LUENGO, P. N87-16945
LUEPKE, DOUGLAS E. N87-17125
LUHMANN, H. J. N87-16939
LUIS, JOSIE ENRIQUE N87-17390
LULLA, K. N87-17332
LUNDEN, B. N87-17244
LUNINE, J. I. N87-17616
LUNINE, JONATHAN I. N87-17637
LUSTMAN, LIVIU R. N87-17088
LUTZ, BARRY L. N87-17617
LYDEN, J. D. N87-17219
N87-17297
LYNN, B. W. N87-17652
LYON, R. J. P. N87-17203
N87-17242
LYONS, MICHAEL G. N87-16871
LYSENKO, V. I. N87-16797
LYZENGA, D. R. N87-17297

M

MACCONE, C. N87-16947
MACDONALD, H. C. N87-17241
N87-17245
N87-17268
MACKLIN, J. T. N87-17335
MACY, WILLIAM N87-17619
MADHAVA, N. M. N87-17070
MADIER, J. P. N87-17253
MAECKEL, R. N87-17173
MAEDA, K. N87-17166
MAETZER, C. N87-17262
MAGUIRE, W. N87-17615
MAHEFKEY, EDWARD T. N87-17005
MAHMOUD, S. F. N87-17198
MAITLAND, A. N87-17068
MALAK, MALAK F. N87-16979
MALILA, A. N87-17164
MALIN, MICHAEL C. N87-17117
MALKAMAEKI, L. J. N87-17567
MANDOLESI, N. N87-17539
N87-17552
MANGALGIRI, P. D. N87-16882
MANLEY, T. O. N87-17222
MARCHESE, P. N87-17056
MARCHETTI, M. N87-16930
MARCKWARDT, W. N87-17353
MARGETSON, J. N87-17072
MARINOS, CHARALAMPUS N87-16875
MARKOV, G. A. N87-17107
MARKWITZ, W. N87-17153
MARLEY, M. N87-17616
MARLOW, MARGARET C. N87-17044
MARON, ADOLFO N87-17390
MARSHALL, ROBERT C. N87-17519
MARSTON, PHILIP L. N87-17498
MARTIN-PINTADO, J. N87-17553
N87-17561
MARTIN, B. D. N87-17384
MARTIN, GLENN L. N87-16793
MARTIN, R. D. N87-17286
MARTIN, R. M. N87-17479
MARTIN, R. N. N87-17568
MARTINEC, J. N87-17317
MARTINEK, S. N87-17610
MARVIN, DEAN C. N87-17523
MASI, SILVIA N87-17539
MASLOVA, N. B. N87-17103
MASUMOTO, H. N87-17508
MASUOKA, T. N87-16892
MATARESE, J. N87-17138
MATERNA, DAVID M. N87-16953
MATHESON, D. N. N87-17569
MATSUMOTO, T. N87-17181
MATSUYAMA, T. N87-17210
MATTHEWS, E. W. N87-16954
N87-16955
MATTILA, K. N87-17559
MATZ, STEVEN MICHAEL N87-17654
MATZLER, C. N87-17223
MAUSEL, P. N87-17332
MAUSER, W. N87-17165
MAXWELL, M. S. N87-17205
MAZUR, V. N87-17271
MCARDLE, JACK G. N87-16825
MCCAULEY, JOHN F. N87-17139
MCCORMICK, M. PATRICK N87-17417
MCCURDY, DAVID A. N87-17483
MCGILLEM, C. N87-17327
MCGRATH, W. R. N87-17572
MCINTOSH, R. E. N87-17307
MCLAURIN, A. P. N87-17291
MCNUTT, L. N87-17189
N87-17229

MCSHERRY, J. N87-16835
MEAUZE, GEORGES N87-16846
MEETHAM, G. W. N87-16905
MEGIER, J. N87-17350
MEI, K. K. N87-17199
MEIER, E. H. N87-17267
MELCHIORRI, FRANCHESCO N87-17539
MENDENHALL, MICHAEL R. N87-16981
MENICHINI, V. N87-16950
MERCER, J. B. N87-17269
METZ, ROGER N. N87-16971
MEYER, P. N87-17273
MEYER, ROBERT T. N87-16849
MIETRACH, D. N87-17032
MIHALY, S. N87-17282
MIKKOLA, P.-V. N87-17343
MILES, JEFFREY H. N87-16799
MILEY, H. S. N87-17652
MILLER, D. N87-17256
MILLER, D. A. N87-17127
MILLER, M. N87-17573
MILLER, S. C. N87-16840
MILNE, GARTH W. N87-16813
MINENO, H. N87-17301
MINER, ELLIS D. N87-17639
MINOMO, M. N87-16933
MIRTICH, MICHAEL J. N87-16875
MITTELMANN, HANS D. N87-17459
MIYAMOTO, Y. N87-17200
MOCK, DONALD R. N87-17110
MOCKOVCIAK, JOHN, JR. N87-17036
MOGNARD, N. M. N87-17386
MOHN, E. N87-17252
MOLCHANOV, S. A. N87-17104
MOLLO-CHRISTENSEN, ERIK N87-17380
MOM, A. J. A. N87-17070
MOMOTA, HIROMU N87-17510
N87-17512
N87-17513
MONALDO, F. N87-17334
MONALDO, FRANK N87-17381
MONGIARDO, M. N87-17261
MONTALVO, E. N87-17509
MOON, W. N87-17293
MOORE, CARLETON J. N87-17039
N87-17040
MOORE, JAMES N87-17052
MOORE, R. K. N87-17188
N87-17217
N87-17240
N87-17278
MOORE, THOMAS N87-17433
MOREL, J. E. N87-17485
MORENO, G. N87-17539
MORGAN, PAUL N87-17649
MORGAN, S. E. N87-16824
MORGANTI, F. N87-16930
N87-16944
MORRIS, A. E. N87-16906
MORRIS, HAYDEN N87-17044
MORTENSEN, R. A. N87-17292
MOSHER, MARIANNE N87-16850
MOTSINGER, R. E. N87-17481
MOUEDDENE, K. N87-17294
MOUGINIS-MARK, P. N87-17245
MU, X. C. N87-17408
MUELLER, BERNHARD N87-16794
MUELLER, P. W. N87-17156
MULLANE, T. N87-17189
N87-17229
MUNZ, H. N87-17226
N87-17257
MURRAY, GENE N87-17126
MURTHY, A. V. N87-16807
MUSIANI, B. N87-17182
MUSIL, DENNIS J. N87-17426
MUTTIT, G. N87-17259
MYERS, PHILIP C. N87-17583

N

NADEAU, F. N87-17066
NAJWIJN, W. M. N87-17463
NAKAMURA, K. N87-17301
NALLASAMY, M. N87-16798
NANAYAKKARA, S. D. F. C. N87-17174
NANOBASHVILI, S. N87-17506
NATHRATH, N. N87-16932
NEE, J. B. N87-16891
NEIDLINGER, H. H. N87-16913
NEJEDLY, G. N87-17274
NELSON, P. J. N87-17016
NEMETH, NOEL N. N87-17087
NEMOTO, YOSHIAKI N87-17145
NEURGAONKAR, R. R. N87-17521
NICHOLS, A. D. N87-17280
NIELSEN, G. N87-16944
NIGRO, L. N87-17238
NIJMEIJER, HENK N87-17452
NILSSON, B. N87-17572
NILSSON, STELLAN N87-16966
NISHIKAWA, K. N87-17358
N87-17360
NISHIMURA, K. N87-17506
NISHINO, H. N87-17358
N87-17360
NIXON, MARK W. N87-16884
NOACK, W. N87-17153
NOLL, K. S. N87-17618
NOMURA, YASUYUKI N87-17512
N87-17513
NOOR, AHMED K. N87-17526
NORBURY, JOHN W. N87-17487
NORMAN, COLIN A. N87-17574
NUESCH, D. R. N87-17267

O

OBARA, CLIFFORD J. N87-16793
OBERLY, CHARLES E. N87-16865
OBERPARLEITER, WOLFRAM N87-17065
OCHIAI, H. N87-17314
OCHOA, M. C. N87-17124
OCHS, G. R. N87-17272
ODA, TOSHIATSU N87-17507
OETTL, HERWIG N87-17162
OFFILER, D. N87-17227
OFFILER, DAVID N87-17382
OHI, SHOICHI N87-17512
N87-17513
OHNISHI, MASAMI N87-17512
N87-17513
OKAMOTO, K. N87-17301
OKAMOTO, MASAO N87-17512
N87-17513
OKAMURA, S. N87-17508
OKIISHI, T. H. N87-16789
N87-16790
OKUYAMA, T. N87-17301
OLAUSSEN, T. N87-17219
OLIVER, J. R. N87-17521
OLIVO, B. N87-17539
OLSON, ROBERT E. N87-17019
OMONT, A. N87-17549
ONEILL, P. E. N87-17302
N87-17303
ONG, CHING CHO N87-16785
ONORATI, G. N87-17243
ONSTOTT, R. N87-17188
ONSTOTT, R. G. N87-17184
N87-17220
OOST, WIEBE A. N87-17376
OREFICE, M. N87-16931
OROFINO, V. N87-17551
ORTON, GLENN S. N87-17600
OTTERMANN, J. N87-17318
OWEN, TOBIAS N87-17617
N87-17638
OWENS, G. A. N87-16887
OZGA, M. N87-17208

P

PACE, A. N87-16936
PAGANA, E. N87-16943
PAJOT, F. N87-17560
PALACIOS, ALEJANDRO FEO N87-16809
PALLUCONI, FRANK D. N87-17113
PALMBERG, BJOERN N87-17094
PALMER, D. J. N87-16967
PAPANICOLOPOULUS, C. D. N87-16962
PARASHAR, S. N87-17229
PAREEK, P. N. N87-16892
PARK, J. S. N87-17003
PARKER, JOHN A. N87-16908
N87-16909
PARKER, R. J. N87-17024
PARRISH, RUSSELL V. N87-16873
PARTRIDGE, B. N87-17552
PARTRIDGE, P. G. N87-17058
PASSERON, L. N87-16926
PASTORINO, M. N87-16926
PATEL, BALVANTRAI N87-17052
PATTON, JAMES M., JR. N87-16815
PAULEY, RANDAL LEE N87-17423
PAULS, T. N87-17573
PAVATE, T. V. N87-17171
PEARSON, D. S. N87-16845
PECKHAM, G. E. N87-17569
PEDERSEN, L. T. N87-17221
PEDROFERNANDES, A. T. N87-17235
PELLETIER, R. E. N87-17124
PENKO, PAUL F. N87-16875
PENNLINE, JAMES A. N87-17441
PEREZ, RIGOBERTO N87-17075
PERSON, LEE H., JR. N87-16849
PESSANHA, L. N87-17207
PETERHERYCH, S. N87-17259
PETERKA, ROBERT J. N87-17431
PETERSEN, DIETER N87-17079
PETERSEN, G. W. N87-17127
PETERSON, D. T. N87-16904
PETRIZILKA, V. A. N87-17504
PETTENGILL, G. H. N87-17138
PEYTURAUX, R. N87-17560
PFEIFFER, GEORGE A. N87-16823
PHILIPS, T. G. N87-17546
PICIORGROS, A. N87-17573
PICKARD, A. C. N87-16838
PIENING, MATTHIAS N87-17065
PIERQUIN, F. N87-17053
PIERSON, W. J., JR. N87-17212
N87-17213
PIKE, T. K. N87-17359
PILEWSKIE, P. A. N87-17270
PINTZ, A. N87-17401
PIRRAGLIA, JOSEPH N87-17634
PITERBARG, L. I. N87-17104
PLANESAS, P. N87-17553
N87-17561
PLATZER, MAX F. N87-17002
PODOLAK, M. N87-17645
POLEY, ADRIAAN D. N87-17015
POLI, LOUIS E. N87-17518
POLLACK, JAMES B. N87-17643
POLLARD, L. WAYNE N87-17494
POMERANTZ, M. A. N87-17560
PONCHAK, GEORGE E. N87-16958
PONTOPPIDAN, KNUD N87-16942
PONZI, U. N87-16931
N87-16952
POPOVA, L. L. N87-17107
POPPEN, WILLIAM A., JR. N87-17442
POSCOLIERI, M. N87-17243
POWELL, D. C. N87-17406
N87-17407
POWELL, REDVERS JOHN N87-17367
POWERS, B. J. N87-17395
PRAKASH, C. N87-17041
PRANGE, M. N87-17138
PRATHAP, GANGAN N87-17080
PRICE, J. C. N87-17265
PRICE, K. N87-17472
N87-17473
PRICE, STEPHEN D. N87-17542
PRINCZ, J. N87-17356
PRONO, D. S. N87-17489
PROULX, H. N87-17287
PUCACCO, G. N87-17539
PUGET, J.-L. N87-17560

Q

QUEEN, LLOYD N87-17126

R

RABITZ, H. N87-16896
RAEISAENEN, A. V. N87-17570
RAGES, KATHY N87-17643
RAGHAVAN, V. N87-17232
N87-17235
RAI, R. K. N87-17233
RAINER, F. N87-17489
RALLO, ROSEMARY A. N87-16848
RAMSEIER, R. N87-17373
RANEY, J. PHILIP N87-16861
RANEY, R. K. N87-17144
N87-17356
RANSOM, V. H. N87-17492
RAST, M. N87-17169
RAU, G. N87-17573
RAUPP, H. N87-16938
RAWSON, R. F. N87-17260
RAYMOND, C. A. N87-17429
RAYNER, B. F. N87-16843
READ, P. L. N87-17630
N87-17633
N87-17635
REAGAN, J. A. N87-17270
REDDOCH, T. W. N87-17400
REDDY, B. R. N87-17433
REEVES, ANTHONY P. N87-17440

REEVES, J. H. N87-17652
REHFIELD, LAWRENCE W. N87-16884
REIBALDI, G. G. N87-16924
REICH, M. N87-17311
N87-17573
REICHART, B. N87-17234
REPAS, GEORGE A. N87-16902
RESPONDEK, WITOLD N87-17452
REUTER, W. G. N87-17093
REVERCOMB, H. E. N87-17623
REYNOLDS, M. L. N87-17169
REYNOLDS, R. N87-16830
RHODES, HENRY W. N87-17044
RICCI, WILLIAM N87-17062
RICHARD, RALPH M. N87-17494
RICHARDS, J. A. N87-17159
RICHARDS, MARK ALAN N87-17409
RICHARDS, P. L. N87-17570
RICHARDSON, K. J. N87-17562
RICKMAN, DOUG N87-17115
RIDDLE, LAURENCE R. N87-17460
RIEGGER, S. N87-17310
RITTER, P. N87-17208
RIVACOBA, J. N87-16946
ROBERTS, B. N87-17505
ROBERTSON, BRENT P. N87-16864
ROBERTSON, N. A. N87-17555
ROBINS, A. G. N87-16993
ROBSON, E. I. N87-17558
RODRIGUEZ, G. N87-17451
RODRIGUEZ, PEDRO I. N87-17455
ROHANI, BEHZAD N87-16914
ROHWER, KLAUS N87-17081
ROLFE, E. J. N87-16923
ROLLINS, FRED P. N87-17035
ROOK, B. J. N87-16960
ROSAKIS, ARES J. N87-17092
ROSBOROUGH, J. R. N87-16978
ROSE, MILTON E. N87-17088
ROSENTHAL, BRUCE N. N87-16917
ROTH, M. N87-17421
N87-17653
ROTH, P. A. N87-17492
ROTHERMEL, JEFFRY N87-17425
ROTHROCK, DREW N87-17151
ROUCOS, SALIM N87-16961
ROWLAND, J. N87-17182
ROWLAND, J. R. N87-17306
ROWLETTE, JOHN J. N87-17397
RUDNER, S. N87-17572
RUDOLPH, L. KEVIN N87-16855
RUED, KLAUS N87-16983
RUF, C. N87-17260
RUFFLES, P. C. N87-16836
RUNGALDIER, H. N87-17216
RUSSELL, JAMES M., III N87-17414
RUTHERFORD, JOHN W. N87-16786
RUZEK, M. J. N87-17156
RUZMAYKIN, A. A. N87-17104

S

SAATCHI, S. N87-17346
SABINS, FLOYD F. N87-17137
SABO, FRANCES E. N87-16802
SACCO, V. M. N87-17328
SACHIDANANDA, M. N87-17271
SADD, MARTIN H. N87-16914
SADER, STEVEN A. N87-17123
SAFFMAN, P. G. N87-17298
SAHAGIAN, CHARLES S. N87-17519
SALVI, S. N87-17243
SAMADANI, R. N87-17186
SAMONDS, M. N87-17041
SAMSON, JAMES A. R. N87-16892
SAMUELSON, ROBERT E. N87-17609
SANKAR, L. N. N87-17001
SANMARTIN, J. GARCIA N87-16940
SANTAVICCA, D. A. N87-16894
SAPPL, E. N87-17359
SATHER, DUANE P. N87-17004
SATO, KUNIHIRO N87-17512
N87-17513
SATO, T. N87-17508
SAWCHUK, A. A. N87-17497
SAWYER, F. G. N87-17322
N87-17361
SCHABER, GERALD G. N87-17139
SCHAEFER, W. N87-16932
SCHAFFAR, E. N87-16926
SCHAFFER, STEVE N87-16784
SCHANDA, E. N87-17178
N87-17347
SCHARLEMANN, E. T. N87-17027
SCHELLENBERG, K. N87-17068
SCHEMPP, WILLIAM N87-17619
SCHENCK, L. R. N87-17348
SCHIAVON, G. N87-17354
SCHMIDT, F. A. N87-16904
SCHNEIDER, G. N87-17174
SCHNUR, G. N87-17559
SCHOEDEL, H. J. N87-16938
SCHOLEN, DOUGLAS E. N87-17125
SCHREIER, G. N87-17153
N87-17231
SCHUCHMAN, R. A. N87-17219
N87-17297
SCHUESSLER, R. N87-17152
SCHUETZ, WALTER N87-17065
SCHULTZ, S. N87-17204
SCHWANIGER, ARTHUR J., JR. N87-17017
SCHWANK, J. R. N87-17524
SCHWARTZ, RICHARD M. N87-16961
SCIACOVELLI, C. N87-16947
SCOTT-FLEMING, I. C. N87-17270
SEDLACEK, Z. N87-17505
SEGALL, ZARY Z. N87-17448
SEIDEL, K. N87-17316
N87-17317
SEKI, T. N87-17314
SENNEFF, J. M. N87-16874
SERABYN, E. N87-17618
SERABYN, EUGENE N87-17614
SERRA, GUY N87-17554
N87-17560
SESSLER, A. M. N87-17488
SETTER, ROBERT N. N87-16851
SEXTON, F. W. N87-17524
SGUBINI, S. N87-16931
N87-16952
SHACKMAN, S. J. N87-17280
SHAFER, R. A. N87-17575
SHAFFER, WILLIAM A. N87-17609
SHANNE, J. J., JR. N87-17280
SHINOHARA, H. N87-17360
SHIRLEY, DAVID NOYES N87-17597
SHIVAKUMAR, K. N. N87-17090
SHMOYS, JERRY N87-17413
SHUCHMAN, R. N87-17223
SHUCHMAN, R. A. N87-17222
SHUCHMAN, ROBERT A. N87-17150
SHUEN, J. S. N87-16827
SHUEN, J.-S. N87-16826
SIDMAN, MICHAEL DAVID N87-17449
SIEBER, A. J. N87-17308
N87-17323
SIEWIOREK, DANIEL P. N87-17448
SIMMER, C. N87-17395
SIMON, M. K. N87-16921
SIMONEAU, ROBERT J. N87-17002
SINGH, R. P. N87-16947
SINGH, RAMBIR N87-17408
SINGHAL, A. K. N87-17041
SINKKO, K. N87-17100
SIPPEL, R. N87-16939
SKELTON, EARL F. N87-17477
SKLAR, H. N87-17403
SKORVE, J. E. N87-17319
SLANEY, V. R. N87-17229
SLIWA, STEVEN M. N87-16815
SLOAT, DAVID N87-17515
SLOGGETT, D. R. N87-17176
SLOTH, P. N87-17221
SLYE, R. N87-17208
SMALLEY, ROBERT R. N87-16851
SMARTT, H. B. N87-17050
SMIGIELSKI, P. N87-17025
SMITH-TAYLOR, RUDEEN N87-17442
SMITH, D. N87-17361
SMITH, LAWSON N87-17128
SMITH, M. P. N87-17186
SMITH, MALCOM G. N87-17538
SMITH, P. N87-17296
SMITH, P. H. N87-17607
SMITH, PAUL L. N87-17426
SMITH, PAUL M. N87-16849
SMITH, PAUL SIDNEY N87-17579
SMITH, WM. HAYDEN N87-17619
SNYDER, HARRY L. N87-17434
SOBIESKI, P. N87-17214
N87-17341
SODERSTON, CANDACE N87-17447
SOFFA, L. L. N87-17067
SOKOLOV, D. D. N87-17104
SOLIMINI, D. N87-17261
N87-17263
SONG, DONG JOO N87-16787
SOVEY, JAMES S. N87-16875
SOWELL, JAMES ROBERT N87-17590
SPAGNA, GEORGE F., JR. N87-17591
SPECTER, C. N87-17170
SPERGEL, D. N. N87-17652
SPERGEL, DAVID NATHANIEL N87-17592
SPINOGLIO, L. N87-17552
SPRING, J. N87-17401
SQUIRE, L. C. N87-17010
SROKOSZ, MERIC A. N87-17365
ST.CLAIR, ANNE K. N87-16911
ST.CLAIR, TERRY L. N87-16911
STACY, JOHN GREGORY N87-17580
STAENZ, K. N87-17273
N87-17318
STANICH, CHUCK N87-17112
STANLEY, TIMOTHY D. N87-17522
STAUTER, RICHIE CHARLES N87-16788
STAVRINIDIS, C. N87-16948
STEEDEN, R. V. N87-16852
STEFFES, PAUL G. N87-17620
STEIN, IRVING N87-17396
STEINHAUSER, L. N87-17059
STELLA, D. N87-16944
STENNE, E. N87-16949
STEPHEN, D. N87-17057
STEVENSON, DAVID J. N87-17637
STEWART, D. S. N87-17436
STEWART, J. A. N87-17050
STIBIG, H.-J. N87-17165
STIMPFLING, A. N87-17025
STOECKEL, J. N87-17506
STOKER, C. N87-17631
STONE, R. H. N87-16883
STONIER, R. N87-16936
STOREY, C. N87-17454
STORVIK, G. N87-17252
STOTZER, E. N87-17262
STOUGH, H. PAUL, III N87-16815
STOYANOV, D. V. N87-17218
STRAZISAR, A. J. N87-16789
N87-16790
STROMOVSKY, L. A. N87-17623
STRUVE, K. W. N87-17489
STUDER, PHILIP A. N87-17038
SUBBARAO, SURAMPUDI N87-17396
N87-17397
SUDER, K. L. N87-16789
N87-16790
SUGGS, R. N87-17603
SULLIVAN, R. L. N87-17400
SUMIDA, J. N87-16922
SUTO, MASAKO N87-16890
N87-16891
SUZUKU, M. N87-17181
SVENDSEN, E. N87-17219
SVENSSON, LARS N87-16868
SWADLING, S. J. N87-17057
SWALLOW, K. C. N87-17430
SWANSON, PAUL N. N87-17571
SWIFT, C. T. N87-17260
SWIFT, CALVIN N87-17386
SZEMPLINSKA-STUPNICKA, WANDA N87-16969

T

TACONET, O. N87-17288
TADMOR, EITAN N87-17453
TAJIMA, T. N87-17509
TAJIMA, TOSHIKI N87-17512
N87-17513
TAKEDA, K. N87-17314
TAKERKIA, H. N87-17352
TAKEUCHI, S. N87-17314
TALMOLA, P. N87-17342
TAN, C. I. N87-17490
TANAKA, K. N87-17358
N87-17360
TANNER, A. N87-17260
TARANIK, JAMES V. N87-17119
N87-17132
TARIQUE, S. M. N87-17235
TARRAS, A. N87-17474
TASCA, DANTA M. N87-16977
TAVARES, C. N87-17207
TAYLOR, F. W. N87-17633
TAYLOR, J. C. N87-17250
TAYLOR, PETER K. N87-17374
TAYLOR, R. G. N87-17063
TEILLET, P. M. N87-17273
TEMAM, ROGER N87-17456
TESTER, JEFFERSON W. N87-17430
THEIS, S. W. N87-17304
THOMAS, J. K. N87-17268
THOMAS, N. L. N87-17501
THOMAS, R. W. N87-17289
THOMAS, V. C. N87-17528
THOMASSON, T. B. N87-17430
THOMPSON, D. R. N87-17147

THOMPSON, K. P. B. N87-17287
THURSTON, GAYLEN A. N87-17086
TIDMAN, D. A. N87-16878
TIGHE, DOUGLAS ROGER N87-16858
TILLEY, D. G. N87-17336
TINGAS, STEPHEN A. N87-16849
TIZZI, S. N87-16930
TOBER, GUSTAV N87 17061
TOGNOLATTI, P. N87-17263
TOKSOZ, M. N. N87-17138
TOKUNAGA, A. T. N87-17618
TOKUNAGA, ALAN N87-17614
TOLMUNEN, T. N87-17342
TOM, V. T. N87-17255
TOMASKO, M. G. N87-17601
N87-17610
N87-17613
TORRENCE, G. W. N87-17306
TOUATI-AHMED, D. N87-17454
TOUZI, R. N87-17265
TOWNSEND, DENNIS P. N87-17033
TOWNSEND, LAWRENCE W. N87-17487
TRACEY, J. P. N87-17324
TRAFTON, L. N87-17602
TRAUGER, J. T. N87-17646
TRAVIS, LARRY D. N87-17598
N87-17647
TRIVERO, PAOLO N87-17392
TSUJI, T. N87-17358
TSUJI, YASUMASA N87-17507
TSUTSUMI, Y. N87-16928
TURKEL, ELI N87-16784
TURNER, JOYCE E. N87-17532
TWILT, FRANK N87-17465

U

UENO, S. N87-17249
N87-17329
UGARTEL, RAFAEL GONZALO N87-17422
ULABY, F. T. N87-17179
N87-17281
N87-17345
ULABY, FAWWAZ T. N87-17160
N87-17393
UNGAR, DAVID M. N87-17437
USHAH, A. N87-17293

V

VANBLARICUM, T. J. N87-16881
VANDEGRIEND, A. A. N87-17303
VANDERBEEK, C. N87-17014
VANDERVELDE, WALLACE E. N87-17529
VANDERVOORT, R. J. N87-16947
VANDESANDE, BRETT DAVID N87-16975
VANDIJK, N. M. N87-17466
N87-17467
N87-17468
VANDISHOECK, EWINE F. N87-17547
VANECK, P. N87-17313
VANGROESEN, E. N87-17014
VANHALSEMA, D. N87-17215
N87-17300
VANHEMELRIJCK, E. N87-17650
VANHOENACKER, D. N87-17214
VANHOVE, P. L. N87-17331
VANOOSTEROM, W. N87-17556
VANPARADIJS, J. N87-17575
VANZYL, J. J. N87-17279
VANZYL, JACOB J. N87-17158
VASILEV, V. L. N87-17218
VASSOUT, P. N87-17432
VECK, N. J. N87-17230
VELTEN, E. H. N87-17191
VERBUNT, F. N87-17575
VESECKY, J. F. N87-17186
VIDAL-MADJAR, D. N87-17288
VINNIKOV, K. YA. N87-17101
VISWANATHAN, VISHU R. N87-16961
VITEK, J. M. N87-17049
VIZARD, D. R. N87-17569
VOGEL, W. J. N87-17306
VONFRESE, RALPH R. B. N87-17418
VONPUTTKAMER, JESCO N87-16856
VORBRUGG, H. N87-16925
VOSS, JANICE E. N87-16867
VUKOBRATOVICH, DANIEL N87-17494

W

WACKER, A. G. N87-17290
WAGNER, R. N87-16939
N87-17152
N87-17357
WAITE, W. P. N87-17241
N87-17245
N87-17268
WAKAHAMA, G. N87-17181
WALKER, DOREEN M. C. N87-16859
WALL, STEPHEN N87-17157
WALLER, G. N87-17355
WALSH, E. J. N87-17380
WALTER, LOUIS S. N87-17129
WANG, J. R. N87-17344
WANG, XIUYAN N87-16891
WANNIER, PETER N87-17548
WARD, IAN A. N87-17391
WARWICK, K. N87-17482
WASA, Y. N87-17200
WATSON, KEN N87-17120
WATT, GRAEME D. N87-17563
WEBB, ALAN W. N87-17477
WEBB, D. D. N87-16910
WEGENER, M. N87-17206
WEGMUELLER, U. N87-17262
WEINERT, HOWARD L. N87-17460
WEINMAN, J. A. N87-17340
WEIR, J. T. N87-17489
WELLS, J. K. N87-16887
WENKERT, DANIEL N87-17424
N87-17843
WENOCUR, MICHAEL L. N87-17470
WESTER, T. N87-17244
WESTMORELAND, H. N87-17240
WESTPHAL, M. N87-16939
WESTWATER, E. R. N87-17339
WEWERINKE, P. H. N87-17435
WEYANDT, C. N87-17472
N87-17473
WHEELER, JOHN T. N87-16877
WHEELOCK, J. T. N87-16904
WHIPPLE, FRED L. N87-17504
WHITCHER, F. S. E. N87-16852
WHITE, C. N87-16830
WHITE, DAWN N87-17062
WHITE, E. RICHARD N87-16828
WHITE, GLENN J. N87-17544
N87-17562
WHITE, LUTHER W. N87-16872
WHITELY, STAN N87-17515
WHITFIELD, DAVID L. N87-16829
WIESBECK, W. N87-17310
WIJKER, J. N87-16948
WILKERSON, JOHN N87-17368
N87-17375
WILLIAMS, C. P. N87-17177
WILLIAMS, F. A. N87-16897
WILLIAMS, JEFFREY P. N87-16848
WILLIAMS, T. H. LEE N87-17188
WILLSHIRE, WILLIAM L., JR. N87-17482
WILMS, G. R. N87-17048
WILSON, D. N87-16887
WILSON, JEFFREY V. N87-17045
WING, R. G. N87-16837
WINGHAM, D. J. N87-17195
WINKLER, D. N87-17572
WINNEWISSER, G. N87-17573
WINOKUR, P. S. N87-17524
WINSOR, N. K. N87-16878
WINTER, R. N87-17231
WITRIOL, NORMAN W. N87-17043
WOLF, L. N87-16985
N87-16986
WRIGHT, ROBERT E. N87-17018
WU, JIUNN-CHI N87-17001
WU, M. K. N87-16900

X

XUE, D. N87-17188

Y

YARMAN, BINBOGA S. N87-16973
YASAKA, T. N87-16933
YETTER, R. N87-16896
YNGVESSON, K. S. N87-17572
YOKOTA, T. N87-17325
YOON, SEOKKWAN N87-16803
N87-16804
N87-16806
YOSHIKAWA, KIYOSHI N87-17512
N87-17513
YOUNG, BRUCE N87-16957
YUEN, H. C. N87-17298
YUNG, Y. L. N87-17636

Z

ZACEK, F. N87-17506
ZAHN, R. W. N87-17256
ZAVESKY, RALPH J. N87-16875
ZDZIARSKI, ANDRZEJ ANTONI N87-17655
ZEBKER, H. A. N87-17279
ZEBKER, HOWARD A. N87-17158
ZEHNDER, ALAN T. N87-17092
ZEMING, J. N87-17183
ZHANG, C. Y. N87-17556
ZHONG, S. N87-17349
ZHONGZHI, Z. N87-17349
ZHU, P. Y. N87-17180
ZICK, ROLF N87-17084
ZIMMERMANN, ROLF N87-17062
ZRNIC, D. S. N87-17271
ZUREK, W. H. N87-17585

Typical Corporate Source Index Listing

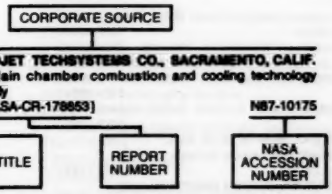

Listings in this index are arranged alphabetically by corporate source. The title of the document provides the user with a brief description of the subject matter. The report number helps to indicate the type of document cited (e.g., NASA report, translation, NASA contractor report). The NASA accession number denotes the number by which the citation is identified. The titles are arranged under each corporate source in ascending accession number order.

A

ADVISORY GROUP FOR AEROSPACE RESEARCH AND DEVELOPMENT, NEUILLY-SUR-SEINE (FRANCE).
Advanced Joining of Aerospace Metallic Materials
[AGARD-CP-398] N87-17051

AERITALIA S.P.A., TORINO (ITALY).
The welding of aluminum alloys: A new technology in space application N87-17056

AERONAUTICAL RESEARCH INST. OF SWEDEN, STOCKHOLM.
Navier-Stokes solution for laminar transonic flow over a NACA0012 airfoil
[FAA-140] N87-16794
A comparison of single-block and multi-block grids around wing-fuselage configurations
[FFA-TN-1986-42] N87-16811
Fatigue life and fastener flexibility of single shear riveted and bolted joints
[FFA-TN-1986-35] N87-17094

AERONAUTICAL RESEARCH LABS., MELBOURNE (AUSTRALIA).
Carbon fibre composite coupons: Static and fatigue behaviour after impact damage
[ARL-STRUC-R-422] N87-16881

AEROSPACE CORP., EL SEGUNDO, CALIF.
Interfacial structure of In/Pt/GaAs heterojunction ohmic contacts
[AD-A175102] N87-17523

AEROVIRONMENT, INC., MONROVIA, CALIF.
HAWT performance with dynamic stall
[DE86-004428] N87-17402

AGRICULTURAL RESEARCH SERVICE, BELTSVILLE, MD.
Applications of remote sensing in the US Department of Agriculture N87-17285

AIR FORCE GEOPHYSICS LAB., HANSCOM AFB, MASS.
Interplanetary dust N87-17542

AIR FORCE WEAPONS LAB., KIRTLAND AFB, N. MEX.
The effect of operating frequency in the radiation induced buildup of trapped holes and interface states in MOS devices
[AD-A173097] N87-17522

ALABAMA UNIV., BIRMINGHAM.
Dynamics and control of flexible manipulators N87-17028

ALFATEH UNIV., TRIPOLI (LIBYA).
The induced current on a long wire due to a vertical electric dipole above dissipative ground N87-17197

AMES LAB., IOWA.
Preparations of rare earth-iron alloys by thermite reduction
[DE86-013753] N87-16904
Abstracts: Review of progress in quantitative NDE
[DE87-000769] N87-17073

ANALYTIC SCIENCES CORP., READING, MASS.
Extracting surface features in multispectral imagery N87-17211
A synergistic approach for multispectral image restoration using reference imagery N87-17255

ARGONNE NATIONAL LAB., ILL.
Supported liquid membranes in 1986: New technology or scientific curiosity
[DE86-007504] N87-16898

ARIZONA STATE UNIV., TEMPE.
Thermal imaging spectroscopy in the Kelso-Baker Region, California N87-17117
Gradient methods for geophysical image inversions N87-17201
A pseudo-arclength continuation method for nonlinear Eigenvalue problems
[AD-A173019] N87-17459

ARIZONA UNIV., TUCSON.
Extrapolation of Earth-based solar irradiance measurements to exoatmospheric levels for broad-band and selected absorption-band observations N87-17270
Dynamic analysis and design of the SIRTF primary mirror mount
[NASA-CR-180158] N87-17494
Modeling the temporal and spatial variations of the vertical structure of Jupiter's atmosphere using observations of the 3-0 hydrogen quadrupole lines N87-17601
The vertical structure of Jupiter's equatorial and tropical regions N87-17607
Constraints on the composition of Jupiter's stratospheric aerosols from ultraviolet photometry N87-17610
The single scattering phase functions of Jupiter's clouds N87-17613
Brown dwarfs and Jovian planets: A comparison N87-17616
Non-solar noble gas abundances in the atmosphere of Jupiter N87-17637
On the oblateness and rotation rate of Neptune's atmosphere N87-17644

ARKANSAS UNIV., FAYETTEVILLE.
Interferometer applications for the rectification of radar images N87-17241
Hawaiian lava flows and SIR-B results N87-17245
Computer-derived height from SIR-B stereo radar images N87-17268

ARMY COLD REGIONS RESEARCH AND ENGINEERING LAB., HANOVER, N. H.
Frost action predictive techniques for roads and airfields: A comprehensive survey of research findings
[DOT/FAA/PM-85/23] N87-16853

ARMY CONSTRUCTION ENGINEERING RESEARCH LAB., CHAMPAIGN, ILL.
Weld quality monitor and control system N87-17062

ARMY ENGINEER SCHOOL, FORT BELVOIR, VA.
Collaborative problem solving for installation planning and decision making
[AD-A174611] N87-17527

ARMY ENGINEER WATERWAYS EXPERIMENT STATION, VICKSBURG, MISS.
The Red River Valley archeological project N87-17128

ASTON UNIV., BIRMINGHAM (ENGLAND).
Discrimation of land features using LANDSAT false colour composite in N Iran N87-17352

ASTRO AEROSPACE CORP., CARPINTERIA, CALIF.
Evaluation of Pactruss design characteristics critical to space station primary structure
[NASA-CR-178171] N87-16870
Batten augmented triangular beam
[NASA-CR-172461] N87-16916

ATMOSPHERIC ENVIRONMENT SERVICE, DOWNSVIEW (ONTARIO).
Application of the Seasat scatterometer to observations of wind speed and direction and Arctic ice/water boundaries N87-17259

AUBURN UNIV., ALA.
Applications of TIMS data in agricultural areas and related atmospheric considerations N87-17124

B

BALLISTIC RESEARCH LABS., ABERDEEN PROVING GROUND, MD.
Atmospheric pressure studies of liquid propellant drops in hot flows
[AD-A174639] N87-16915

BATTELLE INST., FRANKFURT AM MAIN (WEST GERMANY).
General classification of two-phase flow codes N87-16985
Review of present approaches to two-phase flow problems N87-16986

BERN UNIV. (SWITZERLAND).
On microwave scattering properties of heterogeneous two-component mixtures N87-17178
Dielectric and surface parameters related to microwave scatter and emission properties N87-17262
Atmospheric corrections of NOAA-AVHRR data verification of different methods by ground truth measurements N87-17274
L to X-band scatter and emission measurements of vegetation N87-17347

BOLT, BERANEK, AND NEWMAN, INC., CAMBRIDGE, MASS.
Noise-immune multisensor transduction of speech
[AD-A174693] N87-16961

BRITISH AEROSPACE AIRCRAFT GROUP, BRISTOL (ENGLAND).
Diffusion bonding in the manufacture of aircraft structure N87-17057

BROWN UNIV., PROVIDENCE, R. I.
Research program in theoretical high-energy physics
[DE86-013326] N87-17490

BULGARIAN ACADEMY OF SCIENCE, SOFIA.
Spatial dependence on sea spikes N87-17218

C

CAIRO UNIV. (EGYPT).
Determination of resistivity and permittivity profiles of a layered Earth N87-17198

CALIFORNIA INST. OF TECH., PASADENA.
Dynamic fracture initiation and propagation in 4340 steel under impact loading
[AD-A173084] N87-17092
Dynamical models for the Earth's geoid N87-17409
Empirical relations between the Earth's radiation budget, cloudiness, and various meteorological parameters N87-17424
Excitation and transfer of submillimeter molecular transitions N87-17546
Parsec-scale structure in the nuclei of double lobed radio quasars N87-17588
Thermal balance of the atmospheres of Jupiter and Uranus N87-17604
Convection without eddy viscosity: An attempt to model the interiors of giant planets N87-17625

CALIFORNIA UNIV., BERKELEY.
Utility of remote sensing data in renewable resource sample survey N87-17289
The design and evaluation of a high performance smalltalk system
[AD-A173022] N87-17437
Low noise SIS mixer with gain for 80-115 GHz N87-17570
VLA observations of Jupiter at 1.3 - 20 cm wavelengths N87-17606

CALIFORNIA UNIV., BERKELEY. LAWRENCE BERKELEY LAB.
Future accelerator technology
[DE86-013190] N87-17488
Reflection grating spectrometer for the X-ray Multi-Mirror (XMM) space observatory: design and calculated performance
[DE86-013485] N87-17500

CALIFORNIA UNIV., LOS ANGELES.
Microstrip dipoles for EHF and millimeter wave applications
[AD-A173025] N87-16976

A modified loop transfer recovery approach for robust control of flexible structures N87-17029
Lattice filters and adaptive identification of flexible structures N87-17030
Position control of mechanical manipulators by using nonlinear adaptive control algorithm N87-17031
Transmission of atmospheric internal gravity waves into the stratosphere N87-17412
Sound propagation in a superfluid helium filled porous solid: Theory and experiment N87-17478
A numerical study of jet production and accretion disk structure in super-Eddington black hole accretion N87-17586
Magmatic differentiation in partially molten systems: Applications to the moon and the palisades sill N87-17597

CALIFORNIA UNIV., SANTA BARBARA.
The image processing workbench - portable software for remote sensing instruction and research N87-17209

CANADA CENTRE FOR REMOTE SENSING, OTTAWA (ONTARIO).
An alternative multi-mode SAR for RADARSAT N87-17144
An overview of operational SAR data collection and dissemination plans for ERS-1 ice data in Canada N87-17189
Canadian plans for operational demonstrations of satellite imaging radar applications N87-17229
An overview of remote sensing agricultural apcations in North America: Past, present and future N87-17284
Reconsideration of azimuth ambiguities in SAR N87-17356
Canada Center for Remote Sensing (CCRS) Convair 580 results relevant to ERS-1 wind and wave calibration N87-17379

CARLETON UNIV., OTTAWA (ONTARIO).
Computational weld mechanics N87-17052

CARNEGIE-MELLON UNIV., PITTSBURGH, PA.
Fault-free performance validation of fault-tolerant multiprocessors
[NASA-CR-178236] N87-17448
Information processing research
[AD-A173026] N87-17533

CASE WESTERN RESERVE UNIV., CLEVELAND, OHIO.
Oil film thickness measurement and analysis for an angular contact ball bearing operating in parched elastohydrodynamic lubrication
[NASA-CR-179506] N87-16879
Investigation of a GaAlAs Mach-Zehnder electro-optic modulator
[NASA-CR-179573] N87-16953

CATANIA UNIV. (ITALY).
Thermal infrared imagery from helicopter for heat loss calculations in industrial plants N87-17326

CENTRAL ELECTRICITY RESEARCH LABS., LEATHERHEAD (ENGLAND).
An introduction to the numerical modelling of dispersion in the atmospheric boundary layer N87-16993

CENTRE D'ETUDE SPATIALE DES RAYONNEMENTS, TOULOUSE (FRANCE).
A nonparametric supervised multispectral classification method using binary morphological operators N87-17253
Segmentation by mathematical morphology processing hand on the image understanding model in remote sensing N87-17254
Extraction of the backscatter coefficient of agricultural fields from an airborne SAR image N87-17265
Computer-aided interpretation of complex geological patterns in remote sensing N87-17294
New results about diffuse galactic emission at 380 microns N87-17554

CENTRE FOR EARTH SCIENCE STUDIES, TRIVANDRUM (INDIA).
Significance of space image, air photo and drainage linears in relation to west coast tectonics, India N87-17232
Computer-aided analysis of LANDSAT data for mapping geologic and geomorphic features, North Bombay, India N87-17235

CENTRE NATIONAL D'ETUDES DES TELECOMMUNICATIONS, ISSY-LES-MOULINEAUX (FRANCE).
Toward a satellite system to monitor the spatial and temporal behavior of soil water content N87-17288

CENTRE NATIONAL D'ETUDES SPATIALES, TOULOUSE (FRANCE).
VARAN-S radar image interpretation
[CNES-CT/DRT/TIT/RL-54-T] N87-16963
MIZEX VARAN-S radar image characteristics
[CNES-CT/DRT/TIT/RL-55-T] N87-16964

CENTRE NATIONAL DE LA RECHERCHE SCIENTIFIQUE, MEUDON-BELLEVUE (FRANCE).
Spatial variation of the thermal structure of Jupiter's atmosphere N87-17612
A model of the spatial and temporal variation of the Uranus thermal structure N87-17642

CENTRE NATIONAL DE LA RECHERCHE SCIENTIFIQUE, VERRIERES-LE BUISSON (FRANCE).
Submillimeter observation of the integrated galactic emission from the South Pole N87-17560

CENTRE OCEANOLOGIQUE DE BRETAGNE, BREST (FRANCE).
Evaluation of the different parameters in Long's C-band model N87-17370
Using buoys and ships to calibrate ERS-1 altimeter and scatterometer N87-17377

CENTRO STUDI E LABORATORI TELECOMUNICAZIONI, TURIN (ITALY).
Prediction of the electrical performance of Inflatable Space Rigidized Structure (ISRS) offset antenna reflectors and correlation with RF measurements N87-16943

CESKOSLOVENSKA AKADEMIE VED, PRAGUE.
On the possible role of the bootstrap effect in the RF current drive experiments, part 2
[IPPCZ-263] N87-17504

CHALMERS UNIV. OF TECHNOLOGY, GOETEBORG (SWEDEN).
Circumstellar envelopes around evolved stars N87-17548
On the feasibility of constructing an imaging array of slot-antennas integrated with SIS mixers N87-17572

CHAM OF NORTH AMERICA, INC., HUNTSVILLE, ALA.
Discrete element weld model, phase 2
[NASA-CR-179009] N87-17041

CHEVRON OIL FIELD RESEARCH CO., LA HABRA, CALIF.
Space shuttle radar images of Indonesia N87-17137

CHINA RESEARCH INST. OF RADIOWAVE PROPAGATION, XINXIANG.
A spatially homogeneous anisotropic surface model with variable parameters for scattering from bare soil N87-17183
Backscattering power spectrum for randomly moving vegetation N87-17349

CINCINNATI UNIV., OHIO.
Laser Doppler velocimeter measurements and theoretical investigation of three dimensional scroll flow N87-16979

CITY COLL. OF THE CITY UNIV. OF NEW YORK.
Verification results for a two-scale model of microwave backscatter from the sea surface N87-17213

CLARKSON COLL. OF TECHNOLOGY, POTSDAM, N.Y.
Nonlinear wave propagation
[AD-A175073] N87-17461

CLEVELAND STATE UNIV., OHIO.
Design and dynamic simulation of a fixed pitch 56 kW wind turbine drive train with a continuously variable transmission
[NASA-CR-179543] N87-17401

COLBY COLL., WATERVILLE, MAINE.
LEO high voltage solar array arcing response model
[NASA-CR-180073] N87-16971

COLOGNE UNIV. (WEST GERMANY).
Observations from the Gornergrat Observatory (Switzerland) with the University of Cologne 3-m radio telescope N87-17573

COLORADO UNIV., BOULDER.
Orbit determination for low Earth orbit spacecraft based on satellite to satellite tracking techniques via a unique very high altitude relay constellation N87-16858
Selection principles and pattern formation in fluid mechanics and nonlinear shell theory
[NASA-CR-180159] N87-17004

COLUMBIA UNIV., NEW YORK.
International ultraviolet explorer observing program: Ultraviolet observations of selected astronomical sources
[NASA-CR-180155] N87-17584

COLUMBIA UNIV., PALISADES, N.Y.
SAR ice floe kinematics and correlation with mesoscale oceanic structure within the marginal ice zone N87-17222

COMMONWEALTH SCIENTIFIC AND INDUSTRIAL RESEARCH ORGANIZATION, ASPENDALE (AUSTRALIA).
Australian validation plans for ERS-1 N87-17387

COMMUNICATIONS RESEARCH CENTRE, OTTAWA (ONTARIO).
Comparisons of the detection performance of a space-based radar system using different antenna systems and aperture illuminations
[AD-A173094] N87-16960

CONSIGLIO NAZIONALE DELLE RICERCHE, BOLOGNA (ITALY).
On the identification of IRAS deep field sources: The radio counterparts N87-17552

CONSIGLIO NAZIONALE DELLE RICERCHE, FLORENCE (ITALY).
Digital techniques for noise reduction in Automatic Picture Transmission (APT) NOAA satellite images N87-17328

CONSIGLIO NAZIONALE DELLE RICERCHE, FRASCATI (ITALY).
Integrated analysis of geological and remote sensing data aimed at mineral deposits detection in the Monapo area (northern Mozambique) N87-17243

CONSTRUCCIONES AERONAUTICAS S.A., MADRID (SPAIN).
Construcciones Aeronauticas S.A. (CASA) large reflector antenna N87-16935
ERS-1 wind scatterometer antenna: Mechanical aspects N87-16940
Development of mm-wave radiometer antenna reflector N87-16941
Wind Scatterometer Antenna (WSA) release shock loads N87-16945

CONTINUUM, INC., HUNTSVILLE, ALA.
Crystal growth and furnace analysis
[NASA-CR-178998] N87-17516

CONTRAVES CORP., ZURICH (SWITZERLAND).
Development of a 2.8 m offset antenna reflector using inflatable, space-rigidized structures technology N87-16927

CONTRAVES ITALIANA, ROME.
Contraves' antenna tip hinge mechanism for Selenia Spazio's 20/30 GHz antenna N87-16944

CORNELL UNIV., ITHACA, N.Y.
Tectonic geomorphology of the Andes with SIR-A and SIR-B N87-17136
Algorithms and programming tools for image processing on the MPP, part 2
[NASA-CR-180146] N87-17440

CRANFIELD INST. OF TECH., BEDFORD (ENGLAND).
The influence of resampling method and multitemporal LANDSAT imagery on crop classification accuracy in the United Kingdom N87-17250

D

DAEDALUS ENTERPRISES, INC., ANN ARBOR, MICH.
The TIMS instrument N87-17112

DANISH METEOROLOGICAL INST., COPENHAGEN.
The ice conditions in the Greenland waters, 1980
[REPT-551.467.3.068(988)] N87-17428

DARTMOUTH COLL., HANOVER, N.H.
Discrimination of lithologic units using geobotanical and LANDSAT TM spectral data N87-17246

DE HAVILLAND AIRCRAFT CO. OF CANADA LTD., DOWNSVIEW (ONTARIO).
Performance data Aeroc 8.2.AC.20, issue 5, Dash 8, series 100 N87-16817
Performance data Aeroc 8.2.AC.20(300), issue 1 N87-16818

DEFENCE RESEARCH ESTABLISHMENT PACIFIC, VICTORIA (BRITISH COLUMBIA).
Estimation of internal wave currents from SAR and infrared scatterometer imagery N87-17295

DEPARTMENT OF THE AIR FORCE, WASHINGTON, D.C.
A composite aluminum conductor for pulsed power applications at cryogenic temperatures and method of its manufacture
[AD-D012501] N87-16885
Flameholder with removable flameholder attachments
[AD-D012466] N87-16893
Method and apparatus for die forming metal sheets and extrusions
[AD-D012512] N87-16920
ECM (electronic countermoasures) preprocessor or tracker using multi-processor modules
[AD-D012513] N87-16959
A pi-section digital phase shifter apparatus
[AD-D012495] N87-16973
High-voltage Milberger slip slide power conditioner
[AD-D012504] N87-16974
Expandable pulse power spacecraft radiator
[AD-D012498] N87-17005
Universal pressure transducer
[AD-D012499] N87-17019
Unitized high temperature probes
[AD-D012508] N87-17020
Interferometric load sensor and strain gage
[AD-D012509] N87-17021
Switching network for monitoring stations
[AD-D012514] N87-17022
Direct cable attach method
[AD-D012505] N87-17046
Anti-rotation guide vane bushing
[AD-D012510] N87-17047
Metal film light modulator
[AD-D012506] N87-17495

High intensity selectable poly or monochromatic slit light source apparatus for optical instruments
[AD-D012507] N87-17496
Technique for the growth of compositionally ungraded single crystals of solid solutions
[AD-D012488] N87-17519
Low noise polycrystalline semiconductor resistors by hydrogen passivation
[AD-D012492] N87-17520

DEPARTMENT OF THE ARMY, WASHINGTON, D. C.
Free electron diode oscillator
[AD-D012519] N87-16975
Dual channel high electron mobility field effect transistor
[AD-D012474] N87-17518

DEPARTMENT OF THE NAVY, WASHINGTON, D. C.
Fabrication of hollow, cored, and composite shaped parts from selected alloy powders
[AD-D012489] N87-16903
Interpenetrating-network polymeric electrolytes
[AD-D012485] N87-16912
Robotic vision system
[AD-D012481] N87-17043
Metallization for hermetic sealing of ceramic modules
[AD-D012483] N87-17044
Test apparatus for uniform tensioning of long lengths of small cables in simulated environments
[AD-D012487] N87-17045
Apparatus and method for stirring fluid borne particles
[AD-D012486] N87-17477

DEUTSCHE FORSCHUNGS- UND VERSUCHSANSTALT FUER LUFT- UND RAUMFAHRT, BRUNSWICK (WEST GERMANY).
Research on structural analysis at the DFVLR, Brunswick N87-17078
Torsion-tension coupling in rods N87-17079
Field consistency and finite element analysis of multifield structural problems N87-17080
Buckling and postbuckling behavior of shallow shells N87-17081
Optimization of axially compressed Carbon Fiber Reinforced Plastic (CFRP) cylinders N87-17082
An effective substructure technique applied to crack problems N87-17083
Crack propagation in UD (Unidirectional) laminates by the stress intensity factors N87-17084
The static aeroelasticity of a composite wing N87-17085

DEUTSCHE FORSCHUNGS- UND VERSUCHSANSTALT FUER LUFT- UND RAUMFAHRT, OBERPFAFFENHOFEN (WEST GERMANY).
The X-SAR System N87-17162
Stereo Line Scanner (SLS): System considerations on an operational instrument for meteorology and weather forecasts N87-17168
The German ERS-1 SAR postprocessing system plans and concepts N87-17231
The significance of Radar Cross Section (RCS) polarization measurements for tree signatures N87-17306
Radar Cross Section (RCS) data base deduced from radar images N87-17323
Antenna ambiguity investigations for X-SAR N87-17355
Analysis of amplitude nonlinearities in the ERS-1 SAR receiver system N87-17359
X-SAR extends the frequency range of Shuttle Imaging Radar N87-17362
DFVLR flight operation acting as a useful service unit for ERS-1 N87-17378

DEUTSCHE FORSCHUNGS- UND VERSUCHSANSTALT FUER LUFT- UND RAUMFAHRT, PORZ (WEST GERMANY).
Off-line processing of ERS-1 synthetic aperture radar data with high precision and high throughput N87-17153

DORNIER-WERKE G.M.B.H., FRIEDRICHSHAFEN (WEST GERMANY).
Analysis of high precision composite sandwich antennas N87-16929
Development status of the ERS-1 SAR antenna N87-16939
Features and technologies of ERS-1 (ESA) and X-SAR antennas N87-17152
Development status of the ERS-1 payload instruments N87-17191
Numerical modeling of two-dimensional time domain electromagnetic scattering by underground inhomogeneities N87-17199
Quasi real time conversion of ERS-1 scatterometer raw data to sigma zero triplets N87-17226
Recent progress in ERS-1 wind scatterometer design N87-17256
The ERS-1 scatterometer system simulator and its relevance for ground processing design N87-17257
The X-band SAR in a joint mission with the Shuttle Imaging Radar N87-17321
Planar array antenna for ERS-1 synthetic aperture radar N87-17357

DRAPER (CHARLES STARK) LAB., INC., BOSTON, MASS.
Real time identification of large space structures
[NASA-CR-171957] N87-16867

DRAPER (CHARLES STARK) LAB., INC., CAMBRIDGE, MASS.
Reducing shuttle-payload dynamic interaction with notch filters
[NASA-CR-171956] N87-16862

DREXEL UNIV., PHILADELPHIA, PA.
An experimental microcomputer controlled system for synchronized pulsating anti-gravity suit
[AD-A174840] N87-17433

DUISBURG UNIV. (WEST GERMANY).
Theoretical consideration on resistance geoelectrics N87-17196

E

EARTH OBSERVATION SATELLITE CO., VA.
Commercial opportunities in Earth observation from space N87-17177

ECOLE CENTRALE DE LYON (FRANCE).
Numerical methods for two-dimensional and three-dimensional heat transfer calculations N87-16995

EDGERTON, GERMESHAUSEN AND GRIER, INC., IDAHO FALLS, IDAHO.
Heat transfer in gas tungsten arc welding
[DE86-013457] N87-17050
Three dimensional CTOD measurements of elastic-plastic surface flaws
[DE86-013454] N87-17093
ATHENA code manual. Volume 1: Code structure, system models, and solution methods
[DE87-001430] N87-17492

ELECTROTEK CONCEPTS, INC., KNOXVILLE, TENN.
Utility interconnection issues for wind power generation
[NASA-CR-175056] N87-17400

ENVIRONMENTAL RESEARCH INST. OF MICHIGAN, ANN ARBOR.
Imaging radar contributions to a major air-sea-ice interaction study in the Greenland Sea N87-17150
An inter-sensor comparison of the microwave signatures of Arctic sea ice N87-17184
Geophysics of the marginal ice zone from SAR N87-17219
Microwave properties of sea ice in the marginal ice zone N87-17220
Analysis of multichannel SAR data of Spitsbergen N87-17223
Multifrequency-polarimetric SAR for remote sensing N87-17280
Analysis of synthetic aperture radar imagery of surface ship wakes N87-17297
An improved method for the determination of water depth from surface wave refraction patterns N87-17299
Calibrated X and L-band scattering coefficients from a southern US forest N87-17312
Characterisation of internal wave surface patterns on airborne SAR imagery N87-17338

EUROPEAN OFFICE OF AEROSPACE RESEARCH AND DEVELOPMENT, FPO NEW YORK 09510.
Homogenizing surface and satellite observations of cloud
[AD-A174691] N87-17427

EUROPEAN SPACE AGENCY, PARIS (FRANCE).
Proceedings of the Second ESA Workshop on Mechanical Technology for Antennas
[ESA-SP-261] N87-16923
Structural Analysis
[ESA-TT-917] N87-17077
Proceedings of the 1986 International Geoscience and Remote Sensing Symposium (IGARSS '86) on Remote Sensing: Today's Solutions for Tomorrow's Information Needs, volume 1
[ESA-SP-254-VOL-1] N87-17163
Overview and status of the ERS-1 program N87-17190
Proceedings of the 1986 International Geoscience and Remote Sensing Symposium (IGARSS' 86) on Remote Sensing: Today's Solutions for Tomorrow's Information Needs, volume 2
[ESA-SP-254-VOL-2] N87-17283
Shape similarity in remote sensing images using graph matching techniques N87-17330
Proceedings of an ESA Workshop on ERS-1 Wind and Wave Calibration
[ESA-SP-262] N87-17363
Proceedings of an ESA Workshop on a Spaceborne Submillimeter Astronomy Mission. A Cornerstone of the ESA Long Term Science Program
[ESA-SP-260] N87-17535

EUROPEAN SPACE AGENCY. EUROPEAN SPACE RESEARCH AND TECHNOLOGY CENTER, ESTEC, NOORDWIJK (NETHERLANDS).
Antenna mechanical technologies within ESA N87-16924
Giotto spacecraft high gain antenna mechanical design and development N87-16938
Engineering and software interfacing for thermal, structural and dynamic control related with spacecraft activities N87-16948
Beam forming network technologies and related manufacturing processes N87-16951
Concept of a future multispectral Thermal Infrared (TIR) pushbroom mission for Earth observation from space N87-17169
The ESA approach for ERS-1 sensor calibration and performance verification N87-17192
ERS-1 radar altimeter: Performance, calibration and data validation N87-17194
ERS-1 fast delivery processing and products N87-17224
Results of the ESA airborne C-band scatterometer campaigns N87-17225
ERS-1 mission constraints related to wind and wave calibration N87-17364
Far infrared submillimeter wave space telescope (FIRST) observations of stars with large mass loss rates N87-17550
A proposed cornerstone mission: Far infrared submillimeter wave telescope (FIRST) N87-17564

F

FAIRCHILD INDUSTRIES, INC., FARMINGDALE, N.Y.
Assessment of damage tolerance requirements and analysis. Volume 1: Executive summary
[AD-A175110] N87-16822

FEDERAL AVIATION ADMINISTRATION, WASHINGTON, D.C.
Air traffic control radar beacon system transponder performance study and analysis. Volume 2: Appendixes
[DOT/FAA/FS-86/1-VOL-2] N87-16812

FLINDERS UNIV., BEDFORD PARK (AUSTRALIA).
The FRS-68010: A new concept for the acquisition and analysis of NOAA HRPT data N87-17206

FLORENCE UNIV. (ITALY).
Multispectral classification of microwave remote sensing images N87-17238

FLORIDA INTERNATIONAL UNIV., MIAMI.
The transfer of remote sensing technology to developing countries: A survey of experts in the field N87-17170

FLORIDA STATE UNIV., TALLAHASSEE.
Variability in the Earth radiation budget as determined from the Nimbus ERB experiments N87-17410

FLOW SCIENCE, INC., LOS ALAMOS, N. MEX.
SOLA: A basic solution algorithm for flow analysis N87-16996
Applications of SOLA to confined flows N87-16997
Applications of SOLA to free surface flows N87-16998

FORD AEROSPACE AND COMMUNICATIONS CORP., PALO ALTO, CALIF.
Application of adaptive antenna techniques to future commercial satellite communication
[NASA-CR-179566] N87-16954
Application of adaptive antenna techniques to future commercial satellite communication
[NASA-CR-179566] N87-16955
On first passage times and differential equations
[AD-A174648] N87-17470
Communications satellite systems operations with the space station. Volume 1: Executive summary
[NASA-CR-179526] N87-17472
Communications satellite systems operations with the space station, volume 2
[NASA-CR-179527] N87-17473

FOREST SERVICE, ATLANTA, GA.
Locating subsurface gravel with thermal imagery N87-17125

FREIBURG UNIV. (WEST GERMANY).
Comparison of Thematic Mapper (TM) and SPOT simulation data for agricultural applications in south west Germany N87-17165
Radar imagery of the European city influenced by variations in depression angle and look direction N87-17237
Microwave remote sensing: Its applications and limitations in operational tasks of land use inventory and forest management N87-17266

G

G B LAB., INC., SANTA ANA, CALIF.
Development of a drag measurement system for the CERF 6-foot shock tube
[AD-A173087] N87-16854
GA TECHNOLOGIES, INC., SAN DIEGO, CALIF.
RF plugging and tandem mirror experiments in a cusp-anchored mirror device
[IPPJ-800] N87-17508
GARRETT TURBINE ENGINE CO., PHOENIX, ARIZ.
Transition mixing study
[NASA-CR-175062] N87-16830
GENERAL ELECTRIC CO., CINCINNATI, OHIO.
Simulated flight acoustic investigation of treated ejector effectiveness on advanced mechanical suppresors for high velocity jet noise reduction
[NASA-CR-4019] N87-17481
GENERAL ELECTRIC CO., PHILADELPHIA, PA.
High energy surge arrester technology development, part 2
[AD-A173066] N87-16977
GENEVA OBSERVATORY (SWITZERLAND).
Redistribution of angular momentum by nonaxisymmetric instabilities in a thick accretion disk
[PUBL-SER-C-FASC-4] N87-17585
GEOLOGICAL SURVEY, DENVER, COLO.
Simulation modeling and preliminary analysis of TIMS data from the Carlin area and the northern Grapevine Mountains, Nevada N87-17120
GEOLOGICAL SURVEY, FLAGSTAFF, ARIZ.
The megageomorphology of the radar rivers of the eastern Sahara N87-17139
GEOLOGICAL SURVEY, RESTON, VA.
Airborne Thermal Infrared Multispectral Scanner (TIMS) images over disseminated gold deposits, Osgood Mountains, Humboldt County, Nevada N87-17134
GEOLOGICAL SURVEY OF CANADA, OTTAWA (ONTARIO).
Integration of surficial geochemistry and LANDSAT imagery to discover skarn tungsten deposits using image analysis techniques
[CONTRIB-19586] N87-17248
GEOLOGICAL SURVEY OF INDIA, JAIPUR.
Comparative study of LANDSAT MSS, Salyut-7 (TERRA) and radar (SIR-A) images for geological and geomorphological applications: A case study from Rajasthan and Gujarat, India N87-17236
GEORGE WASHINGTON UNIV., HAMPTON, VA.
Flight-vehicle structures education in the US: Assessment and recommendations
[NASA-CR-4048] N87-17526
GEORGIA INST. OF TECH., ATLANTA.
Quantitative analysis of fracture surfaces using computer aided fractography N87-17076
Laboratory measurements of microwave absorption from gaseous atmospheric constituents under conditions for the outer planets N87-17620
GEORGIA TECH RESEARCH INST., ATLANTA.
In-band antenna coupling research
[AD-A175093] N87-16962
GKSS-FORSCHUNGSZENTRUM GEESTHACHT (WEST GERMANY).
Comparison concept of satellite derived wind and wave data with ground truth N87-17373
GOOD SAMARITAN HOSPITAL AND MEDICAL CENTER, PORTLAND, OREG.
Role of orientation reference selection in motion sickness
[NASA-CR-180161] N87-17431
GRENOBLE UNIV. (FRANCE).
Molecular abundances in circumstellar envelopes N87-17549
GRONINGEN RIJKSUNIVERSITEIT (NETHERLANDS).
Review of coherent and incoherent detection techniques: Outlook and limitation N87-17537
Infrared radiation from interface regions in molecular clouds: L1551 and the Serpens nebula N87-17556
GT-DEVICES, ALEXANDRIA, VA.
Investigation of a repetitive pulsed electrothermal thruster
[NASA-CR-179464] N87-16878

H

HARVARD-SMITHSONIAN CENTER FOR ASTROPHYSICS, CAMBRIDGE, MASS.
Interstellar chemistry and submillimeter observations N87-17547
HARVARD UNIV., CAMBRIDGE, MASS.
The astrophysical implications of weakly interacting, massive particles N87-17592
Radiative processes underlying the X-ray and gamma-ray continua of active galactic nuclei and gamma-ray bursts N87-17655
HAWAII UNIV., HONOLULU.
Cyclic unequal error protection codes constructed from cyclic codes of composite length
[NASA-CR-180165] N87-17457
On codes with multi-level error-correction capabilities
[NASA-CR-180166] N87-17458
HELSINKI UNIV. OF TECHNOLOGY, ESPOO (FINLAND).
Dielectric and scattering behavior of snow at microwave frequencies N87-17179
Developpement of algorithms to retrieve the water equivalent of snow cover from satellite microwave radiometer data N87-17264
Classification of forest and surface types by satellite microwave radiometry N87-17305
Retrieval of near-surface wind speed in the Baltic Sea from NIMBUS-7 Scanning Multichannel Microwave Radiometer (SMMR) observations N87-17342
Sea ice studies in the Baltic Sea using satellite microwave radiometer data N87-17343
An 800 MHz bandwidth acousto-optical spectrometer at Helsinki Observatory N87-17567
HOKKAIDO UNIV., SAPPORO (JAPAN).
Snow stratigraphy observed by an FM-CW microwave system N87-17181
HUGHES HELICOPTERS, CULVER CITY, CALIF.
Inertia welding of nitralloy N and 18 nickel maraging 250 grade steels for utilization in the main rotor drive shaft for the AR-64 military helicopter program N87-17067

I

IBM JAPAN.
Evaluation of LANDSAT 5 Thematic Mapping (TM) data for image clustering and classification N87-17251
ILLINOIS UNIV., URBANA.
Pressure gradient effects in the viscous wall region of a turbulent flow
[REPT-7] N87-16980
IMPERIAL COLL. OF SCIENCE AND TECHNOLOGY, LONDON (ENGLAND).
Opportunities and potential for a millimetre wavelength search for the Sunyaev-Zeldovich effect N87-17555
The Saturnian ribbon feature: A baroclinically unstable model N87-17629
INDIAN INST. OF TECH., BOMBAY.
In service training of scientists and engineers: An important method of information transfer in the area of satellite remote sensing and its applications N87-17171
INDIANA STATE UNIV., TERRE HAUTE.
IRSAP: An improved approach in processing remotely sensed data N87-17332
INDUSTRIEANLAGEN-BETRIEBSGESELLSCHAFT M.B.H., OTTOBRUNN (WEST GERMANY).
Influence of welding flaws on the fatigue strength of electron beam weldments in Ti Al6 V4 N87-17065
INSTITUT D'AERONOMIE SPATIALE DE BELGIQUE, BRUSSELS.
A model for an electromotive force generator in the magnetosphere: A source of discrete auroral arcs
[AERONOMICA-ACTA-A-309-1986] N87-17421
The effect of Saturn's rings on the upper-boundary insolation of its atmosphere
[AERONOMICA-ACTA-A-308-1986] N87-17650
The interaction between the solar wind and the comets
[AERONOMICA-ACTA-A-306-1986] N87-17653
INSTITUT FRANCAIS DE RECHERCHE POUR L'EXPLOITATION DE LA MER, BREST (FRANCE).
ERS-1 wind scatterometer: Wind extraction and ambiguity removal N87-17227
INSTITUT FRANCO-ALLEMAND DE RECHERCHES, ST. LOUIS (FRANCE).
Combined density and velocity measurements. Application to the investigation of a free jet
[ISL-CO-206/86] N87-16808
Afterbody shape effects on the near-wake velocity characteristics at Mach numbers between 0.35 and 0.92
[ISL-CO-205/86] N87-17011
Experimental investigation in turbulent flow separation
[ISL-CO-208/86] N87-17012
A new method for compensating and measuring any motion of 3D-objects in holographic interferometry: Recent developments
[ISL-CO-242/85] N87-17025
Biological effects of aerial shock waves: Review of work to date
[ISL-NB-402/85] N87-17432
INSTITUT GEOGRAPHIQUE NATIONAL, PARIS (FRANCE).
Monitoring of large phenomena in developing countries through satellite imagery N87-17172
INSTITUTE OF OCEANOGRAPHIC SCIENCES, WORMLEY (ENGLAND).
The influence of spatial and temporal scales on calibration/validation N87-17365
Requirements and constraints in the calibration and validation of ERS-1 wind and wave parameters N87-17369
Validation of ERS-1 wind data using observations from research and voluntary observing ships N87-17374
INSTITUTE OF PLASMA PHYSICS, PRAGUE (CZECHOSLOVAKIA).
Initial-value problem for the 1-D wave equation in an inhomogeneous medium
[IPPCZ-268] N87-17505
Plasma formation and sustainment by a multijunction grill on the castor tokamak
[IPPCZ-255] N87-17506
INSTITUTO DE PESQUISAS ESPACIAIS, SAO PAULO (BRAZIL).
Environmental modification of metropolitan areas through satellite images: Study of urban design in the tropics N87-17175
INSTITUTO NACIONAL DE METEOROLOGIA E GEOFISICA, LISBON (PORTUGAL).
Digital satellite imagery acquisition and processing N87-17207
INSTITUTO NACIONAL DE TECNICA AEROESPACIAL, MADRID (SPAIN).
The effects of heavy rain on profile aerodynamics
[ETN-87-98848] N87-16809
Profile design in transonic regime
[ETN-87-98849] N87-16810
Ground vibration tests
[ETN-87-98847] N87-17422
INTEGRATED SYSTEMS, INC., PALO ALTO, CALIF.
Adaptive control techniques for large space structures
[AD-A173083] N87-16871
INTERA ENVIRONMENTAL CONSULTANTS LTD., CALGARY (ALBERTA).
Digital terrain mapping with STAR-1 SAR data N87-17269
INTERA ENVIRONMENTAL CONSULTANTS LTD., OTTAWA (ONTARIO).
SAR imagery for forest management N87-17313
Thermal infrared remote sensing: One of today's solutions N87-17324
INTERNATIONAL COUNCIL OF SCIENTIFIC UNIONS, URBANA, ILL.
Middle Atmosphere Program. Handbook for MAP, volume 22
[NASA-CR-180128] N87-17414
ISTANBUL UNIV. (TURKEY).
LANDSAT-5 Thematic Mapping (TM) data applications to land use classification on around the Bosphorus area, Turkey N87-17351

J

JET PROPULSION LAB., CALIFORNIA INST. OF TECH., PASADENA.
Multiple Trellis Coded Modulation (MTCM): An MSAT-X report
[NASA-CR-180134] N87-16921
Coherent versus noncoherent signaling for satellite-aided mobile communications
[NASA-CR-180133] N87-16922
Evaluation of geophysical parameters measured by the Nimbus-7 microwave radiometer for the TOGA Heat Exchange Project
[NASA-CR-180151] N87-17110
The TIMS Data User's Workshop
[NASA-CR-180130] N87-17111
The TIMS investigator's guide N87-17113
Enhancement of time images for photointerpretation N87-17116
Lithologic mapping of silicate rocks using TIMS N87-17118
Application of TIMS data in stratigraphic analysis N87-17121
Infrared spectroscopy for geologic interpretation of TIMS data N87-17130
Calculation of day and night emittance values N87-17131
A geologic atlas of TIMS data N87-17133
The Second Spaceborne Imaging Radar Symposium
[NASA-CR-180131] N87-17135
Geological applications of multipolarization SAR data N87-17140
Spaceborne imaging radar research in the 90's N87-17141
Venus Radar Mapper (VRM): Multimode radar system design N87-17142
Spaceborne Imaging Radar Project N87-17143
Present statue of Japanese ERS-1 Project N87-17145

A scanning radar altimeter for mapping continental topography N87-17146
Ocean waves near Hurricane Josephine from SIR-B N87-17148
The SIR-C ground data system: Digital processor, data products, information flow N87-17155
Multiple incidence angle SIR-B experiment over Argentina N87-17157
Imaging radar polarimetry from wave synthesis N87-17158
SIR-C, the next generation spaceborne SAR N87-17161
Imaging spectrometry: Aircraft and space program N87-17202
Analysis of AIS radiometry at Mono Lake, California N87-17204
Roundoff noise analysis for digital Doppler processors in radar scatterometers N87-17258
Imaging radar polarimetry from wave synthesis N87-17279
Image processing methods in two and three dimensions used to animate remotely sensed data N87-17292
Remote sensing of tree attenuation at 870 MHz along simulated Earth-satellite paths N87-17306
On the relationship between age of lava flows and radar backscattering N87-17348
NASA scatterometer data processing system: Features for validation N87-17366
Satellite scatterometer comparisons with surface measurements: Techniques and Seasat results N87-17372
An overview of the NSCAT/N-ROSS program N87-17384
Safety considerations of lithium-thionyl chloride cells [NASA-CR-180129] N87-17396
The NASA Aerospace Battery Safety Handbook [NASA-CR-180127] N87-17397
Kalman filtering, smoothing and recursive robot arm forward and inverse dynamics [NASA-CR-180135] N87-17451
Vibroacoustic payload environment prediction system (VAPEPS): Data base management center remote access guide [NASA-CR-180132] N87-17528
The large deployable reflector: A NASA submillimeter-infrared orbiting observatory N87-17571
Spatial and temporal variability of infrared-observable properties of the Jovian atmosphere: A partial survey N87-17600
An updated hydrocarbon photochemical model for the Jovian atmosphere from the troposphere through the homopause: A prelude to Galileo N87-17636
The Voyager encounter with Uranus and Neptune N87-17639
The ortho-para H2 distribution on Uranus: Constraints from the collision-induced 3-0 dipole band and 4-0 S(0) and S(1) quadrupole line profiles N87-17640
Radiative-convective equilibrium models of Uranus and Neptune N87-17641
The HD/H2 ratio in the atmosphere of Uranus N87-17646

JOHNS HOPKINS UNIV., BALTIMORE, MD.
Recursive linear smoothing for dissipative hyperbolic systems [AD-A173020] N87-17460

JOHNS HOPKINS UNIV., LAUREL, MD.
Hydrodynamics of internal solitons and a comparison of SIR-A and SIR-B data with ocean measurements N87-17147
Operational wave forecasting with spaceborne SAR: Prospects and pitfalls N87-17149
Rain measurement results derived from a two polarization S-band radar employing frequency diversity at Wallops Island, Virginia N87-17182
Characteristics of a very low altitude spacecraft for collecting global directional wave spectra with spaceborne synthetic aperture radar N87-17333
The SAR image modulation transfer function derived from SIR-B image spectra and airborne measurements of ocean wave height spectra N87-17334
Deriving two-dimensional ocean wave spectra and surface height maps from the Shuttel Imaging Radar (SIR-B) N87-17336
Spatial evolution of wave spectra in the vicinity of the Agulhas current from SIR-B N87-17337
A procedure for estimation of two-dimensional ocean height-variance spectra from SAR imagery N87-17381

JOINT PUBLICATIONS RESEARCH SERVICE, ARLINGTON, VA.
USSR report: Earth sciences [JPRS-UES-86-005] N87-17096
Geophysicist comments on how solar activity may affect weather N87-17097
Thermodynamic estimate of climatic system efficiency N87-17098
Contemporary changes in climate and paleoclimate N87-17099
Determination of nonglobal component against background of global radioactive pollution of atmospheric aerosols N87-17100
Assessment of contemporary changes in global climate N87-17101
Metal content of ocean water studied with radio spectrometer N87-17102
Stochastic model of tidal evolution of Earth-Moon system with cyclic change in resonant frequency of ocean N87-17103
Ocean surface temperature field variability N87-17104
Solution of direct gravimetry problems for vertical cylindrical bodies N87-17105
Development of new aviation technology for gravimetric surveying N87-17106
Modeling of nonlinear effects of plasma wave beams on ionospheric plasma N87-17107
Joint influence of turbulence and wind on signal power in radioacoustic sounding of atmosphere N87-17108

JOINT RESEARCH CENTRE OF THE EUROPEAN COMMUNITIES, ISPRA (ITALY).
Rural land use inventory and mapping in the Ardeche area (France) using multitemporal Thematic Mapping (TM) data N87-17350

K

KANAZAWA INST. OF TECH. (JAPAN).
Bitemporal analysis of Thematic Mapper data for land cover classification N87-17249

KANAZAWA UNIV. (JAPAN).
Radiometric correction method which removes both atmospheric and topographic effects from the LANDSAT-MSS data N87-17329

KANSAS STATE UNIV., MANHATTAN.
Assessing grass canopy condition and growth from combined optical-microwave measurements N87-17286

KANSAS UNIV., LAWRENCE.
Development of a sensitivity analysis technique for multiloop flight control systems N87-16847

KANSAS UNIV. CENTER FOR RESEARCH, INC., LAWRENCE.
Microwave backscatter coefficients of artificially grown first-year sea ice N87-17188
Tower-based broadband backscattering measurements from the ocean surface in the North Sea N87-17217
Determining the vertical pattern of a spaceborne SAR by observation of uniform targets N87-17240
Some trade-offs in modest-resolution radars for space N87-17278

KAPTEYN ASTRONOMICAL LAB., GRONINGEN (NETHERLANDS).
Far infrared and optical study of the high latitude cloud L1642 N87-17559

KARLSRUHE UNIV. (WEST GERMANY).
Hydrogeological research in Peloponnesus (Greece) Karst area by support and completion of LANDSAT-thematic data N87-17234
Results of tectonic and spectral investigations along the Wadi Araba fault in Jordan using special processed Thematic Mapping (TM) data N87-17247
Coherent polarimetric Radar Cross Section (RCS) measurements on trees N87-17310

KOMBINET VEB CARL ZEISS, JENA (EAST GERMANY).
Optical visual evaluation and interpretation of remote sensing data N87-17353

L

LAMONT-DOHERTY GEOLOGICAL OBSERVATORY, PALISADES, N.Y.
Magnetization of the oceanic crust: TRM or CRM? [NASA-CR-179896] N87-17429

LANCHESTER POLYTECHNIC, COVENTRY (ENGLAND).
Submillimetre continuum observations of active galactic nuclei N87-17558

LAVAL UNIV. (QUEBEC).
Analysis of the spatial structure of Synthetic Aperture Radar (SAR) imagery for a better separability of cereal crops, wheat and barley N87-17287

LAWRENCE LIVERMORE NATIONAL LAB., CALIF.
Mechanical properties of graphite epoxy used for Zero CTE Program [DE86-013227] N87-16886
Direct computation of wall bounded aerosol turbulent flow interactions [DE86-013221] N87-17009
Optical modeling of induction-linac driven free-electron lasers [DE87-001432] N87-17027

Interactive wrapper tool for mapping objects to Fortran library functions [DE86-009686] N87-17446
Empirical considerations for laser guided electron beams in the advanced test accelerator [DE86-013218] N87-17489
Nanosecond two-dimensional imaging using tomographic techniques [DE86-008164] N87-17499
Optical thin film monitoring using optical fibers [DE87-001355] N87-17501

LECCE UNIV. (ITALY).
Some results about laboratory dust analysis in the FIR range N87-17551

LIBURDI ENGINEERING LTD., BURLINGTON (ONTARIO).
Repair techniques for gas turbine components N87-17071

LIEGE UNIV. (BELGIUM).
The Extendable Refractable Mast (ERM) thermal analysis: A heat radiation case study via the finite element method N87-16949

LOCKHEED-CALIFORNIA CO., BURBANK.
Flight service evaluation of advanced composite ailerons on the L-1011 transport aircraft [NASA-CR-178170] N87-16883

LOCKHEED MISSILES AND SPACE CO., SUNNYVALE, CALIF.
Space station human productivity study. Volume 4: Issues [NASA-CR-171963] N87-16865
Space station human productivity study. Volume 5: Management plans [NASA-CR-171964] N87-16866
Space station human productivity study. Volume 2: Executive summary and oral review presentation [NASA-CR-171962] N87-16868
Space station human productivity study, volume 1 [NASA-CR-171961] N87-16869

LOS ALAMOS NATIONAL LAB., N. MEX.
Canopy hot-spot as crop identifier [DE86-011258] N87-17395
Recent developments in discrete-ordinates electron transport [DE86-007827] N87-17485

LOUGHBOROUGH UNIV. OF TECHNOLOGY (ENGLAND).
A study of anomalous propagation at radar frequencies and a proposal for a radar coverage forecasting model, book 2 of 2 [ETN-87-98938] N87-16967
Globally convergent hybrid conjugate gradient methods [MR-196] N87-17454

LOWELL OBSERVATORY, FLAGSTAFF, ARIZ.
A possible deuterium anomaly: Implications of the CH3D/CH4 mixing ratios in the atmospheres of Jupiter, Saturn, and Uranus N87-17617

M

M/A-COM, INC., BURLINGTON, MASS.
The 60 GHz IMPATT diode development [NASA-CR-179536] N87-17515

MACDONALD, DETTWILER AND ASSOCIATES LTD., RICHMOND (BRITISH COLUMBIA).
RADARSAT high throughput SAR processor development N87-17154
ERS-1 synthetic aperture radar fast delivery processor N87-17228

MANITOBA UNIV., WINNIPEG.
Application of 2-D Hilbert transform in the interpretation of remotely sensed potential field data N87-17293

MARCONI CO. LTD., CHELMSFORD (ENGLAND).
The UK ERS Data Centre, an offline processing and archiving facility N87-17230
SIR-B observations of ocean waves in the NE Atlantic N87-17335
A scatterometer research program N87-17391

MARCONI SPACE AND DEFENCE SYSTEMS LTD., PORTSMOUTH (ENGLAND).
On-ground verification and in-orbit performance prediction of the ERS-1 wind scatterometer N87-17193
An advanced SAR design for future land missions N87-17322

MARCONI SPACE SYSTEMS LTD., PORTSMOUTH (ENGLAND).
A powerful utility for assessing the performance of the ERS-1 synthetic aperture radar N87-17361

MARTIN MARIETTA CORP., DENVER, COLO.
Tethered orbital refueling study [NASA-CR-171953] N87-16855

MARYLAND UNIV., COLLEGE PARK.
The development of the Goddard Compton gamma-ray telescope and neutral hydrogen N87-17580

MASSACHUSETTS INST. OF TECH., CAMBRIDGE.
Delineation of fault zones using imaging radar N87-17138
Microwave remote sensing of snow-covered sea ice N87-17187
An iterative multi-resolution shape-from-shading algorithm and its application to planetary mapping N87-17331
Supercritical water oxidation of products of human metabolism
[NASA-CR-180144] N87-17430
A research program in advanced information systems
[NASA-CR-180150] N87-17529
Convective adjustment in baroclinic atmospheres N87-17626

MASSACHUSETTS UNIV., AMHERST.
A backscattering model for various foliated deciduous tree types at millimeter wavelengths N87-17307
Intersensor comparisons for validation of wind speed measurements from ERS-1 altimeter and scatterometer N87-17386

MATERIALS QUALITY ASSURANCE DIRECTORATE, LONDON (ENGLAND).
A comparison of two British standard test methods for the determination of resistance to humidity of paint films
[MQAD-TP-918] N87-16906

MATERIALS RESEARCH LABS., ASCOT VALE (AUSTRALIA).
Grinding of steel: A case study
[AD-A174649] N87-17048

MAX-PLANCK-INST. FUER METEOROLOGIE, HAMBURG (WEST GERMANY).
Wave modeling activities of the Wave Modeling (WAM) group relevant to ERS-1 N87-17389

MAX-PLANCK-INST. FUER PHYSIK UND ASTROPHYSIK, GARCHING (WEST GERMANY).
A soft X-ray observation of omega Centauri with EXOSAT
[MPE-PREPRINT-60] N87-17575
Observations of quasi-periodic oscillations in Cyg X-2
[MPE-PREPRINT-61] N87-17576

MAX-PLANCK-INST. FUER RADIOASTRONOMIE, BONN (WEST GERMANY).
Interstellar dust N87-17545
IRAS observations of the Pleiades N87-17557
The submillimeter telescope (SMT) project N87-17568

MESSERSCHMITT-BOELKOW-BLOHM G.M.B.H., AUGSBURG (WEST GERMANY).
Economical manufacturing and inspection of the electron-beam-welded Tornado wing box N87-17055

MESSERSCHMITT-BOELKOW-BLOHM G.M.B.H., LEMWERDER (WEST GERMANY).
Ultrasonic testing techniques for diffusion-bonded titanium components N87-17061

MESSERSCHMITT-BOELKOW-BLOHM G.M.B.H., MUNICH (WEST GERMANY).
Experience gained by sector model testing of an unfurlable mesh/rib antenna N87-16825
Qualification of gridding process for a Polarization Sensitive Reflector (PSR) N87-16932
The stereo-pushbroom scanner system Digital Photogrammetry System (DPS) and its accuracy N87-17167

METEOROLOGICAL OFFICE, BRACKNELL (ENGLAND).
The use of numerical wind and wave models to provide areal and temporal extension to instrument calibration and validation of remotely sensed data N87-17371
The use of aircraft for wind scatterometer calibration N87-17382

METEOROLOGICAL OFFICE, LONDON (ENGLAND).
Quasi-geostrophic free mode models of long-lived Jovian eddies: Forcing mechanisms and crucial observational tests N87-17630
Transport of absolute angular momentum in quasi-axisymmetric equatorial jet streams N87-17635

MICHIGAN STATE UNIV., EAST LANSING.
Experimental investigation of the turbulence production mechanism in boundary layers
[AD-A173091] N87-17007

MICHIGAN UNIV., ANN ARBOR.
Optimal turning at high angle of attack of supersonic and hypersonic vehicles N87-16814
Simultaneous density velocity measurements in premixed turbulent flames to assess a theoretical model N87-16889
SIR-B measurements and modeling of vegetation N87-17160
Components and comparisons of potential information from several imaging satellites N87-17164
Millimeter-wave network analyzer-based scatterometer N87-17281
Microwave dielectric spectrum of vegetation material N87-17345
Microwave dielectric behavior of vegetation material
[NASA-CR-180096] N87-17393
Scale-free models of highly flattened elliptical galaxies N87-17589
Yellow supergiants in open clusters N87-17590
The hydrogen geocorona: Simultaneous optical and radar observations at Arecibo N87-17651

MIDWEST RESEARCH INST., GOLDEN, COLO.
Effect of the size of structural bulk inhomogeneities on the specular transmittance of polymer films
[DE86-010727] N87-16913
Feasibility of using wind power for an aerostat-borne radar system
[DE86-004481] N87-17403
Wind energy technical reading list
[DE86-010704] N87-17404

MINISTERIO DE OBRAS PUBLICAS, MADRID (SPAIN).
Marine climate program N87-17390

MINISTRY OF POSTS AND TELECOMMUNICATIONS, IBARAKI (JAPAN).
Measurement of sea backscatter at extremely low grazing angle by C-band Doppler radar N87-17301

MINNESOTA UNIV., MINNEAPOLIS.
Microwave radiances from horizontally finite precipitating clouds containing ice and liquid hydrometeors N87-17340

MISSISSIPPI STATE UNIV., MISSISSIPPI STATE.
Advanced 3-D viscous SSME turbine rotor stator CFD algorithms
[NASA-CR-178997] N87-16829

MULLARD SPACE SCIENCE LAB., DORKING (ENGLAND).
An automatic tracking mode switching algorithm for the ERS-1 altimeter N87-17195

N

NAGOYA UNIV. (JAPAN).
Annual review, April 1985 - March 1986
[ISSN-0547-1567] N87-17503
The optimum condition of TPD-1 recombining helium plasma for VUV coherent lasing action
[IPPJ-798] N87-17507
RF plugging and tandem mirror experiments in a cusp-anchored mirror device
[IPPJ-800] N87-17508
Implicit particle simulation of electromagnetic plasma phenomena
[IPPJ-799] N87-17509
Tilt stability of field-reversed configurations
[IPPJ-802] N87-17510
A self-consistent modeling of a quasi-steady state compact torus evolving to ignition
[IPPJ-801] N87-17511
Advanced fuels in a field-reversed configuration
[IPPJ-804] N87-17512
Physics considerations on a fusion plasma in a field-reversed configuration
[IPPJ-803] N87-17513

NATIONAL AERONAUTICS AND SPACE ADMINISTRATION, WASHINGTON, D.C.
Stability characteristics of a supersonic boundary layer and their relation to the position of the laminar-turbulent transition point
[NASA-TM-88533] N87-16797
A new day: Challenger and space flight thereafter
[NASA-TM-77717] N87-16856
Transitional boundary layers under the influence of high free stream turbulence, intensive wall cooling and high pressure gradients in hot gas circulation
[NASA-TM-88524] N87-16983
Design of software for design of finite element for structural analysis
[NASA-TM-88528] N87-17089
Training programs in remote sensing for professionals, students and the general public
[NASA-TM-88541] N87-17394
Decentralized control of large-scale systems: Fixed modes, sensitivity and parametric robustness
[NASA-TM-88537] N87-17474
NASA thesaurus supplement (supplement 2)
[NASA-SP-7053(SUPP-2)] N87-17530
Zhamanshin meteor crater
[NASA-TM-88531] N87-17595

NATIONAL AERONAUTICS AND SPACE ADMINISTRATION. AMES RESEARCH CENTER, MOFFETT FIELD, CALIF.
Computation of separation ahead of blunt fin in supersonic turbulent flow
[NASA-TM-89416] N87-16791
Transonic unsteady aerodynamic and aeroelastic calculations about airfoils and wings
[NASA-TM-89417] N87-16800
Computational, unsteady transonic aerodynamics and aeroelasticity about airfoils and wings
[NASA-TM-89414] N87-16801
AFTI/F-111 MAW flight control system and redundancy management description
[NASA-TM-88267] N87-16819
Vinyl stilbazoles
[NASA-CASE-ARC-11429-3CU] N87-16908
Fire and heat resistant laminating resins based on maleimido substituted aromatic cyclotriphosphazene polymer
[NASA-CASE-ARC-11428-2] N87-16909
Elevated waterproof access floor system and method of making the same
[NASA-CASE-ARC-11363-1] N87-16918
Data communication requirements for the advanced NAS network
[NASA-TM-89315] N87-16957
Projection lens scanning laser velocimeter system
[NASA-CASE-ARC-11547-1] N87-17026
Portable EDITOR (PEDITOR): A portable image processing system N87-17208
Profiling under UNIX by patching
[NASA-TM-89316] N87-17443
Vertical structure of aerosols and clouds in the atmospheres of Uranus and Neptune: Implications for their heat budgets N87-17643
Are the aerosols on Uranus and Neptune composed of methane photopolymers? N87-17645

NATIONAL AERONAUTICS AND SPACE ADMINISTRATION. DRYDEN (HUGH L.) FLIGHT RESEARCH CENTER, EDWARDS, CALIF.
Design and initial application of the extended aircraft interrogation and display system: Multiprocessing ground support equipment for digital flight systems
[NASA-TM-86740] N87-16820
Digital program for calculating static pressure position error
[NASA-TM-86726] N87-16821

NATIONAL AERONAUTICS AND SPACE ADMINISTRATION. EARTH RESOURCES LAB., BAY ST. LOUIS, MISS.
Estimation of absolute water surface temperature based on atmospherically corrected thermal infrared multispectral scanner digital data N87-17114
Atmospheric correction of TIMS data N87-17115
Monitoring vegetation recovery patterns on Mount St. Helens using thermal infrared multispectral data N87-17122
Investigation of forest canopy temperatures recorded by the thermal infrared multispectral scanner at H. J. Andrews Experimental Forest N87-17123
Applications of TIMS data in agricultural areas and related atmospheric considerations N87-17124

NATIONAL AERONAUTICS AND SPACE ADMINISTRATION. GODDARD INST. FOR SPACE STUDIES, NEW YORK, N.Y.
The Jovian Atmospheres
[NASA-CP-2441] N87-17598
Vertical cloud structure models for the NTRZ EQZ, SEB and STRZ of Jupiter N87-17608
Astronomical, physical, and meteorological parameters for planetary atmospheres N87-17647

NATIONAL AERONAUTICS AND SPACE ADMINISTRATION. GODDARD SPACE FLIGHT CENTER, GREENBELT, MD.
Radial and torsionally controlled magnetic bearing
[NASA-CASE-GSC-12957-1] N87-17038
The physical basis for spectral variations in thermal infrared emittance of silicates and application to remote sensing N87-17129
Active/passive microwave sensor comparison of MIZ-ice concentration estimates N87-17185
The Electronically Steered Thinned Array Radiometer (ESTAR) N87-17260
Effects of salinity on the microwave emission of soils N87-17302
Discrimination of soil hydraulic properties by combined thermal infrared and microwave remote sensing N87-17303
Snow property measurements correlative to microwave emission at 35 GHz N87-17315
Dependence of snow melting and surface-atmosphere interactions on the forest structure N87-17318
Evaluating roughness models of radar backscatter N87-17344
Microwave backscattering from an anisotropic soybean canopy N87-17346
Oceanographic measurement capabilities of the NASA P-3 aircraft N87-17380
Para hydrogen equilibration in the atmospheres of the outer planets N87-17599
Water vapor in Jupiter's atmosphere N87-17605
Study of the ammonia ice cloud layer in the north tropical zone of Jupiter from the infrared interferometric experiment on Voyager N87-17609
Two micron quadrupole line emission of H2 from the Jovian auroral zone N87-17615

Global dynamics and thermal structure of Jupiter's atmosphere N87-17621
Mesoscale waves as a probe of Jupiter's deep atmosphere N87-17628
Chaotic motion in the Jovian atmosphere N87-17634

NATIONAL AERONAUTICS AND SPACE ADMINISTRATION. LYNDON B. JOHNSON SPACE CENTER, HOUSTON, TEX.

Euler solutions using an implicit multigrid technique [NASA-TM-58276] N87-16792
Self-contained, single-use hose and tubing cleaning module [NASA-CASE-MSC-20857-1] N87-17035
Sun shield [NASA-CASE-MSC-20162-1] N87-17036

NATIONAL AERONAUTICS AND SPACE ADMINISTRATION. LANGLEY RESEARCH CENTER, HAMPTON, VA.

Geometries for roughness shapes in laminar flow [NASA-CASE-LAR-13255-1] N87-16793
Loads and Aeroelasticity Division research and technology accomplishments for FY 1986 and plans for FY 1987 [NASA-TM-89084] N87-16796
Compendium of NASA Langley reports on hypersonic aerodynamics [NASA-TM-87760] N87-16802
Flight investigation of the effect of tail configuration on stall, spin, and recovery characteristics of a low-wing general aviation research airplane [NASA-TP-2644] N87-16815
Over-the-wing propeller [NASA-CASE-LAR-13134-2] N87-16828
Description of the Spacecraft Control Laboratory Experiment (SCOLE) facility [NASA-TM-89057] N87-16848
Piloted simulator study of allowable time delays in large-airplane response [NASA-TP-2652] N87-16849
Structural dynamics and attitude control study of early manned capability space station configurations [NASA-TM-89078] N87-16861
Single frequency multitransmitter telemetry [NASA-CASE-LAR-13006-1] N87-16863
Initial utilization of the CVIRB video production facility [NASA-TM-89036] N87-16873
Effect of adherend thickness and mixed mode loading on debond growth in adhesively bonded composite joints [NASA-TM-88992] N87-16882
Comparison of composite rotor blade models: A coupled-beam analysis and an MSC/NASTRAN finite-element model [NASA-TM-89024] N87-16884
Ethynyl terminated ester oligomers and polymers therefrom [NASA-CASE-LAR-13118-2] N87-16907
Soluble aromatic polyimides for film and coating applications [NASA-TM-89016] N87-16911
A preliminary study of factors affecting the calibration stability of the iridium versus iridium-40 percent rhodium thermocouple [NASA-TM-89086] N87-17018
A parallel solution for the symmetric Eigenproblem [NASA-TM-89082] N87-17086
A three dimensional calculation of elastic equilibrium for composite materials [NASA-CR-178158] N87-17088
Energy dissipation associated with crack extension in an elastic-plastic material [NASA-TM-89032] N87-17090
SAGE aerosol measurements. Volume 3: January 1, 1981 to November 18, 1981 [NASA-RP-1173] N87-17417
Evolution of a localized thermal explosion in a reactive gas [NASA-CR-178231] N87-17436
Line plotting program using DI-3000/Grafmaker routines [NASA-TM-89010] N87-17442
Multigrid applied to singular perturbation problems [NASA-CR-178230] N87-17444
Convenient total variation diminishing conditions for nonlinear difference schemes [NASA-CR-178209] N87-17453
Survey of the status of finite element methods for partial differential equations [NASA-CR-178222] N87-17456
Power cepstrum technique with application to model helicopter acoustic data [NASA-TP-2586] N87-17479
Noise propagation from a four-engine, propeller-driven airplane [NASA-TM-89035] N87-17482
Aircraft noise synthesis system [NASA-TM-89040] N87-17483
Doubly differential cross sections for galactic heavy-ion fragmentation [NASA-TP-2659] N87-17487
Scientific and technical information output of the Langley Research Center for calendar year 1986 [NASA-TM-89065] N87-17531

NATIONAL AERONAUTICS AND SPACE ADMINISTRATION. LEWIS RESEARCH CENTER, CLEVELAND, OHIO.

Comparison of three explicit multigrid methods for the Euler and Navier-Stokes equations [NASA-TM-88878] N87-16784
Measurements of the unsteady flow field within the stator row of a transonic axial-flow fan. 1: Measurement and analysis technique [NASA-TM-88945] N87-16789
Measurements of the unsteady flow field within the stator row of a transonic axial-flow fan. Part 2: Results and discussion [NASA-TM-88946] N87-16790
Euler analysis of the three dimensional flow field of a high-speed propeller: Boundary condition effects [NASA-TM-88955] N87-16798
Spatially growing disturbances in a two-stream, coplanar jet [NASA-TM-88949] N87-16799
Unsteady flows in a single-stage transonic axial-flow fan stator row [NASA-TM-88929] N87-16805
Identification and proposed control of helicopter transmission noise at the source [NASA-TM-89312] N87-16816
Outdoor test stand performance of a convertible engine with variable inlet guide vanes for advanced rotorcraft propulsion [NASA-TM-88939] N87-16825
Particle-laden swirling free jets: Measurements and predictions [NASA-TM-88904] N87-16826
Representation of the vaporization behavior of turbulent polydisperse sprays by equivalent monodisperse sprays [NASA-TM-88906] N87-16827
A distributed data acquisition system for aeronautics test facilities [NASA-TM-88961] N87-16851
Heat exchanger for electrothermal devices [NASA-CASE-LEW-14037-1] N87-16875
Composite space antenna structures: Properties and environmental effects [NASA-TM-88859] N87-16880
Conventionally cast and forged copper alloy for high-heat-flux thrust chambers [NASA-TP-2694] N87-16902
Research opportunities in microgravity science and applications during shuttle hiatus [NASA-TM-88964] N87-16917
A new model for broadband waveguide to microstrip transition design [NASA-TM-88905] N87-16958
Absolute gain measurement by the image method under mismatched condition [NASA-TM-88924] N87-16968
Analysis of viscous transonic flow over airfoil sections [NASA-TM-88912] N87-17001
A general method for unsteady stagnation region heat transfer and results for model turbine flows [NASA-TM-88903] N87-17002
Common problems and pitfalls in gear design [NASA-TM-88858] N87-17033
Surface flaw reliability analysis of ceramic comonents with the SCARE finite element postprocessor program [NASA-TM-88901] N87-17087
A comparison of five benchmarks [NASA-TM-88956] N87-17441
Combustion noise from gas turbine aircraft engines measurement of far-field levels [NASA-TM-88971] N87-17480
Research and technology [NASA-TM-88868] N87-17656

NATIONAL AERONAUTICS AND SPACE ADMINISTRATION. MARSHALL SPACE FLIGHT CENTER, HUNTSVILLE, ALA.

Space shuttle main engine vibration data base [NASA-TM-86576] N87-16876
Statistical analysis of 59 inspected SSME HPFTP turbine blades (uncracked and cracked) [NASA-TM-86584] N87-16877
Electrical properties of Al-In-Sn alloys directionally solidified in high and low gravitational fields [NASA-TM-86569] N87-16900
The effects of gravity level during directional solidification on the microstructure of hypermonotectic Al-In-Sn alloys [NASA-TM-86573] N87-16901
The non-metallic materials sample array [NASA-TM-86578] N87-16910
The 5000 GPM firefighting module evaluation test [NASA-TM-86560] N87-16919
Small computer interface to a stepper motor [NASA-TM-86574] N87-16970
Space shuttle main engine high pressure fuel pump aft platform seal cavity flow analysis [NASA-TP-2685] N87-17000
Interface circuitry for superconducting bolometer [NASA-TM-86581] N87-17016
Low-g measurements by NASA [NASA-TM-86585] N87-17017
Non-backdriveable free wheeling coupling [NASA-CASE-MSC-20475-1] N87-17037
Solid rocket booster joint seal analyses [NASA-TM-86580] N87-17039
SRB O-ring free response analysis [NASA-TM-86582] N87-17040
On the analytical determination of relaxation modulus of viscoelastic materials by Prony's interpolation method [NASA-TM-86579] N87-17455
Welding torch with arc light reflector [NASA-CASE-MFS-29134-1] N87-17493
FY 1986 scientific and technical reports, articles, papers and presentations [NASA-TM-86575] N87-17532
Convective forcing of global circulations on the Jovian planets N87-17624

NATIONAL AERONAUTICS AND SPACE ADMINISTRATION. PASADENA OFFICE, CALIF.

Tank tread assemblies with track-linking mechanism [NASA-CASE-NPO-16321-1CU] N87-17034
High band gap 2-6 and 3-5 tunneling junctions for silicon multijunction solar cells [NASA-CASE-NPO-16526-1CU] N87-17399

NATIONAL AEROSPACE LAB., AMSTERDAM (NETHERLANDS).

Evaluation of DDH and weld repaired F100 turbine vanes under simulated service conditions N87-17070

NATIONAL CENTER FOR ATMOSPHERIC RESEARCH, BOULDER, COLO.

Moisture driven convection on Jupiter: A mechanism to produce the equatorial plumes N87-17631

NATIONAL ENVIRONMENTAL SATELLITE SERVICE, WASHINGTON, D. C.

Validation of wind speed and significant wave height from Geosat N87-17368
Accuracy estimates of wind and wave observations from ships of opportunity in the WMO voluntary observing ship program N87-17375

NATIONAL OCEANIC AND ATMOSPHERIC ADMINISTRATION, BOULDER, COLO.

Remote probing of wind and refractive-index structure using optical scintillation techniques N87-17272
Ground-based microwave radiometric observations of atmospheric geopotential height fluctuations N87-17339

NATIONAL PHYSICAL LAB., TEDDINGTON (ENGLAND).

An implementation of the Hough transform using a linear array processor in conjunction with a PDP/11microprocessor [NPL-DITC-74/86] N87-17438

NATIONAL RESEARCH COUNCIL OF CANADA, BOUCHERVILLE (QUEBEC).

Thermoelastic testing of stratified materials N87-17064
A real time vision system for robotic arc welding N87-17066

NATIONAL SEVERE STORMS LAB., NORMAN, OKLA.

Application of Doppler radar and lidar to diagnose atmospheric phenomena N87-17271

NATIONAL SPACE DEVELOPMENT AGENCY, IBARAKI (JAPAN).

A satellite-borne SAR transmitter and receiver N87-17358
Pulse compression test results of the SAR transmitter and receiver N87-17360

NATIONAL SPACE DEVELOPMENT AGENCY, TOKYO (JAPAN).

Some results of Marine Observation Satellite (MOS-1) airborne verification experiment Multispectral Electronic Self Scanning Radiometer (MESSR) N87-17166

NATIONAL WATER RESEARCH INST., BURLINGTON (ONTARIO).

A two-scale Bragg scattering model for microwave backscatter from wind generated waves N87-17212

NAVAL OCEAN RESEARCH AND DEVELOPMENT ACTIVITY, BAY ST. LOUIS, MISS.

Observations of surface currents at Nantucket Shoals and implications for radar imaging of the bottom N87-17296
N-ROSS validation N87-17385

NAVAL RESEARCH LAB., WASHINGTON, D. C.
Application of Spaceborne Distributed Aperture/Coherent Array Processing (SDA/CAP) technology to active and passive microwave remote sensing N87-17277
NEBRASKA UNIV., LINCOLN.
Total and dissociative photoionization cross sections of N2 from threshold to 107 eV
[NASA-CR-180172] N87-16892
TIMS data applications in Nebraska N87-17126
NEVADA UNIV., RENO.
Detection and mapping of volcanic rock assemblages and associated hydrothermal alteration with Thermal Infrared Multiband Scanner (TIMS) data Comstock Lode Mining District, Virginia City, Nevada N87-17119
Application of Thermal Infrared Multiband Scanner (TIMS) data to mapping of Plutonic and stratified rock and assemblages in accreted terrains of the Northern Sierra, California N87-17132
NEW HAMPSHIRE UNIV., DURHAM.
On the spectra of gamma-ray bursts at high energies N87-17654
NEW MEXICO STATE UNIV., LAS CRUCES.
Seasonal north-south asymmetry in solar radiation at the top of Jupiter's atmosphere N87-17603
A proposal for adopting a standard coordinate system for defining atmospheric nomenclature for the giant planets N87-17632
NEW MEXICO UNIV., ALBUQUERQUE.
Polarimetry and photometry of active quasars at visual and near-infrared wavelengths N87-17579
NEW SOUTH WALES UNIV., KENSINGTON (AUSTRALIA).
Radar signature determination: Trends and limitations N87-17159
NIELSEN ENGINEERING AND RESEARCH, INC., MOUNTAIN VIEW, CALIF.
Prediction of vortex shedding from circular and noncircular bodies in subsonic flow
[NASA-CR-4037] N87-16981
NIPPON TELEGRAPH AND TELEPHONE PUBLIC CORP., YOKOSUKA (JAPAN).
Development of 30/20 GHz satellite antenna structures N87-16933
NORWEGIAN COMPUTING CENTER, OSLO (NORWAY).
A simulation study of some contextual classification methods for remotely sensed data N87-17252

O

OAK RIDGE NATIONAL LAB., TENN.
Microstructural modifications during laser and electron beam welding
[DE86-011076] N87-17049
Programming robotics applications on an advanced hypercube multiprocessor
[DE86-008895] N87-17445
OBSERVATOIRE DE MARSEILLE (FRANCE).
The interstellar medium at submm wavelengths N87-17543
OBSERVATOIRE DE PARIS-MEUDON (FRANCE).
A study of planetary atmospheres in the submillimetric range N87-17540
Submillimeter cometary spectroscopy N87-17541
Enhanced acetylene emission near the north pole of Jupiter N87-17614
OBSERVATORIO ASTROMICO NACIONAL, GUADALAJARA (SPAIN).
Maser and thermal SiO emission in evolved stars N87-17553
Vibrationally excited cyanoacetylene in regions of massive star formation N87-17561
OFFICE NATIONAL D'ETUDES ET DE RECHERCHES AEROSPATIALES, PARIS (FRANCE).
Application of flow calculation methods to transonic and supersonic axial turbomachines
[ONERA-RTS-80/7103-EY] N87-16846
Three-dimensional separation on a cylindrical ellipsoid. Results of the first test campaign on the F2 wind tunnel
[ONERA-RT-16/7252-AN] N87-17013
OHIO STATE UNIV., COLUMBUS.
Basic research for the geodynamics program
[NASA-CR-180137] N87-17415
Improvement of the Earth's gravity field from terrestrial and satellite data
[NASA-CR-180139] N87-17416
OKLAHOMA UNIV., NORMAN.
Estimation and control of distributed models for certain elastic systems arising in large space structures
[AD-A175019] N87-16872
OPERATIONS RESEARCH, INC., ROCKVILLE, MD.
The Sequential Filter Imaging Radiometer (SFIR), a new instrument configuration for Earth observations N87-17205
OSLO UNIV. (NORWAY).
A climatological-hydrological study of lake ice in the southwestern mountain area in Norway by use of satellite sensing N87-17319
OXFORD UNIV. (ENGLAND).
Recursive techniques in identification
[OUEL-1644/86] N87-17482
An electrostatic probe technique for R.F. plasma
[OUEL-1637/86] N87-17514
Investigation of long-lived eddies on Jupiter N87-17633

P

PACIFIC NORTHWEST LABS., RICHLAND, WASH.
Model for simulating rotational data for wind turbine applications
[DE86-010784] N87-17406
Review of wind simulation methods for horizontal-axis wind turbine analysis
[DE86-012223] N87-17407
Ultralow background searches for beta beta-decay, cold dark matter and solar axions
[DE86-013592] N87-17652
PARIS VII UNIV. (FRANCE).
Active optics for the far infrared submillimeter wave space telescope (FIRST): A high angular resolution mode N87-17566
PENNSYLVANIA STATE UNIV., UNIVERSITY PARK.
Transient catalytic combustion
[AD-A173098] N87-16894
On the influence of strain-path changes on fracture
[AD-A172535] N87-17091
The application of remotely sensed data to pedologic and geomorphic mapping on alluvial fan and playa surfaces in Saline Valley, California N87-17127
Use of low energy ion implants in high efficiency crystalline silicon solar cells
[NASA-CR-179971] N87-17408
PHYSICS AND ELECTRONICS LAB. TNO, THE HAGUE (NETHERLANDS).
C and Ku-band scatterometer results from the SCATTMOD internal wave experiment N87-17215
Sea wave measurements using a ship's radar N87-17300
PHYSICS INTERNATIONAL CORP., SAN FRANCISCO, CALIF.
RF plugging and tandem mirror experiments in a cusp-anchored mirror device
[IPPJ-800] N87-17508
POLISH ACADEMY OF SCIENCES, WARSAW.
On routes to chaotic motion in oscillators with unsymmetric and symmetric elastic nonlinearity
[ISSN-0208-5658] N87-16969
POLYTECHNIC INST. OF BROOKLYN, FARMINGDALE, N. Y.
A study of large, medium and small scale structures in the topside ionosphere
[NASA-CR-180068] N87-17413
PRC KENTRON, INC., HAMPTON, VA.
Spacecraft attitude control momentum requirements analysis
[NASA-CR-178219] N87-16864
PRINCETON UNIV., N. J.
Lumped model generation and evaluation: Sensitivity and lie algebraic techniques with applications to combustion
[AD-A174984] N87-16896
Fuels combustion research
[AD-A175040] N87-16897
The study of shock wave and turbulent boundary layer interactions
[AD-A175033] N87-17008
PURDUE UNIV., WEST LAFAYETTE, IND.
Measurement of the three-dimensional aerodynamics of an annular cascade airfoil row N87-16788
Stress intensity factors for fatigue cracks at holes under cyclic stress gradients N87-17075
Analysis of multiple incidence angle SIR-B data for determining forest stand characteristics N87-17156
Parameter space techniques for image registration N87-17327
Improving the geological interpretation of magnetic and gravity satellite anomalies
[NASA-CR-180149] N87-17418
A laboratory investigation of two-celled vortex flows N87-17423

R

RADIO STERRENWACHT, DWINGELOO (NETHERLANDS).
CO observations of the outflow source NGC 7023 N87-17563
RENSSELAER POLYTECHNIC INST., TROY, N.Y.
The theory of finite elastic-plastic deformation with induced anisotropy modelled as combined isotropic-kinematic hardening N87-17074
Research on single-crystal CdTe solar cells
[DE86-010719] N87-17405
A study of spatial models and human navigation within complex computer interfaces N87-17447
Numerical calculations of radiation transport in a dusty medium in disk geometry N87-17591
RESEARCH INST. OF NATIONAL DEFENCE, LINKOEPING (SWEDEN).
Vegetation influence on wave propagation
[FOA-B-30097-3.3] N87-16965
Transmission loss measurements in mobile radio nets
[FOA-B-30098-3.3] N87-16966
RESEARCH INST. OF NATIONAL DEFENCE, STOCKHOLM (SWEDEN).
Damage and repairing of fiber composites, a summary
[FOA-C-20620-2.5] N87-16888
RESEARCH TRIANGLE INST., RESEARCH TRIANGLE PARK, N.C.
Concept definition for space station technology development experiments. Experiment definition, task 2
[NASA-CR-178153] N87-16860
On the stochastic dissemination of faults in an admissible network
[NASA-CR-178238] N87-17469
RHODE ISLAND UNIV., KINGSTON.
A study of explosive wave propagation in granular materials with microstructure
[AD-A173015] N87-16914
RICE UNIV., HOUSTON, TEX.
Aeroassisted coplanar orbital transfer of flight vehicles using the sequential gradient restoration algorithm N87-16857
The distribution of atomic hydrogen in the Jovian atmosphere N87-17611
RICERCHE E PROGETTI S.R.L., TURIN (ITALY).
Dynamics and Control Analysis Package (DCAP): An automated analysis and design tool for structural control of space structures N87-16947
ROCKWELL INTERNATIONAL SCIENCE CENTER, THOUSAND OAKS, CALIF.
Research on millimeter wave dielectric materials
[AD-A173017] N87-17521
ROLLS-ROYCE LTD., DERBY (ENGLAND).
Low aspect ratio turbine design at Rolls-Royce
[PNR90338] N87-16824
Manufacturing cell for the V2500 variable vanes
[PNR90330] N87-16835
Reducing the cost of aero engine research and development
[PNR90341] N87-16836
Burner rig and engine test experience of platinum aluminide coatings
[PNR90342] N87-16837
Component lifing
[PNR90346] N87-16838
Observation of ice/water formations on a model intake section subjected to simulated cloud conditions
[PNR90347] N87-16839
Future trends in propulsion
[PNR90349] N87-16840
An approach to AE monitoring during the rig shop testing of large CFRP aero-engine components
[PNR90350] N87-16841
Gas turbine materials: A review
[PNR90356] N87-16842
The technology of advanced prop-fan transmissions
[PNR90357] N87-16843
Aircraft derivative gas turbine development in China
[PNR90359] N87-16844
Operational aids to engine development
[PNR90362] N87-16845
Preliminary investigations into the microcracking of PMR-15/graphite composites. Part 1: Effect of cure temperature
[PNR90348] N87-16887
Corrosion/oxidation protection of high temperature material
[PNR90355] N87-16905
Observations on the turbulent structure in an unsteady, normal shock/boundary-layer interaction
[PNR90361] N87-17010
Industrial holography: The Rolls-Royce experience
[PNR90351] N87-17024
NDT of electron beam welded joints (micro-focus and real time X-ray) N87-17063
ROLLS-ROYCE LTD., LEAVESDEN (ENGLAND).
Impact of IPS and IRS configuration on engine installation design
[PNR90324] N87-16834

ROME AIR DEVELOPMENT CENTER, GRIFFISS AFB, N.Y.
ICNIA (Integrated Communications Navigation Identification Avionics) HF transmitter system preliminary study
[AD-A173013] N87-16823
ROME UNIV. (ITALY).
Effects of curing stresses on composite structures N87-16930
Thermomechanical characteristics of dichroic subreflectors N87-16952
Antenna pattern correction in scanning radiometry: A singular system analysis N87-17261
Effect of electrical and thermal properties of materials on microwave brightness temperature of the terrestrial crust N87-17263
Effects of rain cells on SAR performance N87-17354
The early universe N87-17539
ROYAL AIRCRAFT ESTABLISHMENT, FARNBOROUGH (ENGLAND).
Developments in data acquisition and processing using an advanced combustion research facility
[RAE-TM-P1089] N87-16852
The contraction of satellite orbits under the influence of air drag. Part 7: Orbits of high eccentricity, with scale height dependent on altitude
[RAE-TR-86013] N87-16859
Diffusion welding of component parts in the aviation and space industries
[RAE-TRANS-2147] N87-17032
The possibility of reducing the cyclic torque fluctuations produced by two-stroke engines using the storage of magnetostatic energy
[RAE-TM-RAD-NAV-265] N87-17042
Diffusion bonding of Al-alloys in the solid state N87-17058
ROYAL ARMAMENT RESEARCH AND DEVELOPMENT ESTABLISHMENT, FORT HALSTEAD (ENGLAND).
Application of modified three parameter Weibull distributions to brittle material design
[RARDE-16/84] N87-17072
ROYAL NETHERLANDS METEOROLOGICAL INST., DE BILT.
The accuracy and availability of operational marine surface wind data for ERS-1 sensor calibration and validation from fixed platforms and free drifting buoys N87-17376
ROYAL OBSERVATORY, EDINBURGH (SCOTLAND).
Status of observational astronomy in the 1990's: Position of submillimetre astronomy N87-17536
ROYAL SIGNALS AND RADAR ESTABLISHMENT, MALVERN (ENGLAND).
Applications of focused ion beams in microelectronics
[RSRE-MEMO-3948] N87-17517
RUTGERS - THE STATE UNIV., NEW BRUNSWICK, N. J.
Calculation of supersonic flow over a compression corner N87-16785

S

SAINT LOUIS UNIV., MO.
A diagnostic approach to obtaining planetary boundary layer winds using satellite-derived thermal data
[NASA-CR-178972] N87-17420
SAN DIEGO STATE UNIV., CALIF.
Measurement of HO2 chemical kinetics with a new detection method
[NASA-CR-180114] N87-16890
CF2 and CFCl fluorescence from VUV excitation of C2F3Cl N87-16891
SANDIA NATIONAL LABS., ALBUQUERQUE, N. MEX.
Monitoring transients in low inductance circuits
[DE86-013756] N87-16978
Performance of polysilicon gate CMOS devices in space and SDI environments
[DE86-009025] N87-17524
SASKATCHEWAN UNIV., SASKATOON.
Image representation via its symmetrical components N87-17290
SCIENCE RESEARCH COUNCIL, CHILTON (ENGLAND).
Gathering and processing a comparative data set for the calibration and validation of ERS-1 data products; preparatory work at the UK-ERS-DC N87-17367
Measurement of the directional spectrum of ocean waves using a conically-scanning radar N87-17383
A 186 GHz radiometer for the microwave limb sounder N87-17569
SELENIA S.P.A., ROME (ITALY).
Development of lightweight dimensionally stable carbon fiber composite antenna reflectors for the INSAT-1 satellite N87-16936
Design and technology of feed array and beam forming network for contoured beam antennas N87-16950
SENER, S.A., MADRID (SPAIN).
A Sener mechanism: Fine adjustment mechanism for the Far Infrared and Submillimeter Space Telescope (FIRST) (F I F) N87-16946
SHEFFIELD UNIV. (ENGLAND).
Model selection and validation methods for nonlinear systems
[RR-292] N87-17095
A prediction error estimate for nonlinear stochastic systems
[RR-295] N87-17471
SLOVAK ACADEMY OF SCIENCES, BRATISLAVA (CZECHOSLOVAKIA).
Results of geomagnetic observations at the Hurbanovo Geomagnetic Observatory in 1985 N87-17419
SMITHSONIAN ASTROPHYSICAL OBSERVATORY, CAMBRIDGE, MASS.
System engineering study of electrodynamic tether as a spaceborne generator and radiator of electromagnetic waves in the ULF/ELF frequency band
[NASA-CR-180156] N87-16956
Investigation of plasma contactors for use with orbiting wires
[NASA-CR-180154] N87-17502
Observations of young low-mass stars in dense cores
[NASA-CR-180152] N87-17583
The study of the physics of cometary nuclei
[NASA-CR-180153] N87-17594
The dynamics and evolution of clusters of galaxies
[NASA-CR-180169] N87-17596
SOCIETE DE FABRICATION D'INSTRUMENTS DE MESURE, MASSY (FRANCE).
High voltage semiconductors for inertial sensors
[SFIM-13293-CP/LS] N87-17525
SOCIETE NATIONALE D'ETUDE ET DE CONSTRUCTION DE MOTEURS D'AVIATION, PARIS (FRANCE).
Study of the electron beam weldability of superalloys through the analysis of melt zone morphology N87-17053
The application of the RBD process to the deposition of anti-wear alloys N87-17069
SOCIETE NATIONALE INDUSTRIELLE AEROSPATIALE, LES MUREAUX (FRANCE).
Mechanical and control study of a 7 m offset unfurlable tracking antenna N87-16926
Structural analysis, manufacturing and development status of large polarization sensitive dual-gridded reflectors N87-16937
SOCIETE NATIONALE INDUSTRIELLE AEROSPATIALE, SURESNES (FRANCE).
Application of diffusion bonding combined with superplastic forming (SPF/DB) to the fabrication of TAGV metal sheet structures N87-17060
SOFTWARE SCIENCES LTD., FARNBOROUGH (ENGLAND).
The design of an international data centre for remote sensing N87-17176
SOUTH CAROLINA UNIV., COLUMBIA.
Advanced alternating frame technology (VISIDEP (TM)) and three-dimensional remote sensing N87-17291
SOUTH DAKOTA SCHOOL OF MINES AND TECHNOLOGY, RAPID CITY.
T-28 data acquisition during COHMEX 1986
[NASA-CR-179001] N87-17426
SPACE TELESCOPE SCIENCE INST., BALTIMORE, MD.
Structure of molecular clouds and space-based sub-millimeter telescopes, for example FIRST N87-17574
SPAR AEROSPACE LTD., STE-ANNE-DE-BELLEVUE (QUEBEC).
Design of a low distortion shared aperture reflector N87-16934
SPECTRON DEVELOPMENT LABS., INC., COSTA MESA, CALIF.
Droplet sizing research program
[AD-A173100] N87-16895
STANFORD LINEAR ACCELERATOR CENTER, CALIF.
Unified formulation for linear accelerator design
[DE86-013441] N87-17491
STANFORD UNIV., CALIF.
The aerodynamics and aeroacoustics of rotating transonic disturbances N87-16786
Identification of a dynamic model of a helicopter from flight tests N87-16813
The influence of wind-tunnel walls on discrete frequency noise N87-16850
Proceedings of the 15th International Symposium on Shock Waves and Shock Tubes
[AD-A173026] N87-17006
Microwave scattering from the ocean surface N87-17109
Spatial analysis of the dynamics of an ecosystem by multistage remote sensing in Kenya N87-17173
Automated remote sensing of sea ice using synthetic aperture radar N87-17186
A knowledge-based software environment for the analysis of spectroradiometer data N87-17203
Interrelationship between field spectra and airborne MSS systems in the Singatse range, (Yerington) Nevada N87-17242
Adaptive control of a flexible structure N87-17449
Adaptive control of mechanical manipulators N87-17450
Far infrared spectroscopy of galaxies from the Kuiper Airborne Observatory N87-17577
Spectral flux from low-density photospheres N87-17578
A search for rapidly modulated emission in bright X-ray sources using the HEAO A-1 data base
[NASA-CR-180148] N87-17593
STATE UNIV. OF NEW YORK, STONY BROOK.
Dark matter and the dynamics of galaxy clustering N87-17587
The abundances of ethane to acetylene in the atmospheres of Jupiter and Saturn N87-17618
The Cassini mission N87-17638
STOCKHOLM UNIV. (SWEDEN).
A statistical approach to select the optimal wavelength bands for separating rocks in the wavelength region 0.4 to 2.3 microns N87-17244
The A-X and B-X band systems of SrH: Wavenumbers and molecular constants
[USIP-86-04] N87-17486
STUTTGART UNIV. (WEST GERMANY).
X and L-band backscattering measurements of agricultural crops, forest stands and single trees N87-17311
Future user requirements and required technological developments of spaceborne synthetic aperture radars N87-17320
SURREY UNIV., GUILDFORD (ENGLAND).
An introduction to numerical methods for flow around bluff bodies N87-16992
SVERDRUP TECHNOLOGY, INC., CLEVELAND, OHIO.
A multigrid LU-SSOR scheme for approximate Newton iteration applied to the Euler equations
[NASA-CR-179524] N87-16803
A high resolution shock capturing scheme for high Mach number internal flow
[NASA-CR-179523] N87-16804
An LU-SSOR scheme for the Euler and Navier-Stokes equations
[NASA-CR-179556] N87-16806
SWISS ALUMINUM LTD., NEUHAUSEN AM RHEINFALL.
Welding of aluminum castings N87-17068
SWISS INST. OF METEOROLOGY, ZURICH.
Forecaster's need in meteorology for the next generation of satellites N87-17275
Real-time application of remotely sensed data N87-17276
SYRACUSE UNIV., N. Y.
Aeroacoustics of supersonic jet flows from contoured and solid/porous conical plug-nozzles
[NASA-CR-178095] N87-17484
SYSTEM DEVELOPMENT CORP., CAMARILLO, CALIF.
Lunar power systems
[NASA-CR-171958] N87-17398

T

TECHNICAL UNIV. OF BUDAPEST (HUNGARY).
A scatterometer operating at 10 GHz N87-17282
TECHNICAL UNIV. OF DENMARK, LYNGBY.
Sea ice in the Greenland sea observed by the Nimbus-7 Scanning Multichannel Microwave Radiometer (SMMR) N87-17221
TECHNISCHE HOGESCHOOL TWENTE, ENSCHEDE (NETHERLANDS).
On variational characterizations of steady vortex rings
[MEMO-577] N87-17014
Effective permeability and macrodispersion in locally heterogeneous aquifers
[MEMO-585] N87-17015
Model of the human controller of a dynamic system
[MEMO-580] N87-17435
Dynamic input-output decoupling of nonlinear control systems
[MEMO-575] N87-17452
A transportation queueing model, solved as a Riemann boundary value problem
[MEMO-573] N87-17463
A representation for piecewise cubic C sup 1-splines on arbitrary triangulations
[MEMO-574] N87-17464
A note on Branin's method for finding the critical points of smooth functions
[MEMO-576] N87-17465
Perturbation theory for unbounded Markov processes with applications to queueing
[MEMO-579] N87-17466

Simple and insensitive bounds for a grading and an overflow model
[MEMO-581] N87-17467
A formal proof for the insensibility of simple bounds for finite multiserver nonexponential tandem queues
[MEMO-582] N87-17468
A note on a core catcher of a cooperative game
[MEMO-572] N87-17475
A construction of solutions of the multicomponent KP-hierarchy
[MEMO-584] N87-17476
Advantageous syndicates in a bilateral market game: The case of the tau-value
[MEMO-583] N87-17534

TECHNISCHE UNIV., MUNICH (WEST GERMANY).
Bonding of superalloys by diffusion welding and diffusion brazing N87-17059

TEXAS A&M UNIV., COLLEGE STATION.
Measurement of heat transfer and pressure drop in rectangular channels with turbulence promoters
[NASA-CR-4015] N87-17003

TEXAS INSTRUMENTS, INC., DALLAS.
The effect of measurement error and confusion from vegetation on passive microwave estimates of soil moisture N87-17304

TEXAS UNIV., ARLINGTON.
Effective medium approximation for effective propagation constant calculation in a dense random medium N87-17180
A scattering model for defoliated vegetation N87-17309

TEXAS UNIV., AUSTIN.
Remote sensing of tree attenuation at 870 MHz along simulated Earth-satellite paths N87-17306
Changes in Saturn's south-temperate haze distribution during the summer of 1973-1980 N87-17602

TEXTRON BELL AEROSPACE CO., BUFFALO, N. Y.
Space station auxiliary thrust chamber technology
[NASA-CR-179552] N87-16874

TICRA A/S, COPENHAGEN (DENMARK).
Simple approach for evaluating mechanical reflector antenna distortions N87-16942

TOBA MERCHANT MARINE COLL. (JAPAN).
Estimation of maximum snow volume distribution using NOAA-AVHRR data N87-17314

TOHOKU UNIV., SENDAI (JAPAN).
Knowledge-based aerial image understanding systems N87-17210

TOKAI UNIV., HIRATSUKA (JAPAN).
RF plugging and tandem mirror experiments in a cusp-anchored mirror device
[IPPJ-800] N87-17508

TOKYO GAS CO. LTD. (JAPAN).
Development of intelligent pipe locator N87-17200

TOKYO UNIV. (JAPAN).
Models for temperature estimation from remotely sensed thermal IR data N87-17325

TOSHIBA RESEARCH AND DEVELOPMENT CENTER, KAWASAKI (JAPAN).
Study on solid surface, deployable antenna reflector N87-16928

TRW ELECTRONIC SYSTEMS GROUP, REDONDO BEACH, CALIF.
The 20 GHz power GaAs FET development
[NASA-CR-179546] N87-16972

TRW SPACE TECHNOLOGY LABS., REDONDO BEACH, CALIF.
Identification of the contribution of Bragg scattering and specular reflection to X-band microwave backscattering in an ocean experiment N87-17216
SAR imaging of bottom topography in the ocean: Results from an improved model N87-17298

TURIN UNIV. (ITALY).
Dielectric support structures for spacecraft antenna feeds N87-16931
Bulk Richardson's number isograms deduced from SAR data N87-17392

U

UNITED KINGDOM INFRARED TELESCOPE UNIT, HILO, HAWAII.
Observations of active galactic nuclei with FIRST N87-17538

UNITED TECHNOLOGIES RESEARCH CENTER, EAST HARTFORD, CONN.
Unsteady aerodynamics of a rotating compressor blade row in incompressible flow. Volume 1: Experimental facilities, procedures and sample data
[AD-A173043] N87-16831
Unsteady aerodynamics of a rotating compressor blade row at low Mach number. Volume 2: Analysis of experimental results and comparison with theory
[AD-A173044] N87-16832
Unsteady aerodynamics of a rotating compressor blade row at low mach number. Volume 3: Experimental data base and users manual
[AD-A173045] N87-16833

UNIVERSITE CATHOLIQUE DE LOUVAIN (BELGIUM).
A modified boundary perturbation approach to microwave scattering and emission by the ocean surface N87-17214
A two-step algorithm for the separate retrieval of ocean surface and atmospheric parameters from microwave radiometers N87-17341

UNIVERSITIES SPACE RESEARCH ASSOCIATION, BOULDER, COLO.
Results from 1984 airborne Doppler lidar wind measurement program. Flight 6: Analysis of line-of-sight elevation angle errors and apparent Doppler velocities
[NASA-CR-178994] N87-17425

UNIVERSITIES SPACE RESEARCH ASSOCIATION, COLUMBIA, MD.
Computation of turbulent boundary layer flows with an algebraic stress turbulence model
[NASA-CR-178967] N87-16982

UNIVERSITY COLL., LONDON (ENGLAND).
Submillimetre wavelength studies of protostars: The role of FIRST N87-17544
Submillimeter HCO+ observations of dense cloud cores N87-17562
The influence of background power on the performance of an ideal bolometer N87-17565

UNIVERSITY OF NORTH-EASTERN HILL, SHILLONG (INDIA).
Structural and geomorphic evolution of Meghalaya plateau, India on LANDSAT imagery N87-17233

UNIVERSITY OF NORTHERN ARIZONA, FLAGSTAFF.
Investigation of the mode of compensation of Venus topography
[NASA-CR-180145] N87-17649

UNIVERSITY OF SOUTHERN CALIFORNIA, LOS ANGELES.
Nonlinear real-time optical signal processing
[AD-A173119] N87-17497

UTAH STATE UNIV., LOGAN.
Model study of the mid-latitude atmospheric interaction with energetic O+ and He+ (20 keV) precipitation during a storm N87-17411

V

VEXCELL CORP., BOULDER, COLO.
Using secondary image products to aid in understanding and interpretation of radar imagery N87-17239

VIGYAN RESEARCH ASSOCIATES, INC., HAMPTON, VA.
Calculation of sidewall boundary-layer parameters from rake measurements for the Langley 0.3-meter transonic cryogenic tunnel
[NASA-CR-178241] N87-16807

VIRGINIA POLYTECHNIC INST. AND STATE UNIV., BLACKSBURG.
Hypersonic nonequilibrium flow over an ablating teflon surface N87-16787
Unitary suprathreshold color-difference metrices of legibility for CRT raster imagery
[AD-A175062] N87-17434
Comparative advantages of graphic versus numeric representation of quantitative data N87-17439

VIRGINIA UNIV. HOSPITAL, CHARLOTTESVILLE.
Mechanisms of helium embrittlement N87-16899

VON KARMAN INST. FOR FLUID DYNAMICS, RHODE-SAINT-GENESE (BELGIUM).
Two-Phase Flows in Major Technological Hazards, volume 3
[VKI-LS-1986-03-VOL-3] N87-16984
Introduction to Numerical Solution of Industrial Flows, volume 1
[VKI-LS-1986-07-VOL-1] N87-16987
Introduction to Numerical Solution of Industrial Flows, volume 2
[VKI-LS-1986-07-VOL-2] N87-16994
Prediction of heat and mass transfer in particulate beds N87-16999

VRIJE UNIVERSITEIT, BRUSSELS (BELGIUM).
An analysis of flow models: From Navier-Stokes to potential flow equations N87-16988
The spatial levels of approximation from three-dimensional to quasi one-dimensional representation N87-16989
Review of discretization techniques and numerical resolution methods N87-16990
The analysis and resolution of numerical schemes N87-16991

W

WASHINGTON STATE UNIV., PULLMAN.
Determining and modeling the response of ytterbium piezoresistance transducers
[AD-A173085] N87-17023
Light scattering theory for bubbles in water: Inverse scattering, coated bubbles and statistics
[AD-A174997] N87-17498

WASHINGTON UNIV., SEATTLE.
Observing the polar oceans with spaceborne radar N87-17151
Eddy processes in the general circulation of the Jovian atmospheres N87-17627

WASHINGTON UNIV., ST. LOUIS, MO.
A detected feature at the expected wavelength for the HD R5(0) line in Jupiter's and Uranus' atmospheres N87-17619

WEAPONS SYSTEMS RESEARCH LAB., SALISBURY (AUSTRALIA).
Linearised theory of stability and resonance for projectiles with aerodynamically induced roll variations
[WSRL-0449-TR] N87-16795

WELDING INST., CAMBRIDGE (ENGLAND).
The application of diffusion bonding and laser welding in the fabrication of aerospace structures N87-17054

WHEATON COLL., NORTON, MASS.
The ionization structure of planetary nebulae. 8: NGC 6826
[NASA-CR-180142] N87-17581
The ionization structure of planetary nebulae. Part 7: New observations in the ring nebula
[NASA-CR-180141] N87-17582

WISCONSIN UNIV., MADISON.
Jupiter: New estimates of mean zonal flow at the cloud level N87-17622
Cloud-top meridional momentum transports on Saturn and Jupiter N87-17623

WOODS HOLE OCEANOGRAPHIC INSTITUTION, MASS.
Analysis of harmonic spline gravity models for Venus and Mars
[NASA-CR-180147] N87-17648

WORLD METEOROLOGICAL ORGANIZATION, GENEVA (SWITZERLAND).
An overview of the implementation of the World Climate Research program N87-17388

Z

ZURICH UNIV. (SWITZERLAND).
Sri Lanka's solution to land use mapping and monitoring for Third World countries development N87-17174
Merging spaceborne image data of optical and microwave sensors N87-17267
Viewing angle corrections of airborne multispectral scanner data acquired over forested surfaces N87-17273
Snow cover recession in an Alpine ecological system N87-17316
Towards snowmelt runoff forecast using LANDSAT-MSS and NOAA/AVHRR data N87-17317

Typical Contract Number Index Listing

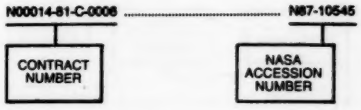

Listings in this index are arranged alphanumerically by contract number. Under each contract number the NASA accession numbers denoting documents that have been produced as a result of research done under that contract are arranged in ascending order. The NASA accession number denotes the number by which the citation is identified.

AF-AFOSR-0005-84 ..... N87-17461
AF-AFOSR-0132-82 ..... N87-17023
AF-AFOSR-0181-84 ..... N87-17497
AF-AFOSR-0224-84 ..... N87-16894
AF-AFOSR-0271-84 ..... N87-16872
AF-AFOSR-0299-85 ..... N87-17427
AF-AFOSR-0315-84 ..... N87-17459
AF-AFOSR-0346-85 ..... N87-16896
AFOSR-85-0230 ..... N87-17570
ARPA ORDER 4871 ..... N87-17437
CAICYT-477/84 ..... N87-17553
CAN-DEPT-COMM-21ST-36100-3-031 ..... N87-16934
CAYCYT-477/84 ..... N87-17561
DA PROJ. 1L1-61102-AH-45 ..... N87-16882
N87-16884
DA PROJ. 1L1-62209-AH-76 ..... N87-17003
DA PROJ. 4A1-61101-A-91-D N87-16914
DAAB07-82-C-J069 ..... N87-16962
DAAG29-83-K-0067 ..... N87-16976
DAAG29-85-G-0079 ..... N87-17006
DAAG29-85-K-0045 ..... N87-17201
DACA39-85-C-0023 ..... N87-16914
DE-AC02-76ER-03130 ..... N87-17490
DE-AC02-83CH-10093 ..... N87-16913
N87-17402
N87-17403
N87-17404
N87-17405
DE-AC03-76SF-00098 ..... N87-17488
N87-17500
DE-AC03-76SF-00515 ..... N87-17491
DE-AC04-76DP-00789 ..... N87-16978
N87-17485
N87-17524
DE-AC05-84OR-21400 ..... N87-17049
N87-17445
DE-AC06-76RL-01830 ..... N87-17406
N87-17407
N87-17652
DE-AC07-76ID-01570 ..... N87-17050
N87-17093
N87-17492
DE-AI01-76ET-20320 ..... N87-17400
N87-17401
DE-AT03-83SF-11713 ..... N87-17506
DFG-SFB-301 ..... N87-17573
DI-14-08-0001-21748 ..... N87-17312
DNA PROJ. Q93-QMXA N87-16854
DNA PROJ. X99-QAXV N87-16977
DNA001-82-C-0241 ..... N87-16977
DNA001-84-C-0438 ..... N87-16854
DRET-84-34-001 ..... N87-16846
DRET-84-411 ..... N87-17525
EMRM-82-0437 ..... N87-17438
ESA-5263/82-NL-GM N87-16941
ESA-5277/82-NL-PP N87-16935
ESA-5285/82 ..... N87-17214
ESA-6153/WL-MS N87-17265
ESTEC-5158/82-NL-PB(SC) N87-16948
ESTEC-5206/82-NL-PB(SC) N87-16925
ESTEC-5494/84-NL-GM N87-16932
ESTEC-5375/85-NL-BI N87-17195
FHWA-8-3-0167 ..... N87-16853
FMV-F-K-82260-84-254-73-001 ..... N87-16811
FMV-FFL-82250-85-076-73-001 ..... N87-17094
FRCU-842019 ..... N87-17196
F04701-85-C-0086 ..... N87-17523
F19628-84-C-0081 ..... N87-17312
F30602-84-C-0068 ..... N87-16961
F33615-81-K-1539 ..... N87-17533
F33615-82-C-3215 ..... N87-16822
F49620-81-C-0068 ..... N87-16831
N87-16832
N87-16833
F49620-83-C-0060 ..... N87-16895
F49620-84-C-0066 ..... N87-17008
F49620-85-C-0002 ..... N87-17007
F49620-85-C-0094 ..... N87-16871
F49620-86-C-0006 ..... N87-16897
F49620-86-C-0022 ..... N87-17470
JAP-MIN-OF-ED-60129032 ..... N87-17249
JPL-956520 ..... N87-17306
JPL-956937 ..... N87-17246
JPL-957126 ..... N87-17408
NAGW-185 ..... N87-17637
NAGW-201 ..... N87-17596
NAGW-284 ..... N87-17413
NAGW-334 ..... N87-17184
N87-17220
NAGW-448 ..... N87-17529
NAGW-661 ..... N87-16890
NAGW-690 ..... N87-17212
N87-17213
NAGW-736 ..... N87-17418
NAGW-792 ..... N87-17648
NAG1-129 ..... N87-17484
NAG1-190 ..... N87-17448
NAG2-220 ..... N87-17494
NAG2-224 ..... N87-17430
NAG2-278 ..... N87-17004
NAG2-330 ..... N87-17649
NAG2-374 ..... N87-17583
NAG3-576 ..... N87-16971
NAG5-270 ..... N87-17187
NAG5-403 ..... N87-17440
NAG5-407 ..... N87-17457
N87-17458
NAG5-480 ..... N87-17393
NAG5-486 ..... N87-17180
N87-17309
NAG5-580 ..... N87-17340
NAG5-596 ..... N87-17429
NAG5-823 ..... N87-17584
NAG8-490 ..... N87-17593
NAG8-551 ..... N87-16956
NAG9-117 ..... N87-17431
NAG9-126 ..... N87-17502
NAS-7-100 ..... N87-17408
NASA ORDER A-32033-C N87-17270
NASA ORDER L-83161-B N87-17270
NASW-4004 ..... N87-16983
N87-17089
NASW-4005 ..... N87-16797
N87-16856
N87-17474
N87-17595
NASW-4006 ..... N87-17394
NASW-4049 ..... N87-17246
NAS1-15069 ..... N87-16883
NAS1-17070 ..... N87-17088
NAS1-17536 ..... N87-16870
N87-16916
NAS1-17639 ..... N87-16860
NAS1-17919 ..... N87-16807
NAS1-17958 ..... N87-16864
NAS1-17962 ..... N87-16981
NAS1-17964 ..... N87-17469
NAS1-18000 ..... N87-16864
NAS1-18107 ..... N87-17088
N87-17436
N87-17444
N87-17453
N87-17456
NAS3-22503 ..... N87-16972
NAS3-23275 ..... N87-17481
NAS3-23339 ..... N87-17515
NAS3-24105 ..... N87-16803
N87-16804
N87-16806
N87-17400
NAS3-24227 ..... N87-17003
NAS3-24253 ..... N87-17472
N87-17473
NAS3-24340 ..... N87-16830
NAS3-24636 ..... N87-16878
NAS3-24656 ..... N87-16874
NAS3-24892 ..... N87-16954
N87-16955
NAS5-28057 ..... N87-17205
NAS7-918 ..... N87-16921
N87-16922
N87-17110
N87-17111
N87-17135
N87-17396
N87-17397
N87-17451
N87-17526
NAS8-33370 ..... N87-17420
NAS8-34010 ..... N87-17425
NAS8-35331 ..... N87-17516
NAS8-35918 ..... N87-16982
NAS8-36486 ..... N87-16829
NAS8-36489 ..... N87-17426
NAS8-36716 ..... N87-17041
NAS9-17059 ..... N87-16855
NAS9-17272 ..... N87-16865
N87-16866
N87-16868
N87-16869
NAS9-17359 ..... N87-17398
NAS9-17422 ..... N87-16855
NAS9-17560 ..... N87-16862
N87-16867
NCC2-387 ..... N87-16957
NCC3-6 ..... N87-17401
NCC3-30 ..... N87-16879
NCC3-54 ..... N87-16953
NGR-28-004-021 ..... N87-16892
NGR-36-008-161 ..... N87-17416
NGR09-010-078 ..... N87-17526
NOAA-NA-80RAD00065 ..... N87-17270
NR PROJ. 657-729 ..... N87-16960
NSERC-A-7400 ..... N87-17293
NSF AST-79-21812 ..... N87-17563
NSF ATM-85-05558 ..... N87-17318
NSF ECS-82-15539 ..... N87-17327
NSF ECS-85-04381 ..... N87-17187
NSF PHY-84-095854 ..... N87-17652
NSF 83-03108 ..... N87-17619
NSG-2403 ..... N87-17430
NSG-5265 ..... N87-17415
NSG-5376 ..... N87-17581
N87-17582
NSG-7082 ..... N87-17594
NSG-7334 ..... N87-17619
N000-14-81-C-0295 ..... N87-17184
N87-17219
N000-14-83-C-0404 ..... N87-17184
N87-17219
N000-14-83-K-0525 ..... N87-17187
N000-14-85-K-0200 ..... N87-17184
N87-17188
N87-17220
N00014-78-CK-0238 ..... N87-17434
N00014-81-C-0259 ..... N87-17222
N00014-81-C-0463 ..... N87-17521
N00014-81-C-0692 ..... N87-17297
N87-17338
N00014-82-K-0324 ..... N87-16960
N00014-83-C-0404 ..... N87-17222
N00014-84-C-2312 ..... N87-17299
N00014-85-C-0132 ..... N87-17222
N00014-85-K-0255 ..... N87-17460
N00014-85-K-0568 ..... N87-17433
N00014-85-K-0596 ..... N87-17092
N00014-86-K-0242 ..... N87-17498

N00014-86-K-0381	N87-17091
N00014-86-K-2001	N87-17340
N00024-85-C-5301	N87-17306
N00039-84-C-0089	N87-17437
N000024-85-C-5301	N87-17182
OSURF PROJ. 711055	N87-17415
OSURF PROJ. 783210	N87-17416
W-31-109-ENG-38	N87-16898
W-7405-ENG-36	N87-17395
W-7405-ENG-48	N87-16886
	N87-17009
	N87-17027
	N87-17446
	N87-17489
	N87-17499
	N87-17501
W-7405-ENG-82	N87-16904
	N87-17073
154-40-80	N87-17598
161-80-15-40-00	N87-17110
199-22-76-01	N87-17487
307-51-00	N87-16953
323-52-52-00	N87-17396
480-43-02	N87-17472
	N87-17473
480-52-05-01	N87-16860
482-58-13-01	N87-16873
483-31-03-01	N87-16861
483-32-03-01	N87-16864
505-31-4K	N87-17003
505-31-04	N87-16784
	N87-16827
505-31-21	N87-16821
505-31-83-01	N87-17068
505-60	N87-16791
	N87-16800
	N87-16801
505-60-01-01	N87-17442
505-61-01-02	N87-16807
505-61-01-05	N87-17018
505-61-11	N87-17484
505-61-41-01	N87-16815
505-61-51-06	N87-17479
505-61-59-03	N87-16884
505-62-3A	N87-17481
505-62-3B	N87-16851
505-62-21	N87-16789
	N87-16790
	N87-16799
	N87-16803
	N87-16804
	N87-16806
	N87-16826
505-62-51	N87-17033
505-62-61-07	N87-16802
505-63-11-03	N87-17086
505-63-21-02	N87-16796
505-63-51-01	N87-17526
505-63-81	N87-16879
505-63-91-01	N87-16911
505-63-91-02	N87-17482
505-66-01-01	N87-16849
505-66-21-01	N87-17448
	N87-17469
505-68-51	N87-16825
505-90-21-01	N87-17436
	N87-17444
	N87-17453
	N87-17456
506-40-31	N87-16878
506-42-22	N87-16902
506-43-11-04	N87-16882
	N87-17090
506-43-41-02	N87-16870
506-44-21	N87-16953
	N87-16958
	N87-16968
	N87-17515
506-46-21-01	N87-16848
506-53-43-01	N87-16916
533-02-01-04	N87-16981
533-02-11	N87-16819
533-02-51	N87-16820
533-05-11	N87-17087
534-06-23-01	N87-16883
535-03-01	N87-16798
	N87-17001
	N87-17480
535-03-11-03	N87-17483
549-01-11-05-00	N87-17451
553-13-00	N87-17002
644-11-00-04-00	N87-17528
650-60-15-01-00	N87-16921
	N87-16922
650-60-26	N87-16954
	N87-16955
650-66-22	N87-16972
665-40-40-01	N87-17417
666-31-01-00-64	N87-17135
674-27-05	N87-16917
677-80-23-01-00	N87-17111
679-40-00	N87-16880

Typical Report Number Index Listing

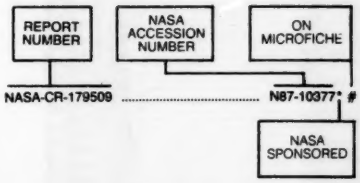

Listings in this index are arranged alphanumerically by report number. The NASA accession number denotes the number by which the citation is identified. An asterisk (*) indicates that the item is a NASA report. A pound sign (#) indicates that the item is available on microfiche.

A-87042 ..... N87-16801* #
A-87047 ..... N87-16791* #
A-87048 ..... N87-16800* #

AAC-TN-1130-REV-A ..... N87-16916* #
AAC-TN-1147-REV-A ..... N87-16870* #

AD-A172535 ..... N87-17091 #
AD-A173013 ..... N87-16823 #
AD-A173015 ..... N87-16914 #
AD-A173017 ..... N87-17521 #
AD-A173019 ..... N87-17459 #
AD-A173020 ..... N87-17460 #
AD-A173022 ..... N87-17437 #
AD-A173025 ..... N87-16976 #
AD-A173026 ..... N87-17006 #
AD-A173028 ..... N87-17533 #
AD-A173043 ..... N87-16831 #
AD-A173044 ..... N87-16832 #
AD-A173045 ..... N87-16833 #
AD-A173083 ..... N87-16871 #
AD-A173084 ..... N87-17092 #
AD-A173085 ..... N87-17023 #
AD-A173086 ..... N87-16977 #
AD-A173087 ..... N87-16854 #
AD-A173091 ..... N87-17007 #
AD-A173094 ..... N87-16960 #
AD-A173097 ..... N87-17522 #
AD-A173098 ..... N87-16894 #
AD-A173100 ..... N87-16895 #
AD-A173119 ..... N87-17497 #
AD-A174611 ..... N87-17527 #
AD-A174639 ..... N87-16915 #
AD-A174640 ..... N87-17433 #
AD-A174648 ..... N87-17470 #
AD-A174649 ..... N87-17048 #
AD-A174691 ..... N87-17427 #
AD-A174693 ..... N87-16961 #
AD-A174984 ..... N87-16896 #
AD-A174997 ..... N87-17498 #
AD-A175019 ..... N87-16872 #
AD-A175033 ..... N87-17008 #
AD-A175040 ..... N87-16897 #
AD-A175062 ..... N87-17434 #
AD-A175073 ..... N87-17461 #
AD-A175093 ..... N87-16962 #
AD-A175102 ..... N87-17523 #
AD-A175110 ..... N87-16822 #

AD-D012466 ..... N87-16893
AD-D012474 ..... N87-17518 #
AD-D012481 ..... N87-17043 #
AD-D012483 ..... N87-17044 #
AD-D012485 ..... N87-16912 #
AD-D012486 ..... N87-17477 #
AD-D012487 ..... N87-17045 #
AD-D012488 ..... N87-17519
AD-D012489 ..... N87-16903 #
AD-D012492 ..... N87-17520
AD-D012495 ..... N87-16973
AD-D012498 ..... N87-17005 #
AD-D012499 ..... N87-17019 #
AD-D012501 ..... N87-16885 #
AD-D012504 ..... N87-16974 #
AD-D012505 ..... N87-17046 #
AD-D012506 ..... N87-17495 #
AD-D012507 ..... N87-17496 #
AD-D012508 ..... N87-17020 #
AD-D012509 ..... N87-17021 #
AD-D012510 ..... N87-17047 #
AD-D012512 ..... N87-16920 #
AD-D012513 ..... N87-16959 #
AD-D012514 ..... N87-17022 #
AD-D012519 ..... N87-16975 #

AERONOMICA-ACTA-A-306-1986 ..... N87-17653 #
AERONOMICA-ACTA-A-308-1986 ..... N87-17650 #
AERONOMICA-ACTA-A-309-1986 ..... N87-17421 #

AFOSR-86-0478TR ..... N87-17470 #
AFOSR-86-0863TR ..... N87-16831 #
AFOSR-86-0864TR ..... N87-17023 #
AFOSR-86-0875TR ..... N87-16895 #
AFOSR-86-0885TR ..... N87-16871 #
AFOSR-86-0903TR ..... N87-17497 #
AFOSR-86-0942TR ..... N87-17007 #
AFOSR-86-1004TR ..... N87-16894 #
AFOSR-86-2106TR ..... N87-16896 #
AFOSR-86-2107TR ..... N87-16897 #
AFOSR-86-2175TR ..... N87-17008 #
AFOSR-86-2192TR ..... N87-17461 #
AFOSR-86-2193TR ..... N87-16872 #

AFSR-4 ..... N87-16883* #

AFWAL-TR-86-1011 ..... N87-17533 #
AFWAL-TR-86-3003-VOL-1 ..... N87-16822 #

AFWL-TR-86-12 ..... N87-17522 #

AGARD-CP-398 ..... N87-17051 #

AIAA-86-0041 ..... N87-16799* #
AIAA-87-0303 ..... N87-16826* #
AIAA-87-0420 ..... N87-17001* #
AIAA-87-0600 ..... N87-16806* #

AR-004-495 ..... N87-16881 #
AR-004-619 ..... N87-16795 #

ARL-STRUC-R-422 ..... N87-16881 #

ARO-19778.10-EL ..... N87-16976 #
ARO-22564.1-EG ..... N87-17006 #

AVSCOM-TM-87-B-2 ..... N87-16884* #

AVSCOM-TR-86-B-2 ..... N87-16882* #
AVSCOM-TR-86-C-25 ..... N87-17003* #

BBN-6114 ..... N87-16961 #

BRL-TR-2768 ..... N87-16915 #

BROWN/HET-586 ..... N87-17490 #

BR99119 ..... N87-16906
BR99145 ..... N87-17042 #
BR99178 ..... N87-17072 #
BR99688 ..... N87-16859 #
BR100130 ..... N87-17517 #
BR100238 ..... N87-16852 #

CAL-1638 ..... N87-17584* #

CECOM-TR-82-J069-F ..... N87-16962 #

CI-FR-0094 ..... N87-17516* #

CNES-CT/DRT/TIT/RL-54-T ..... N87-16963 #
CNES-CT/DRT/TIT/RL-55-T ..... N87-16964 #

CONF-860366-12 ..... N87-17027 #
CONF-860575-17 ..... N87-17488 #
CONF-860610-24 ..... N87-17485 #
CONF-860629-25 ..... N87-17491 #
CONF-860685-12 ..... N87-17489 #
CONF-860682-4 ..... N87-17093 #
CONF-860741-9 ..... N87-17652 #
CONF-860880-19 ..... N87-16913 #
CONF-860880-34 ..... N87-17501 #
CONF-860888-1 ..... N87-17395 #
CONF-860921-1 ..... N87-16898 #
CONF-860950-1 ..... N87-17499 #
CONF-860963-1 ..... N87-17445 #
CONF-860968-1 ..... N87-17524 #
CONF-860967-1 ..... N87-17446 #
CONF-8506110-ABST ..... N87-17073 #
CONF-8510160-19 ..... N87-17050 #
CONF-8511123-5 ..... N87-17500 #
CONF-8609101-1 ..... N87-17049 #
CONF-8609116-1 ..... N87-17009 #

CONTRIB-19586 ..... N87-17248 #

COO-3130TA-379 ..... N87-17490 #

CRC-1401 ..... N87-16960 #

CRREL-86-18 ..... N87-16853 #

CSDL-T-939 ..... N87-16862* #
CSDL-T-941 ..... N87-16867* #

DE86-004428 ..... N87-17402 #
DE86-004461 ..... N87-17403 #
DE86-007504 ..... N87-16898 #
DE86-007827 ..... N87-17485 #
DE86-008164 ..... N87-17499 #
DE86-008895 ..... N87-17445 #
DE86-009025 ..... N87-17524 #
DE86-009686 ..... N87-17446 #
DE86-010704 ..... N87-17404 #
DE86-010719 ..... N87-17405 #
DE86-010727 ..... N87-16913 #
DE86-010784 ..... N87-17406 #
DE86-011076 ..... N87-17049 #
DE86-011258 ..... N87-17395 #
DE86-012223 ..... N87-17407 #
DE86-012364 ..... N87-17408* #
DE86-013190 ..... N87-17488 #
DE86-013218 ..... N87-17489 #
DE86-013221 ..... N87-17009 #
DE86-013227 ..... N87-16886 #
DE86-013326 ..... N87-17490 #
DE86-013441 ..... N87-17491 #
DE86-013454 ..... N87-17093 #
DE86-013457 ..... N87-17050 #
DE86-013485 ..... N87-17500 #
DE86-013592 ..... N87-17652 #
DE86-013753 ..... N87-16904 #
DE86-013756 ..... N87-16978 #
DE87-000769 ..... N87-17073 #
DE87-001355 ..... N87-17501 #
DE87-001430 ..... N87-17492 #
DE87-001432 ..... N87-17027 #

DFVLR-MITT-84-21 ..... N87-17077 #

DNA-TR-86-85-PT-2 ..... N87-16977 #
DNA-TR-86-119 ..... N87-16854 #

DOE/ER-03130/379 ..... N87-17490 #

DOE/NASA/0006-3 ..... N87-17401* #
DOE/NASA/4105-2 ..... N87-17400* #

DOE/NBM-6012364 ..... N87-17408* #

DOT/FAA/FS-86/1-VOL-2 ..... N87-16812 #

DOT/FAA/PM-85/23 ..... N87-16853 #

DR-SE-1093T-VOL-2 ..... N87-16868* #
DR-SE-1093T-VOL-4 ..... N87-16865* #
DR-SE-1093T-VOL-5 ..... N87-16866* #

E-2935 ..... N87-16958* #
E-3103 ..... N87-16804* #
E-3104 ..... N87-16803* #
E-3105 ..... N87-16806* #
E-3126 ..... N87-16784* #
E-3134 ..... N87-17481* #
E-3152 ..... N87-16879* #
E-3164 ..... N87-17003* #
E-3190 ..... N87-16805* #
E-3223 ..... N87-17033* #
E-3225 ..... N87-16880* #
E-3229 ..... N87-17067* #
E-3300 ..... N87-16827* #
E-3304 ..... N87-16902* #
E-3307 ..... N87-16826* #
E-3329 ..... N87-17002* #
E-3340 ..... N87-17001* #
E-3359 ..... N87-16968* #
E-3364 ..... N87-16825* #
E-3393 ..... N87-16789* #
E-3394 ..... N87-16790* #
E-3398 ..... N87-16799* #
E-3399 ..... N87-16798* #
E-3407 ..... N87-17480* #
E-3411 ..... N87-17441* #
E-3417 ..... N87-16851* #
E-3420 ..... N87-16917* #

EGG-J-01586 ..... N87-17050 #

EGG-M-18785 ..... N87-17093 #

EGG-RTH-7397-VOL-1 ..... N87-17492 #

EOARD-TR-87-01 ..... N87-17427 #

EPISODE-9 ..... N87-17584* #

ESA-SP-254-VOL-1 ..... N87-17163 #
ESA-SP-254-VOL-2 ..... N87-17283 #
ESA-SP-260 ..... N87-17535 #
ESA-SP-261 ..... N87-16923 #
ESA-SP-262 ..... N87-17363 #

ESA-TT-917 ..... N87-17077 #

ETN-87-98535 ..... N87-17163 #
ETN-87-98536 ..... N87-17283 #
ETN-87-98773 ..... N87-16834 #
ETN-87-98777 ..... N87-16835 #
ETN-87-98778 ..... N87-16824
ETN-87-98779 ..... N87-16836 #
ETN-87-98780 ..... N87-16837 #
ETN-87-98781 ..... N87-16838 #
ETN-87-98782 ..... N87-16839 #
ETN-87-98783 ..... N87-16687 #
ETN-87-98784 ..... N87-16840 #
ETN-87-98785 ..... N87-16841 #
ETN-87-98786 ..... N87-17024 #
ETN-87-98787 ..... N87-16905 #
ETN-87-98788 ..... N87-16842 #
ETN-87-98789 ..... N87-16843 #
ETN-87-98790 ..... N87-16844 #
ETN-87-98791 ..... N87-17010 #
ETN-87-98792 ..... N87-16845 #
ETN-87-98798 ..... N87-17025 #
ETN-87-98801 ..... N87-17011 #
ETN-87-98802 ..... N87-16808 #
ETN-87-98803 ..... N87-17012 #
ETN-87-98805 ..... N87-17432 #
ETN-87-98806 ..... N87-16963 #
ETN-87-98807 ..... N87-16964 #
ETN-87-98808 ..... N87-16846 #
ETN-87-98810 ..... N87-17525 #
ETN-87-98811 ..... N87-17013 #
ETN-87-98814 ..... N87-17077 #
ETN-87-98834 ..... N87-17535 #
ETN-87-98835 ..... N87-16923 #
ETN-87-98836 ..... N87-17363 #
ETN-87-98838 ..... N87-17421 #
ETN-87-98839 ..... N87-17653 #
ETN-87-98840 ..... N87-17650 #
ETN-87-98843 ..... N87-16984 #
ETN-87-98844 ..... N87-16987 #
ETN-87-98845 ..... N87-16994 #
ETN-87-98847 ..... N87-17422 #
ETN-87-98848 ..... N87-16809 #
ETN-87-98849 ..... N87-16810 #
ETN-87-98900 ..... N87-17585 #
ETN-87-98904 ..... N87-17486 #
ETN-87-98905 ..... N87-17094 #
ETN-87-98906 ..... N87-16811 #
ETN-87-98907 ..... N87-16888 #
ETN-87-98908 ..... N87-16965 #
ETN-87-98909 ..... N87-16966 #
ETN-87-98911 ..... N87-17517 #
ETN-87-98912 ..... N87-17072 #
ETN-87-98913 ..... N87-16852 #
ETN-87-98914 ..... N87-17042 #
ETN-87-98915 ..... N87-16859 #
ETN-87-98916 ..... N87-16906
ETN-87-98917 ..... N87-17438
ETN-87-98929 ..... N87-17514 #
ETN-87-98930 ..... N87-17462 #
ETN-87-98931 ..... N87-17095 #
ETN-87-98932 ..... N87-17471 #
ETN-87-98938 ..... N87-16967 #
ETN-87-98966 ..... N87-17575
ETN-87-98967 ..... N87-17576
ETN-87-99051 ..... N87-17475 #
ETN-87-99052 ..... N87-17463 #
ETN-87-99053 ..... N87-17464 #
ETN-87-99054 ..... N87-17452 #
ETN-87-99055 ..... N87-17465 #
ETN-87-99056 ..... N87-17014 #
ETN-87-99058 ..... N87-17466 #
ETN-87-99059 ..... N87-17435 #
ETN-87-99060 ..... N87-17467 #
ETN-87-99061 ..... N87-17468 #
ETN-87-99062 ..... N87-17534 #
ETN-87-99063 ..... N87-17476 #
ETN-87-99064 ..... N87-17015 #

FAA-140 ..... N87-16794 #

FFA-TN-1986-35 ..... N87-17094 #
FFA-TN-1986-42 ..... N87-16811 #

FOA-B-30097-3.3 ..... N87-16965 #
FOA-B-30098-3.3 ..... N87-16966 #

FOA-C-20620-2.5 ..... N87-16888 #

GALCIT-SM-86-6 ..... N87-17092 #

GARRETT-21-5723 ..... N87-16830* #

GBL-86-036R ..... N87-16854 #

GIT-A-3213 ..... N87-16962 #

GTD86-5 ..... N87-16878* #

H-1284 ..... N87-16821* #
H-1296 ..... N87-16820* #
H-1368 ..... N87-16819* #

HFL/ONR-86-3 ..... N87-17434 #

ICAS-86-1.2.2 ..... N87-17010 #
ICAS-86-3.10.1 ..... N87-16843 #

ICASE-86-51 ..... N87-17088* #
ICASE-86-74 ..... N87-17453* #
ICASE-86-77 ..... N87-17456* #
ICASE-87-1 ..... N87-17444* #
ICASE-87-2 ..... N87-17436* #

ICOMP-86-3 ..... N87-16784* #

IEEE-86CH2268-1-VOL-1 ..... N87-17163 #
IEEE-86CH2268-1-VOL-2 ..... N87-17283 #

IPPCZ-255 ..... N87-17506 #
IPPCZ-263 ..... N87-17504 #
IPPCZ-268 ..... N87-17505 #

IPPJ-798 ..... N87-17507 #
IPPJ-799 ..... N87-17509 #
IPPJ-800 ..... N87-17508 #
IPPJ-801 ..... N87-17511 #
IPPJ-802 ..... N87-17510 #
IPPJ-803 ..... N87-17513 #
IPPJ-804 ..... N87-17512 #

IS-4879 ..... N87-17073 #

ISBN-87-7478-275-4 ..... N87-17428 #
ISBN-91-7056-072-2 ..... N87-16965 #
ISBN-91-7056-072-2 ..... N87-16966 #
ISBN-92-835-0397-X ..... N87-17051 #

ISI-85 ..... N87-16871 #

ISL-CO-205/86 ..... N87-17011 #
ISL-CO-206/86 ..... N87-16808 #
ISL-CO-208/86 ..... N87-17012 #
ISL-CO-242/85 ..... N87-17025 #

ISL-NB-402/85 ..... N87-17432 #

ISSN-0065-3713 ..... N87-17421 #
ISSN-0065-3713 ..... N87-17650 #
ISSN-0065-3713 ..... N87-17653 #
ISSN-0072-6566 ..... N87-17363 #
ISSN-0169-2690 ..... N87-17014 #
ISSN-0169-2690 ..... N87-17015 #
ISSN-0169-2690 ..... N87-17435 #
ISSN-0169-2690 ..... N87-17452 #
ISSN-0169-2690 ..... N87-17463 #
ISSN-0169-2690 ..... N87-17464 #
ISSN-0169-2690 ..... N87-17465 #
ISSN-0169-2690 ..... N87-17466 #
ISSN-0169-2690 ..... N87-17467 #
ISSN-0169-2690 ..... N87-17468 #
ISSN-0169-2690 ..... N87-17475 #
ISSN-0169-2690 ..... N87-17476 #
ISSN-0169-2690 ..... N87-17534 #
ISSN-0208-5658 ..... N87-16969 #
ISSN-0262-5369 ..... N87-17438
ISSN-0281-0263 ..... N87-16965 #
ISSN-0281-0263 ..... N87-16966 #
ISSN-0347-3694 ..... N87-16888 #
ISSN-0379-6566 ..... N87-16923 #
ISSN-0379-6566 ..... N87-17163 #
ISSN-0379-6566 ..... N87-17283 #
ISSN-0379-6566 ..... N87-17535 #
ISSN-0469-4732 ..... N87-17507 #
ISSN-0469-4732 ..... N87-17508 #
ISSN-0469-4732 ..... N87-17509 #
ISSN-0469-4732 ..... N87-17510 #
ISSN-0469-4732 ..... N87-17511 #
ISSN-0469-4732 ..... N87-17512 #
ISSN-0469-4732 ..... N87-17513 #
ISSN-0547-1567 ..... N87-17503 #

IWR-86-R-6 ..... N87-17527 #

JHU/EE-86/19 ..... N87-17460 #

JPL-PUB-86-14 ..... N87-17397* #
JPL-PUB-86-26 ..... N87-17135* #
JPL-PUB-86-38 ..... N87-17111* #
JPL-PUB-86-39 ..... N87-17528* #
JPL-PUB-86-43 ..... N87-16922* #
JPL-PUB-86-44 ..... N87-16921* #
JPL-PUB-86-48 ..... N87-17451* #
JPL-PUB-86-50 ..... N87-17110* #
JPL-PUB-86-015 ..... N87-17396* #

JPRS-UES-86-005 ..... N87-17096 #

L-16070 ..... N87-17479* #
L-16140 ..... N87-17483* #
L-16149 ..... N87-16849* #
L-16177 ..... N87-17417* #
L-16179 ..... N87-17482* #
L-16187 ..... N87-17487* #
L-16194 ..... N87-16815* #
L-16207 ..... N87-16884* #

LA-UR-85-39-53 ..... N87-17535 #
LA-UR-86-1596 ..... N87-17395 #

LBL-20466 ..... N87-17500 #
LBL-21536 ..... N87-17488 #

LC-86-80109-VOL-1 ..... N87-17163 #
LC-86-80109-VOL-2 ..... N87-17283 #

LMSC-F060784/1-VOL-1 ..... N87-16869* #
LMSC-F060784/2-VOL-2 ..... N87-16868* #
LMSC-F060784/4-VOL-4 ..... N87-16865* #
LMSC-F060784/5-VOL-5 ..... N87-16866* #

LR-31032 ..... N87-16883* #

MCR-86-587 ..... N87-16855* #
MCR-86-591 ..... N87-16855* #

MEMO-572 ..... N87-17475 #
MEMO-573 ..... N87-17463 #
MEMO-574 ..... N87-17464 #
MEMO-575 ..... N87-17452 #
MEMO-576 ..... N87-17465 #
MEMO-577 ..... N87-17014 #
MEMO-579 ..... N87-17466 #
MEMO-580 ..... N87-17435 #
MEMO-581 ..... N87-17467 #
MEMO-582 ..... N87-17468 #
MEMO-583 ..... N87-17534 #
MEMO-584 ..... N87-17476 #
MEMO-585 ..... N87-17015 #

MPE-PREPRINT-60 ..... N87-17575
MPE-PREPRINT-61 ..... N87-17576

MQAD-TP-918 ..... N87-16906

MR-196 ..... N87-17454 #

MRL-TN-504 ..... N87-17048 #

MSAT-X-140 ..... N87-16922* #
MSAT-X-141 ..... N87-16921* #

NADC-86119-60 ..... N87-17433 #

NAS 1.15:58276 ..... N87-16792* #
NAS 1.15:77717 ..... N87-16856* #
NAS 1.15:86560 ..... N87-16919* #
NAS 1.15:86569 ..... N87-16900* #
NAS 1.15:86573 ..... N87-16901* #
NAS 1.15:86574 ..... N87-16970* #
NAS 1.15:86575 ..... N87-17532* #
NAS 1.15:86576 ..... N87-16876* #
NAS 1.15:86578 ..... N87-16910* #
NAS 1.15:86579 ..... N87-17455* #
NAS 1.15:86580 ..... N87-17039* #
NAS 1.15:86581 ..... N87-17016* #
NAS 1.15:86582 ..... N87-17040* #
NAS 1.15:86584 ..... N87-16877* #
NAS 1.15:86585 ..... N87-17017* #
NAS 1.15:86726 ..... N87-16821* #
NAS 1.15:86740 ..... N87-16820* #
NAS 1.15:87760 ..... N87-16802* #
NAS 1.15:88267 ..... N87-16819* #
NAS 1.15:88524 ..... N87-16983* #
NAS 1.15:88528 ..... N87-17089* #
NAS 1.15:88531 ..... N87-17595* #
NAS 1.15:88533 ..... N87-16797* #
NAS 1.15:88537 ..... N87-17474* #
NAS 1.15:88541 ..... N87-17394* #
NAS 1.15:88858 ..... N87-17033* #
NAS 1.15:88859 ..... N87-16880* #
NAS 1.15:88868 ..... N87-17656* #
NAS 1.15:88878 ..... N87-16784* #
NAS 1.15:88901 ..... N87-17087* #
NAS 1.15:88903 ..... N87-17002* #
NAS 1.15:88904 ..... N87-16826* #
NAS 1.15:88905 ..... N87-16958* #
NAS 1.15:88906 ..... N87-16827* #
NAS 1.15:88912 ..... N87-17001* #
NAS 1.15:88924 ..... N87-16968* #
NAS 1.15:88929 ..... N87-16805* #
NAS 1.15:88939 ..... N87-16825* #
NAS 1.15:88945 ..... N87-16789* #
NAS 1.15:88946 ..... N87-16790* #
NAS 1.15:88949 ..... N87-16799* #
NAS 1.15:88955 ..... N87-16796* #
NAS 1.15:88956 ..... N87-17441* #
NAS 1.15:88961 ..... N87-16851* #
NAS 1.15:88964 ..... N87-16917* #
NAS 1.15:88971 ..... N87-17480* #
NAS 1.15:88992 ..... N87-16882* #
NAS 1.15:89010 ..... N87-17442* #
NAS 1.15:89016 ..... N87-16911* #
NAS 1.15:89024 ..... N87-16884* #
NAS 1.15:89032 ..... N87-17090* #
NAS 1.15:89035 ..... N87-17482* #
NAS 1.15:89036 ..... N87-16873* #
NAS 1.15:89040 ..... N87-17483* #
NAS 1.15:89057 ..... N87-16848* #
NAS 1.15:89065 ..... N87-17531* #
NAS 1.15:89078 ..... N87-16861* #
NAS 1.15:89082 ..... N87-17086* #
NAS 1.15:89084 ..... N87-16796* #
NAS 1.15:89086 ..... N87-17018* #
NAS 1.15:89312 ..... N87-16816* #
NAS 1.15:89315 ..... N87-16957* #
NAS 1.15:89316 ..... N87-17443* #
NAS 1.15:89414 ..... N87-16801* #
NAS 1.15:89416 ..... N87-16791* #
NAS 1.15:89417 ..... N87-16800* #
NAS 1.21:7053(SUPP-2) ..... N87-17530* #
NAS 1.26:4015 ..... N87-17003* #
NAS 1.26:4019 ..... N87-17481* #
NAS 1.26:4037 ..... N87-16981* #
NAS 1.26:4048 ..... N87-17526* #
NAS 1.26:171953 ..... N87-16655* #
NAS 1.26:171956 ..... N87-17398* #
NAS 1.26:171957 ..... N87-16867* #
NAS 1.26:171958 ..... N87-16862* #
NAS 1.26:171961 ..... N87-16869* #
NAS 1.26:171962 ..... N87-16868* #
NAS 1.26:171963 ..... N87-16865* #
NAS 1.26:171964 ..... N87-16866* #
NAS 1.26:172461 ..... N87-16916* #
NAS 1.26:175056 ..... N87-17400* #
NAS 1.26:175062 ..... N87-16830* #
NAS 1.26:178095 ..... N87-17484* #
NAS 1.26:178153 ..... N87-16860* #
NAS 1.26:178158 ..... N87-17088* #
NAS 1.26:178170 ..... N87-16883* #
NAS 1.26:178171 ..... N87-16870* #
NAS 1.26:178209 ..... N87-17453* #
NAS 1.26:178219 ..... N87-16864* #
NAS 1.26:178222 ..... N87-17456* #
NAS 1.26:178230 ..... N87-17444* #
NAS 1.26:178231 ..... N87-17436* #
NAS 1.26:178236 ..... N87-17448* #
NAS 1.26:178238 ..... N87-17469* #
NAS 1.26:178241 ..... N87-16807* #
NAS 1.26:178967 ..... N87-16982* #
NAS 1.26:178972 ..... N87-17420* #
NAS 1.26:178994 ..... N87-17425* #
NAS 1.26:178997 ..... N87-16829* #
NAS 1.26:178998 ..... N87-17516* #
NAS 1.26:179001 ..... N87-17426* #
NAS 1.26:179009 ..... N87-17041* #
NAS 1.26:179464 ..... N87-16678* #
NAS 1.26:179506 ..... N87-16879* #
NAS 1.26:179523 ..... N87-16804* #
NAS 1.26:179524 ..... N87-16803* #
NAS 1.26:179526 ..... N87-17472* #
NAS 1.26:179527 ..... N87-17473* #
NAS 1.26:179536 ..... N87-17515* #
NAS 1.26:179543 ..... N87-17401* #
NAS 1.26:179546 ..... N87-16972* #
NAS 1.26:179552 ..... N87-16874* #
NAS 1.26:179556 ..... N87-16806* #
NAS 1.26:179566 ..... N87-16954* #
NAS 1.26:179566 ..... N87-16955* #
NAS 1.26:179573 ..... N87-16953* #
NAS 1.26:179896 ..... N87-17429* #
NAS 1.26:179971 ..... N87-17408* #
NAS 1.26:180068 ..... N87-17413* #
NAS 1.26:180073 ..... N87-16971* #
NAS 1.26:180096 ..... N87-17393* #
NAS 1.26:180114 ..... N87-16890* #
NAS 1.26:180127 ..... N87-17397* #
NAS 1.26:180128 ..... N87-17414* #
NAS 1.26:180129 ..... N87-17396* #
NAS 1.26:180130 ..... N87-17111* #
NAS 1.26:180131 ..... N87-17135* #
NAS 1.26:180132 ..... N87-17528* #
NAS 1.26:180133 ..... N87-16822* #
NAS 1.26:180134 ..... N87-16921* #
NAS 1.26:180135 ..... N87-17451* #
NAS 1.26:180137 ..... N87-17415* #
NAS 1.26:180139 ..... N87-17416* #
NAS 1.26:180141 ..... N87-17582* #
NAS 1.26:180142 ..... N87-17581* #
NAS 1.26:180144 ..... N87-17430* #
NAS 1.26:180145 ..... N87-17649* #
NAS 1.26:180146 ..... N87-17440* #
NAS 1.26:180147 ..... N87-17648* #
NAS 1.26:180148 ..... N87-17593* #
NAS 1.26:180149 ..... N87-17418* #
NAS 1.26:180150 ..... N87-17529* #
NAS 1.26:180151 ..... N87-17110* #
NAS 1.26:180152 ..... N87-17583* #
NAS 1.26:180153 ..... N87-17594* #
NAS 1.26:180154 ..... N87-17502* #
NAS 1.26:180155 ..... N87-17584* #
NAS 1.26:180156 ..... N87-16956* #
NAS 1.26:180158 ..... N87-17494* #
NAS 1.26:180159 ..... N87-17004* #
NAS 1.26:180161 ..... N87-17431* #
NAS 1.26:180165 ..... N87-17457* #
NAS 1.26:180166 ..... N87-17458* #
NAS 1.26:180169 ..... N87-17596* #
NAS 1.26:180172 ..... N87-16892* #
NAS 1.55:2441 ..... N87-17598* #
NAS 1.60:2586 ..... N87-17479* #
NAS 1.60:2644 ..... N87-16815* #
NAS 1.60:2652 ..... N87-16849* #
NAS 1.60:2659 ..... N87-17487* #
NAS 1.60:2685 ..... N87-17000* #
NAS 1.60:2694 ..... N87-16902* #
NAS 1.61:1173 ..... N87-17417* #

NASA-CASE-ARC-11363-1 ..... N87-16918* #
NASA-CASE-ARC-11428-2 ..... N87-16909* #
NASA-CASE-ARC-11429-3CU ..... N87-16908* #
NASA-CASE-ARC-11547-1 ..... N87-17026* #

NASA-CASE-GSC-12957-1 ..... N87-17038* #

NASA-CASE-LAR-13006-1 ..... N87-16863* #
NASA-CASE-LAR-13118-2 ..... N87-16907* #
NASA-CASE-LAR-13134-2 ..... N87-16828* #
NASA-CASE-LAR-13255-1 ..... N87-16793* #

NASA-CASE-LEW-14037-1 ..... N87-16875* #

NASA-CASE-MFS-29134-1 ..... N87-17493* #

NASA-CASE-MSC-20162-1 ..... N87-17036* #
NASA-CASE-MSC-20475-1 ..... N87-17037* #
NASA-CASE-MSC-20857-1 ..... N87-17035* #
NASA-CASE-NPO-16321-1CU ..... N87-17034* #
NASA-CASE-NPO-16526-1CU ..... N87-17399* #

NASA-CP-2441 ..... N87-17598* #

NASA-CR-4015 ..... N87-17003* #
NASA-CR-4019 ..... N87-17481* #
NASA-CR-4037 ..... N87-16981* #
NASA-CR-4048 ..... N87-17526* #
NASA-CR-171953 ..... N87-16655* #
NASA-CR-171956 ..... N87-17398* #
NASA-CR-171957 ..... N87-16867* #
NASA-CR-171958 ..... N87-16862* #
NASA-CR-171961 ..... N87-16869* #
NASA-CR-171962 ..... N87-16868* #
NASA-CR-171963 ..... N87-16865* #
NASA-CR-171964 ..... N87-16866* #
NASA-CR-172461 ..... N87-16916* #
NASA-CR-175056 ..... N87-17400* #
NASA-CR-175062 ..... N87-16830* #
NASA-CR-178095 ..... N87-17484* #
NASA-CR-178153 ..... N87-16860* #
NASA-CR-178158 ..... N87-17088* #
NASA-CR-178170 ..... N87-16883* #
NASA-CR-178171 ..... N87-16870* #
NASA-CR-178209 ..... N87-17453* #
NASA-CR-178219 ..... N87-16864* #
NASA-CR-178222 ..... N87-17456* #
NASA-CR-178230 ..... N87-17444* #
NASA-CR-178231 ..... N87-17436* #
NASA-CR-178236 ..... N87-17448* #
NASA-CR-178238 ..... N87-17469* #
NASA-CR-178241 ..... N87-16807* #
NASA-CR-178967 ..... N87-16982* #
NASA-CR-178972 ..... N87-17420* #
NASA-CR-178994 ..... N87-17425* #
NASA-CR-178997 ..... N87-16829* #
NASA-CR-178998 ..... N87-17516* #
NASA-CR-179001 ..... N87-17426* #
NASA-CR-179009 ..... N87-17041* #
NASA-CR-179464 ..... N87-16878* #
NASA-CR-179506 ..... N87-16879* #
NASA-CR-179523 ..... N87-16804* #
NASA-CR-179524 ..... N87-16803* #
NASA-CR-179526 ..... N87-17472* #
NASA-CR-179527 ..... N87-17473* #
NASA-CR-179536 ..... N87-17515* #
NASA-CR-179543 ..... N87-17401* #
NASA-CR-179546 ..... N87-16972* #
NASA-CR-179552 ..... N87-16874* #
NASA-CR-179556 ..... N87-16806* #
NASA-CR-179566 ..... N87-16954* #
NASA-CR-179566 ..... N87-16955* #
NASA-CR-179573 ..... N87-16953* #
NASA-CR-179896 ..... N87-17429* #
NASA-CR-179971 ..... N87-17408* #
NASA-CR-180068 ..... N87-17413* #
NASA-CR-180073 ..... N87-16971* #
NASA-CR-180096 ..... N87-17393* #
NASA-CR-180114 ..... N87-16890* #
NASA-CR-180127 ..... N87-17397* #
NASA-CR-180128 ..... N87-17414* #
NASA-CR-180129 ..... N87-17396* #
NASA-CR-180130 ..... N87-17111* #
NASA-CR-180131 ..... N87-17135* #
NASA-CR-180132 ..... N87-17528* #
NASA-CR-180133 ..... N87-16922* #
NASA-CR-180134 ..... N87-16921* #
NASA-CR-180135 ..... N87-17451* #
NASA-CR-180137 ..... N87-17415* #
NASA-CR-180139 ..... N87-17416* #
NASA-CR-180141 ..... N87-17582* #
NASA-CR-180142 ..... N87-17581* #
NASA-CR-180144 ..... N87-17430* #
NASA-CR-180145 ..... N87-17649* #
NASA-CR-180146 ..... N87-17440* #
NASA-CR-180147 ..... N87-17648* #
NASA-CR-180148 ..... N87-17593* #
NASA-CR-180149 ..... N87-17418* #
NASA-CR-180150 ..... N87-17529* #
NASA-CR-180151 ..... N87-17110* #
NASA-CR-180152 ..... N87-17583* #
NASA-CR-180153 ..... N87-17594* #
NASA-CR-180154 ..... N87-17502* #
NASA-CR-180155 ..... N87-17584* #
NASA-CR-180156 ..... N87-16956* #
NASA-CR-180158 ..... N87-17494* #
NASA-CR-180159 ..... N87-17004* #
NASA-CR-180161 ..... N87-17431* #
NASA-CR-180165 ..... N87-17457* #
NASA-CR-180166 ..... N87-17458* #
NASA-CR-180169 ..... N87-17596* #
NASA-CR-180172 ..... N87-16892* #

NASA-RP-1173 ..... N87-17417* #

NASA-SP-7053(SUPP-2) N87-17530* #

NASA-TM-58276 N87-16792* #
NASA-TM-77717 N87-16856* #
NASA-TM-86560 N87-16919* #
NASA-TM-86569 N87-16900* #
NASA-TM-86573 N87-16901* #
NASA-TM-86574 N87-16970* #
NASA-TM-86575 N87-17532* #
NASA-TM-86576 N87-16876* #
NASA-TM-86578 N87-16910* #
NASA-TM-86579 N87-17455* #
NASA-TM-86580 N87-17039* #
NASA-TM-86581 N87-17016* #
NASA-TM-86582 N87-17040* #
NASA-TM-86584 N87-16877* #
NASA-TM-86585 N87-17017* #
NASA-TM-86726 N87-16821* #
NASA-TM-86740 N87-16820* #
NASA-TM-87760 N87-16802* #
NASA-TM-88267 N87-16819* #
NASA-TM-88524 N87-16983* #
NASA-TM-88528 N87-17069* #
NASA-TM-88531 N87-17595* #
NASA-TM-88533 N87-16797* #
NASA-TM-88537 N87-17474* #
NASA-TM-88541 N87-17394* #
NASA-TM-88858 N87-17033* #
NASA-TM-88859 N87-16880* #
NASA-TM-88868 N87-17656* #
NASA-TM-88878 N87-16784* #
NASA-TM-88901 N87-17087* #
NASA-TM-88903 N87-17002* #
NASA-TM-88904 N87-16826* #
NASA-TM-88905 N87-16958* #
NASA-TM-88906 N87-16827* #
NASA-TM-88912 N87-17001* #
NASA-TM-88924 N87-16968* #
NASA-TM-88929 N87-16805* #
NASA-TM-88939 N87-16825* #
NASA-TM-88945 N87-16789* #
NASA-TM-88946 N87-16790* #
NASA-TM-88949 N87-16799* #
NASA-TM-88955 N87-16798* #
NASA-TM-88956 N87-17441* #
NASA-TM-88961 N87-16851* #
NASA-TM-88964 N87-16917* #
NASA-TM-88971 N87-17480* #
NASA-TM-88992 N87-16882* #
NASA-TM-89010 N87-17442* #
NASA-TM-89016 N87-16911* #
NASA-TM-89024 N87-16884* #
NASA-TM-89032 N87-17090* #
NASA-TM-89035 N87-17482* #
NASA-TM-89036 N87-16873* #
NASA-TM-89040 N87-17483* #
NASA-TM-89057 N87-16848* #
NASA-TM-89065 N87-17531* #
NASA-TM-89078 N87-16861* #
NASA-TM-89082 N87-17086* #
NASA-TM-89084 N87-16796* #
NASA-TM-89086 N87-17018* #
NASA-TM-89312 N87-16816* #
NASA-TM-89315 N87-16957* #
NASA-TM-89316 N87-17443* #
NASA-TM-89414 N87-16801* #
NASA-TM-89416 N87-16791* #
NASA-TM-89417 N87-16800* #

NASA-TP-2586 N87-17479* #
NASA-TP-2644 N87-16815* #
NASA-TP-2652 N87-16849* #
NASA-TP-2659 N87-17487* #
NASA-TP-2685 N87-17000* #
NASA-TP-2694 N87-16902* #

NPL-DITC-74/86 N87-17438

ONERA-RT-16/7252-AN N87-17013 #

ONERA-RTS-80/7103-EY N87-16846 #

OUEL-1637/86 N87-17514 #
OUEL-1644/86 N87-17462 #

PNL-SA-14160 N87-17652 #

PNL-5857 N87-17406 #
PNL-5903 N87-17407 #

PNR90324 N87-16834 #
PNR90330 N87-16835 #
PNR90338 N87-16824
PNR90341 N87-16836 #
PNR90342 N87-16837 #
PNR90346 N87-16838 #
PNR90347 N87-16839 #
PNR90348 N87-16887 #
PNR90349 N87-16840 #
PNR90350 N87-16841 #
PNR90351 N87-17024 #
PNR90355 N87-16905 #
PNR90356 N87-16842 #
PNR90357 N87-16843 #
PNR90359 N87-16844 #
PNR90361 N87-17010 #
PNR90362 N87-16845 #

POLY-MRI-1454-86 N87-17413* #

PUBL-SER-C-FASC-4 N87-17585 #

RADC-TM-86-4 N87-16823 #

RADC-TR-86-87 N87-16961 #

RAE-SPACE-656 N87-16859 #

RAE-TM-P1089 N87-16852 #

RAE-TM-RAD-NAV-265 N87-17042 #

RAE-TR-86013 N87-16859 #

RAE-TRANS-2147 N87-17032 #

RARDE-16/84 N87-17072 #

REPT-7 N87-16980 #
REPT-86SDS4239-PT-2 N87-16977 #
REPT-551.467.3.068(988) N87-17428 #
REPT-1767-MAE N87-17008 #
REPT-4036/6 N87-17041* #
REPT-8911-950001 N87-16874* #

RIACS-TR-86.22 N87-16957* #
RIACS-TR-86.24 N87-17443* #

RR(OH)925 N87-17024 #

RR-292 N87-17095 #
RR-295 N87-17471 #

RSRE-MEMO-3948 N87-17517 #

RTI/3042/07-01F N87-16860* #

R85AEB518 N87-17481* #

S/N-36778 N87-16972* #

SAND-86-0335C N87-17485 #
SAND-86-0845C N87-17524 #

SAPR-22 N87-17594* #
SAPR-23 N87-17594* #
SAPR-24 N87-17594* #

SAR-1 N87-17502* #
SAR-11 N87-17596* #

SASR-1 N87-17583* #
SASR-17 N87-17415* #

SC5345.AR N87-17521 #

SD-TR-86-59 N87-17523 #

SDL-86-2286-15F N87-16895 #

SDSMT/IAS/R-86/08 N87-17426* #

SERI/SP-273-2911 N87-17404 #

SERI/STR-211-2962 N87-17405 #
SERI/STR-217-2732 N87-17402 #
SERI/STR-217-2899 N87-17403 #

SERI/TP-255-2995 N87-16913 #

SFIM-13293-CP/LS N87-17525 #

SLAC-PUB-3981 N87-17491 #

SR-42 N87-17416* #

TR-1 N87-17091 #
TR-88 N87-17459 #
TR-0086(6945-09)-2 N87-17523 #

TRANSL-18511 N87-16844 #

TSL-85-3 N87-17007 #

UCID-20805 N87-16886 #

UCRL-93185 N87-17499 #
UCRL-93752 N87-17489 #
UCRL-94258 N87-17027 #
UCRL-94377 N87-17446 #
UCRL-94800 N87-17009 #
UCRL-94970 N87-17501 #

US-PATENT-APPL-SN-470113 N87-16863* #
US-PATENT-APPL-SN-500046 N87-16918* #
US-PATENT-APPL-SN-550681 N87-16793* #
US-PATENT-APPL-SN-636463 N87-16875* #
US-PATENT-APPL-SN-692745 N87-17026* #
US-PATENT-APPL-SN-692802 N87-17034* #
US-PATENT-APPL-SN-724720 N87-16893
US-PATENT-APPL-SN-725689 N87-17037* #
US-PATENT-APPL-SN-725725 N87-16908* #
US-PATENT-APPL-SN-726558 N87-17520
US-PATENT-APPL-SN-731744 N87-17519
US-PATENT-APPL-SN-760374 N87-16909* #
US-PATENT-APPL-SN-760797 N87-16907* #
US-PATENT-APPL-SN-764805 N87-17036* #
US-PATENT-APPL-SN-767455 N87-16973
US-PATENT-APPL-SN-783886 N87-17035* #
US-PATENT-APPL-SN-783890 N87-17493* #
US-PATENT-APPL-SN-789892 N87-16978 #
US-PATENT-APPL-SN-791972 N87-16904 #
US-PATENT-APPL-SN-800193 N87-17038* #
US-PATENT-APPL-SN-809975 N87-17399* #
US-PATENT-APPL-SN-846462 N87-16828* #
US-PATENT-APPL-SN-849989 N87-16885 #
US-PATENT-APPL-SN-875808 N87-17005 #
US-PATENT-APPL-SN-876618 N87-17045 #
US-PATENT-APPL-SN-877926 N87-17022 #
US-PATENT-APPL-SN-880242 N87-16959 #
US-PATENT-APPL-SN-880245 N87-17019 #
US-PATENT-APPL-SN-880246 N87-16920 #
US-PATENT-APPL-SN-881741 N87-17047 #
US-PATENT-APPL-SN-882059 N87-17021 #
US-PATENT-APPL-SN-882101 N87-17020 #
US-PATENT-APPL-SN-883222 N87-17496 #
US-PATENT-APPL-SN-883249 N87-17043 #
US-PATENT-APPL-SN-884143 N87-16912 #
US-PATENT-APPL-SN-885103 N87-17495 #
US-PATENT-APPL-SN-885116 N87-17046 #
US-PATENT-APPL-SN-887166 N87-17044 #
US-PATENT-APPL-SN-887407 N87-16903 #
US-PATENT-APPL-SN-890201 N87-17477 #
US-PATENT-APPL-SN-891821 N87-16974 #
US-PATENT-APPL-SN-897692 N87-16975 #
US-PATENT-APPL-SN-900126 N87-17518 #

US-PATENT-CLASS-29-576 N87-17520
US-PATENT-CLASS-52-126.5 N87-16918* #
US-PATENT-CLASS-52-309.15 N87-16918* #
US-PATENT-CLASS-52-391 N87-16918* #
US-PATENT-CLASS-52-511 N87-16918* #
US-PATENT-CLASS-52-814 N87-16918* #
US-PATENT-CLASS-60-203.1 N87-16875* #
US-PATENT-CLASS-60-261 N87-16893
US-PATENT-CLASS-134-93 N87-17035* #
US-PATENT-CLASS-134-166C N87-17035* #
US-PATENT-CLASS-135-903 N87-17036* #
US-PATENT-CLASS-136-249 N87-17399* #
US-PATENT-CLASS-156-617 N87-17519
US-PATENT-CLASS-160-23R N87-17036* #
US-PATENT-CLASS-160-265 N87-17036* #
US-PATENT-CLASS-192-46 N87-17037* #
US-PATENT-CLASS-192-67R N87-17037* #
US-PATENT-CLASS-210-282 N87-17035* #
US-PATENT-CLASS-219-124.34 N87-17493* #
US-PATENT-CLASS-219-130.01 N87-17493* #
US-PATENT-CLASS-219-275 N87-16875* #
US-PATENT-CLASS-244-35R N87-16793* #
US-PATENT-CLASS-244-55 N87-16828* #
US-PATENT-CLASS-244-121 N87-17036* #
US-PATENT-CLASS-244-130 N87-16793* #
US-PATENT-CLASS-244-130 N87-16828* #
US-PATENT-CLASS-244-158R N87-17036* #
US-PATENT-CLASS-244-200 N87-16793* #
US-PATENT-CLASS-244-204 N87-16793* #
US-PATENT-CLASS-296-100 N87-17036* #
US-PATENT-CLASS-305-36 N87-17034* #
US-PATENT-CLASS-305-51 N87-17034* #
US-PATENT-CLASS-305-58PC N87-17034* #
US-PATENT-CLASS-305-58R N87-17034* #
US-PATENT-CLASS-310-90.5 N87-17038* #
US-PATENT-CLASS-333-139 N87-16973
US-PATENT-CLASS-340-825.5 N87-16863* #
US-PATENT-CLASS-340-870.18 N87-16863* #
US-PATENT-CLASS-356-28 N87-17026* #
US-PATENT-CLASS-356-28.5 N87-17026* #
US-PATENT-CLASS-371-63 N87-16863* #

US-PATENT-CLASS-375-88 ..... N87-16863* #
US-PATENT-CLASS-428-421 ..... N87-16909* #
US-PATENT-CLASS-428-473.5 ..... N87-16909* #
US-PATENT-CLASS-428-500 ..... N87-16909* #
US-PATENT-CLASS-428-704 ..... N87-16909* #
US-PATENT-CLASS-474-220 ..... N87-17034* #
US-PATENT-CLASS-528-168 ..... N87-16909* #
US-PATENT-CLASS-528-321 ..... N87-16909* #
US-PATENT-CLASS-528-322 ..... N87-16909* #
US-PATENT-CLASS-546-339 ..... N87-16908* #
US-PATENT-CLASS-546-346 ..... N87-16908* #
US-PATENT-CLASS-546-350 ..... N87-16908* #
US-PATENT-CLASS-560-104 ..... N87-16907* #

US-PATENT-4,594,851 ..... N87-16893
US-PATENT-4,602,421 ..... N87-17520
US-PATENT-4,602,979 ..... N87-17519
US-PATENT-4,604,593 ..... N87-16973
US-PATENT-4,608,821 ..... N87-16875* #
US-PATENT-4,619,423 ..... N87-16793* #
US-PATENT-4,626,046 ..... N87-17034* #
US-PATENT-4,626,593 ..... N87-16908* #
US-PATENT-4,629,147 ..... N87-16826* #
US-PATENT-4,631,352 ..... N87-17399* #
US-PATENT-4,631,538 ..... N87-16863* #
US-PATENT-4,632,548 ..... N87-17026* #
US-PATENT-4,633,060 ..... N87-17493* #
US-PATENT-4,634,191 ..... N87-17038* #
US-PATENT-4,634,759 ..... N87-16909* #
US-PATENT-4,635,663 ..... N87-17035* #
US-PATENT-4,635,773 ..... N87-17037* #
US-PATENT-4,637,181 ..... N87-16918* #
US-PATENT-4,637,447 ..... N87-17036* #
US-PATENT-4,638,083 ..... N87-16907* #

USAAVCOM-TR-87-C-2 ..... N87-16816* #

USAAVSCOM-TR-86-C-29 ..... N87-16805* #
USAAVSCOM-TR-86-C-30 ..... N87-16789* #
USAAVSCOM-TR-86-C-31 ..... N87-16790* #

USIP-86-04 ..... N87-17486 #

UTRC/R85-915767-3 ..... N87-16831 #
UTRC/R85-915767-5 ..... N87-16833 #
UTRC/R86-915767-4 ..... N87-16832 #

VKI-LS-1986-03-VOL-3 ..... N87-16984 #
VKI-LS-1986-07-VOL-1 ..... N87-16987 #
VKI-LS-1986-07-VOL-2 ..... N87-16994 #

WDL-TR-10941 ..... N87-16954* #
WDL-TR-10941 ..... N87-16955* #

WES-TR-SL-86-35 ..... N87-16914 #

WSRL-0449-TR ..... N87-16795 #

☆ U.S. GOVERNMENT PRINTING OFFICE: 1987—181-546/60007

FEDERAL DEPOSITORY LIBRARIES

ALABAMA

AUBURN UNIV. AT MONTGOMERY LIBRARY
Documents Department
Montgomery, AL 36193
(205) 279-9110, ext. 253

UNIV. OF ALABAMA LIBRARY
Documents Dept.-Box S
University, AL 35486
(205) 348-7369

ARIZONA

DEPT. OF LIBRARY, ARCHIVES AND PUBLIC RECORDS
Third Floor—State Cap.
1700 West Washington
Phoenix, AZ 85007
(602) 255-4121

UNIVERSITY OF ARIZONA LIB.
Government Documents Dept.
Tucson, AZ 85721
(602) 626-5233

ARKANSAS

ARKANSAS STATE LIBRARY
One Capitol Mall
Little Rock, AR 72201
(501) 371-2326

CALIFORNIA

CALIFORNIA STATE LIBRARY
Govt. Publications Section
P.O. Box 2037
Sacramento, CA 95809
(916) 322-4572

COLORADO

UNIV OF COLORADO LIB.
Government Pub. Division
Campus Box 184
Boulder, CO 80309
(303) 492-8834

DENVER PUBLIC LIBRARY
Govt. Pub. Department
1357 Broadway
Denver, CO 80203
(303) 571-2131

CONNECTICUT

CONNECTICUT STATE LIBRARY
Government Documents Unit
231 Capitol Avenue
Hartford, CT 06106
(203) 566-4971

FLORIDA

UNIV. OF FLORIDA LIBRARIES
Library West
Documents Department
Gainesville, FL 32611
(904) 392-0367

GEORGIA

UNIV. OF GEORGIA LIBRARIES
Government Reference Dept.
Athens, GA 30602
(404) 542-8951

HAWAII

UNIV. OF HAWAII LIBRARY
Govt. Documents Collection
2550 The Mall
Honolulu, HI 96822
(808) 948-8230

IDAHO

UNIV. OF IDAHO LIBRARY
Documents Section
Moscow, ID 83843
(208) 885-6344

ILLINOIS

ILLINOIS STATE LIBRARY
Information Services Branch
Centennial Building
Springfield, IL 62706
(217) 782-5185

INDIANA

INDIANA STATE LIBRARY
Serials Documents Section
140 North Senate Avenue
Indianapolis, IN 46204
(317) 232-3686

IOWA

UNIV. OF IOWA LIBRARIES
Govt. Documents Department
Iowa City, IA 52242
(319) 353-3318

KANSAS

UNIVERSITY OF KANSAS
Doc. Collect—Spencer Lib.
Lawrence, KS 66045
(913) 864-4662

KENTUCKY

UNIV. OF KENTUCKY LIBRARIES
Govt. Pub. Department
Lexington, KY 40506
(606) 257-3139

LOUISIANA

LOUISIANA STATE UNIVERSITY
Middleton Library
Govt. Docs. Dept.
Baton Rouge, LA 70803
(504) 388-2570

LOUISIANA TECHNICAL UNIV. LIBRARY
Documents Department
Ruston, LA 71272
(318) 257-4962

MAINE

UNIVERSITY OF MAINE
Raymond H. Fogler Library
Tri-State Regional Documents Depository
Orono, ME 04469
(207) 581-1680

MARYLAND

UNIVERSITY OF MARYLAND
McKeldin Lib.—Doc. Div.
College Park, MD 20742
(301) 454-3034

MASSACHUSETTS

BOSTON PUBLIC LIBRARY
Government Docs. Dept.
Boston, MA 02117
(617) 536-5400 ext.226

MICHIGAN

DETROIT PUBLIC LIBRARY
Sociology Department
5201 Woodard Avenue
Detroit, MI 48202
(313) 833-1409

MICHIGAN STATE LIBRARY
P.O. Box 30007
Lansing, MI 48909
(517) 373-0640

MINNESOTA

UNIVERSITY OF MINNESOTA
Government Pubs. Division
409 Wilson Library
309 19th Avenue South
Minneapolis, MN 55455
(612) 373-7813

MISSISSIPPI

UNIV. OF MISSISSIPPI LIB.
Documents Department
University, MS 38677
(601) 232-5857

MONTANA

UNIV. OF MONTANA
Mansfield Library
Documents Division
Missoula, MT 59812
(406) 243-6700

NEBRASKA

NEBRASKA LIBRARY COMM.
Federal Documents
1420 P Street
Lincoln, NE 68508
(402) 471-2045
In cooperation with University of Nebraska-Lincoln

NEVADA

UNIVERSITY OF NEVADA LIB.
Govt. Pub. Department
Reno, NV 89557
(702) 784-6579

NEW JERSEY

NEWARK PUBLIC LIBRARY
5 Washington Street
Newark, NJ 07101
(201) 733-7812

NEW MEXICO

UNIVERSITY OF NEW MEXICO
Zimmerman Library
Government Pub. Dept.
Albuquerque, NM 87131
(505) 277-5441

NEW MEXICO STATE LIBRARY
Reference Department
325 Don Gaspar Avenue
Santa Fe, NM 87501
(505) 827-2033, ext. 22

NEW YORK

NEW YORK STATE LIBRARY
Empire State Plaza
Albany, NY 12230
(518) 474-5563

NORTH CAROLINA

UNIVERSITY OF NORTH CAROLINA AT CHAPEL HILL
Wilson Library
BA/SS Documents Division
Chapel Hill, NC 27515
(919) 962-1321

NORTH DAKOTA

UNIVERSITY OF NORTH DAKOTA
Chester Fritz Library
Documents Department
Grand Forks, ND 58202
(701) 777-2617, ext. 27
In cooperation with North Dakota State Univ. Library

OHIO

STATE LIBRARY OF OHIO
Documents Department
65 South Front Street
Columbus, OH 43215
(614) 462-7051

OKLAHOMA

OKLAHOMA DEPT. OF LIB.
Government Documents
200 NE 18th Street
Oklahoma City, OK 73105
(405) 521-2502

OKLAHOMA STATE UNIV. LIB.
Documents Department
Stillwater, OK 74078
(405) 624-6546

OREGON

PORTLAND STATE UNIV. LIB.
Documents Department
P.O. Box 1151
Portland, OR 97207
(503) 229-3673

PENNSYLVANIA

STATE LIBRARY OF PENN.
Government Pub. Section
P.O. Box 1601
Harrisburg, PA 17105
(717) 787-3752

TEXAS

TEXAS STATE LIBRARY
Public Services Department
P.O. Box 12927—Cap. Sta.
Austin, TX 78753
(512) 471-2996

TEXAS TECH. UNIV. LIBRARY
Govt. Documents Department
Lubbock, TX 79409
(806) 742-2268

UTAH

UTAH STATE UNIVERSITY
Merrill Library, U.M.C. 30
Logan, UT 84322
(801) 750-2682

VIRGINIA

UNIVERSITY OF VIRGINIA
Alderman Lib.—Public Doc.
Charlottesville, VA 22901
(804) 924-3133

WASHINGTON

WASHINGTON STATE LIBRARY
Documents Section
Olympia, WA 98504
(206) 753-4027

WEST VIRGINIA

WEST VIRGINIA UNIV. LIB.
Documents Department
Morgantown, WV 26506
(304) 293-3640

WISCONSIN

MILWAUKEE PUBLIC LIBRARY
814 West Wisconsin Avenue
Milwaukee, WI 53233
(414) 278-3000

ST. HIST LIB. OF WISCONSIN
Government Pub. Section
816 State Street
Madison, WI 53706
(608) 262-4347

WYOMING

WYOMING STATE LIBRARY
Supreme Ct. & Library Bld.
Cheyenne, WY 82002
(307) 777-6344

National Aeronautics and
Space Administration
Code NTT-4
Washington, D.C.
20546
Official Business
Penalty for Private Use, $300

SPECIAL FOURTH-CLASS RATE
POSTAGE & FEES PAID
NASA
PERMIT No. G 27

NASA

POSTMASTER: If Undeliverable (Section 158
Postal Manual) Do Not Return

SEP 2.8 1989